

317107

THE LITHOGEOCHEMICAL AND
MINERALOGICAL SETTING
OF TURBIDITE HOSTED
ARSENIC-GOLD
DEPOSITS IN THE
LOWER PALAEOZOIC OF SCOTLAND.

by

Paul R. Duller, B.Sc.

Volume One

Thesis submitted to the
University of Strathclyde for the Degree
of Doctor of Philosophy

Department of Applied Geology,
University of Strathclyde,
GLASGOW,
Scotland,
G1 1XJ.

POST

December 1989.

BEST COPY AVAILABLE.

VARIABLE PRINT QUALITY

The following has been
excluded at the request of
the university

In reference and
bibliography section there
are a couple of journal
articles from p337a to
start of appendices

*There's gold, and it's haunting and haunting;
It's luring me on as of old;
Yet it isn't the gold that I'm wanting,
So much as just finding the gold.*

*It's the great, big, broad land 'way up yonder,
It's the forests where silence has lease;
It's the beauty that thrills me with wonder,
It's the stillness that fills me with peace.*

The Spell of The Yukon, Robert Service.

ORIGINAL RESEARCH PROPOSAL

FORMATION OF SEDIMENTARY EXHALATIVE ARSENIC-ANTIMONY DEPOSITS IN THE SOUTHERN UPLANDS (CASE Studentship).

Supervisors : Dr M.J. Russell (Strathclyde),
Dr M.J. Gallagher (BGS).

Date : 1981.

Stratiform arsenic concentrations recently discovered by the Institute of Geological Sciences in Silurian greywackes of the Southern Uplands are not only significant in themselves and worthy of detailed study but also have pathfinder value for economic antimony mineralization. Stibnite is closely associated with the bedded arsenopyrite but together with other valuable sulphides it is confined to veins of uncertain age and origin. The presence of mass flow deposits in the hostrocks may provide a key to the environment of deposition of the metals. Detailed mineralogical and chemical studies of the extensive sample material (450m of drillcore) may serve to determine the loci of hydrothermal feeders while geochemical analyses of "footwall" rocks, the stratabound sulphide body and "hangingwall" rocks will permit assessment of the chemical and thermal evolution of the hydrothermal system. Isotope studies will be required to elucidate the origin of the sulphur and lead.

Field analyses of arsenic in drainage and overburden samples in conjunction with outcrop mapping of a wide area around the known mineralization will enable criteria to be developed for future exploration. Comparative studies will be made on antimony-arsenic mineralisation elsewhere in the Southern Uplands. Research techniques will be: reflected light microscopy, mass spectrometry, scanning electron microscopy, X-ray diffraction and electron microprobe analysis in mineral characterisation, and atomic absorption and X-ray fluorescence in chemical analysis.

The student will acquire an all-round knowledge of geochemical techniques and an understanding of mineralization which will equip him for work as an economic geologist.

ABSTRACT

Detrital gold is widely dispersed in the Southern Uplands and attributed to minor Au-bearing vein mineralisation hosted by Ordovician and Silurian turbidites. Field, mineralogical and geochemical studies in the Glendinning area indicate the pervasive and laterally extensive nature of hydrothermal alteration and element zonation associated with As-Sb-Au mineralization. Geochemical anomalies are characterised by elevated chalcophile (As, Sb, S, Cu, Pb, Tl, Hg) and depleted siderophile (Fe, Mg, Zn) and alkali group (Na) elements. Broad areas of sodium depletion are indicative of primary hydrothermal activity and together with anomalous arsenic values locate 8 zones of As-Sb-Au-Hg mineralization within 10km of the Glendinning mine and some 60 locations elsewhere in the Southern Uplands of Scotland and the Longford Down, Ireland.

Electron microprobe studies demonstrate that an initial phase of arsenopyrite mineralisation forms the principal locus of submicroscopic and lattice-hosted gold concentration in the Glendinning, Knipe, Caimgarroch Bay and Clontibret As-Sb-Au deposits. Gold deposition was initiated during wallrock alteration and hydraulic brecciation, possibly as a result of fluid chilling, while later stibnite vein deposition was accompanied and overprinted by minor chalcopyrite, sphalerite, galena and a variety of sulphosalts.

Hydrothermal alteration and As-Au mineralisation in the Southern Uplands postdates arc-related volcanism, turbidite deposition and early deformation. The model envisaged invokes the discharge of highly reducing, sulphur-rich hydrothermal fluids, related to the emplacement of structurally constrained, late Silurian calc-alkaline minor intrusives at the close of the Caledonian orogeny. Different levels of crustal emplacement and subsequent exhumation are considered to explain the various styles of As-Sb-Au mineralization exposed in the Southern Uplands.

The complex tectonic history of the Southern Uplands and Longford Down is mirrored by significant variations in the chemical composition of strike parallel greywacke tracts admixed with sediments derived from ophiolites, calc-alkaline volcanic arcs, stable cratons and carbonate shelves. Non-parametric K-means cluster analysis applied to 840 petrographically defined samples, determined the chemical variation within each petrofacies and provides a satisfactory method of classifying individual members. Geochemical traverses through the Southern Uplands and Longford Down reveal lateral continuity over a strike length of 350km.

ACKNOWLEDGEMENTS

This thesis has only been produced with the assistance, support and encouragement of many people over the last six years, to all of whom, for their contributions, I offer my sincere gratitude. In particular I would like to thank Dr Michael Gallagher and Professor Mike Russell who initiated and jointly supervised this research project. I am indebted to them for their advice, innovation and constructive criticism and for providing both the motivation and academic freedom to see this project to completion. Professor's Mike Russell and Peter Baker provided the use of facilities within the Geology Departments of both Strathclyde and Nottingham University, respectively. I am especially grateful to Dr Peter Harvey, Dr Brian Atkin, Adrian Shepard, Don Evans and particularly Dr George Bowes, for their assistance with the many aspects of computing, statistical analysis and data presentation, and for their advice and discussion of the results. The Natural Environment Research Council (NERC) and the British Geological Survey (BGS) jointly supported this CASE research studentship and funded my attendance and participation at the Mineral Deposits Studies Group meetings in Manchester (1983) and Aberdeen (1984). NERC also provided financial assistance to aid my participation at the International Geochemical Exploration Symposium in Toronto (1985) and the Turbidite Hosted Gold Deposits Symposium organised by the Geological Association of Canada, Fredericton (1985). Overseas research visits to Harvard University, the Massachusetts Institute of Technology, the Woods Hole Oceanographic Institute, and my attendance at the Correlation of Caledonian Stratabound Sulphides Symposium, Ottawa (1983) were made possible by the generosity of the Department of Applied Geology. I am indebted to the British Geological Survey for providing a wealth of logistic assistance, at many instances, during field and laboratory studies. Facilities for X-ray fluorescence sample preparation and analysis, wet geochemistry and data processing were provided by the Geology Department of Nottingham University, under the meticulous supervision of Dr Peter Harvey and Dr Brian Atkin. Electron microprobe analytical facilities were generously made available by Dr Richard Patrick, and supervised under the instruction of Dr Tim Hopkins and David Plant within the Department of Geology, Manchester University. Rare earth element analyses were carried out by inductively coupled plasma spectroscopy, under the supervision of Dr Nick Walsh and Simon Chenery, in the Geology Department of King's College, London. Sulphur isotope training and facilities were provided within the Stable Isotope Unit of the British Geological Survey, under the instructions of Dr John Rouse and Malcolm Hunt. The technical staff of both Strathclyde and Nottingham departments donated many hours of their expertise during the tenure of this project, and as such I would like to express my gratitude to Murdoch McLeod, John Gileece, Peter Wallace, Graham Cawson and David Jones. The Scottish Minerals and Lapidary Club in conjunction with the Hopetown Estate are thanked for providing underground access to the Susanna Vein at Leadhills. Detailed investigations in the Glendinning area were only possible due to the cooperation of Lt. Col. R.P. Johnson-Ferguson, the Economic Forestry Group and Tillhill Ltd. They, together with numerous landowners, farmers and shepherds across the Southern Uplands, provided access to land, interest and hospitality. The Captain and crew of the M.V. Apache assisted on numerous occasions during coastal traverses and are warmly thanked. Mr David Wilbur of Munster Base Metals Ltd, made available unpublished company reports and kindly provided access to surface and borehole material from the Clontibret deposit, Co. Monaghan, Eire. Dr John Morris of the Geological Survey of Ireland, acted as both guide and mentor on my numerous visits to the Clontibret area. Mr John Langlands of ACA Howe International Ltd., generously made available unpublished company reports on Southern Scotland. Robert Middleton of Middleton Exploration Services, Chris Cooper of Rio-Finex North Ltd. and Mike O'Neil of O'Neil-McHugh Laboratories, provided complimentary gold data (fire assay and neutron activation analysis) and are gratefully acknowledged. My understanding of Lower Palaeozoic geology and mineralization has benefited from many discussions with survey geologists in both the U.K. and Eire, in particular John Morris, James Floyd, Phillip Stone, Robert Barnes, Neil Fortey, Nick Rock and Richard Gillanders. In addition Dr's Floyd and Morris provided invaluable access to extensive suites of samples from the Southern Uplands and Longford Down respectively. My warmest thanks go to all members of the Department of Applied Geology, especially Allan Hall, George Bowes, Brian Bell and fellow research students Martin Hills, David Banks, Gary Gray, Adrian Boyce, Kerr Anderson and Hanni Mills who provided abundant advice and assistance over the last few years. This work has greatly benefited from discussions held with Robert Middleton, Chris Stanley, Rob Ixer, Iain Samson, John Ashton, Colin Dickinson, David Polya, Robert Scott and Henrik Stendal. Logistic support provided by the Geochem Group during the completion of this thesis is also gratefully acknowledged. Finally, I should like to thank my Parents and Family for their support and encouragement, and especially my Wife, Josie for her patience, hardwork and typing.

CONTENTS

	Page No.
ORIGINAL RESEARCH PROPOSAL.....	i
ABSTRACT.....	ii
ACKNOWLEDGEMENTS.....	iii
CONTENTS.....	iv
LIST OF APPENDICES	vii
LIST OF FIGURES	viii
LIST OF PLATES	xx
LIST OF TABLES	xxi
ENCLOSURES.....	xxix
ABBREVIATIONS AND NOMENCLATURE	xxx

CHAPTER ONE : INTRODUCTION

1.1	Introduction.....	1
1.2	Geological Framework	1
1.3	Gold mineralization in the UK and Ireland.....	2
	1.3.1 Scotland.....	2
	1.3.2 Northern Ireland	7
	1.3.3 Wales.....	7
	1.3.4 Cornwall and Devon	8
	1.3.5 Lake District	9
	1.3.6 Republic of Ireland	9
1.4	Arsenic and antimony mineralization in Scotland.....	10
1.5	The Role of the British Geological Survey.....	12
1.6	Objectives and methodology of the present study.....	13
1.7	Thesis Structure	14

CHAPTER TWO: ANALYTICAL TECHNIQUES AND METHODS OF INTERPRETATION

2.1	Introduction.....	16
2.2	Analytical Techniques	16
	2.2.1 X-Ray fluorescence spectrometry	16
	2.2.2 Electron probe microanalysis.....	17
	2.2.3 Scanning electron microscopy	17
	2.2.4 Fire assay	18
	2.2.5 Instrumental neutron activation analysis	18
2.3	Data Management Techniques	19
	2.3.1 Introduction	19
	2.3.2 The RAW database system	19
2.4	Statistical Techniques	22
	2.4.1 Introduction.....	22
	2.4.2 Simple Statistics	23
	2.4.3 Multivariate Statistics	24
2.5	Graphical Techniques	25

CHAPTER THREE: GEOLOGICAL, GEOCHEMICAL AND MINERALOGICAL STUDIES OF THE GLENDINNING As-Sb-Au DEPOSIT, SOUTHERN SCOTLAND

3.1	Introduction.....	27
3.2	Regional Setting	27
3.3	Geological Environment	28
	3.3.1 Stratigraphy.....	28
	3.3.2 Structure.....	28
	3.3.3 Sedimentology.....	29
3.4	Summary of Previous Investigations	30
	3.4.1 Mining History	31

3.4.2	Recent studies	31
3.4.3	Scope and objectives of this study	31
3.5	Mineralogy.....	34
3.5.1	Ore microscopy	34
3.5.2	Textural and petrographic studies	39
3.5.3	Wallrock alteration	43
3.5.4	Sulphur isotopes	46
3.5.5	Sulphide geochemistry	48
3.6	Geochemical studies	50
3.6.1	Drillcore geochemistry	51
3.6.2	Glendinning regional geochemical traverse	58
3.6.3	Glendinning regional geochemical atlas.....	71
3.6.4	Hydrothermal alteration and geochemical discrimination.....	82
3.7	Soil Geochemistry	86
3.7.1	Overview.....	86
3.7.2	Exploratory data analysis	87
3.7.3	Rams Cleuch	88
3.7.4	Swin Gill	91
3.7.5	Discussion.....	93
3.7.6	Reccomendations.....	95
3.8	Nature and evolution of the hydrothermal system	95
3.9	Summary and conclusions	103

CHAPTER FOUR: TURBIDITE HOSTED ARSENIC-GOLD MINERALIZATION

4.1	Introduction.....	112
4.2	Fluid chemistry	112
4.3	Structural relationships	115
4.3.1	Breccias.....	115
4.3.2	Lineaments.....	117
4.4	Igneous relationships	119
4.4.1	Calc-alkaline associations	119
4.4.2	Lamprophyres.....	121
4.5	Worldwide As-Sb-Au deposits	125
4.5.1	Arsenic dominant deposits	125
4.5.2	Antimony dominant deposits	132
4.5.3	Hot spring geothermal systems	138
4.6	Scottish As-Sb-Au deposits	142
4.7	Genetic models	151
4.8	Summary and conclusions	153

CHAPTER FIVE: REGIONAL LITHOGEOCHEMICAL STUDIES

5.1	Introduction.....	156
5.2	Regional geology	156
5.2.1	Stratigraphy.....	156
5.2.2	Structure.....	157
5.2.3	Sedimentology.....	159
5.2.4	Turbidite petrography and provenance studies	160
5.3	Lithogeochemical studies	163
5.3.1	Aims and objectives	163
5.3.2	Previous investigations and study areas	164
5.3.3	Geochemical classification and mapping	166
5.3.4	Turbidite geochemistry and tectonic setting	173
5.4	Southern Uplands regional studies	179
5.4.1	Southern Uplands composite geochemical traverse.....	179
5.4.2	Marchburn Formation	188
5.4.3	Afton Formation	190
5.4.4	Blackcraig Formation.....	194
5.4.5	Scar Formation	195
5.4.6	Shinnel Formation.....	198

5.4.7	Pyroxenous Formation	198
5.4.8	Intermediate Formation	201
5.4.9	Hawick Group	202
5.4.10	Summary.....	206
5.5	The Rhinns of Galloway geochemical traverses	215
5.5.1	The Corsewell Formation	216
5.5.2	The Kirkcolm Formation	216
5.5.3	The Galdenoch Formation	217
5.5.4	The Portpatrick (Basic Clast) Formation	217
5.5.5	The Portpatrick (Acid Clast) Formation	217
5.5.6	The Pyroxenous Formation	217
5.5.7	The Intermediate Formation	218
5.5.8	The Hawick Formation	218
5.5.9	Lithogeochemical atlas	219
5.6	The Longford Down Geochemical Traverse	224
5.6.1	The Strokestown Group	224
5.6.2	The Gowna Group	226
5.6.3	The Hawick Group	226
5.6.4	Hydrothermal Alteration and Mineralization	227
5.6.5	Longford Down lithogeochemical atlas	228
5.7	Leadhills underground traverse	234
5.8	Interformational studies	235
5.9	Discussion of provenance and tectonic setting	237
5.10	Summary and conclusions	242

CHAPTER SIX: MICROCHEMICAL MAPPING STUDIES

6.1	Introduction.....	245
6.2	Study areas	245
6.3	Sulphide geochemistry and trace element zonation.....	247
6.3.1	Overview.....	247
6.3.2	Deposits.....	250
6.3.2.1	Glendinning.....	250
6.3.2.2	The Knipe	256
6.3.2.3	Cairngarroch Bay	258
6.3.2.4	Talnotry.....	260
6.3.2.5	Clontibret.....	261
6.3.3	Summary.....	263
6.4	Arsenopyrite geothermometry	264
6.4.1	Overview.....	265
6.4.2	Deposits.....	266
6.4.2.1	Glendinning.....	266
6.4.2.2	The Knipe	267
6.4.2.3	Cairngarroch Bay.....	267
6.4.2.4	Talnotry.....	268
6.4.2.5	Clontibret.....	268
6.4	Summary and Conclusions.....	268

CHAPTER SEVEN: CONCLUSIONS

7.1	Introduction.....	270
7.2	Turbidite-hosted arsenic-gold deposits	270
7.3	Turbidite geochemistry and provenance	273
7.4	Recommendations for future work	274

REFERENCES AND BIBLIOGRAPHY.....

<u>APPENDICES.....</u>	1001
<u>FOLDOUTS.....</u>	1196
<u>FIGURES.....</u>	1202
<u>PLATES.....</u>	1778
<u>TABLES.....</u>	1816
<u>ENCLOSURES.....</u>	3084

LIST OF APPENDICES

APPENDIX ONE : X-RAY FLUORESCENCE STUDIES

A1.1	Equipment	1001
A1.2	Sample preparation	1001
A1.2.1	Pressed powder pellet	1001
A1.2.2	Fusion beads	1002
A1.3	Analytical procedures	1004
A1.3.1	XRF analysis	1004
A1.3.2	Ferrous iron determination	1005
A1.3.3	Carbon dioxide determination	1005
A1.3.4	Approximate lower limits of detection	1006
A1.3.5	XRF analytical standards	1006

APPENDIX TWO : INDUCTIVELY COUPLED PLASMA ANALYSIS

A2.1	Equipment	1008
A2.2	REE sample preparation	1008
A2.3	Analytical procedures	1008

APPENDIX THREE : ELECTRON MICROPROBE ANALYSIS

A3.1	Equipment	1010
A3.2	Sample preparation	1010
A3.3	Analytical procedures	1011
A3.4	Analytical conditions, calibration and standards	1012
A3.5	Percentile class intervals	1015
A3.5.1	Arsenopyrite grids.....	1015
A3.5.2	Pyrite grid	1016

APPENDIX FOUR : SULPHUR ISOTOPE STUDIES

A4.1	Equipment	1017
A4.2	Sample preparation	1017
A4.2.1	Hydrofluoric acid digestion	1017
A4.2.2	Diamond drilling	1018
A4.3	Analytical and calibration procedures	1018

APPENDIX FIVE : SAMPLE SITE LOCATIONS

A5.1	Regional greywacke samples	1019
A5.2	West Coast traverse	1026
A5.3	Glendinning exploration samples	1031
A5.4	Wallrock alteration suite	1034
A5.5	Polished thin section index	1035
A5.6	Southern Uplands composite traverse	1037
A5.7	Glendinning regional traverses	1055
A5.8	Longford Down traverse	1066
A5.9	The Rhinns of Galloway traverse	1071
A5.10	Interformational traverses	1077
A5.11	Leadhills Underground traverse	1078
A5.12	Glendinning Borehole traverses	1079

APPENDIX SIX : SEMIQUANTITATIVE X-RAY DIFFRACTION ANALYSIS

A6.1	Whole rock preparation	1083
A6.2	Extraction of clay fractions	1083

APPENDIX SEVEN : COMPUTER PROGRAMS

A7.1	RAW : Numerical database management system	1085
A7.2	HIS : Histograms	1138
A7.3	STA : Univariate statistics	1150
A7.4	RAT : Ratio calculation packages	1162
A7.5	DIS : Simple discriminant analysis	1170
A7.6	TRV : Geochemical traverses	1176
A7.7	SIF : Key input and selection	1183
A7.8	SOR : Sorting/extraction utility	1187

LIST OF FIGURES

Figure No.		Page
1 -	British Isles Location Map (conical projection)	1202
2 -	Thesis methodology and philosophy	1203
3 -	Relationship between the Ordnance survey national numerical grid and the grid reference lettering system	1204
4a-	Major structural lineaments in the UK (after Haszledine 1986).....	1205
4b-	Location of the Glendinning As-Sb-Au deposit with respect to the Southern Uplands Shatter Belt.....	1206
5 -	The occurrence of gold mineralization in the UK (from Collins 1977).....	1207
6 -	Southern Uplands of Scotland Location Map.....	1208
7a-	Location of the Glendinning Deposit in Southern Scotland.....	1209
7b-	Location of Arsenopyrite hosted gold mineralization in the Southern Uplands of Scotland.....	1209
8 -	Occurrences of Gold mineralization in Ireland (after Jones, 1986).....	1210
9 -	Location of the Clontibret deposit in Southern Ireland.....	1211
10-	Detailed mine plans and sections of the Clontibret deposit from Wilbur (1978) and Morris (1986).....	1212
11-	Sites of historical alluvial gold mining in the Leadhills area.....	1214
12-	Distribution of alluvial gold mineralization in the Strath Kildonan (Helmsdale) area of northeast Scotland (after Michie 1974).....	1215
13-	Location map of the principal vein systems in the Loch Tay Area.....	1216
14-	The Leadhills-Wanlockhead Mining District (from Gillanders, 1981).....	1217
15-	Detailed plan of the Susanna Mine, Leadhills and underground sampling site locations.	1218
16-	Geological map of the Southern Uplands showing major lithostratigraphic divisions (from Stone et al 1987).....	1219
17-	Structural map of the Southern Uplands identifying major faults and boundaries between belts (After Leggett 1979).....	1220
18-	Location map of the Southern Uplands defining the position of the Glendinning and Rhinns of Galloway Study areas.....	1221
19-	Comparative lithopetrographic stratigraphy of the Ordovician Rocks of the Southern Uplands (from Floyd 1981).....	1222
20a-	Stratigraphic section through the Ordovician Rocks of the West Nithsdale area of the Southern Uplands (from Floyd 1981).....	1222
20b-	Geological map of the Northern Belt study area (From Floyd 1981).....	1222
20c-	Petrographic traverses displaying the quartz and ferromagnesian mineral content of the Marchburn, Afton, Blackcraig, Scar and Shinnel Formations (after Floyd 1981).....	1223
20d-	QFM diagrams comparing lithopetrographic units in the Northern Belt (after Kelling (1961) and Floyd (1975,1980)).....	1224
21-	Simplified accretionary prism model of the relationships between differing Ordovician petrographic formations during the Early Silurian.....	1225
22-	Geological map of the Fleet granite and surrounding area (from Leake et al.,1978).....	1226
23-	Drainage geochemistry map of the Fleet granite and surrounding area (from Leake et al., 1978)	1228
24-	Location of old metalliferous mines in the vicinity of the Fleet Granite, Southwest Scotland.....	1229
25-	Geological map of the Loch Doon Granite and Surrounding area (from Leake et al., 1981).....	1230
26-	Distribution of alluvial gold in the Loch Doon area (Leake et al., 1981).....	1231
27-	The location of the Marchburn, Afton, Blackcraig, Scar and Shinnel Formations in the Loch Doon area (from Leake et al., 1981).....	1232
28-	Schematic flowchart of the RAW Database management system.....	1233
29-	Sandstone classification diagram (Modified after Dott 1964).....	1234
30-	Measured stratigraphic sections of the Tweed Bridge and Tala Linn study areas.....	1235
31-	Scottish Lamprophyre arsenic and gold geochemistry.....	1236
32-	Histograms showing the distribution of major and trace elements in greywackes from the Glendinning regional Study area.....	1237

33-	Histograms showing the distribution of major and trace elements in mudstones from the Glendinning regional Study area.....	1241
34-	Histograms showing the distribution of major and trace elements in mineralized drillcore from the Glendinning As-Sb-Au deposit.....	1245
35a-	Geochemical Alteration:- Glendinning area SiO_2 (%).....	1249
35b-	Geochemical Alteration:- Glendinning area Al_2O_3 (%).....	1249
35c-	Geochemical Alteration:- Glendinning area TiO_2 (%).....	1249
36a-	Geochemical Alteration:- Glendinning area Fe_2O_3 (%).....	1251
36b-	Geochemical Alteration:- Glendinning area MgO (%).....	1251
36c-	Geochemical Alteration:- Glendinning area CaO (%).....	1251
37a-	Geochemical Alteration:- Glendinning area Na_2O (%).....	1252
37b-	Geochemical Alteration:- Glendinning area K_2O (%).....	1252
37c-	Geochemical Alteration:- Glendinning area MnO (%).....	1252
38a-	Geochemical Alteration:- Glendinning area P_2O_5 (%).....	1253
38b-	Geochemical Alteration:- Glendinning area As (ppm).....	1253
38c-	Geochemical Alteration:- Glendinning area Ba (ppm).....	1253
39a-	Geochemical Alteration:- Glendinning area Cl (ppm).....	1254
39b-	Geochemical Alteration:- Glendinning area Co (ppm).....	1254
39c-	Geochemical Alteration:- Glendinning area Cr (ppm).....	1254
40a-	Geochemical Alteration:- Glendinning area Cu (ppm).....	1255
40b-	Geochemical Alteration:- Glendinning area Ga (ppm).....	1255
40c-	Geochemical Alteration:- Glendinning area La (ppm).....	1255
41a-	Geochemical Alteration:- Glendinning area Ni (ppm).....	1256
41b-	Geochemical Alteration:- Glendinning area Nb (ppm).....	1256
41c-	Geochemical Alteration:- Glendinning area Pb (ppm).....	1256
42a-	Geochemical Alteration:- Glendinning area Rb (ppm).....	1257
42b-	Geochemical Alteration:- Glendinning area Sr (ppm).....	1257
42c-	Geochemical Alteration:- Glendinning area Sb (ppm).....	1257
43a-	Geochemical Alteration:- Glendinning area S (ppm).....	1259
43b-	Geochemical Alteration:- Glendinning area Th (ppm).....	1259
43c-	Geochemical Alteration:- Glendinning area V (ppm).....	1259
44a-	Geochemical Alteration:- Glendinning area Y (ppm).....	1260
44b-	Geochemical Alteration:- Glendinning area Zr (ppm).....	1260
45a-	Geochemical Alteration:- Glendinning area Zn (ppm).....	1261
45b-	Geochemical Alteration:- Glendinning area Tl (ppm).....	1261
46a-	Glendinning Discrimination Diagram:- SiO_2 vs Al_2O_3	1262
46b-	Glendinning Discrimination Diagram:- SiO_2 vs Fe_2O_3	1262
46c-	Glendinning Discrimination Diagram:- SiO_2 vs Na_2O	1262
46d-	Glendinning Discrimination Diagram:- SiO_2 vs K_2O	1262
46e-	Glendinning Discrimination Diagram:- SiO_2 vs Sr.....	1262
46f-	Glendinning Discrimination Diagram:- SiO_2 vs CaO.....	1262
47a-	Glendinning Discrimination Diagram:- SiO_2 vs V.....	1264
47b-	Glendinning Discrimination Diagram:- Al_2O_3 vs TiO_2	1264
47c-	Glendinning Discrimination Diagram:- Al_2O_3 vs Na_2O	1264
47d-	Glendinning Discrimination Diagram:- Al_2O_3 vs K_2O	1264
47e-	Glendinning Discrimination Diagram:- Al_2O_3 vs MgO	1264
47f-	Glendinning Discrimination Diagram:- Al_2O_3 vs CaO.....	1264
48a-	Glendinning Discrimination Diagram:- Al_2O_3 vs Fe_2O_3	1265
48b-	Glendinning Discrimination Diagram:- Al_2O_3 vs Co.....	1265
48c-	Glendinning Discrimination Diagram:- Al_2O_3 vs Sr.....	1265
48d-	Glendinning Discrimination Diagram:- Al_2O_3 vs Rb.....	1265
48e-	Glendinning Discrimination Diagram:- TiO_2 vs Fe_2O_3	1265
48f-	Glendinning Discrimination Diagram:- TiO_2 vs Na_2O	1265
49a-	Glendinning Discrimination Diagram:- TiO_2 vs K_2O	1266
49b-	Glendinning Discrimination Diagram:- TiO_2 vs MgO	1266
49c-	Glendinning Discrimination Diagram:- TiO_2 vs CaO.....	1266
49d-	Glendinning Discrimination Diagram:- TiO_2 vs Rb.....	1266
49e-	Glendinning Discrimination Diagram:- TiO_2 vs V.....	1266
49f-	Glendinning Discrimination Diagram:- Fe_2O_3 vs Na_2O	1266
50a-	Glendinning Discrimination Diagram:- Fe_2O_3 vs K_2O	1268
50b-	Glendinning Discrimination Diagram:- Fe_2O_3 vs MgO	1268
50c-	Glendinning Discrimination Diagram:- Fe_2O_3 vs CaO.....	1268
50d-	Glendinning Discrimination Diagram:- Fe_2O_3 vs Cr.....	1268

50e-	Glendinning Discrimination Diagram:- Fe_2O_3 vs Rb.....	1268
50f-	Glendinning Discrimination Diagram:- Fe_2O_3 vs Sr.....	1268
51a-	Glendinning Discrimination Diagram:- Fe_2O_3 vs Sb.....	1269
51b-	Glendinning Discrimination Diagram:- Fe_2O_3 vs Zr.....	1269
51c-	Glendinning Discrimination Diagram:- Na_2O vs K_2O	1269
51d-	Glendinning Discrimination Diagram:- Na_2O vs Cu.....	1269
51e-	Glendinning Discrimination Diagram:- Na_2O vs Co.....	1269
51f-	Glendinning Discrimination Diagram:- Na_2O vs Cr.....	1269
52a-	Glendinning Discrimination Diagram:- Na_2O vs Ni.....	1271
52b-	Glendinning Discrimination Diagram:- Na_2O vs Rb.....	1271
52c-	Glendinning Discrimination Diagram:- Na_2O vs Sr.....	1271
52d-	Glendinning Discrimination Diagram:- Na_2O vs MgO	1271
52e-	Glendinning Discrimination Diagram:- CaO vs Rb.....	1271
52f-	Glendinning Discrimination Diagram:- CaO vs V.....	1271
53a-	Glendinning Discrimination Diagram:- MgO vs Na_2O	1272
53b-	Glendinning Discrimination Diagram:- MgO vs Rb.....	1272
53c-	Glendinning Discrimination Diagram:- MgO vs V.....	1272
53d-	Glendinning Discrimination Diagram:- MgO vs Ga.....	1272
53e-	Glendinning Discrimination Diagram:- MgO vs Ni.....	1272
53f-	Glendinning Discrimination Diagram:- K_2O vs Sr.....	1272
54a-	Glendinning Discrimination Diagram:- Na_2O vs V.....	1273
54b-	Glendinning Discrimination Diagram:- Co vs Rb.....	1273
54c-	Glendinning Discrimination Diagram:- Cr vs V.....	1273
54d-	Glendinning Discrimination Diagram:- Cr vs Rb.....	1273
54e-	Glendinning Discrimination Diagram:- Cu vs Rb.....	1273
54f-	Glendinning Discrimination Diagram:- Rb vs Sr.....	1273
55a-	Glendinning Discrimination Diagram:- Rb vs V.....	1275
55b-	Glendinning Discrimination Diagram:- Ni vs Rb.....	1275
55c-	Glendinning Discrimination Diagram:- V vs Zr.....	1257
56a-	Southern Uplands Greywacke Formations: SiO_2 (%).....	1276
56b-	Southern Uplands Greywacke Formations: Al_2O_3 (%).....	1276
56c-	Southern Uplands Greywacke Formations: TiO_2 (%).....	1276
57a-	Southern Uplands Greywacke Formations: Fe_2O_3 (%).....	1278
57b-	Southern Uplands Greywacke Formations: MgO (%).....	1278
57c-	Southern Uplands Greywacke Formations: CaO (%).....	1278
58a-	Southern Uplands Greywacke Formations: Na_2O (%).....	1279
58b-	Southern Uplands Greywacke Formations: K_2O (%).....	1279
58c-	Southern Uplands Greywacke Formations: MnO (%).....	1279
59a-	Southern Uplands Greywacke Formations: P_2O_5 (%).....	1280
59b-	Southern Uplands Greywacke Formations: As (ppm).....	1280
59c-	Southern Uplands Greywacke Formations: Ba (ppm).....	1280
60a-	Southern Uplands Greywacke Formations: Co (ppm).....	1281
60b-	Southern Uplands Greywacke Formations: Cr (ppm).....	1281
60c-	Southern Uplands Greywacke Formations: Cu (ppm).....	1281
61a-	Southern Uplands Greywacke Formations: Ga (ppm).....	1283
61b-	Southern Uplands Greywacke Formations: La (ppm).....	1283
61c-	Southern Uplands Greywacke Formations: Ni (ppm).....	1283
62a-	Southern Uplands Greywacke Formations: Nb (ppm).....	1284
62b-	Southern Uplands Greywacke Formations: Rb (ppm).....	1284
62c-	Southern Uplands Greywacke Formations: Sr (ppm).....	1284
63a-	Southern Uplands Greywacke Formations: Pb (ppm).....	1285
63b-	Southern Uplands Greywacke Formations: Sb (ppm).....	1285
63c-	Southern Uplands Greywacke Formations: S (ppm).....	1285
64a-	Southern Uplands Greywacke Formations: Th (ppm).....	1286
64b-	Southern Uplands Greywacke Formations: V (ppm).....	1286
65a-	Southern Uplands Greywacke Formations: Y (ppm).....	1287
65b-	Southern Uplands Greywacke Formations: Zr (ppm).....	1287
65c-	Southern Uplands Greywacke Formations: Zn (ppm).....	1287
66a-	Southern Uplands Greywacke REE study : La (ppm).....	1289
66b-	Southern Uplands Greywacke REE study : Ce (ppm).....	1289
66c-	Southern Uplands Greywacke REE study : Pr (ppm).....	1289
67a-	Southern Uplands Greywacke REE study : Nd (ppm).....	1290
67b-	Southern Uplands Greywacke REE study : Sm (ppm).....	1290

67c-	Southern Uplands Greywacke REE study : Eu (ppm).....	1290
68a-	Southern Uplands Greywacke REE study : Gd (ppm).....	1291
68b-	Southern Uplands Greywacke REE study : Dy (ppm).....	1291
68c-	Southern Uplands Greywacke REE study : Ho (ppm).....	1291
69a-	Southern Uplands Greywacke REE study : Er (ppm).....	1292
69b-	Southern Uplands Greywacke REE study : Yb (ppm).....	1292
69c-	Southern Uplands Greywacke REE study : Lu (ppm).....	1292
70-	Greywacke classification: Marchburn Formation.....	1293
71-	Greywacke classification: Afton Formation.....	1294
72-	Greywacke classification: Blackcraig Formation.....	1296
73-	Greywacke classification: Scar Formation.....	1297
74-	Greywacke classification: Shinnel Formation.....	1298
75-	Greywacke classification: Pyroxenous Formation.....	1299
76-	Greywacke classification: Intermediate Formation.....	1300
77-	Major Element Greywacke classification: Glendinning Greywacke.....	1301
78-	Greywacke classification: Glendinning Mudstone.....	1302
79-	Greywacke classification: Glendinning mineralization.....	1303
80a-	Th-Co-Zr/10 Greywacke classification: Marchburn Formation.....	1305
80b-	Th-Co-Zr/10 Greywacke classification: Afton Formation	1305
80c-	Th-Co-Zr/10 Greywacke classification: Blackcraig Formation.....	1305
80d-	Th-Co-Zr/10 Greywacke classification: Scar Formation.....	1305
81a-	Th-Co-Zr/10 Greywacke classification: Shinnel Formation.....	1306
81b-	Th-Co-Zr/10 Greywacke classification: Pyroxenous Formation.....	1306
81c-	Th-Co-Zr/10 Greywacke classification: Intermediate Formation.....	1306
81d-	Th-Co-Zr/10 Greywacke classification: Hawick Formation.....	1306
82a-	Zr-La-Y Greywacke classification: Marchburn Formation.....	1307
82b-	Zr-La-Y Greywacke classification: Afton Formation.....	1307
82c-	Zr-La-Y Greywacke classification: Blackcraig Formation.....	1307
82d-	Zr-La-Y Greywacke classification: Scar Formation.....	1307
83a-	Zr-La-Y Greywacke classification: Shinnel Formation.....	1308
83b-	Zr-La-Y Greywacke classification: Pyroxenous Formation.....	1308
83c-	Zr-La-Y Greywacke classification: Intermediate Formation.....	1308
83d-	Zr-La-Y Greywacke classification: Hawick Formation.....	1308
84-	Location map of the Glendinning area showing NNE trending structural lineaments identified from aerial photographs (after Gallagher et al 1983).....	1310
85-	Mine section of the Louisa Vein, Glendinning, Southern Scotland (after Dirom, 1850).....	1311
86-	Detailed map of the Glendinning mine area defining the position of BGS traverse lines and Boreholes (after Gallagher et al 1983).....	1312
87-	Geology and topography of the area around the Glendinning mine showing the distribution of antimony in shallow overburden samples (from Gallagher et al 1983).....	1313
88-	Hypothetical E-W trending section through the Glendinning deposit defining width of alteration (stippled) and anastomosing network of mineralized veins (black).....	1314
89-	Summary of geochemical net additions and depletions occurring within the wallrocks adjacent to stibnite vein mineralization at Glendinning.....	1315
90a-	Location map of the Rams Cleuch Area and soil sampling grid.....	1316
90b-	Location map of the Swin Gill Area and soil sampling grid.....	1316
91-	Sample site locations within the Rams Cleuch Soil Grid (200 x 200m).....	1317
92-	Sample site locations within the Swin Gill Soil Grid (300 x 500m).....	1318
93a-	Rams Cleuch Soil Geochemistry Maps: SiO ₂ (%).....	1320
93b-	Rams Cleuch Soil Geochemistry Maps: Al ₂ O ₃ (%).....	1320
93c-	Rams Cleuch Soil Geochemistry Maps: Fe ₂ O ₃ (%).....	1320
93d-	Rams Cleuch Soil Geochemistry Maps: MgO (%).....	1320
93e-	Rams Cleuch Soil Geochemistry Maps: Na ₂ O (%).....	1320
93f-	Rams Cleuch Soil Geochemistry Maps: K ₂ O (%).....	1320
93g-	Rams Cleuch Soil Geochemistry Maps: As (ppm).....	1320
93h-	Rams Cleuch Soil Geochemistry Maps: Sb (ppm).....	1320
94a-	Rams Cleuch Soil Geochemistry Maps: Cu (ppm).....	1322
94b-	Rams Cleuch Soil Geochemistry Maps: Pb (ppm).....	1322
94c-	Rams Cleuch Soil Geochemistry Maps: Zn (ppm).....	1322
94d-	Rams Cleuch Soil Geochemistry Maps: Ba (ppm).....	1322

94e-	Rams Cleuch Soil Geochemistry Maps: S (ppm).....	1322
94f-	Rams Cleuch Soil Geochemistry Maps: Sr (ppm).....	1322
94g-	Rams Cleuch Soil Geochemistry Maps: Rb (ppm).....	1322
94h-	Rams Cleuch Soil Geochemistry Maps: Tl (ppm).....	1322
95a-	Rams Cleuch Soil Geochemistry Maps: Ga (ppm).....	1323
95b-	Rams Cleuch Soil Geochemistry Maps: Co (ppm).....	1323
95c-	Rams Cleuch Soil Geochemistry Maps: Ni (ppm).....	1323
95d-	Rams Cleuch Soil Geochemistry Maps: V (ppm).....	1323
95e-	Rams Cleuch Soil Geochemistry Maps: Eigen Vector 2.....	1323
95f-	Rams Cleuch Soil Geochemistry Maps: Eigen Vector 3.....	1323
96a-	Swin Gill Soil Geochemistry Maps: SiO ₂ (%).....	1325
96b-	Swin Gill Soil Geochemistry Maps: Al ₂ O ₃ (%).....	1325
96c-	Swin Gill Soil Geochemistry Maps: MgO (%).....	1325
96d-	Swin Gill Soil Geochemistry Maps: Fe ₂ O ₃ (%).....	1325
96e-	Swin Gill Soil Geochemistry Maps: K ₂ O (%).....	1325
96f-	Swin Gill Soil Geochemistry Maps: Na ₂ O (%).....	1325
96g-	Swin Gill Soil Geochemistry Maps: As (ppm).....	1325
96h-	Swin Gill Soil Geochemistry Maps: Sb (ppm).....	1325
97a-	Swin Gill Soil Geochemistry Maps: Cu (ppm).....	1326
97b-	Swin Gill Soil Geochemistry Maps: Pb (ppm).....	1326
97c-	Swin Gill Soil Geochemistry Maps: Zn (ppm).....	1326
97d-	Swin Gill Soil Geochemistry Maps: Ba (ppm).....	1326
97e-	Swin Gill Soil Geochemistry Maps: S (ppm).....	1326
97f-	Swin Gill Soil Geochemistry Maps: Sr (ppm).....	1326
97g-	Swin Gill Soil Geochemistry Maps: Sr/Rb.....	1326
97h-	Swin Gill Soil Geochemistry Maps: As/Na.....	1326
98a-	Swin Gill Soil Geochemistry Maps: V (ppm).....	1327
98b-	Swin Gill Soil Geochemistry Maps: Co (ppm).....	1327
98c-	Swin Gill Soil Geochemistry Maps: Ni (ppm).....	1327
98d-	Swin Gill Soil Geochemistry Maps: Eigen Vector 2.....	1327
98e-	Swin Gill Soil Geochemistry Maps: Eigen Vector 3.....	1327
99 -	Swin Gill Composite Soil Anomaly trends: Summary.....	1328
100a-	X-Ray Diffraction Studies: Glendinning Greywacke (CXD1500).....	1330
100b-	X-Ray Diffraction Studies: Glendinning Mudstone (CXD1552).....	1330
101a-	X-Ray Diffraction Studies: Glendinning Greywacke (CXD1551).....	1331
101b-	X-Ray Diffraction Studies: Glendinning Mudstone (CXD2001).....	1331
102a-	X-Ray Diffraction Studies: Glendinning Clay Fraction (CXD1500).....	1332
102b-	X-Ray Diffraction Studies: Glendinning Clay Fraction (CXD1552).....	1332
103a-	X-Ray Diffraction Studies: Glendinning Clay Fraction (CXD1551).....	1333
103b-	X-Ray Diffraction Studies: Glendinning Clay Fraction (CXD2001).....	1333
104-	X-Ray Diffraction Studies: Alunite, Kaolinite and Dickite.....	1334
105-	X-Ray Diffraction Studies: Galena, Arsenopyrite, Stibnite, Pyrite, marcasite and chalcopyrite.....	1335
106-	X-Ray Diffraction Studies: Tetrahedrite, tennantite, jamesonite, pyrrhotite and sphalerite.....	1336
107-	X-Ray Diffraction Studies: Zinkenite, Semseyite and Fuloppite.....	1337
108-	X-Ray Diffraction Studies: Arsenic, antimony, gold and mercury.....	1338
109-	Arsenopyrite Geothermometry: Univariant temperature-sulphur activity diagram (after Kretchmar and Scott, 1976).....	1339
110-	Arsenopyrite Geothermometry: Univariant temperature-antimony (Wt%) diagram (after Gamyandin 1976).....	1341
111-	Arsenopyrite Geothermometry: Arsenic (%) vs. temperature diagram (based upon data provided by Kretchmar and Scott 1976).....	1342
112-	Arsenopyrite Geothermometry: Arsenic (%) vs. sulphur activity (data provided by Kretchmar and Scott 1976).....	1343
113-	Glendinning Stratiform Pyrite Microchemical Mapping studies.....	1344
114-	Glendinning Arsenopyrite (ASP1) Microchemical Mapping Studies.....	1345
115-	Glendinning Arsenopyrite (ASP2) Microchemical Mapping Studies.....	1347
116-	Glendinning Arsenopyrite (ASP5) Microchemical Mapping Studies.....	1349
117-	Glendinning Arsenopyrite (ASP6) Microchemical Mapping Studies.....	1350
118-	The Knipe Arsenopyrite (ASP7) Microchemical Mapping Studies.....	1352
119-	The Knipe Arsenopyrite (ASP8) Microchemical Mapping Studies.....	1354
120-	Talnorty Arsenopyrite (ASP9) Microchemical Mapping studies.....	1355

121-	Cairngarroch Arsenopyrite (ASP10) Microchemical Mapping Studies.....	1358
122-	Cairngarroch Arsenopyrite (ASP11) Microchemical Mapping Studies.....	1360
123-	Cairngarroch Arsenopyrite (ASP12) Microchemical Mapping Studies.....	1361
124-	Cairngarroch Arsenopyrite (ASP13) Microchemical Mapping Studies.....	1363
125-	Clontibret Arsenopyrite (ASP14) Microchemical Mapping Studies.....	1364
126-	Clontibret Arsenopyrite (ASP15) Microchemical Mapping Studies.....	1367
127-	Arsenopyrite geochemistry As-Sb-Au diagram: The Knipe, Talnotry, Cairngarroch and Clontibret deposits.....	1369
128-	Arsenopyrite geochemistry As-Sb-Au diagram: The Glendinning Deposit.....	1370
129-	Arsenopyrite geochemistry S-As-Fe diagram: The Glendinning Deposit.....	1372
130-	Arsenopyrite geochemistry S-As-Fe diagram: The Knipe and Talnotry.....	1374
131-	Arsenopyrite geochemistry S-As-Fe diagram: The Cairngarroch Deposit.....	1376
132-	Arsenopyrite geochemistry S-As-Fe diagram: The Clontibret Deposit.....	1377
133-	A comparative study of the major and trace element chemistry of arsenopyrites from As-Sb-Au deposits in the Southern Uplands of Scotland and Longford Down.....	1378
134-	As-Au diagram of microprobe analyses from disseminated, vein and breccia hosted arsenopyrites from the Glendinning Deposit.....	1381
135-	As-Au diagram of microprobe analyses from vein and wallrock hosted arsenopyrites, Clontibret Deposit.....	1382
136-	As-Au diagram of microprobe analyses from vein and wallrock hosted arsenopyrites, The Knipe Deposit.....	1383
137-	As-Au diagram of microprobe analyses from vein and wallrock hosted arsenopyrites, Talnotry and Cairngarroch Bay Deposits.....	1384
138-	As-Sb diagram of microprobe analyses from stratiform, vein and breccia hosted arsenopyrites in the Glendinning Deposit.....	1385
139-	As-Sb diagram of microprobe analyses from vein and wallrock hosted arsenopyrites, Clontibret Deposit.....	1386
140-	As-Sb diagram of microprobe analyses from vein and wallrock hosted arsenopyrites, Talnotry and Cairngarroch Bay Deposits.....	1388
141-	As-Sb diagram of microprobe analyses from vein and wallrock hosted arsenopyrites, The Knipe Deposit.....	1389
142-	As-S diagram of microprobe analyses from stratiform, vein and breccia hosted arsenopyrites in the Glendinning Deposit.....	1390
143-	As-S diagram of microprobe analyses from vein and wallrock hosted arsenopyrites, Clontibret Deposit.....	1391
144-	As-S diagram of microprobe analyses from vein and wallrock hosted arsenopyrites, Talnotry and Cairngarroch Bay Deposits.....	1392
145-	As-S diagram of microprobe analyses from vein and wallrock hosted arsenopyrites, The Knipe Deposit.....	1393
146-	As-S diagram of microprobe analyses from breccia hosted arsenopyrite, The Glendinning Deposit.....	1394
147-	As-S diagram of microprobe analyses from vein hosted arsenopyrites, The Glendinning Deposit.....	1395
148-	As-S diagram of microprobe analyses from wallrock hosted arsenopyrites, The Glendinning Deposit.....	1396
149-	As-S diagram of microprobe analyses from breccia hosted arsenopyrites, The Glendinning Deposit.....	1398
150-	As-S diagram of microprobe analyses from wallrock hosted arsenopyrites, The Glendinning Deposit.....	1399
151-	As-S diagram of microprobe analyses from Vein hosted arsenopyrites, The Glendinning Deposit.....	1400
152-	As-S diagram of microprobe analyses from wallrock hosted arsenopyrites, The Knipe Deposit.....	1401
153-	As-S diagram of microprobe analyses from vein hosted arsenopyrites, The Knipe Deposit.....	1402
154-	As-S diagram of microprobe analyses from vein hosted arsenopyrites, The Talnotry Deposit.....	1403
155-	As-S diagram of microprobe analyses from vein hosted arsenopyrites, Cairngarroch Deposit.....	1404
156-	As-S diagram of microprobe analyses from vein hosted arsenopyrites, The Clontibret Deposit.....	1406
157-	As-S diagram of microprobe analyses from wallrock hosted arsenopyrites,	

	The Clontibret Deposit.....	1407
158-	Glendinning Regional Lithogeochemical Survey Area: Drainage Map.....	1408
159-	Glendinning Regional Lithogeochemical Survey Area: Contoured Region.....	1409
160-	Glendinning Regional Lithogeochemical Atlas (Greywacke): SiO ₂ (%).....	1411
161-	Glendinning Regional Lithogeochemical Atlas (Greywacke): Al ₂ O ₃ (%).....	1412
162-	Glendinning Regional Lithogeochemical Atlas (Greywacke): TiO ₂ (%).....	1413
163-	Glendinning Regional Lithogeochemical Atlas (Greywacke): Fe ₂ O ₃ (%).....	1414
164-	Glendinning Regional Lithogeochemical Atlas (Greywacke): Na ₂ O (%).....	1415
165-	Glendinning Regional Lithogeochemical Atlas (Greywacke): CaO (%).....	1416
166-	Glendinning Regional Lithogeochemical Atlas (Greywacke): MgO (%).....	1417
167-	Glendinning Regional Lithogeochemical Atlas (Greywacke): K ₂ O (%).....	1419
168-	Glendinning Regional Lithogeochemical Atlas (Greywacke): MnO (%).....	1420
169-	Glendinning Regional Lithogeochemical Atlas (Greywacke): P ₂ O ₅ (%).....	1421
170-	Glendinning Regional Lithogeochemical Atlas (Greywacke): As (ppm).....	1422
171-	Glendinning Regional Lithogeochemical Atlas (Greywacke): Ba (ppm).....	1424
172-	Glendinning Regional Lithogeochemical Atlas (Greywacke): Cl (ppm).....	1425
173-	Glendinning Regional Lithogeochemical Atlas (Greywacke): Co (ppm).....	1426
174-	Glendinning Regional Lithogeochemical Atlas (Greywacke): Cr (ppm).....	1427
175-	Glendinning Regional Lithogeochemical Atlas (Greywacke): Cu (ppm).....	1428
176-	Glendinning Regional Lithogeochemical Atlas (Greywacke): Ga (ppm).....	1429
177-	Glendinning Regional Lithogeochemical Atlas (Greywacke): La (ppm).....	1431
178a-	Glendinning Regional Lithogeochemical Atlas (Greywacke): Ni (ppm).....	1432
178b-	Glendinning Regional Lithogeochemical Atlas (Greywacke): Nb (ppm).....	1433
179-	Glendinning Regional Lithogeochemical Atlas (Greywacke): Pb (ppm).....	1434
180-	Glendinning Regional Lithogeochemical Atlas (Greywacke): Rb (ppm).....	1435
181-	Glendinning Regional Lithogeochemical Atlas (Greywacke): Sr (ppm).....	1436
182-	Glendinning Regional Lithogeochemical Atlas (Greywacke): Sb (ppm).....	1437
183-	Glendinning Regional Lithogeochemical Atlas (Greywacke): S (ppm).....	1439
184-	Glendinning Regional Lithogeochemical Atlas (Greywacke): Th (ppm).....	1440
185-	Glendinning Regional Lithogeochemical Atlas (Greywacke): V (ppm).....	1441
186-	Glendinning Regional Lithogeochemical Atlas (Greywacke): Y (ppm).....	1442
187-	Glendinning Regional Lithogeochemical Atlas (Greywacke): Zn (ppm).....	1444
188-	Glendinning Regional Lithogeochemical Atlas (Greywacke): Zr (ppm).....	1445
189-	Glendinning Regional Lithogeochemical Atlas (Greywacke): TL (ppm).....	1446
190-	Glendinning Regional Lithogeochemical Atlas (Mudstone): SiO ₂ (%).....	1447
191-	Glendinning Regional Lithogeochemical Atlas (Mudstone): Al ₂ O ₃ (%).....	1448
192-	Glendinning Regional Lithogeochemical Atlas (Mudstone): TiO ₂ (%).....	1449
193-	Glendinning Regional Lithogeochemical Atlas (Mudstone): Fe ₂ O ₃ (%).....	1451
194-	Glendinning Regional Lithogeochemical Atlas (Mudstone): Na ₂ O (%).....	1452
195-	Glendinning Regional Lithogeochemical Atlas (Mudstone): CaO (%).....	1453
196-	Glendinning Regional Lithogeochemical Atlas (Mudstone): MgO (%).....	1454
197-	Glendinning Regional Lithogeochemical Atlas (Mudstone): K ₂ O (%).....	1455
198-	Glendinning Regional Lithogeochemical Atlas (Mudstone): MnO (%).....	1456
199-	Glendinning Regional Lithogeochemical Atlas (Mudstone): P ₂ O ₅ (%).....	1457
200-	Glendinning Regional Lithogeochemical Atlas (Mudstone): As (ppm).....	1459
201-	Glendinning Regional Lithogeochemical Atlas (Mudstone): Ba (ppm).....	1460
202-	Glendinning Regional Lithogeochemical Atlas (Mudstone): Cl (ppm).....	1461
203-	Glendinning Regional Lithogeochemical Atlas (Mudstone): Co (ppm).....	1462
204-	Glendinning Regional Lithogeochemical Atlas (Mudstone): Cr (ppm).....	1463
205-	Glendinning Regional Lithogeochemical Atlas (Mudstone): Cu (ppm).....	1464
206-	Glendinning Regional Lithogeochemical Atlas (Mudstone): Ga (ppm).....	1466
207-	Glendinning Regional Lithogeochemical Atlas (Mudstone): La (ppm).....	1467
208-	Glendinning Regional Lithogeochemical Atlas (Mudstone): Ni (ppm).....	1468
209-	Glendinning Regional Lithogeochemical Atlas (Mudstone): Nb (ppm).....	1469
210-	Glendinning Regional Lithogeochemical Atlas (Mudstone): Pb (ppm).....	1470
211-	Glendinning Regional Lithogeochemical Atlas (Mudstone): Rb (ppm).....	1471
212-	Glendinning Regional Lithogeochemical Atlas (Mudstone): Sr (ppm).....	1472
213-	Glendinning Regional Lithogeochemical Atlas (Mudstone): Sb (ppm).....	1474
214-	Glendinning Regional Lithogeochemical Atlas (Mudstone): S (ppm).....	1475
215-	Glendinning Regional Lithogeochemical Atlas (Mudstone): Th (ppm).....	1476
216-	Glendinning Regional Lithogeochemical Atlas (Mudstone): V (ppm).....	1477
217-	Glendinning Regional Lithogeochemical Atlas (Mudstone): Y (ppm).....	1478
218-	Glendinning Regional Lithogeochemical Atlas (Mudstone): Zn (ppm).....	1479

219-	Glendinning Regional Lithogeochemical Atlas (Mudstone): Zr (ppm).....	1481
220-	Glendinning Regional Lithogeochemical Atlas (Mudstone): TL (ppm).....	1482
221-	Glendinning Regional Atlas: Multi-element Greywacke Anomaly Map.....	1483
222-	Glendinning Regional Atlas: Multi-element Greywacke Depletion Map.....	1484
223-	Glendinning Regional Atlas: Multi-element Mudstone Anomaly Map.....	1485
224-	Glendinning Regional Atlas: Multi-element Mudstone Depletion Map.....	1486
225-	Southern Uplands Greywacke Geochemistry: SiO ₂ Histograms	1488
226-	Southern Uplands Greywacke Geochemistry: Al ₂ O ₃ Histograms.....	1489
227-	Southern Uplands Greywacke Geochemistry: TiO ₂ Histograms.....	1490
228-	Southern Uplands Greywacke Geochemistry: Fe ₂ O ₃ Histograms.....	1491
229-	Southern Uplands Greywacke Geochemistry: MgO Histograms.....	1492
230-	Southern Uplands Greywacke Geochemistry: CaO Histograms.....	1493
231-	Southern Uplands Greywacke Geochemistry: Na ₂ O Histograms.....	1494
232-	Southern Uplands Greywacke Geochemistry: K ₂ O Histograms.....	1485
233-	Southern Uplands Greywacke Geochemistry: MnO Histograms.....	1497
234-	Southern Uplands Greywacke Geochemistry: P ₂ O ₅ Histograms.....	1498
235-	Southern Uplands Greywacke Geochemistry: As Histograms.....	1499
236-	Southern Uplands Greywacke Geochemistry: Ba Histograms.....	1500
237-	Southern Uplands Greywacke Geochemistry: Co Histograms.....	1501
238-	Southern Uplands Greywacke Geochemistry: Cr Histograms.....	1502
239-	Southern Uplands Greywacke Geochemistry: Cu Histograms.....	1503
240-	Southern Uplands Greywacke Geochemistry: Ga Histograms.....	1504
241-	Southern Uplands Greywacke Geochemistry: La Histograms.....	1505
242-	Southern Uplands Greywacke Geochemistry: Ni Histograms.....	1506
243-	Southern Uplands Greywacke Geochemistry: Nb Histograms.....	1507
244-	Southern Uplands Greywacke Geochemistry: Pb Histograms.....	1508
245-	Southern Uplands Greywacke Geochemistry: Rb Histograms.....	1510
246-	Southern Uplands Greywacke Geochemistry: S Histograms.....	1511
247-	Southern Uplands Greywacke Geochemistry: Sb Histograms.....	1512
248-	Southern Uplands Greywacke Geochemistry: Sr Histograms.....	1513
249-	Southern Uplands Greywacke Geochemistry: Th Histograms.....	1514
250-	Southern Uplands Greywacke Geochemistry: V Histograms.....	1515
251-	Southern Uplands Greywacke Geochemistry: Y Histograms.....	1516
252-	Southern Uplands Greywacke Geochemistry: Zn Histograms	1517
253-	Southern Uplands Greywacke Geochemistry: Zr Histograms.....	1518
254-	Southern Uplands Greywacke Geochemistry: Al/Si Histograms.....	1519
255-	Southern Uplands Greywacke Geochemistry: K/Na Histograms.....	1520
256-	Southern Uplands Greywacke Geochemistry: K/K+Na Histograms.....	1521
257-	Southern Uplands Greywacke Geochemistry: K+Na Histograms.....	1523
258-	Southern Uplands Greywacke Geochemistry: Rb/Sr Histograms.....	1524
259-	Southern Uplands Greywacke Geochemistry: Mg+Fe Histograms.....	1525
260-	Southern Uplands Greywacke Geochemistry: Fe/Mg Histograms.....	1526
261-	Southern Uplands Greywacke Geochemistry: Ni/Co Histograms.....	1527
262-	Southern Uplands Greywacke Geochemistry: Zr/Nb Histograms.....	1528
263-	Southern Uplands Greywacke Geochemistry: La/Y Histograms.....	1529
264-	Southern Uplands Greywacke Geochemistry: Nb/P Histograms.....	1530
265-	Southern Uplands Greywacke Geochemistry: Nb/Y Histograms.....	1531
266-	Geological Map of the Northern Section of the Rhinns of Galloway.....	1532
267-	Lithogeochemical Atlas of the Rhinns of Galloway, Scotland: SiO ₂ (%).....	1534
268-	Lithogeochemical Atlas of the Rhinns of Galloway, Scotland: Al ₂ O ₃ (%).....	1535
269-	Lithogeochemical Atlas of the Rhinns of Galloway, Scotland: TiO ₂ (%).....	1536
270-	Lithogeochemical Atlas of the Rhinns of Galloway, Scotland: Fe ₂ O ₃ (%).....	1537
271-	Lithogeochemical Atlas of the Rhinns of Galloway, Scotland: MgO (%).....	1538
272-	Lithogeochemical Atlas of the Rhinns of Galloway, Scotland: Na ₂ O (%).....	1539
273-	Lithogeochemical Atlas of the Rhinns of Galloway, Scotland: CaO (%).....	1540
274-	Lithogeochemical Atlas of the Rhinns of Galloway, Scotland: K ₂ O (%).....	1541
275-	Lithogeochemical Atlas of the Rhinns of Galloway, Scotland: MnO (%).....	1542
276-	Lithogeochemical Atlas of the Rhinns of Galloway, Scotland: P ₂ O ₅ (%).....	1544
277-	Lithogeochemical Atlas of the Rhinns of Galloway, Scotland: As (ppm).....	1545
278-	Detailed enlargement of Arsenic anomalies, Southeast of Portpatrick.....	1546
279-	Lithogeochemical Atlas of the Rhinns of Galloway, Scotland: Ba (ppm).....	1547
280-	Lithogeochemical Atlas of the Rhinns of Galloway, Scotland: Co (ppm).....	1548
281-	Lithogeochemical Atlas of the Rhinns of Galloway, Scotland: Cr (ppm).....	1549

282-	Lithogeochemical Atlas of the Rhinns of Galloway, Scotland: Cu (ppm).....	1550
283-	Lithogeochemical Atlas of the Rhinns of Galloway, Scotland: La (ppm).....	1551
284-	Lithogeochemical Atlas of the Rhinns of Galloway, Scotland: Nb (ppm).....	1552
285-	Lithogeochemical Atlas of the Rhinns of Galloway, Scotland: Ni (ppm).....	1554
286-	Lithogeochemical Atlas of the Rhinns of Galloway, Scotland: Pb (ppm).....	1555
287-	Lithogeochemical Atlas of the Rhinns of Galloway, Scotland: Rb (ppm).....	1556
288-	Lithogeochemical Atlas of the Rhinns of Galloway, Scotland: S (ppm).....	1557
289-	Lithogeochemical Atlas of the Rhinns of Galloway, Scotland: Sb (ppm).....	1558
290-	Lithogeochemical Atlas of the Rhinns of Galloway, Scotland: Sr (ppm).....	1559
291-	Lithogeochemical Atlas of the Rhinns of Galloway, Scotland: Th (ppm).....	1560
292-	Lithogeochemical Atlas of the Rhinns of Galloway, Scotland: V (ppm).....	1561
293-	Lithogeochemical Atlas of the Rhinns of Galloway, Scotland: Y (ppm).....	1562
294-	Lithogeochemical Atlas of the Rhinns of Galloway, Scotland: Zn (ppm).....	1564
295-	Lithogeochemical Atlas of the Rhinns of Galloway, Scotland: Zr (ppm).....	1565
296a-	Petrochemical Stratigraphy of the Southern Uplands and Longford Down.....	1566
296b-	Petrographic Greywacke Formations in the Southern Uplands of Scotland.....	1567
297-	Changes in Sea level and associated features through the Lower Palaeozoic stratigraphic Record in the British Isles (from Legget 1981).....	1568
298-	Underground lithogeochemical traverse of the Susanna Vein, Leadhills.....	1569
299-	IUGS Silica-Total Alkali Classification Diagram (after LeBas 1983).....	1574
300-	IUGS Silica-Total Alkali Diagram: Marchburn and Afton Formations.....	1575
301-	IUGS Silica-Total Alkali Diagram: Blackcraig and Scar Formations.....	1576
302-	IUGS Silica-Total Alkali Diagram: Shinnel and Pyroxenous Formations.....	1577
303-	IUGS Silica-Total Alkali Diagram: Intermediate and Hawick Formations.....	1578
304-	IUGS Silica-Total Alkali Diagram: Glendinning Greywacke.....	1580
305-	IUGS Silica-Total Alkali Diagram: Glendinning mineralized Greywacke.....	1581
306-	CaO-Sr Discrimination Diagram: Marchburn Formation.....	1582
307-	CaO-Sr Discrimination Diagram: Afton Formation.....	1583
308-	CaO-Sr Discrimination Diagram: Blackcraig Formation.....	1584
309-	CaO-Sr Discrimination Diagram: Scar Formation.....	1585
310-	CaO-Sr Discrimination Diagram: Shinnel Formation.....	1586
311-	CaO-Sr Discrimination Diagram: Pyroxenous Formation.....	1587
312-	CaO-Sr Discrimination Diagram: Intermediate and Hawick Formation.....	1589
313-	SiO ₂ -MgO Discrimination Diagram: Marchburn and Afton Formation.....	1590
314-	SiO ₂ -MgO Discrimination Diagram: Blackcraig and Scar Formation.....	1591
315-	SiO ₂ -MgO Discrimination Diagram: Pyroxenous and Shinnel Formation.....	1592
316-	SiO ₂ -MgO Discrimination Diagram: Intermediate and Hawick Formation.....	1593
317-	SiO ₂ -Rb Discrimination Diagram: Marchburn and Afton Formation.....	1594
318-	SiO ₂ -Rb Discrimination Diagram: Blackcraig and Scar Formation.....	1595
319-	SiO ₂ -Rb Discrimination Diagram: Pyroxenous and Shinnel Formation.....	1597
320-	SiO ₂ -Rb Discrimination Diagram: Intermediate and Hawick Formation.....	1598
321-	SiO ₂ -CaO Discrimination Diagram: Marchburn and Afton Formation.....	1599
322-	SiO ₂ -CaO Discrimination Diagram: Blackcraig and Scar Formation.....	1600
323-	SiO ₂ -CaO Discrimination Diagram: Pyroxenous and Shinnel Formation.....	1601
324-	SiO ₂ -CaO Discrimination Diagram: Intermediate and Hawick Formation.....	1602
325-	SiO ₂ -Sr Discrimination Diagram: Marchburn and Afton Formation.....	1604
326-	SiO ₂ -Sr Discrimination Diagram: Blackcraig and Scar Formation.....	1605
327-	SiO ₂ -Sr Discrimination Diagram: Pyroxenous and Shinnel Formation.....	1606
328-	SiO ₂ -Sr Discrimination Diagram: Intermediate and Hawick Formation.....	1607
329-	SiO ₂ -Na ₂ O Discrimination Diagram: Marchburn and Afton Formation.....	1608
330-	SiO ₂ -Na ₂ O Discrimination Diagram: Blackcraig and Scar Formation.....	1609
331-	SiO ₂ -Na ₂ O Discrimination Diagram: Pyroxenous and Shinnel Formation.....	1611
332-	SiO ₂ -Na ₂ O Discrimination Diagram: Intermediate and Hawick Formation.....	1612
333-	SiO ₂ -TiO ₂ Discrimination Diagram: Marchburn and Afton Formation.....	1613
334-	SiO ₂ -TiO ₂ Discrimination Diagram: Blackcraig and Scar Formation.....	1614
335-	SiO ₂ -TiO ₂ Discrimination Diagram: Pyroxenous and Shinnel Formation.....	1615
336-	SiO ₂ -TiO ₂ Discrimination Diagram: Intermediate and Hawick Formation.....	1616
337-	SiO ₂ -Fe Discrimination Diagram: Marchburn and Afton Formation.....	1618
338-	SiO ₂ -Fe Discrimination Diagram: Blackcraig and Scar Formation.....	1619
339-	SiO ₂ -Fe Discrimination Diagram: Pyroxenous and Shinnel Formation.....	1620
340-	SiO ₂ -Fe Discrimination Diagram: Intermediate and Hawick Formation.....	1621
341-	(Fe+Mg)-Ti Discrimination Diagram: Marchburn and Afton Formation.....	1622
342-	(Fe+Mg)-Ti Discrimination Diagram: Blackcraig and Scar Formation.....	1623

343-	(Fe+Mg)-Ti Discrimination Diagram: Pyroxenous and Shinnel Formation.....	1625
344-	(Fe+Mg)-Ti Discrimination Diagram: Intermediate and Hawick Formation.....	1626
345-	(Fe+Mg)-(Al/Si) Discrimination Diagram: Marchburn and Afton Formation...	1627
346-	(Fe+Mg)-(Al/Si) Discrimination Diagram: Blackcraig and Scar Formation.....	1628
347-	(Fe+Mg)-(Al/Si) Discrimination Diagram: Pyroxenous and Shinnel Form.	1629
348-	(Fe+Mg)-(Al/Si) Discrimination Diagram: Intermediate and Hawick Form. ...	1630
349-	(Fe+Mg)-(K/Na) Discrimination Diagram: Marchburn and Afton Formation..	1632
350-	(Fe+Mg)-(K/Na) Discrimination Diagram: Blackcraig and Scar Formation.....	1633
351-	(Fe+Mg)-(K/Na) Discrimination Diagram: Pyroxenous and Shinnel Form.	1634
352-	(Fe+Mg)-(K/Na) Discrimination Diagram: Intermediate and Hawick Form....	1635
353-	(Fe+Mg)-(Al/(CaO+Na ₂ O)) Diagram: Marchburn and Afton Formation.....	1636
354-	(Fe+Mg)-(Al/(CaO+Na ₂ O)) Diagram: Blackcraig and Scar Formation.....	1637
355-	(Fe+Mg)-(Al/(CaO+Na ₂ O)) Diagram: Pyroxenous and Shinnel Formation.....	1639
356-	(Fe+Mg)-(Al/(CaO+Na ₂ O)) Diagram: Intermediate and Hawick Formation.....	1640
357-	Th-La Discrimination Diagram: Marchburn and Afton Formation.....	1641
358-	Th-La Discrimination Diagram: Blackcraig and Scar Formation.....	1642
359-	Th-La Discrimination Diagram: Pyroxenous and Shinnel Formation.....	1643
360-	Th-la Discrimination Diagram: Intermediate and Hawick Formation.....	1644
361-	(K/K+Na)-(K+Na) Discrimination Diagram: Marchburn and Afton Form.	1645
362-	(K/K+Na)-(K+Na) Discrimination Diagram: Blackcraig and Scar Formation...	1647
363-	(K/K+Na)-(K+Na) Discrimination Diagram: Pyroxenous and Shinnel Form. ..	1648
364-	(K/K+Na)-(K+Na) Discrimination Diagram: Intermediate and Hawick Form..	1649
365-	(K/K+Na)-(K+Na) Discrimination Diagram: As-Sb-Au mineralization Study..	1650
366-	Fe/Mg-Cr Discrimination Diagram: Marchburn and Afton Formation.....	1651
367-	Fe/Mg-Cr Discrimination Diagram: Blackcraig and Scar Formation.....	1653
368-	Fe/Mg-Cr Discrimination Diagram: Pyroxenous and Shinnel Formation.....	1654
369-	Fe/Mg-Cr Discrimination Diagram: Intermediate and Hawick Formation.....	1655
370-	Y-CaO Discrimination Diagram: Marchburn and Afton Formation.....	1656
371-	Y-CaO Discrimination Diagram: Blackcraig and Scar Formation.....	1657
372-	Y-CaO Discrimination Diagram: Pyroxenous and Shinnel Formation.....	1659
373-	Y-CaO Discrimination Diagram: Intermediate and Hawick Formation.....	1660
374-	Sr-Y Discrimination Diagram: Marchburn and Afton Formation.....	1661
375-	Sr-Y Discrimination Diagram: Blackcraig and Scar Formation.....	1662
376-	Sr-Y Discrimination Diagram: Pyroxenous and Shinnel Formation.....	1663
377-	Sr-Y Discrimination Diagram: Intermediate and Hawick Formation.....	1664
378-	K ₂ O-Rb Discrimination Diagram: Marchburn and Afton Formation.....	1666
379-	K ₂ O-Rb Discrimination Diagram: Blackcraig and Scar Formation.....	1667
380-	K ₂ O-Rb Discrimination Diagram: Pyroxenous and Shinnel Formation.....	1668
381-	K ₂ O-Rb Discrimination Diagram: Intermediate and Hawick Formation.....	1669
382-	K ₂ O-Rb Discrimination Diagram: As-Sb-Au mineralization Study.....	1670
383-	MgO-Sr Discrimination Diagram: Marchburn and Afton Formation.....	1671
384-	MgO-Sr Discrimination Diagram: Blackcraig and Scar Formation.....	1672
385-	MgO-Sr Discrimination Diagram: Pyroxenous and Shinnel Formation.....	1674
386-	MgO-Sr Discrimination Diagram: Intermediate and Hawick Formation.....	1675
387-	Cr-V Discrimination Diagram: Marchburn and Afton Formation.....	1676
388-	Cr-V Discrimination Diagram: Blackcraig and Scar Formation.....	1677
389-	Cr-V Discrimination Diagram: Pyroxenous and Shinnel Formation.....	1678
390-	Cr-V Discrimination Diagram: Intermediate and Hawick Formation.....	1679
391-	Ni-Cr Discrimination Diagram: Marchburn and Afton Formation.....	1681
392-	Ni-Cr Discrimination Diagram: Blackcraig and Scar Formation.....	1682
393-	Ni-Cr Discrimination Diagram: Pyroxenous and Shinnel Formation.....	1683
394-	Ni-Cr Discrimination Diagram: Intermediate and Hawick Formation.....	1684
395-	Zr-Y Discrimination Diagram: Marchburn and Afton Formation.....	1685
396-	Zr-Y Discrimination Diagram: Blackcraig and Scar Formation.....	1686
397-	Zr-Y Discrimination Diagram: Pyroxenous and Shinnel Formation.....	1688
398-	Zr-Y Discrimination Diagram: Intermediate and Hawick Formation.....	1689
399-	Fe/Mg-Zr Discrimination Diagram: Marchburn and Afton Formation.....	1690
400-	Fe/Mg-Zr Discrimination Diagram: Blackcraig and Scar Formation.....	1691
401-	Fe/Mg-Zr Discrimination Diagram: Pyroxenous and Shinnel Formation.....	1692
402-	Fe/Mg-Zr Discrimination Diagram: Intermediate and Hawick Formation.....	1693
403-	Zr-TiO ₂ Discrimination Diagram: Marchburn and Afton Formation.....	1694
404-	Zr-TiO ₂ Discrimination Diagram: Blackcraig and Scar Formation.....	1696
405-	Zr-TiO ₂ Discrimination Diagram: Pyroxenous and Shinnel Formation.....	1697

406-	Zr-TiO ₂ Discrimination Diagram: Intermediate and Hawick Formation.....	1698
407-	La/Y-Nb/Y Discrimination Diagram: Marchburn and Afton Formation.....	1699
408-	La/Y-Nb/Y Discrimination Diagram: Blackcraig and Scar Formation.....	1700
409-	La/Y-Nb/Y Discrimination Diagram: Pyroxenous and Shinnel Formation.....	1702
410-	La/Y-Nb/Y Discrimination Diagram: Intermediate and Hawick Formation.....	1703
411-	Longford Down Lithogeochemical Survey Area: Geological Map.....	1704
412-	Longford Down Lithogeochemical Atlas : SiO ₂ (%).....	1706
413-	Longford Down Lithogeochemical Atlas : Al ₂ O ₃ (%).....	1707
414-	Longford Down Lithogeochemical Atlas : TiO ₂ (%).....	1708
415-	Longford Down Lithogeochemical Atlas : Fe ₂ O ₃ (%).....	1710
416-	Longford Down Lithogeochemical Atlas : Na ₂ O (%).....	1711
417-	Longford Down Lithogeochemical Atlas : CaO (%).....	1712
418-	Longford Down Lithogeochemical Atlas : MgO (%).....	1713
419-	Longford Down Lithogeochemical Atlas : K ₂ O (%).....	1714
420-	Longford Down Lithogeochemical Atlas : MnO (%).....	1715
421-	Longford Down Lithogeochemical Atlas : P ₂ O ₅ (%).....	1716
422-	Longford Down Lithogeochemical Atlas : As (ppm).....	1717
423-	Longford Down Lithogeochemical Atlas : Ba (ppm).....	1719
424-	Longford Down Lithogeochemical Atlas : Co (ppm).....	1720
425-	Longford Down Lithogeochemical Atlas : Cr (ppm).....	1721
426-	Longford Down Lithogeochemical Atlas : Cu (ppm).....	1722
427-	Longford Down Lithogeochemical Atlas : Ga (ppm).....	1723
428-	Longford Down Lithogeochemical Atlas : La (ppm).....	1724
429-	Longford Down Lithogeochemical Atlas : Nb (ppm).....	1725
430-	Longford Down Lithogeochemical Atlas : Ni (ppm).....	1726
431-	Longford Down Lithogeochemical Atlas : Pb (ppm).....	1727
432-	Longford Down Lithogeochemical Atlas : Rb (ppm).....	1728
433-	Longford Down Lithogeochemical Atlas : S (ppm).....	1730
434-	Longford Down Lithogeochemical Atlas : Sb (ppm).....	1731
435-	Longford Down Lithogeochemical Atlas : Th (ppm).....	1732
436-	Longford Down Lithogeochemical Atlas : V (ppm).....	1733
437-	Longford Down Lithogeochemical Atlas : Y (ppm).....	1734
438-	Longford Down Lithogeochemical Atlas : Zn (ppm).....	1735
439-	Longford Down Lithogeochemical Atlas : Zr (ppm).....	1736
440-	Chondrite normalised REE patterns for Archean Greywackes (after Taylor and McClennan 1985).....	1737
441-	Chondrite normalised REE patterns for Phanerozoic Greywackes (after Taylor and McClennan 1985).....	1739
442-	Chondrite normalised REE patterns for Post Archean shale composites and averages (after Taylor and McClennan 1985).....	1740
443-	Chondrite normalised REE patterns for Quartz Rich Greywackes (after Taylor and McClennan 1985).....	1741
444-	Chondrite normalised REE patterns for Quartz Intermediate Greywackes (after Taylor and McClennan 1985).....	1742
445-	Chondrite normalised REE patterns for Quartz Poor Greywackes (after Taylor and McClennan 1985).....	1743
446-	Chondrite normalised REE: Marchburn Formation (A).....	1745
447-	Chondrite normalised REE: Marchburn Formation (B).....	1746
448-	Chondrite normalised REE: Marchburn Formation (C).....	1747
449-	Chondrite normalised REE: Marchburn Formation (B).....	1748
450-	Chondrite normalised REE: Afton Formation (A).....	1749
451-	Chondrite normalised REE: Afton Formation (B).....	1750
452-	Chondrite normalised REE: Afton Formation (C).....	1751
453-	Chondrite normalised REE: Afton Formation (D).....	1752
454-	Chondrite normalised REE: Blackcraig Formation (A).....	1754
455-	Chondrite normalised REE: Scar Formation (A).....	1755
456-	Chondrite normalised REE: Scar Formation (B).....	1756
457-	Chondrite normalised REE: Scar Formation (C).....	1757
458-	Chondrite normalised REE: Scar Formation (D).....	1758
459-	Chondrite normalised REE: Scar Formation (E).....	1759
460-	Chondrite normalised REE: Scar Formation (F).....	1760
461-	Chondrite normalised REE: Shinnel Formation (A).....	1761
462-	Chondrite normalised REE: Shinnel Formation (B).....	1763

463-	Chondrite normalised REE: Shinnel Formation (C).....	1764
464-	Chondrite normalised REE: Pyroxenous Formation (A).....	1765
465-	Chondrite normalised REE: Pyroxenous Formation (B).....	1766
466-	Chondrite normalised REE: Pyroxenous Formation (C).....	1767
467-	Chondrite normalised REE: Pyroxenous Formation (D).....	1768
468-	Chondrite normalised REE: Intermediate Formation (A).....	1769
469-	Chondrite normalised REE: Intermediate Formation (B).....	1770
470-	Chondrite normalised REE: Intermediate Formation (C).....	1772
471-	Chondrite normalised REE: Glendinning Alteration (A).....	1773
472-	Chondrite normalised REE: Glendinning Alteration (B).....	1774
473-	Chondrite normalised REE: Glendinning Alteration (C).....	1775
474-	Chondrite normalised REE: Glendinning Alteration (D).....	1776
475-	A Simplified model of the metallogensis of As-Sb-Au deposits in the British Caledonides.....	1777

LIST OF PLATES

Plate No.	Page No.
1 -	Historical gold mining activity in Scotland..... 1778
2 -	Polished sections of mineralized breccias from the Glendinning deposit..... 1779
3 -	Polished sections of disseminated sulphide mineralization from Glendinning.. 1780
4 -	Polished sections of microprobe analysis grid within arsenopyrite crystals from the Talnotry deposit..... 1781
5 -	Polished sections of microprobe analysis grid within arsenopyrite crystals from the Glendinning and Cairngarroch Bay deposits..... 1782
6 -	Polished sections of vein and wallrock hosted arsenopyrite mineralization from the Glendinning deposit..... 1783
7 -	Polished sections of sulphide assemblages from the Glendinning deposit..... 1784
8 -	Polished sections of fine grained and massive varieties of stibnite mineralization from the Glendinning deposit..... 1785
9 -	SEM study of clay minerals associated with As-Sb mineralization in the Glendinning deposit..... 1786
10 -	Backscatter SEM study of stratiform pyrite and pyrite-magnetite assemblages within greywackes from the Glendinning deposit..... 1787
11 -	Backscatter SEM study of sulphides from the Glendinning deposit..... 1788
12 -	Backscatter SEM study of sulphide hosted gold inclusions and veinlets from the Glendinning deposit..... 1789
13 -	Thin sections of lamprophyres and coeval igneous rocks in the Southern Uplands..... 1790
14 -	Thin sections of arsenopyrite-bearing biotite granite from the Glenhead area, Loch-Doon..... 1791
15 -	Thin sections demonstrating sedimentary textures in mineralized core samples from the Glendinning deposit..... 1792
16 -	Thin section study of Glendinning breccias : Part 1 1793
17 -	Thin section study of Glendinning breccias : Part 2 1794
18 -	Thin section study of Glendinning breccias : Part 3 1795
19 -	Thin sections of Glendinning vein-wallrock relationships..... 1796
20 -	Thin sections of typical unmineralized greywacke from the Glendinning Area 1797
21 -	Thin sections of granodiorite hosted arsenopyrite-pyrite mineralization within the Knipe deposit..... 1798
22 -	Thin section of vein and disseminated arsenopyrite-pyrite mineralization within the Cairngarroch Bay deposit..... 1799
23 -	The Leadhills mining district..... 1800
24 -	BGS drilling program at Glendinning, Winter 1980..... 1801
25 -	The Glendinning Mine Area..... 1802
26 -	Glendinning regional study area : Topography..... 1803
27 -	Glendinning regional study area : Typical Sampling Locations..... 1804
28 -	Glendinning regional study area : Penecontemporaneous Structures..... 1805
29 -	Rams Cleuch Study Area..... 1806
30 -	Rams Cleuch and Swin Gill Overburden Sampling Grids..... 1807
31 -	Corsewall Conglomerate, Corsewall Point, Rhinns of Galloway..... 1808
32 -	Cairngarroch Bay Study Area, Rhinns of Galloway..... 1809
33 -	Cairngarroch Bay Arsenopyrite Vein..... 1810
34 -	Tongerhie Cu-As deposit, Southwest Scotland..... 1811
35 -	Tweed Bridge Interformational Study area..... 1812
36 -	Arsenopyrite hosted gold inclusions..... 1813
37 -	XRF sample preparation equipment, Nottingham University..... 1814
38 -	XRF pressed powder pellets illustrating a diffusive colour index..... 1815

LIST OF TABLES

The enclosed tables have been subdivided into four sections:

- 1 - General
- 2 - Summary Statistics
- 3 - Multivariate Statistics
- 4 - Chemical Analyses

1 - General

Table No.	Page No.
1.00 -	History of the Scottish Goldfields..... 1816
1.01 -	Glendinning X-Ray diffraction analyses..... 1818
1.02 -	Glendinning lithogeochemical 'grey-scale' mapping intervals..... 1819
1.03 -	Sulphur isotope analyses..... 1820
1.04 -	International standard sedimentary REE analyses (after Taylor 1985)..... 1821
1.05 -	Phanerozoic and Archean greywacke REE analyses (after Taylor 1985)..... 1822
1.06 -	A comparison of the oxidation state of iron in mineralized and unmineralized samples from the Glendinning area..... 1823
1.07 -	Enrichment factors associated with Glendinning mineralization..... 1824
1.08 -	Summary of analytical laboratories and gold assay techniques..... 1825
1.09 -	An inter-laboratory study of gold analysis techniques..... 1826
1.10a -	Gold soil geochemistry : Glendinning north-east extension..... 1827
1.10b -	Gold lithogeochemistry : Glendinning mineralized drillcore..... 1827
1.10c -	Gold lithogeochemistry : Glendinning greywacke background..... 1828
1.10d -	Gold lithogeochemistry : Southern Uplands greywacke background..... 1828
1.10e -	Gold lithogeochemistry : Southern Uplands mineralization..... 1828
1.11 -	Glendinning borehole No. 2 : Gold geochemistry (MIBK extraction)..... 1829
1.12 -	Glendinning borehole No. 3 : Gold geochemistry (MIBK extraction)..... 1830
1.13 -	Glendinning borehole geochemistry..... 1831
1.14 -	XRF analyses : Southern Uplands lamprophyre geochemistry..... 1832
1.15 -	Probe mapping studies : grid boundaries..... 1833
1.16a -	Greywacke geochemistry : Marchburn Formation F test statistics..... 1834
1.16b -	Greywacke geochemistry : Afton Formation F test statistics..... 1835
1.16c -	Greywacke geochemistry : Blackcraig Formation F test statistics..... 1836
1.16d -	Greywacke geochemistry : Scar Formation F test statistics..... 1837
1.16d -	Greywacke geochemistry : Shinnel Formation F test statistics..... 1837
1.16e -	Greywacke geochemistry : Pyroxenous Formation F test statistics..... 1838
1.16e -	Greywacke geochemistry : Intermediate Formation F test statistics..... 1838
1.16e -	Greywacke geochemistry : Hawick Formation F test statistics..... 1838
1.17a -	Principal Component analysis : Rams Cleuch Soil Grid..... 1839
1.17b -	Principal Component analysis : Swin Gill Soil Grid..... 1839
1.18 -	Principal Component analysis : Marchburn Formation..... 1840
1.19 -	Principal Component analysis : Afton Formation..... 1841
1.20 -	Principal Component analysis : Blackcraig Formation..... 1842
1.21 -	Principal Component analysis : Scar Formation..... 1843
1.22 -	Principal Component analysis : Shinnel Formation..... 1844
1.23 -	Principal Component analysis : Pyroxenous Formation..... 1845
1.24 -	Principal Component analysis : Intermediate Formation..... 1846
1.25 -	Principal Component analysis : Hawick Formation..... 1847
1.26 -	Principal Component analysis : Glendinning mineralized mudstone..... 1848
1.27 -	Principal Component analysis : Glendinning mineralized siltstone..... 1849
1.28 -	Principal Component analysis : Glendinning mineralized greywacke..... 1850
1.29 -	Principal Component analysis : Glendinning mineralized breccias..... 1851
1.30 -	Principal Component analysis : Leadhills mineralization..... 1852
1.31 -	Principal Component analysis : Clontibret mineralization..... 1853
1.32 -	Petrography of core specimens: BH 1 (after Gallagher et al 1982)..... 1854

1.33a -	Petrography of core specimens: BH 2 (after Gallagher et al 1982).....	1855
1.33b -	Petrography of core specimens: BH 2 (after Gallagher et al 1982).....	1856
1.34a -	Petrography of core specimens: BH 3 (after Gallagher et al 1982).....	1857
1.34b -	Petrography of core specimens: BH 3 (after Gallagher et al 1982).....	1858
1.34c -	Petrography of core specimens: BH 3 (after Gallagher et al 1982).....	1859
1.34d -	Petrography of core specimens: BH 3 (after Gallagher et al 1982).....	1860
1.35 -	Petrography of core specimens: BH 4 (after Gallagher et al 1982).....	1861
1.36 -	Southern Uplands greywacke lithogeochemistry : As-Sb Anomalies.....	1862
1.37 -	Glendinning Area greywacke lithogeochemistry : As-Sb Anomalies.....	1863
1.38 -	Glendinning Area mudstone lithogeochemistry : As-Sb Anomalies.....	1864
1.39 -	Glendinning Region multi-element lithogeochemical anomaly sites.....	1865
1.40 -	Modified K-Means cluster analysis :Seed Points.....	1866
1.41 -	Index to the Southern Scotland Regional Geochemical database.....	1867
1.42 -	Rams Cleuch and Swin Gill soil geochemistry contour levels.....	1870
1.43 -	Components of the Southern Uplands Geochemical Traverse.....	1871
1.44 -	General relationships between elements and their host minerals.....	1872
1.45 -	Southern Uplands regional data set : Percentile class intervals.....	1873
1.46 -	A glossary of Mineral deposits in the Southern Uplands.....	1874
1.47 -	Heavy mineral component of Ordovician Greywacke Formations.....	1875
1.48 -	Comparison of Ordovician Greywacke granule and point count data.....	1876
1.49 -	Southern Uplands Greywacke Classification.....	1878
1.50 -	Microprobe Mapping Studies : Grid size and sample density.....	1879
1.51 -	History of alluvial gold production in SE Ireland.....	1880
1.52 -	Average abundance of chemical elements in the main types of igneous rocks in the lithosphere (after Rosler 1972).....	1881
1.53 -	The Clark values (after Rosler 1972).....	1882
1.54 -	Background gold abundances in different rock types.....	1884
1.56 -	Lamprophyre Geochemistry from the Southern Uplands.....	1885
1.58 -	BGS Gold Pan Sites in the Southern Uplands.....	1886
1.59 -	Provenance Studies of Southern Uplands Greywackes.....	1888
1.60 -	Average trace element content of Greywackes from various tectonic settings after Bhatia and Crook (1986).....	1889
1.61 -	Plate tectonic setting classification of continental margins and oceanic basins (after Bhatia and Crook, 1986).....	1890
1.62 -	Average trace element content of Southern Uplands Greywackes	1891
1.63 -	Tectonic setting discrimination of Southern Uplands Greywackes based upon trace element contents defined by Bhatia and Crook (1986).....	1892
1.64 -	Mean Compositions of Petrographic Formations from the Southern Uplands of Scotland.....	1893
1.65 -	A comparison of the mean compositions of Petrographic Formations from the Southern Uplands.....	1894
1.66 -	The Origin of the Glendinning Breccias.....	1895
1.67 -	Qualitative detrital composition of Principal petrofacies in the Northern Belt and Northern Part of the Central Belt (Morris, 1988).....	1896
1.68 -	A Summary of Discrimination Diagrams.....	1897
1.69 -	Swin Gill Geochemical Structures.....	1898
1.70 -	Microprobe Analysis Raster Study.....	1900

2 - Summary Statistics

2.01 -	Microprobe Analyses : Glendinning Arsenopyrite (ASP1)	1901
2.02 -	Microprobe Analyses : Glendinning Arsenopyrite (ASP2)	1902
2.03 -	Microprobe Analyses : Glendinning Arsenopyrite (ASP3)	1903
2.04 -	Microprobe Analyses : Glendinning Arsenopyrite (ASP4)	1904
2.05 -	Microprobe Analyses : Glendinning Arsenopyrite (ASP5)	1905
2.06 -	Microprobe Analyses : Glendinning Arsenopyrite (ASP6)	1906
2.07 -	Microprobe Analyses : The Knipe Arsenopyrite (ASP7)	1907
2.08 -	Microprobe Analyses : The Knipe Arsenopyrite (ASP8)	1908
2.09 -	Microprobe Analyses : Talnotry Arsenopyrite (ASP9)	1909
2.10 -	Microprobe Analyses : Cairngarroch Arsenopyrite (ASP10)	1910
2.11 -	Microprobe Analyses : Cairngarroch Arsenopyrite (ASP11)	1911
2.12 -	Microprobe Analyses : Cairngarroch Arsenopyrite (ASP12)	1912
2.13 -	Microprobe Analyses : Cairngarroch Arsenopyrite (ASP13)	1913

2.14 -	Microprobe Analyses : Clontibret Arsenopyrite (ASP14)	1914
2.15 -	Microprobe Analyses : Clontibret Arsenopyrite (ASP15)	1915
2.16 -	Microprobe Analyses : Clontibret Arsenopyrite (ASP16)	1916
2.17 -	Microprobe Analyses : Clontibret Arsenopyrite (ASP17)	1917
2.18 -	Microprobe Analyses : Glendinning Au-rich samples (AU1).....	1918
2.19 -	Microprobe Analyses : Glendinning Pyrite (PYTE1)	1919
2.20 -	Microprobe Analyses : Glendinning Pyrite (PYTE2)	1920
2.21 -	Microprobe Analyses : Glendinning Stibnite (STIB1)	1921
2.22 -	Microprobe Analyses : Glendinning Stibnite (STIB2)	1922
2.24 -	Microprobe Analyses : Glendinning Sphalerite (SPTE1)	1923
2.25 -	Microprobe Analyses : Glendinning Tetrahedrite (TET1)	1924
2.26 -	XRF Analyses : Glendinning Greyacke (BEAD1)	1925
2.27 -	XRF Analyses : Glendinning Mudstone (BEAD2)	1926
2.28 -	XRF Analyses : Glendinning mineralization (BEAD3)	1927
2.29 -	XRF Analyses : Regional Greyacke (BEAD4)	1928
2.30 -	XRF Analyses : Marchburn Formation (B1)	1929
2.31 -	XRF Analyses : Afton Formation (B3)	1930
2.32 -	XRF Analyses : Blackcraig Formation (B5)	1931
2.33 -	XRF Analyses : Scar Formation (B7)	1932
2.34 -	XRF Analyses : Shinnel Formation (B9)	1933
2.35 -	XRF Analyses : Pyroxenous Formation (B11)	1934
2.36 -	XRF Analyses : Intermediate Formation (B13)	1935
2.37 -	XRF Analyses : Glendinning Duplicates (DUP1)	1936
2.38 -	XRF Analyses : Glendinning Duplicates (DUP2)	1937
2.39 -	MIBK Analyses : Southern Uplands Gold Data (GOLD1)	1938
2.40 -	AA Analyses : Glendinning mineralization (GOLD2)	1939
2.41 -	INAA Analyses : Rams Cleuch Gold data (GOLD3)	1940
2.42 -	INAA Analyses : Glendinning Core Samples (GOLD4)	1941
2.43 -	INAA Analyses : Glendinning Regional Samples (GOLD5)	1942
2.44 -	INAA Analyses : Southern Uplands Ore Samples (GOLD6)	1943
2.45 -	XRF Analyses : Rams Cleuch Soil geochemistry (GRD1)	1944
2.46 -	XRF Analyses : Swin Gill Soil geochemistry (GRD2)	1945
2.47 -	XRF Analyses : Glendinning Greywacke Suite (GWKE1)	1946
2.48 -	XRF Analyses : Upper Silurian Greywackes (GWKE2)	1947
2.49 -	XRF Analyses : Lower Silurian Greywackes (GWKE3)	1948
2.50 -	XRF Analyses : Regional Greywacke Suite (GWKE4)	1949
2.51 -	XRF Analyses : Marchburn Formation (GWKE8)	1950
2.52 -	XRF Analyses : Afton Formation (GWKE9)	1951
2.53 -	XRF Analyses : Blackcraig Formation (GWKE10)	1952
2.54 -	XRF Analyses : Scar Formation (GWKE11)	1953
2.55 -	XRF Analyses : Shinnel Formation (GWKE12)	1954
2.56 -	XRF Analyses : Pyroxenous Formation (GWKE13)	1955
2.57 -	XRF Analyses : Intermediate Formation (GWKE14)	1956
2.58 -	XRF Analyses : Garnetiferous Formation (GWKE15)	1957
2.59 -	XRF Analyses : Glen Trool Formation (GWKE16)	1958
2.60 -	XRF Analyses : Epidotitic Formation (GWKE17)	1959
2.61 -	XRF Analyses : U.Calcareous Formation (GWKE18)	1960
2.62 -	XRF Analyses : L.Calcareous Formation (GWKE19)	1961
2.63 -	XRF Analyses : Southern Uplands Unassigned (GWKE20)	1962
2.64 -	XRF Analyses : S. Uplands Coastal Traverse (GWKE22)	1963
2.65 -	XRF Analyses : Tweedsmuir Interformation Study (GWKE23).....	1964
2.66 -	XRF Analyses : Tweedsmuir Interoutcrop Study (GWKE2A).....	1965
2.67 -	XRF Analyses : Tweedsmuir Basal-formation Study (GWKE2B).....	1966
2.68 -	XRF Analyses : Additional Trace Elements (GWKE24)	1967
2.69 -	XRF Analyses : Kirkudbright (L. Silurian) (GWKE25)	1968
2.70 -	XRF Analyses : Kirkudbright (U. Silurian) (GWKE26)	1969
2.71 -	XRF Analyses : Kirkudbright Mapping Study (GWKE27)	1970
2.72 -	XRF Analyses : Glendinning Addit.Trace Elements (GWKE28).....	1971
2.73 -	XRF Analyses : Glendinning Addit.Trace Elements (GWKE29).....	1972
2.74 -	XRF Analyses : Glendinning Addit.Trace Elements (GWKE30).....	1973
2.75 -	XRF Analyses : Tweedsmuir Interformation Study (GWKE31)	1974
2.76 -	XRF Analyses : Wigtownshire East Mapping Study (GWKE32)	1975
2.77 -	XRF Analyses : Wigtownshire West Mapping Study (GWKE33)	1976

2.78 -	XRF Analyses : Selkirk Study (GWKE34)	1977
2.79 -	XRF Analyses : Longford Down Traverse (GWKE40)	1978
2.80 -	XRF Analyses : Aghamore Formation (GWKE41)	1979
2.81 -	XRF Analyses : Lackan Formation (GWKE42)	1980
2.82 -	XRF Analyses : Finnalaya Formation (GWKE43)	1981
2.83 -	XRF Analyses : Coronea Formation (GWKE44)	1982
2.84 -	XRF Analyses : Cornhill Formation (GWKE45)	1983
2.85 -	XRF Analyses : Carrickateane Formation (GWKE46)	1984
2.86 -	XRF Analyses : Glen Lodge Formation (GWKE47)	1985
2.87 -	XRF Analyses : Red Island Formation (GWKE48)	1986
2.88 -	XRF Analyses : Slieve Glah Formation (GWKE49)	1987
2.89 -	XRF Analyses : Hawick Equiv. Formation (GWKE50)	1988
2.90 -	XRF Analyses : Slieve na Calliagh Formation (GWKE51)	1989
2.91 -	XRF Analyses : Marchburn Formation + Ratios (FOR1)	1990
2.93 -	XRF Analyses : Blackcraig Formation + Ratios (FOR5)	1991
2.94 -	XRF Analyses : Scar Formation + Ratios (FOR7)	1992
2.95 -	XRF Analyses : Shinnel Formation + Ratios (FOR9)	1993
2.96 -	XRF Analyses : Pyroxenous Formation + Ratios (FOR11)	1994
2.97 -	XRF Analyses : Intermediate Formation + Ratios (FOR13)	1995
2.98 -	XRF Analyses : Garnetiferous Formation + Ratios (FOR15)	1996
2.99 -	XRF Analyses : Glen Trool Formation + Ratios (FOR17)	1997
2.100 -	XRF Analyses : Epidiotitic Formation + Ratios (FOR19)	1998
2.101 -	XRF Analyses : U. Calcareous Formation + Ratios (FOR21)	1999
2.102 -	XRF Analyses : L. Calcareous Formation + Ratios (FOR23)	2000
2.103 -	XRF Analyses : Glendinning mineralization (FORM1)	2001
2.104 -	XRF Analyses : Leadhills mineralization: Hole 1 (LEAD1)	2002
2.105 -	XRF Analyses : Leadhills mineralization: Hole 2 (LEAD2)	2003
2.106 -	ICP Analyses : Glendinning mineralization (MED1)	2004
2.107 -	ICP Analyses : Tweedsmuir Interformational Study (MED2)	2005
2.108 -	XRF Analyses : Glendinning mineralized Core (MINE1)	2006
2.109 -	XRF Analyses : Glendinning Hole No. 1 (MINA1)	2007
2.110 -	XRF Analyses : Glendinning Hole No. 2 (MINB1)	2008
2.111 -	XRF Analyses : Glendinning Hole No. 3 (MINC1)	2009
2.112 -	XRF Analyses : Glendinning Hole No. 4 (MIND1)	2010
2.113 -	XRF Analyses : Glendinning mineralized breccia (MINF1)	2011
2.114 -	XRF Analyses : Glendinning mineralized greywacke (MING1)	2012
2.115 -	XRF Analyses : Glendinning mineralized siltstone (MINS1)	2013
2.116 -	XRF Analyses : Glendinning mineralized mudstone (MINM1)	2014
2.117 -	XRF Analyses : Clontibret mineralized greywacke (MINE2)	2015
2.118 -	XRF Analyses : Clontibret mineralized greywacke (MINE3)	2016
2.119 -	XRF Analyses : Leadhills mineralized greywacke (MINE4)	2017
2.120 -	XRF Analyses : Cairngarroch mineralization (MINE5)	2018
2.121 -	XRF Analyses : Tongerhie mineralization (MINE6)	2019
2.122 -	XRF Analyses : Miscellaneous mineralization (MINE7)	2020
2.123 -	XRF Analyses : Glendinning Regional mudstone (MUD1)	2021
2.124 -	XRF Analyses : Glendinning BGS pan concentrates (PAN1)	2022
2.125 -	ICP Analyses : S. Uplands REE (Chondrite Normalised) (NORM1)	2023
2.126 -	ICP Analyses : S. Uplands REE (NASC Normalised) (NORM2)	2024
2.127 -	ICP Analyses : Glendinning REE (Chondrite Normalised) (NORM4)	2025
2.128 -	ICP Analyses : Glendinning REE (NASC Normalised) (NORM5)	2026
2.129 -	ICP Analyses : Mineralization (Chondrite Normalised) (NORM7)	2027
2.130 -	ICP Analyses : Mineralization (NASC Normalised) (NORM8)	2028
2.131 -	ICP Analyses : Tweedsmuir REE (Chondrite Normalised) (NORM10)	2029
2.132 -	ICP Analyses : Tweedsmuir REE (NASC Normalised) (NORM11)	2030
2.133 -	ICP Analyses : S.Uplands Regional greywacke REE (REES)	2031
2.134 -	ICP Analyses : Glendinning greywacke REE Study (REEG)	2032
2.135 -	ICP Analyses : Glendinning wallrock REE Study (REEM)	2033
2.136 -	ICP Analyses : Tweedsmuir Interunit REE Study (REET)	2034
2.137 -	ICP Analyses : Marchburn Formation REE Study (REE1)	2035
2.138 -	ICP Analyses : Afton Formation REE Study (REE3)	2036
2.139 -	ICP Analyses : Blackcraig Formation REE Study (REE5)	2037
2.140 -	ICP Analyses : Scar Formation REE Study (REE7)	2038
2.141 -	ICP Analyses : Shinnel Formation REE Study (REE9)	2039

2.142 -	ICP Analyses : Pyroxenous Formation REE Study (REE11)	2040
2.143 -	ICP Analyses : Intermediate Formation REE Study (REE13)	2041
2.144 -	ICP Analyses : Garnetiferous Formation REE Study (REE15)	2042
2.145 -	ICP Analyses : Standard KC10 Duplicates (STD1)	2043
2.146 -	ICP Analyses : Standard 1005 Duplicates (STD2)	2044
2.147 -	XRF Analyses : Marchburn Formation Petrography.....	2045
2.148 -	XRF Analyses : Afton Formation Petrography.....	2046
2.149 -	XRF Analyses : Blackcraig Formation Petrography	2047
2.150 -	XRF Analyses : Scar Formation Petrography.....	2048
2.151 -	XRF Analyses : Shinnel Formation Petrography.....	2049
2.152 -	XRF Analyses : Hawick Formation (Normalised CaO free).....	2050
2.153 -	XRF Analyses : Cratonic derived greywacke formations.....	2051
2.154 -	XRF Analyses : Volcanic derived greywacke formations.....	2052
2.155 -	F-Test Comparison of Volcanic and Cratonic derived greywackes.....	2053
2.156 -	T-Test Comparison of Volcanic and Cratonic derived greywackes.....	2054
2.157 -	Chi-squared test: Cratonic derived greywackes.....	2055
2.158 -	Chi-squared test: Volcanic Derived greywackes.....	2056
2.159 -	Median and inter-quartile ranges of the major and trace element chemistry of Cratonic, Volcanic and Hawick formation greywackes.....	2057

3 - Multivariate Statistics

3.00 -	Correlation Coefficients : Glendinning mineralized Greywackes.....	2058
3.01 -	Correlation Coefficients : Marchburn Formation.....	2060
3.02 -	Correlation Coefficients : Afton Formation.....	2062
3.03 -	Correlation Coefficients : Blackcraig Formation.....	2064
3.04 -	Correlation Coefficients : Scar Formation.....	2066
3.05 -	Correlation Coefficients : Shinnel Formation.....	2068
3.06a -	Principal Component Analysis : Rams Cleuch soil grid.....	2070
3.06b -	Principal Component Analysis : Swin Gill soil grid.....	2070
3.07 -	Principal Component Analysis : Marchburn Formation.....	2071
3.08 -	Principal Component Analysis : Afton Formation.....	2072
3.09 -	Principal Component Analysis : Blackcraig Formation.....	2073
3.10 -	Principal Component Analysis : Scar Formation.....	2074
3.11 -	Principal Component Analysis : Shinnel Formation.....	2075
3.12 -	Principal Component Analysis : Pyroxenous Formation.....	2076
3.13 -	Principal Component Analysis : Intermediate Formation.....	2077
3.14 -	Principal Component Analysis : Hawick Formation.....	2078
3.15 -	Principal Component Analysis : Clontibret mineralization.....	2079
3.16 -	Principal Component Analysis : Leadhills mineralization.....	2080
3.17 -	Principal Component Analysis : Glendinning greywacke.....	2081
3.18 -	Principal Component Analysis : Glendinning breccia.....	2082
3.19 -	Principal Component Analysis : Glendinning mudstone.....	2083
3.20 -	Principal Component Analysis : Glendinning siltstone.....	2084
3.21 -	Discriminant Analysis : Southern Uplands greywacke formations.....	2085
3.22 -	Correlation Coefficients : Cratonic derived greywacke petrofacies.....	2086
3.23 -	Correlation Coefficients : Volcanic derived greywacke petrofacies.....	2088
3.24 -	Correlation Coefficients : Rams Cleuch soil grid.....	2090
3.25 -	Correlation Coefficients : Swin Gill soil grid.....	2091

4 - Chemical Analyses

4.01 -	Microprobe Analyses : Glendinning Arsenopyrite (ASP1) (7).....	2092
4.02 -	Microprobe Analyses : Glendinning Arsenopyrite (ASP2) (3).....	2099
4.03 -	Microprobe Analyses : Glendinning Arsenopyrite (ASP3) (4).....	2102
4.04 -	Microprobe Analyses : Glendinning Arsenopyrite (ASP4) (6).....	2106
4.05 -	Microprobe Analyses : Glendinning Arsenopyrite (ASP5) (33).....	2112
4.06 -	Microprobe Analyses : Glendinning Arsenopyrite (ASP6) (10).....	2145
4.07 -	Microprobe Analyses : The Knipe Arsenopyrite (ASP7) (5).....	2155
4.08 -	Microprobe Analyses : The Knipe Arsenopyrite (ASP8) (7).....	2162
4.09 -	Microprobe Analyses : Talnotry Arsenopyrite (ASP9) (20).....	2167
4.10 -	Microprobe Analyses : Cairngarroch Arsenopyrite (ASP10) (57).....	2187

4.11 -	Microprobe Analyses : Cairngarroch Arsenopyrite (ASP11) (26).....	2244
4.12 -	Microprobe Analyses : Cairngarroch Arsenopyrite (ASP12) (7).....	2269
4.13 -	Microprobe Analyses : Cairngarroch Arsenopyrite (ASP13) (15).....	2276
4.14 -	Microprobe Analyses : Clontibret Arsenopyrite (ASP15) (4).....	2291
4.15 -	Microprobe Analyses : Clontibret Arsenopyrite (ASP16) (11).....	2295
4.16 -	Microprobe Analyses : Clontibret Arsenopyrite (ASP17) (7).....	2306
4.17 -	Microprobe Analyses : Clontibret Arsenopyrite (ASP18) (5).....	2313
4.18 -	Microprobe Analyses : Glendinning Au-rich samples(AU1) (2).....	2318
4.19 -	Microprobe Analyses : Glendinning Pyrite (PYTE1) (18).....	2320
4.20 -	Microprobe Analyses : Glendinning Pyrite (PYTE2) (3).....	2338
4.21 -	Microprobe Analyses : Glendinning Stibnite (STIB1) (1).....	2341
4.22 -	Microprobe Analyses : Glendinning Stibnite (STIB2) (1).....	2342
4.23 -	Microprobe Analyses : Glendinning Stibnite (STIB3) (1).....	2343
4.24 -	Microprobe Analyses : Glendinning Sphalerite (SPTE1) (2).....	2344
4.25 -	Microprobe Analyses : Glendinning Tetrahedrite (TET1) (1).....	2346
4.26 -	XRF Analyses : Marchburn Formation (B1) (3).....	2347
4.27 -	XRF Analyses : Afton Formation (B3) (3).....	2350
4.28 -	XRF Analyses : Blackcraig Formation (B5) (1).....	2353
4.29 -	XRF Analyses : Scar Formation (B7) (4).....	2357
4.30 -	XRF Analyses : Shinnel Formation (B9) (3).....	2360
4.31 -	XRF Analyses : Pyroxenous Formation (B11) (3).....	2363
4.32 -	XRF Analyses : Intermediate Formation (B13) (2).....	2365
4.33 -	XRF Analyses : Glendinning Duplicates (DUP1) (1).....	2366
4.34 -	XRF Analyses : Glendinning Duplicates (DUP2) (1).....	2367
4.35 -	XRF Analyses : Rams Cleuch Soil geochemistry (GRD1) (20).....	2368
4.36 -	XRF Analyses : Swin Gill Soil geochemistry (GRD2) (30).....	2388
4.37 -	XRF Analyses : Glendinning Greywacke Suite (GWKE1) (31).....	2418
4.38 -	XRF Analyses : Glendinning Greywacke (BEAD1) (1).....	2449
4.39 -	XRF Analyses : Glendinning Mudstone (BEAD2) (1).....	2450
4.40 -	XRF Analyses : Glendinning mineralization (BEAD3) (1).....	2451
4.41 -	XRF Analyses : Regional Greywacke Suite (BEAD4) (20).....	2452
4.42 -	XRF Analyses : Regional Greywacke Suite (GWKE4) (70).....	2472
4.43 -	XRF Analyses : Marchburn Formation Petrography (1).....	2542
4.44 -	XRF Analyses : Afton Formation Petrography (1).....	2543
4.45 -	XRF Analyses : Blackcraig Formation Petrography (1).....	2547
4.46 -	XRF Analyses : Scar Formation Petrography (1).....	2548
4.47 -	XRF Analyses : Shinnel Formation Petrography (1).....	2550
4.48 -	XRF Analyses : Marchburn Formation Granule Petrography (1).....	2552
4.49 -	XRF Analyses : Afton Formation Granule Petrography (1).....	2553
4.50 -	XRF Analyses : Blackcraig Formation Granule Petrography (1).....	2554
4.51 -	XRF Analyses : Scar Formation Granule Petrography (1).....	2555
4.52 -	XRF Analyses : Shinnel Formation Granule Petrography (1).....	2556
4.53 -	XRF Analyses : Marchburn Formation (GWKE8) (5).....	2557
4.54 -	XRF Analyses : Afton Formation (GWKE9) (9).....	2562
4.55 -	XRF Analyses : Blackcraig Formation (GWKE10) (7).....	2578
4.56 -	XRF Analyses : Scar Formation (GWKE11) (10).....	2585
4.57 -	XRF Analyses : Shinnel Formation (GWKE12) (8).....	2595
4.58 -	XRF Analyses : Pyroxenous Formation (GWKE13) (5).....	2603
4.59 -	XRF Analyses : Intermediate Formation (GWKE14) (8).....	2608
4.60 -	XRF Analyses : Gametiferous Formation (GWKE15) (2).....	2616
4.51 -	XRF Analyses : Glen Trool Formation (GWKE16) (1).....	2618
4.62 -	XRF Analyses : Epidotitic Formation (GWKE17) (2).....	2619
4.63 -	XRF Analyses : U.Calcareous Formation (GWKE18) (5).....	2621
4.64 -	XRF Analyses : L.Calcareous Formation (GWKE19) (26).....	2626
4.65 -	XRF Analyses : Southern Uplands Unassigned (GWKE20) (11).....	2652
4.66 -	XRF Analyses : S. Uplands Coastal Traverse (GWKE22) (28).....	2663
4.67 -	XRF Analyses : Tweedsmuir Interformation Study(GWKE23) (2).....	2691
4.68 -	XRF Analyses : Tweedsmuir Interoutcrop Study(GWKE2A) (2).....	2693
4.69 -	XRF Analyses : Tweedsmuir Basal-formation Study(GWKE2B) (1).....	2695
4.70 -	XRF Analyses : Additional Trace Elements (GWKE24) (10).....	2696
4.71 -	XRF Analyses : Kirkudbright (L. Silurian) (GWKE25) (2).....	2706
4.72 -	XRF Analyses : Kirkudbright (U. Silurian) (GWKE26) (2).....	2708
4.73 -	XRF Analyses : Kirkudbright Mapping Study (GWKE27) (3).....	2710

4.74 -	XRF Analyses : Glendinning Additional Trace Elements(GWKE28) (2).....	2713
4.75 -	XRF Analyses : Glendinning Additional Trace Elements(GWKE29) (1).....	2715
4.76 -	XRF Analyses : Glendinning Additional Trace Elements(GWKE30) (1).....	2716
4.77 -	XRF Analyses : Tweedsmuir Multi-element Study (GWKE31) (2).....	2717
4.78 -	XRF Analyses : Wigtownshire East Mapping Study (GWKE32) (8).....	2719
4.79 -	XRF Analyses : Wigtownshire West Mapping Study (GWKE33) (10).....	2727
4.80 -	XRF Analyses : Selkirk Study (GWKE34) (1).....	2737
4.81 -	XRF Analyses : Longford Down Traverse (GWKE40) (30).....	2738
4.82 -	XRF Analyses : Aghamore Formation (GWKE41) (1).....	2768
4.83 -	XRF Analyses : Lackan Formation (GWKE42) (1).....	2769
4.84 -	XRF Analyses : Finnalayta Formation (GWKE43) (6).....	2770
4.85 -	XRF Analyses : Coronea Formation (GWKE44) (4).....	2776
4.86 -	XRF Analyses : Cornhill Formation (GWKE45) (1).....	2780
4.87 -	XRF Analyses : Carrickateane Formation (GWKE46) (1).....	2781
4.88 -	XRF Analyses : Glen Lodge Formation (GWKE47) (1).....	2782
4.89 -	XRF Analyses : Red Island Formation (GWKE48) (1).....	2783
4.90 -	XRF Analyses : Slieve Glah Formation (GWKE49) (1).....	2784
4.91 -	XRF Analyses : Hawick Equiv. Formation (GWKE50) (8).....	2785
4.92 -	XRF Analyses : Slieve na Calliagh Formation (GWKE51) (1).....	2793
4.93 -	XRF Analyses : Marchburn Formation + Ratios (FOR1) (5).....	2794
4.94 -	XRF Analyses : Afton Formation + Ratios (FOR3) (16).....	2799
4.95 -	XRF Analyses : Blackcraig Formation + Ratios (FOR5) (6).....	2815
4.96 -	XRF Analyses : Scar Formation + Ratios (FOR7) (10).....	2822
4.97 -	XRF Analyses : Shinnel Formation + Ratios (FOR9) (8).....	2832
4.98 -	XRF Analyses : Pyroxenous Formation + Ratios (FOR11) (5).....	2840
4.99 -	XRF Analyses : Intermediate Formation + Ratios (FOR13) (8).....	2845
4.100 -	XRF Analyses : Garnetiferous Formation + Ratios (FOR15) (2).....	2853
4.101 -	XRF Analyses : Glen Trool Formation + Ratios (FOR17) (1).....	2855
4.102 -	XRF Analyses : Epidotitic Formation + Ratios (FOR19) (2).....	2856
4.103 -	XRF Analyses : U. Calcareous Formation + Ratios (FOR21) (5).....	2858
4.104 -	XRF Analyses : L. Calcareous Formation + Ratios (FOR23) (26).....	2862
4.105 -	XRF Analyses : S. Uplands Unassigned Greywackes (FOR25) (11).....	2888
4.106 -	XRF Analyses : Glendinning mineralization (FORM1) (17).....	2899
4.107 -	XRF Analyses : Leadhills mineralization: Hole 1 (LEAD1) (2).....	2916
4.108 -	XRF Analyses : Leadhills mineralization: Hole 2 (LEAD2) (1).....	2918
4.109 -	ICP Analyses : Glendinning mineralization (MED1) (2).....	2919
4.110 -	ICP Analyses : Tweedsmuir Interformational Study (MED2) (3).....	2921
4.111 -	XRF Analyses : Glendinning mineralized Core (MINE1) (17).....	2924
4.112 -	XRF Analyses : Glendinning Hole No. 1 (MINA1) (4).....	2941
4.113 -	XRF Analyses : Glendinning Hole No. 2 (MINB1) (5).....	2945
4.114 -	XRF Analyses : Glendinning Hole No. 3 (MINC1) (8).....	2950
4.115 -	XRF Analyses : Glendinning Hole No. 4 (MIND1) (2).....	2958
4.116 -	XRF Analyses : Glendinning mineralized Breccia (MINF1) (3).....	2960
4.117 -	XRF Analyses : Glendinning mineralized Greywacke (MING1) (5).....	2963
4.118 -	XRF Analyses : Glendinning mineralized Siltstone (MINS1) (7).....	2968
4.119 -	XRF Analyses : Glendinning mineralized Mudstone (MINM1) (2).....	2975
4.120 -	XRF Analyses : Clontibret mineralized Greywacke(MINE2) (3).....	2977
4.121 -	XRF Analyses : Clontibret mineralized Greywacke(MINE3) (1).....	2980
4.122 -	XRF Analyses : Leadhills mineralized Greywacke(MINE4) (3).....	2981
4.123 -	XRF Analyses : Cairngarroch mineralization (MINE5) (1).....	2984
4.124 -	XRF Analyses : Tongerhie mineralization (MINE6) (1).....	2985
4.125 -	XRF Analyses : Miscellaneous mineralization (MINE7) (1).....	2986
4.126 -	XRF Analyses : Glendinning Regional Mudstone (MUD1) (20).....	2987
4.127 -	XRF Analyses : Glendinning BGS Pan Concentrates (PAN1) (1).....	3007
4.128 -	ICP Analyses : S. Uplands Regional REE Study (REES) (23).....	3008
4.129 -	ICP Analyses : Glendinning Greywacke REE Study (REEG) (1).....	3031
4.130 -	ICP Analyses : Glendinning mineralization Study (REEM) (1).....	3032
4.131 -	ICP Analyses : Tweedsmuir Inter-Unit REE Study (REET) (1).....	3034
4.132 -	ICP Analyses : Marchburn Formation REE Study (REE1) (3).....	3036
4.133 -	ICP Analyses : Afton Formation REE Study (REE3) (3).....	3039
4.134 -	ICP Analyses : Blackcraig Formation REE Study (REE5) (1).....	3042
4.135 -	ICP Analyses : Scar Formation REE Study (REE7) (4).....	3043
4.136 -	ICP Analyses : Shinnel Formation REE Study (REE9) (3).....	3047

4.137 -	ICP Analyses : Pyroxenous Formation REE Study (REE11) (3).....	3050
4.138 -	ICP Analyses : Intermediate Formation REE Study (REE13) (3).....	3053
4.139 -	ICP Analyses : Garnetiferous Formation REE Study (REE15) (1).....	3056
4.140 -	ICP Analyses : Standard KC10 Duplicates (STD1) (2).....	3057
4.141 -	ICP Analyses : Standard 1005 Duplicates (STD2) (3).....	3059
4.142 -	XRF Analyses : Glendinning Greywacke Anomalies (As) (1).....	3062
4.143 -	XRF Analyses : Glendinning Greywacke Anomalies (Sb) (1).....	3064
4.144 -	XRF Analyses : Glendinning Greywacke Anomalies (Cu) (1).....	3066
4.145 -	XRF Analyses : Glendinning Greywacke Anomalies (Pb) (1).....	3067
4.146 -	XRF Analyses : Glendinning Greywacke Anomalies (Zn) (1).....	3069
4.147 -	XRF Analyses : Glendinning Greywacke Anomalies (Na ₂ O) (1).....	3070
4.148 -	XRF Analyses : Glendinning Greywacke Anomalies (Zn ₂ O) (1).....	3072
4.149 -	XRF Analyses : Glendinning Mudstone Anomalies (As) (1).....	3073
4.150 -	XRF Analyses : Glendinning Mudstone Anomalies (Sb) (1).....	3075
4.151 -	XRF Analyses : Glendinning Mudstone Anomalies (Cu) (1).....	3076
4.152 -	XRF Analyses : Glendinning Mudstone Anomalies (Pb) (1).....	3077
4.153 -	XRF Analyses : Glendinning Mudstone Anomalies (Zn) (1).....	3079
4.154 -	XRF Analyses : Glendinning Mudstone Anomalies (Na ₂ O) (1).....	3081
4.155 -	XRF Analyses : Glendinning Mudstone Anomalies (Zn ₂ O) (1).....	3083

10 -	SOUTHERN ISLANDS OF THE SOUTHERN OCEAN	10
11 -	SOUTHERN ISLANDS OF THE SOUTHERN OCEAN	11
12 -	SOUTHERN ISLANDS OF THE SOUTHERN OCEAN	12
13 -	SOUTHERN ISLANDS OF THE SOUTHERN OCEAN	13
14 -	SOUTHERN ISLANDS OF THE SOUTHERN OCEAN	14
15 -	SOUTHERN ISLANDS OF THE SOUTHERN OCEAN	15
16 -	SOUTHERN ISLANDS OF THE SOUTHERN OCEAN	16
17 -	SOUTHERN ISLANDS OF THE SOUTHERN OCEAN	17
18 -	SOUTHERN ISLANDS OF THE SOUTHERN OCEAN	18
19 -	SOUTHERN ISLANDS OF THE SOUTHERN OCEAN	19
20 -	SOUTHERN ISLANDS OF THE SOUTHERN OCEAN	20
21 -	GEOLOGICAL MAP OF THE SOUTHERN OCEAN	21
22 -	PETROCHEMICAL STRATIGRAPHY OF THE SOUTHERN OCEAN	22

LIST OF ENCLOSURES

- 1 - SOUTHERN UPLANDS GEOCHEMICAL ATLAS : SiO_2 (%)..... (1:250,000).
- 2 - SOUTHERN UPLANDS GEOCHEMICAL ATLAS : TiO_2 (%)..... (1:250,000).
- 3 - SOUTHERN UPLANDS GEOCHEMICAL ATLAS : Fe_2O_3 (%)..... (1:250,000).
- 4 - SOUTHERN UPLANDS GEOCHEMICAL ATLAS : MgO_2 (%)..... (1:250,000).
- 5 - SOUTHERN UPLANDS GEOCHEMICAL ATLAS : CaO (%)..... (1:250,000).
- 6 - SOUTHERN UPLANDS GEOCHEMICAL ATLAS : Na_2O (%)..... (1:250,000).
- 7 - SOUTHERN UPLANDS GEOCHEMICAL ATLAS : As (ppm)..... (1:250,000).
- 8 - SOUTHERN UPLANDS GEOCHEMICAL ATLAS : Co (ppm)..... (1:250,000).
- 9 - SOUTHERN UPLANDS GEOCHEMICAL ATLAS : Cr (ppm)..... (1:250,000).
- 10 - SOUTHERN UPLANDS GEOCHEMICAL ATLAS : La (ppm)..... (1:250,000).
- 11 - SOUTHERN UPLANDS GEOCHEMICAL ATLAS : Nb (ppm)..... (1:250,000).
- 12 - SOUTHERN UPLANDS GEOCHEMICAL ATLAS : Ni (ppm)..... (1:250,000).
- 13 - SOUTHERN UPLANDS GEOCHEMICAL ATLAS : Pb (ppm)..... (1:250,000).
- 14 - SOUTHERN UPLANDS GEOCHEMICAL ATLAS : Rb (ppm)..... (1:250,000).
- 15 - SOUTHERN UPLANDS GEOCHEMICAL ATLAS : Sb (ppm)..... (1:250,000).
- 16 - SOUTHERN UPLANDS GEOCHEMICAL ATLAS : Sr (ppm)..... (1:250,000).
- 17 - SOUTHERN UPLANDS GEOCHEMICAL ATLAS : V (ppm)..... (1:250,000).
- 18 - SOUTHERN UPLANDS GEOCHEMICAL ATLAS : Y (ppm)..... (1:250,000).
- 19 - SOUTHERN UPLANDS GEOCHEMICAL ATLAS : Zr (ppm)..... (1:250,000).
- 20 - SOUTHERN UPLANDS LOCATION MAP (1:250,000).
- 21 - GEOLOGICAL MAP OF THE SOUTHERN UPLANDS..... (1:250,000).
- 22 - PETROCHEMICAL STRATIGRAPHY OF THE SOUTHERN UPLANDS.

ABBREVIATIONS AND NOMENCLATURE

The positions of all surface localities are given as their full ten figure, numeric National Grid References (G.R.) and orientations of geological features are described relative to Grid North.

Unless otherwise stated, all references to the ten major rock forming elements (Si, Al, Ti, Fe, Mg, Ca, Na, K, Mn, and P) presented in this work, are quoted in terms of their oxide weight percentage. In addition, all computer programs and geochemical data generated during the tenure of this thesis, are deposited in computer readable form, within the National Geochemical Data Base (NGDB) of the British Geological Survey.

CHAPTER ONE

This thesis was word processed on an IBM-PC using Multimate Advantage and typeset using Aldus Pagemaker. Simple tables were output using a Juki 6100 daisywheel printer whereas both text and complex tables were printed on a Qume Script 10 laser printer. The main body of text in this thesis (Chapters 1 to 7) was typeset using a Times Roman font, 15 point line spacing and 18, 14 and 9 point sizes used for headings, subheadings and general text, respectively.

CHAPTER ONE

CHAPTER ONE

INTRODUCTION

1.1 INTRODUCTION

The Lower Palaeozoic turbidite sequences of the Southern Uplands of Scotland and the Longford Down Inlier in the Republic of Ireland host numerous small baryte-base metal vein deposits (Morris, 1986). This baryte-lead-zinc mineralization is considered by Russell (1978) to have a close association with major normal faulting and basin development processes which formed large stratiform base metal deposits in central Ireland. In addition to these vein systems a small number of highly unusual polymetallic deposits also occur in a variety of geological settings. These include both sediment hosted (greywacke or shale) stratiform or stratabound deposits and igneous hosted vein and disseminated (porphyry style) deposits.

This thesis presents a study of one group of these deposits, namely those associated with arsenic-antimony-gold mineralization, and investigates the application of lithogeochemistry to both exploration for, and detailed evaluation of, their related hydrothermal systems in a turbidite terrain. In addition, it also attempts to define the nature, origin and timing of the As-Sb-Au mineralization and to detail the relationships between deposits and igneous, tectonic and orogenic processes.

1.2 GEOLOGICAL FRAMEWORK

The Southern Uplands occupies an area of 18,000 square km and is bounded to the north by the Southern Upland and Stinchar faults and to the south by the Northumberland Trough. Although the granitic intrusions in the SW of this area give rise to peaks in excess of 700m (ie. Merrick at 842m and the Rhinns of Kells, 813m) a smooth well rounded topography typifies the greater part of this region and results from the general uniformity of the Southern Uplands sediments (Greig, 1971).

The Southern Uplands and also the Longford Down Inlier are principally occupied by an Ordovician-Silurian greywacke/shale sequence which is generally steeply inclined with a consistent NE-SW regional strike. This region is subdivided by a series of major NE-SW trending strike-parallel faults into a number of stratigraphic tracts each of which predominantly young to the NW but becomes sequentially younger to the SE (Stone et al., 1987). Within each unit, the beds are disrupted and repeated by folding and minor strike faulting (Eales, 1979). This turbidite succession was deposited at the northern margin of the Iapetus ocean (Phillips et al., 1976) and has been compared to modern accretionary prisms currently developing on active continental margins where successively younger sedimentary units are underthrust below the continental margin (Leggett et al., 1979). This palaeo-forearc analogy was recently subjected to intense scrutiny by Stone et al. (op.cit) who provided evidence for an alternative depositional environment, invoking both back-arc basin sedimentation and thin-skinned tectonics to explain the observed facts. Chemical evidence in support of a back-arc model is presented in Chapter 5.

Orogenic processes relating to the closure of the Iapetus ocean included intermittent, syn- to post-tectonic granitoid and gabbroid plutonism from around 490-395Ma (Brown et al., 1979; Powell and Phillips, 1984; Rock et al., 1987).

Emplacement of an extensive dyke swarm of lamprophyres and associated intermediate acidic minor intrusions commenced before 420Ma and continued until after 395Ma (Rock et al., 1986). Thus, the earliest syn-tectonic lamprophyres are sheared and predate many of the Late Caledonian granites (eg. Doon, Fleet and Criffel) whereas the latest, post-tectonic lamprophyres postdate even the commencement of post-orogenic molasse sedimentation and represent the last event in Caledonian magmatism.

In the past, this region has been subjected to intense exploration activity for alluvial gold and has yielded in excess of 40,000oz (Gillanders, 1981) from production dating back to the 16th century. One serendipitous result of this activity was the discovery of a number of Pb-Zn-Ba deposits, most notably the Leadhills-Wanlockhead vein system, which have been worked with various measures of success over the last 400 years (Gillanders op cit.).

1.3 GOLD MINERALIZATION IN THE UK and IRELAND

Gold has been exploited from a variety of locations and settings within the British Isles since pre-Roman times (Collins, 1977). The location of the more important of these historical deposits is presented in figures 5 and 8. On the British mainland a significant portion of all exploration activity carried out over the last 20 years has centred upon gold exploration, with the bulk of this work undertaken in Scotland and Wales. This activity has met with varying amounts of success. However, late in 1983 one of the most significant gold discoveries in north-west Europe during this century was made in the Curraghinalt area of the Sperrin Mountains, 15 km north-east of Omagh in Northern Ireland (Earls et. al., 1989).

In 1988 the thirteenth annual commodity meeting of the Institution of Mining and Metallurgy focused upon gold, with emphasis on recent exploration. The resulting proceedings summary (Trans. Inst. Min. Metall. Vol.98) presents the most recent review of exploration activity, techniques and methodology currently applied within the British Isles, and supplements the historical discussions presented in this chapter.

1.3.1 Scotland

Although gold is widely distributed throughout the UK, a number of areas in Scotland have yielded concentrations of gold in economic or sub-economic quantities, namely:

a) Leadhills-Crawford Moor area

Historical records show that mining was being carried out in the Leadhills area as early as the thirteenth century (Wilson, 1921) but it is quite probable that mining activity was also undertaken here as in other parts of the British Isles as early as Roman times. MacGibbons (1935) estimated that the total value of gold, both registered and that illegally exported, obtained from this goldfield was in the region of £200,000 sterling. At the prices pertaining during the peak of production, prior to 1600, this would account for approximately 40,000 ounces of gold, or in present day terms, in excess of £ 10 million.

Until the sixteenth century, the focus of mining activity in Scotland centered upon the exploitation of base metal mineralization for its silver content. During the middle of the sixteenth century the emphasis was switched to gold, due to the discovery of alluvial gold mineralization in vein quartz pebbles and as fine nuggets within stream gravels from the Leadhills area (Duff, 1985). However successful the alluvial deposits proved to be, the possible existence

of gold veins in this district has preoccupied entrepreneurs and adventurers over the last 400 years (Gillanders, 1977).

A chronological account of the history of the Southern Uplands (Crawford Moor) and other Scottish goldfields presented in Table 1.00 based upon a review by Langlands (1980), with additional information derived from Atkinson (1619); Lauder Lindsay (1868,1869); Porteous (1876); Cochran-Patrick (1878); Mitchell Cash (1917); MacGibbon (1935); Snout (1967); Collins (1975); Harvey and Downs-Rose (1975); Gillanders, (1977); Dawson et al. (1979); and Fraser et al. (p.c.m). The widespread distribution of alluvial gold in this area, led to the supposition that a number of auriferous quartz veins existed, however during the following 400 years of subsequent exploration activity, both at surface and underground, no such vein systems were ever formally documented.

Following a period of intense gold exploration and production during the sixteenth and early seventeenth centuries, the Leadhills-Wanlockhead area fell into a period of relative inactivity. However, previous attempts to locate the source of the gold by trenching, had led to the discovery of a large number of Pb-Zn vein deposits in a district where the surface indications of such veins were virtually absent, thus lending considerable impetus to the resurgent lead mining industry (Gillanders, 1977). These veins were the subject of considerable mining activity over the next four hundred years and contributed a greater portion of lead metal to the economy of Scotland than any other mining district.

Temple (1955) detailed two major periods of mineralization in the Leadhills area, with the first phase producing quartz veins containing gold and muscovite, followed by later galena and sphalerite bearing veins. However, the report of a single gold-bearing quartz vein in this area by Temple (op. cit.) is in fact misquoted; Temple was actually, referencing a quotation from Atkinson (1619), found in the treatise on the history of mining in this area by Porteous (1876), where it was stated that the Elizabethan mining expert, George Bowes had 'apparently' located a small gold-bearing quartz vein. This record reports that Bowes swore all his workmen to secrecy and concealed the location of their workings. Due to the untimely departure of George Bowes, in an accident at the bottom of a copper mine in Keswick, the vein was never worked and its location (if it ever actually existed) lost forever. Given the difficulties faced by entrepreneurs such as Bowes in raising the necessary funds to undertake exploration in this area (knightships were even offered by James VI as a form of remuneration for such an investment), it is quite probable that exaggerated claims of potential/proven reserves could have been made and may have found their way into Scottish records of this period. Given also, the fact that none of the workers involved with this apparently major discovery pursued the matter further following Bowes death, it is fair to assume that this report lies more within the realms of Scottish folklore than Scottish mining history. The remaining portion of Temple's mineralogical studies provided the first systematic and detailed account of the nature and diversity of the deposit found in the Leadhills area, although his conclusions that the mineralization had a 'deep seated' origin, was emplaced at temperatures of 143-281°C and was Hercynian in origin have recently been the subject of critical review (Samson,1984).

b) Strath Kildonan area (Helmsdale), Sutherland

Gold exploitation in the Strath Kildonan area of Sutherland was carried out in the latter part of the eighteenth century. In the New Statistical account of Scotland (1845) the discovery of a gold nugget weighing more than half an ounce was reported in Kildonnán Burn. Newspapers of the time recorded further discoveries of alluvial gold in a number of the local burns (or streams) by Gilchrist, a native of Sutherland and a successful prospector, who

upon his return from the Australian goldfields, initiated the first systematic search for gold in 300 years. These reports heralded the start of the famous 1868 Scottish gold rush. Within a few months of the initial discovery over 400 "miners" had moved into the area to seek their fortune and, upon payment of a prospecting fee of £1 per month to the landowner (the Duke of Sutherland) they were assigned sole rights to a 40 foot square claim (Pledger, 1973). Initially a large tented encampment was established at a spot known today as Carn-nam-Burth (place of tents) which was later replaced by a small shanty town (plate 1a and 1b) on the north bank of Kildonnan Burn at a locality known as Baile-an-Or (the Bridge of gold).

Historical records indicate that individual "miners" were producing somewhere in the order of one ounce of gold a week by hand panning and in three years of production over 3000oz of gold was recovered and deposited at the Helmsdale Bank. Given that all gold found at this time was subject to royalty payments it is safe to assume that this figure only partially reflects the amount of gold actually recovered. Exploitation in this region was brought to a rapid halt in 1870 following the removal of mining permission by the Duke of Sutherland. It is reported (Dunbar, 1970) that the Duke considered the wool and mutton from his sheep farm more valuable and less inconvenient than the mining operations and all that they entailed and the miners were therefore given orders to quit.

Since this time a number of individual and commercial attempts have been made to produce gold from this area and have met with a varying measure of success. In 1885 an English firm (under licence from the Duke) attempted mining around the Suisgill Burn but departed from the area shortly afterwards. This aborted attempt was followed by similar action by the Sutherland Mining Company in 1889. A further attempt was made to locate the "mother lode" by the Sutherland County Council early in the 1900's. This operation, involving sixteen miners under the direction of a Mr. Heath (a Californian gold mining expert), also resulted in failure, much to the delight of the local farmers and fishermen who, with a wry sense of humor presented Mr. Heath with a gold watch and chain upon his departure.

In 1964 the British Geological Survey carried out an evaluation of this area and concluded that due to "the rough flaky and granular texture of the alluvial gold and its irregular distribution in streams draining the north-east flanks of Strath Kildonan" the gold mineralization was derived from late-stage hydrothermal mineralization associated with the emplacement of granite plutons. The gold recovered by the BGS survey occurred predominantly in the size fraction 0.25 to 0.75mm. However, approximately 10% of the total number of grains recovered were of 1 to 3mm in size. Small scale hydraulic sluicing techniques were suggested as an optimum method of economic exploitation of these deposits, though it was pointed out that further detailed studies were required to assess the true economic reserves of the area. It is worthy of note that the report of this assessment (Dawson et al. 1965) included amongst its conclusions a provisional estimate that "at least as much gold still exists in this area as was won by the 400 or more gold diggers operating during the years 1868-1870".

In 1969 the Radioactive and Rare Minerals Unit of the BGS re-examined the gold workings in Strath Kildonan and showed that the distribution of the alluvial gold was more extensive than previously believed, covering an area of approximately 80 sq. km. (Phillipson, A.D. 1969) and in addition this study demonstrated a close spatial relationship between gold sites and a zone of migmatites in the Moine series. Furthermore, it was suggested that the gold and base metals may have been derived from complex sulphide ore bodies originally present in the Dalradian meta-sediments which now form the migmatite zones, although it was recognized that large bodies of Newer Caledonian granites intrude the migmatite complexes with the development of local skarns (Michie, 1974).

Following initial examination of the 128 panned concentrates collected by this study, the alluvial gold was considered to have been liberated during tropical erosion and later redistributed by ice action. Detailed microprobe studies of the gold grains (Fortey 1979) revealed that they were in fact gold-silver alloys (electrum) containing minor amounts of platinum and copper. The silver content of individual grains was demonstrated to vary from 10 to 30 wt%. The discovery that the rims of each grain were depleted in silver (up to 98 wt% gold) with respect to the core, was attributed to leaching processes within the alluvium. However, the presence of thin, incomplete rim-zones was used to suggest a nearby source for the alluvial gold of this area.

c) Stronchullin area, Argyllshire

At Stronchullin a 38-46cm wide quartz vein containing galena, sphalerite and chalcopyrite, crosscutting quartzites of Dalradian age, was discovered in the early 1900's. Subsequent assays of the vein mineralization revealed arsenic and antimony contents ranging from 5 to 12% and both gold and silver values of up to 4oz per ton (BGS Gold Files). Following its discovery this deposit was worked as an opencut into the hillside and the remains of these workings are still visible in the form of a 25m long trench, 1 to 2m in width and excavated to a depth of between 4-6 metres. On the basis of these dimensions it can be calculated that approximately 750 tons of material were extracted by this operation, though the exact proportions of ore to waste are unknown.

In the Loch Fyne area of Argyllshire, pyritiferous schists occur within the Ardrishaig phyllite series. Outcrops of this unit on the shore of Loch Fyne have yielded minor gold and silver values associated with galena and sphalerite mineralization.

d) Loch Tay area, Perthshire

The Loch Tay area of Perthshire has been known as a site of alluvial gold for over 130 years. Mining activity in this area was initiated by the Marquis of Breadalbane in the early part of the nineteenth century. In 1838 the Marquis retained Odernheimer, a German mineralogist, to examine the mineralization and mines on his estate, particularly the Tomnadashan copper deposit, on the south bank of Loch Tay and the Corrie Buie lead veins, near the summit of Meall nan Ogrieg.

In 1860 Thoust, in his detailed account of the geology and mineral deposits on the south side of Loch Tay, reported the discovery of a 2oz nugget of gold from Glen Quaich and also noted abundant pyrite and hematite in this area. Three large gold nuggets (weighing 4, 5 and 6oz respectively) were found at Corrie Buie during the process of lead mining (Perthshire Courier, 2-3-1852). Argentiferous galena from this quartz vein deposit historically yielded 40-600 ounces of silver per ton. In addition, arsenical pyrites was reported from a small trial pit in the Lochearnhead area which yielded 6oz of gold per ton. These discoveries linked with the location of native gold in the River Almond (Perthshire Courier, 23-3-1852) appears to have stirred the exploration interests of the local community. Lindsay (1870) reported that a digging "mania" swept this region during 1852. A daily average of 300 "diggers" in this area was not uncommon and exploration extended over an area of twenty square miles including opposite shores of the Forth of Tay. Gold fever reached its peak on the 15th May, 1852 when over 1700 'gold seekers' congregated on west Lomond Hill.

Recently this area has been the subject of intense exploration activity by a joint partnership of two Canadian mining companies (Colby and East West Resources) under the management of R.S. Middleton Exploration Services, based

in Timmins, Ontario. Following an earlier reappraisal of the Tomnadashan mine area by the Canadian Boylen Group which revealed gold assays of up to 0.06oz per ton, and detailed literature surveys, this group obtained an exclusive Crown licence to explore for gold and silver, over an area covering 185 square miles of Upper Dalradian strata (118,400 acres) south of Loch Tay. Initial work confirmed the location of twenty historical sites of alluvial gold mineralization in this area, and defined further alluvial gold localities in a 5 km long east-west trending zone, on the southern flanks of Ben Chonzie in Glen Almond, paralleling the outcrop of a metabasite unit. This activity furthered press speculation of a new "Scottish Klondike" (Daily Express, 4-3-86) in the Loch Tay area. In 1986 a regional geological, geochemical and geophysical assessment of five major estates in this area (resulting in panned concentrate assays of up to 100,000 ppb gold) resulted in a 3000 ft drilling program within the Auchnafree estate (owned by Sir James Whittaker). Although the results of this investigation were inconclusive, this area still remains one of the most attractive sites for potential gold deposits outwith the Southern Uplands and, in light of the Ennex discovery in the Sperrin Mountains of Northern Ireland (Earls et. al., 1989) should merit further investigation.

e) Tyndrum area

Ennex has also been actively evaluating the gold potential of the Dalradian rocks in the highlands of Scotland, where investigations centred upon the Cononish Farm, west of Tyndrum. Here gold-bearing quartz veins containing 0.45oz/ton gold and 1.3oz silver have to date been traced by trenching over lengths of up to 330 ft (Ennex Annual Report, 1984; Parker pers. comm.). By the end of 1987 a total of 100,000 oz of reserves had been proven at this site (Parker, 1987) and to date ore reserves stand at 925,000 short ton with grades averaging 0.22 oz Au/short ton cut (0.35 oz Au/short ton uncut) and 1.18 oz Ag/short ton. The company received planning permission for an 850m exploration adit in 1988 and development is well under way to confirm the continuity of mineralization and ore reserves (Mining Magazine, January, 1989).

f) Gairloch area, Wester Ross

In 1907 a 'copper-bearing limestone' was reported by Peach et al. in the Gairloch area in northwest Scotland. This deposit was not subjected to further investigation until 1978, when Consolidated Gold Fields, Ltd. began an evaluation of this area. In 1983, Jones et al. presented summary results of this study and detailed the location of an extensive stratiform mineralized horizon containing significant gold and zinc. This horizon occurs within the Lewisian Loch Maree Group, a supracrustal sequence of mafic volcanics, greywackes, limestones, shales and banded iron formations, unconformably overlying an older Lewisian high-grade metamorphic complex (Winchester et al. 1980). A submarine exhalative origin was proposed for this deposit (Jones, op.cit) and it was tentatively compared with deposits of Besshi and Kieslager types. Although the mineralization is exposed over a relatively small area, diamond drilling by Consolidated Gold fields delineated vertical and lateral extensions to this deposit. In addition, further sulphide-rich gossans were reported in the general area.

g) Shetland Isles

Hedde in 1919 reported the occurrence of native gold associated with ilmenite sands on the Island of Unst, near Berwick, and suggested a possible association with local quartz veins cross cutting an epidotic syenite. In the most recent study of mineralization in this region, Lord and Pritchard (1989) detailed the widespread distribution of low-level concentrations of Au (10-100ppb) and demonstrated a primary magmatic association with chromite-rich or clinopyroxene-dominated ultramafic rocks of ophiolitic affinity.

1.3.2 Northern Ireland

The Sperrin Mountains discovery made by Ennex International Ltd. occurs in Dalradian metasedimentary rocks of the Southern Highlands Group. This deposit is located in the Curraghinalt Burn area and is hosted by a WNW trending quartz-vein swarm (0.4 to 1.1m in width) to the northwest of the Omagh Thrust (Clifford, 1986; Earls et al., 1989). Furthermore, drilling in juxtaposed Ordovician volcanics to the south of the Curraghinalt area, south of the Omagh Thrust is reported to have intersected narrow zones of low grade base metal values with associated gold. However, no intersections of economic widths/grades were located (Ennex Ltd. Quarterly Report, June, 1986).

Mineralogically, the Curraghinalt deposit appears simple, with electrum present as both intergrowths and fracture infills within pyrite, arsenopyrite and chalcopyrite. Free gold is present and ranges in size from 20-130 microns (Earls et al., op.cit.). Lithogeochemical studies have established an intimate sympathetic relationship between Au, Ag, Bi and Fe but Au appears unrelated to Cu, Pb, Hg and As. Current ore reserves of this Dalradian hosted quartz vein-gold deposit are 1 million short ton at a grade of 0.28 oz Au/short ton cut (Ennex Ltd, Quarterly Report, September, 1986). The gold-bearing vein systems are known to be open both at depth (up to 500 ft) and along strike. An underground exploration programme, including the development of a 1,400 ft adit to enable detailed underground examination (at depths of 170 ft) of the five veins on which the ore reserve calculations are based is currently underway. Recent exploration activity in Northern Ireland has also included an evaluation by Dungannon Exploration Ltd. of licence D5, an area to the north of the Ennex deposit, approximately 25 km south of Londonderry (Continental Carlisle Douglas Newsletter 1986). In this area the identification of a number of alluvial gold anomalies led to the discovery of two auriferous vein systems in the Golan Burn area. Details of the results of this study are still, for the most part confidential however, assays of 0.23oz/ton over 8.125 ft and 0.27oz/ton over 1.4 ft have been announced (26-9-86). Internal geological reports have speculated that the mineralization located in the Golan Burn area is a lateral extension to that of Ennex's adjacent property. However, a considerable investigation is still required before this claim may be justified.

1.3.3 WALES

a) Ogofau

Mining at this site has been undertaken since Roman times and it has been estimated by Annells (pers. com. 1983) that production was in the order of 4-5,000 oz gold. From the late 1880's this site witnessed sporadic activity by predominantly cornish miners and in 1888 a small mill was built on the site. In the early 1900's the Roman adits were extended and a small number of new adits dug, but it was not until the formation of British Goldfields Ltd. in 1931, that full-scale exploitation of this mine began. In the period that followed a 480 ft shaft was dug with a series of levels at 100 ft intervals and approximately 2-3000 tons of ore were extracted. Work ceased at the mine prior to the onset of the second world war due to the high arsenic content of the mill concentrate and other geological problems.

The deposit is hosted by pyritic Ordovician siltstones and shales at the junction with the overlying Silurian turbidites. Geochemical studies in the mine area reveal similar wallrock alteration characteristics to the Glendinning deposit namely, arsenic enrichment and zinc depletion (with the lode zone itself is enriched in zinc).

Fluid inclusion and sulphur isotope studies infer deposition temperatures of the gold bearing quartz veins between 338-372°C (Steed pers com. 1985).

b) The Dogellau Gold Belt

The Dogellau Gold Belt is situated on the south eastern flank of the Harlech Dome a periclinal structure composed of Cambrian sediments, recently described by Allen et al. (1985). A number of gold bearing quartz-sulphide veins occur in a 'belt' roughly coincident with the outcrop of the Clogau Formation, a sequence of black silty mudstones of Cambrian age. Gold exploitation and mining in this area dates from the mid nineteenth century and in excess of twenty mines and thirty known trials have been recorded. This region has produced approximately 130,000 oz of gold since the 1850's (Hall, 1975) and while interest centres upon the Clogau and Gwynfyndd Mines (80,000 and 40,000 oz production respectively) it should be noted that between 1890-1910 twenty substantial deposits were actively mined in this area. Integrated structural, textural and geochemical studies of the Gwynfyndd deposit were undertaken by Ashton (1981) who assigned the gold mineralization a Late Caledonian age and proposed that the deposits formed as result of extension and major normal faulting.

The forest of Coed-y-Brenin, five miles NNE of Dogellau was famed for its deposits of Turf Copper, an extensive low-lying peat bog enriched with copper sulphate. Historical exploitation of copper at this site was undertaken during the nineteenth century by burning the peat in kilns and extracting native copper from the ashes. This area was the subject of intense exploration activity during the period 1965-1973 by Riofinex Ltd (Rice et al. 1974) who delineated the presence of an extensive, low-grade (0.2%) disseminated copper deposit, hosted by late Cambrian diorites. This deposit displayed many features commonly associated with 'porphyry copper' deposits, such as a phyllic-propylitic alteration envelopes and associated metal zonation patterns, and was ascribed a Caledonian age. To date, little discussion of the gold potential of this deposit has been published and in comparison with similar deposits elsewhere, the suggestion that any gold present could be extracted as a by-product during copper production cannot be discounted.

In the mid-late 1970's this deposit was the subject of a major public enquiry, due to its location within the Snowdonia National Park. Unfortunately, the enquiry sided with the arguments raised by a strong nature conservation lobby and refused to allow any further development of the Coed-y-Brenin deposit. Recently, the Gold-Belt area was the subject of a geochemical drainage survey, undertaken by the British Geological Survey as part of their on-going Mineral Reconnaissance Programme (Cooper et al. 1985). This study delineated the metallogenic potential of this region and defined a series of anomalous areas related to a variety of different styles of mineralization including: Gold Belt vein deposits; granite-related deposits; disseminated 'porphyry-style' copper deposits; and stratabound and epigenetic manganese deposits.

1.3.4 Cornwall and Devon

Although the south-west of England is best known for its tin mining industry, a large number of sites of alluvial gold occur throughout Cornwall and Devon, the most famous being at the head of the Restronget Creek in the Falmouth Estuary. The earliest review of gold mineralization in this area is presented by McLaren (1908) who noted that very little of this alluvial gold had been traced back to its bedrock source. The principal site of gold mineralization in Devon is North Molton, where in 1850 "vein gossans" crosscutting Devonian aged strata within

the Britannia and Poltimore mine, yielded over 1.3oz of gold per ton and total production from this source was in the order of approximately 150oz. The gossan has been described as a “friable ironstone containing copper” (Anon, BGS Gold file) which most probably formed by the decomposition of gold-bearing sulphides, predominantly pyrite (Collins, 1975). A further potential source of alluvial gold in the Port Issiac area of North Cornwall was identified by Stanley (pers.com.) where both native gold and electrum inclusions are present in tetrahedrites hosted by metabasites.

Leake et. al. (1989) documented the results of a detailed drainage survey and gold exploration programme in south Devon. Microchemical investigation of detrital gold grains from both drainage and overburden samples (for Au, Ag, Pd, Cu and Fe) revealed the presence of considerable compositional variation. Zoned Pd-bearing gold (Pd 3-10%) displays similar composition to dendritic gold from Hope’s Nose, and as such is inferred by Leake et. al. (op.cit.) to represent the original composition of gold mineralization in this region.

1.3.5 Lake District

One of the earliest records of gold mining activity in the UK is attributed to Roman activity at the Goldscope Mine, in the Vale of Newlands, to the south-west of Keswick. Mining activity resumed at this mine during the reign of Elizabeth I and the succession of workings for both lead and copper at this site are detailed by Postlethwaite (1913). The general geology of the mine area consists of a major E-W trending vein set dominated by chalcopyrite but also containing pyrite, arsenopyrite, native bismuth and microscopic inclusions of native gold and electrum (Stanley, 1986 pers.com). The vein system cross cuts Ordovician graphitic siltstones in close proximity to the contact with the overlying Borrowdale Volcanic Group. The Dale Head North vein, 2 km to the south of the Goldscope Mine is also reported to contain gold bearing sulphides (Stanley 1986 pers com.).

The origin of these chalcopyrite-arsenopyrite-pyrite veins was discussed in detail by Firman (1986) who proposed a volcanic source for the mineralizing fluids and in addition, tentatively suggested a model for the recirculation of volcanic exhalative fluids, driven by Lower Devonian granite intrusion. Detailed mineralogical studies by Ixer et al. (1979) upon a wide variety of cobalt-, nickel- and iron-bearing sulpharsenides from the Lake District also led to the inference of a magmatic component to this form of mineralization. An additional point worthy of note in relation to both of the above deposits is the presence of tourmaline in association with the sulphide-gold mineralization. Thus, the pathfinder elements Cu, As, Bi, Sb and B could prove useful in any form of geochemical survey for this type of mineralization.

Small quantities of arsenic-bismuth-molybdenum mineralization have been described by Young (1985) from a quartz-topaz greisen located at the margin of the Eskdale Granite [SD 1525 9723]. The age relationships of this mineralization is unclear but it was proposed that the mineralization was genetically related to the granite and developed during the final stages of emplacement, thus implying an early Silurian episode of mineralization.

1.3.6 Republic of Ireland

Small quantities of gold have historically been located in various parts of Ireland (Fig 8). A detailed review of gold in Ireland is presented by Reeves (1971) and more recently McArdle (1989) summarising the wealth of historical literature from sources including Boat (1652), Kane (1845), Calvert (1853), Holdsworth (1857), Kinghan (1878),

Ball (1895) and Simoens (1921). In addition to the predominantly alluvial deposits described above, in-situ gold mineralization has also been reported from the Avoca district in southeast Ireland, South Mayo, the Longford Down Inlier and the west of Ireland (McArdle, op.cit.).

Gold is currently the principal focus of mineral exploration for most companies in the Republic of Ireland (Morris, 1986; McArdle, op.cit.). Exploration activity has been encouraged by the definition and detailed investigation of a number of prospects, including Clontibret (Munster Base Metals Ltd.); Westport, County Mayo (Tara Prospecting Ltd.) and the Sperrin Mountains (Ennex plc Ltd.). Historical gold production in the Republic of Ireland was confined to a number of placer occurrences in the Goldmines River area of the Wicklow Mountains, south of Dublin where approximately 50,000oz of gold were liberated between 1790-1850 (a similar figure to the gold production estimates of the Leadhills area in Southern Scotland). A chronological account of the history of alluvial gold production in the Gold Mines River area, Co. Wicklow presented in table 1.51, is based upon this review with additional information derived from Mills (1801), Weaver (1821), and MacLaren (1903).

In 1986 Tara Prospecting announced the discovery of a significant vein and placer gold mineralization, near Westport in County Mayo. The deposit is located at the fault-bounded contact between Silurian turbidites, Dalradian metasediments and an undated ophiolitic complex. Auriferous quartz vein systems have been traced over a strike length of approximately 12 km and in one location preliminary diamond drilling delineated reserves of 7000 tonnes grading 4.9g/tonne (0.16oz/tonne) Morris (1986). Recently, Riofinex plc announced the discovery of a new group of gold-bearing veins three km west of Omagh, County Tyrone and reported strike extensions of up to 3000ft (Mew Quarrying and Mining 15th Feb, 1988). Furthermore, significant gold mineralisation associated with massive sulphide deposits have been reported by Ovoca Gold Exploration PLC from their exploration programme in Dalradian rocks in Connemara, western Ireland (McArdle, 1989).

In County Monaghan, the Clontibret (Lisglassan-Tullybuck) deposit, historically worked for antimony (Morris, 1985) has since 1979, been subjected to an intense exploration program by Munster Base Metals Ltd. This study has defined a number of NNW trending stibnite-quartz lodes, and a stratabound stringer-vein zone, within Ordovician turbidites. The stringer-vein zone has been traced along strike for more than 500m, delineating a broad zone of low grade gold mineralization (ie. 0.88g/tonne over 41.3m and 0.93g/tonne over 25.7m). The lode zones, defined by Morris (1986) as vein/fault zones enveloped by disseminated auriferous arsenopyrite and pyrite in pervasively altered (phyllitic) greywacke, have yielded higher grades over considerably narrower widths (ie. 36g/tonne over less than 2m). Detailed geological studies by Morris and Steed (1985, 1986 and 1987) suggest that this deposit is Caledonian in age and related to minor igneous activity.

1.4 ARSENIC AND ANTIMONY MINERALISATION IN SCOTLAND

Antimony, historically a strategic element because of its role in the explosives industry, has been recovered from a number of deposits in the British Isles. In all instances however, production was carried out on a limited scale and in each case the ore was confined to erratically distributed pods of stibnite within narrow quartz veins. A summary of the internal and published BGS records relating to arsenic and antimony deposits in Scotland (Dewey, 1920) is presented below:

1.4.1 Talnotry

Here a 1.3m wide arsenopyrite-quartz vein occurs along a faulted junction between the Cairnsmore Granite and Silurian slates and greywackes. Arsenopyrite occurs as both coarse masses up to 5cm in diameter within the vein and as fine grained disseminations in the host rocks (Duller and Harvey, 1984). Historical workings dating from the late 1800's, consist of a shaft 32m in depth with a side level driven for a few tens of metres.

1.4.2 Glendinning

The Louisa Mine at Glendinning, 12 miles north-west of Langholm was discovered in 1760 during a search for lead mineralization. At this site a stibnite-quartz vein was located outcropping in the Glenshanna Burn, which on detailed examination was also found to contain minor sphalerite and traces of galena, pyrite and chalcopyrite. This vein remained for the most part unexploited until 1793 when the Glendinning Antimony Mine Company began regular production. In the six years that followed (1793-98) approximately 100 tons of antimony metal was refined on site, valued at this time at £8,400. During this period approximately 40 people were employed on site and paid wages of £23-26 per year. In 1888 exploitation of this deposit resumed and during the period 1888-91 a further 88 tons of metal were extracted. Mining activity appeared to have ceased abruptly in 1891 and approximately 10 tons of ore was left on the sorting floor. Further work at the mine appears to have been undertaken during the period of the first world war (1914-18) but few details or records of production are available.

The only cross-section of this mine located to date is that presented on General Dirom's County Map of Dumfriesshire (circa 1850) which forms the basis of Figure 85. The mine was worked on three main levels by a process of open-stopping. However, access to the old workings is currently restricted to twenty metres of the adit level, the remaining 100 metres of this adit is sealed off by a roof collapse and other levels are inaccessible due to the (pre-1920) collapse of the main shaft. In 1979 this deposit was investigated by the British Geological Survey as part of its Mineral Reconnaissance Program in Scotland. This survey led to the discovery of apparent stratiform arsenopyrite mineralization in close proximity to the vein stibnite deposit and recognized the association of arsenic and antimony in the surrounding area (Gallagher et al. 1981 and 1983).

1.4.3 The Knipe

The Knipe Antimony Mine, 3 miles SSE of New Cumnock, was first reported by Alexander Rose in 1845. The deposit is located near the centre of a small granodioritic cupola of Lower Devonian age intruding a Lower Ordovician (Arenig-Llandeilo) series of greywackes and shales, and gives rise to the prominent upland areas of Hare Hill and the Knipe (Khan, 1968; Fowler, 1976; Rollin, 1983; Naden and Caulfield, 1989). The orebody consists of a N-S trending 30-50 cm wide vein containing acicular stibnite and quartz. Underground workings consisted of an adit driven into the hillside for a distance of approximately 55 metres. However, as the entrance to this adit has now collapsed, underground exposures are inaccessible. A second stibnite vein 15-20cm wide trending N010° was reported by Fowler (op cit.) to the west of the main vein, outcropping within the old boundary walls of the Dalhana property (Blackadams Burn). This vein was traced by Fowler (op cit.) over a strike length of 400m during a VLF geophysical survey of the mine area. Immediately north of the main mine area a N-S trending fine grained microgranite ('felsite') dyke outcrops within Garepool Burn. Disseminated arsenopyrite has been located by the author within the wallrocks to the main stibnite vein (sericitised granodiorite) and the dyke (hornfels

greywacke) and as such a tentative link between the dyke and the As-Sb mineralization is inferred. Little information is currently available as to the exact timing of exploitation at this site or regarding the amount and value of ore extracted. This deposit was recently the subject of detailed evaluation by BP Minerals Ltd and the results of a fluid inclusion and stable isotopic study of this deposit is presented by Naden and Caulfield (1989).

1.5 THE ROLE OF THE BRITISH GEOLOGICAL SURVEY

The British Geological Survey was established by the Government in 1835 with the specific charter to produce geological maps of the country in order to aid the assessment of national mineral wealth and assist the construction of land utilisation policies (Wilson, 1977). Geological mapping of Scotland began in 1854 and for the first 20 years concentrated upon the rapid survey of central Scotland and the Southern Uplands. Subsequent to this survey, Lapworth (1884) established the importance of graptolites in the interpretation of the geology of the Southern Uplands and as a result, a major resurvey of this area was undertaken by Peach and Horne between 1888 and 1898, resulting in the 1899 publication of revised maps and their now classic memoir.

Since this time the British Geological Survey has actively undertaken a wide variety of studies in the Southern Uplands, including the remapping and publication of individual 1:50,000 scale geological maps and accompanying sheet memoirs and a detailed assessment of the sand and gravel resources of this region. This work has been supplemented to a great extent by detailed individual studies in a wide variety of disciplines, particularly the Department of Trade and Industry funded Mineral Reconnaissance Programme (MRP). It should be noted that the recent releases of drainage geochemical data relevant to this region from the Geochemical Survey Programme (GSP) are not reviewed here. The MRP programmes instigated in the mid-1970's centred upon a detailed (re)examination of many of the known areas of historical mining activity or recorded mineralization. In addition, the technique of stream sediment sampling was used during these studies to aid the assessment of the mineral potential of the surrounding areas and proved extremely effective in delineating previously unreported mineralization. The following areas and styles of mineralization were investigated by the Survey:

- a) Stratabound arsenic and vein antimony mineralization in Silurian greywackes at Glendinning, Southern Scotland (Gallagher et al. 1983).
- b) Base-metal mineralization associated with an Ordovician shale sequence in south-west Scotland (Stone et al. 1983).
- c) Investigations of small intrusions in Southern Scotland (Cooper et al. 1982).
- d) Mineral exploration in the area of the Fore Burn igneous complex, south-western Scotland (Allen et al. 1982).
- e) Gold mineralization at the Southern margin of the Loch Doon granitoid complex, south-west Scotland (Leake et al. 1981).
- f) Copper-bearing igneous rocks at Cairngarroch Bay, south-west Scotland (Allen et al. 1981).
- g) Porphyry style copper mineralization at Black Stockarton Moor, south-west Scotland (Allen et al. 1980).
- h) Mineral reconnaissance survey of the Abington-Biggarr-Moffat area, South-Central Scotland (Dawson et al. 1979).
- i) A geochemical drainage survey of the Fleet granitic complex and its environs (Leake et al. 1978).
- j) A reconnaissance geochemical drainage survey of the Criffel-Dalbeattie granodiorite complex and its environs (Leake et al., 1978).

- k) A mineral reconnaissance survey of the Doon-Glenkens area, south-west Scotland (Dawson et al. 1977).
- l) Lead, zinc and copper mineralization in basal Carboniferous rocks at Westwater, south Scotland (Gallagher et al., 1977).
- m) Geophysical surveys around Talnotry Mine, Kirkcudbrightshire, Scotland (Parker, 1977).

The above reports present the most extensive and up to date source of reference for potential mineralization in Southern Scotland. They have been used extensively by mineral exploration companies to delineate potential targets within this region and as such are responsible for actively promoting further 'private sector' exploration. Where appropriate the results of pertinent reports are discussed further within chapters 3-6.

1.6 OBJECTIVES AND METHODOLOGY

This research was initiated in 1982 with the objective being to characterise the geochemical effects of hydrothermal alteration in the Glendinning deposit and test the hypothesis that lithogeochemical surveys could be used to identify potential areas of similar As-Sb-Au mineralization. In the period 1982-83, field work concentrated upon subsampling of the available BGS drillcore, chip sampling in the immediate area of the Louisa Mine and the implementation of a regional lithogeochemical sampling program between Glendinning and Hawick. During this period sampling of many of the polymetallic vein deposits in the Southern Uplands was also undertaken in conjunction with several visits to the turbidite hosted arsenic-gold deposit at Clontibret in the Republic of Ireland. By the end of 1983 initial geochemical results clearly defined a number of anomalous lithogeochemical sites to the north east of the Louisa Mine area, which were then investigated by a program of shallow soil sampling and overburden geochemistry.

The success of these studies clearly merited the assessment of lithogeochemistry as a potential tool in gold exploration on a much wider scale. To this end, simultaneous cross-strike traverses were undertaken by the author and Dr R. Barnes (across the south-west coast of Scotland) and Dr J. Morris of the Geological Survey of Ireland (across the Longford Down). In addition, a suite in excess of 1000 petrographically studied greywacke samples were made available for chemical study by Dr J. Floyd of the British Geological Survey from his own research areas in the Northern and Central belts of the Southern Uplands. Automated XRF, electron microprobe and more traditional 'wet' chemical analysis was carried out in 1983-1984 within the geochemical laboratories of Nottingham and Manchester Universities and Kings College, London. The third year of this study was dominated by geochemical data assessment, interpretation, presentation and review, linked by intensive computer programming activity.

This research initially set out to characterise the chemical effects of mineralizing hydrothermal fluids upon their turbidite host rocks and to test the hypothesis that lithogeochemistry could be used effectively to detect the presence of stratabound As-Au mineralization in any turbidite terrain. Lithogeochemical studies of greywackes, shales and mineralized drillcore were used to define a 'chemical fingerprint' for the hydrothermal (wallrock) alteration effects associated with As-Au deposits in southern Scotland and successfully delineated new areas of potential mineralization. The resulting geochemical data were also used to provide detailed information upon the variation in chemistry of the mineralizing fluids with time, and were augmented by detailed petrographic, mineralogical, micro-chemical and isotopic studies.

Lithogeochemical data from samples collected on a regional scale across the Southern Uplands of Scotland and Longford Down in the Republic of Ireland were used to define "geochemical signatures" for a series of petrographically distinct turbidite units and to generate a regional lithogeochemical 1:250,000 atlas of this region (see enclosures) linking a number of detailed inset maps produced at scales of 1:100,000 and 1:50,000.

1.7 THESIS STRUCTURE

This thesis describes a geological, mineralogical and geochemical investigation of stratabound arsenopyrite-gold mineralization in the Lower Palaeozoic turbidite succession of the Southern Uplands of Scotland. This attempt to define the nature and genesis of these deposits also includes an evaluation of the application of lithogeochemistry to regional studies in this terrain.

The research proposal (for this study) was developed during 1979, following the discovery by the Mineral Reconnaissance Program of the British Geological Survey (formerly known as the Institute of Geological Sciences) of stratiform arsenopyrite mineralization in close proximity to the Louisa Mine, near Glendinning, 13 km NW of Langholm (Gallagher et al. 1981 and 1983). The original investigation by the BGS was regarded as a reconnaissance; detailed studies were required to elucidate the origin and genesis of the deposit and evaluate the potential of the region for similar occurrences. This project was proposed to and supported by the Natural Environment Research Council, in the form of a CASE studentship supervised jointly by Professor M.J. Russell of the Department of Applied Geology, Strathclyde University and Dr M.J. Gallagher of the British Geological Survey, Edinburgh (see page iv for details of the original proposal).

This chapter reviews the geological and historical background to gold mineralization in the UK, defining the area of investigation and outlining the methods and philosophy followed during the tenure of the research programme. In chapter two, details of the analytical, computational, data management and interpretation techniques applied within this study are presented and discussed. The Glendinning As-Sb-Au deposit is evaluated in detail within chapter three. The broad spectrum of observational scales described in this chapter is used to test a number of possible hypotheses relating to ore genesis and alteration processes. In chapter four a critical review of the global association of arsenic and antimony deposits with gold mineralization is presented. This includes a discussion of the nature, origin and genesis of such deposits and the structural control, occurrence and igneous association of gold mineralization in Scotland.

The results of the systematic lithogeochemical sampling program in both Scotland and Ireland is described in chapter five. This study is used to evaluate the origin and provenance of Scottish greywackes within their regional geological context and define the relationships between turbidite petrography and geochemistry. mineralized and unmineralized greywackes are also compared in order to distinguish the effects of ore forming processes from the effects of turbidite provenance. Chapter six details the results of a series of micro-chemical mapping studies upon a number of individual sulphide crystals and discusses the application of this technique to both mineral exploration and processing. In the final chapter the conclusions generated within this thesis are summarised and their significance discussed. Opportunities for future studies and their application with regard to outstanding problems are also presented. During the tenure of this research program interim reports were presented in the form of short lectures at a series of local and international conferences and subsequently published (see References and bibliography). A summary of the analytical studies undertaken is presented below:

Microprobe Analysis

Sulphide	Analyses
Arsenopyrite	1743
Pyrite	206
Stibnite	20
Sphalerite	12
Tetrahedrite	7
Gold Inclusions	16
Total.....	2004

X-Ray Fluorescence Analysis

Rock Type	Pressed Pellet	Fused Bead
Greywacke	1847	200
Mudstone	197	10
Mineralized Core	167	10
Soil Samples	495	-
Mineralization	84	-
Total.....	2790	220

Inductively Coupled Plasma Analysis

Rock Type	Samples
Greywacke	213
Mineralized Rocks	15
Total.....	228

The geochemical database formed by the above data contains in excess of 100,000 elemental analyses together with approx. 30,000 calculated values (ie. ratios, totals, norms, formula units and atomic proportions). Listings of all data and computer programs are presented within the tables and appendices of this thesis. Copies of the geochemical data in a computer readable format are lodged with the British Geological Survey and form part of the National Geochemical Database.

CHAPTER TWO

ANALYTICAL TECHNIQUES AND METHODS OF INTERPRETATION

2.1 INTRODUCTION

The trend towards large-scale multi-element geochemical studies over recent years has not only yielded increasing large numbers of geochemical analyses, but also an increasingly wide selection of chemical elements for each sample. Twenty nine major, minor and trace elements were routinely analysed by XRF techniques during this study and these were augmented by an additional 20+ elements analysed by ICP, neutron activation or other specialised techniques. In a project of this size, considerable benefits were gained by the use of computer-based data processing techniques, particularly in the fields of data management, statistical processing and automated cartography and plotting. Computer programming and data analysis were carried out within the Applied Geology Department of Strathclyde University whereas XRF data processing, discriminant analysis and grey scale mapping were carried out in the XRF laboratory within the Geology Department of Nottingham University. An account of all sample preparation and analytical procedures is provided within the appendices of this report.

2.2 ANALYTICAL TECHNIQUES

2.2.1 X-Ray Fluorescence Spectrometry

X-ray fluorescence spectrometry is a well established analytical technique, capable of producing reliable, high precision geochemical data. It is only with recent developments in instrumentation and computer technology that the speed of analysis has been increased to a point where the technique has become cost effective for use in geochemical exploration (Harvey and Atkin, 1985).

These techniques are based upon the theory that X-rays (short wavelength electromagnetic radiation) may be produced by bombarding matter with high energy particles or radiation. If the bombarding particles possess sufficient energy they will be able to knock out electrons from the inner shells of atoms in the target area, leaving holes. Electrons from outer energy shells of the atoms will fall back into the holes in the inner shells and in so doing, emit electromagnetic radiation. The wavelengths of the fluorescent radiation emitted are determined by the atomic energy levels and are characteristic of the element emitting them.

Sequential wavelength dispersive spectrometers are capable of determining most elements from atomic number nine (F) upwards over a compositional range of a few parts per million, or less, up to 100% (Galson et. al. 1983). The development and availability of a high power (3kW) rhodium anode X-ray tube was highly significant, as the tube can be used to determine almost all elements of geological interest (with the exception of Ag, Cd and In) thereby minimising the need to change X-ray tubes within analytical runs. Quality control procedures were undertaken during geochemical analysis in order to ensure that the final analysis is within acceptable/predicted error bounds. This involve the analysis of "known" samples (ideally Certified Reference Standards) in order to

check the “accuracy” and the repeat analysis of either “known” or “unknown” samples to check the precision (Harvey and Atken, 1985). As the concentration of an element decreases its measurement precision deteriorates until the Lower Limit of Detection (LLD) where the precision is $\pm 100\%$ is reached (NB. The LLD may within reason, be raised or lowered by altering the counting times). Standard analysis runs involved the frequent analysis of an instrument “monitor”, the analysis of several Certified Reference Standards, in-house Reference Standards and the unknown samples.

Harvey et. al. (1973) described a technique for X-ray fluorescence analysis of fusion beads based upon the method of Norrish and Hutton (1964) but modified to enable more rapid preparation and processing of samples without any loss of accuracy. This method was followed during the preparation and analysis of greywacke samples during the tenure of this project. Because of the non-destructive nature of the XRF technique, an identical set of standards were used for all analysis runs, thereby ensuring that the data obtained from individual runs remained compatible even in the low ppm range, throughout this project. Full details of the sample preparation techniques and analytical procedures are presented in appendix one.

2.2.2 Electron Probe Microanalysis

A detailed summary of the principles of electron probe microanalysis is provided by Craig and Vaughan (1981). In summary, a beam of electrons generated in a potential of 20kV may be focused into a 1 micron diameter beam and directed at the sample under analysis. This beam then excites the emission of X-rays characteristic of the elements present in the sample, the intensities of which are calibrated against those of known standards in order to provide a quantitative analysis of element concentration.

The Manchester probe comprises a Cameca Camebax system fitted with two wavelength dispersive spectrometers (WDS) and a Link 860-500 EDS system. A 20kv accelerating potential voltage was used with a 40° take-off angle, 14.5nA beam current and 2 micron beam width. Spectra software was used to deconvolute overlapping X-ray peaks and subtract a background radiation by reference to a previously obtained library of standard peak profiles. Standards consisted of a mixture of pure metal and synthetics (see appendix 3). Arsenic analyses were calibrated in relation to a secondary standard with respect to Kretchmar 200, the international arsenopyrite standard.

2.2.3 Scanning Electron Microscopy

If a microprobe's electron beam is made to raster across the surface of a specimen (rather than remain stationary) secondary and backscattered electrons are produced. When these electrons are detected and the signal amplified, a magnified image of the specimen surface can be produced on a cathode ray oscilloscope in a similar manner to a television picture. The backscatter electron image forms a powerful tool in the study of small-scale mineralogical structures as it provides good atomic number contrast with a resolution of approximately 50nm. The CAMECA Camebax at Manchester University uses four solid state diodes to detect the backscattered electrons. In addition the Camebax can also be used as a high performance scanning electron microscope (resolution 10nm) by detecting secondary electrons, however this image gives poor contrast between most silicate phases.

2.2.4 Fire Assay

Although the special position held by fire assay in analysing the precious metals is under threat by other techniques, the unique chemical properties of precious metals and their common association with complex matrices ensures that the fire assay technique is still an essential analytical tool. In its simplest form, the fire assay technique is based upon the affinity of precious metals for molten lead. In detail, individual samples are heated with a mixture of lead oxide, a reducing agent and a flux. The resulting high temperature lead metal forms alloys with the precious metals contained within the sample and collects as a lead (Dore) bead, leaving the remaining material to form a glassy slag. Following cooling and separation, the Dore bead is placed within a bone-ash crucible and heated in a direct air flow. This oxidises the lead which is partially absorbed by the porous crucible and partially evaporated. Since the precious metals are inert they remain in the crucible and at the end of this 'cupellation' stage, form a small bright button ('prill') which is then weighed. In the absence of platinum group elements it is a simple matter to digest the silver content of this bead in nitric acid, leaving the relatively more noble gold as a residue to be collected and weighed. The silver content may then be calculated from the difference between initial and final bead weight. When platinum group metals are present a complex series of chemical separations are also performed on the bead. The limitation of this procedure is the smallest amount of gold that can be weighed reliably, and most laboratories report a detection limit of ~0.01 ounce per short ton (0.343ppm) using a 30g sample.

This technique has been modified within the isotope laboratories of McMaster University, where the standard Dore bead is irradiated prior to instrumental neutron activation analysis (INAA). This pre-concentration of gold and other precious metals within a lead bead prior to irradiation, serves to reduce many of the matrix effects inherent in whole rock samples, increasing sensitivity and providing detection limits as low as 1ppb for Au. Full details of the determination of gold by neutron activation analysis are provided by Hoffman and Brooker (1983).

Considerable confusion exists in the terminology and units used in analytical and economic assessments of gold deposits. This is compounded by the fact that fire assay results are generally reported in ounces per ton, whereas geochemical results are reported in parts per million (ppm). As such, simple conversion factors between these two forms of data are presented below:

10 ppb	= 0.00033 oz/long ton	(2240 pounds)
10 ppb	= 0.00029 oz/short ton	(2000 pounds)
1 ppm	= 0.033 oz/long ton	(1000ppb)
30.61 ppm	= 1 oz/long ton	
34.28 ppm	= 1 oz/short ton	= 1.120 oz/long ton
100 ppm	= 2.917 oz/short ton	= 3.267 oz/long ton

2.2.5 Instrumental Neutron Activation Analysis

Instrumental neutron activation analysis is an analytical technique dependent on the measurement of the number and energy of gamma and x-rays emitted by radioactive isotopes produced within a sample, following irradiation with neutrons from a nuclear reactor. This neutron-induced radioactivity emits a characteristic gamma-ray energy spectrum for each element (ie. an individual nuclear fingerprint) which can be measured and quantified using a gamma-ray spectrometer.

The analytical facilities of the McMaster Nuclear Reactor Center, Ontario, Canada were used during the tenure of this project. The McMaster nuclear reactor operates at a 2MW power level and allows simultaneous irradiation of a large number of samples under a variety of conditions. This facility caters for an industrial requisite of large numbers of routine gold analyses. This technique provides a highly sensitive method for gold and platinum assay and is further enhanced when used in conjunction with the classical fire assay collection of gold in a Dore bead prior to irradiation (detection limit 1ppb).

Until recently, restrictions in funding have prevented BGS from preparing geochemical maps for either gold or its pathfinder elements such as arsenic and antimony. With supplementary support from the private sector, a highly successful program of re-analysis of stream sediment samples from large tracts of northern Scotland (for As, Au, Sb and other elements) by non-destructive INAA techniques is underway.

2.3 DATA MANAGEMENT TECHNIQUES

2.3.1 Introduction

The geochemical exploration programme instigated during this study is characterised by large, multivariate data sets. Plant and Moore (1979) noted that the preparation of a systematic geochemical database provides a fundamental requisite of regional exploration programmes.

The logistical problems of handling, manipulating and processing the large volume of data generated by this study presented numerous problems. IBM-PC database and spreadsheet packages such as dBASE and Lotus 1-2-3 had only recently been introduced to the UK at this time (1982-3) and were unavailable to the author. As such, this problem was resolved by the creation of a purpose built, relational data management system (RAW) written in Fortran 77 for use on the VAX 8600 mainframe computer.

2.3.2 The RAW Database Management System

Fundamental to the success of this project was the standardisation upon a flexible datafile structure. The RAW format defined by Harvey and Atken (1982 pers. com.) was deemed to be most appropriate, based upon the philosophy that each data set could be 'self-formatting' and carry its own detailed description which could be read by other programs (ie. title, number of variables, number of samples, variable names and data formats) in addition to the actual sample names and data values. Complete listings of the RAW system programs are presented in appendix seven. Once developed, the initial RAW program allowed the user to:

- 1) CREATE - This option allows the user to CREATE a RAW database file from data input via the keyboard.

Upon CREATION the DATABASE contains the following information:

TITLE - Title for the data and pages of REPORT output.

VARIABLES - A list of the user defined VARIABLE names.

M and N - The number of VARIABLES and SAMPLES/ROWS.

SAMPLE No's - A name for each RECORD of data in the file.

RECORDS - An array containing the numeric data input for each SAMPLE/ROW of the "M" VARIABLES.

This file may be edited from with RAW or by use of the screen editors.

2) **DELETE** - Any variable or sample record can be removed from the RAW datafile.

3) **APPEND** - This section allows the user to both read and append RAW formatted data files.

As in the **CREATE** routine, additional data **RECORDS** may be input, then added to an existing file. Output from this program is in the form of an incremented version of the original RAW filename. Extreme care is therefore required with system **PURGE** commands after any **APPEND**. The naming, number and order of the variables are defined previously by the RAW file which will be appended. The ability to modify the output file generated by this program, is incorporated within the RAW package, and may be accessed through the **EDIT** option.

4) **MERGE** - The **MERGE** option allows a number of similar RAW files to be linked together to form a larger **DATABASE** file. Two possible forms of **MERGE** may be undertaken:

- 1) Additional samples records may be added to existing variables.
- 2) Additional variables may be added to existing sample records.

Note that in each case, all variables (1) or samples (2) must exist in both files for this operation to succeed.

5) **EDIT** - This section allows the user to both read, manipulate and/or correct RAW formatted datafiles. Numerous options are available to allow data conversions and these fall into two main editing categories:

a) **SAMPLE ORIENTATED** : This editor allows individual sample records to be accessed and allows the modification of items from any specific file. Any number of selected samples/rows may be corrected in this way before returning to the main **EDIT** option and exiting. An added function of this program is the ability to delete individual records by their unique sample/row name. By the careful use of **CREATE**, **APPEND** and **EDIT** most, if not all data handling and manipulation operations may be carried out, on an interactive basis in a user friendly mode.

CORRECT : This option allows mistakes within one or more individual **SAMPLE RECORDS** to be corrected. Records are located by their respective **SAMPLE** numbers and any item of data relating to that sample may then be modified.

DELETE : This option has the ability to delete any or all **SAMPLE RECORDS** from a data file and **REINSTATE** any or all of the deleted records.

SELECTIVE DELETE : This function allows individual sample records to be deleted by **SAMPLE** name.

TOTAL DELETE : This function deletes all sample records within the datafile, thereby allowing a large number of individual records to be deleted by a single command. Individual sample records may be "undeleted" by the use of the **REINSTATE** command. Please note that sample records may not be **REINSTATED** once the user **EXIT**'s from the RAW program.

b) **VARIABLE ORIENTATED** : This editor allows data to be modified, created or deleted by **VARIABLE**. New names have to be **GENERATED**, and are placed at the end of the variable list. Variable data may then be **INSERTED** by direct input from the keyboard or produced by a **TRANSFORM** applied to one or more variables. Pre-existing variables may also be **TRANSFORMED** using the math options; **DELETED** from the datafile or **MOVED** to a different position.

INSERT : This option may be used to systematically insert new data into any given variable for all or a selected number of records. No discrimination is made between existing variables and those created within the EDIT section by the GENERATE command. In unforeseen circumstances, if it is necessary to EXIT before the INSERT operation is completed, type 999.999. The program will then provide you with the last completed record number which should be noted and input later in the SELECTIVE INSERT option to continue the INSERT from the last known position.

TRANSFORM : This program allows the user to mathematically convert one or more variables for each sample record in the datafile, by the use the mathematical commands: add (+); subtract (-); divide (/); multiply (*); \log^{10} (L); exponential (P); or none (N).

Examples:

VARIABLE 1 + VARIABLE 2	= VARIABLE 3 (addition)
VARIABLE 1 L	= VARIABLE 3 (log transform)
VARIABLE 1 N	= VARIABLE 3 (copy)

Variable names 1, 2 and 3 are requested individually. However, a CONSTANT can replace names 1 or 2 by typing / when prompted for either name 1 or 2.

6) **REPORT** - Analytical data contained in a RAW file may be output in a user defined, tabular format. Two styles of TABULATED REPORTS are provided by this option:

Style 1 - **SAMPLES** by **VARIABLES** (ie. Samples across and variables down).

Style 2 - **VARIABLES** by **SAMPLE/ROWS** (ie. Variables across and samples down).

The creation of the RAW program provided a powerful data management tool, which was fully utilised by this project. The natural development of the RAW program was its integration of with existing programs in both the department and university. To this end, interfaces were developed with the Computer Centre's PLOTLIB plotting package and a number internal geochemical mapping programs developed by Dr Bowes in the Applied Geology Department.

A major drawback in the speed of analysis of the geochemical data was the cumbersome manner in which relatively simple summary statistics were obtained using SPSS. Once generated (by 'batch' processing) the statistical data would have to be manually edited to create even the most simple summary tables. As such, it was decided to write an interactive statistical package which would not only interact directly with RAW datafiles, but also provide tabulated, 'report-ready' output. Statistical algorithms were obtained from Davis (1973) and other sources (see program listings for details) and used to develop the STA program. This program provided both standard univariate statistics (from a selection of min, max, mean, range, standard deviation, skewness, kurtosis, geometric mean and coefficient of variation) and correlation coefficients. When linked to a local daisywheel printer, report quality tables were then able to be rapidly generated with minimum user interaction. Following completion of the STA program, additional programs were written to assist the processing of the geochemical data, including:

- 1) **SOR** A series of sorting and file extraction utilities used directly with RAW files.
- 2) **SIF** A utility to input and edit a series of KEY's (ie. lithology, stratigraphy or Formation Codes). SIF may also be used to subdivide RAW files on the basis of the KEY value.
- 3) **HIS** This program may be used to create histograms cumulative frequency plots (or both superimposed) using three modes of operation:

- a) Manual histograms created for any element with a user defined range
 - b) Fully Automated histograms automatically created for each and every variable with the range of each defined by MIN and MAX values.
 - c) Preset histograms automatically created for each variable using pre-defined ranges, presented in a separate RAW file.
- 4) TRV This program automated the production of simple bar charts and may be applied to any variable for a user defined range. NB. the size of the diagram is controlled by the number of samples, as each sample within the RAW file is represented by a single line bar.

This collective group of programs is referred to as the RAW System (Duller, 1984). Although time consuming in development, this system and its interfaces to both plotting and mapping packages proved invaluable during the collection, collation, statistical and graphical assessment of the data presented in this thesis. The RAW system was incorporated into the Strathclyde University Computer Centre's library of utility programs in 1984 and provides a 'user-friendly' interface to their PLOTLIB plotting system. In 1986, the RAW System was evaluated and accepted by the GEOCHEM Group Ltd and now forms the kernel of their data processing system.

The recent development of 4GL database systems such as Oracle and advent of standard query languages (SQL) provides a level of sophistication, far in excess of that required by the general (geological) user. Small and highly variable data sets are generally required to be rapidly input, processed and transformed into report-ready tables, statistics and diagrams with a minimum of user interaction, prior to the interpretative phase of any study. In a commercial geological environment, high throughput and rapid turnaround form the prerequisites of any information processing system. The simple project orientated file structure provided by the RAW system, linked with the ability of the user to generate high quality, report-formatted output with minimal effort, provides the user with a powerful data management and analytical tool.

2.4 STATISTICAL TECHNIQUES

2.4.1 Introduction

Exploratory data analysis is an initial investigation of one or more data sets carried out with no explicit ideas on the patterns or structure within the data. It is designed to assist the detection of patterns within complex data sets, and aid generation of hypotheses about the underlying mechanisms. Ideally, it should be followed by confirmatory analysis, in which the proposed hypothesis can be tested using independent data collected in the same way but not used to formulate the original hypothesis. Exploratory data analysis techniques included ordering of data, identification of outliers, simple univariate statistics, t-, F- and χ^2 tests, correlation coefficients, principal component analysis, simple discriminant analysis, and k-Means clustering methodologies. Graphical techniques included the presentation of summary histograms and bar diagrams, cumulative frequency curves, point source and contoured geochemical maps, compositional envelopes, summary geochemical logs, crossplots, triangular plots, and spider diagrams.

2.4.2 Simple Statistics

The STA program (see chapter 2.3) is used to calculate the following univariate statistical parameters:

- 1) Minimum (the lowest value);
- 2) Maximum (the highest value);
- 3) Mean (the arithmetic average);
- 4) Range (the difference between maximum and minimum);
- 5) Standard Deviation (a measure of the distribution of analytical values with respect to the mean);
- 6) Skewness (a measure of the symmetry of the distribution compared to the normal population);
- 7) Kurtosis (a measure of the 'peakedness' of the distribution compared to a normal population);
- 8) Geometric Mean (the multiplicative average, for use with highly skewed data);
- 9) Coefficient of variability (A comparison of the degree of scatter between elements requires the use of a statistic that is independent of the magnitude of the variables concerned (Taylor et. al., 1984). The coefficient of variability (CV%) is one such parameter and expresses the residual variance as a percentage of the mean:

$$CV\% = \frac{\text{residual variance}}{\text{mean}} \times 100$$
- 10) Correlation Coefficients : To estimate the degree of interrelation between two variables the correlation coefficient (a dimensionless number ranging from +1 to -1) is calculated for each possible pair of variables.

These parameters are used to rapidly assess the nature and distribution of individual variables within each dataset, and in the case of correlation coefficients, to identify possible relationships with other individual variables. It should be noted that a correlation coefficient approaching +1 may be used to infer a direct relationship between the variables, whereas a correlation approaching -1 is indicative of an inverse relationship. Coefficients close to 0 indicate the lack of any linear relationship. The actual value of a correlation coefficient may be influenced by the number of samples, particularly in large datasets ($n > 50$). In order to evaluate the significance of individual coefficients, a 'critical value' (associated with a specific confidence level) is assigned to the correlation matrix. The 'critical value' is dependant up the sample population and the level of confidence required (ie. 90, 95 or 99%). Snedecor (1956) tabulated a series of critical values for the 0.05 and 0.01 confidence levels of correlation coefficients. Correlation coefficients were calculated following the procedures outlined by Davies (1973) in order to identify which major and trace elements displayed similar or opposing behavior.

Data evaluation using correlation coefficients may be partially distorted by the 'Closure Effect'. This may be explained in terms of the abundance and variability of the most significant element, normally silica (50-80%) coupled with the fact that the major element values always sum to 100%. These factors result in an apparent negative correlations between SiO_2 and all other oxides. This problem can be partly overcome by recalculating the major element analyses as a percentage of the 'non- SiO_2 ' fraction of the rock. Although this eliminates the problem of the dominance of SiO_2 , a similar, albeit smaller problem is then posed by the next most significant variable. An alternative approach to this problem would be the application of 'power transforms' as described by Howarth (1981) and Aitchison (1984). Examination of the results of alternative types of transform on the Glendinning data set revealed a considerable range of variation. As it appears that there is no simple solution to the examination of closed data sets, simple correlation coefficients calculated using the program STA (appendix 7.3) are presented in the context of this thesis. Ahrens (1957) demonstrated that the majority of minor elements show a lognormal distribution and that they are positively skewed. As such, all lithogeochemical data was subjected to χ^2 analysis to check whether they are normally or lognormally distributed.

2.4.3 Multivariate Statistics

Critical reviews of multivariate procedures in the analysis of geochemical data are presented by Miesch (1969), Closs and Nichol (1975) and Howarth (1984). Multivariate data analysis techniques, are applicable in many areas of geological and geochemical research, however they need to be used with considerable care and thought. These techniques enable large data sets may be summarised in such a way that inherent albeit cryptic patterns may be observed more clearly. Consequently, the aim of more detailed statistical analysis was to define any unknown or unexpected patterns within the individual datasets.

Principal Component Analysis

Principal components, the eigenvectors of a variance-covariance or a correlation matrix (Davis, 1973) provide a useful tool in the analysis of structure within a data matrix and are interpreted in a similar manner to factors. Full details of the calculation of principal component scores and loadings are provided by Davis (op. cit). In principal component analysis (PCA) the interelement covariance matrix for m elements is decomposed into an orthogonal (intercalated) set of new variables which are linear combinations of the original element values. The eigenvectors and related eigenvalues are extracted in such a way that the first eigenvector (which may be regarded as the coefficients of the first linear transform equation) accounts for as much as possible of the total variability of the data, the second for as much as possible of the residual variance, and so on (Howarth and Martin, 1979). Therefore, each successive component chosen contains as much as possible of the remaining information and is uncorrelated with all preceding components. In summary, principle component analysis is used to orthogonalize both major and minor element data in order to produce a new set of variables, that tend to be geological-process orientated, rather than chemical-response orientated (Garrett, 1983). As such, the interpretation of principal component loadings ('reification') of geochemical data can provide insights into relatively cryptic chemical associations present within differing mineralogical phases of the samples. An example of such a study is provided by Garrett (op. cit) in studies of lithogeochemical data from Canada.

Discriminant Analysis

Discriminant analysis is a multivariate statistical technique that involves the 'Formulation' of a decision rule which partitions the data into mutually exclusive groups, and the 'Application' of a decision rule to assign observations to the group to which they have greatest resemblance (Chork and Govett, 1985). A number of different methods of discriminant analysis including linear, piecewise and polynomial discriminant functions are reviewed by Howarth (1973) and Chork and Govett (1985). Discriminant function analysis assumes that the two populations (datasets) are different and computes a function (a factor for each element) which will best discriminate between the populations. After the computation of the function for each sample, the mean position of all the samples in each formation is calculated and the distance between the two mean positions (the Mahalanobis distance) then forms a measure of the discrimination (Davies, 1973). Using this method, several variables are combined into a single new variable which optimizes the distinction between two sample populations. A representative set of known samples (the training set) from each population is necessary to form the discriminant equation.

The role of discriminant analysis and its application to the analysis of geochemical data has been described by authors including Davis (1973) and Howarth (1983). Specific exploration related studies include: lithogeochemical surveys (Cameron et al., 1971; Govett, 1976.; Whitehead and Govett, 1974) the classification of gossans (Joyce and

Clema, 1974) and regional stream sediment surveys (Howarth, 1971). In addition, studies by Rose (1979) combined geochemical, geophysical and geological data to classify different areas according to their exploration potential. In general terms, discriminant analysis is a multivariate statistical technique in which the variables are combined in such a way as to maximise the difference among a number of previously defined groups. In geochemistry, a two-group classification (eg. mineralized vs. barren) is the most common case. A discriminant function computed for these groups, known as 'training' sets, can be used to classify unknown samples.

Cluster Analysis

In pattern classification of geochemical data it is commonly required to group without prior knowledge, a set of multi-element data into clusters that are geologically meaningful (Chork and Govett, 1985). The procedures followed to accomplish these aims are known as cluster analysis (Davis, 1973) and have been discussed in detail by Parks (1966), Gower (1967) and Howarth (1973).

Factor Analysis

Factor analysis is a statistical technique applicable to the analysis of large data matrices. Factoring methods attempt to resolve the interrelation of multivariate geochemical data, in terms of much simpler relationships. However, factor analysis forms one of the most controversial methods of multivariate analysis of geochemical data (Blackith and Reyment, 1971) and as such, is deemed outwith the scope of this current study.

2.5 GRAPHICAL TECHNIQUES

In this study every attempt was made, where possible, to display the geochemical data spatially. The treatment of such large data sets containing multiple components for each sample, required the extensive use of automated cartographic procedures. The following presentation styles were selected in order to display and interpret various types of geochemical data:

- 1) X-Y Crossplots: This format is used to display simple inter-relationships between both individual elements and ratios, and is used to erect simple discriminant diagrams. Scatterplots provide an effective technique for demonstrating trends and relationships between pairs of variables. The relationships may be quantified by regression or correlation techniques. However, a problem arises with this form of data evaluation in that only pairs of variables are correlated and any trends involving several variables (eg. the association of As, Sb, Na, Ca, K and Fe during hydrothermal alteration) are not readily recognised. As such, principal component analysis (PCA) was used in order to identify inter-relationships between all variables within a dataset.
- 2) X-Sample Traverses: It is difficult to compare differing multi-element data sets whilst retaining the individual contributions of each sample. To this end the geochemical traverses (foldout 1-7) were prepared in order to aid visual assessment and correlation. This format is used to display the results of successive sampling (ie. boreholes or traverses) in order to highlight systematic trends and variations within individual datasets.
- 3) X-Y-Z Triangular Diagrams: This format is used to present three component data, such as the Fe-As-S compositions of arsenopyrite and provide a further discrimination diagram.

- 4) **REE diagrams:** This format is used to present chondrite normalised data for a number of rare earth elements. Normalised REE analyses for each sample are joined by a line and the relative shape of individual sample lines are compared with known standards.
- 5) **X-Y-Z Crossplots:** This format is similar to the X-Y cross plot however the size of individual symbols is controlled by the value of Z. This format is also used to generate geochemical base maps by providing the grid reference of each sample site in the form of an easting (x) and northing (y) followed by the element concentration (z). Symbol size may be directly related to concentration or controlled by a series of arbitrarily established ranges. Rose et. al. (1979) noted that computer-generated maps may be used in large multi-element surveys to present individual elemental concentrations and via a process of contouring to establish broader trends and patterns within the data.
- 6) **Histograms and Bar Charts:** This format is used to present the results of univariate and frequency statistics and provide a simple graphical summary of data distribution.
- 7) **Grey-Scale Maps:** This format is applied to closely sampled geochemical data (ie. soil or microprobe grid data) and provides a contoured, shaded area summary map. Element concentration is represented by an increasing scale of grey shading .

As automated contouring of geochemical data plays a major role in this study it is important that the fundamentals of contouring, as discussed by Walden (1972) are fully understood. The first stage in any contouring exercise was to superimpose a fine rectangular grid over the area to be mapped and interpolate element values at each grid intersection (node) from the raw sample data. A second interpolation procedure is then used to connect all points of equal value (using the grid node values rather than the raw data). It should however, be noted that a number of factors affect both gridding procedures and the resulting contour maps:

- 1) fewer samples are required to estimate a smooth surface, than are needed to estimate a complex one;
- 2) random sample distributions form the most satisfactory arrangement for general purpose studies, however concentrated sampling in areas where the greatest changes of gradient occur would generate a more accurate estimate of the true surface than purely random samples;
- 3) the smoothness of individual contour lines is directly proportional to the size (or 'fineness') of the primary grid;
- 4) increases in the sample population have a positive influence in the estimation of the surface, increasing the reliability of the entire map;
- 5) surface correlation decreases slightly with increased grid size.

In conclusion, graphical techniques applied within this study include summary histograms and bar diagrams, cumulative frequency curves, point source and contoured geochemical maps, compositional envelopes, summary geochemical traverses (or logs), crossplots, triangular plots, and spider diagrams.

CHAPTER THREE

GEOLOGICAL, GEOCHEMICAL AND MINERALOGICAL STUDIES OF THE GLENDINNING As-Sb-Au DEPOSIT, SOUTHERN SCOTLAND

3.1 INTRODUCTION

The greywacke-shale sequences of the Southern Uplands of Scotland has been known as a gold province for many centuries. In the Leadhills area alone it has been estimated that prior to 1876 over 25,000 oz of alluvial gold valued at over £10 million had been extracted by the exploitation of river gravels. No matter how successful these alluvial deposits proved to be, the possible existence of gold veins in the Southern Uplands has preoccupied entrepreneurs over the last four hundred years. Recently gold has been detected by panning in over 100 streams draining the Silurian and Ordovician rocks of the Southern Uplands (Dawson et al., 1979). However, the presence of gold had not been confirmed in situ, prior to a series of mineral reconnaissance studies by the British Geological Survey. The first in-situ gold record in Southern Scotland was made by Leake et al., (1980) who located a series of gold bearing arsenopyrite quartz veins within the contact margin of the Loch Doon granite (Fig 2b).

The field characteristics of turbidite hosted gold mineralization in the Glendinning area of the Southern Uplands of Scotland was studied in detail as part of the original research proposal. The mineralogical and geochemical setting of stratabound arsenopyrite mineralization at Glendinning is detailed together with the nature and genesis of As-Sb-Au mineralization in the region. Furthermore, the validity of a sedimentary model for this deposit proposed by Gallagher et al., (1983) is tested. The stratabound appearance of the mineralization and the occurrence of intraformational breccias or debris flows is re-interpreted. An alternative genetic model indicates that sediments present in the Glendinning area do not contain evidence of exhalative input. The As-Sb-Au enrichments are associated with late Caledonian hydrothermal fluids which migrated along and through the fracture and breccia zones identified in this deposit and resulted in extensive wallrock alteration and the formation of the disseminated and vein mineralization. These conclusions are discussed in the next chapter, where comparison is made between the Glendinning As-Sb-Au hydrothermal system, similar deposits in the Southern Uplands and Longford Down, active hydrothermal systems and historical examples reported from the literature.

3.2 REGIONAL SETTING

The disused Louisa Mine at Glendinning occurs 13km NNW of Langholm [NY 3313 5967] in the southeastern part of the Southern Uplands (Fig 79 and 85). It is an isolated NNE trending vein deposit, crosscutting Llandoverly greywackes, remote from other mining district districts in Scotland, unrelated to major faulting and distant from any contemporaneous volcanicity or igneous intrusion (Gallagher et al., op.cit).

The Silurian hostrocks at Glendinning form part of a systematic sequence of stratigraphically distinct, steeply dipping greywacke-shale units trending NE-SW across the Southern Uplands. Bedding is steeply inclined, dipping SE and younging both NW and SE as a result of tight folding, with hinge zones plunging steeply WSW, superimposed upon sub-horizontally hinged folds (Gallagher, 1981).

The location of the Glendinning deposit in relation to the Southern Uplands and Scotland is presented in Fig. 7a, while the position of the Glendinning study area is presented in Fig. 18.

3.3 GEOLOGICAL ENVIRONMENT

3.2.1 Stratigraphy

Lapworth and Wilson (1871) defined the Hawick Group as consisting of 'very arenaceous grey and purple sandstones and schists'. In detail, this division consists of dominantly flaggy greywackes with interbedded siltstones and grey-green and red mudstones. Over 50% of the succession is represented by dark bluish-grey greywackes with a grain size varying from medium (0.25-1.0mm) to fine (<0.25mm) grained (Warren, 1964). Many greywacke-siltstone beds display both laminated and small-scale current bedding, load, flute, prod and other penecontemporaneous structures (plate 28).

Oliver (1988) in summarising the results of recent systematic studies of regional metamorphism within the Paratectonic Caledonides of the British Isles, attributed tectonic burial within an accretionary prism as the dominant mechanism of metamorphism within the Southern Uplands and Longford Down. The Glendinning sediments have been affected zeolite facies metamorphism leading to the generation of prehnite and pumpellyite from the minor basic volcanic clasts within the greywackes.

3.2.2 Structure

Intense folding and cleavage in the Hawick rocks, first recognised by Lapworth (1874) and Peach and Horne (1899), has been the subject of intense study (Craig and Walton, 1959; Rust, 1963, 1965; Weir, 1968, 1969, 1979; Treagus, 1972; Stringer, 1975; Stringer and Treagus, 1980, 1981; Webb, 1983; and Barnes et al., 1986, 1988). Warren (1964) presented a detailed description of the stratigraphy and structure of the Silurian (Wenlock) rocks south of Hawick. A series of major faults trending 015°-195° was interpreted on field evidence to represent a set of sinistral wrench-faults. A subordinate series of dextral and second-order sinistral wrenches were also defined, trending 120°-300° and 170°-350°. Williams (1945) demonstrated that the wrench component of these faults is pre-Devonian whereas later normal faulting is of post-Caledonian age.

Geological relationships observed at exposures indicate that the As-Sb-Au mineralization is structurally controlled. The Glendinning deposit may be viewed as a series of intersecting high-angle faults and breccia zones that acted as the principal channelways for the ore-forming solutions. Numerous steeply-dipping normal faults cut and offset altered and mineralized wallrock. In the smaller fractures the fault gouge is clay-rich (dickite). Breccia veins exhibit a close spatial relationship with the larger quartz veins and appear in borehole section to have been fed directly by them. The mineralized faults form laterally persistent features, consisting of wide areas of extensive brecciation, containing variable quantities of quartz and sulphides in highly altered greywacke. This area is also characterised by a strong component of brittle deformation in the form of intense fracturing and small scale faulting.

The Glendinning deposit lies structurally within a high angle, NNE trending, sinistral strike-slip fault zone. This pattern of high angle, sinistral faulting was first described in this area by Warren (1964) and discussed more recently by Kemp (1985). Prominent N 015° trending fractures provide the major structural controls upon the principal geophysical and geochemical anomalies defined by Gallagher et al., (1981). Although Gallagher et al., (1983) noted that “no significant structural control was apparent”, it is tentatively suggested that this ‘Glendinning trend’ forms a southerly extension to a major regional fault structure, trending N 010° and termed the Southern Uplands Shatter Belt (Fig.4b).

This Shatter Belt was first identified by Peach and Horne (1889) and may be traced over 30km from its intersection with the Southern Uplands Fault to 8km east of Meggat, where it intersects the Leadhills line. The orientation of this major linear breccia zone has previously been interpreted as converging with the Leadhills strike-fault zone and thereby altering its trend to NE-SW. Although outcrop is sparse, this belt is represented by a 500-1000m wide zone of brecciated, weathered/altered greywackes and mudstones. A detailed southerly extrapolation of this Belt using 1:50,000 scale ordnance and geological survey maps, delineates a feature which passes within 1km of the Glendinning deposit. It is tentatively suggested that the southerly extension of the Shatter Belt may be of importance in providing both structural and genetic controls upon the Glendinning deposit. To date, little if any metallogenic significance has been placed upon this lineament and to the authors knowledge this zone has not been subjected to detailed exploration activity.

3.3.3 Greywacke Sedimentology

The Southern Uplands of Scotland are underlain by a series of petrographically distinct, steeply inclined turbidite units, separated by major strike faults. The sediments present in the Glendinning area represent a series of turbidity current deposits, consisting of a fining upwards sequence of thinly bedded greywacke sandstones, the Bouma B/C units, together with interbedded mudstones, the Bouma E unit (Plate 27). They exhibit a wide range of sedimentary structures including graded bedding, load, flute and groove casts, as well as flame and other dewatering structures (Plate 28). The proposed environment of deposition of the sediments in this study area is that of a mid to lower turbidite fan (Walker, 1979). Because of the interbedded nature and differing depositional mechanisms it was decided to sample both greywacke sandstones (the B/C unit) and mudstones (the E unit) at each site, whenever possible.

Glendinning Breccias

The Glendinning deposit is proposed by Gallagher et al., (1981,1983) to represent a synsedimentary sulphide accumulation deposited within a proximal/mid fan environment, later overprinted by a succession of vein mineralization. Clemmy (1979) in a discussion of discrimination between ‘sedimentary’ and ‘tectonic’ structures in ore deposits noted that correct identification is critical to the genetic model of the deposit and hence exploration philosophy. As such, it is necessary to review this interpretation in considerable detail.

A debris flow is defined by Carter (1975) as a slurry-flow transport mechanism (or the deposits of such a flow) in which appreciable numbers of suspended clasts are present in the slurry. Stow (1984) provided a succinct definition of a debris flow as “a highly concentrated, highly viscous, sediment-fluid dispersion that moves downslope under the influence of gravity”. Most debris flow are composed of clasts carried in a watery mud matrix and supported by a combination of clast buoyancy and matrix yield strength (Johnson, 1970; Hampton, 1972). Submarine debris-

flow deposits have been described from many ancient flysch successions, including those of the northern Apennines where they are commonly called olistostromes (Abbate et al., 1970) and, more rarely from the modern deep sea (Embley, 1976; Moore et al., 1976; Flooe et al., 1979). Submarine debris flows are commonly considered as part of a continuum between slumping and turbidity currents (Rupke, 1978) and may be a very important process of resedimentation in the deep sea (Hampton, 1972).

Studies by Stow (1984) revealed the logarithmic nature of the relationship between bed thickness and maximum clast size in debris flows. This relationship can be used to predict the approximate maximum clast size expected from the intraformational breccias at Glendinning, assuming a debris flow model for deposition. On the above evidence, the estimated maximum clast size of 30-40cm is however ten times that identified in the Glendinning breccias and as such casts doubt upon the validity of the BGS interpretation. On the basis of this study the BGS model is disputed and an alternative explanation of the textures described by Gallagher et al., (op.cit) is proposed, based upon comparisons with similar deposits in Scotland, Ireland and Canada, namely that:

- 1) The inter-formational breccia units at Glendinning represent part of a continuing spectrum of the vein breccias described by Gallagher (op.cit) and were formed by intense hydraulic brecciation of wallrock. This brecciation event forms the earliest manifestation of mineralization and alteration in the Glendinning deposit. It should be noted however, that brecciation was polycyclic and continued throughout the life cycle of the hydrothermal system.
- 2) The major spatial control placed upon the occurrence of disseminated arsenopyrite is the distribution of synsedimentary pyrite/magnetite which provided localised areas of reduction and a loci for arsenopyrite precipitation within the greywacke unit. In many instances arsenopyrite nucleation sites now mirror the original bedded nature of the pyrite, however the apparently bedded arsenopyrite occurs only in close proximity to the vein mineralization (<15 m) and as such in the authors view, had previously been mistakenly interpreted as primary synsedimentary mineralization.

A summary of the characteristic features of both hydraulic and sedimentary breccias in comparison with those displayed in the Glendinning Deposit is presented in table 1.66. From this study it is concluded that a debris flow model is incompatible with the structural, geochemical and petrographic evidence and it is proposed that the small variety of breccias located within the Glendinning deposit represent part of a continuum of hydraulic fracturing and intense hydraulic brecciation. The similarities between some tectonic and sedimentary structures are well known (Cosgrove, 1979). However, on the evidence presented above, the inter-formational breccias of Gallagher et al., (1983) can be confidently described as tectonic, fault-related structures.

3.4 SUMMARY OF PREVIOUS INVESTIGATIONS

3.4.1 Mining History

A detailed review of the mining history of the Louisa Mine at Glendinning is presented in chapter 1.4.2. In addition to the documented mine history it should be noted that recent investigation by the author revealed the existence of a second subsidiary adit, branching eastwards from but aligned parallel to, the High Level Forehead (Fig.85) approximately 14m from the adit entrance. This secondary adit extends for a length of approximately 12m, indicating the possible position of a second, structurally controlled ore zone. In addition, the remnants of another

small trial adit were identified by this study, immediately north of the Powder Hut, displayed on a detailed plan of the Glendinning mine area (Fig. 86).

3.4.2 Recent Studies

Prior to the late 1970's little previous geological work had been carried out in this study area. In 1979 this deposit was investigated by the British Geological Survey as part of its Mineral Reconnaissance Programme in Scotland. Studies by Gallagher et al., (op.cit) revealed that the Silurian greywackes of the Glendinning area contain As, Sb, Hg Cu, Pb and Zn drainage anomalies which extend up to 5km NE of the deposit. This work has recently been extended by both Riofinex (Hazleton per.com) and European Gold Exploration, up to 10km from the Glendinning deposit. Based upon the location of these highly anomalous metal values (Sb > 20ppm) and the value of antimony itself, a detailed investigation of the mine area was undertaken. As exposure was extremely poor in the mine area, soil sampling and geophysics formed the major exploration techniques. These initial studies yielded coincident VLF-EM and As/Sb soil anomalies (defined by the 40ppm Sb contour) trending N 015° to N-S within both the area of known extraction and in an adjacent zone where little or no evidence of earlier workings existed (Fig. 84 and 87). A detailed plan of the Louisa Mine area is presented in Fig. 86 which defines the position of BGS traverse lines and boreholes in the Louisa Mine area.

On the basis of these studies four shallow boreholes were drilled in 1980 (Fig. 86) which intersected stratabound mineralization including a 'stratiform' pyrite-arsenopyrite assemblage (in which the sulphides are frequently concentrated into individual bands parallel to original bedding) exhibiting drillcore intersections of 0.7% As over 12m and a series of reported 'intraformational' breccia units in close proximity to the vein stibnite deposit. Gallagher et al., (op.cit) proposed that the deposit was formed by a synsedimentary mineralizing event and interpreted the intraformational breccias to have formed by the penecontemporaneous fragmentation and redeposition of sulphide sediment and sulphide mud within a sedimentary debris flow in a mid or lower fan environment, where euxinic conditions periodically developed. After an initial study of the available drillcore, hand specimens and thin sections it became obvious to the author that the interpretation was not as straightforward as proposed by the original BGS study.

This chapter presents a considerable wealth of evidence in support of an alternative, much simpler model for Glendinning mineralization than that proposed by BGS, invoking intense hydraulic brecciation and pervasive wallrock alteration processes to account for all observed features of the deposit.

3.4.3 Scope and Objectives of this Study

This chapter documents the mineralogical and geochemical characteristics of both vein mineralization and wallrock alteration at Glendinning and critically reviews the possible genetic models for the formation this deposit. This deposit had not been studied to any extent, prior to investigation by the British Geological Survey during 1979-80 (Gallagher et al., 1981). The principal objective of this study was to examine the mineralogical and lithogeochemical characteristics of the As-Sb-Au mineralization at Glendinning and compare and contrast these results with the other deposits in the Southern Uplands and Longford Down. In the current study, geochemical surveys in the Glendinning area were undertaken to provide:

- 1) Evidence of existing mineralization and wallrock alteration profiles.
- 2) Controlled sampling in areas of potential mineralization.
- 3) Regional assessment of fundamental geochemical variation in composition.

The results of a number of analytical techniques including petrography, ore microscopy, XRD, XRF, ICP, SEM, fluid inclusion and sulphur isotopes are integrated to provide a detailed evaluation of this deposit. Mineralogical and geochemical correlation between wallrock alteration and sulphide mineral assemblages are documented. Features such as veins, zoning, pervasive alteration patterns were quantified on a local scale. These studies are also used to characterise the products of hydrothermal alteration and assist the interpretation of the geochemical data. In this study the wallrock geochemistry, alteration mineralogy, ore textures and sulphide geochemistry were examined with particular emphasis placed upon arsenic chemistry and mineralisation. As a result, this study has identified the presence of arsenopyrite hosted gold mineralization dominantly concentrated within the wallrocks to the stibnite-quartz vein system.

At the onset of this study, the size and nature of geochemical dispersions at Glendinning were unknown, and there was a possibility that they could extend beyond the area of BGS investigations identified by Gallagher et al., (op. cit). One of the major drawbacks of the B.G.S. reconnaissance in this area was the actual limitation of area investigation. One aspect of this project was to evaluate the potential for a strike extension to the known mineralization and establish the role of the Glendinning deposit in Scottish metallogenic models. An orientation survey was carried out over the known mineralization at Glendinning, to establish the nature of geochemical dispersion, and define the appropriate sampling and interpretational procedures required to evaluate possible strike extensions within the regional study area. The results of this orientation were then compared and contrasted with variations in background geochemical data obtained from a detailed lithogeochemical survey of over 200 sq km of Upper Silurian strata, centred upon the Glendinning deposit. This survey resulted in the location of previously unrecorded As-Sb-Au mineralization in this area and defined broad scale metallogenic correlation patterns in this region.

Sampling

The Glendinning area consists of high moorland with a thin peat and residual soil cover (Plate 26). Although valleys contain substantial thicknesses of boulder clay, exposure is not as poor as one would first expect. Stream sections and various sized quarries provided suitable sites for sampling, but by far the most useful exposures in this area were the numerous, recently excavated roadways created by various forestry groups. Many of these road provided virtually complete exposure of cross-strike sections and were sampled in detail (Plate 27). The general sampling philosophy followed was to collect from a series of 10km long traverses spaced 1500m apart, at 150m intervals across strike. Due to the paucity of outcrop in some areas, all major exposures in the survey area were also sampled. Because of the interbedded nature and differing depositional mechanisms of the interbedded sediments it was decided to sample both the greywacke sandstone of the bouma B/C horizon and the mudstones of the D/E horizon at each site, whenever possible.

It was demonstrated by Govett and Nichol (1979) that the application and success of lithogeochemistry, forms a function directly related to the availability of adequate samples, from bedrock exposure and/or drill core. The recent expansion of forestation and the accompanying development of extensive roadways, crosscutting large areas of Scottish moorland, now enables such a study now be undertaken. The object of the regional sampling program in

the Glendinning area was to sample at regular interval throughout the entire stratigraphic thickness. At each site fresh, unveined chip samples were collected across both complete greywacke and mudstone units in order to:

- 1) Remove any chemical bias which might otherwise be created due to grain size variations close to either the top or the base of the greywacke unit.
- 2) Facilitate the study of element partitioning within the two differing sedimentological environments of each unit and any subsequent geochemical alteration. Approximately 4kg of greywacke and 1kg of mudstone rock chips were collected from each sample location to provide a representative sample of the outcropping units.

The main objectives in undertaking the Glendinning study were to detect and quantify the anomalous geochemical patterns related to mineralization within the deposit (ie. the nature, shape and extent of trace element dispersion and alteration in the vein wallrock) in order to recognise similar anomalies superimposed upon background values elsewhere in this region. To collect representative samples from each location, each turbidite unit was chip sampled. Extreme care was taken during sampling to collect only those chips representative of un-weathered and un-veined bedrock. Following crushing and grinding of these samples, the resulting powders were analysed by automated XRF for 31 elements at the University of Nottingham. The mineralized drillcores from Glendinning were also re-analysed using the same technique and standards to that of the regional samples in order to provide comparable multi-element data for the target mineralization and place some constraints on the nature and source of the mineralizing fluids in this environment. The distribution and variation of between 29 and 52 elements were examined in 170 mineralized samples selected from four boreholes and compared with unmineralized greywacke (n=305) and mudstone (n=195) samples collected from an area of 200 sq km surrounding the mine. However, an assessment of the geochemical dispersion within the Louisa Mine was not possible due to the unstable nature of the historical underground workings and restricted access caused by roof collapse. Following multi-element XRF and ICP analysis the resulting geochemical database was used to:

- 1) Model the geochemical environment('s) within the Southern Uplands.
- 2) Test hypothesis relating to mineralization
- 3) Explore for and assess the strike extension of the Glendinning deposit in areas previously regarded as barren.

A sampling program was devised to obtain representative suites of samples from both mineralized, potentially mineralized and barren regions. Samples of stibnite dominant mineralisation were obtained from the sorting floors adjacent to the main adit and arsenopyrite dominant samples were obtained from the BGS drillcore. The mineralogy of the Glendinning deposit was studied in hand specimen, and both thin and polished section. Both reflected light and transmitted light studies were undertaken to evaluate the nature and inter-relationship of sulphide mineralization and hydrothermal alteration in this deposit. Transmitted light studies of Glendinning core samples were initiated in order to study the effects of ore-forming hydrothermal solutions, whereas ore microscopy and microchemical studies were carried out in order to determine the mineralogical sites and distribution of the known ore-forming elements. Clay mineral assemblages were identified by detailed X-ray diffraction techniques, whereas sulphide composition data was obtained by electron-probe microanalysis. The extensive analyses of individual arsenopyrite crystals were undertaken following the recognition of their auriferous potential. An integrated approach to the problem of data analysis was undertaken. In an initial evaluation of the Glendinning datasets, numerous techniques were used to discern the variations in element concentration related to hydrothermal

alteration and mineralization (see Chapter 2). The geochemical analyses were then assessed in terms of the mineralogical study of the vein and wallrock assemblages, in order to provide evidence for, and fundamental controls upon the variability and characteristics of greywacke provenance.; chemical nature of the As-Sb ore forming fluids; and mineralogical controls upon element mobility during hydrothermal alteration and sulphide deposition. The result of these investigations are documented in the following sections of chapter three.

3.5 MINERALOGY

The main aim of this section is to describe the nature of both vein and disseminated sulphide and silicate mineralogy in the Glendinning deposit, within the context of the textural development of this deposit. Samples obtained from borehole cores have been used, whenever possible to provide a suite of fresh, unweathered material from which the effects of hydrothermal alteration may be characterised. In most instances the identity of the ore minerals was determined using reflected light microscopy. Supplementary evidence was provided by stained and polished thin sections and X-ray diffraction (Figs. 105-110). Where subject to supergene alteration in the near surface environment the primary sulphide minerals are commonly altered to 'secondary' phases, as demonstrated in the upper 3-8m of the BGS boreholes.

3.5.1 Ore Microscopy

Ore minerals, with the exception of arsenopyrite and pyrite (which are most abundant in the wallrocks to vein mineralisation and breccia zones) are confined to fractures and immediate marginal areas (2-5mm in width) associated with stibnite-bearing quartz veins. These prominent quartz-stibnite veins appear confined to the areas of strongest hydrothermal alteration and are observed to cross cut zones of earlier brecciation. The dominant vein mineralogy consists of intergrown coarse-grained aggregates of stibnite-rich and sphalerite-rich ore in a matrix of quartz and ankerite. At the vein margins, stibnite may be observed to form individual or clusters of acicular crystals. The polymetallic vein assemblages comprise of quartz, stibnite, dolomite, calcite, baryte, dickite, pyrite, arsenopyrite, galena, sphalerite, semseyite, bourmonite, chalcopyrite, tetrahedrite and tennantite (Gallagher et al., 1983). The detailed textural and mineralogical relationships identified within this deposit are outlined in the following section. In general, disseminated, irregular shaped aggregates and framboidal masses of pyrite occur sporadically throughout unmineralized greywacke units. Pyrite, stibnite and sphalerite form the dominant sulphides visible in hand specimens of vein material. Scarce chalcopyrite, galena and arsenopyrite may also be identified within mineralized quartz-carbonate veins, whereas disseminated, minute, well developed arsenopyrite needles (<1mm long) may be identified in bleached, altered greywacke lithologies. Two distinctive ore assemblages occur in separate settings within the Glendinning deposit. In the Clontibret deposit, virtually identical assemblages are inferred to represent two phases of deposition within a single mineralizing cycle (Steed, 1982). The component phases of the Glendinning mineralization are discussed below:

Arsenopyrite (FeAsS)

The commonest sulphide mineral in polished section is arsenopyrite which generally forms near euhedral, arrowhead to needle shaped crystals. These prismatic, crystals display a 'needle-like' habit with length/width ratios up to 10:1. Fine grained arsenopyrite crystals are ubiquitous in wallrock samples from the Glendinning mine dumps and readily identified by their physical characteristics and tin-white color in hand

specimen. The high reflectivity, rhombic habit and strong anisotropy (strong blue-green to brownish-yellow) formed diagnostic features in polished section. In the disseminated, wallrock hosted mineralization, arsenopyrite forms by far the most dominant sulphide species (~80% of total opaques) followed by subordinate pyrite and remnants of magnetite grains. The breccia hosted mineralisation is also dominated by disseminated arsenopyrite which commonly tends to concentrate around the silicified rims of breccia fragments, and is inferred to represent an extremely early phase of ore formation in the Glendinning deposit. Arsenopyrite veinlets are subordinate to disseminations and are typically 1-2mm in width and a few cm in length. Veinlets occur commonly as penetrations into breccia fragments that terminate at fracture margins and are ubiquitous throughout the wallrocks to the mineralized zones. Although extensive arsenopyritisation occurs at fracture margins, the growth of notably coarser, individual arsenopyrite crystals is observed within siltstone and greywacke sandstones distal from the fractures.

Although individual crystals exhibit evidence of moderate post-depositional deformation and brittle micro-fracturing, no evidence for dissolution, alteration or replacement was located. The euhedral nature of arsenopyrite crystals within both breccia and wallrock hosted samples serve to illustrate the resilient nature of arsenopyrite and absence of interaction with later fluid phases. Stylolitic, corroded crystal margins, as described by Muff (1978) were not identified in any of the deposits studied in the Southern Uplands or Longford Down.

Arsenopyrite concentrations at Glendinning are observed in some instances to form a pseudo-lamination following and controlled by both grain size and the occurrence of detrital/syndiagenetic pyrite and magnetite accumulations. However, the arsenopyrite crystals are observed as randomly orientated overgrowths upon pre-existing bedding parallel sulphides with crystals projecting radially into overlying and underlying microlaminii. This feature provides further evidence of post-sedimentation mineralization as opposed to the deposition of fine grained crystals in the form of a sulphide mud.

Arsenopyrite is predominantly located within wallrocks to the quartz-stibnite vein mineralization, displaying a chemical correlation with elevated gold values and forming the mineralogical loci of gold deposition. The fine grain size of the arsenopyrite mineralization may be used to infer that the crystals were deposited rapidly, essentially as a single event indicating that the mineralizing fluids were active for a relatively restricted period concomitant with breccia formation. The presence of arsenopyrite early in the history of this deposit may be used to suggest a period of relatively high initial temperatures which were short-lived due to rapid cooling. The widespread nature of arsenopyrite mineralization, hosted by fracture and breccia systems supports a hydrothermal origin related to large scale tectonic and igneous processes, rather than a sedimentary genesis.

Pyrite (FeS₂)

Tiny crystals of euhedral and anhedral pyrite are found disseminated throughout a major part of the Glendinning drillcore. Pyrite is one of the most abundant sulphide phases and may occur in association with other sulphides, alone in barren quartz veins or disseminated in bedding-parallel 'stratiform' zones. Pyrite was readily identified by its physical properties in hand specimen. In reflected light microscopy it was recognised by its color, polishing hardness and idiomorphic habit. Textural evidence may be used to infer the existence of four major types of pyrite in the Glendinning deposit:

- 1) Detrital pyrite (small, rounded pyrite crystals, transported into the depositional environment).
- 2) Synsedimentary pyrite (rounded blebs or mosaic-like framboidal aggregates formed within the depositional environment and represent the most common form of iron sulphide in sedimentary rocks (Ostwald and England, 1977; Taylor, 1982)).
- 3) Authigenic pyrite (recrystallised anhedral pyrite grains formed post-deposition, commonly displaying growth zones)
- 4) Quartz-stibnite vein-hosted pyrite (present as skeletal, granular and euhedral forms, and also observed as inclusions in sphalerite, stibnite and galena).

Using SEM techniques, pyrite was observed to passively replace small, anhedral detrital grains of magnetite (by a highly intensive phase of sulphidation) with brecciation observed to accelerate the process. The resulting metablastic texture is displayed in plate 10. Kelling (1961) noted the presence of both euhedral and framboidal forms of pyrite in Ordovician greyackes from the Southern Uplands which were interpreted to represent low grade metamorphic recrystallisation and late-diagenetic effects, respectfully. Anhedral pyrite grains are generally found in association with, and form a nucleation site for disseminated, wallrock hosted arsenopyrite. In opposition to pyrite, the arsenopyrite crystals display homogenous internal structures and lack any form of optical internal zonation.

Nair and Ray (1977) noted the following syndepositional features in pyrite rich orebodies: layering (thin alternating layers of pyrite and pyritic shale); scour and fill structures (crosscutting longitudinal sections of layered pyrite); flame structures (exhibited by the disruption and 'pulling out' of pyrite layers); and intraformational breccias (fragments of pyrite rich sediments incorporated into overlying sediment horizons). In addition, the following diagenetic features were also observed in pyrite: load folds (resulting from differential compaction during diagenesis), warping around scattered clasts, microfaulting of layered pyrite (giving rise to displacements up to 5mm); matrix filled fractures within intraclasts; and diagenetic flowage of pyrite and shale layers. It should be noted that few if any of these textures has been recognised in this deposit, providing further evidence in favour of their epigenetic origin.

Stibnite (Sb_2S_3)

Examples of stibnite-quartz vein material located on the sorting floor contain fragments of brecciated siltstone and sandstone which display a range of wallrock alteration effects ('bleaching') and contain sub-angular quartz grains in a matrix of sericite, muscovite, carbonate, disseminated pyrite and arsenopyrite. Stibnite crystals occur in acicular, bladed and prismatic habits and form massive clusters, crustified veins, thin fracture fills and films. In polished section, stibnite is readily recognised by its strong reflection pleochroism and anisotropy. In general, stibnite and quartz are intergrown and display overlapping periods of crystallization. Three distinct textural types of stibnite can be distinguished in polished section, closely associated with and replaced by ankerite:

- 1) Coarsely crystalline stibnite, which occurs in small veins and fracture infills in the form an intergrown mass of large, elongate crystals (up to 2cm in length) exhibiting both simple and complex twinning. Coarse grained crystals exhibit complex pressure lamellae (slightly offset portions of grains that exhibit undulatory extinction or slightly different extinction positions) formed in response to deformation processes.
- 2) Cementing material in brecciated wallrock, with similar characteristics to (1).

- 3) Finely crystalline stibnite, exhibiting equidimensional grains, 120° triple junctions, and granoblastic textures (see plate 8).

Oxidation of the sulphide ores on the sorting floors of the mine area resulted in the development of a small suite of secondary metal oxides. This assemblage is dominated by stibiconite, forming a fine grained boxwork-like texture, penetrating stibnite along grain boundaries and fractures. Oxidation products of stibnite, identified by XRD studies include stibiconite, cervantite and kermesite.

The absence of berthierite in the stibnite phase of mineralization may be used to suggest an excess of Fe over Sb in the mineralizing fluid. The late-stage formation of stibnite may correspond to an increase in sulphur activity, or more likely, a simple decrease in temperature. It is inferred that sulphur saturation of ore fluids was present throughout all phases of As-Sb-Au mineralization. (NB. A useful field test to identify stibnite is its ability to be melted within a match flame).

Sphalerite (ZnS)

Sphalerite, the most common ore mineral located on the Glendinning sorting floors, was readily identified by its physical properties (hardness, color and lustre). It is particularly notable for its wide range of color (grey, gold and brown). Coarse- to medium grained intergrowths of sphalerite, galena and stibnite are distributed in a coarsely crystalline gangue of euhedral quartz and calcite together with minor dickite. Sphalerite is an important, but erratically distributed mineral which occurs in coarsely crystalline masses associated in part with coarse grained stibnite mineralization. In polished section, sphalerite was recognised by its deep grey color, low reflectivity, internal reflection and isotropism. It precedes and may be replaced by galena and tetrahedrite and often displays cusped boundaries. Sphalerite contains a patchy distribution of tiny (<2mm) sheaf-like aggregates of stibnite which appear epitaxially orientated to the (110) cleavage direction of sphalerite.

Galena (PbS)

Galena was identified in hand specimen by its physical properties, and found to represent a minor component of the Glendinning mineralization. In reflected light, galena was identified by its color, reflectivity, isotropy, polishing hardness and triangular cleavage pits. Galena although closely associated with sphalerite, is also observed to form fine grained replacements and overgrowths with pyrite, sphalerite, tetrahedrite, carbonates and quartz. Vein calcite frequently contains minute acicular crystals of galena. Numerous pulses of sphalerite and galena deposition are indicated by a variety of inter-related crosscutting and replacive textures. Semiquantitative microprobe scans indicated that up to 0.45 wt% Ag is contained within the galena lattice. The general paragenesis of stibnite followed by Pb-Sb sulphides and then galena was observed, inferring that the hydrothermal system may be characterised by decreasing antimony and increasing lead content with time. Moelo et al., (1978) described the occurrence of a small Pb-Sb deposit at Brestree, France in which a similar stibnite to galena paragenesis was observed.

Gold (Au)

Coarse grained, visible gold is absent in both the Glendinning and Clontibret deposits. In primary material, gold is rarely identified as discrete grains, sulphide hosted inclusions or micro-fracture infills by reflected

light techniques. However, backscatter SEM studies (plate 12) revealed the presence of small, discrete gold grains (up to 12x20 microns in diameter) and a network of small gold filled fractures (0.1 to 1.0 microns in width) in arsenopyrites. Semiquantitative assessments of gold fineness ($(\text{Au}/(\text{Au}+\text{Ag})) \times 1000$) in these instances reveal values >950.

Data released by the British Geological Survey in 1988 defined the location of 95 positive and 30 possible sightings of gold grains in pan concentrate samples, collected during stream sediment sampling programs of the Clyde and Borders sheets. It is worthy of note that out of 61 sites identified on the Borders sheet over 25% occur within or in relative proximity to the Glendinning Regional Study area (as defined by the Ordnance Survey Sheet 79) in an area historically regarded as having little if any potential for gold mineralization. Traces of gold have been identified by the author in panned concentrate samples collected downstream of the Glendinning deposit where it is intergrown with limonite and hematite. Although gold was not identified by this survey in streams draining the Swin Gill or Rams Cleuch study areas, due to time commitments, recent work undertaken by European Gold Exploration (pers com, 1987) confirmed the presence of both native gold and cinnabar in these areas.

Tetrahedrite ((CuFeAg)₁₂Sb₄S₁₃)

In this study, tetrahedrite was only recognised in hand specimen after it had been identified by reflected light microscopy, where it was distinguished from sphalerite by its lighter grey color, higher reflectivity and isotropy. Tetrahedrite forms subhedral to anhedral grains <1mm in diameter and comprises <0.5% of the vein material in the Glendinning deposit. In rare instances, tetrahedrite is observed to contain minute inclusions of sphalerite, chalcopyrite, pyrite and arsenopyrite. In general the tetrahedrite is observed in close association with pyrite, sphalerite and stibnite. Tetrahedrite is also known to form minute inclusions in galena where it acts as host to silver mineralization (Patrick, 1981). Electron microprobe analyses (table 2.25) reveal elevated silver levels (up to 0.62 wt%) which increase as a function of Sb content, within tetrahedrites from the Glendinning deposit. Asselborn (1982) observed that minor Tl substitution can occur within the tenantite-tetrahedrite series. Lead-antimony sulphosalts such as fulopite, palagionite and semseyite described by Jambor (1969) were however, not identified within the Glendinning deposit.

Cinnabar (HgS)

Detrital cinnabar has been identified at a number of localities within the Glendinning study area, however it is interesting to note that these occurrences parallel those defined by lithogeochemical As-Sb values (European Gold Plc, pers. com.) possibly inferring a genetic link between these elements. Cinnabar is identified in pan concentrate samples by its high specific gravity, scarlet red color, uneven fracture and near metallic, adamantine lustre. In addition, the presence of cinnabar was also confirmed by X-ray diffraction. The quantity of cinnabar in the Glendinning ore is extremely difficult to estimate in reflected light because of the fine grain size and irregular distribution, as inclusions within other sulphide phases. A similar Hg association was noted by Otkhnezuri and Dolidze (1981) who identified a quartz-dickite-cinnabar assemblage in numerous As-Sb-Hg deposits from the USSR.

Discussion

It is proposed that the earliest phase of mineralization at Glendinning was that of sulphidation of wallrocks coupled with the introduction of As-rich fluids. Due to the absence of orpiment and realgar from the deposit it may be inferred that deposition took place at temperatures exceeding their invariant points and that arsenopyrite was precipitated from fluids in excess of 265°C (Hall and Yund, 1964). The Glendinning deposit is represented by a linear core of quartz-stibnite vein mineralization enveloped by an extensive zone of anastomosing fracture controlled and pervasive arsenopyritisation. Pyrite and auriferous arsenopyrite were the first sulphides introduced during a period of initial brecciation of the host rocks and were deposited contemporaneously with wallrock alteration. Subsequent minor movements may have reopened or created new fluid conduits for hydrothermal solutions depositing minor amounts of pyrite, galena, sphalerite, bournonite, tetrahedrite, tennantite, quartz and carbonate. However, the minor sulphides formed late in the hydrothermal episode after gold deposition. The growth of ore minerals in open veins is commonly characterised by the formation of crystals with well-developed faces and colloform or zoned monomineralic bands (Craig and Vaughan, 1981). Due to the complex nature of fracturing, alteration and brecciation within this deposit, simple crustified veins, showing a successive deposition of sulphides and a simple paragenetic sequence were not readily observed in this deposit. Detailed ore microscopy has revealed a classical three stage hydrothermal paragenesis, with early pyrite and arsenopyrite (As-Fe-S-Sb-Au-Hg), followed by stibnite and sphalerite (Sb-Zn-Cu), finally overprinted by a later phase of galena, sphalerite and barite (Pb-Zn-Ba-Cu) mineralization. After their primary emplacement the ores were subjected to low-grade regional metamorphism was caused by tectonic burial (Oliver, 1981). However, the effects of low-grade metamorphism provided little if any modification to the textural or mineralogical composition of the sulphides. On the basis of their textural relationships, it is suggested that:

- 1) Syn-diagenetic sulphide phases were limited to pyrite (and/or its precursor minerals).
- 2) Early pyrite framboids and/or pyrite euhedra formed by the sulphidation of detrital magnetite grains acted as cores and nucleation sites to wallrock hosted arsenopyrite crystals.
- 3) Little if any remobilisation of wallrock hosted As-Fe sulphides occurred during the successive stages of mineralization.
- 4) Stibnite deposition postdates the major phase of arsenic-gold mineralization.

All the geological, mineralogical and textural evidence presented within the context of this study suggests that the Glendinning ores were deposited from complex hydrothermal solution. Depositional sites were controlled by the location of extensive fracture systems and breccia zones. The presence of pyrite and arsenopyrite in the vein assemblages, restricts the fS_2 to a relatively narrow range. The upper limit of fS_2 is controlled by the pyrite-arsenopyrite reaction, because the pyrite + native arsenic assemblage is not observed in this deposit. It may be inferred that the ore solutions were saturated with sulphur due to the absence of metallic antimony and berthierite in all phases of the ore. Late-stage deposition of arsenopyrite and stibnite on fractures and in calcite veins which cut the disseminated core, together with the change from arsenopyrite dominant to stibnite dominant sulphides in Glendinning-type deposits can be explained by decreased sulphur activity and/or temperature during the waning stage of hydrothermal activity.

3.5.2 Textural and Petrographic Studies

Petrographic studies in the Southern Belt are hampered by the predominant fine grain size of the compositionally mature, quartz-rich sandstones and their interbedded mudstones (Kemp, 1985). The Silurian Hawick Group greywackes in the Glendinning study area have a distinct and relatively uniform mineralogy. In thin section the greywackes are poorly sorted with angular to subrounded, elongate quartz and subordinate carbonate grains (0.5-0.2mm) contained within a fine grained matrix (0.01-0.02mm) of carbonate and clays. Quartz is the dominant framework mineral (35-60%) feldspar is present in variable but low amounts (2-5%). Rock fragments are common and consist of chert, mudstone and quartz-arenite. Heavy minerals identified in decreasing order of abundance are zircon, monazite, opaques, apatite and sphene. The most distinctive feature of the Hawick Group greywackes is the presence of oxidised micas, magnetite and carbonate (Warren, 1963; Kemp, 1985). Biotite grains exhibit slight to pervasive haematization which accounts for the strong reddening of the mica grains. Warren (1963) in a detailed petrographic study of the Hawick and Riccarton groups, classified the Hawick Group on the basis of an abundant 'reddish-brown' biotite and noted that magnetite constitutes between 5 and 10% of the total rock composition. Detrital angular particles of plagioclase feldspar are common, though partly or totally replaced by sericite in proximity to the mine area, where coarse grained hydrothermally altered greywacke sandstones were found to contain disseminated arsenopyrite intimately associated with anhedral pyrite. In this area, the rock matrix contains a felted mass of sericite flakes, quartz and carbonate. In addition, quartz grains were observed to undergo dissolution along microcrystalline boundaries.

In Hawick Group greywackes, the modal carbonate content can be >30% of and as such are more appropriately termed calcareous sandstones (Kemp, 1985). The high carbonate content of the Hawick Group greywackes, may be invoked as a possible source of CO₂ enrichment associated with hydrothermal alteration at Glendinning. However, mantle degassing during magma generation cannot be rejected as a possible source for the CO₂.

Breccias

The cause and effects of hydraulic fracturing and its relation to mineralization was presented by Phillips (1970, 1972) who demonstrated that the accumulation of a body of hydrothermal solution on a fault zone under pressures greater than the pore water pressure would result in the extension of the fault by hydraulic fracturing. The abrupt drop in pressure of the hydrothermal solution when fracturing occurs results in the 'bursting' apart of the rock into which the hydrothermal solution has permeated under high pressure, and the formation of angular breccias. Under these conditions, Phillips (op. cit.) showed that the dip of each extension to the normal fault increases up to the point where the fracture forms a vertical breccia zone.

Following the initial explosive brecciation of the host rocks during the earliest phase of hydrothermal activity, it is probable that both the porosity and effective permeability of the host rocks rapidly increased. These factors were later reduced (to possibly less than its original pre-mineralization state) owing to the effects of wallrock alteration and the precipitation of hydrothermal minerals, particularly quartz in pores, vugs and fractures. Considerable evidence of structural disruption is observed, with thin beds of greywacke, siltstone and mudstones dislocated and brecciated by a series of closely spaced fractures. Polyphase brecciation is evident with wallrock fragments displaying earlier veining, cemented and then re-brecciated. The presence of a fine-grained quartz cement throughout the polyphase breccias may be used to infer that the hydrothermal fluids were able to recharge after their hydrothermal expansion into the brecciated zone (cf. Berger, 1985). The larger veins contain a high proportion of

gouged and sheared wallrock. Fragments of brecciated wallrock enclosed within the quartz-stibnite vein contain disseminated arsenopyrite-pyrite mineralization. These textures are interpreted to represent a series of hydraulic fracturing along a conduit during successive episodes of fluid discharge.

Commonly, zones of micro-brecciation are developed in both vein and wallrock. In addition networks of micro-veins of a similar mineralogy pervade the wallrocks adjacent to the quartz stibnite veins. Hydraulic fracturing may have enhanced permeability on a microscopic scale by the opening of grain boundaries and microfractures, although it is probable that each episode of fracturing and brecciation was followed by 'self-sealing' with silica.

Texturally the evidence provided by Gallagher et al., (op.cit) does not provide clear, conclusive proof that the breccias recorded in the Glendinning boreholes were derived from debris flows. Detailed examination of representative samples of intraformational breccia revealed that the clasts were formed by brittle fracture of lithified and veined sediments, with fragment boundaries displaying straight edges and sharp angular corners. Breccia fragments exhibit interiors of argillic alteration, enveloped by margins of siliceous alteration. Feldspar is virtually absent from the breccia fragments, wallrock and matrix and has been replaced by fine grained sericite and dickite. In addition this study noted that the breccia is generally clast rather than matrix supported, in opposition to that inferred on the basis of the 'debris flow' model. The present study demonstrates that extensive hydraulic brecciation of lithified sediments resulted in the generation of a wide variety of breccia textures which have previously been interpreted by Gallagher et al., (op.cit) in terms of intraformational breccias or debris flows. This epigenetic model could be refuted however, if it was found that stratiform metalliferous cherts exist in the vicinity of the Glendinning deposit and/or arsenic-rich stratiform horizons occur throughout the Glendinning study area.

The formation of extensive brecciation in this deposit was probably assisted by fluid boiling and the loss of CO_2 to the vapour phase. It is tentatively suggested that these breccias formed relatively early in the history of the geothermal system, as later, steam-dominated phases of such systems have a tendency to produce un- or poorly-cemented breccia zones (Berger, 1985). The extensive nature of rebrecciated and recemented sulphide and greywacke clasts provide further evidence that extensive fault-related deformation occurred contemporaneously with mineralization. As such, it is inferred that mineral deposition was accompanied by episodic periods of brecciation and shearing in a structurally active environment. The development of mineralization in the Glendinning deposit may be characterised by three discrete but temporally overlapping events, including: initial fracturing, brecciation and wallrock alteration; arsenopyrite-pyrite-gold mineralization; and stibnite dominant polymetallic mineralization.

Vein Mineralogy

Quartz

Quartz-carbonate veins (1-10cm wide) occur in both mineralized and unmineralized areas within the Glendinning region. In the mineralized zones, these veins contain abundant disseminated pyrite crystals, fine grained masses of pyrite and if mineralized, fine grained disseminated arsenopyrite needles. Pale grey and white to clear microcrystalline quartz occurs throughout the drillcore and was deposited as irregular to massive cavity and fracture fills, often cementing portions of the brecciated drillcore. Silica appears to be one of the earliest hydrothermal minerals deposited in the drillcore, though it commonly contains disseminated, minute crystals of pyrite and arsenopyrite. In thin section the average quartz vein is composed of anhedral interlocking grains of quartz

which display irregular crystal margins. Rosettes of coarse quartz, up to 3.5mm in diameter, are located within a matrix of finer mosaic-like quartz. Sulphide minerals within the vein system have grown at sites on quartz grain boundaries, preferentially associated with the finer-grained mosaic quartz. Radiating crystal clusters of small (usually less than 2mm) clear quartz crystals are present in a small number of cavities and fractures throughout the drillcore. Crystalline quartz appears to be an early hydrothermal mineral, and was most probably deposited immediately following hydraulic brecciation. A number of generations of quartz deposition have been identified associated with differing phases of sulphide mineralization. Silica was a major component of the hydrothermal fluids and formed a weakly silicified zone around both the breccias and veins. Silicification is the general term relating to several processes which involve silica transport, and is defined by Meyer and Hemley (1967) as an increase in the proportion of quartz and silica to other minerals in an altered rock.

Carbonate

XRD studies of unmineralized greywacke and mudstone samples from the Hawick Group revealed the major carbonate component (15-35% of the sample) to be ankerite (cf. ferroan dolomite - $\text{Ca}(\text{Mg,Fe})(\text{CO}_3)_2$). Cavities and fractures in the Glendinning drillcore are lined by ubiquitous, white to pale pink, bladed calcite crystals (up to 1cm long). Calcite appears to have formed relatively late in the paragenetic sequence of minerals, and generally postdates the arsenopyrite mineralization.

Clay Mineralogy

A small subset of mineralized samples were subjected to whole rock and clay fraction analysis by the X-ray diffractometry (XRD) techniques proposed by Bridges (1987). Four representative greywacke and mudstone samples were selected from BGS borehole 3 for semiquantitative whole rock and clay fraction XRD analysis. The results of this study are presented in Figs. 100-103 and Table 1.01. Whole rock analyses revealed the samples to be composed of quartz, illite/mica and carbonate with minor quantities (<2%) of K-feldspar, plagioclase, chlorite, dickite and pyrite. Mudstone samples may be distinguished from their coarser grained counterparts by systematically lower levels of K-feldspar and plagioclase. Clay fraction studies revealed that illite forms the major clay mineral component in greywacke samples (35-70%) accompanied by subordinate dickite (up to 65%) illite-smectite (2.5-7%) and chlorite (in order of decreasing abundance). Mudstone samples are characterised by increased dickite content and relatively reduced illite values. In comparison with unmineralized samples these results demonstrate that the total clay mineral content increases and that feldspar and lesser chlorite decrease in mineralized material. In addition, the proportion of kaolinite (dickite) forming the clay mineral fraction in altered material is substantially increased. The clay content of mudstone lithologies display reduced illite and illite-smectite contents. However, the relative proportions of illite-smectite is increased in comparison with illite. The chlorite and dickite contents of mudstone lithologies are considerably enhanced in comparison with their greywacke counterparts (Table 1.01). In addition, sericite and mixed layer illite-smectite occurs as open space fillings and as a whole rock alteration product throughout the drillcore.

XRD studies of clay minerals located in core samples (Fig 100-104) defined the powder diffraction profiles for the mineral dickite, a structurally well ordered and morphologically well formed, polytypic variety of kaolinite. Brindley and Brown (1980) noted that higher temperatures and hydrothermal pressures favour dickite rather than kaolinite formation. Brilliant white to yellow-stained dickite is present in fractures, vugs and throughout the drillcore. In thin section, dickite is observed to form pseudomorphous aggregates with sericite and finely divided

quartz and is found in association with pyrite, arsenopyrite, smectite, sericite and quartz. The results of a detailed SEM examination of the morphology of hydrothermal dickite are presented in plate 9. The formation of dickite results from the hydrolysis of sodic feldspar, which by coincidence releases sodium to the aqueous phase (Table 1.01 and Fig. 100-105) following the reaction :



Note that the Na^+ cation is transferred from mineral to the fluid phase and is removed in solution whereas H^+ enters the solid phase (dickite). This mechanism is interpreted as the major cause of the sodium depletion associated with the Glendinning deposit and implies both a genetic relationship with the As-Sb-Au mineralisation and the concept of a pathfinder element. This reaction also provides an upper limit to the temperature of alteration as a dehydration reaction occurs between kaolinite group minerals and quartz to generate pyrophyllite and water at temperatures exceeding 300°C .

Hydrothermal minerals containing sodium as the dominant cation are commonly associated with hot spring activity such as analcime, clinoptilolite, mordenite, Na-smectite and aegirine (Bargar and Beeson, 1985). These minerals are however absent whereas minerals containing significant amounts of potassium, such as illite-smectite were located in drillcore samples together with hydrothermal silica, dickite, sericite and chlorite. Due to the absence of both gypsum and alunite from any of the mineral assemblages present in the Glendinning drillcore it is inferred that the deposit was not formed in a near-surface environment (ie the upper 100m) of a geothermal system, as it was not subjected to the form of acid (H_2SO_4) alteration characteristic of the Yellowstone (Muffer and Barger, 1974) and Steamboat Springs (Schoen et al., 1974) types of deposits. The absence of discharge sinters in the Glendinning deposit provides further evidence for sub-surface deposition.

Summary

Petrographic, geochemical and XRD studies of borehole and outcrop samples suggest the development of three distinct but overlapping chemical and mineralogical zones surrounding the deposit:

- 1 - Outer: characterised by depletion of Na, Zn, Fe and Mg; the destruction of primary plagioclase and ferromagnesian minerals and the development of secondary hydrated physicalists such as sericite and dickite and chlorite.
- 2 - Inner: characterised by an abrupt increase in As and S, and is mineralogically defined by the presence of a halo disseminated and fracture hosted arsenopyrite and pyrite marginal to a quartz-stibnite ore zone.
- 3 - Core: characterised by high CaO , SiO_2 As, Sb and S contents and the presence of quartz-carbonate-stibnite veining.

Geochemical alteration halos (Outer Zone) have been identified up to 400m WSW of the Louisa Mine area, The maximum extent of the sericitic alteration and the disseminated sulphide mineralisation in the host rocks to this deposit has not been fully evaluated and is limited by the extent of sparse outcrop and diamond drilling in the mine area.

3.5.3 Wallrock Alteration

Greywackes at Glendinning are extensively bleached and provide a visual indication of hydrothermal activity. Geochemical alteration patterns in the host rocks in the immediate vicinity of the mine were established on the basis of 170 samples from 4 diamond drill holes and 25 outcrop samples. Alteration is defined within the context of this study as the mineralogical, textural and chemical changes resulting from the interaction of circulating hydrothermal solutions with their host rocks. Meyer and Hemley (1967) defined 10 major types of alteration, 5 of which are important in the context of this study, and include:

- 1) **Advanced argillic alteration:** characterised by the presence of dickite, kaolinite, quartz (\pm alunite). Sericite is usually present together with pyrite and amorphous clay minerals. This type of intense alteration is often present in breccia pipe deposits associated with acidic intrusions; in hot spring environments; and in shallow precious metal deposits. This alteration may be characterised by extreme leaching of alkalis from aluminous phases such as feldspars and micas, but is only present if aluminium is not appreciably mobilised.
- 2) **Sericitization:** characterised by the presence of sericite (fine grained muscovite) pyrite, quartz and minor kaolinite. Zones of sericitization are commonly enveloped by zones of lower grade intermediate argillic alteration. Sericitic alteration in this instance is represented by the assemblage sericite-quartz-pyrite-carbonate-clays and is the most widespread form of alteration in the Glendinning deposit. Phyllic and advanced phyllic alteration is distinguished from sericitic alteration on textural grounds. Phyllic alteration is typified by very fine grained intergrowths of sericite-illite/dickite-quartz associated with intense (>10 vol%) sulphide mineralization. It may be regarded as overprinting sericitic alteration assemblages in the Glendinning deposit.
- 3) **Intermediate argillic alteration:** The principle mineralogy of this form of alteration includes both kaolin- and montmorillonite-group minerals occurring mainly as alteration products of plagioclase and accompanied by appreciable leaching of calcium, sodium and magnesium.
- 4) **Propylitic alteration:** characterised by the assemblage chlorite, epidote, albite (\pm carbonate) with minimal depletion of alkalis. H_2O , CO_2 and sulphur may be added.
- 5) **Silicification:** This form of alteration involves an increase in the proportion of quartz or cryptocrystalline silica in the altered zone. Silica may be introduced from the hydrothermal solution or derived as a by product of feldspar alteration.

Alteration occurs in two forms within this deposit. The replacement of feldspar by sericite represents one aspect of the most intense form of alteration, which is referred to within the context of this thesis as pervasive alteration. The deposition of minerals within fractures, between breccia fragments and in voids is termed flooding. In both instances the bulk composition has been changed, however the original mineralogy is changed only by pervasive alteration. As demonstrated in section 3.5.2, wallrock alteration processes associated with fracturing, hydrothermal brecciation and vein formation include silicification, sericitisation and dickitisation. Greywacke and mudstone samples located in both breccia and fault zones exhibit clear evidence of all three forms of alteration. Because of this, sericitisation is attributable to the development of primary feldspars (cf. section 3.5.1).

the small grain size of the alteration products XRD techniques were used to indicate the change in mineralogy from unmineralized to mineralized country rock. In summary, a number of characteristic features relating to alteration have been observed, in the Glendinning deposit including:

- 1) Both alteration and mineralisation exhibit cross-cutting relationships with stratigraphy.
- 2) Greywackes are more susceptible to alteration than their finer grained counterparts.
- 3) Silicification is an important factor in areas immediately adjacent to the breccia zones, whereas sericitization is the dominant alteration process in wallrock samples.
- 4) Arsenopyritisation is pervasive and laterally widespread throughout this deposit.

The earliest evidence of hydrothermal alteration is identified by the appearance of clay mineral alteration of plagioclase and the weak sericitization of primary micas. The mineralogical changes that occurred during alteration, developed as a result of the destruction of primary feldspars and ferromagnesian minerals to form zones of silicification and sericitisation. Although kaolinisation of feldspars is the commonest type of clay alteration, extensive argillic alteration of rock fragments and ferromagnesian minerals by kaolinite/dickite was also observed. The development of kaolinite (dickite) may be used to infer that the hydrothermal fluids which attacked the feldspars were acidic (Scott and Taylor, 1982).

The initial phase of wallrock alteration which resulted in the dissolution of Na-feldspar is inferred to have resulted in a marked increase in permeability and the development of favourable zones for the ore-bearing solutions. The chemical breakdown of feldspars, particularly plagioclase is a major mechanism for the creation of secondary porosity (McBride, 1985). As such it is clear that the initial alteration events at Glendinning served to increase the relative porosity of the greywacke wallrock prior to the main phase of mineralization.

Magnetite, a somewhat refractory mineral, exhibits extensive evidence of alteration and varying degrees of replacement by pyrite in the vicinity of the mine area, and provides an indication of the highly reducing conditions present during alteration. X-ray diffraction, petrography, SEM and electron microprobe investigations indicate that the both the progressive destruction of primary feldspars and a replacement of magnetite by pyrite (plate 10) correlate with depletion halos of Na and Fe respectively. Similar processes were noted by Colvine et al., (1984) invoking the sulphidation of iron oxides and silicates as virtually ubiquitous in Archean gold deposits. It is tentatively suggested that the removal of magnetite by reduction with the hydrothermal fluid may have resulted in the formation of a 'magnetic hole' associated with the alteration zone, however this hypothesis remains untested.

Geochemical alteration halos (Outer Zone) have been identified up to 400m laterally from the Louisa Mine area. The maximum extent of sericitisation, dickitisation and disseminated sulphide mineralisation in the host rocks to this deposit has not been fully evaluated and is limited by the extent of diamond drilling and sparse outcrop in the mine area. The extensive nature of wallrock alteration may be used to infer gross chemical disequilibrium between the hydrothermal fluids and greywacke host lithologies. The wallrock alteration associated with the mineralising event at Glendinning required the introduction of large volumes of hydrothermal fluid (in excess of the volume of altered material) through structurally induced zones of high permeability. The fault controlled breccia zone acted as a structural trap, or conduit through which hydrothermal fluids were transported, reacting with the wallrock and precipitating the observed mineralization. Wallrock alteration may be interpreted in terms of a chemical exchange between ore forming solutions and host rocks. The REE provide sensitive indicators of alteration and mineralization, directly attributable to the destruction of primary feldspars (cf. section 3.6).

In most hydrothermal ore deposits at least some of the alteration is contemporaneous with ore deposition because the fluids normally do not deposit ore when they are chemically in equilibrium with the wallrock. The greater the extent of alteration the more useful a guide to ore. Alteration may precede the ore but it has been found that this has led to an increased porosity and permeability of the host rock and the development of fluid channelways. The nature and extent of the alteration is dependent upon the host rock lithology, petrology and geochemistry. The width of alteration present in the Glendinning deposit is dependent upon a number of physical parameters including both porosity and permeability. Furthermore, the increased porosity of the greywacke in comparison to that of the mudstone indicates that a more extensive alteration envelope would be developed in the greywackes. It is clear that the early pervasive phase of hydraulic brecciation and wallrock alteration enhanced porosity and permeability and was rapidly followed by arsenopyritisation of wallrocks. The destruction of the original greywacke texture is a major feature of the mineralized alteration zone at Glendinning. It may be demonstrated that the changes in mineralogy and texture of the wallrocks enclosing the ore are far more extensive and obvious than the fine grained, disseminated nature of the arsenopyrite-gold mineralization.

Altered rocks may be extremely useful in the interpretation of the chemical and physical conditions of ore deposition. The assemblage of hydrothermal minerals forms a valuable supplement to the actual ore minerals as they provide a wider range of elements compared to the ore itself. Detailed alteration studies therefore provide not only a guide to the ore mineralization in the field but also an indication of the character of the fluids associated with ore deposition. In general, the hydrothermal alteration identified in the breccia-fault zones associated with As-Sb-Au mineralization resembles a compacted porphyry copper zonation.

A visual indication of the effects of hydrothermal alteration takes the form of a progressive bleaching of the greywacke, up to areas adjacent to the main breccia zones. On the basis of this investigation, the hydrothermal alteration at Glendinning can be subdivided into an inner core (or stockwork) containing the sulphide mineralization and a surrounding halo of intensely altered and bleached greywacke. In addition, the presence of extensive kaolinite group minerals adds to the characteristic pale nature of the sediments. Samples collected from the Glendinning area exhibit a continuum ranging from unaltered dark grey greywacke to buff colored greywacke containing visible disseminated sulphide and stringers of vein mineralization (Plate 38). The drab colors were developed under reducing conditions by the reduction of ferric oxide and/or ferric oxide hydrate, with the resulting ferrous iron incorporated into pyrite and other sulphides. This bleaching effect has been recognized elsewhere within the regional survey area and proved extremely useful in 'prelocating' geochemically anomalous zones, prior to analysis. It is therefore suggested that a qualitative system of diffusive colour charts arranged in matrix form, such as the USGS or Methuen systems, could form the basis of an empirical field guide to alteration and form an aid to the exploration geologist. Although such colour changes appear dramatic when viewed side by side, the differences present in the field are more subtle as they may extend gradationally over a considerable area. Only by careful study and qualitative colour classification can these changes be monitored during cross strike traverses. The resulting ability to recognize areas of hydrothermal input and potential targets prior to the receipt of the geochemical data, has many useful applications and advantages. Although the colour changes shown in Plate 38 appear dramatic, when compared in hand specimen, the colour differences between mineralized and unmineralized greywackes in the field can be subtle, as they extend gradationally over a considerable area. Although geochemical, petrological and isotopic techniques provide extremely useful academic parameters, they are not always immediately applicable for use by the exploration geologist in the field. Only by careful study and qualitative classification can these changes be monitored during cross strike traverses. However, the ability to recognise areas

of hydrothermal input and potential areas of stratabound mineralization prior to any geochemical study has considerable benefits and applications.

3.5.4 Sulphur Isotopes

Sulphur isotopic ratios are widely used in recent studies of ore genesis. The determination of sulphur isotopic ratios of vein minerals facilitated two aspects of the As-Sb-Au mineralization to be addressed, including the source of the reduced sulphur and the potential for isotopic equilibrium in the vein system. Sulphur isotopic analyses of both arsenopyrite and stibnite samples are presented in Table 1.03. These samples closely cluster around the $-2^{0/00}$. The isotopic difference between mineral pairs (arsenopyrite-pyrite and stibnite-sphalerite) are minimal and infer the close genetic relationship between arsenopyrite mineralization and wallrock hosted pyrite grains.

In the Glendinning deposit disseminated arsenopyrite ($0.042^{0/00}$) and pyrite ($-2.81^{0/00}$) concentrates from wallrock samples were analysed together with both microcrystalline ($-2.55^{0/00}$) and massive ($-2.81^{0/00}$) vein stibnite and granular vein sphalerite ($-2.743^{0/00}$). These values corresponded closely with values obtained for vein stibnite in both the Knipe ($-3.41^{0/00}$) and Clontibret ($-3.95^{0/00}$) deposits. The extremely narrow range of sulphur values defined by this reconnaissance study may be used to infer the existence of isotopic equilibrium between the vein minerals, while the lack of isotopically light (strongly negative) sulphur values, precludes the derivation of sulphur from the greywacke wallrocks. The relatively narrow range of sulphur isotope values suggest that the fluids were dominated by reduced-sulphur species and that fluid oxidation during sulphidation was minimal (Perring et al., 1987). The results are consistent with derivation of sulphur from juvenile fluids, or by leaching of magmatic sulphides during metamorphism (Ohmoto and Rye, 1979).

Sulphur isotopic determinations for all sulphide phases at Clontibret closely group within a -4 to $+6^{0/00}$ range, centered upon a mean of $-0^{0/00}$ (Morris and Steed, 1985). Individual ranges for pyrite, arsenopyrite and stibnite closely mirror those observed in the Glendinning deposit and were used to suggest a magmatic or magmatic related source for the mineralizing fluids. Limited sulphur isotope studies provide evidence for a sulphidisation model for gold mineralization and may be used to demonstrate that the removal of sulphur from solution due to sulphidisation of the wallrocks may have been sufficient to cause the required change in gold solubility and subsequent precipitation. Sulphur isotope values delineated a single grouping of samples at $-2 \pm 2^{0/00}$. Although isotopic fractionation factors for systems containing stibnite have not been determined, a comparison with the sulphur isotope studies of Robinson and Farrand (1982) indicates that the sulphides were precipitated from an ore fluid containing mantle derived reduced sulphur in solution (dominantly H_2S) at temperatures around $200-250^\circ C$. Little evidence of the acquisition of sedimentary sulphur was identified.

Preliminary sulphur isotope data of background and Pb-Zn mineralised sediments in the Southern Uplands and Longford Down has been presented by Anderson et al., (1989). In the Southern Uplands, this study centred upon the diagenetic pyrite component of Late Ordovician-Early Silurian Moffat Shales, and revealed a ^{34}S range from $-0.6^{0/00}$ to $-17.1^{0/00}$ as anticipated following normal bacteriogenic fractionation (-30 to $-40^{0/00}$) of contemporaneous seawater sulphate. While Anderson et al., (1989) consider that the Pb-Zn vein sulphides at Wanlockhead represent leached and homogenized Lower Palaeozoic diagenetic sulphide, the origin of sulphides in the Late Silurian/Early Devonian Glendinning and Clontibret As-Au deposits is more problematical. It has been demonstrated in this study, that the Glendinning deposit is hosted by sulphur-poor (mean 50ppm) greywackes, deposited in a relatively well

oxygenated, carbonate-rich environment. As such, isotopic data derived from the pyrite-rich Moffat Shale (Anderson et al., 1989) cannot be directly equated with the greywackes host rocks to this deposit, and further investigation of the background isotopic composition is required.

The extremely narrow range of sulphur isotope values identified in all phases from the Glendinning deposit define an isotopically homogenous source of sulphur from depth, exhibiting typical magmatic values. This statement requires qualification, in as much as a magmatic source cannot be identified on the basis of these values without due reference to the sulphur isotope values of the host (unmineralized) sediments, however the likelihood of a magmatic derivation cannot be precluded. On the basis of the limited evidence available to date, it may be inferred that hydrothermal, seawater sulphur was not involved in this deposit to any great extent, and that a magmatic source of sulphur is quite probable. As such, there is no evidence of the involvement of reduced seawater sulphate in the deposition of arsenopyrite, as would be expected in an exhalative sulphide deposit. Furthermore, close isotopic similarities exist between:

- 1) Vein and wallrock hosted sulphides in the Glendinning deposit.
- 2) Differing vein-hosted sulphide phases in the Glendinning deposit.
- 3) Stibnite samples from Sb-deposits across the Southern Uplands and Longford Down (including Glendinning, The Knipe and Clontibret).

It is clear from this reconnaissance study that the As-Sb-Au mineralisation in the Southern Uplands and Longford Down display a tightly constrained range of values, clearly distinct from those identified by Anderson et al., (1989) for Lower Carboniferous vein and stratiform deposits. These results provide further evidence in support of the hypothesis invoking a major magmatic component to the Glendinning deposit. However, detailed studies of this and other As-Sb-Au deposits and their host rocks in the Southern Uplands are required to substantiate this hypothesis.

3.5.5 Sulphide Geochemistry

The following section details the results of electron probe microanalysis of individual sulphide phases from the Glendinning deposit.

Arsenopyrite

Lithogeochemical analysis of the mineralized greywackes and mudstones from the Glendinning deposit demonstrated a correlation between arsenic, gold and the presence of visible arsenopyrite. Reflected light, electron probe and SEM studies revealed that gold is commonly found intimately associated with arsenopyrite, but rarely in its free (native) state. Arsenopyrite is potentially one of the most useful indicator of temperature and sulphur activity during mineralization in this deposit due to the application of Kretzmar and Scott's (1976) arsenopyrite geothermometer, a detailed discussion of which is presented in chapter six. Electron microprobe mapping studies revealed that arsenopyrites, particularly those hosted by wallrock contain significant amounts of sub microscopic gold. Similar features have been observed within the Knipe, Talnotry, Cairngarroch and Clontibret deposits (cf. chapter six). In summary, this study provides evidence for: the cryptic enrichment, substitution and zonation of gold and associated trace elements within a sulphide lattice; the coexistence of two possible sites for gold deposition within arsenopyrite crystals; and the preferential deposition of gold within areas of greatest thermal

gradients and maximum fluid-rock interaction. As such, cooling of the ore solution by 'quenching' is proposed as the most viable mechanism for the precipitation of early sulphide-gold phases.

In the earliest stage of mineralization, conditions of gold deposition were attained due to fluid/rock reaction which lead to both precipitation of arsenopyrite and pyrite and a resulting decrease in sulphur activity. The arsenopyrite-gold assemblage was deposited in a restricted zone where suitable chemical, physical and structural zones coincided. These conditions occurred where high temperature As-Au-S bearing fluids interacted with a large surface area of highly permeable, sulphide-rich rocks and were rapidly chilled. Estimates of mineralization temperatures in the Southern Uplands based upon the use of the arsenopyrite geothermometer, mineral assemblages and compositions range from ~250-380°C, with an average of ~300°C.

Sphalerite

The FeS content of sphalerite coexisting with pyrite and pyrrhotite varies as a function of pressure, and has been calibrated for use as a geobarometer (Scott, 1983). However, this geobarometer may only be applied to coexisting samples of sphalerite, pyrite and pyrrhotite, whilst avoiding grains that contain or coexist with chalcopyrite. Traverses made across two sphalerite grains provided little indication of zoning and defined generally low Fe contents (0.0-0.54 wt%). In general, the trace element contents (table 2.24) were low, however the importance of As, Sb, Cd, Ag and Pb (900, 3300, 6900, 1600 and 8300ppm max., respectively) should be evaluated further. The low Fe content of sphalerite from the Glendinning deposit may be used to infer a low FeS activity and high sulphur activity which serves to preclude the development of pyrrhotite. The absence of coexisting pyrrhotite in the Glendinning deposits also precludes the use of the sphalerite geobarometer.

Stibnite

Although limited in extent, a pilot geochemical study, using the electron microprobe to analyse both coarse (n=6) and fine (n=7) grained stibnite crystals uncovered rather surprising results: the coarse grained crystals (table 2.21) displayed relatively low trace element contents, close to the detection limits of the technique (As - 0.31; Ag - 0.02; and Au - 0.00 wt%) whereas the finer grained fraction (table 2.22) demonstrated considerably elevated values (As - 4.72; Ag - 0.06; and Au - 0.10 wt%).

Tetrahedrite

Tetrahedrite-tennantite is a naturally occurring sulphosalt in which many substitutions can take place (Patrick, 1981). The general formula for the tetrahedrite-tennantite series is $(\text{Cu}, \text{Ag})_{10}(\text{Zn}, \text{Fe}, \text{Cu})_2(\text{Sb}, \text{As}, \text{Bi})_4\text{S}_{13}$. This series is defined by the substitution of Sb for As, forming a complete solid solution in which both As-rich, Sb-rich and intermediate varieties are common. In the Glendinning deposit tetrahedrites (table 2.25) form the dominant host mineral to Ag mineralization (up to 0.62 wt%) and are associated with elevated Sb and notably high Tl levels (9.50 and 0.25 wt% maximum respectively) and are Cd poor (0.33ppm max). Microprobe analyses of tetrahedrite inclusions from Glendinning demonstrated that an As-rich phase of precipitation was followed by an Sb-rich phase.

Pyrite

Following the methodology of Scott (1986) syngenetic/diagenetic pyrite may be distinguished from epigenetic pyrite by extremely low chalcophile element (As and Sb) content. A reconnaissance evaluation of the trace-element

content of syn-diagenetic framboidal pyrite located peripheral (~50m) to the Glendinning deposit, revealed the absence of both arsenic and gold. As such, the presence of synsedimentary As-Au mineralization could not be substantiated. Sulphidation processes were most intense in the margins of the quartz-stibnite vein system, where magnetite rich bands and framboidal clusters were preferentially replaced and/or overgrown by pyrite. Frequently, these pyrite euhedra contain arsenical margins, indistinguishable from the core zones in reflected light, but which containing up to 5% As.

Levels of cobalt and nickel and the Co:Ni ratio in pyrite can provide reliable indicators of the origin of the pyrite and the host sulphide deposit (Willan and Hall, 1980). Using this model pyrite samples associated with mineralization in the Glendinning deposit, fall outwith the fields defined for both sedimentary/diagenetic pyrite and synsedimentary massive sulphide deposits of hydrothermal origin. Early minerals introduced into the Glendinning deposit include arsenical pyrite and auriferous arsenopyrite. Trace element studies of arsenian pyrite crystals and rim zones from the Glendinning deposit (table 2.19 and 2.20; n=206) revealed the presence of elevated As, Cd, Hg and Au values (5.39, 1.87, 1.09 and 0.20 wt% max., respectively). Pyrite associated with the As-Au phase of mineralization contains high As, Sb, Hg and Ag values and displays slightly elevated Au levels. Their high As/Sb ratio and association with intense wallrock alteration suggests a relatively high formation temperature. Vein pyrite exhibits similar patterns of trace element enrichment but with a significant reduction in the As/Sb ratio due to increased Sb content in the vein mineralization. The lower Sb content of wallrock hosted pyrite may reflect the relative mobility of Sb in the fluid system.

3.6 GEOCHEMICAL STUDIES

Grigoryan (1974) in a classic paper on the application of lithogeochemistry to mineral exploration, noted that hydrothermal mineral deposits are always accompanied by primary multi-element geochemical halos, and their recognition and classification may be used to provide effective prospecting criteria for the identification of concealed ('blind') deposits. In addition, Grigoryan (op. cit.) recognised that these anomalies may be both horizontally and vertically zoned and proposed the use of multiplicative geochemical halos in defining the presence of the ore zones. In general, primary geochemical halos surrounding ore bodies, can be classified as either dispersions of chalcophile and siderophile elements, or zones of visible or cryptically altered wallrock. In a discussion of the application of lithogeochemistry in detecting blind sulphide deposits, Govett and Goodfellow (1975) demonstrated the presence of individual and multi-element halos associated with massive sulphide deposits. In a summary of lithogeochemistry in mineral exploration, Govett and Nichol (1979) noted that chemical alteration halos may be more intense and therefore detectable over greater distances than mineralogical halos, since the lattice substitution of elements may be detected chemically without having any mineralogical representation. Selinus (1981) in an assessment of the application of lithogeochemistry to mineral exploration in northern Sweden, recorded distinct primary halos associated with known ore bodies and additional areas containing previously unrecorded mineralization.

An advantage of lithogeochemical surveys providing fresh rock is available, is the direct measurement of deep-seated dispersion patterns which are unaffected by complications from the secondary environment. This study is used to demonstrate the more widely dispersed nature of alteration related elements, present in concentrations several orders of magnitude greater than the ore-related elements. By comparing the geochemistry of unaltered equivalents with host rocks from the hydrothermal environment, a semi-quantitative approach to chemical mass transfer during alteration is attained.

3.6.1 Drillcore Geochemistry

The results of multi-element geochemistry upon a series of interbedded greywackes, siltstones and mudstones of Wenlock age sampled from four boreholes in proximity to the Louisa Antimony Mine, Glendinning are graphically displayed upon fold-out No.3. Samples from each borehole have been grouped in ascending numerical order and combined to create a composite geochemical profile (n=170). The chemical effects of hydrothermal alteration and mineralization have been assessed in relation to background geochemical variations by both statistical and graphical techniques, and by a direct comparison with fold-out No.1 (Section 3.6.2). Histograms of element distribution in greywacke, mudstone and altered core samples from the Glendinning study area are presented in Figs. 32-34, respectfully. In addition, bar diagrams comparing and contrasting the effects of hydrothermal alteration upon greywacke and mudstone lithologies are presented for individual elements in Figs. 37a-45b. Elements intimately associated with mineralization processes (ie Na, As, Sb, Ni, Pb, Cu, S, Ba and Zn) display positively skewed and highly kurt populations. The mean values, notably of As and S are affected by this distribution and the geometric means (692 and 1243ppm respectively) display considerable variation from their arithmetic counterparts. Major rock forming elements display lower or negatively skewed, less kurt populations with a trend towards a more normal distribution. Detailed lithological descriptions of the core samples are provided in tables 1.32 to 1.35. Geochemical data, summary statistics and correlation coefficients relating to this study are presented in tables 4.111-4.119, 2.108-2.116 and 3.00 respectively. A detailed discussion of the drillcore geochemistry is presented below:

SiO₂

SiO₂ displays relatively consistent background values, upon which two forms of anomaly are superimposed: slight increases, attributable to the effects of silicification, and major increases (81.40% max) resulting from brecciation and intense quartz-stibnite veining. Increases in SiO₂ content correlate directly with both disseminated and vein hosted ore forming elements. This is reflected in a skewed distribution and slight increase in the mean composition (Fig. 35a) of mineralized samples (59.41%) in comparison with background values displayed in the Hawick Formation (58.89%). Discrimination diagrams used to distinguish greywackes, mudstones and altered samples are displayed in Figs. 46a to 47a. SiO₂ values are positively correlated with, in order of significance: Fe, Co, Sb, S, As, Fe/Mg and Al/Ca+Na and inversely correlated with Al, Ti, Mg, Ca, K, Mn, P, Cr, Rb, Sr, V, Zn and Al/Si. A detailed discussion of these correlation pairs was not undertaken at this time.

Al₂O₃

Al₂O₃ displays variable background values with depletions directly related to increased SiO₂ content and enrichments related to both mineralization and lithic-related element groups. This is reflected in a slight increase in the mean composition of mineralized samples (18.01%) in comparison with background values displayed in the Hawick Formation (14.23%). Discrimination diagrams used to distinguish greywackes, mudstones and altered samples are displayed in Figs. 46a and 47b to 48d. Al₂O₃ values are positively correlated with Ti, K, V, Rb, As, Cr, Cu, Ga, La, Ni, Nb and Y; and inversely correlated with Si and Co.

TiO₂

Highly consistent TiO₂ values display little systematic variation with the exception of an inverse relationship to SiO₂ anomalies. This pattern is interpreted, simply in terms of silica enrichment and detrital/lithic depletion (a

'dilution effect') and bears little if any relation to alteration processes. This is exemplified by minimal variation in mean composition between mineralized samples (0.81%) and background values in the Hawick Formation (0.84%). Discrimination diagrams used to distinguish greywackes, mudstones and altered samples are displayed in Figs. 47b and 48e to 49e. TiO_2 values are positively correlated with Al, K, P, V, Cr, Ga, La, Ni, Nb, Rb, Th, Sr, V and Zr; and inversely correlated with Si, Co and S.

Fe_2O_3

Fe_2O_3 displays a relatively variable distribution and marked inverse correlation with anomalous arsenic and antimony values. This is reflected in a slight decrease in the mean composition of mineralized samples (5.39%) in comparison with background values displayed in the Hawick Formation (5.96%). Discrimination diagrams used to distinguish between hydrothermally altered and unaltered samples are displayed in Figs. 46b, 48a, 48e and 49f to 51b. Fe_2O_3 values are positively correlated with Mg and Na; and inversely correlated with As and Sr.

MgO

Systematic variations in MgO content are observed in all boreholes with values inversely related with mineralization. This is reflected by a slight decrease in the mean composition of mineralized samples (6.99%) in comparison with background values in the Hawick Formation (7.40%). Discrimination diagrams used to distinguish greywackes, mudstones and altered samples are displayed in Figs. 47e, 49b, 50b, 52d and 53a-53e. MgO values are positively correlated with Fe, Ca, Mn, Na, P and Y; and inversely correlated with As, Sb, Co and S.

CaO

As with MgO, this element displays systematic variations in all boreholes, inversely related to and counterbalanced by the sulphide group elements. This is reflected in a slight decrease in the mean composition of mineralized samples (6.99%) in comparison with background values in the Hawick Formation (7.4%). Discrimination diagrams used to distinguish greywackes, mudstones and altered samples are displayed in Figs. 46f, 47f, 49c, 50c, 52e and 52f. CaO values are positively correlated with Mg, Mn, Na, P and Y; and inversely correlated with Si, As, Co and S.

Na_2O

Apart from the sulphide group elements (As, Sb, Pb, Cu, Ni and S) Na_2O provides the single most useful indicator of hydrothermal alteration and cryptic, low-grade As-Sb-Au mineralisation. This major element exhibits extensive depletions in proximity to quartz-stibnite veins and disseminated As-rich sulphides, and defines broad alteration envelopes associated with hydrothermal alteration. The effects of Na depletion result from the hydrolysis of sodic feldspar and the creation of dickite (a high temperature polymorph of kaolinite). Almost total depletion of Na_2O is quantified by a major decrease in the mean composition of mineralized samples (0.20%) in comparison with background values in the Hawick Formation (1.55%). Discrimination diagrams used to distinguish greywackes, mudstones and altered samples are displayed in Figs. 46c, 47c, 48f, 49f, 50a, 51c-52d, 53a and 54a. Na_2O values are positively correlated with Fe, Mg, P and Zr; and inversely correlated with Al, K, As, Rb, Sr, Sb and S.

K₂O

The K₂O content displayed throughout all four boreholes is relatively variable, but positively correlated with clay mineral, detrital and mineralization group elements. This is reflected in a slight increase in the mean composition of mineralized samples (3.36%) in comparison with background values displayed in the Hawick Formation (2.21%). Discrimination diagrams used to distinguish altered and unaltered samples are displayed in Figs. 46d, 47d, 49a, 51c and 53f. K₂O values are positively correlated with Al, Rb, Ti, P, Cr, Cu, La, Ni, Nb, Sr, V and Y; and inversely correlated with Si, Na, As, Co and S.

MnO

Highly consistent MnO values are displayed throughout all boreholes with the only deviations in concentration directly related to major increases in SiO₂ content ('quartz dilution') and indirectly, the effects of mineralization. This is reflected in a slight decrease in the mean composition of mineralized samples (0.09) in comparison with background values in the Hawick Formation (0.11). MnO values are positively correlated with Mg, P, Y and Zr; and inversely correlated with Si, As, S, Co, S and Sb.

P₂O₅

Highly consistent P₂O₅ values are displayed in all four borehole sections with no variation between the mean composition of mineralized samples and background values. P₂O₅ values are positively correlated with Al, Ti, Mg and Ca; and inversely correlated with Si, As, Co and S.

As

Highly elevated As levels (up to 25,994ppm) displayed in all boreholes are controlled by the presence of sulphides, predominantly arsenopyrite (FeAsS) with minor contributions attributable to substitution in both pyrite and stibnite (see chapter six). Mean arsenic concentrations in mineralized samples (2766ppm) demonstrate considerable enrichment with respect to background levels in the Hawick Formation (3.5ppm). Arsenic concentrations are particularly important in this study due to the positive chemical correlation between As and Au and the identification of an arsenopyrite host to gold mineralisation in this deposit (see chapter six). Arsenic values are positively correlated with S, Si, Sb, Co, Pb, Cu and La; and inversely correlated with Na, Mg, Fe and Ca.

Ba

Consistent patterns of background Ba values are displayed, upon which is superimposed a small number of sizeable anomalies (max 5363ppm). No major correlation between barium and sulphide group elements was noted, however subtle correlations may be discerned on the fold-out diagram, between Ba anomalies and fracture-controlled SiO₂ enrichment. This association suggests minor baryte mineralization, unrelated to the As-Sb-Au phase of deposition (and alteration) to be the most probable source of contamination. This pattern is reflected in a slight increase in the mean composition of mineralized samples (386ppm) in comparison with background values in the Hawick Formation (280ppm).

Co

Co displays variable, systematic patterns throughout all four boreholes with enrichment associated with sulphide group elements, notably As and S. This is reflected in a slight increase in the mean composition of mineralized samples (33ppm) in comparison with background values in the Hawick Formation (26ppm). Discrimination diagrams used to distinguish greywackes, mudstones and altered samples are displayed in Figs. 48b, 51e and 54b. Co values are positively correlated with Si, As, S, Zn and Fe; and inversely correlated with Mg, Al, Ti, Ca, Mn, K, P, La, Nb, Rb, Sr, V, Y, Zr and Tl.

Cr

Cr displays a consistent, systematic pattern of values inversely related to silica, positively correlated with clay and lithic group elements, but unrelated to the sulphide group values. No variation is noted between mineralized and background mean Cr content (both 142ppm). Discrimination diagrams used to distinguish greywackes, mudstones and altered samples are displayed in Figs. 50d, 51f, 54c and 54d. Cr values are positively correlated with Ti, Al, K, Rb, V, P, Y, La, Nb, Ga, Zr, Ni, Sr, and Th; and inversely correlated with Si only.

Cu

Cu displays variable, systematic trends related to both sulphide and clay mineral group elements (Max. 103ppm). This is reflected by an increase in the mean composition of mineralized samples (34ppm) in comparison with background in the Hawick Formation (24ppm). Discrimination diagrams used to distinguish greywackes, mudstones and altered samples are displayed in Figs. 51d and 54e. Cu values are positively correlated with Al, K, As, La, Ni, Rb, Sb and V; and inversely correlated with Ca.

Ga

Relatively variable Ga values are displayed over a restricted range of concentration. These values may be correlated with both detrital lithic, clay mineral and sulphide group elements, and are inversely related to alkali group elements. No variation is observed between the mean composition of mineralised samples and background values. Ga values are positively correlated with Al, Ti, V, As, Rb, Cr, Cu, Y, La, Ni, Nb, Pb, Sb, Sr and Zn; and inversely correlated with Na, K and Ca.

La

Consistent La values are displayed within all four boreholes, elevated with respect to background values and correlated with both clay and detrital group elements. A slight increase in the mean composition of mineralized samples (38ppm) is observed in comparison with background values displayed by the Hawick Formation (32ppm). La values are positively correlated with Al, Ti, K, Cr, Nb, Ga, Ni, Rb, Sr, V, Y and Zn; and inversely correlated with Si and Co.

Ni

Consistent Ni values are displayed throughout the succession. A slight increase in the mean composition of mineralized samples (72ppm) is observed in comparison with background values in the Hawick Formation

(58ppm). Discrimination diagrams used to distinguish greywackes, mudstones and altered samples are displayed in Figs. 52a, 53e and 55b. Little systematic correlation exists between Ni and the sulphide group elements with the exception of Pb. Ni values are positively correlated with Al, Ti, Cr, V, Pb, Rb, La, Nb, Sr, Y and Zr.

Pb

Although a generally low background Pb content (14ppm) occurs in the Hawick Formation, Boreholes 1, 2 and 4 display anomalies which correspond to both SiO₂ and As enrichment. In addition, borehole 3 displays highly elevated (max 1717ppm) Pb levels throughout the upper 120m of core, which are strongly correlated with pervasive arsenopyrite mineralization. This is reflected in a significant increase in the mean composition of mineralized samples (70ppm) in comparison with background values.

Rb

Slightly elevated Rb values display a positive relationship with clay mineral group elements. This is reflected in a slight increase in the mean composition of mineralized samples (119ppm) in comparison with background values in the Hawick Formation (71ppm). Discrimination diagrams used to distinguish greywackes, mudstones and altered samples are displayed in Figs. 48d, 49d, 50e, 52a, 52b, 52e, 53b, 54b, 54d, 54f, 55a and 55b. Rb values are positively correlated with K, Al, Ti, V, P, La, Cr, Y, Ni, Nb and Sr; and inversely correlated with Si, Na, Co and S.

Sr

Consistently low Sr values are present in all boreholes with the pattern of variation closely mirroring that of CaO. This is reflected in a slight decrease in the mean composition of mineralized samples (121ppm) in comparison with background (151 ppm). Discrimination diagrams used to distinguish greywackes, mudstones and altered samples are displayed in Figs. 46e, 48c, 50f, 52c, 53f and 54f. Sr values are positively correlated with Ca, Al, Ti, K, P, Ti, Cr, La and Nb; and inversely correlated with Si, Fe and Co.

Sb

Antimony (Sb) forms a key member of the sulphide group elements and displays patterns of variation which closely mirror that of Pb. In particular, samples from borehole 3 display considerably elevated and widespread values (in comparison to the remaining holes) which are interpreted as reflecting the stockwork-like nature of the quartz-stibnite vein system and the extensive nature of fracturing and brecciation. Given the nature of this deposit it is no surprise that highly elevated Sb levels are present (max 956ppm) in mineralized samples (mean 77ppm) in comparison with background values (mean 2ppm) displayed in the Hawick Formation (Fig. 42c and 51a). Sb values are positively correlated with As, Cu, Pb, Zn and S; and inversely correlated with Ca, Na, Fe, Mn, Mg and Th.

S

Highly elevated sulphur concentrations (max 26,000ppm) in the core samples display a similar range and distribution to arsenic (As) values. This is reflected by a major increase in the mean composition of mineralized samples (3334ppm) in comparison with background values in the Hawick Formation (47ppm). S values are positively correlated with Si, As, Co and Sb; and inversely correlated with Mg, Ca, Na, Mn, Ti, P, Nb, Y and Zn.

Th

Highly consistent Th values (mean 9ppm) are present throughout the succession which display no significant variation in composition in comparison with background values (8.5ppm). Th values are positively correlated with Al, K, P, Cr, Nb, V, Y and Zr; and inversely correlated with Si, As, Sb and S.

V

Highly consistent V values displaying no direct correlation with sulphide group elements are present throughout this succession. No significant variation in composition between mineralized samples (mean 116ppm) and background values could be defined. Discrimination diagrams used to distinguish greywackes, mudstones and altered samples are displayed in Figs. 47a, 49e, 52f, 53c, 54a-54c and 55a. V values are positively correlated with Al, Ti, K, P, Cr, Ga, La, Ni, Nb, Rb, Sr, Th and Y; and inversely correlated with Si and Co.

Y

Extremely consistent Y values, displaying no direct correlation with sulphide group elements are located in all boreholes. No variation in composition between mineralized and background samples was observed. Y values are positively correlated with Ti, K, Mg, Al, P, Cr, La, Ni, Nb, Rb, Sr, Th, V and Zn; and inversely correlated with Si, Co and S.

Zn

The upper section of borehole 1 displays relatively unaltered background values; however, a rapid decrease in occurs with depth which may be directly linked with the effects of both mineralization and hydrothermal alteration. The systematic decrease in Zn concentration displayed by all boreholes is quantified by a decrease in the mean composition of mineralized samples (45 ppm) in comparison with background values (66 ppm). Similar progressive leaching of zinc was located by Stone (1985) to the west of this deposit in the Loch Doon area. Here, zinc depletion is accompanied by the introduction of arsenic and lead vein mineralization. Notable zinc anomalies (max 1846 ppm) are present in the upper part of borehole 3, which correlate with Pb, S, Sb, As, Ba, Co, Ni, Pb, SiO₂, quartz-sulphide veining and the presence of sphalerite in polished section. At the base of borehole 3, Zn values approach background levels. In general Zn values are positively correlated with and Pb and Sb; and inversely correlated with Ni, As and Co.

Zr

Highly consistent Zr values are displayed throughout all borehole profiles with little systematic variation in response to mineralization. A minor decrease in the mean composition of core samples (177 ppm) is noted in comparison with background values in the Hawick Formation (202 ppm). Discrimination diagrams used to distinguish greywackes, mudstones and altered samples are displayed in Figs. 51b and 55c. Zr values are positively correlated with Ti, P, Na, Mn, Cr, La, Nb, Sr, Th and Y; and inversely correlated with Si, As, Co and S.

Tl

A considerable portion (approx.85%) of all samples analysed contained Tl levels below the detection limits of the XRF (1- 2ppm). As such the Tl (max 7ppm) profile was not included in this fold-out diagram. Statistically, there appears to be little variation between the mean composition of background and mineralized samples. However, in the Glendinning regional study, relatively low Tl levels are closely associated with As-Sb mineralization and provide useful clues to the genesis of this type of deposit. It is worthy of note that the Tl values are positively correlated with K and possibly Sr, and inversely correlated with Co.

Element Ratios

In addition to the major, minor and trace element profiles a number of element ratios were calculated and displayed in a similar format. These ratios are presented as fold-out diagrams and are used for tasks including discrimination and the identification of hydrothermal alteration. The application of these ratios to the Glendinning borehole data (mineralization) and a comparison with the Glendinning Regional study (background) is summarised below:

- a) **Al/Si:** this ratio closely mirrors the Al_2O_3 profile and is relatively increased in comparison to background levels.
- b) **K/Na:** this ratio displays highly elevated values (30-40) in comparison to both background greywacke (mean=1) and mudstone samples (mean=3), and as such provides an extremely useful index to alteration. This ratio may be used to demonstrate that all samples with the exception of the upper portion of borehole 1 have been subjected to intense hydrothermal alteration. On this basis, it is clear that the boreholes were drilled within the alteration envelope of the mineralization and did not intersect "unaltered" samples even at depth. As such it is proposed that the nature of hydrothermal alteration at Glendinning was both pervasive and laterally extensive, and the deposit itself is open at depth.
- c) **K+Na:** The total alkali content of mineralized samples is consistently lower than background values.
- d) **K/Na+K:** This ratio may be used in a similar manner to K/Na and clearly defines the position of hydrothermally altered samples throughout all boreholes (with the exception of samples 1-3 in hole 1). This alteration index provides further, conclusive evidence of extensive nature of the alteration envelope to the Glendinning deposit.
- e) **Fe+Mg:** A systematic decrease in Fe+Mg content is displayed throughout all borehole samples in comparison with background values.
- f) **Fe/Mg:** Considerably lower Fe/Mg ratios are displayed in all borehole samples in comparison with background levels displayed in the Hawick Formation (fold-out 1). Although both Fe and Mg are inversely related to mineralization this ratio may be used to demonstrate a disproportionate reduction in Fe content in comparison with Mg.
- g) **Al/Ca+Na:** A slight increase in the alteration index is noted in comparison with with background values. This 'alteration' index is little use in the Hawick Formation as the effects of Na depletion are masked by the exceptionally high Ca content of the greywackes.

- h) Nb/Y: This ratio displays no variation between mineralized and background values.
- i) Nb/P: This ratio displays no variation between mineralized and background values.
- j) Rb/Sr: High values in greywacke samples can provide a useful guide to alteration, however increased variability in background mudstone samples could result in samples being misclassified. This ratio may only be used to identify the effects of hydrothermal alteration in lithologically controlled sampling programs.
- k) Ni/Co and Cu/Co: Both ratios display slight increases in mineralized core samples, compared with background values.
- l) Zn/Co: Considerably lower values are identified throughout all borehole profiles in comparison with background values. The dominant control upon this variation is zinc depletion (see Zn section).
- m) Zr/Nb: highly consistent values are displayed in both mineralized and background samples.

In comparison with the mean values of additional trace element studies in the Southern Uplands (n=170) mineralized greywacke samples from Glendinning (n=29) display relatively elevated concentrations of Ag, Cs, Sc, Mo, W and Ce with maximum values of 4, 59, 27, 11, 951 and 262ppm respectively. No variations in Cd, Bi, Se, Sn, Te, U and Hf values were detected by XRF.

3.6.2 Glendinning Regional Geochemical Traverse

This section reviews the results of a multi-element geochemical study upon a series of interbedded greywackes and mudstones of Late Llandovery and Wenlock and Ludlow age, located in the Glendinning-Hawick-Eskdalemuir area and defined as the Hawick Group. In this study, interbedded greywacke (n=305) and mudstone (n=197) samples were collected from the same locality (whenever possible) on a series of cross-strike traverses centred upon the Glendinning As-Sb-Au deposit. A location and drainage map of the survey area is presented in Fig. 158. Separate point-source and contour maps for each element and lithology are displayed in Figs. 160-220 and summary multi-element anomaly maps in Figs. 221-224. Samples were grouped on the basis of stratigraphy, lithology and numerical order to aid the assessment and are graphically displayed in Fold-out No. 1. Correlation coefficients for both mudstone and greywacke samples display close similarities. As such, all reported correlations are defined with respect to greywacke lithologies in order to facilitate a direct comparison with other units in the Southern Uplands.

Differences between the geochemistry of greywackes and mudstones from the Hawick Formation may be attributed to an overriding mineralogical control provided by an increased clay fraction in the finer grained lithologies. Enhanced clay mineral content provides both enrichment (in mineralogically related elements such as Al, K, Rb, V, Mn and Na) and depletion due to the effects of clay dilution upon lithic components. In a comparison of variance using the F test statistic the major and trace element data for both Ludlow and Wenlock sediments display similar variances. In addition the average composition of each stratigraphic division display close similarities and the results of a Student T test indicate a high probability that both Ludlow and Wenlock sediments were both derived

from the same parent population/terrain. As such, in the following description of element variation, only trends and patterns relating to lithological variations are discussed:

SiO₂

Hawick Formation greywackes display relatively uniform silica values throughout this succession. No systematic variation in composition is defined, however, values are enhanced by 4-5 wt% with respect to their interbedded, mudstone counterparts. The spatial distribution of this data for both greywacke and mudstone lithologies is presented in Fig. 160 and 190, respectfully. A single example of vein material from the Louisa Mine at Glendinning is clearly distinguished from its host greywackes by its elevated SiO₂ (quartz) content. SiO₂ values are positively correlated with, in order of significance: Al, Ti, P, Co, Fe/Mg and Rb/Sr; and inversely correlated with Ca, Sr, Mn, Mg and Na.

Al₂O₃

Al₂O₃ values in greywacke samples exhibit considerably more variation than the relatively higher, but more systematic values defined by mudstone lithologies. The most notable variation in Al₂O₃ values within both greywacke and mudstone lithologies display strong antipathetic relationships with CaO. The spatial distribution of this data for both greywacke and mudstone lithologies is presented in Figs. 161 and 191, respectively. Al₂O₃ values are positively correlated with, in order of significance: Ti, Fe, K, Rb, Ga, Ni, V, P, Ba, Cu, Nb, Th, Y and Zn; and inversely correlated with both Ca and Sr.

TiO₂

TiO₂ values display little variation in greywacke samples and marginally lower values than in their finer grained counterparts. The spatial distribution of this data is presented in Figs. 162 and 192. TiO₂ values are positively correlated with, in order of significance: Al, Fe, P, Cr, Ni, V, Zn, K, Ba, Ga, La, Rb, Th, Y and Zr; and inversely correlated with Ca and Sr.

Fe₂O₃

The Fe₂O₃ content of greywacke samples display generally lower values than their interbedded mudstones. Anomalous Fe₂O₃ values superimposed upon the general background variation reflect increases in arsenic (As) content. However, it should be noted that similar arsenic enrichment in mudstone lithologies corresponds with a subtle decrease in Fe₂O₃ content. The spatial distribution of this data is presented in Fig. 163 and 193. Fe₂O₃ values are positively correlated with, in order of significance: Ti, Al, Mg, K, As, Ba, Ni, V, Cr, Zn, Rb and K/K+Na; and inversely correlated with Ca and Sr.

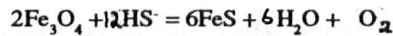
FeO

The ratio of the ferrous to total iron content of silicate and metal oxide minerals was determined for greywacke and mudstone samples of both mineralized and unaltered material, according to the procedure described by Kerrich et al., (1977) and the results are compiled in Table 1.06. Although sulphur has clearly been introduced there is considerable evidence of iron mobility. Detailed analytical studies (XRF fused bead, CO₂, LOI and FeO analysis)

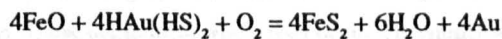
reveal a significant depletion in the total Fe content of mineralized greywackes compared to background values linked to increases in both $\text{Fe}^{2+}/\text{Fe}^{3+}$ and $\text{Fe}^{2+}/\text{Total Fe}$. These features infer that both iron reduction and iron depletion are characteristics of the hydrothermal system at Glendinning.

<u>Ratio</u>	<u>Greywacke</u>	<u>Mineralized Greywacke</u>
	Total Iron >	Total Iron
$\text{Fe}^{2+}/\text{Fe}^{3+}$	1.97	2.68
$\text{Fe}^{2+}/\text{Total Fe}$	0.62	0.71

Based upon the actual decrease in total iron content within mineralized samples it is suggested that the source of iron required in the formation of arsenopyrite may well have been locally derived with Fe^{2+} obtained from the alteration of iron bearing minerals such as pyroxenes, amphiboles or magnetite. Detrital magnetite bands have been located using petrographic techniques from greywackes in the Glendinning mine area. The magnetite is composed of small (<1mm) euhedral-subhedral grains containing fine ilmenite lamelli. SEM analysis of mineralized samples revealed that the detrital magnetite had undergone partial or complete replacement by pyrite. As pyrite and magnetite normally coexist this feature provides detailed constraints upon the nature of the fluids at the time of ore deposition/replacement. For pyrite to replace magnetite a sulphidation reaction is required following the equation outlined below:



This sulphidation reaction is similar to that observed in the Carrock Fell deposit (Hall, Pers. Com.) and when coupled with the pyrite replacement of magnetite may be used to infer that the ore bearing solution was Fe deficient (otherwise FeS would have been precipitated directly). The reduction of magnetite may be used to account for a considerable part of the total Fe reduction observed in the wallrock samples from the Glendinning deposit. As alteration in the form of a sulphidation reaction is clearly observed to affect magnetite bearing greywacke horizons in the Glendinning area and as arsenopyrite exhibits an epitaxial relationship with both pyrite and magnetite it is inferred that these horizons could also provide an indirect locii for As and Au precipitation in this area. In summary, it is proposed that bands of syndiagenetic pyrite and altered magnetite served as nucleation sites for the localisation of arsenopyrite precipitation in the Glendinning deposit. In addition, the alteration of detrital magnetite to pyrite provided a major source of free iron in the fluid phase, and mechanism for gold deposition following the general equation:



Kerrick et al., (1977) in studies of gold bearing quartz veins from the Yellowknife district in Canada observed that a significant reduction in the oxidation state of primary iron was due to large scale interaction of wallrocks with ascending, reducing hydrothermal fluids (water/rock ratio >3:1). As described above, a significant mineralogical redistribution of iron had taken place, with iron liberated from detrital magnetite, incorporated into sulphide phases or released to the aqueous phase. In general, the alteration zone is characterised by extreme reduction and the net removal of total iron. Chemical studies of the oxidation state of the remaining iron present in mineralized samples provides evidence for large scale fluid interaction processes, similar to that described by Kerrich (op. cit). Chemical reduction appears to have formed a critical mechanism in the precipitation of ore phases. In addition, sulphidation of detrital iron oxides (a reducing process) occurs over a greater extent than the deposition of arsenopyrite itself.

MgO

Highly uniform MgO Values are displayed across the traverse with higher background levels established within mudstone lithologies. In addition, systematic depletions of MgO are mirrored by significant levels of arsenic enrichment in both lithologies. The spatial distribution of this data is presented in Fig. 164 and 194. MgO values are positively correlated with, in order of significance: Fe, Ti, V, K, Rb, Ba, Zn and Na+K; and inversely correlated with Ca, Mn and As.

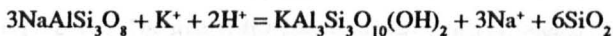
CaO

In greywacke lithologies the CaO content displays a strong antipathetic relationship with SiO₂. Within finer grained lithologies however, the CaO content is highly variable with anomalous values closely correlated with arsenic enrichment. This data is presented in Figs. 165 and 195. CaO values are positively correlated with, in order of significance: Sr and Mn; and inversely correlated with Si, Al, Ti, Fe, Pb, V, Na+K, Mg, K, P, Co, La, Ni, Y, Zn and Zr.

Na₂O

The Na₂O content of greywacke samples displays highly consistent values with the exception of depleted zones associated with arsenic enrichment (Fig. 166 and 196). Lower background Na₂O values are displayed by the finer grained, mudstone lithologies. Depletions of Na₂O associated with arsenic enrichment are still present in the finer grained lithologies, however the magnitude of variation is smaller and therefore more cryptic. Na₂O values are positively correlated with Zr; and inversely correlated with Fe, K, As, Sb, Ca, Ni and Nb.

The mineralization at Glendinning is also be characterized by major depletion of sodium (0.5% Na₂O depletion threshold) and zinc which define an envelope 400m in diameter surrounding the mine area. The sodium depletion and potassium enrichment associated with the mineralization at Glendinning correspond closely with observed mineralogical changes (ie. the kaolinitisation of albite and the alteration of chlorite to sericite). The decrease in plagioclase content may be explained in terms of a kaolinitisation (dickitisation) process following the general reaction:



The distribution pattern of Na₂O in both greywacke and mudstone samples in the vicinity of the deposit is indicative of extensive Na₂O depletion. These depletions, where they occur, are significant, with values falling to below 50% of background. The Na depletion is accompanied by that of Zn and less obvious, Mg and Fe. These depletions, together with a well defined arsenic anomaly associated with the Glendinning deposit may be followed for a distance of up to 1 km NNE. All samples intersected by the BGS boreholes in the Glendinning deposit show clear evidence of hydrothermal alteration and major sodium depletion. The extent of sodium depletion was not restricted even within 'bottom hole' samples and as such the Glendinning deposit remains 'open' at depth.

Studies by Schouwstra and Villiers (1988) describing similar geochemical and mineralogical patterns of alteration associated with gold mineralization noted that this type of alteration was detectable at least 5-10m away from individual mineralized fracture zones. It is proposed that the broad sodium depletion envelope surrounding the

Glendinning deposit extends beyond the limits of both As and Sb anomalies and was formed as a result of extensive hydraulic brecciation at this site. This brecciation provided an anastomosing network of fractures forming conduits to the mineralizing fluids and resulted in the development of a 'stockwork-like' zone of mineralization and alteration. In a discussion of geochemical dispersion in wallrocks associated with the Norbec deposit in Quebec, Pirie and Nichol (1981) noted that Na_2O depletion is closely associated with sericitic alteration. Volume changes during alteration are insignificant and as such are not responsible for 'artificial' trace element enrichments and depletions (cf. Kerrich and Fyfe, 1981; Ludden et al., 1984). In comparison with the model proposed by Carten (1986) for sodium-calcium metasomatism it is suggested that sodic alteration occurred at temperatures below 360°C . In summary, the most significant change in major element values approaching the Glendinning deposit is the increase in the $\text{K}_2\text{O}/\text{Na}_2\text{O}$ ratio and decrease in Na_2O values, both well known indicators of hydrothermal alteration (Meyer and Hemley, 1967; Boyle, 1974). This change is accompanied by widespread sericitization and bleaching of greywackes.

K_2O

Very consistent K_2O patterns are displayed throughout this succession. Anomalous values displayed within greywacke units may be directly related to areas of As enrichment, however similar enrichments within the mudstone lithologies are less obvious and masked by higher background levels. The increase in K_2O reflects the increasing abundance of sericite and white mica, accompanied by the pervasive alteration of plagioclase and loss of Na_2O . The spatial distribution of this data is presented in Fig. 167 and 197. K_2O values are positively correlated with, in order of significance: Al, Ti, Fe, Rb, V, Ba, Ni, Th and Zn; and inversely correlated with Ca, Na and Sr.

Lickley et al., (1987) proposed that primary variations in K_2O content were sufficient to mask changes in K_2O resulting from hydrothermal alteration. It is clear from the results of geochemical studies in the Glendinning area, that this hypothesis is weak and virtually invalid in any form of multi-element study, where sufficient attention to orientation studies and sampling procedures is made, and elemental ratios (ie. $\text{K}_2\text{O}/\text{Na}_2\text{O}$) are determined.

MnO

Highly consistent MnO levels are displayed by both greywacke and to a lesser extent, mudstone lithologies. Enhanced MnO levels are directly attributable to increases in CaO content and as such a carbonate host mineral for Mn is proposed. The spatial distribution of this data is presented in Figs. 168 and 198. MnO values are positively correlated with, Ca, Y, K/Na and Fe/Mg; and inversely correlated with Mg and Na.

P_2O_5

Virtually constant P_2O_5 values occur throughout both greywacke and mudstone lithologies, which are positively correlated with Ti, Cr, V, Al, La and Zr; and inversely correlated with Ca and Sb.

As

Arsenic is the third member of group VA of the periodic table, which also includes nitrogen, phosphorus, antimony and bismuth. In nature, four oxidation states are possible, which enable a wide variety of soluble As complexes and complex compounds to be formed. In a review of the geochemistry of arsenic, Onishi and Sandell (1955)

detailed the average arsenic content of a series of igneous rock types, including granites ($n = 50$; $As = 1.7 \pm 0.3$ ppm) basalts ($n = 40$; $As = 1.9 \pm 0.3$ ppm) and ultramafic rocks ($n = 19$; $As = 1.0 \pm 0.2$ ppm); and indicated that the arsenic content of the lithosphere, is ~ 2 ppm. Boyle and Jonasson (1973) presented a review of the geochemistry of arsenic with particular reference to its use as an indicator element in geochemical prospecting.

Background arsenic levels established from the Glendinning regional study area are generally below the detection limits of the XRF (1-2 ppm). The highest levels of arsenic in the Mine area occur within greywacke lithologies and breccias marginal to the quartz-stibnite vein systems and closely correlate with the presence of disseminated arsenopyrite and subordinate pyrite. Govett (1983) noted that most dispersion halos around vein and replacement deposits, demonstrate a logarithmic decay pattern away from mineralization, reaching background within 1-30m. A linear rather than log-linear decrease in As values away from the main area of mineralization at Glendinning is indicative of extensive permeation of the hydrothermal fluids and widespread alteration. The shape of the trace element dispersion halos may be used to suggest that the hydrothermal fluids permeated away from the veins under the influence of a pressure gradient.

Analytical results indicate a highly significant, positive correlation between As and Au (correlation coefficient 0.84) and a poor correlation between Sb and Au. Such concentrations within greywacke and siltstone lithologies indicates a strong lithological control upon the sulphide deposition within this deposit. This control may be indirectly related to grain size, porosity, permeability and the relative availability of iron within the individual lithologies. Regional lithogeochemical studies reveal a range of As values from below the detection limits, to 65 ppm As and 55 ppm Sb. Arsenic and antimony anomalies are scattered throughout this region, and the prominent correlation between As and Sb is reflected in the occurrence of many coincident As and Sb anomalies. Each of the data sets appears to be unimodal and conforms approximately to a lognormal distribution. The sediments immediately adjacent to the vein mineralization are enriched in As and Sb, with the Sb enriched sediments forming a core to the much broader zone of As enriched sediments.

Kerrich and Fryer (1981) demonstrated that As, Sb, Hg, and B are typically present in association with hydrothermal gold deposits and have been concentrated by a factor of 10^3 - 10^4 compared with host rocks. In a comparison between the mineralization and regional greywacke suite, arsenic is observed to be enriched by a factor of 1000 when compared to a regional threshold of 15 ppm. Similar enrichments at the 95 percentile level are observed in Sb (11 ppm); Pb (26 ppm); Cu (43 ppm); Ni (81 ppm); S (400 ppm); Co (37 ppm) and Rb (100 ppm). The background Au abundances determined in this study, mirror those reported by Boyle (1979) in similar terranes. Arsenic concentrations greater than or equal to 15 ppm are present in 23 ($\sim 5\%$) of samples from the study area.

Arsenic enrichment occurs in both greywacke and mudstone lithologies. However, due to higher background levels in mudstone lithologies, cryptic As enrichment is more clearly identified in greywackes (figs. 170 and 200). Furthermore, the effects of arsenic enrichment are mirrored by Sb, Pb, S, Cu and Fe (sulphide group elements); K and Rb (clay mineral/alteration group elements); Na and Zn (depletion group elements) and K/Na, K/Na+K and Al/Ca+Na (alteration indices). Arsenic values are positively correlated with, in order of significance: Sb, S, K/Na, K, Cu, Pb and Rb; and inversely correlated with Na, Sr and Na+K. Large (1981) and Russell (1974, 1983) have noted enrichment of Mn and Zn in ore-horizons associated with submarine exhalative activity. However, no evidence has been detected by this study for the existence of a similar stratiform enrichment of As, Sb or Zn in the Glendinning study area.

Au

Background Au values (< 1ppb) within both mudstone and greywacke were established in order to evaluate the relative abundance in each rock type and determine their likelihood in forming the source of Au in the Glendinning deposit. The lower limits of detection use for gold in this study vary between analytical techniques. Although MIBK solvent extraction and fire assay techniques define detection limits of ~50 ppb Au, instrumental neutron activation analysis (INAA) limits are as low as 1 ppb. Gold in unmineralized samples from the Glendinning area were generally below detection limits (ie. < 1ppb or 0.001 g/t). It is low (<100ppb) within quartz-stibnite vein samples from sorting floor, but in arsenopyritised breccia and wallrock samples up to 840ppb (0.84ppm) is present marginal to the main fault zone. This study demonstrates the occurrence of areas of significant precious-metal enrichment (up to 500ppb Au). Background gold values at Glendinning (<1ppb) may be used to infer a 500 fold increase in Au concentration associated with mineralization.

Ba

Barium displays consistent patterns throughout the traverse with generally elevated levels in the mudstone lithologies compared with their coarser grained counterparts. Anomalous Ba values correlate well with zones of arsenic enrichment, particularly in greywackes (figs. 171 and 201). Ba values are positively correlated with, in order of significance: Fe, Mg, Rb, S, V, Zn, Al, K, Cu, Ni, and Y; and are inversely correlated with Ca and Sr.

Co

Highly consistent values occur in both mudstone and greywacke lithologies, however anomalous values may be positively correlated with arsenic enrichment. The spatial distribution of this data is presented in Fig.173 and 203. Co values are positively correlated with Cr, Ti, La, S and Zr; and inversely correlated with Ca and Sr.

Cr

Both greywacke and mudstones display similar, highly consistent values throughout the succession. The spatial distribution of this data is presented in Fig.174 and 204. Cr values are positively correlated with, in order of significance: Ti, Fe, P, V, Zr, Mg, La and Ni; and inversely correlated with Sb and Cu.

Cu

Relatively consistent values are displayed by greywackes as opposed to more variable, elevated levels in mudstones. Anomalous values in both lithologies correspond to zones of arsenic enrichment. A diverse distribution of copper anomalies unrelated to the As-Sb anomalies, may be explained in terms of the widespread presence of low-grade Cu-dolomite veins throughout this area. The spatial distribution of this data is presented in Fig.175 and 205. Cu values are positively correlated with Fe, Ba, Al, Mg, K, Rb, Ni, V and Zn; and inversely correlated with Na and Zr. The positive correlation observed between Cu, Pb, Zn and Sb in the Glendinning deposit may be explained in terms of the sulphide mineralogy identified within the quartz-stibnite vein system, which included: sphalerite (ZnS) galena (PbS) boumonite ($2\text{PbS} \cdot \text{Cu}_2\text{S} \cdot \text{Sb}_2\text{S}_3$) semseyite ($9\text{PbS} \cdot 4\text{Sb}_2\text{S}_3$) chalcopyrite (CuFeS_2) tetrahedrite (Cu_3SbS_3) and tennantite (Cu_3AsS_3). The limited Cu content in the ore deposit may possibly indicate the relative instability of copper-rich bisulphide complexes at low temperatures rather than a scarcity of Cu in the hydrothermal solution (cf. Lambert and Scott, 1973).

CO₂ and H₂O

The possibility that hydrothermal alteration was accompanied by a gain in H₂O levels was investigated by wet geochemistry. H₂O values were estimated from the total LOI subtracted from the CO₂ content. Thirty nine samples were analysed in duplicate from mineralized and unaltered lithologies and the results are presented in tables 2.26 to 2.28. CO₂ and LOI levels in Hawick Formation greywackes (means = 6.44% and 2.03% respectively) and mudstones (means = 4.01% and 2.5% respectively) reflect the abundance of carbonate and clay. Mineralised samples from the Glendinning mine area display elevated levels of CO₂ (mean 7.64%) and to a lesser extent, H₂O (mean 2.85%) reflecting hydrolysis (H⁺ metasomatism) and carbonate alteration. Elevated As, Sb and S in mineralised samples correlate with CO₂ and H₂O enrichment. The average CO₂ content of mineralized samples is enriched in comparison to both greywacke and mudstone lithologies by 1.2-3.6wt% (mean) and 0.9-1.7wt% (maximum) respectively. Average and maximum H₂O contents of mineralized samples are higher compared with greywacke and mudstone by 0.3-0.8wt% and 1.0-1.7wt% respectively, reflecting wallrock hydrolysis. The rocks of the Glendinning deposit are therefore inferred to be water-rich compared to the surrounding sediments, a feature reflected in the increased proportions of clay minerals in the altered sediments.

Ga

Highly consistent Ga values are displayed by both greywacke and mudstone lithologies (figs. 176 and 206) with increased background values in the finer grained samples. Ga values are positively correlated with Al, K, Rb, Ti and Fe; and inversely correlated with Ca and Sr.

La

Consistent La values are displayed throughout the succession with a slight increase in the background levels of mudstones. Subtle enrichments in La values correlate with zones of arsenic enrichment (figs. 177 and 207). La values are positively correlated with, in order of significance: Al, Ti, Ni, Nb, V, Zr, Fe, K, P, Co, Cr, Rb, Th, Y and Zr; and inversely correlated with Ca.

Ni

Consistent Ni values are displayed in both of the studied lithologies with increased background values in mudstones and subtle increases associated with arsenic enrichment (figs. 178 and 208). Ni values are positively correlated with Al, Ti, Fe, V, K, Rb, Zn, Mg and Y; and inversely correlated with Ca, Sr and Na.

Nb

A consistent pattern displaying slight (2-3ppm) increases in the background value of mudstone samples compared with their coarser grained greywacke counterparts (figs. 179a and 209). Nb values are positively correlated with, in order of significance: Zr, Ga, La, Th, Y, Al, Na, K and Rb.

Pb

Consistent background levels are displayed in both of the studied lithologies. Anomalous Pb values correlate closely with arsenic and copper enrichment (figs. 179b and 210). Pb values are positively correlated with Fe, K and Zn; and inversely correlated with Na.

Rb

The element pairs potassium-rubidium and calcium-strontium display similar ionic radii, electronegativity and ionic potentials (Schouwstra and Villiers, 1988), thereby providing evidence for the association of Rb in potassium minerals and Sr in calcium minerals. The Rb/Sr ratio was proposed by Plimmer and Elliot (1979) to provide a sensitive indicator of hydrothermal activity and wallrock alteration. Rb forms a pathfinder to gold-pyrite mineralization in the Oggofau deposit, south Wales (Al-Atia, 1974). Elevated levels in greywacke correlate with zones of arsenic enrichment whereas those in mudstones appear less sensitive to the effects of arsenic enrichment and hydrothermal alteration (figs. 180 and 211). Rb values are positively correlated with: Al, Ti, Fe, as, K, Ba, Ni, Zn, Mg, Nb, Th, V and La, and inversely correlated with Na, Ca and Sr. It is inferred that element enrichment occurred as a result of substitution in K-mica formed during sericitisation. The increase in Rb/Sr ratio in mineralized zones correlates with the alteration of plagioclase and increasing illite content.

Sr

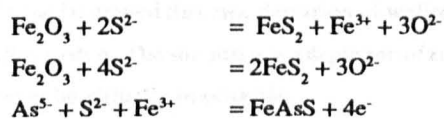
Mudstone lithologies display systematically lower values than their greywacke counterparts (figs. 181 and 212). Sr values are positively correlated with Ca and Mn, and inversely with Al, Ti, Ni, V, Fe, Rb, K and Zn.

Sb

The lowest Sb value recorded in a 250m traverse across the Glendinning Mine area was 1ppm with elevated values reaching a maximum of 387ppm marginal to the vein outcrop. No apparent variation was observed in background levels between mudstone and greywacke, unlike those displayed by arsenic. Samples containing > 5ppm Sb are considered anomalous relative to the crustal abundances (0.2-0.5ppm) identified by Evans and Peterson (1986) and define areas of hydrothermal Sb input and proximity to mineralization (figs. 182 and 213). Sb values are positively correlated with As and inversely correlated with Na, Sr, Zn, Ti, Mg, P, Cr and La.

S

Background levels in the Hawick Formation (generally <50ppm) are the lowest in any of the Southern Uplands greywacke Formations and are discussed in detail in chapter 5. Extensive sulphidation of host rocks to the Glendinning deposit is apparent with levels in excess of 25,000ppm recorded from breccia and wallrock samples, with possible sulphidation reactions including:



In the Glendinning study area anomalous levels of sulphur correspond with zones As and Sb enrichment (figs. 183 and 214). In general, sulphur values are positively correlated with As, Ba and Co.

Th

Th values in greywacke lithologies display generally low but erratic concentrations together with minor enrichments in interbedded mudstone lithologies. No relationship is displayed with hydrothermal alteration or trace element

enrichment associated with As-Sb-Au mineralization (figs.184 and 214). Th values are positively correlated with Al, Ti, V, Fe, K, La, Ni, Nb, Rb, Y, Zn and Zr; and inversely correlated with Ca and Sr.

V

Minor increases occur within mudstone lithologies which correlate directly with increased Th content (figs. 185 and 216). There is a positive correlation with Th, Al, Ti, Fe, K, Ni, Rb, Zn, Mg, P, Ba, Cr, Cu, Ga and La, and an inverse correlation with Ca, Sr and Sb.

Y

Minor enrichments mirroring those of Th and V are displayed in fig.186 and 217. Values are positively correlated with Al, Ti, Ni, Nb, Fe, K, Rb, Th, V, Ba and La, and inversely correlated with Ca, Sr and Sb.

Zn

The Glendinning deposit is enveloped by a Zn depletion zone up to 400m in diameter. With the exception of the quartz-stibnite vein system, all lithologies adjacent to the mineralization contain ~50ppm less Zn than background values. Correlation coefficients reveal a cryptic, inverse relationship between Zn and As whereby As mineralization may be characterised by subtle levels of Zn depletion. It should be noted that narrow zones (<1m in width) of Zn enrichment associated with sphalerite deposition occur in association with the mineralised fracture system. Data presented in figs. 187 and 218 show that Zn values are positively correlated with Al, Ti, Fe, Ni, V, K, Rb, S, Th, Y, Ba, Cu, Ga and La, and inversely correlated with Ca, Sr and As.

Similar progressive leaching of zinc was identified by Stone (1985) to the west of the Glendinning deposit in the Loch Doon area where it is accompanied by arsenic and lead vein mineralization. Large-scale zinc mobilization processes may have been instigated by mineralizing As-rich hydrothermal fluids. Stendal (1981) in a study of the geochemistry and genesis of arsenopyrite mineralization in late Precambrian sediments from central East Greenland noted that Zn is depleted in mineralized samples compared with semipelitic quartzite host rocks. Although Zn does not occur in conjunction with the arsenopyrite mineralization, it is associated with later quartz veins. Base metal leaching has been observed at high levels within developing porphyry systems (Cyr et al., 1984) and extreme Zn depletion has been observed by Ludden et al., (1984) in visible alteration zones within the wallrocks to gold-bearing feldspathic porphyry dykes. Zinc depletion has also been observed in the Oggafau As-Au deposit (see chapter 1). It can be argued that zinc depletion of wallrock may have contributed to the sphalerite phase of mineralization in this system. The simultaneous depletion of zinc in the wallrocks and enrichment in the juxtaposed veins would however be virtually impossible.

Zr

Consistent Zr values are displayed in both greywacke and mudstones with a subtle decrease in concentration in the finer grained lithologies. The spatial distribution of this data is presented in Fig.188 and 219. Zr values are positively correlated with Nb, Ti, Th, and Y; and inversely correlated with Ca and Sb.

Tl

Tl enrichment halos were predicted around many base and precious metal deposits by Ewers and Keays (1977). Although in excess of 95% of all samples analysed in this study contained Tl values below the detection limits of the XRF, elevated Tl values (up to 17 ppm) have been identified in the regional study area (ie Rams Cleuch) and define sites of major exploration interest (figs. 189 and 220). In general, Tl values are weakly correlated with Al, K, Rb, As and Sb, and inversely correlated with Na and Zn.

Hg

Limited investigations of the Hg distribution has revealed cryptic enrichment in mineralized samples, however, the distribution of Hg in the Glendinning deposit is sporadic and inferred to result from minute cinnabar inclusions, too small to be determined under the optical microscope.

W

Sporadic, elevated W values located in Glendinning drillcore samples may be interpreted in terms of a minor W component (inferring a Lake District type As-Sb-W assemblage). However, it is possible that these values resulted from W contamination of BGS samples during grinding. As such, it is impossible to ascertain the level of W enrichment within the core samples and as such detailed resampling and analysis of core material should be considered a priority for further studies.

Element Ratios

A number of element ratios are displayed in fold-out 1 which may be used to distinguish between mudstone and greywacke, and between unaltered and mineralized samples. In addition, multi-element ratios are used to reduce the effects of local reversals in zoning and analytical variation. Additive and multiplicative halos and ratios are favored by Soviet geochemists in preference to regression and discrimination techniques, commonly used outside of the USSR (Govett and Nichol, 1979). The ratio's Al/Si, Rb/Sr, Ni/Co, Cu/Co, Zn/Co, Fe+Mg, Nb/Y, K/Na and K/(K+Na) display relatively higher values in mudstones, as opposed to both Nb/P and Zn/Nb which display higher values in greywacke lithologies. Boyle (1974) discussed the use of major element ratios in lithogeochemical exploration and concluded that the K_2O/Na_2O ratio provided the best parameter for estimating proximity to mineralization. As such, the ratio K_2O/Na_2O was used to evaluate any consistent increase in proximity to mineralization, thereby reflecting the corresponding effects of potassium metasomatism and sodium depletion. It was found that the alkali alteration indices K/Na and K/(K+Na) clearly illustrate the effects of sodium depletion, dickitisation and potassium metasomatism associated with hydrothermally altered samples. A decrease in the total alkali content of altered samples is displayed by the K+Na profile, whereas an increase in both Fe/Mg and Fe+Mg values associated with arsenic enrichment and alteration, demonstrates the clear addition of iron from the hydrothermal system.

REE : REVIEW

The rare earth elements (REE) or 'lanthanides' comprise a group of elements with atomic numbers 57 to 71 (Haskin et al., 1968) and occur primarily as trace elements in rock forming minerals. The ionic radii of the REE decrease

with atomic number from 1.14A for La to 0.85A for Lu. The REE behave coherently during most geological processes because of their similar chemical properties. The REE may be divided into two subgroups: those from La to Sm (lower atomic numbers and masses) which are referred to as the light rare earth elements (LREE) and those from Gd to Lu (higher atomic numbers and masses) referred to as the heavy rare earth elements (HREE). REE data are normally presented in the form of a rare earth element pattern, constructed by plotting the normalised concentration of each element versus the element name, thereby enabling the relative enrichments and depletions of the REE in a sample to be readily observed (Haskin et al., 1968). The standard against which other samples are generally normalised, is the distribution of REE in chondritic meteorites. In studies of sedimentary rocks, however, additional standards such as NASC (north American shale composite) and PAAS (post Archean average shale) have been used. The REE form a coherent group, because of their systematic decrease in atomic radii, with increasing atomic number and predominant +3 oxidation state. The fact that two members of the group, Ce and Eu are often found in anomalous oxidation states, adds to the groups use (Klinkhammer, 1983). REE data have been used extensively for examining the compositions of hydrothermal fluids in many types of deposit (Graf, 1977; Kerrich and Fryer, 1981; Jenner et al., 1981; Mitropoulos, 1982; Taylor and Fryer, 1978, 1982, 1983; Klinkhammer et al., 1983; Wilton, 1985).

Graf (1977) demonstrated the use of REE's as hydrothermal traces during the formation of massive sulphide deposits. Because of the coherent and predictable geochemical properties of the REE, it was suggested that they could be used to monitor the alteration reactions between hydrothermal fluids and their host rocks. This coherent group behavior in hydrothermal alteration processes was noted to reflect changing fluid characteristics and behavior (Taylor and Fryer, 1978). For example, in a porphyry environment, magmatic hydrothermal fluids produce potassic alteration, with strong enrichment in the light rare earths (LREE) reflecting high pH and low water/rock ratios. Increasing water/rock ratios and decreasing pH accompanying a progressive involvement of meteoric fluids and propylitic/phyllitic alteration, all REE are leached, with LREE leached more severely than the HREE. Taylor and McLennan (1981) presented a detailed review of the composition and evolution of the continental crust, based upon REE evidence from sedimentary rocks. It was demonstrated by Taylor and Fryer (1982) that LREE are enriched and HREE are depleted during potassic alteration of granodiorites. Subsequent overprinting by meteoric-hydrothermal solutions and the development of a quartz-sericite-pyrite assemblage, results in progressive leaching of all REE. A detailed review of rare earth element geochemistry, was presented by Henderson (1984). The rare earth elements, lanthanum to lutetium (atomic numbers 57-71) are members of Group IIIA in the periodic table and all have very similar chemical and physical properties. Despite the similarity in their chemical behavior, these elements can be partially fractionated by petrological, mineralogical and alteration processes. Chatterjee and Strong (1984) in lithogeochemical studies in southwestern Nova Scotia, noted the progressive depletion of LREE in the early stages of alteration, associated with K-metasomatism and sericitization. Similar leaching of all rare earth elements, accompanying the destruction of the preexisting mineralogy has been observed in porphyry-type mineral deposits (Taylor and Fryer, 1983). Bence and Taylor (1985) in a discussion of the REE patterns associated with hydrothermal alteration processes noted that Eu may be selectively mobilized and that the selective removal of LREE by the hydrothermal fluids, results in a severe depletion relative to HREE. In studies of REE patterns associated with metasedimentary rocks adjacent to the Land's End granite, in southwest England, Mitropoulos (1982) demonstrated LREE enrichment relative to HREE, and a general increase in REE content relative to unaltered sediments, due to the introduction of REE from the granite by the action of hydrothermal fluids. Felsic volcanics derived by minor partial melting of a mafic source are also characterised by HREE depletion (Jenner et al., 1981). In granitic rocks the REE are mainly concentrated

in accessory minerals such as sphene, apatite and monazite. These minerals tend to concentrate the LREE and consequently, whole rock samples are frequently enriched in LREE. Plagioclase, K-feldspar and biotite act as host for the remaining REE, in order of relative abundance.

Trivalent REE such as Ce and Eu are highly susceptible to changes in the oxidation state of individual samples, and display trends which differ from the systematic fractionation associated with other REE group members (Moller et al., 1981). Eu^{3+} can be reduced to Eu^{2+} during hydrothermal alteration, which due to an accompanying large change in ionic radii, results in a notable fractionation or 'anomaly'. In general, feldspars form the most common group of minerals which exhibit positive Eu anomalies. During hydrothermal alteration and the destruction of feldspars in the Glendinning deposit, Eu was passed into solution. It is proposed that the Eu was then reduced to Eu^{2+} and unable to follow the other trivalent ions in coprecipitation with Ca^{2+} ions, was removed in solution, thereby resulting in the observed strong negative Eu anomaly. It is predicted that vein calcite crystals would also display negative europium anomalies, indicative of precipitation from the same mineralizing solution.

REE : RESULTS

Chondrite normalised REE plots illustrating the effects of hydrothermal alteration upon mineralized Hawick Formation greywackes in the Glendinning deposit are presented in Figs. 471 to 473. Samples CXD1005, 1006, 1030, 1050, 1051, 1052, 1053, 1159, 1160, 1165, 1166, 1168, 1077 and 1078 display REE patterns parallel to those of PAAS with similar if not slightly elevated total REE values; subtle evidence of LREE enrichment and the presence of negative Eu-anomalies. On the basis of REE evidence, mineralized Hawick Formations samples display characteristics typical of post-Archean upper crust, as indicated by PAAS. Fractionation of REE in the form of LREE enrichment and relative HREE depletion associated with hydrothermal alteration at Glendinning (Fig. 471-474) is interpreted in terms of leaching of the HREE during intense hydrothermal activity and provides further evidence of extensive water-rock interaction. This pattern is similar to that defined by Kerrich and Fryer (1981) for Au-bearing veins and precious-metal hydrothermal systems in the Abitibi Greenstone Belt of Canada, but is opposite to that defined by Graf (1977) associated with stratiform, exhalative deposits in New Brunswick.

3.6.3 Glendinning Regional Lithogeochemical Atlas

The Glendinning Regional Study area is located within the central portion of Ordinance Survey sheet 79 (Scale 1:50,000). This area consists of high moorland with a thin peat and residual soil cover. Although valleys contain substantial thicknesses of boulder clay, exposure is not as poor as one would first expect. Stream sections and various sized quarries provide suitable sites for sampling, but by the far the most useful exposures in this area were the recently excavated roadways on forestry ground (Plate 27). Many of these roads provide virtually complete cross-strike traverses and have been sampled in detail. The general philosophy followed in the Glendinning study area was to sample along a series of 10km long traverses spaced 1500m apart, at 100m intervals across strike. However, due to the paucity of outcrop in some areas, all major exposures in the region were also sampled. Orientation studies in the Glendinning mine area involved the collection of a closely spaced set of samples in proximity to the vein and a more widely spaced set downstream of the deposit. This group of samples was augmented by the BGS borehole material.

To collect representative samples from each location, the entire unit in question was chip sampled. Care was taken during sampling to collect chips representative of unweathered and unveined bedrock. A 4kg sample of greywacke was collected from each site and where possible, 1kg of mudstone was also selected. Plate 27 displays the remnants of a roadside exposure after one such sampling exercise. This sampling programme yielded 305 greywacke and 197 mudstone samples which formed the basis of a 31 element geochemical study, carried out by automated XRF at the University of Nottingham. Samples of Glendinning borehole material (n=167) provided by BGS were also reanalysed for major, trace and REE using both XRF (major and trace elements) and ICP (REE's) techniques in order to provide comparable multi-element data for the target As-Sb-Au mineralization. Upon completion, the multi-element geochemical data was transferred to the VAX mainframe computer system at Strathclyde University and processed using software developed by the author (see chapter 2).

The drillcore samples were divided into three lithological groups (greywacke, siltstone and mudstone) and subjected to univariate statistical analysis. The variations in the distribution of the major and trace elements between the immediate mine environment and the surrounding area are compared in a series of histograms presented in Figs. 32-34. In addition, a series of major and trace element discrimination diagrams which serve to distinguish mineralized from unaltered lithologies are presented in figs. 46a to 55c and discussed at length later in this section. Following XRF analysis a geochemical database containing over 22,000 values together with grid references was created for the Glendinning area and manipulated by various univariate and multivariate statistical procedures including correlation coefficients, principal component and discriminant analysis. This database combined with site locations was used to automate the production of a 1:100,000 lithogeochemical atlas for greywacke and mudstone lithologies (figs. 158-224). As lithogeochemical information is most easily evaluated in terms of its spatial distribution, data are presented with accompanying topographic and drainage maps. Large scale (1:100,000) maps were plotted on acetate sheets, using a high speed drum printer and form a series of geochemical overlays for geological, geophysical and site location maps in this area. The scale on each map is indicated by the scale bar and by the 1km ticks along the margins. On each of the single element maps sample sites are represented by a graduated series of circles, the size of which is related to the concentration present of the element with respect to a percentile classification of the sample population, the largest circles being indicative of anomalous or at least threshold values. The close sample spacing and level of reduction necessary to present the geochemical atlases on an A4 sized diagram, has made it impossible to identify individual sample sites by their corresponding sample number. The use of proportional point source symbols has also been adopted as the principal method of presentation for BGS regional geochemical data (Plant and Moore, 1979). The interpretation of point source geochemical maps may be greatly assisted by contouring or 'grey-scale' mapping which highlights important anomalous areas.

Due to the paucity of sample sites at the margins of the Glendinning atlas boundary lines were defined enclosing a pentagonal region of high sample density (Fig. 159). This area of approximately 15km² defines the margins of the area which was subjected to grey-scale contouring (Figs.160-220). The margins of the contour plots do not however, directly correspond with the margins of the point-source maps, with figure 159 most clearly illustrating this relationship. Although, contour intervals may be selected at perceived inflection points on histograms or cumulative frequency plots in this study specific percentiles were chosen for each population. All contouring was carried out using computerized data processing algorithms in order to minimize the subjectivity and increase both reliability and repeatability. Grid nodes were calculated using a weighted average of the 8 nearest data points and an inverse-square distance weighting was used to determine the value of the grid points.

Geochemical profiles of the geochemistry of greywacke, mudstone and mineralized drillcore are also presented on fold-out diagrams 1 and 2. It should be noted that a geochemical map is a specialised form of geological map, that enhances the known geology and provides a powerful tool in mineral exploration (Plant et al., 1988). As such, the Glendinning atlas and geochemical sections provide invaluable data as to the spatial distribution of the primary geochemical environment and may be used to model the mineralization. Natural groupings (or clusters) of anomalous samples may also be used to define target areas for further assessment and evaluation. Isochemical plots of element composition superimposed upon each sample location were used to pinpoint zones of enrichment or depletion relative to their surrounding area. In summary, the Glendinning atlas was compiled from litho-geochemical data during a reconnaissance survey:

- 1) to evaluate areas adjacent to known gold-sulphide mineralization.
- 2) To establish regional geochemical thresholds for mineralisation related element (the 95th percentile).
- 3) To define localities favourable for disseminated and/or vein mineralization for further evaluation by trenching, overburden sampling, geophysics and/or diamond drilling.
- 4) To assess geochemical partitioning between the greywacke and mudstone and the spatial distribution to known mineralization.

Glendinning Atlas

This atlas (figs. 160-224) details the spatial and elemental variation in greywacke and mudstone lithologies. Point-source data is presented with the position of individual sample sites identified by circles and in the lower right hand corner of each page a contoured, grey-scale map of element concentration is located with contour intervals defined on the basis of a percentile classification (0-50, 50-75, 75-90, 90-95 and >95). The margins of the contour area correspond to those defined by the shaded zone in Fig. 159 and do not correspond with the edge of the larger, rectangular survey area and point source geochemical maps. Geochemical data, summary statistics and histograms related to this survey area are presented in tables 4.37, 2.47 and figs 32, 33 and 34 respectively and summarized graphically on foldout No. 1. The location of individual As and Sb anomalies (the main pathfinders for gold mineralization) are presented in tables 1.37 (greywacke) and 1.38 (mudstone). Composite multi-element anomalies are detailed in table 1.39 and the spatial position of trace element (As-Sb-Cu-Pb-Zn) anomalies defined in figs 221 (greywacke) and 223 (mudstone); the position of Na and Zn depletion anomalies are presented in figs 222 (greywacke) and 224 (mudstone). Anomaly sites identified by this study and documented in table 1.39 include: the Glendinning Deposit (G); Black Syke (BS); Rams Cleuch (RC); Swin Gill (SC); Wisp Hill (WH); Philhope Loch (PL); Cat Rig (CR); Greatmoor Hill (GH); Rashigrain (R); The Shoulder (TS); Stibbiegill Head (SH); Stennies Water (SW); Linhope Burn (LB); Phaup Burn (PB); Meggat Water (MW) and Upper Stennies Water (US).

SiO₂

The small range of SiO₂ values located in Hawick Formation greywacke and mudstone (figs. 160 and 190 respectively) display little spatial variation with relatively uniform silica values throughout. Samples in close proximity to the mine area display little evidence of enrichment, and values are attributed to be directly related to the detrital quartz content of the sediments. In comparison with mudstone (fig.190) a increase of 4-5wt% is observed in greywacke samples.

Al₂O₃

The alumina values defined upon the point source geochemical maps (figs. 161 and 191) display little systematic variation and bear little relation to mineralization related trace element values (ie. As or Sb). They may be directly related to the clay mineral content of the greywacke and indirectly related to grain size of the samples (ie. finer grain size - greater clay mineral content). In the greywackes a strong inverse relationship exists between Al₂O₃ and CaO, whereas in the mudstone samples Al₂O₃ values are positively correlated with Fe, K, Rb and V; and inversely related to both CaO, Mn and Sr.

TiO₂

Values defined within both greywacke and mudstone lithologies (figs. 162 and 192) display little spatial variation and like samples close to the mine area display little evidence of enrichment associated with wallrock alteration processes. Marginally higher values are defined within the mudstone lithologies as opposed to their coarser grained greywacke counterparts. The close correlation observed between TiO₂, MgO and Fe₂O₃ values may be directly related to the detrital ferromagnesian mineral content of the sediments.

Fe₂O₃

The wide range of Fe values displayed by greywacke lithologies (figs. 163 and 193) are generally lower than their mudstone counterparts and display little systematic variation throughout the survey area. However, anomalous values (>95%) are closely related to sites of anomalous As and Sb values including Black Syke, Rams Cleuch and Wisp Hill. This pattern is also reflected, albeit to a lesser extent within mudstone lithologies (Fig. 193). Although three main sources of iron have been identified within the greywacke (ferromagnesian minerals, Fe-rich carbonates and iron bearing sulphides) sulphidation processes associated with hydrothermal alteration are deemed to be responsible for the observed anomalous Fe values. An increase in both Fe/Mg and Fe+Mg values associated with arsenic enrichment and alteration provides additional evidence of the addition of iron from the hydrothermal fluids.

Na₂O

The Na₂O contents of greywacke and mudstone (figs. 164 and 194) are consistent except in depleted zones associated with areas of arsenic enrichment and hydrothermal activity. Na₂O has previously been identified as inversely related to the elements As and Sb. This relationship may be explained mineralogically, as the dominant host mineral for sodium within these greywacke is sodic feldspar, which when subjected to hydrothermal alteration is converted to dickite (a high temperature polymorph of kaolinite) and water together with the release of sodium to the aqueous phase. As such, sodium depletion is characteristic of the mineralization processes operating within this area. Note the relative position of 'sodium holes' surrounding the Glendinning, Swin Gill, Rams Cleuch, Greatmoor Hill, Phaup Burn, Linhope Burn, Stibbiegill Head and Greatmoor Hill anomalous zones (figs. 164 and 194).

CaO

The large range of elevated CaO values results from addition of major detrital carbonate. This component displays a strong antipathetic relationship to SiO₂ (a 'closure' effect). The high carbonate content of the greywackes masks the subtle effects of CaO enrichment associated with hydrothermal alteration. The contour plot details a slight

increase in CaO level in the south western portion of the study area. A highly variable, diverse range of CaO values was identified within Hawick Group mudstone. In both greywacke and mudstone, CaO values display a strong inverse relationship with SiO_2 . However, in mudstone samples CaO enrichment is more easily associated with the effects of hydrothermal alteration and mineralization. Anomalous CaO values occur at Glendinning, Swin Gill, Phaup Burn and Rams Cleuch.

MgO

MgO values defined on point source geochemical maps (figs. 166 and 196) are highly uniform with little systematic variation within the study area. Greywackes display a relatively restricted range compared with mudstones. In addition, a positive correlation is defined with 'depletion' related elements such as Na and Fe, whereas an inverse relationship is observed between MgO and hydrothermally enriched elements associated with As-Sb-Au mineralization (ie. As, Sb, Cu, Pb). The contour plot displays a narrow belt of MgO depletion extending from the Glendinning and Black Syke areas eastwards to Swin Gill. Depletion is also associated with smaller peripheral zones marginal to the Rams Cleuch, Greatmoor Hill and Wisp Hill As-Sb anomaly zones.

K₂O

Consistent K₂O values in greywacke and mudstone (figs. 167 and 197) decrease in the south western portion of the survey area. A notable exception to this trend is an enrichment zone surrounding the Glendinning and Black Syke localities. In general K₂O values are enriched within both greywacke and mudstone lithologies in the vicinity of hydrothermal alteration and As-Sb mineralization, however enrichment within mudstone are less obvious and masked by higher background levels. Examples of this feature are displayed by the Swin Gill, Cat Rig, Rams Cleuch, Wisp Hill and Greatmoor Hill anomaly sites.

MnO

Highly consistent MnO values within both greywacke and mudstone (figs. 168 and 198) display a generally low and an extremely narrow range of values throughout the survey area. No spatial or mineralization related variation in MnO values can be observed, however enhanced MnO levels are directly attributable to increases in CaO content and as such, a carbonate host mineral for much of the Mn is proposed.

P₂O₅

As with MnO, P₂O₅ values for both lithologies (figs. 169 and 199) are generally low and display an extremely restricted (virtually constant) range throughout the survey area.

As

Arsenic, forming the main 'pathfinder' element of arsenopyrite hosted gold mineralization in this area, provides an extremely useful guide to hydrothermal activity and As-Sb mineralization. Lithogeochemical studies (figs. 170 and 200) reveal that the Glendinning deposit forms a small part of a much larger mineralization center with dimensions of ~10x10km. The full extent of As-Sb mineralization in this region is unknown due to the limited extent of detailed sampling in this area. The Glendinning deposit has been the focal point of all previous investigations due to its historical importance as an antimony mine and the lack of any regional geochemical data

outwith the mine area. Although arsenic is enriched in both greywacke and mudstone because of the higher background levels in mudstones, cryptic As enrichment is more clearly identified in greywackes. The effects of As enrichment are mirrored by Sb, Pb, S, Cu and Fe (sulphide group elements); K and Rb (clay mineral/alteration group elements); Na and Zn (depletion group elements) and K/Na, K/Na+K and Al/Ca+Na (alteration indices). This study has identified the presence of 8 further sites of hydrothermal activity and As-Sb enrichment which exhibit a multi-element chemical signature equal to, if not greater than that of the Glendinning deposit itself. These sites (fig. 221) include Black Syke (BS) the NNE extension to the mine area; Rams Cleuch (RC); Swin Gill (SG); Wisp Hill (WH); Philhope Loch (PL); Cat Rig (CR); Greatmoor Hill (GH); Rashigrain (R); The Shoulder (TS); Stibbiegill Head (SH); Stennies Water (SW); Linhope Burn (LB); Phaup Burn (PB); Meggat Water (MW) and Upper Stennies Water (US). Sites of As enrichment in mudstone as well as in greywacke samples, include: The Shoulder (TS), Stennies Water (S), Stibbiegill Head (SH), Linhope Burn (LP) and Phaup Burn (PB) (refer to fig 223 and 224). Grid references and element signatures relating to these sites are given in tables 1.37, 1.38 and 1.39.

Ba

Barium is relatively consistent throughout the survey area, generally increasing in the southeast (figs. 171 and 201). Greywackes display a restricted range of values compared with mudstones. Anomalous Ba values correlate well with zones of arsenic enrichment, particularly in greywackes. Note the N-S orientated zone of Ba anomalies displayed on the contour map, extending from Swin Gill in the south, through to Rashigrain and The Shoulder, in the north. The presence of low grade Pb-Zn-Ba mineralization in this zone is the most probable source of Ba enrichment observed in a small number of samples (max: 912ppm Ba) unrelated to, but occasionally superimposed upon As-Sb-Au mineralization in the survey area, due to the continued use of the same structural controls and fluid pathways.

Cl

Elevated Cl values are located in both the northern and southern sections of the survey area while centrally there is a broad belt of relatively restricted values (figs. 172 and 202). Slightly elevated Cl values are associated with the Glendinning Mine, Swin Gill, Rams Cleuch, Wisp Hill, and the Philhope Loch areas. Problems of Cl contamination during sample preparation invalidate use of this data in geochemical modelling

Co

Co values on the greywacke geochemical map (fig. 173) are highly consistent and there is a strong systematic variation within the study area. Although Co values display a restricted range (11-66ppm) anomalous values may be positively correlated with arsenic enrichment and areas of hydrothermal activity. Individual sites of Co enrichment include Glendinning, Black Syke, Swin Gill and Rams Cleuch. The trend towards high Co values throughout all samples collected within Stennies Water, to the east of the mine area is as yet unexplained, however it does result in the development of a major anomaly zone in the south western corner of the contour map. Co values within mudstone (fig. 203) display a slightly enlarged compositional range (13-76 ppm) as opposed to their interbedded greywacke counterparts (range 11-66ppm). Anomalous Co values correlate with zones of arsenic enrichment, with maximum values contained within the central portion of the survey area, in proximity to the Rams Cleuch, Cat Rig, The Shoulder and Rashigrain anomaly zones. Other sites of Co enrichment, outwith this central zone, include Black Syke and Phaup Burn.

Cr

As observed within the Southern Uplands Study Area, the distribution of Cr values is directly related to the proportion of detrital Cr-bearing mineral phases present within the sample (ie. ferromagnesian minerals, detrital chromite, and mafic lithoclasts). Within the Glendinning study area both greywacke and mudstone (figs. 174 and 204) display similar, highly consistent values; a small, relatively restricted range composition (49-290 ppm) and no systematic spatial relationship with either stratigraphic or mineralization related trends. Mudstones display a much narrower range of compositions (100-188ppm) than their interbedded greywacke counterparts, with the maximum values spatially concentrated in a strike parallel belt, occupying the northwestern half of the survey area. No mineralization related trends are observed.

Cu

Copper within greywacke lithologies (fig 175) exhibit relatively consistent values over a small range (7-70 ppm) as opposed to more variable, elevated levels in mudstones (fig. 205). Although, anomalous values in both rock types correlate with zones of As enrichment, only two of the eight sites identified above (Wisp Hill and Rashigrain) which contain a mineralized or hydrothermally altered geochemical signature could be identified by anomalous copper values. In addition, however a number of isolated Cu anomalies occur throughout the survey area unrelated to either As-Sb-Au or Pb-Zn-Ba phases of mineralization (see fig. 221). Copper values in mudstones exhibit relatively variable values over the range (5-109ppm) as opposed to the more static, lower levels displayed by greywackes. A small number of Cu anomalies are grouped in the central portion of the study area (similar in spatial distribution to the trend identified by Co anomalies in Fig.203). It was observed that anomalous Cu values may correlate with zones of As enrichment. In particular, five sites (Black Syke, Stennies Water, The Shoulder, Rashigrain and Greatmoor Hill) containing a mineralized multielement geochemical signature are also identified by anomalous copper values. In addition, a number of isolated Cu anomalies are identified, unrelated to either As-Sb-Au or Pb-Zn-Ba geochemical anomalies, and are attributed to the widespread occurrence of low grade Cu-dolomite vein mineralization in this region.

Ga

Highly consistent Ga values are displayed by both lithologies within the survey area (figs. 176 and 206). Greywackes exhibit an extremely narrow range of values (6-24ppm) somewhat lower than the mudstones (7-36 ppm) and display no spatial or mineralization related variation.

La

La defined on the point source geochemical maps (figs. 177 and 207) display consistent values and a relatively systematic pattern of variation. Although these values display a restricted range (12-56ppm) they are positively correlated with mineralization related elements such as As and Sb. Individual sites of major La enrichment include: Glendinning, Swin Gill, Wisp Hill Rashigrain and Rams Cleuch. In addition, the contour plot displays the presence of a strike parallel belt containing elevated La values, crosscutting the contour map in a NE-SW direction. In general, mudstone values display an increase in background values (range 28-60ppm) compared with their coarser grained counterparts. Subtle enrichments of La correlate with arsenic enrichment and anomalies of other mineralization related elements such as Sb, S, K, Cu, Pb and Rb. Elevated La values are concentrated in the vicinity

of the Glendinning and Black Syke locations, with additional anomalous values are located in the vicinity of both Rams Cleuch and Phaup Burn anomaly zone.

Ni

As observed within the Southern Uplands Study Area, the distribution of Ni values is related to both Cr and Fe values. Within the Glendinning study area Ni values (fig. 178a) exhibit a small, restricted range of composition (12-100 ppm) and display a subtle association with mineralization. Anomaly sites identified containing elevated Ni levels include: Black Syke, Wisp Hill, Phaup Burn, Greatmoor Hill, Rams Cleuch, Cat Rig and Rashigrain. In mudstone lithologies (fig. 208) Ni values exhibit an increase in background values (range 0-222ppm) compared with their coarser grained counterparts and display a subtle association with As enrichment and mineralization. Elevated Ni values are concentrated within a strike parallel belt occupying the northwestern half of the survey area. Within this belt, anomaly sites containing elevated Ni levels include: Black Syke, Rams Cleuch and The Shoulder. In addition, note the N-S orientation of Ni anomalies in the central portion of the survey area and the concentration of minor anomalies immediately SW of the Glendinning deposit.

Nb

Highly consistent Nb values defined on the point source geochemical maps (figs. 178b and 209) display a relatively cryptic pattern of variation within the study area and display a restricted range (4-37ppm). In general the maximum Nb values are located in the northern section of the survey area, however the contour plot displays the presence of a strike parallel belt containing elevated Nb values in the central portion of the diagram, which crosscuts the map in a NE-SW direction. In mudstone lithologies Nb displays a slight increase in background levels (minimum 10ppm) in comparison with their interbedded greywacke counterparts (minimum 4ppm). Both lithologies are weakly correlated with mineralization related elements (As/Sb) and positively correlated with Zr, La, Th, Na, K and Rb.

Pb

Highly consistent background levels are displayed by both greywacke and mudstone lithologies (figs. 179 and 210). Anomalous Pb values are defined on both maps and display a close correlation with both arsenic and copper enrichment. Although these values display a restricted range (0-53ppm) individual sites of Pb enrichment within the survey area are clearly identified and mirror a number of locations defined as As anomalies in fig.170. These sites include: Swin Gill, Rams Cleuch, Cat Rig, Stennies Water, The Shoulder, Linhope Burn, Phaup Burn and Philhope Loch. Mudstone values display an enlarged compositional range (5-209ppm) in comparison with their interbedded greywacke counterparts. Note the similarity and relative position of the centres of mineralization highlighted on both As and Pb contour plots and the N-S orientation of anomalies in the central portion of the study area.

Rb

In greywacke lithologies (fig. 180) Rb values display a relatively restricted range of values (15-136ppm) with anomalous values correlating with zones of arsenic enrichment. Although Rb values in mudstones (fig. 211) are considerably enriched (64-182 ppm) in comparison with their coarser grained counterparts, they appear less sensitive to the effects of As enrichment and hydrothermal alteration. A number of individual sites of Rb

enrichment within the survey area mirror anomalous As-rich locations (refer to fig.170). These sites include: The Glendinning Mine area, Swin Gill, Rams Cleuch, The Shoulder, Phaup Burn and Philhope Loch. The concentration of minor values to the immediate SW of the Glendinning deposit should be noted together with the general NNE-SSW orientation of Rb anomalies crosscutting the Glendinning deposit on the contour plots.

Sr

Sr display a generally consistent values throughout the survey area. In general, mudstone lithologies display systematically lower values (20-278 ppm) than their coarser grained counterparts. Spatially, Sr values correlate with both Ca and Mn values and display an inverse relationship with Rb, Al, Ti, Ni, V and K throughout the survey area. Note the general depletion envelope surrounding both the Mine area and Swin Gill anomaly zones.

Sb

The Louisa Mine at Glendinning formed a historically important source of antimony (stibnite) and was one of only two such mines in Scotland. Despite historical exploration activity in this region the Glendinning deposit was regarded prior to this study as a single isolated example of this form of turbidite hosted Sb-mineralization. Antimony (Sb) forms the main pathfinder element for quartz hosted stibnite mineralization and also acts as a secondary guide to gold mineralization in this area. Background levels of 0-2ppm may be used to infer that detectable values (>5ppm) define areas of hydrothermal Sb input and proximity to mineralization. Individual sites of Sb enrichment within the survey area are clearly identified and mirror a number of locations defined as As anomalies in fig.170. No apparent variation in background levels between mudstone and greywacke are observed, unlike those displayed by arsenic. This feature may be explained by the relative pervasive nature of arsenic as opposed to antimony mineralization and/or the transgressive, crosscutting nature of Sb emplacement. Note the similarity and relative position of the centres of mineralization highlighted on both As and Sb contour plots. Despite the low levels of Sb in regional greywacke and mudstone samples, this evaluation details the presence of 8 further sites of hydrothermal activity and As-Sb-Au enrichment, up to 10km from the mine area. The anomaly sites located by this study are identified within in fig 221-223 and include: Black Syke (BS); Rams Cleuch (RC); Swin Gill (SG); Wisp Hill (WH); Cat Rig (CR); Great moor Hill (GH); Rashigrain (R); The Shoulder (TS); Phaup Burn (PB); Stibbiegill Head (SH); Stennies Water (SW); and Linhope Burn (LB). The contour plot clearly illustrates the isolated nature of the zones of Sb enrichment and hydrothermal activity. A number of additional sites have been located which exhibit evidence of alteration and/or weak mineralization. These sites, together with their respective grid references and element signatures are detailed in tables 1.37-1.39. It should be noted that although no direct spatial orientation of Sb anomalies is defined by these plots, both the Rams Cleuch Swin Gill and The Shoulder/Rashigrain anomaly zones are contained within a relatively narrow N-S or NNE-SSW trending zone. Note the relatively small geochemical signature of the Glendinning-Swin Gill anomaly zone and compare this with both the Wisp Hill, Stennies Water, Rams Cleuch, Rashigrain and Phaup Burn anomaly zones.

S

Although sulphur displays a wide range of values (0-2755 ppm) a comparison with greywacke samples collected from other formations in the Southern Uplands indicates that background values are remarkably low (mean 48ppm) within the Study Area (Hawick Formation). The maximum sulphur concentrations are located within a relatively narrow, strike parallel belt, along the south eastern margin of the survey area. The strong spatial association between sulphur values and As anomalies, is best exemplified within the Black Sike, Swin Gill and Rams Cleuch

zones. Sulphur values in mudstone samples display a relative restricted range of composition (0-592ppm) in comparison with their greywacke counterparts. Anomalous levels of sulphur define areas subjected to the effects of sulphidation associated with hydrothermal alteration and As enrichment. These include: Swin Gill, Rashigrain, The Shoulder, Phaup Burn and Rams Cleuch. The concentration of anomalous sulphur values in the tributaries of the Swin Gill zone, at the southern margin of the study area should also be noted.

Th

A highly consistent pattern of Th values occur throughout the study area. Mudstone lithologies (fig. 215) display minor enrichments in composition (range 0-30ppm) compared with their interbedded greywacke counterparts (fig. 184). Slightly elevated Th levels occupy a strike parallel belt on the northwestern flank of the survey area. However, no direct relationship with hydrothermal alteration or As-Sb-Au mineralization is displayed.

V

Vanadium displays highly consistent values throughout the survey area. A minor increase in concentration occurs within the mudstone lithologies, and minor enrichments correlate directly with increases in Th content. Maximum V levels are concentrated in a strike parallel belt on the northwestern flank of the survey area. In general vanadium enrichment is inversely correlated with Ca, Sr and Sb, however a subtle enrichment in V values occurs in proximity to the Glendinning mine area.

Y

In both greywacke and mudstone lithologies (figs. 186 and 217) Y displays highly consistent values throughout the survey area with minor enrichments mirroring those of Th and V. The variation in Y composition closely follows that of V and values are inversely correlated with Ca, Mn and Sr. In addition a weak inverse relationship between Y and mineralization related elements is observed within the study area, however the application of Y geochemistry in predicting areas of hydrothermal alteration and possible mineralization is extremely limited.

Zn

Zinc displays relatively consistent values in greywackes with slightly elevated levels in mudstone lithologies. Two differing relationships exist between zinc values and mineralization in this area (Duller and Harvey, 1983 and 1984): The first, a cryptic inverse relationship between Zn and As allows Glendinning type As-Au deposits to be characterised by subtle levels of Zn depletion within their wallrock; Whereas secondly, anomalous Zn levels pinpoint areas of low grade Pb-Zn mineralization which due to overriding structural controls, is often superimposed upon earlier phases of As-Sb-Au mineralization. Zinc depletion is by far the more pervasive of the two styles of anomaly and may be used to identify a depletion zone approximately 400m wide in the vicinity of the Glendinning deposit. Zn enrichment is characteristic of a number of As anomaly sites in the survey area including; Swin Gill, Rams Cleuch, Rashigrain, Cat Rig and The Shoulder. The N-S orientated zone of Zn anomalies located on the contour map, crosscutting the central portion of the survey area should be noted. Similar zinc depletion processes were located by Stone (1985) to the west of the Glendinning deposit in the Loch Doon area, where Zn depletion accompanied both As and Pb vein mineralization. In mudstone lithologies Zn displays slightly elevated levels (range 18-718ppm) in comparison with its interbedded greywacke counterparts. Zn enrichment is characteristic

of a number of As anomaly sites in the survey area including: Stibbiegill Head, Rashigrain, Cat Rig and The Shoulder whereas Zn depletion sites (see fig. 224) include: Glendinning, Upper Stennieswater, Swin Gill, Rams Cleuch, Wisp Hill and Phaup Burn.

Zr

Consistent Zr values are displayed in both greywacke and mudstones lithologies (figs. 188 and 219) throughout the survey area. A slight decrease in concentration is observed within the finer grained mudstone lithologies, however no evidence of mineralization related variation is observed. This feature may be explained due to the fact that the main host for Zr is zircon (ZrSiO_4), a detrital mineral, highly resistant to the effects of hydrothermal activity. Zr values are positively correlated with Ti, Th, Y and Nb and inversely correlated with Ca and Mn.

Tl

Over 95% of all samples analysed within the survey area contain Tl values below detection limits (1-2ppm). Of the remaining samples, Tl levels up to 7ppm were located within the Glendinning deposit, whereas values up to 17ppm were detected outwith the Mine area and define areas of considerable exploration, given their close association with As-Sb anomalies. Sites of Tl enrichment include: Rams Cleuch, Black Syke, Cat Rig, Wisp Hill, Philhope Loch and Rashigrain.

Summary

A summary of composite multi-element anomalies located within greywacke samples from the Glendinning Study Area is presented in fig. 221. Details of each individual site including name, grid reference and multi-element signature are presented in table 1.39. The most significant eight sites within this study area are identified by a one or two letter abbreviation and include: Glendinning (G); Black Syke (BS); Rams Cleuch (RC); Swin Gill (SC); Wisp Hill (WH); Philhope Loch (PL); Cat Rig (CR); Greatmoor Hill (GH); Rashigrain (R). A number of additional anomaly sites were identified in studies of mudstone geochemistry within this area and are presented in Fig. 223. The sites include: The Shoulder (TS); Stibbiegill Head (SH); Stennies Water (SW); Linhope Bum (LB); Phaup Burn (PB); Meggat Water (MW) and Upper Stennies Water (US). A summary of element depletion sites used to characterise the location of zones of hydrothermal activity in greywacke samples from the Glendinning Study area is presented in fig. 222. The location of sites of Na and Zn depletion are indicated by diamond and circle symbols, respectively. These maps clearly illustrate the extensive zone of sodium and zinc depletion in the Glendinning/Black Syke area; the zinc depletion at Swin Gill; and the extensive sodium depletion at Rams Cleuch.

A summary of composite multi-element anomalies located within mudstone samples collected from the Glendinning Study area is presented in fig. 223. Note the large number of single element anomalies contained within mudstone lithologies in direct contrast to the much smaller number of single element anomalies defined by greywacke samples (Fig. 221). Details of each individual site including name, grid reference and element signature are presented in tables 1.38 and 1.39. Mudstone depletion sites used to characterise the location of zones of hydrothermal activity are presented in fig. 224. The location of sites of Na and Zn depletion are indicated by diamond and circle symbols, respectively. Sodium depletion anomalies highlight the position of the Glendinning area and point to zones of hydrothermal activity to the southwest of the main mine area. As with the greywacke samples, zinc depletion is a characteristic of the Swin Gill, Phaup Burn and Rams Cleuch zones whereas sodium

depletion is located in the Wisp Hill, Linhope Burn, Stibbiegill Head, Meggat Water, and Upper Stennies Water and Stennies Water sites.

In summary, target areas of potentially economic arsenopyrite-gold mineralization may be detected by the recognition of visual, mineralogical and primary geochemical indicators of pervasive hydrothermal alteration. The use of major and trace element depletion holes may provide evidence for the existence of a hydrothermal activity and rapidly delineate target areas for further detailed studies. On the basis of the reconnaissance survey, eight target areas for priority follow-up surveys were identified and mineralization-related alteration was traced for approximately 1000m north of the Glendinning mine area.

3.6.4 Hydrothermal Alteration and Geochemical Discrimination

Hydrothermal alteration may be classified into five types, each characterized by particular mineral assemblages, alteration textures and spatial relationships to the vein mineralization. These include propylitization, intermediate argillic, advanced argillic, quartz-sericite and siliceous alteration styles. Geochemical halos are associated with distinct mineralogical zones that have developed out from the orebody in response to progressive decreases in intensity of alteration. These halos may persist from greater distances along primary or induced zones of permeability and porosity in the host rocks.

Element associations identified by correlation coefficients and lithogeochemical concentrations can be easily matched with petrographic and mineralogical observations relating to alteration. In particular the highest K_2O and Al_2O_3 values correspond with intense sericitisation. A substantial reduction in K/Rb ratios associated with altered samples suggests that the alteration may have been produced by fluids from a late magmatic source (Ambrust and Gannicott, 1980). A model for the development of the alteration zone may be created based upon the assumption of localised equilibrium conditions. Within an alteration sequence the width of alteration varies due to lateral changes in the physical parameters at the reaction fronts (ie porosity, fluid availability etc). On the basis of the geochemical study of the borehole samples it was clear that the alteration was highly pervasive and as no unaltered samples were intersected at the bottom of the four holes, this deposit may be regarded as open at depth.

Wallrock alteration and trace element dispersion patterns associated with the Glendinning deposit are both cryptic and laterally extensive. The comparison of altered and unaltered greywackes enables the geochemical effects of the hydrothermal ore forming fluid to be evaluated, the results of which are summarized in figure 89. Net additions resulting from hydrothermal interaction within the fluid conduit include major silica, arsenic, antimony, sulphur, lead, copper and nickel; minor enrichments of cobalt, potassium, strontium, rubidium, gold and thallium while sodium and zinc as well as subordinate iron and magnesium underwent depletion. The only grains that show no evidence of alteration or dissolution are the common ultrastable heavy minerals, including zircon, tourmaline and rutile. Within mineralized samples, TiO_2 , Zr, Y and Nb were shown to be relatively immobile during alteration by comparison with their unaltered counterparts. Many arsenic-gold deposits are surrounded by chemical alteration halos defined by anomalous abundances of various elements. These zones are spatially larger than their respective ore deposits and they provide a considerably enlarged target area.

The host rocks in the immediate vicinity of the deposit are marked by the development of distinctive chemical and mineralogical zones representing an outward gradation in alteration intensity. Chemical variation within samples of wallrock alteration are directly related to the relative intensity of alteration. Systematic variations such as those

observed within the Glendinning deposit may be inferred to reflect distance from the source of hydrothermal input and the pervasive nature of the alteration. The geochemical effects of the hydrothermal ore forming fluid upon greywacke geochemistry are summarised in figure 89. The geometry and size of any alteration zone is dependant upon the primary permeability, as well as the chemical reactivity of the rocks being altered. The permeability of the host rocks is one of the most important physical parameters affecting the hydrothermal fluid and is therefore an important control on hydrothermal alteration and trace element zonation.

The observed alteration effects are not confined to geochemistry alone. A visual indication of hydrothermal alteration takes the form of a progressive bleaching of the greywacke, up to areas adjacent to the main fluid conduits. Samples (Plate 38) from the Glendinning area typify this effect, moving from unaltered dark-grey greywacke through to pale grey greywacke marginal to mineralization. This bleaching effect can, and has been recognised within the regional survey area, and has proved extremely useful in pre-locating geochemically anomalous zones. The salient chemical changes associated with alteration of greywacke, are major additions of Sb, As, S and volatiles, which correspond to the precipitation of metal sulphides and the formation of hydrated silicates such as sericite. In addition, Fe, Mg and Na have been removed, whereas K was added and represents the hydrolysis of feldspar and biotite, to muscovite and clay minerals. The alteration envelope is characterised by Na, Zn, Fe and Mg depletion and As, Sb, Pb enrichment. Because these depleted patterns occur within samples, displaying obvious hydrothermal mineralogy, the depletion is attributed to alteration produced by hydrothermal overprinting.

It was evident that extensive fracturing and brecciation of the wallrock to the vein mineralization had occurred. Field relations suggest that the major N10°E trending fault structures in the Glendinning deposit formed the major fluid conduit for all episodes of hydrothermal activity, alteration and mineralization. The morphology of this deposit is reinterpreted in terms of a fracture related elongate breccia pipe and associated stockwerk zone (Fig.88). The spatial relationships between the various alteration types are envisaged as an elongate halo grading outward from the quartz-stibnite veining to unaltered greywackes. Argillic alteration may host stibnite, but this is always fracture controlled and clearly later than the arsenopyritization. Although the hydrothermal fluids were initially weakly acidic, it is suggested that they became neutral or slightly alkaline by reaction with wallrock.

The scale and intensity of changes in the chemistry of the host rock is a function of the genesis of the ore, the chemistry of the host rock, and the nature of secondary processes (Govett and Nichol, 1979). These chemical and mineralogical changes are associated with and envelope the ore zones, and provide an enlarged target for mineral exploration, of significantly greater width than the vein mineralisation. Bailey and McCormick (1974) noted that wallrock alteration halos may enlarge the target area for a vein deposit by a factor >10. The depletion envelopes associated with the Glendinning deposit define an approximate symmetrical halo which is 2-3 orders of magnitude wider than the vein system. Gold exploration in the Glendinning area is still in its early stages and the search for additional centres of hydrothermal activity is continuing. Only by a detailed and systematic study of each mineralization centre can the full potential of this region be properly assessed.

Geochemical Distribution

The distribution of major and trace elements in greywackes and mudstones from the regional study area and mineralised drillcore from the Glendinning deposit are displayed in a series of histograms in Figs. 32, 33 and 34. Bar diagrams displaying this variation in detail are presented in figs. 35a to 45b: A general increase in Si, Al, K,

Mn, As, Co, Cu, La, Ni, Pb, Rb, Sr, Sb, S, Th, and Tl, and decrease in Fe_2O_3 , MgO , Na_2O and Zn composition was identified in altered samples with respect to their unmineralized counterparts. In general, the mudstone lithologies are lower in SiO_2 , CaO and Na_2O ; and higher in Ti, Al, Fe, K, Rb, Ba, $\text{Al}_2\text{O}_3/2\text{Na}_2\text{O}$ and $\text{K}_2\text{O}/\text{Na}_2\text{O}$ when compared to their interbedded greywacke counterparts, reflecting the increased abundance of clay minerals. As Ga substitutes for Al, it follows that Ga should be preferentially concentrated in the finer grained clay-rich fraction of the sediments, a feature clearly displayed in the Glendinning mudstone samples. In addition, both Ba and Rb correlate with and follow the distribution of K in clay minerals.

Sulphidation is observed to have formed a major process during alteration and has imposed considerable enrichments in both greywacke and mudstone samples. Altered greywacke samples are enriched in sulphur by a factor of 100% compared to their altered mudstone equivalents inferring that greywacke lithologies were considerably more susceptible to this process of alteration. Although a slight increase in minimum V content is observed between greywacke and altered greywacke samples no major changes in V content can be directly attributable to the mineralizing processes. A minor increase in average altered greywacke composition is counterbalanced by decreases in altered mudstone composition. Although characteristic decreases in maximum Zr contents are observed in both altered greywacke and mudstone samples the average composition is relatively unaffected by alteration and although possibly affected by minor dilution effects, Zr has remained immobile during the mineralization processes. It is important to note that zinc unlike other base metals displays a major depletion effect associated with altered greywacke (mean 30ppm) and mudstone (mean 60ppm) samples. Although the maximum Zn content in greywackes is highly enriched (max 2000ppm) this value may be due to the incorporation of sphalerite (ZnS) in the sample.

A summary diagram detailing the geochemical net additions and depletions within the wallrocks adjacent to the vein mineralisation at Glendinning is presented in fig. 89. In general, all chalcophile elements are enriched during the alteration processes, whereas lithophile elements exhibit varying degrees of depletion. It should be noted that the Glendinning mineralisation is also characterised by slight increases in both CO_2 and volatile components. The depletion of Zn and Na_2O coupled with the levels of trace element enrichment defined previously, provides a chemical fingerprint for the location and identification of Glendinning type deposits in this terrane.

Discrimination Diagrams

This section details the results of the application of a number of different forms of discrimination diagram to the Glendinning regional and mineralised datasets and display the major chemical characteristics of greywacke, mudstone and hydrothermally altered samples. Following the classification scheme defined by Blatt et al., (1972) and Crook (1974) samples from the Glendinning regional study area within the Hawick Formation (fig. 77) may be classified as Fe-rich, quartz rich greywackes/lithic sandstones. Total alkali contents extend outwith the field defined by Maynard et al., (1982) for Lower Palaeozoic greywackes. The majority of values are emplaced above the $\text{Na}/\text{K}=1$ threshold, indicative of a major increase in K_2O content, resulting from the cratonic nature of these sediments. In addition, the effects of hydrothermal alteration within the Hawick Formation samples may be directly correlated with Na depletion. Using a $\text{Na}_2\text{O}=1.0\%$ depletion threshold, sixteen samples may be immediately identified as altered and subjected to detailed study. Mudstone samples from the Hawick Formation (fig. 78) demonstrate a positive enrichment in K_2O content with respect to their coarser grained counterparts. The total alkali diagram demonstrates a clear inverse relationship between Na_2O and K_2O contents which extend outwith the field defined by Maynard et al. (1982) for Lower Palaeozoic greywackes. All values are emplaced above the $\text{Na}/\text{K}=1$

threshold. The effects of hydrothermal alteration and Na depletion may be directly assessed using a $\text{Na}_2\text{O}=0.8\%$ depletion threshold. Mineralized samples from the BGS Glendinning boreholes (fig. 79) demonstrate the major effects of Na depletion associated with hydrothermal alteration upon the host rock geochemistry. Sample populations in both plots illustrate the virtually complete removal of Na from all samples and justifies the use of Na depletion in the identification of hydrothermally altered samples in the regional sample set.

The SiO_2 vs Al_2O_3 diagram (fig. 46a) provides a chemical classification to differentiate between mudstone and greywacke samples from the Glendinning regional study area. The discrimination boundary is defined on the basis of a 95% significance level. The SiO_2 vs Fe_2O_3 diagram (fig. 46b) clearly demonstrates the chemical differentiation of mudstone and greywacke samples on the basis of major element composition. Particularly noteworthy in the SiO_2 vs Na_2O diagram (fig. 46c) is the differentiation between greywacke and mudstone, and the effects of hydrothermal fluids on upon both lithologies, namely the sodium depletion associated with wallrock alteration. The SiO_2 vs K_2O diagram (fig. 46d) details the increased potassium content of mudstone samples which is interpreted as reflecting an increased clay mineral content. The IUGS Silica-Total Alkalii diagram (fig. 304) displays the position of cratonic derived Hawick Formation greywackes from the Glendinning regional study area, and illustrates the relatively narrow, restricted range of total alkalii content which displays a weak positive correlation with silica values. Silica values (fig. 303) have been systematically depleted by the introduction of carbonate detritus and are located within the basaltic-andesite and andesite fields. Mineralized Hawick Formation greywackes from the Glendinning deposit are also presented in this format in fig. 305, where values are concentrated in the basaltic-andesite and andesite fields, and display a decrease in minimum and increase in range of alkalii values compared with their unmineralized counterparts. In addition, a small subset of samples are located within the dacite field ($\text{SiO}_2 > 61\%$) which indicate silica enrichment (silicification) together with major alkalii depletion (dickitisation) within this deposit. The SiO_2 vs Sr diagram (fig. 46e) clearly illustrates the addition of strontium to both greywacke and mudstone samples and provides a discrimination between individual lithologies as well as cryptic mineralisation. The SiO_2 vs CaO diagram (fig. 46f) clearly illustrates the relationship between these elements in both greywackes and mudstones and may be used to chemically differentiate between the two lithologies. The SiO_2 vs V diagram (fig. 47a) displays an increased vanadium content in mudstones which correlates well with similar increases in both potassium and alumina contents, thereby inferring a clay mineral host for this element.

The Al_2O_3 vs TiO_2 diagram (fig. 47a) may be used to differentiate between greywacke, mudstone and hydrothermally altered equivalents, due predominantly to potassium metasomatism in wallrock samples. The Al_2O_3 vs Na_2O diagram (fig. 47b) may be used to distinguish between altered and unaltered lithologies and provides a further discrimination diagram for use in pinpointing cryptic mineralization. The Al_2O_3 vs K_2O diagram (fig. 47d) demonstrates the clear linear relationship between Al and K content, thus inferring a clay mineral association. Mudstone and greywacke samples may be clearly differentiated by the relative abundance of these two elements (ie. their relative clay content). In the Al_2O_3 vs MgO diagram (fig. 47e) the effects of magnesium depletion in wallrock samples is superimposed upon the linear relationship between alumina and magnesium in all unmineralized samples. The Al_2O_3 vs CaO diagram (fig. 47f) clearly illustrates the combination of clay mineral alteration and increase in CaO content (predominantly as carbonate) within altered samples. In the Al_2O_3 vs FeO (fig. 48a) the effects of iron depletion in hydrothermal alteration, superimposed upon the linear relationship between Al and Fe in all unmineralized samples. The Al_2O_3 vs Co diagram (fig. 48b) displays the uniform levels of cobalt in both greywacke and mudstone samples and identified the sporadic nature of cobalt enrichment associated with mineralized samples. The Al_2O_3 vs Sr diagram (fig. 48c) clearly illustrates the combination of clay mineral

alteration and increase in strontium content associated with wallrock alteration processes. The correlation between strontium and CaO infers a close mineralogical association and as such it is proposed that the predominant host mineral for Sr is CaCO_3 . In the Al_2O_3 vs Rb diagram (fig. 48d) a linear relationship between alumina and rubidium is displayed with threshold values between greywacke and mudstone lithologies controlled by clay mineralogy (as identified in figs. 47d and 48a).

The TiO_2 vs Fe_2O_3 diagram (fig. 48e) clearly displays a linear relationship between titanium and iron in both greywacke and mudstone samples whereas the TiO_2 vs Na_2O diagram (fig. 48f) may be used to differentiate between greywacke and mudstone samples together with the effects of wallrock alteration processes. The TiO_2 vs K_2O diagram (fig. 49a) provides a suitable means for discriminating between greywacke, mudstone and wallrock alteration samples, with an increase in K content relative to Ti in the altered sample suite. TiO_2 vs MgO diagram (fig. 49b) illustrates the approximate linear relationship between titanium and magnesium in both greywacke and mudstone lithologies and the effects of magnesium depletion associated with the alteration processes. In the TiO_2 vs CaO diagram (fig. 49c) an inverse linear relationship between titanium and calcium contents is displayed, with the highest titanium values occurring in mudstone lithologies. The TiO_2 vs Rb diagram (fig. 49d) clearly illustrates the addition of rubidium during hydrothermal alteration of both lithologies. In the TiO_2 vs V diagram (fig. 49e) a linear relationship between titanium and vanadium in both lithologies is clearly identified, possibly inferring a similar host mineral.

The Fe_2O_3 vs Na_2O diagram (fig. 49f) illustrates a direct relationship between iron and sodium content of both greywacke and mudstone lithologies. The greywacke samples are relatively enriched in sodium compared to their finer grained counterparts however the iron content of mudstones is considerably enriched in preference to greywacke samples. Note the pronounced effects of sodium depletion associated with hydrothermal alteration. In the Fe_2O_3 vs K_2O diagram (fig. 50a) a linear relationship between Fe and K is displayed together with the combined effects of potassium enrichment and iron depletion upon the wallrock alteration suite of samples. In addition, the Fe_2O_3 vs MgO diagram (fig. 50b) Note the approximate linear relationship exhibited between iron and magnesium. This positive correlation is interpreted to reflect the nature of a joint parent mineral. The Fe_2O_3 vs CaO diagram (fig. 50c) displays an inverse relationship between iron and calcium, similar in many respects to that displayed in fig. 49c between titanium and calcium, and illustrates a decrease in Ca content with grain size. In the Fe_2O_3 vs Cr diagram (fig. 50d) an apparent linear relationship is displayed between iron and chromium inferring a possible host mineral association. Sporadic high concentrations of Cr in greywacke samples is inferred to result from the inclusion of a separate, possibly monomineralic source, such as detrital chromite grains. The Fe_2O_3 vs Rb diagram (fig. 50e) illustrates the strong positive correlation between iron and rubidium and the effects of iron depletion and rubidium enrichment in the alteration suite. The Fe_2O_3 vs Sr diagram (fig. 50f) displays an apparent inverse relationship between iron and strontium reflecting a similar trend to that observed with calcium and thereby reaffirming the mineralogical association of both calcium and strontium. The Fe_2O_3 vs Sb diagram (fig. 51a) display generally low levels of antimony (<3ppm) in all unaltered lithologies and the lack of a significant correlation between antimony and iron enrichment in wallrock samples. The Fe_2O_3 vs Zr diagram (fig. 51b) displays the increased variation in Zr content in greywacke samples as opposed to their mudstone equivalents (inferred to be due to variances in grain size distribution) and exhibits a sharp cutoff between the two lithologies on the basis of iron content.

The Na_2O vs K_2O diagram (fig. 51c) illustrates an inverse relationship between sodium and potassium content. Potassium enrichment in the finer grained lithologies is attributed to an increase in the proportion of clay minerals, whereas sodium enrichment appears concentrated within the coarse grained fraction of the sample population and is interpreted as representing an increase in detrital feldspar content. In the Na_2O vs Cu diagram (fig. 51d) a general increase in abundance of copper is noted within the mudstone lithologies and is attributed to the scavenging effects of clay minerals. Here again, the effects of sodium depletion and minor copper enrichment are displayed in the hydrothermally altered samples. The Na_2O vs Co diagram (fig. 51e) displays a narrow range of cobalt composition in both lithologies and the effects of minor cobalt enrichment during hydrothermal alteration. In the Na_2O vs Cr diagram (fig. 51e) an approximate bimodal relationship between sodium and chromium is displayed. A simple inverse relationship between both lithologies is overprinted by a range of high chromium values concentrated in greywacke lithologies and interpreted in terms of detrital components. In the Na_2O vs Ni diagram (fig. 52a) displays an inverse linear relationship between sodium and nickel and the effects of hydrothermal alteration. The Na_2O vs Rb diagram (fig. 52b) clearly illustrates the inverse relationship between sodium and rubidium and the effects of Na depletion and Rb enrichment in altered samples. In the Na_2O vs Sr diagram (fig. 52c) an approximate linear relationship between sodium and strontium is displayed in both greywacke and mudstone lithologies, together with the effects of Sr enrichment and Na depletion in wallrock samples.

The CaO vs Rb diagram (fig. 52e) may be used to clearly differentiate between greywacke, mudstone and hydrothermally altered material. Wallrock alteration is identified by enrichment of both calcium and rubidium. In the CaO vs V diagram (fig. 52f) a general inverse relationship between calcium and vanadium is defined with elevated vanadium values concentrated predominantly within the finer grain lithologies. The MgO vs Na_2O diagram (fig. 53a) displays a preferential concentration of magnesium values in finer grained lithologies, together with the effects of both sodium and magnesium depletion in altered samples. The MgO vs Rb diagram (fig. 53b) illustrates the linear relationship between magnesium and rubidium, the increased values of both elements present in finer grained sediments and the profound effects of magnesium depletion and rubidium enrichment in hydrothermally altered samples. In the MgO vs V diagram (fig. 53c) the linear relationship between magnesium and vanadium is displayed, together with the limited effects of magnesium depletion on the sample population. The MgO vs Ga diagram (fig. 53d) displays an approximate linear relationship between magnesium and gallium in both lithologies and displays the effects of magnesium depletion during alteration. In the MgO vs Ni diagram (fig. 53e) a linear relationship between nickel and magnesium content is identified in both lithologies with the highest values present in the finer grained sediments.

The K_2O -Rb diagram (fig. 382) displays the relative position of cratonic derived Hawick Formation greywackes and their mineralized equivalents obtained from boreholes through the Glendinning As-Sb-Au deposit. A narrow compositional trend and strong positive correlation is displayed by unmineralized Hawick Formation samples. Elevated levels ($>3\text{wt}\%$ K_2O and $>100\text{ppm}$ Rb) and expanded range are displayed by hydrothermally altered samples from the Glendinning deposit. The positive correlation displayed between K_2O and Rb is formed as a result of strong mineralogical control, with clay minerals (potassium aluminium silicates) forming the main host to Rb values. The $(\text{K}/\text{K}+\text{Na})$ -($\text{K}+\text{Na}$) diagram (fig. 365) also displays the relative position of cratonic derived Hawick Formation greywackes and their mineralized equivalents. A narrow $\text{K}+\text{Na}$ range of values is displayed by unmineralized Hawick Formation samples, whereas a small subset of altered samples is defined by $\text{K}/\text{K}+\text{Na}$ values in excess of 75-80% and/or $\text{K}+\text{Na}$ values less than 3wt%. In addition, a marked concentration of mineralized samples occur in a narrow, elliptical field defined by $\text{K}/\text{K}+\text{Na}$ values in excess of 90%, which display the lowest

recorded total alkali content of any greywacke in the Southern Uplands. The K_2O vs Sr diagram (fig. 53f) clearly identifies an inverse relationship between potassium and strontium content in both lithologies and the effects of K and Sr enrichment during mineralization.

The Na_2O vs V diagram (fig. 54a) illustrates an inverse relationship between sodium and vanadium as a function of grain size. This trend is also observed with nickel, rubidium, potassium, iron, aluminium and copper when compared with their corresponding sodium values. In the Co vs Rb diagram (fig. 54b) a clear distinction between greywacke and mudstone lithologies is observed, together with the limited effects of cobalt enrichment during alteration. In the Cr vs V diagram (fig. 54c) a bimodal distribution of chromium values is displayed. The linear relationship between Cr and V is disrupted by a secondary population of high Cr values which has previously been interpreted as resulting from the inclusion of detrital chromite grains in greywacke samples.

The Cr vs Rb diagram (fig. 54d) identified a linear relationship between chromium and rubidium in both lithologies and displayed the enrichment of both elements in the finer grain samples. In the Cu vs Rb diagram (fig. 54e) a confined range of greywacke compositions is identified in comparison with the finer grained, mudstone lithologies. This diagram has limited use of in differentiating between altered and unaltered material. The Rb vs Sr diagram (fig. 54f) displays clear differentiation pattern between greywacke and mudstone geochemistry with rubidium and strontium inversely related and both subjected to enrichment during wallrock alteration. In the Rb vs V diagram (fig. 55a) a positive correlation between rubidium and vanadium is displayed by both lithologies, with the concentration of these elements in the finer grained (mudstone) lithologies. The Ni vs Rb diagram (fig. 55b) defines the linear relationship between nickel and rubidium in both lithologies. The effects of rubidium enrichment during alteration are also clearly illustrated. The V vs Zr diagram (fig. 55c) illustrates the narrow range of Zr content defined in both greywacke and mudstone lithologies, however the boundaries between the two sediments may be defined on the basis of vanadium content alone.

Principal Component Analysis

To aid the understanding of the complex relationships present within this geochemical data, principal component analysis was applied to both Hawick Formation greywackes and the individual lithologies present in Glendinning borehole sections. The principal component analyses and component scores are presented in tables 3.14 to 3.20. The geochemical associations defined by this study are discussed below:- three eigen vectors are presented, the first of which displays the chemical associations which account for the greatest proportion (approx.65%) of element variation in the dataset; the second and third account for significantly less of the total variation and are used to define more subtle associations superimposed upon the general background. In the Hawick Formation greywackes the following geochemical associations were identified:

Eigen vector 1: Ca-Sr, Sb-S-Pb-Co, Fe-Ti-K-Al-Rb-V-Ni, Mg-La-Cr-Nb-P, As-Ba-Cu-Zn, Si-Zr-P.

Eigen vector 2: Ca-Sr, As-Pb-S-Ba-Mg, K-Rb-Zn-Ni, Ti-La-Y-Nb, Co-Cr and Si-Zr-P.

Eigen Vector 3: Ca-Zr, Cu-Mn, Al-Y-Zn, K-Rb, As-Sb-S, P-Sr-Th-Fe, Ti-Na and Co-Cr.

In comparison, hydrothermally altered greywackes from Glendinning display the following associations:

Eigen Vector 1: Ca-Mn-Mg, Fe-Na, Y-Zr-Th, Nb-Cr, Sb-K-Ba, Si- Ti-La, As-S, Pb-Zn-Co-Ni.

Eigen Vector 2: Ca-Fe-Mg-Cr, As-Sb-S-Pb-Cu-Zn-Co-Ni- Na-S and K-Al-Rb-Sr-Ti-Nb-P.

Eigen Vector 3: Ca-As-Sb-S-Pb-Mg-V, Fe-K-Al-Rb-Ti, Si-P-Ti-Y.

These elemental groupings appear complex, however they may be interpreted by reference to their petrographic and mineralogical associations and classified in terms of alteration, sulphide, carbonate, ferromagnesian, silicic and accessory group members. It should be noted that the subtle mineralization group associations are defined within the Hawick Formation samples, formed in response to the presence of weakly altered samples within the regional dataset. The As-Sb-S association however, is not defined until eigen vector 3, thereby demonstrating the reduced influence of mineralization in the regional data set. Although similar element associations are defined in the siltstone, mudstone and 'breccia' lithologies from the Glendinning core, a strong As-Sb-S-Tl-Pb-Cu-Si association is particularly noteworthy in the breccia samples (eigen vector 1) as is a Na-Zn-Mg (depletion) association identified in all lithologies (eigen vector 1). In principal component studies of mineralized sample data from the Clontibret deposit, similar element associations were defined (table 3.15). In addition, both loss on ignition (LOI) and CO₂ were defined in close association with CaO, whereas gold (Au) occurs in association with As, Fe, Cu and Zn. In comparison with As-Sb-Au dominant deposits, a geochemical study of altered wallrock samples from the Susannah Vein at Leadhills reveals major differences in the nature of element associations characterised by the Pb-Zn-Cu vein mineralization (table 3.16). In particular, principal component analysis indicates that the As-Sb relationship dominant at Glendinning and Clontibret is replaced by As-Pb and Sb-Zn-Cu associations.

Discriminant Analysis

Grunsky (1986) demonstrated that the spatial presentation of lithogeochemical data combined with discrimination and clustering techniques can be used to delineate both geology, zones of alteration, and other lithogeochemically anomalous zones. Selinus (1983) detailed the application of factor and discriminant analysis to lithogeochemical data from central Sweden. Several different geochemical populations relating to distinct multi-element halos were distinguished. At the onset of this project it was proposed that discriminant analysis of the lithogeochemical data based upon the defined geochemical associations within the Glendinning deposit could be used to assess the significance of any target area prior to more detailed geological examination. Chemical analysis of 170 mineralized greywacke samples were statistically compared with ~2,000 regional samples. On the basis of this study a number of factors have been recognised, resulting from either the regional variation in rock chemistry or hydrothermal alteration. These factors may be used to aid the identification of sites containing hydrothermally altered and/or cryptically mineralized greywackes from regional sample sets.

Given 'a priori' knowledge of the geochemical characteristics of the mineralized area, discriminant analysis may then be used to isolate further anomalous zones. In this study, discriminant analysis was performed upon two groups; unmineralized Hawick Formation greywackes and As-rich greywackes from the Glendinning deposit, using four different classifiers (table 3.21). Classifier 1, included the total data set (31 variables) and gave an exceptionally good separation with only 1.7% of the total population misclassified. Further classification based upon relatively restricted variable sets including Na, K, As, Co, Ni, Pb and Zn (Classifier 2); Na only (Classifier 3); and Na+K (Classifier 4) resulted in a progressive increase in rate of misclassification (4.0%, 5.2% and 6.1% respectively). All the discriminant classifiers used in this study are effective in the classification of As-Sb-Au mineralization. However, the most successful results obtained to date using the largest number of variables (n=31), thereby inferring the complex inter-element relationships associated with hydrothermal alteration and mineralization. On a cost effective basis however, it is clear that a small subset of carefully selected elements (classifier 2) could provide similar levels of discrimination. As a sufficiently high proportion of the samples (>95%) are correctly classified, this technique may be applied to unknown samples from this region.

The results of simple discriminant analysis applied to both greywacke and mudstone lithologies from the Glendinning regional geochemical data set are presented in table 1.39. Threshold values were established, based upon simple mean + 2 standard deviations (enrichment) and mean - 2 standard deviations (depletion) levels for each lithology. In the Glendinning study area, simple discriminant analysis has revealed the following anomalous samples (prefixed by DJR):

Greywacke -	As :	063, 064, 066, 784, 785, 788, 863, 903, 946, 947.
	Sb :	053, 063, 064, 065, 066, 704, 785, 787, 788, 809, 863, 900, 903, 946.
	Cu :	006, 700, 712, 734, 809, 903.
	Pb :	003, 004, 021, 761, 768, 775, 787, 788, 858, 857, 893, 910, 936.
	Na ⁺ :	033, 049, 063, 064, 065, 066, 766, 785, 786, 787, 788, 858, 863, 888.
	Zn ⁺ :	010, 063, 066, 715, 731, 863, 886, 946.
Mudstone -	As :	1021, 1023, 1031, 1048, 1053, 1056, 1761, 1784, 1802, 1811, 1815, 1817, 1830, 1864, 1908, 1910, 1943.
	Sb :	1023, 1053, 1704, 1900, 1903, 1942.
	Cu :	1003, 1008, 1734, 1802, 1811, 1872, 1898, 1919, 1926, 1942.
	Pb :	1002, 1023, 1777, 1784, 1801, 1814, 1845, 1883, 1916, 1929, 1943.
	Na ⁺ :	1011, 1021, 1033, 1037, 1048, 1049, 1053, 1766, 1784, 1874, 1888, 1909, 1910, 1911, 1921, 1943.
	Zn ⁺ :	1010, 1011, 1049, 1057, 1791, 1815, 1851, 1900, 1950.

To aid the interpretation of the multivariate, bi-lithology data a simple numbering system was adopted which distinguished each site (and greywacke sample) with a 3 digit number (ie. 900), and identified mudstone samples from the same site by prefixing the site number with '1'. Thus, sample number 1900 represents a mudstone sample collected from an turbidite unit at sample position 900 and may be compared directly with its interbedded greywacke counterpart (sample 900). This simple attempt at 'codification' provided considerable benefits in both sample preparation, XRF and wet chemical analysis, data handling and interpretation. In general, two types of anomaly site are defined by this study; the first associated predominantly with greywacke anomalies, whereas; the second concentrated upon anomalies defined by mudstone lithologies only (figs 220-223). It is clear that in conjunction with the Glendinning deposit, the Black Syke, Rams Cleuch, Swin Gill and Wisp Hill Zones display very similar characteristics. Sb-Zn anomalies (with no arsenic enrichment or sodium depletion) are detailed in the vicinity of Greatmoor Hill and Rashigrain, whereas Pb-Zn anomalies are located near Philhope Loch and Cat Rig, respectively. Arsenic anomalies which occur in mudstone lithologies only, have been detected in five locations; At Stennies Water and Linhope Bum, arsenic enrichment is associated with sodium depletion only, whereas; at both The Shoulder and Stibbiegill Head an additional zone of Cu-Pb-Zn anomalies are superimposed upon the arsenic rich zones. In both Meggat Water and Upper Stennies Water, combined Na+Zn depletion zones were defined which lack any apparent form of metal enrichment. Although these sites have a relatively low priority in any follow-up study of this area, these two sites should still be evaluated as the Na+Zn depletions indicate the presence of hydrothermally altered samples (Outer Zone 1) and infer the close proximity of As-Sb mineralization. In summary, multi-element geochemical studies in the Glendinning Regional Project area have pinpointed several new sites of As-Sb-Au mineralization, and numerous primary target areas for further evaluation. In addition, this study has detailed the presence of an additional Pb-Zn-Cu phase of mineralization, quite separate, although occasionally superimposed upon the As-Sb-Au target.

This study demonstrates that although successful discrimination can be made using certain covariance element relationships (eg. Ba/Rb, Zr/Rb) it is clear that the application of discriminant analysis to the analytical data guarantees >95% success in separating the barren and the ore-bearing groups. From the results of the discriminant analysis, the following elements, As, Sb, Pb, Na, Zn and Mg were found to be most useful in distinguishing the altered from the unaltered greywackes. As such, it is recommended that discriminant analysis should be utilized during the orientation survey stage of a lithogeochemical exploration program. This allows an optimum set of pathfinder elements to be chosen from the multi-element analyses carried out on a relatively small sample populations thereby avoiding the subsequent analyses of hundreds or thousands of rock samples for variables that prove to be ineffective in defining geochemically anomalous rocks. In summary, the results of this comparison showed that As, Sb and Pb provide the best anomaly contrast, together with Na and Zn depletion. Simple ratios including K/Na, Fe/Mg, Rb/Sr although identifying sites of potential mineralization failed to extend the anomaly width defined by individual elements. The readily identifiable geochemical halos associated with the Glendinning deposit, may be used to infer that As, Sb, S and Na₂O form the best combination of elements to use in further lithogeochemical exploration. Geochemical evidence points to at least eight centers of mineralization and hydrothermal activity in the Glendinning study area. The exploration significance of all geochemical anomalies in the Glendinning area has not been established, however their multi-element geochemical signature, is indicative of probable undiscovered mineralization. In addition, it should be noted that this study has revealed similar anomalous patterns related to As-Sb-Au mineralization in the Leadhills, Loch Doon and Cairngarroch Bay areas.

3.7 SOIL GEOCHEMISTRY

3.7.1 Overview

The aim of the initial lithogeochemical reconnaissance survey in the Glendinning region was to determine the mineral potential of a relatively large area (200 sq km) eliminate barren ground and draw attention to local areas of interest. These studies identified a number of target areas containing a mineralized geochemical signature which have been investigated in order of decreasing magnitude. The three major anomalous areas, Rams Cleuch, Swin Gill and Black Sike provided priority targets for further exploration. In order to establish the extent of the identified lithogeochemical anomalies this study was then extended to a second stage follow-up study including field investigation, soil sampling and geochemistry and reconnaissance panning. Subsequent to lithogeochemical survey heavy mineral separates were collected from the Glendinning, Swin Gill and Rams Cleuch areas and examined by binocular reflected light microscopy. Both stibnite and realgar were identified in all three locations, providing evidence for the location of new As-Sb mineralization in this region; the importance of mercury; and the possible genetic association between As-Sb-Au and Hg.

Arsenic anomalies at Black Sike occur approximately 1km along strike from the mine workings at Glendinning. A detailed site investigation indicated the presence of an ~400m wide zone of hydrothermal alteration/bleaching, similar to that associated with both the Glendinning and Clontibret Sb-As-Au deposits. XRD studies of gossans from Black Syke identified limonite and quartz as the dominant phases, with accessory constituents, including a variety of sulfates, arsenates, carbonates, silicates, and clay minerals (predominantly dickite). Given the high correlation between overburden geochemical anomalies and subcropping mineralization at Glendinning it was proposed that shallow soil sampling would prove the most appropriate technique for detailed site investigation of the Swin Gill and Rams Cleuch target areas. As such, two follow-up geochemical soil sampling programs were

undertaken on a grid basis in the vicinity of the target areas with the objectives to determine the nature, trend, extent and element associations of the primary dispersion pattern related to low grade As-Sb (-Au) mineralization at each site.

Orientation studies by Leake et al., (1981) over several arsenic vein systems in the Loch Doon area concluded that the arsenic levels in soil samples from either A or B/C horizon can be directly compared. As such, samples from either horizon are deemed equally applicable to future sampling programs in the Glendinning region. Soil sampling was then applied to detailed survey areas where lithogeochemistry and reconnaissance sediment sampling indicated potential for hydrothermal alteration and/or metal enrichment. A rectilinear sampling grid was set out over each area using a Watts theodolite, leveling staff and ranging poles, and the baselines were identified by 2"x2" wooden stakes. Traverse lines were laid out in an E-W direction, at a right angle to the known mineralization trend. In comparison with the soil survey carried out by BGS at Glendinning (Gallagher et al., 1983) sample intervals of 20 and 30m were selected for the Rams Cleuch and Swin Gill sites respectively, thereby ensuring that at least two points would fall within each anomaly of interest. Both soil grids were oriented with respect to the National grid and the location of individual sample sites are identified by a unique 12 figure grid reference.

Approximately 50-100g of B/C horizon soils were collected from each site at depths of 90-120 cm using a shallow soil auger and placed into 3"x8" water resistant 'Kraft' paper bags. In both areas the soils are well drained and similar to those described by Gallagher et al.(op cit) in the vicinity of the Glendinning deposit. They consist of well oxidised yellow-brown silty clays with a variable content of angular lithic fragments generally increasing with depth. The samples were air dried, but not sieved (in order to preserve the lithic component) and ground to <300#. Each sample was then analysed by automated X-ray fluorescence for six major and 14 trace elements including: Si, Al, Fe, MgO, Na, K, As, Ba, Co, Cu, Ga, Ni, Pb, Rb, Sr, V, Zn, S, Sb and Tl. In addition to the above oxides and elements the following ratios were also calculated: Si/Al, As/Na, Sb/Na, Cu/Na, Sr/Rb, together with the multiplicative variable As*Mg.

Potential sources of contamination in this region included human habitation, agricultural operations, forestry development and previous mining activity. The position of both Rams Cleuch and Swin Gill surveys areas in high, well drained upland areas, remote from industrial activity and habitation, tends to preclude environmental contamination as a major factor for consideration in this study. The most northern portion of the Rams Cleuch map forms a topographically high area of relatively flat-lying ground whereas both the south western and north eastern quadrants of the Swin Gill grid are topographically high and form the flanks steeply incised hillside. Given the lack of potential sources of environmental contamination in the vicinity of either soil grid all geochemical anomalies are defined to be directly attributable to variations in subcropping bedrock mineralization.

3.7.2 Exploratory Data Analysis

The first phase in exploratory data analysis of the soil geochemistry from both grids comprised an assessment of histograms for each variable. This then enabled both the nature and order of magnitude of element variation to be assessed and approximate contour levels, background and threshold values to be selected. Studies of the frequency distribution of elements in rocks and other natural materials suggest that in many cases the log-transformed concentrations are distributed approximately normally (Ahrens, 1954 and 1957). Percentile classifications are used within the study as opposed to the use of more common parameters such as mean and standard deviation because

of they are less effected by the extreme values present in a skewed distribution and more reliably describe the nature of the frequency distributions. In addition, elements that are below the detection limit in some of the samples are easier to handle statistically (Nurmi,1985). NB. The nth percentile is the value below which n% of the data occur. The geochemical data was contoured using an interactive grey-scale mapping package incorporating a nearest neighbour contouring algorithm. Class intervals chosen for each map represent (with increasing grey density) the 0-50, 50-75, 75-90 and 95-100 percentile intervals, respectively. The GRD mapping program (Harvey, 1981) used for this study incorporated a nearest neighbour grid model using a d^2 inverse distance weighting with six nearest neighbours. Careful selection of the grey scale shading symbols enabled any increase in contrast or element concentration to be mirrored.

Grey-scale geochemical maps were drawn for each variable and for many of the calculated ratios (Boyle,1974). These maps provided considerably more information than ordinary point source symbol maps. Contour levels for both oxide and trace element data for the Rams Cleuch (grid 1) and Swin Gill (grid 2) survey sites are presented in table 1.42. The frequency distribution of data for each element was divided into 5 classes (in order to best reflect spatial trends and features within the data) defined on the basis of the 0-50, 50-75, 75-90, 90-95 and 95-100 percentiles intervals. The individual element threshold for each percentile level are presented in table 1.42. Grey scale/level symbol maps (figs.93-98) illustrate the distribution of samples that have concentrations within each class. Total element concentrations determined for the soil samples from the Rams Cleuch and Swin Gill surveys are presented in tables 4.35 and 4.36. Gold analyses from a subset of the Rams Cleuch samples are displayed in table 2.41. Location maps of the Rams Cleuch and Swin Gill soil sampling grids are presented in in figs. 90a and 90b, individual sample sites are displayed in figs. 91 and 92, and summary statistics are displayed in tables 2.45 and 2.46. For the Rams Cleuch exercise a 20x10m rectangular sampling grid was mapped to a 10x10 primary grid by the creation of intermediate 'traverses' estimated by using the four nearest neighbours and a weighting factor of two. A secondary or 'plotting' grid 94x64 was then used to provide the necessary details for grey scale contouring. (This grid was designed to generate a map 8x8" using a line printer set to 12 cpi horizontally and 8 cpi vertically). A composite anomaly trend map for the Swin Gill area is presented in fig. 99. These geochemical trends are closely supported by aerial photographic observations of this area. Threshold level was set to isolate the samples present in the sub-populations related to mineralization. The 50th percentile interval was taken as the upper threshold for the background values and the 90th percentile as the threshold for mineralization. Although these values appear arbitrarily selected their calculation is relatively simple and they do provide a detailed measure of the distribution of data within the sample population. Suitable alternative graphical techniques have been proposed by Sinclair (1983) and Lepeltier (1979) where threshold selection is defined on the basis of significant 'breaks' of the gradient when the data is displayed upon cumulative probability plots.

Both element ratios and multiplicative values provide an extremely simple technique for the enhancement of inherent variations within the soil geochemical dataset particularly in instances where elements are highly correlated. The definitions of areas associated with two positively correlated (enriched) elements may be enhanced by a multiplicative technique (ie. $As \cdot Sb$ or $As \cdot MgO$) element ratios however are best applied where two variables are negatively correlated and they may be used to demonstrate the presence of either enrichment or depletion dependent upon the variable selected as the exponent (ie. As/Na).

Statistical treatment of the analytical data was restricted by the complex form of most element distributions, however element association were examined using correlation and principal component analysis. Correlation coefficients were calculated from each soil survey area (Table 3.22 and 3.23). Tables of summary statistics for grid

1 and grid 2 overburden geochemistry are presented in Table 2.45 and 2.46 respectively. As part of the statistical assessment of the multi-element soil geochemistry individual principal component scores relating to each sample site were contoured for both eigenvectors 2 and 3. A total of 20 computer generated isochemical maps summarising the analytical results for each grid area are presented in figs. 93-99. NB. All anomaly widths are measured on the basis of the 90-100th percentile intervals.

3.7.3 Rams Cleuch

At Rams Cleuch, 8km northeast of the Glendinning mine area, on the north western flank of Commonbrae Hill (800-1100ft) a clearly defined N15°E trending fault zone provided the main locii of exploration activity and the center of the soil grid (200x200m). In outcrop, the fault comprised a ten metre wide zone of a highly altered and brecciated mixture of sulphidic greywacke, siltstone and minor mudstone clasts (<15cm in diameter) hosted by clay gouge. Dickite was present on joints and fractures within the breccia zone. In addition to lithogeochemically anomalous As and Sb results, Tl values up to 17ppm were detected in breccia samples. A relatively close sample spacing was selected using 10m x 20m intervals. A grid was laid out in the vicinity of the major bedrock anomaly and extended to cover an area of 40,000 m² (Fig. 90a and 91). Two hundred soil samples were then collected.

With reference to the soil geochemical maps, the maximum concentration of As, Sb, Cu, Pb, Zn, Ba and Tl occur in two near parallel, NNE trending linear zones with the major structure transecting the western half of the grid area while a second somewhat smaller structure occurs in the north western corner and extends over approximately 50% of the grid. Visually there is an excellent spatial correlation between As, Sb, Cu, Pb, Zn, Ba, Co, Ni, Sr, Tl and to a limited extent Al and Fe. The highest values of these elements occur within a prominent NNE trending zone cross cutting the western half of the grid area. The arsenic background figures for fresh, unmineralized rock in each of the areas studied is less than 1ppm. At Rams Cleuch a broad, irregular, secondary dispersion pattern nearly 300m in length was defined by values >30ppm arsenic. This concentration however, falls linearly with distance from the vein structure, and background values are usually reached within 50m from the peak of the anomaly. Within the mineralized zones arsenic values found to be very erratic, reflecting indirectly the nature of the fracturing and brecciation within individual lode zones.

The normal background level of antimony in soils is <1ppm (Wedapohl, 1978). Approximately 30% of all samples analysed in grid 1 and 2 contain significantly higher level than this and as such, were considered anomalous. It appears from the figures obtained, however, that the primary dispersion pattern of As is broader than that for Sb, extending into the wallrock for at least 10m on either margin of the feeder vein. The degree of mineralization and hydrothermal alteration decreases outwards from the feeder zone and defines a gradational transition to unaltered rock. A small As anomaly occurs on the eastern side of the Rams Cleuch grid, yielding a maximum value of 17ppm and measuring 20 x 100m (at the 90 percentile level). It is possible that the slope of the hillside, albeit gentle, contribute to the broadening of the more relatively mobile trace element concentrations by either drainage effects of downward dispersal of particulate matter. As the top of the map is topographically high yet relatively flat, this may explain the encroachment of the two anomalous zones. In general, the shape of the As-Sb soil anomalies reflects the way in which these elements exist in bedrock. The As anomalies form a relatively broad envelope to narrow Sb anomalies, thereby reflecting the extensive nature of arsenopyritisation marginal to the quartz-stibnite vein mineralization. The highest anomalous members of the sample population are either directly related to the presence of subcropping mineralized material in the soil samples whereas the 50-70 percentile level of values may

be attributed to secondary dispersion. The total chemical variation within this site may be attributed to the presence of a mineralized fault breccia transecting the survey grid. In comparison with the Glendinning deposit this pattern is interpreted as a similar stibnite dominant quartz vein system, contained within an extensive zone of arsenopyritisation (note the arsenic envelope and associated sodium 'hole'). Contour plots of As, Sb, Cu, Pb, Zn, Ba, Co and Ni showed spatially related high and anomalous levels of these elements thus indicating a similar source of variation. The interelement correlation of major and trace elements within this grid infers the considerable extent of interaction between wallrock alteration processes and the mineralizing fluids.

In order to define the element associations present, principal component analysis was applied to the Rams Cleuch and Swin Gill soil geochemistry datasets. In both cases all analysed elements were compared and it was noted that, three eigen vectors account for >95% of the variance. The results of this study are displayed in table 3.06a and 3.06b and discussed below. Simple distributions are caused by the dominants of a single source of variation such as the presence of arsenopyrite (arsenic enrichment) and stibnite (antimony enrichment). In the Rams Cleuch dataset the following geochemical associations are identified by principal component analysis:

- Eigen vector 1: As-Sb-Pb-Tl-Mg, K-Al-Rb-V-Ni, Cu-Zn-Ba-Fe and Si-Na-S.
- Eigen vector 2: As-Sb-Pb-Fe-S, K-V-Rb-Sr-Cu-Tl, Na-Mg-Si.
- Eigen vector 3: As-Sb-Pb-Zn-Cu-Ni, K-Rb-V, Fe-S-Tl, Co-Sr-Mg-Na and Si-Al.

In addition to the single element contour maps, two further maps are also presented, named EV-2 and EV-3. These maps present a spatial analysis of the structure of the correlation matrix for the total multi-element data set and were generated by the extraction of component scores for each sample site, with respect to both eigenvectors 2 and 3 (EV-2 and EV-3 respectively) during principal component analysis of the the data. Evaluation of the eigenvector values indicate that the EV-2 map summaries the spatial distribution of a group of elements either positively or negatively correlated with respect to either arsenic and antimony mineralization. The EV-3 map delineates a second suite of mineralization related elements, dominated by copper, lead, zinc and barium. One possible interpretation of these diagrams is that two geochemically distinct phases of mineralization are present within the survey area. The Cu-Pb-Zn-Ba association appears spatially related to, but more laterally extensive than the As-Sb association and as such it is tentatively suggested that although the Cu-Pb-Zn-Ba mineralizing fluids migrated along the same structural conduits as those of the As-Sb-Au fluids, they did so at a later stage.

Wallrock alteration is strongest in the vicinity of mineralised fractures. Secondary minerals identified by XRD studies include quartz, potassium feldspar, biotite, dickite and sericite. Na, K, and Mg have a low anomaly contrast and form broad but slightly dispersed depletion anomalies surrounding and immediately above the main mineralised structures. These depletion envelopes provide further evidence of the extensive nature of wallrock alteration in this area. Potassic alteration is best defined by the distribution of K values although Rb, Rb/Sr and Al/Ca show comparable anomaly patterns. The broadest depletion halos occur in the Western part of the grid and again identify the principal mineralized zone. The elements Si, Ga and V show no consistent pattern related to the identified mineralized structure.

Rank Spearman correlation coefficients for the Rams Cleuch samples are presented in Table 3.22. These coefficients clearly illustrate a number of factors; The main ore forming elements, arsenic and antimony are positively correlated with Cu, Pb, Zn and S, but inversely correlated with both Na and Mg. Arsenic in particular

is strongly correlated with iron whereas antimony correlates well with potassium and strontium. Other pertinent correlations worthy of note include the strong negative relationship between Mg and Sr, and Zn and S.

Aluminium is positively correlated with a number of ore forming elements; Ba, Cu, Ni and Zn together with K_2O and Sr, however it appears inversely correlated with sulphur. The problem of a closed dataset as illustrated by the inverse correlation of SiO_2 with all other elements with the exception of sodium. The removal of oxide copper due to rapid runoff of the groundwater may explain the zone of low copper geochemistry on the sloping flanks of the grid.

Due to both time and cost factors, gold analyses were only undertaken on the soil samples across a single traverse in grid 1 at Rams Cleuch. The gold content of 20 samples forming a single E-W traverse across the grid was determined by conventional fire assay followed by instrumental neutron activation analysis (detection limit 1 ppb). The results of this study yielded gold values of 0-20ppb. It is worthy of note that the maximum gold value in the samples occurred coincident with arsenic and antimony maxima (27ppm As and 20ppm Sb). As such it can be quite readily observed that the gold values mirror the arsenic dispersion pattern. These factors thus provide additional evidence for the presence of minor, structurally constrained arsenic-gold mineralization at this site and demonstrate quite clearly the effectiveness of arsenic as a pathfinder element for gold mineralization in this region. The dispersion represented by >10ppb Au within the soil sample defines a zone 30m in width and effectively outlines the projected breccia zone and zone of arsenopyritisation. As wallrock arsenopyrite is reported to act as a host for gold in this region (see Chapter 5) this linear anomaly should form the locus for future exploration in this area.

In summary, at Rams Cleuch a combination of lithogeochemistry and overburden geochemistry led to the definition of a NNE trending brecciated fault zone containing As-Sb-Au mineralisation. A systematic geochemical zoning pattern was present in all samples from the Rams Cleuch area providing a clear reflection of bedrock mineralization. Although the magnitude of the geochemical values is small these undisputed arsenic anomalies provide clear evidence of a subcropping mineralized fracture system in the area and define detailed targets for further evaluation, as the full extent of the As/Sb soil anomalies have yet to be identified. The presence of dickite on fracture surfaces within the breccia zone provides further cryptic evidence for potential gold mineralization at this site.

3.7.4 Swin Gill

Swin Gill, on the southwestern flank of Sole Hill, was previously identified as a potential target area by a limited BGS stream sediment survey of this and the surrounding drainage systems and yielded maximum antimony pan concentrate anomaly values of 127ppm near the its headwaters, in the vicinity of the lithogeochemical anomalies and the site of the soil survey grid. At Swin Gill, the lithogeochemical anomalies were however, more widespread than those at Rams Cleuch with less apparent structural control and no obvious target. As such, the field of investigation and size of soil grid were expanded accordingly (300x500m). At this site 300 soil samples were collected at 10m intervals along traverse lines spaced 50m apart. The sampling grid was laid out over the widespread lithogeochemical anomaly zone in the western headwaters of Swin Gill (Fig. 90b and 92) covering an area of 150,000m² at a height of 1100-1500 ft. Although most of the metallic constituents from this site were dissolved in the course of weathering, appreciable amounts were absorbed or coprecipitated with the ubiquitous hydrous Fe-oxides as evident from the anomalous (As-Sb) stream sediment samples collected by BGS in this area

(Gallagher et al., 1983). The elements associated with the As-Sb-Au mineralization show rather dispersed anomaly patterns as might be expected from the Rams Cleuch study. Elements having significant positive or negative correlation coefficient with either As or Sb reflect albeit cryptically, the nature of the mineralization processes. The distribution of the anomalies appears more complex in the Swin Gill study area but the cross strike trend is still apparent. The main anomalies and associated higher values occur in a series of parallel linear features in an area where there is no evidence of previous mineralization or mining activity.

The geochemical anomalies (Fig. 96-98) from the Swin Gill area, define far more complex pattern than were detected within the Rams Cleuch grid (fig. 93-95). This may be due in part to the four fold increase in grid area (40,000 to 150,000m²) and the two fold increase in traverse spacing (20 to 50m) as opposed to a 50% increase in the number of samples. This detailed soil survey both up and downslope from the original lithogeochemical anomalies located a number of linear structures. These structures, their orientation and chemical associations are presented in Fig. 99 and table 1.69. In general two major groups of linear structure are observed in the grid area. The first group comprises of nine N10°E trending parallel features each separated by approx. 50m, extending across the entire grid. The second group are represented by approximately four NW-SE trending zones. The relative position of both sets of features are summarised in Fig 99. Each separate structure has been assigned an identification number (1-13) which is used for reference purposes in the following discussion of the individual geochemical maps.

Arsenic forms a broad W-shaped envelope enclosing a number of smaller lobate zones (>90th percentile interval) and define both NNE (1,2,3,4,5,6 and 8) and W (10,11) trending anomalies. Antimony distribution mirrors that of arsenic in the central and south western portion of the grid section (anomalies No.7, 8 and 9) but not in the eastern sector. The distribution of arsenic and antimony differs particularly in the north eastern quadrant of the survey area. In the north of the area As and Sb anomalies are sparse and generally of much smaller amplitude. Neither the intensity nor the contrast or spatial extent of the antimony anomalies are as pronounced as those for arsenic. The highest antimony content was 34ppm (sample no.311) while the lowest value was below detection limits. It is suggested therefore, that antimony displays a much narrower secondary dispersion pattern than arsenic in this area, and as such it is concluded that the antimony distribution is directly related to and controlled by subcropping Sb-quartz vein mineralization.

Within the Swin Gill study area there is a narrow 'peak' of high values rising to 65ppm As (sample 382) and 34ppm Sb (sample 311) immediately over the suboutcrop of the main structure. It is possible, however, that multiple parallel veins are responsible for the single composite anomaly displayed in figure 96-98. However, a major component of the elemental variations present within this area may be attributed to an increase in the spatial complexity of underlying mineralization. A disparity between the two anomalous zones may be noted; the most western structure at Swin Gill comprises of a localised zone of antimony anomalies contained within an envelope of enriched arsenic values, whereas the easterly structure, containing the strongest arsenic values and exhibiting similar alteration patterns (Rb, Sr, Cu and Pb enrichment associated with Na depletion) contains few antimony values above detection limits. The differences between the two geochemical signatures can be reconciled by a model invoking:

- 1) Early hydraulic brecciation and associated As (+Au) enrichment, with the hiatus of brecciation concentrated on the westerly zone.

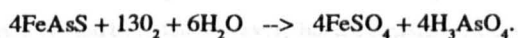
- 2) Later, antimony-bearing fluids followed existing fluid conduits with deposition concentrated within areas of highest permeability (predominantly in the western zone).
- 3) Reactivation of both NNW trending fault structures and overprinting during a later phase of Cu-Pb-Zn-Ba mineralization.

The results of zinc analysis show that except in the quartz-stibnite vein, all wallrocks adjacent to the mineralization contain ~50ppm less Zn than those marginal to the deposit. Thus this element shows a 'negative' anomaly (or depletion) with respect to mineralization and suggests that zinc has been mobilised by the mineralizing fluids. The apparent antipathetic relationship between arsenic and silica is deemed insignificant due to the closure effect inherent within this form of dataset.

3.7.5 Discussion

Although many elements in poorly developed soils occur as partially weathered grains of the parent material, a small portion of the metal values liberated by weathering may be held in organic material, or as ions adsorbed onto both clays and/or colloidal Fe-Mn oxides (Rose, 1979). Most mobile or semi-mobile metals in freely drained residual soils overlying oxidised ores are firmly associated with clays and Fe-Mn oxides. Mather (1959) demonstrated that high concentrations of arsenic in soils occur predominantly in the form of Fe-arsenate. In oxidised soil samples arsenic is positively correlated and chemically associated with iron, presumably in the form of arsenate adsorbed on ferric oxides and hydroxides or of precipitated FeAsO_4 (Kenanori, 1965; Ferguson and Gravis, 1972; Price, 1976 and Farmer and Lovell, 1981). Where highly acid conditions prevail and where the supergene solutions encounter low amounts of carbonate minerals, arsenic is relatively mobile and may migrate for considerable distances. Where the solutions are weakly acid, neutral, or alkaline, soluble arsenic is relatively immobile because of hydrolysis phenomena and coprecipitation with various natural compounds, particularly hydrous iron oxides (limonite, etc). Iron cobalt, nickel, lead, and zinc in solution react readily with soluble arsenates forming a number of secondary minerals. Scorodite, erythrite, and annabergite are particularly common among the secondary arsenates, however none of these minerals have been identified to date within the grid area.

During the weathering of rocks and deposits containing arsenic the element enters the exogene (surficial) cycle mainly as soluble arsenates in which the element is in the (V) oxidation state. The oxidation of arsenic minerals is a complex process involving numerous step-wise reactions, however the oxidation of arsenopyrite can be expressed as follows:



Residual hydrous Fe-oxide derived from the oxidation of Fe-bearing sulfides and carbonates has long been of significance in mineral exploration (Rose et al., 1979). Accumulations of hydrous Fe-oxide are known as gossans and are commonly formed from the weathering of pyrite, arsenopyrite (FeAsS), siderite (FeCO_3) and ankerite ($\text{Ca}(\text{Mg.Fe})(\text{CO}_3)_2$). Precipitation of the small amounts of arsenic from surface waters takes place by adsorption on mineral particles, clays and gels, and by adsorption and/or chelation or other forms of organic binding by humic constituents. Natural hydrous iron oxides are particularly good scavengers of arsenic, as are also certain types of natural precipitates containing hydrous iron oxides, manganese oxides, and humic constituents by the positive iron colloids (gels). Manganese oxides, on the other hand carry a negative charge, and tend to repel the anions. Wad and other manganese oxides do not, therefore contain large amounts of arsenic and antimony and as such MnO was not determined in this study.

Investigation of arsenic and antimony dispersion pattern in soils over a number of antimonial gold deposits in Southern Rhodesia were made by James (1957). The results showed that anomalous arsenic values are commonly found in the immediate vicinity of gold mineralization. In detail, the gold mineralisation was found to occur in association with fracture controlled and disseminated phases of pyrite-arsenopyrite mineralization. Similar lithogeochemical and soil geochemical surveys have defined additional areas of As-Sb-Au-Hg mineralization up to 10km north of the Glendinning mine area, thus adding considerable importance to this region as a metallogenic center within the Southern Uplands. Relatively broad primary halos are associated with all four occurrences. The halos are characteristic of each particular occurrence. As, Sb, Pb, Zn, and Na seem to be useful pathfinder for this form of cryptic occurrence. Sulphur halos are however, smaller and often erratic. Mineralogically, the trace elements presented on the soil maps reflect both primary sulphides (As, Sb, Pb, Zn, Cu, Tl) and sulphates (Ba) whereas the major element chemistry relates to wallrock alteration processes particularly the loss of sodic feldspars during K-metasomatism and sericitisation. Trace elements, most notably As and Sb form elliptical, narrow, 30m wide anomaly zones the strike of which correspond to those of fracture zones observed in bedrock (Rams Cleuch) or within aerial photographs (Swin Gill).

Although the order of magnitude of As and Sb values are relatively small (max 65 and 34ppm respectively) the anomalies detected in both grid 1 and grid 2 compare favorably with the results of the BGS soil survey at Glendinning (55ppm Sb and 350ppm As), particularly when environmental contamination from the historical mining activity is taken into consideration. Although the background arsenic content of the unaltered rock was found to be <1ppm, alteration zones are defined by soil geochemistry upto 30m in width which yield arsenic values >50ppm. The width of the primary dispersion pattern however, is unknown due to the limited exposure within the grid area.

From the orientation of soil geochemical anomalies located to date it is clear that the arsenic concentrations are directly related to the weathering of wallrock hosted arsenopyrite associated with fracture controlled quartz-stibnite mineralisation rather than being derived from stratiform, syndimentary concentrations of arsenic within the underlying greywackes as proposed by Gallagher et al., (1983). In any appraisal of the possible economic significance of soil anomalies a number of factors merit consideration, namely: the magnitude of the values (ie. the contrast between peak and background); the size and shape of the anomaly zone; and the geological setting.

Magnitude: It should be noted that in comparison with the Glendinning Deposit, the heavy metal content of soil samples overlying the mineralization were several orders of magnitude lower than the bedrock source. Thus, relatively low metal values in soil samples are of considerable importance and may be used to infer details of the primary mineralization. It should be noted however, that the classification of anomalies solely on this basis, making the fundamental assumption that a reliable correlation exists between anomaly contrast and ore grade is rarely justified in practice (Rose, op.cit).

Size and Shape: Soil geochemistry in the Rams Cleuch site defined two parallel, NNE trending, coincident, linear As-Sb anomalies approximately 40m in width. These anomalies are most strongly developed in the central portion of the grid area, however, it is clear that they are open at both ends and as such the strike length of this mineralized fault system is unknown. In the Swin Gill study area a number of linear NNE trending anomalies were identified traversing the grid. It is clear from this study that both arsenic and antimony enrichment is considerably more widespread in this area than previously reported.

Geological Setting: Both the Rams Cleuch fault/breccia zone and the Swin Gill survey area display close geochemical, petrographic and structural similarities with the Glendinning deposit; They are hosted by greywackes of the same carbonate rich petrofacies, and both follow the same NNE structural trend. Evidence of hydrothermal activity at Rams Cleuch is present in the form of trace element enrichment, sodium depletion, bleaching and dickitisation, features characteristic of outcrop samples from the Glendinning deposit.

Webster (1986) showed that secondary gold remobilization in this form of disseminated deposit can often be attributed to gold complexing by sulphur-bearing ligands. The nature and mineral association of secondary gold in oxidised zone of Glendinning type disseminated gold deposits in the Southern Uplands may therefore have been ultimately responsible for the widespread distribution of coarsely crystalline alluvial gold, consistent with prior remobilization as a thiosulphate complex. Reconnaissance stream sediment sampling by the British Geological Survey (Gallagher, Pers.Com) within the tributaries of Ewes Water defined a series of arsenic, antimony and base metal anomalies in heavy mineral concentrates contained within 1.5km section of Swin Gill (with maximum concentrations 127ppm Sb and 43ppm As). Unfortunately this sampling program did not extend northwards to the Rams Cleuch site area however recent surveys carried out by European Gold Exploration Limited following the authors recommendations have defined the presence of arsenic, antimony and mercury anomalies within this area. These results clearly outline the widespread potential for further discoveries of As-Sb-Au-Hg mineralization within the Glendinning study area and the importance of this region in Scottish metallogenic models.

3.7.6 Recommendations

The systematic sampling of residual soils in the search for anomalies directly overlying suboutcropping mineralized vein systems has been outstandingly successful in the Glendinning study area. Soil Geochemistry provides an effective tool in exploration for and the delineation of fracture controlled shallow of blind As-Sb-Au mineralization. These results provide clear diagnostic features of As-Sb-Au mineralization and assist the preparation of conceptual models and criteria for further exploration in this region. In summary, this study has demonstrated that anomalous levels of arsenic can be directly used as pathfinder for As-Sb-Au mineralization in this region, and that shallow soil sampling can serve as a powerful exploration tool for Glendinning type As-Sb deposits where outcrop is sparse and bedrock largely unknown. As such, it is recommended that the lateral extensions of both soil grid areas be evaluated and large scale E-W traverses be undertaken to detect further parallel structures. The anomalies defined by this further studies should then be investigated by trenching, detailed geological mapping, lithogeochemical bulk sampling and diamond drilling.

3.8 NATURE AND EVOLUTION OF THE HYDROTHERMAL SYSTEM

The hypothesis presented here to account for the origin of As-Sb-Au deposits in the Southern Uplands, involves the focused discharge of magmatic/geothermal fluids. The resulting hydrothermal system is closely linked to the emplacement of late Silurian calc-alkaline minor intrusives and is structurally constrained by the extent of hydraulic fracturing in a tension zone at the close of the Caledonian orogeny.

3.8.1 Overview

The Glendinning deposit exhibits close structural, chemical and mineralogical similarities with both the Clontibret deposit in Eire (hosted by Ordovician greywackes) described by Morris and Steed (1985,1989), the Sheba Mine in South Africa, hosted by Archaean turbidites (Schouwstra and Villiers, 1988) and a number of Early Devonian high-temperature As-Cu-Co (270-350°C) deposits from the Lake District detailed by Stanley and Vaughan (1982). In a comparison of the Glendinning and Clontibret deposits, the most notable differences include the extent of both brecciation and wallrock alteration. The broader zones of both features identified at Glendinning are inferred to be indicative of relatively shallower, near-surface emplacement (see fig. 475).

The definition of multi-element halos around gold deposits in the Southern Uplands, relies upon the ability to define background abundances in the surrounding country rocks. As such, geochemical investigations of the Glendinning deposit were extended over the general area, outwith the area of known mineralization, and also undertaken on a regional scale.

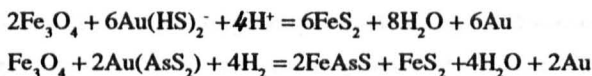
To aid the understanding of ore genesis within the Glendinning deposit, indirect arguments based on the geochemistry of the mineralization and its hydrothermal alteration products become critical. Even though the exact chemical composition of the mineralizing fluid is not known, a number of parameters may be closely constrained. Factors affecting the formation of hydrothermal minerals at Glendinning include temperature, permeability, fluid composition, greywacke composition and pressure (important in determining the depth of boiling). Permeability is an important control since most mineralogical changes are not isochemical and the rocks must be open for exchange of constituents (Weissburg et al., 1979).

The key factors in any discussion of the genesis of the Glendinning deposit, relate to whether the mineralization is essentially syngenetic and related to some form of early volcanic or volcano-sedimentary processes (Gallagher et al., 1983), or whether it is truly hydrothermal and related to igneous and tectonic processes (Rock et al., 1986; Gallagher et al., 1989; Duller (this thesis)). A number of features are considered to support an epigenetic origin for the As-Sb-Au mineralization at Glendinning, including the absence of true chemically precipitated cherts; the structural control upon mineralization and hydrothermal alteration and the close mineralogical and geochemical similarity with epigenetic deposits throughout this terrane. Detailed evidence for and against both models have been presented in the previous sections of this chapter and it is concluded that considerable support exists for the epigenetic/epithermal nature of Au-As mineralization. On the basis of this study, it is proposed that the hydrothermal arsenic-gold mineralization resulted from extensive geothermal activity related to the high heat flow and minor intrusive activity.

A number of parameters constraining the origin and subsequent history of the ore-forming fluids may be established from the chemical composition of vein and alteration minerals, redox patterns, fluid inclusions, and sulphur isotopes. Barnes (1979) proposed that although precipitation may result from changes in temperature and pressure, chemical reactions between the hydrothermal fluid and wallrock form one of the most important factors in the onset of sulphide deposition. In the Glendinning deposit K^+ and H^+ metasomatism led to kaolinitisation and sericitisation with the release of Na, Mg, Zn and Fe. All four elements were removed to varying extents by the hydrothermal solution, resulting in a depletion zone associated with alteration. The mechanisms resulting in the onset of initial sulphide (arsenopyrite) deposition were also directly responsible for gold mineralization in this deposit. On the

basis of mineralogical and geochemical evidence it may be inferred that the gold was transported in an arsenic-sulphur-bearing fluid containing minor quantities of antimony, mercury, lead and copper. Although Fe, Ni and Zn are present in sulphide phases, a comparison of mineralized and unmineralized host rock geochemistry indicates that these elements were most probably obtained from primary constituents of the host rock. The broad scale nature of metal zonation in the Glendinning mine area, is indicative of dispersion methods, related to high permeability rather than those simply controlled by diffusion.

Mineralogical studies indicate that ore deposition took place from sulphide rich, alkaline to neutral, H_2O-CO_2 solutions. Gold was transported by reduced sulphur complexes and precipitated during wallrock alteration by the following reactions:



Auriferous mineralisation is spatially and genetically related to extensive wallrock alteration including carbonatization, arsenopyritization and sulphidation. Gold-bearing arsenic rich fluids were channeled into the main conduit, which then flooded the highly permeable breccia and stockwork zones. Temperature and/or pressure changes can be used to explain the deposition mechanisms operating within this deposit. Alternatively, a decrease in reduced sulphur activity caused by rapid sulphide deposition offers a possible explanation for the mechanism of gold deposition. Arsenopyrite geochemistry indicates that gold mineralization was dominantly controlled by temperature with precipitation resulting from a temperature drop through $300^\circ C$, below which the solubility of Au declines rapidly (Kay and Strong, 1983). The chemical composition of the hydrothermal fluid was constantly changing due to the dissolution of rock-forming minerals and the primary crystallization of sulphide minerals. However, in this model it is proposed that As, Sb and Au were of hydrothermal origin and that they were deposited from a sulphur rich fluid containing a strong magmatic component.

3.8.2 Breccias

An area of mineralization related alteration (a stockwork zone) has been outlined in the vicinity of the abandoned Louisa mine at Glendinning. This stockwork zone is characterised by multistage brecciation and infilling by sulphides and silica, accompanied by pervasive arsenopyritization, sericitization and the obliteration of many primary textures. It is proposed that the widespread nature of mineralization in the Glendinning deposit formed as a result of large-scale faulting and brecciation processes which provided a broad conduit for numerous pulses of hydrothermal fluid. In detail, it is proposed that large but short lived overpressures in the geothermal reservoir, probably triggered by sudden magmatic activity, induced hydraulic shear, tensile fracturing and extensive brecciation processes in this deposit. The consequence of high fluid pressure, is that these hydraulic fractures will tend to propagate towards the surface. The hydraulic brecciation identified in the vein system at Glendinning is indicative of relatively shallow (<1km) mineralization (cf. Phillips, 1972; Pattick et al., 1983).

These breccia zones are interpreted as the the main hydrothermal flues (cf. Berger, 1985) with clasts in the breccia representing the remnants of this or earlier periods of explosive brecciation and self-sealing, thereby indicating that repeated activity was focused in the same hydrothermal conduit. The number of brecciation events is however, difficult to quantify. Extensive fluid-rock interaction in large scale breccia zones, resulted in major chemical and thermal exchange between the two and may be used to explain the relative lack of zoning in the breccia zone,

compared to the vein mineralization. These observations can be used to define further exploration targets in the Southern Uplands and Longford Down. It should be noted that breccias similar to those at Glendinning are widely reported in the literature, and reviewed in detail in chapter four.

3.8.3 Fluid Inclusion Studies

Samson (1983) demonstrated that Base metal vein deposits in the Southern Uplands of Scotland formed from ~80 to 150°C solution which had salinities mostly in the range of 18-30 wt%. The Knipe antimony deposit in the Southern Uplands of Scotland was deposited from higher temperature, and lower salinity fluids formed at ~185 to 215°C from a 5-8wt% NaCl fluid. In this study, eight polished wafers of Glendinning vein material were studied in transmitted light. All wafers exhibited a general paucity of fluid inclusions. However, of the inclusions located, ~95% occur within late stage milky white quartz, are extremely small (~1 micron in diameter) and contain a single fluid phase implying temperatures of deposition less than 60°C. A smaller number of complex CO₂ rich three phase inclusions (<5 microns in diameter) were identified within quartz veining associated with early arsenopyrite mineralization. Microthermometric studies of both types of inclusions proved extremely difficult. The limited results obtained to date, however infer low salinities (0-3 wt% NaCl) and depositional temperatures in excess of 250°C for the arsenopyrite-quartz mineralization. In general, fluid inclusions are rarely preserved in the quartz veins, but where present they indicate CO₂-rich fluids of low salinities similar to those in quartz veins from the Clontibret deposit (Morris and Steed 1986). These liquid + vapour CO₂ rich fluid inclusions associated with arsenopyrite mineralization may be used to infer periods of sporadic boiling. These results are however, too few to be statistically valid, and as such are not discussed further.

If a comparison is made between paragenetic and published thermochemical data, an estimate can be made of the conditions of deposition present during mineralization in the Glendinning deposit. Deposition was initiated by rapid physical and chemical changes, such as major decreases in temperature; concentration due to the separation of steam; and the loss of CO₂ and H₂S to the steam phase. In close proximity to a hydrothermal vein system it can be argued on the grounds of fluid pressure alone, that an outward migration of ore-elements is more likely to have occurred rather than the remobilization effects proposed by Gallagher et al., (1981; 1983). The shape and extent of the alteration zones, suggest formation in vertical zones of high permeability by a process of fluid flow rather than diffusion. The dispersion profile of As and the intense nature of arsenopyritisation may be used to infer that pressurized hydrothermal fluids entered the wallrock by permeation. The resulting fluid/wallrock interaction resulted in the destabilization of metal complexes and led to the deposition of gold-rich sulphides during episodic boiling.

It is proposed that the rapid precipitation of gold and arsenopyrite took place in several pulses of fluid flow associated with hydrothermal brecciation. If, as suggested above, boiling did occur, the resulting vapour phases would stream upward. Retrograde boiling would therefore result in a loss of CO₂, brecciation of arsenopyrite and deposition of calcite. In a comparison with the studies of Kay and Strong (1983) it is proposed that the initial vein formation resulted from early CO₂ rich fluids. Decreasing CO₂ content and temperature with time, resulting in the transition from As-rich to Sb-rich mineralization. It should be noted that the reaction of clay minerals with carbonates during deep burial diagenesis provides a powerful mechanism for generating large quantities of CO₂ by inorganic origin (McBride, 1985). This study demonstrates that the Glendinning ore solutions differ from the modern hot springs of the east Pacific Rise, in that they were boiling, and had lower discharge of temperatures.

The presence of a pressure gradient between the hydrothermal fluids in vein and wallrock was used to explain why peak metal values not occur immediately adjacent to vein (Phillips, 1971; Ashton, 1981). As diffusion controlled alteration never ventures more than 10m or so from the vein wallrock (Ashton, op.cit) it is suggested that a system of open fractures were present at the time of mineralization/alteration allowing the fluids to permeate wallrocks over a much greater extent. This hydrothermal flooding model may be used to explain the broad nature of the observed hydrothermal alteration at Glendinning. Romberger (1986) noted that under conditions of stability of pyrite and argillic alteration assemblages, gold will be transported as bisulfide complexes. In systems such as this, containing significant amounts of arsenic, thioarsenide complexes may be important with oxidation, dilution and cooling promoting gold deposition under these conditions. In addition, adsorption and coprecipitation are possible mechanisms of deposition for gold. The acidity required to generate sericite alteration may have been provided by the condensation of acid volatiles (cf. Vivian et al., 1987). The boundary conditions of the ore-bearing hydrothermal solution have been summarised above. In the following discussion the factors responsible for the changes in the hydrothermal solution chemistry responsible for the observed paragenesis are reviewed.

pH : Factors invoked in order to suggest that the pH of the hydrothermal solution was probably near neutral or slightly acidic, include a comparison with the pH of currently active high temperature geothermal systems at depth and the fact that the interaction between the hydrothermal solution and carbonate-rich wallrocks will have a neutralizing effect upon the solution.

Temperature : The temperature of the hydrothermal solution may decrease as a result of three processes, including: fluid chilling during interaction with large surface areas of relatively cold hostrocks; fluid mixing with cooler solutions (meteoric or seawater); and adiabatic boiling of the solutions prior to exhalation. The development of alteration began with the infiltration of hydrothermal fluids into open extensional fractures and fracture related breccia zones.

3.8.4 Oxygen Fugacity

The destabilization of metal complexes in the fluids may have been caused by a change in fluid buffering from a pyrite-magnetite assemblage to a pyrite-arsenopyrite assemblage in the host rocks. To estimate the oxygen fugacity it is necessary to follow an indirect approach. A rapid deposition of sulphides without re-equilibration with the source fluid would drastically decrease the activity of reduced sulphur in solution thus causing a drop in gold solubility. In comparison with studies by Seaward (1973) it may be shown that the change from pyrite-magnetite fO_2 buffering to pyrite-arsenopyrite should be accompanied by an increase in the fugacity of hydrogen with the resultant deposition of gold. Mineralized greywackes which are crosscut by gold-bearing hydrothermal veins, display a strongly reduced state of iron, relative to the oxidation state of unmineralized material. This extreme reduction may be used to infer the extensive interaction with fluids originating under high-temperature reducing conditions. Estimates of minimum fluid-rock ratios obtained from shifts in the oxidation state following the methodology of Kerrich et al., (1977) are >3:1. In addition, there is evidence for the reduction and replacement of iron oxides on a meso- and microscopic scale. The withdrawal of sulphide and arsenide ions by reaction with iron in the host rocks (ie. the formation of pyrite and arsenopyrite) may also lead directly to the breakdown of gold complexes and the consequent precipitation of gold. The redox condition of the hydrothermal solution are normally reported in the form of oxygen fugacity (fO_2). Modern hydrothermal solutions display a pO_2 ($\sim fO_2$) of $10^{-42.5}$ to 10^{-35} bars at temperatures in the range 225-300°C (Ellis, 1979). On the basis of investigations by Large (1980) in the

Fe-S-O system it may be demonstrated that the fO_2 of the mineralising solution lies within the range 10^{-30} to 10^{-40} (atm). The mineralizing fluids were buffered to a near-neutral pH and had their redox and sulphidation states buffered by Fe phases in the wallrocks and veins. Precipitation is enhanced by decreasing temperature, increasing pressure, reduction of alkalinity or dilution of the fluids.

It is possible to construct a quantitative hypothesis for the mineralization process at Glendinning, based upon the oxidation state of iron in the context of the arguments presented by Kerrich et al., (1977) and Rock et al., (1987). Late Silurian minor intrusive activity in the Glendinning region provided the energy source and conditions of high permeability required for the creation of a convective instability to drive hydrothermal fluids up conduits within fracture zones. A diffusional model for fluid transport and ore deposition is rejected on the grounds that the low water/rock ratios involved could not account for the extensive reduction of iron in the mine area. It should be stressed that unless a fluid is moving over a large T-P gradient, the reduction of iron observed in both the Yellowknife and Glendinning deposits is virtually impossible. Thus, the extensive iron reduction within the Glendinning deposit may be used to infer a high water/rock ratio; high geothermal gradient; and the presence of a large-scale hydrothermal system (Kerrich et al., 1977).

3.8.5 Proposed Mineralization Model

Any potential model for hydrothermal activity and ore deposition must account for the observed chemical and mineralogical variations within the Glendinning deposit. In the Glendinning deposit it is proposed that the initial phase of arsenic-gold mineralization was relatively short-lived ($\sim 10^5$ y) sulphur-rich hydrothermal system. The reduction of fluid temperatures during successive mineralization phases may in itself have resulted in thermal stressing, increasing both permeability and circulation and leading to further heat loss.

A four stage sequence of events are recognised in the Glendinning deposit: The initial phase of activity occurred during the Late Silurian and involved the onset of large-scale faulting; the initiation of hydraulic fracturing and brecciation propagating from depth (cf. Allison and Kerrich, 1981); and the formation of pathways for subsequent hydrothermal fluids. The second phase of activity followed concomitant with the first and led to the development of extensive alteration zones and the deposition of disseminated As-Au mineralization. The third phase of mineralization involved the deposition of quartz-stibnite veins; with the final phase of mineralization following much later (?Lower Carboniferous) and represented by Pb-Zn-Cu-Ba vein mineralization. The geometry of the vein systems at Glendinning indicate formation by hydraulic fracturing under conditions of very high fluid pressures. The prediction of the style of mineralization to be expected in this terrane may have a profound influence upon the design of geochemical and geological exploration programmes.

The vertical extent of geochemical halos above a deposit depends upon the permeability and structural controls for the deposit. Beus and Grigorian (1977) indicated that primary halos extend 200-800m above most types of hydrothermal deposit controlled by steeply dipping fracture zones. On the evidence described in this chapter, it is quite probable that an extensive vertical zonation profile exists in the Glendinning deposit, however the relatively shallow borehole investigations undertaken to date, have not allowed this hypothesis to be tested. The vertical extent of the alteration at Glendinning is difficult to assess due to limited underground access and diamond drilling carried out on the property. Limited published data have been used to propose a generalized metal zonation in precious-metal systems which is defined by Tl, Hg, As and Sb at surface or shallow depths, followed by Au and

Ag with increasing Ag/Au with depth, towards a base metal rich mineralized zone (Celenek, 1987). If this model is applied to the Glendinning deposit, it may be used to infer the presence of a high level (Au-poor) portion of a zoned hydrothermal system and more importantly, considerable potential for higher grade Au mineralization at depth. It also follows that, if the elevated gold values identified in the Clontibret deposit form a feature mirroring the depth of emplacement, then considerable potential exists for the discovery of 'bonanza' type zones at below the currently evaluated levels of the Glendinning deposit, or within the surrounding area. Furthermore, a number of factors favour a magmatic origin/component for the hydrothermal fluid, including:

- 1) Sulphur isotopes, with low to nil fractionation, resemble those of magmatic sulphides.
- 2) The As-Sb veins appear to have been deposited at a higher temperature than subsequent Pb-Zn veins.
- 3) The common association of gold mineralization with minor intrusive activity
- 4) The high deposition temperatures.
- 5) The consistent proximity of As-rich veins to minor intrusives and their adjacent fracture systems.
- 6) The geochemical similarity to other vein systems genetically related to acid magmatism (cf. Kay and Strong, 1983).

The absence of an As enriched ore-equivalent horizon in proximity to the Glendinning deposit provides further evidence in favour of an epigenetic model for mineralisation. In a comparison of the Glendinning deposit with volcanic epithermal environments, a number of similarities are observed, including: metal associations (As-Sb-Au-Hg) and hydrothermal alteration (silicification, sericite, kaolinite-dickite and K-feldspar). In addition, a number of arguments proposed in favour of a hydrothermal model for this deposit, which include: geological field relationships; the vein type mineralization; the pervasive nature of wallrock alteration, the polymetallic, multiphase nature of mineralization; the regional distribution of arsenopyrite mineralization associated with minor intrusive activity and major structural controls.

It is possible that this deposit represents an early stage of development of a downward excavating hydrothermal convection system, similar to that proposed to account for the development of the Leadhills-Wanlockhead Pb-Zn vein system (Russell, 1986). However, the As-Sb-Au-Hg bearing mineral assemblages, structural and igneous associations, and limited sulphur isotope data point towards a single, magmatic source for the hydrothermal solutions. Furthermore, in order to explain the observed paragenetic sequence, a fall in temperature throughout the lifetime of the hydrothermal system is required. These variations are in direct opposition with the model proposed by Russell (1978, 1986) and invoked by Patrick (1981) to account for the Pb-Zn vein mineralisation at both Tyndrum and Leadhills.

This investigation suggests that the Glendinning deposit was developed coeval with minor intrusive activity and ?volcanism, and is epithermal in nature. As-Au mineralizing events may be constrained by a relatively consistent Late Silurian/Early Devonian age of mineralisation. From the evidence presented in this chapter, three possible genetic sources may be invoked, namely: direct hydrothermal evolution from granitic intrusions or basic intrusions; hydrothermal processes resulting in the selective concentration from associated black shales or pre-existing sulphides; and ore solutions derived from a deep source near the crust-mantle boundary.

Although a source for the ore fluid cannot be unequivocally defined by existing data, considerable evidence is presented for the involvement of juvenile components, in the ore fluid and their association with volatile-rich Au-bearing lamprophyres. Although no igneous intrusions were encountered within the mine area, the presence of a relatively shallow minor intrusion is invoked as a source for the metals. It is therefore proposed that structurally controlled, minor intrusives provided the Au-bearing fluids, and acted as a localised heat source.

The association of As-Sb-Au-Hg±Ag identified in the Glendinning deposit is similar in many respects to the element suite identified by White (1985) in active geothermal systems associated with epithermal deposits. A common chemical and mineralogical zonation of alteration assemblages and sulphide phases occurs throughout this region. The elemental and mineralogical composition of the ores and alteration products is similar to that of demonstrably epigenetic deposits elsewhere in the Southern Uplands and Longford Down, reflecting a similar fluid source and origin. In addition, because of their close mineralogical and geochemical similarities the Glendinning and Clontibret deposits are inferred to have been formed by similar processes.

On the basis of this study in Southern Uplands and Longford Down it is proposed that gold deposition was most likely to occur at/or within the margins of the fluid conduit, but precipitation was greatly increased in situations that resulted from incipient hydraulic brecciation and fracturing, where relatively 'hot' fluids were rapidly introduced to large surface areas of relatively 'cold' wallrock and rapidly chilled. As the mineralizing event proceeded, temperature gradients may migrate away from the zones of initial sulphide deposition and fluid/rock thermal exchange, allows the system to return to temperatures approaching that of the parental fluid. This model is invoked to explain the large variations in temperature observed in both disseminated and breccia hosted arsenopyrite crystals.

It was noted by Colvine et al., (1984) that silicification, sulphidation and alkali metasomatism, although directly associated with gold mineralisation in Archean lode gold deposits, does not give rise to broad alteration halos. It may be concluded that the processes that resulted in the depletion halos associated with the Glendinning deposit, were not dominated by diffusion, but controlled by fluid flow in a permeable medium, with the limits of the halos approximating to the limits of permeability (the fracture system) at that time. The variety of alteration products in brecciated samples indicate an incomplete wallrock reaction indicative of a short lived event and/or the existence of small scale chemical potential gradients. The precipitation of gold, sulphides and quartz, together with the extensive reduction of iron are all consistent with the behavior of ascending and cooling hydrothermal fluids.

The high frequency of mineralised veins and breccias in the vicinity of the Glendinning deposit is inferred to have formed as a result of a particularly violent upwards flow of fluids. CO₂ forms the most abundant gaseous component that is discharged at modern hydrothermal centres. As such, the CO₂ content of the hydrothermal solution at Glendinning played a critical role in metal transport and deposition processes. In addition, the relatively high content of CO₂ in the hydrothermal solution will have reduced the solubility of Ca²⁺ (Large, 1980).

It may be tentatively suggested that the breccia zone at Glendinning represents the feeder zone to, and is spatially related with, stratiform precious metal deposits, similar in many respects to that identified at Rhynie by Rice et al., (1987). The inferred surface features of the Glendinning geothermal system, most probably included sulphur deposition around vents, high and low pressure steam vents, and metalliferous sediments. The metal rich sediments were deposited within porous/highly permeable units such as breccia and fault zones, interpreted as a sub-surface fissure system associated with continental hot springs.

Alteration zones due to hydrothermal activity from fumarolic fluids, have been recognised below massive sulphide deposits (Govett and Goodfellow 1975). Compared to volcanogenic massive sulphide deposits, the Glendinning deposit differs in the lack of magnesium enrichment associated with alteration and displays a lower base metal content in the sulphide ores.

3.8.6 Summary

In a comparison of As-Sb-Au mineralization in Scotland it is proposed that one or more minor intrusions may be present at shallow depths below As-Sb-Au mineralized fault breccias and hydrothermally altered wallrocks at Glendinning. Additional intrusions may also be responsible for the observed zones of mineralization in the Glendinning study area. A model is proposed for the Glendinning deposit invoking the development of a hydrothermal system genetically related to and driven by intrusive heat sources. Different levels of crustal emplacement/exhumation may be invoked to explain the various styles of As-Sb-Au mineralization exposed in the Southern Uplands. A summary diagram illustrating the pertinent points of this model is presented in figure 89b. In this model it is proposed that hydrothermal activity commenced coeval with a period of lamprophyric intrusion and the formation of hydrothermal breccias. Precious metal bearing solutions were transported through fault breccia systems, permeating wallrock and depositing gold rich assemblages in sites of high fluid-rock interaction (ie. wallrock and breccias). The interaction of carbonate rich greywacke with high temperature hydrothermal fluids may have led to the dissolution of carbonate and the addition of both CaO and CO₂ components to the aqueous phase.

Zones of intense, pervasive hydrothermal alteration are spatially associated with Sb mineralization confined to small, localized structures including parallel fault systems and hydrothermal breccias. Auriferous fluid flow was focussed preferentially into highly fractured, brittle greywacke at points of high competency contrast. Major NNE trending fault zones acted as high permeability zones which controlled the emplacement of sulphide mineralisation. An epigenetic origin is supported by the available structural, mineralogical and isotopic data. It should be noted that the size and duration of the hydrothermal convective system, driven by heat released from the intrusion, places important constraints upon the development of economic gold concentrations in this region. Hydrothermal fluids containing the As-Au association were expelled upwards and laterally away from the cooling intrusion and deposited minerals of sequentially lower temperature facies with time.

At the onset of this project the author proposed that in comparison with modern day hot springs, the element thallium could prove to be an extremely useful pathfinder element for gold mineralization in the Southern Uplands. However, at Glendinning the distribution of thallium is relatively low and sporadic (max 8ppm). Although concentrations of 17 ppm have been recorded in the Rams Cleuch Breccia Zone, Tl values cannot be generally applied as a guide to hydrothermal alteration in the region. Where thallium is present in significant quantities, it is located within the immediate vicinity of As-Sb-Au vein mineralization (ie Rams Cleuch) and as such has an important bearing upon the nature of the hydrothermal processes responsible for this form of deposit. In comparison with studies elsewhere in the Southern Uplands by Caulfield and Naden (1988) it is proposed that the fault system at Glendinning probably remained active for a period of 10-30 million years and provided important structural controls throughout a series of relatively short-lived hydrothermal events.

3.9 SUMMARY AND CONCLUSIONS

The integration of mineralogical, textural, structural and lithogeochemical data provided a powerful tool in the examination of ore genesis in this deposit. This study has identified a number of structural and mineralogical controls upon the location of gold within the Glendinning deposit. In addition, this deposit has been evaluated in respect of its regional context and numerous geochemically similar deposits have been identified within a ten km radius of the mine area. In addition, detailed inspection of mine workings, drill core logging, mapping of individual deposits and literature review have shown that the Glendinning mineralization has many similarities to other deposits in this class, on both a local, regional and global scale.

Field observations, petrographic and geochemical studies of 304 greywacke and 197 mudstone samples collected from the Glendinning regional study area indicate that there is extensive, cryptic hydrothermal alteration and trace element zonation associated with the Glendinning As-Sb-Au deposit. The effects of similar alteration processes active throughout the study area are readily observed, and serve to pinpoint further examples of As-Sb-Au mineralization. The most important features of the Glendinning deposit investigated by this study, include: structural controls, hydrothermal alteration, lithogeochemical zonation, overburden geochemistry and sulphide hosted gold mineralization.

3.9.1 Structural controls

Fault or breccia structures provide the single most important control upon gold distribution in this region. Sillitoe (1985) noted that breccia related deposits are often misclassified as 'sedimentary' in origin when they were actually, tectonically derived. In the Glendinning deposit hydrothermally altered clasts and fragments of both sulphides and gangue minerals are common and provide evidence of multiple alternating episodes of brecciation and mineralization. The Glendinning deposit is interpreted to have formed during a period of major fracturing and minor intrusive activity, as a precursor to and possibly developed coeval with, granite emplacement. This deposit may be regarded as an elongated breccia pipe intruded into the Hawick formation and contains pyrite, arsenopyrite, stibnite, sphalerite and minor gold.

3.9.2 Hydrothermal alteration

One of the major problems with exploration geochemistry in the past has been the prerequisite to isolate extremely localised anomalous areas within a larger field area. In addition, because of the rapid increase in exploration over the last two decades, and subsequent major discoveries we are now rapidly exhausting the supply of near surface deposits. A new generation of exploration techniques and models must be based upon the recognition and location of crypto-chemical signatures (areas of weak hydrothermal alteration or depletion) which provide broader target areas for further detailed study.

In this study geochemical criteria have been established to define cryptic hydrothermal alteration of greywackes associated with As-Sb-Au mineralization. A primary halo is identified enveloping the Glendinning deposit, yielding coherent and extensive geochemical anomalies, and which may be located by using a relatively low sampling density. The location of ore zone itself requires a larger number of samples, since the alteration halo (zone 1 and 2) is several times as extensive as the ore outcrop (zone 3). Alteration is uniformly pervasive and is characterised by distinct mineralogical and lithogeochemical signatures. Altered greywackes are characterised by extreme depletion of Na_2O and subordinate Zn, Fe and Mg. Arsenic and sodium, however form the most efficient pathfinder elements for Glendinning-type deposits in this environment.

This work defines the presence of widespread alteration zones in the Glendinning area, accompanied by at least three periods of hydrothermal activity. In addition, eight types of hydrothermal alteration processes are associated with the As-Sb-Au mineralization at Glendinning; carbonatisation, silicification, potassium metasomatism, sericitisation, dickitisation, sulphidation, pyritisation and arsenopyritisation. The recognition of the visual indications and geochemical characteristics of As-Sb-Au deposits forms an important component of any exploration programme in this region.

3.9.3 Lithogeochemical Zonation

This study demonstrates that lithogeochemical halos can be recognised in surface samples at a considerable distance from As-Au deposits. Lithogeochemistry has been applied at three levels of exploration:

- 1) Regional scale reconnaissance - the identification of geochemical provinces and mineralization centres.
- 2) Local scale reconnaissance - the recognition of local halos related to individual deposits within a study area.
- 3) Mine scale - the recognition of wallrock anomalies related to individual alteration profiles, veins and structures.

On a local scale, mineralized zones may be characterised by elevated chalcophile (As, Sb, S, Cu, Pb, Tl, Hg) and depleted siderophile (Fe, Mg, Zn) and alkalis (Na) elements. The resulting geochemical halo has a minimum width of 300 to 400m. As such, sampling on cross-strike 'mega-traverses' using a spacing of 200-250m is adequate to delineate lithogeochemical halos associated with Glendinning-type deposits in this terrane. The location of broad zones of sodium depletion provide a primary indicator of hydrothermal activity. Anomalous arsenic values may be used directly as a guide to pinpoint the position of arsenopyrite-gold rich fracture zones within the sodium depletion envelope. All anomalous As and Sb values located within this region, infer the presence of bedrock As-Sb-Au mineralization and provide primary targets for detailed exploration. Samples collected from surface outcrop northeast of the mine area indicate similar enrichments and depletions (As 65ppm) at sites predicted by the extrapolation of the vein mineralization at Glendinning, inferring a minimum NNE strike extension of 1km to the known vein system. On the basis of a lithogeochemical study of the Hawick Formation greywackes hosting the Glendinning deposit, it is considered that no evidence of synsedimentary enrichment of As and Au exists.

Broad, primary halos are associated with a series of anomaly zones identified within the Glendinning study area. As, Sb, Pb, Zn, and Na form the most useful pathfinder elements for this form of cryptic occurrence. Sulphur halos are smaller and often erratic. The broad-scale nature of these geochemical anomalies suggest, that such studies may be successfully applied as a primary exploration tool. In addition, this form of study provides considerable benefits in detailed exploration around known mineral occurrences. It should be noted however, that the lithogeochemical anomalies identified in the Glendinning study are do not constitute exact drilling targets; detailed sampling and geophysical techniques are required to define the location, structure and size of the primary mineralization, prior to trenching and/or diamond drilling. In summary, this study has proved conclusively that anomalous levels of arsenic can be directly used as pathfinder for As-Sb-Au mineralization in this region. In addition, the recognition of the nature and processes responsible for alteration in the Glendinning deposit has important exploration and conceptual value in our understanding of the parental hydrothermal system.

3.9.4 Overburden Geochemistry

Mineralogically, the trace elements presented on the soil geochemical maps from the Rams Cleuch and Swin Gill areas reflect both primary sulphides (As, Sb, Pb, Zn, Cu, Tl) and sulphates (Ba) whereas the major element chemistry relates to wallrock alteration processes particularly the loss of sodic feldspars during K-metasomatism and sericitisation. Trace elements, most notably As and Sb form elliptical, narrow, 30m wide anomaly zones the strike of which correspond to those of fracture zones observed in bedrock (Rams Cleuch) or within aerial photographs (Swin Gill). It should be noted that although the order of magnitude of As and Sb values are relatively

small (max 65 and 34ppm respectively) the anomalies detected in both the Rams Cleuch and Swin Gill grids compare favorably with the results of the BGS soil survey at Glendinning (55ppm Sb and 350ppm As) particularly when environmental contamination from the historical mining activity is taken into consideration. The width of the primary dispersion pattern however, is unknown due to the limited exposure within the grid area.

This study has demonstrated that the systematic sampling of residual soils in the search for secondary dispersion anomalies directly overlying suboutcropping mineralized vein systems has been outstandingly successful in the Glendinning study area. Soil Geochemistry provides an effective tool in exploration for and the delineation of fracture controlled shallow of blind As-Sb-Au mineralization. These results provide clear diagnostic features of As-Sb-Au mineralization and assist the preparation of conceptual models and criteria for further exploration in this region. It is considered that there are sufficient indications of As-Sb-Au mineralization in the Glendinning area to justify further investigations. Specifically, the lithogeochemical and shallow overburden anomalies defined at Rams Cleuch and Swin Gill, together with six further geochemically anomalous sites, should be investigated further.

3.9.5 Sulphide hosted gold Mineralization

This study has demonstrated that an initial phase of arsenopyrite-pyrite mineralisation formed the principal locus of gold mineralisation in both the Glendinning and Clontibret deposits. The presence of submicroscopic and lattice-hosted gold associated with low grade, disseminated arsenopyrite-pyrite assemblage in a structurally controlled breccia suggests that there is considerable potential for the discovery of a large scale turbidite hosted gold deposit in the Glendinning area. The fundamental controls of temperature, pressure, ore-fluid chemistry and wallrock composition were clearly important in the genesis of this deposit.

3.9.6 Conclusions

Target areas of potentially economic arsenopyrite-gold mineralization may be detected by the recognition of primary mineralogical and geochemical indicators of pervasive hydrothermal alteration, including:

- 1) Visual - a progressive decrease in diffusive colour.
- 2) Mineralogical - the presence of dickite within veins or fractures.
- 3) Geochemical - the location of primary arsenic and associated trace elements anomalies.
- 4) Depletion - the location of primary sodium and zinc geochemical depletion anomalies may be used to delineate broader targets than those associated with primary sulphide mineralization.

It is proposed that the location and occurrence of gold in the Glendinning deposit is structurally controlled and hydrothermal in origin. The Glendinning deposit may be classified as an auriferous polymetallic vein-type epigenetic deposit, in which disseminated arsenopyrite mineralization forms the loci for gold deposition. On the basis of geochemical, mineralogical and isotopic evidence it may also be tentatively suggested that the Glendinning deposit represents a hydromagmatic breccia-hosted As-Sb-Au deposit related to minor intrusive activity. In comparison with similar hydrothermal systems (cf. chapter 4) it is proposed the the As-Sb-Au phase of mineralization took place over a period of ~150,000 to 500,000 years.

Using the above model, geochemical atlas and multi-element anomaly maps a number of target areas were delineated in the Glendinning study area which merit further attention. To date both gossans and two new vein systems have been located by the application of lithogeochemistry in this region and the strike length of the known As-Sb-Au vein mineralization at Glendinning (or at least its geochemical alteration envelope) has been extended over a distance of 1km NNE from the main adit. From an evaluation of the Glendinning deposit and soil investigations of two target areas (Rams Cleuch and Swin Gill) it is concluded that As-Sb-Au mineralization in this region is structurally controlled and located with a series of NNE trending fracture zones.

The economic potential of the mineralization around the Louisa Mine at Glendinning is difficult to assess from the limited information obtained from the geochemical surveys and drilling conducted to date, and due to the poor exposure to the east of the deposit. No evidence of coarse grained gold has been found in vein samples, and geochemical evidence suggests that virtually all gold within this deposit is preferentially located within an arsenopyrite host. This work has shown that arsenic may be used as a pathfinder element for As-Sb-Au mineralization in this region, in both lithogeochemical reconnaissance and detailed overburden sampling programmes. In addition, this study has revealed the presence of numerous vein and vein swarms in the Glendinning study area and suggest that the Glendinning deposit forms an important new mineralization centre in Southern Scotland. In light of the evidence presented in chapter four, and the timing of igneous activity in Scotland, a late Silurian-Early Devonian age is proposed for the mineralizing event at Glendinning. Although no examples of late Silurian minor intrusions were detected in boreholes through the Glendinning deposit, numerous local intrusions (hornblende lamprophyres, monzonites and quartz-porphyry dykes) provide favourable environments for gold-rich mineralization in the Glendinning study area. Further exploration for similar deposits in Scotland may be restricted to areas where three fundamental conditions coincide namely, the presence of a suitable fracturing system, the identification of metal enriched primary or secondary anomalies and the location of an intrusive heat source.

Prior to the BGS investigation (Gallagher et al., 1983) the Louisa Mine at Glendinning was regarded as an isolated antimony deposit, historical subjected to mining activity and unrelated to other deposits in this region. It has been demonstrated by this study that the Glendinning deposit contains a previously unreported phase of As-Au mineralisation and that the surrounding area hosts numerous sites of As-Sb-Au mineralisation. As such, potential exists for the discovery of similar, if not larger deposits to that identified at Glendinning.

The Southern Uplands greywacke terrane and its continuation into the Longford Down, host four major centres of mineralisation, including: Clontibret, Newtonards, Leadhills and Newton Stewart. Lithogeochemical and soil geochemical surveys have defined additional areas of As-Sb-Au-Hg mineralization up to 10km north of the Glendinning mine area, thus adding considerable importance to this region as a metallogenic center within the Southern Uplands. In view of the widespread nature of As-Sb-Au vein mineralization identified by this study, the Glendinning area is proposed as the fifth major mineralisation centre, in this region.

CHAPTER FOUR

CHAPTER FOUR

CHAPTER FOUR

TURBIDITE HOSTED ARSENIC-GOLD MINERALIZATION

4.1 INTRODUCTION

Interest in the location of arsenic deposits across the Southern Uplands has rapidly increased during the last decade, due to the recognition of the arsenic-gold association and the potential for economic gold mineralization in this region. This chapter summarises the empirical features and geological setting of As-Sb-(Au) deposits and presents a review of their lithogeochemical, mineralogical and genetic characteristics in order to establish the background to chapter's 3, 6 and 7. In addition, this study documents the contention that Lower Palaeozoic sediments in southern Scotland form the host to a range of gold-bearing epithermal deposits.

It should be noted that the origin of mineral deposits has been the subject of considerable debate throughout the last five centuries, if not earlier. A detailed review of the historical background to such metallogenic studies is presented by Emblin (1978): As early as 1546, Agricola recognised that ore bodies were emplaced in older rocks by circulating currents of various origins and also that the shape and orientation of the emplacement was controlled by the structure of the host rock. Steno (1669) suggested that ores were a condensation product of vapors which ascended through open fissures from deep in the crust. Henkel (1725) and Zimmerman (1746) both applied the term 'hydrothermal solution' to Steno's vapors and proposed that these solutions should contain material dissolved from the country rock through which they had ascended. Hutton (1788) and Werner (1791) initiated what has since been termed the Plutonist/Neptunist argument. Hutton proposed that deposits were derived from deep molten magmas (plutonism) and had been transported by ascending fluids, whereas Werner maintained that mineral veins originated as chemical precipitates in structural cracks that developed on the floors of primeval oceans (Neptunism). Lindgren (1933) developed a hierarchy of genetically separate mineralizing mechanisms which, while allowing for syngenetic and diagenetic ores, placed considerable emphasis on igneous-hydrothermal activity. This hierarchy forms the basis of a fundamental classification system still in use at this time. The term 'hydrothermal' when used in the context of this study is taken to imply the formation from a hot, aqueous fluid of unspecified origin. A comprehensive review of hydrothermal ore deposits is presented by Barnes (1979).

4.2 FLUID CHEMISTRY

Two major mechanisms for the formation of trace element halos in essentially unaltered wallrocks are widely discussed in the literature, namely diffusion and permeation. Diffusion is the process by which trace elements enter wallrock due to concentration gradients between the hydrothermal fluid (in the vein) and the pore fluids (in the host rocks) whereas permeation is the process by which trace elements are transported by circulating hydrothermal fluids through pore spaces, and/or other voids, in the wallrock under the influence of a pressure gradient between the vein fluid and the pore water pressure. It has been demonstrated by this study (chapter 3) that epigenetic gold deposits in the Southern Uplands are enveloped by laterally extensive multi-element halos, formed during the pervasive alteration of country rocks by fluid permeation.

The transport of gold in solution has been investigated by numerous authors and is the subject of considerable debate. Precipitation mechanisms may include the decomposition of gold complexes in solution due to changes in pH, Eh and wallrock reactions; and the adsorption and/or coprecipitation of soluble gold complexes and colloids. Helgeson and Garrels (1968) in a discussion of the hydrothermal transport and deposition of gold, suggested that gold-quartz veins are formed from weakly acid solutions and are generally precipitated above 175°C. Fife and Henley (1973) demonstrated that the solubility of gold in chloride solutions increases from 10ppm at 300°C to 1000ppm at 510°C, thus enabling large amounts of gold to be transported at high temperature before precipitation at ~300°C. Seward (1973) in studies of the transport of gold in hydrothermal ore solutions, concluded that three thio gold complexes contributed to the solubility of gold in aqueous sulphide solutions. The complex $\text{Au}_2(\text{HS})_2\text{S}^{2-}$ predominated in alkaline solution, the $\text{Au}(\text{HS})_2^-$ complex occurred in the neutral pH region, and in the acid pH region $\text{Au}(\text{HS})^0$ complex was present. In addition, Fyfe et al., (1984) included CO and COS as possible ligands. It was therefore proposed that gold is transported in hydrothermal ore solutions as both thio and chloro complexes and may be deposited in response to changes in temperature, pressure, pH, oxidation potential and sulphur activity. The absence of igneous intrusions and the extensive nature of hydrothermal alteration in numerous deposits, led to the development of a model by Fyfe and Henley (1973) invoking the concentration of gold by the circulation of fluids during metamorphism. They concluded that dehydration/metamorphic fluids in which chlorides are present, could move gold from large volumes of rock into shear zones and faults where it is concentrated by precipitation at lower temperatures and pressures. Additional mechanism for precipitation from solution include changes in temperature, pressure, pH, oxidation state and other chemical disequilibria, resulting from the interaction with wallrock, boiling and mixing with groundwater or other fluids (Barnes, 1973).

Experimental work by Ewers and Keays (1977) demonstrated that decreasing temperatures are highly effective in controlling the deposition of As and Sb sulphides. In addition, the fugacities of H_2S and H_2 in a number of Broadlands drillholes are ~0.1 bars, which indicate the reducing nature of the solutions. Studies by Rytuba and Dickson (1974) indicated that in a reducing environment, chloride ions are not effective in transporting gold. Hutchinson (1983) demonstrated that most deeply circulated metalliferous hydrothermal fluids are strongly reduced, with very low Eh or fO_2 . Seward (1983) however, noted that even very low gold concentrations, close to those of seawater values, may still lead to economic concentrations of gold (eg. Broadlands Geothermal system, New Zealand). Seaward (1984) proposed that the most important complexes involved in the transportation of gold are those involving Cl^- , sulphur donor ligands such as HS^- and S^{2-} , thioarsenite ligands such as AsS_2^- , or NH_3 . Ore bodies such as those located within the Carlin deposit were formed where hydrothermal solutions flowing along fault and breccia zones penetrated outward and reacted with the wallrocks, depositing hydrothermal silica, pyrite, arsenopyrite and gold. The decrease in pressure as solutions are discharged at the surface and the resulting losses of H_2S through boiling, tend to reduce the stabilities of metal complexes and contribute to the surface enrichment of As, Sb and Au (Ewers and Keays, 1977). Harris and Radtke (1976) demonstrated the use of statistical assessment of lithogeochemical data to test hypotheses on the origin and geochemical paragenesis of disseminated gold mineralization in the Carlin deposit, Nevada. They concluded that the hydrothermal solution responsible for the Carlin ores was weakly alkaline and contained excess dissolved sulphur.

Finlow-Bates and Large (1978) documented the effects of water depth upon the formation of submarine exhalative ore deposits, and demonstrated that boiling in the feeder zones due to low pressures would cause cooling of the solution and precipitation of the least soluble sulphide phases as a crosscutting (disseminated, breccia filling, vein-type or stockwork) facies prior to exhalation. In hypogene environments, the loss of alkalis during wallrock

reaction (sericitization) leads to a shift in the pH towards acidic compositions, the decomposition of alkaline complexes and the precipitation of native gold (Boyle 1979). Weissburg et al., (1979) also noted that cooling, oxidation and decreasing pH were important factors in the deposition of gold bearing precipitates in New Zealand hot springs (accompanied by high arsenic, antimony, mercury and thallium). Boyle (1979) however, noted that the oxidation processes in gold deposits are complex and depend essentially on the Eh and pH.

Active geothermal systems have been considered to be modern analogues of epithermal systems (White, 1985; Weissberg et al., 1979). The trace element chemistry of modern geothermal systems has been studied by numerous authors including Weissberg et al., (1979), Ewers and Keays (1977), White (1985) and Henley (1985). These studies documented high concentrations of As, Sb, Hg and Tl in the upper portions of geothermal systems in addition to Au and Ag. Dilute geothermal waters may transport and deposit sufficient amounts of Au, Ag, Hg, As and Sb to account for many 'epithermal' deposits in spite of the extremely low concentrations of metals, provided that sufficiently high flow rates persist for long periods of time (Weissburg et al., 1979).

A consequence of the transport and deposition of gold from reduced sulphur complexes is the distinctive elemental composition of the ores, characterised by high concentrations of Au, Sb, Hg, As, Bi, B (Kerrick, 1977; Kerrich and Fryer, 1979; Phillips et al., 1984). Phillips and Groves (1983) have argued that the enriched elements form weakly charged cations (or soft acids) that complex selectively with larger polarizable ligands (or soft bases), such as bisulphide ions.

Temperature forms the main control on SiO_2 solubility in hydrothermal aqueous solutions, with the solubility increasing with increasing temperature, while decreases in temperature result in precipitation. Active hot-spring hydrothermal systems are generally saturated with silica and Ellis (1967) identified values ranging from 250-750ppm SiO_2 in solution in surface waters. It should be noted that if the confining pressure upon the hydrothermal solution is exceeded by the vapour pressure, the solution will commence to boil. Such fluid boiling will result in a loss of CO_2 (and H_2S). Furthermore, if gold, arsenic and antimony are present as thio complexes, their coprecipitation is enhanced by the removal of reduced sulphur (as H_2S) through boiling and to a minor extent, by precipitation of iron sulphides (Weissburg et al., 1979).

Heinrich and Eadington (1986) demonstrated the application of thermodynamic calculations to predict the speciation of arsenic in hydrothermal solutions and the solubility of arsenic minerals. This evaluation revealed that at neutral to acid pH the aqueous species H_3AsO_3^0 may account for the transport of arsenic. The As mineral associations: 1) Orpiment + realgar + native arsenic + pyrite; 2) Arsenopyrite + pyrite; and 3) Arsenopyrite \pm pyrrhotite \pm loellingite \pm pyrrhotite were predicted to reach As solubilities high enough to account for hydrothermal transport at progressively higher temperatures in systems containing excess iron sulphide. In addition, host rock buffers were proposed to have dominated the chemical evolution of fluids in disseminated breccia ores which exhibit penetrative wallrock alteration. Rosenbauer and Bischoff (1983) in studies of the hydrothermal alteration of greywacke by NaCl-rich fluids at 350°C, noted that 67% of the original greywacke was converted to albite and smectite. In addition the rock gained Na and released Ca, K, heavy metals and CO_2 to solution. The fluid composition combined with ore element association and the intimate relationship between Au and Fe-As-sulphides, may be used to suggest that reduced-sulphur complexes formed the major transporting agents for gold mineralization (Phillips and Groves, 1983). Groves et al., (1983) suggested that the majority of Archaean volcanic hosted gold deposits of western Australia formed from CO_2 -rich fluids of low salinity at temperatures 350°C \pm

50°C. The composition of these fluids (CO₂ rich, low NaCl) appears incompatible with a seawater source. In relation to Scottish deposits, Russell (1986) proposed that the elements As, Sb, Bi, Cu and Au could have partitioned into the Caledonian melts to be precipitated from late stage magmatic hydrothermal solutions on loss of CO₂ and near surface boiling.

Henley (1985) identified the coincidence of high gas flux (CO₂ + H₂S) and gold and proposed a hypothesis that the gas was derived from a deep crustal (or even upper mantle) source. This work was extended by Cole (1986) who demonstrated the direct relationship between the vertical extent of gold mineralization, the depth of deposition, the initial CO₂ content of the solution prior to boiling and the amount of gold deposited during the boiling event. High CO₂-bearing systems were demonstrated by Cole (op. cit) to have vertically extensive mineralization over depths of ~600m. Cole and Drummond (1986) noted that the depth at which boiling commences becomes shallower with either decreasing temperature and/or CO₂ concentration for a constant salinity. Their model predicted zones of intense gold enrichment near the top of the boiling interval (analogous to high grade bonanza ores) associated with high water-rock ratios, in order to deposit concentrations typical of most epithermal deposits.

Krupp and Seaward (1987) in a study of the Rotokawa geothermal system, New Zealand, identified 12 different hydrothermal explosion breccias. Clasts within these breccias commonly contain pyrite and yield sub-economic gold values (<0.1ppm). Thermal waters discharging at this time are currently depositing ore grade gold, arsenic and antimony-rich muds which also contain high concentrations of thallium and mercury. Perring et al., (1987) identified a number of constraints upon the source of auriferous fluids for Archaean gold deposits. Most models emphasise the focusing of H₂O-CO₂, low-salinity fluids along fault or shear zones to dilational sites where fluid-rock reactions caused Au precipitation under suitable P-T conditions, in contrast, hypotheses concerning the source of ore fluid and ore components, including Au, are diverse. The separation of a vapour phase during boiling or direct exsolution of gaseous phases from magmas, coupled with the interaction between hot vapour and cold groundwater, may lead to the explosive escape of vapour and the generation of hydrothermal eruption vents (Foster, 1986). Recent studies of the Broadlands geothermal system (Henley, 1985) have indicated that almost all gold precipitation may be accounted for by boiling. In a comparison with the above features and those documented in chapter three, hydrothermal fluids implicated in the Glendinning deposit were present at 320° ± 40°C, and underwent transient effervescence of CO₂.

4.3 STRUCTURAL RELATIONSHIPS

This section details the major structural relationships identified within the literature, which provide dominant controls upon the location of As-Sb-Au deposits.

4.3.1 Breccias

An epithermal ore deposit is defined by Silberman and Berger (1985) as a relatively near-surface deposit, formed in a hydrothermal system under low to moderate pressure and a temperature range below ~300°C. Epithermal deposits occur in a continuum of settings ranging from shallow stockwork and breccias (the 'hot spring' environment) to relatively deep veins and fissures (the 'Bonanza' environment). Brecciation processes including hydrothermal explosions and hydrofracturing result in the rapid decrease of both temperature and pressure. Simultaneously, nonvolatile dissolved components are enriched in the residual liquid, whereas the partitioning of

gasses into the steam fraction will result in changes to both the pH and Eh of the solution (cf. Fournier, 1985). As such, hydrothermal brecciation creates the ideal conditions for the deposition of silica minerals, sulphides and gold.

Explosive brecciation in a relatively near-surface environment provides evidence to indicate that the hydrothermal system had become overpressured, with a consequent violent and sudden release of energy. As such, the formation of a seal or cap to this system forms a necessary requisite for the development of the extensive breccia zones identified in the Glendinning deposit (cf. Berger, 1985). A number of mechanisms are proposed to explain the origin of breccia pipes including hydrothermal stoping (Sillitoe and Sawkins, 1971), fluidization (Gilmour, 1977) and phreatomagmatic explosion (Wolfe, 1980). Phreatomagmatic explosions and the resulting brecciation occur when a rising body of magma encounters a voluminous supply of water, which instantly flashes to steam. After numerous repetitions of this process the resultant breccias may be sealed from crystallization from the hydrothermal fluids. In a review of ore-related breccias in volcano-plutonic arcs, Sillitoe (1985) defined six possible mechanisms for sub-surface brecciation, including:

- 1) Release of magmatic-hydrothermal fluids from high-level hydrous magma chambers.
- 2) Magmatic heating and expansion of meteoric pore fluids.
- 3) Interaction of ground waters with sub-surface magma and the generation of phreatomagmatic explosions.
- 4) Magmatic-hydrothermal brecciation caused by decompression and eruption of the top portion of an underlying magma chamber.
- 5) The mechanical disruption of the wallrocks during sub-surface movement of magma (any intrusion related deposit may include such intrusion breccias).
- 6) Tectonic breccias resulting from fault displacement.

Hydraulic Fracturing

In 1972, Phillips proposed a model for vein genesis which explains both lateral variations in structure and mineralization along the veins, as well as providing the broad stratigraphic control on ore formation. In summary, he proposed that pressurized hydrothermal fluids accumulated on normal shear fractures, causing extension of the fractures and brecciation resulting from episodic bursts of hydraulic fracturing. Hydraulic fracturing occurs when $P_{\text{fluid}} > P_{\text{lithostatic}} + \text{tensile strength of the rock}$, and is a likely mechanism where fluid from deep level plutons penetrate upwards to higher crustal levels. Furthermore, Sibson et al., (1975) noted that as a consequence of the dilatency/fluid-diffusion mechanism for shallow earthquakes, considerable volumes of fluid are rapidly redistributed in the crust following seismic faulting. It was therefore proposed that a seismic pumping mechanism may have been involved in the generation of hydrothermal vein deposits. This dilatency/fluid-diffusional model of Sibson et al., (op.cit) provides one explanation for the intermittent flow of hydrothermal fluids in and around fault zones, and may be used to infer that seismic faulting acts as a pumping mechanism for the mineralizing fluids. Norris and Henley (1976) noted that where interconnected hydraulic fracture systems developed over more than 100 to 200m in vertical extent, the fractures become unstable and the process will tend to be self-perpetuating. This process is most successful with wrench faults because differential stresses associated with normal faulting are relatively low.

Beach (1980) described the processes of hydraulic fracturing in which load parallel (tensile) or load oblique (shear) fractures are produced through the action of a fluid under pressure within a crack. Hydraulic fracturing of rocks occurs during the burial, dewatering and metamorphism of sedimentary sequences as very large volumes of water are released (Holland and Lambert, 1969; Fyfe, 1976, Norris and Henley, 1976). It is highly probable that the decrease in pressure caused by breccia development, resulted in boiling and the rapid precipitation of fine grained silica and sulphide phases. High-power discharge of metalliferous fluids may occur through breccia pipes and vents generated by hydrothermal explosion. Subsequent events may result in the brecciation of both ore and stockwork.

Sillitoe (1985) noted that a continuum exists between many of these breccia types, and as such it is difficult to identify unique criteria for their unambiguous distinction. Phillips (1986) presented a classic study of the effects of hydraulic fracturing in the formation of gold-bearing vein mineralization in mid-Wales and noted that many of the normal mineralized faults tend to pass laterally into vertical, dilational breccia zones. This feature was interpreted in terms of a three stage process, involving: a slow build up of the differential stress until the critical failure conditions are reached; abrupt fracturing that results in a release of elastic strain energy, a temporary reduction in fluid pressure, which results in brecciation, and a small reduction in the differential stress near the fault; and permeation of the pore water into the fracture.

In volcanogenic deposits the diameter of the alteration pipe increases upwards until coincident with that of the massive ore (Sangster, 1972). Volatile separation during the ascent of a granitic magma, could raise the pressure sufficiently in the magmatic system to fracture surrounding country rock and produce pathways for fluid flow and zones for the precipitation of lode deposits (Burnham and Ohmoto, 1980).

Evidence for a relatively high crustal level of intrusion in the Southern Uplands is provided by Leake and Cooper (1983) who detailed the occurrence of breccia pipes and breccia dykes in the Black Stockarton Moor subvolcanic complex. According to the model for porphyry copper systems developed by Sillitoe (1973) the probable depth of this complex and its associated mineralization would be ~2km below the pre-existing land surface. In borehole sections, in the Black Stockarton Moor complex, there is abundant evidence of tensional fracturing and brecciation in the turbidites immediately above many of the sheet intrusions, reflecting a rise in hydraulic pressure due to retrograde boiling (Phillips, 1973; Leake and Cooper, 1983).

4.3.2 Lineaments

Lineaments are 'pattern disruptions' expressed in rock outcrop patterns, volcanic elongations, magnetic or gravity anomalies, folds, faults or joints (Haszeldine, 1987). In the UK, these form N-S ($\pm 10^\circ$) alignments, extending up to 400km across different basement terranes and the Iapetus Suture. Their first manifestation occurs during the late Silurian (Pridoli) times immediately after the closure of Iapetus, where lamprophyre dykes and coeval 415-400 Ma granodiorites were orientated N-S (Rock et al., 1987, Haszeldine, 1987). These lineaments provided major structural controls upon mineralization, sedimentation, rifting and volcanism throughout the Devonian and Carboniferous periods and influenced Permian, Triassic, Jurassic and early Tertiary sedimentation and volcanism. The series of major N-S lineaments identified by Haszeldine (1987) during research upon structural controls of Carboniferous sedimentation are presented in fig. 4a. Within the Southern Uplands exceptionally regular N-S structures were identified by Russell (1971, 1972) and Haszeldine, (1987). These lineaments acted as a focii for igneous activity as demonstrated by the Loch Doon granite and its surrounding lamprophyre and porphyrite dykes

(Haszeldine, 1987). As such, the hypothesis postulated within this thesis is that there is a significant correlation between lineaments, intrusions and gold mineralization in Southern Scotland.

Plant *et. al.* (1988) have demonstrated the effective use of regional geochemical and other databases in identifying fundamental crustal blocks and lineaments in basement terranes. In the Scottish Caledonides metalliferous mineralization is found in association with granites only when they are also associated with major fault systems (Atherton and Plant, 1986). Plant (1988) demonstrated that in Scotland all metalliferous granites are located along major lineaments. Geochemical changes are therefore not progressive across Scotland as suggested by Thirlwall (1980) but are discontinuous and related to the emplacement of granites (and other minor intrusions) in deep crustal lineaments. Stephens (1986) however, in studies of the Late Caledonian granites in Scotland, concluded that deep crustal boundaries do not correlate well with the surface traces of major faults.

Russell (1971) proposed that north-south trending faults as well as crustal inhomogeneity in central Scotland were formed in response to E-W tensional activity within the lithosphere. Russell (1971) identified the occurrence of the Buckhaven-Innerleithen lineament 45km east of the postulated Alva-Thornhill structure. Although Russell (*op. cit.*) noted that no major mineralization exists along this structure, it is interesting to note that this structure corresponds with the approximate position of the Southern Uplands 'Shatter Belt', and also the Glendinning deposit. This study demonstrates that many, if not all of the As-Sb-Au deposits in the Southern Uplands and Longford Down occur in close proximity to major fracture-related lineaments.

Haszeldine (1987) noted that major structural lineaments may affect areas several km in width, on either side of a central structure. In a discussion of the origin of these major structural lineaments, Haszeldine (1987) proposed that they formed as a result of epirc tensional forces, unrelated to local plate tectonic activity. N-S trending fault structures generated by extensional tectonics, together with extensive strike-parallel shear zones, were intruded by felsic, lamprophyric and porphyry dykes and stocks and served to localize widespread hydrothermal alteration and As-Sb-Au mineralization. A further manifestation of these lineaments is displayed at the western margin of Black Stockarton Moor (Leake and Cooper, 1983) where they control the orientations within lamprophyre and/or subvolcanic complexes. Preliminary analysis suggests that large scale crustal lineaments, provided an important structural control upon the location of gold deposits in this region.

Jahoda *et al.*, (1989) identified the relationship between en-echelon fault offsets ('jogs'), igneous activity, hydrothermal breccias and As-Au mineralisation in northwest Spain. The recognition of jogs that have been the loci of intrusive magmatism ('hot jogs') is of fundamental importance in the genesis of gold mineralisation and may have particular application within the British Caledonides. The mineralized zone at Glendinning lies within the extension of a major linear feature identified as 'the Southern Uplands Shatter Belt'. The importance of similar structures in localizing mineralization is emphasized and guidelines are suggested, upon which future exploration for similar deposits may be based. The proposed structural controls are considered to be extremely important and may be used to assist the choice of target areas at both local and regional scale. Similar lineaments have been identified in Canadian greenstone terranes and are interpreted by McNeil and Kerrich (1986) as trans-crustal listric normal faults, which initially accommodated rifting and acted as conduits for mantle derived alkalic magmas. These structures also provided major structural controls upon hydrothermal fluids and the siting of gold deposits.

4.4 IGNEOUS RELATIONSHIPS

This section details the major igneous relationships identified during this study which provide dominant controls upon the location of As-Sb-Au deposits.

4.4.1 Calc Alkaline Volcanics

During the last decade there has been a dramatic increase in the search for low-grade, large-tonnage and near-surface gold deposits. This was due to higher gold prices accompanied by technological improvements in bulk mining capability. Most of the major discoveries since the 1970's have been restricted to areas of calc-alkaline volcanism in the circum-pacific region, including western USA, Chilli, southern Japan, Fiji and Papua New Guinea (Celenek, 1987).

Stephenson and Ehmann (1971) proposed that mafic intrusions provided the source rocks to numerous gold deposits. Marakushev (1977) proposed that the relationship between auriferous deposits, diorites and granodiorites was related to endogenic concentration during the early stages in granitoid magmatism. Boyle (1979) demonstrated a trend towards progressively decreasing gold content from mafic to calc-alkaline rock types. Unfortunately, Govett and Nichol (1979) noted that vein deposits associated with intrusive rocks, represent one of the smallest targets for mineral exploration.

Halliday et al., (1979) in a study of the Rb-Sr and U-Pb isotopic systems of Caledonian granitic plutons in Scotland and northern England concluded that, in strong contrast to the ~550 Ma and ~460 Ma granitoids, the ~400 Ma magmas were largely hybrids derived from the mantle and/or 'new' lower crust with varying degrees of assimilation of upper crustal material. In detailed studies of the Rb-Sr and O isotopic systems within zoned Caledonian granitic plutons, Halliday et al., (1980) demonstrated that the magmas responsible for the Loch Doon, Criffel and Fleet plutons were derived by melting of mantle and/or 'new' basic lower crust and metasediments. Isotopic variations between the three plutons were interpreted to have formed as a result of incomplete hybridization between magmas derived from these differing sources. Stanton and Ramsay (1980) in a discussion of the relationship between calc-alkaline volcanics and mineralization, noted that fractional crystallization forming the calc-alkaline suite of rocks was also responsible for the generation of an aqueous volatile-rich phases. Thirlwall (1981) in a study of the geochemistry of Lower Devonian volcanic rocks in northern Britain, noted that volcanic and plutonic rocks south of the Southern Uplands fault were probably unrelated to subduction activity.

Eugster (1985) in a study of the relationship between granites and hydrothermal ore deposits noted that large highly charged cations (LHC) elements including As, Sb, W, Sn and Mo may become enriched in the roof of an acid magma chamber via transportation mechanisms enhanced by the formation of hydrous complexes. According to computer models, the development of convective circulation in, and around intrusions is an inevitable outcome of magma emplacement, the magnitude of which is dominantly controlled by permeability (Shepherd and Allan, 1985). Stephens (1980) provided detailed evidence that calc-alkaline magmatism may be generated by processes other than subduction at destructive margins, and demonstrated that collision tectonics may provide suitable crustal protoliths for calc-alkaline magmas.

Plant et al., (1983) in studies of metalliferous Caledonian granites, noted their association with major deep seated fracture systems and suggested that the development of mineralization associated with granites is dependant upon both the chemistry of the intrusion and the crustal setting in which it is emplaced. Furthermore, Colvine et al., (1984) demonstrated that many Archean lode gold deposits are temporally associated with alkaline magmatism and dioritic to granodiorite batholith emplacement in a similar manner to that observed by this study in the Southern Uplands.

Plant et al., (1985) in a study of the geochemistry of high heat production granites in the British Caledonides, identified three main groups of granite which can be related to classifications based upon metalliferous associations, including: granites emplaced at constructive plate margins and in extensional marginal basins associated with high heat flow and the rise of basic magma into the crust; calc-alkaline granites emplaced at destructive plate margins; and alkaline- and sub-alkaline granites which were emplaced post-orogenically or in anorogenic rift zones. The post orogenic granites in Scotland and Ireland display juvenile isotopic compositions and were emplaced through deep lineaments, comparable to the granites of the Peruvian coastal batholith (Atherton and Plant, 1986). In addition, Plant (1986) documented a series of models for granites and their mineralizing systems in the British and Irish Caledonides.

Stephens (1988) reviewing granitoid plutonism in the Caledonian orogen of Europe noted that early magmatism N of the Iapetus suture line was dominantly S-type resulting from crustal anatexis of dominantly metasedimentary rocks. Later plutonism (400–410 Ma) in the Southern Uplands is dominated by concentrically zoned I-type plutons, with the exception of the Cairnmore of Fleet pluton which exhibits S-type characteristics. A detailed overview of Ordo-Silurian volcanism in the Caledonian-Appalachian Orogen was presented by Stillman (1988) who demonstrated that the primary controls upon volcanism were plate-margin dynamics resulting from the change from a spreading to closing ocean basin with the development of converging margins, volcanic arcs, marginal basins, active continental margins and arc trench systems. Detailed studies of Wenlock to mid-Devonian volcanism of the Caledonian orogen were presented by Thirlwall (1988) who noted the presence of abundant calc-alkaline volcanism in Scotland (410 Ma) which he related to subduction processes on the NW margin of the Iapetus ocean. Cu porphyries ('I' type granites) have the most primitive geochemistry and characterise the early stages of subduction under conditions of high pH_2O in the mantle and lower crust (Plant, 1986). The association between magma genesis of metalliferous granites and movement on deep faults is particularly relevant in Southern Scotland. Intrusions of porphyry Cu association occur dominantly in the south and southwest Grampian Highlands and in the Southern Uplands of Scotland. These intrusions are composed of small calc-alkaline complexes associated with ultramafic or mafic rocks and have juvenile isotopic compositions and relatively unfractionated trace element patterns (Plant, 1986).

During the final stages of the Caledonian orogeny, numerous granitoid plutons were intruded into the Caledonian rocks of Scotland and northern England. In the Southern Uplands of Scotland metalliferous granites were emplaced into relatively-cool crust. The intrusions are geochemically and structurally discordant and their spatial positions suggest a relationship with deep seated, sub-crustal processes. Initial igneous activity in the Southern Uplands consisted of an initial phase of numerous small, volatile-rich, fracture-controlled intrusions, in contrast to the final phases of Caledonian igneous activity are characterised by the development of large-scale plutons. The identification of centres of minor igneous activity in Southern Scotland is hampered by the fact that the published geological maps of do not necessarily reflect the abundance of such intrusions (Leake, et al., 1981). Stone (1981)

invoked the presence of pre-tectonic minor intrusions to suggest the presence of local areas of high geothermal gradients.

During the initial stage of emplacement of granitoid batholiths, calc-alkaline volcanics were developed comagmatically. The occurrence of early Devonian andesitic lavas in the Cheviots in addition to other centers further north (Leake and Cooper, 1983) provides further evidence that volcanism was developed coeval with granite intrusion. Stone and Leake (1983) proposed that the abundance of metal-rich minor intrusions in the Glenhead area provides strong circumstantial evidence in favour of an igneous source for all mineralisation. This hypothesis may also be applied on a wider regional scale in the Southern Uplands and in addition, metalliferous mineralization associated with granites from the Longford Down is favored by the contemporaneous age of the intrusions with the metalliferous suite in Southern Scotland. It was however proposed by Stone and Gallagher (1984) that the association of gold with minor intrusive activity was a result of remobilization from a greywacke source rather than of primary origin. As such, the spatial association between As-Sb-Au deposits and minor intrusions, does not provide unequivocal evidence for a genetic link between the two, and further lines of evidence must be sought.

4.4.2 Lamprophyres

This section details the results of the first attempt to classify the economic/auriferous potential of lamprophyre dykes and their associated breccia pipes and stocks in Scotland. As part of the geochemical investigations undertaken during the tenure of this project, over 100 samples of lamprophyre dyke material collected across Scotland by BGS, were analysed for As-Sb in order to assess the source potential of these rocks for As-Sb-Au mineralization.

In general, the Southern Uplands of Scotland consist of an Ordovician-Silurian greywacke-mudstone sequence associated with rare ophiolites, intruded by large granitoid plutons (ca 400 Ma; Harmon et al., 1984), many thousands of lamprophyre, "porphyrite" and "porphyry" dykes and associated subvolcanic complexes (ca 425-395 Ma; Barnes et al., 1987; Macdonald et al., 1985; and Rock et al., 1986). Many similarities exist between the Southern Uplands and the Californian goldfields described by Rock, Duller, Haszeldine and Groves (1987); both are accreted oceanic terranes with ophiolites, intruded by plutons and lamprophyre dyke swarms. Rock et al., (1986) noted that although the origin of calc-alkaline lamprophyres is both obscure and contentious, their closest chemical allies, the lamproites, are derived by minor partial melting, at >100 km depth, of mantle peridotite metasomatically enriched in K, Ba, REE etc., by mantle 'plumes' from the core-mantle boundary. Lamproites are as such of deeper origin than any other terrestrial rocks, with the exception of kimberlites, and their genesis is essentially independent of lithospheric plate activity. Rock et al., (1987) presented a detailed overview of the nature and origin of lamprophyres, in which it was stated that they represent primitive if not primary magmas. Calc-alkaline lamprophyres were demonstrated to represent parental magmas to a range of hydrous alkaline intrusives, including potassic pyroxenite, diorite, shonkinite, syenite, and granite plutons.

Macdonald et al., (1985) demonstrated that mafic lamprophyre dykes in northern England were emplaced immediately following the final closure of the Iapetus Ocean at the end of the Caledonian orogeny. Three components were recognised in the lamprophyre chemistry, including: a depleted mantle source; a H₂O-rich subduction zone component; a CO₂-rich phase formed from the degassing of the mantle after ocean closure. Rock et al., (1986) noted that dyke swarms formed the most neglected aspect of Late Caledonian igneous activity in the

British Isles and identified a regional SW-NE trending zone in the Southern Uplands, ~10km wide and >300km long containing Siluro-Devonian calc-alkaline lamprophyre dykes. It was then demonstrated that the lamprophyres were locally emplaced, contemporaneously with small (<400 x 200m) subvolcanic vents of greywacke/mudstone agglomerate.

Anderson (1986) demonstrated that the hiatus of sinistral movements followed the deformation of early pre- and post- S1 vein sets and was expressed in the form of widespread wrench faulting associated with the intrusion of lamprophyre dykes at ~400 Ma. These dykes present several paradoxes in the current models for the development of the Southern Uplands, namely: volcanic, subvolcanic and plutonic magmatism is juxtaposed in both time and space; the lamprophyres were derived from an excessively deep mantle source unrelated to the subduction zone; and they display similar chemistry over a 700km wide zone from northern England to the western and northern Isles of Scotland. These studies, revealed that lamprophyres are rocks of exceptionally deep mantle origin (>130km) with a unique chemistry which would have been lost had they been intruded through a volatile-rich subducting plate (Rock et al., 1988). Furthermore, recent evidence suggests that lamprophyres intrusion began before turbidite deposition in the Southern Uplands ceased and compositional changes in lamprophyre geochemistry across the province mirror those of central Scotland. Both features are difficult to reconcile with a simple accretionary prism model for the Southern Uplands (Rock et al., 1986, 1988 and Rock, 1989).

The subvolcanic complex at Black Stockarton Moor, which immediately predates the Criffel pluton, is probably the most remarkable example of lamprophyric magmatism in the Southern Uplands. It forms a low-grade Cu-porphyry deposit with minor As (<300ppm), Au (<60ppb) and Sb (<200ppm) and consists of small granite cupolas, breccia vents and vast numbers of lamprophyre-porphyrite dykes intruded as four distinctly orientated swarms. The latter cumulatively produced up to 50% crustal extension over an area of approximately 30 km² (Leake and Cooper, 1983). Elsewhere in the Southern Uplands, extensions due to dyke emplacement commonly reached 6% (Barnes et al., 1986) but are probably nearer the 1 to 2 percent on a regional scale. There is no lack of evidence for the explosive, forceful nature of emplacement, particularly in the upper most margins of some dykes (cf. Leake and Cooper, 1983).

A series of six subvolcanic vents accompanied by calc-alkaline porphyrite and lamprophyre dyke swarms were identified by Rock et al., (1986) near Kirkcudbright in southwest Scotland. Although considerable geochemical studies have been undertaken on these intrusions (Macdonald et al., 1985; Rock et al., 1986; Rock 1987) the absence of both As and Sb analyses precluded the identification of zones of As-Sb-Au enrichment.

Gold mineralization in the Southern Uplands, as demonstrated within this study, generally consists of anastomosing quartz-stibnite vein systems surrounded by an envelope of disseminated auriferous arsenopyrite and pyrite. These veins are associated with intense fracturing and explosive brecciation. As in the Abitibi Belt (Kerrick, 1979) wallrock enrichment in K, Rb, Ba, Co, Ni, Si, As, Sb, Ca, Pb, Tl and S (as well as Au) and depletions in Na, Fe, Mg and Zn, closely mirror the chemistry of lamprophyres themselves, which are characteristically enriched in K, Rb, Co and Ni relative to common igneous rocks of similar Si content (note that both the gold deposits and lamprophyres possess lithophile-element enrichments).

The ultimate source of gold in the Southern Uplands remains problematical: the granitoid plutons and country rock greywackes are essentially barren of Au and its associated As and Sb; there is no evidence for any form of structural,

temporal or genetic association between the plutons and the Glendinning Deposit; other potential source-rocks (eg. serpentinites and stratiform mafic volcanics) are rare and their occurrence does not correlate with gold deposits in this region. This limited study undertaken during the tenure of this project recognised the widespread association of lamprophyres (deep crustal melts) with gold mineralization.

One of the earliest accounts of lamprophyre related gold association was documented by Buturlinov and Latysh (1970) who identified values up to 80ppb Au in lamprophyres in the Donets Basin, USSR. Boyle (1979) noted that some varieties of monchiquite, camptonite, odonite and other lamprophyre rocks were enriched in gold (and silver). McNeil and Kerrich (1986) demonstrated the close relationship between lamprophyre dykes, mafic magmas, deep crustal structures and gold mineralization in the Canadian Arrow deposit, Matheson, Canada. In the Canadian Arrow deposit, ductile shear zones and gold mineralization were developed preferentially in lamprophyre dykes (McNeil and Kerrich, 1986). Gold values ranging from 380-2700ppb Au were identified in hydrothermally altered lamprophyres. Rock et al., (1987) demonstrated that major gold deposits may be aligned along crustal-scale lineaments, which may form syn-basinal faults or major shear zones.

The close spatial association of gold mineralisation with both major and minor igneous intrusions throughout the Southern Uplands and Longford Down is the first line of evidence, invoked to suggest a genetic association between As-Sb-Au mineralisation and magmatic activity. However, a number of differing models may be invoked to explain the origin of the gold-lamprophyre association identified in Southern Scotland. Preliminary evidence presented below enables each hypothesis to be assessed on its relative merits:

In 1985, the author proposed that in comparison with breccia pipe structures produced by lamprophyres and the orientation of the dykes themselves, a genetic association with the Glendinning breccias might exist. (NB. hydrothermal pipes, vents and dykes may be differentiated by their width/length aspect ratios. Pipes display an essentially elliptical/sub-surface outcrop pattern whereas vents display irregular, elongated outcrops and dykes are more elongated still (Rock et al., 1987)). In the Southern Uplands, hydrothermally altered lamprophyres display LREE depletion and HREE enrichment relative to the assumed parental lamprophyre dyke, and define a similar pattern to that previously described in Archaean gold deposits by Kerrich and Fryer (1981).

Following a review of the structural and igneous controls upon in-situ gold mineralization in Southern Scotland it was noted that all gold sites were related to, if not confined by areas in close proximity to major N-S trending lineaments identified by Hazledene (1986). The predominant trend of the related vein mineralization is N10°E as opposed to the regional lamprophyre strike NE-SW. However, lamprophyre dykes in the vicinity of these lineaments have a trend closer to N-S than NE (Rock et al., 1987). In view of the global gold-lamprophyre associations identified above, a small subset (n=119) of lamprophyres were selected from the BGS collection of more than 3000 fresh dykes from the whole of Scotland, in order to assess possible relationships with As-Sb-Au mineralization. These samples were analysed by automated XRF spectroscopy at Nottingham University. The results of this study clearly demonstrated a preferential arsenic-antimony enrichment in samples intruding the Lower Palaeozoic turbidite succession, south of the Southern Uplands fault. The lamprophyre suite comprised of both fresh and altered samples of hornblende, biotite and mica rich varieties collected from the Wigtown, Glen Luce, Hawick, and St Abbs Head.

All analysed lamprophyres invading the Proterozoic and Archaean schists and gneisses of the Scottish Highlands contained As and Sb values below detection limits. Arsenic, a well-known pathfinder element for gold mineralization (Boyle, 1979; Rose et al., 1979) reaches levels >50ppm, over thirty times higher than the average arsenic content for intermediate igneous rocks (Wedepohl, 1979). Eleven of these enriched dykes representing the upper tenth percentile of the Sb and As distributions were then analysed by fire assay/neutron activation at the McMaster University Research Reactor Centre. This study revealed extraordinary Au enrichments (mean 137ppb and median 90ppb) and As-Au correlations (0.98) significant above the 99.9% level. Lamprophyres showing the highest Au values are hornblende (spessartites), fine grained and rich in felsic magmatic segregations (the 'globular' structures of Rock, 1987) which are locally cored by sulphides. These results provided clear evidence for considerable As-Au enrichment however, in comparison with the initial 100+ samples, this As-Sb rich group is interpreted as representing a potentially mineralized or hydrothermally altered subset and as such, the trend observed between As-Au cannot be assumed to be characteristic of the remaining 90% of the sample population.

In comparison with the initial 100+ samples, the group of 11 samples represent a mineralized/hydrothermally altered subset and as such the relationship between As-Au may not be observed in the remaining 90% of the population, which contain arsenic values below detection limits. These systematically high gold values appear elevated in comparison with gold values reported for other igneous rock types (Wedepohl, 1979; Keays, 1984, Mutschler et al., 1985). However a number of working models may be invoked to explain the observed relationship between gold and lamprophyres in the Southern Uplands, including:

- 1) Au is from the mantle, transported as primary gold in the lamprophyre dykes.
- 2) Au is incorporated into mantle-derived lamprophyres by crustal contamination during ascent.
- 3) Au is derived from the terrane around the dykes, leached out by small-scale hydrothermal cells set up in the wallrocks to the dykes.
- 4) Lineaments provided discharge pathways for Au-bearing fluids and also conduits controlling lamprophyre emplacement (ie. the gold and lamprophyres have no direct genetic connection).

All known primary gold localities in the Southern Uplands occur close to major lineaments, which in turn are spatially related to lamprophyre dykes (Fig 1 Rock, Duller, Haszeldine and Groves, 1987). Most dykes and the Criffel and Fleet Plutons are elongated NE-SW parallel to the regional Caledonian trend. However in a few narrow zones, the dyke orientations deviate towards crosscutting N-S trends, one of which coincides with the axis of the Loch Doon pluton. Similar N-S lineaments exist both 43km east and 43km west of this lineament, and all extend axially for tens of kilometers. Less well developed N-S lineaments occur between and east of these major lineaments at spacings of approximately 11 or 22km. Dykes or veins associated with these lineaments in the Glendinning, Cairngaroch, and Loch Doon deposits show high As and/or Au contents (Duller and Harvey, 1985a, b). The earliest manifested activity of the lineaments is in relation to the dyke orientations within the Black Stockarton Moor subvolcanic complex, however the same N-S lineaments later controlled the location of Carboniferous - Permian sedimentary basins, and the Carboniferous Pb-Zn veins at Leadhills and Wanlockhead (Russell, 1972). Haszeldine (1987) considered the lineaments to have originated within the mid- or lower crust due to epeirogenic tensional forces commencing after Iapetus closure and unconnected with contemporaneous European plate-tectonic movements. Increasing crustal contributions to the Criffel, Doon and Fleet plutonic melts with time (Halliday et al., 1980) confirm progressively decreasing crustal tension. It is speculated that lamprophyre magmas may be Au-bearing because they form deeper in the mantle (>150km) than any other igneous rocks; in

fact, from mantle which was previously metasomatised by fluids which may have originated as deep as the core-mantle boundary, and may therefore carry Au scavenged from both core and mantle. When emplaced into the crust, lamprophyres generate large volumes of felsic (syenitic or granitic) magmas by combined differentiation and crustal anatexis, and release large quantities of metasomatising fluids rich in CO_2 , K and related elements. Therefore lamprophyres have the potential to explain many general features of gold deposits, such as the origin of gold and the ore fluid; the indirect association between gold and felsic intrusions; and the associated metasomatism.

On the basis of As-Sb-Au geochemistry, structural and temporal evidence it is proposed that lamprophyre dyke-swarms were genetically related to Au-bearing quartz-arsenopyrite-stibnite deposits in the Southern Uplands. Both lamprophyres and mineralization are in turn related to crustal lineaments which first became active synchronous with lamprophyre emplacement, and continued to influence mineralization events into the Carboniferous. The conjunction of lamprophyric rocks, major structures and gold deposits are therefore interpreted in terms of trans-crustal fractures, utilised as a conduit for alkalic magmas from the mantle, and for discharge of hydrothermal fluids from a magmatic reservoir. It is speculated that lamprophyre magmas may be Au-bearing because they form deeper in the mantle (>150km) than any other igneous rocks; in fact, from mantle which was previously metasomatised by fluids which may have originated as deep as the core-mantle boundary, and may therefore carry Au scavenged from both core and mantle. When emplaced into the crust, lamprophyres generate large volumes of felsic (syenitic or granitic) magmas by combined differentiation and crustal anatexis, and release large quantities of metasomatising fluids rich in CO_2 , K and related elements.

Whatever the mode of origin for gold enrichment in lamprophyre, the intersection and combination of lamprophyres with major structural lineaments originating from epiroc tensional forces unconnected with local plate tectonic activity, provides a major new gold exploration target. Calc-alkaline lamprophyres thus deserve careful assessment as both gold sources and potential exploration targets in the Southern Uplands of Scotland, and elsewhere.

4.5 WORLDWIDE As-Sb-Au DEPOSITS

4.5.1 Arsenic Dominant Deposits

Arsenic is a relatively mobile element in hydrothermal systems and is commonly associated with several types of sulphide ore deposits particularly those containing chalcophile elements and gold, for which it is used as a pathfinder (Zhou, 1987). Arsenic is associated with most types of gold deposit, usually within the ore zone and, more importantly, in the supra-ore assemblage, which makes it particularly useful in prospecting for a wide variety of different types of mineral deposits, enriched in a range of metals, including: Cu, Ag, Au, Zn, Cd, Hg, U, Sn, Pb, Sb, Bi, Mo, W, Co, Ni, Pt metals and S.

Both organic and inorganic arsenic compounds are commonly used in agricultural chemicals including herbicides, plant desiccants and defoliants, insecticides, soil sterilizers, insect baits and sheep dips (Loebenstein, 1980). Other industrial applications of arsenic include its use in wood preservatives, floatation agents, glass manufacture, chemical catalysts, pharmaceuticals, and semiconductors.

Boyle and Jonasson (1973) noted the strong coherence between arsenic and gold in practically all types of gold deposit and the frequently close relationship between arsenic, antimony and bismuth in many polymetallic deposits. Detailed reviews of the application of As, Sb and Bi as pathfinder elements in geochemical exploration have been presented by numerous authors (Hale, 1981; Boyle and Jonasson, 1973).

The chalcophile nature and relative mobility of arsenic leads to the development of broad primary halos in the vicinity of many gold deposits (Hale, 1981). These deposits occur in a wide variety of settings, ranging from massive sulphides, volcanic breccias, skarns and hydrothermal veins. A comprehensive review of the geochemistry and nature of gold occurrences worldwide is presented by Boyle (1979). Craig and Vaughan (1981) noted that gold in quartz vein hosted deposits occurs primarily within, or marginal to pyrite and/or arsenopyrite, and is generally very fine grained. Arsenic occurs as an essential element in a range of mineral types from arsenides, sulphides, sulphosalts and arsenates through to oxides and the native element. In the Southern Uplands, the principle As mineral is arsenopyrite, however elevated arsenic levels have also been defined in both pyrite, stibnite and tetrahedrite.

In southern Rhodesia, James (1957) studied the geochemical dispersion patterns related to As-Sb rich gold deposits. Wilson (1973) in studies of wallrock alteration, in the Ashanti gold mine, Ghana, noted that the mineralization was accompanied by sericitization, carbonate enrichment and arsenopyrite depletion. Webb et al., (1973) detailed the results of a geochemical stream sediment survey of Northern Ireland, undertaken to evaluate the application regional datasets to mineral exploration, agriculture, pollution and public health. Arsenic anomalies (>20ppm) were located in association with major shear zones in NE Antrim, Omagh and Central Tyrone; and peripheral to the north-west margin of the Newry granodiorite - a composite intrusion hosted by Lower Palaeozoic greywackes and associated with dioritic and monzonitic minor intrusions (O'Connor, 1986) (Note that the Omagh Thrust zone forms a prominent structural feature associated with economic gold deposits in the Sperrin Mountains).

Cooper et al., (1985) in a reconnaissance geochemical drainage survey of the Harlech Dome in North Wales, noted the presence of arsenic (+?Au) anomalies associated with Ordovician acid volcanics, ranging in composition from dolerite to microtonalite. Historical gold mining activity in this area was concentrated on the south-eastern side of the Harlech Dome in the 'Dolgellau gold-belt' which coincides with the outcrop of the Cloggau Formation. A series of quartz-sulphide veins form the host of the gold mineralization, with gold occurring as either 'free gold' dispersed within the quartz, or intimately associated with sulphides including: pyrite, pyrrhotite, chalcopyrite, arsenopyrite, galena and sphalerite. Examples of gold forming replacement or exsolution blebs in pyrite and arsenopyrite were also identified.

In studies of the geological and fluid controls on Lower Palaeozoic hydrothermal veins in the Moretons Harbour area, Newfoundland, Kay and Strong (1983) defined the occurrence of three types of vein mineralization, including: arsenopyrite dominant (Au rich); stibnite dominant (Au poor); and base metal + arsenopyrite dominant (Au + Ag rich). The arsenopyrite dominant vein mineralization was deposited from CO₂-rich, low salinity fluids at temperatures > 300°C, whereas the stibnite dominant veins were deposited from relatively saline, low-CO₂ fluids at temperatures < 220°C.

In a detailed description of the mineralogy, paragenesis and origin of Ag-Ni, Co arsenide mineralization in the Camswell River area, N.W.T. Canada, Badham (1975) noted that the location of individual mineral veins were controlled by contacts of earlier intrusions; rock chemistry; the presence of sulphides in the host rock; and the

position of tensional fractures. Wojak and Sinclair (1984) in a detailed description of the Equity Silver mine (an Ag-Cu-Au-Sb deposit in British Columbia) noted the presence of concentric clay-rich alteration zones up to 300m in width, enveloping a finely disseminated mixture of pyrite, arsenopyrite, chalcopyrite and tetrahedrite contained within the matrix of a volcanic breccia. An epithermal model was proposed for this genesis deposit invoking the intrusion of quartz monzonite which heated acidic meteoric water and contributed a saline magmatic component in order to create the ore fluid. Perrault et al., (1984) demonstrated the existence of auriferous halos associated with gold deposits in the Val d'Or area of northwestern Quebec. Two distinct forms of halo were identified: a >3ppb zone, enclosing a broad area interpreted as an ore-field halo; and a >10ppb zone enveloping all known ore zones and defined as the ore-zone halo. These ore-zone halos however, do not constitute exact drilling targets and further geophysical or geochemical methods are required to define the nature of mineralization within individual halos. In addition it was noted that the presence of slightly elevated gold values could be used to define to position of auriferous ore-field (>3ppb) and ore-zone (>10ppb) halos. Robert and Brown (1986) in a study of hydrothermal alteration in the Sigma Mine, Quebec noted that deposition of vein minerals may be attributed to chemical changes in the fluid resulting from progressive wallrock alteration.

In a study of arsenopyrite-gold mineralization from the Yuzhnoye deposit, in the USSR, Atabekyants (1972) noted the significant distribution of lamprophyre and dioritic dykes in close proximity to mineralization. The main host rocks to the mineralization are a series of brecciated sandstones and mudstones, impregnated with sulphides and dominated by pyrite and arsenopyrite which host the majority of the gold. Luzgin and Shepelenko (1975) detailed the relationship between mercury, arsenic and antimony deposits in the Gomy Altay region of the USSR. In the Baley gold deposit in eastern Transbaikalia, Au-bearing veins display As-Sb-Hg anomalies which widen and coalesce upward forming a zone in excess of 300m in width near and above the ore, which can be detected at least 250m above the zone of ore grade mineralization (Rose et al., 1980). These deposits lie within the arsenic-, antimony-, or mercury-bearing base metal vein-type deposits described by Craig and Vaughan (1981) and exemplified by the Butte (Montana), Getchell (Nevada) and Almaden (Spain) deposits, respectively. A feature common to all three types of deposit is the development of feldspathization, sericitisation, argillization and bleaching in the wallrocks to the sulphide ores (Craig and Vaughan, op. cit).

Sillitoe, Baker and Brook (1984) in studies of gold deposits associated with hydrothermal eruption breccias in Papua, New Guinea, noted that fluid over pressures, which developed at depths of >100m triggered hydrothermal eruptions which gave rise to a ramifying system of irregular veins and bodies of hydrothermal breccia. Self-sealing was caused by early quartz carbonate vein mineralization, which also may be found in fragments of later breccias.

Pamir (1974) in a short description of gold-bearing arsenopyrite veins from the Sobice Mountains in Turkey, noted an inverse relationship between vein thickness and gold content; an intimate association of gold and arsenopyrite; and grades up to 129ppm.

Stephens et al., (1988) presented a review of massive sulphide deposits in the Caledonian-Appalachian Orogen. The Buchans deposit in Newfoundland is a polymetallic, stratiform, volcanogenic massive sulphide deposit associated with submarine fumarolic activity, formed during the quiescent phases of calc-alkaline volcanism, and exhibits numerous similarities to the Kuroko deposits of Japan (Thurlow et al., 1975). Henley and Thomley (1979) in a discussion of polymetallic massive sulphide formation noted that these deposits result from transient discharge to the seafloor from submarine geothermal systems. Low-power discharges result in metalliferous sediments or banded massive sulphide ores whereas short-lived high-power discharges through stockwork zones formed by hydrothermal brecciation, result in the formation of Kuroko and Archaean type massive sulphide deposits.

In a detailed summary of mineralization in the English Lake District, Stanley and Vaughan (1982) identified two major types of mineralization which include both Lower Devonian (Caledonian) Cu-As-Fe deposits and early Carboniferous Pb-Zn deposits. Stanley and Vaughan (1982) in studies of the Bonsor vein deposit, in the English Lake District, demonstrated that an early phase of arsenopyrite mineralization had penetrated the cleaved and altered wallrocks to this deposit. Where the Cu-As-Fe mineralization is closely associated with granite intrusions, more complex assemblages involving W or Mo bearing phases were found to occur.

In the western United States sediment hosted precious metal deposits have been identified in carbonaceous, silty dolomites and limestones or calcareous siltstones and mudstones. Gold mineralization is disseminated in the host sedimentary rocks and is exceedingly fine grained, usually <1 micron in size, in unoxidised ore. These deposits are commonly associated with As, Hg, Sb, and Tl and are classified by Bagby and Berger (1985) as sediment-hosted, disseminated precious-metal deposits. Boyle (1981) noted that extensive replacement/alteration may be developed in calcareous pelites and psammities and other thinly bedded carbonate rocks by the intrusion of granitic stocks, porphyry dykes and sills. Deposits of this type are widely distributed throughout the world and are commonly referred to as 'Carlin-type'. In studies of gold bearing quartz veins in the Alleghany district of California, Ferguson and Gannett (1972) identified the widespread association of gold with arsenopyrite, and noted that arsenopyrite is most abundant in veins crosscutting Fe-rich wallrocks, such as gabbro and serpentinite.

The principal ore minerals in hydrothermal gold deposits such as those at the Cortez Mine, Carlin, Nevada are arsenopyrite and pyrite (Wells and Mullens, 1973). Gold is rarely observed even at 15,000 x magnifications, yet assays of sulphide concentrates reveal grades of up to 200 oz/ton. Springer (1985) presented a graphical summary of the submicroscopic gold content of both arsenopyrite and pyrite from numerous deposits around the world. The highest values were located in oxidised ores at the Carlin Mine (Wells and Mullens, 1973) containing up to 2500ppm Au in arsenopyrite and 700-1500ppm Au in pyrite. Radtke (1976) reported an average content of 506ppm As and 126ppm Sb in unoxidized ore from the Carlin deposit. Evans and Peterson (1986) in lithogeochemical studies in the vicinity of the Carlin deposit, Nevada noted that hydrothermal alteration and gold mineralization are present in all rock types within the mine area, but are intensely developed along faults and breccia zones. Gold-bearing quartz veins occur in and near major fault zones in deformed oceanic and island arc lithologies west of the Sierra Nevada composite batholith (Bohlke 1986). It was proposed that the mineralizing fluids were mobilised by deep seated magmatic activity, related to subduction processes along the western margin of North America.

Greenstone belts have produced over 20,000 metric tons of gold mainly from Canada, Australia, Zimbabwe, South Africa, Brazil and India. Within the greenstone belts, two general types of gold deposits may be recognised. The first, is vein-associated occurring dominantly in metavolcanic and metasedimentary rocks, whereas the second is represented by stratiform-stratabound deposits in banded iron formations. Despite the stratabound nature of vein sets, critical evidence for an epigenetic origin of the vein associated deposits was defined including their transgressive nature. Anhaeusser (1976) presented a review of the nature and distribution of Archean mineralization in southern Africa and noticed that although gold mineralization is generally stratabound, it had been remobilised by structural and metamorphic events following the intrusion of a range of granites and other minor intrusions. In a study of trace element mobility in alteration zones associated Archean Au vein deposits, Ludden et al., (1984) noted the presence of a cryptic alteration zone characterised by rare earth element leaching accompanied by sericitic alteration. An integrated model for the origin of Archean lode gold deposits was presented by Colvine et al., (1984). It was noted that gold deposits occur within linear tectonic zones (transcurrent or thrust systems) and

were formed by dynamic, evolving hydrothermal systems which produced several forms of permeability and styles of mineralisation, within individual deposits. Kerrich (1981) in a synthesis of stable isotope and geochemical relations, noted that wallrocks associated with Archean gold-bearing veins, display a strong iron reduction anomaly compared to background. In addition, it was suggested that the distinctive suites of metals in vein gold deposits, when compared to massive base-metal sulphides, reflect fundamentally different properties and conditions of deposition within a hydrothermal system. Burrows, Wood and Spooner (1986) presented carbon isotope evidence for a magmatic origin of Archean gold-quartz vein deposits.

Gold abundances in ultramafic rocks have been the subject of recent research (Saager, et al., 1982; Fyon, et al., 1984). Tilling et al., (1973) observed that mafic rocks contain more gold than felsic and intermediate rocks in both plutonic and volcanic suites. It was also demonstrated that gold tends to be more abundant in early crystallizing minerals, such as mafic silicates than in later quartz and feldspar. Buisson and Leblanc (1985) noted that arsenic, gold, mercury and Co-Ni arsenides may be located in carbonate-bearing ultramafic rocks (termed 'listwaenites') located along the borders of Alpine-type ultramafic massifs. Lithochemical studies reveal a strong positive correlation between As-Au and As-Au-K, with Sb, Bi and Ag also associated with high gold values. Mineralogically, the concentration of gold is related to gold rich sulphides, sulphoarsenides, or arsenides. Listwaenites are developed during the late stage tectonic emplacement of serpentinized ultramafic massif, along deep seated suture zones, and formed by CO_2 -Ca metasomatism within a large-scale hydrothermal system.

Gold deposits in California, although widely scattered, show a marked preference for oceanic and island-arc terranes that have been invaded by granitoid plutons (Albers, 1981). The association of gold deposits with oceanic and island-arc derived sediments in California was suggested by Albers (op. cit) to infer that the gold was derived from these two types of material and that lesser amounts of gold would be available in areas of continental crust. Buisson and Leblanc (1985) reported the location of several gold occurrences in carbonate-rocks located along the margins of serpentinized ultramafic massifs, related to various ophiolite complexes. These carbonate rich rocks (listwaenites) were formed during CO_2 -Ca metasomatism of ultramafic rocks, and contain elevated gold values (1 to 10ppm) in areas of cobalt-arsenide mineralization and display a strong positive correlation between As-Au-S.

A number of papers reviewing recent developments in the exploration and genesis of turbidite hosted gold mineralisation, were presented in 1985, at the turbidite hosted gold mineralisation symposium during the joint JAC/MAC annual general meeting at Fredricton, Canada. Authors and their respective areas of interest included: Boyle (overview); Foster et al., (Zimbabwe); Ruitenberg (New Brunswick); Smith (Nova Scotia); Sandiford and Keays (Victoria, Australia); Paterson (New Zealand); Steed and Morris (Ireland); Duller and Harvey (Scotland); Goldfarb et al., (Alaska); Bow (Ywoming); Padgham (Northwest Territories); Tomkinson (Southern Appalachians); and Crockett et al., (Nova Scotia). Boyle (1985) noted the widespread distribution of turbidite hosted gold mineralisation, noted the widespread distribution deposits throughout the world, which occur in rocks ranging in age from Archean to Tertiary. Since the mid 1800's when gold was first discovered in Nova Scotia, the Lower Palaeozoic Meguma group of turbidites has gained world recognition as a type-example of turbidite hosted gold deposits, with more than 60 producing mines, yielding over 1,000,000 oz gold. Typically, wallrocks to in this region have been subjected to intense arsenopyritisation and sericitization and display many similar characteristics to the vein systems identified in the Southern Uplands.

Smith (1985) in an evaluation of turbidite hosted gold mineralization in the eastern Meguma terrane of Nova Scotia, proposed a tentative genetic model in evoking a Devonian granitoid intrusion, as the hydrothermal pump

responsible for introducing mineralization along a shear zone. Haynes (1985) in studies of gold deposits of the Meguma Terrane suggested that tectonically activated fault zones acted as feeders for hydrothermal hot-spring systems, which precipitated gold, arsenic, mercury and other metals from low density buoyant plumes ('white smokers') as laminated siliceous exhalites, exhibiting structures similar to modern geyserites. In the underlying hydrothermal system and vertical fluid conduits, silicification, sericitization and arsenopyritization at temperatures of 300-350°C were responsible for the development of extensive stockwork zones.

In a study of mineral deposits in New Brunswick, Ruitenberg and Fyffe (1982) noted the association of gold-bearing quartz veins (hosted by Ordovician siltstones and shales) with contemporaneous granitic and mafic intrusions. Numerous gold-bearing veins (\pm Pb-Zn sulphides) are associated with granitic intrusions along the Bay of Fundy Coast in New Brunswick, Canada (Ruitenberg and Fyffe, 1982). In addition, Ruitenberg (1985) identified a low grade gold-arsenopyrite bearing argillic alteration zone enveloping quartz-stibnite vein mineralization, hosted by Silurian turbidites in the Lake George deposit, New Brunswick.

Wilton (1985) detailed the results of a REE and Au geochemical study of gold mineralization associated with the Cape Ray Fault Zone in southwestern Newfoundland. Wallrocks to gold bearing quartz veins in both schists and granite, exhibited LREE depletion probably due to leaching by hydrothermal solutions. Baldwin (1980) reported the occurrence of stratabound arsenopyrite mineralization hosted by Precambrian volcanic-derived turbidites in the Churchill Province of Manitoba, Canada. This deposit has been subjected to regional amphibolite-grade metamorphism and all primary sulphides have been remobilized into sulphide-rich bands, conformable with metamorphic layering. Turbidite hosted gold vein mineralization is widespread throughout the Yellowknife Supergroup, of the northwest territories, Canada, and is currently the subject of extensive exploration programmes.

In an investigation of turbidite hosted Au-Sb deposits in Otago, New Zealand, Paterson (1985) identified the general occurrence of sericitic-propylitic wallrock alteration assemblage enveloping vein mineralisation which formed at \sim 300°C. Sandiford and Keays (1985) in a study of turbidite hosted gold deposits in Australia, attributed the source of gold to metamorphism and dehydration of deep seated crustal rocks associated with the generation of late to post-tectonic granites. In studies of the origin and structural control of gold-rich deposits in deformed turbidites from the Cobar mining district in Australia, Glen (1987) noted that Au-Cu deposits previously interpreted as remobilized syngenetic ores are structurally controlled and lie in zones of silicification on or adjacent to major faults. Robertson (1987) in studies of the Cobar deposit in Australia, noted that the mineralization was surrounded by unusually extensive depletions in Na and K in the host metasediments. These zones are marked by the virtual absence of feldspar in proximity to the ore and an increase in sericite.

The geochemistry of hydrothermal arsenopyrite mineralization in late-Precambrian sediments of Central East Greenland was reported by Stendal (1981; 1983). Two types of arsenopyrite mineralization were noted: the first, a stratabound occurrence was restricted to fracture zones and their respective wallrocks crosscutting semipelitic quartzites. This style of arsenic mineralization was found to contain gold values up to 650ppb and was associated with zinc depletion; the second, vein hosted arsenopyrite mineralization crosscuts both quartzite and semipelitic lithologies and occurs together with galena and chalcopyrite. Evidence for the hydrothermal origin of both styles of mineralization were cited, based upon field relationships, including: the vein type mineralization; arsenic impregnation associated with fracture zones; decreasing metal contents of wallrocks with distance from the vein systems; the regional distribution of deposits; and polymetallic nature of the mineralization. In a re-evaluation of the genesis of this mineralization based upon field and geochemical evidence, Stendal (op.cit) discounted earlier

models of syn-sedimentary/diagenetic arsenopyrite formation with later remobilisation, in favour of a pneumatolytic-hydrothermal origin for the widespread arsenic mineralization located in this terrane. Stendal and Ghisler (1984), in studies in east Greenland, noted the occurrence of widespread arsenopyrite mineralization which were deposited from boiling CO₂-bearing fluids of low salinity at temperatures 225° to 260°C. Mineralized fracture zones were found to contain an average 5.5% As and are generally enriched in Pb, Cu, B and Co. It is proposed that the occurrences of hydrothermal mineralization in east Greenland displays many features in common with Caledonian magmatic activity and mineral deposits in Scotland.

Pedersen and Stendal (1987) in an investigation of the geology and geochemistry of W-Sb-As (-Au) vein mineralization in central east Greenland, established a Caledonian age for the mineralizing event. In general, early arsenopyrite-pyrite-gold mineralization is superimposed by later phase of stibnite (\pm scheelite). It was proposed that these deposits form examples of lineament controlled, precious metal-bearing geothermal systems, in which antimony and gold are concentrated at shallow depth.

Brill (1983) in studies of polymetallic deposits from the French Massif Central, noted that early crystallization of arsenopyrite is always a precursor to stibnite mineralization. Brill (op. cit) identified two types of paragenesis originating from complex low salinity, CO₂-rich fluids. These included a high temperature (~350°C) As-W-Au deposits and lower temperature (~260°C) stibnite occurrences. A later, lower temperature phase of Pb-Zn mineralization, deposited from highly saline fluids resulted in some remobilisation of antimony, which was redeposited with Pb in the form of sulphosalts.

Breccia-hosted arsenopyrite-gold mineralisation occurs within Cambro-Ordovician metasediments in the Monteroso deposit in northwest Spain (Jahoda et al., 1989). The hydrothermal system responsible for this deposit was associated with minor mafic-granodioritic intrusions emplaced within a dilational fault zone. Numerous close similarities exist between the Glendinning deposit and the carbonate-quartz-stibnite-sphalerite-gold deposits identified by Gumiel and Arribas (1987) in the Iberian Peninsula. These deposits are characterised by the early deposition of pyrite, arsenopyrite and gold. Other minerals which complete the paragenesis include sphalerite, chalcopyrite, tetrahedrite and berthierite. Examples of such deposits include the Ribeiro da Igreja mine (Portugal) and the Pilar mine (Badajoz). Such a re-interpretation is not unique; Allen and Easterbrook (1978) suggested that the Glasdir mine in the Dolgellau gold belt in central Wales, previously regarded as a vein deposit, was a mineralized breccia pipe associated with intermediate and basic intrusions formed during Lower Palaeozoic magmatic activity.

A variety of origins have been suggested for turbidite-hosted gold deposits in a detailed review by Boyle (1985) including igneous, hydrothermal and lateral secretion: According to Meyer and Hemley (1967) the most abundant alteration minerals in Precambrian gold deposits are chlorite, sericite and complex carbonate assemblages, especially magnesium and iron-rich types (ie., ankerite). In most of these deposits sericitic alteration is associated with sulphide deposition. The compositions of hydrothermal fluids and the nature of gold transport mechanisms have been the subject of critical debate (Fyfe and Henley, 1973). Several mechanisms can be invoked resulting in the destabilization of soluble Au complexes (Henley, 1973; Seaward, 1973 and 1976) with a decrease in temperature forming one of the simpler mechanisms.

Kerrich and Fryer (1981) detailed the REE compositional variations, associated with Archean precious-metal hydrothermal systems in the Abitibi Greenstone belt of eastern Canada. Oxidation accompanying hydrothermal

alteration in proximity to the seafloor has been discussed by Spooner and Fife (1973) and Spooner et al., (1977). The chemical composition of fluid inclusions in As-Sb-Hg deposits in the USSR was investigated by Otkhnezuri and Dolidze (1981). In a study of trace element mobility within alteration zones associated with Archean Au vein deposits, Ludden et al., (1984) noted that zones of incipient sericitic and cryptic alteration may be characterised by REE leaching, developed within a low pH environment. A range of criteria were used by Kay and Strong (1983) to suggest that the ore fluids were derived from a felsic magma.

A common association exists between CO₂ rich fluids and As-Sb-Au deposits (Kay and Strong, 1983; Smith et al., 1969). Phillips and Groves (1983) suggested that Au deposition occurred by selective sulphidation of Fe-rich rocks, with concomitant destabilization of reduced-sulphur Au complexes. Novgorodova et al., (1984) in a study of the geochemistry of trace elements in gold-bearing quartz veins, demonstrated a marked correlation between Au, As, Sb, Na and REE (La, Eu and Sm). In studies of the Macassa gold deposit in Ontario, Kerrich and Watson (1984) noted that the hydrothermal fluids had not fractionated the REE, during interaction with wallrock. This data is consistent with a fluid which evolved from a dehydration of volcanic/igneous rocks, which ascended by hydrofracture along pre-existing faults and fractures, into which sulphide and gangue phases were precipitated.

In studies of hydrothermal alteration associated with gold mineralization in northwest Spain, Harris (1980) identified a disseminated pyrite, arsenopyrite, molybdenite and stibnite assemblage within a Hercynian granodioritic complex. The mineralization and accompanying hydrothermal alteration were inferred to have formed from episodic influxes of sporadically boiling fluids, rich in CO₂, H₂O, S, Sb and As. This form of hydrothermal brecciation and associated silicification may be used to indicate proximity to fluid upflow and boiling (Hedenquist and Henley, 1985).

It has been widely recognised that certain types of deposit are concentrated in specific regions of the world. These regions are known as metallogenic provinces and may be delineated by reference to one or more metals or metal associations. On the basis of this study, the Lower Palaeozoic turbidite succession of the Southern Uplands and Longford Down (and their lateral extensions) may be regarded as a As-Sb-Au metallogenic province. The recognition of the development of this type of gold province is of fundamental importance to the exploration geologist. As such, detailed lithogeochemistry can be a very potent technique in the exploration for As-Sb-Au deposits in this terrane.

4.5.2 Antimony Dominant Deposits

The word antimony is derived from the Greek 'anti plus monos' which means "a metal seldom found alone" and aptly defines the polymetallic nature of this metal in its natural form (Rathjen, 1980). The most important property of antimony is that it expands, rather than contracts upon cooling. Antimony has many industrial applications, the most important of which is its use as a hardener in antimonial lead used in storage batteries, protective sheathing for power cables, sheets, pipes, collapsible tubes and foil. Other applications of antimony include flame retardants, casting alloys, semiconductors, pigments, glasses, glazes, electroplating, Britannia metal and pewter, ammunition, flares, tracer shells and bullets, vulcanizing rubber and pharmaceuticals.

Antimony deposits may be classified into two types - those which are mineralogically and structurally simple and those which are complex. In the first category, deposits are generally small in extent, discontinuous, and consist

mainly of quartz and stibnite. They are considered to have been formed from hydrothermal solutions at low temperatures and shallow depths, and are normally associated with granitic rocks. Deposits of this type do not usually contain more than several thousand tonnes of ore, but are represented by some of the world's most productive antimony deposits, including those of Bolivia, Mexico, China, Peru, South Africa, Italy and Japan. In the second category, antimony occurs as a constituent of other metalliferous ores; either as stibnite in gold-quartz veins or as a constituent of Cu-Pb-Zn sulphide bodies where it occurs in minerals such as tetrahedrite.

South Africa is the world's leading exporter of antimony with production of ~16,000 tons accounting for ~23% of the world's annual output. The other major world producers are Bolivia and Mexico. In addition, China and Russia together produce about 22,000 tons/year, however their production is normally consumed internally. Sahli (1961) noted that the first phase of mineralization in the Murchison range was the emplacement of pyrite-arsenopyrite-gold deposits. With decreasing temperature the succeeding phase was dominated by the emplacement of ubiquitous stibnite-gold mineralization, and overprinted by cinnabar deposition.

Muff (1978) presented a major review paper on the antimony deposits in the Murchison Range, South Africa and identified the association of As, Sb and Hg in terms of a 'hot spring' or 'mobile element' factor. Muff and Sager (1979) in a review of metallogenic studies of antimony deposits in the Murchison greenstone belt noted the presence of a stratabound, banded pyrite-arsenopyrite ore in addition to a separate, almost monomineralic stibnite ore. It was proposed that this pyrite-arsenopyrite assemblage formed the precursor of, and was genetically related to primary antimony ores, formed by synsedimentary volcanogenic submarine-hydrothermal processes. At an early stage of fumarolic activity the high-temperature mineral assemblages of the banded pyrite-arsenopyrite ore were formed. With decreasing temperatures the fluids became enriched in volatile elements, silica and carbon dioxide. As a result, the mineral assemblages changed gradually from pyrite-arsenopyrite ore to stibnite ore. During the waning phase of volcanic activity and mineralization the mineralizing solutions were enriched in Sb, Hg, As, CO₂ and SiO₂ and depleted in Fe, Cu and Zn. A genetic link between gold and komatiitic rocks has been suggested to explain the distribution of gold deposits in South Africa (Viljoen, 1982, 1984). The close association between gold mineralization and tonalite-granodiorite intrusions in Zimbabwe, was explained by a number of complex and inter-related parameters, including the igneous source, diapiric nature, timing of emplacement and the generation of low fO₂, high SO₂-H₂S fluids capable of efficient gold transport (Foster, 1988).

Mitchell (1975) speculated that the location of antimony deposits in Burma and China, on the continental side of tin-bearing granite belts suggests that antimony mineralization was related to a rise in volatiles from a depth of several hundred km. Submarine-hydrothermal Sb-Hg-W deposits were investigated in Turkey (Holl, 1966), Spain (Maucher and Saupe, 1967) and in Austria and Yugoslavia (Holl and Maucher, 1967).

Jankovic (1960) in studies of Yugoslavian antimony deposits noted their genetic association with Tertiary volcanics, and identified the following associations: Sb only; Sb-As-Hg; Sb-Pb-Zn-Cu; Sb-W; Sb-As-Ni-Co-U; Sb-Cu-Mo. In subsequent studies, Jankovic et al., (1977) noted the association of Sb-As-Pb-Zn and provided detailed evidence of the genetic relationship between mineralisation and Tertiary granodioritic intrusions.

In a geological and geochemical study of the Senator antimony deposit in Turkey, Bernasconi et al., (1980) defined the presence of a hydrothermal breccia pipe containing Sb-mineralization composed almost entirely of oxides (stibiconite, scorodite, dusserite) with lesser amounts of amorphous sulphides (metastibnite). This deposit was formed by hot spring/fumarolic activity associated with Late Tertiary-early Quaternary volcanic activity.

Antimony bearing vein mineralization has been observed in the Brioude-Massiac district of the Massif Central, France (Roger, 1969). The dominant ore mineralogy comprised of stibnite, berthierite and minor sulphosalts in a gangue of quartz and carbonate: in narrow veins hosted within a series of NNE trending faults and sub-concordant fractures. Bril (1983) in a study of the metallogeny of antimony mineralization in the Brioude-Massiac district in the French Massif Central, noted that ore deposition took place at relatively elevated temperatures (300°-400°C) from complex low salinity, CO₂ rich fluids. A metallogenic model was proposed invoking extensive fluid circulation resulting from thermal anomalies caused by late magmatism and fracturing events.

In a review of antimony deposits in the Iberian Peninsula, Gumiel and Arribas (1987) defined eight mineralogical associations including: quartz-stibnite; quartz-stibnite-gold; carbonate-quartz-stibnite-sphalerite-gold; carbonate-quartz-stibnite-galena-silver; quartz-stibnite-sphalerite, quartz-stibnite-scheelite; quartz-stibnite-cinnabar; quartz-stibnite-copper. Three phases of antimony mineralization were observed (Lower Ordovician, Silurian-Devonian, and Lower Carboniferous) and interpreted to be the result of pre-orogenic volcanism. In all instances of antimony mineralization recorded from the Iberian Peninsula, arsenopyrite deposition forms a precursor to the main phase of stibnite deposition. The Almaden mercury deposit in Southern Iberia is particularly noteworthy. This deposit, recently described by Saupe (1987) is responsible for one third of the cumulative world production of mercury and as such, may be regarded as a giant orebody of its type. This deposit occurs as both stratabound and diatreme related mineralization hosted by Lower Silurian (Llandovery) quartzites which have been subjected to low grade (anchizone) metamorphism. Three periods of major volcanic activity are recorded from this region (Llandeilo, Llandovery-Wenlock and Middle Devonian) during which abundant basic volcanic rocks (spilites and diabases) were erupted or extruded together with the intrusion of dykes and sills of dolerite, microgranites and lamprophyres. It is clear that the tectonic environment during mineralization exhibits many close similarities with that of the Southern Uplands. The cinnabar is interpreted by Saupe (op.cit) to have been deposited at, or just below the seafloor at temperatures of approx. 300°C. Sulphur isotope fractionation studies of pyrite associated with cinnabar indicate that hydrothermal circulation of Silurian seawater provided a partial sulphur source. Possible sources of the mercury include, thermal remobilization from Silurian black shales or volcanics, and mantle degassing, genetically related to basic Silurian volcanism.

The geochemistry of the ore-bearing fluids for similar Californian deposits has been investigated by Barnes and Seward (1987) who developed a general genetic model for these deposits, invoking low grade metamorphism of subducted marine sediments to provide the necessary ore forming solutions and subsequent syngenetic, diagenetic or shallow epigenetic deposition of sulphides which resulted from either cooling or a decrease in pH. Gumiel and Arribas (1987) classify most if not all, stibnite-cinnabar deposits as epithermal (mostly volcanic) origin and they proposed that all antimony deposits in the Iberian Peninsula were genetically related either to volcanic exhalative processes or the emplacement of intrusive rocks.

In a study of polymetallic deposits from Sardinia, Schneider (1972) noted the presence of stratabound As-rich ores (± stibnite) constrained by Lower Palaeozoic (mainly Silurian) sediments, associated with acid, submarine volcanism. In a more recent evaluation of Sardinian antimony deposits Carmignani et al., (1982) detailed the occurrence of a major, lineament controlled, tectonic breccia hosted by Lower Silurian black shales, containing extensive stibnite mineralisation. Although a number of possible origins were considered, field and geochemical evidence pointed towards a magmatic-hydrothermal model for this deposit.

In a discussion of exploration for antimony deposits in Italy, Dehm et al., (1983) demonstrated the application of overburden sampling in extending the patterns of known mineralization and identifying neighbouring anomalies. Furthermore, Dehm et al., (op.cit) proposed a genetic model for the Sb deposits invoking deep seated mobilization of Sb rich fluids, transport along major structural features and near-surface precipitation.

In 1948, Ahlfeld presented a review of antimony deposits in Argentina. Of particular importance in this study were the detailed descriptions of vertical zonation within numerous working deposits. The Puyita mine vein (which yielded 300 tons of antimony ore) is unusual in that it is vertically zoned and it passes at depth to a sphalerite-dominant system. In the Pabellon deposit, stibnite veins hosted by Ordovician turbidites pass with depth into a gold bearing (stibnite absent) quartz vein.

Threadgold (1958) documented the occurrence of antimony-gold mineralization at Steel's Creek, Victoria, Australia. In this deposit the ore occurs as a series of narrow, near vertical veins, hosted by a quartz-feldspar porphyry, which itself intrudes a Silurian turbidite succession. These veins exhibit similar morphology, mineralogy and alteration to that observed in the Southern Uplands. Balitsky et al., (1968) in studies of the formation of natural antimony and stibnite noted that a H_2S deficiency is the most important controlling factor for the formation of antimony in a hydrothermal deposit. It may be demonstrated therefore that in hydrothermal solutions a temperature decrease and increase in H_2S activity lead to the formation of stibnite.

Leonard (1965) documented the occurrence of a cinnabar-bearing stibnite deposit in central Idaho, USA. This deposit occurs in a sheared, silicified zone hosted by granodiorite and cut by basic dykes. Although the principle ore mineral is stibnite, it is associated with fine grained and disseminated cinnabar, pyrite, arsenopyrite, sphalerite, and boulangerite. Cinnabar, one of the commonest forms of mercury sulphide, occurs sporadically in stibnite and quartz as groups of discreet granules and as coatings of very small crystals. Cinnabar is readily overlooked in massive stibnite which may be cut by hairlike veinlets of cinnabar.

Stibnite vein mineralization is commonly found in association with granitic intrusions. Srikanthia (1977) recorded the presence of a series of polymetallic stibnite veins in the Lahaul-Spiti District of India which assayed up to 1.52% As, 1.4dw/ton Au and 50 oz/ton Ag. Farrand (1979) in a study of stibnite mineralization in Australia presented a model for the origin of antimony from the troilite phase of the deep mantle. One of the major controls of stibnite mineralization in Australia was demonstrated to be the landward projection of major transform faults related to calc-alkaline volcanic activity and extensional tectonics. Furthermore, Farrand (op.cit) noted the close similarity of stibnite mineralization in the Central Asian Mercury Belt to that in New England, Australia which he related to plume activity and possibly a failed spreading axis. It should be noted that stibnite mineralization is widespread throughout the eastern margin of Australiasia and extends discontinuously throughout the eastern coastal area of Australia. New England is a focus of stibnite deposits with production centered on the Hillgrove-Metz mining field, 30 km SE of Armidale (Robinson and Farrand, 1982). This area is currently responsible for 2-3% of world antimony production.

Maucher (1968) showed that Sb-W-Hg formations in the Mediterranean and eastern Alps were related to early Palaeozoic volcanism. The coincidence of Cretaceous-Tertiary Sb-Hg deposits with the early Palaeozoic sequences is widespread and as such it was proposed that the younger deposits represented mobilization from early Palaeozoic Sb-Hg-rich formations. In 1978, Maucher presented an extensive review of stratabound Hg-Sb-W

deposits, with examples from the Mediterranean and eastern Alps. It was noted that the fundamental metal supply took place during the early Palaeozoic period, and was genetically connected with basic volcanism and its alkali-rich acidic differentiates, and closely linked with major structural lineaments. The metals Sb, Hg, W, Be, Bi, As, Au and Ag were derived from the mantle and transported by deep seated volcanic processes.

Holl (1977) in studies of Sb-As-Hg mineralization in north west Europe identified the widespread occurrence of minor scheelite (CaWO_4) mineralization in association with these deposits. In addition, it was reported that stibnite and cinnabar occurrences in the eastern Alps are spatially, temporally and genetically connected with subduction related basic, locally ultramafic and acid volcanism, and with igneous related hydrothermal activity during the Upper Ordovician and Silurian. Holl (1979) defined a simplistic model for Sb-W-Hg deposits in the eastern Alps, invoking a series of parallel belts above a subduction zone system. In this model Hg deposits were produced near the trench whereas Sb-As-W deposits were produced further from the trench and related to a more deep seated origin. Furthermore, Holl (1979) noted that many stratabound stibnite and cinnabar deposits in northern Europe show close temporal and genetic relationships to deposits hosted within Archean greenstone belts.

Stumpfl and Reimann (1980) noted the close association of ocean-floor basalts and associated mafic volcanics with stibnite mineralisation in the Southern Central Alps. The genetic model of Maucher (1978) involving a direct association between Sb-Hg mineralization and mafic rocks has been somewhat modified by the detailed studies of Reimann and Stumpfl (1981) to include submarine volcanicity of basic to acid affinity, associated with exhalative activity and intermittent clastic sedimentation. This model may be extended further to incorporate the features identified in the Southern Uplands by the inclusion of both terrestrial and subvolcanic categories. In addition, Reimann and Stumpfl (1981) in studies of stratabound stibnite mineralization in the Kreuzeck mountains, Austria noted that both arsenopyrite and pyrite are present in stratabound and vein-type ores. Previous authors have stressed an exclusive association of stibnite mineralization with basic volcanic rocks, however this study demonstrated that, intermediate to acid volcanic rocks play an important role in the development of the mineralization.

A 10m wide phyllic alteration zone were identified by Morris and Steed (1985) in the immediate vicinity of vein mineralisation in the Clontibret As-Sb-Au deposit. This zone was enclosed within a propylitic alteration envelope of indeterminate width. The Clontibret deposit (see Chapter 1) consists of several NNW-trending lode zones and was worked historically for antimony. Two principle mineralization episodes are present, with early disseminated arsenopyrite-pyrite followed by a localised stibnite veining. Wallrock alteration is characterised by progressive K_2O enrichment and Na_2O depletion, in proximity to the ore body. Furthermore, mineralogical studies by Morris et al., (1985) were used to infer that the most intensive, and highest temperature phase of mineralization in the Clontibret deposit, is represented by the arsenopyrite-pyrite assemblage. In contrast, the stibnite phase of mineralization is relatively localised and unaccompanied by any form of distinctive wallrock alteration. Igneous intrusions are both rare and poorly exposed, in the vicinity of the Clontibret deposit, however drilling by Munster Base Metals limited, has identified several minor mafic intrusions (?sills) immediately east of the deposit. In addition a small area of hornfelsed greywacke is exposed ~2km SE of the deposit, unassociated with any visible igneous rocks. Elsewhere in the Longford Down, similar hornfels is associated with small intermediate intrusions (? monzodiorite) of Caledonian age (Morris et al., 1986). Immediately south of the Clontibret Sb deposit, further mineralization comprising of a dense stockwork of veins, displaying prominent, internal, cataclastic deformation textures was identified and considered to be a precursor to the main mineralization event (Morris et al., 1986).

In the Wadebridge area of southwest England antimony occurs in small quartz vein deposits and has been historically mined. Jamesonite is the principal antimony mineral associated with subsidiary amounts of chalcopyrite and galena. Edwards (1976) using metallogenic maps, showed that a spatial relationship exists between the antimony mineralization and spilitic lavas which outcrop in this area and suggested a genetic relationship between the two. The association of Sb-rich spilites and metasediments were compared by Edwards (op. cit.) with the stratabound, volcanogenic stibnite deposits from Ballao-Villasalta (Holl, 1966) and Turkey (Maucher, 1972). Stanley et al., (1989) detailed the mineralogical and structural setting of gold-antimony vein mineralization in southwest England. NW-SE trending, quartz-carbonate veins at Loddiswell were found to contain native gold, tetrahedrite, boumonite, bismuthian jamesonite, antimonian bismuth, chalcopyrite, covellite, gersdorffite, acanthite and sphalerite. A model for this mineralization was proposed invoking the interaction of volcanic rocks (spilites and dolerites) with a series of major NW-SE lineaments.

Rundle (1979) concluded that the Eskdale granite was altered as a result of hydrothermal activity during the Late Silurian to Early Devonian period. In addition, Fortey et al., (1985) noted the relatively widespread distribution of antimony mineralization in the Lake District of northern England. In a study of scheelite-ferberite-chalcopyrite mineralization hosted by granodiorite at Buckbarrow Beck in the Lake District, Young et al., (1986) noted that the mineralization formed part of a minor episode of hydrothermal activity related either to emplacement of the Early Silurian Eskdale granite or to the end-Silurian Caledonian orogenic event.

It is interesting to note that stibnite mineralisation occurs along a major shear zone separating Ordovician and Silurian turbidites in New Brunswick, Canada (Ruitenberg and Fyffe, 1982). In a study of fracture controlled antimony mineralization in the Lake George deposit, New Brunswick, Scratch et al., (1984) detailed the mineralogy, geochemistry and alteration products of a deposit which exhibits many close similarities with the Glendinning and Clontibret deposits. This deposit comprises of a series of stibnite-bearing quartz veins crosscutting a Silurian turbidite succession. The vein system passes at depth into a siliceous skarn intruded by granite porphyry dikes, which was preceded by, or developed contemporaneous with, an argillaceous alteration halo. In the Lake George deposit, a series of stibnite bearing quartz veins, crosscut tightly folded Silurian turbidites, within the contact metamorphic aureole of a small granodiorite porphyry intrusion. Wallrock alteration accompanying stibnite quartz vein emplacement involved major additions of Sb, As, S and volatiles, with minor introduction of K_2O , Rb and Si. In addition Fe_2O_3 , MgO , CaO and Na_2O together with Co, Ni and Zn were depleted. The dominant fracture controlled argillic alteration zone, containing quartz-stibnite veins and disseminated arsenopyrite, was developed at 360° to 490°C and pressures of 600-900 bars and may be directly related to small granodiorite porphyry. An argillic alteration zone envelopes the stibnite bearing veins and is developed over distances of 30m from the major vein. This alteration is characterised by a fine grained assemblage of quartz, sericite, illite, kaolinite, dickite, arsenopyrite and pyrite. In addition a siliceous alteration zone, 3-5 cm thick surrounds the main stibnite-bearing quartz veins, overprinting the previously formed argillic alteration and formed contemporaneous with vein emplacement. The ore forming solutions, were proposed to have been late-stage magmatic in origin, evolved from the granitic intrusion, itself derived from partial melting of Sb-enriched sediments. It is interesting to note however, that Sb enrichment within the granodiorite porphyry occurred during alteration, rather than as a primary feature, and a lamprophyre dyke swarm occurs parallel to, and is transected and altered by the stibnite bearing quartz vein. The quartz-stibnite veins also host native antimony (the only other mineral of economic importance) arsenopyrite, pyrite, pyrrhotite, tetrahedrite, boumonite, boulangerite, cubanite, sphalerite, chalcopyrite, molybdenite, bornite, kermasite and senarmonite. In summary, the stibnite-quartz vein mineralization in the Lake George

deposit, is related to, but slightly later than, the arsenopyrite-rich argillic alteration and both are directly controlled by the fracture system. Scratch et al., (1984) proposed that Sb, As and Au in the Lake George deposit, New Brunswick were derived from either the direct leaching of metal enriched Cambro-Ordovician black shales or a late-stage magmatic fluid, with secondary Sb enrichment resulting from a magma derived from partial melting of the Cambro-Ordovician sediments.

Two possible schemes for the hydrothermal system of the Lake George Sb deposit were proposed by Scratch et al., (1984). The first, involved the generation of an ore fluid by thermally driven convection of meteoric surface waters through the sedimentary sequence. The early phase of argillic alteration may have been induced by the escape of the vapour phase, followed by stibnite-quartz deposition from the residual saline liquid (Scratch et al., 1984). The second model invoked the expulsion of Sb-rich magmatic fluids from an intrusion associated with a coeval meteoric water convection cell. Seal et al., (1987) in a discussion of W-Mo mineralization in the Lake George deposit, New Brunswick noted that a Late Silurian complex hydrothermal center was spatially and temporally related to a biotite monzogranite stock, and porphyry and lamprophyric dykes.

4.5.3 Hot Spring Geothermal Systems

De La Beeche (1839) divided the more rational of early views on metallogenesis into two categories, namely the sublimation of substances driven by heat from below; and the filling of fissures in rocks by chemical deposits from substances in solution in the fractures. Using contemporary ideas the first 'hot spring' model was developed, generated by the natural geothermal gradient with metalliferous components derived from indigenous rocks.

The characteristics of epithermal precious-metal deposits have been recorded by numerous authors including Lindgren (1933), White (1943, 1985), Henley and Ellis (1983), Berger and Eimon (1983) and Hendenquist and Henley (1985). In addition, a detailed account of the geological and geochemical features of hot spring precious-metal deposits is presented by Berger (1985). These deposits may be distinguished from their deeper-seated epithermal counterparts by extensive near-surface silicification, elevated As, Au, Hg, Sb and Tl values, and widespread hydrothermal brecciation. Similarities between epithermal ore deposits and active geothermal systems have been recognised by numerous authors including White (1974, 1981), Ewers and Keays (1977), Sillitoe et al., (1984). Evidence supporting a genetic link between geothermal activity and precious metal mineralization has accumulated over the last decade from research into active geothermal systems and from studies of precious metal deposits in hot spring environments.

Epithermal Au-As-Sb-Hg vein deposits are common in volcanic areas of north America, parts of the USSR, New Zealand and elsewhere. The association with volcanic activity, and the limited vertical range of mineralization has been invoked to suggest near surface deposition in an environment similar to modern day hot springs (Ewers and Keays, 1977; Rose et al., 1979). Hemley and Jones (1964) discussed the characteristic effects of hydrogen metasomatism, within different types of hydrothermal alteration. The hydrolysis of feldspars to form a kaolinite-quartz bearing assemblage is characteristic of both hot spring and epithermal Au deposits and represents an intense form of hydrogen metasomatism.

The transport chemistry of the epithermal group of metals has been reviewed in detail by Barnes (1979), Weissberg et al., (1979), Henley (1985), and Henley and Brown (1985). Hg and Sb deposits are reported from several sites

of hot spring activity in the western United States. White (1967) described the frequent association of mercury deposits with hot springs. Stibnite and amorphous silica are deposited at/or near surface in the Steamboat Springs deposit (Dickson and Tunell, 1968). Further examples of hot springs associated with As-Sb-Hg sulphides include Boiling Springs, Idaho; Sulphur Bank, Amedee Springs, and Skagga Springs, California and Norris Basin, Yellowstone National Park (White, 1967). The nature of gold deposition at modern hot springs indicates that the gold was originally deposited as disseminations of sub-microscopic grains. Subsequent metamorphism may have resulted in an increase in grain size. The processes involved in exhalative sulphide deposition and their application to existing ore bodies has been discussed by Hutchinson (1983), Sangster and Scott (1976) and Solomon (1980) and a general correlation between As and Au was observed in discharge material.

Schoen et al., (1974) presented a detailed account of the argillization process associated with present-day hot spring activity in the Steamboat Springs area, Nevada. It was demonstrated that sulphuric acid formed by oxidation of exsolved hydrogen sulphide formed the active altering agent. Rose and Burt (1979) in a study of alteration in hot springs and epithermal deposits noted that the character of alteration and mineral deposition may be changed by cooling and/or boiling. Cooling results in super saturation of the fluid components, whereas boiling selectively removes CO_2 , H_2S and other volatile compounds, and increases pH. Moore et al., (1983) identified As-Sb-Hg-Au-rich surface discharges at the Roosevelt Hot Springs thermal system in Utah. Mercury and arsenic were demonstrated to form the most widely distributed trace element anomalies in soil samples overlying the thermal system, with the highest concentrations of Hg and As (5.5 and 26ppm respectively) occurring in soils within 300m of the thermal discharge. Stauffer and Thompson (1984) demonstrated that both arsenic and antimony were present at elevated levels in geothermal waters, from the Yellowstone National Park, Wyoming. Berger and Silberman (1985) in a discussion of trace element zonation patterns within hot spring type precious metal deposits noted that epithermal mineralization generally precipitated within 100-300m of the surface and emplaced as small veins, stockworks and explosive breccias in association with non-marine volcanism, generally calc-alkaline in composition (NB. phreatic eruptions occur in areas where the heat flow is sufficiently high to locally exceed the boiling point-depth relationship). Furthermore, in 1985, Silberman and Berger proposed a vertical zonation scheme through active geothermal systems.

Tooker (1985) noted the similarity between disseminated gold deposits formed from near surface, low-temperature, silica-rich hydrothermal solutions and those associated with hot-spring systems. In a study of hydrothermal eruption mechanisms and hot spring gold deposits, Nelson and Giles (1985) noted that episodes of gold mineralization in hot spring environments are directly related to hydrothermal eruption events, their accompanying breccias and peripheral stockwork zones. Antimony and mercury deposition from hot springs has also been reported from several localities in the western United States, in the USSR and on Hokkaido, Japan (Muff, 1978); for example, the Mayacmas district of California contains a 40km long NW trending belt of mercury deposits and thermal springs hosted by Franciscan greywacke and shales.

Henley (1985) in a discussion of terrestrial, magma-related hydrothermal systems noted that alteration assemblages correspond closely to those encountered in epithermal and porphyry-style mineral deposits. The major difference between the discharge behavior of terrestrial and submarine systems is that the excess pressure due to overlying seawater (for the latter) leads to relatively higher temperatures in the near surface systems and renders boiling less common.

The element thallium (Tl) displays close chemical affinities with As, Au and Sb within many epithermal precious metal systems. The geochemistry of thallium was reviewed by Shaw (1957) who noted that Tl replaces K in both feldspars and mica in a similar manner to that of Rb. It should be noted however, that in minerals, Tl only substitutes substantially for K, during hydrothermal alteration. Weissberg (1969) in a description of the chemistry of precipitates from active hot spring and drill hole discharges from New Zealand noted the following maximum values: 2% As; 85ppm Au; 500ppm Ag; 2000ppm Hg; and 1000ppm Tl. Lambert and Scott, (1973) in a geochemical study of the host rocks to the McArthur Zn-Pb-Ag deposit, Australia, noted that Tl is preferentially concentrated in the ore deposit (with values ~100ppm). Ewers (1975) determined the distribution of Au, As, Sb, Tl, Ag, Bi, Pb, Zn, Te, Se and Co in the sulphide fraction of borehole samples from the Broadlands Geothermal System, New Zealand. Two main zones of sulphide deposition were located in which pyrite, was found to contain up to 1.30 ppm Au. The geochemical association of Au-As-Sb-Hg and Tl corresponds closely with that found in the Broadlands (New Zealand) hot spring gold deposits forming at this moment in time. Tl enrichment/primary dispersion halos, were predicted by Ewers and Keays (1977). Emsley (1978) detailed the historical background to the discovery of thallium and described the nature of its toxicity. Polymetallic vein deposits containing elevated Tl levels, are related to either volcanic or plutonic acidic magmatism (Jankovic, 1980). The enrichment of Tl during late stage of magmatic differentiation, follows closely to that of potassium. On the basis of element mobility Hg, Tl, As and Sb will travel upward and outward to form large, near-surface halos (White, 1985). Duchesne et al., (1983) noted the occurrence of elevated Tl levels (30 to 6800 ppm) in Fe-sulphides, associated with Belgian Pb-Zn vein deposits. In addition, Ikramuddin et al., (1983) presented a detailed review of the geochemistry of thallium and its application as a potential guide to mineralization. In the north Moccasin gold deposit of Arizona, low Tl values (1.84ppm) were regarded as highly significant in comparison to background values (0.52ppm). In addition, it was demonstrated that the high abundance of Tl in altered rocks and the significant positive correlations with both K and Rb in the mineralized rocks, infers that Tl was concentrated in the hydrothermal fluids. Relatively low temperature hydrothermal solutions associated with epithermal gold deposits were demonstrated to have a much greater abundance of Tl than high temperature fluids associated with Cu-Mo deposits (Ikramuddin et al., 1983). The source of Tl in the As-Sb-Au deposits located in the Glendinning study area, may thus be linked to a magmatic component.

In New Zealand a number of geothermal systems have been identified by Weissberg et al., (1969; 1979) along the eastern margin of the Taupo volcanic zone (regional Mesozoic greywacke basement) at Rotokaua, Broadlands, Waiotapu and Waimangu. These systems are characterised by amorphous arsenic and/or antimony rich sulphide precipitates which contain highly elevated gold, silver, mercury and thallium values. Detailed investigation indicated a zoned deposition pattern with Zn, Pb and Cu sulphides at depth and a near-surface element suite of As, Sb, Hg, Tl, Ag and Au. In general, the element association Sb-As-Au-Hg-Tl identified in hot spring deposit worldwide is similar to the associations identified in the Glendinning deposit.

In a study of precious metal zoning in the Broadlands geothermal field, New Zealand, Ewers and Keays (1977), noted that the deposition of Tl occurred solely in response to decreasing fluid temperature, while other elements were precipitated through the combined effects of decreasing temperature and boiling within permeable zones. This study demonstrated the existence of a crude metalliferous zoning with As, Sb, Au and Tl enriched in near-surface regions while Ag, Se, Te, Bi, Pb, Zn, Cu and Co are concentrated mainly at depths of ~1.0-1.4km. Blakestad and Stanley (1986) defined the characteristics of monotonic and prograding geothermal systems. Monotonic systems display little if any spatial variation whereas, prograding systems display steep geothermal gradients,

explosive breccias, complex veining and mineralisation. Arnannsson et al., (1986) presented a detailed study of the Theistareykir high-temperature geothermal area in Iceland, and noted that geothermal activity may occur in areas as large as 20km².

In a study of submarine exhalative gold mineralization, Mangan et al., (1984) noted the close spatial association of submarine epiclastic volcanic debris and exhalative chemical sediments. These deposits were believed to have formed by processes analogous to those currently active in the Atlantis II Deep of the Red Sea. Silica rich, hypersaline brines discharged through fractures in the sea floor, ponded in a local basin and were subjected to episodic influx of clastic debris. Hedenquist and Henley (1985) proposed a model of the origin of hydrothermal eruptions in the Waiotapu geothermal system and their relationship to precious metal mineralization. In opposition to the fluid overpressure models of Sillitoe et al., (1984) this mechanism invoked the transmission of deeper reservoir pressures by the evolution of a compressible cap of exsolved gas (dominantly CO₂). In addition, two chemical environments were recognised in which arsenopyrite deposition and coprecipitation of gold and other metals may occur, namely: boiling and H₂S in the fracture network and conduit below an eruption crater and/or surface heat loss and pH buffering.

Hedenquist and Henley (1985) emphasized the correlation of epithermal precious metal deposits and active geothermal systems, and detailed the characteristics and origin of hydrothermal eruptions and associated breccias at Waiotapu, New Zealand. Zhu Bingqiu et al., (1986) demonstrated the direct application of As-Sb-Hg geochemistry in the identification of active geothermal areas in China. Average anomaly values of 19ppm As and 2.7ppm Sb correspond favorably with those identified in the Glendinning study area. It is therefore proposed that As-Sb-Au mineralization was deposited by analogous processes, from fluids of similar chemical composition, forming part of a major hydrothermal episode. The results of this study may be used to infer the presence of a highly active geothermal system in this area during late Silurian-early Devonian period, similar in many respects to that currently located in the Broadlands area, New Zealand.

Recent studies by Silberman and Berger (1985) have linked fossil hot-spring systems to the more deeply emplaced bonanza-type epithermal vein deposits by documenting a continuum of features from surface springs to the deep veins. A bonanza-type epithermal precious metal deposit is defined by Harris et al., (1988) as a relatively near-surface deposit formed in a hydrothermal system under low to moderate lithostatic pressures (less than 300m) at temperatures below 300°C. The potential for the discovery of such a deposit in the Glendinning area therefore cannot be ignored.

Many epithermal deposits may be closely associated with convergent plate boundaries and are characterised by recent volcanism, high heat flow, tectonic activity, and by the presence of active and recently active geothermal systems. Mitchell (1985) noted that epithermal gold mineralization in magmatic arcs is commonly associated with the start of transform faulting that follows either arc rotation or oblique collision (such as that associated with the closure of the Iapetus Ocean, in the Southern Uplands). Within arc systems epithermal gold mineralization is mainly confined to sub-volcanic or plutonic intrusions, their contact margins and overlying pre-intrusion host rocks. It should be noted that epithermal deposits in the Circum-Pacific region produce ~30 million grams of gold annually together with a larger but indeterminate amount of silver.

Foster and Furber (1985) in discussions on calc-alkaline related exhalative and volcanoclastic-hosted gold mineralisation in Zimbabwe, noted that typical end member models of lode-gold and massive sulphide mineralisation

were not applicable in the Shamva deposit. Foster (1986) proposed that felsic-related fumarolic activity may be accompanied by gold, arsenic and other metals. This analogy may also be applied in the British Caledonides, where outcropping mineralisation forms a part of a continuum related to depth of exposure, depth of emplacement and proximity to igneous intrusions.

The analogy between epithermal ore deposits and geothermal systems is supported by the identification of economic concentrations of Au and Ag and other associated elements from several active geothermal systems including Steamboat Springs, Nevada; Ohaaki, Broadlands and Waiotapu, New Zealand and elsewhere (Weissberg, 1969; Weissberg et al., 1979; Ewers and Keays, 1977; and Silberman and Berger, 1985). The discovery of economic precious-metal deposits related to physical-chemical processes in the near-surface portions of high-temperature hot-spring systems has led to intensive exploration efforts for similar types of deposit. James (1984) identified a large number of gold environments within the Philippines. These depositional environments are geologically complex and mirror those of the Southern Uplands in many respects (metamorphic basement, accreted terranes and calc-alkaline volcanics). Furthermore, many of the hot spring systems in both New Zealand and Nevada are associated with felsic volcanics and porphyry dykes, features also characteristic of Au deposits in the Southern Uplands.

Mineral assemblages similar to those identified in the Southern Uplands are also reported from recent volcanic and hot spring areas worldwide. In addition, a number of close similarities were observed between the Glendinning, Clontibret and Lake George deposits (Duller and Harvey, 1985; Morris and Steed, 1985; and Ruitenberg, 1984). Although the surface expression of Palaeozoic hot-spring systems are rarely preserved in the stratigraphic record, Cunneen and Sillitoe (1989) have identified a Late Devonian hot-spring sinter in the Drummond Basin, Australia. Disseminated gold occurrences first reported in western USA are now recognised in similar (if older) accreted terranes such as the Southern Uplands and as such, the conclusions and models detailed in this study may have widespread application to exploration programmes in other turbidite terranes.

4.6 SCOTTISH As-Sb-Au DEPOSITS

The Southern Uplands may be regarded as a turbidite dominant, complex intrusive-volcano-sedimentary terrane characterised by numerous epigenetic gold deposits. Particles of gold and gold-bearing secondary oxidation products are readily identified in stream sediment samples and panned concentrates in the vicinity of numerous historical mines in the Southern Uplands. In a study of the morphology and composition of placer gold from this region, Naden et al., (1985) noted that the alluvial gold shows evidence of short transport distances (<10km). In addition compositional variations related to the greywacke petrography, included relatively 'silver-rich' grains associated with acidic lithologies (cratonically derived); and 'gold-rich' grains associated with basic clast lithologies (volcanically derived).

This study provides an attempt to elucidate the broad metallogenic relationships between diverse types of As-Sb-Au deposits in this terrane and details the evolution of the hydrothermal systems with time. Three main type of metalliferous mineralization were identified in this study, namely: As-Sb-Au vein-type deposits; Cu-Mo-As-Au deposits directly associated with Caledonian igneous intrusions; and late stage Pb-Zn-Ba-Cu vein mineralization.

The relative positions of the five main arsenopyrite-gold deposits studied within the Southern Uplands are presented in figure 7b and superimposed upon the relative position of juxtaposed petrographically and geochemically

distinct turbidite formations within the study area in fig. 296b. Despite the apparent differences between As-Sb-Au deposits in southern Scotland, there is a marked similarity in the nature of the geochemical dispersion and alteration features. Sericitization is almost ubiquitous and often accompanied by silicification and carbonatization, and sodium is found to be strongly depleted in the vicinity of all deposits. In addition, a frequent association exists between tourmaline with gold-bearing igneous rocks in the Southern Uplands.

This section summarised the results of a series of highly pertinent British Geological Survey M.R.P. reports relating to mineralization in the Southern Uplands, re-examined or newly discovered since 1973 and is combined with the results of a literature survey.

The Doon-Glenkens Area

Dawson et al., (1977) reported the results of an integrated reconnaissance survey of the Doon-Glenkens area in south-west Scotland undertaken between 1972-75, by the British Geological Survey. It is interesting to note that five out of the seven previously unknown examples of exposed mineralization defined by this study contained arsenopyrite and were located in close proximity to panned gold anomalies: Four sites were contained within altered tonalite-diorite intrusions/dykes (Burnhead, Kirreoch Burn, Milldown and Kishinnoch Burn) whereas at the fifth site (Step of Trool [NX 420797]) a 30cm wide, mineralized greywacke breccia was found to contain pyrite and arsenopyrite together with traces of galena and sphalerite.

The Abington-Biggarr-Moffat Area

Dawson et al., (1979) in a mineral reconnaissance study of 195 panned heavy mineral concentrates from the Abington-Biggarr-Moffat area (immediately east of the Leadhills mining district) revealed numerous new occurrences of Pb, Cu, and Ba minerals together with the widespread distribution of fine grained particulate gold. In addition, the mercury mineral, cinnabar (HgS) was identified for the first time in Scotland, at three locations in close proximity to the Southern Uplands Fault. Chromiferous spinel was recognised as a major constituent of panned concentrates. It also forms a detrital component in greywackes from this region and infers derivation from an ultrabasic source. Although no antimony minerals were identified in pan concentrates, XRF analysis revealed a small number of anomalies (25-45ppm) concentrated in tributaries of the River Tweed. Arsenic mineralization dominated by arsenopyrite, was identified in trace amounts within a small number of pan concentrates. XRF studies defined 10 samples containing arsenic values >90ppm which cluster in close proximity to the Ordovician-Silurian boundary.

The Fleet Granite

The results of a regional geochemical drainage programme centred upon the Fleet granitic complex were reported by Leake et al., (1978). These results provided evidence for the existence of eight geochemical units within the turbidite sequence, separated by presumed major strike faults adjacent to belts of black shales. The most northerly unit in this area is correlated with the Afton Formation, and characterised by greywackes rich in quartz but poor in ferromagnesian minerals (Dawson et al., 1977; and Floyd, 1984). Six panned concentrate samples from this study were found to contain detectable Sb levels. The highest concentration (25ppm) was located in Craigshinnie Burn, draining historical Pb-Zn-Cu trials whilst other samples occur near the headwaters of Penkiln Burn, associated with base metal mineralization and plumbogummite rich gossans. Unfortunately, arsenic was not analysed within either

stream sediment or pan concentrate samples, and as such a comparison with the Loch Doon and Glendinning areas could not be made. The location of old metalliferous mines in the vicinity of the Fleet Granite, Southwest Scotland is displayed in fig. 24. Arsenopyrite was reported as a minor constituent of a series of NW-SE and NNE-SSW trending, lead-zinc bearing veins on the south-west flank of the Cairnmore of Fleet granite (Wilson, 1921; Leake et al., 1978). Temple (1955) considered on the basis of field evidence, that the veins were Permo-Carboniferous in age, due to their field, however Leake et al., (op.cit) invoked their association with the aureole of the Cairnmore of Fleet granite to suggest a Caledonian age for emplacement.

Cairngarroch Bay

Two complex intrusions comprising of microtonalite, granodiorite, quartz porphyry, porphyritic quartz-microdiorite and quartz-microdiorite are emplaced within a folded succession of Silurian sedimentary rocks at Cairngarroch Bay (Allen et al., 1981). Investigations during the late 1970's by the Mineral Reconnaissance Unit of the British Geological Survey, revealed the presence of localised zones of intense hydrothermal alteration, network fracturing, brecciation and pyritisation. Rare chalcopyrite crystals were identified as sparse disseminations and hosted by pyrite rich quartz-veins; and arsenopyrite was located in wallrocks adjacent to the main Bay complex. Lithogeochemical studies indicated the presence of pervasive but patchy Cu-Fe-As-Mo mineralization in all rock types, accompanied by irregular Ba, K and Sr enrichment. Arsenic levels were highly variable with values including: microtonalite (max 89ppm); microdiorite (max 123ppm); mineralized greywacke (max 531ppm) and quartz sulphide veins (max >1000ppm). The nature of mineralization and alteration identified within this deposit exhibit characteristics of a small, low-grade copper porphyry system.

Loch Doon

In an evaluation of gold mineralization at the southern margin of the Loch Doon granitoid complex, Leake et al., (1981) reported the discovery of native gold and arsenopyrite hosted by quartz veins intruding turbidites within Glenhead Burn, south-east of Loch Trool. Lithogeochemical samples from this deposit reveal a strong correlation between arsenic and gold. Furthermore, swarms of concordant minor intrusives including quartz monzonite, granodiorite and hornblende lamprophyres predate the pluton and are located within its aureole (fig. 25). In detail, two phases of gold-bearing, arsenic-rich mineralization were recognised by Leake et al., (op.cit) in the Loch Doon area, namely:

- 1) Early disseminations of pyrrhotite, arsenopyrite and pyrite in the margins of monzonitic minor intrusions and disseminations of arsenopyrite in the adjacent hornfelsed metasediments. This style of mineralization occurs in zones up to 18m wide, containing arsenic and gold levels of upto 3000ppm and 0.16ppm respectively.

- 2) A superimposed a stockwerk of discordant N-S trending quartz veins, crosscutting all rock types in this area, containing pyrite, arsenopyrite (up to 3.5% As) and native gold (8.8ppm max). Wallrocks adjacent to these veins are strongly sericitised and contain abundant disseminated arsenopyrite. (NB. A separate, later phase of sphalerite and galena mineralization also occur within this area).

A N-S trending elongate, complex pattern of chemical and petrographic zonation occurs within the 'granite' with peripheral diorite, norite and tonalite surrounding a granite and transitional granite core (fig. 25). Furthermore, the

widespread distribution of alluvial gold throughout this region and the concentration in areas marginal to small igneous intrusions is displayed in fig. 26. Pervasive metasomatism has affected all sedimentary rocks in this area. Two forms of alteration were identified in the turbidite sediments, dominated by Ca and subordinate Mn and Sr enrichment, and accompanied by Mg, Ni, Zn, Rb and Ba depletion.

A genetic model of mineralization in the Loch Doon area was presented by Leake et al., (op. cit) which attributed gold deposition to metasomatic and hydrothermal events within an evolving cycle of magmatism in which phases from granodiorite to diorite were emplaced at a moderately high levels (>3km) in the crust. The association of arsenic and gold with minor intrusive igneous activity was clearly demonstrated in the Glenhead Burn. Furthermore, the abundance of CO₂-rich fluid inclusions in the later, discordant gold-bearing quartz veins was used by Leake et al., (op.cit) to infer a magmatic source for this phase of mineralization, however the location of this deposit is also subject to major structural controls.

Penkiln Burn

Significant secondary base metal anomalies were located in a N-S trending fracture zone, 2.3km in length, across the Penkiln Burn area on the SW margin of the Loch Doon pluton (Stone et al., 1983). These anomalies were located within a broadened section of Moffat shales containing an abundant dyke swarm (porphyritic homblende microdiorite, spessartite lamprophyres, microtonalites and quartz-microdiorites); and spatially associated with weakly disseminated and fracture controlled Pb-Zn-Cu mineralization. Lithogeochemical studies of extensively altered dyke material from within a fault zone south east of Lamachan Hill revealed arsenic levels in excess of 10,000ppm. Due to the level of alteration, no crystalline arsenic minerals were detected and it was proposed by Forthey (1981) that the arsenic was hosted within hydrated iron oxides. Subsequent borehole investigations by the British Geological Survey revealed elevated As and Sb levels within all minor intrusions (As - 1560ppm max; Sb - 42ppm max). Extensively veined and hydrothermally altered minor intrusions display evidence of potassic metasomatism and sericitisation accompanied by sodium, magnesium and zinc depletion. The virtual absence of zinc within altered samples may be used to indicate the extensive nature of leaching within the fracture zones. A genetic model of Penkiln Burn mineralization was tentatively proposed by Stone (op. cit.) invoking the presence of minor intrusions and resulting high geothermal gradients to initiate localised hydrothermal convection cells. It should be noted that mineralized sites within the Penkiln area occur within 1-3km south of the known Au-As-Base metal mineralization at Glenhead, where concordant minor intrusions are believed to control the early phase of mineralization (Leake et al., 1981). Close geochemical similarities exist between the Penkiln Burn and Glendinning deposits, however the Glendinning deposit is distinguished by the 'apparent' absence of intrusive rocks in the immediate mine vicinity. It should be noted that Leake et al., (1981) noted a localised 60° flexure of strike in the Glenhead Burn area, inferred to have produced the tensional stress regimes necessary to facilitate the emplacement of minor intrusions and mineralization.

Fore Burn

Allen et al., (1982) detailed the results of a mineral reconnaissance investigation of the Fore Burn igneous complex, immediately north of the Southern Uplands Fault, 24km east of Girvan. This early Devonian complex comprises of concordant and semiconcordant bodies of quartz-microdiorite, tonalite and feldspar porphyry. The complex hosts several small intrusion breccias and a zone of monolithic breccia, located along a 2km long fault zone following the drainage pattern defined by the Fore Burn. Extensive sericitic alteration, sodium metasomatism and the wide distribution of tourmaline serve to characterise this area.

Drainage geochemistry revealed elevated levels of B and As (2310ppm and >3000ppm max. respectively) over an area of 4km², which was interpreted to represent the presence of Cu-As-B-Au-Mo mineralization, concentrated along the Fore Burn breccia zone. Lithogeochemical studies noted the enrichment of Cu (>10,000ppm max), As (>3,000ppm max), Mo (410ppm max), Au (1390ppb max), Sb (1404 ppm max), Bi (521ppm max), Co, Ni, Pb and Zn in mineralized breccia samples; and mineralogical investigations defined the presence of arsenopyrite, pyrite and chalcopyrite together with traces of tennantite, tetrahedrite, cobaltite and native gold. In a comparison with the work of Drummond and Goodwin (1976) in western Canada, Allen et al., (op. cit.) proposed that the Fore Burn complex represented the upper and outer portions of a Cu-Mo-Au porphyry system. Charley et al., (1988) in studies of the Fore Burn igneous complex in the Southern Uplands (an eroded volcanic core) demonstrated the presence of gold and silver mineralization hosted by mineralogically complex quartz-tourmaline-sulphide veins within volcanic breccias, acid to intermediate lavas, agglomerates and small dioritic intrusions. Both hydrothermal mineralization and alteration were defined to have 'porphyry' affinities.

Black Stockarton Moor

Porphyry type copper mineralization has been reported by Brown et al., (1979) at Black Stockarton Moor in southwest Scotland. This mineralization is associated with a subvolcanic complex of intersecting dykes and breccia pipes on the western margin of the Criffel granodiorite. The mineralogical and geochemical parameters associated with porphyry copper mineralization were detailed by Henley and McNabb (1978). The Black Stockarton Moor subvolcanic complex described by Leake and Cooper (1983) is composed of a series of intersecting porphyrite dyke swarms, granodioritic sheet intrusions, small granodiorite stocks and breccia pipes of Late Caledonian age, emplaced within the Lower Palaeozoic turbidite succession of the Southern Uplands. An evolution from subvolcanic to plutonic igneous regimes, was identified with the successive intrusion of dykes, sheets, stocks and the adjacent Bengaim and Criffel plutonic complexes. Breccia pipes identified by Leake and Cooper (1983) in this complex display many close similarities with the Glendinning breccias. For example, a breccia pipe located at Pennan Hill [733 565] is composed of irregular, mainly angular fragments of randomly orientated, silicified mudstone and greywacke, ~2cm in diameter. The margins of most fragments are silicified and the breccia matrix consists of crypto-crystalline silica. Although there are no traces of igneous rocks in the breccia matrix, this pipe appears to be associated with the top of a small granodiorite stock and as such it was suggested that the pipe formed by hydraulic fracture or violent degassing of the magma.

Minor Intrusions

An investigation of sixteen small intermediate intrusions throughout Southern Scotland were undertaken by Cooper et al., (1982) in order to define the potential for disseminated porphyry copper style mineralization at or near surface. Unfortunately, this study concluded that there were few indications of this type of mineralization within the studied locations. This study however provides invaluable lithogeochemical and panned concentrate data, of considerable importance in the assessment of the As-Sb-Au potential in this region. Although the significance of the arsenic geochemistry was not fully appreciated in this evaluation, highly elevated arsenic levels (1019ppm max) were defined within hydrothermally altered microdiorites from both Glenluce (NX 214569) and the Mull of Galloway (NX 140308), together with elevated arsenic levels (89ppm max) in microtonalites from Cairngarroch Bay. In addition, altered greywackes from the wallrocks of the Tonderghie copper mine (NX 439384) 2.5km north-west of Burrow Head revealed As levels up to 386ppm. Furthermore, although antimony levels were only analysed in panned concentrates, samples from Cockburnlaw (NT 772589) in the north-east of Scotland

revealed values up to 207ppm (NB. arsenic was not analysed in pan concentrates). At Cockburnlaw a complex hybrid intrusion together with numerous lamprophyre and quartz-porphyry dykes intrude Silurian turbidites. It should be noted that tourmaline, the dominant indicator of Cu-As-Au-Sb mineralization within the Fore Burn igneous complex, occurs locally throughout this area. In comparison with the Glendinning and Fore Burn deposits, these factors may be used to infer the presence of Sb mineralization and as such, this area provides a new target for possible As-Sb-Cu-Au mineralization in this region.

Caulfield and Naden (1988) presented the results of a fluid inclusion and isotopic study upon quartz-pyrite-arsenopyrite vein mineralization associated with granitoid intrusions at Hare Hill, Moorbrock Hill, Stobshiel and Glenhead Burn. Low salinity (3.4-5.8 equiv.wt% NaCl) two and three phase fluid inclusions yielded temperatures of 220-280°C. In addition, this study revealed that extensive fluid un-mixing had not taken place during mineralization, which was suggested to have occurred at different structural levels.

Culvenan Fell

Reconnaissance geochemical and geophysical surveys were carried out by BGS at Culvenan Fell to investigate the potential for porphyry copper style mineralization associated with the Culvenan diorite (Parker, 1981). Exploration centred upon the west of the intrusion where numerous intermediate dykes and three small intrusion breccias crosscut Silurian greywackes from the Gala Group. Narrow geophysical anomalies associated with sulphide concentrations in both sediments and dykes were associated with low-grade, localised Cu-As-Fe-Pb mineralization with arsenic values including: intrusion breccias (900ppm max); sandstones (137ppm max); hornblende lamprophyres (56ppm max) and quartz veins containing >1000ppm As.

The Cheviots

Leake and Haslam (1978) presented the results of a panned concentrate geochemical survey of the Cheviot area in northern England. This study is of importance to this discussion in that:

- 1) The Cheviot granite hosted by Lower Devonian volcanics, intrudes Silurian greywackes at depth, petrographically similar to those hosting the Glendinning deposit, 35km to the southwest.
- 2) The igneous rocks of this area are cut by a suite of contemporaneous dykes and by a number of fault, shear and breccia zones of predominantly NE and NNW trend.
- 3) Although arsenic and gold values were not generally determined, anomalous antimony values (>10ppm) define a NNW trending 'Kingsseat' lineament on the southwestern margin of the Cheviot granite, paralleling the trend defined by Breamish fault zone (Leake and Haslam, op. cit.).
- 4) The most anomalous antimony values were defined at the northern margin of this lineament, within gossanous samples from Kingseat Burn (NT 869 182) containing 130ppm Sb; 110ppm Cu; 20ppm Ag; and 40ppm As.
- 5) Antimony anomalies are also located in the headwaters of the River Coquet, draining greywackes of Wenlock age, and forming the southwestern extension of the trend established by Harthope Burn, following a major NE-SW trending shear zone, crosscutting the central portion of this study area.

Although Leake and Haslam (op. cit.) clearly identified a number of discrete Cu, Pb, Zn and Ba mineral occurrences in this area the importance of the antimony (-arsenic-silver) anomalies and their relationship with major structural features, was somewhat overlooked. In comparison with the Glendinning deposit, it is proposed that the Cheviot

area is host to a previously unidentified, fracture related phase of As-Sb-Ag-?Au mineralization, and as such forms a further target area for gold exploration in this region.

The Knipe

The first recorded evidence of the existence of an antimony deposit at this site was made by Alexander Rose, a mineral surveyor from Edinburgh, who in 1845 at the bequest of the Marquis of Bute evaluated the deposit and reported that the main vein was 51-56cm in width and contained a stibnite to quartz ratio of 2:1. The second vein was also evaluated and found to be 15-20cm in width and of a similar N10°E trend to the main vein (cf. an identical trend to the stibnite-quartz vein mineralisation at Glendinning). On the basis of this report, mining operations were commenced early in 1847 and an adit was driven for approximately 55m into the hillside, following the main vein mineralisation. It is interesting to note that the discovery of both veins within the margins of the intrusion was not fortuitous - the granodiorite forms a topographically high feature, rising above a broad area of ground covered by peat bog. It is highly probable that both vein systems extend into the hornfelsed greywacke host rocks, below the extensive drift/peat cover.

A reconnaissance study of stibnite vein mineralisation at the Knipe revealed that the vein occurs at the contact margin of a small biotite-hornblende granodiorite intruding Lower Ordovician turbidites in close proximity to the Southern Uplands fault. Although exposure in the mine area is poor and the adit at the time of this study was inaccessible, fragments of highly altered, sericitised granodiorite and possibly greywacke are identified within quartz-stibnite vein material from the mine dump. It should be noted that the stibnite vein occurs immediately south of a N-S trending biotite-hornblende porphyrite dike that extends over a strike length of 1km, which may be directly related to the mineralisation. Disseminated and vein hosted arsenopyrite mineralisation was identified in samples from the mine area and, perhaps more importantly disseminated in hornfelsed greywackes within the margin of the porphyrite dike, ~800m north of the main mine area in Garepool Burn.

Rollin (1976) defined the presence of highly magnetic (ultrabasic) rocks between the mine area and the Southern Uplands fault. Detailed mapping revealed a sequence of Arenig cherts, spilites, dolerite and gabbros of ophiolitic affinity, NW of the mine area. A geochemical and geophysical investigation of the Knipe deposit, near New Cumnock, Ayrshire was undertaken by Fowler (1976) in which the position of a second N-S trending vein in the headwaters of Blackdams Burn, in proximity to the old boundary walls of the Dalhana property was also investigated. VLF studies were used to trace the extent of both veins trending in a similar N-S direction over distances of ~400m.

Talnotry

Sample collected from a quartz-arsenopyrite vein within Palnure Burn, 300m SE of the Talnotry nickel mine (NX 477 701), close to the margin of the Cairnmore of Fleet granite. Although gold values at this site lay below detection limits, assays of ore samples from the nearby Talnotry nickel mine (a lens of diorite containing pentlandite, chalcopyrite, pyrrhotite, niccolite, smaltite and arsenopyrite, intruding lower Palaeozoic turbidites) revealed gold values up to 2ppm (Dawson et al., 1977).

Leadhills

During the last quarter of the 18th century, John Tyler, who was the then manager of the Lead mines at Wanlockhead, recognised a close correlation between the increasing abundance of alluvial gold and the outcrop of lead-zinc veins. Many factors could contribute to such an observation, but the existence of disseminated auriferous arsenopyrites within the wallrocks to the vein systems, could not only explain this trend, but also provide an explanation as to why in-situ particulate gold had never been recorded from within the veins of this area. This hypothesis was then tested by detailed wallrock sampling along a crosscut to the Susannah vein, the detailed results of which are presented in chapter five.

Kilmelford

Zhou (1988) presented the results of a detailed petrographic and lithogeochemical study of a gold and silver-bearing Late Caledonian subvolcanic centre, near Kilmelford, Argyllshire. At Lagalochoan, the field relationships between igneous rocks including porphyrite, flow-banded dacites, pyroclastics and several bodies of hydrothermal breccia, were used to infer subvolcanic emplacement near a volcanic vent. This subvolcanic zone acted as a conduit to mineralizing fluids which were responsible for widespread sericitic alteration, and the deposition of anomalously high concentrations of Au (0.67ppm), Ag (10.1ppm), As (35ppm), Cu, Mo, Zn and Pb, with the maximum concentrations located within a zone of hydrothermal breccias. This area has been the subject of intense exploration activity since the middle 1970's during which time porphyry-related disseminated copper mineralization was discovered by the British Geological Survey (Ellis, et al., 1977) 5km south-west of the Lagalochoan deposit. An extensive three year exploration programme was undertaken in this area by B.P. Minerals from 1982 to 1986. Harris et al., (1988a) detailed the results of an initial top-of-bedrock geochemical survey which yielded strong Au-Ag-Cu-(Mo or As) anomalies and accurately pinpointed the periphery of a zone of intense hydrothermally alteration and mineralization. This mineralization was shown to comprise of a shear-related As-Sb-Au-Ag-Pb-Zn assemblage that occurs peripheral to an earlier, hypogene Cu-Au-(Mo) stage associated with breccias and calc-alkaline, granodiorite-diorite intrusives (Harris et al., 1988b).

It was proposed by Harris et al., (op. cit.) that the Lagalochoan complex represented the basal section of a vented phreatomagmatic event, complexly intruded by stocks, dyke sheets and breccia bodies, with intrusive activity accompanied by base- and precious metal mineralization and associated sericitic/phyllitic hydrothermal alteration. To date, however, the BP investigations have proved unsuccessful in defining large-scale ore reserves in this area.

Discussion

Low grade copper mineralization has been identified in association with small calc-alkaline porphyry intrusions of Caledonian age throughout Scotland. One such deposit at Garbh Achadh (Ellis 1978) is located within a small stock of biotite-feldspar porphyry, 0.25km² in area, intruded into a sequence of Dalradian schists and quartzites. Hydrothermal alteration is extensive and characterised by the widespread development of sericite and kaolinite.

The Scottish 'Newer Granite' complexes (characterised by large negative gravity anomalies and strong magmatic trends) are relatively enriched in incompatible elements and often associated with metalliferous mineralization (eg. Grudie (Mo, Cu, Bi) Ellis, 1977; Kilmelford (Cu, Mo) Evans, 1977; Ballachulish (Cu, Mo), Gallagher, 1974; Helmsdale (U, Mo, As) Plant, et al., 1979). These igneous complexes are believed to be derived from modified

Upper Mantle and emplaced in a subvolcanic, continental margin environment. This environment is typical of a low grade, porphyry style, copper-gold deposits. Sillitoe (1985) has recently discussed the occurrence of gold-rich porphyry copper deposits (defined as containing more than 0.4ppm Au). Economic gold values are normally associated with potassic alteration. Secondary biotite, potassium feldspar and sericite are typical.

Simpson et al., (1988) noted that gold mineralization present in the Dalradian ensialic basin of Scotland is associated with both late porphyries (temporarily and spatial related to the emplacement of post-tectonic granites) and deep crustal lineaments crosscutting turbiditic sediments. A model was proposed invoking the initial concentration of gold in organic enriched turbidites with subsequent enrichment in both porphyry and lineament controlled systems. The significance of iron in depositing gold from solutions in which gold is carried in the AuHS complex was emphasized.

Zhou (1987) detailed the results of a lithogeochemical survey of the Kilmelford district, in the Grampian Highlands of Scotland and identified an area exhibiting high levels of Ag, As, Cu, Rb, Cd, Pb and Zn in the northeast of the study area near Lagalochoan. This association of elements was interpreted as similar to that around porphyry copper deposits and was used to propose that this area may contain significant copper and gold mineralization. Elevated gold values (up to 0.67ppm) identified in selected rock samples from Lagalochoan were used to confirm this conclusion. The association of As and Sb may occur up to 150m from gold deposits whereas, simple As anomalies located along shear zones may extend as much as 600m above the ore zone (Zhou, 1987).

Russell (1986) in a detailed assessment of the evolution of the Scottish mineral sub-province, identified a mantle and subduction related contribution to Au, As and Sb, which he proposed were remobilised during the later stages of Caledonian magmatism. Furthermore, the geological evidence provided by the Glenhead Burn, Black Stockarton Moor, Caimgarroch Bay, Fore Burn and Talnotry deposits, suggests a close genetic relationship between Late Silurian minor igneous activity, mineralization and hydrothermal alteration. The close spatial and temporal relationship between ore formation and magmatism form provide fundamental evidence for a magmatic source for the ore bearing fluids. The Glendinning deposit may therefore represent an earlier phase of hydrothermal activity and/or a precursor to intrusive activity. Implicit from the above discussion is that the As-Sb-Au mineralisation in this region is directly associated with Late Silurian/Early Devonian magmatic activity and controlled by deep-seated structural lineaments.

Rice and Trewin (1987, 1988) identified a Lower Devonian gold-bearing hot spring system near Rhynie, in the Grampian region of Scotland. Elevated levels of Au, As and Sb (maximum 0.18, 300 and 71ppm respectively) were identified in the Rhynie chert (interpreted as a siliceous sinter) and in a silicified fault zone (forming a feeder zone to the stratiform chert) developed during the final stages of Caledonian magmatism in a linear, fault-bounded basin. In terms of both the regional tectonic (orogenic) and local magmatic setting, hot spring activity at Rhynie was similar to that which occurs in the western USA and New Zealand. Deposits of this type were generated in hydrothermal systems analogous to the present-day Taupo volcanic zone of New Zealand and the Yellowstone caldera of the USA.

Given the large-scale exposure of Lower Devonian andesitic lavas in the Cheviot area of Northern England and the identification of precious-metal hot spring systems of similar age at Rhynie (Rice and Trewin, 1987, 1988) this area offers considerable potential for the generation and preservation of similar stratiform deposits. It should be

noted however, that the relatively shallow origin of these deposits may have resulted in the loss by erosion of a significant portion of the deposits in this terrane. It is therefore proposed that hot spring sinters such as those identified at Rhynie by Rice and Trewin (op.cit) characterise the paleosurfaces above epithermal As-Sb-Au deposits in the Southern Uplands. Unfortunately, little if any consideration has been given to the surface expression of the vein systems during mineralization. The model proposed in Fig. 475 may be used to illustrate the likelihood that the fault systems were open to the surface during mineralization.

The Newry granodiorite which intrudes Silurian greywackes in the Longford Down is associated with a suite of ultramafic, dioritic and monzonitic lithologies in the northeastern end of the pluton. In comparison with the Loch Doon area of Southern Scotland, this site is predicted to host extensive As-Sb mineralization and should be regarded as a priority target for further exploration.

In view of the known mineralogical and geochemical association of arsenic and gold in the studied deposits, the use of arsenic as a pathfinder element for gold exploration in the Southern Uplands is strongly recommended. As such, the forthcoming publication by BGS of a regional stream sediment atlas of Southern Scotland (including extensive arsenic data) will form an fundamental basis for future gold exploration in this region.

4.7 GENETIC MODELS

In the last 60 years, many investigators have advocated a magmatic hydrothermal origin for all gold deposits. This extreme view was however believed by many authors, including Boyle (1979) to be fundamentally wrong, because it failed to consider many of the geochemical features of gold, particularly its behavior within the weathering cycle, and the role played by metamorphism.

This review of individual deposits throughout the Southern Uplands and Longford Down provides fundamental evidence to suggest that rather than representing a variety of individual deposit types generated over a wide period of time, they form part of a continuum of styles related to a single, composite Late Silurian/Early Devonian mineralising event (Fig. 475). The timing of hydrothermal activity may be considered in two different manners. On a very broad scale, hydrothermal activity may be related to its relative time position within the tectonic evolution and development of the Southern Uplands. Smaller scale studies of the absolute timing of mineralization relative to the host rocks, is also of considerable importance.

The fundamental requirements pertaining to the origin and genesis of epithermal As-Sb-Au deposits in the Southern Uplands, namely a heat source at depth and a fracture system to facilitate convective circulation of the hydrothermal fluid. As demonstrated earlier, gold mineralization in the Southern Uplands occurs within fault-related structures on a regional and local scale. These structural lineaments are inferred to have provided pathways for the introduction of heat, hydrothermal fluids and igneous intrusions. Since the As-Sb-Au mineralization exhibits a close relationship with major structural features it is inferred to be related to deep seated processes.

The mechanisms of hydrothermal convection in ore-forming systems have been reviewed by Henley (1973). According to the general exhalative model of Hutchinson (1983), Solomon (1974), and Russell (1975, 1978, 1983, 1986) normal seawater initially descends along faults and permeable strata (forming a downward excavating convection cell) increasing in temperature with depth. These hot fluids react with the surrounding rocks and become

relatively reduced, slightly alkali solutions which are able to leach and transport metals in solution, predominantly as Cl^- complexes. If these hot, metalliferous fluids are convected upwards through faults and fractures and exhaled onto the sea floor, a distinctive suite of oxides, sulphides and silicates will be precipitated as the brine mixes with the cooler, oxidizing seawater. Russell et al., (1981) in a discussion of the genesis of sediment-hosted, exhalative Zn-Pb deposits, noted that these ores formed in local basins on the seafloor as a result of protracted hydrothermal activity accompanying continental rifting. A downward-penetrating convection cell model was proposed to account for the general characteristics and features of such deposits. This large scale fluid convection model contrasts strongly with the relatively restricted zones and high geothermal gradients related/induced by magmatic intrusion.

Available data from a wide variety of lower Palaeozoic As-Sb-Au deposits point towards an epigenetic model for mineralization. Low salinity, $\text{H}_2\text{O}-\text{CO}_2$ fluids carrying Au in the form of reduced sulphur complexes were focused along dilational zones, where gold was deposited at $300^\circ \pm 50^\circ\text{C}$ and 2 ± 1 kb in response to a decrease in temperature and fluid rock reactions. The development of metalliferous mineralization associated with granitoid intrusion is dependant upon magma emplacement in an adequately hydrous environment (Plant et al., 1983). The recently deposited turbidite sequence in the Southern Uplands provides a classic example of this form of hydrous environment. Fluid circulation was probably driven by thermal convection, related to the cooling of the underlying intrusion. During the initial stages of intrusive activity, tectonic contacts acted as channelways for As-Sb-Au-S- CO_2 rich fluids focusing the mineralization processes. Arsenopyrite, gold, stibnite and other sulphides were accumulated in the Glendinning deposit by different mechanisms as the hydrothermal system evolved. Petrographically similar breccia dykes (up to 200m long) were interpreted by Rock et al., (1986) to represent arrested stages in the formation of subvolcanic vents, related to explosive, deep seated, K-rich magmatism. Relatively slow, controlled explosive expansion and brecciation of a partly consolidated intrusion may give rise to an environment suitable for the formation of an extensive disseminated mineral deposit.

Fluid transport was concentrated along major crustal structures (lineaments) which also served to focus both major and minor igneous activity. The genetic significance of these structures remains speculative at this time. It is proposed however, that rather than simply reflecting a common tectonic environment in which minor intrusions and gold mineralization is localised, the regional faults are directly responsible for the focusing of magmatic activity, and transport of fluids. Water and metal components were most probably derived ultimately from the zone of magma generation, reaching the upper crust by transport within convecting magma and subsequent exsolution as a fluid phase. It is therefore concluded that both the hydrothermal fluids and gold were most probably derived from primary material in the upper mantle.

It is suggested that the association of gold-bearing hydrothermal vent breccias and intrusive rocks, could be explained in terms of a ascending magma encountering a ponded hydrothermal reservoir, where P fluid is greater than P load. Under these conditions the fluid would penetrate the magma, and result in explosive volcanism. Jahoda et al., (1989) recognised that the intrusion of magma into dilational jogs was most probable along major shear zones, several tens or hundreds of kilometres in length, which had the greatest potential for tapping deep seated magma. Close analogies may be drawn between this model and that of Rock et al., (1986) invoked to explain the association of deep-seated lamprophyric magmatism and arsenic-gold mineralisation. This model may also be tentatively applied to the structural setting and tectonic environment of the Lower Devonian gold-bearing hot spring deposit at Rhynie, in northeast Scotland.

A general genetic model for stratiform Au mineralisation involves the syngenetic concentration of As, Sb, Au, Ag, Hg, S (from hydrothermal fluids) near discharge sites in the anoxic portions of small depressions or basins. In light of the re-interpretation of the Glendinning breccias it should be noted that the specific criteria required in a stratiform-stratabound model were proposed by Phillips et al., (1984). For example, mineralization should not be restricted to specific fold or fault structures, or zones of intense fracturing and brecciation and gold grades should not be related to transgressive features such as fractures and faults

Based upon the regional tectonic and lithologic framework for these deposits, it was obvious that a single genetic model could not be invoked to account for all observed features. As such a simplified model of the metallogenesis of As-Sb-Au deposits in the British Caledonides was derived, and presented in Fig. 475 (after Duller and Harvey, 1985; Rock et al., 1988; Gallagher et al., 1983; Leake et al., 1981; Morris and Steed, 1985, 1986). Eight major types of deposit are recognised, including:

- 1) Metalliferous hot springs (eg. Rhynie)
- 2) Mineralized breccias and fault systems (eg. Glendinning)
- 3) Mineralized fault systems (eg. Clontibret)
- 4) Mineralized fault systems and minor intrusions (eg. Penkiln Burn, Glenhead, Talnotty Copper mine)
- 5) Vein mineralization:- marginal to or at the contact with major intrusions (eg. Glenhead, Talnotty, Cairn Garroch, The Knipe)
- 6) Vein and disseminated mineralisation:- hosted by major intrusions (eg. Black Stockton Moor)
- 7) Vein and disseminated mineralisation:- hosted by igneous breccias and agglomerates (eg. Fore Burn, Kilmelford)

It is not suggested that each different style of mineralisation is present in every deposit, however a tentative model is proposed relating the nature of the deposit to depth of emplacement, and an increasing igneous component with depth. It is also proposed that the syngenetic or exhalative mineralization identified by Rice and Trewin (1987, 1989) may correspond to the sub surface geothermal systems which led to the formation of the Glendinning and other deposits in the Southern Uplands. It is concluded that As-Au mineralization may have been instigated up to 10 Ma before the emplacement of the granite plutons and as such may represent deposition from precursor fluids, forming part of a continuum culminating in granite emplacement. As such, it is proposed that the development of an economic deposit in the Southern Uplands requires that the high temperature phase of mineralization was sustained by an ample heat supply, in the form of a single large body of magma or multiple intrusions. Centres of minor intrusive activity, particularly those in close proximity to the margins of plutonic complexes therefore provide primary geological targets for exploration in this region. Further data concerning the nature of individual hydrothermal systems and deposits will lead to an expanded and more complex genetic model, however, it is hoped that this study will provide the basis for further classification.

Silberman and Berger (1985) noted that there may be considerable variation in the pathfinder elements associated with precious-metal mineralisation. The ubiquitous association of arsenopyrite with gold mineralisation throughout the Southern Uplands and Longford Down is however, at odds with their findings and suggests that arsenic forms the single-most effective pathfinder element for gold mineralisation in this terrane. In addition, the presence of As-Sb-Au mineralization in comparable geological environments within both the British and North American Caledonides may be used to suggest the existence of a precious-metal province/terrane, genetically related to large-

scale tectonic controls, and it is proposed that the recognition of potential fault structures may assist further exploration in this terrane.

Geological and genetic models of gold deposits should be given due consideration at both the planning and interpretation stages of any major programmes. Although the identification of orebodies is not necessarily model dependant, using the wrong model, the wrong terrane may be examined with the wrong techniques. A detailed understanding of ore genesis within individual terranes should lead to the development of better models and the possible recognition of previously unidentified types of deposit.

4.8 SUMMARY AND CONCLUSIONS

This study has revealed the general characteristics of As-Sb-Au deposits in the Southern Uplands, their genetic processes and inter-relationships. It is clear that a wide continuum of inter-related processes were involved in the formation of the diversity of deposits now observed. The development of plate tectonic theory and models has had a major impact upon our understanding of ore genesis.

This review has identified remarkably similar characteristics of both ore fluids, ore-element associations (As-Sb-Au-Hg-Ag) and wallrock alteration assemblages in a wide variety of turbidite-hosted gold deposits. As such, the identification of the geological features developed in association with As-Sb-Au mineralization in the Southern Uplands is critical to further exploration in this terrane.

On the basis of this study, four possible genetic sources may be invoked:

- 1) Direct hydrothermal evolution from granitic intrusions
- 2) Direct hydrothermal evolution from basic intrusions
- 3) Hydrothermal processes resulting in the selective concentration from associated black shales or pre-existing sulphides
- 4) Ore solutions from a deep source near the crust-mantle boundary

It was suggested by Harris and Radtke (1976) that independent variables which display the strongest mathematical correlation to any dependant variable (ie. arsenic) have the strongest physical relation to the phenomenon being studied. The distribution of arsenic anomalies in the Southern Uplands are so extensive that they cannot be attributed to a single ore district, and as such it is suggested that they represent extensive clusters of small sub-economic deposits. In addition, it is advocated that both As and Sb should be analysed routinely in any geochemical study (regional or otherwise) within this region.

Both dip-slip and strike-slip fault systems may develop extensional/shear fractures in pull-apart zones. During the opening of such zones, suctional forces are created allowing large volumes of fluid to enter the dilating fracture system from the wallrocks (Jahoda et al., 1989). Where faulting intersects active magmatic systems, magma would have entered the fracture system and igneous activity would have been focused at dilational fault offsets, the 'hot jogs' of Jahoda et al., (1989). This study has demonstrated the temporal and spatial association of As-Au mineralisation in the Southern Uplands and elsewhere with extensive alteration zones and major fault systems. The fundamental process in the formation of such deposits therefore involved the flow of large volumes of fluid, through structurally controlled zones of high permeability. Furthermore, hydrothermal activity associated with Caledonian

granites and minor intrusions is widespread and metal concentrations, along major fault and thrust zones distal to the known granites occur on a regional scale. The common spatial coincidence of As-Sb-Au mineralization with minor intrusions may be used to infer a magmatic origin for both fluids and metals in the Southern Uplands.

This study has recognised the presence of significant As-Sb-Au mineralization in the vicinity of small calc-alkaline volcanic centres in the British Isles. It is proposed that under favourable tectonic conditions exhalative gold deposits were formed, overlying areas of calc-alkaline activity, together with a complex suite of Au-bearing epigenetic deposits. However, the present erosion level in Scotland may be used to infer that a significant proportion of all mineralization has been lost (Russell, 1986).

In summary, it is suggested that in the Southern Uplands of Scotland and its continuation into the Longford Down, gold mineralization is spatially and temporally associated with a characteristic group of clastic sediments and igneous rocks, spatially controlled by major N-S trending structural lineaments. It is suggested that the antimony component of these deposits was generated as a result of partial melting of the upper mantle, associated with a linear zone of anomalous heat flow and tectonism.

On the basis of this study, it is clear the no individual single-stage model may be invoked to account for all observed features related to mineralization in the Southern Uplands. Varying levels of erosion have led to the exposure of successive stages of mineralization across this region. The primary As-Sb-Au mineralization was linked with the physiochemical processes responsible for the generation of deep-seated, lineament controlled, igneous activity during Late Silurian-Early Devonian times. During this period the region became a hot spring province with intermittent exhalative activity continuing throughout the Early Devonian penecontemporaneous with epithermal gold mineralization.

In summary these deposits form part of a continuum related to igneous, hydrothermal and fumarolic activity. It is concluded that this model offers an explanation for the observed geological parameters associated with As-Sb-Au mineralization in this region, and it may have a wider application to mineral exploration in Lower Palaeozoic turbidite terranes, in general. Even though the source of gold itself remains enigmatic, a spatial association between lineaments, lamprophyres and gold mineralization occurs in the Southern Uplands. The intersection of major structural lineaments and igneous intrusions provide both fluid conduit and source for the development of these deposits and as such should be regarded as a priority target for future exploration.

CHAPTER FOUR

Geological and Petrographical Studies of the Southern Uplands

4.1 INTRODUCTION

The Southern Uplands of Scotland are a region of great geological interest. This chapter discusses the geological structure of the Southern Uplands, which is one of the main parts of the Scottish Highlands. The geological structure of the Southern Uplands is described in terms of a number of geological and tectonic provinces, which are defined on the basis of their geological structure. The detailed geological structure of the Southern Uplands is described in terms of a number of geological provinces, which are defined on the basis of their geological structure. The detailed geological structure of the Southern Uplands is described in terms of a number of geological provinces, which are defined on the basis of their geological structure. The detailed geological structure of the Southern Uplands is described in terms of a number of geological provinces, which are defined on the basis of their geological structure.

CHAPTER FIVE

Geological and Petrographical Studies of the Southern Uplands. This chapter discusses the geological structure of the Southern Uplands, which is one of the main parts of the Scottish Highlands. The geological structure of the Southern Uplands is described in terms of a number of geological and tectonic provinces, which are defined on the basis of their geological structure. The detailed geological structure of the Southern Uplands is described in terms of a number of geological provinces, which are defined on the basis of their geological structure. The detailed geological structure of the Southern Uplands is described in terms of a number of geological provinces, which are defined on the basis of their geological structure. The detailed geological structure of the Southern Uplands is described in terms of a number of geological provinces, which are defined on the basis of their geological structure.

1. To determine whether the Southern Uplands can be distinguished geologically from one another.
2. To apply the results of the geological studies to a regional scale as well as to geological mapping.
3. To define the position of hydrogeologically distinct ranges related to potentially economic gas- and oil-accumulation.

The main aim of this chapter is to provide a detailed geological and petrographical study of the Southern Uplands. The chapter is divided into two main parts: the first part is devoted to the geological structure of the Southern Uplands, and the second part is devoted to the petrographical studies. The results of the geological and petrographical studies are discussed in terms of a number of geological provinces, which are defined on the basis of their geological structure. The detailed geological structure of the Southern Uplands is described in terms of a number of geological provinces, which are defined on the basis of their geological structure.

5.2 REGIONAL GEOLOGY

5.2.1 Stratigraphy

The regional geology of the Southern Uplands is based upon the study by Lumsden (1889), which was subsequently revised and extended by Peach and Horne (1891) who divided Lower Palaeozoic gneisses in the

CHAPTER FIVE

REGIONAL LITHOGEOCHEMICAL STUDIES

5.1 INTRODUCTION

The importance of greywackes in the development of continental crust is evident from their abundance in the geological column. They are generally deposited in tectonically active regions, and in earlier parts of the Precambrian, form the dominant sandstone (Peterman et al., 1981). This chapter describes the results of a systematic lithogeochemical sampling programme undertaken in both Southern Scotland and Ireland in order to define the relationships between turbidite petrography, tectonic setting, provenance and geochemistry. As detailed petrographic studies had previously been undertaken (Kelling, 1961; Floyd, 1982) the major objectives in this study were to establish the nature and magnitude of chemical variation within individual formations and investigate the application of geochemistry as an aid to stratigraphic correlation in the Southern Uplands and Longford Down.

Using the automated XRF facilities of the Geology Department of Nottingham University, 2295 greywacke samples were analysed for Si, Al, Ti, Fe, Mg, Ca, Na, K, Mn, P, As, Ba, Cr, Co, Ga, La, Ni, Nb, Pb, Rb, Sr, S, Sb, Th, V, Y, Zn and Zr. In addition around 10% of the total sample population were submitted for fused bead preparation (and major element analysis) and re-analysed for CO₂, LOI and FeO and the following elements: Ag, Bi, Br, Cd, Ce, Cs, Hf, Mo, Sc, Se, Sn, Ta, Te, U, W, Cl and Tl (by XRF); and La, Ce, Pr, Nd, Sm, Eu, Gd, Tb, Dy, Ho, Er, Tm, Yb and Lu (by ICP). It should be noted that if the ICP data is included, the largest number of elements determined for an individual sample is 55. In detail, the application of geochemical techniques to stratigraphic problems in the Southern Uplands, had three main objectives:

- 1) To determine whether individual formations can be distinguished chemically from one another
- 2) To apply the resulting chemical parameters on a regional scale as an aid to geological mapping
- 3) To define the position of hydrothermally altered samples related to potentially economic As-Sb-Au mineralization

Preliminary spatial and statistical analysis of the resulting geochemical database (and accompanying geochemical maps) facilitated the chemical subdivision of the petrographically distinct turbidite units and the recognition of fundamental differences between mineralized and unmineralized samples. It was recognised that the results of these initial investigations offered considerable potential for extending the field area along strike into the Longford Down.

5.2 REGIONAL GEOLOGY

5.2.1 Stratigraphy

The classical stratigraphy of the Southern Uplands is based upon the study by Lapworth (1889) which was subsequently revised and extended by Peach and Horne (1899) who divided Lower Palaeozoic greywackes in the

Southern Uplands into three strike-parallel belts. Morris (1983) defined the lateral equivalents of two of these, the Northern and Central belts in the Longford Down Inlier. Recent interpretations of the geology of the Southern Uplands are based upon the recognition of at least 10 linear, fault-bounded tracts of Lower Palaeozoic sediments and volcanics. These tracts contain the results of 55 million years of sedimentation, tectonism and volcanic activity on the northern margin of the Iapetus ocean. Each individual tract displays a distinctive stratigraphy and petrography with little if any along-strike variation, but at least in the Northern Belt, sharp contrasts with juxtaposed units (Anderson, et al., 1986).

In 1986, a meeting was held at the Geological Society in order to discuss the application of the accretionary prism model developed by Mitchell and McKerrow (1975); McKerrow et al., (1977); and Leggett et al., (1979, 1982) to the Southern Uplands of Scotland. This meeting was entitled 'The Southern Uplands Controversy' and served as a forum for the presentation of critical reviews and reassessments of this model; and resulted in the publication of a thematic edition of the Journal of the Geological Society, in 1987. In addition, Harris and Fettes (1988) present a major synthesis of the Caledonian-Appalachian Orogen and detailing orogenic, faunal and sedimentological processes active from Pre-Arenig to Permian times.

5.2.2 Structure

The Southern Uplands are characterised by a repetitive sequence of greywackes and black shales, considered by the original surveyors, Peach and Horne (1899) to be the result of isoclinal folding and associated local strike-slip faulting (Webb, 1983). Recent studies have increasingly stressed the importance of the strike faulting (Leggett et al., 1979) and have drawn analogies between the Southern Uplands structure and that of accretionary wedges developed at modern active plate margins (Mitchell and McKerrow, 1975; McKerrow et al., 1977; Leggett et al., 1979). A plate tectonic model for the Caledonides of the British Isles was presented by Phillips et al., (1976) invoking three non-parallel lower Ordovician-lower Devonian subduction systems. In addition, evidence was also presented for the oblique closure of the Iapetus ocean from the late Ordovician to early Devonian, and subsequent dextral strike-slip movement on the resulting suture, based on the migration of an unstable trench - trench transform triple point junction.

A series of structural blocks, each characterised by distinctive petrography, stratigraphy and bounded by major strike faults have been established throughout the Southern Uplands of Scotland (McKerrow et al., 1977; Leggett et al., 1979; Floyd, 1982; Hepworth et al., 1982; and Stone et al., 1986). Barnes, Lintern and Stone (1989) simplified the historically complex deformational sequence in the Southern Uplands into three main phases. It was tentatively suggested by Needham and Knipe (1986) that the observed deformational phases/features could be related to downslope gravity-driven deformation, accretion-related deformation, collision-related deformation and post collision adjustments.

Leggett and Casey (1982) demonstrated a number of implications and controls on the structural development of subduction complexes using the Southern Uplands as a type-example of an accretionary prism. It is clear that strike-slip displacements were important during the closure of the Iapetus Ocean and affected the Grampian Highlands, Midland Valley (Bluck, 1983) and the Southern Uplands (Leggett, et al., 1981). In a discussion of movements upon the Southern Uplands Fault, Elders (1987) demonstrated that sediment provenance studies could be used to provide direct evidence of the magnitude of strike-slip displacements. Furthermore, McKerrow and Elders (1989) used a

comparison of clasts in mass flow conglomerates with granites in western Newfoundland to suggest large-scale Ordovician and Silurian strike-slip movements.

A detailed summary of the imbricate structure of Silurian greywackes across part of the Central Belt of the Southern Uplands was described by Webb (1983). This study presented evidence for the formation of major structural features in response to the progressive shearing of early folds which formed penecontemporaneously with the deposition of the sediments; and predicted that the imbricated greywackes extend to depths of 3km rather than the 15km predicted by the LISPB profile.

Needham and Knipe (1986) presented a model of accretion- and collision- related deformation in the Southern Uplands which was considered to be a large-scale 'pop-up' structure formed between a fore thrust, the Iapetus suture and a back thrust, which partially obducted it northwestward. Oliver et al., (1986) demonstrated that the southern boundary of the Midland Valley with the Southern Upland terrane is marked by the Southern Upland Fault and Lammermuir Fault and used detailed fault fabric studies to provide evidence of early sinistral brittle strike-slip motion, which also deformed felsite dykes in a ~200m wide zone parallel to the faults.

Stone et al., (1987) detailed the existence of southerly-derived turbidites containing fresh andesitic detritus, derived from a volcanic island arc situated to the South of the Southern Uplands. Northerly derived turbidites displayed more mature, quartz-rich characteristics. These observations led to the development of a back-arc model for the Southern Uplands, comprising of a mature continental landmass to the north and a rifted continental fragment containing an active volcanic arc to the south. The Hawick Group and the Wenlock sequences of the Southern Belt were considered by Stone et al., (op.cit) to have been deposited in a southward-migrating foreland basin ahead of a rising thrust stack. Mid to Late Silurian sinistral strike-slip movements were also proposed by Stone et al., (1986, 1987) to have produced the transpressional environment in which mantle derived lamprophyres were intruded along major, deep-seated structures. The British Caledonides were recognised by Oliver (1988) as composed of a number of regionally metamorphosed tectonostratigraphic terranes brought into juxtaposition during closure of the Iapetus Ocean. The suspicion exists that strike-slip motions formed important controls on the major faults now separating the various terranes. It was concluded that regional metamorphism of these terranes did not necessarily occur at the same time or in the same relative geographical positions that they now occupy.

A concise summary of the discovery and development of the terrane concept, and its application to the study of displaced terranes in Britain and Ireland was presented by Soper et al., (1989). The recognition of potential, large scale, transcurrent fault movements along active plate margins was a critical factor in the development of the terrane concept. Initial definition of tectonostratigraphic terranes as 'fault bounded units of regional extent, each characterised by a geological history which is distinct from that of neighboring terranes' (Jones et al., 1983) have been superseded by more cautious, restrictive description (Keppie, 1989): 'A terrane is an area characterised by internal continuity of geology, that is bounded by faults, melanges representing a trench complex, or suture zones across which neighbouring terranes may have a distinct geological record not explicable by facies changes, or a similar record that can only be distinguished by the presence of a terrane boundary representing oceanic lithosphere'. This concept has had considerable impact upon the interpretation of geotectonic processes and resulted in the evolution of 'terrane analysis' methodologies incorporating palaeontological, sedimentological, geophysical, isotopic and palaeomagnetic techniques, in order to reconstruct the evolution of an orogen by defining its constituent terrains and their displacement histories.

Trench et al., (1989) presented palaeomagnetic evidence of a near equatorial palaeo-latitude for the Southern Uplands terrane; and demonstrated that the Grampian Highlands, Midland Valley and Southern Uplands terranes had docked by late Silurian-early Devonian times. Thirlwall (1989) presented evidence that the chemical and isotopic differences present in Ordovician-Devonian igneous rocks of northern Britain were attributable to subduction-related and collision magmatism processes, incorporating a variety of mantle and crustal sources. Igneous rocks south of the Southern Uplands Fault were reported to be chemically different from those in the Midland Valley of Scotland; displaying element concentrations incompatible with the subduction model of Thirlwall (1981); and interpreted as indicative of significant transcurrent or across-strike displacement.

5.2.3 Sedimentology

The Southern Uplands of Scotland is composed of a series of stratigraphic sequences of Ordovician and Silurian greywackes, shales and conglomerates, occasionally associated with basalts and cherts and separated by strike-parallel faults. The term greywacke is used within the context of this study to denote sandstones of a wide mineralogical range, deposited by turbidity currents or other mass-flow processes, and characterised by typical Bouma sequences (Bouma 1962). A diversity of sedimentological studies have been undertaken during the last two decades across the Southern Uplands and Longford Down: In a study of the sedimentology and diagenesis of Silurian greywackes from Kirkcudbrightshire, Weir (1974) noted that the greywackes dominantly cluster in the lithic greywacke field of Pettijohn (1957) and contain an average of 35% feldspar and rock fragments (quartzites and pelitic schists) and in excess of 20% matrix. The turbidite systems identified in the Northern, Central and older portions of the Southern Belt essentially fit the model of 'highly efficient' fans of Mutti (1979) and are characterised by remarkable lateral continuity. Fan progradation is generally indicated by coarsening upwards sequences (bD -> BD -> aBD -> Ad). Hepworth et al., (1981) presented a detailed study of the sedimentology, volcanism, structure and metamorphism of the Bail Hill - Abington area of the Southern Uplands.

Short-lived, but extensive regressions occurred at or near the base and top of the Arenig series (extending into the lower Llandeilo) with a major regressive event at the top of the Ashgill, associated with contemporary glaciation (Brenchley and Cocks, 1982; Fortey and Cocks, 1988). Subsequent transgressions occur throughout much of the Arenig, Llanvim, Caradoc and Llandovery series. Although local tectonic and volcanic processes may override the effects of transgressive and regressive cycles, shore lines associated with continental masses and volcanic island arcs will generally be enlarged in times of regression (as more land emerges) whereas transgressive phases spread epicritic habitats far across shallow shelves and also bring more oceanic biofacies shelfwards (Fortey and Cocks, op. cit.) Following late Ordovician glaciation, a steady transgression occurred throughout Llandovery times, with flooding of shelves and continental margins. Leggett et al., (1981) noted that a 'greenhouse effect' occurred worldwide during the early Silurian (Llandovery-early Wenlock). During this period (~12 Ma) sea levels were high and the accompanying transgressions resulted in highly productive shelf seas containing a diverse benthic biota. Highly oxygenated conditions were recorded from the mid to late Silurian (post early Wenlock age), and may explain the widespread absence of black shales and mudstones from sediments of this age in Southern Scotland. The major eustatic oscillations in the Ordovician and Silurian affected the dominant styles of sedimentation (Leggett et al., 1981). The NW margin of the Iapetus Ocean was highly active from Llanvirn times into the mid-Silurian, with typical Llandovery shelf faunas such as the Stricklandia community accompanying turbidites, olistostromes and paraconglomerates (Fortey and Cocks, op. cit.). Elevated detrital carbonate levels result from the interplay between biofacies disposition on the former continental shelves and slopes, and the siting

of the continental landmass relative to the palaeo-equator (Fortey and Cocks, 1988). A detailed study of the Late Silurian sedimentary and tectonic evolution of the Southern Belt in the Southern Uplands was presented by Kemp (1985) and is divided into two main phases:

- 1) Early Wenlock sedimentation dominated by small scale, high-gradient sandy fans and SW-flowing axial currents
- 2) Middle Wenlock sedimentation involving the development of extensive meandering channel systems, and associated channel mouth and depositional lobe facies.

Examples of epicontinental (Wenlock) carbonate sedimentation from southeastern Norway were described by Olaussen (1981). Both marls and carbonates were deposited upon the Precambrian shield in supratidal, intertidal and restricted subtidal environments. Red arenaceous dolomites reflect minor progradations of the adjacent continental facies. In addition, the identification of celestite within sediments from the high intertidal-supratidal environment provides evidence for evaporitic conditions within this uppermost marine sequence.

Mutti (1985) demonstrated that long-term global sea level variations and local tectonic controls form the basic framework within which turbidite sediments develop as a response to breaks in the equilibrium between shelf and basin sedimentation. It was therefore proposed by Mutti (op.cit) that large-volume turbidite sandstones were derived from adjacent shelf areas that underwent phases of tectonic uplift or eustatic fall of sea level, shortly after periods characterised by high rates of terrigenous sedimentation. The frequent lowering of sea level, produced by tectonic uplift in an active structural setting can lead to suitable conditions for turbidite development, however the volumes of resedimented deposits will be less, due to insufficient recharge in adjacent shelves.

Pickering and Siveter (1986) using faunal evidence from ostracods, demonstrated that opposing Ordovician plates may have been in closer proximity than previously supposed. In addition, as there appears to be little if any evidence for an ocean floored by oceanic crust in post-Caradoc times it was proposed that subduction-accretion had ceased in both Newfoundland and Ireland by the Early Silurian (Llandovery). Fortey and Cocks (1988) however, in a review of the controls upon Arenig to Llandovery faunal distributions in the Caledonides, noted that contemporary transgressive-regressive cycles were the dominant cause of diachronous shifts of biofacies belts.

5.2.4 Turbidite Petrography and Provenance Studies

The term greywacke, is defined within the context of this study following the terminology of Pettijohn (1963) as 'a sandstone consisting of quartz, feldspar and rock particles of sand size embedded in a silt-clay-sized matrix'. Recent studies have demonstrated the numerous inter-relationships between greywacke mineralogy, provenance and tectonic setting (Crook, 1974; Schwab, 1975; Dickinson and Suczek, 1979; Maynard, et al., 1982; Bhatia, 1983 and Bhatia and Crook, 1983). A comprehensive multi-element geochemical study of crystalline basement and continental sediments from both Russia and North America was provided by Ronov and Migdisov (1971) who noted the close similarity between continental basement and the average composition of the overlying sediments. Four distinct settings of greywacke deposition were recognised by Dickinson (1971) and Karig (1971) including: Trench fill; Arc-trench gap; Interarc basins; and Marginal basins (ie. behind the arc). Murray and Condie (1973) in petrographic and geochemical studies of greywackes from the eastern Klamath subprovince of Northern California, demonstrated that Ordovician greywackes display strong cratonic (plutonic-metamorphic) character-

istics in comparison with later, calc-alkaline volcanic dominated greywackes of Silurian to Jurassic age. The relationship between sandstone composition and tectonic environment was recognised by Schwab (1975) who expanded the work of Crook (1974), to include varieties of sandstone other than greywacke in this classification scheme. In general, quartz-rich rocks characterise continental margins, quartz-poor rocks are derived from island arcs and intermediate quartz contents associated with active continental margins and orogenic belts.

In studies of Lower Ordovician greywackes from New Zealand, Nathan (1976) identified the distinctively quartzose nature of Greenland Group sediments and inferred a polycyclic origin related to a plutonic source. Cabby et al., (1977) in studies of the geochemistry of Upper Proterozoic greywackes from northwestern Algeria, identified dominantly andesitic characteristics formed as a result of erosion of a pencontemporaneous calc-alkaline volcanic suite, emplaced in Upper Proterozoic shelf sediments. Furthermore, Dickinson and Suczek (1979) recognised and developed a model correlating sandstone petrography and plate tectonic setting. Moore (1979) demonstrated the existence of two tectonostratigraphic units on Nias Island, Indonesia, representative of trench and trench-slope deposits. The trench-slope sediments were shown to be enriched in polycrystalline quartz and K-feldspar in relation to the trench deposits, a feature interpreted in terms of a non-volcanic (cratonic) source terrane on the west coast of Sumatra, composed of Palaeozoic/Mesozoic metamorphic and plutonic lithologies. In addition, Bhatia (1983) suggested that the chemical composition of greywackes could be used to designate environmental features.

Whole rock geochemistry may be used to characterise the provenance of sandstones and greywackes and is of particular importance in samples where the original detrital mineralogy is only partially preserved during diagenesis (Bhatia, 1983). The concentration of certain elements, notably Mg, Fe, Cr, Ni and Ti strongly reflect the primary chemistry of the source material as these elements are located within resistant mineral phases or are readily adsorbed by clay minerals. In particular, high concentrations of Cr and Ni are good indicators of an ophiolitic source (Hiscott, 1984).

The foundations for petrographic and geochemical classification of greywacke formations in the Southern Uplands were laid by Walton (1957,1961) who recognised the importance of lithic fragments in both mapping and provenance studies and identified three different greywacke groups (the Pyroxenous, Intermediate and Garnetiferous). In addition, Walton (1961) presented the chemical analysis of six greywacke samples and distinguished the Pyroxenous (Formation) group from other greywackes on the basis of silica content alone. Detailed descriptions of the petrography of individual greywacke formations in the Southern Uplands and Longford Down is provided by numerous authors including Floyd (1975, 1982), Morris (1983) and Kemp (1985) (Fig. 16). Greywackes from the Central and Northern belts contain a diverse assemblage of lithic fragments including pyroxene and hornblende andesite, metabasalt, rhyolite, felsite, tuff, granite, biotite granite, hornblende gabbro, hornblende granodiorite, quartzite, schist, shale, siltstone and greywacke. Detrital minerals include quartz, feldspar, hornblende, biotite, muscovite, clinopyroxene, glaucophane, epidote, spinel, garnet, prehnite, ilmenite, magnetite and staurolite (Walton, 1961, 1963, 1965; Kelling, 1964; Oliver and Leggett, 1980; Floyd, 1982). Most of the greywackes contain between 15 and 30% matrix composed of very fine grained quartz, calcite, chlorite and sericite (phengite). In the Southern Belt, greywackes contain abundant detrital quartz and albite, which together with white mica and biotite, are hosted by a matrix of calcite, chlorite and sericite.

Condie and Snansiang (1971) in petrographic and geochemical studies of Ordovician and Silurian greywackes from Northern California, demonstrated the existence of two different sources/tectonic settings. An inverse picture to

that observed in the Southern Uplands was defined however, with Ordovician greywackes dominated by sediments derived from plutonic-metamorphic terranes and Silurian greywackes dominated by increasing contributions of calc-alkaline volcanics. Similar studies on modern deep-sea sands revealed similar correlations between composition and environment (Maynard et al., 1982).

During an extensive mapping study of specific areas in the Southern Uplands by the British Geological Survey, in excess of 700 'fresh' greywacke samples were collected from individual localities and subjected to petrographic examination, with modal compositions determined by standard 1000 point count analysis. This investigation (Floyd, 1975) revealed that the Northern Belt of the Southern Uplands is composed of at least four petrographically distinct lithostratigraphic greywacke formations. The observed petrographic contrasts are indicative of contrasting provenance areas within either cratonic or volcanic terranes. Petrographic examination of the Blackcraig, Scar and Pyroxenous formation greywackes suggest that the sediments were derived from an active calc-alkaline volcanic arc, whereas greywackes of the Afton, Shinnel and Intermediate formations were supplied from a more cratonic provenance, comprising of sedimentary metamorphic and felsic igneous rocks (the general relationships between chemical elements, mobility, associations and host minerals is presented in table 1.44). The cratonic and volcanic petrofacies suites described within the context of this study broadly equate with the Metaclast and Basic Clast petrofacies of Morris (1987) respectively.

The cratonic suite may be characterised by a mixed felsic igneous and metamorphic detrital composition derived from a continental terrain (Kelling, 1961, 1964; Morris, 1983) whereas the volcanic suite contains abundant calc-alkaline detritus derived from a volcanic arc source terrain and plutonic/ metamorphic root zone. Metamorphic rocks are represented by polycrystalline quartz fragments with strain shadows, sutured grains and orientated flakes of muscovite. Fragments of chert and dark mudstone are also present. The detrital plagioclases identified in thin section have a refractive index less than quartz and were identified as Na-rich albite. Possible sources of the albite include: Calc-alkaline volcanics; Low grade chlorite-biotite schists; and altered basic and ultrabasic rocks from the Ballantrae Ophiolite. In the Northern and Central belts, Oliver and Leggett (1980) suggested that much of the albite was of metamorphic origin, formed by the in situ breakdown of detrital calcic plagioclase, releasing both Ca and Al to the fluid phase.

Floyd (1982) identified five formations in the Northern Belt of the Southern Uplands, on the basis of lithological and petrographical evidence derived from their type area in West Nithsdale and correlated his results throughout large tracts of the Northern Belt, in Southwest Scotland. These petrographically defined samples were subsequently provided by Dr Floyd to the author for chemical analysis. In addition, samples collected during Dr Floyd's continued research in the Southern Uplands (extensions of the original field area) were also supplied for analysis. This suite of point counted and petrographically classified samples provided an invaluable training set for geochemical and statistical evaluation and together with the Glendinning Region, form the 'type' areas for this study.

Due to the manner in which the definition and naming of different petrofacies has evolved over the last 30 years (with some form of standardisation only recently appearing) the naming conventions defined by Floyd (1982) used to define the respective members of the training set, are followed throughout this study. Where applicable, local formation and/or Group names are also used and reported in conjunction with their equivalent petrofacies from the training set. A table defining the qualitative detrital composition and principal petrofacies in the Northern and

Central Belts was presented by Morris (1987) and is included for reference purposes (Fig 1.55). It should be noted that the 'volcanic' derived greywackes although containing a high proportion of volcanic detritus, also contain significant volumes of plutonic, metamorphic and sedimentary rock fragments. The most notable feature of the volcanic greywackes is the relative abundance and freshness of the pyroxenes in both rock fragments and single mineral clasts (Styles et al., 1989). In addition, Floyd and Trench (1989) demonstrated the presence of consistent differences in magnetic susceptibility, which parallel differences in petrography and are directly related to variations in detrital magnetite content.

Lapworth and Wilson (1871) assigned rocks south of the Ettrick Valley thrust as the Hawick rocks and the Selkirk beds. The Selkirk division has fallen into disuse and the southern part of the Central belt is regarded as Hawick rocks (Cook, 1979). The Southern Belt was originally classified on the basis that it contained only Wenlock rocks, the Riccarton and Raeberrie Castle formations. In a discussion of greywackes from St Abbs Head, in the northeast of the Southern Uplands, Greig (pers. com., 1985) noted that carbonate, rarely present to the north-west of St Abbs Head, becomes an important part of the greywacke matrix in the Coldingham Bay area and to the south of Eymouth. Rust (1965) in a study of the sedimentology and diagenesis of Silurian turbidites from Wigtownshire identified the presence of a characteristic red mica (muscovite with a fine grained hematite coating) in Hawick greywackes, and its absence from the Riccarton group. Well preserved masses of the colonial coral *Heliolites* cf. *megastoma* were also located. Diagenetic carbonate replacement of feldspar was noted as common, and formed in response to the distribution of primary carbonate in the sediment. A two stage chemical weathering process involving the derivation of Silurian greywackes from the erosion and weathering products of Ordovician greywackes results in the creation of a relatively mature greywacke succession, as demonstrated by Wyborn and Chappell, (1983). This model has significant implications in the development of the Hawick formation in southern Scotland.

The Highlands of Scotland have been historically regarded as the source area for Southern Uplands greywackes (Peach and Horne, 1899). However, Elders (1984, 1987) demonstrated that the Scottish Highlands, Midland Valley and Ireland were unable to provide the range of granitic detritus identified in the Southern Uplands and inferred a source area in NW Newfoundland, with sediments transposed by subsequent strike-slip displacement. The first substantiated report of prehnite-pumpellyite facies regional metamorphism in the British Isles was located by Oliver (1978) in County Cavan, Ireland. Oliver and Leggett (1980) extended this study into southern Scotland, confirming the presence of albite, prehnite, pumpellyite, phengite, calcite, hematite and quartz bearing metamorphic assemblages in basalts and basic-clast greywackes in the Southern Uplands. Regional prehnite-pumpellyite facies metamorphism was attributed to tectonic burial processes, related to accretion during the closure of the Iapetus Ocean. Please note that the following six samples have been reassigned from their original classification groupings on the basis of petrographic evidence provided by Floyd (1987, pers. com.): S-212 (Afton); S-4 (Pyroxenous); S-6 (Shinnel); S-250 (Intermediate); S-251 and S-252 (Scar).

5.3 LITHOGEOCHEMICAL STUDIES

5.3.1 Aims and Objectives

The purpose of regional lithogeochemical studies in the Southern Uplands and Longford Down was to delineate broad-scale patterns of primary element distribution related to bedrock petrography, hydrothermal alteration and mineralization. In addition, it was proposed that the resulting database could also be used to assist the delineation

of suspect agricultural areas of clinical and sub-clinical trace element disorders in crops and livestock; and provide a reference for a variety of environmental studies. In addition, this data may also serve as a useful source of fundamental scientific information, when viewed in the context of British Caledonide geology.

5.3.2 Previous Investigations and Study Areas

Alsayegh (1971, 1972, 1973) presented the results of an initial geochemical investigation of Lower Palaeozoic greywacke geochemistry in the Southern Uplands. Geochemical studies centered upon the southwestern margin of this region and resulted in the analysis of 327 samples for both major and trace elements. Samples were grouped on the basis of the stratigraphy erected by Kelling (1961) and individual populations were compared using simple univariate tests of significance. Pronounced variations in Ce, La, Nb, Zr, Sr and CaO were observed between specific areas which were found to correspond closely with the identified stratigraphy. This pioneering work provided an important contribution to the geology of the Southern Uplands, however the philosophy adopted by Alsayegh (1971) during this early attempt at geochemical mapping suffered from a number of fundamental problems, including:

- 1) The virtual absence of any form of petrographic control or interpretation relating to the chemistry of individual samples.
- 2) The absence of any form of correlation between chemically similar units across the Southern Uplands.
- 3) The failure to equate distinct mineralogical characteristics of stratigraphic units with the geochemical data.
- 4) The over-simplistic comparison of Ordovician versus Silurian geochemistry (Alsayegh, 1973) was undertaken despite the known mineralogical variation displayed by individual formations, which as such, renders such a comparison virtually meaningless.
- 5) The absence of both As or Sb values rendered this investigation of little economic use.

The petrographic character of greywacke samples from the Marchburn, Afton, Blackcraig, Scar, Shinnel, Pyroxenous and Intermediate Formations have been investigated by Floyd (1975, 1982). Floyd (1975) demonstrated on petrographic grounds, that contrasting source areas characterised by volcanic and cratonic derived detritus, dominated the sediment supply, at different times throughout the history of the Southern Uplands. Hawick Group samples were investigated by Duller and Harvey (1984, 1985) within the context of this study. The type area of the Marchburn Formation defined by Floyd (1982) occurs immediately SE of the Southern Uplands Fault and SW of the Sanquhar coalfield, with the formation named after its type section in the March Burn [NS 67 12]. On the basis of petrography and relative position, this formation was correlated with the Corsewall (Kelling, 1961) and Glen App (Walton, 1961) groups along strike in SW Scotland. The type area of the Afton Formation defined by Floyd (1982) occurs between the Carcrow Fault and the Leadhills Line and is bounded to the SW by the Afton Water and to the NE by the Sanquhar coalfield. This formation is distinguished from the Marchburn Formation by its elevated quartz content and the virtual absence of ferromagnesian minerals.

The Blackcraig Formation identified by Floyd (1982) is named after Blackcraig Hill [NS 647 065] in the type area of Upper Glen Afton. The type section extends from Blackcraig Farm [NS 636 082] across the western edge of Blackcraig Hill and along Afton Water up to the Afton Reservoir [NS 630 048]. Floyd (1982) recognised that this formation is dominated by thickly-bedded, coarse grained greywackes rich in ferromagnesian minerals, and correlated this formation with the Galdenoch Group of Kelling (1961). The type area of the Scar Formation

identified by Floyd (1982) is bounded by the River Nith, Scaur Water and the Leadhills and Fardingmullach faults. This formation was originally named after the Scaur Water (originally 'Scar') and is characterised by quartz-poor greywackes rich in feldspar and ferromagnesian minerals. The type area of the Shinnel Formation defined by Floyd (1982) occurs between the Fardingmullach Fault and the northwestern limit of the Silurian greywackes of the Central Belt, and is bounded to the NE and SW by the River Nith and Scaur Water, respectively. This formation derives its name from the nearby Shinnel Water and is typified by quartz-rich greywackes. The southeastern limit of this formation is marked by the presence of greywackes containing brown hornblende, which form the lateral equivalent of the Pyroxenous Group (Lower Llandoverly) identified by Walton (1955) in the Peebles area. The Shinnel Formation was correlated by Floyd (1982) with the Portpatrick (acid-clast) division of Kelling (1961).

The study was undertaken with particular reference to the tectonic discrimination of petrographically distinct turbidite formations from the Southern Uplands. The greywacke data sets used for this purpose were compiled from the analysis of samples, carefully screened in terms of location, stratigraphic position, lithology and petrography.

Lithogeochemical studies have had widespread application in the USSR and have led to the successful detection of blind ore bodies, at depths up to a few hundred metres. The recognition and identification of a standard scheme of vertical geochemical zonation (Grigoryan, 1974) is used in order to assess whether the geochemical anomaly reflects probable economic mineralization or simply the root zone of a deposit in which the economic portion has been eroded away. As such, lithogeochemical studies were carried out on alteration zones associated with a number of mineral occurrences in Southern Scotland, however considerable care was taken in the field preparation of rock samples in order to avoid contamination from both veined and weathered material. Information regarding the location of individual samples (the full numerical grid reference) were appended to the geochemical datafiles in the form of two additional, numerical variables (North and East). Petrographic classifiers together with analytical, mineralization, alteration and lithology codes were added to their respective samples in the form of a set of 'keys' or indexes (see RAW system notes in chapter 2) which were then used to rapidly sort or subdivide individual samples into a variety of different datafile formats.

Plant and Moore (1979) presented a detailed summary of a series of regional geochemical atlases prepared, or in preparation, by the British Geological Survey. In a similar manner, the database resulting from this study was used to construct a regional geochemical atlas of the Southern Uplands (see enclosures) and is presented at a scale of 1:250,000 together with topographic, geological and classification summary maps. This atlas presents a broad view of both the nature and extent of this geochemical programme in Southern Scotland and presents the results of 19 of the 29 elements analysed in the form of single element, point source geochemical maps (proportionally sized circles, centred upon the sample site location are used to represent element concentration).

ATLAS	No. of Samples	Datafile	Scale	Rock type	No. of Elements	Area (km)
GLENDINNING	306	GWKE1	1:100K	Greywacke	31	22x22
GLENDINNING	197	MUD1	1:100K	Mudstone	31	22x22
S.UPLANDS	1454	ATLAS	1:250K	Greywacke	29	210x140
RHINNS	279	GWKE22	1:100K	Greywacke	29	30x50
LONGFORD DOWN	297	GWKE40	1:400K	Greywacke	29	110x40

It should be noted that grid references of samples from the Longford Down study area have been transferred from the alphanumeric Irish National Grid reference to a fully numeric grid in order to facilitate computer aided drafting of the geochemical atlas for the region. As opposed to the UK system of prefixing a eight figure grid reference with a two letter mnemonic (ie NX), the Irish National Grid relies upon a single character to identify a 100 x 100km grid across the country. An example of the transformation of Irish grid reference is shown below:

Original Reference: N 9820 8300

Transformed Reference: 29820 28300

This study facilitated the investigation of variations in element groups and ratios, providing a new approach to the problems of provenance, depositional environment and tectonic setting of greywacke formations in the Southern Uplands.

5.3.3 Geochemical Classification and Mapping

It is now standard practice for geochemists to collect a suite of basalts from a deformed terrane and then infer former tectonic settings using trace element geochemistry. Sedimentary geochemistry has, until recently, been ignored together with the implications of fingerprinting an actual provenance rather than a petrological hypothesis (Boyle, 1985). Lithogeochemical studies of turbidite terranes enable not only the discrimination of constituent stratigraphic units/formations, but also allow a fundamental assessment of both provenance, depositional environment and hydrothermal history to be undertaken.

Overview

An extensive review of computer based techniques in the compilation, mapping and interpretation of exploration of exploration geochemical data was presented by Howarth and Martin (1979). This review stressed the need for correct organization of field sampling programs and laboratory quality control to minimize bias in the data. In addition, proper attention to cartographic design and the use of multivariate statistical analysis techniques (principal component, factor and cluster analysis) were proposed as major areas for development and research, in order to improve the standard of quantitative data analysis. Howarth (1973) presented a keynote review of pattern recognition techniques and their application in applied geochemistry. Feature selection, pattern classification (discriminant analysis) and pattern analysis (cluster-seeking techniques) were discussed with reference to regional stream sediment survey data from south-west England and it was noted that non-parametric methods provide a more effective classification tool than their parametric counterparts. The terminology associated with pattern recognition was detailed by Howarth (1973) and includes:

- Measurement - One of several numerical values (eg. element concentrations) which form a component of the pattern.
- Pattern - A collection of measurements characterizing the sample.
- Cluster - A set of points (corresponding to the patterns) contained in a high-dimensional (measurement) space.
- Training set - A set of data in which the class membership of each sample is known.
- Testing set - A set of data in which the classes are known, that has been treated as a set of unknown samples.

From a classification of the true and assigned classification of the testing set samples, a measure of the overall classification success rate is achieved (Howarth, 1971). Roth et al., (1972) applied principal component, discriminant and cluster analysis techniques to semi-quantitative mineralogical data from a series of distinct, bioclastic carbonate turbidite units from the Blake Basin. Brotzen (1975) noted that large datasets can be subdivided by the analysis of corresponding point distributions in multidimensional space, where the separate dimensions are represented by chemical variables. As distinct groups of samples are represented by different clusters of points in multivariate space, it follows that an analysis and recognition of such clusters could be used to produce chemical groupings. If transitions occur between two groups, the corresponding clusters will be joined by transitional points in zones of reduced point density. A number of recent publications have debated the application of log-, power- and other forms of transforms in the assessment of geochemical data (Mancey and Howarth, 1980). Transforms are applied to datasets in order to reduce skewness; produce a relatively more normal (Gaussian) distribution; and to make the use of parametric statistics more reliable. It should be noted that no transforms were applied to the data.

Winchester, et al., (1981) demonstrated the use of multi-element geochemistry in an assessment of the inter-relationship between psammites and pelitic lithologies from the western part of the Moinian. Hickman and Wright (1982) demonstrated the applicability of lithogeochemistry as a tool in stratigraphic correlation in the Appin Group metasediments from Argyll, Scotland and proposed that the correlation of stratigraphic units by similarities in their chemistry should be referred to as chemostratigraphical correlation. Boyle and Robertson (1983) demonstrated the use of chemical fingerprinting techniques in provenance studies of fine grained sediments whereas Van de Kamp and Leake (1986) demonstrated the use of Niggli numbers in an attempt to combine petrographic and chemical characteristics within a single discrimination diagram. This approach has considerable academic merit however, the general lack of familiarity with Niggli numbers displayed by most scientists and the additional data processing overheads incurred by such procedures invalidates this approach to all but the most adventurous researchers.

Data Analysis

Data was collected and processed following the methodology described in chapter 2, and submitted for both univariate and multivariate statistical analysis. Major and trace element geochemistry for the above formations were determined by XRF spectrometry following the methodology of Norrish and Hutton (1969) and Harvey and Aitken (1981, 1982). In addition, a subset of ~200 samples were analysed for REE at Kings College, London, following the methodology of Walsh et al., (1981). In order to investigate the application of chemical fingerprinting of greywackes, it was necessary to commence this study with samples displaying strong stratigraphic and petrological controls. This 'training set' was obtained from the personal collection of Dr J. Floyd and that of the British Geological Survey. Following an initial evaluation of this data it was clear that individual formations, if not chemically unique, displayed considerable variation and differences with their juxtaposed counterparts. Subsequently, their lateral equivalents in southwest Scotland and the Longford Down were examined with a view to establishing the continuity of these formations, and geochemical mapping. A variety of data analysis techniques have been employed to quantify the chemical differences between individual formations and mineralized/unmineralized samples. Where possible, a visual representation of this data is presented. Trace element parameters and discrimination diagrams provide a useful tool in the characterisation of greywacke provenance (Bhatia and Crook, 1986) and may be used to interpret the nature and tectonic setting of the host environment.

Greywacke Chemistry

In 1983, the IUGS Subcommittee on the Systematics of Igneous Rocks produced a classification of igneous rocks based on mineralogy (Lebas, 1983) and subsequently a chemical classification based on the 'alkali-silica' diagram was proposed. Fifteen categories of igneous rocks were delineated by the combined use of 15,594 analyses from both the CLAIR and PETROS databases. The resulting discriminant diagram (Fig. 299) although not immediately applicable to the classification of sedimentary rocks (*sensu-stricto*) has been used as a basis of the initial evaluation and classification of the Southern Uplands Turbidite Geochemistry Database (figs. 300-305). In comparison with the IUGS diagram, the Marchburn Formation samples plot within the basalt-andesite field (fig. 300) as opposed to the juxtaposed Afton Formation which plot within the andesite-dacite field. Samples from the volcanic derived Blackcraig and Pyroxenous Formations are tightly constrained within the andesite field whereas the Scar Formation although centred upon the andesite field, extends to a dacite composition (fig. 301 and 302). The cratonic derived Shinnel and Intermediate Formations samples are constrained predominantly by the dacite field whereas the Hawick Formation samples lie within the andesite-basaltic andesite field (fig. 303). The shift in SiO_2 composition in the Hawick Formation away from that expected for cratonic derived sediments, may be explained by the addition of a major CaO component (predominantly carbonate) to the greywackes. When the effects of CaO are removed by normalisation of the remaining major element contents the Hawick Formation samples plot in the expected dacite field. In a comparison of unmineralized and mineralized samples (Figs. 304 and 305) the unmineralized data set display a relatively narrow, restricted range of alkali content (with 13 samples below a 3wt% threshold) whereas the mineralized data set displays the direct effects of SiO_2 enrichment and total alkali depletion with samples skewed to the bottom right hand corner of the diagram (depletion threshold 3wt%). On the basis of a statistical evaluation of the mineralized data set it is observed that sodium is almost completely removed by alteration processes. In comparison with this trend Fig. 305 clearly illustrates a relatively static if not slightly elevated total alkali level, thereby inferring the considerable effect of potassium metasomatism upon the samples.

On the basis of major, trace and immobile element abundances and ratios, a number of chemically distinct suites of samples were identified, each characterised by different ratios and trends. The minor chemical differences that exist between greywackes from cratonically derived formations, are still sufficient to facilitate a significantly high probability of classification. Major and trace element crossplots provide a visual method for the rapid discrimination of greywackes derived from cratonic and volcanic terranes. Cratonic derived greywackes are in general represented by simple quartz rich, feldspar/pyroxene poor petrography as opposed to greywackes derived from volcanic sources which exhibit relatively quartz poor, feldspar/pyroxene rich facies. The geochemical data exhibit unusually sharp boundaries between juxtaposed cratonic and volcanic derived greywacke formations. An F-test was applied to sets of populations to determine if two populations have a common standard deviation. Unless both populations possess nearly identical standard deviations any further evaluation to test that the means of the two populations differ (Student t-test) is invalid. Multivariate statistical techniques are of assistance in classifying multi-element geochemical data, into petrographic and metal associations which characterise specific geological environments and processes and, thereby contribute to an improved interpretation of the data (Closs and Nichol, 1975).

Discriminant Analysis

Discriminant function analysis forms a powerful tool in the classification of individual cases (samples) into pre-defined groups on the basis of multivariate data. Discriminant analysis techniques have been widely applied in

the classification of geochemical data: Clausen and Harpoth (1983) demonstrated the use of this technique in classifying panned heavy mineral concentrates.

In general, the aims of discriminant analysis are to classify samples of unknown type into one of a number of pre-defined groups (eg. mineralized or Unmineralized) on the basis of their elemental compositions. In all methods, irrespective of the decision rule (discriminant function) used, the starting point is to have an established 'training set' of samples representative of each group. Once the decision criteria have been determined, an independent 'test set' of samples should be classified on the basis of the established decision rules to find out how well they perform before applying them to known data (Howarth, 1973; Howarth and Martin, 1979).

Discriminant function analysis was applied by Middleton (1962) to distinguish the tectonic setting of a number of sandstone units. Howarth (1971) detailed the application of an empirical discrimination method to the geochemical classification of a diverse range of sedimentary and igneous rocks grouped into 7 main classes. This technique achieved an overall classification success of 80%. Many different forms of discrimination function exist, including the linear, piecewise linear and polynomial discriminant function, however the linear discriminant functions are the widest used in geochemical applications (Howarth, 1972).

Hawkins and Rasmussen (1973) demonstrated the use of discriminant analysis for geochemical classification of strata in sedimentary successions within the Witwatersrand Basin. A linear discriminant function was used by Campbell (1978) to locate and place a boundary between two soil mapping units. For each discriminant function, Wilks' lambda indicates the statistical significance, whereas the canonical correlation coefficient signifies the strength of the discrimination function, and eigenvalue indicates the percentage of variation expressed by the function in the original data (Bhatia, 1983). Furthermore, Bhatia (1983) used major element discrimination function analysis to determine the tectonic setting of derived sandstones. Rock et al., (1984) detailed the application of discriminant and correlation analysis, in the identification of Lewisian, Moinian and Dalradian limestones from the Highlands of Scotland.

It is important to consider the number of samples in evaluating the significance of sample variants and historical studies. Typically, small populations of 10-20 samples in total are common in geochemical studies undertaken during the 1960's, 70's and early eighties. With such small sample populations it is unlikely that the sample population provides a true estimate of the actual population, and as such lowers the confidence limits which can be applied to this data (Huff, 1983). In most published studies, authors have been content to confine themselves to the discrimination of two or at most three quite distinct units/formations (eg. Weber and Middleton (1961); Rogers (1965); Condie and Snansiang (1971); Nathan (1976); Clayton (1982); Lambert et al., (1982); Winchester et al., (1981); Wyborn and Chappel (1983); Haselock (1984); Rock et al., (1984); Orth et al., (1986); Floyd and Leveridge (1987)). This study attempts to classify a minimum of eight petrographically distinct formations in the Southern Uplands of Scotland and relate them to their along-strike equivalents in the Longford Down. A further complication arises in this study, resulting from hydrothermal overprinting related to As-Sb-Au mineralization. However, altered samples are considered to form a further distinct group of records and are classified accordingly. A larger number of samples collected from a number of different localities provides a more statistically acceptable technique to assess compositional variation and identify the specific characteristics of individual formations.

Discriminant analysis was undertaken on the differing petrographic tracts in the Southern Uplands and provided a further test procedure to evaluate the relationship between juxtaposed formations. Training sets were established

using petrographically defined samples identified by Floyd (1981). The results of this classification study are presented in table 3.21. Simple discriminant analysis was performed using two group classifiers upon these juxtaposed, petrographically defined greywacke formations from the Southern Uplands (table 3.21). This classifier included all available variables ($n=29$) and gave good separations (maximum 5.1% misclassified) for all units with the exception of the Intermediate:Hawick Formation classification (7.2% misclassified). The most distinct Formations within the Southern Uplands are represented by the Marchburn and Afton Formations, with only 1.1% of samples misclassified. Here again, further attempts at discrimination utilizing restricted variable sets, led to increased levels of misclassification.

Discriminant analysis on the different petrographic formations produced an imperfect classification, however when the formations were grouped into their respective volcanic, cratonic and carbonate-rich groups, a significantly higher overall classification rate (~85-90%) was achieved. The Mahalanobis distance, D^2 , between two groups is highly significant. The usefulness of the discriminant function was evaluated using both background and anomalous samples. The covariance matrices for the background and anomalous groups are significantly different at a level of 0.001. Limitations of this technique inherent in the nature of the data merited a slightly different approach to the problem of classification. Parametric statistical methods, including discrimination analysis are most effective when applied to data which has a near-normal or lognormal distribution. This requirement is in many cases difficult to satisfy due to the polymodal distribution displayed by mineralized data. This form of data can be classified using an empirical discriminant function which does not require normality (Howarth, 1971) or alternatively, non-parametric techniques such as K-means cluster analysis need to be invoked.

Cluster Analysis

The initial training set has been both modally and chemically analysed, and provides an invaluable database (~800 samples analysed for 29-54 elements). Cluster analysis may be used to separate the sample population into a number of distinct groups and identify individual samples that have been subjected to hydrothermal alteration or are weakly mineralized. In addition, this procedure may be applied to remove the effects of closure within this dataset.

Using an assumption of no 'a priori' knowledge, the number of naturally occurring clusters within the training set ($n=840$) were determined as part of the clustering technique, by setting the number of clusters (k) to 2, 3, 4, 5, 6, 7, 8, 9, and 10; and then interpreting some measure of "goodness of fit". In this study, a significant break of slope on the X-Y plot (No of clusters vs. summed deviation about the centroids) was observed at $k=3$ (interpreted as representative of cratonic, volcanic and carbonate-rich greywackes) together with a relatively more subtle break in slope at $k=8$. Greywackes were divided petrographically into seven groups and verified by linear discriminant analysis of the chemical data. As some of the geochemical differences between petrographic formations are relatively subtle, a classification scheme was required to enable the identification of not only cratonic and/or volcanic characteristics, but also differentiate between individual formations. Following the methods described by Shepherd et al., (1985) and identification algorithm was developed involving a combination of empirical and statistical techniques including: simple discriminant analysis (eg. $Cr > 500$ ppm; $CaO > 10\%$) giving a true or false answer; and non-hierarchical K-means clustering techniques (MacQueen, 1967; Shephard et al., 1985). This algorithm facilitated the rapid identification of hydrothermally altered and/or mineralized samples reflecting As, Sb and base metal mineralization (eg. $As > 10$ ppm; $Na < 0.5\%$). In addition, samples from the most distinct greywackes formations (Marchburn and Hawick) were readily identified, increasing their classification success

by a factor of 5 to 7% over that of 'clustering only' methodologies. It should be noted however that the less chemically distinct formations benefit little from the application of simple discriminant analysis and are separated by K-means clustering using seed centroids for all the 'known' groups (or Formations).

This classification procedure was then applied (using the same 'a priori' seed points) to 297 'unknown' samples from a coastal traverse of the Rhinns of Galloway. Unknown samples were compared against the 'known' centroids and assigned the identity of the one it most closely resembled or defined as 'unclassified'. At approximately two thirds of these sites (notably within the Northern and Central parts of this traverse) it was possible to check the predicted classification with previous geological mapping and petrographic studies (Kelling, 1969). Here again, a 70-80% success rating was observed in a comparison between the position of individual petrographic units and their predicted classification. This approach to geochemical mapping and boundary identification has significant applications in delineating differing petrographic units on both a local and regional scale, within superficially monotonous sedimentary sequences, and may be used to identify areas favourable for mineralization. This study demonstrated that non-parametric statistical techniques can provide an important processing aid in the analysis of multi-element geochemical data, with advantages including, the unnecessary requirement for a normal population distribution or many of the other assumptions made for parametric statistical methods; ease of use; rapid operation; and its ability to process very large data arrays (Shepherd et al., op. cit.). The inclusion of spatial/locational information in the form of (x,y) coordinates in the training sets served only to reduce the relative success of the classification algorithm, most probably due to the NE-SW strike orientation of the individual greywacke formations under evaluation.

The nearest-neighbour classification rule states that a sample may be assigned to the same group as its nearest neighbour in measurement space, or to the class most frequently represented among its 'r' nearest neighbours. The applicability of non-hierarchical cluster analysis to greywacke classification, was tested using a modified convergent form of the MacQueen's k-means method of clustering devised by Shephard (1985). Non-hierarchical techniques are partitioning methods where samples are classified into a specific number of mutually exclusive groups or clusters (Anderberg, 1973). An initial evaluation was undertaken using eight 'a priori' seed points defined by the average chemical compositions of a series of 'undisputedly' distinct greywacke formations defined by Floyd (1981). In total, a training set of 819 petrographically defined samples of 'known' composition were submitted to the modified K-means program for classification. Convergence was reached after four iterations and the results of this classification are presented below:

Seed Point	Formation Name	Petrographically Defined	Geochemically Defined	Success (%)
1	Marchburn	44	28	63.63
2	Afton	140	110	78.57
3	Blackcraig	57	42	73.68
4	Scar	99	76	76.76
5	Shinnel	62	51	82.25
6	Pyroxenous	43	31	72.09
7	Intermediate	79	57	72.15
8	Hawick	<u>295</u>	<u>274</u>	<u>92.88</u>
	Total	819	666	80.47

These results clearly demonstrated the success of this technique, which may be adopted for operational use to form the basis of a lithogeochemical classification scheme, assessing 'unknown' samples with respect to petrographic formations in the Southern Uplands. This optimum classification achieved an overall 80.47% success rate (range 63-92%) comparable in many respects to that defined by Howarth (1971) for a more diverse range of sedimentary rocks. Higher success rates could only have been achieved if a wider, more clearly distinct range of geochemical values/rock types was present. This form of classification procedure has not been widely applied to sedimentary provenance or geochemical exploration projects due to the practical difficulties associated with obtaining adequate sample data for constructing training sets. Once a discriminant function has been established, subsequent classification is extremely rapid, even when several thousand samples are involved.

Factor Analysis

R-mode factor analysis was used by Lambert, et al., (1982) to identify the controlling factors in lateral variations in chemistry detected within the Leven Schists. Four factors were required to resolve 98% of the variance. R-mode principle component analysis is used to group related variables into a smaller number of parameters called 'factors'. The positive and negative loadings of related variables in each factor may be used to suggest similar or opposite trends. The results of principle component analysis upon greywacke formations from the Southern Uplands is presented in table 1.18 to 1.27. Factor analysis provides a powerful tool in the interpretation of geochemical inter-relationships within individual data sets, however its detailed application is beyond the scope of this project.

Summary

Univariate and multivariate statistical tests (including principal component, discriminant and K-means cluster analysis) were initially applied to a representative training set of approximately 900 petrographically defined samples in order to determine the significance of the chemical variation within each petrofacies and define a suitable classification system. It was initially proposed that these classification algorithms would provide a satisfactory method for the identification for greywackes of unknown origin. A chemical 'fingerprint' would be used to classify each sample into its respective petrofacies or alternatively define the sample as 'altered' and of exploration interest. The scale of sampling within this program facilitated:

- 1) the chemical definition of the nature, origin and evolution of differing provenance sources.
- 2) the assessment of the nature and magnitude of the chemical variation between different turbidite units and the development of a series of chemical classification systems for each distinct petrographic unit.
- 3) the evaluation of lithogeochemistry as a tool in regional stratigraphic correlation, terrain boundary identification and mineral exploration.
- 4) the identification of areas of chemical alteration related to tectonism, igneous intrusion and/or hydrothermal activity.

Discriminant and k-means cluster analysis techniques provided complementary tools for geochemical data analysis. The discrimination and clustering procedures applied within this study appear to accurately delineate the boundary between individual formations. The effectiveness of this classification was confirmed by comparison with a petrographically defined 'testing set' of samples from the Rhinns of Galloway. These composite traverses may be directly compared, and provide an aid to the correlation of sequences and regional geochemical stratigraphies in these two regions. Furthermore, the accurate placement of boundaries between petrographically

distinct Formations in the Southern Uplands using both discriminant and cluster analysis techniques applied to lithogeochemical data, provides an important new tool in the compilation of geological maps of this region.

5.3.4 Turbidite Geochemistry and Tectonic Setting

It is generally recognised that plate tectonics provide the dominant controls upon source rocks, sandstone detritus and depositional environment (Condie and Snarseng, 1971; Crook, 1974; Schwab, 1975; Dickinson and Suczek, 1979; Bhatia and Taylor, 1980, 1981; Clayton, 1982). This section presents a detailed review of the application of geochemical studies to greywacke provenance and depositional setting.

Weber and Middleton (1961) demonstrated that gravity settling processes result in the concentration of a suite of heavy minerals at the base of turbidite beds which displays accompanying trace element (Zr, Ti, Ni) enrichment. In a similar manner it was proposed that the elements B, Ba and V which are precipitated from sea water or adsorbed onto clays, would be concentrated in the upper, clay-rich part of the bed. Pettijohn (1963) proposed that greywackes display a tightly restricted range of chemical compositions that are not duplicated by other lithologies. Rogers (1965) investigated the geochemistry of greywackes from western Oregon and Washington and identified close similarities between the volcanic clast assemblages and the Greater Antilles island-arc. An initial greywacke classification incorporating both petrographic and major element data was proposed by Crook (1974) which divided greywackes into quartz-rich, quartz-intermediate and quartz-poor categories on the basis of SiO_2 content, $\text{K}_2\text{O}/\text{Na}_2\text{O}$ ratios and the proportion of modal quartz. Quartz-rich greywackes being derived from passive (trailing-edge/atlantic-type) continental margins; quartz-intermediate varieties derived from continental-arc (Andean-type) margins; and quartz-poor greywackes are derived from fore-arc basins of island arcs.

Lajoie et al., (1974) in studies of Lower Palaeozoic greywackes in the eastern Canadian Appalachians, identified a Grenvillian metamorphic source for Early Ordovician greywackes. Graham et al., (1976) demonstrated that fore-arc areas are characterised by predominantly volcanic and subordinate metamorphic/lithic grains derived from an eroded continental margin arc. Continental back-arc areas may be characterised by a volcanic and variable sedimentary/lithic component from the rifted continental margin, Floyd and Leveridge (1987). In most greywackes the majority of the Na_2O is held in feldspar and rock fragments, while K_2O is held largely in the clay matrix (Nathan, 1976). The $\text{K}_2\text{O}/\text{Rb}$ ratio shows little variation with increasing K_2O values, suggesting that both elements are held in a single clay phase. Cabry et al., (1977) in studies of the geochemistry of Upper Proterozoic greywackes from northwestern Algeria, identified dominantly andesitic characteristics formed as a result of erosion of a penecontemporaneous calc-alkaline volcanic suite, emplaced in Upper Proterozoic shelf sediments. Ingersoll (1978) documented the petrologic evolution of a Late Cretaceous fore-arc basin in California, whereas Redfern (1979) detailed the results of a geochemical study of Silurian greywackes south of the Shap granite in the Lake District. Jakes et al., (1979) demonstrated the chemical similarity between Proterozoic greywackes from the Tepla-Barrandian area of Czechoslovakia with that of recent island-arc volcanism as well as material derived from recent continental margins (Andean volcanism) or their metamorphic equivalents, and suggested a similar origin. Lambert et al., (1981) proposed that the characteristic trace element ratios of the chemically mature Appin Group semi-pelites could be used to distinguish between Appin Group (Dalradian) and Moine semi-pelites. Peterman et al., (1981) identified both felsic components and a mafic source in a geochemical study of the provenance of greywackes from the Flournoy formation, Oregon. However, they failed to recognise the important implications relating to provenance caused by significant variations in geochemistry between formations.

Clayton (1982) presented the results of a preliminary investigation of the geochemistry of greywackes from South Georgia Island and distinguished greywackes displaying typical calc-alkaline characteristics (the Cumberland Bay Formation) from those of a more acidic provenance (the Sandebugten Formation), using simple tests of significance and univariate statistical procedures. In addition, it was noted that the nature and magnitude of chemical variation within turbidites is controlled by a number of factors including provenance, erosion rates, transport and deposition, and depositional environment. Dickinson (1982) confirmed that sandstones from circum-Pacific fore-arc basins display similar chemical compositions reflecting varying degrees of dissection of magmatic arc terranes.

Lambert et al., (1982) applied petrographic and geochemical techniques to the discrimination of Dalradian, Leven Schists and Grampian division Monadhliath Schists in the central Highlands. In studies of recent deep sea sands, Maynard et al., (1982) demonstrated a clear distinction between active and passive plate tectonic settings on both petrographic and chemical grounds. It was noted however, that major element geochemistry was unable to distinguish different types of arc-related sandstones. Wyborn and Chappell, (1983) in studies of the geochemistry of Ordovician and Silurian greywackes from the Snowy Mountains of southeastern Australia, demonstrated distinctive geochemical variations between Ordovician and Silurian sediments, interpreted in terms of detrital feldspar content, and related to the extent of chemical weathering.

As certain elements are characteristically concentrated in basic rather than acid rocks, and vice versa, an estimate of the provenance of individual formations may be made. Bhatia and Taylor (1981) demonstrated the use of the elements La, Th, U and Hf in discriminating arc derived greywackes (andesitic source rocks) from relatively mature greywackes derived from rifted continental margins and marginal basins (granitic and sedimentary source rocks). A simplified plate tectonic classification of continental margins and oceanic basins was proposed by Bhatia and Crook (1986) in which four types are recognised:

- 1) Oceanic island arc - deposition within a sedimentary basin adjacent to an oceanic island arc or an island arc partially formed on thin continental crust
- 2) Continental island arc - deposition within a sedimentary basin adjacent to island arcs formed on a well-developed continental crust or on thin continental margins
- 3) Active continental margins - deposition within a sedimentary basin developed on/or adjacent to a thick continental crust composed of granite-gneisses, and uplifted basement
- 4) Passive margins - composed of rifted continental margins of Atlantic type developed along the edges of continents, remnant ocean basins adjacent to collision orogens and inactive or extinct convergent margins

Bhatia (1983) demonstrated that tectonism is the primary control upon sandstone composition and provided mean values attributed to the four major tectonic settings together with an estimate of uncertainty. In addition, Bhatia (1983) developed a tectonic setting discrimination algorithm used to distinguish the representative members of the transitional groups defined by oceanic island arc (OIA), continental island arc (CIA), active continental margin (ACM) and passive margin (PM) on the basis of a progressive decrease in $\text{FeO}+\text{MgO}$, TiO_2 and $\text{Al}_2\text{O}_3/\text{SiO}_2$ and a progressive increase in $\text{K}_2\text{O}/\text{Na}_2\text{O}$ and $\text{Al}_2\text{O}_3/(\text{CaO}+\text{Na}_2\text{O})$. The ratio $\text{Al}_2\text{O}_3/\text{SiO}_2$ provides an indication of the relative proportions of quartz to clay, whereas the ratio $\text{K}_2\text{O}/\text{Na}_2\text{O}$ forms a measure of the K-feldspar and clay vs. plagioclase content. The average Zr/Th ratio for active continental margin greywackes as defined by Bhatia and Crook (1986) is 9.5 ± 0.7 in comparison with 21.5 ± 2.5 and 19.1 ± 5.8 for continental island arc and passive margin

greywackes respectively. Oceanic island arc sediments are dominantly derived from calc-alkaline andesites and are characterised by a higher abundance of TiO_2 , Al_2O_3 , Na_2O and Fe_2O_3 and a lower abundance of SiO_2 and K_2O compared with all other sandstones/greywackes. In general oceanic island arc greywackes are characterised by extremely low abundances of La, Th, U, Zr, Nb, Th/U and La/Y.

The La/Y ratio provides a general indication of the enrichment of LREE (represented by La) over HREE (represented by Y). Oceanic island arcs are characterised by low La/Y (generally <0.5), continental island arc greywackes are discriminated by values between 0.5 and 1.0, and active continental margin greywackes have high La/Y ratios >1 (Bhatia and Crook, 1986). Furthermore, the average composition of active continental margin type greywackes is characterised by equal amounts of K_2O and Na_2O with a bulk composition similar to that of crystalline basement in the upper continental crust (Bhatia, 1983).

Active continental margin sediments dominantly derived from uplifted basement, reflect the composition of upper continental crusts in their higher SiO_2 and K_2O levels with $\text{K}_2\text{O}/\text{Na}_2\text{O} \sim 1$. Continental island arc sediments, dominantly derived from felsic volcanic rocks, are characterised by higher SiO_2 , K_2O and $\text{K}_2\text{O}/\text{Na}_2\text{O}$ ratio (~ 0.6) and lower $\text{Fe}_2\text{O}_3 + \text{MgO}$ than their oceanic island arc counterparts. Continental island arc setting may be characterised by increasing abundances of La, Th, U, Zr and Nb. In general, active continental margin (ACM) and passive margin (PM) greywackes may be discriminated by the Th/Zr ratio, however the most important characteristic of passive margin type greywackes is the increased abundance of Zr, high Zr/Th and lower Ba, Rb, Sr and Ti/Zr ratio compared to active continental margin sediments. Passive margin sediments display a large variation in composition which may overlap with that of the active continental margin. In general, they are significantly enriched in SiO_2 and depleted in Al_2O_3 , TiO_2 , Na_2O and CaO , and have a $\text{K}_2\text{O}/\text{Na}_2\text{O}$ ratio >1 . Passive margin greywackes can be identified by their higher Zr, Zr/Nb, Zr/Th and lower Ba, Rb, Sr, V and Ti/Zr ratios. These characteristics form as a result of the polycyclic nature of the passive margin sediments and the resulting depletion of feldspar and labile fragments and the increased abundance of heavy minerals.

Bhatia and Crook (1986) recognised four distinct provenance and tectonic settings of Australian Palaeozoic turbidites on the basis of their variation in trace element composition. Oceanic island arc, continental island arc, active and passive continental margin settings may be distinguished by a systematic increase in light rare earth elements (La, Ce, Nd), Th, Nb and the Ba/Sr, Rb/Sr, La/Y and Ni/Co ratios; and decrease in V, Sc and the Ba/Rb and K/Th ratios. In general, the average composition of oceanic island arc sandstones is similar to that of andesites (Bhatia, 1983) whereas the average composition of continental island arc greywackes is similar to that of continental calc-alkaline rocks (Bhatia, 1983). A mineralogical maturity index (MI) was proposed by Bhatia and Crook (1986) in which the ratio of quartz to quartz+feldspar+rock fragments is calculated, thereby providing a 'sliding-scale' index of the relative maturity of the sediments.

Geochemical studies of Palaeozoic greywackes from eastern Australia have demonstrated a large variation in the immobile trace elements (La, Ce, Nd, Th, Zr, Nb, Y, Sc and Co) which form useful discriminators of distinct provenance types and tectonic settings including oceanic island arc, continental island arc, active continental margin and passive margins (Bhatia and Crook, 1986). Huff (1983) demonstrated the use of major and trace element analysis in the correlation of Middle Ordovician K-rich bentonites from southwestern Ohio and northern Kentucky. Six separate bentonite horizons were classified using simple discriminant analysis and traced over a maximum distance of $\sim 300\text{km}$.

Haselock (1984) demonstrated the existence of systematic geochemical variations between two tectonically separate successions in the Grampian division of the Dalradian Supergroup. With regard to the Southern Uplands, evidence provided by Simon (1986) regarding the provenance and setting of Lower Palaeozoic conglomerates in Northern Ireland, exhibit close similarities with those of central Scotland (Bluck, 1983) and support the hypothesis of Phillips, et al., (1976) that island-arcs were developed to the north of the Longford Down Massif during the Ordovician. Orth, et al., (1986) documented a detailed geochemical study across the Ordovician/Silurian boundary on Anticosti Island, Quebec. This boundary marks one of the largest extinction events in the fossil record, second only to the Permian/Triassic extinction. This extinction has been attributed to changes in the physical environment, caused by worldwide glacio-eustatic withdrawal of epicontinental seas and climatic deterioration.

Rock et al., (1986) demonstrated the use of comparative geochemical studies of pelitic rocks from the Grampian Highlands of Scotland. Using discriminant analysis upon a multi-element data set it was possible to distinguish Lewisian, Moinian and Dalradian pelites from each other (Lewisian samples exhibit the lowest Al, K, Ti, P, Rb, Y, Nb, Ce, Pb and highest Fe, Mg, Ca and Cr contents). Van de Kamp and Leake (1986) demonstrated that greywacke sandstones generally reflect provenance source regions better than comparative studies of mudstones and shales, and noted that it is not possible to distinguish mafic volcanic and mafic plutonic sources with any degree of confidence. In conclusion, Van de Kamp and Leake (1986) noted that, despite the need for large data sets, the chemical composition of sandstones provides an important source of information relating provenance sources and plate tectonic settings of deposition.

Taylor and McClennan (1985) demonstrated that both ancient and modern sedimentary environments may be classified according to plate tectonic setting. They distinguished fundamental differences between passive (or trailing-edge) settings and active margin settings, with the former being related to continental rifting and separation, whereas the latter are more complex and are subdivided into categories including collision and subduction zones. Furthermore, Taylor and McClennan (op.cit) noted that some care is needed in simple tectonic interpretations based upon K and Na abundances, as these variations are dominantly controlled by feldspar distribution (with the abundance of volcanogenic plagioclase providing a key index of tectonic setting). Albitization processes (the replacement of Ca and K by Na) in feldspars during diagenesis may have considerable influence upon this ratio.

In general, trace element data particularly for the REE are scarce and as such represent a major gap in our understanding of sedimentary geochemistry (Taylor and McClennan, 1985). A detailed review of rare earth element geochemistry, was presented by Henderson (1984). The rare earth elements, lanthanum to lutetium (atomic numbers 57-71) are members of Group IIIA in the periodic table and all have very similar chemical and physical properties. Despite the similarity in their chemical behavior, these elements can be partially fractionated by petrological, mineralogical and alteration processes. The REE may be divided into two subgroups: those from La to Sm (lower atomic numbers and masses) which are referred to as the light rare earth elements (LREE) and those from Gd to Lu (higher atomic numbers and masses) referred to as the heavy rare earth elements (HREE). The REE form a coherent group, because of their systematic decrease in atomic radii, with increasing atomic number and predominant +3 oxidation state. The fact that two members of the group, cerium and europium, are often found in anomalous oxidation states, adds to the groups use (Klinkhammer, 1983). In general, the fractionation of REE in greywackes results from the abundance of primary and secondary mineral phases. In granitic rocks the REE are mainly concentrated in accessory minerals such as sphene, apatite and monazite. These minerals tend to

concentrate the LREE and consequently, whole rock samples are frequently enriched in LREE. Plagioclase, K-feldspar and biotite act as host for the remaining REE, in order of relative abundance.

Floyd and Leveridge (1987) presented a geochemical study of Devonian sandstones in south Cornwall. Petrographic and geochemical data indicated that the sandstones were derived from a dissected continental magmatic arc displaying a composition similar to average upper continental crust, but with an admixture of minor intermediate/basic material. Lash (1987) in a petrographic study of Middle Ordovician turbidites from the Central Appalachian orogen, detailed the presence of both volcanic and cratonic derived formations which exhibit close similarities to formations of similar age in the Southern Uplands and Longford Down. This comparison however, is somewhat tentative and requires considerable further investigation.

Merriman and Roberts (1988) in geochemical studies of ~100 bentonites from Dob's Linn, Moffat, identified trace element characteristics indicative of dacitic to rhyolitic compositions with volcanic arc to predominantly within-plate characteristics typical of back-arc basin volcanism. Chemical fingerprinting has been used successfully in tracing and correlating Ordovician bentonites (Huff, 1983) and offers a possible means of differentiating Palaeozoic greywackes in the Southern Uplands. The geochemistry of sandstones and greywackes can be used to infer the provenance type and plate tectonic setting of ancient sedimentary basins (Bhatia, 1983). As such, the relationship between sediment composition and plate tectonics provides a powerful tool in the recognition of ancient tectonic settings.

Discriminant Diagrams

A diversity of greywacke discrimination diagrams have been presented by authors, including Blatt (1972); Crook (1974); Ricci (1976); Caby (1977); Clayton (1982); Pearce (1982); Lambert and Holland (1982); Cathelineau (1983); Lebas (1983); Bell (1984); Bhatia (1983, 1985) and Rock (1985). Upon review a subset of 33 X-Y diagrams and 3 X-Y-Z diagrams were selected to compare the nature of the variation in the Southern Uplands with that reported elsewhere (table 1.68). Petrographically classified samples from each formation were plotted on a series of geochemical crossplots. Each individual plot defines the data fields for successive pairs of formations, including; the Marchburn and Afton; Blackcraig and Scar, Shinnel and Pyroxenous; Intermediate and Hawick; and Mineralised and Un-mineralized groups. To assist the generation of both X vs Y and triangular plots the following variables were created/calculated for each sample using the TRANSFORM option in the RAW program and appended to the geochemical database: K_2/Na_2O ; Al_2O_3/SiO_2 ; Fe_2O_3+MgO ; $Al_2O_3/(CaO+Na_2O)$; La/Y ; Nb/Y ; Nb/P_2O_5 ; Rb/Sr ; Ni/Co ; Cu/Co ; Zn/Co ; Zr/Nb ; $(K_2O/(K_2O+Na_2O)) * 100$; and K_2O+Na_2O .

A series of discrimination diagrams (figs. 306-410) are presented in order to display the major chemical characteristics of greywacke formations located within the Southern Uplands Study Area. All samples (with the exception of the Hawick Formation) have been subjected to petrographic examination (Floyd, 1981) and classified into their respective Formations on the basis of point-count and spatial information. Summary statistics relating to each formation are presented in tables 2.50-2.58, and a table listing the most widely used greywacke discrimination diagrams and their respective authors is presented in table 1.68.

The silica-total alkali classification diagram (fig.299) was developed by the IUGS based upon the petrographic study and geochemical analysis of over 15000 igneous rock samples. This discrimination diagram is used to provide a framework for simple geochemical classification of greywacke samples from the Southern Uplands study area.

The Th-Co-Zr/10 discrimination diagram (fig.80) defined by Bhatia (1985) may also be applied in a classification of the distinct provenance types and tectonic setting in the Southern Uplands. Four categories are recognised, namely: Oceanic Island Arc (OIA); Continental Island Arc (CIA); Active Continental Margin (ACM); and Passive Margins (PM). OIA greywackes are characterised by their high Th/Co ratio and plot close to the Co pole. ACM greywackes are characterised by Low Th/Co ratios and plot close to the Th pole. Passive margin greywackes characterised by a high Zr/Th ratio and plot near the Zr pole.

For comparative purposes the REE abundances have been normalised to an average chondrite abundance and plotted against the relative ionic radii of individual elements in figs 440 to 474. In detail, figure 440 displays the chondrite normalised REE patterns of selected Archean greywacke samples (after Taylor and McLennan, 1985) including: DD9 (Knife Lake); YK2 (Yellowknife); KH44 (Kalgoorlie); C28 (Fig Tree); and G21 (South Pass). Note that although samples are derived from different source terranes, their REE patterns are all generally similar, with no substantial Eu-anomalies and fairly steep HREE patterns. In comparison with post-Archean greywackes, these samples exhibit some similarity with the quartz-poor varieties (Fig. 445) with both groups lacking negative Eu-anomalies, however HREE patterns differ in their steepness. In opposition, figure 441 displays a range of chondrite normalised REE patterns of from selected Phanerozoic greywacke samples including: Quartz-Poor M277 and M285 (Devonian Baldwin Formation, Australia); Quartz-Intermediate MK64 (Silurian-Devonian Waterbeach Formation, Australia) and T82/324 (Triassic Torlesse Group, New Zealand); and Quartz-Rich P39803 (Ordovician Greenland Group, New Zealand) and MK97 (Ordovician Bendigo Trough, Australia). The quartz-poor samples are derived from volcanogenic (andesite) sources whereas quartz-rich samples are derived from a polycyclic source of plutonic derived material. The individual REE patterns are discussed in detail in figures 443, 444 and 445. The chondrite normalised REE patterns of post-Archean shale composites NASC and ES (North American shale composite and European shale composite respectively) and the PAAS (Post-Archean average Australian shale) are presented in Fig. 442 and display a strong uniformity of patterns with high abundances (compared to chondritic meteorites) light REE enrichment, relatively flat heavy REE patterns and most importantly, a significant negative Eu-anomaly. The enrichment or depletion of europium (Eu) is assessed in relation to the neighbouring REE, samarium (Sm) and gadolinium (Gd) following the calculation of the theoretical Eu concentration (assuming a smooth REE pattern in the region Sm-Eu-Gd). These patterns most closely resemble granodioritic compositions and are interpreted by Taylor and McLennan (1985) to support the view that sedimentary REE patterns reflect the upper continental crust exposed to weathering and erosion.

Figure 445 displays chondrite normalised REE data from selected quartz-poor greywackes plotted against PAAS for comparison. Samples include both M277 and M285 from the Devonian Baldwin Formation of the Tamworth Trough, Australia. These samples are volcanogenic (andesite) in origin and a fore-arc setting for deposition with an undissected magmatic arc provenance (Chappell, 1968 and Nance, 1977). The REE patterns displayed by the quartz-poor samples include lower total REE and La/Yb (compared to PAAS) with no Eu depletion. It is clear that calc-alkaline andesitic rocks were the primary source for these sediments. Chondrite normalised REE data from selected quartz-rich greywackes plotted against PAAS are displayed in fig. 443. Samples include P39803 (Ordovician Greenland Group, New Zealand) and MK97 (Ordovician Bendigo Trough, Australia). The REE patterns displayed by the quartz-rich samples include LREE enrichment ($La_N/Y_N > 8$) and strong Eu depletion (similar in magnitude to PAAS). As such, quartz-rich greywackes are indistinguishable from typical post-Archean upper crust in terms of REE (as indicated by PAAS).

5.4 SOUTHERN UPLANDS REGIONAL STUDIES

In general, previous chemical studies have attempted to relate greywacke compositions with tectonic environment (Bhatia and Taylor, 1981; Bhatia, 1983) however, these studies have lacked detailed petrographic data on the same sample sets. This study has attempted to overcome this deficiency by the analysis of petrographically defined samples from within the study area. The resulting petrographic and geochemical database and their inferred provenance, has allowed the tectonic setting discrimination indices of numerous authors to be evaluated during this study. In general, this study demonstrates that the major and trace element composition of both cratonic and volcanic derived greywacke samples reflects their distinctive modal compositions. However, the direct application of the specific discrimination parameters outlined by Bhatia and Crook (1986) to greywackes of the Southern Uplands results in a number of conflicting interpretations.

5.4.1 The Southern Uplands Composite Geochemical Traverse

The results of multi-element geochemistry upon a series of petrographically defined greywacke formations in the Southern Uplands are displayed in fold-out 2. Samples from each formation have been grouped in ascending numerical order and combined with other formations to create a composite geochemical profile (n=861). Of the eight formations studied, the Marchburn (n=44) Blackcraig (n=61) Scar (n=100) and Pyroxenous (n=63) Formations were defined by Floyd (1983) on petrographic evidence to have been derived from one or more volcanic terrains as opposed to the Afton (n=154) Shinnel (n=71) and Intermediate (n=79) Formations which were derived from a cratonic terrain. The Hawick Group (n=306) is defined by this study as a cratonic derived greywacke formation containing a significant proportion of carbonate. It should be note that an inverted stratigraphy is displayed on fold-out 2 in order to mirror the actual north-south juxtaposition of each formation across the Southern Uplands. The identified trends and variations in element concentration defined by the 24,969 analytical and 12,915 calculated values relating to this study are discussed below:

SiO₂

All margins between the cratonic and volcanic petrographically defined formations are also clearly defined by respective increases and decreases in SiO₂ content. The mean composition of volcanic derived greywackes is generally lower than the cratonic group (<62%). Note that both the Blackcraig and Scar Formations are derived from a volcanic terrain. In the Hawick Group, a relative decrease in SiO₂ content mimics the expected values for volcanic derived sediments. This decrease is however, counter-balanced by an increase in CaO content brought about by the addition of a major carbonate component from the source terrane. SiO₂ values in the cratonic formations are inversely correlated with, in order of significance; Fe, Mg, Cu, V, Al, Ti, Ca, K, Mn, Cr, Ni and Sr. No significant positive correlations were identified. SiO₂ values in the volcanic formations are positively correlated with, in order of significance; Na, Fe/Mg and Nb/P; and inversely correlated with Ti, Fe, Mg, Ca, Mn, P, Co, Cr, Ni, V and Zn. A notable geochemical feature of the greywacke geochemistry in general is the inverse linear relationship between SiO₂ and many of the remaining major and trace elements. This feature is a reflection of the dilutant effects of quartz and exemplifies the problem of closure in such a data set.

Al₂O₃

The sporadic Al₂O₃ values defined by this study indicate that although the element has a tendency towards higher values in the more finer grained samples it has no significant use in greywacke discrimination and terrain boundary identification. In general, Al₂O₃ values in the cratonic formations are positively correlated with, in order of significance; K, Rb, Ba, Co, Cu, La, Nb; and inversely correlated with Ca, whereas Al₂O₃ values in the volcanic formations are positively correlated with; K, Rb, Sr, Pb, Ba, Co, Cu and La; and inversely correlated with Ti, Fe, Ca and Y.

TiO₂

An overall decrease in TiO₂ content occurs across this succession with time. Particularly high values occur in the Marchburn and Blackcraig Formations (volcanic) whereas the lowest values are found in the Hawick Group. The mean TiO₂ content of Ordovician volcanic greywackes is generally 0.3-0.5% higher than their cratonic counterparts. Slightly elevated values, higher than those expected on the basis of a simple volcanic/cratonic division occur in the Afton Formation, together with corresponding lower values in the Scar and Pyroxenous Formations. These values may be used to infer major differences in the source terrane of each formation. TiO₂ values in the cratonic formations are positively correlated with, in order of significance; Fe, Nb, V, P, Cu, Y; and inversely correlated with Al and Ca, whereas TiO₂ values in the volcanic formations are positively correlated with; Fe, V, Y, Mg, Mn, Nb and Zn; and inversely correlated with K, Rb, Sr, Al, Ba, La and Pb.

Fe₂O₃

The Fe₂O₃ values mirror that of TiO₂ with an overall trend towards decreasing values across the succession. Superimposed upon this trend the volcanic derived greywacke formations (Marchburn, Blackcraig, Scar and Pyroxenous) exhibit increased iron content in comparison with their cratonic counterparts, whereas the Intermediate Formation and Hawick Group contain the lowest Fe₂O₃ contents in the succession. In general, the mean Fe₂O₃ value in the volcanic derived sediments is 2-3% higher than juxtaposed cratonic greywackes. Fe₂O₃ values in the cratonic formations are positively correlated with, in order of significance; Mg, Ga, V, Cu and Zn; and inversely correlated with P. Fe₂O₃ values in the volcanic formations are positively correlated with; Ti, Mg, Mn, V, Y and Zn; and inversely correlated with Rb, K, Sr, Al, Ba, La, Sr and Zr.

MgO

MgO values closely follow that of TiO₂ and Fe₂O₃ with the highest contents occurring in the Marchburn Formation. The remaining volcanic derived formations exhibit similar levels of enrichment compared to their juxtaposed cratonic counterparts. The MgO content of greywackes provides a useful index for the discrimination of cratonic and volcanic derived greywackes. (NB. the average volcanic is 1.5-3.0% higher than its cratonic counterpart). MgO values in the both cratonic and volcanic formations are positively correlated with, in order of significance; Fe, Cr, V and Ni.

However, it is noteworthy that the Hawick Group contains slightly elevated MgO values compared with the neighbouring Intermediate Formation. Given the close petrographic similarity between the non-carbonate xenolithology of these two formations, the strong positive correlation between CaO and MnO may be used to infer that Mn carbonate was the most probable source of MnO enrichment at this time. MnO values in the cratonic

CaO

The CaO content varies systematically across the traverse. With the exception of the Hawick Group the cratonic derived greywackes have a 2-3% lower CaO content than their volcanic counterparts. The Hawick Group is however, characterised by the highest CaO content of any unit in this succession, due to a significant input of carbonate from the source terrain. CaO values in the cratonic formations are positively correlated with Mn and inversely correlated with Al, Na, Nb, La, Rb/Sr. In opposition, CaO values in the volcanic formations are positively correlated with Mn, and inversely correlated with Al, K, Rb, Sr, Ba, La, and Nb.

Na₂O

The Na₂O content reflects the variation in petrography across the Southern Uplands with high values associated with volcanic derived greywackes and relatively lower values associated with their cratonic counterparts (the mean volcanic composition is 0.8% higher than cratonic). The only variation to this pattern occurs in the Pyroxenous Formation (volcanic) where values differ little from the juxtaposed Shinnel Formation (cratonic). However, both the Intermediate Formation and Hawick Group (south of the Pyroxenous Formation) show marked decreases in Na₂O content with respect to the Pyroxenous Formation. Throughout the succession the effects of hydrothermal alteration are displayed dramatically by the virtual total depletion of Na₂O in altered samples. This factor, linked with the enrichment of major and trace elements in the vicinity of alteration systems provides a powerful guide to the recognition of primary targets for further mineral exploration. Na₂O values in the cratonic formations are positively correlated with Sr and P; and inversely correlated with Ca, As, Rb/Sr, K and Ni. In the volcanic formations Na₂O values are positively correlated with Sr, and inversely correlated with K, Al, Mg, Ca, Cr, Rb, Mg/Fe and Rb/Sr.

K₂O

Systematic differences in K₂O content between cratonic and volcanic derived greywacke formations are only clearly illustrated during Ordovician times, between the Marchburn, Afton, Blackcraig and Scar Formations (mean volcanic content is 0.5 wt% lower than cratonic). Thereafter, variation is minimal with the exception of samples associated with hydrothermal activity/mineralization which show marked increases in K₂O content, counterbalanced by decreased Na₂O values. K₂O values in the cratonic formations are positively correlated with Rb, Ba, La, Al, Ni, Rb/Sr and Y; and inversely correlated with Na. In opposition, K₂O values in the volcanic formations are positively correlated with Al, Rb, Ba, La, Sr, and Zr; and inversely correlated with Ti, Fe, V, Ca, Na, Mn and Y.

MnO

Although the MnO content of all samples was low (<0.25%) systematic variations can be observed between cratonic and volcanic derived greywackes with the former relatively depleted with respect to its volcanic counterpart (mean volcanic composition is 0.05% higher than cratonic). This trend prevails throughout the succession, however it is noteworthy that the Hawick Group contains slightly elevated MnO values compared with the neighbouring Intermediate Formation. Given the close petrographic similarity between the non-carbonate mineralogy of these two formations, the strong, positive correlation between CaO and MnO may be used to infer that Mn rich carbonate was the most probable source of MnO enrichment at this time. MnO values in the cratonic

formations are positively correlated with Ca, Sr, V and K/Na, whereas MnO values in the volcanic formations are positively correlated with Ti, Fe, Ca, V and Mg+Fe and Fe/Mg; and inversely correlated with Al, K, Pb, Rb and Rb/Sr.

P₂O₅

Detailed study of the diagram reveal a subtle trend towards decreasing P₂O₅ content across the succession, with notably higher values occurring in the Marchburn Formation (volcanic). P₂O₅ values in the cratonic formations are positively correlated with Ti, Na, La, Sr, V, Y, Zr and Mg+Fe. P₂O₅ values in the volcanic formations are positively correlated with La, Nb, Sr, Al, Ba, Co, Ga, Zr, Al/Si, La/Y and Nb/Y.

As

The background values of arsenic in greywackes from the Southern Uplands lies close to or below the detection limit of the XRF (2-3ppm). The mean composition of volcanic greywackes is 1-2ppm lower than the cratonic samples. In addition, numerous occurrences of As levels in excess of 10ppm define samples of considerable exploration interest. If support in the form of additional major and trace element enrichment (or sodium depletion) is identified, the sample may be defined as hydrothermally altered and the location earmarked for future evaluation. As values in the cratonic formations are positively correlated in order of significance, with Sb, Fe/Mg, Rb/Sr, Na/K, and K/Na+K; and inversely correlated with Na. As values in the volcanic formations are positively correlated with Sb, Zn, Rb/Sr and Al/Ca+Na.

Ba

Although there is no systematic variation in Ba content across the succession, individual formations exhibit sharp contrasts with juxtaposed units. This feature is most clearly illustrated by the Blackcraig and Scar formations. Ba values in the cratonic formations are positively correlated in order of significance, with K, Al, Rb, Sr, Al/Si, Na+K, Ga and La. Ba values in the volcanic formations are positively correlated with K, Ti, Fe, Ca, V and Y.

Co

The Co content of the greywackes is highly variable throughout the succession. The Ordovician volcanic greywackes are on average 5-8ppm lower than juxtaposed cratonic. In addition, the Intermediate Formation displays high and erratic values in comparison with the Hawick Group. Co values in the cratonic formations are positively correlated with Al and Al/Si; and inversely correlated with Th and Nb/Y. Co values in the volcanic formations are positively correlated with Al, Al/Si, Mg, P, V and Ga.

Cr

A systematic trend of decreasing Cr values across this succession occurs with average volcanics 30-150ppm higher than their cratonic counterparts. Extremely high Cr values (up to 900ppm) characterise the Marchburn Formation and are indicative of a greater proportion of basic/ultrabasic lithologies in the source terrain (in comparison with the other volcanic formations present in the Southern Uplands). Possible host minerals include chromium-rich

magnetite, spinel, chromite and olivine. Cr values in the cratonic formations are positively correlated with Mg, Ni, V, Fe, Mg+Fe, Ni/Co and Zr/Nb; and inversely correlated with Nb/Y. In the volcanic formations Cr values are positively correlated with Mg, Ni, Ti, Fe, V, Mg+Fe, Ni/Co and basic clasts.

Cu

Volcanic derived greywacke formations display slightly elevated Cu values compared to their cratonic counterparts. Very high Cu levels are associated with a variety of mineralization styles and should be viewed in light of additional trace element enrichment in order to more clearly define the nature of the hydrothermal input. In general, Cu values in the cratonic formations are positively correlated with Fe, V, Zn, Ba, S, Al, Ti, and Mg+Fe, whereas Cu values in the volcanic formations are positively correlated with Al, Al/Si, Pb and Ga.

Ga

Highly consistent Ga values are displayed across the entire succession, with subtle variation (3-4ppm) in composition between volcanic (higher) and cratonic (lower) derived formations. Ga values in the cratonic formations are positively correlated with Al, Ti, Fe, Ba, Rb, La, V and Mg+Fe; whereas Ga values in the volcanic formations are positively correlated with Zn, Al, Fe, Ti, Mg, Na, P, Cu, Sr, V, and Mg+Fe.

La

Systematic variations in La content occur across the entire succession with cratonic formations exhibiting levels 10-15ppm greater than their volcanic counterparts. La values in the cratonic formations are positively correlated with Al, K, Rb, Y, Nb, Ti, P, Ba, Ga, Th, and Zr; and inversely correlated with CaO, whereas in the volcanic formations La values are positively correlated with Al, Ba, P, Nb, Rb, Sr, Zr, K and Th; and inversely correlated with Fe, Ca and V.

Ni

A general decrease in Ni content is observed across the succession, with volcanic derived units defined by values 40-60ppm higher than their cratonic counterparts. The Marchburn Formation is again characterised by extremely high Ni values (>250ppm). Ni values in the cratonic formations are positively correlated with Mg, Cr, K, V and Y; and inversely correlated with Na. In opposition, Ni values in the volcanic formations are positively correlated with Mg, Cr, Cu, Ti and Fe; and inversely correlated with Na and Y.

Nb

Subtle systematic variations in Nb content occur throughout the succession with volcanic formations 5-15ppm lower than their juxtaposed cratonic counterparts. Particularly sharp contrasts occur between the Afton and Blackcraig/Scar Formations. Nb values in the cratonic formations are positively correlated with Ti, Ga, La, Al, Th and Zr; and inversely correlated with Ca, whereas Nb values in the volcanic formations are positively correlated with La, P, Y and Zr; and inversely correlated with Ca.

Pb

Highly consistent Pb values occur throughout the succession. No systematic variation is observed however, anomalous values are indicative of proximity to mineralization. Pb values in the cratonic formations are positively correlated with K, Ba, Zn and Zr/Co; whereas in the volcanic formations Pb values are positively correlated with Al, La/Y, Na, K, Ba, Cu, Rb and Sr; and inversely correlated with Ti, Fe, Mn, V, Y and Mg+Fe.

Rb

A systematic increase in Rb values are observed across the succession with volcanic derived formations 20-30ppm lower than their juxtaposed counterparts. Rb values in the cratonic formations are positively correlated with Al, K, Ba, La, Ga and Y; whereas Rb values in the volcanic formations are positively correlated with K, Al, Sr, Ba, La, Zr and Na/K; and inversely correlated with V, Y, Ti, Fe, Ca, Na and Mn.

Sr

Systematic variations in Sr content occur throughout this succession with the mean composition of volcanic formations 130-200ppm higher than the cratonic derived greywackes. Sr values in the cratonic formations are positively correlated with Na, Ba, Mg, Mn, P and Na+K; and inversely correlated with Nb/Y. Sr values in the volcanic formations are positively correlated with Rb, La, Al, P, Ba, Pb, Na+K and Zr; and inversely correlated with Ti, Fe and Nb/Y. It should be noted that high Ca-Sr ratios may be used to imply the influence of carbonate input.

Sb

With the background level of Sb close, if not below the detection limits of the XRF (1-3ppm) all values in excess of 5ppm define metal anomalies worthy of further investigation. The average Sb content of the volcanic formations is 0.4-1.6ppm lower than that defined for the cratonic units. Sb values in the cratonic formations are positively correlated with As and inversely correlated with Na; whereas Sb values in the volcanic formations are positively correlated with As, Cu and Cu/Co.

S

A systematic decrease in S content across the succession is clearly identified, with volcanic formations containing 200-1000ppm higher values than their juxtaposed cratonic counterparts. The Hawick Group is characterised by extraordinarily low values (<50ppm) which may be inversely correlated with increases in CaO content. S values in the cratonic formations are positively correlated with Fe, Cu, Zn and V; whereas S values in the volcanic formations are positively correlated with Fe, Ti, V and Ga; and inversely correlated with Sr, Zr and La/Y.

Th

A consistent pattern of Th values occur throughout the succession with volcanic derived greywackes generally 4-6ppm lower than their juxtaposed cratonic counterparts. Th values in the cratonic formations are positively

correlated with Ti, Fe, K, La and Ni/Co; and inversely correlated with Co. Th values in the volcanic formations are positively correlated with K, La, Rb, Ba, Sr, Zr and La/Y; and inversely correlated with V, Ti, Fe, Ca, and Co. In general, a positive correlation between Th and LREE is identified.

V

A systematic decrease in V content occurs across the succession with volcanic derived formations exhibiting concentration 50-100ppm higher than their juxtaposed cratonic sediments. Vanadium is typically located as a trace element within ferromagnesian minerals which reside with the mafic component of the greywacke. V values in the cratonic formations are positively correlated with Ti, Fe, Mg, Cu, Cr, Mn, P, Y and Zn; whereas V values in the volcanic formations are positively correlated with Ti, Fe, Mn, Mg, Ca, S, Y, Zn, and Mg+Fe; and inversely correlated with K, Rb, Ba, Sr, Ga, La, Th and Zr.

Y

The Y values throughout this succession are highly consistent and display no systematic variation. The Scar Formation displays the lowest values in the sequence, whereas the highest values are located in the Hawick Group. Y values in the cratonic formations are positively correlated with P, La, Al, Ti, Fe, Ca, As and Rb/Sr; whereas in the volcanic formations Y values are positively correlated with Ti, Fe, V, Mn, Nb, Zn and Fe/Mg; and inversely correlated with Rb, La/Y, Al, Mg, K, Ni, Pb and Sr.

Zn

A systematic variation in Zn content is observed across the succession with volcanic derived greywackes 10-30ppm higher than juxtaposed cratonic sediments. Zn values in the cratonic formations are positively correlated with Cu, Ga, Al, Ti and Fe; whereas Zn values in the volcanic formations are positively correlated with Ti, Fe, Ga, V, Y, As and Nb.

Zr

A systematic variation in Zr content occurs across the succession with volcanic derived greywackes displaying values 100-150ppm lower than juxtaposed cratonic greywackes. The Hawick Group however, displays significantly lower values than expected when compared to the adjacent Intermediate Formation (cratonic). This factor may be attributed to the dilution effects caused by the addition of 10-15% carbonate to the Hawick (Wenlock) greywackes. Zr values in the cratonic formations are positively correlated with La, Ti, Cr and P; whereas Zr values in the volcanic formations are positively correlated with La, Nb, Rb, Ba, Sr, Th and P; and inversely correlated with Ti, Fe, S and V. It should be noted that Ti, Zr, Y and Nb are all high field strength elements (charge/radius ratio) which are not usually transported in aqueous fluids and as such, are relatively unaffected by hydrothermal alteration.

Al/Si

The highly variable Al/Si content across the succession displays no systematic pattern of variation.

Fe/Mg

This ratio displays a systematic decrease with time across the succession, is relatively consistent and as such of little use in distinguishing between volcanic and cratonic provenance.

Fe+Mg

This variable mirrors the pattern displayed by its two components and displays a systematic decrease across the succession with volcanic formations higher than the cratonic formations. Notably high values occur in the Marchburn Formation.

K+Na

The total alkali content of the greywackes is highly variable throughout the section, with the volcanic formations generally higher than the cratonic. The Hawick Group provides the lowest values of any formation in the Southern Uplands.

K/Na

This variable is very consistent throughout the succession with the volcanic formations generally lower than their cratonic counterparts. In addition this ratio serves to enhance the effects of hydrothermal activity, present in the form of sodium depletion and/or potassium metasomatism (ie. alkali exchange) and provides a useful geochemical guide to mineralization.

K/(K+Na)

This ratio defines a consistent pattern of values, with the volcanic formations slightly lower than their cratonic counterparts. The consistent background values define a threshold level above which, an alteration index is superimposed. This ratio may be used in a similar manner to K/Na however, it is the authors contention that the simpler of the two ratios is more applicable to exploration, as the variation between background and anomaly levels is considerably enhanced.

Al/Ca+Na

With the exception of the Hawick Group, a systematic pattern of variation occurs throughout the succession with volcanic formations generally lower than their juxtaposed cratonic counterparts. Confusion arises in the Hawick Group due to both the general increase in CaO and the depletion of Na₂O associated with hydrothermal activity.

La/Y

Although highly variable, a systematic pattern of variation is observed across the succession with the Ordovician volcanic derived formations characterised by low values than their cratonic counterparts.

Nb/P

A systematic variation occurs across the entire succession with the volcanic derived formations characterised by lower values than their cratonic counterparts.

Nb/Y

This ratio mirrors that of Nb/P however the characteristic low values defining the Blackcraig Formation should be noted for future reference.

Rb/Sr

This ratio provides a clear illustration and discrimination index between volcanic derived greywackes (low) and their cratonic counterparts (high). Note the anomalous values in the Hawick Group which correspond to enrichments in As content and hydrothermal activity.

Ni/Co

A systematic decrease across the succession is defined by this ratio, with the volcanic formations displaying higher values than their juxtaposed counterparts. Ni/Co values correlate well with both Fe and S inferring a possible pyrite host mineral.

Cu/Co

The Cu/Co ratio displays highly erratic values and little if any systematic variation attributable to petrographic changes.

Zn/Co

The Zn/Co ratio displays variable, erratic values and no significant patterns, even within individual formations.

Zr/Nb

This ratio displays subtle variations which may be attributed to petrographic differences between formations. In general, the volcanic derived greywackes exhibit lower values than their more acidic counterparts. However, when using this ratio for source terrain discrimination the Pyroxenous Formation is indistinguishable from its juxtaposed cratonic counterparts.

Discussion

Taylor and McClennan (1985) noted that in greywackes, the most distinctive geochemical parameters are K_2O/Na_2O and $FeO+MgO$. Trailing edge greywackes typically have $FeO+MgO < 5\%$ and $K_2O/Na_2O > 1$. Forearc greywackes have $FeO+MgO > 8\%$ and $K_2O/Na_2O < 0.5$. Greywackes in back-arc basins and leading-edge basins

have intermediate values, consistent with their petrography. In comparison with greywackes from the Southern Uplands, this form of simple discrimination identified forearc settings for the Marchburn and Blackraig formations, trailing edge settings for the Afton and Intermediate Formations and the Hawick Group, and back-arc settings for the Scar, Shinnel and Pyroxenous formations. In summary, these results indicate a trend across the Southern Uplands, typified by early forearc/continental margin environment, which evolved with time into a back-arc basin and subsequent passive margin. The geochemistry of the individual formations identified in the Southern Uplands are reviewed in detail in the following sections.

5.4.2 The Marchburn Formation

The Marchburn formation is correlated on stratigraphic, petrological and lithological criteria (Floyd, 1982) with the Traboyack Division of the Tappins Group (Williams, 1962) located between Girvan and Barhill. Greywackes of this formation are rich in feldspar and rock fragments, and quartz poor (~14%). Analytical data for the Marchburn Formation greywackes are given in table 2.51 and summarised statistically in table 2.30. It should be noted that the samples are presented in ascending sample number which bears little if any relationship to relative stratigraphic position. Marchburn Formation greywackes have a SiO_2 range of 50-65 wt%, high $\text{Fe}_2\text{O}_3 + \text{MgO}$ contents of between 11 and 25 wt%, and low K/Na ratios with a mean of 0.47 (cf. table 2.91). Following the methodology defined by Blatt et al., (1972) and Crook (1974) samples from the Marchburn Formation may be classified as a highly Fe-rich, quartz intermediate greywackes (table 1.49). Total alkali contents lie within the field defined by Maynard et al., (1982) however, note the concentration of values below the $\text{Na/K}=1$ threshold.

Marchburn Formation samples plot (fig 80a) within the Oceanic Island Arc field defined by Bhatia (1983). In the Zr-La-Y triangular diagram (fig.82a) Marchburn Formation samples define a broad elliptical group which plots close to the Zr pole and defines a field for volcanic derived greywackes in the Southern Uplands. The relatively calcium-rich geochemistry of this formation is reflected by subtle increases in plagioclase content. Principal component analysis of Marchburn Formation samples identified mafic/ultramafic (Fe-Mg-Ti-Ni-Cr-V), sulphide (As-Sb-S) and feldspar/Clay (K-Rb-Al) related groupings. Of particular importance to this study of the Marchburn Formation is the Cr geochemistry, which is discussed in detail below:

Cr

The abnormally high Cr contents (up to 905ppm) identified in the Marchburn Formation, represent the most basic/ultrabasic components of any greywacke recorded in any literature, to date and place severe constraints upon the nature of their parental source material. Ricci and Sabatini (1976) demonstrated that high Cr contents (up to 450ppm) located in greywackes from Central Sardinia, were derived from dominantly mafic igneous sources. It is therefore proposed on geochemical grounds that the Marchburn Formation received a substantial input from an ultramafic source. In general, the elevated Cr content can be correlated with the influx of basic/ultrabasic clasts, which are generally limited elsewhere in this succession. In addition, the negative correlation between Cr and Fe/Mg (fig. 366) may be used to suggest a close magmatic relationship within the source material and to rule out any geochemical differentiation of Cr relative to Mg in the sedimentary or diagenetic environments. Both Cr-rich pyroxenes and/or Cr-rich spinels provide the likely sources of Cr enrichment, however elevated Ni values (particularly within the Marchburn Formation) indicate olivine to be a further potential source of Cr enrichment.

The most northerly, geochemically defined formation in the Southern Uplands can be traced along a narrow, strike-parallel tract immediately to the south of the Southern Upland Fault (SUF) linking the Marchburn Formation in Nithsdale (Floyd, 1982) through the Glen App Group south of Ballantrae, to the Corsewall Group on the Rhinns Peninsula (Kelling et al., 1987). It should however, be noted that the Marchburn Formation does not fit the relatively simplistic cratonic/volcanic model for the Southern Uplands. This feature was also recognised by Floyd (1982) and characterised by the presence of lavas and cherts interbedded with greywackes. Furthermore, Fe, Mg, Ni and Cr vs. SiO_2 crossplots, indicate that Marchburn Formation samples are incompatible with a simple andesitic derivation model.

Although mafic rocks contribute to the components of common sandstones, as demonstrated by the occurrence of chromite, pyroxene and other minerals of exclusively mafic igneous origin, sandstones with abundant mafic mineralogy are rare in the stratigraphic record (Van de Kamp and Leake, 1986). Cr and Ni values are of particular interest as high values of both elements require an ultramafic-basic source rock in the provenance area. Chromite is particularly diagnostic and has been used to identify the former presence of now eroded ophiolite sheets from its presence in greywackes (Hiscott, 1984; Van de Kamp and Leake, 1986). It is therefore proposed that high values of Cr, Ni, Ti and Mg identified in the Marchburn Formation are indicative of detritus derived from mafic and ultramafic sources. It should be noted however, that similar high abundances of chrome and nickel ($604 \pm 80\text{ppm}$, $352 \pm 101\text{ppm}$ respectively) identified in the Pilbara Supergroup, western Australia, by McLennan et al., (1983) did not fit easily into their proposed provenance model and were interpreted to result from secondary enrichment processes.

Henley (1970) discussed the application of factor analysis of a series of slates, siltstones and greywackes from the Perranporth area, Cornwall. High Cr and REE values were identified in the Meadfoot Beds (slates) in sharp contrast to the juxtaposed Gramscatho sediments (greywackes, siltstones and slates). It was proposed that the chromium values were associated with a detrital illite or muscovite due to the fact that chromium is strongly adsorbed onto detrital phyllosilicates during transport and only weakly desorbed after deposition. The absence of detailed petrographic controls upon these samples does not preclude the presence of a Cr-bearing mineral phase, such as chromite. Van de Kamp and Leake (1986) noted that mafic-rich sediments derived from mafic volcanic or plutonic rocks preserve an essentially mafic igneous chemistry and as such could form protoliths of amphibolites which grade into metasediments.

It was noted that certain analogies exist between the proposed source area and the Southern Highlands Group of the Dalradian Belt, with its associated serpentinitised units and mafic character. In addition, Young et al., (1988) suggested that Lower Palaeozoic 'volcanic terrains' in Northwest Europe, Newfoundland, Canada and North-western USA were potential hosts for gold deposits. During lithogeochemical exploration within Ordovician and Silurian turbidite successions in Co. Mayo, Young et al., (op.cit) identified high Cr and Ni ($>500\text{ppm}$) in Lower Ordovician units, and interpreted the Cr enrichment in terms of the presence of Cr-mica (fuchsite). Wrafter and Graham (1989) in a more detailed study of trace element enrichments in Ordovician greywackes of South Mayo, noted that enhanced Cr values result from the presence of both detrital chromite grains and Mg-rich chlorite, and proposed an ophiolitic (ultramafic) origin. In opposition, greywackes containing high Ti and Fe values only, were interpreted as mafic in origin.

REE

Figures 446-449 display a series of chondrite normalised REE profiles of Marchburn Formation greywackes from the Southern Uplands. It is probable that the REE are located in fine-grained accessory phosphate minerals such as apatite and monazite. In detail, petrographically defined samples (A232, A233, A234, N237, N241, N292, N294, A297, A299, W379, W380, N413, N426, C472, AX54, AX156, AX214 and AX215, AX216, AX217, AX224, AX292, AX293 and AX294) display LREE enrichment; lower LREE and total REE compared to PAAS; relatively flat HREE patterns and lack the negative Eu-anomaly associated with quartz-rich, cratonic derived sediments. On the basis of the REE evidence presented in Figs. 446-449 it is clear that calc-alkaline andesitic rocks were the most probable primary source for Marchburn Formation greywackes.

Summary

On both petrographic and geochemical grounds (ie. Cr up to 900ppm) the Marchburn Formation samples show a geochemical affinity with basic/ultrabasic igneous material. In general the high Cr and Ni values are indicative of a source area composed of a considerable portion of ultrabasic material. In addition, the geochemistry of the Marchburn Formation suggests that the sources were more varied with a greater proportion of mafic/ultramafic material than at any other time in the development of the Southern Uplands. In summary, the Marchburn Formation greywackes form the most chemically distinct units in the Southern Uplands and are interpreted in terms of a mixed calc-alkaline and basic/ultrabasic provenance.

5.4.3 The Afton (Kirkcolm) Formation

Greywackes of the Afton Formation are characterised by moderate amounts of quartz, rare or absent ferromagnesian minerals and minor feldspar. Afton Formation samples have a SiO_2 range of 56-85 wt%, low $\text{Fe}_2\text{O}_3 + \text{MgO}$ contents of between 4 and 16 wt%, and high K/Na ratios with a mean of 0.95 (refer to tables 2.52 and 2.92 for a complete statistical review). Following the classification scheme defined by Blatt et al., (1972) and Crook (1974) samples from the Afton Formation may be classified as Fe-rich, quartz intermediate/rich greywackes/lithic sandstones (fig.71). Total alkali contents lie within the field defined by Maynard et al., (1982) however, the concentration of values centered upon the $\text{Na/K}=1$ threshold is indicative of a considerable increase in K_2O content in cratonic derived sediments as opposed to their volcanic counterparts. Afton Formation samples displayed on the Th-Co-Zr/10 triangular diagram are skewed towards the Zr pole, and plot within the Continental Island Arc/Passive Margin field defined by Bhatia (op.cit). Afton Formation samples displayed on the Zr-La-Y triangular diagram, plot within a narrow elliptical zone which in comparison to the Marchburn Formation plot closer to the Zr pole but distant from the Y pole and defines a field for cratonic derived greywackes in the Southern Uplands. Figure 450-453 presents a series of chondrite normalised REE profiles of Afton Formation greywackes from the Southern Uplands. Petrographically defined samples (A222, E452, K462, A463, C471, AX131, AX132, AX133, AX134, AX135, AX136, AX137, AX140, AX141, AX149, AX170, AX171, AX172, AX202, AX204, AX222, AX223 and AX296) display highly consistent REE patterns essentially parallel to those of PAAS but with slightly lower LREE enrichment (particularly notable in the relatively flat HREE profile); and (with the exception of samples E452 and K462) Eu depletion (with slightly higher Eu/Eu^* compared with PAAS). On the basis of REE evidence presented in Figs. 450-453 Afton Formation greywackes display characteristics typical of post-Archean upper crust (as indicated by PAAS).

Discriminant Diagrams

Figure 300 displays the relative positions of Marchburn and Afton Formation greywackes on the IUGS classification diagram. Volcanic derived, Marchburn Formation samples are located within the Basaltic-Andesite and Andesite fields whereas the cratonic Afton Formation samples occupy the Andesite and Dacite fields. Afton Formation members form a relatively restricted, consistent range of alkali values as opposed to the Marchburn Formation, where a strong positive relationship exists between silica and alkali.

The CaO-Sr discrimination diagram defined by Caby (1977) is used in figs. 306-312 to display the chemical variation present in the major petrographically distinct formations located in the Southern Uplands Study Area. Figure 306 displays the relative position of Marchburn Formation greywackes on the CaO-Sr discrimination diagram. Note the relatively restricted CaO range (2-5%); the wide range of Sr values (88-857ppm); and the lack of any form of correlation between CaO and Sr. Figure 307 displays the relative position of cratonic derived Afton Formation greywackes and demonstrates a shift towards lower 'cratonic' values compared with their volcanic counterparts; the relatively restricted CaO and Sr range; and the lack of any significant correlation between CaO and Sr.

The SiO_2 -MgO discrimination diagram (fig.313) defined by Bhatia (1983) displays the relative position of volcanic derived Marchburn and cratonic derived Afton Formation greywackes. An inverse relationship is displayed between MgO and SiO_2 in both formations, whereas elevated MgO and restricted SiO_2 values displayed by the Marchburn Formation allow a classification boundary to be erected between the two groups. The SiO_2 -Rb discrimination diagram (fig.317) defined by Bhatia (1983) presents the relative position of Marchburn and Afton Formation greywackes. In summary, this plot displays a weak inverse relationship displayed between Rb and SiO_2 in the Afton Formation, with elevated Rb and SiO_2 values displayed by this formation used to construct a the classification boundary between the two groups. In general, the Marchburn Formation displays restricted SiO_2 and relatively low Rb values.

The SiO_2 -CaO discrimination diagram (fig. 321) defined by Bhatia (1983) is used to display the relative position of Marchburn and Afton Formation greywackes. Note the weak inverse relationship displayed between CaO and SiO_2 in both formations; the relatively elevated CaO and restricted SiO_2 values displayed by the Marchburn Formation; the generally lower CaO values displayed by the Afton Formation; and the approximate position of a classification boundary between cratonic and volcanic derived formations. The SiO_2 -Sr discrimination diagram (fig. 325) defined by Bhatia (1983) may also be used to display the relative position of Marchburn and Afton Formation greywackes. Note the weak inverse relationship displayed between Sr and SiO_2 in the Afton Formation and the stronger positive correlation in the Marchburn Formation; the relatively elevated Sr and restricted SiO_2 values displayed by the Marchburn Formation (mirroring the trend defined by CaO); the generally lower Sr values displayed by the Afton Formation; and the position of a classification boundary between cratonic and volcanic derived formations, controlled predominantly by SiO_2 content.

The SiO_2 - Na_2O discrimination diagram (fig. 329) defined by Bhatia (1983) defines the strong positive correlation displayed between Na_2O and SiO_2 in both Formations; the relatively restricted SiO_2 and slightly elevated Na_2O values within the Marchburn Formation; the parallel trends defined by both formations; the generally lower Na_2O values displayed by the Afton Formation; and the position of a classification boundary between cratonic and volcanic derived formations, controlled predominantly by SiO_2 content.

The SiO_2 - TiO_2 discrimination diagram (fig. 333) defined by Bhatia (1983) is used to display the strong inverse correlation displayed between TiO_2 and SiO_2 in both formations; the relatively restricted SiO_2 and elevated TiO_2 values displayed by the Marchburn Formation; the single SiO_2 - TiO_2 trend defined by both formations; the generally lower TiO_2 values displayed by the Afton Formation; and the position of a classification boundary between cratonic and volcanic derived formations controlled predominantly by SiO_2 content.

The SiO_2 - Fe_2O_3 discrimination diagram (fig.337) defined by Bhatia (1983) is used to display the strong inverse correlation displayed between Fe_2O_3 and SiO_2 in both formations (mirroring the trend defined by TiO_2); the relatively restricted SiO_2 and elevated Fe_2O_3 values displayed by the Marchburn Formation; the single SiO_2 - Fe_2O_3 trend defined by both formations; the generally lower Fe_2O_3 values displayed by the Afton Formation; and the approximate position of a classification boundary between cratonic and volcanic derived formations (controlled predominantly by SiO_2 content).

The $(\text{Fe}_2\text{O}_3+\text{MgO})$ - TiO_2 discrimination diagram (fig.341) defined by Bhatia (1983) details the strong positive correlation displayed between these variables in both formations; the relatively low $\text{Fe}+\text{Mg}$ values displayed by the Afton Formation; the single trend defined by both formations; the generally lower TiO_2 values displayed by the Afton Formation; and the approximate position of a classification boundary between cratonic and volcanic derived formations. The $(\text{Fe}+\text{Mg})$ -(Al/Si) discrimination diagram (fig.345) defined by Bhatia (1983) is used to display the weak positive correlation displayed between these variables in both formations; the relatively low Fe_2O_3 + MgO values displayed by the Afton Formation; the single trend defined by both formations; the generally higher Al/Si values displayed by the Marchburn Formation; and the approximate position of a classification boundary between cratonic and volcanic derived formations.

The $(\text{Fe}+\text{Mg})$ -(K/Na) discrimination diagram (fig.394) defined by Bhatia (1983) is used to display the weak positive correlation displayed between these variables in both Formations; the relatively low $\text{Fe}+\text{Mg}$ values displayed by the Afton Formation; the generally higher K/Na ($>0.5\text{wt}\%$) values displayed by the Afton Formation; and the approximate position of a boundary between cratonic and volcanic derived formations.

The $(\text{Fe}+\text{Mg})$ -($\text{Al}/(\text{Ca}+\text{Na}))$ discrimination diagram (fig. 353) defined by Bhatia (1983) details the poor correlation displayed by both Formations; the relatively low $\text{Fe}+\text{Mg}$ values displayed by the Afton Formation; the elevated $\text{Al}/(\text{Ca}+\text{Na})$ ($>2.5\text{wt}\%$) values displayed by the Afton Formation; and the position of a classification boundary between cratonic and volcanic derived formations. With the exception of the Hawick Group, anomalous $\text{Al}/(\text{Ca}+\text{Na})$ values provide an alteration index relating sodium depletion and clay alteration with hydrothermal activity.

The Th-La discrimination diagram (fig.357) defined by Bhatia (1985) displays the positive correlation displayed by both Formations; the relatively low La and Th values displayed by the Marchburn Formation; the elevated La ($>20\text{ppm}$) and Th ($>5\text{ppm}$) values displayed by the cratonic Afton Formation; and the position of a approximate discrimination boundary between cratonic and volcanic derived formations.

The $(\text{K}/\text{K}+\text{Na})$ -($\text{K}+\text{Na}$) diagram (fig.361) defined by Cathelineau (1983) details the wide scatter and poor correlation displayed by both Formations; the relatively low $\text{K}/\text{K}+\text{Na}$ values (<45) displayed by the Marchburn Formation; and the relatively consistent total alkali levels displayed by both Formations. The $\text{K}/\text{K}+\text{Na}$ variable is used by Cathelineau (op. cit) to assess the level of potassic metasomatism present within individual samples,

and this is compared with the total alkali content of the samples in order to assess the possible effects of sodium addition or depletion. In addition, it should be noted that the position of a discrimination boundary between cratonic and volcanic derived formations may be defined on the basis of K/K+Na content alone.

The (Fe/Mg)-Cr discrimination diagram defined by Ricci and Sabatini (1976) was originally used to demonstrate the relationship between the presence of mafic clast components and elevated Cr values (up to 450ppm). In addition, the negative correlation between Cr and Fe/Mg was also used to suggest a close magmatic relationship within the source material and to rule out any geochemical differentiation of Cr relative to Mg in the sedimentary, diagenetic or metamorphic environments. Both Cr-rich pyroxenes and/or Cr-rich spinels provide the likely sources of Cr enrichment in the Southern Uplands Study area. In addition, elevated Ni values (particularly the Marchburn Formation) indicate olivine to be a further potential source of Cr enrichment. Figure 366 displays the relative position of Marchburn and Afton Formation greywackes on this diagram. Note the inverse correlation displayed by both formations (inferring a positive correlation between Mg and Cr); the relatively low Cr values (<250ppm) displayed by the Afton Formation; the highly elevated Cr values (max 905ppm) and restricted Fe/Mg values (<2.2) displayed by the Marchburn Formation; and the position of a discrimination boundary between cratonic and volcanic derived formations which may be defined on the basis of Cr content alone.

The Y-CaO discrimination (fig.370) diagram defined by Lambert and Holland (1982) details the narrow, restricted range of Y values defined by each formation; the poor correlation displayed by both formations; and the relatively elevated Sr levels (>150 ppm) displayed by the Marchburn Formation, controlling the position of a discrimination boundary between cratonic and volcanic derived formations. The Sr-Y discrimination diagram (fig.374) also defined by Lambert and Holland (1982) displays the narrow, restricted range of Y values defined by both formations; the poor correlation displayed by both formations; and the relatively elevated CaO levels (>1.5 wt%) displayed by the Marchburn Formation. The position of a discrimination boundary between cratonic and volcanic derived formations is poorly constrained by this diagram. The K₂O-Rb discrimination diagram (fig.378) defined by Rock (1985) is used to detail the narrow compositional range, single trend and positive correlation displayed by both formations; the overlapping compositional ranges; and the elevated Rb and K₂O levels displayed by the Afton Formation. The position of a discrimination boundary between cratonic and volcanic derived formations is poorly constrained on this diagram due to the level of overlap between the two groups.

The MgO-Sr discrimination diagram (fig.383) defined by Rock (1985) displays the wide scatter and inverse relationship displayed between MgO and Sr in the Marchburn Formation; the narrow restricted range of MgO and Sr values (MgO <6wt% and Sr <200wt%) displayed by the Afton Formation; and the classification boundary between the two groups. The Cr-V discrimination (fig.387) diagram defined by Rock (1985) details the narrow, relatively restricted range of V values (<150ppm) defined by the Afton Formation; the strong positive correlation displayed by both groups; and the elevated V and Cr levels (>130ppm and 200-905ppm respectively) displayed by the Marchburn Formation. The position of a discrimination boundary between cratonic and volcanic derived formations may be identified solely on the basis of V content (Cratonic Formations <130ppm). The Ni-Cr discrimination diagram (fig. 391) defined by Clayton (1982) is used to display the narrow, relatively restricted range of Cr (<250ppm) and Ni values (<100ppm) defined by the Afton Formation; the strong positive correlation and single trend displayed by both groups; the elevated Ni and Cr levels (>100ppm and >250ppm respectively) displayed by the Marchburn Formation; and the position of a discrimination boundary between cratonic and volcanic derived formations.

The Zr-Y discrimination diagram (fig.395) defined by Clayton (1982) details the strong positive correlation displayed between both formations; the low Zr values ($<230\text{ppm}$) displayed by the Marchburn Formation; the generally higher Zr ($>230\text{ppm}$) values displayed by the Afton Formation; the relatively restricted Y values (20-30ppm) displayed by both Formations; and the position of a boundary between cratonic and volcanic derived formations based upon the $\text{Zr}=230\text{ppm}$ threshold. The (Fe/Mg)-Zr discrimination diagram (fig.399) defined by Clayton (1982) is used to detail the strong positive correlation displayed by Marchburn Formation samples; the wide scatter and elevated Zr values ($>230\text{ppm}$) displayed by the Afton Formation; the generally lower Zr ($<230\text{ppm}$) values displayed by the Marchburn Formation; and the position of a boundary between cratonic and volcanic derived formations based upon the $\text{Zr}=230\text{ppm}$ threshold. The Zr-TiO₂ discrimination diagram (fig.403) defined by Pierce (1982) is used to display the relative position of Marchburn and Afton Formation greywackes. Note the strong positive correlation displayed both Marchburn and Afton Formation samples; the elevated Zr ($>230\text{ppm}$) and relatively restricted TiO₂ values ($<1.4\text{wt}\%$) displayed by the Afton Formation; the generally lower Zr ($<230\text{ppm}$) and elevated Ti values displayed by the Marchburn Formation; and the position of a boundary between cratonic and volcanic derived formations based upon the $\text{Zr}=230\text{ppm}$ and $\text{TiO}_2=1.4\text{wt}\%$ thresholds.

The (La/Y)-(Nb/Y) discrimination diagram (fig.407) defined by Bell (pers. com, 1984) details the positive correlation and single trend displayed by both Marchburn and Afton formations; the elevated La/Y (>1) and Nb/Y (>0.55) values displayed by the Afton Formation; the generally lower La/Y (<1) and Nb/Y (<0.55) values displayed by the Marchburn Formation; and the position of a boundary between cratonic and volcanic derived formations defined on the basis of the $\text{La/Y}=1.00$ threshold. The higher La/Y values displayed by relatively acid, cratonically derived Afton Formation greywackes may be used to infer the relative enrichment of LREE.

5.4.4 Blackcraig Formation

Blackcraig Formation greywackes have a SiO₂ range of 51-68 wt%, high Fe₂O₃ + MgO contents of between 10 and 14 wt%, and low K/Na ratios with a mean of 0.42 (refer to table 2.93 for a complete statistical review). Following the classification scheme defined by Blatt et al., (1972) and Crook (1974) samples from the Blackcraig Formation (fig.72) may be classified as Fe-rich, quartz intermediate greywackes. Total alkali contents lie within the field defined by the Marchburn Formation, and provided further evidence of the volcanic affinities of the Blackcraig Formation.

The Th-Co-Zr/10 classification diagram (fig.80c) may be used to demonstrate that the Blackcraig Formation samples are more closely constrained than the Marchburn samples and plot within the Oceanic Island Arc field defined by Bhatia (1983). The Zr-La-Y classification diagram (fig.82c) depicts Blackcraig Formation samples within a similar field to that of the Marchburn Formation, with a slight shift of the center of the cluster towards the Y pole. A series of chondrite normalised REE profiles are presented in fig.454 which may be used to define the composition of six petrographically defined samples from the Blackcraig Formation (A20, A21, A45, AX288, AX289 and AX290). These samples display lower total REE compared to PAAS; low, relatively flat HREE patterns; and lack the negative Eu-anomaly associated with quartz-rich, cratonic derived sediments. On the basis of the REE evidence, calc-alkaline andesitic rocks were the dominant primary source of Blackcraig Formation greywackes.

5.4.5 Scar Formation

The Scar Formation (now a junior synonym of the Portpatrick Formation) is characterised by quartz-poor greywackes, rich in feldspar, ferromagnesian minerals and andesitic lithoclasts. Though stratigraphically younger than the Galdenoch Formation, it displays similar petrography and calc-alkaline volcanic island-arc provenance (Stone et al., 1987). In general, Scar Formation greywackes have a SiO_2 range of 53-76 wt%, high $\text{Fe}_2\text{O}_3 + \text{MgO}$ contents of between 6 and 17 wt%, and moderate K/Na ratios with a mean of 0.60 (table 2.94). Following the methodology defined by Blatt et al.(1972) and Crook (1974) samples from the Scar Formation (fig.73) may be classified as Fe-rich, quartz intermediate greywackes. Alkali contents lie within the field defined by the volcanic Marchburn Formation (below the $\text{Na/K}=1$ threshold) and provide further evidence for the volcanic affinity of this formation. The Th-Co-Zr/10 classification diagram (fig.80d) displays the position of Scar Formation greywackes (fig.80d) within the Oceanic Island Arc/Continental Island Arc fields defined by Bhatia (1983). Further evidence of a volcanic derivation is displayed by the Zr-La-Y classification diagram (fig.82d) in which Scar Formation samples are closely grouped within the center of the field originally defined by the Marchburn Formation.

Chondrite normalised REE profiles of Scar Formation greywackes from the Southern Uplands are presented in Figs. 455-460. Petrographically defined samples analysed include: S102, S105, S110, S111, S116, E117, S118, S119, S121, S122 S124 and S126, S127, S128, E136, E139 and E140, AX111, AX112, AX117, AX119, AX124, AX157, AX158, AX159, AX181, AX190, AX191, AX200, AX210, AX211, AX213, AX275, AX277, AX278 and AX279) In detail, these profiles display a highly constrained pattern of REE values with LREE enrichment; lower total REE compared to PAAS; low, relatively flat HREE patterns; and significantly no negative Eu-anomaly (normally associated with quartz-rich, cratonic derived sediments). On the basis of the REE evidence it may be inferred that calc-alkaline andesitic rocks formed a major primary component of Scar Formation greywackes.

Discrimination Diagrams

The relative positions of Blackcraig and Scar Formation greywackes are displayed using the IUGS classification diagram (fig.301). Petrographically, both formations display strong volcanic affinities, and in this diagram, samples are concentrated within the Basaltic-Andesite and Andesite fields. It should be noted that although both formations display similar ranges, the Scar Formation displays slightly elevated alkali values in comparison with the Blackcraig Formation. The CaO-Sr discrimination diagram (fig.308) displays the relative position of volcanic derived Blackcraig Formation greywackes a details a shift towards higher values compared with their cratonic counterparts; a highly restricted range of CaO and Sr values; and the lack of correlation between CaO and Sr. Figure 309 displays the relative position of Scar Formation greywackes on the CaO-Sr discrimination plot and details the positive shift and extended range of Sr values compared with the Blackcraig Formation and the weak positive correlation between CaO and Sr. The relative position of Blackcraig and Scar Formation greywackes on the SiO_2 -MgO discrimination diagram is displayed in fig.314. Here, a strong inverse relationship exhibited between SiO_2 and MgO in both formations. In addition, elevated MgO values are identified in the Scar Formation and both groups overlap the volcanic field, defined in fig.316.

The SiO_2 -Rb discrimination diagram (fig.318) displays the lack of correlation between both elements; the grouping of Blackcraig Formation samples below the $\text{Rb}=30\text{ppm}$ threshold; the relatively elevated Rb values present in the Scar Formation; and the overlapping position of 75% of both groups within the volcanic field (defined in fig.317). The SiO_2 -CaO discrimination diagram (fig.322) identifies the lack of correlation between both elements and the

overlapping position of both formations with the volcanic field previously defined by the Marchburn Formation (fig.321). The SiO_2 -Sr discrimination diagram (fig.326) displays the relatively restricted Sr content of Blackcraig Formation greywackes ($\text{Sr} < 300\text{ppm}$) and the overlapping position of both groups within the volcanic field previously defined in figure 325.

Figure 330 displays the relative position of Blackcraig and Scar Formation greywackes on the SiO_2 - Na_2O discrimination diagram and reveals the weak positive correlation defined between both elements; the restricted SiO_2 content and generally elevated Na_2O values identified by both formations; and the overlapping position of both groups within the volcanic field defined in fig. 329. The SiO_2 - TiO_2 discrimination diagram (fig.334) details the weak inverse correlation defined between both elements; the separation of both volcanic formations on the basis of their TiO_2 content (Scar Formation $< 1.15\text{wt}\%$ TiO_2); the restricted SiO_2 values identified by both Formations; and the position of both groups within the volcanic field defined in Fig. 329, with the Blackcraig Formation exhibiting a close chemical affinity to the Marchburn Formation.

The SiO_2 - Fe_2O_3 discrimination diagram (fig.338) details a weak inverse correlation defined between both elements; the separation of both volcanic formations on the basis of their Fe content (Scar Formation $< 8.3\text{wt}\%$ Fe_2O_3); the low, restricted SiO_2 values identified by both formations; the position of both groups within the volcanic field defined by the Marchburn Formation in Fig. 337. Here again, the Blackcraig Formation exhibits a close chemical affinity with the Marchburn Formation.

The (Fe+Mg)-Ti discrimination diagram (fig.342) displays the strong positive correlation defined between both elements; the separation of both volcanic formations on the basis of their TiO_2 content (Scar Formation $< 1.1\text{wt}\%$ TiO_2); the relatively high Fe_2O_3 +MgO values identified in both Formations; the position of both groups within the volcanic field defined by the Marchburn Formation (fig.341). The (Fe+Mg)-(Al/Si) discrimination diagram (fig.346) details a positive correlation defined between both variables; the overlapping nature of both volcanic formations; the relatively high Fe_2O_3 +MgO values identified in both formations; and the position of both groups within the volcanic field defined by the Marchburn Formation (fig.345). The (Fe+Mg)-(K/Na) discrimination diagram (fig.350) revealed a poor correlation defined between both variables; the overlapping nature of both volcanic formations with high Fe+Mg ($> 11\text{wt}\%$) and low K/Na values identified in both Formations; and the position of both groups within the volcanic field defined by the Marchburn Formation (fig.349).

The (Fe+Mg)-(Al/(Ca+Na)) diagram (fig.354) displays a poor correlation defined between both variables; the overlapping nature of both volcanic formations; the high Fe+Mg ($> 11\text{wt}\%$) and low Al/(Ca+Na) values identified in both Formations; and the position of both groups within the volcanic field defined by the Marchburn Formation in Fig. 353. The Th-La discrimination diagram (fig.358) displays a weak positive correlation defined between La and Th; the overlapping compositional fields and generally low ($< 10\text{ppm}$) Th levels in both formations; the relatively low La values ($< 17\text{ppm}$) identifying Blackcraig Formation samples; and the concentration of both groups within the volcanic field defined by the Marchburn Formation in (fig.357). The (K/K+Na)-(K+Na) diagram (fig.362) displays the relative position of Blackcraig and Scar Formation greywackes and details the weak positive correlation defined by Blackcraig Formation samples; the overlapping compositional fields and low (< 45) K/K+Na levels in both Formations; the relatively lower K+Na values ($< 4\text{wt}\%$) characteristic of Blackcraig Formation samples; and the concentration of a large proportion ($> 80\%$) of samples within the volcanic field defined by the Marchburn Formation in Fig. 361.

The Fe/Mg-Cr diagram (fig.367) displays the weak inverse correlation defined by both Formations; the relatively low Fe/Mg ratio (<1.6) and elevated Cr values (max 476ppm) defined by the Scar Formation; the discrimination of both formations on the basis of Fe/Mg content; and the relatively low Cr levels (<200ppm) displayed by the Blackcraig Formation samples; and the grouping of a large portion (>95%) of samples within the volcanic field defined by the Marchburn Formation in Fig. 366. The Y-CaO diagram (fig.371) displays a poor correlation within both formations; the relatively low Y values displayed by the Scar Formation; the distinct compositional fields of both Blackcraig and Scar Formations separated by the Y=25ppm threshold; and the slight positive shift in CaO values displayed by the volcanic Blackcraig Formation.

The Sr-Y discrimination diagram (fig.375) displays the relative position of Blackcraig and Scar Formation greywackes and details the weak positive correlation defined by both formations; the relatively low Y and elevated Sr values displayed by the Scar Formation; the distinct compositional fields of both Blackcraig and Scar Formations separated by the Y=25ppm threshold; and the restricted Sr values (<300ppm) displayed by the volcanic Blackcraig Formation. The K₂O-Rb discrimination diagram (fig.379) displays the narrow compositional range, single trend and strong positive correlation defined by both formations; the relatively restricted Blackcraig Formation values; and the overlapping compositional fields of both Blackcraig and Scar Formations. The MgO-Sr discrimination diagram (fig.384) details the wide scatter, and poor correlation displayed between Sr and MgO in the Scar Formation; the weak positive correlation and relatively restricted MgO and Sr values (MgO <6wt% and Sr <200wt%) present in the Blackcraig Formation; and the overlapping position of both groups within the volcanic field defined by fig. 383.

The Cr-V discrimination diagram (fig.388) displays the relative position of Blackcraig and Scar Formations and details the strong positive correlation, relatively narrow Cr values and elevated V levels (>130ppm) defined by the Blackcraig Formation; the poor correlation and restricted V levels displayed by the Scar Formation; and the overlapping position of both groups within the volcanic field defined by the Marchburn Formation. The Ni-Cr Discrimination Diagram (fig.392) displays the strong positive correlation and single trend displayed by both groups; the relatively restricted Ni and Cr values (>100ppm and >250 ppm respectively) displayed by the Blackcraig Formation (ie. a 'cratonic' signature); the relatively elevated Ni and Cr levels defined by the Scar Formation; and the slight overlap of both groups within the cratonic field defined by the Afton Formation. The Zr-Y discrimination diagram (fig.396) displays the parallel trend displayed by both groups; and the relatively restricted Y values (<24ppm) displayed by the Scar Formation; and the location of both formations within the volcanic field defined by the Marchburn Formation. The Fe/Mg-Zr discrimination diagram (fig.400) displays the weak inverse correlation and single trend displayed by both formations; the restricted (Fe/Mg) values (<1.7) displayed by the Scar Formation; the low Zr values (<200ppm) displayed by both Formations; and the position of both groups within the volcanic field defined by the Marchburn Formation.

The Zr-TiO₂ discrimination diagram (fig.404) details the parallel geochemical trends displayed by the Blackcraig and Scar Formations; the restricted TiO₂ (<1.2wt%) and Zr (<230ppm) values displayed by the Scar Formation; the elevated TiO₂ (>1.2wt%) and low Zr values (<200ppm) displayed by the Blackcraig Formation; and the overlapping position of both groups within the volcanic field defined by the Marchburn Formation. The La/Y-Nb/Y discrimination diagram (fig.408) displays the correlation and single trend displayed by both Formations; the elevated La/Y (>1) values displayed by the Scar Formation; the relatively low La/Y and Nb/Y values identifying the Blackcraig Formation; and the overlapping position of both groups within the volcanic field defined by the Marchburn Formation.

5.4.6 Shinnel Formation

Shinnel Formation greywackes have a SiO_2 range of 55-77 wt%, low $\text{Fe}_2\text{O}_3 + \text{MgO}$ contents of between 4 and 9 wt%, and moderate to high K/Na ratios with a mean of 0.82 (table 2.95). Following the methodology defined by Blatt et al., (1972) and Crook (1974) samples from the Shinnel Formation (fig.74) may be classified as Fe-rich, quartz intermediate greywackes. Alkali contents are centred upon the $\text{Na/K}=1$ threshold, though skewed towards the $\text{Na/K}=0.7$ threshold and as such provide conflicting evidence for the affinity of this formation. The Zr-La-Y classification diagram details the position of Shinnel Formation samples within the field originally defined by the cratonic derived Afton Formation. Furthermore, the Th-Co-Zr/10 discrimination diagram (fig.81a) details a positive skewed towards the Zr pole, with samples concentrated within the Continental Island Arc/Passive Margin field defined by Bhatia (1983). Chondrite normalised REE profiles of Shinnel Formation greywackes from the Southern Uplands are displayed in figs. 461-463. Petrographically defined samples (S54, S56, S58, S64, N400, N401, N456, S466, S492, S494, AX1, AX36, AX38, AX164, AX177, AX226, AX229, AX235, AX236 and AX276) display REE patterns parallel to those of PAAS with slightly lower total REE levels; and Eu depletion anomalies. On the basis of the REE evidence and in comparison with PAAS, Shinnel Formation greywackes clearly display characteristics typical of post-Archean upper crust.

5.4.7 Pyroxenous Formation

Pyroxenous Formation greywackes have a SiO_2 range of 53-70 wt%, high $\text{Fe}_2\text{O}_3 + \text{MgO}$ contents of between 9 and 17 wt%, and moderate to high K/Na ratios with a mean of 0.75 (table 2.96). Following the methodology defined by Blatt et al.(1972) and Crook (1974) samples from the Pyroxenous Formation may be classified as Fe-rich, quartz intermediate greywackes. Alkali contents are tightly constrained, lie within the field defined by the volcanic Marchburn Formation (below the $\text{Na/K}=1$ threshold) and provide evidence for the volcanic affinity of this formation. The immature characteristics of volcanic derived greywackes may also be used to infer that volcanism, plutonism and greywacke deposition were penecontemporaneous. Using the Zr-La-Y classification diagram (fig.83b) it may be demonstrated that volcanic derived Pyroxenous Formation samples plot slightly closer to the Y axis in comparison with the Afton Formation within a field most closely related to the Marchburn Formation. The Th-Co-Zr/10 diagram (fig.81b) details the position of Pyroxenous Formation samples within the Oceanic Island Arc field defined by Bhatia (1983). In general, these greywackes fall into the volcanic-lithic category of Valloni and Maynard (1981) which characterise both the back-arc basins of island arcs and the forearc basins of continental margins.

Chondrite normalised REE profiles of Pyroxenous Formation greywackes from the Southern Uplands are defined in figs. 465-467. Petrographically defined samples (AX151, AX182, AX194, AX195, AX196, AX197, AX198, AX199, AX221, AX238, AX274, AX286, AX657, AX659, AX781, AX782, AX783, AX784, AX785, AX789, AX789, AX790, AX791, AX796, AX797 and AX834) display tightly constrained values with parallel but lower REE compared to PAAS; relatively flat HREE patterns; and evidence of weak negative Eu-anomalies with slightly higher Eu/Eu^* ratios than their cratonic counterparts. On the basis of the REE evidence, Pyroxenous Formation greywackes display characteristics derived from sources including recycled orogenic, continental block and dissected magmatic arcs. Both the absolute and relative REE abundances in this formation is similar to that of andesites, indicating that the REE have not been significantly depleted or enriched during weathering, erosion or diagenesis.

Discrimination Diagrams

The IUGS Silica-Total Alkali diagram (fig.302) displays the relative positions of Shinnel and Pyroxenous Formation greywackes. Volcanic derived, Pyroxenous Formation samples are predominantly located in the Andesite field whereas the Shinnel Formation samples occupy the Andesite and Dacite fields. Pyroxenous Formation samples form a relatively restricted range of values as opposed to the Shinnel Formation where a weak inverse relationship exists between silica and total alkali content. The CaO-Sr discrimination diagram (fig.310) displays the relative position of cratonic derived Shinnel Formation greywackes and details the shift towards lower values compared with their juxtaposed volcanic counterparts; the extended CaO range; and the strong positive correlation between both elements. Using this diagram, the relative position of volcanic derived Pyroxenous Formation greywackes are displayed (fig.311) and reveal the positive shift and extended range of Sr values compared with their cratonic counterparts; the reduced range of CaO values; and the weak positive correlation between both elements.

The SiO_2 -MgO discrimination diagram (fig.315) details the strong inverse relationship displayed between MgO and SiO_2 in both formations; the elevated MgO and restricted SiO_2 values displayed by the Pyroxenous Formation (the volcanic field); and the low MgO and elevated SiO_2 values displayed by the Shinnel Formation. The SiO_2 -Rb discrimination diagram (fig.319) documents the weak inverse relationship displayed between Rb and SiO_2 in the cratonic Shinnel Formation; the elevated SiO_2 values displayed by the Shinnel Formation (identifying the cratonic field); and the restricted SiO_2 values displayed by the Pyroxenous Formation. The SiO_2 -CaO discrimination diagram (fig.323) details the weak inverse relationship displayed between CaO and SiO_2 in the Shinnel Formation; the elevated SiO_2 values displayed by the Shinnel Formation (identifying the cratonic field); and the restricted SiO_2 values displayed by the Pyroxenous Formation (occupying the volcanic field defined in fig. 321). The SiO_2 -Sr discrimination diagram (fig.327) displays the weak inverse relationship displayed between Sr and SiO_2 in the Shinnel Formation (mirroring the trend defined by CaO); the elevated SiO_2 values displayed by the Shinnel Formation (identifying the cratonic field); and the elevated Sr and restricted SiO_2 values displayed by the Pyroxenous Formation (occupying the volcanic field defined in fig. 325).

The SiO_2 - Na_2O discrimination diagram (fig.331) details the weak positive relationship displayed between Na_2O and SiO_2 in both formations; the elevated SiO_2 values displayed by the Shinnel Formation (identifying the cratonic field); the position of a small subgroup of samples displaying relatively depleted Na values, possibly indicative of hydrothermal alteration; and the relatively elevated Na_2O and restricted SiO_2 values displayed by the Pyroxenous Formation (occupying the volcanic field defined in fig. 329). The SiO_2 - TiO_2 discrimination diagram (fig.335) displays the poor correlation displayed between TiO_2 and SiO_2 in both formations; the elevated SiO_2 values displayed by the Shinnel Formation (identifying the cratonic field); and the restricted TiO_2 content of the volcanic Pyroxenous Formation (<1.15wt%) displaying similar characteristics to the Scar Formation (fig.334).

The SiO_2 - Fe_2O_3 discrimination diagram (fig.339) displays the relative position of Pyroxenous and Shinnel Formation greywackes and details the inverse correlation displayed between Fe_2O_3 and SiO_2 in both formations; the elevated SiO_2 values displayed by the Shinnel Formation (identifying the cratonic field); the single SiO_2 - Fe_2O_3 trend defined by both formations; and the elevated Fe_2O_3 content of the volcanic Pyroxenous Formation (<6 wt%) displaying similar characteristics to the Scar and Blackcraig formations. The (Fe+Mg)-Ti discrimination diagram (fig.343) details the weak positive correlation displayed between Fe+Mg and TiO_2 in both formations; the restricted Fe_2O_3 +MgO values displayed by the Shinnel Formation (identifying the cratonic field); and the elevated

$\text{Fe}_2\text{O}_3 + \text{MgO}$ content of the volcanic Pyroxenous Formation (<14 wt%) displaying similar characteristics to that of the Scar and Blackcraig formations. The (Fe+Mg)-(Al/Si) discrimination diagram (fig.347) displays the positive correlation and single compositional trend displayed between Fe+Mg and Al/Si in both formations; the restricted Fe+Mg values displayed by the Shinnel Formation (identifying the cratonic field); and the elevated Fe+Mg content of the Pyroxenous Formation (<14 wt%) displaying similar characteristics to the Scar and Blackcraig formations. The (Fe+Mg)-(K/Na) discrimination diagram (fig.351) details the poor correlation displayed by both variables; the restricted Fe+Mg values (<11 ppm) displayed by the Shinnel Formation (identifying the cratonic field); the low K/Na values and elevated Fe+Mg (>11wt%) content of the volcanic Pyroxenous Formation displaying similar characteristics to the Scar and Blackcraig formations.

The (Fe+Mg)-(Al/(Ca+Na)) diagram (fig.355) details the poor correlation displayed within both formations; the restricted (<11wt%) Fe+Mg values displayed by the Shinnel Formation (identifying the cratonic field); and the elevated Fe+Mg (>11 wt%) content of the volcanic Pyroxenous Formation (which displays similar attributes to both the Scar and Blackcraig Formations). The Th-La discrimination diagram (fig.359) details relatively restricted (<10ppm) Th values displayed by the Pyroxenous Formation (identifying the volcanic field); and the overlapping nature of both compositional fields. The Shinnel Formation samples display similar attributes to both the Afton Formation samples (Fig. 357). The (K/K+Na)-(K+Na) discrimination diagram (fig.363) details the wide scatter and poor correlation displayed both Formations; the large range of K/K+Na values displayed by the Shinnel Formation; the narrow, restricted range of K+Na values displayed by the Pyroxenous Formation and the overlapping nature of both compositional fields.

The Fe/Mg-Cr diagram (fig.368) details the narrow range of Fe/Mg and Cr values displayed by the Pyroxenous Formation (located within the volcanic field); the apparently bimodal grouping of values within the Shinnel Formation (a high Cr group displaying an inverse relationship with Fe/Mg and a low Cr group displaying a poor correlation with Fe/Mg); and the overlapping nature of both compositional fields. The Y-CaO discrimination diagram (fig.372) displays the narrow, restricted range of Y values detailed by both formations; the poor interelement correlation displayed within both formations; the large range of CaO values (max 12.27wt%) displayed by the Shinnel Formation; the elevated range of CaO values displayed by the volcanic Pyroxenous Formation; and the overlapping nature of both compositional fields. The Sr-Y discrimination diagram (fig.376) details the narrow, restricted range of Y values displayed and the poor interelement correlation displayed by both formations; the elevated Sr levels identifying Pyroxenous Formation samples (>300ppm) and the restricted Sr levels (<300ppm) displayed by the cratonic Shinnel Formation. The K_2O -Rb discrimination diagram (fig.380) displays a similar trend to previous K_2O -Rb plots with a narrow compositional range, single trend and strong positive correlation displayed by both Formations; and the closely overlapping compositional fields of both groups. The MgO-Sr diagram (fig.385) details the weak positive correlation displayed between MgO and Sr in both formations; the elevated MgO and Sr values displayed by the Pyroxenous Formation (the volcanic field); and the extremely low MgO and Sr values displayed by the Shinnel Formation. The Cr-V diagram (fig.389) displays the strong positive correlation displayed between V and Cr in the Shinnel Formation; the wide scatter, poor correlation and elevated V values (>130ppm) displayed by the Pyroxenous Formation. The Ni-Cr discrimination diagram (fig.393) displays the overlapping position of both Formations; the strong positive correlation displayed between Cr and Ni in the Pyroxenous Formation; and the apparent bimodal nature of Shinnel Formation, with the first group distinguished by low Ni and Cr values and a strong positive correlation, and the second group identified by relatively higher Cr and Ni values, a wide scatter and poor correlation.

The Zr-Y discrimination diagram (fig.397) details slightly overlapping compositional fields; the positive correlation and elevated Zr values (>200ppm) displayed by the Shinnel Formation; the narrow, restricted range of both Y and Zr values (20-28 and 150-250ppm respectively) displayed by the Pyroxenous Formation; and the position of the Shinnel Formation within the cratonic field defined by the Afton Formation (Fig. 395). The Fe/Mg-Zr discrimination diagram (fig.401) displays the wide scatter and poor correlation displayed by the Shinnel Formation; the restricted Zr and Fe/Mg values (<230ppm and <2 respectively) displayed by both groups; the elevated Zr values displayed by the Shinnel Formation; the location of the Pyroxenous Formation within the volcanic field defined by the Marchburn, Blackcraig and Scar formations; and the position of the Shinnel Formation in the cratonic field defined by Afton Formation greywackes. The Zr-TiO₂ discrimination diagram (fig.405) displays the wide scatter, elevated Zr levels (>200ppm) and weak positive correlation displayed by Shinnel Formation samples; the restricted Zr and TiO₂ values (<230ppm and 0.75-1.1wt% respectively) displayed by the Pyroxenous Formation; the location of the Pyroxenous Formation within the volcanic field defined by the Marchburn, Blackcraig and Scar formations; and the location of both formations within the cratonic field defined by Afton Formation greywackes.

The La/Y-Nb/Y discrimination diagram (fig.409) detail the wide scatter, elevated Nb/Y levels (>0.5) and weak positive correlation displayed by the Shinnel Formation; the narrow, restricted range of Nb/Y values (0.35-0.50) displayed by the Pyroxenous Formation; the location of the Pyroxenous Formation in the volcanic field defined by the Marchburn Formation; and the correlation of the Shinnel Formation within the cratonic field defined by Afton Formation greywackes.

5.4.8 Intermediate Formation

Intermediate Formation greywackes have a SiO₂ range of 50-78 wt%, low to moderate Fe₂O₃ + MgO contents of between 5 and 18 wt%, and high K/Na ratios with a mean of 1.68 (table 2.97). Following the classification scheme defined by Blatt et al., (1972) and Crook (1974) samples from the Intermediate Formation (fig.76) may be classified as Fe-rich, quartz intermediate-rich greywackes/lithic sandstones. Total alkali contents lie within the field defined by Maynard et al., (1982) however, values are centered upon the Na/K=1 threshold, indicative of an increase in K₂O content with respect to the juxtaposed Pyroxenous Formation, and the cratonic nature of these sediments.

Using the Zr-La-Y greywacke classification diagram (fig.83c) Intermediate Formation samples are located within a narrow field initially defined by the Afton Formation. The Th-Co-Zr/10 classification diagram reveals that Intermediate Formation samples plot in a similar position to the Shinnel Formation, but are skewed towards the Zr pole and lie within the Continental Island Arc/Passive Margin field defined by Bhatia (1983). Chemical data supporting the acidic nature of the greywackes is exhibited by the chondrite normalised patterns for the REE (figs. 468-470). Petrographically defined samples (AK502, AK674, AX44, AX46, AX48, AX94, AX96, AX97, AX107, AX108, AX109, AX272, AX280, AX281, AX283, AX107, AX108, AX109, AX272, AX280, AX281 and AX283) display REE patterns parallel to those of PAAS with slightly lower total REE values and subtle evidence of negative Eu-anomalies. On the basis of REE evidence and in comparison with PAAS, Intermediate Formation greywackes are inferred to display characteristics typical of post-Archean upper crust.

5.4.9 Hawick Group

The southern half of the Central Belt is occupied by rocks of Late Llandovery age, generally assigned to the Hawick Group. The Hawick Group greywackes have a SiO_2 range of 46-85 wt%, low to moderate $\text{Fe}_2\text{O}_3 + \text{MgO}$ contents of between 3 and 18 wt%, and high K/Na ratios with a mean of 2.44 (table 2.102). The Zr-La-Y triangular diagram (fig.83d) illustrates that Hawick Group samples display the widest distribution and extending further away from the Zr pole than any previous group, however this trend may be partially attributed to the dilution effects of added carbonate upon the system. The Th-Co-Zr/10 triangular diagram (fig.81d) display a tightly constrained range of values which plot within the Continental Island Arc field defined by Bhatia (1983).

Correlation coefficients indicate that most elements correlate positively with Al (clay fraction) and negatively with Ca (carbonate fraction) and present a similar pattern to those observed in shallow marine carbonate sequences (Orth, et al., 1986). The increase in Ca and decrease in elements that correlate with the clay content, suggest that either the rate of carbonate precipitation increased, or that the input of detrital material decreased. In general, this variation reflects differences in the nature of the source material, and to a much lesser extent reflects the conditions of deposition and diagenesis. The dominant fine grain size and compositional maturity of sandstones in Late Llandovery and Wenlock sediments was inferred by Kemp (1985) to be due to the arid weathering and erosion of uplifted greywacke sandstones from the emergent trench-slope break, and subsequent breakdown of the sandstones into their constituent grains and the decomposition of feldspars and mafic components.

Discussions regarding the nature and origin of the carbonate fraction of these greywackes, are widely documented. Peach and Home (1899) were the first to identify fragments of corals and brachiopods in coarse grained greywackes in the Central Belt. In studies of the Gatehouse area, Weir (1974) proposed that a considerable portion of the carbonate was introduced from an external (magmatic or groundwater) source. Carbonate is first observed as a detrital component of greywacke sandstones in rocks of uppermost Llandovery age, immediately south of the Ettrickbridgend fault line (Kemp, 1985) and forms a major component of both Hawick and Riccarton groups where it forms matrix, cement and detrital grains. In these greywackes the cement is micritic to sparry calcite with subordinate amounts of phyllosilicate and silica cement. In general however, it is extremely difficult to distinguish between calcite cement, recrystallized matrix and fine grained carbonate skeletal fragments. In the Hawick Group low Sr values and Ca/Sr ratios may be used to infer a contribution from shallow and littoral limestones, rather than their deep-sea counterparts (Hickman and Wright, 1982). The extensive evidence of bioclastic material and detrital carbonate grains presented by Kemp (1985) was used to suggest that a considerable portion of all carbonate originated as fine grained, micritic detritus which has been redistributed during diagenesis.

To investigate the contribution made by CaO addition (dominantly in the form of carbonate) to the Hawick Group, the geochemical data (excluding CaO) was normalised and then compared with other formations in the Southern Uplands, particularly the juxtaposed Intermediate Formation. Summary statistics of normalised major element geochemistry from the Hawick Group is presented in Table 2.152. In a comparison of variance using the F test statistic, CaO free, normalised major element data from the Intermediate Formation and Hawick Group displayed similar variances and average compositions (differing by as little as 0.02 wt%). Furthermore, the results of a student T test, comparing the two formations indicated a high probability that they were both derived from the same parent population. It is clear from this study that the Hawick Group was derived from a similar source terrane to that of the Intermediate Formation, if not the Intermediate Formation itself. The addition of a carbonate component

however, provides the major discriminating factor between these two formations, and serves to dilute the cratonic/acidic geochemical components of the Hawick Group.

Moore (1979) demonstrated the increasing carbonate component of trench-slope greywackes in comparison to trench deposits and suggested that any primary carbonate in the trench sediments may have been dissolved during diagenesis and burial metamorphism. Kemp (1985) identified significant quantities of bioclastic material including brachiopod, crinoid and bryozoan fragments in medium-course grained sandstones. In finer grained lithologies however, these grains were not readily identified. This bioclastic material was invoked by Kemp (1985) to suggest the presence of shallow marine areas and/or fringing reefs around emergent land in the source area. In addition, the abundance of finely comminuted carbonate material was used to suggest the derivation of carbonate mud from extensive shallow marine areas. Intermittent tectonic pulses resulted in the creation of carbonate rich turbidite flows derived from carbonate platform and ramp detritus. Furthermore, Kemp (1985) proposed that a considerable portion of the material in the Hawick Group is consistent with derivation by erosion of rocks from the Northern and Central belts of the Southern Uplands. On geochemical grounds it may be shown that the Hawick Group sediments display (CaO-free) geochemical values statistically comparable with those of the Intermediate Formation sediments.

Although global sea level rose steadily throughout the early Cambrian period, it was unusually low by the end of the Ordovician. Evidence of glaciation at this time has been located in Africa (Anderton, 1979) and it has been demonstrated that melting of extensive ice sheets early in the Silurian, produced a widespread (global) rise in sea level (transgression) together with more equable climates. Carbonate deposition was initiated following the culmination of a worldwide transgression in Llandovery times (Anderton et al., 1981) following a Late Ordovician glaciation. Sea level rose sharply at the beginning of the Silurian and the resulting particularly high levels drowned many continental shelves, led to a retreat of shorelines away from the shelf margins and sharply reduced the supply of clastic material reaching the basin. The onset of carbonate deposition is characteristic of the Late-Llandovery - Wenlock period and is clearly defined in the sedimentary succession of the Southern Uplands by the major enrichments in CaO content. The virtual absence of sulphur identified in the Hawick Group may be attributable to variations in one or more of the following inter-related parameters; seawater sulphate content, availability of organic material, presence of bacteria and reducing conditions. Geochemical studies reveal that the depleted sulphur values are inversely correlated with increased CaO content (predominantly in the form of carbonate) and derived by the mixing of cratonic sediment with biogenic carbonate, prior to turbidite deposition. The proposed depositional environment would not be conducive to the formation of barrier reefs or lagoons, features which could have led to restricted seawater circulation and possible reducing conditions. Moreover, this environment would have contained considerable organic material and a high bacterial content. It is therefore proposed that the most likely cause of sulphur depletion is the high energy, oxidised conditions prevalent on the shelf and the subsequent rapid deposition of carbonate-rich turbidites. A further characteristic feature of the Hawick Group greywackes is the presence of red mica flakes and sporadic red mudstone horizons inferring oxidation of the detrital components prior to deposition. The presence of oxidised material in the Hawick Rocks is also attributed by McKerrow (1988) to the Upper Llandovery marine transgression. In summary, it is suggested that carbonate deposition took place in the form of isolated reef developments on a shallow, but relatively steep, high energy, unstable shelf. This environment would have facilitated the rapid build-up of an admixture of cratonic sediments and carbonate debris, coeval with episodic turbidite deposition.

It should be noted that in the south-west of Scotland this study has geochemically located the presence of Hawick Group greywackes in the Mull of Galloway, and at Burrow Head, west of Wigtown Bay.

Discrimination Diagrams

The IUGS Silica-Total Alkalii diagram (fig.303) displays the relative positions of the cratonic Intermediate Formation and Hawick Group greywackes. Although the carbonate-free fraction of both formations are petrographically identical, the input of carbonate detritus into Hawick Group greywackes however, resulted in the dilution of major element values notably Si, by Ca and a shift towards lower silica content from andesite-dacite fields to basaltic-andesite and andesite. Hawick Group members display a narrow range of total alkalii values. In addition a small number of samples ($\text{Na}+\text{K} < 3\text{wt}\%$) are attributed to represent the effects of hydrothermal alteration.

The CaO-Sr discrimination diagram (fig.312) displays the relative position of cratonic derived Intermediate Formation and Hawick Group greywackes. The Intermediate Formation displays typical cratonic characteristics (low Ca and Sr values) whereas the Hawick Group displays strongly highly elevated CaO values (0-19%); a narrow, restricted range of Sr values; the strong positive correlation between both elements; and the position of a discrimination line which may be used to classify the samples into their respective formations.

The SiO_2 -MgO diagram (fig.316) details the weak inverse relationship displayed between SiO_2 and MgO in both formations and the location of the Hawick Group within the volcanic field (formed by the negative shift in SiO_2 values within the Hawick Group, as a direct result of the input of carbonate detritus and associated CaO dilution of all other major element components). The SiO_2 -Rb diagram (fig.320) displays the weak inverse relationship displayed between SiO_2 and Rb in both formations; the relatively enriched Rb levels located in both formations (compared with all other greywacke formations in the Southern Uplands); the presence of a small subset of anomalous Rb values ($\text{Rb} > 100\text{ppm}$) associated with hydrothermal alteration and As-Sb-Au mineralization; and the location of the Hawick Group within the volcanic field defined previously.

The SiO_2 -CaO diagram (fig.324) details the major inverse relationship displayed between SiO_2 and CaO and the considerably elevated CaO levels present in the Hawick Group (max 24.36%) together with correspondingly low SiO_2 levels; the lack of any form of inter-element correlation in the Intermediate Formation; the relatively enriched SiO_2 levels located in the Intermediate Formation; and the location of the Hawick Group within the volcanic field defined previously in fig. 321. The SiO_2 -Sr diagram (fig.328) displays an inverse relationship displayed between SiO_2 and Sr in the Hawick Group together with correspondingly low SiO_2 levels; the weak inter-element correlation in the Intermediate Formation; the relatively enriched SiO_2 levels located in the Intermediate Formation; and the location of the cratonic derived Hawick Group within the volcanic field defined previously in fig. 325.

The SiO_2 - Na_2O discrimination diagram (fig.332) details the weak positive correlation between SiO_2 and Na_2O in the Hawick Group together with correspondingly low SiO_2 levels; the relatively weak inter-element correlation in the Intermediate Formation; the enriched SiO_2 levels located in the Intermediate Formation; the position of highly Na depleted samples within both formations inferring the association with hydrothermal alteration and As-Sb-Au mineralization (see chapter 3); and the location of the cratonic derived Hawick Group within the volcanic field defined previously in fig. 329. The SiO_2 - TiO_2 discrimination diagram (fig.336) details the poor correlation and wide scatter of SiO_2 and TiO_2 values in both Formations; the relatively low SiO_2 levels in the Hawick Group; and the position of Hawick Group samples within the volcanic field defined by both Scar and Pyroxenous Formations

in figs. 334 and 335, respectively. The SiO_2 -Fe discrimination diagram (fig.340) displays the poor correlation and wide scatter of SiO_2 and Fe_2O_3 values in both formations; the relatively low SiO_2 level in the Hawick Group; and the position of Hawick Group samples within the volcanic field defined by both Scar and Pyroxenous formations in figs. 338 and 339, respectively.

The (Fe+Mg)-Ti discrimination diagram (fig.344) details the strong inter-element correlation and relatively low Fe_2O_3 +MgO levels (<14wt%) in both formations; and the slight reduction of Fe_2O_3 +MgO levels in the Hawick Group compared with Intermediate Formation values. In addition, the (Fe+Mg)-(Al/Si) diagram (fig.348) displays similar trends with a strong inter-element correlation; the relatively low Fe+Mg levels (<14wt%) in both formations (defining the cratonic field); and the slight reduction in Fe+Mg and Al/Si levels in the Hawick Group compared with the juxtaposed Intermediate Formation. The (Fe+Mg)-(K/Na) discrimination diagram (fig.352) depicts the relatively low Fe+Mg levels (<13wt%) in both formations (the cratonic field); and the slight reduction in Fe+Mg and elevated K/Na levels both formations compared with other formations in the Southern Uplands. The (Fe+Mg)-(Al/(Ca+Na)) diagram (fig.356) details the strong inter-element correlation; relatively low Fe+Mg levels (<13wt%) in both formations (the cratonic field); and the reduction in Al/(Ca+Na) levels in the Hawick Group samples (due to the influx of detrital carbonate and accompanying sharp increase in CaO values).

The Th-La diagram (fig.360) displays the wide scatter and poor inter-element correlation displayed by members of both units; the strongly overlapping compositional fields of both Intermediate Formation and Hawick Group greywackes; and a positive shift in both La and Th values away from that defining the volcanic Blackcraig and Scar formations.

The (K/K+Na)-(K+Na) discrimination diagram (fig.364) details the wide scatter and poor inter-element correlation displayed by the Intermediate Formation; the relatively restricted compositional field and the narrow K+Na range of values displayed by the Hawick Group; the positive shift in values of both formations to within the cratonic field ($\text{K}/(\text{K}+\text{Na}) > 45$); the strongly overlapping compositional fields of both Intermediate Formation and Hawick Group greywackes; and the small subset of hydrothermally altered samples defined by K/K+Na values in excess of 75-80%. Note the presence of altered samples in both units and the reduction in total alkali content formed as a result of sodium depletion and dickitisation processes.

The Fe/Mg-Cr diagram (fig.369) details the relatively wide scatter and poor inter-element correlation displayed by the Intermediate Formation; the relatively restricted compositional field and the narrow range of Cr values displayed by the Hawick Group (50-200ppm); the strongly overlapping compositional fields of both Intermediate Formation and Hawick Group greywackes; and the small subset of hydrothermally altered Hawick Group samples defined by Fe/Mg values in excess of 1.7wt%.

The Y-CaO diagram (fig.373) details the elevated range of CaO values (max 18.35wt%) displayed by the Hawick Group, the restricted range of CaO values displayed by the Intermediate Formation (<3wt%) and the relatively wide range of Y values (20-45ppm) displayed by both units. The CaO values identified within the Hawick Group display the highest levels of all greywacke formations present in the Southern Uplands and serve to identify the influx of carbonate rich detritus from the source terrane.

The Sr-Y diagram (fig. 377) displays the relatively restricted range of Sr values (max 263ppm) displayed by the

Hawick Group, the elevated range of Sr values displayed by the Intermediate Formation (max 510ppm) and the comparatively wide range of Y values (20-45ppm) displayed by both units. The K_2O -Rb diagram (fig.381) depicts the narrow compositional range, single trend and strong positive correlation displayed by both units; the overlapping compositional fields of both groups; and the elevated values ($>3\text{wt}\% K_2O$ and $>100\text{ppm Rb}$) indicative of hydrothermally altered samples (see Fig. 382). The MgO-Sr diagram (fig.386) displays the poor correlation and restricted range displayed by the Hawick Group; the overlapping compositional field of both units; the elevated Sr values identified in the Intermediate Formation (max 485ppm); and the location of the Hawick Group greywackes within the cratonic field defined by both Afton and Shinnel formations.

The Cr-V diagram (fig.390) details the strong positive correlation, overlapping compositional field and restricted Cr and V values displayed by both formations; and the location of both Hawick Group and Intermediate Formation greywackes within the cratonic field defined by both Afton and Shinnel formations. The Ni-Cr diagram (fig.394) also displays both strong positive correlation, overlapping compositional field and restricted Cr and Ni values displayed by both formations; the elevated Cr (max 505ppm) and Ni (max 243ppm) values identified in the Intermediate Formation; and the location of both Hawick Group and Intermediate Formation greywackes within the cratonic field defined by both Afton and Shinnel formations.

The Zr-Y diagram (fig.398) displays the elevated Y and Zr values, positive correlation and partially overlapping compositional fields displayed by both formations; the highly elevated Zr values displayed by the Intermediate Formation (230-410ppm); and the location of both Hawick Group and Intermediate Formation greywackes within the cratonic field defined by both Afton and Shinnel formations. The Fe/Mg-Zr diagram (402) details the poor correlation and wide scatter of Zr and Fe/Mg values in the Intermediate Formation; the relatively restricted Fe/Mg levels (1.2-1.5) in the Hawick Group (with the exception of hydrothermally altered Fe-rich samples); the position of Hawick Group samples within the volcanic field defined by the Scar and Pyroxenous formations; and the location of Intermediate Formation samples within the cratonic field defined by the Afton and Shinnel formations. The Zr-TiO₂ diagram (fig.406) displays the poor correlation and wide scatter of Zr and TiO₂ values in both Formations; the relatively elevated Zr levels ($>230\text{ppm}$) in the Intermediate Formation; the negative shift in Zr values displayed by the Hawick Group in comparison with Intermediate Formation samples; and the location of the Intermediate Formation within the cratonic field defined by both the Afton and Shinnel formations.

The La/Y-Nb/Y diagram (fig.410) details the strong correlation of Nb/Y and La/Y values in both formations; the overlapping nature of both formations; the relatively reduced Nb/Y and La/Y levels in the Hawick Group greywackes; the location of Hawick Group samples in the volcanic field defined by the Marchburn Formation (Fig. 407); and the position of the Intermediate Formation within the cratonic field defined by both the Afton and Shinnel formations.

5.4.10 Summary

Juxtaposed, petrographically distinct formations throughout the Southern Uplands exhibit numerous chemical differences that can be recognised by a comparison of their modal compositions. These variations may also be examined using specific discrimination diagrams in which individual formations plot in separate, or slightly overlapping fields. A series of individual element compositional envelopes (figs. 56-69) document the variations

displayed by differing petrographic formations across the Southern Uplands. In detail, the eight greywacke formations described, may be subdivided into two main categories in order to aid interpretation, namely: cratonic (Afton, Shinnel, Intermediate formations and Hawick Group) and volcanic derived (Marchburn, Blackcraig, Pyroxenous and Scar formations). The Hawick Group is particularly noteworthy in that both the major and trace element contents are diluted by a major addition of CaO (predominantly as carbonate). This dilution has resulted in the assignment of a 'volcanic' chemical signature to this formation (petrographically defined as cratonic in origin). In addition, summary histograms for each element and ratio determined by this study are presented in figs. 225-265. Here again, samples have been classified and sorted into one of eight petrographically distinct formations within the Southern Uplands. These histograms serve to compliment the compositional envelopes (figs.56-69) and provide additional information on the distribution of element values within each formation. Geochemical data relating to these formations are presented in tables 4.53-4.63 with corresponding summary statistics in tables 2.47-2.57.

SiO₂

The volcanic Marchburn, Blackcraig, Scar and Pyroxenous formations (fig. 56a and 225) display notably lower, negatively skewed SiO₂ population in comparison with their cratonic counterparts. In general, all histograms display highly kurt distribution. Note the low Si distribution of the Hawick Group. A small overlap of compositional fields is present, however most of the samples plot outside the compositional field of their juxtaposed formations.

Al₂O₃

Little systematic variation in Al₂O₃ composition (fig. 56b and 226) is observed between volcanic and cratonic formations. As such this element is deemed to have no significant role in greywacke discrimination and/or terrane boundary identification.

TiO₂

A general decrease in TiO₂ distribution occurs across the succession (figs. 56c and 227) with volcanic formations displaying relatively higher populations and mean values than their juxtaposed cratonic counterparts. Particularly noteworthy is the positively skewed distribution in the Marchburn Formation.

Fe₂O₃

The Fe₂O₃ content of volcanic derived formations (fig. 57a and 228) display relatively higher (minimum and mean) values than their cratonic counterparts mirroring Ti distributions with a trend towards decreasing composition across the succession.

Na₂O

The Na₂O content (figs. 58a and 231) reflects variations in petrography across the succession with the mean compositions and distribution of volcanic derived greywackes up to 0.8% higher than their cratonic counterparts.

The effects of Na depletion associated with hydrothermal activity are most clearly observed in the cratonic Afton and Intermediate formations and Hawick Group.

MgO

MgO values (figs. 57b and 229) closely follow that of Ti and Fe with the highest values and widest distribution occurring in the volcanic derived Marchburn Formation. In general, volcanic compositions are 1.5-3.0% higher than the distribution of juxtaposed cratonic sediments and as such provides a useful discrimination index. In addition, the MgO/CaO ratio may be used to demonstrate the effects of low-temperature diagenetic processes. CaO is often depleted relative to MgO and results in MgO/CaO ratios that are higher than for most igneous rocks of similar SiO₂ content (Peterman, et al., 1981).

CaO

CaO contents (figs. 57c and 230) vary systematically throughout the petrographic units, and with the exception of the Hawick Group, cratonic derived greywackes have 2-3% lower contents than their volcanic derived counterparts. The Hawick Group is however, characterised by the highest Ca content of any unit in this study due to a substantial input of carbonate from the source terrane. In addition, the high concentrations of TiO₂, Fe₂O₃ and CaO may be related with the concentration of 'heavy' detrital minerals such as ilmenite, rutile and epidote.

K₂O

Systematic differences in distribution exist between the cratonic and volcanic derived formations (fig.58b and 232). In general the volcanic formations display mean values 0.5% lower than their cratonic counterparts, particularly during Ordovician times. From a comparison of the modal analyses of the individual formations, it is clear that the higher concentration of K₂O in the volcanic derived formations can be attributed to a higher proportion of K-feldspar and suggests that the sediments are relatively immature.

MnO

Although the MnO content (figs. 58c and 233) is generally low (<0.25%) systematic variations between cratonic and volcanic derived greywacke formations exist with the former relatively depleted with respect to its volcanic counterpart. The mean volcanic composition is generally 0.05% higher than cratonic formations.

P₂O₅

Figures 59a and 234 illustrate the highly consistent distribution of P₂O₅ values within all formations. Particularly noteworthy are the elevated values identified within the volcanic Marchburn Formation.

As

Both the minimum and mean As content of greywackes from this succession (figs. 59b and 235) lie close to, if not below the analytical detection limit of the XRF (2-3ppm). In general, the mean composition of volcanic derived

greywackes is 1-2 ppm lower than that of cratonic samples and both formations display a negatively skewed, highly kurt (leptokurtic) distribution of values. In addition the diagrams illustrate the occurrence of elevated arsenic levels (several tens of ppm) across this succession.

Ba

Although there is no systematic variation in Ba content across this succession, individual formations (figs. 59c and 236) exhibit significant contrasts with juxtaposed units and detail the major increase in Ba content within the Intermediate Formation. In general, Ba occupies the same site as K in crystal lattices and the plot of Ba against K demonstrates a reasonable correlation.

Co

The Co content (figs 60a and 237) is highly variable through all formations. In general, volcanic derived greywackes are on average 5-8 ppm lower than their juxtaposed cratonic equivalents. A bimodal distribution of values is displayed in the Shinnel, Pyroxenous and Intermediate formations together with the restricted compositional range within the Hawick Group.

Cr

A systematic trend of decreasing Cr values (figs. 60b and 238) occurs throughout the studied formations with the distribution of volcanic derived greywackes generally 30-150ppm higher than their juxtaposed cratonic counterparts. Elevated Cr values (up to 1100ppm) characterise both the Marchburn and Blackcraig Formation and indicate an ultrabasic contribution from the source terrane. These enrichments are accompanied by elevated Fe, Ti and Ni values and are indicative of a high mafic mineral content and suggest derivation from a poorly differentiated source.

Cu

Volcanic derived greywacke formations (figs. 60c and 239) display slightly elevated Cu populations compared to their cratonic counterparts. Anomalous Cu values are related to a variety of differing styles of mineralization and identify targets of possible exploration interest.

Ga

Highly consistent Ga values (figs. 61a and 240) are displayed throughout all formations with volcanic formations (3-4ppm) higher than their juxtaposed cratonic equivalents. In general, gallium occupies lattice positions in illite, kaolinite and montmorillonite.

La

Systematic variations in La content occur throughout all formations (figs. 61b and 241) with cratonic derived greywackes exhibiting levels 10-15 ppm greater than their volcanic counterparts.

Ni

A general decrease in Ni contents of cratonic formations is identified (figs. 61c and 242) with populations 40-60ppm lower than their volcanic counterparts. In particular, the Marchburn Formation is characterised by extremely high Ni values (>250ppm).

Nb

Subtle systematic variations in Nb content occur throughout all formations (figs. 62a and 243) with volcanic derived populations 5-15ppm lower than their juxtaposed cratonic counterparts.

Pb

Highly consistent Pb values occur within all formations (figs. 63a and 244). No systematic variation is observed between volcanic and cratonic formations, however anomalous values indicate the proximity to mineralization.

Rb

A systematic increase in Rb values are observed throughout all formations, (figs. 62b and 245) with volcanic derived populations 20-30ppm lower than their juxtaposed cratonic counterparts. The Rb levels provide an indication of the relative proportion of clay minerals present, whereas Ba values provide a measure of the total feldspar content.

S

A systematic decrease in S content is observed throughout all formations, (figs. 63c and 246) with volcanic populations 200-1000 ppm higher values than their juxtaposed cratonic counterparts. The Hawick Group in particular, is characterised by low sulphur values (<50ppm) which are inversely correlated with an increased CaO content.

Sb

The background level of Sb are close, if not below the detection limits of the XRF (1-3ppm). No variation in antimony concentrations are observed within these formations (fig. 63b and 247) however on the basis of a statistical assessment of this data the average antimony content of the volcanic formations were found to be 0.4-1.6ppm lower than that defined for the cratonic units.

Sr

Systematic variations in Sr content occur throughout all formations (fig. 62c and 248) with volcanic derived populations 130-200ppm higher than their cratonic derived counterparts. Although a diverse range of values is present in the Marchburn Formation, a highly restricted range of values is defined by the Hawick Group. In general, Sr is concentrated in sediments containing elevated carbonate levels, however a substantial control by clay minerals is also inferred.

Th

A consistent pattern of Th values occur throughout the succession (figs. 64a and 249) with volcanic derived greywackes generally 4-6 ppm lower than their juxtaposed cratonic counterparts.

V

A systematic decrease in V content occurs throughout the individual formations (figs. 64b and 250) with volcanic derived units exhibiting concentrations 50-100ppm higher than their juxtaposed cratonic counterparts. In general, vanadium tends to be enriched in sediments that are deposited in organic-rich, poorly aerated environments (Large, 1981).

Y

Y values (figs 65a and 251) are highly consistent throughout all formations and display no systematic variation. The highest values located within any formation are contained within the Intermediate Formation and Hawick Group.

Zn

A systematic variation in Zn content is observed throughout all formations (figs. 65c and 252) with volcanic derived greywackes displaying populations 10-30ppm higher than their juxtaposed cratonic counterparts.

Zr

A systematic variation in Zr content occurs throughout all formations (figs. 65b and 253) with volcanic derived greywackes displaying populations 100-150ppm lower than juxtaposed cratonic units. The Hawick Group displays significantly lower values than expected when compared to the adjacent Intermediate Formation. This factor which may be attributed to the dilution effects caused by the addition of 10-15% carbonate to the Hawick Group greywackes. In general, high Zr contents are controlled by the abundance of detrital zircon and may be correlated with SiO₂ content in the cratonically derived samples. Finlow-Bates and Stumpfl (1981) presented evidence that the 'immobile' elements Y, Sc and Nb are in fact extremely mobile during hydrothermal alteration and as such, only Zr and TiO₂ may be used with any reliability to identify the level of magmatic differentiation in hydrothermally altered rocks.

Al/Si

Highly consistent Al/Si distributions (fig.254) display no systematic variation between the individual formations. Average Al₂O₃/SiO₂ ratios are variable (0.17 to 0.24) and dominantly reflect grain-size variation, with the coarser grained units displaying the lowest ratios. In general, large-ion-lithophile (LIL) elements such as K, Rb, Cs, Sr, La, Th and U demonstrate large concentration ranges, however specific element pairs display relatively consistent values throughout the stratigraphic sequence.

K/Na

Highly consistent K/Na distributions (fig.255) are defined by all formations with systematically lower values located in volcanic derived formations as opposed to their cratonic counterparts. Note the low, extremely narrow range of values displayed by the Blackcraig Formation. Elevated K/Na values serve to illustrate the effects of hydrothermal activity, sodium depletion/potassium metasomatism, and provide a useful index of mineralization potential.

K/K+Na

A systematic variation in K/K+Na content occurs throughout all formations (fig.256) with volcanic derived greywackes displaying populations relatively lower than the juxtaposed cratonic counterparts. This ratio is closely associated with the K/Na ratio defined in Fig. 255 and may also be used to identify the effects of hydrothermal activity.

K+Na

The total alkali content of all greywacke formations display a highly variable range of values (fig.257) with volcanic derived units exhibiting a wider range and higher maximum values than their cratonic counterparts.

Rb/Sr

Little variation in Rb/Sr content occurs throughout all formations (fig.258) although volcanic derived greywackes displaying populations slightly higher than their juxtaposed cratonic counterparts. In general, Rb and Sr exhibit rather erratic distributions and Rb/Sr ratios have a relatively restricted range which suggests that these rocks are unsuitable for Rb/Sr age determinations.

Mg+Fe

A systematic variation in Mg+Fe content occurs throughout all formations (fig. 259) with volcanic derived greywackes displaying populations relatively higher than cratonic counterparts.

Fe/Mg

Highly consistent Fe/Mg distributions occur within all formations (fig.260) with the smallest range of values displayed by the Hawick Group.

Ni/Co

A systematic variation in Ni/Co content occurs throughout all formations (fig.261) with volcanic derived greywackes displaying relatively higher populations than their cratonic counterparts.

Zr/Nb

Subtle variations in Zr/Nb content are noted with volcanic derived formations (fig.262) displaying relatively lower populations than their juxtaposed cratonic counterparts.

La/Y

Although variable, a systematic pattern of La/Y variation is observed within all formations (fig.263) with volcanic derived units characterised by relatively lower distributions than their cratonic counterparts.

Nb/P

A systematic variation in Nb/P content occurs throughout all formations (fig.264) with volcanic derived greywackes displaying relatively lower distributions than their juxtaposed cratonic counterparts.

Nb/Y

Variations in Nb/Y content (fig.265) mirror those of Nb/P (Fig. 264) with volcanic derived greywackes displaying populations relatively lower than their cratonic counterparts.

La

REE element analyses of 213 greywacke samples were undertaken by ICP following the techniques outlined in chapter 2, with normalized REE profiles of representative samples from each formation displayed in figs. 440 to 474. Although La displays relatively consistent values, figure 66a shows the mean composition of volcanic derived formations to be comparatively lower (6-8ppm) than their juxtaposed cratonic counterparts. In addition, a systematic decrease in range, coupled with an increase in minimum values is observed across the succession.

Ce

Figure 66b illustrates the comparative increase in Ce content of cratonic derived greywackes as opposed to their volcanic counterparts. A systematic increase in the Ce content of volcanic greywackes across the succession is counterbalanced by respective decreases in cratonic greywackes.

Pr

The Pr content of cratonic derived greywackes is 1-2ppm higher than their volcanic counterparts (fig.66c). The general REE trend of increasing minimum and decreasing range (IMDR) across the succession is also demonstrated by this element.

Sm

Sm displays markedly similar element variations to that of the previous REE.

Nd

The Nd content of the cratonic derived greywackes displayed in fig.67a is again higher than their volcanic counterparts, with the IMDR trend is also present.

Eu

Eu displays a notably different profile (fig.67c) compared to that of the previous REE, with the mean values of volcanic derived greywackes higher than their cratonic counterparts and a general trend towards a decrease in composition across this succession. The slightly elevated levels of Eu/Eu^* observed in quartz-intermediate greywackes is interpreted to reflect a component of volcanogenic (andesitic) material which dilutes the upper crustal REE signature.

Gd

Little if any systematic trend is apparent between cratonic and volcanic derived greywacke formations (fig.68a) with highly consistent values present across the entire succession.

Dy

The tightly constrained range of the Blackcraig Formation on this diagram (fig.68b) provides the only misnomer on an otherwise highly consistent pattern of values.

Ho

The Blackcraig Formation again shows a tightly constrained, leptokurtic population with distribution positively skewed with respect to the remaining formations (fig.68c) which display highly consistent values across the succession.

Er

In general Er values (fig.69a) display similar patterns and trends to both Dy and Ho.

Yb

Yb values (fig.69b) display similar patterns and trends to Dy, Ho and Er. Here again the Blackcraig Formation provides the only disparity within a relatively consistent series of values.

Lu

The weakest concentrations of REE elements (fig.69c) are displayed by this element (0.19-0.5ppm) yet a remarkable similarity in compositional envelope pattern is displayed between this element and Dy, Ho, Er and Yb. With the exception of the Blackcraig Formation values are highly consistent, with a trend towards decreasing range across the succession. In general, the volcanic formations exhibit the greatest variability in both magnitude and range.

5.5 The Rhinns of Galloway Geochemical Traverses

This area was first mapped by Irvine in 1872 as part of the Geological Survey of Southern Scotland. Due to problems of cliff access and an almost total lack of exposure inland, nearly all previous work has been concentrated along about half of the 55km of coastal exposure. In a re-examination of the stratigraphy and structure of the northern portion of the Rhinns of Galloway, Kelling (1961) erected a stratigraphic succession which subdivided four main groups (Corsewall, Kirkcolm, Galdenoch and Portpatrick) on the basis of their distinctive petrography. The southern portion of the Rhinns has been subjected to considerably less investigation than the north, where lithostratigraphic controls are more clearly defined. However, the detailed stratigraphy of Kelling (op.cit) was extended southwards by Barnes et al., (1987). The results of multi-element geochemistry upon greywackes sampled at approximately 200m intervals, during this study of the Rhinns are graphically displayed in fold-out diagram no. 4. This diagram may be divided into three sections:

- 1) Traverse A-B from Currarie Point [20550,57790] south to Laight [20598,57030] relates to sampling on the eastern margin of Loch Ryan, as opposed to:
- 2) Traverse C-D from Milleur Point [20200,57370] south to Clachan [20350,57040] on the western margin.
- 3) The remaining samples (forming the major part of this investigation) were collected on a 42km traverse of the western margin of the Rhinns of Galloway; from Corsewall Point in the North, south to the Mull of Galloway.

It should be noted that the Corsewall, Kirkcolm and Portpatrick formations (Kelling, 1969) are correlated with the Marchburn, Afton, Scar (Portpatrick basic clast division) and Shinnel (Portpatrick acid clast division) formations of Floyd (1982). This study clearly delineates the location of a further volcanic group (the Pyroxenous Formation) south of Portpatrick, juxtaposed against cratonic derived sediments defined as Intermediate Formation equivalents. In addition, carbonate rich sediments characteristic of the Hawick Group are identified in the most southerly apex of the Rhinns, the Mull of Logan. Similar major and trace element patterns are displayed throughout both traverse C-D and the lower two thirds of traverse A-B. Variations in concentration clearly define the division of volcanic and cratonic derived sediments in each section (equivalents of the Marchburn and Afton formations) and facilitates geochemical mapping of the contact.

In addition, this study defines the presence of a further distinct group of greywackes, north of the Southern Upland Fault, in the initial third of traverse A-B. This group is predominantly composed of cratonic detritus, however samples 1, 2 and 3 display exceptional Mg, Cr and Ni values, clearly derived from volcanic material. The spatial distribution of samples collected from this area are defined upon a series of point-source, 1:325,000 scale geochemical maps (Figs. 267-296). Each map displays the results of individual elemental determinations, with concentrations directly related to increases in symbol size. A key defining the specific ranges of concentration for each element (defined on a percentile basis) with their corresponding symbol size, is presented on each map. The sharp contrast in values produced by the juxtaposition of volcanic and cratonic derived greywackes is clearly displayed by systematic variations in symbol size across the traverse. The twenty nine elemental maps may be grouped together to provide a geochemical atlas of the Rhinns and an effective tool in identifying differing petrographic tracts and the effects of granite intrusion, hydrothermal alteration and mineralization.

The problem of differing lateral variation within individual formations in the Rhinns has previously been rendered difficult due to the lack of adequate marker horizons (Kelling, 1969). This problem is not aided by the presence of intense tectonic deformation, and as such it was proposed that lithogeochemical studies of this area might be used to define more precise chemical constraints upon the stratigraphy. The following discussion relates to the major part of this study, namely the Western Margin Traverse of the Rhinns. Geochemical results are compared directly with both stratigraphic position and the characteristic chemical patterns identified in the Southern Uplands Composite Traverse (training set). Note the segmentation of the lower portion of the traverse, which is used to identify the relative position occupied by the Portencorkrie granodiorite intrusion.

5.5.1 The Corsewell Formation

The Corsewell Formation defined by Kelling (1961) forms the northern margin of the Rhinns and forms the lateral equivalent of the Marchburn Formation. Petrographically, these greywackes comprise a high proportion of angular rock fragments together with almost equal amounts of feldspar and quartz. Detrital grains of augite, epidote, hornblende and apatite are prominent with sodic plagioclase, the dominant feldspar. Clast mineralogy include acid, intermediate and basic igneous, metamorphic and sedimentary rock types. Igneous rock types include diorite, hornblende-dolerite, hornblende-granulite, andesite, serpentinite and vesicular spilite. Scarce fragments of glaucophane schist are also present. This volcanic derived formation is clearly identified on the geochemical traverse by relatively:

Low - Si, Al, La, Nb, Rb, Th, Al/Si, Nb/P, Rb/Sr, Ni/Co and Fe/Mg; and
High - Ti, Fe, Mg, Na, Mn, P, Sr, V, Fe+Mg and K+Na;

The high sulphur values found within volcanic derived greywacke formations correlate with increased framboidal pyrite content (Kelling, 1961).

5.5.2 The Kirkcolm Formation

The Kirkcolm Formation is composed of greywackes (up to 2m thick) separated by pale-blue silty bands and occasional thicker beds (up to 30m) of flaggy blue-grey siltstone and mudstone with seams of black graptolitic shale (Walton, 1961). This formation is generally more fine grained than the Corsewell Formation and contains no detrital ferromagnesian minerals, a higher proportion of metamorphic quartz and detrital mica, and less detrital feldspar. Rock fragments include ubiquitous meta-quartzites and phyllite, garnet-muscovite schists and hornfelsic rocks. Here again, sodic plagioclase is the most predominant feldspar and although muscovite is the dominant variety of mica, both biotite and chlorite are also common. The Kirkcolm Formation (samples 81-144) derived from a cratonic terrane, is clearly identified on the geochemical traverse (fold-out 5) juxtaposed against the Corsewell Formation by relatively:

Low - Ti, Fe, Mg, Ca, Na, Mn, P, Ba, Cr, Co, Ni, Sr, S, and V; and
High - Si, Al, K, La, Nb, Rb, Th, Y, Zr, La/Y, Nb/Y, Nb/P, Rb/Sr, Zn/Co and Fe/Mg.

Non-faulted boundaries between different greywacke formations have been identified (Styles, et al., 1989) within both the Kirkcolm and Portpatrick Formation.

5.5.3 The Galdenoch Formation

An added complexity occurs within a small subset of samples (No. 107-111) included in the Kirkcolm Formation and defined by a “?” on the traverse. These samples display more volcanic chemical affinities (ie higher Ti, Fe and Mg) and in comparison with the investigations of Kelling (1961,1969) correspond with the Galdenoch Group (a lateral equivalent of the Blackcraig Formation). Greywackes from this formation were defined by Kelling (op. cit.) to contain abundant rock fragments, detrital grains of hornblende, augite, epidote and apatite together with more quartz than feldspar. Rock fragments include spilite, andesite and acid igneous clasts together with a relatively restricted suite of metamorphic rock fragments, predominantly low-grade chlorite schists and phyllites. This formation is identified on the traverse by relatively:

Low - Si, Al, Rb, La/Y, Nb/P, Rb/Sr, K/K+Na; and

High - Ti, Fe, Mg, Na, Mn, V, Ba, Co, Cr, Cu, Ni, Sr, S, Fe+Mg, K+Na.

5.5.4 Portpatrick (Basic-Clast) Formation

This formation is composed of greywackes rich in fresh detrital pyroxene, amphibole, epidote, rock fragments, plagioclase and subordinate quartz. Augite, the main ferromagnesian mineral is accompanied by actinolite and rare glaucophane. This group is also characterised by the abundance of detrital biotite. Rock fragments include spilite, chert, acid igneous, metamorphic, rhyolitic tuffs and abundant andesite (giving the greywackes a primary tuff-like appearance). In general terms, this formation is characterised by relatively:

Low - Si, La, Rb, Th, Zr, Al/Ca+Na, La/Y, Nb/Y, Nb/P, Rb/Sr, Zn/Co.

High - Fe, Mg, Ca, Mn, V, Ba, Cu, Ga, Sr, V, Zn, Fe+Mg, K+Na.

5.5.5 Portpatrick (Acid-Clast) Formation

In general, this formation is more poorly sorted than its volcanic counterpart and contains a greater portion of quartz, acid igneous and metamorphic rock fragments and considerably less feldspar, basic igneous fragments and ferromagnesian minerals. This formation is characterised by an abundance and wide variety of metamorphic rock types, ranging from phyllites to tremolite-schists and garnetiferous gneisses. Geochemically, this formation is defined by relatively:

Low - Fe, Mg, Ca, Mn, V, Ba, Cu, Ga, Sr, V, Zn, Fe+Mg and K+Na; and

High - Si, La, Rb, Th, Zr, Al/Ca+Na, La/Y, Nb/Y, Nb/P, Rb/Sr and Zr/Co.

This formation forms the lateral equivalent of the Shinnel Formation (Floyd, 1982).

5.5.6 The Pyroxenous Formation

The location of a pyroxenous-rich greywacke formation, south of the Portpatrick (Acid-Clast) Group was first proposed by the author in 1985 on the basis of the geochemical data discussed below, and later defined on petrographic grounds by Barnes et al., (1987) who limited the occurrence of pyroxenous greywackes to a 400m

wide tract within the Money Head Block. On the basis of a comparative geochemical study of the Pyroxenous Formation in the Central Belt, it is proposed that the width of this tract is closer to 3-4km and bounded by the Standfoot and Cairngarroch fault zones. The Pyroxenous Formation may be identified on this traverse by relatively:

- Low - Si, Nb/Sr, Nb/P; and
- High - Ti, Mg, Ca, Na, K, Mn, Cr, Ni, Sr, K+Na and Fe/Mg.

5.5.7 The Intermediate Formation

South of the Money Head Block, Barnes et al., (op. cit) defined seven further blocks; the Float Bay, Ardwell Point, Mull of Logan, Port Logan, Clanyard, Cardrain and Mull of Galloway blocks, defined upon structural style and separated by strike-parallel faults. The first six blocks may be grouped together and defined on their component geochemistry as Intermediate Formation equivalents, composed of cratonic derived detritus. The Intermediate Formation may be characterised on this traverse by relatively:

- Low - Al, Ti, Fe, Mg, Ca, Na, K, Mn, P, Co, Cr, Ga, Ni, Sr, V, Zn,
Fe+Mg, Nb/P, K+Na, Fe/Mg; and
- High - Si, La, Rb, Th, Zr, Al/Ca+Na, La/Y and Rb/Sr.

Portencorkrie Granodiorite

The effects of igneous intrusion upon Intermediate Formation greywackes are illustrated diagrammatically and with reference to samples 247-250 and 251-254, representing traverses towards and away from the north and south contact margins of the Portencorkrie granodiorite, respectfully. The effects of alteration are particularly well displayed on the southern margin of the granodiorite where exposure was less restricted. (NB. Sample 251 was collected 40m from the contact margin). The progressive geochemical effects of intrusion upon the host greywackes may be defined in terms of subtle:

- Enrichment - Fe, Ca, K, As, Ba, Cu, Pb, Rb, Sr, S and K+Na;
- Depletion - Na, Zn, Al/Ca/Ca+Na, Rb/Sr.

It should be noted that this pattern of element enrichment and depletion is also characteristic of that associated with hydrothermal alteration and As-Sb-Au mineralization elsewhere in the Southern Uplands.

5.5.8 The Hawick Group

The outcrop of greywackes defined on the basis of their component geochemistry as members of the Hawick Group, lie within an area identified by Barnes et al., (1987) as the Mull of Galloway Block, south of the Tarbet Fault, which forms the most southerly promontory of the Rhinns. Barnes et al., (op.cit) identified greywackes from the Cardrain Block (an area between the Portencorkrie granodiorite and the Tarbet Fault) as also belonging to the Hawick Group. Litho-geochemical studies however, indicate that although both blocks contain cratonic derived sediments, major differences exist in their respective carbonate contents, which mimic those observed between Intermediate Formation and Hawick Group elsewhere in the Southern Uplands. It is clear from this study that Hawick Group greywackes are only present south of the Tarbet Fault and may be distinguished from their northerly counterparts

by relatively:

- Low - Si, Al, Ti, Fe, Na, K, P, Ba, Ga, La, Nb, Pb, Th, Y, Zn, Zr,
Al/Ca+Na, Rb/Sr, Zn/Co, Zr/Nb, Fe/Mg; and
High - CaO, Sr and possibly Sb.

5.5.9 Lithogeochemical Atlas

The relative positions of differing petrographic formations identified by Kelling (1969, 1971) in the northern half of the Rhinns of Galloway are displayed in fig.266. The results of a geochemical study of 279 greywacke samples collected during a coastal traverse of the western margin of the Rhinns of Galloway are presented as a series of single-element maps (figs. 267-296). These maps may be grouped together to form a multi-element lithogeochemical atlas of this region. Within each map, individual sample sites are represented by circles, the size of which is directly proportional to concentration, and controlled by the percentile ranges (0-50, 50-75, 75-90, 90-95 and >95%). Major variations in chemical composition are attributed to differences in the petrographic character of individual greywacke formations, and the cryptic effects of hydrothermal alteration and As mineralization. The sharp contrast in values produced by the juxtaposition of volcanic and cratonic derived greywackes are clearly displayed by systematic variations in symbol size across the traverse. The scale of each map is displayed by the 1km tick marks on the southern and western axes and by the 10km grid covering the study area. It should be noted that the Corsewall, Kirkcolm and Portpatrick formations (Kelling 1969) are correlated with the Marchburn, Afton, Scar (Portpatrick basic) and Shinnel (Portpatrick acid) formations of Floyd (1983). In addition the position of the (Silurian) Pyroxenous (Kilfillan) and Intermediate (Queensbury) formations and Hawick Group are identified by this study. A graphical summary of the chemical data contained within these maps is presented in fold-out no. 5. A detailed discussion of the individual geochemical maps is presented below:

SiO₂

Sharply contrasting, systematic variations in SiO₂ concentration may be used to identify the positions of juxtaposed volcanic and cratonic derived greywacke units within the Rhinns of Galloway survey area (fig.267). Formations identified by this map include the Corsewall, Kirkcolm, Portpatrick, Shinnel, Kilfillan, Queensbury formations and Hawick Group. Note the low values associated with volcanic units as opposed to their higher cratonic counterparts.

Al₂O₃

Systematic variations in Al₂O₃ concentration may be used to identify the relative position of the Corsewall, Queensbury formations and Hawick Group within the Rhinns of Galloway survey area (fig.268). No differentiation between the Kirkcolm, Portpatrick and Shinnel formations could be made using this element. Note the relatively low values associated with volcanic units as opposed to their higher cratonic counterparts.

TiO₂

Sharply contrasting variations in TiO₂ content may be used to identify the boundaries between the Corsewall-Kirkcolm; Kirkcolm-Portpatrick; Kilfillan-Queensbury; and Queensbury Formation-Hawick Group in the Rhinns of Galloway survey area (fig.269). Differentiation between the Portpatrick and Shinnel formations however, was not possible using the class intervals selected for this diagram, although in general, higher values are associated with volcanic units as opposed to their relatively lower cratonic counterparts.

Fe₂O₃

Systematic variations in Fe₂O₃ concentration may be used to identify the relative position of the Corsewall, Kirkcolm, Portpatrick, Shinnel, Kilfillan, Queensbury formations and Hawick Group within the Rhinns of Galloway survey area (fig.270). Note the relatively high values associated with volcanic units as opposed to their lower cratonic counterparts.

MgO

Sharply contrasting, systematic variations in MgO content may be used to identify the positions of both volcanic and cratonic derived greywacke units within the Rhinns of Galloway (fig.271). Formation boundaries identified by this element include the Corsewall-Kirkcolm; Kirkcolm-Portpatrick; Shinnel-Kilfillan, Kilfillan-Queensbury and Queensbury-Hawick group boundaries. In general, extremely high MgO values are associated with volcanic units as opposed to their lower cratonic counterparts.

Na₂O

Contrasting variations in Na₂O content may be used to identify the boundaries between the Corsewall-Kirkcolm; Kirkcolm-Portpatrick; Portpatrick-Shinnel; Shinnel-Kilfillan; Kilfillan-Queensbury; and Queensbury-Hawick Group in the Rhinns of Galloway survey area (fig.272). Relatively high Na values are associated with volcanic units as opposed to their lower cratonic counterparts.

CaO

Subtle systematic variation in CaO content occurs through out the Rhinns survey area and may be used to identify the positions of both volcanic and cratonic derived greywacke units (fig.273). Formation boundaries identified by this element include the Corsewall-Kirkcolm; Kirkcolm-Portpatrick; Shinnel-Kilfillan, Kilfillan-Queensbury and Queensbury-Hawick Group boundaries. Note the extremely high CaO values associated with the cratonic derived Hawick Group greywackes.

K₂O

Contrasting variations in K₂O content may be used to identify the boundaries between the Corsewall-Kirkcolm and Portpatrick-Shinnel formations in the Rhinns of Galloway (fig.274).

MnO

Sharply contrasting, systematic variations in MnO content may be used to identify the positions of both volcanic and cratonic derived greywacke units within the Rhinns of Galloway (fig.275). Formation boundaries identified by this element include the Corsewall-Kirkcolm; Kirkcolm-Portpatrick; Kilfillan-Queensbury and Queensbury-Hawick Group boundaries. In general relatively high MnO values are associated with volcanic units in the northern section of the Rhinns.

P₂O₅

Systematic variations in P₂O₅ concentration may be used to identify the relative position of the Corsewall, Kirkcolm, Portpatrick, Shinnel, Kilfillan and Queensbury formations and Hawick Group within the Rhinns of Galloway survey area (fig.276). Relatively higher values are associated with volcanic units as opposed to their lower cratonic counterparts.

As

Extremely low arsenic values (<3ppm) occur within all greywacke formations from the Rhinns of Galloway study area (fig.277). Anomalous arsenic values defined at three main sites south of Portpatrick. Figure 278 presents a partial enlargement of the arsenic map (Fig.277) covering an area 10x20km south of Portpatrick, containing all major arsenic anomalies located within this region, to date. The three anomaly sites identified include: Morroch Bay, Cairngarroch Bay and Grennan Point. The Cairngarroch Bay anomalies have been evaluated in detail by the author where anomalous arsenic values were traced to a series of quartz-arsenopyrite veins and widespread arsenopyritisation at the margins of a small composite igneous intrusion (see plates 32 and 33).

Ba

Contrasting variations in Ba content may be used to identify the boundaries between the Corsewall-Kirkcolm; Kirkcolm-Portpatrick; Portpatrick-Shinnel; Shinnel-Kilfillan; Kilfillan-Queensbury; and Queensbury-Hawick Group in the Rhinns of Galloway survey area (fig.279). In detail, elevated Ba values are associated with volcanic derived units as opposed to their lower cratonic counterparts.

Co

Subtle variations in Co content occur throughout the Rhinns survey area and may be used to identify the positions of both volcanic and cratonic derived greywacke units (fig.280). Formation boundaries identified by this element include the Corsewall-Kirkcolm; Kirkcolm-Portpatrick; Shinnel-Kilfillan formation boundaries. In general, slightly elevated values are associated with volcanic units as opposed to their lower cratonic counterparts.

Cr

Systematic variations in Cr concentration may be used to identify the relative position of the Corsewall, Kirkcolm, Portpatrick, Shinnel, Kilfillan, Queensbury and Hawick Group within the Rhinns of Galloway survey area (fig.281). In addition, the Corsewall Formation may be subdivided into the Flaggy and Conglomeratic divisions on the basis of their differing elevated Cr contents. Highly elevated Cr values are associated with volcanic units as opposed to their lower cratonic counterparts.

Cu

Figure 282 displays a lack of chemical differentiation between volcanic and cratonic derived units with respect to their copper geochemistry.

La

Subtle systematic variation in La content occurs through out the Rhinns survey area and may be used to identify the positions of both volcanic and cratonic derived greywacke units (fig.283). Boundaries identified by this element include the Corsewall-Kirkcolm; Kirkcolm-Portpatrick; Kilfillan-Queensbury and Queensbury-Hawick Group boundaries. In general, relatively low La values are associated with volcanic units as opposed to their elevated cratonic counterparts.

Nb

Contrasting variations in Nb content may be used to identify the boundaries between the Corsewall-Kirkcolm; Kirkcolm-Portpatrick; Portpatrick-Shinnel; Shinnel-Kilfillan; Kilfillan-Queensbury; and Queensbury-Hawick Group in the Rhinns of Galloway survey area (fig.284). Extremely low values Nb values are associated with volcanic units in comparison with their higher cratonic counterparts.

Ni

Systematic variations in Ni concentration may be used to identify the relative position of the Corsewall, Kirkcolm, Shinnel, Kilfillan and Queensbury formations, and Hawick Group within the Rhinns of Galloway (fig.285). Relatively low Ni values are associated with volcanic units as opposed to their higher cratonic counterparts.

Pb

Highly consistent Pb values are displayed by both volcanic and cratonic formations (fig.286) throughout the Rhinns study area.

Rb

Subtle variations in Rb content occur throughout the Rhinns survey area which may be used to identify the positions of both volcanic and cratonic derived greywacke units (fig.287). Boundaries identified by this element include the Corsewall-Kirkcolm; Kirkcolm-Portpatrick; Portpatrick-Shinnel; Shinnel-Kilfillan; Kilfillan-Queensbury and Queensbury-Hawick Group boundaries. Note the lower Rb values associated with the volcanic units as opposed to their higher cratonic counterparts, and the elevated Rb levels are displayed by the Queensbury (Intermediate) Formation.

S

Sharply contrasting variations in sulphur content may be used to identify the boundaries between the Corsewall-Kirkcolm; Portpatrick-Shinnel; Shinnel-Kilfillan; Kilfillan-Queensbury; and Queensbury-Hawick Group in the Rhinns survey area (fig.288). Note the extremely low values sulphur values identified in both the Corsewall (Lower Ordovician) and Hawick (Silurian) formations.

Sb

Consistently low Sb values (<4ppm) are displayed throughout the succession (fig.289). A small number of anomalies are identified, located in both Morroch and Cairngarroch Bay's (areas also pinpointed by arsenic geochemistry, see figs. 277 and 278) Logan Bay and the Mull of Galloway. Also noteworthy is the general increase in the background Sb content of greywackes in close proximity to major igneous intrusions.

Sr

Systematic variations in Sr concentration may be used to identify the relative position of the Corsewall, Kirkcolm, Portpatrick, Shinnel, Kilfillan, Queensbury formations and Hawick Group within the Rhinns of Galloway study area (fig.290). Here, the elevated Sr values associated with volcanic units as opposed to their lower cratonic counterparts.

Th

Weakly contrasting variations in Th content may be used to identify the boundaries between the Corsewall-Kirkcolm; Kirkcolm-Portpatrick; Portpatrick-Shinnel; Shinnel-Kilfillan; Kilfillan-Queensbury; and Queensbury-Hawick Group in the Rhinns survey area (fig.291). In general, low Th values are associated with volcanic units as opposed to their subtly higher cratonic counterparts.

V

Sharply contrasting variations in V content may be used to identify the boundaries between volcanic and cratonic derived greywacke units (fig.292). Formation boundaries identified on the basis of variations in V content include; the Corsewall-Kirkcolm; Kirkcolm-Portpatrick; Portpatrick-Shinnel; and Shinnel-Kilfillan boundaries in the Rhinns of Galloway survey area. Extremely elevated V values are associated with volcanic units as opposed to their lower cratonic counterparts.

Y

Subtle variations in Y content occur within greywackes throughout the Rhinns survey area (fig.293). These variations may be used to identify the positions of both volcanic and cratonic derived greywacke units and their associated boundaries. Formation boundaries identified by Y chemistry include the Corsewall-Kirkcolm; Kirkcolm-Portpatrick; Kilfillan-Queensbury and Queensbury-Hawick Group boundaries. Note the low values associated with volcanic units as opposed to their relatively higher cratonic counterparts.

Zn

Relatively consistent Zn values displayed in the northern section of the Rhinns and the lower values associated with the Kilfillan Formation (fig.294). Zinc depletion envelopes are located in both Morroch and Cairngarroch Bay (associated with hydrothermal alteration and As-Sb mineralization) and within the margins of the Portencorkrie granodiorite at the southern margin of the survey area.

Zr

Systematic variations in Zr concentration may be used to identify the relative position of the Corsewall, Kirkcolm, Portpatrick, Shinnel, Kilfillan, Queensbury formations and Hawick Group within the Rhinns of Galloway study area (fig.295). In general, extremely low Zr values associated with the volcanic derived units as opposed to their considerably higher cratonic counterparts.

5.6 THE LONGFORD DOWN GEOCHEMICAL TRAVERSE

Leggett (1979) presented a correlation between the Northern Belt in the Southern Uplands and greywacke formations identified in the northern and central portions of the Longford Down Inlier, Ireland. Three strike parallel tracts separated by strike faults were recognised and distinguished by differences in both stratigraphy and greywacke petrography. In subsequent studies, Morris (1987) demonstrated that the Northern Belt of the Southern Uplands/Longford Down contains two compositionally distinct petrofacies suites, each ranging from mid-to late Ordovician age. Both suites extend throughout the length of the belt and are generally separated by strike faults: The first, metaclast petrofacies of Morris (1987) is characterised by felsic, igneous and metamorphic detritus derived from a continental source to the NW, whereas the second, southeastern basic clast petrofacies contains abundant calc-alkaline detritus derived from an island arc complex to the south.

The results of this study to evaluate the application of lithogeochemistry to correlation and geochemical mapping within the Longford Down Inlier, are graphically displayed in fold-out diagram No.4. This reconnaissance study was based upon a suite of petrographically defined greywacke samples provided for geochemical analysis by Dr John Morris of the Irish Geological Survey. Samples were assigned to their respective formations on the basis of petrographic examination (Morris, 1983) grouped in ascending numerical order and combined with other formations to create a geochemical profile (n=225). This profile presents a composite section across three, regional scale stratigraphic units, namely: the Strokestown, Gowna and Hawick Groups.

The Strokestown Group, defined by Morris (1987) comprises five formations: Aghamore, Lackan, Finnalayhta, Coronea and Cornhill, which range in age from Llanvirn to Lower Silurian; whereas the Llandeilo-Caradoc Gowna Group consists of three formations: Carackateane, Glen Lodge and Red Island. The Hawick Group however, is not subdivided in this study, but is separated from the Gowna Group by the Slieve Glah Shear Zone. The spatial distribution of samples collected during this survey are defined upon a series of point-source 1:400,000 scale geochemical maps (Figs 411-441). The geochemistry of each group is defined below and discussed in comparison with their strike extensions in the Southern Uplands.

5.6.1 The Strokestown Group

The Corn Hill Formation

The Corn Hill Formation (Llanvirn age) is the oldest formation exposed in the Longford Down and is composed of greywackes rich in feldspar, quartz and rock fragments which, although dominated by argillite lithologies also include arenite, mafic, volcanoclastic and conglomeratic lithologies. This formation, despite its mafic components

is characterised by cratonic affinities (ie high SiO_2 - Low MgO) and may be clearly differentiated from volcanic (basic-clast) petrofacies by relatively:

High - Si, Ti, La, Nb, Rb, Th, Y, Zr, Fe/Mg, Rb/Sr, Al/Ca+Na, Nb/Y and Nb/P; and
Low - Fe, Mg, Ca, Na, Cr, Sr, V, Fe+Mg and Zr/Nb.

The Coronea, Finnalayhta and Lackan formations

The Coronea, Finnalayhta and Lackan formations are assigned by Morris (1987) to the Metaclast (cratonic) petrofacies. They are characterised by quartz, metamorphic and felsic igneous detritus and are correlated with the Afton Formation (Floyd, 1981); Abington Formation (Hepworth et al., 1982) and Kirkcolm Formation (Kelling, 1962). These formations are characterised by strong cratonic affinities and are clearly distinguished from volcanic petrofacies by relatively:

High - Si, Ti, La, Nb, Rb, Th, Y, Zr, Fe/Mg, Rb/Sr, Nb/Y, Nb/P; and
Low - Fe, Mg, Ca, Na, Cr, Sr, V, Fe+Mg and Zr/Nb.

Both the Coronea and Lackan formations display similar variances (F test statistic) and similar mean compositions. In addition the results of a student T test indicate a high probability that the two formations were both derived from the the same parent population/source terrane. The Lackan Formation however, may be distinguished from both the Finnalayhta and Coronea counterparts by a highly variable chemical composition. The reasons for this increase in range of composition are at first unclear. If however, the Lackan Formation is subdivided into an upper and lower unit, the range of variation is reduced (within unit). In addition the two units display close chemical affinities with their juxtaposed counterparts, namely the stratigraphically higher Aghamore and lower Finnalayhta formations. (Nb The detailed geochemistry of the Aghamore Formation is described in the next section).

It is tentatively proposed that, on the basis of these results the Lackan Formation represents a transitional unit between the Aghamore and Finnalayhta formations, and is composed of varying proportions of material derived from the source areas of both formations, with their respective contributions controlled by stratigraphic position. In summary, the geochemical evidence presented to date, suggest that the Comhill, Coronea, Finnalayhta and Lower Lackan formations were derived from the same source terrane. Little if any variation in the nature of sediment supply was observed, until the Upper Lackan and Aghamore formations were deposited from a considerably more acidic source.

The Aghamore Formation

This formation is the youngest member of the Strokestown Group (Early Silurian) and consists of a series of greywackes intercalated with spilitic lavas, volcanoclastics and black cherts. Although the intercalated nature of the greywackes would suggest a probable volcanic derivation, the Aghamore Formation is remarkable in that it displays the most cratonic chemical characteristics of all the formations in the Strokestown Group. The Aghamore Formation may be distinguished from the Finnalayhta and Coronea formations by relatively:

High - Si, Fe/Mg, La/Y, Nb/P; and
Low - Ti, Fe, Mg, Mn, P, Co, Cr, Ni, Nb, V, Y, Zn, Rb/Sr and Ni/Co.

A simple quartz (SiO_2) dilution model cannot be invoked to explain the major depletions in Ti, Fe and Mg content. It is clear from this study that a significant change in source area/ provenance is defined by this formation, with the removal of a considerable portion of the mafic component of the sediments. In comparison with the Southern Uplands, this formation exhibits clear similarities with the Intermediate Formation.

5.6.2 The Gowna Group

Red Island Formation

The Red Island Formation, a volcanic-lithic greywacke, forms the oldest unit in the Gowna Group and is defined in detail by Sanders and Morris (1978) and Morris (1979,1983). This formation together with the Glen Lodge Formation is identified by Morris (1987) as the lateral equivalent of the Basic Clast Division of the Portpatrick Formation (Kelling, 1961) and Scar Formation (Floyd, 1982). It is characterised by andesitic mineral and lithic fragments together with minor blueschist detritus. Geochemically, both the Red Island and Glen Lodge Formation exhibits strong volcanic (basic-clast) characteristics in comparison with the Strokestown Group formations, and close similarities with the Scar Formation in the Southern Uplands. Both formations may be distinguished from their juxtaposed cratonic equivalents by relatively:

High - Mg, Ca, Na, Cr, Ni, Sr, V, Fe+Mg; and

Low - Si, Ti, K, La, Nb, Pb, Th, Y, Zr, K/Na, Nb/P and Rb/Sr.

The Glen Lodge and Carrickateane formations

The Glen Lodge and Carrickateane formations are differentiated from the Red Island Formation on the basis of variations in stratigraphic position as defined by graptolite faunas and the increased abundance of intercalated spilitic lavas and cherts. Based upon variations in detrital mineralogy the Glen Lodge Formation is defined by Morris (1987) as the lateral equivalent of the Scar Formation, whereas the Carrickateane Formation is equated with the Galdenoch Formation (cf. Blackcraig Formation, Floyd, 1982). On the basis of this study and limited sample density, the Glen Lodge Formation may be differentiated from the Red Island and Carrickateane formations by relatively low Ca, Sr and V values and high MnO content. It is worthy of note that the P_2O_5 content increases systematically throughout this group in direct opposition to both Cr and Ni values.

The Carrickateane Formation (cf. Blackcraig Formation) may be distinguished from other members of this group by relatively lower Cr, Ni, Ni/Co, Nb/P and Nb/Y; and higher Na and P contents. The Nb/Y values determined in this formation are the lowest identified in greywackes from the Longford-Down and in comparison with the Southern Uplands correlate well with the characteristically low values defined for the Galdenoch (Blackcraig) petrofacies.

5.6.3 The Hawick Group

Greywacke samples from the lateral equivalents of the Hawick Group were collected on a cross-strike traverse across the central part of the Longford Down. Petrographically, this group exhibits close similarities with the Hawick Group in the Southern Uplands, with greywackes composed of quartz, feldspar, lithic fragments and

detrital carbonate. Rock fragments including felsic igneous and metamorphic lithologies are characteristic of a cratonic source terrane. Geochemically, this group may be characterised on the basis of CaO and S content alone, however it may also be distinguished from:

- 1) The Strokestown Group, on the basis of relatively:
High - Ca and Sr; and
Low - Si, Al, Ti, Fe, Na, Mn, Ba, Cr, Ga, La, Nb, S, V, Zn, Zr, Fe+Mg, Fe/Mg, La/Y, Nb/Y, Al/Ca+Na and Nb/P.
- 2) The Gowna Group, on the basis of relatively:
High - Ca, Nb, Th, Y, Zr, K/Na, Nb/P, Rb/Sr;
Low - Al, Fe, Mg, Na, Mn, P, Ba, Co, Cr, Ga, Ni, Sr, V, Zn, Fe+Mg, Al/Ca+Na, K+Na.

Slieve Glah Shear Zone

The boundary between the Northern and Central belts in the Longford Down, is marked by a major strike fault, the Slieve Glah shear zone (Oliver, 1978; Morris et al., 1985). Three greywacke samples collected from the Slieve Glah Shear Zone exhibit close similarities with Gowna Group volcanic (Basic Clast) greywackes. Subtle variations, possibly related to the effects of alteration associated with shearing include both decreases in Ca, K, Sr, K/Na and K/K+Na; and increases in Na, Rb and Fe/Mg. The sample density in this formation is too low to provide a statistically acceptable assessment of shear related alteration, however in comparison with alteration studies in the Southern Uplands, there appears little chemical similarity between shear and As-Sb-Au related alteration processes.

5.6.4 Hydrothermal Alteration and Mineralization

Arsenic anomalies (>20ppm) are located in the Aghamore and Lackan Formation and Hawick Group equivalents, in areas previously recorded as having little if any mineral potential. In each instance, the samples display similar patterns of major and trace element alteration to that associated with As-Sb-Au mineralization in Scotland, namely:

Enrichment -	As, Sb, S, K, Ba, Pb, Co, La, K/Na; and
Depletion -	Na, Zn and Mg.

As such, each site provides a primary target for mineral exploration and should be subjected to detailed evaluation to ascertain the nature and magnitude of the mineralization. In addition to anomalies related to As-Sb-Au mineralization a small number of Ba, Cu, Pb and Zn anomalies were also identified in apparently unmineralized greywackes and are interpreted in relation to the low temperature Pb-Zn-Cu mineralization reported from this area (Morris, 1985). Regional arsenic lithogeochemical studies in the Longford Down have revealed anomalies values from samples located in close proximity to major shear zones. Such shear-associated anomalies are regarded as excellent gold targets elsewhere in the world and these sites provide favourable environments for gold mineralisation in Ireland.

5.6.5 Longford Down Lithogeochemical Atlas

A summary geological map of the Longford Down Study Area in the Republic of Ireland (after Morris, 1978, 1979 and 1985) is presented in fig. 411. This area includes counties Louth and Monaghan, a substantial part of County Cavan and parts of Counties Leitrim, Longford, Meath and Roscommon. This area was mapped by the Geological Survey of Ireland during the 19th century, a study which resulted in the publication of summary 1 inch:1 mile scale geological maps and memoirs. Subsequent to this study various parts of the inlier have been remapped by both the Geological Survey and individual researchers. Unfortunately, the metallic mineral deposits which occur in the inlier have in general been subjected to little investigation, however Morris (1984) presented a summary of all metallic mineral deposits of the Longford-Down.

In general, the Longford-Down Inlier is composed of Ordovician and Silurian rocks which continue along strike into similar age rocks in the Southern Uplands, and form part of the Caledonides of Britain, Scandinavia and the Appalachians of eastern North America (Morris, 1984). Ordovician rocks are constrained in a NE-SW trending belt along the northern margin of the inlier, whereas Silurian rocks dominate the central and southern parts of the inlier. A suite of igneous intrusions were emplaced during the Late Silurian-Early Devonian Caledonian Orogeny, which range from minor sills and dykes to stocks and plutons. Mafic, locally ultramafic and intermediate compositional igneous rocks dominate the earliest phase of igneous intrusion in contrast to more felsic compositions in later intrusions (Morris, op.cit). Figure 411 may also be used to illustrate the position of the late Caledonian NE-SW trending, strike parallel Navan-Collon, Carrickateane and Orloch Bridge (Slieve Glah) Fault Zones (comparable with major fault structures in the Southern Uplands); the position of Silurian and Ordovician greywackes (shaded dark grey and light grey respectively); the location of Carboniferous (Courceyan) and younger clastic sediments unconformably overlying the Lower Palaeozoic sequence; and the position of the Late Silurian-Early Devonian (430-400my) Crossdoney granodiorite.

The results of a geochemical study of 297 greywacke samples collected for this study by Dr John Morris (Geological Survey of Ireland) on a 'dog leg' traverse across the Longford Down Study Area are presented in a series of 1:400,000 scale maps which together form a multi-element lithogeochemical atlas of this region (Figs 411-441). The sampling pattern selected in this study was chosen to maximise coverage, include areas with strong stratigraphic and petrographic controls and avoid the Clontibret region and other mineralized areas. Individual sample sites are represented by circles, the size of which is proportional to concentration, and controlled by specific percentile ranges (0-50, 50-75, 75-90, 90-95 and >95%) of each element. Major variations in chemical composition are attributed to differences in the petrographic character of individual greywacke formations, and the cryptic effects of hydrothermal alteration and As-Sb-Au mineralization. The sharp contrast in values produced by the juxtaposition of volcanic and cratonic derived greywackes is displayed by systematic variations in symbol size across the traverse. The scale of each map is displayed by the 10km tick marks on the southern and western axes which may be used to identify the relative position of samples within the 100km Irish Survey grid cells G, H, M and N covering the study area. The chemical data contained within these maps is located in table 4.81-4.92 and presented graphically as a number of composite profiles within foldout no. 4.

Three regional scale stratigraphic units are defined in this study area, namely the Strokestown, Gowna and Hawick Groups. The Strokestown Group (Morris, 1987) comprises five formations: Aghamore, Lackan, Finnalayhta, Coronea and Cornhill, which range in age from Llanvirn to Lower Silurian; whereas the Llandeilo-Caradoc Gowna

Group consists of three formations: Carackateane, Glen Lodge and Red Island. The Hawick Group however, is not subdivided in this study, but is separated from the Gowna Group by the Slieve Glah Shear Zone. For the purposes of the following discussion the survey area may be divided into the following 5 sectors:

- Sector 1 - the Strokestown Inlier, this forms the western margin of the field area and contains both Marchburn and Kirkcolm Formation equivalents.
- Sector 2 - the Arva area - occupying the northwestern margin of the main inlier this area is bounded to the southwest by the Carrickateane Fault and contains Kirkcolm Formation equivalents.
- Sector 3 - the Gowna area is located immediately to the southeast of sector 2; contains Portpatrick Formation equivalents and is bounded in the southwest by the Orloch Bridge Fault.
- Sector 4 - the Bailieborough area - occupying a greater portion of the study area than any other sector, this area is bounded to the north by the Orloch Bridge Fault (Slieve Glah Shear Zone) and to the south by a line drawn from Jonesborough (in the NE) to Loch Glore (in the SE). This sector contains the Silurian Pyroxenous and Intermediate Formation equivalents.
- Sector 5 - the Castletown area, is located to the southeast of sector 4, occupying the remaining portion of the Inlier and defines the position of Hawick Group equivalents.

The relationship between these sectors and their underlying bedrock geochemistry is discussed in the following section:

SiO₂

Sharply contrasting, systematic variations in SiO₂ concentration may be used to identify the positions of juxtaposed volcanic and cratonic derived greywacke units within the Longford Down survey area (fig.412). Cratonic formations identified by this element are detailed in chapter 5 and include the Cornhill, Coronea, Finnalayhta, Aghamore and Hawick units which may be distinguished from the volcanic Red Island, Glen Lodge and Carackateane formations. Note the generally low values associated with volcanic units (clearly observed within sector 3) as opposed to their higher cratonic counterparts (sectors 2 and 4). Samples from sector 5 (displayed along the eastern margin of the geochemical map) define restricted values more appropriate to a volcanic derivation than their petrography suggests. This silica-poor feature may be explained by the addition of considerable CaO addition (predominantly in the form of carbonate) and the resulting dilution of all other major elements accordingly. The marked rise in CaO content is characteristic of the Hawick Group in the Southern Uplands and may be used as a mapping tool to identify the boundary between Intermediate and Hawick Group equivalents in the Longford Down.

Al₂O₃

Little systematic variation in composition is observed between volcanic and cratonic formations (fig.413). As such this element plays no significant role in greywacke discrimination and/or terrain boundary identification.

TiO₂

Sharply contrasting variations in TiO₂ content may be used to identify the boundaries between the positions of juxtaposed volcanic and cratonic derived greywacke units within the Longford Down survey area (fig.414). Cratonic formations identified by this element include the Cornhill, Coronea, Finnallyhta, Aghamore and Hawick units; and may be distinguished from the volcanic Red Island, Glen Lodge and Carackateane formations by the relatively higher values. Note the general decrease in Ti values across the succession with volcanic formations displaying relatively higher values than their juxtaposed cratonic counterparts; and the marked drop across the Ordovician-Silurian boundary.

Fe₂O₃

Volcanic derived formations display higher Fe values than their cratonic counterparts and mirror TiO₂ compositions with a trend towards decreasing values across the succession (fig.415). Note the position of juxtaposed volcanic and cratonic derived greywackes in the Longford Down survey area; the sharp boundary between sector 3 and 4, and the extremely low Fe values displayed by Sector 5 (Hawick equivalents).

Na₂O

The Na content reflects variations in petrography across the Longford Down with the compositions of volcanic derived greywackes elevated in comparison with their cratonic counterparts (fig.416). The effects of Na depletion associated with hydrothermal activity are markedly developed in sectors 1, 2 and 5.

CaO

With the exception of the Hawick Group, CaO values vary systematically across the Longford Down (fig.417). Cratonic derived greywackes display values 2-3% lower than their juxtaposed volcanic counterparts. Note the elevated values in sector 1 (Marchburn Formation equivalents) and the northern portion of sector 4 (Pyroxenous Formation equivalents). Hawick Group equivalents located on the eastern margin of the survey area (sector 5) are characterised by the highest CaO content of any formation in this study, with elevated levels formed in response to the input of carbonate from the source terrain. As such CaO values alone may serve to distinguish between the Silurian Intermediate and Hawick Group equivalents.

MgO

MgO values closely follow that of Ti and Fe within the Longford Down survey area (fig.418) with the highest values located in unit 3 (volcanic derived Pyroxenous Formation equivalents). Volcanic composition are in general 1.5-3.0% higher than their juxtaposed cratonic counterparts and as such this element provides a useful discrimination index.

K₂O

Systematic differences in composition between juxtaposed cratonic and volcanic derived greywacke formations are located in the Longford Down survey area (fig.419). Volcanic derived formations display values relatively lower than their cratonic counterparts particularly in sectors 1 and 3.

MnO

Although the MnO content is generally low (<0.25%) systematic variations between cratonic and volcanic derived greywacke formations are observed within the Longford Down survey area (fig.420) with cratonic derived formations relatively depleted with respect to their volcanic counterparts. Note the elevated values displayed within sector 3 in contrast to the cratonic sector 2, 4 and 5.

P₂O₅

This diagram illustrates a subtle trend towards decreasing P₂O₅ content across the Longford Down (Fig.421). Note the high P₂O₅ values occurring in the sector 1 and 4 (Marchburn and Intermediate Formation equivalents) and the extremely low values located in sector 4 on the eastern flank of this study area (Hawick Group equivalents).

As

Arsenic values in greywackes from the Longford Down lie close to, or below the analytical detection limit of the XRF (2-3ppm). As such, a comparison between background levels in volcanic and cratonic derived formations could not be made. Figure 422 however, illustrates the position of numerous arsenic anomalies (>8ppm) which may be used to pinpoint new areas of hydrothermal alteration and As-Sb-Au mineralization. Note the position of major arsenic anomalies on the southeastern margin of sector 5 (max 55ppm) located in the Dunleer township, adjacent to the Navan-Collon Fault zone. Arsenic anomalies are also observed in the western section of the study area adjacent to a major fault (Fergus Shear Zone) marking the western edge of the Strokestown Inlier.

Ba

Although little systematic variation in Ba content is observed across the Longford Down, individual formations exhibit sharp contrasts with juxtaposed units (fig.423). This feature is most clearly illustrated between sectors 3, 4 and 5. In addition, extremely reduced Ba levels occur in sector 5 (Hawick Group equivalents).

Co

The Co content is highly variable across the Longford Down (fig.424). Volcanic derived greywackes display slightly (5-8 ppm) lower values than their juxtaposed cratonic equivalents. Note the elevated Co levels concentrated on the northwestern margin of sector 4 (Pyroxenous group equivalents).

Cr

A systematic trend of decreasing Cr values is observed across the Longford Down (fig.425) with volcanic compositions 30-150ppm higher than their juxtaposed cratonic counterparts. Elevated Cr values up to 590ppm are characteristic of sector 3 and the northwestern margin of sector 4 are indicative of an ultrabasic/basic contribution from the source terrain. Note the consistently low Cr values displayed within the Hawick Group equivalents (sector 5).

Cu

Volcanic derived greywacke formations in the Longford Down display slightly elevated Cu values compared to their cratonic counterparts (fig.426). Anomalous Cu levels may be related to Cu mineralization and identify targets of possible exploration interest. Note the restricted Cu levels displayed by sectors 4 and 5 and the elevated Cu values adjacent to the Navan-Collon Fault.

Ga

Highly consistent Ga values are displayed across the entire succession. Subtle variations (3-4ppm) are observed between volcanic (higher) and cratonic (lower) derived formations (fig.427) with relatively restricted Ga levels displayed within sectors 4 and 5.

La

Systematic variations in La content occur across the Longford Down (fig.428) with Ordovician cratonic formations (sector 2) exhibiting levels 10-15 ppm greater than their volcanic counterparts (sectors 1 and 3). Note the relatively elevated levels displayed by Intermediate Formation equivalents (sector 4) in comparison with depleted Hawick Group samples (sector 5). La depletion in sector 5 is attributed to the effects of CaO dilution.

Nb

Subtle systematic variations in Nb content occur throughout the Longford Down study area (fig.429) with volcanic formations displaying values 5-15ppm lower than their juxtaposed cratonic counterparts. Particularly noteworthy are the restricted values displayed by samples in sector 3 and the northwest margin of sector 4.

Ni

A general decrease in Ni content is observed across the Longford Down succession, with volcanic units defined by values 40-60ppm higher than their cratonic counterparts (fig.430). Note the elevated values displayed within sector 3 and the northwestern margin of sector 4; and the restricted levels contained within sector 5 (Hawick Group equivalents).

Pb

No systematic variation is observed within the Longford Down (Fig.431) however anomalous values particularly those associated with the Navan-Collon Fault and Castle Fergus shear zone are indicative of proximity to mineralization.

Rb

A systematic increase in Rb values are observed across the Longford Down with volcanic derived formations 20-30ppm lower than their juxtaposed counterparts (fig.432). Note the elevated levels displayed within sectors 4 and 5.

Sb

The background level of Sb are close, if not below the detection limits of the XRF (1-3ppm). As such, a comparison between background levels in volcanic and cratonic derived formations could not be made. The Sb geochemical map (fig.433) however, illustrates the position of numerous Sb anomalies (>5ppm) which may be used to pinpoint new areas of hydrothermal alteration and accompanying As-Sb-Au mineralization. Note the concentration of antimony anomalies (max 14ppm) on the eastern margin of the study area within sector 5. In this area, Sb anomalies are more widely distributed than their As counterparts, and located adjacent to Tallanstown, Mansfieldstown, Dromin and the Navan-Collon Fault zone. In addition, a concentration of weak Sb anomalies is also identified 4km southeast of Cavan, in proximity to the Slieve Glah shear zone, at the junction between sector 3 and 4.

S

A systematic decrease in S content across the Longford Down is clearly identified (fig.434) with volcanic formations containing 200-1000ppm higher values than their juxtaposed cratonic counterparts. Hawick Group equivalent greywackes displayed in sector 5 are characterised by extremely low values (<50ppm) which are inversely correlated with CaO content. Note that anomalous S values occur in proximity to the Navan-Collon Fault and coincide with both As, Sb, Pb, and Cu anomalies. Elevated S levels are also detected in the Sb anomaly zone located within the Slieve Glah Shear Zone, southeast of Cavan.

Th

A consistent pattern of Th values occur throughout the Longford Down with volcanic derived greywackes generally 4-6 ppm lower than their juxtaposed cratonic counterparts (fig.435). Note the restricted values displayed in sector 3 compared with the relatively elevated values in sectors 2 and 4.

V

A systematic decrease in V content occurs across the Longford Down with volcanic derived formations exhibiting concentration 50-100ppm higher than their juxtaposed cratonic sediments (fig.436). Note the elevated V values displayed in sectors 1 and 3; and the extremely low contents displayed by the Intermediate Formation and Hawick Group equivalents (sectors 4 and 5).

Y

Y values throughout the Longford Down are highly consistent and display little if any systematic variation (fig.437) however, the highest values in this sequence are located in the cratonic derived formations of sectors 2, 4 and 5.

Zn

A systematic variation in Zn content is observed across the succession with volcanic derived greywackes (sector 3 and the northwestern margin of sector 4) displaying values up to 30ppm higher than juxtaposed cratonic sediments (fig.438). Restricted Zn levels are displayed within sector 5 and in addition low Zn values (depleted samples) are found in association with As, Sb, Pb and Cu anomalies associated with major shear zone related fault zones.

Zr

A systematic variation in Zr content occurs across the succession with volcanic derived greywackes displaying values up to 150ppm lower than juxtaposed cratonic greywacke (fig.439). Note the restricted Zr levels displayed by sector 1, 3 and the northwestern margin of sector 4. In addition, sector 5 (Hawick Group equivalents) display significantly lower values than those predicted from a comparison with adjacent sector 4 (Intermediate Formation equivalents). This feature may be attributed to dilution effects formed by the addition of a major (10-15%) carbonate component to sector 5 greywackes.

5.7 LEADHILLS UNDERGROUND TRAVERSE

A detailed description of the geological setting, mining history and mineralization in the Leadhills-Wanlockhead district of Scotland is presented by Temple (1956), Mackay (1959) and Gillanders (1981). Temple (1956) recognised the existence of two distinct periods of mineralization in the Leadhills-Wanlockhead region. The first, consisted of Caledonian quartz veins containing minor gold mineralization, whereas the second constituted extensive Permo-Carboniferous lead-zinc vein mineralization. Although alluvial gold is widespread throughout the Leadhills district, particularly favourable localities include the Long Cleuch and Windgate Burns.

The results of multi-element geochemistry upon 29 greywacke samples collected from a 200m long underground traverse perpendicular to the Susanna Pb-Zn vein system at Leadhills are displayed in figure 298. In addition, a plan of the Susanna Mine detailing underground sample site locations is presented in fig.15. The geochemical data relating to this study is also presented in tables 4.122 and 2.119. Altered greywackes from the Susanna mine traverse at Leadhills are composed of poorly sorted grains of quartz, sodic plagioclase, detrital flakes of white mica, fine grained igneous rock fragments and interstitial clay. Detrital feldspar are partially or completely replaced by fine grained sericitic aggregates whereas detrital mica is altered to a colorless low birefringent clay mineral, possibly kaolinite.

The Susanna Vein:

Fe, As, Ba and Fe/Mg values are elevated in proximity to the Susanna vein whereas La, Pb, Sb, S, Th, K/Na, Al/Ca+Na, Nb/P, Rb/Sr, Ni/Co and Cu/Co exhibit varying degrees of depletion with respect to the average greywacke composition.

The Humby Vein:

Al, K, As, Ba, Cu, La, Pb, Rb, Sb, Zn and K/Na, Fe/Mg, Al/Ca+Na, Rb/Sr and Cu/Co values are elevated in proximity to the vein whereas Na, Fe, Mg and Ca exhibit variable levels of depletion with respect to the average greywacke composition.

The McDonalds Vein:

Fe, Mg, Ca, Pb, Zn, Cu and Sr values are elevated in proximity to the McDonalds vein whereas Na, K, Mg, Fe, Rb, K/Na, Al/Ca+Na, Rb/Sr are depleted.

In general Si, Mn, P, Cr, Nb, V, Y, Zr and Al/Si display relatively consistent values throughout the traverse. With the exception of wallrock samples from the Susanna Vein, sodium exhibits widespread depletion ($Na < 1\%$) and indicates the extensive nature of wallrock alteration throughout the traverse. Potassium values demonstrate an inverse relationship with sodium and exhibit elevated values across the central portion of the traverse. Arsenic

levels are all generally above detection limits, with elevated values located marginal to Pb-Zn-Ba (\pm Cu) vein mineralization. Maximum Pb values are located adjacent to the McDonalds vein however elevated values are defined throughout the traverse and illustrate the pervasive nature of Pb mineralization in this deposit. Sb values correlate with both Pb, As, Cu, Rb, S, Zn and the alteration index K/Na, and serve to illustrate the complex geochemical relationships present within this deposit. To aid the understanding of the inter-relationships present within this geochemical data, principal component analysis was undertaken. The principal component results and component scores are presented in table 3.16. In the hydrothermally altered/mineralized greywackes marginal to the Susannah Vein at Leadhills, the following associations are identified:

Eigen Vector 1: Na-Sr, Mg-Ti-Mn-Cr, Si-Fe-Zr, Pb-As-S-V-La, Zn-Sb-Ni-Y, Al-Cu and K-Rb.

Eigen Vector 2: Na-Sb, Mg-Ti-Fe-Cr-V, Pb-Zn-Cu-Co-Ni, As-S-Ca-Sr-Ba and K-Al-Rb.

Eigen Vector 3: Na-Sr-Mn, Sb-Cu-Zn-Ca, As-Co-Ni-Ba-Si, Mg-Ti-Fe-Cr-Al-Rb, Pb-S and V-Y.

This study reveals major differences in the nature of element associations characterised by the Pb-Zn-Cu vein mineralization. In particular, the dominant As-Sb relationship at Glendinning and Clontibret is replaced by As-Pb and Sb-Zn-Cu associations.

5.8 INTERFORMATIONAL STUDIES

Weber (1959) undertook one of the earliest studies of inter-unit variation within a greywacke succession and although limited in both elemental range and sample population, he was able to demonstrate that greywackes tend to retain the minor element distribution pattern of parental material in the provenance area. In 1961, Weber and Middleton presented one of the first studies upon chemical differentiation of turbidites and proposed that a change in the source environment during the relatively short period of time between successive turbidite deposits was unlikely.

This investigation details the results of two multi-element geochemical studies undertaken to evaluate the effects of inter-formational variation within a greywacke sequence in the Southern Uplands (fold-out No. 6). Samples of greywacke were obtained from two carefully measured stratigraphic sections composed of interbedded mudstones and greywackes. The first study, The Tweed Bridge Section (Pyroxenous Formation) defines the nature of element variation present within a single, massive turbidite bed, whereas the second study, The Talla Linn Section (Intermediate Formation) details element variation present within a succession of closely spaced, interbedded greywacke units sampled over a 30m long traverse.

5.8.1 Tweed Bridge

At Tweed Bridge [30977,62434] a single, relatively homogenous, 4m thick turbidite unit (T_{abe} horizon) was sampled at 30cm intervals across its outcrop. Grain size present in outcrop ranged from granular sand at its base (0-50cm) grading upwards through coarse and medium sand to fine sand/silt in the upper 30cm of the unit. This form of inter-bed comparison was attempted on a rather more limited scale (n=10) by Maynard et al., (1982).

Although subtle, systematic variations in geochemistry are displayed throughout this section, which may be directly related to both grain size and clay mineral content. These variations include systematic increases in Al,

Fe, Mg, Na, K, Rb, P, La, V and Al/Si; and decreases in Si, Ca, Pb, S and particularly Sr which correspond to both decreased grain size and stratigraphic position within the unit (fig. 30). It should be noted however, that the elements Ti, Mn, As, Co, Cr, Cu, Ga, Ni, Nb, Sb, Th, Y, Zn and Zr display no variation in composition throughout the unit. In addition, the chondrite normalised REE patterns of 10 greywacke samples from the Tweed Bridge study area are presented in fig. 474. Petrographically defined samples (AX97201, 97203, 97205, 97207, 97209, 97211, 97213, 97215, 97217 and 97219) display highly consistent, tightly constrained REE patterns with lower total REE compared to PAAS; relatively flat HREE patterns; and lack the negative Eu-anomaly associated with quartz-rich, cratonic derived sediments. On the basis of this evidence it is clear that calc-alkaline andesitic rocks were the primary source for Pyroxenous Formation greywackes in this study area.

Discriminant analysis was also performed upon two groups of interbedded lithologies from the Hawick Group. Greywacke and mudstone samples from the Glendinning study area were assessed using a single two-group classifier (table 3.21). This classifier included all available variables (n=29) and gave a good separation with 5.6% of the population misclassified. Further attempts at discrimination based upon relatively restricted variable sets, led to increased levels of misclassification, as such these results are not discussed further.

5.8.2 Talla Linn

A detailed review of the geochemical variation within Intermediate Formation greywackes from the Talla Linn section [31415,62009] reveals subtle, systematic changes in composition throughout the succession. In general, two broad patterns of variation are identified, the first characterised in the SiO_2 profile and mirrored by Na, P, La, Sr, Th, and Zr; whereas the second, displayed in the Al_2O_3 profile is mirrored by Fe, Mg, K, Ba, Co, Cu, Ga, Ni, Nb, Rb, V, Y, Zn and Al/Si. No apparent variation is displayed by Mn, As, Pb or Sb, however erratic, highly variable values are recorded in both CaO and S. Within the individual turbidite beds, Rb shows the greatest variation and is directly related to the clay fraction a similar, progressively decreasing variation is observed for Ni, Zn, Pb, Cu and Co, all of which are present in clay minerals as both adsorbed, exchangeable ions and hosted within the phyllosilicate structure.

Given the relatively homogenous gross mineralogy of the greywacke samples, variations within these two inversely correlated groups of elements are interpreted as reflecting minor changes in petrographic composition, controlled predominantly by respective increases and decreases in clay mineral and detrital quartz/lithic components. Obvious mineralogical associations (ie. Al_2O_3 with Fe, Rb and V in clay minerals) correlate particularly well with the observed trends. In summary, detailed sampling of individual outcrops and graded units illustrate minimal geochemical variation within metre-scale sections, both parallel and perpendicular to bedding. It may be demonstrated that these subtle systematic variations in chemical composition may occur within a turbidite succession in direct response to a decrease in grain size and a corresponding increase in clay mineral content. It should be noted however, that the order of magnitude in element variation within individual formations is far smaller than the variation displayed between different petrographic formations, particularly where cratonic and volcanic derived greywackes are compared.

5.9 DISCUSSION OF PROVENANCE AND TECTONIC SETTING

The Southern Uplands of Scotland constitute an example of a single suspect terrane in the British sector of the Caledonide orogen (Anderson, 1986). The geology of the Southern Uplands closely mirrors that of California as described by Albers (1981) with various terranes of oceanic and island-arc crust accreted upon older sialic crust, intruded by granitoid batholiths and a diversity of minor intrusions.

Petrographic and geochemical evidence indicates that a wide diversity of source rock lithologies exist for the Ordovician turbidite succession in the Southern Uplands and Longford Down, with individual greywacke formations within this region characterised by discrete petrographic and geochemical attributes related to subsets of these lithologies. In general, the framework mineralogy and geochemical data exhibit remarkable consistency within individual greywacke formations, however the differences in lithic populations are attributed to different source terranes. The chemical classification of the major greywacke formations in the Southern Uplands indicate that the greywackes can be considered in terms of admixtures of varying proportions of cratonic and volcanic (and carbonate in Wenlock sediments) detritus, represented by two antithetic 'end member' compositions.

In the Northern Belt, individual petrographic tracts derived from varied source areas have been traced over strike lengths of up to 130km (Floyd, 1975, 1982; Dawson et al, 1977, 1979). The petrography of greywackes from the Central Belt is less varied than that of the Northern Belt. The northernmost tract of the Central Belt is characterised by the presence of pyroxene and forms the Pyroxenous Group of Walton (1957). Immediately south two further tracts were identified by Walton including the Intermediate and Garnetiferous groups. In studies of Lower Palaeozoic sediments from North Down, Craig (1984) demonstrated close affinities with the Southern Uplands of Scotland. North Down was demonstrated to represent a continuation of the Northern Belt of the Southern Uplands into Ireland, forming a tract bounded to the south by the Orlock Bridge Fault. Prior to studies by Elders (1985, 1987) it had generally been assumed that the source areas for basic, acid and metamorphic detritus could be identified in Scotland within the Scottish Highlands or in Ballentrae-type basic igneous complexes.

Changes in sea level through both Ordovician and Silurian periods have had profound effects upon the nature of sediment supply, benthos and biota (Leggett, 1981). The decrease in black shales recorded in the Silurian follows the hiatus of an Upper Ordovician glaciation and coincides with a worldwide marine transgression throughout Llandovery times (fig. 297). Brenchley (1984) presented a detailed study of Late Ordovician extinctions and their relationship to the Gondwana glaciation. The resulting transgression culminated at the end of the Llandovery and slowly regressed throughout Wenlock and Ludlow times. Furthermore, the cessation of the marine transgression allowed relatively stable shelf conditions to be established over large areas and resulted in the dominantly shelly type area recorded worldwide during this period. With regard to this investigation, major and trace element abundances and elemental ratios for each of the studied formations are presented in tables 2.91 to 2.102. Geochemical correlation coefficients are presented in tables 3.00 to 3.05 and composite volcanic and cratonic groupings in table 3.21 and 3.22, respectively.

Bhatia (1983) demonstrated that in most basins SiO_2 is enriched, and Na_2O and CaO are depleted in greywackes, compared to their source rock composition (Bhatia, 1983). The apparent sensitivity of Co, Ni, Ti, Zr and REE to the sediment source is controlled primarily by the behavior of refractory mineral phases (ie. magnetite, ilmenite, zircon, sphene and apatite) which resist chemical breakdown during weathering, erosion and diagenesis. In

addition, the large cation group (K, Rb and Pb), large highly charged cations (Th, U, Zr and Nb) and LREE (La, Ce and Nd) are positively correlated with Si, indicating that these elements are associated with the quartzose components of the source rocks. It is obvious therefore that several processes have contributed to the variations of these elements. One of the salient features of metal distribution within the Southern Uplands is the predominance of arsenic concentrations in the Hawick Group.

In studies of the petrogenetic implications of Ti, Zr, Y and Nb variations in volcanic rocks, Pearce and Norry (1979) demonstrated that following fractional crystallization from basic to acid magmas, these elements could be used to identify the change in crystallizing mafic phases from island arcs (clinopyroxene-dominated) to Andean-type arcs (amphibole \pm biotite-dominated). In general, the ferromagnesian elements (Fe, Ti, Mg and V) and small cations (Na, Ca and Sr) display an inverse correlation with Si (dominantly quartz) and suggests their probable correlation with chemically unstable components such as feldspar, pyroxenes and volcanic rock fragments (Bhatia and Crook, 1986). This study demonstrates that greywackes derived from active volcanic arcs, differ significantly with those derived from more mature, cratonic sources. In general, the cratonic and volcanic settings are broadly supported by the geochemistry of their derived sediments.

Elders (1985) demonstrated that the source terrane of granitic detritus in the Southern Uplands, was unlike anything exposed in Scotland at this time. However, the long range provenance in northwest Newfoundland contain similar granites together with abundant ophiolitic terranes, and provides a possible source area for all components of the Southern Uplands greywackes. As such it was concluded that the Southern Uplands sediments were deposited west of their present day position relative to the Scottish highlands, with subsequent large-scale sinistral faulting resulting in the current configuration. Furthermore, Elders (1986) demonstrated that undeformed granite clasts from the Southern Uplands turbidite succession display Rb-Sr ages from 1,200 to 460my, with most falling in the range 1,200 to 900my and 500 to 460my. It was proposed that as few undeformed plutons of these ages occur within Scotland, they were derived from the north and west of Newfoundland and displaced by strike-slip motions which commenced in the Late Ordovician. Albers (1981) in studies of the geology of California, noted that chromite is confined to ultramafic rocks, much of which occupy suture zones separating various accreted terranes (Albers, 1981). All available petrographic and geochemical data relating to the Marchburn Formation indicates that this unit had a magmatic arc derived provenance which displays basic/ultrabasic characteristics (?ophiolitic) possible derived within a forearc basin.

Sanders and Morris (1978) proposed that the andesitic detritus identified in greywackes from the Longford Down, were derived from calc-alkaline pyroclastics generated as a result of Caledonian subduction at a continental margin. However, powerful sedimentological evidence is now available, which suggests that a considerable portion of all volcanic material was derived from an offshore source to the south (Kelling et al., 1987; Stone et al., 1987; and Styles et al., 1989). Furthermore, Morris (1987) recognised a distal continental source to the northwest and a proximal arc source to the south of the Northern Belt in the Longford Down, and concluded in favour of a back-arc model for the Southern Uplands/Longford Down. This southern volcanic terrane has not been preserved in the stratigraphic record and as such its nature and characteristics may only be deduced from the mineralogy and geochemistry of its detritus. Barnes et al., (1987) detailed a number of along-strike stratigraphic and structural features of the Southern Uplands central belt in the Rhinns of Galloway and Co. Down, NE Ireland, and noted in particular, that the distinctive Hawick Group lithologies facilitated a correlation across three, coastal profiles. This study demonstrates that volcanic derived greywackes preserve most of the geochemical and petrographic

characteristics of the primary volcanic material and as such are important guides in our understanding of the nature of volcanic events where the products and/or source has been completely removed. The high alkali greywackes of the Blackcraig, Scar and Pyroxenous formations display gross chemical similarities with andesite, whereas a more basaltic (and perhaps ultramafic) component is reflected in Marchburn Formation greywackes. The low Sr abundances in cratonic greywackes correlate with a lack of Ca-bearing detrital minerals, specifically calcic plagioclase which is found in relative abundance in the volcanic derived formations. In summary therefore, the Blackcraig, Scar and Pyroxenous formations exhibit trace element abundances typical of calc-alkaline volcanic rocks, and support a model for their calc-alkaline volcanic provenance. This study provides further evidence in support of the work of Styles et al., (1989) who demonstrated that the abundant, fresh clinopyroxenes identified within volcanic rich greywackes of southerly provenance, occur both as individual crystals and phenocrysts in lithic fragments and display compositions indicative of a calc-alkaline island arc origin.

Taylor and McLennan (1981) presented a detailed review of the composition and evolution of the continental crust, based upon REE evidence from sedimentary rocks. Geochemically, the Afton, Shinnel and Intermediate Formation greywackes display no statistically significant enrichment or depletion relative to the average crustal abundances defined by Weber and Middleton (1961) and are inferred to display close similarities in concentration with undifferentiated crustal material. The tectonic setting of individual formations has also been inferred by comparison of the REE geochemistry and previously published chemical criteria (Taylor and McLennan, 1985; Bhatia and Crook, 1986). The four major tectonic settings proposed by Bhatia and Crook (1986) represent 'end members' which may evolve from one to another during their depositional history, due to plate tectonic activity. The REE patterns identified within this study provide considerable support for the model proposed by Stone et al., (1987) which inferred a calc-alkaline island arc origin for the Galdenoch, Portpatrick and Pyroxenous formations.

The identification of plutonic igneous, volcanic, metamorphic or sedimentary source terranes provides an important constraint in plate tectonic reconstructions of a suspect terrane (Van de Kamp and Leake, 1986). As a result of this investigation, extremely high confidence limits may be placed upon the hypothesis, that a number of juxtaposed Ordovician and Lower Silurian formations were derived from differing source areas. The widespread acceptance of the fossil accretionary prism model, proposed by McKerrow et al., (1978) dominated all aspects of research in this area up to 1986. This accretionary prism model is heavily dependant upon stratigraphic sedimentological, structural and metamorphic data and hypotheses, many of which are interdependent (Murphy and Hutton, 1986). This model has however, been the subject of detailed review, and recent research which has served to undermine some of the fundamental concepts presented by McKerrow et al., (1977) and led to the development of alternative hypotheses and models.

Both petrographic and geochemical data may be used to infer the presence of volcanic arcs at the northern margin of the Iapetus Ocean during the Ordovician and Early Silurian periods. The resulting volcanoclastic detritus formed a major component of the Blackcraig, Scar and Pyroxenous formations. It was suggested by Leggett (1987) that the volcanic detritus was derived from seamounts and/or local volcanos, however a consideration of the volumes of sediment involved, and the lateral continuity of the volcanic-rich formations tends to invalidate this hypothesis. In recent arc-trench systems, arc-derived detritus is deposited within elongate sedimentary basins, seaward of the volcanic arc. Three depositional basin environments were identified by Moore (1979) including the trench, lower trench-slope and the forearc (upper slope) basin. Murphy and Hutton (1986) also presented an alternative model to that of the imbricate prism (Leggett and reinterpreted the Silurian rocks of the Southern Uplands in terms of a

turbidite filled, successor basin that formed following the closure of Iapetus at the end of the Ordovician. Furthermore, Murphy and Hutton (1986) proposed that the ending of subduction in the Southern Uplands was not marked by the youngest identified sediments (upper Wenlock-Ludlow) but by the ending of synchronous arc-like magmatism on both margins of Iapetus in the Late Ordovician, and illustrated by the deposition of similar remnant arc and metamorphic detritus deposited in Lower Silurian sediments from both sides of the closed ocean.

Anderson (1986) demonstrated that the Northern Belt, of Upper Ordovician age is separated from the Central Belt by the major Orlock Bridge Fault, which may be traced over 400km, and displays a sinistral displacement probably greater than the exposed strike length of the fault. In response to these criticisms, Leggett (1987) proposed that the Southern Uplands sediments were not deposited in a marginal basin as prescribed by the model of Stone et al., (1987), and proposed an analogy with areas along the SW Japan forearc, where active submarine arc-type volcanism occurs on the seaward side of a currently growing accretionary prism. It should be noted however, that the Japanese suites of rhyolites, granites, etc. cited by Leggett (op.cit) are totally dissimilar to the Southern Uplands lamprophyres identified by Rock (1989).

Although Kelling et al., (1987) proposed that a volcanic island arc was briefly juxtaposed against the northern forearc region by strike-slip faulting, an alternative explanation was proposed by Stone et al., (1987) and supplemented by Styles et al., (1989) in which the Southern Uplands greywackes were deposited in a back-arc environment. In detail, Stone et al., (op.cit) presented new palaeocurrent and compositional evidence from Llandeilo to mid-Llandovery age turbidites in the northern part of the Southern Uplands and demonstrated that turbidites derived from the south contain significant quantities of fresh andesitic detritus whereas those from the north are represented by more mature quartz-rich formations. On the basis of this evidence a back-arc environment was proposed in which sediments were deposited in a basin with a relatively mature continental landmass to the north and a rifted continental segment hosting an active volcanic arc to the south. Following the cessation of subduction, underthrusting of the southern margin initiated a SE-propagating thrust stack, which deformed the back-arc basin sequence and possibly ramped over the remains of the volcanic arc. In summary, recent evidence, including the contrasting provenance and sediment supply, and the extensive presence of mantle-derived lamprophyres was difficult to reconcile with a forearc accretionary prism interpretation, and as such, an alternative model is proposed, invoking the development of an essentially ensialic, Late Ordovician back-arc basin in which the relatively volcanoclastic greywacke tracts, were derived from a composite continental-volcanic terrane to the south.

The closure of Iapetus during the Llandovery, resulted in the cessation of subduction and the transfer of compression into the Southern Uplands back-arc basin, and the development of a southeastward propagating thrust stack (Stone et al., 1986, 1987). This thrust stack provided the source area to a foreland basin developed above the compressed forearcs on either side of the oceanic suture and gave rise to the Late Llandovery, carbonate-rich Hawick Group sediments. In addition the presence of syntectonic lamprophyre dykes (418-395 Ma) derived from a deep mantle source, was used to suggest that emplacement occurred several hundred kilometres behind the active trench (Stone, et al., 1986, 1987) and was intimately associated with the development of As-Sb-Au mineralization in this region.

Morris (1987) proposed that on the basis of distinct petrofacies suites and other aspects of regional geology, the Northern Belt sediments were deposited within a back-arc basin and provides further evidence in support of the

thrust duplex model proposed by Stone et al., (1987). The major change in facies from the classical turbidites of Late Llandovery and Early Wenlock to the extensive meandering channel systems of mid-Wenlock was inferred by Kemp (1985) to indicate that by mid-Wenlock times the topographic trench had been filled and sediments were developing over the remnant Iapetus basin.

Wrafter and Graham (1989) in studies of Ordovician sediments from the western Irish Caledonides demonstrated major variations in major and trace element geochemistry throughout the succession. High Cr, Ni and Mg concentrations together with the presence of detrital chromite and Mg-rich chlorite were used to infer an ultramafic derivation of sediments which succeed high Ti and Fe (with low Mg, Cr and Ni) units of mafic provenance. The geochemical patterns are interpreted as resulting from the progressive unroofing of an ophiolite sequence from its upper mafic portion down to its lower ultramafic components. In addition, the significant volumes of continental debris located within the succession was cited as evidence for obduction of the source ophiolite onto continental crust. The progressive dissection of a ensialic volcanic arc and the erosion of its plutonic roots and continental basement leads to the development of a 'unroofing stratigraphy' with sediments indicating more cratonic characteristics with time.

Styles et al., (1989) provided further mineralogical evidence as to the nature of greywackes provenance in the Southern Uplands and reported that quartzo-feldspathic greywackes units derived from the north are interbedded with volcanic rich greywacke of southerly provenance. Abundant fresh clinopyroxenes are recorded in the latter group, both as single crystals and phenocrysts in lithic fragments, with compositions that indicate a calc-alkaline island arc origin. Furthermore, Styles et al., (op.cit) concluded that in any attempt at regional terrane modelling:

- 1) A continental margin, volcanic arc to the north is incompatible with recent sedimentological studies.
- 2) The calc-alkaline Borrowdale Volcanic Group in the Lake District, initially considered as a possible source, is inapplicable on the basis of both faunal provinciality and petrography.
- 3) Interpolation volcanics such as the Bail Hill Complex, could only have contributed to the Blackcraig Formation.
- 4) The large volume of volcanoclastic sediments involved suggest that the source terrane was of considerable size and extent.

Detrital mica ages from Southern Uplands greywacke formations were determined by ^{40}Ar - ^{39}Ar laser probe techniques (Kelley and Bluck, 1989) which defined the range 458-502 Ma. The results of this highly innovative study were used to propose a basement provenance for these sediments. Although Grenvillian samples have not been recorded, southerly derived, detrital volcanic clasts defined cooling ages of 530-560 Ma interpreted to represent a non-contemporaneous, arc terrane provenance of uncertain affinities. This interpretation is in direct opposition with the models proposed by Hutton and Murphy (1987), Morris (1987) and Stone et al., (1987) which require the presence of a contemporaneously active arc. It is interesting to note that an alternative plate tectonic model for the Southern Uplands has been recently proposed by Mitchell (1989) in which the Northern Belt is interpreted as an Ordovician forearc basin, in a northwest-facing arc which collided with Laurentia in Late Ordovician times and reversed direction. This model was not supported in the accompanying discussion where faunal and structural evidence presented by McKerrow and Cocks, and Stone tended to refute this interpretation. In addition, the petrographic differences in greywacke petrography from the Lake District and Southern Uplands (Styles, et al., 1989) were cited as further evidence against this interpretation.

5.10 SUMMARY AND CONCLUSIONS

This study has attempted to correlate petrographic and geochemical characteristics of a series of fault-bounded tracts of compositionally distinct greywackes located in the Southern Uplands and Longford Down. Field evidence, petrography and geochemistry indicate the presence of a diverse range of greywackes in the Southern Uplands, derived from varied source areas on the northern margin of the Iapetus Ocean during the Ordovician and Silurian periods. The chemical composition of Lower Palaeozoic greywackes provides significant information on the nature of the source terranes and the plate-tectonic setting of the depositional basin. Bhatia and Crook (1986) proposed a simple discrimination scheme for characterizing provenance and tectonic setting on the basis of the most discriminating trace elements. It is clear from their preliminary study based upon medium/fine grained greywackes from eastern Australia, that the principles of this classification are valid. However, the quantification of their results may be inapplicable to specific areas, such as the Southern Uplands, and should only be applied following detailed orientation studies of the suspect terrane. In detail, the scale of sampling within this programme facilitated:

- 1) The chemical definition of the nature, origin and evolution of differing provenance sources and tectonic settings.
- 2) The assessment of the nature and magnitude of the chemical variation between different turbidite units
- 3) The development of a chemical classification system for distinct petrographic units
- 4) The evaluation of lithogeochemistry as a tool in regional stratigraphic correlation, terrane boundary identification and mineral exploration
- 5) The identification of areas of chemical alteration related to tectonism, igneous intrusion and/or hydrothermal activity.

Van de Kamp and Leake (1986) noted that despite innumerable commercial studies, there is little published systematic information relating to the chemical compositions of sedimentary suites of known provenance. The significant chemical variation noted between juxtaposed formations mimics previously described petrographic variation and corresponding changes in provenance and source area. This study demonstrates that there are persistent and significant differences in geochemistry between the eight major greywacke formations of the Southern Uplands. In addition these differences are explained in terms of detrital mineralogy, provenance and depositional environment. Furthermore, the application of Bhatia's criteria to the Southern Uplands of Scotland, is in general agreement with the tectonic settings proposed by Stone, et al., (1987). These results also reflect a significant similarity with Bhatia's investigations however, the precise magnitude of trace element variation between differing provenances is suspect. It is therefore proposed that lithogeochemistry provides a powerful tool in distinguishing individual formations in the Southern Uplands, as the elemental concentrations may be directly related to variations in the detrital components of the original sediments, which mirror variations in provenance. In addition, the geochemical and mineralogical differences between juxtaposed formations across the Southern Uplands provide detailed further for the variability of provenance and the lateral continuity of individual source areas. The repeated interbedding of antithetic greywacke types in the Southern Uplands, indicates that provenance was either bimodal or that more than one source area was involved (Styles et al., 1989). In summary, three major distinct lithogeochemical signatures can be recognised across the Southern Uplands, including cratonic and volcanic derived greywackes and a carbonate-rich subset.

Both major and trace element geochemistry display marked variations between cratonic and volcanic derived units. In addition more subtle differences occur between individual formation members, in both of these two major groups. Detailed geochemical mapping of extensive coastal profiles in southwest Scotland and numerous regional traverses within both the Southern Uplands and Longford Down, have demonstrated a remarkable lateral continuity of individual formations across this region. By analysing petrographically defined formations from their type area, it has been possible to establish their characteristic chemical compositions and determine probable along-strike stratigraphic correlations. This study has demonstrated that the 70km wide belt of petrographically distinct stratigraphic sequences recognised in the Southern Uplands and Longford Down may be mapped geochemically over a strike length of over 350km. In general, it was not possible to subdivide the petrographically classified formations further, on geochemical grounds. Individual samples were however, identified exhibiting anomalous compositions worthy of further investigation.

It is clear from this study that both major and trace element geochemistry provides a powerful technique in the identification of source terranes and in particular to differentiate between a cratonic (acid) and volcanic (calc-alkaline, basic or ultrabasic) provenance. In detail, the volcanic derived greywacke formations display higher Ti, Fe, Mg, Ca, Na, Mn, Cr, Ga, Ni, Sr, S, V and Zn values than their cratonic counterparts. In opposition, the cratonic derived greywackes display higher Si (with the exception of the Hawick Group) K, As, Co, La, Nb, Rb, Sb, Th and Zr. Furthermore, on the basis of the REE geochemistry, volcanogenic provenances (typically andesitic) may be readily distinguished from granitic/cratonic sources.

Most of the geochemical correlations identified agree with the geological observations, however some correlations revealed subtle relationships previously unrecognized. Multivariate techniques applied to geochemical data from the Southern Uplands, all gave similar general results. Univariate and multivariate statistical tests including principal component, discriminant and non-parametric K-means cluster analysis, were employed on a representative training set composed of ~900 petrographically defined samples to determine the significance of chemical variation within each petrofacies and define suitable classification algorithms. These algorithms provide a satisfactory method of identification for greywackes of unknown origin as the chemical fingerprint can be used to classify each sample into its respective petrofacies or defining the sample as 'altered'. The resulting petrochemical stratigraphy of the Southern Uplands and Longford Down is summarized in fig. 296a. Important features emerging from this study include:

- 1) The greywackes of the Lower Palaeozoic of Scotland and Eire, exhibit systematic cross-strike contrasts in their patterns of element variation (a 'geochemical stratigraphy')
- 2) The obvious correlation between petrofacies and geochemistry is controlled by consistent differences in the ratio of quartz and feldspar, and the abundance of ferromagnesian, carbonate and accessory minerals related to differing provenance/tectonic setting
- 3) The applicability of regional lithogeochemical studies to boundary identification and geochemical terrane mapping.
- 4) The successful identification of new areas of potentially economic As-Sb-Au mineralization in both Scotland and Eire
- 5) The petrographic and chemical compositions of individual formations from the Ordo-Silurian greywacke-mudstone succession of the Southern Uplands reflect their respective tectonic setting.
- 6) Volcanogenic greywackes from the Marchburn, Blackcraig, Scar and Pyroxenous formations display REE patterns which are dissimilar to typical post-Archean upper crust, but similar to their andesitic source rocks.

- 7) Greywackes from the Afton, Shinnel and Intermediate formations and Hawick Group have REE patterns similar to the upper crust.
- 8) The provenance of Ordo-Silurian greywackes in the Southern Uplands includes a diversity of lithologies, such as felsic and mafic volcanics, acid and calc-alkaline material, recycled metamorphic and sedimentary rocks and detrital bioclastic material.
- 9) Individual tracts display relatively consistent widths (~4km) which may be traced over 300km along strike.

The use of petrofacies concepts in conjunction with lithogeochemical data and tectonic models provide a powerful interpretive tool in the study of the Southern Uplands. Furthermore, the results of this study reveal that rapid multi-element lithogeochemistry provides a valuable technique for distinguishing otherwise uniform sedimentary sequences on the basis of their component mineralogy and forms a viable technique for greywacke identification and correlation over distances of at least 300km. From a review of similar studies, it is proposed that the extensive multi-element data presented in this study forms the most complete geochemical investigation of any sedimentary terrane undertaken to date.

Lithogeochemistry has been applied on a regional scale to the identification of mineralized areas in the Southern Uplands turbidite terrane. On a local scale, geochemical dispersion halos of both major and trace elements have been shown in association with As-Sb-Au deposits. Both Na, Fe, Mg and Zn depletions, together with characteristic trace element enrichment form a general feature in this terrane. Although this data details the regional variations in As and Sb content of turbidites, distinct groups of geochemical anomalies interpreted as hydrothermal centres were also identified. In excess of 60 sites of possible As-Sb-Au mineralization were identified from a suite of 1847 greywacke samples in the Southern Uplands and Longford Down. This study has affirmed the conclusions of Alsayegh (1971) and demonstrated that lithogeochemistry may be used as a mapping tool across not only the Southern Uplands but also the Longford Down. Although few analyses are available for comparative study in the Appalachian orogen, it is hoped that this study may provide the impetus for further geochemical investigations of Ordo-Silurian sequences in Canada and the USA. It should be noted that geochemical studies of greywackes can only be fully utilized where strong underlying petrographic and mineralogical controls are available. Although lithogeochemistry provides invaluable information regarding the composition of individual samples, this data may only be correctly interpreted in terms of provenance/tectonic setting when viewed in conjunction with detailed petrographic evidence. Chemical and/or isotopic studies on specific mineral phases within individual samples may be utilized to provide further details on the nature and origin of greywackes, the most complex of all sedimentary rocks.

This section is ended on a cautionary note to all future workers preparing to embark upon any major sampling and analytical programme. Large geochemical datasets, although providing 'safety in numbers', create formidable logistic problems in storage, manipulation, interpretation and presentation. These problems can only be successfully overcome by the widespread application of computer technology and data management throughout the tenure of such projects in areas as far removed as data capture, computer graphics, statistical assessment and report generation. Unless such facilities are both available and/or planned for in the initial proposal, any attempt to implement a large-scale program of sampling and analysis will be doomed to failure. In order to avoid such problems, individual workers should therefore carry out a logistic/feasibility study of the facilities available to them and the time constraints placed upon different analytical and interpretational techniques prior to the commencement of any sampling programme, thereby constraining the limits of the proposed project within a realistic time framework.

TABLE 1

ANALYTICAL METHODOLOGY

ANALYTICAL METHODOLOGY

The analytical methodology employed in this study is described in detail in the following sections. The methodology is based on the use of a scanning electron microscope (SEM) equipped with an energy-dispersive X-ray (EDS) detector. The SEM was used to examine the morphology and composition of the samples. The EDS detector was used to determine the elemental composition of the samples. The results of the SEM and EDS analyses are presented in the following sections.

The analytical methodology employed in this study is described in detail in the following sections. The methodology is based on the use of a scanning electron microscope (SEM) equipped with an energy-dispersive X-ray (EDS) detector. The SEM was used to examine the morphology and composition of the samples. The EDS detector was used to determine the elemental composition of the samples. The results of the SEM and EDS analyses are presented in the following sections.

CHAPTER SIX

6.1 STUDY AREAS

6.1.1 Introduction

The analytical methodology employed in this study is described in detail in the following sections. The methodology is based on the use of a scanning electron microscope (SEM) equipped with an energy-dispersive X-ray (EDS) detector. The SEM was used to examine the morphology and composition of the samples. The EDS detector was used to determine the elemental composition of the samples. The results of the SEM and EDS analyses are presented in the following sections.

The next stage of the investigation involved the detailed analysis of individual sample-bearing mineral phases including arsenopyrite, pyrite and arsenic-bearing pyrite, as determined by microprobe analysis. Following an initial evaluation of the variation of gold and other trace elements in arsenopyrite, it was obvious that the relationships were not simple. As each individual arsenopyrite crystal was analysed for major and trace elements, one grid

CHAPTER SIX

MICROCHEMICAL MAPPING STUDIES

6.1 INTRODUCTION

The presence of insitu gold mineralization was confirmed in the Southern Uplands in 1980 when Leake et al. traced alluvial gold to a series of gold bearing arsenopyrite-quartz veins within the contact margin of the Loch Doon granite. Accurate identifications of alluvial gold are now known in over 100 streams draining the Ordovician and Silurian turbidite succession of the Southern Uplands. It may be inferred that the presence of polymetallic vein deposits and the dispersion of alluvial gold across this region are favourable to the existence of gold deposits.

The initial aim of this study was to undertake a detailed examination of the nature of the major and trace element zonation patterns within individual sulphide phases, from a variety of settings within individual As-Sb-Au deposits throughout the Southern Uplands and Longford Down. Polished sections of vein and wallrock samples from the Glendinning, Knipe, Talnotry and Cairngarroch Bay deposits in the Southern Uplands were examined using transmitted and reflected light techniques in an attempt to determine the location and association of gold mineralization. In view of the close geochemical association of gold and arsenic particular attention was paid to arsenopyrite and pyrite. Detailed optical studies (cf. Chapter 3) however, failed to identify either inclusions or discrete sulphide-free particles of gold. The trace element content of arsenopyrite crystals from these deposits were investigated using an electron microprobe. Instrumental and analytical procedures were varied in order to test the validity of the initial gold analyses. Test procedures (see appendices) included a comparison of short and long count times upon gold-rich and gold-free arsenopyrites; the geochemical analysis of arsenopyrite rich samples; the determination of average compositions of individual crystals by raster beam study; the investigation of the effects of relief at the margin of the arsenopyrite grain; and the monitoring of spot deterioration (due to electron 'burning' and the formation of a carbon annulus).

6.2 STUDY AREAS

Glendinning

Geochemical analysis of wallrock samples from the Glendinning deposit (cf. Chapter 3) show a high correlation between gold and arsenic inferring a strong genetic relationship. This correlation posed a puzzling problem, in that discrete gold grains or inclusions within sulphides could not be identified by reflected light microscopy, even within samples from the highest grade drillcore intersections. It therefore became evident that the chemical relationship between gold and arsenic had some form of overriding cryptic mineralogical control.

The next stage of this investigation involved the detailed analysis of individual arsenic bearing mineral phases including arsenopyrite, pyrite and tetrahedrite by multi-element electron microscopy. Following an initial evaluation of the variation of gold and other trace elements in arsenopyrite, it was obvious that the relationships were not simple. As such, individual arsenopyrite crystals were analysed for major and trace elements on a grid

system covering all or half of each crystal. The microprobe analyses were then processed through an interactive grey scale mapping package to produce a series of contour maps of each crystal, with shading/contour levels controlled directly by element concentration. This mapping technique permitted the rapid identification of geochemical trends and inter-relationships and stoichiometric modelling. Although the Glendinning deposit is considered by Gallagher et al., (1983) to display both stratabound and vein characteristics, a textural study of this deposit (cf. Chapter 3) indicates that it formed as a result of hydraulic brecciation, wallrock alteration and fracture vein mineralization.

Cairngarroch Bay

Although minor disseminated arsenopyrite was noted by Allen et al., (1981) within the wallrock to one of the two igneous complexes present in this area, the significance of a potential arsenic-gold association within this failed porphyry copper system was clearly not evaluated. In this study, the Cairngarroch Bay area was initially identified by a reconnaissance lithogeochemical traverse of this coastline (cf. Chapter 5.5). Detailed site investigation revealed numerous small arsenopyrite - quartz veins 1-2 cm in width, associated with intense hydrothermal alteration. A new arsenopyrite vein comprising of an 11cm wide quartz-arsenopyrite core surrounded by an 80 cm wide rim of silicified and brecciated country rock, containing a much greater proportion of disseminated arsenopyrite than the vein core, was identified. The predominant orientation of the mineralized vein system is NNE with the thicker vein located at the contact margin between a granodiorite intrusion and a small wedge of greywacke hornfels.

Talnotty

At Talnotty, a mineralized diorite sill contains chalcopyrite, pentlandite, pyrrhotite, niccolite and arsenopyrite as both massive sulphide and wallrock disseminations. Gregory (1927) proposed that the ore was not a magmatic segregation but was in fact derived from the interaction and alteration of the dyke by hydrothermal solutions.

Clontibret

Steed (1981) in a mineralogical and geochemical assessment of the Clontibret deposit, noted the following features:

- 1) A close geochemical correlation between Pb and Sb, reflecting the presence of boulangerite.
- 2) The broad correlation of gold and arsenic values.
- 3) Wallrock samples containing up to 35ppm Au (sample 79-3/181).
- 4) A poor correlation between gold inclusions and mine assay results.
- 5) No gold particles occur in association with stibnite.
- 6) Rarely, large particles of gold were observed in complex grains, intergrown with galena, boulangerite and boumonite.
- 7) Gold particles contain ~10.5% silver.
- 8) Exceptionally small arsenopyrite grains contain up to 2500ppm Au.

One of the initial and most important conclusions in a study of the Clontibret deposit (Steed, op. cit) was that gold is geochemically associated with arsenopyrite-pyrite rather than stibnite mineralization. Although some native gold was identified, a substantial proportion of the gold is located in solid-solution within arsenopyrite and pyrite. Morris and Steed (1985) noted that the most widespread and significant mineralization is auriferous arsenopyrite

and pyrite disseminated within the wallrocks and brecciated rock fragments. A major proportion of all gold identified within this deposit is contained in solid solution within arsenopyrite crystals, a factor reflected by the strong correlation between Au and As values. Fluid inclusion studies demonstrated a sharp peak for homogenization temperatures in quartz associated with arsenopyrite-pyrite (gold) between 280° and 300°C, and a less clearly defined peak for quartz and carbonates associated with stibnite between 240° and 280°C. In both cases, the estimated pressure correction added to these values is 40°-50°C. Inclusions from the arsenopyrite-pyrite (gold) assemblage exhibit high concentrations of CO₂ with an aqueous phase containing about 2% by weight NaCl equivalent.

6.3 SULPHIDE GEOCHEMISTRY AND TRACE ELEMENT ZONATION

6.3.1 Overview

Gold is often reported in association with other sulphides. Investigations on the nature of gold (and silver) in host minerals have been carried out by numerous authors and reviewed in detail by Boyle (1979) who noted that gold is a common microconstituent in a large number of sulphides and sulphide-arsenides, dominantly concentrated in the Cu, Ag and Sb species and in pyrite and arsenopyrite. In these minerals gold was believed to occur as both occluded native inclusions (Boyle, 1981) and lattice constituents (plate 36). In addition, gold is commonly located in pyrite and arsenopyrite and associated but not directly correlated with elevated Ag, As, Sb values. Although gold bearing sulphides have been recorded from many deposits around the world, the amount of visible (> 0.1mm) or microscopic (> 0.001mm) gold present in any deposit only accounts for a small proportion of the total gold contained within the ore. The remaining 'cryptic gold' is generally assigned the term 'invisible', and is only liberated by roasting of the sulphide concentrate.

Arsenopyrite is particularly abundant sulphide mineral in a wide variety of deposits hosted by aluminosilicate-rich rocks such as granites, acid volcanics and pelitic to quartzo-feldspathic sediments (Heinrich and Eadington, 1986). In general two views dominate the literature concerning the nature of sulphide hosted gold, namely that either gold is present in some form of chemical combination with the host sulphides; or gold is present in a finely divided, possibly even colloidal, submicroscopic state (<0.5 microns).

Microchemical analysis provides major and trace element values for individual mineralogical phases which may be interpreted in terms of phase equilibria and sulphidation data, and may be used to estimate a variety of formation parameters. Akright et al., (1972) in a study of the trace element content in the Carlin deposit, Nevada, noted that the gold mineralization was deposited in micron- to submicron-sized particles, disseminated along bedding planes to form a stratabound deposit. Wells and Mullen (1973) found in the Carlin and Cortez deposits in Nevada that a significant proportion of gold was present in a sub-microscopic form (<0.5 microns) in minute grains of arsenian pyrite, thin rims of larger pyrite grains and small arsenopyrite crystals. Fripp (1976) noted from stratabound gold deposits hosted by Archaean banded iron formations that gold in arsenopyrite-bearing samples displayed a quantitative relationship with arsenic and was therefore occluded/absorbed within arsenopyrite crystals. Electron microprobe analyses (Scratch et al., 1984) of arsenopyrites in direct contact with stibnite from the Lake George Sb-As deposit, New Brunswick, reveal zonation from pure FeAsS in the core to Sb-rich rims containing up to 3.2% Sb, an inverse trend to that defined at Glendinning. In addition, El-Bouseily et al., (1985) detailed the mineralogical and geochemical characteristics of gold-bearing sulphide minerals from the El Sid gold mine, Egypt.

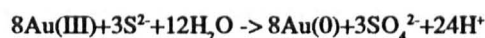
Structurally, arsenopyrite is a member of the disulphide group of minerals (pyrite, marcasite and arsenopyrite), similar in many respects to a NaCl structure. Because it is highly refractory, arsenopyrite does not readily re-equilibrate on cooling. In a discussion of the mineralogical associations of microscopic and submicroscopic gold, Springer (1985) noted that pyrite and arsenopyrite form the principal hosts for invisible gold, with sulphide concentrates containing > 30 oz/ton Au (> 1000 ppm). In synthetic systems gold is more soluble in arsenopyrite than pyrite and it was suggested that an increase in arsenic content of the pyrite lattice also increases the solubility for gold. In conclusion, it is clear that arsenopyrite forms the main gold-bearing mineral in numerous hydrothermal deposits, where its average Au content may reach 1000-3000ppm (Cathelineau et al., 1989).

Wiessberg (1970) noted that maximum gold solubility in sulphide-rich brines is dependant upon the formation of a gold-thio complex (AuS^-) and maximum gold solubility in aqueous sulphide solutions is reached at temperatures below 350°C at neutral pH. As the transport of gold is dependant upon the formation of thio-complexes, deposition may take place as the result of changes in temperature, pressure, pH, oxidation potential and/or total sulphur content of the fluid system. Seaward (1973) and Foster et al., (1980) presented a model invoking the complexes $\text{Au}(\text{AsS}_2)^0$ and $\text{Au}(\text{AsS}_3)^{2-}$ as transport mechanisms for gold in order to explain the coexistence of gold and arsenopyrite. The restricted distribution of gold within arsenopyrites from the Glendinning deposit indicate a strong geochemical/temperature control upon the solubility of gold in arsenopyrite, a relationship controlled by the availability of arsenic deficient sites for gold within the arsenopyrite lattice. In a mathematical study of zoning and precious metal distribution within base metal sulphides, Brimhall et al., (1984) demonstrated a technique using generalized inverse methods whereby the concentration of minor and trace elements in host mineral phases is estimated by utilizing a general relationship between whole-rock composition (ie., assays, mineral composition and abundance and modal data). Electron probe microanalysis however, enables a precise determination of arsenopyrite composition.

The mechanism of transport and precipitation of Sb- and Hg- bearing minerals was first discussed by Barnes and Czamanske (1967). According to Barton (1974) the solution of gold in sulphides can take place only in the presence of excess sulphur. Boyle (1979) postulated that early, high temperature pyrite and arsenopyrite will tend to take up gold and silver in solid solution, or as atomic layers on the growing faces of the sulphide minerals and inferred that gold deposition was controlled by changes in redox conditions and volatile equilibria. Furthermore, Boyle (op.cit) noted that up to 2000 ppm gold could be substituted in either a pyrite or arsenopyrite lattice. Because of the similarity in the covalent radius of arsenic and gold (1.39 and 1.40 Angstroms, respectively) it is proposed that direct arsenic-gold substitution was proposed (Boyle, 1981). In addition the small degree of metallic bonding within arsenopyrite may well impart a degree of alloying properties to the sulphides allowing other metals such as gold, nickel and antimony to reside within the lattice without excessive distortion.

Boyle (1979) presented a number of theoretical reasons to infer that gold may enter the structure of pyrite and arsenopyrite. In laboratory studies gold is observed to form three rather unstable artificial sulphides, AuS , Au_2S and Au_3S_2 , indicating that a bond with sulphur (although weak) is possible. This work suggests that gold may substitute in the iron sites of pyrite and arsenopyrite because of similar octahedral radii and weak affinity for sulphur. There may also be some substitution of gold for arsenic in arsenopyrite because of the similar radii and charges of the two elements. The presence of antimony in auriferous pyrites and arsenopyrites may be more than circumstantial, serving to neutralize any charge differences sufficiently to bind gold to the sulphide lattice. Once growth was initiated, the arsenopyrites became active sites for the precipitation of gold. In general, gold substitution within arsenopyrite may take the form of coupled ($2\text{As}^{3+} = \text{Sb}^{5+} + \text{Au}^+$) or trivalent substitution ($\text{As}^{3+} = \text{Au}^{3+}$).

Champness et al., (1981) discussed the application of quantitative analytical electron microscopy to ultra thin geological specimens. This technique was applied at an evaluation level in this study, however the problems encountered during sample preparation and electron beam thinning proved prohibitive in this investigation. Bancroft and Jean (1982) observed native gold depositing as thin layers on sulphides at room temperature and proposed a mechanism for the inclusion of invisible gold in sulphides, above the limits of solid solubility. In further studies, Bancroft and Jean (1982) and Jean and Bancroft (1985) demonstrated the application of X-ray photoelectron spectroscopy (XPS) and scanning electron microscopy in an evaluation of the mechanisms of adsorption and reduction of gold solutions on sulphides. Specific sites of abnormally high Au concentrations, were used to suggest that the adsorption of Au(III) and Au(I) by sulphide minerals followed by reduction of the gold by the sulphide:



This mechanism forms an important process for gold deposition from low concentration solutions and results in the formation of irregularly shaped granules which, following subsequent sulphide deposition, form microscopic and/or sub-microscopic inclusions in the host sulphide. Experimental data on the hydrothermal solubility of arsenopyrite or theoretical investigations of the solution transport of arsenic and its precipitation as arsenopyrite have been reported by Heinrich and Eadington (1986). Recently this approach has been extended by Cathelineau et al., (1989) to include secondary ion mass spectrometry and Mossbauer spectroscopy, and provides additional evidence in support of the conclusions of Duller and Harvey (1984, 1985) who proposed that gold occurs as both native gold inclusions and in a combined state within the arsenopyrite crystal lattice

Cathelineau et al., (1989) in a study of the location, state and genesis of gold in arsenopyrite, noted that individual crystals exhibit heterogeneous gold contents varying from a few ppm to over 1%. and reported that Au-rich arsenopyrites crystallize at low $f\text{O}_2$ (which approximate to the Ni-NiO oxygen buffer) at relatively low temperatures (170-250°C). In addition they noted that the efficiency of coprecipitation is dominantly controlled by $f\text{S}_2$ and T. A fractional crystallization model for the deposition of argentian tetrahedrite was presented by Hackbarth and Peterson (1984) who noted that the composition of samples varied systematically within individual deposits and led to the development of a model to show that heterogeneity within a single sample could result when an individual depositional site receives more or less evolved fluids at different times.

Gamyanin et al., (1981) in studies of the Urultun near-surface Sb-As deposit (Kolyma River basin, Russia), located a variety of arsenopyrite containing 1.8-11.1 wt% Sb associated with subvolcanic rocks. They concluded that heterogeneous isomorphism of Sb^{5+} and As^{3+} atoms was involved in this substitution and they proceeded to determine the limits of solubility of Sb in arsenopyrite at 550, 450, and 325°C. Their experiments resulted in concentrations of 14.5, 8, and 3.4 wt% Sb, respectively and the development of an 'antimony geothermometer' ($\text{Sb-T}^\circ\text{C}$ curve, see fig. 110). In addition it was demonstrated that a large temperature gradient (200°C) from the commencement of the hydrothermal system until its end was one of the main factors responsible for changing the composition of the Sb-As ores deposited under subvolcanic near-surface conditions.

6.3.2 Deposits

The mineralogy and paragenesis of vein and wallrock hosted mineralization has been studied from specimens collected insitu, from borehole material and from mine dumps/sorting floors. Polished sections of the ore samples were examined using standard reflected and transmitted light techniques. The negative results of optical examination do not directly imply the presence of gold 'in solution' within arsenopyrite but pointed towards a sub-microscopic occurrence of gold within these samples. As such, major and trace element compositions of selected crystals were determined using a Cameca Camebax electron microprobe, at the University of Manchester under the guidance of Dr R.A. Patrick. All analyses were produced using crystal spectrometry. In any reference to these analyses it should be noted that the detection limits for Cd-Fe-Cu-Zn-As-Ag-Ni and S were close to 100 ppm whereas those of Sb-Pb-Hg were nearer 200 ppm. Although the detection limits of an electron microprobe may fall to as low as 25 to 50 ppm for some elements the detection level for gold in a pyrite or arsenopyrite matrix is approximately 200 ppm. Using a pure gold microprobe standard and counting times of 120 seconds, concentrations of gold up to 0.34 at% were measured in arsenopyrite. Note that these levels are significantly higher than the detection limit. Individual samples were also studied by back scattered X-ray emission using a SEM (plates 10, 11 and 12). The resulting backscattered electron images were used to locate particulate gold associated with complex sulphide grains in the Glendinning deposit.

Internal zoning in arsenopyrites is a large scale feature and as such is not readily detectable by backscatter electron or X-ray scan photography on the microprobe (Kretchmar and Scott, 1976). As such, the application of microchemical mapping techniques for monitoring the major and trace element content and the distribution of gold within individual arsenopyrite crystals was developed by Duller and Harvey (1984; 1985). Systematic grid sampling of individual crystals was undertaken to:

- 1) Avoid any possible bias inherent in random sampling
- 2) Define the exact center of the zoned grain
- 3) Detail the nature of internal major and trace element zonation within each crystal
- 4) Investigate the nature of gold mineralization within individual crystals
- 5) Illustrate the internal chemical variation within individual sulphide crystals.

The arsenopyrite compositional data generated in this study display considerable variability on both regional, inter-deposit and single crystal scales. The variations form systematic patterns in each of the studied deposits, and suggest the presence of a common controlling mechanism. Most of the samples show internal compositional variability and yield correlation bands for As vs. Sb within each sample. All zoning observed within the studied samples is broadly concentric, if somewhat irregular, with no reversals.

6.3.2.1 Glendinning

The lowest As and highest gold contents lie in the core zones of early euhedral arsenopyrites which formed in sericitised wallrocks marginal to fracture and breccia zones. Arsenopyrite rims and vein hosted arsenopyrites exhibit higher As values but considerably reduced Au values. If constant sulphur activity is assumed, the As contour levels may be directly related to temperature. The extensive zonation observed in individual crystals reflects rapidly changing conditions during the formation of the arsenopyrites and provides further evidence of the resistance to internal homogenization.

With regard to the trace elements, although complexly zoned there appears to be a general increase in concentration away from the rim of the grain. Antimony is preferentially located in areas of arsenic deficiency, and thus provides clear evidence of a solid solution relationship. Nickel appears at first sight to be randomly distributed, but does show antipathetic tendencies towards mercury. Within disseminated (wallrock hosted) arsenopyrites two distinct gold populations are observed, the first of a similar order of magnitude to the breccia hosted mineralization, namely 0-3000ppm, while the second presents values of 0.5 to 3.0%. The first population is related to major and trace element zonation in the arsenopyrite and is inferred to be a result of similar processes (ie trace element substitution within the arsenopyrite lattice). The second population is more problematic, due to the relatively high concentration and random nature of gold distribution within the crystal (fig. 116). This population is however interpreted in terms of the presence of individual sub-microscopic inclusions of native gold occluded within the arsenopyrite.

The strong correlation between Au and As, coupled with the virtual absence of particulate gold is used by Duller and Harvey (op.cit) to suggest that the gold was most probably dispersed within the sulphide phases. Neither arsenopyrite or any other sulphide in the Glendinning deposit exhibit Te levels above detection limits. As such, it is concluded that tellurides were not concentrated within this form of hydrothermal system. Low concentrations of gold in the transporting solutions, combined with the significant solubility of gold as bisulfide complexes and the variation in range of gold content within the arsenopyrite crystals lead to the suggestion that the hydrothermal solutions responsible for this type of deposit are rarely saturated with gold and as such, coprecipitation with sulfides may be an important initial depositional process.

The cobalt content of sedimentary and vein pyrites all lie below detection limits of the microprobe (<300ppm) and invalidates the use of discriminant plots such as the Co-Ni plot used by Willan (1983). Stibnite was shown to contain little gold within its lattice. However in the Clontibret deposit, Steed (1981) and Morris and Steed (1985) demonstrated that gold when present in association with stibnite, occurs predominantly in its native form, as aurostibnite, or in admixed sulphosalts.

A microchemical investigation of the trace element content of a framboidal pyrite cluster and accompanying authigenic/epigenetic overgrowths associated with mineralization are presented in fig. 113. Microprobe analysis were undertaken using a 20 micron grid spacing (n=174) within a 250x250 micron grid. The analytical results of this study are presented in table 4.19 together with summary statistics in table 2.19. Sulphur values illustrate a concentric structure defining the approximate extent of relic framboidal pyrite. This cluster is crosscut by a series of fractures the most notable of which is infilled by authigenic pyrite exhibiting a low sulphur and high trace element content associated with the euhedral epigenetic overgrowth. Antimony values correlate with areas of low sulphur content peripheral to the pyrite framboid and also occupy the crosscutting fracture zone. This trend is again apparent in a review of the gold geochemistry with only minor enrichments associated with the fracture zone, the major area of gold enrichment is concentrated in the northeastern corner of the grid. Mercury is dominantly concentrated in the peripheral zone of the crystal and given the relatively low content in the fracture zone, may have been deposited later than Sb. Cadmium follows a similar trend to Sb and is concentrated both marginally to the framboid core and within the crosscutting fracture zone.

A number of individual arsenopyrite crystals were selected from different settings within deposit for detailed mapping studies, the results of which are presented below. It should be noted that each crystal is referenced within the text, tables and diagrams by a unique reference number, prefixed by the letters ASP.

ASP1

Figure 114 presents grey-scale contour maps detailing the results of a microchemical investigation of the major and trace element content of breccia hosted arsenopyrite from the Glendinning deposit. Microchemical analyses were undertaken over one half of a rhombic shaped arsenopyrite crystal (180x60 microns in cross-section) using a 10 micron analysis grid (n=72). The results of this study are presented in table 4.01 together with summary statistics in table 2.01. Grid sizes, coordinates and mapping boundaries for all microchemical studies are presented in table 1.15 and 1.50. The atomic %Fe in arsenopyrite (Fe%Aspy) plot illustrates a relatively sporadic distribution. Note that Fe values (range: 32.85-33.60 at.%S) exhibit minimal variation with respect to either As or S. The atomic %As in arsenopyrite (As%Aspy) plot exhibits clear evidence for an As enriched margin (max: 31.97 at.%As) and depleted core (min: 27.93 at.%As) to the crystal. The atomic %S in arsenopyrite (S%Aspy) plot displays a relatively enriched core zone (max: 38.38) and depleted margin (min: 34.74) a trend inversely related to that of arsenic. Au values (max: 1500 ppm) indicate a preferential enrichment in areas of low arsenic/high sulphur values within the crystal core and illustrate an inverse relationship with arsenic concentration. Sb values are notably enriched within the crystal core (max: 7400ppm) and exhibit a marked concentric zonation parallel to crystal margins. Sb is positively correlated with sulphur and inversely correlated with arsenic values. Ni values (max: 1700ppm) follow the trends identified by both Au and Sb and are concentrated in low arsenic/high sulphur zones within the core of the crystal. It should be noted however that the greatest concentration of both Ni and Au coincide within this zone, and are located marginally to the highest Sb concentrations. Hg values (max: 5200ppm) follow the trends identified by Ni and Au, and form a peripheral zone to areas of highest Sb content.

ASP2

Fig 115 presents grey-scale contour maps of the major and trace element content of breccia hosted arsenopyrite. Microchemical analyses (n=25) were undertaken over a small, rhomb shaped arsenopyrite crystal (40x20 microns in cross-section) using a 10 micron analysis grid. The results of this study together with a statistical summary, grid sizes, coordinates and mapping boundaries are presented in tables 4.02 and 2.02, 1.15 and 1.50 respectively. The atomic %Fe in arsenopyrite plot illustrates a relatively concentric distribution with an enriched margin (max: 33.90 at.% Fe) and depleted core (min: 32.14 at.% Fe). Note that the range of Fe%Aspy values is considerably lower than that of As or S. The atomic %As in arsenopyrite plot exhibits similar trends to Fe and provides clear evidence for As enriched margins (max: and core depletion. The atomic %S in arsenopyrite plot displays a strongly enriched core zone (max: 38.60 at.% S) and depleted margin (34.90 at.% S) a trend inversely related to that of arsenic. Au values (max: 1200 ppm) indicate a preferential enrichment in areas of low arsenic/high sulphur values within the core of the crystal and illustrate a strong positive correlation with sulphur concentration. Sb values are notably enriched (max: 4100 ppm) within the crystal core and exhibit a marked positive correlation with sulphur and inverse correlation with As values. Hg values (max: 10,500 ppm) display little systematic variation with respect to either As or S. Ni values (max: 700ppm) are relatively enriched within the core of the crystal and follow the trends identified by both Au and Sb. Please note that although the ASP4 crystal data was not amenable to contouring, it is discussed later in this section.

ASP5

Grey-scale contour maps of the major and trace element content of a wallrock hosted arsenopyrite crystal are presented in fig. 116. Microchemical analyses were undertaken upon a rhomb shaped arsenopyrite crystal (250

microns in width) using a 5 micron sampling grid (n=323). The results of this study are presented in table 4.05 together with summary statistics, grid size, coordinates and mapping boundaries are presented in table 2.05, 1.15 and 1.50, respectively. The atomic %Fe in arsenopyrite plot illustrates a relatively systematic distribution with values concentrated in the margin of the crystal (max: 29.40 at.% Fe). Note that Fe values exhibit minimal variation with respect to either As or S. The atomic %As in arsenopyrite plot exhibits clear evidence for preferential As enrichment in the crystal margins (max: 33.28 at.% As) and depletion (min: 26.25 at.% As) in the crystal core. The plot of atomic %S in arsenopyrite is antipathetic to arsenic, illustrated by a relatively enriched core zone (max: 41.23 at.% S) and depleted margin (min: 33.44 at.% S). Sb values (max: 7300ppm) are notably enriched within the crystal core and exhibit a strong concentric zonation parallel to the crystal margin. Sb is positively correlated with S and inversely correlated with As values. Au values (1000-3000ppm) indicate a preferential enrichment in areas of low arsenic/high sulphur values and illustrate an inverse relationship with arsenic concentration. The total Au plot illustrates the relatively random distribution of gold values in excess of 3000ppm (max: 29000ppm) interpreted within the context of this study as sub-microscopic gold inclusions. Hg values (max: 8500ppm) follow the trends identified by Au and form a peripheral zone to areas of highest Sb content. Ni values (max: 13000ppm) follow the trends identified by both Au and Sb and are concentrated in low arsenic/high sulphur zones within the core of the crystal.

ASP6

Figure 117 shows grey-scale contour maps of the major and trace element content of a wallrock hosted arsenopyrite crystal. Microchemical analyses were undertaken over one half of an arsenopyrite rhomb (120x150 microns in cross-section) using a 5 micron analysis grid (n=97). Note that the central portion of the crystal is situated on the right of each diagram. The results of this study are presented in table 4.06 together with summary statistics, coordinates and mapping boundaries in tables 2.06, 1.15 and 1.50. The atomic %Fe in arsenopyrite plot illustrates the concentration of values (max: 33.58 at.% Fe) in a broad linear zone crosscutting the central portion of the crystal. However the Fe values exhibit minimal variation with respect to either As or S. The atomic %As in arsenopyrite plot indicates an As enriched crystal margin (max: 32.86 at.% As) and a depleted core (min: 28.44 at.% As). The atomic %S in arsenopyrite plot displays an inverse relationship with arsenic; a relatively enriched core zone (max: 39.39 at.% S) and depleted crystal margin (min: 35.50 at.% S). Au values (max: 23,700ppm) indicate preferential enrichment in areas of low arsenic values within the crystal. Sb values (max: 7500ppm) are enriched in areas of arsenic deficiency, notably within the crystal core. Sb is positively correlated with sulphur and, to a lesser extent Au and inversely correlated with arsenic. Hg values (max: 14,900ppm) follow the general trends identified by sulphur values and highlight peripheral zones adjacent to areas of highest Sb content. Ni values (max: 8400ppm) follow the trends identified by Sb and are concentrated in low arsenic/high sulphur zones within the core of the crystal.

Discrimination Diagrams

The As-Sb-Au triangular diagram (fig. 128) illustrates major differences in arsenopyrite geochemistry between individual crystals studied in the Glendinning deposit and compares and contrast trends relating to their host lithology (vein, breccia or wallrock hosted). The first diagram (ASP1) defines the compositional fields for a breccia hosted crystal (n=72) containing high levels of Sb and moderate Au values. A weak trend towards bimodal distribution is observed with both high Au/low Sb and high Au/high Sb end-members present. The second diagram (ASP2) of a further breccia hosted sample illustrates a relatively restricted distribution (n=25) in comparison to

the previous crystal, and lacks the low Sb concentrations depicted in ASP1. The final breccia hosted crystal (ASP3) follows a similar trend to that established by the first example (ASP1) and contains a wide range of Sb values and moderate Au levels (n=35). The fourth diagram (ASP4) illustrates the trends associated with vein hosted arsenopyrite (n=56) in this deposit, namely: a wide range of Sb content with little or no systematic evidence of Au enrichment. Two examples of wallrock hosted arsenopyrite ASP5 and ASP6 (n=323 and 97) are presented which define a somewhat different pattern to the previous samples, with highly elevated Au values located in the low Sb field of each diagram. Two composite plots summarising the major differences between breccia and wallrock hosted ('stratiform') arsenopyrites are presented in the top-right and bottom-left corners of the diagram. Note that the breccia-hosted plot displays a wide range of Sb values and moderate Au content whereas wallrock hosted samples, although displaying a similar Sb content, exhibit a considerably enlarged range of gold values (max: 29,400ppm).

The S-As-Fe triangular diagram (fig. 126) is used to illustrate the variation in major element composition between individual crystals in the Glendinning deposit, and compare and contrast trends relating to their host lithology (vein, breccia or wallrock hosted). The first plot (ASP1) defines the compositional range for a breccia hosted crystal (n=72) containing high levels of Sb and moderate Au values. This narrow linear zone of values occurs adjacent to the FeS_2 - FeAs_2 tie line in the central portion of the Fe-As-S system and demonstrates a slight iron deficiency, similar to crystals grown synthetically by Kretchmar and Scott (1976). This compositional range reflects the effects of chemical zonation within the crystal which, as observed in fig. 114 is concentric if slightly irregular with no reversal. The high Au/low Sb values defined in fig. 128 are located at the bottom end of this solid-solution series whereas the high Au/high Sb members form the upper portion of this trend. In the second diagram (ASP2) a further breccia hosted sample illustrates a similar, albeit restricted distribution (n= 25). The third breccia hosted crystal (ASP3) follows a similar trend to that established by the first example and contains a wide range of Sb values and moderate Au levels. The fourth diagram presents a composite plot of all (n= 133) breccia hosted analyses and serves to illustrate the trends associated with this group, namely a narrow range of Fe content and linear solid-solution relationship between As and S formed as a result of chemical zonation. The vein hosted crystal (ASP4) displays an increased range of Fe composition and the concentration of values above the As%=36 contour level. Two wallrock hosted arsenopyrites (ASP5 and ASP6) (No. of analyses = 323 and 97, respectively) define a somewhat different pattern to the previous samples, with an increased range of As and S values and a proportionate decrease in Fe composition. Elevated Au values are located within the sulphur rich end-members of the As-S solid solution series. The As-Au plot of microprobe analyses from disseminated, vein and breccia hosted arsenopyrites from the Glendinning deposit (fig. 134) displays little direct correlation between As (at.%) and Au (ppm) content. Gold values are generally enriched in disseminated, wallrock hosted samples as opposed to their vein and breccia hosted counterparts. Furthermore, an As-Sb plot of probe data from the same environments (fig. 135) identifies the inverse relationship between As and Sb values in different host lithologies from the Glendinning deposit and illustrates a broad trend towards a decrease in antimony content with increasing arsenic concentration. In general, the highest antimony levels are developed in both breccia and wallrock hosted crystals.

Arsenic-sulphur plots are presented (figs.142-157) in order to quantify the trends identified in Fe-As-S triangular diagrams. Figure 142 illustrates the strong inverse relationship between the arsenic and sulphur content of arsenopyrites from the Glendinning deposit. Note the presence of two parallel trends formed by the differing chemistry of wallrock and vein/breccia hosted samples. The positive shift in composition within wallrock samples (ASP5 and ASP6) may be directly correlated with a decrease in iron and increased trace element content. Figure

146 details the strong negative correlation between arsenic and sulphur in arsenopyrite samples from breccia hosted samples from the Glendinning deposit as described previously in diagram 142. However, this diagram differs in that the concentration of a third variable is represented by a variable sized symbol proportional to the log Au (ppm) concentration. Note the general trend towards increasing gold content with decreasing arsenic values. In vein hosted crystals from Glendinning (fig. 147) this relationship between arsenic and gold was not observed. The As-S crossplot in figure 148 defines the general negative correlation between arsenic and sulphur in wallrock hosted arsenopyrite samples from Glendinning, with the concentration of log Au (ppm) represented by proportionally sized symbols.

In figure 149 and 150, As-S plots detail a strong negative correlation in arsenopyrite samples from breccia and wallrock hosted samples from Glendinning. In addition, the concentration of a third variable, in this case log Sb (ppm) is represented by a proportionally variable symbol size and indicates a general trend towards increasing Sb content with decreasing As values. Vein hosted sample fig. 151 displays a grouping of high Sb values within areas containing low As concentrations.

Summary

In disseminated, wallrock hosted samples the earliest phase of arsenopyrite deposition contains relatively high values of Sb, Au and Hg which decrease as crystal development progresses. In addition, within sample ASP5 from the Glendinning deposit, clear evidence of the random location of gold-rich zones (?inclusions) are observed. Although most of the gold located within this deposit is contained as a minor component of arsenopyrite, rare 'free' gold inclusions up to 12x20 microns have been located by SEM in association with galena and Pb-Sb-sulphosalts (plate 12b). In addition, narrow (0.1-1.0 micron) gold filled fractures are identified in arsenopyrite crystals (plate 12a, c and d).

Stanley and Vaughan (1982) in studies of the Dale Head Vein in Cumbria, noted As-rich cores and As-depleted rims in arsenopyrites, consistent with continued growth either under conditions of falling temperature in a sulphur activity buffered assemblage or at constant temperature in an unbuffered or changing buffer system. Breccia and wallrock samples from the Glendinning deposit, display As-depleted auriferous cores and an inverse zonation to that defined by Stanley and Vaughan (op.cit). Figures 127-133 display a progressive increase in gold content within the fields As-Sb-Au and As-Ni-Au from vein arsenopyrites towards breccia hosted arsenopyrites to that of wallrock hosted crystals.

Rytuba (1985) demonstrated that under conditions of consistent temperature and pressure, the relative stability of arsenic minerals is a function of sulfur activity. At high sulfur activity, orpiment is the stable phase, as it decreases, more sulphur-deficient arsenic phases become stable with the progressive formation of realgar, native arsenic, arsenopyrite, and finally, loellingite. On the basis of this study the main period of gold deposition in the Glendinning deposit, occurred when sulfur activity was low enough for arsenopyrite to be stable but sufficiently high to preclude the formation of loellingite. Native arsenic was also adsorbed onto the surface of preexisting pyrite grains to form arsenian pyrite. Wallrock hosted arsenopyrites define complex trace element zonation patterns similar to breccia hosted crystals, which may be used to infer a probable epigenetic rather than syngenetic origin. The relatively restricted zonation patterns defined in vein hosted arsenopyrites may simply reflect equilibrium growth conditions, slow rates of cooling and relatively uniform shifts in sulphur activity with time. Although up to 55% FeS can be synthetically incorporated in sphalerite at high a_{FeS} (Craig and Scott, 1974) the Glendinning

samples contain only 700 to 5400 ppm Fe (table 2.24) thereby inferring a low a_{FeS} in the ore forming solution at the time of deposition.

6.3.2.2 The Knipe

A detailed investigation of the major and trace element content of wallrock (ASP7) and vein (ASP8) hosted arsenopyrite crystals from the Knipe deposit is presented below:

ASP7

Figure 118 presents grey-scale contour maps of the major and trace element content of a wallrock hosted arsenopyrite crystal. Analyses were undertaken over one half of a rhombic shaped arsenopyrite crystal (70 x 50 microns in cross-section) using a 5 micron analysis grid (n=49). Note that the central portion of the crystal is situated at the top of each diagram. The results of this study are presented in table 4.07 together with summary statistics, coordinates and mapping boundaries in tables 2.07, 1.15 and 1.50. The atomic %Fe in arsenopyrite plot illustrates the enrichment of values (max: 33.78 at.% Fe) adjacent to the crystal margin. However, Fe values exhibit minimal variation with respect to either As or S. The atomic %As in arsenopyrite plot exhibits enriched crystal margins (max: 29.69 at.% As) and a deficient core zone (min: 24.79 at.% As). The atomic %S in arsenopyrite plot displays an inverse relationship with arsenic, with a relatively enriched core zone (max: 41.55 at.% S) and a depleted crystal margin (min: 36.89 at.% S). Gold values (max 1800ppm) are enriched in zones adjacent to the crystal margin and are positively correlated with As, Sb, Hg and Cd. Ag values (max 600ppm) display a close correlation with S enrichment and As deficiency. Sb values are enriched (max: 8600ppm) in zones of weak arsenic deficiency (notably within the crystal core) and positively correlated with Au, Hg, Cd. Hg values (max: 6600ppm) follow the general trend identified by sulphur and correlate with Au, Sb and Cd. Cd values (max: 800ppm) follow the trends identified by Fe, S, Sb and Hg whereas Ni values (max: 500 ppm) present an small, isolated, linear anomaly perpendicular to the crystal margin. In general, the chemical zonation identified within this wallrock hosted arsenopyrite from the Knipe deposit exhibits close similarities with wallrock hosted arsenopyrite from the Glendinning deposit.

ASP8

Grey-scale contour maps of elements in a quartz-stibnite vein hosted arsenopyrite crystal are shown in fig. 119. Microchemical analyses were undertaken upon a rhombic shaped crystal (50x30 microns) using a 5 micron analysis grid (n=61). The results of this study are presented in table 4.08 together with summary statistics, coordinates and mapping boundaries in tables 2.08, 1.15 and 1.50, respectively. The atomic %Fe in arsenopyrite plot illustrates a relatively sporadic distribution of values (max: 35.26 at.% Fe) which may be grouped into two zones, crosscutting the southern half and northern quarter of the crystal. The Fe anomaly zones (>90th percentile) exhibit some similarity with Hg, Au, Ag and S enrichment. The atomic %As in arsenopyrite plot defines an As enriched zone (max: 32.99 at.% As) in the eastern section of the crystal which virtually subdivides the crystal into two halves. The atomic %S in arsenopyrite plot displays an inverse relationship with arsenic and defines an enrichment zone (max: 38.72 at.% S) occupying the western half of the crystal. The highest As and S zones occur adjacent to the crystal margins. Gold values up to a maximum of 1100ppm define a concentric, approximate rhomb shaped pattern of enrichment, crosscutting zones defined by high arsenic and high sulphur content. The patterns defined by Au exhibit similarities with those of Ag, Hg and to a lesser extent Fe. Anomalous Ag values (max: 600ppm) reflect Au

and correlate with Ni, Fe and to a lesser extent Hg. Antimony values (max: 6900ppm) are enriched in areas of arsenic depletion, notably within the left-hand half of the crystal, mirroring sulphur. Antimony is positively correlated with S and to a lesser extent Hg and Ni; and inversely correlated with As. Ni values (max: 600ppm) follow the trends identified by Sb and Hg but are unrelated to Au and Ag anomalies. Sporadic Hg values (max: 6100ppm) follow the general trends identified by Sb values and form peripheral zones adjacent to areas of highest Sb content. Cu values are enriched in both the crystal core and in areas of anomalous Hg values in the crystal margin. Cu values (max: 1000ppm) appear unrelated to Au and Ag anomalies. An As-Au plot (fig. 136) details the variation in arsenic and gold composition in wallrock and vein hosted samples from the Knipe deposit. There is a difference in arsenic content between the two host lithologies with lower values concentrated in the wallrock samples; and the trend towards increasing gold content with arsenic abundance. In addition, the As-Sb plot (fig. 141) identifies the inverse relationship between Sb and As in arsenopyrite samples from the Knipe deposit.

Discrimination Diagrams

The As-Sb-Au triangular diagram (fig. 127) can be used to compare and contrast major differences in arsenopyrite geochemistry within the studied deposits. The first two plots in fig. 127 define the compositional fields of vein and wallrock samples from the Knipe deposit. Plot ASP7 illustrates the enrichment of Sb within vein hosted arsenopyrite whereas ASP8 defines Sb depletion and corresponding Au enrichment within wallrock hosted samples. The third plot, ASP9 defines the composition of massive vein hosted arsenopyrite from the Talnотry deposit; note the extremely low Sb and Au composition of the sample and the restricted compositions. The fourth plot represents a composite study of three arsenopyrite crystals from the Cairngarroch Bay deposit, ASP11, ASP12 and ASP13, and illustrates the general trend towards low Sb content with consistently higher Au levels than within the Knipe or Talnотry deposits. The final two plots define the compositional range of both vein and wallrock samples ASP15, ASP16, ASP17 and ASP18 from the Clontibret Sb-As-Au deposit, in Southern Ireland. This diagram illustrates the enriched levels of Sb and low Au values within vein hosted samples; and the reduced Sb and elevated Au content of wallrock hosted samples. Note that in the Clontibret plots Au and Sb appear inversely related. In light of the spatial distribution of Sb and Au in both crystals (figs 125 and 126) it is concluded that the major controls upon substitution in the respective crystals are the level of As at.% (and by inference T°C and sulphur activity) and availability of both Sb and Au at the time of deposition. The S-As-Fe triangular diagram (fig. 130) is used to illustrate the variation in major element composition of arsenopyrite crystals from the Knipe, Talnотry and Cairngarroch Bay deposits, and compare and contrast trends relating to their host lithology (vein/breccia/wallrock). The first plot (ASP7) defines the compositional range for a wallrock hosted crystal from the Knipe deposit. With reference to the arsenic geothermometer of Kretz and Scott (1976) the observed trends may be used to infer that the wallrock hosted Au-rich samples were deposited at a relatively lower temperature and sulphur activity than their vein hosted counterparts. Vein hosted sample ASP8 from the Knipe displays evidence of arsenic enrichment in comparison with wallrock samples and defines a bimodal population with analyses clustering into an Sb rich and Sb poor group along the similar linear field. The third diagram (ASP9) illustrates the restricted composition of massive arsenopyrite from the Talnотry deposit (n=74) located in a similar field to the antimony poor variety of vein and breccia hosted arsenopyrites from the Knipe and Glendinning deposits. The final diagram in figure 127 illustrates a composite plot (n=462) of all vein hosted arsenopyrite crystals from the Cairngarroch Bay deposit and displays an increase in Fe range and the shift in composition away from that defined by the Talnотry samples towards a more S and Sb rich trend. Figure 137 defines the range of As and Au compositions of arsenopyrites from the Talnотry and Cairngarroch Bay deposits. Note the increased As values present in samples from the Talnотry deposit, which also exhibit slightly reduced Au values.

The As-S crossplot (fig.145) demonstrates the strong inverse relationship between arsenic and sulphur in arsenopyrite samples from the Knipe. An extremely narrow linear trend is defined by both vein and wallrock hosted crystals, with the clustering of vein hosted samples at the high arsenic end of this compositional range. This range may be interpreted in terms of depositional temperature, with relatively high temperature vein fluids chilled by interaction with wallrock and resulting in the deposition of lower temperature arsenopyrites. In figure 152 a similar trend is displayed, however as the symbol size is directly controlled by the log Sb (ppm) content it can be observed that high Sb samples are closely grouped in the lowest As fraction of this population. Figure 153 displays an increase in As concentration in comparison with the wallrock hosted samples from this deposit (Fig. 152) and demonstrates the clustering of Sb rich samples at the low arsenic end of this compositional range.

6.3.2.3 Cairngarroch Bay

ASP10

Figure 121 presents grey-scale contour maps of the major and trace element content of a vein hosted arsenopyrite crystal. Microchemical analyses were undertaken on a square shaped arsenopyrite crystal (50 microns in diameter) using a 5 micron sampling grid (n=74). The results of this study are presented in table 4.10 together with summary statistics, grid size, coordinates and mapping boundaries are presented in tables 2.10, 1.15 and 1.50, respectively. The atomic %Fe in arsenopyrite (Fe%Aspy) plot illustrates a relatively systematic distribution with values concentrated in the bottom half of the crystal, notably close to the crystal margins (max: 35.13 at.% Fe). The atomic %As in arsenopyrite (As%Aspy) plot exhibits evidence for the preferential enrichment in the crystal margins, notably in the western quadrant (max: 32.92 at.% As) and depletion (min: 28.47 at.% As) in the crystal core. The atomic %S in arsenopyrite (S%Aspy) plot displays an inverse relationship with both As and Fe anomalies, illustrated by a small relatively enriched core zone (max: 40.38 at.% S) and northern margin. Sb values (max: 1000ppm) are notably enriched within the crystal core and in areas of both S and Fe enrichment. Sb is positively correlated with both S and Fe; and inversely correlated with As values. Au values (max: 8700ppm) indicate a preferential enrichment in areas of low arsenic/high iron+sulphur concentrations, and are poorly related to Sb values. Ag values (max:700ppm) follow the trends identified by Au; are concentrated within the core zone, and occur marginal to areas of high Sb content. Ni values (max: 1000ppm) define isolated anomaly zones marginal to the crystal rims and follow trends identified by both Fe and Sb and are concentrated in high arsenic/high iron zones within the rim of the crystal.

ASP11

Grey-scale contour maps of the major and trace element content of a further vein hosted arsenopyrite crystal are presented in fig. 122. Microchemical analyses were undertaken on a rhomb shaped arsenopyrite crystal (200x200 microns in size) using a 5 micron grid (n=254). Analytical results are presented in table 4.11 together with summary statistics, grid size, coordinates and mapping boundaries are presented in tables 2.11, 1.15 and 1.50, respectively. The atomic %Fe in arsenopyrite plot illustrates a relatively systematic distribution with values generally concentrated in the margins of the crystal (max: 35.13 at. % Fe). The atomic %As in arsenopyrite plot exhibits evidence for preferential enrichment in the rim zones of the crystal (max: 32.43 at.% As) and depletion (min: 29.19 at.% As) in the crystal core. The atomic %S in arsenopyrite plot displays an inverse relationship with As anomalies, illustrated by a relatively enriched core zone (max: 37.99 at.% S) and western margin. Sb values (max: 1000 ppm) are notably enriched within the crystal core following the trends identified by S enrichment and As deficiently. Sb

is positively correlated with both S and Fe; and inversely correlated with As. Au values (max: 8700ppm) indicate a sporadic enrichment in the core of the crystal, in areas of low As and/or high Fe + S concentrations. Au values also follow the trends identified by Sb and Ag anomalies. Ag values (max: 700ppm) follow the trends identified by both Sb and Au, and are concentrated within the core zone. Ni values (max: 400ppm) define isolated anomaly zones concentrated within the crystal core and follow trends identified by both Sb and Ag.

ASP12

Figure 123 presents grey-scale contour maps of the major and trace element content of a further vein hosted arsenopyrite crystal. Microchemical analyses were again undertaken on a rhomb shaped arsenopyrite crystal (60x60 microns in size) using a 5 micron grid (n=64). The results of this study are presented in table 4.12 together with summary statistics, grid size, coordinates and mapping boundaries are presented in tables 2.12, 1.15 and 1.50, respectively. The atomic %Fe in arsenopyrite plot illustrates a relatively systematic distribution with values generally concentrated (max: 33.68 at.% Fe) in the core of the crystal (an inverse trend to that of the previous crystal from this deposit). The atomic %As in arsenopyrite plot exhibits evidence for preferential enrichment in the core and north eastern rim zone of the crystal (max: 32.92 at.% As) and depletion (min: 29.04 at.% As) in the remaining crystal margins. The atomic %S in arsenopyrite plot displays an inverse relationship with As anomalies, and exhibits enriched crystal margins (max: 40.38 at.% S). Sb values (max: 800ppm) are enriched both within the crystal core and in marginal areas exhibiting S enrichment. Sb is positively correlated with both S and Fe; and inversely correlated with As. Au values (max: 1500 ppm) are enriched in the rim zones of the crystal in areas of low arsenic and high sulphur concentration. Au values also follow many of the anomaly trends identified by both Sb and Ag. Ag values (max: 700ppm) follow the trends identified by both Sb and Au, and are concentrated within the marginal rim zones. Ni values (max: 1000ppm) define isolated anomaly zones concentrated within the crystal core and north eastern margin, and follow the patterns identified by As.

ASP13

Grey-scale contour maps detailing the results of a microchemical investigation of the major and trace element content of a further vein hosted arsenopyrite crystal are presented in fig. 124. Microprobe analyses were undertaken over a rhomb shaped arsenopyrite crystal (130x100 microns in cross-section) using a 10 micron analysis grid (n=144). The results of this study are presented in table 4.13 together with summary statistics, grid sizes, coordinates and mapping boundaries in table 2.13, 1.15 and 1.50. The atomic %Fe in arsenopyrite plot illustrates a relatively sporadic distribution (range: 32.20-33.80 At.%Fe). The atomic %As in arsenopyrite plot exhibits clear evidence for an As enriched margin (max: 31.40 at.%As) and depleted core (min: 29.26 at.%As). The atomic %S in arsenopyrite plot displays a relatively enriched core zone (max: 38.26) and depleted margin (min: 35.70 at.%S) a trend inversely related to that of arsenic. Au values (max: 2000ppm) indicate a preferential enrichment in areas of low arsenic/high sulphur values within the crystal core and southwestern margin. Sb values are notably enriched within the crystal core (max: 900ppm) and exhibit a marked concentric zonation parallel to crystal margins. Sb is positively correlated with sulphur and inversely correlated with arsenic values. Ni values (max: 300ppm) are generally low, forming isolated anomalies following the trends identified by both S and Sb. In general Ni values are concentrated in low arsenic/high sulphur zones within the core of the crystal. Ag values (max: 600ppm) follow the trends identified by S, Sb and Au.

Discrimination Diagrams

The S-As-Fe triangular diagram (fig.131) illustrates the variation in major element composition of vein hosted arsenopyrite crystals from the Cairngarroch Bay deposit. The three crystals represented in this figure ASP11, ASP12 and ASP13 illustrate a number of common features, including a tightly constrained As-S composition; an increase in Fe range compared with that of Glendinning vein and breccia hosted samples and a shift in composition away from that defined by the Talnotry vein samples towards more S rich compositions. The As-Sb crossplot (fig.140) illustrates the extremely low concentration of antimony (<1000ppm) in arsenopyrites from the Talnotry and Cairngarroch Bay deposits, and a general increase in arsenic content within the crystals analysed from the Talnotry deposit.

6.3.2.4 Talnotry

ASP9

Figure 120 shows grey-scale contour maps of the major and trace element content of a massive, vein hosted arsenopyrite crystal. Analyses were undertaken upon a rectangular shaped area (100x200 microns) within a massive arsenopyrite hosted by vein quartz (plate 4) using a 10 micron sampling grid (n=74). The results of this study are presented in table 4.09 together with summary statistics, grid size, coordinates and mapping boundaries are presented in table 2.09, 1.15 and 1.50, respectively. It is immediately obvious that the patterns of concentric zonation displayed in the previous studies, are absent from this crystal. Element distribution within this massive crystal is restricted in range but highly variable, with no apparent structural or mineralogical control. In detail the atomic %Fe in arsenopyrite plot illustrates a highly irregular distribution with values concentrated along the upper and lower margins of the crystal and within the centre of the grid area (max: 34.18 at.% Fe). The atomic %As in arsenopyrite plot exhibits a complex, convoluted distribution with some evidence for As enrichment in areas of low Fe content (max: 33.31 at.% As). The atomic %S in arsenopyrite plot displays a relatively more subtle inverse relationship with arsenic, illustrated by an enrichment on the right margin of the grid, particularly in the lower right quadrant (max: 36.80 at.% S). Antimony values (max: 900ppm) are notably lower than those observed in both the Glendinning and Knipe deposits. Elevated Sb values are tentatively correlated with S enrichment however the extremely low values and variable distribution make such spatial correlation problematic. Gold values (max: 1400ppm) are preferentially enriched in areas of high Sb content and exhibit a weak association with Fe values. Silver values (max: 300ppm) occur close to the analytical detection limits. Although weak, Ag anomalies follow the trends identified by Au and Sb. Ni values (max: 500ppm) are also considerably lower in this deposit and exhibit trends following Fe and to a lesser extent Au and Ag. Cu values (max: 900ppm) are irregularly distributed, however anomalous values display similar trends to that of As and Sb.

The As-Sb plot (fig. 154) reflects the strong negative correlation between arsenic and sulphur in arsenopyrite samples from the Talnotry deposit, and details the clustering of samples at the high arsenic/low sulphur end of this compositional range. Although the symbol size is proportional to Log Sb (ppm) content, little if any systematic variation in antimony content occurs within this group.

6.3.2.5 Clontibret

ASP14

Figure 125 presents grey-scale contour maps detailing the results of an investigation of the major and trace element content of a vein hosted arsenopyrite crystal from the Clontibret Sb-As-Au deposit, in Southern Ireland. Microchemical analyses were undertaken over a rhomb shaped arsenopyrite crystal (100x80 microns in cross-section) using a 5 micron analysis grid (n=108). The results of this study are presented in table 4.14 together with summary statistics, grid sizes, coordinates and mapping boundaries in tables 2.14, 1.15 and 1.50, respectively. The atomic %Fe in arsenopyrite plot illustrates a relatively sporadic distribution (max: 33.17 At.%Fe). The atomic %As in arsenopyrite plot exhibits clear evidence for an As enriched margin (max: 32.32 at.%As) and depleted core (min: 30.01 at.%As). The atomic %S in arsenopyrite plot displays a relatively enriched core zone (max: 36.92 at.%S) and depleted margins (min: 34.74 at.%S) a trend inversely related to that of arsenic. Sb values are notably enriched within the crystal core (max: 48000ppm) and exhibit a concentric zonation, parallel to crystal margins. Sb is positively correlated with S and inversely correlated with As values. Au values (max: 1700ppm) indicate preferential enrichment in areas of high arsenic/low sulphur values within the crystal margin. Ag values (max: 100ppm) are concentrated within the core of the crystal, however their low concentration, close to that of the analytical detection limit invalidated the observed relationship. Ni values (max: 500ppm) are generally low, and cluster in the margins of the crystal. These values closely follow the trends identified by Fe and to a lesser extent Sb. Cu, Zn and Co values all lie below the analytical detection limit and are not discussed further.

ASP15

Grey-scale contour maps detailing the results of an investigation of the major and trace element content of a wallrock hosted arsenopyrite crystal are presented in fig. 126. Microchemical analyses were undertaken over a small, rhombic shaped arsenopyrite crystal (70x50 microns in cross-section) using a 5 micron analysis grid (n=102). The results of this study are presented in table 4.15 together with summary statistics, grid sizes, coordinates and mapping boundaries in tables 2.15, 1.15 and 1.50, respectively. The atomic %Fe in arsenopyrite plot illustrates a relatively sporadic distribution (max: 32.95 At.%Fe). The atomic %As in arsenopyrite plot exhibits clear evidence for an As enriched margin (max: 32.53 at.%As) and depleted core (min: 30.13 at.%As). The atomic %S in arsenopyrite plot displays a relatively enriched core zone (max: 37.36 at.% S) and depleted margins (min: 34.87 at.%S); a trend inversely related to that of arsenic. Sb values are notably enriched within the crystal core (max: 5400ppm) and exhibits a zonation pattern mirroring that of S, inversely related to As values. Au values (max: 3200ppm) are higher than their vein hosted counterparts and may be used to indicate preferential enrichment in areas of high arsenic - low sulphur values within the crystal margin. Ag values (max: 200ppm) follow the trend identified for Au and are concentrated within the margin of the crystal. The low Ag concentration however, close to the analytical detection limit of this technique casts doubt upon the validity of the observed relationship. Ni values (max: 600ppm) are generally low, clustering in the core of the crystal and forming an envelope to zones of Fe enrichment. In general Ni values are concentrated in low arsenic/high sulphur zones within the core of the crystal. Cu, Zn and Co values all lie below the analytical detection limit and are not discussed further.

Discrimination Diagrams

The S-As-Fe triangular diagram (fig.132) illustrates the variation in major element composition between vein and wallrock hosted arsenopyrite crystals from the Clontibret Sb-As-Au deposit in Southern Ireland. The first plot defines the compositional range of vein hosted sample ASP15 whereas the remaining three plots detail the composition of wallrock hosted samples ASP16, ASP17 and ASP18, respectfully. All four diagrams illustrate a relatively restricted range of Fe values and a small range of As-S values which form a narrow, linear trending compositional envelope. Vein hosted samples are concentrated in the more arsenic rich portion of envelope, whereas wallrock hosted samples exhibit a population skewed towards the sulphur rich end-members of this group. Enriched levels of Sb and low Au values are observed within stibnite vein hosted samples, whereas reduced Sb and elevated Au values are recorded in the wallrock hosted samples. This relationship is inferred to have an overriding mineralogical control with both Sb and Au rich samples clustering around the two end-members of the Fe-As-S solid-solution series. The three wallrock hosted crystals in this figure display a restricted As-S composition and exhibit close geochemical similarities to the breccia hosted samples from Glendinning. However, in opposition to the trends identified in wallrock hosted samples from the Glendinning deposit, gold at Clontibret is concentrated within the As rich rims of wallrock samples as opposed to As depleted core zones. The As-Au crossplot (fig.135) displays a general correlation between increased gold composition and arsenic content within both vein and wallrock hosted arsenopyrites from the Clontibret deposit. Note the increased range of gold compositions in wallrock hosted samples from this deposit and the positive increase in arsenic composition in comparison with samples from the Glendinning deposit (fig.134). In addition the As-Sb crossplot (fig.139) details the inverse relationship between antimony and arsenic in arsenopyrite samples from the Clontibret deposit in Southern Ireland. Note the extended range values in the wallrock hosted samples and the concentration of vein hosted samples in the low (<1000ppm) antimony/high arsenic (>31 at.%) values.

The As-S diagram (fig.143) reveals the inverse relationship between arsenic and sulphur in vein and wallrock arsenopyrites in the Clontibret deposit. Values are confined within a narrow linear range. In vein hosted samples (fig.156) extremely low levels of antimony are accompanied by the lack of any systematic pattern of variation within this compositional range, whereas in wallrock samples (fig.157) enhanced levels of antimony are tightly grouped at the low arsenic end of this range.

6.3.3 Summary

Compositional envelopes (fig. 133) illustrate variation in minimum, mean and maximum and two compositional ranges present within 18 microchemical studies (n=1627) of arsenopyrite crystals from the Southern Uplands and Longford Down. The respective deposits and details of individual crystals studied are presented below:

<u>Crystal</u>	<u>Deposit</u>	<u>Analyses</u>	<u>Host/Lithology</u>
ASP1	Glendinning	72	Greywacke breccia
ASP2	Glendinning	26	Greywacke breccia
ASP3	Glendinning	35	Greywacke breccia
ASP4	Glendinning	56	Quartz-stibnite vein
ASP5	Glendinning	323	Greywacke wallrock
ASP6	Glendinning	97	Greywacke wallrock
ASP7	The Knipe	49	Greywacke wallrock
ASP8	The Knipe	61	Quartz-stibnite vein
ASP9	Talnotry	74	Quartz-arsenopyrite vein
ASP11	Cairngarroch Bay	254	Quartz-arsenopyrite vein
ASP12	Cairngarroch Bay	64	Quartz-arsenopyrite vein
ASP13	Cairngarroch Bay	144	Quartz-arsenopyrite vein
ASP15	Clontibret	32	Quartz-stibnite vein
ASP16	Clontibret	102	Greywacke wallrock
ASP17	Clontibret	69	Greywacke wallrock
ASP18	Clontibret	50	Greywacke wallrock

The Fe contents display a relatively systematic distribution with tightly constrained mean values disrupted only by Glendinning wallrock hosted samples ASP5 and ASP6 which exhibit strong depletion effects. The As content plot displays highly variable compositions between crystals from differing deposits and host lithologies. The most marked variation is displayed by extremely low minimum and mean values associated with wallrock samples from the Knipe deposit (ASP7); and by the highest minimum and mean values displayed within the Talnotry sample (ASP9). Note the consistent mean values of samples from the Glendinning deposit (ASP1-ASP6) and the relatively increased As content of samples from the Clontibret deposit. Sulphur contents are again highly variable with the highest mean compositions displayed by the Knipe sample (ASP7) and largest ranges displayed by the Glendinning (ASP5) and Cairngarroch Bay (ASP12) samples. The gold content plot summarises a number of features including the increase in gold content from Glendinning vein through breccia to wallrock hosted crystals; the increase in mean gold compositions of samples from the Cairngarroch and Clontibret deposit (ASP11 to ASP18) in comparison with samples from the Knipe and Talnotry deposits; and the low gold content of vein hosted arsenopyrites from the Southern Uplands. Antimony values are highly variable, with the largest mean and maximum antimony values present in quartz-stibnite vein hosted samples from the Knipe and Clontibret deposits; and the extremely low Sb values located in the Cairngarroch and Talnotry deposits (ASP9-ASP13). This study provides evidence for a greater complexity of internal zonation and trace element substitution within arsenopyrite crystals than had been previously considered. Microprobe analysis has revealed widely varying mean gold contents of the different sulphide minerals. Gold is preferentially concentrated in wallrock-hosted arsenopyrite and to a lesser extent pyrite

(cf. Chapter 3). Although tetrahedrite and tennantite contain traces of silver, all other sulphides (ie. stibnite, sphalerite and galena) contain gold levels close to or below the detection limits of this technique. In general, significant gold levels were detected by microprobe in arsenopyrite grains, particularly those hosted by greywacke wallrocks. Distinct chemical compositions characterise individual depositional environments in each deposit. On the basis of electron microprobe and SEM studies, three modes of gold occurrence were distinguished: arsenopyrite-hosted gold; pyrite-hosted gold; free native gold particles associated with stibnite, galena and sulphosalts (plate 12).

6.4 ARSENOPYRITE GEOTHERMOMETRY

6.4.1 Overview

The theoretical background to arsenopyrite geothermometry has been established for some time (Clark, 1969; Barton, 1969; Kretschmar, 1973; Kretschmar and Scott, 1976) and applied by numerous authors including Lowell and Gasparri (1982); Berglund and Ekstrom (1980); Scott (1983); Sundblad et al., (1985); Stanley and Vaughan (1979, 1982). Kretschmar and Scott's 1976 proposal that the physical conditions present during crystal growth provided an overriding control upon the arsenic content of the arsenopyrite has been widely used in order to ascertain temperatures of ore deposition or metamorphism. The fundamental assumption made in each case is that the mineralizing fluid is in equilibrium with its host rocks, and as such single core and rim analyses are usually sufficient to characterise the arsenopyrite. In addition, the presence of arsenopyrite contained within or in contact with arsenian pyrite is accepted as evidence for the coexistence of the two minerals. Kretschmar and Scott (op.cit) also noted that zonation from S-rich cores to As-rich rims is common in S-rich (As-poor) fluid systems and may reflect local disequilibrium conditions during arsenopyrite growth. In addition they demonstrated a clear correlation between decreasing formation temperatures and the extent of zoning and proposed the use of arsenopyrite compositions as a 'sliding-scale' geothermometer.

Scott (1983) noted that arsenopyrite chemistry may be applied to estimate either sulphur activity or temperature during mineral formation. This study (chapter 3) has demonstrated that arsenopyrite-pyrite mineralization was developed coeval with wallrock alteration and a common textural relationship was developed in which arsenopyrite grains are found in close association if not nucleated upon pre-existing pyrite grains. Since arsenopyrite is in equilibrium intergrowth with arsenical pyrite but not with pyrrhotite, the minimum temperature of formation can be inferred from the Fe-As-S system (Kretschmar and Scott, op.cit). As such, the atomic weight percent of As in arsenopyrite, coexisting with pyrite, is inferred to form a direct function of the temperature of formation and is only mildly affected by variations in pressure (Kretschmar and Scott, 1976; Scratch et al., 1984). If arsenopyrite formed in equilibrium with syndiagenetic pyrite the results of Kretschmar may be extrapolated to much lower temperatures (cf. Stanley, 1982). Using the sulphur activity-temperature projection of Kretschmar and Scott (op.cit) and mineralogical data from As-Sb deposits presented here, it was possible to identify a restricted stability field in which pyrite and arsenopyrite coexist, but native arsenic, loellingite and pyrrhotite are excluded.

Kretschmar and Scott (1976) dealt with point analyses only (ie. rim and core) whereas systematic geochemical mapping of individual crystals is adopted here. As with all geothermometers the techniques proposed by Kretschmar and Scott, (1976) must be applied with caution and other independent checks on temperature should be undertaken if possible. Sulphidation curves representing the arsenopyrite compositions identified within the

studied deposits were plotted on a series of diagrams (fig. 109-112) relating sulphur activity to temperature following the methods of Stanley and Vaughan (1982) in extrapolating Kretchmar and Scott's (1976) sulphidation curves to temperatures lower than 300°C. Sundblad et al., (1985) presented a detailed study of sphalerite geobarometry and arsenopyrite geothermometry of metamorphosed sulphide ores in the Swedish Caledonides. Arsenopyrite studies revealed that significant compositional variations may exist within individual deposits, due either to growth zoning or elevated Ni, Co and/or Sb levels. High Sb contents (>0.2 wt%) apparently resulted in temperature determinations that were too low in comparison with other geological features. It was concluded that this technique provides an accurate method for determining metamorphic temperatures if enough attention is paid to the minor element content.

Gamyranin (1981) reported the first discovery of an antimonial variety of arsenopyrite from the Urultun Sb-As deposit in the Kolyma River basin of the U.S.S.R.. Methods of dry and hydrothermal synthesis were employed to determine limits of Sb solubility in arsenopyrite at 550, 450 and 325°C which were then used to generate an Sb content vs. temperature curve. This data forms the basis of an antimony content geothermometer and may be used to provide a temperature estimate in samples where the total trace element content exceeds 1%. (fig. 110). Note the general substitution line ($T^{\circ}\text{C} = 20 \times \text{Sb wt\%} + 255$) and error bars ($\pm 10^{\circ}\text{C}$). In general, analyses of arsenopyrites from the Southern Uplands plot within the shaded field on this diagram within a highly restricted 255-280°C ($\pm 10^{\circ}\text{C}$) range. In opposition to the trend identified by arsenopyrite geothermometry (see below) involving the decrease of formation temperature with Sb substitution, this study reveals a relative increase in formation temperature with increasing Sb content.

In studies of a previously unrecorded ENE-WSW trending, quartz-antimony vein at Wet Swine Gill (NY 3144 3215) Fortey et al., (1984) noted the assemblage stibnite-berthierite-arsenopyrite-zinckenite-fulopite and semseyite. In addition, XRF studies revealed traces of silver and mercury. Although arsenopyrite forms a rare, minor component of this deposit, extraordinarily high Sb contents were located in core zones containing up to 7 wt% Sb. Fortey et al., (op. cit.) inferred that the pattern of Sb-rich cores and Sb-poor margins could represent either true growth zoning of retrogressive leaching during cooling. Using the 'antimony content' geothermometer of Gamyranin et al., (1981) depositional temperatures in excess of 300°C were recorded for the arsenopyrite mineralization. This vein was interpreted as a lateral extension of the nearby Early Devonian Carrock W-As deposit; however it should be noted that the Wet Swine Gill vein occurs parallel to a series of quartz-dolerite dykes.

6.4.2 Deposits

In this investigation, 1743 analyses of arsenopyrite are reported from 5 Caledonian As-Sb-Au deposits in the Southern Uplands and Longford Down (Glendinning, Knipe, Talnotry, Caimgarroch Bay and Clontibret). Fe, As, Sb, Au, Co, Ni were determined in all samples and Cu, Ag and Hg were also analysed in approximately 70% of the sample population. Emphasis was placed on arsenopyrite grains enclosed or in contact with arsenian pyrite. In all instances Co values rarely exceeded the detection limits. Using the electron microprobe, a grid pattern of analyses over 12 arsenopyrite crystals from different environments/deposits in the Southern Uplands and Longford Down was erected. All analyses were undertaken using an arsenopyrite standard prepared by the British Museum, and calibrated with respect to the Asp 200 standard of Kretchmar and Scott (1976).

Multi-element studies of arsenopyrites from each deposit, demonstrate the importance of determining the minor element content before geothermometric evaluations are made. Kretchmar and Scott (1976) recommended that

arsenic grains with total Sb+Ni+Co values > 1.00 wt% should not be used for geothermometric determination. Furthermore, given the intense chemical zonations defined within arsenopyrites from the Glendinning deposit it was deemed inappropriate to determine an 'average' composition by XRD analysis (using the d_{131} interplanar spacing) following the methodology of Kretchmar and Scott (1976). It was not possible to independently estimate sulphur activity during arsenopyrite formation due to the absence of coexisting additional sulphur activity dependant assemblages (ie. pyrite-pyrrhotite).

6.4.2.1 Glendinning

ASP1

Both temperature and sulphur activity during crystal formation may be obtained using the arsenopyrite geothermometer of Kretchmar and Scott (1976). Arsenic zonation in fig. 114 reflects the presence of a low temperature core and relatively high temperature margin (range 240-350°C) with a greater portion of values confined to a 290-330°C range. Sulphur activity (a_{S_2}) is also lower in the crystal core (10^{-14} to 10^{-11}) than the margin (10^{-11} to 10^{-6}) with average values in the 10^{-11} to 10^{-7} field. In addition, the antimony substitution geothermometer defined by Gamyranin (1981) displayed in fig. 110 may be used to infer an alternative set of depositional temperatures in the range 255-270°C ($\pm 10^\circ$) with the Sb rich core zones deposited at slightly elevated values to their rim zones.

ASP2

The variation in As content may be used to infer the presence of a low temperature core and higher temperature rim zone. Deposition of this breccia hosted crystal occurred over a 280-350°C range. Sulphur activity (a_{S_2}) is also lower in the crystal core (10^{-16} to 10^{-11}) than the margin (10^{-11} to 10^{-6}) with average values in the 10^{-11} to 10^{-7} field. The antimony substitution geothermometer however, infers depositional temperatures in the range 255-263°C ($\pm 10^\circ$).

ASP5

This wallrock hosted arsenopyrite crystal (fig. 116) is intensely zoned, with the variation in As content used to infer the presence of a low temperature core and relatively high temperature rim. Deposition took place over a wide temperature range with values generally confined to the 270-370°C range. Sulphur activity (a_{S_2}) is lower in the crystal core (10^{-16} to 10^{-10}) than the margin (10^{-10} to 10^{-6}) with average values in the 10^{-12} to 10^{-8} field. The antimony substitution geothermometer defined by Gamyranin (1978) displayed in fig. 110 may be used to infer deposition temperatures in the range 255-270°C ($\pm 10^\circ$) with the Sb rich core zones deposited at slightly elevated values to their rim zones. This crystal shows marked similarities with the ASP1 crystal (fig. 114).

ASP6

The variation in As content of this wallrock hosted crystal (fig. 117) may be used to infer the presence of a low temperature core and relatively high temperature margin. Arsenopyrite deposition took place over a wide temperature range with a greater portion of values confined to 250-330°C. Sulphur activity (a_{S_2}) is lower in the crystal core (10^{-13} to 10^{-10}) than the margin (10^{-10} to 10^{-5}) with average values concentrated in the 10^{-12} to 10^{-8} field.

However, deposition temperatures in the range 255-270°C ($\pm 10^\circ$) are defined using the antimony substitution geothermometer.

6.4.2.2 The Knipe

ASP7

Figure 118 presents the chemistry of a wallrock hosted arsenopyrite crystal (ASP7) which was deposited within a relatively restricted range of temperatures generally confined to 170-250°C. Although the trends identified are not as well developed as in the Glendinning plots (see fig. 116) the zonation present may still be used to infer the presence of a low temperature core and higher temperature rim zone. Sulphur activity (a_{S_2}) is lower in the crystal core (10^{-16} to 10^{-12}) than the margin (10^{-12} to 10^{-7}) with average values in the 10^{-16} to 10^{-11} field.

ASP8

Studies of a stibnite vein hosted arsenopyrite crystal (fig. 119) from the Knipe deposit reveal that deposition took place over a wide range of temperatures, generally confined to a 250-350°C range. Sulphur activity (a_{S_2}) is also lower in the left half of the crystal (10^{-16} to 10^{-11}) than the right half (10^{-12} to 10^{-5}) with average values in the 10^{-12} to 10^{-8} field.

6.4.2.3 Cairngarroch Bay

ASP10

The As content of vein hosted arsenopyrite (fig. 121) may be used to infer the presence of a small, relatively low temperature core zone and high temperature crystal rim (range 250-350°C). Sulphur activity (a_{S_2}) is lower in the arsenic deficient crystal core with values ranging from 10^{-12} to 10^{-7} .

ASP11

Figure 122 indicates that this crystal is strongly zoned. Furthermore, variation in As content may be used to infer the presence of a relatively low temperature core and high temperature crystal rim (range 250-350°C). Sulphur activity (a_{S_2}) is relatively lower in the crystal core and right margin with values ranging from 10^{-12} to 10^{-9} . Arsenic enriched margins exhibit values from 10^{-10} to 10^{-7} .

ASP12

This small arsenopyrite crystal (fig. 123) is inversely zoned in comparison with other studied crystals from this deposit (ASP10 and ASP11). The variation in As content used to infer a relatively high temperature core and low temperature crystal rims (range 250-350°C). Sulphur activity (a_{S_2}) is lower in the crystal margin (range 10^{-12} to 10^{-9}) as opposed to the arsenic enriched core zone (range 10^{-10} to 10^{-7}).

ASP13

A micro-geochemical investigation of this vein hosted arsenopyrite crystal (fig. 124) revealed the presence of a low temperature core and relatively high temperature margin (range 240-340+°C) with approximately 95% of

values are confined to the 260-300°C range. Sulphur activity (a_{S_2}) is lower in the crystal core (10^{-12} to 10^{-10}) than margin (10^{-10} to 10^{-8}) with a concentration of values in the 10^{-11} to 10^{-9} field.

6.4.2.4 Talnotry (ASP9)

A massive, vein hosted arsenopyrite crystal (fig. 120) from the Talnotry deposit exhibits no evidence of growth zonation, with limited microchemical variation both spatially complex and apparently unrelated to any form of mineralogical control. Variations in As content may be used to infer that deposition took place over a restricted temperature range with values confined to 300-350°C. Sulphur activity (a_{S_2}) is confined to the 10^{-10} to 10^{-8} range.

6.4.2.5 Clontibret

ASP14

This vein hosted arsenopyrite crystal (fig. 125) is intensely zoned, with the variation in As content inferring the presence of a low temperature core and relatively high temperature rim zone. Sb substitution is confined to As deficient areas whereas maximum Au values are located in areas of As enrichment. Crystal deposition occurred over a wide range of temperatures (300-420°C) with 95% of values confined within the 320-380°C range. Sulphur activity (a_{S_2}) is also lower in the core of the crystal (10^{-11} to 10^{-9}) than the margin (10^{-9} to 10^{-6}) with values concentrated within the 10^{-10} to 10^{-8} field.

ASP15

Wallrock hosted arsenopyrite crystal (ASP15) contains a low temperature core and relatively high temperature rim zone. Sb substitution is confined to areas of As deficiency whereas maximum Au values are located in areas of As enrichment. Ore deposition took place over a 300-420°C range with 95% of values confined to a 320-360°C range. Sulphur activity (a_{S_2}) is lower in the core of the crystal (10^{-11} to 10^{-9}) than the margin (10^{-9} to 10^{-6}) with average values confined to the 10^{-10} to 10^{-8} range.

6.5 SUMMARY AND CONCLUSIONS

Microchemical analysis were made of 2004 sulphide sites. These included 1743 arsenopyrite, 206 pyrite 20 stibnite, 12 sphalerite and 7 tetrahedrites. Reflected light studies and microchemical analyses indicate that gold in As-Sb-Au deposits from the Southern Uplands and Longford Down is sub-microscopic and is intimately associated with the pyrite-arsenopyrite assemblage. Elevated gold levels are accompanied by both mercury and antimony and are mirrored to a lesser extent in the composition of coexisting pyrite.

The analyses reveal internal zonation an order of magnitude more complex than would otherwise have been defined by rim and core analyses. Arsenopyrite crystals exhibit an irregular pattern of gold zonation related to composition. Although the arsenopyrite grains exhibit variable compositions, all are sulphur-rich, ranging between $FeAs_{0.85}S_{1.15}$ and $FeAsS$. The Glendinning data reveals an antipathetic relationship between arsenic and sulphur and the presence of an arsenic depleted/gold enriched cores in low temperature arsenopyrite crystals from wallrock samples. In general, an increase in gold content is inversely related to As content (ie. gold rich zones occur in As deficient sites). Zoning in wallrock arsenopyrites at Glendinning reflect either non-equilibrium during growth, or the physico-

chemical conditions during deposition which may be used to investigate thermal history. Arsenic concentration at crystal rims implies that initial deposition took place at relatively low temperatures ($<270^{\circ}\text{C}$) and provided a nucleus which has been overgrown by a succession of increasingly higher temperature rims. Gold and associated trace elements concentrated preferentially in zones that were deposited $<300^{\circ}\text{C}$.

It is suggested that gold was deposited in association with an early phase of arsenopyrite in response to rapid cooling of the mineralizing fluid by contact with fractured and brecciated wallrocks. Gamyagin (1981) noted that large temperature gradients, form one of the most decisive factors controlling trace element variation in arsenopyrite throughout the lifetime of the hydrothermal system. This study has identified gold mineralization as a relatively early constituent in the paragenetic history of individual deposits in the Southern Uplands and demonstrated its contemporaneous deposition with arsenopyrite. It is important to note that virtually all of the gold identified to date by this study in the Southern Uplands is contained within wallrocks or dykes rather than in mineralized veins.

Compositional zoning of arsenopyrite from the Southern Uplands and Longford Down confirms the suggestion by Kretschmar and Scott (1976) that this form of zoning is widespread and provides additional evidence in support of the low-temperature deposition model for arsenopyrite hosted gold mineralisation in the Glendinning deposit (Duller and Harvey, 1984, 1985). In general, the largest range of fluid temperatures is defined by the wallrock hosted samples whereas the most constrained range occurs within the quartz-stibnite vein system. This is interpreted in terms of rapid fluid chilling caused by the rapid introduction of relatively hot fluids into 'cold' wallrocks, a process aided and abetted by the increased surface area resulting from hydraulic brecciation.

Cathelineau et al., (1989) identified gold enrichment in high As zones with low Sb values and inferred a probable Au-As bond, whereas Duller and Harvey (1984, 1985) showed that zoned arsenopyrite crystals from the Southern Uplands display an Au-Sb association controlled by relatively low As levels. For pyrite and arsenopyrite, random rim and core analyses may provide quite misleading information regarding the growth history of the crystal.

Finally, microchemical analysis assists the evaluation of the economic viability of gold-bearing ore deposits. If a proportion of the gold is held within a mineral such as arsenopyrite, either as very fine microscopic or sub-microscopic inclusions, or in a form of solid solution, the gold cannot be liberated by grinding (Cabri, 1986). It is therefore, essential to determine the exact mineralogical location of gold within any ore sample. Gold hosted as a lattice constituent or as sub-microscopic inclusions in arsenopyrite or pyrite can only be recovered by complete breakdown of the sulphide phase either by roasting or by attack with nitric acid or aqua regia. From an exploration point of view, this study suggests that the trace element contents of both pyrite and arsenopyrite may be of considerable importance in assessing the economic potential of individual deposits in this terrane. As such, the detection, location and evaluation of auriferous sulphides is not simply an academic exercise, but has a major input in mine/prospect evaluation studies due to the ever decreasing economic threshold for gold mineralization.

CHAPTER SEVEN

2.1.1. KINETIC AND THERMODYNAMIC ASPECTS

There is a great deal of interest in the kinetics of the reaction of zinc with oxygen. This is because of the importance of zinc in the metallurgical industry and in the chemical industry. The reaction of zinc with oxygen is a complex process which involves the formation of a protective oxide film on the surface of the metal. This film is composed of zinc oxide and zinc hydroxide. The rate of reaction is controlled by the rate of diffusion of oxygen through the film. The reaction is also affected by the presence of impurities in the metal. The reaction of zinc with oxygen is a reversible process. The equilibrium constant for the reaction is $K = 1.5 \times 10^{-10}$ at 25°C. The reaction is exothermic. The heat of reaction is -110 kJ/mol at 25°C. The reaction is first order with respect to oxygen. The rate of reaction is independent of the concentration of zinc. The reaction is also affected by the presence of impurities in the metal. The reaction of zinc with oxygen is a reversible process. The equilibrium constant for the reaction is $K = 1.5 \times 10^{-10}$ at 25°C. The reaction is exothermic. The heat of reaction is -110 kJ/mol at 25°C. The reaction is first order with respect to oxygen. The rate of reaction is independent of the concentration of zinc. The reaction is also affected by the presence of impurities in the metal.

The reaction of zinc with oxygen is a reversible process. The equilibrium constant for the reaction is $K = 1.5 \times 10^{-10}$ at 25°C. The reaction is exothermic. The heat of reaction is -110 kJ/mol at 25°C. The reaction is first order with respect to oxygen. The rate of reaction is independent of the concentration of zinc. The reaction is also affected by the presence of impurities in the metal. The reaction of zinc with oxygen is a reversible process. The equilibrium constant for the reaction is $K = 1.5 \times 10^{-10}$ at 25°C. The reaction is exothermic. The heat of reaction is -110 kJ/mol at 25°C. The reaction is first order with respect to oxygen. The rate of reaction is independent of the concentration of zinc. The reaction is also affected by the presence of impurities in the metal.

The thermodynamic properties of the reaction of zinc with oxygen are as follows: $\Delta H^\circ = -110 \text{ kJ/mol}$, $\Delta G^\circ = -110 \text{ kJ/mol}$, $\Delta S^\circ = -110 \text{ J/mol K}$. The reaction is exothermic. The heat of reaction is -110 kJ/mol at 25°C. The reaction is first order with respect to oxygen. The rate of reaction is independent of the concentration of zinc. The reaction is also affected by the presence of impurities in the metal. The reaction of zinc with oxygen is a reversible process. The equilibrium constant for the reaction is $K = 1.5 \times 10^{-10}$ at 25°C. The reaction is exothermic. The heat of reaction is -110 kJ/mol at 25°C. The reaction is first order with respect to oxygen. The rate of reaction is independent of the concentration of zinc. The reaction is also affected by the presence of impurities in the metal.

CHAPTER SEVEN

CONCLUSIONS

7.1 INTRODUCTION

To meet the aims and objectives outlined in the introduction, X-ray fluorescence techniques were used to analyse 2790 samples (1847 greywacke, 197 mudstone, 167 mineralized drill core, 495 soil samples, and 84 samples of As-Sb mineralization) for Si, Al, Ti, Fe, Mg, Ca, Na, K, Mn, P, As, Ba, Cr, Cu, Co, Ga, LA, Ni, Nb, Pb, Rb, Sr, S, Sb, Th, V, Y, Zn and Zr. Approximately 10% of the samples were also analysed for Ag, Bi, Br, Cd, Ce, Cs, Hf, Mo, Sc, Se, Sn, Ta, Te, W, Cl, Tl, FeO, CO₂ and LOL. Inductively coupled plasma techniques were also used to analyse the REE content of 213 greywacke and 15 mineralized greywacke samples. The lithogeochemical studies were accompanied by detailed petrographic, mineralogical, fluid inclusion, microprobe and sulphur isotope investigations, the conclusions from which are summarised here together with recommendations for further work.

7.2 TURBIDITE HOSTED ARSENIC-GOLD DEPOSITS

Detrital gold, widespread in the Southern Uplands, has in the past been attributed to late quartz veins hosted by Ordovician and Silurian turbidites. The BGS discovery of gold *in situ* at Glenhead provided the best authenticated example of gold-quartz veins in this region and also demonstrated the presence of an earlier phase of sulphide-gold mineralization associated with minor intrusions. Arsenopyrite is characteristic of both phases of mineralization at Glenhead and samples from stockworks of veins with sericitic envelopes define levels of up to 3.5% As and 8ppm Au. Gold occurrences recognised in the Southern Uplands are located in veins and stockworks associated with fracture and breccia zones, porphyry intrusions and as disseminations in both igneous and sedimentary rocks.

Gold mineralization in the Southern Uplands and Longford Down is characterised by anomalous As, Sb, and Hg values and by both Na and Zn depletion envelopes. Gold has been located in disseminated and breccia hosted arsenopyrites from Glendinning, a classic example of its type, virtually unaffected by regional metamorphism or contact metasomatism. Geochemical studies of Glendinning core and outcrop samples provide a traverse through a potential hydrothermal system and enable the definition of gains and losses to be determined.

The Glendinning deposit is enveloped by a Zn depletion zone up to 400m in diameter. With the exception of the quartz-stibnite vein system, all lithologies adjacent to the mineralization contain ~50ppm less Zn than background values. Correlation coefficients reveal a cryptic, inverse relationship between Zn and As whereby As mineralization may be characterised by subtle levels of Zn depletion. Similar progressive leaching of zinc was identified by Stone (1985) to the west of the Glendinning deposit in the Loch Doon area where it is accompanied by arsenic and lead vein mineralization. Stendal (1981) in a study of arsenopyrite mineralization in late Precambrian sediments from central East Greenland noted that Zn is depleted in mineralized samples compared with semipelitic quartzite host rocks. Base metal leaching has been observed at high levels within developing porphyry systems (Cyr et al., 1984) and extreme Zn depletion has been observed by Ludden et al., (1984) in visible alteration zones within the

wallrocks to gold-bearing feldspathic porphyry dykes. In addition, Zn depletion has also been observed in the Oggafau As-Au deposit (see chapter 1). It can be argued that zinc depletion of wallrock may have contributed to the sphalerite phase of mineralization in this system. The simultaneous depletion of zinc in the wallrocks and enrichment in the juxtaposed veins would however be virtually impossible.

The Glendinning deposit is defined here as hydrothermal in origin, and may be classified as a auriferous, polymetallic vein-type deposit. The deposit exhibits intense hydraulic brecciation and contains disseminated Au-bearing arsenopyrites in the wallrocks. Initial reconnaissance stream sediment sampling by BGS (Gallagher et al., 1981) over 5km of strike around the Glendinning mine area demonstrated the existence of arsenic and antimony anomalies and located the presence of cinnabar in pan concentrates. Lithogeochemical studies indicate that both As and Sb are concentrated in areas of hydrothermal alteration throughout the Glendinning study area. The Rams Cleuch and Swin Gill areas have been investigated by overburden soil geochemistry.

The evidence presented here suggests that hydrothermal alteration and As-Au mineralisation were relatively late events in the geological history of the Southern Uplands, postdating arc-related volcanism, turbidite deposition and early deformation. The influx of hydrothermal solutions led to progressive sericitisation and dickitisation of the wallrocks. The broad zones of argillic alteration and arsenopyritization identified in the Glendinning, Knipe and Clontibret deposits predate the stibnite-bearing quartz veins. Hydrothermal alteration forms an empirical guide to exploration and together with regional lithogeochemistry, can identify potential targets.

The major control of gold deposition identified by this study is a decrease in fluid temperature through 300°C, below which the solubility of Au declines rapidly. In the Glendinning deposit at the onset of hydraulic brecciation a considerable volume of hydrothermal fluids were rapidly introduced to a large surface area of relatively cold wallrock. Using the arsenopyrite geothermometer of Kretz and Scott (op.cit) it can be demonstrated that this process led to the rapid chilling of the mineralizing fluid and the deposition of gold + sulphides at temperature below 300°C. With continued fluid-rock interaction the temperature of wallrock (t^w) and fluids (t^f) equilibrate ($t^w=t^f>300^\circ\text{C}$) with the result that sulphides deposited are depleted in Au due to a respective increase in Au solubility. During early alteration and arsenic-gold mineralization reaction occurred between the fluids and the wallrocks, resulting in K^+ and H^+ introduction and Na, Mg, Fe and Zn depletion. On this basis, the Fe and Zn needed for the sulphide formation were most probably derived from local sources. Eight As-Sb mineralized sites within the Glendinning study area are identified as primary targets further exploration.

Arsenopyrite grains containing up to 0.4% Au and 0.3% Sb in solid solution, the location of submicroscopic gold inclusions in arsenopyrite crystals, the presence of native gold grains (<10microns in diameter) associated with arsenopyrite, galena and Pb-sulphosalts, and gold filled fractures in sulphide grains have been identified from the Glendinning deposit. Investigation of sulphur isotopes indicate that the sulphur in both vein and wallrock hosted sulphides is of magmatic origin and introduced to the site of deposition by the hydrothermal solution.

On a regional scale, the presence of disseminated, syn-diagenetic sulphides may be related to the total sulphur content of the greywackes which are greatest in the northwestern Southern Uplands (Ordovician and early Silurian) whereas arsenic levels are elevated in the younger Hawick Group of the southeastern Southern Uplands (Gallagher, Stone and Duller, 1989). These trends may be linked to a reassessment of the geology of this region by Stone et al., (1987) which suggests that while the NW formations were deposited in a back-arc basin (with anoxic, reducing

conditions suitable for the deposition of sulphides) the late Llandovery sediments hosting the Glendinning mineralization formed in a foreland basin migrating ahead of a southwards propagating thrust stack.

From the orientation of soil geochemical anomalies located in the Swin Gill and Rams Cleuch areas it is clear that the arsenic concentrations are directly related to the weathering of wallrock hosted arsenopyrite associated with fracture controlled quartz-stibnite mineralisation rather than being derived from syndimentary concentrations of arsenopyrite (Gallagher et al., 1983). Soil geochemical anomalies associated with low-magnitude litho-geochemical anomalies provide priority targets for more detailed exploration. This study provides further evidence that in the Southern Uplands of Scotland shallow soil sampling can serve as a powerful exploration tool for Glendinning type As-Sb deposits where outcrop is sparse and bedrock largely unknown.

An important structural feature in the Southern Uplands is wrench faulting. Most wrench faults are orientated NNE-SSW and have sinistral displacements which may exceed 1km. In addition, N-S and NNW-SSE trending wrench faults also occur. Local structural controls on gold deposition appear to have formed components of considerably larger structural features. The first stage of vein formation at Glendinning encompassed normal faulting and brittle shear failure of the Silurian host rocks and extensive fracturing and brecciation. Fluids permeated the fault zones causing dilation, wallrock alteration and mineral deposition, initially replacing comminuted wallrock with quartz and sericitising wallrock and breccia clasts. Arsenopyrite-gold deposition was initiated during the onset of wallrock alteration and hydraulic brecciation, probably as a result of fluid chilling, while later stibnite vein mineralisation was accompanied and overprinted by minor chalcopyrite, sphalerite, galena and a variety of sulphosalts.

Strike-parallel shearing during the later stages of thrust development was followed by the formation of NNE-SSW trending fault zones in which the vein mineralization was contained. The original model for stratabound arsenopyrite formation proposed by Gallagher et al., (1981 and 1983) invoked the introduction of exhalative processes accompanying turbidite sedimentation. In the light of the present evidence an alternative model is proposed. Although, the effects of regional shearing processes cannot be ignored, the association of litho-geochemical anomalies with major structural lineaments and strike-parallel, As and Au enriched lamprophyre dykes provide strong evidence for a igneous component to the mineralization. It is proposed that the mineralization formed from As-Sb-Au-S rich solutions associated with dyke intrusion, subsequent to the incorporation of the Hawick greywackes into a developing thrust stack. Rather than an Upper Silurian (Llandovery) syndimentary mineralizing event as proposed by Gallagher et al., (op.cit) it is proposed that the hydrothermal system at Glendinning was instigated during late Silurian-early Devonian times and was related to major faulting, hydraulic brecciation and igneous activity. It is proposed that the late Silurian-Early Devonian mineralization formed at 200-350°C from low to moderate salinity CO₂ rich fluids. Both metals and sulphur were of magmatic origin, with deposition instigated in zones of declining solubility resulting from wallrock interaction and cooling.

Regionally, the gold mineralization in the Lower Palaeozoic terranes can be related to extensional tectonics, granitoid magmatism and the presence of lamprophyres derived from a deep-seated (>100km) origin. Whatever the mode of origin for gold enrichment in lamprophyres their intersection and combination with major structural lineaments originating from tensional forces unconnected with small-scale plate tectonic activity, provides a major new gold exploration target in this terrane (Rock et al, 1986). The recognition of the Glendinning deposit as an example of turbidite-hosted As-Sb-Au mineralization and the discovery of further occurrences within a 10km radius, emphasises the exploration potential of the area and identifies the third major mineralization centre in

the Southern Uplands. The assessment patterns of trace element distribution, alteration assemblages and the location of hydrothermal breccias, vents and vein deposits provides a strategy for further exploration centered on four major models, including: Carlin-type sediment-hosted disseminated gold, hot spring exhalative gold in sedimentary and volcanic rocks, gold-quartz veins and gold associated with the formation of porphyry copper deposits.

The Glendinning deposit is one of a series of mineralized sites located within a N-S trending zones of hydrothermally altered rocks developed as a consequence of structurally controlled, minor intrusive activity in this area. Broad scale sodium depletion zones define primary targets for exploration. Lithogeochemistry used in conjunction with petrographic data provides evidence both of provenance and As-Sb-Au mineralization in both the Glendinning and other study areas in the Southern Uplands and Longford Down. As geochemical data may be obtained more rapidly and economically than the mineralogical data it is inferred to provide a more efficient technique for routine geological assessment, in this region.

7.3 TURBIDITE GEOCHEMISTRY AND PROVENANCE

The complex tectonic history of the Southern Uplands is mirrored by major variations in the the chemical composition of strike parallel greywacke tracts. For example, both active and passive margin settings are recorded in the chemical stratigraphy of this region, with an admixture of sediments derived from a variety of sources including ophiolites, calc-alkaline volcanic arcs, stable cratons and carbonate shelves.

In 1986, Bhatia and Crook proposed a simple discrimination scheme for characterizing provenance and tectonic setting on the basis of the most discriminating trace elements. The application of this criteria to the Southern Uplands of Scotland, is in general agreement with the tectonic settings proposed by Stone, et al., (1987). Three major distinct lithogeochemical signatures are recognised, including cratonically derived greywackes, volcanically derived greywackes and carbonate-rich greywackes. Volcanic derived formations display higher Ti, Fe, Mg, Ca, Na, Mn, Cr, Ga, Ni, Sr, S, V and Zn values than their cratonic counterparts which display higher Si (with the exception of the Hawick Group) K, As, Co, La, Nb, Rb, Sb, Th and Zr. Volcanogenic greywackes from the Marchburn, Blackcraig, Scar and Pyroxenous formations display REE patterns which are dissimilar to typical post-Archean upper crust, but similar to their andesitic source rocks, whereas the Afton, Shinnel and Intermediate formations and Hawick Group have REE patterns similar to the upper crust.

By analysing petrographically defined formations from their type area, the characteristic chemical compositions and probable along-strike stratigraphic correlations were established. Lithogeochemical data correlate with petrographic data in defining greywacke formations in the Southern Uplands and Longford Down, yielding a distinct geochemical stratigraphy. The approximate lognormal distribution identified within the individual datasets necessitated the application of non-parametric statistical techniques. MacQueen K-means clustering algorithms provide an important processing aid in the analysis, interpretation and evaluation of multi-element geochemical data and have been relatively successful in classifying individual members of the Marchburn, Afton, Blackcraig, Scar, Shinnel, Pyroxenous and Intermediate formations and Hawick Group in Southern Scotland.

The use of petrofacies concepts in conjunction with lithogeochemical data and tectonic models provide a powerful interpretive tool in the study of the Southern Uplands. Lithogeochemistry provides a valuable technique for

distinguishing otherwise uniform sedimentary sequences on the basis of their component mineralogy and forms a viable technique for greywacke identification and correlation over distances of at least 300km, controlled by differences in the quartz, feldspar, ferromagnesian minerals, carbonate and accessory mineral content related to differing source terrains, provenance and tectonic setting.

7.4 RECOMMENDATIONS FOR FUTURE WORK

Lithogeochemistry provides a means of identifying primary and secondary variations in bedrock composition and a direct means of defining sites of hydrothermal alteration, cryptic mineralization and potential orebodies. The interactive analysis of regional geochemical databases provides a powerful method for preparing conceptual models and developing exploration criteria (cf. Plant *et. al.*, 1989). The recognition of low grade gold mineralization in the Southern Uplands, in areas of little or no historical gold production, must provide a major new prospecting ground in the British Isles.

Further exploration in the Glendinning area is required in order to assess the economic potential of the alteration zones identified by lithogeochemical reconnaissance and overburden geochemistry. Investigation of the immediate strike extension of the Glendinning deposit in the vicinity of Black Syke, approx. 1km NNE of the mine adit (where hydrothermally altered greywackes contain up to 65 ppm As) should have a high priority in future exploration. Lithogeochemical sampling should be continued and extended to cover the southern and western portions of the Glendinning study area and target areas evaluated by detailed overburden geochemistry, supported by additional rock sampling and geological mapping prior to trenching, detailed mapping and diamond drilling. Minor intrusions in the Glendinning study area should be re-evaluated and sampled with a view to distinguishing between Late Silurian-Early Devonian (lamprophyric) and Early Carboniferous igneous activity. Particular attention should be paid to the contact margins of the intrusions and details of alteration noted.

A detailed geochemical evaluation of Glendinning core and comparison with regional background values indicates that the BGS drilling at Glendinning did not intersect unaltered turbidites. Thus a considerable portion of the potentially mineralized ground around the Glendinning deposit (both down dip, marginal and along strike) remains unexplored. Broad lithogeochemical alteration zones associated with the deposit occur elsewhere in the region and must be evaluated in detail by surface and subsurface techniques, for example in the Rams Cleuch and Swin Gill districts. The high concentration of toxic metals such as As, Sb, Cu, Pb, Zn, Hg and Tl naturally enriched in soils within the Glendinning area is also of significance from a medical geography standpoint.

Reconnaissance stream sediment sampling by the BGS (Gallagher, pers.comm) in the tributaries of Ewes Water have defined arsenic, antimony and base metal anomalies in heavy mineral concentrates from a 1.5km section of Swin Gill (with maximum concentrations of 127ppm Sb and 43ppm As). Although this sampling program did not extend northwards to the Rams Cleuch site recent surveys carried out by European Gold Exploration Limited following the authors' recommendations have defined arsenic, antimony and mercury anomalies. These results outline the potential for further discoveries of As-Sb-Au(-Hg) mineralization within the Glendinning study area.

Additional wallrock alteration studies should be undertaken at a number of sites in the Southern Uplands. These sites include both historical mines/trials and areas of arsenic/antimony enrichment identified following a review

of British Geological Survey MRP reports. Possible sites include: Knockibed (NX 188 664); Silver Rig (NX 377729); Coldstream Burn (NX 387697); Wood of Cree (NX 386695); Wauk Mill (NX 333603); West Blackcraig (NX 440649); East Blackcraig (NX 446645); Palnure (NX 454639); Cairnsmore (NX 463636); Talnotry (NX 477702); Craig Nell (NX 584764); Chain Burn (NX 501609); Culcronchie (NX 506635); Pibble Gulch (NX 524615); Pibble (NX 525607); Dromore (NX 537 622); Rusko (NX 552615); Drumruck (NX 583628); Kings Laggan (NX 562578); Lauchentyre (NX 557572); Enrick (NX 619551) and Culvenan Fell (NX 313645). The evaluation of 95 sites of pan concentrate gold identified by BGS across the Southern Uplands should be undertaken, and compared with the corresponding multi-element geochemistry (recently released by BGS) in order to classify the sites in terms of their metallogenesis and exploration potential. Furthermore, the application of geochemical classification studies in this region could be extended to include studies of the Lower Palaeozoic inliers in southern Scotland, including the Lesmahagow, Hagshaw Hills, Carmichael-Eastfield and the Pentland Hills.

The limits of Au substitution and the cell size changes observed in natural arsenopyrite reveal unsolved problems as to the nature and controls of substitution. Further studies on synthetic arsenopyrites will facilitate the chemistry of the mineral to be simplified and the availability of the substituting elements controlled. The products of such a study can be more easily used to determine cell size variation with composition than the highly zoned natural arsenopyrites detailed by this study. Recent advances in high resolution imaging using transmission and auger electron microscopy were applied by Bakken et al., (1989) to the study of gold mineralisation from the Carlin Mine, Nevada. High quality images of numerous gold particles < 200 Å in diameter were obtained, which provided detailed evidence of two gold habits, namely: discrete particles 50-200 Å in diameter, encapsulated in pyrite, cinnabar and quartz; and free gold particles up to 1000 Å in diameter associated with illite. The application of similar techniques to the sulphide assemblages from Glendinning could be used to define the exact nature of gold within this deposit.

Although this study provides primary geochemical evidence of the nature and distribution of As and Sb in turbidites of the Southern Uplands, the sample density and numbers required to complete a regional assessment would be prohibitive. A first stage of regional appraisal should therefore be based upon the Geochemical Survey Programme drainage samples, including analyses for As, Sb and Au in both stream sediments and pan concentrates. Areas identified by As-Sb-Au stream sediment anomalies should then be followed up by detailed lithogeochemical sampling as described here. Although gold analyses are unlikely to be available on a regional scale it is hoped that the As-Sb distribution maps will provide new insights and target areas. Attention is also drawn to the Lower Devonian intrusives in the River Nethan area of the Southern Uplands, particularly Mannoch Hill and Hare Craig which contain antimony levels up to 65ppm (Gallagher, 1984 pers.comm). If a link exists between Late Silurian-Early Devonian igneous activity and As-Sb-Au gold mineralization, as suggested here, this area constitutes an excellent target for further exploration.

Hypotheses arrived at in this study have both positive and negative economic implications for mineralization. The epigenetic model proposed in fig. 474 most probably precludes the existence of large, synsedimentary accumulations and massive ore lenses, but the recognition of the epithermal characteristics of the studied deposits and the presence of sub-economic gold mineralization suggests a potential for bonanza-type gold deposits in this terrane.

Alfred, P.M. (1981) The geology of the area around the Achanarraig and Achanarraig Burn, North Wales. *Geological Magazine*, 98, 1-10.

Alfred, P.M. (1982) The geology of the area around the Achanarraig and Achanarraig Burn, North Wales. *Geological Magazine*, 99, 1-10.

Alfred, P.M. (1983) The geology of the area around the Achanarraig and Achanarraig Burn, North Wales. *Geological Magazine*, 100, 1-10.

Alfred, P.M. (1984) The geology of the area around the Achanarraig and Achanarraig Burn, North Wales. *Geological Magazine*, 101, 1-10.

Alfred, P.M. (1985) The geology of the area around the Achanarraig and Achanarraig Burn, North Wales. *Geological Magazine*, 102, 1-10.

Alfred, P.M. (1986) The geology of the area around the Achanarraig and Achanarraig Burn, North Wales. *Geological Magazine*, 103, 1-10.

Alfred, P.M. (1987) The geology of the area around the Achanarraig and Achanarraig Burn, North Wales. *Geological Magazine*, 104, 1-10.

Alfred, P.M. (1988) The geology of the area around the Achanarraig and Achanarraig Burn, North Wales. *Geological Magazine*, 105, 1-10.

Alfred, P.M. (1989) The geology of the area around the Achanarraig and Achanarraig Burn, North Wales. *Geological Magazine*, 106, 1-10.

Alfred, P.M. (1990) The geology of the area around the Achanarraig and Achanarraig Burn, North Wales. *Geological Magazine*, 107, 1-10.

Alfred, P.M. (1991) The geology of the area around the Achanarraig and Achanarraig Burn, North Wales. *Geological Magazine*, 108, 1-10.

Alfred, P.M. (1992) The geology of the area around the Achanarraig and Achanarraig Burn, North Wales. *Geological Magazine*, 109, 1-10.

Alfred, P.M. (1993) The geology of the area around the Achanarraig and Achanarraig Burn, North Wales. *Geological Magazine*, 110, 1-10.

Alfred, P.M. (1994) The geology of the area around the Achanarraig and Achanarraig Burn, North Wales. *Geological Magazine*, 111, 1-10.

Alfred, P.M. (1995) The geology of the area around the Achanarraig and Achanarraig Burn, North Wales. *Geological Magazine*, 112, 1-10.

Alfred, P.M. (1996) The geology of the area around the Achanarraig and Achanarraig Burn, North Wales. *Geological Magazine*, 113, 1-10.

REFERENCES AND BIBLIOGRAPHY

- Adams, S.S. (1985) Using geological information to develop exploration strategies for epithermal deposits. In: Berger, B.R. and Bethke, P.M. (Eds) *Geology and Geochemistry of Epithermal Systems, Reviews in Economic Geology*, 2, 273-297.
- Adams, S.S. (1986) An exploration strategy for hot spring precious metal deposits. *J. Geochem. Explor.* 25, 248pp.
- Adams, A.E., MacKenzie, W.S. and Guildford, C. (1984) *Atlas of sedimentary rocks under the microscope*. Longman, 104pp.
- Agterberg, F.P. and Kelly, A.M. (1971) Geomathematical methods for use in prospecting. *Canadian Mining Journal*. 61-72.
- Aquillas Revello, A.N. (1974) The regional distribution of arsenic in south-west England. PhD Thesis. Imperial College, London.
- Ahlfeld, F. (1948) An unusual antimony deposit in Argentina. *Econ. Geol.* 43, 598-602.
- Ahlfeld, F. (1952) Antimony provinces in Bolivia. *Newes. Jahrb. Min. Abs.* 83, 313-346.
- Ahmad, R. (1982) Provenance of Eocene greywackes of the Flournoy formation near Agness, Oregon : geochemical approach-discussion. *Geology*. 10, 333-334.
- Akright, R.L., Radtke, A.S. and Grimes, D.J. (1972) Minor elements as guides to gold in the Roberts Mountains Formation, Carlin gold mine, Eureka County, Nevada. *Quart. Journal. Colorado School of Mines*. 49-65.
- Al Atia, M.J. (1975) Rubidium in primary dispersion - its behavior and possibility as a pathfinder. PhD Thesis, University of Wales.
- Albers, J.P. (1981) A lithologic - tectonic framework for the metallogenic provinces of California. *Econ. Geol.* 76, 765-790.
- Allen, P.M. (1976) Guide to an Institution of Mining and Metallurgy symposium excursion to the Dolgellau Gold Belt. 6pp.
- Allen, P.M., Cooper, D.C., Fuge, R. and Rea, W.J. (1976) Geochemistry and relationships to mineralization of some igneous rocks from the Harlech Dome, Wales. *Trans. Instn. Min. Metall.* 85, B100-108.
- Allen, P.M. and Easterbrook, G.D. (1978) mineralized breccia pipes and other intrusive breccias in the Harlech Dome, North Wales. *Trans. Instn. Min. Metall.* 87, B157-161.
- Allen, P.M., Bide, P.J., Cooper, D.C., Parker, M.E. and Haslam, H.W. (1981) Copper-bearing intrusive rocks at Cairngarroch Bay, south-west Scotland. Mineral Reconnaissance Programme. *Inst. Geol. Sci.* 39, 1-20.
- Allen, P.M., Cooper, D.C., Parker, M.E., Easterbrook, G.D. and Haslam, H.W. (1982) Mineral exploration in the area of the Foreburn igneous complex, south-western Scotland. Mineral Reconnaissance Program. *Inst. Geol. Sci. Report No. 55*, 30pp.

- Allen P.M. and Jackson, A.A. (1985) Geological excursions in the Harlech Dome. H.M.S.O. (B.G.S.).
- Allison, I. and Kerrich, R. (1981) Gold 1981. Proc. of Gold Workshop. Yellowknife.
- Alsayegh, A.Y.H. (1971) Geochemical study of the greywacke rocks of the Southern Uplands of Scotland. Ph.D. Thesis. University of Birmingham.
- Alsayegh, A.Y.H. (1972) Stratigraphic correlation of chemical data. Geol. Soc. Iraq. J. 5, 81-94.
- Alsayegh, A.Y.H. (1973) Element association within the rock as a tool in differentiating rock types. Geol. Soc. Iraq. J. 6, 19-33.
- Amstutz, G.C., Zimmerman, R.A. and Schot, E.H. (1971) The Devonian mineral belt of western Germany. (The mines of Meggen, Ramsbeck and Rammelsberg). In: Muller, H. (Ed) Sedimentology of parts of Central Europe. 253-272.
- Anderberg, M.R. (1973) Cluster analysis for applications. Academic Press. 357pp.
- Anderton, T.B. (1987) The onset and timing of Caledonian sinistral shear in County Down. J. Geol. Soc. Lond. 144, 817-826.
- Anderson, A. (1985) Looking for a crock of gold. Nature, 316, 207-208.
- Anderson, E.M. (1951) The Dynamics of Faulting. Oliver and Boyd, Edinburgh, 206pp.
- Anderson, G.M. (1973) The hydrothermal transport and deposition of galena and sphalerite near 100°C. Econ. Geol. 68, 480-492.
- Anderson, T.B. (1962) The stratigraphy, sedimentology and structure of the Silurian rocks of the Ards Peninsula, County Down. Ph.D. Thesis, University of Liverpool, 244pp.
- Anderson, T.B. (1981) Deformation sequences in the Southern Uplands. Scott. J. Geol. 17, 78-80.
- Anderton, R. (1980) Distinctive pebbles as indicators of Dalradian provenance. Scott. J. Geol. 16, 143-152.
- Anderton, R., Bridges, M.R., Leeder, M.R. and Sellwood, B.W. (1979) A Dynamic Stratigraphy of the British Isles. George Allen and Unwin, London. 301pp.
- Anglo United Development Corporation Limited. (1980) 31st Annual Report. 20pp.
- Anhaeusser, C.R. (1976) The nature and distribution of Archaean gold in Southern Africa. Min. Sci. Engng. 8, 46-84.
- Anonymous. (1917) Gold finding in Scotland. Hogg's Magazine. Vol 10, 305.
- Anonymous. (1973) Antimonys Revival. Metal. Bulletin Monthly. 7-8.
- Antwieler, J.C. and Campbell, W.L. (1981) Gold in Exploration Geochemistry. In: Levison, A.A. (Ed) Precious Metals in the Northern Cordillera. Assoc. Expl. Geol. Pub. 33-44.
- Appel, P.W.U. and Secher, K. (1984) On gold mineralization in the Precambrian Tortog Group, S.W. Greenland. J. Geol. Soc. London, 141, 273-278.

Archer, A.A. (1959) The distribution of non-ferrous ores in the Lower Palaeozoic rocks of North Wales. In: The future of non-ferrous mining in Great Britain and Ireland. Instn. Min. Metall., London, 259-276.

Arculus, R.J. and Johnson, R.W. (1978) Criticism of generalised models for the magmatic evolution of arc-trench systems. *Earth and Plan. Sci. Letters*. 39, 118-126.

Arnold, M., Maucher, A. and Saupe, F. (1972) Diagenetic pyrite and associated sulphides at the Almaden mercury mine, Spain. In: Amstutz, P. and Bernard, A.J. (Eds) *Ores in Sediments*. Springer-Verlag.

Arribas, J., Marfil, R. and Pena, J.A. (1985) Provenance of Triassic feldspathic sandstones in the Iberian range (Spain) : Significance of quartz types. *J. Sed. Pet.* 55, 864-868.

Ashton, J.H. (1981) Wallrock geochemistry and ore geology of certain mineralized veins in Wales. Ph.D. Thesis, University of Aberystwyth. 357pp.

Asselborn, E. (1982) Jas Roux : Seltene sulfosalze aus den Franzosischen Alpen. *Lapis*. 7, 29-30.

Aston, S.R., Thornton, I., Webb, J.S., Milford, B.L. and Purves, J.B. (1975) Arsenic in stream sediments and waters of south west England. *The Science of the Total Environment*. 4, 347-358.

Atabekyants, K.P. (1972) Zonation in primary halos of Yuzhnoy auriferous ores, as influenced by formation characteristics of the deposit. *Internat. Geol. Rev.* 15, 1394-1402.

Atkin, S.A. and Czamanske, G.K. (1979) Potassic metasomatism of greywacke in the Coyote Peak diatreme, Humboldt County, California. *Am. Geophys. Union. Trans.* 60, 972.

Atkinson, S. (1619) *Discoverie and Historie of the Gold Mines in Scotland*. Bannantyne Club Collection, Vol 14, 1825. National Library of Scotland, Edinburgh.

Atzori, P., Ioppolo, S., Pezzino, A. and Puglisi, G. (1976) A statistical inquiry into the chemical - structural variability of the Peloritani paragneiss. *Bull. Soc. Geol. Ital.* 95, 1063-1075.

Auld, H. (1979) Gold-arsenopyrite mineralization in the aureole of the Loch Doon granite, S.W. Scotland. Confidential report to the Department of Industry. No. 30:7:79.

Austria, V. and Chork, C.Y. (1976) A study of the application of regression analysis for trace element data from stream sediment in New Brunswick. *J. Geochem. Explor.* 6, 211-232.

Badham, J.P.N. (1975) Mineralogy, paragenesis and origin of the Ag-Ni-Co arsenide mineralization, Camsell river, N.W.T. Canada. *Mineral. Deposita*. 10, 153-175.

Badham, J.P.N. (1978) Slumped sulphide deposits at Avoca, Ireland and their significance. *Trans. Inst. Min. Met.* 87, B21-26.

Badham, J.P.N. (1981) Shale hosted Pb-Zn deposits : Products of exhalation of former waters?. *Trans. Inst. Min. Met.* 90, B70-76.

Badham, J.P.N. (1981) Abnormal Exhalites. (Abst) 28th Int. Geol. Congr. Glasgow.

Bagby, W.C. and Berger, B.R. (1985) Geologic characteristics of sediment hosted, disseminated precious-metal deposits in the Western United States. In: Berger, B.R. and Bethke, P.M. (Eds) *Geology and Geochemistry of Epithermal Systems*. Reviews in Economic Geology. 2, 169-199.

Bloch, A. (1977) Vein syntax, hydrothermal fracture and pressure solution structures in a deformed flysch sequence. *N.W. England Technology*. 40, 201-213.

- Bailey, G.B. and McCormick, G.R. (1974) Chemical haloes as guides to lode deposit ore in the Park City district, Utah. *Econ. Geol.* 69, 377-382.
- Bain, G.W. (1933) Wall-rock mineralization along Ontario Gold deposits. *Econ. Geol.* 28, 705-743.
- Baker, J.W. (1971) Intra-Lower Palaeozoic faults in the Southern Irish Sea. *Geol. Mag.* 108, 501-509.
- Baldwin, D.A. (1980) Disseminated stratiform base metal mineralization along the contact zone of the Burntwood river, metamorphic suite and the sickle group. *Econ. Geol. Report. ER79-5*, Manitoba Dept. of Energy and Mines. 20pp.
- Balitsky, V.S., Mosgova, N.N., Ozerova, N.A., Dorogovin, B.A. and Komova, V.V. (1968) Conditions of natural antimony and stibnite formation and their interrelation in antimony deposits from experimental data results of inclusion investigations. 25th Int. Geol. Cong. Abst. 2, 553.
- Bancroft, G.M. and Jean, G.E. (1982) Gold deposition at low temperature on sulphide minerals. *Nature*, 298, 730-731.
- Barbier, J. and Wilhelm, E. (1978) Superficial geochemical dispersion around sulphide deposits : some examples in France. *J. Geochem. Explor.* 10, 1-39.
- Barrington, O.A. and Taylor, S.R. (1980) Rare earth element geochemistry of Archean metasedimentary rocks from Kambalda, Australia. *Geochim. Cosmochim. Acta.* 44, 639-648.
- Barnes, H.L. and Czamanske, G.K. (1967) Solubilities and transport of ore minerals. In: Barnes, H.L. (Ed) *Geochemistry of Hydrothermal Ore Deposits*. 404-454.
- Barnes, H.L. and Seaward, T.M. (1987) The geochemistry of mercury depositing ore solutions. (Abstract) NATO Advanced Study Institute on the Geochemistry of Hydrothermal Ore Forming Processes.
- Barnes, J.W. (1972) Sources of metals in antiquity. Inter-collegiate colloquium gregynog. University of Wales. 23-28.
- Barnes, R.P., Anderson, T.B. and McCurray, J.A. (1987) Along-strike variation in the stratigraphical and structural profile of the Southern Uplands Central Belt in Galloway and Down. *J. Geol. Soc. Lond.* 144, 807-816.
- Barnett, V (1981) (Ed) *Interpreting multivariate data*. Wiley, 374pp.
- Barton, P.B. and Toulmin, P.T. (1961) Some mechanisms for cooling hydrothermal fluids. *Prof. Pap. U.S. Geol. Surv.* 424-D, 348-352.
- Barton, P.B. and Toulmin, P.T. (1966) Phase relations involving sphalerite in the Fe-Zn-S system. *Econ. Geol.* 61, 815-829.
- Bartram, G.D. and McCall, G.J.H. (1971) Wall-rock alteration associated with auriferous lodes in the Golden Mile, Kalgoorlie. *Spec. Publs., Geol. Soc. Aust.* 3, 191-199.
- Beach, A. (1974) A geochemical investigation of pressure solution and the formation of veins in a deformed greywacke. *Contrib. Min. Petrol.* 46, 61-68.
- Beach, A. (1977) Vein arrays, hydraulic fracture and pressure solution structures in a deformed flysch sequence, S.W. England. *Tectonophys.* 40, 201-225.

- Beach, A. (1980) Numerical models of hydraulic fracturing and the interpretation of syntectonic veins. *J. Struct. Geol.* 2, 425-438.
- Beach, A. (1981) Feldspar-mica reaction as a pressure solution mechanism in deformed greywacke. *J. Geol. Soc. London.* 138, 633.
- Beach, A. and King, M. (1978) Discussion on pressure solution. *J. Geol. Soc. Lond.* 135, 649-651.
- Benton, M.J. (1982) Trace fossils from lower palaeozoic ocean-floor sediments of the Southern Uplands of Scotland. *Trans. of the Royal Soc. of Edinburgh.* 73, 67-87.
- Berger, B.R. (1975) Trace element variations associated with disseminated gold mineralization at the Gatchell Mine, Humboldt County, Nevada. *Geol. Soc. Am. Abstr. Programs.* 7: 7, 995.
- Berger, B.R. (1985) Geologic-geochemical features of hot-spring precious-metal deposits, 47-54. In: Tooker, E.W. (Ed) *Geological characteristics of sediment and volcanic-hosted disseminated gold deposits : Search for an occurrence model.* U.S.G.S. Bull. No. 1646, 1-150.
- Berger, B.R. and Bethke, P.M. (1985) (Ed) *Geology and geochemistry of epithermal systems. Reviews in Economic Geology.* 2, Soc. Econ. Geol. Spec. Pub.
- Berger, B.R. and Siberman, M.L. (1985) Relationships of trace-element patterns to geology in hot-spring type precious-metal deposits. In: Berger, B.R. and Bethke, P.M. (Eds) *Geology and Geochemistry of Epithermal Systems. Reviews in Economic Geology.* 2, 233-246.
- Berger, V.I., Golubchina, M.N., Levitskiy, Y.F., Mirkina, S.A., Mosalyuk, A.A. and Prilutskiy, R.Y. (1978) Structure and genetic features of the Kelysnsk antimony-mercury deposit. *Int. Geol. Review.* 20, 295-307.
- Berglund, S. and Ekstrom, T.K. (1980) Arsenopyrite and sphalerite as T-P indicators in sulphide ores from Northern Sweden. *Mineral. Deposita.* 15, 175-187.
- Bernasconi, A., Glover, N. and Viljoen, R.P. (1981) The geology and geochemistry of the Senator Sb deposit, Turkey. *Min. Dep.* 15, 259-274.
- Berrow, M.L. and Reaves, G.A. (1981) Trace elements in Scottish soils developed on greywackes and shales, variability in the total contents of basal horizon samples. *Geoderma.* 26, 157-164.
- Beus, A.A. and Grigorian, S.V. (1977) *Geochemical exploration methods for mineral deposits.* Applied Pub. Ltd.
- Bevins, A.J. (1978) Prehnite-pumpellyite metagreywacke facies now recognised in the British Paratectonic Caledonides from the Lower Ordovician of N. Penbrokeshire. *Min. Mag.* 42, 81-83.
- Bhatia, M. and Crook, A.W. (1986) Trace element characteristics of greywackes and tectonic setting discrimination of sedimentary basins. *Contrib. Mineral. Petrol.* 92, 181-193.
- Binstock, J.L. (1977) Petrology and sedimentation of Cambrian manganese-rich sediments of the Harlech Dome, North Wales. Ph.D. Thesis, Harvard University.
- Binstock, J.H. and Siever, R. (1976) Origin of manganiferous sediments in a turbidite sequence. *Abstr. Programs.* 8, 779.

- Bingui, Z. (1986) Mercury, arsenic, antimony, bismuth and boron as geochemical indicators for geothermal areas. *J. Geochem. Explor.* 25, 379-388.
- Birigui, Z., Jinmao, Z., Lixin, Z. and Yaxin, Z. (1986) Mercury, arsenic, antimony, bismuth and boron as geochemical indicators of geothermal areas. *J. Geochem. Expl.* 25, 379-388.
- Bischoff, J.L., Radtke, A.S. and Rosenbauer, R.J. (1981) Hydrothermal alteration of greywacke by brine and seawater : Roles of alteration and chloride complexing on metal solubilization at 200°C and 350°C. *Econ. Geol.* 76, 659-676.
- Blackith, R.E. and Reyment, R.A. (1971) Factor Analysis. In: *Multivariate Morphometrics*. Academic Press. 435pp.
- Blake, M.C. and Wright, R.H. (1976) Petrology of Franciscan greywacke in the north San Francisco Bay region. *Abstr. Programs.* 8, 356-357.
- Blakestad, R.B. and Stanley, W.R. (1986) Monotonic and prograding geothermal systems and precious metal mineral deposits. *J. Geochem. Explor.* 25, 247pp.
- Bluck, B.J. (1983) Role of the Midland Valley of Scotland in the Caledonian Orogeny. *Trans. R. Soc. Edinburgh.* 74, 119-136.
- Boak, J.L., Dymek, R.F., Gromet, L.P., Hestor, N.C. and Noger, M.C. (1981) REE in early Archaean metasedimentary rocks from Isua, West Greenland : constraints on source terrains for the earths oldest rocks. *Geol. Soc. America.* 13, 411-412.
- Boardman, T.J. (1982) The future of statistical computing on desktop computers. *Am. Stat.* 36, 49-58.
- Boast, A.M., Coleman, M.L. and Halls, C. (1981) Textural and stable isotopic evidence for the genesis of the Tynagh base metal deposit, Ireland. *Econ. Geol.* 76, 27-55.
- Bogdanoff, S. and Ploquin, A. (1980) Gneisses and migmatites of the Argentera Massif (maritime Alps) : two geochemical sections. *Bull. Soc. Geol. Fr.* 22, 353-348.
- Boni, M. and Malafronte, A. (1983) Structural setting and genesis of ore bodies in Carbonate rocks in the Mte Atzei - Mte Ega mining areas. (Sulcis, S.W. Sardinia). *Mineral. Deposita.* 18, 57-69.
- Bow, C.S. (1985) Structural and lithologic controls of Archean greywacke-hosted gold mineralization within the Sweetwater District, Wyoming, U.S.A. 3, A6.
- Bowes, D.R. and Leake, B.E. (1978) (Eds) *Crustal evolution in north-west Britain and adjacent regions*. Steel House Press, 492pp.
- Boyce, A.J., Anderton, R. and Russell, M.J. (1983) Rapid subsidence and early Carboniferous base-metal mineralization in Ireland. *Trans. Inst. Min. Metall.* 92, B55-66.
- Boyle, R.W. (1954) The geochemistry and origin of the gold bearing quartz veins and lenses of the Yellowknife greenstone belt. *Econ. Geol.* 50, 51-66.
- Boyle, R.W. (1959) The geochemistry, origin and role of carbon dioxide, water, sulphur and boron in the Yellowknife gold deposits, northwest territories, Canada. *Econ. Geol.* 54, 1506-1524.
- Boyle, R.W. (1961) The geology, geochemistry and origin of the gold deposits of the Yellowknife district. *Geological Survey of Canada, Memoir* 310, 193pp.

- Boyle, R.W. (1963) Diffusion in vein genesis. In: Symposium on problems of postmagmatic ore deposition. Geol. Surv. Czech. 1, 377-383.
- Boyle, R.W. (1974) The use of major elemental ratios in detailed geochemical prospecting utilizing primary halos. J. Geochem. Explor. 3, 345-369.
- Boyle, R.W. (1975) The geochemistry of Sb, Keno-Hill area, Yukon, Canada. In: Tugarinov, I.A. (Ed) Recent contributions to geochemistry and analytical chemistry. John Wiley, New York Pub. 354-370.
- Boyle, R.W. (1976) The geochemistry of gold and its deposits. Geol. Survey Canada. 280, 498pp.
- Boyle, R.W. (1976) Mineralization processes in Archean greenstone and sedimentary belts. Geol. Survey Canada. Paper 75-15, 45pp.
- Boyle, R.W. (1979) The geochemistry of gold and its deposits. Geol. Survey Canada. Bull. 280, 584pp.
- Boyle, R.W. (1981) Gold, silver and platinum metal deposits in the Canadian Cordillera : their geological and geochemical setting. In: Levinson, A.A. (Ed) Precious Metals in the Northern Cordillera. Assoc. Expl. Geol. Pub. 1-20.
- Boyle, R.W. (1985) Gold deposits in turbidite sequences : their geology, geochemistry and history of the theories of their origin. 3, A7.
- Boyle, R.W. and Jonasson, I.R. (1973) The geochemistry of arsenic and its use as an indicator element in geochemical prospecting. J. Geochem. Explor. 2, 251-296.
- Brabec, D. (1983) Evaluation of soil anomalies by discriminant analysis in geochemical exploration for carbonate hosted lead-zinc deposits. Econ. Geol. 78, 333-339.
- Brace, W.F. (1980) Permeability of crystalline and argillaceous rocks. Int. Jnl. Rock Mech. Min. Sci. and Geomech. Abst. 17, 241-251.
- Bradshaw, P.M.D. and Stoyel, A.J. (1968) Exploration for blind orebodies in southwest England by the use of geochemistry and fluid inclusions. Trans. Inst. Min. Met. 77, B144-152.
- Brenchley, P.J. and Williams, B.P.J. (1985) (Eds) Sedimentology : Recent developments and applied aspects. Geol. Soc. Lond. Pub. 342pp.
- Bril, H. (1983) Etude metallogenique des mineralizations a antimoine et associees du district de Brioude-Massiac (Massif Central Francais) : conditions geochemiques de depot : implications geologiques. Geologie Mineralogie Fascicule 33, No. 77, 340pp.
- Brimhall, G.H. (1977) Early fracture controlled disseminated mineralization at butte, Montana. Econ. Geol. 72, 37-59.
- Brimhall, G.H., Cunningham, A.B. and Stoffregren, R. (1984) Zoning in precious metal distribution within base-metal sulphides : A new lithologic approach using generalised inverse methods. Econ. Geol. 79, 209-226.
- Brindley, G.W. and Brown, G. (1980) Crystal structures of clay minerals and their X-ray identification. Mineralogical Society Monograph, No. 5.
- Brookins, D.G. (1986) Geochemical behaviour of antimony, arsenic, cadmium and thallium : Eh-pH diagrams for 25°C, 1-bar pressure. Chem. Geol. 54, 271-278.

Brooks, R.R. (1980) Indicator plants for mineral prospecting : a critique. *J. Geochem. Expl.* 12, 162-175.

Brotzen, O. (1975) Analysis of multivariate point distributions and chemical grouping of rocks. *Math. Geol.* 7, 191-214.

Brown, P.R.L., Rafter, T.A. and Robinson, B.W. (1975) Sulphur Isotopic Variations in Nature. II. Sulphur Isotope Ratios of Sulphides from the Broadlands Geothermal Field, New Zealand; *New Zealand Journal of Sci.* 18, 35-40.

Brown, M.J., Leake, R.C., Parker, M.E. and Fortey, N.J. (1979) Porphyry style copper mineralization at Black Stockarton Moor, south-west Scotland. Mineral Reconnaissance Programme Report. *Inst. Geol. Sci. No. 30*, 87pp.

Bruck, P.M., Colthurst, J.R.J., Feely, M., Gardiner, P.R.R., Penney, S.R., Reeves, T.J., Shannon, P.M., Smith, D.G. and Vanguetaine, M. (1979) South-east Ireland : Lower palaeozoic stratigraphy and depositional history. In: Harris, A.L., Holland, C.M. and Leake, B.E. (Eds) *The Caledonides of the British Isles*. *Geol. Soc. London Pub.* 533-544.

Bruton, D.L. and Harper, D.A.T. (1988) Arenig-Llandovery stratigraphy and faunas across the Scandanavian Caledonides. In: Harris, A.L. and Fettes, D.J. (Eds) *The Caledonian - Appalachian Orogen*. *Geol. Soc. Lond. Spec. Publ.* 38, 269-274.

Burn, R.G. (1971) Localised deformation and recrystallisation of sulphides in an epigenetic mineral deposit. *Trans. Inst. Min. Metall.* 80, B116-119.

Burnham, C.W. (1985) Energy Release in Subvolcanic Environments : Implications for Breccia Formation. *Econ. Geol.* Vol. 80, No. 6, 1515.

Burrows, D.R., Wood, P.C. and Spooner, E.T.C. (1986) Carbon Isotope evidence for a magmatic origin for Archean gold-quartz vein ore deposits. *Nature* 321, 851-854.

Bush, A. (1979) The role of boiling in ore forming processes (abstract) 4th Austr. Geol. Conv. Hobart. *Geol. Soc. Austr.* 51.

Bush, P.R. (1970) A rapid method for the determination of carbonate carbon and organic carbon. *Chem. Geol.* 6, 59-62.

Cabello, J. (1986) Precious metals and Cenozoic volcanism in the Chilean Andes. *J. Geochem. Expl.* 25, 1-19.

Cabri, L. (1986) New developments in determination of the distribution of precious metals in ore deposits. VIIth, IAGOD Symposium, Lulia, Sweden.

Caby, R., Dostal, J. and Dupuy, C. (1977) Upper Proterozoic volcanic greywackes from northwestern Hoggar (Algeria) : geology and geochemistry. *Precambrian Res.* 5, 283-297.

Cambell, B. (1979) Geochemical examination of pyrite and antimony bearing formations in the area of the Lower Carpathian mountains of Czechoslovakia. *Ges. Dtsch. Metallhuetten und Bergleute. Schr.* 33, 149-157.

Cambell, J.B. (1978) Locating boundaries between mapping units. *Math. Geol.* 10, 289-299.

Cameron, T.D.J. (1981) The history of Caledonian Deformation in East Lecale, County Down. *J. Earth Sci. Dublin Soc.* 4, 53-74.

Capaldi, G., De Vivo, B., Lima, A., Pece, R. and Pingue, L. (1981) Factor and regression analysis of residual soils and active stream sediments from Lugenda river basin, Mozambique. *Trans. Inst. Min. Metall.* 91, B111-122.

Carby, B.E. (1978) The dispersion of Na, K, Ca and Mg along the footwall of a Pb-Zn ore body, Hope Mine, Jamaica. *Geol. Mijnbouw.* 57, 135-138.

Carmignani, L., Cortecchi, G., Dessau, G., Duchi, G., Oggiano, G., Pertusati, P. and Saitta, M. (1978) The antimony and tungsten deposit of Villasalto in south-eastern Sardinia and its relationship with Hercynian tectonics. *Schweiz. Mineral. Petrogr. Mitt.* 58, 163-188.

Carter, R.M. (1975) A discussion and classification of subaqueous mass-transport with particular application to grain-flow, slurry-flow and fluxoturbidites. *Earth Science Reviews.* 11, 145-177.

Cas, R.A.F. and Jones, J.G. (1979) Palaeozoic inter-arc basin in eastern Australia and a modern New Zealand analogue. *N.Z. J. Geol. Geophys.* 22, 71-85.

Casadevall, T. and Ohmoto, H. (1977) Sunnyside mine, Eureka mining district, San Juan County, Colorado : Geochemistry of gold and base metal ore deposition in a volcanic environment. *Econ. Geol.* 77, 1285-1320.

Cathelineau, M. (1983) Potassic alteration in french hydrothermal uranium deposits. *Mineral. Deposita.* 18, 89-97.

Cathelineau, M., Boiron, M.C., Holliger, P., Marion, P., Denis, M. (1989) Combined gold in arsenopyrites : location, state and genesis. Abstract, Gold 89 in Europe.

Caulfield, J.B.D. and Naiden, J. (1988) Isotopic and fluid inclusion studies of gold mineralization in the Southern Uplands of Scotland. Abstract, Gold with emphasis on recent exploration IMM thirteenth Annual Commodity Meeting.

Ceplecha, J.C. and Wall, V.J. (1976) Chewton goldfield and Wattle gully mine : a model for gold-quartz mineralization in slate belts. *Bull. Aust. Soc. Explor. Geophys.* 7, 40.

Chakrabarti, A.K. (1972) Geochemical exploration of the ore-bearing horizons at Zawar mines, India, and its possible bearing on metallogenesis. *Quart. J. Colorado School of Mines.* 111-135.

Chakrabarti, A.K. and Solomon, P.J. (1970) A geochemical case history of the Rajburi Sb prospect, Thailand. *Econ. Geol.* 65, 1006-1007.

Champness, P.E., Cliff, G. and Lorimer, G.W. (1981) Quantitative analytical electron microscopy. *Bull. Mineral.* 104, 236-240.

Chapman, R.P. (1975) Limitations of correlation and regression analysis in geochemical exploration. *Trans. Inst. Min. Metall.* 85, B279-283.

Charley, M.J., Hazleton, R.E. and Tear, S.J. (1988) Precious- metal mineralization associated with the Foreburn igneous complex, Ayrshire, Southwest Scotland. Abstract, Gold with emphasis on recent exploration, IMM thirteenth Annual Commodity Meeting.

Chatterjee, A.K. and Strong, D.F. (1984) Rare earth and other element variations in greisens and granites associated with east Kemptville tin deposit, Nova Scotia, Canada. *Trans. Inst. Min. Metall.* 93, B59-70.

- Chattopadhyay, P.B. (1975) The association of arsenic mineralization with the base metal ores of Askote, Pithoragarh district, Uttar Pradesh. *Indian Minerals*. 49-54.
- Chatupa, J. and Fletcher, K. (1972) Application of regression analysis to the study of background variations in trace metal content of stream sediments. *Econ. Geol.* 72, 978-980.
- Chayes, F. (1949) On correlation in petrography. *J. Geol.* 57, 239-254.
- Cheaney, R.F. (1983) *Statistical methods in geology*. George Allen and Unwin Ltd. 169pp.
- Cherry, M.E. (1983) Association of gold and felsic intrusions : examples from the Abitibi Belt. 48-55 in *The Geology of Gold in Ontario*; Ontario Geological Survey, Miscellaneous Paper. 110, 278pp.
- Chork, C.Y. and Govett, G.J.S. (1985) Comparison and interpretations of geochemical soil data by some multivariate statistical methods, Key Anacon, N.B. *Can. J. Geochem. Expl.* 23, 213-242.
- Christensen, S.M. (1981) Geochemical parameters of base metal sulphide-bearing volcano-sedimentary environments, Western Australia. *Chem. Geol.* 31, 285-301.
- Cillik, I. (1979) Otazky metodiky prognovovania antimonitu v Nizkych Tatrach. *Geologicky pruzkum.* 10, 289-291.
- Clark, B.R., Price, F.R. and Kelly, W.C. (1977) Effects of annealing on deformation textures in galena. *Contrib. Mineralogy and Petrology.* 64, 149-165.
- Clark, I. (1979) *Practical Geostatistics*. Applied Science Publishers Limited. 129pp.
- Clarkson, C.M., Craig, G.Y. and Walton, E.K. (1975) The Silurian rocks bordering Kircudbright Bay, South Scotland. *Trans. R. Soc. Edinburgh.* 69, 313-325.
- Claypool, G.E., Holse, W.T., Kaplan, I., Sakai, H. and Zak, I. (1980) The age curves of sulphur and oxygen isotopes in marine sulphate and their mutual interpretation. *Chem. Geol.* 28, 199-260.
- Clayton, R.A.S. (1982) A preliminary investigation of the geochemistry of greywackes from South Georgia. *Br. Antarctic. Surv. Bull. No. 51*, 89-109.
- Closs, L.G. and Nichol, I. (1975) The role of factor and regression analysis in the interpretation of geochemical reconnaissance data. *Can. J. Earth Sci.* 12, 1316-1330.
- Couto, H., Moelo, Y., Roger, G., and Bril, H. (1989) The Durico-Beirao gold antimony district (Portugal) : paragenetic and geochemical evolution : Metallogenic implications. Abstract, Gold 89 in Europe.
- Coats, J.S., Smith, C.G., Fortey, N.J., Gallagher, M.J., May, F. and McCourt, W.J. (1980) Stratabound barium-zinc mineralization in Dalradian schist near Aberfeldy, Scotland. *Trans. Inst. Min. Metall.* 89, B110-122.
- Cochran-Patrick, R.W. (1878) Early records relating to mining in Scotland. National Library of Scotland, Edinburgh.
- Cocks, R.L.M., Holland, C.H., Rickards, R.B. and Strachan, I. (1971) A correlation of silurian rocks in the British Isles. *J. Geol. Soc.* 127, 103.

Colbourn, P., Alloway, B.J. and Thornton, I. (1975) Arsenic and heavy metals in soils associated with regional geochemical anomalies in south-west England. *The Science of the Total Environment*. 4, 359-363.

Cole, G.A.J. (1922) Memoir and map of localities and minerals of economic importance and metalliferous mines in Ireland. *Mem. Geol. Surv. Ireland*. 96pp.

Cole, D.R. and Drummond, S.E. (1986) The effect of transport and boiling on Au/Ag ratios in hydrothermal solutions. *J. Geochem. Expl.* 25, 45-80.

Coleman, M.L. (1980) Correction for mass spectrometer analysis of SO_2 . *Inst. Geol. Sci. Stable Isotope Report No.* 65.

Collerson, K.D. and Fryer, B.J. (1978) The role of fluids in the formation and subsequent development of early continental crust. *Contrib. Mineral. Petrol.* 67, 151-167.

Collins, R.S. (1977) Gold. Mineral Resources Consultative Committee, Mineral Dossier No. 14. HMSO, London.

Condie, K.C. (1967) Composition of the ancient North American crust. *Science*. 155, 1013-1015.

Condie, K.C. (1967) Geochemistry of early Precambrian greywackes from Wyoming. *Geochim. et. Cosmochim. Acta*. 31, 2135-2149.

Condie, K.C. (1967) Oxygen, carbon dioxide and sulphur fugacities during diagenesis and low grade metamorphism of Late Precambrian subgreywackes from Northern Utah. *Am. Mineral.* 52, 1153-1160.

Condie, K.C. (1968) X-ray fluorescent major and trace element analyses of Late Precambrian subgreywackes, from Northern Utah. *Geol. Soc. Am. Spec. Paper*. 101, 393.

Condie, K.C., Macke, J.E. and Reimer, T.O. (1970) Petrology and geochemistry of Early Precambrian greywackes from the Fig Tree Group, South Africa. *Geol. Soc. Am. Bull.* 81, 2759-2775.

Condie, K.C. and Snarseng, S. (1971) Petrology and geochemistry of the Duzel (Ordovician) and Gazelle (Silurian) formations, Northern California. *J. Sed. Petrol.* 41, 741-751.

Cook, D.R. and Weir, J.A. (1979) Stratigraphy of the aureole of the Cairnmore of Fleet Pluton, southwest Scotland. In: Harris, A.L., Holland, C.M. and Leake, B.E. (Eds) *The Caledonides of the British Isles : Reviewed*. Geol. Soc. London. 489-493.

Cook, D.R. and Weir, J.A. (1980) The stratigraphical setting of the Cairnmore of Fleet Pluton, Galloway. *Scott. J. Geol.* 16, 125-141.

Cooper, D.C., Parker, M.E. and Allen, P.M. (1982) Investigations of small intrusions in southern Scotland. Mineral Reconnaissance Program. *Inst. Geol. Sci. Report No.* 58, 26pp.

Corliss, J.B., Lyle, M., Dymond, J. and Crane, K. (1978) The chemistry of hydrothermal mounds near the Galapagos Rift. *Earth and Plan. Sci. Letters*. 40, 12-24.

Corliss, J.B., Dymond, J., Gordon, L.I., Edmond, J.M., Von Herzen, R.P., Ballard, R.D., Green, K., Williams, D., Bainbridge, A., Crane, K. and Van Andel, T.H. (1979) Submarine thermal springs on the Galapagos Rift. *Science*. 203, 1073-1083.

- Cotton, M.T. (1972) The geochemistry of wallrock alteration in West Cornwall with particular reference to the Mount Wellington mine. Ph.D. Thesis, Kings College, University of London.
- Cowan, P. (1979) The gold content of interflow metasedimentary rocks in the Red Lake area. M.Sc. Thesis, McMaster University, Ontario.
- Craig, G.Y. and Duff, P.McL.D. (1975) The geology of the Lothians and Southeast Scotland : an excursion guide. Scottish Academic Press.
- Craig, G.Y. and Walton, E.K. (1959) Sequence and structure in the Silurian rocks of Kirkcudbrightshire. *Geol. Mag.* 96, 209-220.
- Craig, J.R., Chaing, L.L.Y. and Lees, W.R. (1973) Investigations in the Pb-Sb-S system. *Canadian Mineral.* 12, 199-206.
- Craig, J.R. and Vaughn, D.J. (1987) Ore Mineral Stabilities. (Abstract) NATO Advanced Study Institute on the Geochemistry of Hydrothermal Ore Forming Processes.
- Craig, L.E. (1984) Stratigraphy in an accretionary prism : the Ordovician rocks in North Down, Ireland. *Trans. R. Soc. Edin.* 74, 183-191.
- Crerar, D.A. and Barnes, H.L. (1976) Ore solution chemistry v. solubilities of chalcopyrite and chalcocite assemblages in hydrothermal solution at 200°C to 350°C. *Econ. Geol.* 71, 772-794.
- Cressie, N. and Hawkins, D.M. (1980) Robust estimation of the variogram. *Mathematical Geology.* 12, 115-125.
- Crocket, J.H., Fueten, F., Clifford, P.M., Kabir, A. and Henderson, J. (1985) The distribution of gold and arsenic in turbidites at Hartigan Cove, Nova Scotia : implications on gold mineralization. GAC/MAC Program with abstracts. 10, A12. Fredericton.
- Crook, K.A.W. (1974) Lithogenesis and geotectonics : the significance of compositional variation in flysch arenites (greywackes). *Society of Economic Palaeontologists and Mineralogists. Spec. Publ.* 19, 304-310.
- Crosbie, T.R. (1981) Polished wafer preparation for fluid inclusion and other studies. *Trans. Inst. Min. Metall.* 90, B82-83.
- Crosby, G.M. (1969) A preliminary examination of trace mercury in rocks, Coeur d'Alene district, Idaho. *Quart. J. Colorado School of mines.* 64, 169-194.
- Cubitt, J.M. (1983) Quantitative stratigraphic correlation. John Wiley and Sons.
- Cummins, W.A. (1962) The greywacke problem. *Liverpool and Manchester Geol. Journal.* 3, 51-72.
- Cunningham, C.G. (1985) Characteristics of boiling-water-table and carbon dioxide models for epithermal gold deposition. 43-46. In: Tooker, E.W. (Ed) Geological characteristics of sediment and volcanic-hosted disseminated gold deposit : search for an occurrence model. USGS, Bull. No. 1646, 1-150.
- Dandurand, J.L., Fortune, J., Perami, R., Schott, J. and Tollon, F. (1972) On the importance of mechanical action and thermal gradient in the formation of metal bearing deposits. *Mineralium Deposita.* 7, 339-350.

- Date, A.R. (1982) Geological reference materials with particular emphasis on multi-element trace analysis. *Anal. Proc.* 7-12.
- Daurer, A. and Schoenlaub, H.P. (1976) Anmerkungen zur Basis der Noerdlichen Grauwackenzone. (The base of the Northern Greywacke Zone). *Mitt. Oesterr. Geol. Ges.* 69, 77-88.
- David, T.W.E. and Browne, R.W. (1956) The Geology of the Commonwealth of Australia. Vol. 2, 333pp.
- Davidson, A.J. and Pirie, I.D. (1985) The Rea gold-massive sulphide deposits, Adams Lake, B.C. : A geochemical exploration case history. 11th IGES Program and abstracts. 11, 48.
- Davies, J.F., Grant, R.W.E. and Whitehead, R.E.S. (1979) Immobile trace element and Archean volcanic stratigraphy in the Timmins mining area, Ontario. *Can. J. Earth Sci.* 16, 305-311.
- Davis, J.C. (1973) Statistics and data analysis in geology. John Wiley and Sons. 550pp.
- Dawson, J., Floyd, J.D. and Phillip, P.R. (1979) A mineral reconnaissance survey of the Abington-Biggarr-Moffat area, south-central Scotland. HMSO Mineral Reconnaissance Program, Inst. Geol. Sci. Report No. 28, 1-34.
- Dawson, J., Floyd, J.D., Phillip, P.R., Burley, A.J., Allsop, J.M., Bennett, J.R.P., Marsden, G.R., Leake, R.C. and Brown, M.J. (1977) A mineral reconnaissance survey of the Doon Glenkens area, south-west Scotland. Mineral Reconnaissance Programme. Inst. Geol. Sci. Report No. 18, 114pp.
- Dawson, K.M. and Sinclair, A.J. (1974) Factor analysis of minor element data for pyrites, Enadako molybdenum mine, B.C. Canada. *Econ. Geol.* 69, 404-411.
- Deer, W.A., Howie, R.A. and Zussman, J. (1964) Rock Forming Minerals. (5 vols). Longmans Green, London.
- Dehm, R.M., Klemm, D.D., Muller, C., Wagner, J. and Weber-Diefenbach, K. (1983) Exploration for antimony deposits in southern Tuscany, Italy. *Mineral. Deposita.* 18, 423-434.
- Deneke, E. and Gunther, K. (1981) Petrography and arrangement of Tertiary greywacke and sandstone sequences of the northern Apennines. *Sediment Geol.* 28, 189-230.
- De Vore, G.W. (1955) Role of absorption in the fractionation and distribution of elements. *J. Geol.* 63, 159-190.
- Dewey, H. (1920) Arsenic and antimony ores. *Memoirs of the Geological Survey. Special reports on the mineral resources of Great Britain.* Vol. XV. Arsenic and antimony ores. 59pp.
- Dickson, F.W. and Tunell, G. (1968) Antimony and mercury deposits associated with hot springs in the western United States. In: Ridge, J.D. (Ed) Ore deposits of the United States. American Inst. Min. Metall. Pub. 1673-1701.
- Dimitrescu, R. and Cocirta, C. (1980) Note on various sedimentary rocks of the Fagaras series. *An. Stiint. Univ. Al. I. Cuza. Iasi.* 26, 75-77.
- Divi, S.R., Thorpe, R.I. and Franklin, J.M. (1980) The use of discriminant analysis to evaluate compositional controls of stratiform deposits in Canada. *Math. Geol.* 11, 391-406.

Dowty, E. (1976) Crystal structure and crystal growth. The influence of internal structure on morphology : sector zoning in minerals. *Am. Min.* 61, 445-459.

Dubertret, L. (1973) (Ed) Explanatory text of the geological map of Turkey. *Maden. Tetkik. ve. Enstitusu. Yayinlarindan*, Ankara. 110pp.

Dubov, R.J. (1973) A statistical approach to the classification of geochemical anomalies. In: Jones, J.M. (Ed) *Geochemical Exploration. Inst. Min. Metall. Pub.* 275-284.

Duchesne, J.C., Rouhart, A., Schoumacher, C. and Dillen, H. (1984) Thallium, nickel, cobalt and other trace elements in iron sulphides from Belgian lead-zinc vein deposits. *Mineral. Deposita.* 18, 303-313.

Dudgeon, P. (Undated) Historical notes on the occurrence of gold in the south of Scotland. Advocates Library Collection. National Library of Scotland, Edinburgh.

Duller, P.R. (1982) Metamorphism and mineralization in southwest England. Internal Report. Southampton University. 140pp.

Duller, P.R. (1984) A sulphur isotope study of the Navan Orebody, Eire and comparisons with coeval deposits in southern Scotland. Preliminary Stable Isotope Report. British Geological Survey.

Duller, P.R. (1985) Contribution to discussions. In: Andrews, C.J. et. al. (Eds) *The Geology and Genesis of Mineral Deposits in Ireland. I.A.E.G. Special Publication.*

Duller, P.R. (1986) RAW : A database management system for numerate scientists, (Documentation and Systems Program), Strathclyde University Computer Centre, Internal Publication.

Duller, P.R. and Harvey, P.K. (1983) Lithogeochemical exploration for stratabound arsenopyrite-gold deposits in the Southern Uplands, Scotland. Mineral Deposits Studies Group, Manchester University. (Abstract).

Duller, P.R. and Harvey, P.K. (1984) Turbidite hosted gold mineralization in Southern Scotland. Mineral Deposits Studies Group, Aberdeen University. (Abstract).

Duller, P.R. and Harvey, P.K. (1985) Turbidite hosted gold mineralization in Southern Scotland. GAC/MAC Program with Abstracts. 10, A15. Fredericton.

Duller, P.R. and Harvey, P.K. (1985) Lithogeochemical exploration for arsenopyrite-gold mineralization in Southern Scotland. The 11th International Geochemical Exploration Symposium Programme and Abstracts. p51.

Dunham, K.C. (1971) mineralization by deep formation waters : a review. *Trans. Inst. Min. Metall.* 80, B50-66.

Dunham, K.C., Beer, K.E., Ellis, R.A., Gallagher, M.J., Nutt, M.J.C. and Webb, B.C. (1980) United Kingdom. In: *Mineral deposits of Europe, Vol. 1, Northwest Europe. Inst. Min. Metall. Publication.*

Dunoyer De Segonzac, G. (1970) The transformation of clay minerals during diagenesis and low grade metamorphism. *Sedimentology*, 15, 281-346.

Durney, D.W. (1972) Solution-transfer, an important geological deformation mechanism. *Nature*, 235, 315-316.

- Durney, D.W. (1976) Pressure solution and crystallisation and deformation. *Phil. Trans. R. Soc. London. A*, 283, 229-240.
- Durocher, M.E. (1983) The nature of hydrothermal alteration associated with the Madsen and Starratt-Olsen Gold deposits, Red Lake Area. In: Colvine, A.C. (Ed) *The geology of gold in Ontario*, Ontario Geological Survey, Misc. Paper No. 110, 123-140.
- Dvorak, J. (1981) Problem concerning the origin of clastic quartz in the quartzites of the Horre-Gommern-Zone. *Neues. Jahrb. Geol. Palaontol. Monatsh.* 81, 303-306.
- Dzulynski, S. and Walton, E.K. (1965) *Sedimentary features of Flysh and Greywackes*. Amsterdam.
- Eakins, P.R. (1962) Geological setting of the gold deposits in the Malaritic District. Province of Quebec, Department of Natural Resources, Report 99, 133pp.
- Eales, M.H. (1979) Structure of the Southern Uplands. In: Harris, A.L., Holland, C.H. and Leake, B.E. *The Caledonides of the British Isles : Reviewed*. *Geol. Soc. London.* 269-273.
- Ebbutt, F. (1948) Relationships of minor structures to gold deposition in Canada. In: *Structural geology of Canadian ore deposits*, 1, Canadian Inst. Min. Metall. Montreal, 64-77.
- Edmunds, F.R. (1977) Multivariate analysis of petrographic and chemical data from the Aldridge Formation, Southern Purcell Mountain Range, British Columbia, Canada. *Diss. Adstr. Int.* 38, 5.
- Elders, C.F. (1984) Provenance studies of Southern Uplands sediments using isotope methods and their tectonic implications. Poster presentation. The Caledonian-Appalachian Orogen Conference, Glasgow University.
- Elders, C.F. (1987) The provenance of granite boulders in conglomerates of the Northern and Central Belts of the Southern Uplands. *J. Geol. Soc. Lond.* 144, 853-863.
- Elliott, R.B. (1960) The carboniferous volcanic rocks of the Langholm district. *Proc. Geol. Assoc.* 71, 1-24.
- Ellis, A.J. and Mahon, W.A.J. (1967) Natural hydrothermal systems and experimental hot water - rock interactions. *Geochim. Cosmochim. Acta.* 31, 519-538.
- Ellis, T.M.R. (1982) A structural approach to Fortran 77 programming. *International Computer Science Series*. Addison-Wesley Pub. 349pp.
- Emmons, W.H. (1937) *Gold deposits of the world*. McGraw Hill, 562pp.
- Emsley, J. (1978) The trouble with thallium. *New Scientist.* 79, 392-394.
- Ertl, R.F. (1982) Goldwashen. *Lapis.* 7, 15-27.
- Esbensen, K.H., Wold, S., Ludholm, I. and Lindquist, L. (1985) Taking a close-up of the background : multivariate data analysis in geochemical prospecting. 11th IEGS Program and Abstracts. 11, 53.
- Esson, J., Stevens, R.H. and Vincent, E. (1965) Aspects of the geochemistry of As and Sb. Exemplified by the Skaergaard intrusion. *Min. Mag.* 35, 88-107.
- Eugster, H.P. (1985) Granites and hydrothermal ore deposits : A geochemical framework. *Min. Mag.* 49 (Pt. 1), 7-23.

Evans, E.M. (1980) An introduction to ore geology. Blackwell, 231pp.

Evans, A.M. and Maroof, S.I. (1976) Basement controls on mineralization in the British Isles. *Ming. Mag.* 134, 401-411.

Everitt, B. (1978) Graphical techniques for multivariate data. Heinemann, 117pp.

Ewers, G.R. (1977) Experimental hot water - rock interactions and their significance to natural hydrothermal systems in New Zealand. *Geochim. Cosmochim. Acta.* 41, 143-150.

Ewers, G.R. and Keays, R.R. (1977) Volatile and precious metal zoning in the Broadlands geothermal field, New Zealand. *Econ. Geol.* 72, 1337-1354.

Farmer, J.G. and Lovell, M.A. (1986) Natural enrichment of arsenic in Loch Lomond sediments. *Geochim. et Cosmochem. Acta.* 50, 2059-2067.

Farrand, M.G. (1979) Antimony in New England, Australia : A plume - generated mineralization?. *Search.* 10, 230-232.

Fedikow, M.A.F. and Turek, A. (1983) The application of stepwise discriminant analysis to geochemical data from the host rocks of the Sullivan Pb-Zn-Ag deposit, Kimberly, Canada. *J. Geochem. Explor.* 18, 231-244.

Fedikow, M.A.F. and Govett, G.J.S. (1985) Geochemical alteration halo's around the Mount Morgan gold-copper deposit, Queensland, Australia. *J. Geochem. Expl.* 24, 247-272.

Ferguson, H.G. and Gannett, R.W. (1932) Gold-quartz veins of the Alleghany district, California. *U.S.G.S. Prof. Paper.* 172, 39-81.

Field, D. and Raheim, A. (1979) A geologically meaningless Rb-Sr total rock isochron. *Nature.* 282, 497-499.

Fienberg, S.E. (1979) Graphical methods in statistics. *Am. Stat.* 33, 165-178.

Fililic, E.Z. (1982) Spilitization, mineralization and vertical metal zonation at the Stekenjokk stratabound sulphide deposit, Central Scandanavian Caledonides. *Trans. Inst. Min. Metall.* 91, B192-199.

Finlay, S., Romer, D.M. and Cazlet, P.C.D. (1984) Lithogeochemical studies around the Navan Zn-Pb orebody in County Meath, Ireland. *Prospecting in areas of Glaciated Terrain. Inst. Min. Metall. Pub.*

Finlow-Bates, T. (1980) The chemical and physical controls on the genesis of submarine exhalative orebodies and their implications for formulating exploration concepts. A review. *Geol. Jb. D40*, 131-168.

Finlow-Bates, T. and Large, D.E. (1978) Water depth as a major control on the formation of submarine exhalative ore deposits. *Geol. Jb. D30*, 27-39.

Finlow-Bates, T. and Stumpfl, E.F. (1981) The behaviour of so-called immobile elements in hydrothermally altered rocks associated with volcanogenic submarine exhalative ore deposits. *Mineral Deposita.* 16, 319-328.

Fitton, J.G. and Hughes, D.J. (1970) Volcanism and plate tectonics in the British Ordovician. *Earth planet. Sci. Lett.* 8, 223-228.

- Floyd, J. and Leveridge, M. (1987) Tectonic environment of the Devonian Gramscatho basin, South Cornwall : Framework mode and geochemical evidence from turbiditic sandstones. *J. Geol. Soc. Lond.* 144, 531-542.
- Floyd, J.D. (1975) The Ordovician rocks of West Nithsdale. Ph.D. Thesis, St. Andrews University.
- Floyd, J.D. (1977) Mineral reconnaissance survey of the Doon-Glenkens area, Southwest Scotland. *Trans. Inst. Min. Metall.* 86, B219-220.
- Floyd, J.D. (1982) Stratigraphy of a flysch succession : the Ordovician of West Nithsdale, Southwest Scotland. *Trans. R. Soc. Edinburgh.* 73, 1-9.
- Floyd, J.D. and Trench, A. (1989) Magnetic susceptibility contrast in Ordovician greywackes of the Southern Uplands. *J. Geol. Soc. Lond.* 146, 77-83.
- Foglierini, F., Samama, J.C. and Rey, M. (1980) The Largentiere (Ardeche) stratiform deposit (Pb+Ag+Zn+Sb). *Fr. Bur. Rech. Geol. Minieres. Mem.* 112: Gisments Francais Fascicule E4, 54pp.
- Fortey, N.J. (1979) Au/Ag ratios in gold grains from the Helmsdale placer deposit, Sutherland. *Appl. Min. Unit. Report No.* 248. B.G.S. 15pp.
- Fortey, N.J., Ingham, J.D., Skilton, B.R.H. and Young, B. (1985) Antimony mineralization at Wet Swine Gill, Caldbeck Fells, Cumbria. *Min. Mag.* (in press).
- Fortey, R.A. and Cocks, L.R.M. (1988) Arenig to Llandovery faunal distributions in the Caledonides. In: Harris, A.L. and Fettes, D.J. (Eds) *The Caledonian - Appalachian Orogen.* *Geol. Soc. Lond. Spec. Publ.* 38, 269-274.
- Foster, R.P. (1980) The controls of gold precipitation in Archean gold deposits; *Mining and Engineering (Zimbabwe)*, June, 21-25.
- Foster, R.P. (1986) Gold Update '85-'86. Conference notes, Southampton University.
- Foster, R.P. (1988) Archean gold metallogeny, crustal evolution and mineral exploration in Zimbabwe. Abstract, Gold with emphasis on recent exploration, IMM thirteenth Annual Commodity Meeting.
- Foster, R.P., Furber, M.J. and Green, D. (1985) Shamva Gold Mine, Zimbabwe : A product of calc-alkaline linked exhalative, volcanoclastic and epiclastic sedimentation in the Late Archean. *GAC/MAC Program with Abstract.* 10, A18.
- Foster-Smith, J.R. (1967) The non-ferrous metal mines of south-west Scotland. Individual survey series. The Northern Cavern and Mine Research Society, Yorkshire. 2, 1-25.
- Fournier, R.O. (1985) Silica minerals as indicators of conditions during gold deposition. 15-26. In: Tooker, E.W. (Ed) *Geological characteristics of sediment and volcanic-hosted disseminated gold deposits : Search for an occurrence model.* *USGS. Bull. No.* 1646, 1-150.
- Fowler, J.D. (1976) Geochemical and V.L.F. investigations in the region of the Knipes Stibnite deposit, Ayrshire. M.Sc. Thesis, St. Andrews.
- Fralick, P.W., Scott, B.M. and Macdonald, A.J. (1985) The genesis of auriferous vein systems in Archean, iron formation bearing submarine fans, Geraldton area, Ontario. *GAC/MAC Program with Abstract.* 10, A19. Fredericton.

Fraser, I. Researcher at School of Scottish Studies into old and ancient place names (Tel: 031 667 1011).

Freshney, E.C. (1960) An extension of the Silurian succession in the Craighead Inlier, Girvan. Trans. Geol. Soc. Glasgow. 24, 27.

Frey, M. (1970) The step from diagenesis to metamorphism in pelitic rocks during Alpine orogenesis. Sedimentology, 15, 261-279.

Friedman, I. and O'Neil, J.R. (1977) Compilation of stable isotope fractionation factors of geochemical interest. U.S. Geol. Survey. Prof. Paper No. 440.

Fripp, R.E.P. (1976) Stratabound gold deposits in the Archean banded iron formation, Rhodesia. Econ. Geol. 71, 58-75.

Frost, F.B. (1976) The geochemistry of the sedimentary rocks of the Harlech Dome, North Wales. Ph.D. Thesis, University of Aston, Birmingham.

Fryer, B.J. and Hutchinson, R.W. (1976) Generation of metal deposits on the sea floor. Can. J. Earth. Sci. 13, 121-135.

Fryer, B.J. and Kerrich, R. (1978) Analysis of precious metals at ppb level in rocks by a combined wet chemical and flameless atomic absorption method. Atomic Absorption Newsletter. 17, 4-6.

Fryer, B.J., Kerrich, R., Hutchinson, R.W., Pierce, M.G. and Rogers, D.S. (1979) Archean precious metal hydrothermal systems, Dome Mine, Abitibi Greenstone Belt. 1. Patterns of alteration and metal distribution. Can. J. Earth Sci. 16, 421-439.

Fuge, R. (1976) The automated colorimetric determination of fluorine and chlorine in geological samples. Chem. Geol. 17, 37-43.

Fukunaga, K. (1972) Introduction to statistical pattern recognition. Academic Press.

Fyfe, W.S. (1973) Dehydration reactions. Bull. Am. Assoc. Petrol. Geol. 57, 190-197.

Fyfe, W.S. (1974) Low grade metamorphism : Some thoughts on the present situation. Can. Mineral. 12, 439-444.

Fyfe, W.S. (1976) Chemical aspects of rock deformation. Phil. Trans. R. Soc. London. 283, 221-226.

Fyfe, W.S. and Henley, R.W. (1973) Some thoughts on chemical transport processes with particular reference to gold. Miner. Sci. Engng. 5, 295-303.

Fyfe, W.S., Price, N.J. and Thompson, A.B. (1978) Fluids in the earth's crust. Elsevier. 320pp.

Fyon, J.A. (1980) Seawater alteration of Early Precambrian (Archean) volcanic rock and exploration criteria for stratiform gold deposits, Porcupine Camp, Abitibi Greenstone Belt, Ontario. M.Sc. Thesis, McMaster University, 238pp.

Fyon, J.A., Schwarcz, H.P. and Crocket, J.H. (1984) Carbonatisation and gold mineralization in the Timmins area, Abitibi Greenstone Belt : Genetic links with Archean mantle CO₂. GAC/MAC Program with Abstracts. 9, 65. London, Ontario.

Gallagher, D. (1940) Albite and gold. Econ. Geol. 35, 698-736.

- Gallagher, M.J. (1969) Portable X-ray spectrometers for rapid ore analysis. 9th Commonwealth Mining and Metall. Cong. I.M.M. Pub.
- Gallagher, M.J. (1980) Exploration for stratabound mineralization in the Scottish Caledonides. (Abst). Norges. Geol. Unders. 360, 285.
- Gallagher, M.J. (1981) Stratabound arsenic and vein antimony mineralization in Silurian greywackes at Glendinning, south Scotland. (Abst). Trans. Inst. Min. Metall. 90, B58.
- Gallagher, M.J., Stone, P. and Duller, P.R. (1988) Gold bearing arsenic-antimony concentrations in Silurian Greywackes, South Scotland. Abstract, Gold with emphasis on recent exploration, IMM thirteenth Annual Commodity Meeting.
- Gallagher, M.J., Stone, P. and Duller, P.R. (1988) Arsenic, antimony and gold distribution in Lower Palaeozoic greywacke of South Scotland. GAC-MAC Montreal, Canada. Program with Abstracts.
- Gallagher, M.J. and Redwood, S.D. (1989) Metallogenic diversity in the gold deposits of Scotland. Abstract, Gold 89 in Europe.
- Gallagher, M.J., Stone, P., Kemp, A.E.S., Hills, M.G., Jones, R.C., Smith, R.T., Peachey, D., Vickers, B.P., Parker, M.E., Rollin, K.E. and Skilton, B.R.H. (1983) Stratabound arsenic and vein antimony mineralization in Silurian greywackes at Glendinning, south Scotland. Mineral Reconnaissance Programme Report. Inst. Geol. Sci. No. 59, 81pp.
- Galloway, W.E. (1974) Deposition and diagenetic alteration of sandstone in northeast Pacific arc-related basins : implications for greywacke genesis. Bull. Geol. Soc. Amer. 85, 379-390.
- Galson, D.A., Atkin, B.P. and Harvey, P.K. (1983) The determination of low concentrations of U, Th and K by XRF spectrometry. Chem. Geol. 38, 225-237.
- Gamyanin, L.A. (1981) The first discovery of an antimonial variety of arsenopyrite. Mineralogical Zhurnal. 3, 87-96.
- Garrels, R.M. and MacKenzie, F.T. (1978) Evolution of Sedimentary Rocks. W.W. Norton and Co. Publ.
- Garrett, R.G. (1969) The determination of sampling and analytical errors in exploration geochemistry. Econ. Geol. 64, 568-569.
- Garrett, R.G. (1983) Sampling methodology. In: Howarth, R.J. (Ed) Statistics and data analysis in geochemical prospecting. Handbook of exploration geochemistry. 2, 83-110.
- Garrett, R.G. (1983) Opportunities for the 80's. Math. Geol. 15, 358-398.
- Gavelin, S., Parwel, A. and Ryhage, R. (1960) Sulphur isotopic fractionation in sulphide mineralization. Econ. Geol. 55, 510-530.
- Ghosh, D.B., Sastry, B.B.K., Rao, A.J. and Rahim, A.A. (1970) Ore environment and ore genesis in Ramagiri Gold Field. Andra Pradesh. India. Econ. Geol. 65, 801-814.
- Gilbey, J.W.G. (1968) The mineralogy, paragenesis and structure of the ores of the Dolgellau Gold Belt, Merionethshire and associated wallrock alteration. Ph.D. Thesis, Kings College, University of London.

- Gill, J.B. (1970) Geochemistry of Viti Levu, Fiji and its evolution as an island arc. *Contr. Miner. Petrol. (Beitr. Miner. Petrogr.)* 27, No.3, 179-203.
- Gill, J.E. (1969) Experimental deformation and annealing of sulphides and interpretation of ore textures. *Econ. Geol.* 64, 500-508.
- Gillanders, R.J. (1977) History of the search for gold veins in the Leadhills - Wanlockhead district. *The Edinburgh Geologist*, 1-80.
- Gillanders, R.J. (1981) The Leadhills - Wanlockhead district, Scotland. *The Mineralogical Record*. 235-250.
- Giordano, T.H. and Barnes, H.L. (1979) Ore solution chemistry VI. PbS solubility in bisulphide solutions to 300°C. *Econ. Geol.* 74, 1637-1646.
- Glasson, M.J. and Keays, R.R. (1978) Gold mobilisation during cleavage development in sedimentary rocks from the auriferous slate belt of Central Victoria, Australia : some important boundary conditions. *Econ. Geol.* 73, 496-511.
- Goldfarb, R.J., Leach, D.L., Miller, M.L. and Pickthorn, W.J. (1985) Geology, metamorphic setting and genetic constraints of epigenetic lode-gold mineralization within the Cretaceous Valdez Group, Alaska. *GAC/MAC Program with Abstracts*. 10, A22.
- Gordon, A.J. (1962) The Lower Palaeozoic rocks around Glenluce, Wigtownshire. Ph.D. Thesis, Edinburgh University.
- Govett, G.J.S. (1976) Detection of deeply buried and blind sulphide deposits by measurement of H⁺ and conductivity of closely spaced surface soil samples. *Journ. Geochem. Explor.* 6, 359-382.
- Govett, G.J.S. and Goodfellow, W.D. (1975) Use of rock geochemistry in detecting blind sulphide deposits : A discussion. *Trans. Inst. Min. Metall.* 84, B134-140.
- Govett, G.J.S. and Nichol, I. (1979) Lithogeochemistry in mineral exploration. In: *Geophysics and geochemistry in the search of metallic ores*. *Geol. Surv. Canada. Econ. Geol. Report No. 31*, 339-362.
- Graf, J.L. (1977) Rare earth elements as hydrothermal tracers during the formation of massive sulphide deposits in volcanic rocks. *Econ. Geol.* 72, 527-547.
- Grant, J.A. (1980) A revised petrogenetic grid for partial melting of pelitic rocks. *Int. Geol. Congr.* 46pp.
- Grant Wilson, J.S. and Cadell, H.M. (1884) The Breadalbane Mines. *Proceedings of the Royal Physical Society of Edinburgh*. 8, 189-207.
- Gray, D.R. (1977) Differentiation associated with discrete crenulation cleavages. *Lithos*, 10, 89-101.
- Gray, G. (1982) Extensive trace element aureoles in host-rocks to exhalative-sedimentary mineral deposits and their use in mineral exploration. *Mineral deposits studies group, University of Strathclyde. Abstract*.
- Green, A.H., Donnelly and Keays, R.R. (1982) Evolution of gold bearing veins in dykes of the Woods Point Dyke Swarm, Victoria. *Mineral. Deposita*. 17, 175-192.
- Green, T. (1985) The new world of gold (revised edition) 272pp. Weidenfield and Nicholson, London.

- Greig, D.C. (1971) *The South of Scotland*. (3rd edition). British Regional Geology. H.M.S.O. 125pp.
- Green, P.M. (1984) Digital image processing of integrated geochemical and geological information. *J. Geol. Soc. Lond.* 141, 941-950.
- Grigoryan, S.W. (1974) Primary geochemical haloes in prospecting and exploration of hydrothermal deposits. *Int. Geol. Rev.* 16, 12-28.
- Gromet, I.P., Dymek, R.F., Haskin, L.A. and Korotev, R.L. (1984) The North American Shale Composite : its composition, major and trace element characteristics. *Geochim. Cosmochim. Acta.* 48, 2469-2482.
- Grunsky, E.C. (1986) Recognition of alteration in volcanic rocks using statistical analysis of lithogeochemical data. *J. Geochem. Expl.* 25, 157-184.
- Gruzdev, V.S. (1972) Galkhaite : A new mineral from arsenic, antimony, mercury deposits of the U.S.S.R. *Doklady Akad. Nauk. U.S.S.R.*, 205, 150-153.
- Gruzdev, V.S., Volgin, V.Y., Shumkova, N.M., Chernistova, N.M. and Ivanov, V.S. (1975) Wakabayashilite from arsenic, antimony, mercury deposits of the U.S.S.R. *Doklady Akad. Nauk. U.S.S.R.*, 224, 418-421.
- Guild, P.W. (1977) Distribution of metallogenic provinces in relation to major earth faetures. *Venez. Dir. Geol. Bol. Geol. Publ. Esp.* 7, 2459-2463.
- Haas, J.L. (1971) The effects of salinity on the maximum thermal gradient of a hydrothermal system at hydrostatic pressure. *Econ. Geol.* 66, 940-946.
- Hackbarth, C.J. and Peterson, U. (1984) A fractional crystallisation model for the deposition of argentian tetrahedrite. *Econ. Geol.* 79, 448-460.
- Hak, J. (1968) The mineralogy and geochemistry of antimony deposits in the Nizke Tatry Mounts. *Min. Abst.* 19, 101.
- Hale, M. (1981) Pathfinder applications of arsenic, antimony and bismuth in geochemical exploration. *J. Geochem. Expl.* 15, 307-323.
- Hall, G.W. (1975) *The Gold Mines of Merioneth*. Griffin. 120pp.
- Hall, A.J. and Willan, R.C.R. (1981) The behaviour of sulphide minerals during regional metamorphism : Evidence from the study of Dalradian metasediments. (Abst.), Conference on sulphide mineralogy. Mineral Soc. Applied Mineralogy Group, Birmingham.
- Hall, J., Powell, D.W., Warner, M.R., El-Isa, Z.H.M., Adesanya, O. and Bluck, B.J. (1983) Seismological evidence for shallow crystalline basement in the Southern Uplands of Scotland. *Nature.* 305, 418-420.
- Hall, R.S., Hodgson, C.J. and Helmstaedt, H. (1985) Stratigraphy, metamorphism and structural deformation at the Muscelwhite stratabound gold prospect, N.W. Ontario. GAC/MAC Program with Abstract. 10, A24. Fredericton.
- Hallbauer, D.K. and Joughin, N.C. (1972) Distribution and size of gold particles in the Witwatersrand Reefs and their effects on sampling proceedures. *Inst. Min. Metall.* 82, 110-119.

- Halliday, A.N. and Mitchell, J.G. (1983) K-Ar ages of clay concentrates from Irish orebodies and their bearing on the timing of mineralization. *Trans. R. Soc. Edinb.* 74, 1-14.
- Haszeldine, R.S. (1987) Deep crustal lineaments control major Carboniferous rift basins : onshore British Isles.
- Harbaugh, J.W. and Merriam, D.F. (1968) *Computer applications in stratigraphic analysis.* Wiley.
- Harries, W.J.R. (1972) *Geochemical exploration in South Wales.* Inter-collegiate colloquium Gregynog, University of Wales.
- Harris, J.F. (1981) Sampling and analytical requirements for effective use of geochemistry in exploration for gold. In: Levison, A.A. (Ed) *Precious Metals in the Northern Cordillera.* Assoc. Explor. Geol. Pub. 53-68.
- Harris, M. (1980) Gold mineralization at Salave gold prospect, northwest Spain. *Trans. Inst. Min. Metall.* 89, 81-84.
- Harris, M. (1980) Hydrothermal alteration at Salave gold prospect, northwest Spain. *Trans. Inst. Min. Metall.* 89, B5-15.
- Harris, M. and Radtke, A.S. (1976) Statistical study of selected trace elements with reference to geology and genesis of the Carlin gold deposit, Nevada. U.S. Geol. Survey. Prof. Paper No. 960, 21pp.
- Hart, P.E., Duda, R.O. and Einaudi, M.T. (1978) Prospector : A computer-based consultation system for mineral exploration and resource assessment. *Math. Geol.* 10, 589-610.
- Hartigan, J.A. (1975) *Clustering Algorithms.* John Wiley and Sons.
- Harvey, P.K. and Atkin, B.P. (1981) The rapid determination of Rb, Sr and their ratios in geological materials by X-ray fluorescence spectrometry using a rhodium X-ray tube. *Chem. Geol.* 32, 291-301.
- Harvey, P.K. and Atkin, B.P. (1983) Automated X-ray fluorescence analysis. Special volume : Sampling and analysis for the mineral industry. *Inst. Min. Metall. Pub.* 17-26.
- Harvey, P.K. and Atkin, B.P. (1985) Automated XRF spectrometric analysis : A rapid cost effective analytical technique for the mineral industry. 11th IGES. Program with Abstracts. 11, 60-61.
- Harvey, P.K., Taylor, D.M., Hendry, R.D. and Bancroft, F. (1973) An accurate fusion method for the analysis of rocks and chemically related materials by X-ray fluorescence spectrometry. *J. X-ray. Spect.* 2, 33-44.
- Harvey, W.S. and Downs-Rose, G. (1975) Men of the Lowther Hills. Leadhills and Wanlockhead. 22p.
- Haselock, P.J. (1984) The systematic geochemical variation between two tectonically separate successions in the southern Monadhliaths, Invernesshire. *Scott. J. Geol.* 20, 191-205.
- Haskins, L.A., Haskins, M.A., Frey, F.A. and Wildeman, T.R. (1968) Relative and absolute terrestrial abundances of the rare earths. In: Ahrens, L.H. (Ed) *Origin and distribution of the elements.* Intern. Ser. Monographs. Earth. Sci. 30, 899-912.
- Hattori, K. (1975) Geochemistry of ore deposition at the Yatani lead-zinc and gold-silver deposit, Japan. *Econ. Geol.* 70, 677-693.

- Hawkes, H.E. (1976) The downstream dilution of stream sediment anomalies. *J. Geochem. Explor.* 6, 345-358.
- Hawkes, H.E. and Webb, J.S. (1962) *Geochemistry in Mineral Exploration*. Harper and Row, New York. 415pp.
- Hawkins, D.M. and Rasmussen, S.E. (1973) Use of discriminant analysis for classification of strata in sedimentary successions. 5, 163-177.
- Hawkins, J.W., Bloomer, S.H., Evans, C.A. and Melchior, J.T. (1984) Evolution of intra-oceanic arc-trench systems. *Tectonophysics*. 102, 175-205.
- Haynes, S.J. (1985) Geology and chemistry of turbidite hosted gold deposits, Greenschist facies, Eastern Nova Scotia. GAC/MAC Program with Abstracts. 10, A25. Fredericton.
- Hedenquist, J.W. and Henley, R.W. (1985) Hydrothermal eruptions in the Waiotapu Geothermal System, New Zealand : Their origin, associated breccias and relation to precious metal mineralization. *Econ. Geol.* Vol. 80, No. 6, 1640.
- Helgeson, H.C. (1964) *Complexing and hydrothermal ore deposition*. Pergamon Press, 128pp.
- Helgeson, H.C. and Garrels, R.M. (1968) Hydrothermal transport and deposition of gold. *Econ. Geol.* 63, 622-635.
- Hellman, P.L., Smith, R.E. and Henderson, P. (1977) Rare earth element investigation of the Cliefden outcrop, N.S.W. Australia. *Cont. Min. Pet.* 65, 155-164.
- Hellman, P.L., Smith, R.E. and Henderson, P. (1979) The mobility of the rare earth element. Evidence and implication from selected terrains affected by burial. *Cont. Min. Petr.* 71, 23-44.
- Hemley, J.J. and Jones, W.R. (1964) Chemical aspects of hydrothermal alteration with emphasis on hydrogen metasomatism. *Econ. Geol.* 59, 538-569.
- Henderson, P. (1976) Rare earth element abundances in rocks and minerals from Greenland. *Earth and Plan. Sci. Letters*. 30, 37-49.
- Henderson, P. (1984) Rare earth element geochemistry, (Developements in Geochemistry 2). Elsevier.
- Henley, R.W. (1971) *Geochemistry and genesis of Precambrian gold deposits*. Ph.D. Thesis, University of Manchester.
- Henley, R.W. (1973) Solubility of gold in hydrothermal chloride solutions. *Chem. Geol.* 11, 73-87.
- Henley, R.W. (1985) The geothermal framework for epithermal deposits. In: Berger, B.R. and Bethke, P.M. (Eds) *Geology and geochemistry of epithermal systems*. Reviews in Econ. Geol. 2, 1-21.
- Henley, R.W. and McNabb, A. (1978) Magmatic vapour plumes and ground-water interaction in porphyry copper emplacements. *Econ. Geol.* 73, 1-20.
- Henley, R.W. and Thornley, P. (1979) Some geothermal aspects of polymetallic massive sulphide formation. *Econ. Geol.* 74, 1600-1612.
- Henley, R.W., Norris, R.J. and Paterson, C.J. (1976) Multistage ore genesis in the New Zealand geosyncline, a history of post-metamorphic lode emplacement. *Mineralium Deposita*, 11, 180-196.

- Henley, S. (1970) An application of statistical methods to the geochemistry of an area around Perranporth, Cornwall. *Proc. Ussher. Soc.* 2, 210-216.
- Henrich, C.A. and Eadington, P.J. (1986) Thermodynamic predictions of the hydrothermal chemistry of arsenic and their significance for the paragenetic sequence of some cassiterite-arsenopyrite-base metal sulphide deposits. *Econ. Geol.* 81, 511-529.
- Hepworth, B.C., Oliver, G.J.H. and McMurtry, M.J. (1982) Sedimentology, volcanism, structure and metamorphism of the northern margin of a Lower Palaeozoic accretionary complex : Bailhill-Abington area of the Southern Uplands of Scotland. In: Leggett, J.K. (Ed), *Trench-Forearc Geology*. Geol. Soc. London. Spec. Pub. No. 10, 521-534.
- Heroux, Y., Chagnon, A. and Bertrand, R. (1979) Compilation and correlation of major thermal maturation indicators. *Am. Assoc. Petrol. Geol. Bull.* 63, 2128-2155.
- Hickman, A.H. and Wright, A.E. (1982) Geochemistry and chemostratigraphical correlation of slates, marbles and quartzites of the Appin Group, Argyll, Scotland. *Trans. R. Soc. Edinburgh.* 73, 251-278.
- Hiroshi, O. and Sandell, E.B. (1955) Geochemistry of Arsenic. *Geochim. Cosmochim. Acta.* 7, 1-33.
- Hirst, D.M. (1961) The geochemistry of modern sediments from the Gulf of Paria - II, The location and distribution of trace elements. *Geochem. Cosmochem. Acta.* 26, 1147-1187.
- Hobbs, B.E., Means, W.D. and Williams, P.F. (1976) *An outline of structural geology*. John Wiley and Sons, New York, 571pp.
- Hoda, S.N. and Chang, L.L.Y. (1975) Phase relations in the pseudo-ternary system $PbS-Cu_2S-Sb_2S_3$ and the synthesis of meneghinite. *Canadian Mineralogist.* 13, 388-393.
- Hodder, R.W. and Petruk, W. (1980) (Eds) *Geology of Canadian gold deposits : proceedings of the CIM gold symposium, September 1980*. Canadian Inst. Min. Metall. Special Vol. No. 24, 286pp.
- Hodgson, J.M. (1976) *Soil Survey Field Handbook*. Tech. Monogr. Soil Surv. GB, No.5.
- Hodgson, C.J. and Lydon, J.W. (1977) Geological setting of volcanogenic massive sulphide deposits and active hydrothermal systems : Some implications for exploration. *Geology and Exploration*. C.I.M. Bull. 95-106.
- Hoffman, E.L. and Brooker, E.J. (1981) The determination of gold by neutron activation analysis. In: Levinson, A.A. (Ed) *Precious Metals in the Northern Cordillera*. Assoc. Explor. Geol. Pub. 69-78.
- Hoffman, E.L. and Pidruczny, A. (1985) The application of multielement data by neutron activation analysis, suitable for exploration geochemical techniques. 11th IEGS Program with Abstracts. 11, 62-63.
- Holl, R. (1977) Early Palaeozoic ore deposits of the Sb-W-Hg formation in the Eastern Alps and their genetic interpretation. In: Klemm, D.D. and Schneider, H.J. (Eds) *Time and stratabound ore deposits*. Springer-Verlag. 169-198.
- Holland, H.D. (1967) Gangue minerals in hydrothermal deposits. In: Barnes, H.L. (Ed) *Geochemistry of Hydrothermal Ore Deposits*. Holt, Rinehart and Winston, New York. 670pp.
- Holmes, A. (1930) *Petrographic Methods*.

Holmyard, E.J. (1957) *Alchemy*. Penguin Books.

Hopkins, T. and Plant, D. (1984) *Microanalysis Course Notes*. Manchester University. 38pp.

Home, R. (1975) Possible transverse fault control of base metal mineralization in Ireland and Britain. *Irish Nat. J.* 18, 140-144.

Home, R. (1975) Traverse fault systems in fold belts and oceanic fracture zones. *Nature*, 255, 620-621.

Hovorka, D. (1975) The lithology and chemical composition of the metasediments of the Jaraba Group, West Carpathians. *Krystalinikum*. 11, 87-99.

Howarth, R.J. (1971) Empirical discriminant classification of regional stream sediment geochemistry in Devon and east Cornwall. *Trans. Inst. Min. Metall.* 80, B142-149.

Howarth, R.J. (1971) Fortran IV program for grey-level mapping of spatial data. *Math. Geol.* 3, 95-121.

Howarth, R.J. (1973) The pattern recognition problem in applied geochemistry. In: Jones, M.J. (Ed) *Geochemical Exploration 1972*. Inst. Min. Metall. London. 259-273.

Howarth, R.J. (1976) Three component colour maps from lineprinter output. *Trans. Inst. Min. Metall.* 85, B234-237.

Howarth, R.J. (1983) (Ed) *Statistics and data analysis in geochemical prospecting*. Handbook of Exploration Geochemistry. Vol. 2. Elsevier. 437pp.

Howarth, R.J. (1983) Mapping. In: Howarth, R.J. (Ed) *Statistics and data analysis in geochemical exploration*. Handbook of Exploration Geochemistry. Vol. 2. Elsevier, 111-205.

Howarth, R.J. (1984) Statistical applications in geochemical prospecting : a survey of recent developments. *J. Geochem. Explor.* 21, 41-61.

Howarth, R.J. and Earle, S.A. (1979) Application of a generalised power transformation to geochemical data. *Math. Geol.* 11, 45-62.

Howarth, R.J. and Lowenstein, P.L. (1971) Sampling variability of stream sediments in broad scale regional geochemical reconnaissance. *Trans. Inst. Min. Metall.* 80, B363-372.

Howarth, R.J. and Martin, L. (1979) Computer-based techniques in the compilation, mapping and interpretation of exploration geochemical data. In: *Geophysics and geochemistry in the search for metallic ores*. Geol. Survey of Canada. Econ. Geol. 31, 545-574.

Howarth, R.J. and Sinding-Larsen, R. (1983) Multivariate statistics. In: Howarth, R.J. (Ed) *Statistics and data analysis in geochemical prospecting*. Handbook of Exploration Geochemistry. Vol. 2. Elsevier. 207-209.

Hower, J., Eslinger, E.V., Hower, M.E. and Perry, E.A. (1976) Mechanism of burial metamorphism of argillaceous sediments : 1. Mineralogical and chemical evidence. *Geol. Soc. America. Bull.* 87, 725-735.

Howarth, R.J. and Turner, M.J. (1987) Statistical graphics in geochemical journals. *Math. Geol.* 19 (1), 1-24.

Huff, W.D. (1983) Correlation of Middle Ordovician K-bentonites based on chemical fingerprinting. *J. Geol.* 91, 657-669.

- Humphris, S.E. and Thompson, G. (1978) Hydrothermal alteration of oceanic basalts by seawater. *Geochim. Cosmochim. Acta.* 42, 107-125.
- Humphris, S.E. and Thompson, G. (1978) Trace element mobility during hydrothermal alteration of oceanic basalts. *Geochim. Cosmochim. Acta.* 42, 127-136.
- Hurley, T.D. and Crocket, J.H. (1984) A gold-sphalerite association in a volcanogenic sulphide occurrence at Tilt Cove, Newfoundland. *GAC/MAC Program with Abstracts.* 9, 75. London, Ontario.
- Hutchinson, M.N. and Scott, S.D. (1980) Sphalerite geobarometry applied to metamorphosed sulphide ores of the Swedish Caledonides and U.S. Appalachians. *Norges. Geol. Unders.* 360, 59-72.
- Hutchinson, R.W. (1976) Lode gold deposits : the case for volcanogenic derivation. In: *Proc. Vol. Pacific Northwestern Min. Metals. Conf. Oregon Dep. Geol. Mineral Ind.* 64-105.
- Hutchinson, R.W. (1983) Hydrothermal Concepts : the old and the new. *Econ. Geol.* 78, 1734-1741.
- Hutchinson, R.W., Fyfe, W.S. and Kerrich, R. (1980) Deep fluid penetration and ore deposition. *Min. Sci. Engng.* 12, 107-120.
- Hutton, D.H.W. and Murphy, F.C. (1987) The Silurian of the Southern Uplands and Ireland as a successor basin to the end-Ordovician Closure of Iapetus. *J. Geol. Soc. Lond.* 144, 765-772.
- Hundman, D., Vitaliand, C.J. and Suttner, L.J. (1980) Granite II - Near surface batholiths, related volcanism, tectonism sedimentation and mineral deposition. *Geology.* 8, 107-110.
- Ikramuddin, M., Asmeron, Y., Nordstrom, P.M., Kinart, K.P., Martin, F.N., Digby, S.J.M., Elder, D.D., Ninjak, W.F. and Afemari, A.A. (1983) Thallium : A potential guide to mineral deposits. *J. Geochem. Explor.* 19, 465-490.
- Ikramuddin, M., Besse, L. and Nordstrom, P.M. (1986) The relationship between Tl, Rb and K in the Carlin-type gold deposits. *J. Geochem. Explor.* 25.
- Ineson, P.R. (1969) Trace element aureoles in limestone wallrocks adjacent to lead-zinc-barite-fluorite mineralization in the northern Pennine and Derbyshire ore fields. *Trans. Inst. Min. Metall.* 78, B29-40.
- Ineson, P.R. (1970) Trace element aureoles in limestone wallrocks adjacent to fissure veins in the Eyam area of the Derbyshire ore field. *Trans. Inst. Min. Metall.* 79, B239-245.
- Ingersoll, R.V. (1978) Petrofacies and petrologic evolution of the late Cretaceous Fore-arc basin, northern and central California. *J. Geol.* 86, 335-352.
- Ingersoll, R.V. and Suczer, C.A. (1979) Petrology and Provenance of Neogene sands from Nicobar and Bengal Fans, DSDP Sites 211 and 218. *J. Sed. Petrol.* 1217-1228.
- Issiagonis, M.J. (1980) Occurance of disseminated gold deposits in porphyries in Archean Albitibi belt, northwestern Quebec, Canada. *Trans. Inst. Min. Metall.* B157-158.
- Jakes, P., Zoubek, J., Zoubkova, J. and Franke, W. (1979) Greywackes and meta greywackes of the Tepla-Barrandian Proterozoic area. *Sb. Geol. Ved. Geol.* 33, 83-122.
- Jambor, J.L. (1968) New lead sulphantimonides from Madoc, Ontario. Part 3 : synthesis, paragenesis, origin. *Canadian Mineralogist.* 9, 505-521.

- Jambor, J.L. (1969) Sulphosalts of the plagioclite group. *Mineralogical Mag.* 37, 288.
- Jambor, J.L. and Plant, A.G. (1975) The composition of the lead sulphantimonide, robinsonite. *Canadian Mineralogist*. 13, 415-417.
- James, C.H. (1957) The geochemical dispersion of As and Sb related to Au mineralization in S. Rhodesia. *Geochem. Prosp. Res. Centre, Imperial College, London. Tech. Comm. No. 12.*
- James, C.H. (1964) The potential role of mercury in modern geochemical prospecting. *Ming. Mag.* London. 112, 23-32.
- James, C.H. (1967) The use of the terms "primary" and "secondary" dispersion in geochemical prospecting. *Econ. Geol.* 62, 997-999.
- James, D.M.D. and James, J. (1969) The influence of deep fractures on some areas of Ashgillian-Llandoveryan sedimentation in Wales. *Geol. Mag.* 106, 562-582.
- Jankovic, S. (1960) Yugoslavian Antimony Deposits. *Neves. Jahab. Min. Abh.* 94, 506-538.
- Jankovic, S., Mozgova, N.N. and Borodaev, Y.S. (1977) The complex Sb-Pb-Zn deposit at Rujevac, Yugoslavia : its specific geochemical and mineralogical features. *Mineral Deposita*. 12, 381-392.
- Jean, G.E. and Bancroft, G.M. (1985) An XPS and SEM study of gold deposition at low temperatures on sulphide mineral surfaces : concentration of gold by adsorption/reduction. *Geochim. Cosmochim. Acta.* 49, 979-987.
- Jenner, G.A., Fryer, B.J. and McLennan, S.M. (1981) Geochemistry of the Archean Yellowknife supergroup. *Geochim. Cosmochim. Acta.* 45, 1111-1129.
- Jolly, W.T. (1974) Behaviour of Cu, Zn and Ni during prenite-pumpellyite rank metamorphism of the Keeweenawan Basalts, N. Michigan. *Econ. Geol.* 69, 1118-1125.
- Jones, E.M., Rice, C.M. and Tweedie, J.R. (1983) Lower Proterozoic stratiform Cu-Zn-Au mineralization near Gairloch, Wester Ross, northwest Scotland. *Trans. Inst. Min. Metall.* 92, B160-161.
- Jones, T.A. (1969) Skewness and kurtosis as criteria of normality in observed frequency distributions. *J. Sed. Pet.* 39, 1622-1627.
- Joreskog, K.G., Klován, J.E. and Reymont, R.A. (1976) *Geological factor analysis.* Elsevier.
- Kantor, J. (1974) Sulphur isotopes of the stratiform pyrite deposit Tureckývrch and stibnite deposit Pezinok, in the Male Karpaty Mountains, Czechoslovakia. *Geol. Zb. (Slov. Akad. Vied.)*. 25, 311-334.
- Kamilli, R.J. and Ohmoto, H. (1977) Paragenesis, zoning, fluid inclusion and isotopic studies of the Finlandia Vein, Colqui District, Central Peru. *Econ. Geol.* 72, 950-982.
- Kamp, P.C. van de, and Leake, B.E. (1986) Petrography and geochemistry of feldspathic and mafic sediments of the northeastern Pacific margin. *Trans. Roy. Soc. Edin.* 76, 411-449.
- Karig, D.E. and Moore, G.F. (1975) Tectonically controlled sedimentation in marginal basins. *Earth. Plan. Sci. Letters*. 26, 233-238.
- Karvinen, W.O. (1978) The Porcupine Camp : A model for gold exploration in the Archean. *Can. Min. J.* September, 48-53.

- Kay, A. and Strong, D.F. (1983) Geologic and fluid controls on As-Sb-Au mineralization in the Moretons Harbour area, Newfoundland. *Econ. Geol.* 78, 1590-1604.
- Keays, R.R. and Scott, R.B. (1976) Precious metals in ocean ridge basalts : implications for basalts as source rocks for gold mineralization. *Econ. Geol.* 71, 705-720.
- Kelling, G. (1961) The stratigraphy and structure of the Ordovician rocks of the Rhinns of Galloway. *Q. J. Geol. Soc. London.* 117, 37-75.
- Kelling, G. (1964) The turbidite concept in Britain. In: Bouma, A.H. and Brouwer, A. (Eds) *Turbidites*. Elsevier.
- Kelling, G., Davies, P. and Holroyd, J. (1987) Style, scale and significance of sand bodies in the Northern and Central Belts, Southwest Southern Uplands. *J. Geol. Soc. Lond.* 144, 787-806.
- Kemp, A.E.S. (1985) The later (Silurian) sedimentary and tectonic evolution of the Southern Uplands accretionary terrain. Ph.D. thesis, University of Edinburgh.
- Kemp, A.E.S. (1987) Tectonic development of the Southern Belt of the Southern Uplands accretionary complex. *J. Geol. Soc. Lond.* 144, 827-838.
- Kemp, A.E.S. and White, D.E. (1985) Silurian trench sedimentation in the Southern Uplands, Scotland : implications of new age data. *Geol. Mag.* (in press).
- Kerrick, R. (1977) Yellowknife mineralization, the product of metamorphic degassing. *Geol. Soc. Am. (Abst.)* 9, 1048-1049.
- Kerrick, R., Fyfe, W.S., Gorman, B.E. and Allison, I. (1977) Local modification of rock chemistry by deformation. *Contrib. Mineral. Petrol.* 65, 183-190.
- Kerrick, R., Fyfe, W.S. and Allison, I. (1977) Iron reduction around gold-quartz veins, Yellowknife District, Northwest Territories, Canada. *Econ. Geol.* 72, 657-663.
- Kerrick, R. and Allison, I. (1978) Vein geometry and hydrostatics during Yellowknife mineralization. *Can. Journal Earth Science.* 15, 1653-1660.
- Kerrick, R. and Fryer, B.J. (1981) The separation of rare elements from abundant base metals in Archean lode gold deposits : Implications of low water-rock source regions. *Econ. Geol.* 76, 160-166.
- Kerrick, R. and Watson, G.P. (1984) The Macassa mine Archean lode gold deposit, Kirkland Lake, Ontario : Geology, patterns of alteration and hydrothermal regimes. *Econ. Geol.* 79, 1104-1130.
- Kerrick, R. and Walker, H. (1981) Auriferous metamorphic fluid venting with peripheral seawater convection. Chadbourne Gold Mine, Noranda, Quebec. *Geol. Soc. America. Abstracts with Programs.* 486.
- Khan, S.A.A. (1968) Geology and origin of the Knappe Antimony deposit, Ayrshire. A report on the application of geochemical prospecting for the exploration of blind antimony deposits. Diploma of Science and Technology, Strathclyde University.
- Kisch, H.J. (1980) Incipient metamorphism of Cambro - Silurian clastic rocks from the Jamtland supergroup, central Scandinavian Caledonides, W. Sweden : Illite crystallinity and vitrinite reflectance. *J. Geol. Soc.* 137, 271-288.

- Kishida, A. (1984) Hydrothermal alteration zoning and gold concentration at the Kerr-Addison mine, Ontario, Canada. Unpub. Ph.D. Thesis, University of Western Ontario.
- Klau, W. and Large, D.E. (1980) Submarine exhalative Cu-Pb-Zn deposits : A discussion of their classification and metallogenesis. *Geol. Jb.* D40, 13-58.
- Klemm, D.D. (1979) Secondary concentration of stratabound deposits through thermal activity. In: Maucher, A. (Ed) *Beitrage zu problem der zeit und schichtgebundenen lagerstaettenbildung*. Ges. Dtsch. Metallhuetten und Berg. Schr. 33, 183-196.
- Knapp, R.B. and Knight, J.E. (1977) Differential thermal expansion of pore fluids : Fracture propagation and micro earthquake production in hot plume environments. *J. Geophys. Res.* 82, 2515-2522.
- Knight, N.D. (1978) Australian Antimony Deposits. Min. Resources Report No. 8. Australian Government Pub. Service.
- Knopf, A. (1929) The Mother Lode System. Prof. Pap. US. Geol. Surv. 157, 137pp.
- Kokelaar, B.P. and Howells, M.F. (1984) (Eds) Marginal Basin Geology. *Geol. Soc. Lond. Spec. Pub.* No. 16, 322pp.
- Konta, J. (1977) Modern views on geochemical processes in pelite sediments. *Acta. Univ. Carol. Geol.* 77, 51-70.
- Komerup, A. and Wanscher, J.H. (1981) The Methuen Handbook of Colour. Eyre Methuen Pub. 252pp.
- Krauskopf, K.B. (1967) Introduction to Geochemistry. McGraw, 721pp.
- Krebs, W. and Wachendorf, H. (1973) Proterozoic - Palaeozoic geosynclinal and orogenic evolution of Central Europe. *Bull. Geol. Soc. America.* 84, 2611-2630.
- Kretschmar, U. and Scott, S.D. (1976) Phase relations involving arsenopyrite in the system Fe-As-S and their application. *Can. Mineral.* 14, 364-386.
- Krige, D.E. and Magri, E.J. (1982) Studies of the effects of outliers and data transformation on variogram estimates for a base metal and gold orebody. *Math. Geol.* 14, 557-564.
- Krumbein, W.C. (1965) An introduction to statistical models in geology. McGraw Hill.
- Lagios, E. and Hipkin, R.G. The Tweeddale granite : a newly discovered batholith in the Southern Uplands. *Nature.* 280, 672-675.
- Lajoie, E., Heroux, Y. and Mathey, B. The Precambrian shield and the Lower Palaeozoic Shelf : The unstable provenance of the Lower Palaeozoic flysch sandstones and conglomerates of the Appalachians between Beaumont and Bic, Quebec. *Can. J. Earth. Sci.* 11, 951-963.
- Lakind, J.S. and Brown, P.E. (1984) Characterisation of the gold-bearing fluid at Red Lake, Ontario. GAC/MAC Program with Abstracts. 9, 80. London, Ontario.
- Lambert, I.B. and Scott, K.M. (1973) Implications of geochemical investigations of sedimentary rocks within and around the McArthur zinc-lead-silver deposit, northern territory. *J. Geochem. Explor.* 2, 307-330.

- Lambert, R.S. and McKerrow, W.S. (1978) Comparison of the San Andreas Fault system with the Highland Boundary Fault system of Scotland. *Geol. Mag.* 115, 367-372.
- Lambert, R. J. St., Holland, J.G. and Winchester, J.A. (1982) A geochemical comparison of the Dalradian Leven Schists and the Grampian Division Mondhliath Schists of Scotland. *J. Geol. Soc. London.* 139, 71-84.
- Landes, K.K. (1966) A scrutiny of the abstract, II. *Bull. Amer. Assoc. Petrol. Geol.* 50, 1992-1999.
- Langlands, J. (1985) A history of the Southern Uplands Goldfield. Unpublished Company Report, A.C.A. Howe International Ltd. 5pp.
- Large, D.E. (1979) Proximal and distal stratabound deposits : A discussion of paper by Plimer, I.R. *Min. Deposita.* 14, 123-124.
- Large, D.E. (1980) Geological parameters associated with sediment hosted submarine exhalative Pb-Zn deposits : An empirical model for mineral exploration. *Geol. Jb.* D40, 59-129.
- Large, D.E. (1981) The geochemistry of sedimentary rocks in the vicinity of the Tom Pb-Zn-Ba deposit, Yukon Territory, Canada. *J. Geochem. Expl.* 15, 203-217.
- Lauder Lindsay, W. (1868) The gold fields of Scotland. *Journal of the Royal Geological Society of Ireland.*
- Lauder Lindsay, W. (1869) Recent gold digging in Scotland : a history and a commentary.
- Leake, R.C., Auld, H.A., Stone, P. and Johnson, C.E. (1981) Gold mineralization at the southern margin of the Loch Doon granitoid complex, southwest Scotland. *Mineral Reconnaissance Program. Inst. Geol. Sci. Rept. No. 46*, 41pp.
- Leake, R.C., Brown, M.J., Smith, T.K. and Date, A.R. (1978) A geochemical drainage survey of the fleet granite complex and its environs. *Mineral Reconnaissance Program. Inst. Geol. Sci. Report No. 21.*
- Leake, R.C. and Cooper, C. (1983) The Black Stockarton Moor subvolcanic complex, Galloway. *J. Geol. Soc. London.* 140, 665-676.
- Leake, R.C. and Haslam, H.W. (1978) A geochemical survey of the Cheviot area in Northumberland and Roxburghshire using panned mineral concentrates. Report 78/4, British Geological Survey, 37pp. HMSO.
- Leggett, J.K. (1987) The Southern Uplands as an accretionary prism : the importance of analogues in reconstructing palaeogeography. *J. Geol. Soc. Lond.* 144, 737-752.
- Leggett, J.K. and Casey, D.M. (1982) The Southern Uplands accretionary prism : implications for controls on structural development of subduction complexes. In: *Studies in Continental Margin Geology. Am. Assoc. Petrol. Geol. Memoir 34*, 377-393.
- Leggett, J.K., McKerrow, W.S., Cocks, L.R.M. and Rickards, R.B. (1981) Periodicity in the early Palaeozoic marine realm. *J. Geol. Soc. London.* 138, 167-176.
- Leggett, J.K., McKerrow, W.S. and Earles, M.H. (1979) The Southern Uplands of Scotland : a Lower Palaeozoic accretionary prism. *J. Geol. Soc. London.* 136, 775-770.

- Leggett, J.K., McKerrow, W.S., Morris, J.H., Oliver, G.J. and Phillips, W.E.A. (1979) The north western margin of the Iapetus Ocean. In: Harris, A.L., Holland, C.H. and Leake, B.E. (Eds) *The Caledonides of the British Isles : reviewed*. Scottish Academic Press, Edinburgh, 499-512.
- Leggett, J.K. and Smith, T.K. (1980) Fe - rich deposits associated with Ordovician basalts in the Southern Uplands of Scotland : Possible Lower Palaeozoic equivalents of modern active ridge sediments. *Earth. Plan. Sci. Letters*. 47, 431-440.
- Le Maitre, R.W. (1982) *Numerical petrology*. Elsevier. 281pp.
- Leonard, B.F. (1965) Mercury bearing antimony deposit, between Big Creek and Yellow Pine, Central Idaho. U.S. Geol. Survey. Prof. Paper 525B, 23-28.
- Lepeltier, C. (1969) A simplified statistical treatment of geochemical data by graphical representation. *Econ. Geol.* 64, 538-550.
- Levinson, A.A. (1980) *Introduction to Exploration Geochemistry*. Applied Publishing. 612pp.
- Lickley, W.P., Whitehead, R.E. and Davies, J.F. (1987) The use of sorting curves in studying alteration in interbedded greywackes and argillite. *J. Geochem. Expl.* 27, 299-311.
- Lister, C.R.B. (1975) On the penetration of water into hot rock. *Geophys. J. Roy. Astron. Soc.* 39, 465-509.
- Longman, C.D., Bluick, B.J. and Breemen, Van. O. (1979) Ordovician conglomerates and the evolution of the Midland Valley. *Nature*. 280, 578-581.
- Lowell, J.D. and Guilbert, J.M. (1970) Lateral and vertical alteration and mineralization zoning in porphyry ore deposits. *Econ. Geol.* 65, 383-408.
- Lowell, G.R. and Gasparri, C. (1982) Composition of arsenopyrite from Topaz greisen veins in southeastern Missouri. *Mineral. Deposita*. 17, 229-238.
- Loebenstein, J.R. (1980) Arsenic. In: *Mineral Facts and Problems*. U.S. Bureau of Mines. Bull. 671.
- Lombard, S.M., Marlow, T.W. and Tanner, J.T. (1971) The determination of Sb in standard rocks by instrument neutron activation analysis. *Analytical. Chem.* 55, 13-17.
- Ludden, J.N., Daigneault, R., Robert, F. and Taylor, R.P. (1984) Trace element mobility in alteration zones associated with Archean Au Lode deposits. *Econ. Geol.* 79, 1131-1141.
- Lumsden, G.I., Tulloch, W., Howells, M.F. and Davies, L. (1967) The geology of the neighbourhood of Langholm. *Mem. Geol. Surv. Scotland*. 255pp.
- Lusk, J. (1972) Examination of volcanic exhalative and biogenic origins for sulphur in the stratiform massive sulphide deposits of the New Brunswick. *Econ. Geol.* 67, 169-183.
- Lusk, J., Campbell, F.A. and Krouse, H.R. (1975) Application of sphalerite geobarometry and sulphur isotope geothermometry to ores of the Quemont Mine, Noranda, Quebec. *Econ. Geol.* 70, 1070-1083.
- Luzgin, B.N. and Shepelenko, L.I. Relationship between mercury and arsenic mineralization in the Sarasa ore zone (Gornyy Altay). *Internat. Geol. Rev.* 18, 329-333.
- Manning, S. (1977) The role of fluid inclusions in gold mineralization. In: *Colvins, A.C. (Ed) The geology of gold in Canada*. Canadian Geological Survey, Misc. Paper 110, 2/3pp.

- Lyndon, J.W. and Galley, A. (1986) Chemical and Mineralogical zonation of the Mathiati alteration pipe, Cyprus and its genetic significance. 46-67. In: *Metallogeny of basic and ultrabasic rocks*. Gallagher, M.J., Ixer, R.A., Neary, C.R. and Pritchard, H.M. (Eds) IMM Publication.
- MacDonald, A.J. and Ray, G.E. (1984) Fluids responsible for lode gold deposition in the Cordillera and Superior Province. Implications for a cost-effective exploration technique. Cordillera Section GAC Symposium. *Cordillera Geology and Mineral Exploration : status and future trends*, Vancouver.
- MacDonald, J.G. and Whyte, F. (1981) Petrogeochemical evidence for the genesis of a Lower Carboniferous basaltic suite in the Midland Valley of Scotland. *Trans. R. Soc. Edinburgh*. 72, 75-88.
- MacDonald, R., Thorpe, R.S., Gaskarth, W.G. and Grindrod, A.R. (1985) Multi component origins of Caledonian lamprophyres of Northern England. *Min. Mag.* 49, 485-494.
- MacGibbon, J. (1935) Scottish gold fields and their history. *Scottish Bankers Magazine*, January, 299-309.
- Mackay, R.A. (1959) The Leadhills-Wanlockhead Mining District. In: *Symposium on the future of non-ferrous mining in Great Britain and Ireland*. Inst. Min. Metall. 49-64.
- Mackenzie, F.T. and Pigott, J.D. (1981) Tectonic controls of Phanerozoic sedimentary rock cycling. *J. Geol. Soc. London*. 138, 183-196.
- Mackie, J.D. (1984) *A history of Scotland*. Penquin. 414pp.
- Mackintosh, D.M. (1967) Quartz-carbonate veining and deformation in Namurian turbidites sandstones of the Crackington Measures, N. Cornwall. *Geol. Mag.* 104, 75-85.
- MacLennan, S.M., Taylor, S.R. and Eriksson, K.A. (1978) Geochemistry of Archean shales from the Pilbara Supergroup, Western Australia. *Geochim. Cosmochim. Acta*. 47, 1211-1222.
- Macpherson, H.G. and Livingstone, A. (1981) Glossary of Scottish Mineral Species. *Scott. J. Geol.* 1-47.
- Macrae, N.D. and Nesbitt, H.W. (1980) Partial melting of common meta-sedimentary rocks, a mass balance approach. *Cont. Min. Pet.* 75, 21-26.
- Maher, S.W. (1971) Regional distribution of mineral deposits beneath the pre-middle Ordovician unconformity in the Southern Appalachian. *Econ. Geol.* 66, 744-747.
- Mancey, S.J. (1982) Cluster analysis in geology. In: Horder, M.F. and Howarth, R.J. (Eds) *Computer applications in geology I and II*. Geol. Soc. London Misc. Pub. 89-102.
- Mancey, S.J. and Howarth, R.J. (1979) Power transform removal of skewness from larger data sets. *Trans. Inst. Min. Metall.* 198, B92-97.
- Mangan, M., Craig, J.R. and Rimstidt, J.D. (1984) Submarine exhalative gold mineralization at the London-Virginia Mine, Buckingham County, Virginia. *Mineral. Deposita*. 19, 227-236.
- Marakushev, A.A. (1977) Geochemical properties of gold and conditions of its endogenic concentration. *Mineral. Deposita*. 12, 123-141.
- Marmont, S. (1983) The role of felsic intrusions in gold mineralization. In: Colvine, A.C. (Ed) *The geology of gold in Ontario*. Ontario Geological Survey, Misc. Paper. 110, 278pp.

- Marshall, B. and Taylor, B.E. (1981) Origin of hydrothermal fluids responsible for gold deposition, Alleghany District, Sierra County, California. In: Silberman, M.L. (Ed) Proceedings of the Symposium on Mineral Deposits of the Pacific Northwest. 281-293.
- Massa, P.J. and Ikramuddin, M. (1986) Thallium in gold-silver bearing quartz veins and associated volcanic rocks from the Como mining district, Nevada, USA. *Chem. Geol.* 54, 27-34.
- Mattinen, P.R. and Bennett, G.H. (1986) The green mountain massive sulphide deposit, Besshi-style mineralization within the Californian foothills copper-zinc belt. *J. Geochem. Explor.* 25, 185-200.
- Maucher, A. (1972) Time and stratabound ore deposits and the evolution of the earth. *Int. Geol. Congr. Abstr. Resumes No. 24*, 137.
- Maucher, A. (1976) The stratabound cinnabar-stibnite-scheelite deposits. In: Wolf, K.H. (Ed) *Handbook of stratabound and stratiform ore deposits*. 7, 477-503.
- Maucher, A. and Holl, A. (1968) The significance of geochemical-stratigraphic guide horizons for determining the age of the Schläining stibnite deposit in Burgenland, Austria. *Mineral. Deposita*. 3, 272-285.
- Mawdsley, J.B. (1937) Late gold and some of its implications. *Econ. Geol.* 32, 194-210.
- Mawer, C.K. (1985) Development of gold-quartz veins, Meguma Terrane, Nova Scotia. *GAC/MAC Program with Abstracts*. 10, A38. Fredericton.
- Maynard, J.B., Valloni, R. and Yu, H.S. (1982) Composition of modern deep-sea sands and arc related basins. In: Leggett, J.K. (Ed) *Trench-Forearc Geology*. *Geol. Soc. London. Spec. Pub. No. 10*, 551-576.
- McAllister, W.D.N. (1979) The mineralization, stream sediment and soil geochemistry of the southwest Lake District. Ph.D. Thesis, University of Nottingham.
- McCammon, R.B., Botbol, J.M., Sinding-Larsen, R. (1984) The new characteristic analysis (NCHARAN) program. *US Geological Survey Bull.* 1621, 27pp.
- McGibbon, N. (1977) Economic mineral deposits of the Catorce mining district, San Luis Potosi, Mexico. *Abst. Programs*. 9, 63-64.
- McKenzie, D. (1974) Some remarks on the development of sedimentary basins. *Earth. Pla. Sci. Letters*. 40, 25-32.
- McKerrow, W.S. (1987) Introduction: The Southern Uplands Controversy. *J. Geol. Soc. Lond.* 144, 735-736.
- McKerrow, W.S. (1988) The development of the Iapetus Ocean from the Arenig to the Wenlock. In: Harris, A.L. and Fettes, D.J. (Eds) *The Caledonian - Appalachian Orogen*. *Geol. Soc. Lond. Spec. Publ.* 38, 269-274.
- McKerrow, W.S. and Elders, C.F. (1989) Movements on the Southern Upland Fault. *J. Geol. Soc. Lond.* 146, 393-396.
- McKerrow, W.S. and Ziegler, A.M. (1972) Silurian paleogeographic development of the Proto-Atlantic Ocean. *24th Int. Geol. Cong. Section 6*, 4-10.
- McKerrow, W.S., Leggett, J.K. and Eales, M.H. (1977) Imbricate thrust model of the Southern Uplands of Scotland. *Nature* 267, 273-239.

- McKinley, T.D., Heinrich, K.F.J. and Wittry, D.B. (Eds) The electron-microprobe. John Wiley and Sons. 1035pp.
- McKinstry, H.E. and Ohle, E.L. (1949) Ribbon structure in gold-quartz veins. *Econ. Geol.* 44, 87-109.
- McLaren, M. (1908) *Geochemistry of Gold*. London.
- McLennan, S.M., Nance, W.B. and Taylor, S.R. (1980) Rare earth element : thorium correlations in sedimentary rocks and the composition of the continental crust. *Geochim. et. Cosmochim. Acta.* 44, 1833-1840.
- McNeil, A.M. and Kerrich, R. (1986) Archean lamprophyre dykes and gold mineralization, Matheson, Ontario : the conjunction of LILE - enriched mafic magmas, deep crustal structures and Au concentration. *Can. J. Earth. Sci.* 23, 324-343.
- Meisel, W.S. (1972) *Computer orientated approaches to pattern recognition*. Academic Press.
- Mercer, W. (1976) Minor elements in metal deposits in sedimentary rocks : a review of the recent literature. 1-27. In: Wolf, K.H. (Ed) *Handbook of stratabound and stratiform ore deposits*. Elsevier.
- Merriman, R.J. and Roberts, B. (1988) Bentonites in the Moffat Shale Group of the Southern Uplands : trace element evidence of back-arc basin volcanism. *Volcanic research in progress (Abst.) Geol. Soc. Lond. Newsletter*.
- Metzger, F.W., Kelly, W.C., Nesbitt, B.E. and Essance, G. (1977) Scanning electron microscopy of daughter minerals in fluid inclusions. *Econ. Geol.* 72, 141-153.
- Meyer, C. and Hemley, J.J. (1967) Wallrock alteration. In: Barnes, H.L. (Ed) *Geochemistry of Hydrothermal Ore Deposits*. Holt, Rinehart and Winston, New York, 670pp.
- Meyer, M. and Sanger, R. (1985) The gold content of some Archean rocks and their possible relationships to epigenetic gold quartz vein deposits. *Min. Deposita.* 20, 284-289.
- Middleton, G.V. and Hampton, M.A. (1973) Sediment gravity flows : mechanics of flow dispersion. In: *Turbidites and deep water sedimentation. (S.E.P.M. Pacific section, Short Course)*, 1-38.
- Miesch, A.T. (1969) Critical review of some multivariate procedures in the analysis of geochemical data. *Math. Geol.* 1, 171-184.
- Miller, J.M. and Taylor, K. (1963) Uranium mineralization near Dalbeattie, Kirkcudbrightshire. *Bull. Geol. Survey.* 25, 1-18.
- Mineral Resources Consultative Committee. (1975) *Gold*. H.M.S.O. Pub. 56pp.
- Minghau, Z., Bing, Z. and Dequan, S. (1981) Geologic and metallogenic characteristics of a stratiform deposit with gold and silver in China. *Acta. Geol. Sin.* 55, 55-66.
- Mironov, A.G., Zhmodik, S.M. and Maksimova, E.A. (1981) An experimental investigation of the Sorption of gold by pyrites with different thermoelectric properties. *Geochem. Int.* 18, 153-160.
- Mironov, A.G. and Geletiy, V.F. (1979) Experimental study of gold distribution in sulphides. *Doklady Arad. Nauk. SSR.* 247, 194-197.

- Mitchell, A.H.G. and Garson, M.S. (1981) Mineral deposits and Global Tectonic settings. Academic Press.
- Mitchell, A.H.G. and McKerrow, W.S. (1975) Analogous evolution of the Burma orogen and the Scottish Caledonides. *Bull. Geol. Soc. Am.* 86, 305-315.
- Mitchell Cash, (1917) Scottish Topography, Mines and Minerals.
- Mirsal, I.A. (1980) About the diagenesis and origin of the carbonate cement in the Lower Carboniferous greywackes of Elnhausen Schichten near Marburg-on-the-Lahn. *Geol. Palaeontol.* 14, 189-194.
- Mitropoulos, P. (1982) REE patterns of the metasedimentary rocks of the Lands End granite aureole (Southwest England). *Chem. Geol.* 35, 265-280.
- Moelo, Y., Fouquet, Y., Laforet, C. and Chauris, L. (1978) L'indice plombo antimonifere de Bestree (Cap Sizun, Finistere), *Bull. Mineral.* 101, 363-367.
- Moller, P., Dulski, F.S., Luck, J. and Szacki, W. (1981) A new way of interpreting trace element concentrations with respect to modes of mineral formation. *J. Geochem. Explor.* 15, 271-284.
- Moore, G.F. (1979) Petrography of subduction zone sandstones from Nias Island, Indonesia. *J. Sed. Pet.* 49, 71-84.
- Moore, J.N., Capuano, R.M. and Christensen, D.D. (1983) Geochemical indicators of a high temperature geothermal system. *J. Geochem. Expl.* 19, 347-348.
- Morad, S. (1983) Diagenesis and geochemistry of the Visingsö Group (Upper Proterozoic) Southern Sweden : a clue to the origin of colour differentiation. *J. Sed. Petrol.* 53, 51-65.
- Morgan, J.W. and Woodless, A. (1980) Rare earth element distribution in some hydrothermal minerals and its evidence for crystallographic control. *Geochim. Cosmochim. Acta.* 44, 973-980.
- Morganti, J.M. (1981) Ore Deposit Models 4 : Sedimentary type stratiform ore deposits : some models and a new classification. *Geoscience Canada* 8, 65-75.
- Morris, H.T. and Lovering, T.S. (1952) Supergene and hydrothermal dispersion of heavy metals in wallrocks near orebodies, Tintic district, Utah. *Econ. Geol.* 47, 685-716.
- Morris, J.H. (1983) The stratigraphy of the Lower Palaeozoic rocks in the western end of the Longford-Down inlier, Ireland. *J. Earth. Sci. R. Dublin soc.* 5, 201-218.
- Morris, J.H. (1984) The metallic mineral deposits of the Lower Palaeozoic Longford-Down inlier, in the Republic of Ireland. *Geol. Surv. Ire. Rep. Series, RS84/1*, 72pp.
- Morris, J.H. (1987) The Northern Belt of the Longford-Down Inlier, Ireland and The Southern Uplands, Scotland : an Ordovician back-arc basin. *J. Geol. Soc. Lond.* 144, 773-786.
- Morris, J.H., Steed, G.M. and Wilbur, D.G. (1985) Gold in the Hills of Co. Monaghan. In: Andrews, C.J. (Ed) *The Geology and Genesis of Mineral Deposits in Ireland : Proceedings of the Dublin conference.* Irish Assoc. Econ. Geol. Spec. Pub. (In Press).
- Morris, J.H. and Steed, G.M. (1989) Gold mineralization in the Remnant Ordovician Arc-Backarc system of the Southern Uplands and Ireland. Abstract, Gold 89 in Europe.

- Morrissey, C.J. (1986) New Trends in Geological Concepts. Trans. Inst. Min. Metall. 95, B54-57.
- Morrissey, C.J. and Ruitenberg, A.A. (1980) Geology of the Lake George antimony deposit, southern New Brunswick. Can. Inst. Min. Bull. 73, 79-84.
- Mozgova, N.N., Borodaev, Yu.S., Ozerova, N.A. and Paakkonen, V. (1977) New minerals of the group of iron antimonides and arsenides from Seinajoki deposit, Finland. Bull. Geol. Soc. Finland. No. 49, Part 1.
- Muff, R. (1978) The antimony deposit in the Murchison Range of the north-eastern Transvaal, Republic of South Africa. Monograph series on mineral deposits, 16. Gebruder Borntraeger, Berlin Pub.
- Murray, M. and Condie, K. (1973) Post-Ordovician to early Mesozoic history of the eastern Klamath Subprovince, Northern California. J. Sed. Pet. 43, 505-515.
- Naden, J., Dawson, J., Ixer, R.A. and Vaughn, D.J. (1985) Morphology and composition of placer gold of the Southern Uplands, Scotland. MDSG Abstracts, Strathclyde University.
- Nakamura, N. (1974) Determination of REE, Ba, Mg, Na and K in carbonaceous and ordinary chondrites. Geochim. Cosmochim. Acta. 38, 757-775.
- Nance, W.B. and Taylor, S.R. (1976) Rare earth element patterns and crustal evolution. Geochim. Cosmochim. Acta. 40, 1539-1551.
- Nathan, S. (1976) Geochemistry of the Greenland Group (Early Ordovician), New Zealand. N. Z. J. Geol. Geophys. 19, 683-706.
- Needham, D.T. and Knipe, R.J. (1986) Accretion and collision related deformation in the Southern Uplands accretionary wedge, southwestern Scotland. Geology 14, 303-306.
- Nelson, C.E. and Giles, D.L. (1985) Hydrothermal Eruption Mechanisms and Hot Spring Gold Deposits. Econ. Geol. Vol. 80, No. 6, 1633.
- Nesbitt, H.W. (1979) Mobility and fractionation of rare earth elements during weathering of a granodiorite. Nature. 279, 206-210.
- Neuman R.B. (1988) Palaeontological evidence bearing on the Arenig-Caradoc development of the Iapetus Ocean basin. In: Harris, A.L. and Fettes, D.J. (Eds) The Caledonian - Appalachian Orogen. Geol. Soc. Lond. Spec. Publ. 38, 269-274.
- Nichol, I. (1986) Geochemical exploration for gold deposits in areas of glaciated overburden : Problems and new developments. In: Prospecting in Areas of Glaciated Terrains 1986. Inst. Min. Metall. Pub. 7-17.
- Nie, N.H. (1975) (Ed) SPSS: Statistical Package for the Social Sciences. McGraw Hill.
- Norman, D.I. and Sawkins, F.J. (1985) The Tribag Breccia Pipes : Precambrian Cu-Mo Deposits, Batchawana Bay, Ontario. Econ. Geol. Vol. 80, No. 6, 1593.
- Norris, R.J. and Henley, R.W. (1976) Dewatering of a metamorphic pile. Geology, 4, 333-343.
- Norrish, K. and Hutton, J.T. (1964) An accurate X-ray spectrographic method for the analysis of a wide range of geological samples. Geochim. Cosmochim. Acta. 33, 431-454.

- Norton, D. and Knapp, R. (1977) Transport phenomena in hydrothermal systems : the nature of porosity. *Am. J. Sci.* 277, 913-936.
- Novgorodova, M.I., Vertennikov, V.M., Boyarskaya, R.V. and Drykin, V.I. (1984) Geochemistry of trace elements in gold bearing quartz. *Geochim. Int.* 21, 101-129.
- Obial, R.C. (1970) Cluster analysis as an aid in the interpretation of multi-element geochemical data. *Trans. Inst. Min. Metall.* 79, B175-180.
- O'Brien, B.H. (1985) Syntectonic veining and hydraulic fracturing : some examples from the Meguma Group of Nova Scotia. GAC/MAC Program with Abstracts, 10, A45. Fredericton.
- Oderheimer, F. (1840) On the mines and minerals of the Breadalbane Highlands. Prize essays and transactions of the Highland and Agricultural society for Scotland. 13, 541-556.
- O'Hara, K. (1986) Tectonic implications of Late Paleozoic metamorphism in southeastern New England. *Geology*, 14, 430-432.
- Ohmoto, H. and Rye, R.O. (1979) Isotopes of sulphur and carbon. In: Barnes, H.L. (Ed) *Geochemistry of Hydrothermal Ore Deposits*. Wiley. 509-563.
- Olaussen, S. (1981) Formation of celestite in the Wenlock, Oslo Region Norway : evidence for evaporitic depositional environments. *J. Sed. Pet.* 51, 37-46.
- Oliver, G.J.H. (1978) Prehnite-pumpellyite facies metamorphism in County Cavan, Ireland. *Nature*, 274, 242-243.
- Oliver, G.J.H. (1986) Low Grade Metamorphism and Terrain Analysis. 33rd Inter-University Geological Congress, University of Nottingham.
- Oliver, G.J.H. (1988) Arenig to Wenlock regional metamorphism in the Paratectonic Caledonides of the British Isles : a review. In: Harris, A.L. and Fettes, D.J. (Eds) *The Caledonian - Appalachian Orogen*. *Geol. Soc. Lond. Spec. Publ.* 38, 269-274.
- Oliver, G.J.H. and Leggett, J.K. (1980) Metamorphism in an accretionary prism : Prehnite-pumpellyite facies metamorphism of the Southern Uplands of Scotland. *Trans. Roy. Soc. Edin.* 71, 235-246.
- Oliver, G.J.H. and McKerrow, W.S. (1984) Seismological evidence for shallow crystalline basement in the Southern Uplands, Scotland: A discussion. *Nature*. 309, 89-90.
- Omori, T. (1966) Singular characteristics of chemical composition of the Permian greywacke from the Kiso mountains, central Japan. *Econ. Geol.* 55, 145-159.
- O'Neil, J.R. and Silberman, M.L. (1974) Stable isotope relations in epithermal Au-Ag deposits. *Econ. Geol.* 69, 902-909.
- Onishi, H. and Sandell, E.B. (1955) The Geochemistry of Arsenic. *Geochim. Cosmochim. Acta.* 7, 1-33.
- Ondrick, C.W. and Griffiths, J.C. (1969) Frequency distribution of elements in Rensselaer greywacke, Troy, New York. *Geol. Soc. Am. Bull.* 80, 509-518.
- Ondrick, C.W. and Griffiths, J.C. (1969) Trend surface analysis applied to the Rensselaer greywacke and its implications to the taconics. *J. Sed. Pet.* 39, 176-186.

Ondrick, C.W. and Suher, N.H. (1969) Error and the spectrographic analysis of greywacke samples. *Chem. Geol.* 4, 429-437.

Oosterom, M.G., Busink, R.W. and Vriend, S.P. (1984) Lithogeochemical studies of aureoles around the Panasqueira Tin-Tungsten Deposit, Portugal. *Mineral. Deposita.* 19, 283-288.

Orth, C.J., Gilmore, J.S., Quintana, L.R. and Sheehan, P.M. (1986) Terminal Ordovician extinction : Geochemical analysis of the Ordovician/Silurian boundary, Anticosti Island, Quebec. *Geology*, 14, 433-436.

Otkhmezuir, Z.V. and Dolidze, I.D. (1981) Chemical composition of fluid inclusions in the ore forming minerals of antimony, mercury, arsenic deposits. *Bull. De Min.* 104, 361-368.

Padgham, W.A. (1985) Turbidite hosted gold deposits of Northwest Territories. GAC/MAC Program with Abstracts, 10, A46. Fredericton.

Palmer, D., Johnston, J.D., Dooley, T. and Maguire, K. (1989) The Silurian of Cley Bay, Ireland : part of the Midland Valley of Scotland?. *J. Geol. Soc. Lond.* 146, 389-392.

Paterson, C.J. (1984) Structural control on the distribution and orientation of gold-tungsten-antimony lodes in metamorphic terrains. GAC/MAC Program with Abstracts, 9, 95. London, Ontario.

Paterson, C.J. (1985) Controls on gold mineralization, Otago, New Zealand. GAC/MAC Program with Abstracts, 10, A47. Fredericton.

Paterson, C.J. and Rankin, P.C. (1979) Trace element distribution in the schist surrounding a quartz-scheelite lode, Glenorchy, New Zealand. *N. Z. J. Geol. Geophys.* 22, 329-338.

Pattee, H.H., Cosslett, V.E. and Engstrom, A. (1963) (Eds) X-ray optics and X-ray microanalysis. Academic Press. 622pp.

Patrick, R.A.D. (1981) The vein mineralization at Tyndrum, Scotland and a study of substitutions in Tetrahedrites. Unpublished Ph.D. Thesis, University of Strathclyde, Glasgow.

Patrick, R.A.D., Coleman, M.L. and Russell, M.J. (1983) Sulphur isotopic investigation of vein lead-zinc mineralization at Tyndrum, Scotland. *Mineral. Deposita.* 18, 477-485.

Patrick, R.A.D. and Hall, A.J. (1983) Silver substitution into synthetic zinc, cadmium and iron tetrahedrites. *Min. Mag.* 47, 441-451.

Park Jnr., C.F. and MacDiarmid, R.A. (1978) Ore Deposits. Freeman and Co. Pub.

Parker, M.E. (1977) Geophysical surveys around the Talnotry mine, Kirkcudbright, Scotland. *Min. Recon. Prog. Inst. Geol. Sci. Report No. 10*, 10pp.

Parker, M.E., Cooper, D.C., Bide, P.J. and Allen, P.M. (1981) Mineral exploration in the area around Culvennan Fell, Kirkcowan, south-western Scotland. *Min. Recon. Prog. Inst. Geol. Sci. Report No. 42*, 1-18.

Parks, J.M. (1966) Cluster analysis applied to multivariate geologic problems. *J. Geol.* 74, 703-715.

Peach, B.N. and Horne, J. (1889) The Silurian rocks of Britain and Scotland. *Mem. Geol. Surv. Scotland.* 714pp.

- Pearce, J.A. (1982) Trace element characteristics of lavas from destructive plate boundaries. In: Thorpe, R.S. (Ed) *Andesites*. Wiley. 525-548.
- Pearce, J.A. (1983) Role of sub-continental lithosphere in magma genesis at active continental margins. In: Hawkesworth, C.J. and Norry, M.J. (Eds) *Continental Basalts and Mantle Xenoliths*. Shiva. 230-249.
- Peatce, J.A. and Norry, M. (1979) Petrogenetic implications of Ti, Zr, Y and Nb variations in volcanic rocks. *Contrib. Mineral. Petrol.* 69, 33-47.
- Pekka, A.N. (1985) Lithogeochemistry in exploration for Proterozoic porphyry-type molybdenum and copper deposits, Southern Finland. *J. Geochem. Expl.* 23, 163-191.
- Perrault, G., Trudel, P. and Bedard, P. (1984) Auriferous halo's associated with gold deposits at Lamaque mine, Quebec. *Econ. Geol.* 79, 227-238.
- Peterman, Z.E., Coleman, R.G. and Bunker, C.M. (1981) Provenance of Eocene greywackes of the Flournoy Formation near Agness, Oregon : a geochemical approach. *Geology*. 9, 81-86.
- Pettet, J. (1981) Site surveying and leveling. *Hutchison*. 128pp.
- Phillips, G.N. and Groves, D.I. (1983) The nature of gold bearing fluids as deduced from gold deposits of western Australia. *J. Geol. Soc. Australia*. 30, 25-39.
- Phillips, G.N., Groves, D.I. and Martyn, J.E. (1984) An epigenetic origin for Archean banded iron formation hosted gold deposits. *Econ. Geol.* 79, 162-171.
- Phillips, W.E.A. (1981) Correlation of geological, geochemical and geophysical data with satellite imagery, west-central Ireland. E.E.C. Contract No. MPP-159-81-EIR, project report, 1-46.
- Phillips, W.E.A., Stillman, C.J. and Murphy, T. (1976) A Caledonian plate-tectonic model. *J. Geol. Soc. London*. 132, 579-609.
- Phillips, W.J. (1956) The Criffell-Dalbeattie Granodiorite Complex. *J. Geol. Soc. London*. 112, 221-239.
- Phillips, W.J. (1970) The mechanical effect of hydrothermal solutions with reference to the formation of the mineralized normal faults and breccia zones in Cardiganshire. In: *Mineral Exploration, Proc. University Wales Colloquium, Cardiff*. 18-24.
- Phillips, W.J. (1972) Hydraulic fracturing and mineralization. *J. Geol. Soc. London*. 128, 337-359.
- Phillips, W.J. (1974) The development of vein and rock textures by tensile strain crystallisation. *J. Geol. Soc. London*. 130, 441-448.
- Phillips, W.J. (1986) Hydraulic fracturing effects in the formation of mineral deposits. *Trans. Inst. Min. Metall.* 95, B17-24.
- Pilipchuk, M.F. (1974) New data on As distribution in Black Sea Water. *Geochem. Int.* 11, 235-238.
- Piper, D.Z. (1974) Rare earth elements in the sedimentary cycle : a summary. *Chem. Geol.* 14, 285-304.
- Pirie, I.D. and Nichol, I. (1981) Geochemical dispersion in wallrocks associated with the Norbec deposit, Noranda, Quebec. *J. Geochem. Explor.* 15, 159-180.

- Pitcher, W.S. (1979) The nature, ascent and emplacement of granite magmas. *J. Geol. Soc. London*. 136, 627-662.
- Plant, J. and Moore, P.J. (1979) Regional geochemical mapping and interpretation in Britain. *Phil. Trans. R. Soc. London*. B288, 95-112.
- Plant, J., Jeffery, K. and Fage, C. (1975) The systematic determination of accuracy and precision in geochemical exploration data. *J. Geochem. Explor.* 4, 467-486.
- Plant, J., Simpson, P.R., Green, P.M., Watson, J.V. and Fowler, M.B. (1983) Metalliferous and mineralized Caledonian granites in relation to regional metamorphism and fracture systems in northern Scotland. *Trans. Inst. Min. Metall.* 92, B33-42.
- Plant, J.A., Breward, N., Forrest, M.D. and Smith, R.T. (1988) The gold pathfinder elements As, Sb and Bi : their distribution and significance in the Southwest Highlands of Scotland. Abstract. Gold with emphasis on recent exploration, IMM thirteenth Annual Commodity Meeting.
- Plimer, I.R. (1978) Proximal and distal stratabound ore deposits. *Mineral. Deposita*. 13, 345-353.
- Plimer, I.R. and Finlow-Bates, T. (1978) Relationship between primary iron sulphide species sulphur source, depth of formation and age of submarine exhalative sulphide deposits. *Mineral. Deposita*. 13, 399-410.
- Porteous, Rev. J.M. (1876) *God's Treasure House in Scotland*. National Library of Scotland, Edinburgh.
- Porter, E.K. and Peterson, P.J. (1975) Arsenic accumulation by plants on mine waste, (United Kingdom). *The science of the total environment*. 4, 365-371.
- Porter, E.W. and Ripley, E. (1985) Petrologic and stable isotope study of the gold-bearing breccia pipe at the Golden Sunlight Deposit, Montana. *Econ. Geol.* Vol. 80, No. 6, 1689.
- Postma, D. (1982) Pyrite and siderite formation in brackish and freshwater swamp sediments. *American Journ. Sci.* 282, 1151-1183.
- Potts, P.J. and Pritchard, H.M. (1986) Mineralogical applications of neutron activation induced beta autoradiography : the search for gold mineralization in thin section. In: Gallagher, M.J., Ixer, R.A., Neary, C.R. and Pritchard, H.M. (Eds) *Metallogeny of Basic and Ultrabasic Rocks*. IMM Publication.
- Powell, C.M.A. (1979) A morphological classification of rock cleavage. *Tectonophysics*. 58, 21-34.
- Prabhakaran Nair, K.P. and Cottenie, A. (1971) A statistical evaluation of the inter-relationships between particle size fractions, free iron oxide and trace elements. *J. Soil. Sci.* 22, 203-209.
- Press, S. (1986) Detrital spinels from alpinotype source rocks in Middle Devonian sediments of the Rhenish Massif. *Geologische Rundschau*, 75, 333-340.
- Pretorius, D.A. (1976) Gold in the Proterozoic sediments of south Africa. Systems, Paradigms and models. 1-27. In: Wolf, K.H. (Ed) *Handbook of stratabound and stratiform ore deposits*. Vol. 7. Elsevier.
- Price, N.J. (1966) *Fault and joint development in brittle and semi-brittle rocks*. Pergamon Press, London. 176pp.
- Pulkkinen, E. Ollila, J. Manner, R. and Koljonen, T. (1986) Geochemical exploration for gold in the Sattasvaara komatiite complex, Finnish Lapland. In: *Prospecting in areas of Glaciated Terrains* (1986) *Inst. Min. Metall.* 7-17.

- Pye, E.G. and Roberts, R.G. (1981) Genesis of Archean volcanic hosted gold deposits. Ontario Geological Survey Misc. Paper No. 97, 169pp.
- Radtke, A.S. (1976) Geology of the Carlin gold deposits, Nevada. U.S.G.S. Prof. Paper No. 960.
- Radtke, A.S., Rye, R.O. and Dickson, F.W. (1980) Geology and stable isotope studies of the Carlin gold deposits, Nevada. *Econ. Geol.* 75, 641-672.
- Radtke, A.S. and Scheiner, B.J. (1970) Studies of hydrothermal gold deposition (I) Carlin gold deposit, Nevada : The role of carbonaceous materials in gold deposition. *Econ. Geol.* 65, 87-102.
- Ramdohr, P. (1969) *The Ore Minerals and their Intergrowths*. Pergamon Press. 1174pp.
- Ramsey, J.G. (1967) *Folding and Fracturing of Rocks*. McGraw. 568pp.
- Ramsey, J.G. and Graham, R.H. (1970) Strain variation in shear belts. *Can. J. Earth. Sci.* 7, 786-813.
- Rankin, D.W., Harald-Furnes, A.C., Bishop, B., Cabanis, D.J., Milton, S.J., O'Brien, S.J. and Thorpe, R.S. (1988) Plutonism and volcanism related to the pre-Arenig evolution of the Caledonide-Appalachian orogen. In: Harris, A.L. and Fettes, D.J. (Eds) *The Caledonian - Appalachian Orogen*. *Geol. Soc. Lond. Spec. Publ.* 38, 269-274.
- Rao, A.N. (1952) Trace element variation in hydrothermally altered rocks associated with mineralization. Ph.D. Thesis, Imperial College, University of London.
- Rathjen, J.A. (1980) Antimony. In: *Mineral facts and problems*. US Bureau of Mines. Bull. 671.
- Raybould, J.G. (1976) The influence of pre-existing planes of weakness in rocks on the localisation of vein-type ore deposits. *Econ. Geol.* 71, 636-641.
- Rea, W.J. (1972) Igneous activity and metallogenesis in the Ordovician of north Wales : A review. In: *Mineral exploitation and economic geology, University of Wales Colloquium, Gregnog*. 45-49.
- Reading, H.G. (1986) (Ed) *Sedimentary Environments and Facies*. Blackwell.
- Redfern, P. (1979) The geology of the Silurian rocks, south of the Shap granite, with special reference to the Birkbeck tunnel. Ph.D. Thesis, University of Nottingham.
- Reid, R.R., Caddey, S.W. and Rankin, J.W. (1975) Primary refraction control of ore shoots with examples from the Coeur d'Alene district, Idaho. *Econ. Geol.* 70, 1050-1061.
- Reimann, C. and Stumpfl, E.F. (1981) Geochemical setting of stratabound stibnite mineralization in the Kreuzeck Mountains, Austria. *Trans. Inst. Min. Metall.* 90, B126-132.
- Reimer, T. (1971) Strontium depletion in Early Precambrian sediments. *Neues. Jahrb. Mineral. Monatsh.* 12, 527-541.
- Ricci, C.A. and Sabatina, G. (1976) An example of sedimentary differentiation in volcano-sedimentary series the high chromium meta-greywackes of central Sardinia (Italy). *Neues. Jb.* 76, 307-319.
- Ricci-Luchi, F. (1975) Depositional cycles in two turbidite formations in Northern Italy. *J. Sed. Pet.* 45, 3-45.

- Rice, C.M. and Trewin, N.H. (1987) The Rhynie chert, a precious metal-bearing hot spring system. MDSG. Newcastle.
- Rice, C.M. and Trewin, N.H. (1988) Lower Devonian gold-bearing hot spring system near Rhynie, Scotland. Abstract, Gold with emphasis on recent exploration, IMM thirteenth Annual Commodity Meeting.
- Rice, R. and Sharp, G.J. (1976) Copper mineralization in the forest of Coed-y-Brenin, North Wales. Trans. Inst. Min. Metall. 85, B1-13.
- Rickard, D.T. (1973) Limiting conditions for synsedimentary sulphide ore formation. Econ. Geol. 68, 605-617.
- Ridge, J.D. (1974) Note on boiling of ascending ore fluids and the position of volcanic exhalative deposits in the Modified Lindgren classification. Geology. 2, 287-288
- Ridler, R.H. (1973) Exhalite concept : a new tool for exploration. Northern Miner.
- Ridler, R.H. (1976) Stratigraphic keys to the gold metallogeny of the Abitibi Belt. Can. Min. J. 97, 81.
- Rieck, K. (1975) First geological and geochemical investigation of an antimony occurrence near Sta. Cruz Cuchilla in Honduras, Central America. Erzmetall. 20, 7-8.
- Ripley, E.M. and Nichol, D.L. (1979) Sulphur isotope studies of Archean slates and greywackes from north-central Minnesota : evidence for the existence of sulphate-reducing bacteria. Geol. Soc. Am. 11, 503-504.
- Robert, F. and Brown, A.C. (1986) Archean gold bearing quartz veins at the Sigma Mine, Parts I and II. Econ. Geol. 81, 578-616.
- Roberts, F.I. (1982) Trace element chemistry of pyrite. A useful guide to the occurrence of sulphide base metal mineralization. J. Geochem. Explor. 42, 50-62.
- Roberts, R.J., Radtke, A.S. and Coats, R.R. (1971) Gold bearing deposits in north-central Nevada and south-western Idaho. Econ. Geol. 66, 14-33.
- Roberts, S. (1988) Ophiolitic chromite formation : A marginal basin phenomenon?. Econ. Geol. 83, 1034-36.
- Robinson, B.W. and Christie, A.B. (1980) Epithermal silver-gold mineralization, Maratoto Mine, New Zealand. Stable Isotopes and Fluid Inclusions. Proceedings of the fifth quadrenial IAGOD symposium. Germany. 719-730.
- Robinson, B.W. and Farrand, M.G. (1982) Sulphur isotopes and the origin of stibnite mineralization in New England. Mineral. Deposita. 17, 161-174.
- Robinson, B.W. and Kusakabe, M. (1975) Quantitative preparation of sulphur dioxide for sulphur isotope analysis, from iron sulphides by combustion with cuprous oxide. Analytical Chemistry. 47, 1179-1181.
- Rock, N.M.S. (1987) The nature and origin of lamprophyres : an overview. In: Fitton, J.G. and Upton, B.G.J. (Eds) Alkaline igneous rocks. Geol. Soc. Lond. Special Publ. No. 30, 191-226.

- Rock, N.M.S. and Duffy, T. (1985) Documentation for SPIDER : A Fortran-77 program for plotting MORB and Chondrite normalised petrology 'spidergrams' of trace and rare earth element data. Mineralogy and Petrology Report No. 85/86. 21pp. British Geological Survey.
- Rock, N.M.S., Jeffreys, L.A. and MacDonald, R. (1984) The problem of anomalous limestone-pelite succession within the Moine outcrop, I : Metamorphic limestones of the Great Glen Area, from Ardgow to Nigg. *Scott. J. Geol.* 20, 383-406.
- Rock, N.M.S., Gasgarth, J.W. and Rundle, C.C. (1986) Late Caledonian dyke-swarms in Southern Scotland : A regional zone of primitive K-rich lamprophyres and associated vents. *J. Geology.* 505-522.
- Rock, N.M.S., MacDonald, R., Szucs, T. and Bower, J. (1986) The comparative geochemistry of some Highland pelites. *Scott. J. Geol.* 22, 107-126.
- Rock, N.M.S., Duller, P.R., Haszeldine, R.S. and Groves, D.I. (1987) Lamprophyres as potential gold exploration targets : some preliminary observations and speculations. In: Groves, D.I. and Ho, S.E. (1987) Recent advances in understanding Archean gold deposits. University W. Australia, Geology Department and University Extension Publication. No. 11.
- Rock, N. M.S. and Groves, D.I. (1988) Can lamprophyres resolve the genetic controversy over mesothermal gold deposits?. *Geology*, 16, 538-541.
- Roedder, E. (1984) Fluid inclusion evidence bearing on the environment of gold deposition. In: *Proc. Gold 82. Geol. Soc. Zimbabwe. Spec. Pub. 1.* Balkema, Holland.
- Roger, G. (1966) Some observations on the relations of the antimony veins in the vicinity of the Collet-De-Deze (Lozere) to their geologic environment. *Soc. Geol. Fr. Bull. Ser. 7.* 8, 577-584.
- Rogers, J.J.W. (1966) Geochemical significance of the source rocks of some greywackes from Western Oregon and Washington. *Texas J. Science.* 5-20.
- Rogers, J.J.W., Condie, K.C. and Mahan, S. (1970) Significance of thorium, uranium and potassium in some Early Precambrian greywackes from Wyoming and Minnesota. *Chem. Geol.* 5, 207-213.
- Romberger, S.B. (1986) Mechanisms of deposition of gold in low temperature hydrothermal systems. *J. Geochem. Explor.* 25, 237pp.
- Ronov, A.B. and Migdisov, A.A. (1971) Geochemical history of the crystalline basement and the sedimentary cover of the Russian and North American platforms. *Sedimentology.* 16, 137-185.
- Rosasco, G.J., Roedder, E. and Simmons, J.H. (1975) Laser excited Raman Spectrography for non destructive partial analysis of individual phases in fluid inclusions. *Mineral Science.* 190, 557-560.
- Rose, A.W., Dahlberg, E.C. and Keith, M.L. (1970) A multiple regression technique for adjusting background values in stream sediment geochemistry. *Econ. Geol.* 65, 156-165.
- Rose, A.W., Hawkes, H.E. and Webb, J.S. (1979) *Geochemistry in mineral exploration.* Academic Press Pub.
- Rosenbauer, R.J., Bischoff, J.L. and Radtke, A.S. (1983) Hydrothermal alteration of greywacke and basalt by 4 M NaCl. *Econ. Geol.* 78, 1701-1710.
- Roslyakova, N.V. and Roslyakova, N.A. (1975) Endogenic aureoles of gold deposits. Nauka Press, Novosibirsk, 130pp. (Translation available from Geological Survey of Canada, Ottawa, Ontario.).

- Roth, H.D., Pierce, J.W. and Huang, T.C. (1972) Multivariate discriminant analysis of bioclastic turbidites. *Math. Geol.* 4, 249-261.
- Roy, A. (1981) Application of cluster analysis in the interpretation of geochemical data from the Sargipalli lead-zinc mine area, Sundergarh District, Orissa (India). *J. Geochem. Explor.* 14, 245-264.
- Royle, A.G. and Newton, M.J. (1972) Mathematical models, sample sets and ore-reserve estimation. *Trans. Inst. Min. Metall.* 82, 78-85.
- Royle, A.G., Newton, M.J. and Sarin, V.K. (1972) Geostatistical factors in design of mine sampling programmes. *Trans. Inst. Min. Metall.* 82, 71-77.
- Rugless, C.S. and Teale, G. (1985) Lithogeochemical exploration for polymetallic Sn-Cu-Ag-Au-Pb-Zn vein mineralization at the north Mammoth prospect, northeast Victoria, Australia. 11th IGES Program with Abstracts. 11, 78.
- Ruitenbergh, A.A. (1972) Metallisation episodes related to tectonic evolution, Rolling Dam and Mascarene : Nerepis Belts, New Brunswick. *Econ. Geol.* 67, 434-444.
- Ruitenbergh, A.A. (1984) Gold bearing structures in the Bay of Fundy Coastal Zone of southern New Brunswick. GAC/MAC Program with Abstracts. 9, 101.
- Ruitenbergh, A.A. and Fyffe, L.R. (1982) Metallic mineral zonation related to tectonic evolution of the New Brunswick Appalachians. In: St. Julian, D. and Beland, J. (Eds) Major structural zones and faults of the northern Appalachians. *Geol. Assoc. Can. Special Paper*, 24.
- Ruitenbergh, A.A. and Fyffe, L.R. (1982) Mineral deposits associated with granitoid intrusions and related subvolcanic stocks in New Brunswick and their relationship to Appalachian tectonic evolution. *Geology of Ore Deposits. Can. Inst. Min. Bull.* 75, 1-15.
- Russell, A. (1917) Report on the Clontibret Antimony Mine, Castleblayney, Co. Monaghan. Unpublished report to the Ministry of Munitions : Open file report, Mineral Resources Division, Geological Survey of Ireland.
- Russell, M.J. (1968) Structural controls of base metal mineralization in Ireland in relation to continental drift. *Trans. Inst. Min. Metall.* B117-128.
- Russell, M.J. (1971) North-south geofractures in Scotland and Ireland. *Scott. J. Geol.* 8, 75-84.
- Russell, M.J. (1973) The geological environment of Post-Caledonian base metal mineralization in Ireland. Ph.D. Thesis, University of Durham.
- Russell, M.J. (1973) Base metal mineralization in Ireland and Scotland and the formation of the Rockall Trough. In: Tarling, D.H. and Runcorn, S.K. (Eds) Implications of continental drift to the earth sciences. 1, 581-597. Academic Press.
- Russell, M.J. (1974) Manganese halo surrounding the Tynagh ore deposit, Ireland : a preliminary note. *Trans. Inst. Min. Metall.* 83, B65-66.
- Russell, M.J. (1975) Lithogeochemical environment of the Tynagh base metal deposit, Ireland and its bearing on ore deposition. *Trans. Inst. Min. Metall.* 84, B128-133.
- Russell, M.J. (1975) Incipient plate separation and possible related mineralization in lands bordering the north Atlantic. *Geol. Assoc. Canada. Special paper.* 14, 337.

- Russell, M.J. (1978) mineralization in a fractured craton. In: Bowes, D.R. and Leake, B.E. (Eds) Crustal evolution in northwest Britain and adjacent regions. Geol. Journ. Special issue. No. 10.
- Russell, M.J. (1978) Downward excavating hydrothermal cells and Irish type deposits : the importance of an underlying thick Caledonian prism. Trans. Inst. Min. Metall. 87, B168-171.
- Russell, M.J. (1983) Major sediment hosted exhalative zinc and lead deposits : formation from hydrothermal convection cells that deepen during crustal extension. In: Sangster, D.F. (Ed) Short course handbook, sediment hosted stratiform lead-zinc deposits. Min. Assoc. Canada. 251-282.
- Russell, M.J. (1984) A New Breed of Geologists. Educational courses in Britain and America. 4, 21. Dominion Press.
- Russell, M.J. (1986) The evolution of the Scottish mineral sub-province. Scott. J. Geol. 21, 513-545.
- Russell, M.J. and Samson, I.M. (1981) Solutions feeding Irish Zn + Pb (+Ba) and other non-volcanogenic exhalative deposits. Abst. J. Geol. Soc. London.
- Russell, M.J., Solomon, M. and Walshe, J.L. (1981) The genesis of sediment hosted, exhalative zinc + lead deposits. Min. Deposita. 16, 113-127.
- Russell, M.J., Willan, R.C.R., Anderton, R., Hall, A.J., Nicholson, K. and Smythe, D.K. (1981) Genetic model and tectonic setting for Dalradian strataform mineral deposits, Grampian Highlands. In: Hal, A.J. and Gallagher, M.J. (Eds) Caledonian-Appalachian stratabound sulphides. 24-29.
- Russell, M.J., Hall, A.J. and Duller, P.R. (1985) The implications of chemical garden growth to the understanding of certain ore morphologies in the Navan orebody. Bull. Min. Soc. 64, 2-3.
- Rust, B.R. (1963) The geology of the area around Whithorn, Wigtownshire. Ph.D. Thesis, Edinburgh University.
- Rust, B.R. (1965) The stratigraphy and structure of the Whitehorn area of Wigtownshire, Scotland. Scott. J. Geol. 1, 101-133.
- Rust, B.R. (1965) The sedimentology and diagenesis of Silurian turbidites in south-east Wigtownshire, Scotland. Scott. J. Geol. 1, 231-246.
- Ryan, P.D., Floyd, P.A. and Archer, J.B. (1980) The stratigraphy and petro-chemistry of the Loch Nafoeey Group (Tremadocian), Western Ireland. J. Geol. Soc. London. 137, 443-458.
- Rye, R. (1985) A model for the formation of carbonate-hosted disseminated gold deposits based on geologic, fluid-inclusion, geochemical and stable-isotope studies of the Carlin and Cortez deposits, Nevada. 35-43. In: Tooker, E.W. (Ed) Geological characteristics of sediment and volcanic-hosted disseminated gold deposit : search for an occurrence model. USGS. Bull. No. 1646, 1-150.
- Rytuba, J.J. (1985) Geochemistry of hydrothermal transport and deposition of gold and sulphide minerals in Carlin-type gold deposits. 27-34. In: Tooker, E.W. (Ed) Geological characteristics of sediment and volcanic-hosted disseminated gold deposit : search for an occurrence model. USGS. Bull. No. 1646, 1-150.
- Rytuba, J.J. (1986) Arsenic minerals as indicators of conditions of gold deposition in Carlin-type gold deposits. J. Geochem. Explor. 25, 237pp.
- Ryzin, J.V. (1977) (Ed) Classification and Clustering. Academic Press. 467pp.

- Saager, R. and Sinclair, A.J. (1974) Factor analysis of stream sediment geochemical data from the Mount Nansen area, Yukon Territory, Canada. *Mineral. Deposita*. 9, 243-252.
- Sabine, P.A. (1969) Geochemistry of sedimentary rocks, 1. Petrography and chemistry of arenaceous rocks. Great Britain. *Inst. geol. Sci. Rept. No. 69/1*, 68pp.
- Sabine, P.A., Harrison, R.K. and Lawson, R.I. (1985) Classification of volcanic rocks of the British Isles on the total alkali-oxide-silica diagram, and the significance of alteration. *B.G.S. Report*, Vol. 17, No. 4. HmSo Pub.
- Sakai, H. (1968) Isotopic properties of sulphur compounds in hydrothermal processes. *Geochem. J. (Japan)*. 2, 29-49.
- Samson, I.M. and Russell, M.J. (1983) Fluid inclusion data from Silvermines base-metal-baryte deposits, Ireland. *Trans. Inst. Min. Metall.* 92, B67-71.
- Sanders, I.S. and Morris, J.H. (1978) Evidence for Caledonian subduction from greywacke detritus in the Longford-Down inlier. *J. Earth Sci. R. Dublin Soc.* 1, 53-62.
- Sandiford, M. and Keays, R.R. (1985) Structural and metamorphic constraints on the origin of turbidite hosted gold deposits, Victoria, Australia. *GAC/MAC Program with Abstracts*. 9, A 54. London, Ontario.
- Sangster, D.F. (1972) Precambrian volcanogenic massive sulphide deposits in Canada : A review. *Geol. Surv. Canada. Paper*, 72-22, 36pp.
- Sarkisyan, G.A. (1973) Lampophre dykes of the Azatek gold-antimony district. *Dolk. Akad. Nauk. Arm. Ssr.* 57, 84-88.
- Saski, A. and Kajiwar, Y. (1971) Evidence of isotope exchange between seawater sulphate and some syngenetic sulphide ores. *Soc. Min. Geol. (Japan) Spec. Pub. No. 3*, 289-294.
- Sato, T. Behaviours of ore forming solutions in seawater. *Mining Geology*. 22, 31-42.
- Saupe, F. (1987) The Almaden Mercury Deposit. NATO Advanced Study Institute on the Geochemistry of Hydrothermal Ore Forming Processes. (Abstract)
- Sawkins, F.J. (1976) Metal deposits related to intra - continental hotspot and rifting environments. *J. Geol.* 84, 653-671.
- Sawyer, E.W. (1986) The influence of source type, chemical weathering and sorting on the geochemistry of clastic sediments from the Quetico metasedimentary belt, Superior Province, Canada. *Chemical Geology*. 55, 77-95.
- Scheps, W. and Friedrich, G. (1983) Geochemical investigations of Palaeozoic shales and carbonates in the Aachen region. *Mineral. Deposita*. 18, 411-421.
- Scherkenblanch, D.A., Sawkins, F.J. and Seyfried, W.E. (1985) Geologic, fluid inclusion and geochemical studies of the mineralized breccias at Cumobabi, Sonora, Mexico. *Econ. Geol.* 80, 1566-1567.
- Schoen, R., White, D.E. and Hemley, J.J. (1974) Argillization by descending acid at Steamboat Springs, Nevada. *Clay and Clay Minerals*. 22, 1-22.
- Schouwstra, R.P. and deVilliers, J.P.R. (1988) Gold mineralization and associated wallrock alteration in the Main Reef Complex at Sheba Mine, South Africa. *Trans. Inst. Min. Metall.* 97, B158-170.

- Schroeder, B., Thompson, G., Sulanowska, M. and Ludder, J.N. (1980) Analysis of geologic materials using an automated X-ray fluorescence system. *X-ray Spect.* 9, 198-205.
- Schoeller, W.R. (1941) Observations on the alteration products of stibnite. *Min. Mag.* 26, 94-96.
- Schneider, H.J. (1972) Stratabound polymetallic and Fe-Ba-deposits of the Sarrabus-Gerrei region, S.E. Sardinia. *Newes. Jb.* H12, 529-541.
- Schmitt, R.A., Smith, R.H. and Olehy, D.A. (1964) Rare earth, Y and Sc abundances in meteoric and terrestrial matter. *Geochim. Cosmochim. Acta.* 28, 67-86.
- Schwab, F.L. (1975) Framework mineralogy and chemical composition of continental margin-type sandstone. *Geology.* 487-490.
- Schwartz, G.M. (1944) The host minerals of native gold. *Econ. Geol.* 39, 371-411.
- Scottish Land Survey Mineral Files : Gold. BGS Records Office (Unpubl.).
- Scott, H.S. (1948) The decrepitation method applied to minerals with fluid inclusions. *Econ. Geol.* 43, 637-654.
- Scott, K.M. (1986) Sulphide geochemistry and wallrock alteration as a guide to mineralization. Mammoth area, N.W. Queensland, Australia. *J. Geochem. Expl.* 25, 283-308.
- Scott, S.D. and Barnes, H.L. (1971) Sphalerite geothermometry and geobarometry. *Econ. Geol.* 66, 653-669.
- Scott, S.D. (1983) Chemical behaviour of sphalerite and arsenopyrite in hydrothermal and metamorphic environments. *Min. Mag.* 47, 427-435.
- Selinus, O. (1983) Factor and discriminant analysis applied to lithogeochemical prospecting in an area of Central Sweden. *J. Geochem. Explor.* 19, 619-642
- Seward, T.M. (1973) Thio-complexes of gold and the transport of gold in hydrothermal ore solutions. *Geochim. Cosmochim. Acta.* 37, 379-399.
- Seaward, T.M. (1984) The transport and deposition of gold in hydrothermal systems. In: Foster, R.P. (Ed) *Gold '82. The geology, geochemistry and genesis of gold deposits.*
- Sharp, W.E. (1965) The deposition of hydrothermal quartz and calcite. *Econ. Geol.* 60, 1635-1644.
- Shaw, D.M. (1957) The geochemistry of gallium, indium, thallium : a review. In: Ahrens, L.H., Press, F., Rankama, K. and Runcorn, S.K. (Eds) *Physics and Chemistry of the Earth.* Pergamon.
- Shepherd, A., Harvey, P.K. and Leake, R.C. (1985) The geochemistry of residual soils as an aid to geological mapping and mineral exploration : a statistical approach. 11th IGES Program with Abstracts. 80-81.
- Shepherd, T.J. and Allen, P.M. (1985) Metallogenesis in the Harlech Dome, north Wales : a fluid inclusion interpretation. 20, 159-168.
- Shepherd, T., Rankin, A.H. and Alderton, D.H.M. (1985) A practical guide to fluid inclusion studies. Blackie. 239pp.

Sheppard, S.M.F. (1977) Identification of the origin of ore-forming solutions by the use of stable isotopes. In: Volcanic processes in ore-genesis. Geol. Soc. Lond. Spec. Publ. No. 7, 25-41.

Sibson, R.H. (1981) Controls on low-stress hydro-fracture dilatancy in thrust, wrench and normal fault terrains. *Nature*. 289, 665-667.

Sibson, R.H., Moore, J.M. and Rankin, A.H. (1975) Seismic pumping : a hydrothermal fluid transport mechanism. *J. Geol. Soc. London*. 131, 653-659.

Siegel, S. (1956) Non-parametric statistics for behavioural sciences. McGraw.

Silberman, M.L. and Berger, B.R. (1985) Relationship of trace element patterns to alteration and morphology in epithermal precious-metal deposits. In: Berger, B.R. and Bethke, P.M. (Eds) *Geology and Geochemistry of Epithermal Systems*. Reviews in Economic Geology. 2, 203-230.

Sillitoe, R.H. (1973) The tops and bottoms of porphyry copper deposits. *Econ. Geol.* 68, 799-815.

Sillitoe, R.H. (1976) Andean mineralization : a model for the metallogeny of convergent plate boundaries. *Geol. Assoc. Can. Spec. Paper*, 14, 59-100.

Sillitoe, R.H. (1985) Ore-related Breccias in Volcano-plutonic Arcs. *Econ. Geol.* Vol. 80, No. 6, 1467.

Sillitoe, R.H., Graubeger, G.L. and Elliot, J.E. (1985) A Diatreme-hosted Gold Deposit at Montana Tunnels, Montana. *Econ. Geol.* Vol. 80, No. 6, 1707.

Simon, J.B. (1986) Provenance and setting of some Ordovician and Silurian conglomerates in northern Ireland. *Scott. J. Geol.* 22, 63-76.

Simpson, P.R. (1988) Gold and the evolution of extensional volcano-sedimentary basins in the Albitibi Belt, Canada, and the Scottish Dalradian. Abstract, Gold with emphasis on recent exploration, IMM 13th Annual Commodity Meeting.

Sinclair, A.J. (1974) Selection of threshold values in geochemical data using probability graphs. *Journ. Geochem. Explor.* 3, 129-149.

Sinclair, A.J. (1983) Univariate analysis. In: Howarth, R.J. (Ed) *Statistics and data analysis in geochemical prospecting*. Handbook of Exploration Geochemistry. Vol. 2. Elsevier, 59-81.

Sirkantia, S.W. (1977) Geology of antimony occurrences near Barashigri Glacier, Lahaul-Spiti district, Himachal Pradesh. *Geol. Surv. India. Misc. Pub.* 27, 145-155.

Sleeman, P.J. and Ingham, M.N. (1981) An investigation into the grinding efficiency of three mills used in the preparation of samples for X-ray Fluorescence analysis. Analytical Chemistry Unit. Report No. 118. British Geological Survey, Geochemistry and Petrology Division.

Smith, C.G. (1978) Investigation of stratiform sulphide mineralization at Meall Mor, south Knapdale, Argyll. *Inst. Geol. Sci. Mineral Reconnaissance Program*. Report No. 15, 39pp.

Smith, G.F.H. (1918) Semseyite from Dumfriesshire. *Min. Mag.* 18, 354-359.

Smith, P.K. (1985) The Cochrane Hill gold deposits : an amphibolite grade turbidite hosted shear zone. GAC/MAC Program with Abstracts. 10, A58.

- Smith, R.E. (1968) Redistribution of major elements in the alteration of some basic lavas during burial metamorphism. *J. Petrology*. 9, 191-219.
- Smith, R.T., Gallagher, M.J. and Fortey, N.J. (1978) Controls of lead-zinc mineralization in basal Carboniferous rocks near Langholm, Scotland. *Trans. Inst. Min. Metall.* 87, 140-143.
- Snout, T.C. (1967) Lead mining in Scotland 1650-1850. In: Payne, P.L. (Ed) *Studies in Scottish Business History*.
- Soler, A. and Ayora, C. (1989) Gold bearing arsenopyrite massive bodies in skarns from the SW contact of the Andorra granite (central Pyrenees, Spain). Abstract, Gold 89 in Europe.
- Solomon, M. (1980) Hot water plumes on the ocean floor, clues to submarine ore formation. *Journ. Geol. Soc. Australia*. 27, 89-90.
- Soper, N.J. (1988) Timing and geometry of collision, terraine accretion and sinistral strike-slip events in the British Caledonides. In: Harris, A. and Fettes, D.J. (Eds) *The Caledonian Appalachian Orogen*. *Geol. Soc. Lond. Spec. Publ.* 38, 481-492.
- Spilsbury, W. and Fletcher, K. (1973) Application of regression analysis to interpretation of geochemical data from lake sediments in central British Columbia. *Can.J. Earth. Sci.* 11, 345-348.
- Spry, A. (1969) *Metamorphic textures*. Pergamon Press, Oxford. 350pp.
- Stanley, C.J. and Vaughan, D.J. (1982) Copper, lead, zinc and cobalt mineralization in the English Lake District : Classification, conditions of formation and genesis. *J. Geol. Soc. London*. 139, 569-579.
- Stanley, C.J. and Vaughan, D.J. (1982) mineralization in the Bonser Vein, Coniston, English Lake District : Mineral assemblages, paragenesis and formation conditions. *Min. Mag.* 46, 343-350.
- Stanley, C.J., Halls, G.S., Cammes, G.S. and James, J. (1989) Gold antimony mineralization at Loddiswell, Devon. Abstract, Gold 89 in Europe.
- Stanley, C.R. and Sinclair, A.J. (1985) Anomaly recognition for multi-element geochemical data : A background characterisation approach. 11th IGES Program with Abstracts. 11, 87.
- Stanton, R.L. and McDonald, A.J. (1962) Fielddetermination of Sb in soil and sediment samples. *Bull. Inst. Min. Metall.* 517-522.
- Stanton, R.L. and Ramsey, W.R.H. (1980) Exhalative ores, volcanic loss and the problems of the island arc calc-alkaline series : A review and hypothesis. *Norges. Geol. Unders.* 360, 9-58.
- Steed, G.M. (1981) Mineralogical and geochemical results for drill core samples from the Clontibret Gold Prospect, Part 1. Munster Base Metals Ltd., Unpub. Company Report. 12pp.
- Steed, G.M. (1982) Gold mineralization within the Clontibret area : Mineralogical and geochemical results, Part 2. Munster Base Metals Ltd., Unpub. Company Report. 15pp.
- Steed, G.M. and Annels, A.E. (1980) *The Ogofau Gold Mines. Mining field centre guide*. Univ. College, Cardiff Publications. 1-4.
- Steed, G.M., Annels, A.E., Shrestha, P.L. and Tater, P.S. (1976) Geochemical and biogeochemical prospecting in the area of the Ogofau gold mines, Dyfed, Wales. *Inst. Min. Metall.* B109-117.

- Steed, G.M. and Morris, J.H. (1985) Gold mineralization in Ordovician greywackes at Clontibret, Ireland. GAC/MAC Program with Abstracts. 10, A59.
- Stegena, L. (1983) Leaching in rocks, some physical properties. In: Augustithis, S.S. (Ed) Leaching and diffusion in rocks and their weathering products. Theophrastus Pub. Athens.
- Stendal, H. (1981) Geochemistry and genesis of arsenopyrite mineralization in Late Precambrian sediments in central east Greenland. Trans. Inst. Min. Metall. 91, B187-191.
- Stephens, W.E (1988) Granitoid plutonism in the Caledonian orogen of Europe. In: Harris, A.L. and Fettes, D.J. (Eds) The Caledonian - Appalachian Orogen. Geol. Soc. Lond. Spec. Publ. 38, 269-274.
- Stern, W.B. (1976) On trace element analysis of geological samples by X-ray fluorescence. J. X-ray Spectrometry. 5, 56-60.
- Stewart, D. (1799) The report of Donald Stewart, Itinerant Mineralogist to the Dublin Society. Trans. Dublin Soc. 1, 142pp.
- Stewart, J.W. (1984) The auriferous carbonate exhalite concept re-examined. Geol. Soc. America. Prog. Abst. 4-7. Reno, November.
- Stillman, C.J. (1988) Ordovician to Silurian volcanism in the Appalachian-Caledonian Orogen. In: Harris, A.L. and Fettes, D.J. (Eds) The Caledonian - Appalachian Orogen. Geol. Soc. Lond. Spec. Publ. 38, 269-274.
- Stone, P. (1981) Geological relationships within an Ordovician shale belt in Galloway. J. Scott. Geol. 17, 205-214.
- Stone, P. (1983) Base metal mineralization associated with an Ordovician shale sequence in southwest Scotland. British Geological Survey Mineral Reconnaissance Programme Report No. 69.
- Stone, P. and Leake, R.C. (1983) Disseminated and epigenetic lead - zinc mineralization in Ordovician mudstone, southwest Scotland. Scott. J. Geol. 20, 181-190.
- Stone, P. and Gallagher, M.J. (1984) Mineral exploration in Lower Palaeozoic turbidites of southern Scotland. In: Prospecting in Areas of Glaciated Terrain. Inst. Min. Metall. Pub. 201-211.
- Stone, P., Floyd, J.D., Barnes, R.P. and Lintern, B.C. (1987) A sequential back-arc and foreland basin thrust duplex model for the Southern Uplands of Scotland. J. Geol. Soc. Lond. 144, 753-764.
- Stow, D.A.V. (1984) Anatomy of debris flow deposits. In: Hay, W.W. (Ed) Initial Reports of the Deep Sea Drilling Project. LXXV, 801-807.
- Stow, D.A.V. and Piper, D.J.W. (1984) (Eds) Fine grained sediments. Geological Society of London. Special Pub. No. 15, 659pp.
- Streckeisen, A.L. (1973) Plutonic Rocks. Classification and nomenclature recommended by the IUGS Subcommittee on the systematics of igneous rocks. Geotimes, 18, 26-30.
- Stringer, P. and Treagus, J.E. (1980) Non-axial planar S1 cleavage in the Hawick Rocks of the Galloway area, Southern Uplands, Scotland. J. Struct. Geol. 2, 317-331.
- Stringer, P. and Treagus, J.E. (1981) Asymmetrical folding in the Hawick Rocks of the Galloway area, Southern Uplands, Scotland. Scott. J. geol. 17, 129-148.

- Strong, D.F. (1974) Plate tectonic setting of Appalachian-Caledonian mineral deposits as indicated by Newfoundland examples. Society of Mining Engineers, A.I.M.E., 256, 121-128.
- Stumpfl, E.F. and Riemann, C. (1980) Ocean floor basalts, associated volcanics and stibnite mineralization in the Southern Central Alps. IGCP Project No. 169. Athens Conference Abstracts.
- Styles, M.T., Stone, P. and Floyd, J.D. (1989) Arc detritus in the Southern Uplands : mineralogical characterisation of a 'missing' terraine. J. Geol. Soc. Lond. 146, 397-400.
- Sun, S. (1980) Lead isotope study of young volcanic rocks from mid-oceanic ridges, ocean islands and ocean arcs. Phil. Trans. Roy. Soc. London. A297, 409-445.
- Suppel, D.W. (1980) The Xikouangshan Antimony Mines. In: Renwick, A. (Ed) The Australian Geological Delegation to China. Austr. Gov. Pub. 54-56.
- Sunblad, K., Zachrisson, E., Smeds, S.A., Berglund, S. and Alinder, C. (1985) Sphalerite geobarometry and arsenopyrite geothermometry applied to metamorphosed sulphide ores in the Swedish Caledonides. Econ. Geol. 79, 1660-1668.
- Sweeney, R.E. and Kaplan, I.R. (1973) Pyrite framboid formation : Laboratory synthesis and marine sediments. Econ. Geol. 68, 618-634.
- Syers, J.K., Williams, J.D.H., Walker, T.W. and Chapman, S.L. (1970) Mineralogy and forms of inorganic phosphorus in a greywacke soil-rock weathering sequence. Soil. Sci. 110, 100-106.
- Tatsch, J.H. (1975) Gold deposits-origin, evolution and present characteristics. Tatsch Associates Pub. 275pp.
- Taylor, B.E. (1981) Hydrothermal fluids in the Mother Lode Gold Deposits. E.O.S. 62, 1059.
- Taylor, G.R. (1982) A mechanism for framboid formation as illustrated by a volcanic exhalative sediment. Mineral Deposita. 17, 23-36.
- Taylor, G.R., Gwatkin, C.C. and Chork, C.Y. (1984) Statistical interpretation of element distribution within distal volcanic exhalative mineralization near Mount Chalmers, Queensland, Australia. Trans. Inst. Min. Metall. 93, B99-108.
- Taylor, H.P. (1974) The application of oxygen and hydrogen isotope studies to the problems of hydrothermal alteration and ore deposition. Econ. geol. 69, 843-883.
- Taylor, R. (1982) Sediments and stratabound economic minerals. Geotimes. 215-216.
- Taylor, S.R. (1964) Abundance of chemical elements in the continental crust : A new table. Geochem. Cosmochem. Acta. 28, 1273-1285.
- Taylor, S.R. and McLennan, S.M. (1981) The composition and evolution of the continental crust : Rare earth element evidence from sedimentary rocks. Phil. Trans. R. Soc. London. A301, 381-399.
- Taylor, S.R. and McLennan, S.M. (1985) The continental crust : Its composition and evolution. Blackwell.
- Temple, A.K. (1955) The Leadhills-Wanlockhead lead and zinc deposits. Trans. R. Soc. Edinburgh. 63, 85-113.

- Thirwell, M.F. (1981) Implications for Caledonian plate tectonic models of chemical data from volcanic rocks of the British Old Red Sandstone. *J. Geol. Soc. London*. 138, 123-138.
- Thirlwall, M.F. (1988) Wenlock to mid-Devonian volcanism of the Caledonian - Appalachian orogen. In: Harris, A.L. and Fettes, D.J. (Eds) *The Caledonian - Appalachian Orogen*. *Geol. Soc. Lond. Spec. Publ.* 38, 269-274.
- Thirlwall, M.F. (1989) Movement on the proposed terrane boundaries in Northern Britain : constraints from Ordovician-Devonian igneous rocks. *J. Geol. Soc. Lond.* 146, 373-377.
- Thomson, J.F.H., Lessman, J. and Thompson, A.J.B. (1986) The Temora Gold-Silver Deposit : A newly recognised style of high sulphur mineralization in the Lower Palaeozoic of Australia. *Econ. Geol.* 81, 732-738.
- Thompson, M. and Walsh, J.N. *A Handbook of Inductively Coupled Plasma Spectrometry*. Blackie, Glasgow, 273pp.
- Thompson, R.N. (1982) Magmatism of the British Tertiary Volcanic Province. *Scott. J. Geol.* 18, 49-107.
- Thompson, T.B., Trippel, A.D. and Dwelley, P.C. (1985) mineralized Veins and Breccias of the Cripple Creek District, Colorado. *Econ. Geol.* Vol. 80, No. 6, 1669.
- Thorpe, R.I. and Thomas, G.M. (1976) Gold content of greywacke and slate of the Goldenville Formation, Nova Scotia, as determined by neutron activation analysis. *Pap. Geol. Surv. Can.* 76, 319-326pp.
- Thost, Gustav, C.H. (1860) On the rocks, ores and other minerals on the property of the marquess of Breadalbane in the highlands of Scotland. *Q. J. Geol. Soc. Lond.* 16, 421-428.
- Threadgold, I.M. (1958) Antimony - gold mineralization at Steels Creek, near Yarra Glen, Victoria. In: Stillwell, F.L. *Anniversary Volume*. *Aust. Inst. Metall. Pub.* 241-248.
- Thurlow, J.G., Swanson, E.A. and Strong, D.F. (1975) Geology and lithochemistry of the Buchans polymetallic sulphide deposits, Newfoundland. *Econ. Geol.* 70, 130-144.
- Tidball, R.R. (1984) Geochemical classification by factor analysis of Missouri agricultural soils. *USGS Prof. Paper*. 954. 1, 1-19.
- Tilling, R.I., Gottfried, D. and Rowe, J.J. (1973) Gold abundance in Igneous rocks : bearing on gold mineralization. *Econ. Geol.* 68, 168-186.
- Tindle, A.G., McGarvie, D.W. and Webb, P.C. (1988) The role of hybridization and crystal fractionation in the evolution of the Cairnmore of Carsphairn Intrusion, Southern Uplands of Scotland. *J. Geol. Soc. Lond.* 145, 11-21.
- Tomkinson, M.J. (1985) A shear zone hosted gold deposit in the Carolina Slate Belt, Southern Appalachians, USA. *GAC/MAC Program with Abstracts*. 10, A63.
- Tooker, E.W. (1985) (Ed) Geological characteristics of sediment and volcanic-hosted disseminated gold deposits : Search for an occurrence model. *USGS Bull.* 1646, 150pp.
- Tooker, E.W. (1985) Discussion of the disseminated gold ore occurrence model. 107-150. In: Tooker, E.W. (Ed) *Geological characteristics of sediment and volcanic-hosted disseminated gold deposit : Search for an occurrence model*. *USGS Bull.* 1646, 1-150.

- Torrance, K.E. and Chan, V.W.C. (1980) A model of hydrothermal convection in an aquifer. *J. Geophys. Research.* 85, 2554-2558.
- Toulmin, P. and Clark, S.P. (1967) Thermal aspects of ore formation. In: Barnes, H.L. (Ed) *Geochemistry of Hydrothermal Ore Deposits*. Holt, Rinehart and Winston, New York. 670pp.
- Trench, A., Dentith, M.C., Bluck, B.J., Watts, D.R. and Floyd, J.D. (1988) Palaeomagnetic constraints on the geological terrane models of the Scottish Caledonides. *J. Geol. Soc. Lond.* 146, 405-409.
- Tukey, J.W. (1977) *Exploratory Data Analysis*. Addison-Wesley. 506pp.
- Tukey, P.A. and Tukey, J.W. (1981) Graphical display of data sets in three or more dimensions. In: Barnett, V. (Ed) *Interpreting Multivariate Data*. Wiley. 189-275pp.
- Turekian, K.K. and Wedepohl, K.H. (1961) Distribution of the elements in some major units of the earth's crust. *Bull. Geol. Soc. America.* 72, 175-192.
- Turner, J.S. and Gustafson, L.B. (1978) The flow of hot saline solutions from vents in the sea floor : some implications for exhalative massive sulphide and other deposits. *Econ. Geol.* 73, 1082-1100.
- Underwood, M.B. and Karig, D.E. (1980) Role of submarine canyons in trench and trench-slope sedimentation. *Geology.* 8, 432-436.
- Van de Kamp, P.C. and Leake, B.E. (1986) Petrography and geochemistry of feldspathic and mafic sediments of the north eastern Pacific margin. *Trans. Roy. Soc. Edin.* 76, 411-449.
- Vaughan, D.J. and Craig, J.R. (1978) *Mineral chemistry of metal sulphides*. Cambridge University Press. 493pp.
- Velleman, P.F. and Hoaglin, D.C. (1981) *Applications, basics and computing of exploratory data analysis*. Duxbury Press. 354pp.
- Viljoen, R.P., Sangster, R. and Viljoen, M.J. (1970) Some thoughts on the origin and processes responsible for the concentration of gold in the early Precambrian of Southern Africa. *Mineralium Deposita.* 5, 164-180.
- Vine, J.D. and Tourtelot, E.B. (1970) Geochemistry of black shale deposits : A summary report. *Econ. Geol.* 65, 253-272.
- Vlasimsky, P. (1979) On the geochemistry of Proterozoic rocks of the Pribram ore district. *Cas. Mineral. Geol.* 24, 113-133
- Voin, M.I. (1978) Neutron activation analysis in the detection of Sb aureoles from subsurface deposits. *Geochem. Inst.* 15, 63-67.
- Vokes, F.M. (1968) Regional metamorphism of the palaeozoic geosynclinal sulphide ore deposits of Norway. *Trans. Inst. Min. Metall.* 77, B53-59.
- Vokes, F.M. (1980) Some aspects of research into the Caledonian stratabound sulphide deposits of Scandinavia. *Norges. Geol. Unders.* 360, 77-93.
- Vokes, F.M. (1989) Gold in Norwegian Caledonian Ophiolites. Abstract, Gold 89 in Europe.

- Vulchin, Y.I., Zelizna, S.T., Fedushchak, M.Y. and Radchenko, L.M. (1978) Micro elements in the black argillites of the Ukrainian Carpathians. *Geol. Geokhim. Goryuch. Iskop.* 50, 38-42.
- Walden, A.R. (1972) Quantitative comparison of automated contouring algorithms. KOX Project, Technical Report. Kansas Geological Survey. 115pp.
- Walker, R.G. (1978) Deep-water sandstone facies and ancient submarine fans : Models for exploration for stratigraphic traps. *Am. Assoc. Pet. Geol. Bull.* 62, 932-966.
- Walker, R.G. (1979) Facies Models 8. Turbidites associated coarse clastic deposits. *Geosci. Canada. Reprint Series.* 1, 91-104.
- Walker, R.G. and Mutti, E. (1973) Turbidite facies and facies associations. In: *Turbidites and deep water sedimentation, (S.E.P.M. Pacific Section, short course)*, 119-158.
- Walker, R.R., Matulich, A., Amos, A.C., Watkins, J.J. and Mannaed, G.W. (1975) The geology of the Kidd Creek Mine. *Econ. geol.* 70, 80-89.
- Wall, V.J. (1976) Gold and pyrophyllite mineralization in the Devonian acid volcanics of the Yawal-Eden belt. *Bull. Aust. Soc. Explor. Geophysicists.* Vol. 7, No. 1.
- Walsh, J.F., Frederick, M. and Kesler, S.E. (1984) Fluid inclusion analysis of auriferous vein quartz from the Porcupine District, Ontario. *GAC/MAC Program with Abstracts.* 9, London, Ontario.
- Walsh, J.N., Buckley, F. and Barker, J. (1981) The simultaneous determination of the rare earth elements in rocks using inductively coupled plasma source spectrometry. *Chemical Geology.* 33, 141-153.
- Walsh, J.N. and Howie, R.A. (1986) Recent developments in analytical methods : uses of inductively coupled plasma source spectrometry in applied geology and geochemistry. *Applied Geochemistry* 1, 161-172.
- Walton, E.K. (1957) Two Ordovician conglomerates in south Ayrshire. *Trans. Geol. Soc. Glasgow.* 22, 133.
- Walton, E.K. (1961) Some aspects of the succession and structure in the Lower Palaeozoic rocks of the Southern Uplands of Scotland. *Geol. Rdsch.* 53, 63-77.
- Walton, E.K. (1984) Lower Palaeozoic : Structure and Palaeogeography. In: Craig, G.Y. (Ed) *Geology of Scotland.* Oliver and Boyd. 139-166.
- Walton, E.K. (1984) Lower Palaeozoic : Stratigraphy. In: Craig, G.Y. (Ed) *Geology of Scotland.* 105-137.
- Wang Chung, Y. (1952) Antimony, its geology, metallurgy, industrial use and economics. Charles Griffin and Co. Pub. 170pp.
- Warren, P.T. (1963) The petrography, sedimentation and provenance of the Wenlock rocks near Hawick, Roxburghshire. *Trans. Ed. Geol. Soc.* 19, 225-255.
- Warren, P.T. (1964) The stratigraphy and structure of the Silurian rocks southeast of Hawick, Roxburghshire, Scotland. *Quart. J. Geol. Soc.* 120, 193-222.

- Wass, S.Y. and Rogers, N.W. (1980) Mantle metasomatism. *Geochim. Cosmochim. Acta.* 44, 1811-1823.
- Watkins, R. and Stensrud, H.L. (1983) Age of sulphide ores in the west Shasta and east Shasta districts, Klamath Mountains, California. *Econ. Geol.* 78, 340-343.
- Watson, J.V. (1984) Continental crust regimes as factors in the formation of sedimentary ore deposits. *J. Geol. Soc. Lond.* 141, 215-220.
- Watson, J.V. (1984) The ending of the Caledonian Orogeny in Scotland. *J. Geol. Soc. London.* 141, 193-214.
- Weaver, B. and Tarney, J. (1984) Empirical approach to estimating the composition of the continental crust. *Nature.* 310, 575-578.
- Webb, J.S. (1959) Notes on geochemical prospecting for lead-zinc deposits in the British Isles. In: *The future of non-ferrous mining in Great Britain and Ireland.* Inst. Min. Metall. London. Pub. 419-436.
- Webb, J.S., Nichol, I., Foster, R., Lowenstein, P.L. and Howarth, R.J. (1973) Provisional Geochemical Atlas of Northern Ireland. Technical Communication No. 60. Applied Geochemistry Research Group. Imperial College, London.
- Weber, J.N. (1959) The geochemistry of some greywackes and some shales. M. Sc. Thesis. McMaster University.
- Weber, J.N. and Middleton, G.V. (1961) Geochemistry of the turbidites of the Normanskill and Charny Formations. *Geochem. Cosmochim. Acta.* 22, 200-243.
- Webster, J.G. (1986) The solubility of gold and silver in the system Au-Ag-S at 25°C at 1 atmosphere. *Geochim. et Cosmochim. Acta.* 50, 1837-1845.
- Wedepohl, K.H. (1978) (Ed) *Handbook of Geochemistry.* Springer-Verlag. 845pp.
- Wehrenberg, J.P. and Silvermn, A. (1965) Studies of base metal diffusion in experimental and natural systems. *Econ. Geol.* 60, 317-350.
- Wei, Dui-Tin, and Saukov, A.A. (1961) Physicochemical factors in the genesis of antimony deposits. *Geochemistry.* 6, 510-516.
- Weir, J.A. (1968) Structural history of the Silurian rocks to the west of Gatehouse, Kircudbright. *Scott. J. Geol.* 31-52.
- Weir, J.A. (1974) The sedimentology and diagenesis of the Silurian rocks on the coast, west of Gatehouse, Kirkcudbrightshire. *Scott. J. Geol.* 10, 165-186.
- Weir, J.A. (1979) Tectonic contrasts in the Southern Uplands. *Scott. J. Geol.* 15, 168-186.
- Weir, J.A. (1981) Tectonic contrasts in the Southern Uplands. *J. Scott. Geol.* 17, 73-74.
- Weir, J.A. (1981) Deformation sequences in the Southern Uplands : A reply. *J. Scott. Geol.* 17, 81-82.
- Weissburg, B.G. (1969) Gold and silver ore-grade precipitates from New Zealand thermal waters. *Econ. geol.* 64, 95-108.

- Weissberg, B.G., Brown, P.R.L. and Seaward, T.M. (1979) Ore metals in active geothermal systems. In: Barnes, H.L. (Ed) *Geochemistry of hydrothermal ore deposits*. Wiley.
- Wellmer, F.W. and Giroux, G.H. (1980) Statistical and geostatistical methods applied to the exploration work of the Nanisivik Zn-Pb mine, Baffin Island, Canada. *Math. Geol.* 12, 321-337.
- Wells, J.D. and Mullens, T.E. (1973) Gold bearing arsenian pyrite determined by microprobe analysis. Cortez and Carlin gold mines, Nevada. *Econ. Geol.* 68, 187-201.
- Welsh, W. (1964) The Ordovician rocks of north west Wigtownshire. Ph.D. Thesis, Edinburgh University.
- Welsh, W. (1981) Tectonic contrasts in the Southern Uplands : Comment. *J. Scott. Geol.* 17, 83-84.
- Wendel, C.A. (1967) A unique mineral assemblage in Turkey. *Econ. geol.* 62, 276-278.
- Wenrich, K.J. (1986) Geochemical exploration for mineralized breccia pipes in Northern Arizona, USA. *Applied Geochemistry*. 1, 469-485.
- Wheatley, C.J.V. (1971) Aspects of metallogenesis within the Southern Caledonides of Great Britain and Ireland. *Trans. Inst. Min. Metall.* 80, B211-223.
- White, W.H. (1943) The mechanism and environment of gold deposition in veins. *Econ. Geol.* 38, 512-532.
- White, D.E. (1985) Vein and disseminated gold-silver deposits of the Great Basin through space and time. 5-14. In: Tooker, E.W. (Ed) *Geological characteristics of sediment and volcanic-hosted disseminated gold deposits : Search for an occurrence model*. USGS Bull. No. 1646, 1-150.
- Whitehead, R.E.S. and Govett, G.J.S. (1974) Exploration rock geochemistry : Detection of trace element halos at Heath Steele mines (N.B. Canada) by discriminant analysis. *J. Geochem. Explor.* 3, 371-386.
- Whitley, G. (1915) The Ictis of Diodorus in the light of modern theories. *Trans. Royal Geol. Soc. Cornwall.* 15, 55-70.
- Wildeman, T.R. and Condie, K.C. (1973) Rare earths in Archean greywackes from Wyoming and from the Fig Tree group, South Africa. *Geochim. Cosmochim. Acta.* 37, 439-435.
- Willan, R.C.R. (1980) Stratabound sulphide mineralization in the Dalradian supergroup of the Grampian Highlands, Scotland. *Norges. Geol. Unders.* 360, 241-258.
- Willan, R.C.R. (1981) Geochemistry of host rocks to the Aberfeldy Baryte deposit, Scotland. In: Hall, A.J. (Ed) *Caledonian-Appalachian Stratabound Sulphides, Scotland*. 46-53.
- Willan, R.C.R. and Coleman, M.L. (1983) Sulphur isotope study of the Aberfeldy barium, zinc, lead deposits and minor sulphide mineralization in the Dalradian metamorphic terrain, Scotland. *Econ. Geol.* 78, 1619-1656.
- Willan, R.C.R. and Hall, A.J. (1980) Sphalerite geobarometry and trace element studies on stratiform sulphide from McPhuns Cairn, Loch Fyne, Argyll, Scotland. *Trans. Inst. Min. Metall.* 90, B31-40.
- Williams, A. (1962) The Barr and Lower Ardmillam Series (Caradoc) of the Girvan district, southwest Ayrshire. *Mem. Geol. Soc. London.* 3.

- Williams, G.J. (1974) Gold mineralization in Early Palaeozoic rocks. *Aust. Inst. Min. Metall.* 4, 33-40.
- Williams, J. (1810) *Natural history of the mineral kingdom*. Edinburgh. 365pp.
- Williams, J. (1964) The mineralogical collections of the Dumfries Burgh Museum. *Trans. Dumfries and Galloway Natural Hist. and Antiq. Soc.* 41, 201-215.
- Williams, J. (1965) Further notes on mineralogy in Dumfries and Galloway. *Trans. Dumfries and Galloway Natural Hist. and Antiq. Soc.* 42, 14-24.
- Williams, P.J. and Badham, J.P.N. (1986) Application of lithogeochemistry to prospecting in the northwestern Iberian meta-ophiolite belt. In: Gallagher, M.J., Ixer, R.A., Neary, C.R. and Pritchard, H.M (Eds) *Metallogeny of basic and ultrabasic rocks*. IMM Publication.
- Williamson, D.R. and Thomas, T.L. (1972) Trend analysis of Alluvial deposits by use of rolling mean techniques. *Inst. Min. Metall.* 80, 94-101.
- Wilson, G.V. (1921) Lead, zinc, copper and nickel ores of Scotland. *Spec. Rept. Min. Res.* Vol. XVII, 13pp.
- Wilson, I.R. (1973) Wallrock alteration studies at Ashanti mine, Ghana and at Geevor mine, Cornwall. Ph.D. Thesis, University of Leeds.
- Winchester, J.A., Lambert, R.St.J. and Holland, J.G. (1981) Geochemistry of the western part of the Moinian assemblage. *Scott. J. Geol.*
- Winchester, J.A. and Max, M.D. (1989) Discussion on the provenance of granite boulders in conglomerates of the Northern and Central Belts of the Southern Uplands. *J. Geol. Soc. Lond.* 146, 359-360.
- Winkler, H.G.F. (1971) *Petrogenesis of the metamorphic rocks*. Springer-Verlag.
- Witton, D.H.C. (1985) REE and background Au/Ag evidence concerning the origin of hydrothermal fluids in the Cape Ray electrum deposits, southwest Newfoundland. *CIM Bull.* 78, 48-60.
- Witton, D.H.C. and Strong, D.F. (1986) Granite related gold mineralization in the Cape Ray fault zone of southwestern Newfoundland. *Econ. Geol.* 81, 281-295.
- Wolfe, J.A. (1980) Fluidisation verses phreatomagmatic explosions in breccia pipes. *Econ. Geol.* 75, 1105-1109.
- Woolenberg, H.A., Harold, A., Smith, A.R. and Bailey, E.H. (1967) Radioactivity of the Upper Mesozoic greywackes in the northern Coast Ranges, California. *J. Geophys. Res.* 72, 4139-4150.
- Wood, S.A., Crearar, D.A. and Borcsik, M. (1983) GAC/MAC Program with Abstracts. 8, 722.
- Worthington, J.E. and Kiff, I.T. (1970) A suggested volcanogenic origin for certain gold deposits in the slate belt of the Northern Carolina Piedmont. *Econ. Geol.* 65, 529-537.
- Wrafter, J.P. and Graham, J.R. (1989) Ophiolitic detritus in the Ordovician sediments of South Mayo, Ireland. *J. Geol. Soc. London* 146, 213-215.
- Wyborn, D. (1982) Basement geology of northern Victoria Land and some possible relations with south-eastern Australia. *J. Aust. Geol. Geoph.* 7, 145-146.

OMISSIONS

- Abbate, E., Bortolotti, V. and Passerini, P. (1970) Olistostromes and Olistoliths. *Sediment. Geol.* 4, 521-57.
- Agricola, G. (1546) *De Ortu et Causis Subterraneorum*.
- Agricola, G. (1556) *De Re Metallica*.
- Anderson, T.B. and Oliver, G.J.H. (1986) The Orlock Bridge Fault: A major late Caledonian sinistral fault in the Southern Uplands terrane, British Isles. *Trans. Royal Soc. Edinburgh*, 77, 203-222.
- Anderson, T.B. (1987) The onset and timing of Caledonian sinistral shear in County Down. *J. Geol. Soc. Lond.* 144, 817-825.
- Anderson, I.K., Andrew, C.J., Ashton, A.J., Boyce, A.J., Caulfield, J.B.D., Fallick, A.E. and Russell, M.J. (1989) Preliminary sulphur isotope data of diagenetic and vein sulphides in the Lower Palaeozoic strata of Ireland and Southern Scotland: implications for Zn+Pb+Ba mineralisation. *J. Geol. Soc. Lond.* 146, 715-720.
- Armannsson, H. and Darling, W.G. (1986) Stable isotopic aspects of fluid flow in the Krafla, Namafjall and Theistareykir geothermal systems of northeastern Ireland. *Chemical Geology* 76.
- Atkinson, S. (1619) The discovery and historie of the gold mynes in Scotland. (manuscript written in 1619) The Bannatyne Club, 1825. James Ballantyne and Co. Edinburgh.
- Bakken, B.M., Hochella, M.F., Marshall, A.F. and Turner, A.M. (1989) High-resolution microscopy of gold in unoxidized ore from the Carlin Mine, Nevada. *Econ. Geol.* 84, 174-179.
- Barnes, H.L. (1967) *Geochemistry of hydrothermal ore deposits*. New York, 670p.
- Barnes, H.L. (1979) Solubilities of ore minerals. In: Barnes, H. L. (ed) *Geochemistry of hydrothermal ore deposits*. New York (2nd Edition).
- Barnes, R.P., Rock, N.M.S. and Gaskarth, J.W. (1986) Late Caledonian dyke swarms in Southern Scotland. *Geol. Journal* 21, 101-125.
- Barnes, R.P., Lintern, B.C. and Stone, P. (1989) Timing and regional implications of deformation in the Southern Uplands of Scotland. *J. Geol. Soc. London* 146, 905-908.
- Barton, P.B. (1969) Thermochemical study of the system Fe-As-S. *Geochim. et Cosmochim. Acta*, 33, 841-857.
- Bell, B. (1984) *Igneous petrochemistry course notes*, Department of Applied Geology, Strathclyde University.
- Bhatia, M.R. (1983) Plate tectonics and geochemical composition of sandstones. *J. Geol.* 91, 611-643.
- Bhatia, M.R. and Taylor, S.R. (1981) Trace element geochemistry and sedimentary provinces: a study from Tasman geosynclines, Australia. *Chemical Geology*, 33, 115-25.
- Blatt, H., Middleton, G. and Murray, R. (1972) *Origin of sedimentary rocks*. Prentice Hall.
- Bohlke, J.K. and Kistler, R.W. (1986) Rb-Sr, K-Ar and stable isotopic evidence for the ages and sources of fluid components of gold-bearing quartz veins in the Northern Sierra Nevada Foothills metamorphic belt, California. *Econ. Geol.* 81, 296-322.
- Bouma, A.H. (1962) *Sedimentology of some flysh deposits*. Elsevier, 168pp.
- Bouma, A.H. and Nota, D.J.G. (1962) Detailed graphic logs of sedimentary formations. *Rept. Int. Geol. Cong.* 21, 52-73.
- Brenchley, P.J. and Cocks, L.R.M. (1982) Ecological associations in a regressive sequence: the latest Ordovician of the Oslo-Asker district, Norway. *Palaentology* 25, 783-815.

- Xin, W. and Delbove, F. (1989) Hydrothermal synthesis of gold bearing arsenopyrite. Abstract, Gold 89 in Europe.
- Yin, W.D. and Saukov, A.A. (1961) Physicochemical factors in the genesis of antimony deposits. *Geokhimiya*. 6, 510-516.
- Young, B. (1985) mineralization associated with the Eskdale Intrusion, Cumbrian. Rep. Program. Dir. A. Br. Geol. Surv. No. PDA2 85/3.
- Young, B., Fortey, N.J. and Nancarrow, P.H.A. (1986) An occurrence of tungsten mineralization in the Eskdale Intrusion, West Cumbria. *Proc. York. Geol. Soc.* 46, 15-21.
- Young, T.Y. and Calvert, M. (1974) Classification, Estimation and Pattern Recognition. American Elsevier Publishing Co. Inc.
- Zairi, N.M., Sher, S.D., Strizhev, V.P., Batrak, V.N. and Panratyeva, L.D. (1978) Isotopic composition of sulphur from the zone of gold bearing sulphide impregnation. *Int. Geol. Rev.* 29, 935-941.
- Zajac, I.S. (1974) The stratigraphy and mineralogy of the Sokoman Formation in the Knob Lake area, Quebec and Newfoundland. *Can. Geol. Surv. Bull.* No. 220, 159pp.
- Zhou, J.X. (1987) An occurrence of shoshonites near Kilmelford in the Scottish Caledonides and its tectonic implications. *J. Geol. Soc. Lond.* 144, 699-706.
- Zhou, J.X. (1987) Geology of a copper-bearing intrusive suite near Kilmelford Argyllshire, Scotland. *Trans. Inst. Min. Metall.* 96, B179-186.
- Zhou, J.X. (1987) Lithogeochemical exploration for copper and gold in the Kilmelford district, Argyllshire, Scotland. *Trans. Inst. Min. Metall.* 96, B187-194.
- Ziserman, A. and Serment, D. (1976) Typological classification of large antimony deposits. *Soc. Geol. Fr. Mem. Hors. Ser.* 7, 285-294.
- Zuffra, G.G. (1985) Provinces of Arenites. Reidel Pubs.

OMISSIONS

- Anderson, I.K., Andrew, C.J., Ashion, A.J., Boyce, A.J., Caulfield, J.R.D., Fallick, A.E. and Russell, M.J. (1989) Preliminary sulphur isotope data of diagenetic and vein sulphides in the Lower Palaeozoic strata of Ireland and Southern Scotland: implications for Zn+Pb+Ba mineralisation. *J. Geol. Soc. Lond.* 146, 715-720.
- Bakken, B. M., Hochella, M. F., Marshall, A.F. and Turner, A. M. (1989) High-resolution microscopy of gold in unoxidized ore from the Carlin Mine, Nevada. *Econ. Geol.* 84, 174-179.
- Cumeeen, R. and Sillitoe, R. H. (1989) Palaeozoic hot spring sinter in the Drummond Basin, Queensland, Australia. *Econ. Geol.* 84, 135-142.
- Earls, G., Clifford, J.A. and Meldrum, A.H. (1989) Carraghianalt gold deposit, County Tyrone, Northern Ireland. Proceedings of the 13th annual commodity meeting. *Trans. Inst. Min. Metall.* 98, B50-51.
- Gallagher, M.J., Stone, P. and Duller, P.R. (1989) Gold-bearing arsenic-antimony concentrations in

- Bridges, P. (1987) X-ray diffraction sample preparation techniques. Internal technical notes, The Geochem Group Ltd, Unpub.
- Brown, M. (1980) Porphyry style copper mineralization at Black Stockarton Moor, Southwest Scotland. BGS Mineral Reconnaissance Program Report 30.
- Buisson, G. and Leblanc, M. (1985) Gold in carbonatized ultramafic rocks from ophiolite complexes. *Econ. Geol.* 80, 2028-29.
- Buturlinov, N.V. and Latysh, I.K. (1970) Gold and silver in magmatic rocks of the Donets Basin. *Geol. Zh. (Kiev)* 30, 69-75.
- Clark, L.A. (1960) The Fe-As-S system: Phase relations and applications. *Econ. Geol.* 55, 1345-1381.
- Clemmy, H. (1979) Tectonic and sedimentary breccias: Nature and origin. *Trans. Inst. Min. Metall.* B78.
- Clifford, J.A. (1986) A note on gold mineralization in Co. Tyrone. 45-49. In: Andrews, C.J., Crowe, R.W.A., Finlay, S., Pennell, W.M. and Pyne, J.F. (Eds) *Geology and genesis of mineral deposits in Ireland*. Special Pub. Irish Assoc. Econ. Geology.
- Colvine, A.C. (1984) An integrated model for the origin of Archean lode gold deposits. Open file Report, Ontario Geological Survey 5524, 98pp.
- Cooper, D.C., Bide, P., Cameron, D.G., Parker, M.E., Haslam, H.W., Easterbrook, G.D. and Basham, I.R. (1985) Exploration for porphyry-style copper mineralisation near Llandeloy, Southwest Dyfed. BGS Mineral Reconnaissance Program Report 79.
- Cooper, D.C., Bide, P., Cameron, D.G., Bell, N. and Allen (1985) A reconnaissance geochemical drainage survey of the Harlech Dome, North Wales. BGS Mineral Reconnaissance Program Report 74.
- Craig, J.R. and Vaughan, D.J. (1981) *Ore Microscopy and Ore Petrography*. John Wiley pubs.
- Cunneen, R. and Sillitoe, R. H. (1989) Palaeozoic hot spring sinter in the Drummond Basin, Queensland, Australia. *Econ. Geol.* 84, 135-142.
- Dawson, J. (1965) Re-examination of gold occurrences Strath Kildonan, Sutherland, Scotland. Geological Survey of Great Britain, Atomic Energy Division Report 265.
- De La Beche (1839) Report on the Geology of Cornwall, Devon and West Somerset. Memoir Geol. Survey UK.
- Dickinson, K. (1971) Tectonics and sedimentation. SEPM Special Paper.
- Dickinson, W.R. and Suczek, C.A. (1979) Plate tectonics and sandstone composition. *Bull. Am. Assoc. Petrol. Geol.* 63, 2164-72.
- Drummond, A.D. and Goodwin, C.I. (1976) Hypogene mineralisation: an empirical evaluation of alteration zoning. In: Sutherland-Brown (Ed) *Porphyry deposits of the Canadian Cordillera*. Can. Inst. Min. Metall. Spec. Volume 15, 52-63.
- Duff (1985) Chapter 5. In: Craig, G.Y. (ed) *Geology of Scotland*. Scottish Academic Press.
- Dunbar, A. (1970) Gold in Scotland. *Glasgow Herald*.
- Earls, G., Clifford, J.A. and Meldrum, A.H. (1989) Curraghinalt gold deposit, County Tyrone, Northern Ireland. Proceedings of the 13th annual commodity meeting. *Trans. Inst. Min. Metall.* 98, B50-51.
- Edwards, R.R. (1976) Aspects of trace metal and ore distribution in Cornwall. *Trans. Inst. Min. Metall.* 85, B83-90.

- Ellis, R.A., Coats, J.S., Fortey, N.J. and Johnson, C.E. (1977) Investigation of disseminated copper mineralisation near Kilmelford, Argyllshire, Scotland. BGS Mineral Reconnaissance Program Report 9.
- Ellis, R.A., Marsden, G.R. and Fortey, N.J. (1978) Disseminated sulphide mineralisation at Garbh Achadh Argyllshire, Scotland. BGS Mineral Reconnaissance Program Report 23.
- Emblin, R. (1978) A pennine model for the diagenetic origin of base-metal ore deposits in Britain. Bull. Peak District Historical Soc. 7, 5-20.
- Firman, R.J. and Lee, M.K. (1986) Age and structure of the concealed English Lake District batholith and its probable influence on subsequent sedimentation, tectonics and mineralisation. In: Geology in the real World. Institute of Mining and Metallurgy, 117-127.
- Fortey, N.J. (1981) Drillcore specimens from Penkiln Burn, Southwest Scotland. Inst. Geol. Sci. Appl. Mineral. Unit. Scientific and Technical Report 81/2.
- Gallagher, M.J. (1977) Lead, Zinc and copper mineralization in basal Carboniferous rocks at Westwater, south Scotland. BGS Mineral Reconnaissance Program Report 17, 80pp.
- Gallagher, M.J., Stone, P. and Duller, P.R. (1989) Gold-bearing arsenic-antimony concentrations in Silurian greywackes, south Scotland. Proceedings of the 13th annual commodity meeting. Trans. Inst. Min. Metall. 98, B58-60.
- Gilmour, P. (1977) Mineralized intrusive breccias as guides to concealed porphyry systems. Econ. Geol. 72, 290-298.
- Glen, R.A. (1987) Copper and gold-rich deposits in deformed turbidites at Cobar, Australia: Their structural control and hydrothermal origin. Econ. Geol. 82, 124-140.
- Gumiel, P. and Arribas, A. (1987) Antimony deposits in the Iberian Peninsula. Econ. Geol. 82, 1453-1463.
- Halliday, A.N., Aftalion, M., Van Breemen, O. and Jocelyn, J. (1979) Petrogenetic significance of Rb-Sr and U-Pb isotope systems in the c.400ma old British Isles granitoids and their hosts. In: Harris, A.L., Holland, C.H. and Leake, B.E. (Eds) The Caledonides of the British Isles - Reviewed. Special Pub. Geol. Soc. London.
- Halliday, A.N., Stephens, W.E. and Harmon, R.S. (1980) Rb-Sr and O-isotopic relationships in 3 zoned Caledonian granite plutons, Southern Uplands, Scotland: Evidence for varied sources of hybridisation of Magmas. J. Geol. Soc. London. 137, 329-349.
- Hampton, M.A. (1972) The role of subaqueous debris flows in generating turbidity currents. J. Sed. Petrol. 42, 775-93.
- Harris, A.L. and Fettes, D.J. (1988) Eds - The Caledonian Appalachian Orogen. Geol. Soc. Lond. Spec. Pub. 38.
- Harris, M., Kay, E.A., Widnall, M.A., Jones, E.M. and Steele, G.B. (1988) Geology and mineralization of the Lagaloan intrusive complex, Western Argyll, Scotland. Trans. Inst. Min. Metall. 97, B15-27.
- Haselock, P.J. (1984) The systematic geochemical variation between two tectonically separate successions in the Southern Monadhliaths, Invernesshire. Scott. J. Geology.
- Heddle, M.F. (1878) A brief description of the maps of Shetland. Min. Mag. 2, 253-285.
- Heddle, M.F. (1919) Geology and Mineralogy of Scotland.
- Henkel, J.F. (1725) Pyritologia oder Keishistorie, Leipzig.
- Henley, R.W. and Brown, K.L. (1985) A practical guide to the thermodynamics of geothermal fluids and hydrothermal ore deposits. 25-44 In: Berger, B.R. and Bethke, P.M. (Eds) Geology and Geochemistry of Epithermal Systems. Reviews in Economic Geology Volume 2.

- Hiscott, R.N. (1981) Deep-sea fan deposits in the Macigno Formation of the Gordana Valley, Northern Apennines, Italy. *J. Sed. Pet.* 51, 1015-1033.
- Holl, R. and Maucher, A. (1976) The stratabound ore deposits in the Eastern Alps. In: Wolf, K.H. (ed) *Handbook of stratabound and stratiform ore deposits*, Elsevier.
- Hutton, J. (1788) *Theory of the Earth*. Trans. Roy. Soc. Edinburgh 1, 204-304.
- Ixer, R.A., Stanley, C.J. and Vaughan, D.J. (1979) Cobalt-, Nickel- and Iron-bearing sulpharsenides from the North of England. *Min. Mag.* 43, 389-95.
- Jahoda, R., Andrews, J.H. and Foster, R.P. (1989) Structural controls of Monterroso and other gold deposits in northwest Spain - fractures, jogs and hot jogs. *Trans. Inst. Min. Metall.* B98, 1-6.
- Kane, R. (1845) *The Industrial resources of Ireland*. Hodges and Smith, Dublin.
- Karig, D.E. (1983) Temporal relationships between back-arc basin formation and arc volcanism with special reference to the Philippine Sea. In Hayes, D.E. (ed) *the tectonic and geological evolution of southeast Asian seas and islands*. American geophysical union monograph 23, 318-23.
- Karig, D.E. and Sharman, G.F. (1971) Subduction and accretion in trenches. *Bull. Geol. Soc. America*. 86, 377-89.
- Keays, R.R. (1984) Archaean gold deposits and their source rocks: the upper mantle connection 17-51. In: Foster, R.P. (ed) *Gold '82: The geology, geochemistry and genesis of gold deposits*. Balkema, Rotterdam.
- Keppie, J.D. (1989) Northern Appalachian terranes and their accretionary history. *Geol. Soc. America. Spec. Paper* 230.
- Kelley, S. and Bluck, B.J. (1989) Detrital mineral ages from the Southern Uplands using ^{40}Ar - ^{39}Ar laser probe. *J. Geol. Soc. Lond.* 146, 401-404.
- Kelling, G. (1958) *The Ordovician rocks of the Rhinns of Galloway* Ph.D. Thesis, University of Edinburgh.
- Kinahan, G.H. (1889) *Economic geology of Ireland*. J. R. Geol. Soc. Ireland 8, 514pp.
- Kretschmar, U. (1973) Phase relations involving arsenopyrite in the system Fe-As-S and their application. Unpub. Ph.D. thesis, Univ. Toronto.
- Krupp, R.E and Seaward, T.M. (1987) The Rtokawa geothermal system, New Zealand: An active epithermal gold depositing environment. *Econ. Geol.* 82, 1109-29.
- Lapworth, C. (1878) Recent discoveries among the Silurians of South Scotland. *Trans. Geol. Soc. Scotland*.
- Lapworth, C. (1884) *The Silurian of Galashiels*. B.G.S. Mus. Pam.
- Lapworth, C. and Wilson, J. (1871) On the Silurian rocks of the Counties of Roxburgh and Selkirk. *Geol. Mag.* 8, 456.
- Leake, R.C., Cameron, D.G., Bland, D.J., Styles, M.T. and Rollin, K.E. (1989) Exploration for gold in south Devon, England. *Proceedings of the 13th annual commodity meeting*. *Trans. Inst. Min. Metall.* 98, B76-77.
- Lebas, M. (1983) The IUGS classification of igneous rocks. Abstract. *Geochemical expression of mineralization. Mineral deposits studies group meeting*, Geol. Soc. London.
- Lepettier, C. (1969) A simplified statistical treatment of geochemical data by graphical representation. *Econ. Geol.* 64, 538-550.
- Lindgren, W. (1935) *Mineral Deposits*. New York.

Lithogeochemical Exploration For Stratabound Arsenopyrite-Gold Mineralisation in the Southern Uplands, Scotland

Duller, P.R. and Harvey, P.K. (1985)

11th International Geochemical Exploration Symposium,
Toronto, Canada. Programme and Abstracts, 51.

A study of the fundamental geochemical composition of stratigraphically distinct lithopetrographic units within a Lower Palaeozoic turbidite succession, included the survey of over 200 km² of Upper Silurian strata, centred upon the known stratabound arsenopyrite-gold and vein stibnite mineralisation at Glendinning in Southern Scotland. Preliminary evaluation of some 22,000 major and trace element lithogeochemical analyses from both regional and mineralised drillcore samples indicate that:-

- a) the changes in chemical composition of greywacke, due to alteration are larger than those related to initial compositional variations.
- b) pervasive hydrothermal alteration at Glendinning may be characterised by the extensive depletion of sodium, which together with minor depletions of iron and magnesium is counterbalanced by silicification and potassic metasomatism. In general, Al, P, Ca and Ti are immobile.
- c) a zinc depletion zone ('zinc hole') surrounds the known mineralisation.
- d) the presence of gold in solid-solution within the arsenopyrite justifies the use of arsenic as a pathfinder element for stratabound gold mineralisation in this region.

The geochemical nature of the alteration may be summarised as follows: The following elements, in order of importance, have undergone addition, As, Sb, S, Pb, Cu, Ni, K₂O, SiO₂, Sr, Rb, Co, V, Au and Tl; whilst the following elements, again in order of importance, have undergone depletion, Na₂O, Zn, Fe₂O₃ and MgO.

An exploration model is proposed based upon the recognition of depletion zones to delineate broad target areas for detailed study. As the visual and mineralogical changes within the greywacke are more extensive and obvious than the disseminated sulphides a diffusive colour system is suggested as an empirical field guide, to detect areas of hydrothermal bleaching (up to 400m wide) and thus potential mineralisation. This investigation extends the strike length of the stratabound mineralisation at Glendinning to over 1km and has pinpointed at least four prospective areas for further study.

- Lord, R.A. and Pritchard, H.M. (1989) An igneous source for gold in the Shetland ophiolite. Proceedings of the 13th annual commodity meeting. Trans. Inst. Min. Metall. 98, B44-46.
- MacQueen, J.B. (1967) Some methods for classification and analysis of multivariate observations. Proc. of Symposium Math. Strat. and Prob., 5th, Berkeley, 1: 281-297. University of California Press, Berkeley.
- Maucher, A. (1976) The stratabound cinnabar-stibnite-scheelite deposits. In: Wolf, K. H. (ed) Handbook of stratabound and stratiform ore deposits. Elsevier.
- McArdle, P. (1989) Geological setting of gold mineralization in the Republic of Ireland. Trans. Inst. Min. Metall. 98, B7-11.
- McArdle, P. (1989) Geological setting of gold mineralization in Ireland. Proceedings of the 13th annual commodity meeting. Trans. Inst. Min. Metall. 98, B55.
- McBride, E.F. (1985) Diagenetic process that affect provenance determinations in sandstone. In Zuffa, G.G. (ed) Provenance of Arenites. Reidel Pubs.
- Michie, U. McL. (1974) Uranium in the Old Red Sandstone of NW Caithness. Institute of Geological Sciences. Radiogeology and Rare Minerals Unit Report, 304.
- Mitchell (1989) Arc Reversal in the Scottish Southern Uplands ?. J. Geol. Soc. Lond. 146, 736-738.
- Mitropoulos, P. (1982) REE Patterns of the metasedimentary rocks of the Lands End Granite aureole. Chemical Geology 35, 279-280.
- Moore, T.C. and Heath, G.R. (1976) Survival of deep sea sedimentary sections. Earth Planet. Sci. Lett. 37, 71-80.
- Morris, J.H. (1979) The geology of the Western end of the Lower Palaeozoic Longford Down Inlier, Ireland. Ph.D. thesis, University of Dublin, Ireland.
- Morris, J.H. (1986) Gold Exploration in Ireland. International Liason Group on Gold Mineralisation Newsletter.
- Morris, J.H. and Steed, G.M. (1986) Gold-Antimony mineralisation in Ordovician Greywackes near Clontibret, County Monaghan. Irish Assoc. Econ. Geol. Ann. Rev. 1986, 27.
- Murphy, F.C. and Hutton, D.H.W. (1986) Is the Southern Uplands of Scotland really an accretionary prism? Geology, 14, 354-7.
- Mutti, E. (1985) Turbidite systems and their relations to depositional sequences. In Zuffa, G.G. (ed) Provenance of Arenites. 65-93. Reidel Pubs.
- Mutti, E. and Ricci, L.F. (1985) Facies Analysis. Am. Assoc. Petrol Geology.
- Naden, J. and Caulfield, J.B.D. (1989) Fluid inclusion and isotopic studies of gold mineralization in the Southern Uplands of Scotland. Proceedings of the 13th annual commodity meeting. Trans. Inst. Min. Metall. 98, B46-48.
- Parker, R.T.G., Clifford, J.A. and Meldrum, A.H. (1989) The Connonish gold-silver deposit, Perthshire, Scotland. Abstract. Trans. Inst. Min. Metall. 98, B51-52.
- Patrick, R.A.D. and Russell, M.J. (1989) Sulphur isotopic investigation of Lower Carboniferous vein deposits of the British Isles. Min. Deposita. 24, 148-153.
- Peach, B.N. and Horne, J. (1899) The Silurian Rocks of Britain 1 : Scotland. Mem. Geol. Survey. G.B.
- Peach, B.N., Horne, J., Gunn, W., Clough, C.T., Hinxman, L.W. and Teal, J.J.H. (1907) The geological structure of the Northwest Highlands. Mem. Geol. Survey G.B.
- Pedersen, J.L. and Stendal, H. (1987) Geology and geochemistry of tungsten-antimony vein mineralization on Ymers O, East Greenland. Trans. Inst. Min. Metall. 96, B31-36.

Turbidite Hosted Gold Mineralisation in Southern Scotland, U.K.

Duller, P.R. and Harvey, P.K. (1985)

Turbidite Hosted Gold Deposits Symposium,
Joint Annual Meeting of the Geological Association
of Canada and Mineralogical Association of Canada.
Program with Abstracts, Volume 10, A15.

The Lower Palaeozoic turbidite succession of the Southern Uplands of Scotland is host to a diverse assemblage of vein and polymetallic deposits. The technique of microgeochemical mapping of individual arsenopyrite crystals was developed and applied to both wallrock and vein samples from many of these deposits. This involved the quantitative analysis of grains by electron microprobe (for As, S, Fe, Sb, Hg, Co, Ni, Cu, Ag and Au) on a grid system covering all or half of the crystal. The analyses were then processed through a geochemical mapping package to produce both elemental distribution and stoichiometric maps for each element, within each crystal.

These maps provide detailed evidence for -

- 1 - The cryptic enrichment and preferential zonation of gold within the core of arsenopyrite crystals from wallrocks to the studied deposits.
- 2 - The substitution of gold and associated trace elements within the arsenopyrite lattice.
- 3 - The existence of two chemically distinct gold populations (0-3000ppm and 1-3%) representing both zoned lattice constituents and randomly distributed native gold inclusions respectively.
- 4 - Arsenopyrite geothermometry indicates that the gold zonation is confined to a low temperature field, below 280°C.

The type of small scale hydrothermal system envisaged as responsible for such zonation may be linked with such factors as incipient hydraulic fracturing and brecciation in association with wallrock alteration processes. Any exploration model for turbidite hosted gold should therefore include the evaluation of the wallrocks to known vein deposits, as the processes controlling wallrock alteration may be intimately linked with gold concentration.

- Perring, C.S., Groves, D.I. and Ho, S.E. (1987) Constraints on the source of auriferous fluids for Archean gold deposits. In: Ho, S.E. and Groves, D.I. (Eds) Recent advances in understanding Precambrian gold deposits. University of Western Australia Pub. 11.
- Pettijohn, F.J. (1963) Chemical composition of sandstones, excluding carbonate and volcanic sands. In: Fleischer (Ed) Sandstones.
- Plant, J.A., Breward, N., Forrest, M.D. and Smith, R.T. (1989) The gold pathfinder elements As, Sb and Bi - their distribution and significance in the Southwest Highlands of Scotland. Proceedings of the 13th annual commodity meeting. Trans. Inst. Min. Metall. 98, B4.
- Postlethwaite, J. (1913) Mines and mining in the (English) Lake District. 3rd Edition. Moss, Whitehaven.
- Reeves, T.J. (1980) Age and provenance of the Carrigmore Diorite, Co. Wicklow. Bull. Geol. Survey of Ireland. No.2, 307-314.
- Rollin, K.E. (1980) I.P. logging of mineral boreholes at the Glendinning Antimony Mine, Dumfriesshire. Inst. Geol. Sci. Appl. Geophys. Unit 3pp.
- Rollin, K.E. (1983) Preliminary appraisal of the geophysical anomalies in the Southern Uplands. BGS Applied Geophysics Unit Report 155.
- Rose, A.W. and Burt, D.M. (1979) Hydrothermal alteration. 173-227. In: Barnes, H.L. (ed) Geochemistry of hydrothermal ore deposits. Wiley.
- Rundle, C.C. (1979) Ordovician intrusions in the English Lake District. J. Geol. Soc. London 136, 29-38.
- Rupke, N.A. (1978) Deep clastic seas. In: Reading, H.G. (Ed) Sedimentary Environments and Facies. 372-95. Blackwell.
- Sahli, W.E. (1961) Antimony in the Murchison Range of the Northeastern Transvaal: Commonwealth Mining Metall. Congr. 7th. South Africa. 181-199.
- Samson, I.M. (1983) Fluid inclusion and stable isotope studies of the Silvermines orebodies Ireland and comparisons with Scottish vein deposits. Unpub. Ph.D. thesis, University of Strathclyde, Glasgow 290p.
- Samson, I.M. and Banks, D.A. (1988) Epithermal base-metal mineralisation in the Southern Uplands of Scotland: nature and origin of the fluids. Min. Deposita 23, 1-8.
- Scratch, R.B. (1981) Geologic, structural, fluid inclusion and oxygen isotope study of the Lake George antimony deposit, Southern New Brunswick. Ph.D. thesis, Univ. Western Ontario, 211pp.
- Scratch, R.B., Watson, G.P., Kerrich, R. and Hutchinson, R.W. (1984) Fracture controlled antimony quartz mineralization, Lake George Deposit, New Brunswick. Mineralogy, Geochemistry, Alteration and Hydrothermal regimes. Econ. Geol. 79, 1159-1186.
- Seal, R.R., Clark, A.H. and Morrissey, C.J. (1987) Stockwork tungsten-molybdenum mineralization, Lake George, Southwestern New Brunswick. Econ. Geol. 82, 1259-1282.
- Sillitoe, R.N. and Sawkins, F.J. (1971) Geologic, mineralogic and fluid inclusion studies relating to the origin of copper-bearing tourmaline pipes, Chile. Econ. Geol. 66, 1028-1041.
- Sillitoe, R.H., Baker, E.M. and Brook, W.A. (1984) Gold deposits and hydrothermal eruption breccias associated with a maar volcano at Wau, Papua New Guinea. Econ. Geol. 79, 638-655.
- Soper, N.J., Gibbons, W. and McKerrow, W.S. (1989) Displaced terranes in Britain and Ireland. J. Geol. Soc. Lond. 146, 365-368.
- Sponer, E.T.C. and Fyfe, W.S. (1973) Subsea floor metamorphism, heat and mass transfer. Contrib. Mineral. Petrol. 42, 287-304.

Gold bearing arsenic-antimony concentrations in Silurian Greywackes, South Scotland.

Gallagher, M.J., Stone, P. and Duller, P.R. 1988
Abstract Appalachian-Caledonian Volcanogenic and
stratabound sulphide mineralisation Symposium,
GAC/MAC meeting, Montreal.

Gold is a widespread detrital mineral in drainage from Ordovician and Silurian turbidite sequences of the Southern Uplands of Scotland. It is principally known from late quartz veins but recently traces have been recognised in stratabound arsenopyrite assemblages adjacent to a stibnite vein deposit at Glendinning. In the Silurian greywackes of this area, drainage anomalies in arsenic, antimony and minor mercury extend along 5km of strike. Drill intersections of 0.7% As over 12m have been obtained in which stratabound arsenopyrite grains contain up to 0.4% Au and 0.3% Sb. These metal concentrations as synsedimentary sulphide indicate contemporaneous volcanism although only a few thin tuff horizons are present in the turbidite sequence. Volcanic exhalative mineralisation in the Glendinning area may have preceded deeper seated magmatism represented by a lamprophyre dominant syntectonic dyke swarm. Lithogeochemical studies of Lower Palaeozoic turbidites from the Southern Uplands illustrates that arsenic is concentrated at levels of tens to a few hundreds of ppm in several districts where mineralisation has not previously been recognised. They are based upon determinations of 10 major elements and 20 minors by automated XRF analysis of some 2000 greywacke and 400 shale samples from controlled regional traverses. The data point not only to new areas for sulphide and gold exploration but are also indicative of chemical variation between turbidite facies, possible hydrothermal alteration and the nature of provenance areas.

- Springer, J. (1983) Invisible gold. Ontario Geological Survey Misc. Paper. 110, 240-249.
- Stendal, H. (1982) Geochemistry and genesis of arsenopyrite mineralization in Late Precambrian sediments in Central East Greenland. Trans. Inst. Min. Metall. 91, B187-191.
- Stendal, H. and Ghisler, M. (1984) Stratabound copper sulphides and non-stratabound arsenopyrite and base metal mineralization in the Caledonides of East Greenland - A review. Econ. Geol. 79, 1574-1584.
- Steno, N. (1669) De solido intra solidum naturaliter contento, Florence.
- Stone, P., Floyd, J.D., Barnes, R.P. and Lintern, B.C. (1986) Comment on: Is the Southern Uplands of Scotland really an accretionary prism?. Geology, 14, 1046-8.
- Taylor, R.P. and Freyer, B.J. (1983) Rare earth element lithogeochemistry of granitoid mineral deposits. CIM Bull. 76, 74-84.
- Taylor, S.R. (1982) Residual lower continental crustal composition. LPS XIV 781.
- Taylor, S.R. and McLennan, S.M. (1985) The Continental Crust: Its composition and Evolution. Blackwell, 312pp.
- Viljoen, M.J. (1982) The nature and genesis of Archean gold mineralisation in South Africa. Rev. Brasileria. Geosci. 12, 522-530.
- Webb, B. (1983) Imbricate structure in the Ettrick area, Southern Uplands. Scott. J. Geol. 19, 387-400.
- Werner, B. (1791) Neu Theorie von der Entstehung der gangue mit Anwendung auf den Bergbau besonder den freibergischen. Frieberg.
- White, D.E. (1968) Hydrology, activity and heatflow of the Steamboat Springs thermal system, Nevada. US Geol. surv. Prof. Paper 458-C, 104pp.
- White, D.E. (1981) Active geothermal systems and hydrothermal ore deposits. Econ. Geol. 75th Anniversary Volume, 392-423.
- Wojdak, P.J. and Sinclair, A.J. (1984) Equity Silver Ag-Cu-Au deposit: Alteration and Fluid Inclusion Studies. Econ. Geol. 79, 969-990.
- Wyman, D. and Kerrich, R. (1988) Lamprophyres a source of gold. Nature 332, 209-210.
- Young, R.D., Burns, D.J. and McCullough, H.M. (1988). Gold associated with Ordovician volcanic sequences in County Mayo, Ireland. Gold, with emphasis on recent exploration. Abstract, Thirteenth annual commodity meeting, Inst. Min. Metall.
- Zimmerman, C.F. (1746) Unteradischem Beschreibung der meissenischen Erzgebirges, Dresden.

The following has been
excluded at the request of
the university

In reference and
bibliography section there
are a couple of journal
articles from p337a to
start of appendices

APPENDICES

APPENDIX I: INTRODUCTION TO THE DATA COLLECTION	
A1.1. Introduction	
A1.2. Sampling procedure	
A1.2.1. Core sample collection	
A1.2.2. Sample preparation	
A1.3. Sample preparation	
A1.3.1. Sample preparation	
A1.3.2. Sample preparation	
A1.3.3. Sample preparation	
A1.3.4. Sample preparation	
A1.3.5. Sample preparation	
A1.4. Sample preparation	
A1.5. Sample preparation	
APPENDIX II: DATA COLLECTION AND ANALYSIS	
A2.1. Data collection	
A2.2. Sample preparation	
A2.3. Analysis	
A2.4. Analysis	
A2.5. Analysis	
APPENDIX III: DATA COLLECTION AND ANALYSIS	
A3.1. Data collection	
A3.2. Sample preparation	
A3.3. Analysis	
A3.4. Analysis	
A3.5. Analysis	
APPENDIX IV: DATA COLLECTION AND ANALYSIS	
A4.1. Data collection	
A4.2. Sample preparation	
A4.2.1. Sample preparation	
A4.2.2. Sample preparation	
A4.3. Analysis	
APPENDIX V: DATA COLLECTION AND ANALYSIS	
A5.1. Regional groundwater sampling	
A5.2. Well Case history	
A5.3. Groundwater exploration results	
A5.4. Wellhead observation data	
A5.5. Detailed hydrologic data	
A5.6. Southern Illinois groundwater data	
A5.7. Groundwater regional flow rates	
A5.8. Groundwater flow rates	
A5.9. The Illinois Geological Survey	
A5.10. Environmental data	
A5.11. Environmental data	
A5.12. Environmental data	
APPENDIX VI: DATA COLLECTION AND ANALYSIS	
A6.1. Whole rock preparation	
A6.2. Extraction of clay fractions	
APPENDIX VII: COMPUTER PROGRAMS	
A7.1. PAN - Numerical database management system	
A7.2. HES - Homogeneous	
A7.3. STA - Univariate statistics	
A7.4. RAT - Basic calculator program	
A7.5. GDS - Single dimension analysis	
A7.6. TRV - Geostatistical software	
A7.7. SIP - Key report site selection	
A7.8. SOR - Surface sampling utility	

LIST OF APPENDICES

APPENDIX ONE : X-RAY FLUORESCENCE STUDIES

A1.1	Equipment	1001
A1.2	Sample preparation	1001
A1.2.1	Pressed powder pellet	1001
A1.2.2	Fusion beads	1002
A1.3	Analytical procedures	1004
A1.3.1	XRF analysis	1004
A1.3.2	Ferrous iron determination	1005
A1.3.3	Carbon dioxide determination	1005
A1.3.4	Approximate lower limits of detection	1006
A1.3.5	XRF analytical standards	1006

APPENDIX TWO : INDUCTIVELY COUPLED PLASMA ANALYSIS

A2.1	Equipment	1008
A2.2	REE sample preparation	1008
A2.3	Analytical procedures	1008

APPENDIX THREE : ELECTRON MICROPROBE ANALYSIS

A3.1	Equipment	1010
A3.2	Sample preparation	1010
A3.3	Analytical procedures	1011
A3.4	Analytical conditions, calibration and standards	1012
A3.5	Percentile class intervals	1015
A3.5.1	Arsenopyrite grids	1015
A3.5.2	Pyrite grid	1016

APPENDIX FOUR : SULPHUR ISOTOPE STUDIES

A4.1	Equipment	1017
A4.2	Sample preparation	1017
A4.2.1	Hydrofluoric acid digestion	1017
A4.2.2	Diamond drilling	1018
A4.3	Analytical and calibration procedures	1018

APPENDIX FIVE : SAMPLE SITE LOCATIONS

A5.1	Regional greywacke samples	1019
A5.2	West Coast traverse	1026
A5.3	Glendinning exploration samples	1031
A5.4	Wallrock alteration suite	1034
A5.5	Polished thin section index	1035
A5.6	Southern Uplands composite traverse	1037
A5.7	Glendinning regional traverses	1055
A5.8	Longford Down traverse	1066
A5.9	The Rhinns of Galloway traverse	1071
A5.10	Interformational traverses	1077
A5.11	Leadhills Underground traverse	1078
A5.12	Glendinning Borehole traverses	1079

APPENDIX SIX : SEMIQUANTITATIVE X-RAY DIFFRACTION ANALYSIS

A6.1	Whole rock preparation	1083
A6.2	Extraction of clay fractions	1083

APPENDIX SEVEN : COMPUTER PROGRAMS

A7.1	RAW : Numerical database management system	1085
A7.2	HIS : Histograms	1138
A7.3	STA : Univariate statistics	1150
A7.4	RAT : Ratio calculation packages	1162
A7.5	DIS : Simple discriminant analysis	1170
A7.6	TRV : Geochemical traverses	1176
A7.7	SIF : Key input and selection	1183
A7.8	SOR : Sorting/extraction utility	1187

APPENDIX ONE : X-RAY FLUORESCENCE STUDIES

A1.1 : XRF EQUIPMENT

X-ray fluorescence spectrometry provides a rapid, cost effective, multi-element analytical tool for the production of high precision geochemical data. The recent availability of a high power (3kW) rhodium anode X-ray tube now enables almost all elements of geological interest to be determined from atomic number nine (F) upwards, over an elemental range of a few parts per million, or less up to 100% (Harvey and Aitkin, 1985). All quantitative X-ray fluorescence analyses undertaken during this study were carried out using a Phillips PW1400 sequential spectrometer within the Geology Department of Nottingham University, under the direct supervision of Dr B. Atkin and Dr P.K. Harvey. The PW1400 spectrometer was purchased together with a 72 position automatic sample changer by Nottingham University with the aid of NERC grant No. GR3/3948. A DEC 11/23 computer running under the RMS-11M was connected to the spectrometer and used to communicate with the microprocessor controlling the XRF and for data storage, processing and subsequent analysis. A detailed account of the principles and operation of an automated X-ray fluorescence spectrometer is provided by Harvey and Atkin, 1983; 1984; and 1985.

A1.2.1 : PREPARATION OF PRESSED POWDER PELLETS

Method:

1. The rock sample should be ground to a grain size that is less than 200 B.S. mesh. One and a half minutes in a chrome steel swing mill or five minutes in an agate swing mill will normally suffice assuming a 50g load in a 250 ml barrel. No sieving is necessary.
2. Place a (homogeneous) sample of about 7 grams of the finely ground powder in a disposable plastic vial. Make a hole in the centre of the powder with a spatula and fill this with 7 to 20 drops of the PVP/Methyl cellulose binder (see below). The number of drops will vary with rock type, more granular samples generally needing the greater amount of binder.
3. Mix the binder and rock powder thoroughly with a spatula. Tip the mixture into a 32 mm die (ideally between tungsten carbide platens) and press at 10 tons pressure. Remove the pellet, label on the side and dry in an oven at 100°C for at least 15 minutes.
4. When removed from the die the sample should be damp but not wet, if the correct amount of binder has been used. If too little binder has been used the edges of the pellet will tend to crumble. If in doubt add a little extra binder; a crumbling sample could explode under vacuum. If this happens it can take several days to completely clean the spectrometer.

As this method of preparation involves no weighing, samples may be prepared at a rate of 10 to 15 pellets per hour.

Preparation of PVP/methyl cellulose binder.

Chemicals: Polyvinylpyrrolidone; BDH Product No. 29579 4F.

Methyl Cellulose; BDH Product No. 29779 4N.

(High Substitution).

Method:

Solution A : Dissolve 70 gm Polyvinylpyrrolidone (PVP) in 250 mls ethanol by slowly adding the PVP powder to the ethanol on a magnetic stirrer.

Solution B : Boil 400 mls of distilled/deionised water in a 1 litre beaker and whilst boiling slowly add 40 gms of methyl cellulose. Place the beaker on a magnetic stirrer and stir vigorously as the liquid cools. At this stage take care that the beaker is not thrown off the stirrer as the viscosity of the liquid increases as it cools and the methyl cellulose dissolves. When solution B has cooled to approximately 70°C, slowly add solution A, continuing to stir vigorously. The resulting solution is then used as the binder for pressed powder pellets as described above.

A1.2.2 : FUSION BEADS

Fusion beads for major element analysis were prepared according to the method of Norrish and Hutton (1969) as modified by Harvey et. al. (1973). The equipment required is as stated in Harvey et. al. (1973) except that the bead diameter has to be increased to 31.5 mm for the PW-1400.

Preparation of Equipment.

1. Switch on the hot plates, muffle furnace and blast-burner.
2. Set the muffle furnace temperature to 1000°C, hot plate 1 to 220-230°C and hotplate 2 to 200°C.
3. Adjust the blast-burner temperature to 1000°C by placing about 0.5g of NaF in a Pt/Au crucible and adjusting the gas-air mixture until the NaF just melts. The flame should then appear as a set of fine blue inverted cones.
4. All the heating units need time to achieve equilibrium before use (usually about 2 hours).

Making the Fusion Beads.

1. The flux used for the fusion beads is the Lithium Borate + Lithium Carbonate + Lanthanum Oxide mixture recommended by Norrish and Hutton (1969) and obtainable from Johnson and Mathey under the trade name Spectroflux 105. Only flux supplied from the X-ray laboratories at Nottingham University should be used in conjunction with the Nottingham calibration coefficients. The flux should be dried at 400°C for 8 hours (large Ni crucibles are good containers) then cooled and stored in a dessicator. The weight loss of the dried flux should be determined immediately prior to use and used in the calculation of flux weight, (see below).
2. Weigh accurately about 0.3700 g of rock powder into a Pt/Au crucible (size 122). Place in the furnace (1000°C) for 15 minutes then remove and cool in dessicator. Reweigh and determine the loss on ignition of the rock.

$$\% \text{ Loss on Ignition (LOI)} = \frac{\text{Wt loss on rock}}{\text{Initial Wt of rock}} \times 100$$

3. Having previously determined the LOI of the flux, weigh onto the rock powder an amount of flux to produce a rock-flux ratio of 1:5.405.

$$\text{Weight of flux} = \frac{\text{Wt of rock powder} \times 5.405}{100 - \% \text{LOI of flux}} \times 100\text{g}$$

4. Place the crucible back in the furnace for 10-15 minutes or until the fusion is complete.

1. NEVER place hot crucibles on anything but aluminium.
2. DO NOT touch the beads with hot tongs.
3. DO NOT touch the melt with tongs.
4. DO NOT handle the beads with your fingers.
5. A long pair of Pt tipped tongs are supplied for removing hot crucibles from the furnace.
6. Clean the discs and plunger face THOROUGHLY after making EACH bead.
7. After use THOROUGHLY clean the bench and all equipment.
8. Switch everything off when finished.

Notes 1 to 8 are extremely important - for reasons of safety, expense and analytical purity.

9. Store any small beads of melt (after cooling) with the complete bead. They may be useful if the bead needs remelting at any time.
10. Work with carbonates suggests that at least 30% Silica needs to be present for a stable bead to form, therefore the use of pressed powder pellets for major element analysis of carbonates, is advised.
11. To clean the crucibles after use, let them cool down and immerse in 50 % HCL overnight. The cleaning solution may be heated to speed up the cleaning process. (The fusion mixture is soluble in HCL).

Wash off the acid in distilled water and dry with Kleenex tissue.

It is advisable to ignite the crucibles and place in dessicator before use.
12. Label as follows:

(12) Flux Mix Number.

DJR-999 User Code / Sample Number
13. The preparation of fusion beads is speeded up if the weight loss of the rock (step 2) is carried out separately. It is recommended that this is done on a 1 gm sample before the fusion beads are prepared. Step 2 can then be reduced to:
(2) Weigh accurately about 0.3700 g of rock powder into a Pt/Au crucible.

- 1 - correction for instrumental drift during the duration of the analysis run, by reference to an internal instrument monitor standard analysed at numerous intervals within a single batch of samples.
- 2 - determination of the measured values for the 12 reference standards present in each batch and a comparison with their 'known' or 'accepted' values (thus providing a measure of the accuracy and stability of the machine).
- 3 - Calculation of the element concentration of the 'unknown' samples (in a similar manner to 2 above) and transfer of the results to a .VAL file.

A1.3.2 : Ferrous Iron Determination

Technique: Ferrous sulphate is determined by attacking the rock powder with HF/H₂SO₄ and titrating directly with potassium dichromate. At the titration stage boric acid is added to complex the fluoride and phosphoric acid to remove ferric iron.

Reagents: Potassium dichromate: 2.73 g in 2000 cm³ H₂O.

Acid HF: Equal volumes of 50% H₂SO₄ and H₃PO₄, saturated boric acid and barium diphenylamine indicator.

Method:

1. Weigh out accurately approximately 0.5 g of rock powder into a platinum crucible.
2. Moisten with a few drops of water and add a mixture of conc. HF and 8 ml H₂SO₄.
3. Heat on a hotplate so that simmering takes place for 15 minutes.
4. While the crucible(s) is heating prepare a 400 ml conical beaker containing 30 ml of acid mix and dilute with 200 ml water.
5. Transfer the crucible, lid and contents to the beaker and titrate with the dichromate after addition of 3 drops of indicator. Titrate until the purple colour persists for 15 seconds.
6. The ferrous iron content is calculated by reference to the equation: $6\text{Fe}^{2+} + \text{Cr}_2\text{O}_7^{2-} + 14\text{H}^+ = 6\text{Fe}^{3+} + 2\text{Cr}^{3+} + 7\text{H}_2\text{O}$
(ie. 0.002g FeO = 1cm³ Cr₂O₇)

A1.3.3 Carbon Dioxide Determination

A rapid and accurate determination of the carbonate hosted carbon dioxide content of individual samples was obtained following a method modified after Bush (1970). This technique has a major advantage over similar alternatives in that the presence of sulphides (Such as within Glendinning mineralised samples) and other impurities do not interfere with the analysis. This method involved the reaction of 1g of finely ground sample with 10ml of ortho-phosphoric acid. The mixture was heated using a bunsen burner for 5 minutes to drive off all carbon dioxide. The resulting gas was drawn through an empty U-tube (acting as a primary water trap) and then through a U-tube containing finely divided anhydrous copper sulphate. The dry gas was then reacted with 50ml of barium hydroxide which, upon completion of the above reaction, was titrated using 0.2M HCl with a thimolphthalein indicator. A 'Blank' value was obtained by repeating the procedure described above, but with the sample omitted and the reaction was calibrated with reference to a standard (0.1g of 'Analar' calcium carbonate) substituted for the sample (as above). Duplicate determinations were made for all 'Unknowns', 'Blanks' and 'Standards'. The formula required to calculate the %CO₂ content of the unknown sample is presented below and outlined in detail in Bush (op cit):

Wt of Calcium Carbonate Standard	= W1 g
Wt of Sample	= W2 g
Volume of HCl used for Blank	= V1 ml
Volume of HCl used for Standard	= V2 ml
Volume of HCl used for Sample	= V3 ml

$$\% \text{CO}_2 (\text{Sample}) = (((V1-V3)*W1*(44.01/100.09))/(V1-V2))/W2)*100$$

A1.3.4 : Approximate Lower Limits of Detection (XRF)

<u>Element</u>	<u>LLD</u>	<u>Element</u>	<u>LLD</u>
*Ag	1.0	Ni	1.7
Au	1.5	Pb	1.5
As	1.1	Rb	0.7
Ba	8.3	S	3.5
Bi	1.0	*Sb	1.4
Ce	7.0	*Sc	0.8
Cl	6.0	*Sn	2.0
Co	2.5	Sr	0.9
Cr	2.8	Ta	1.9
*Cs	1.1	Th	0.6
Cu	0.8	U	1.4
Ga	1.3	V	1.9
Hf	2.9	W	1.6
La	4.0	Y	1.2
Mo	0.9	Zn	3.0
Nb	1.2	Zr	3.1

(* : Cr X-ray tube; all others: Rh X-ray excitation).

- These figures represent the approximate lower limits of detection (LLD) in ppm, based either on W-1 or the Nottingham Andesite N-1005.
- Individual limits of sensitivity vary with matrix and may also be significantly affected by interfering (line overlap) elements.
- These limits are based on 'normal' counting times - they may, within reason, be lowered (or raised) by changing these times as the spectrometer is sufficiently stable to allow this approach.

A1.3.5 : XRF Analytical Standards.

	Name	Standard
1	GSP-1	United States Geological Survey (USGS) : Granodiorite.
2	STM-1	United States Geological Survey (USGS) : Syenite.
3	BHVO-1	United States Geological Survey (USGS) : Basalt.
4	SCO-1	United States Geological Survey (USGS) : Shale.
5	AGV-1	United States Geological Survey (USGS) : Andesite.
6	N-1007	Nottingham University Internal Standard : Delabole Slate.
7	N-1011	Nottingham University Internal Standard : Bunter Sandstone.
8	ST-2	Nottingham University Internal Standard : Greenstone.
9	ST-5	Nottingham University Internal Standard : Siltstone.
10	ST-6	Nottingham University Internal Standard : Shale.
11	ST-29	Nottingham University Internal Standard : Greywacke.
12	NIM-G	South African Institute of Metallurgy : Granite.

A1.2.1.3.5 Sample Preparation

Soil samples : collected by hand, washed, ground

Granodiorite and syenite : ground (USGS, BSM 100, 75/100)

Basalt, shale, sand, silt, and clay : ground (USGS, BSM 100, 75/100)

APPENDIX TWO : INDUCTIVELY COUPLED PLASMA ANALYSIS

A2.1.1 : ICP Equipment

Inductively coupled plasma source spectrometry (ICP) provides a technique for the rapid simultaneous analysis of a wide range of elements in solution. A detailed account of the development and principles of ICP is presented by Walsh and Howie (1986) and summarised below: A solution containing the sample for analysis is introduced into an ICP flame via a nebuliser where it is converted into an aerosol and intimately mixed with argon. Following initial spark ignition, inductive heating of the ICP flame generates temperatures of 6-10,000 K. As no chemical bonds remain stable at these temperatures 'atomisation' of the solution is virtually complete and in addition many atoms are ionised. The light emitted by the ICP is formed by different elements at different wavelengths with the intensity of the light directly related to concentration. This light is focused into a multi-channel spectrometer (polychromator) where a diffraction grating resolves the light into its component wavelengths and onto a series of light sensitive photo-multiplier tubes located at precise wavelengths in the diffracted light spectrum. The resulting electrical signal from the photomultiplier is fed to a capacitor and then to a digital voltmeter. As a linear relationship occurs between the signal and the concentration of each respective element, the analysis may be calibrated with reference to a series of standard solutions.

A2.1.2 : ICP Analytical Procedures

ICP studies were undertaken under the supervision of Dr N. Welsh and S. Chenery using the analytical facilities of the Geology Department of Kings College, London. Sample preparation however, was carried out within the geochemical laboratories of the Geology Department of Nottingham University. The low detection limits (sub ppm) offered by ICP analysis provided an extremely suitable analytical technique for the rare-earth elements (La, Ce, Pr, Nd, Sm, Ho, Er, Yb, Lu). However, concentration of the elements Tb, Tm and Pm were not determined (NB. Pm does not exist naturally). The routine analytical procedure was to run a set of internal Kings College standards (Ba250, Fe100, Zr100 and Ca500) at the start and finish of a sample batch which was then followed by sets of 8 'unknown' samples and two REE standards (COMP and Ce20). A further quality control check was imposed by the inclusion of a Nottingham University REE standard and a BLANK which were prepared in an identical manner to the 'unknown' samples and located as the 7th and 8th member of each sample set. Following analysis the raw analytical data relating to both standards, unknowns and blanks was transferred to the Nottingham computer system where the data was validated and corrections then applied for element interferences, machine and analytical variation. REE data was then transferred to a .RAW file format prior to further assessment.

A2.2 : REE Sample Preparation

Reagents: Sodium Hydroxide, analytical grade.

Hydrofluoric acid, assay grade 39-43%, BDH No. 28514.

Hydrochloric acid, analytical grade, pronalysis AR (1.75g/cc), May and Baker.

Method:

1. Weigh 0.5 g of rock powder into a platinum crucible.
2. Add 4 mls of HClO_4 and 15 mls of HF and digest to dryness so that no HClO_4 remains.
3. Cool, then add 5 mls of concentrated HCl and half fill the crucible with distilled water, then warm until dissolved.
4. Filter this solution using number 42 filter paper.
5. Rinse the filter paper with warmed 5% HCl , then rinse well with distilled water, collecting filtrate in a 100 ml beaker.
6. Ignite the filter paper in a silver crucible, starting the furnace from room temperature and taking it up to 800°C (leave for half an hour at 800°C).
7. Remove crucible from furnace, cool and add 5 pellets of NaOH . Return to furnace for further half an hour at 800°C .
8. Remove again, swirling the mixture until it solidifies. Cool, then add approximately 5 mls of distilled water to digest the cake.
9. Add approximately 3 mls of concentrated HCl carefully and stir with a rubber policeman to dissolve the cake.
10. Add this to the filtered portion and make it up to approximately 100 mls with distilled water.
11. Load the column with clean resin to a height of 12 cms. Rinse with distilled water, then load the sample onto the column.
12. When the sample has passed through, elute the column with 600 mls of 1.7 N HCl . Discard this portion.
13. Place a filter funnel with number 42 filter paper under the column and elute the column with 600 mls of 4.00 N HCl , saving the eluted portion.
14. Evaporate, until approximately 15 mls remain. Transfer this to a 50 ml beaker and take down to dryness. Cover the beaker with parafilm.
15. After using the column, rinse it with approximately 200 mls of distilled water, then return to 1.

A3.2 Equipment

All probe analyses presented in tables in this thesis were generated using Phoenix and Spectro software of the Geology Department of McMaster University. The Phoenix system provided all values, MSA/CA Converter (a custom software) based on the Phoenix output files produced the values in this thesis. The MSA/CA Converter was developed and published by the University of Minnesota and MSA/CA Converter was completed in July, 1993.

APPENDIX THREE : ELECTRON MICROPROBE ANALYSIS

The use of a microprobe in a mineralogical study has considerable advantages over more traditional techniques such as XRF analysis, in that very small 'spots' (1-2 microns in diameter) may be analysed. This feature is particularly useful when applied to the analysis of small grains, fine intergrowths and zoned phases. Detailed geochemistry of individual phases enables the mineral formulae to be calculated. In addition the data may be applied to provide details of element substitutions in solid solution series (particularly in zoned phases) and geothermometry/geobarometry calculations upon both silicates and sulphides (eg sphalerite geobarometry and arsenopyrite geothermometry).

A3.1 Principles

Electron microprobe analysis is based upon the principle that when a finely focused beam of electrons hits the surface of a solid material it gives rise to a characteristic X-ray spectrum. The wavelengths and intensity of the peaks in the spectrum are used to identify the elements present in the sample and their concentration is measured by a comparison with the intensities from standards of known concentration (Hopkin and Plant, 1984). Two devices for detecting the resulting X-rays are available, namely: An Energy dispersive Spectrometer (EDS) : an electronic device based upon a lithium doped silicon crystal used to simultaneously detect elements from Na to U (detection limits approximately 0.2 Wt%); and a Wavelength dispersive Spectrometer (WDS) : a mechanical device used to detect individual elements (from B to U) using diffraction from a crystal of known lattice spacing (detection limits approx. 0.002 Wt%).

Individual specimens comprised highly polished thin sections (mounted on 48x26mm glass slides) vacuum coated with a 20nm layer of carbon. Low magnification photomicrographs of the entire specimen provided a precise guide to previously defined areas of interest. These areas are then positioned under the electron beam by use of a reflected light optical microscope. The property of some minerals to fluoresce when bombarded by an electron beam (cathode luminescence) was used to align the light optics to the exact position of the electron beam prior to microanalysis (Hopkin and Plant, op cit).

If the electron beam remains stationary on a specimen for longer than thirty seconds a small round ring of carbonaceous contamination (derived from hydrocarbons in the pump oil being 'cracked' by the beam) is built up around the area of interest. This contamination is not detrimental to the analysis; however it does provide a further check upon the position of the beam. In addition, when analysing sulphide samples (particularly those rich in Ag and Sb) the electron beam vaporises extremely small volumes of material (directly under the beam) and forms a minute analysis 'pit' on the specimen surface.

A3.2 Equipment

All probe analyses presented within the context of this thesis were generated using Electron microprobe facilities of the Geology Department of Manchester University. The Manchester system consisted of a C.A.M.E.C.A Camebax electron microprobe fitted with two wavelength dispersive spectrometers (WDS) and a Link Systems 860-500 EDS system. The machine was purchased jointly by the University of Manchester and NERC, and installation was completed in July, 1981.

A3.3 Operating Conditions

The Camebax operating conditions are as follows:

- 15 kV accelerating potential
- 40 degree take off angle
- 14.5 nA beam current for EDS and WDS analysis.

Following measurement of the raw X-ray intensity the SPECTRA software (used to control both EDS and WDS analysis) applies a series of correction procedures to the data. The software deconvolutes overlapping X-ray peaks and subtracts a background radiation by reference to a previously obtained library of standard peak profiles (Hopkin and Plant, op cit). X-ray intensities are automatically ZAF corrected using a procedure based upon the TIMI program of Duncumb and Jones (1969). The atomic number correction of Duncumb and Reed (1968) is used together with a fluorescence correction (Reed, 1965). Absorption effects were calculated using Philbert's equation as calculated by Yakowitz et al (1973).

The SPECTRA software has the ability to record the exact position of up to 1024 analysis points and then automatically analyse each site following a pre-defined set of instructions. By using both WDS simultaneously to detect different elements it was possible to perform a single analysis of arsenopyrite (AsFeS) for As, Fe, S, Au, Sb, Co, Ni and Hg (with extended counting times for Au) in approximately 8 minutes. Although this time appears prohibitive, when correctly calibrated, programmed and left to run overnight a large number of analyses could be obtained from any predefined grid area.

As certain phases (eg Sb-rich sulphides) are relatively unstable in the electron beam, the more 'volatile' elements (Sb,Hg) were always determined first. Because of the problems associated with element interferences, the presence of high atomic number elements and the required detection limits (for 'trace' element analysis) WDS techniques were selected in preference to EDS for all sulphide analyses. Using WD methods trace elements such as Sb, Hg, Cu, Co, Ni and Au were determined down to levels of approx 100-200ppm.

During the period of analytical work at Manchester University, no facilities for data processing or data transfer were available. As such the only output media for the resulting probe analyses consisted of a single computer printout.

All microprobe results were manually re-entered into a series of datafiles using the RAW database manager (see chapter 2) at either Nottingham or Strathclyde University. Atomic proportions and formula units were then calculated, and submitted to both statistical and spatial/graphical analysis.

References

- Duncumb, P. and Reed, S.J.B. (1968) Quantitative electron probe micro-analysis. N.B.S. Spec. Pub. 298, 133-154.
- Heinrich, K.F.J.(1967) 2nd National Conference on Electron Probe Micro-analysis, Boston, USA. Paper No. 7.
- Hopkins, A. and Plant, D. (1984) Electron Microprobe Analysis. Course Notes, Manchester University.
- Philbert, J. (1967) X-ray optics and X-ray microanalysis. Academic press.
- Reed, S.J.B. Brit. J. appl. Phys. 16, 913.
- Stanham, P.J. (1977) Analytical Chemistry 49, 2149-2154.
- Yakowitz, H. Mykleburst, R.L. and Heinrich, K.F.J. (1973) Frame : An on-line correction procedure for quantitative electron probe micro-analysis. N.B.S. Tech. Note 796.

A3.4 : Analytical Conditions, Calibration and Standards.

The following tables detail the analytical conditions set, to undertake quantitative sulphide micro-analysis on the Camecia Wavelength Dispersive Analytical System, within the Department of Geology, Manchester University.

WD STANDARDS FILE NO. 10.

NO.	ELEMENT	KV	ED/WD	VAL	CONC %	SP XTAL
1	Fe : KA	20.00	WD	2	46.55	1 LIF
2	Co : KA	20.00	WD	2	100.00	1 LIF
3	Ni : KA	20.00	WD	2	100.00	1 LIF
4	Cu : KA	20.00	WD	2	100.00	1 LIF
5	Zn : KA	20.00	WD	2	67.09	1 LIF
6	As : KA	20.00	WD	1	41.32	1 LIF
7	S : KA	20.00	WD	2	32.91	2 PET
8	Sb : KA	20.00	WD	3	48.87	2 PET
9	Au : KA	20.00	WD	2	100.00	2 PET
10	Ag : KA	20.00	WD	1	28.31	2 PET
11	Hg : MB	20.00	WD	2	86.22	2 PET

PEAK.

No.	COUNTS	TIME	POSITION	COUNT RATE
1	80000	.0000	.48083	1754.39
2	80000	.0000	.44411	4073.86
3	80000	.0000	.41149	3799.93
4	80000	.0000	.38255	2801.12
5	40000	.0000	.35610	1722.77
6	40000	.0000	.29143	440.72
7	80000	.0000	.61405	2140.18
8	40000	.0000	.39295	2470.75
9	40000	.0000	.66710	865.42
10	40000	.0000	.47467	968.99
11	40000	.0000	.62027	631.91

BACKGROUND.

No.	COUNTS	TIME	LOW	HIGH	COUNT RATE
1	0	5.0000	.47762	.48983	13.1073
2	0	5.0000	.43830	.45030	18.7307
3	0	5.0000	.40575	.41775	21.2965
4	0	5.0000	.37661	.38861	19.5041
5	0	5.0000	.35043	.36243	14.5387
6	0	10.0000	.28543	.29743	11.8501
7	0	5.0000	.59134	.63335	6.3890
8	0	5.0000	n/r	.40444	26.8007
9	0	5.0000	.65473	.67488	12.9268
10	0	5.0000	.46395	.48662	15.7444
11	0	5.0000	n/r	.63291	15.4002

On the basis of the instrumental conditions defined overleaf, the results of a standard analysis are presented below together with the relevant counting statistics and detection limits.

No.	ELEMENT	TIME	PEAK (sec)	BACKGROUND (c/s)	(c/s)	TOTAL COUNT	DETECTION LIMIT TIME (sec)
1	Fe: KA		30	1780.94	14.1177	35	200ppm
2	Co: KA		60	4026.46	18.1642	90	350ppm
3	Ni: KA		60	3810.07	20.7311	90	310ppm
4	Cu: KA		60	2954.21	19.5764	90	290ppm
5	Zn: KA		60	1730.79	18.2728	90	340ppm
6	As: KA		30	428.54	12.3002	35	180ppm
7	S : KA		30	2129.93	5.4864	35	100ppm
8	Sb: LA		60	2525.38	28.0008	120	270ppm
9	Au: MA		120	831.95	13.4357	180	370ppm
10	Ag: LA		60	964.79	14.2839	90	300ppm
11	Hg: MA		60	743.77	13.2002	120	500ppm

(NB. The Detection limit is defined at the 95% confidence level).

APPENDIX A3.5.1 : Percentile Class Intervals - Arsenopyrite Grids

Grid	%	As	Fe	S	Ni%	Sb%	Hg%	Au%	Ag%	Cu%
Grid1	50%	30.25	30.20	36.00	0.01	0.09	0.35	0.02	-	-
	75%	30.80	33.35	37.10	0.04	0.38	0.40	0.04	-	-
	90%	31.10	33.45	37.65	0.06	0.50	0.44	0.06	-	-
	95%	31.40	33.55	37.90	0.08	0.60	0.48	0.10	-	-
Grid2	50%	30.25	30.20	36.00	0.04	0.24	0.72	0.07	-	-
	75%	30.80	33.35	37.10	0.05	0.28	0.82	0.08	-	-
	90%	31.10	33.45	37.65	0.06	0.31	0.92	0.09	-	-
	95%	31.40	33.55	37.90	0.07	0.35	1.20	0.10	-	-
Grid5	50%	30.50	31.70	37.20	0.03	-	0.30	0.02	-	-
	75%	31.25	32.25	38.00	0.12	-	0.36	0.04	-	-
	90%	32.00	33.00	38.50	0.30	-	0.40	0.06	-	-
	95%	32.25	33.40	39.00	0.55	-	0.48	0.10	-	-
Grid6	50%	30.70	37.00	31.80	0.05	0.08	-	0.02	-	-
	75%	31.20	37.60	32.20	0.15	0.12	-	0.05	-	-
	90%	31.70	38.20	32.80	0.30	0.24	-	0.10	-	-
	95%	32.20	38.50	33.10	0.40	0.28	-	0.30	-	-
Grid7	50%	26.70	33.30	39.00	0.02	0.35	0.38	0.02	0.02	0.03
	75%	28.40	33.50	40.00	0.03	0.55	0.44	0.04	0.03	0.04
	90%	29.00	33.60	40.50	0.04	0.60	0.50	0.06	0.04	0.06
	95%	29.40	33.70	40.90	0.05	0.65	0.55	0.08	0.05	0.07
Grid8	50%	31.50	33.20	34.50	0.02	0.18	0.38	0.02	0.02	0.04
	75%	32.20	33.35	35.70	0.03	0.22	0.44	0.04	0.03	0.06
	90%	32.40	33.50	36.70	0.04	0.40	0.50	0.06	0.04	0.07
	95%	32.60	33.65	37.30	0.05	0.45	0.55	0.10	0.05	0.08
Grid9	50%	33.18	32.25	34.45	0.01	0.03	-	0.01	0.00	0.02
	75%	33.50	32.55	34.65	0.02	0.05	-	0.03	0.01	0.04
	90%	33.70	32.80	34.95	0.03	0.06	-	0.05	0.015	0.05
	95%	33.90	32.95	35.25	0.04	0.07	-	0.06	0.02	0.06
Grid10	50%	30.10	33.00	37.00	0.00	0.02	-	0.05	0.03	-
	75%	30.40	33.20	37.25	0.01	0.03	-	0.08	0.04	-
	90%	30.80	33.30	37.70	0.02	0.05	-	0.11	0.05	-
	95%	31.40	33.40	37.85	0.03	0.06	-	0.13	0.06	-
Grid11	50%	30.50	33.10	36.10	0.00	0.03	-	0.02	0.03	-
	75%	30.90	33.30	36.50	0.005	0.05	-	0.06	0.04	-
	90%	31.10	33.50	36.80	0.01	0.07	-	0.10	0.05	-
	95%	31.30	33.70	37.10	0.02	0.08	-	0.12	0.06	-
Grid12	50%	30.70	33.00	36.00	0.00	0.01	-	0.05	0.03	-
	75%	31.00	33.25	36.40	0.01	0.02	-	0.09	0.04	-
	90%	31.50	33.45	36.70	0.02	0.03	-	0.11	0.05	-
	95%	31.70	33.50	38.00	0.03	0.04	-	0.12	0.06	-
Grid13	50%	30.30	32.95	36.65	0.01	0.02	-	0.05	0.03	-
	75%	30.50	33.25	36.80	0.02	0.04	-	0.07	0.04	-
	90%	30.85	33.40	37.10	0.03	0.06	-	0.10	0.05	-
	95%	30.95	33.50	37.40	0.04	0.07	-	0.11	0.06	-
Grid14	50%	31.00	32.50	36.30	0.20	0.20	-	0.03	0.00	0.01
	75%	31.50	32.62	36.60	0.30	0.25	-	0.06	0.01	0.02
	90%	32.00	32.75	36.80	0.40	0.35	-	0.20	0.02	0.03
	95%	32.20	32.85	37.00	0.50	.45	-	0.25	0.03	0.04
Grid15	50%	32.00	32.30	35.40	0.04	0.05	-	0.05	-	-
	75%	32.20	32.50	35.70	0.06	0.09	-	0.08	-	-
	90%	32.40	32.62	36.20	0.10	0.22	-	0.11	-	-
	95%	32.50	32.70	37.20	0.18	0.30	-	0.14	-	-

(NB. Arsenic, Iron and sulphur values are presented in the form of their atomic percentage in arsenopyrite).

APPENDIX FOUR : SULPHUR ISOTOPE STUDIES

Sulphur isotope geochemistry can provide an important contribution in the interpretation of ore genesis particularly when applied within a framework of detailed geological, mineralogical and other geochemical studies. The sulphur isotopic composition of individual hydrothermal mineral phases is controlled both by the physical/chemical conditions of the fluid during deposition (T, pH etc) and the initial sulphur isotopic composition of the ore-bearing fluid. Important sources of sulphur in ore deposits include deep-seated (mantle or homogenised crust) local country rocks, and sea water or marine evaporites (Rye and Ohomoto, 1974). Sulphur isotope analyses were undertaken during the tenure of this Ph.D within the Stable Isotope Laboratory, Isotope Geology Unit, British Geological Survey.

A4.1 Analytical Procedures

Sulphur isotope ratios were determined for mono-mineralic sulphide samples by reacting an intimate mixture of the specimen and excess cuprous oxide at a temperature of 800°C following the preparation method outlined by Robinson and Kusakabe, 1975. Following the separation of CO₂ (by fractional sublimation) and water from the liberated gas, pure sulphur dioxide was then analysed by mass spectrometry. A mass spectrometer is a device designed to separate charged atoms and molecules on the basis of their masses based on their motions in electrical and/or magnetic fields. Separated ions may be detected electronically and their presence converted into a digital signal. A mass analysis of an element, composed of several isotopes (or isotopic masses) is obtained by varying a magnetic field in such a way that separated ion beams are focused on the detector in succession. The resulting signals then form a mass spectrum of the element with the relative intensity of each signal proportional to a discrete isotopic concentration (Fawe 1977).

A4.2.1 : Hydrofluoric Acid Digestion

A sulphide concentrate may be prepared from disseminated sulphide mineralisation by digesting the matrix of the host rock with hydrofluoric acid.

Reagents: Hydrofluoric acid, assay grade 39-43% BDH No. 28514.

Hydrochloric acid, analytical grade.

Method:

1. Weigh out multiples of approximately 0.5g of rock chips (<2mm) into a platinum crucible.
2. Moisten with a few drops of water.
3. Add 20mls of HF (40%) and digest overnight on a steam bath.
4. Evaporate to dryness on hot plate and allow to cool.
5. Add 5mls of concentrated HCl (to remove fluoride complexes) and 10mls of H₂O. Heat on hotplate for 15 minutes.
6. Filter residue through '42' Whatman filter paper and dry in oven at 90°C

The sulphide concentrate can then be subdivided using a variety of techniques dependant upon the mineral assemblage present (ie. handpicking, gravitational or electromagnetic methods).

A4.2.2 Diamond Drilling

An alternative method of sample preparation to that outlined above is the careful use of a dentist-type diamond drill to extract selective sub-samples of individual mineral phases. This technique has a number of advantages particularly where detailed inter-sample traverses are undertaken, or sample extraction is required from a cut slab or polished block. In addition the resulting fine grained powder is immediately amenable to both XRD analysis (to monitor sample quality) and isotopic study, with little if any further preparation. This technique was used to generate sulphur isotope samples from massive and large bladed crystals of stibnite from the Glendinning, Knipe and Clontibret deposits.

A4.3 Correction Procedures

As the isotopic composition of the reference gas is not assumed, results are first standardised with respect to the composition of a BGS reference standard (CPI) included within in each batch of samples. A correction equation is then calculated for the reference standard with respect to the isotopic abundance of the standard troilite phase of the Canyon Diablo meteorite and the measured values are corrected accordingly. Full details of the isotopic data corrections including isobaric, instrumental and internal standardisation procedures and their related algorithms are presented by Coleman (1979).

APPENDIX A5.1 : Regional Greywacke Sample Locations.

AX 1	Cape Cleuch, Leithen Water.	AX123	Low Cawer Wood.
AX 2	Bowbeat Rig, Leithen Water.	AX124	Cardorcan.
AX 4	Hunters Knowe, Leithen Water.	AX125	Wood of Cree.
AX 5	Fair Hope, Leithen Water.	AX126	Wood of Cree.
AX 36	Hornshill Quarry, Snowdon.	AX127	near Barskeoch Mains.
AX 37	Papana Water.	AX128	near Craigencallie.
AX 38	Papana Water.	AX129	near Drannadow.
AX 40	Frigg Gas Trench.	AX130	near Larg.
AX 43	Frigg Gas Trench.	AX131	near Laglanny.
AX 44	Frigg Gas Trench.	AX132	near Craigenrae.
AX 46	Frigg Gas Trench.	AX133	High Mill Burn.
AX 47	Frigg Gas Trench.	AX134	near Loch Dow.
AX 48	Frigg Gas Trench.	AX135	Highlandman's Rig.
AX 51	Frigg Gas Trench.	AX136	near Corrafeckloch.
AX 54	Frigg Gas Trench, Knock Leaven.	AX137	High Mill Burn area.
AX 62	Frigg Gas Trench, White Hill.	AX138	near Drumjohn.
AX 63	Frigg Gas Trench, Netherton Fm.	AX139	Loch Doon area.
AX 67	Frigg Gas Trench, Elvanfoot Fm.	AX140	Loch Doon area.
AX 68	Frigg Gas Trench, Elvanfoot Fm.	AX141	Loch Doon area.
AX 73	Frigg Gas Trench, Harryburn.	AX143	near Polharrow Bridge.
AX 75	Frigg Gas Trench, Harryburn.	AX149	Knocklach Burn.
AX 79	Frigg Gas Trench, Rivox Moor.	AX150	River Tweed, Tweedsmuir.
AX 80	Frigg Gas Trench, Rivox Moor.	AX151	Talla Dain.
AX 83	Frigg Gas Trench, White Knowe.	AX155	Talla Water.
AX 87	Frigg Gas Trench, Beld Knowe.	AX156	Coulter Craigs Quarry.
AX 94	Talla Water.	AX157	Knock Burn.
AX 95	Quarry, Henderland.	AX158	Coulter Waterhead Dain.
AX 96	Garlie Cleuch, Winterhope.	AX159	Culter Water.
AX 97	Winterhope Burn.	AX163	Hare Burn.
AX 99	Gool Knowe, Shielhope.	AX164	Hare Burn.
AX100	Glengaber Burn.	AX166	Kingledoors Burn.
AX101	Glengaber Burn.	AX167	Upper Olive Dod Area.
AX102	Glengaber Burn.	AX168	Kings Beck.
AX103	Glengaber Burn.	AX169	Kings Beck.
AX104	Poultrybuie Hill.	AX170	Birthwood.
AX105	Poultrybuie Hill.	AX171	Nisbet.
AX106	Corse Burn area.	AX172	Nisbet.
AX107	Munwhul.	AX177	Cat Shoulder, Camps.
AX108	Munwhul.	AX178	Slate Brae.
AX109	Fore Burn.	AX179	March Burn.
AX110	Munwhul.	AX180	Read Gill, Camps.
AX111	Brigton.	AX181	Fall Hill.
AX112	Pulniskie Burn.	AX182	Tippet Hill, Beattock Summit.
AX113	Larg Fell.	AX185	East Water, Harecleuch.
AX114	Pulniskie Burn area.	AX187	East Water, Harecleuch.
AX115	Ferrach Burn area.	AX188	Harecleuch Farm.
AX116	Ferrach Burn area.	AX189	Harecleuch Farm.
AX117	Ferrach Burn area.	AX190	Grains Burn, Camps.
AX118	Black Burn area.	AX191	Camps Dam.
AX119	Jenny's Hill.	AX194	Frigg Gas Trench, Little Clyde
AX121	Borgan.	AX195	Frigg Gas Trench, Little Clyde
AX122	Larg.	AX196	Frigg Gas Trench, Little Clyde

AX197	Frigg Gas Trench, Little Clyde	AX276	A7, Stagebank.
AX198	Frigg Gas Trench, Tippet Hill.	AX277	Cakemuir Burn.
AX199	Frigg Gas Trench, Tippet Hill.	AX278	Falahill.
AX200	Grains Burn, Camps.	AX279	Heriot Station.
AX201	Grains Burn, Camps.	AX280	A7, Buckholm.
AX202	Big Swagill, Cowgill.	AX281	Bow Quarry.
AX203	Big Swagill, Quarry.	AX282	Bowland Station.
AX204	Cowgill Rig.	AX283	Bowland.
AX206	Stone Gill, Culter Water.	AX284	Stow Station.
AX210	Culter Water.	AX285	Lugate Farm.
AX211	Brecks Burn, Culter Dam.	AX286	Cortleferry Quarry.
AX212	Culter Water.	AX287	Halltree Farm.
AX213	Culter Water.	AX288	Glengap Burn.
AX214	Hartside Burn.	AX289	Todholes Hill.
AX215	Hartside Quarry.	AX290	Todholes Hill.
AX216	Devonshaw Hill.	AX292	Fingland Burn.
AX217	Devonshaw Hill.	AX293	Fingland Burn.
AX218	Frigg Gas Trench, Fopperbeck.	AX294	Fingland Burn.
AX219	Frigg Gas Trench, Dead Side.	AX296	Kiln Burn, Bail Hill.
AX220	Frigg Gas Trench, Dead Side.	AX298	Sow Burn, Bail Hill.
AX221	Frigg Gas Trench, Clydes Burn.	AX299	Kiln Burn, Bail Hill.
AX222	Gair Gill, Culter Water.	AX300	Kiln Burn, Bail Hill.
AX223	Gair Gill, Culter Water.	AX301	Kiln Burn, Bail Hill.
AX224	Culter Craigs Quarry.	AX302	Kiln Burn, Bail Hill.
AX225	Frigg Gas Trench, Hill End.	AX304	Kiln Burn, Bail Hill.
AX226	Frigg Gas Trench, Hill End.	AX305	Kiln Burn, Bail Hill.
AX227	Frigg Gas Trench, Hill End.	AX306	Kiln Burn, Bail Hill.
AX229	Scar Water.	AX307	Kiln Burn, Bail Hill.
AX230	Scar Water.	AX308	Kiln Burn, Bail Hill.
AX231	Scar Water.	AX311	Kiln Burn, Bail Hill.
AX232	Scar Water.	AX604	Talla Linn.
AX233	Scar Water.	AX657	Tweedsmuir.
AX234	Scar Water.	AX659	A701, Hawkshaw, Tweedsmuir.
AX235	Frigg Gas Trench, Buch.	AX753	Dreva Hill.
AX236	Frigg Gas Trench, Buch..	AX755	A701, Stanhope.
AX237	Frigg Gas Trench, Errickstane.	AX781	Badlien Quarry.
AX238	Frigg Gas Trench, Errickstane.	AX782	Badlien Quarry.
AX239	Frigg Gas Trench, Buch.	AX783	Glenwhappen Burn.
AX241	Frigg Gas Trench, Buch.	AX784	Fingland Burn.
AX243	Frigg Gas Trench, Buch.	AX785	Fingland Burn.
AX244	Frigg Gas Trench, Buch.	AX789	Fingland Burn.
AX245	River Tweed.	AX790	Fingland Burn.
AX246	Stobo Quarry.	AX791	Hawkshaw Burn.
AX247	Dob's Linn.	AX796	Craigmaid.
AX248	Dob's Linn.	AX797	Fingland Hill.
AX249	Dob's Linn.	AX800	Glenbreck Burn.
AX251	Pim Quarry, Innerleithen.	AX802	Glenbreck Burn.
AX271	Craigend Quarry.	AX803	Peddirie Dod, Glenbreck.
AX272	Old Quarry, Stow.	AX805	Old Burn, Fingland.
AX273	Buckholm.	AX833	Black Grain, Fingland.
AX274	A7, Fountainhall.	AX834	Ballaman Hill, Fruid.
AX275	Hangingshaw Quarry.	AX835	Muckle Burn, Badlieu.

AX840	Colin Craig, Cor Water.	A	1	Glen Afton.
AX841	River Tweed, Tweedhopefoot.	A	2	Glen Afton.
AX842	Priest Burn, Tweedhopefoot.	A	6	Glen Afton.
AX844	Kirkhope Burn, Manor Water.	A	7	Glen Afton.
AX847	Whitehope Burn, Earlshaugh.	A	9	Glen Afton.
AX849	Annanhead Hill.	A	12	Glen Afton.
AX851	Powskein Burn, Earlshaugh.	A	13	Glen Afton.
AX852	Ram Gill.	A	14	Glen Afton.
AX857	Shank Houp, Cowgill.	A	15	Glen Afton.
AX858	Shank Houp, Cowgill.	A	17	Glen Afton.
AX861	Pipershole Burn, Tweedsmuir.	A	18	Glen Afton.
AX864	Snaip Hill, Coulter.	A	19	Glen Afton.
AX865	Cow Gill, Coulter.	A	20	Glen Afton.
AX866	Wool Gill.	A	21	Glen Afton.
AX868	Tweedhopefoot.	A	22	Glen Afton.
AX873	Nisbet Burn.	A	23	Glen Afton.
		A	24	Glen Afton.
DTIA 2	Dalry, A713.	A	26	Glen Afton.
DTIA 3	Dalry, A713.	A	33	Glen Afton.
DTIA 5	Dalry, A713.	A	35	Blackcraig Hill.
DTIA 27	Bennan.	A	36	Blackcraig Hill.
DTIA 39	Benbrack.	A	43	Blackcraig Hill.
DTIA 41	Benbrack.	A	45	Blackcraig Hill.
DTIA 42	Benbrack.	A	46	Blackcraig Hill.
DTIA 47	Drumbuie.	A	49	Blackcraig Hill.
DTIA 48	Stranfasket Hill.			
DTIA103	Polharrow Burn, Fore Bush.	S	54	Scar Water.
DTIA104	Polharrow Burn, Fore Bush.	S	56	Scar Water.
DTIA131	Cairnsgarroch.	S	57	Scar Water.
DTIA133	Meikle Craigtarson.	S	58	Scar Water.
DTIA135	Cairnsgarroch.	S	59	Scar Water.
DTIA211	Marbrack Farm.	S	60	Scar Water.
DTIA212	Gallow Rig.	S	62	Scar Water.
DTIA292	Clatteringshaws Loch.	S	64	Scar Water.
		S	65	Scar Water.
		S	67	Scar Water.
		S	70	Scar Water.
		S	75	Scar Water.
		S	77	Scar Water.
		S	85	Glenwhargen Craig.
		S	88	Glenwhargen Craig.
		S	93	Glenwhargen Craig.
		S	95	Glenwhargen Craig.
		S	96	Glenwhargen Craig.
		S	97	Glenwhargen Craig.
		S	99	Glenwhargen Craig.
		S	100	Scar Water.
		S	101	Scar Water.
		S	102	Scar Water.
		S	103	Scar Water.
		S	104	Scar Water.
		S	105	Scar Water.

S 107 Scar Water.
S 108 Scar Water.
S 110 Scar Water.
S 111 Scar Water.
S 113 Scar Water.
S 114 Scar Water.
S 115 Scar Water.
S 116 Scar Water.
S 117 Glenmaddie Craig.
S 118 Glenmaddie Craig.
S 119 Glenmaddie Craig.
S 120 Stell Burn.
S 121 Stell Burn.
S 122 Stell Burn.
S 123 Stell Burn.
S 124 Stell Burn.
S 125 Stell Burn.
S 126 Scar Water.
S 127 Scar Water.
S 128 Scar Water.
S 129 Scar Water.
S 130 Scar Water.
S 131 Scar Water.
S 133 Scar Water.
S 134 Scar Water.

E 135 Glenmaddie Craig.
E 136 Glen Burn.
E 138 Glen Burn.
E 139 Birk Burn.
E 140 Birk Burn.
E 142 Birk Burn.
E 146 Glen Burn.
E 148 Glen Burn.
E 150 Glen Burn.
E 151 Glen Burn.
E 152 Glen Burn.
E 153 Glen Burn.
E 155 Glen Burn.
E 156 Glen Burn.
E 157 Glen Burn.
E 159 Euchar Water.
E 160 Euchar Water.
E 161 Euchar Water.
E 162 Barr Moor.
E 163 Barr Moor.
E 164 Barr Moor.
E 165 Barr Moor.
E 166 Barr Moor.
E 168 Barr Moor.
E 171 Barr Moor.
E 172 Brunt Rig.

E 173 Brunt Rig.
E 174 Brunt Rig.
E 175 Drumbuie Moorhead.
E 176 Drumbuie Moorhead.
E 177 Drumbuie Moorhead.

A 178 Blacklorg Hill.
A 181 Craig Burn.
A 185 Craig Burn.
A 186 Craig Burn.
A 187 Craig Burn.
A 188 Craig Burn.
A 189 Craig Burn.
A 190 Craig Burn.
A 191 Craig Burn.
A 192 Craig Burn.
A 193 Craig Burn.
A 195 Craig Burn.
A 197 Craig Burn.
A 198 Craig Burn.
A 199 Blackcraig Hill.
A 200 Blackcraig Hill.
A 201 Blackcraig Hill.
A 202 Blackcraig Hill.
A 203 Blackcraig Hill.
A 204 Blackcraig Hill.
A 205 Blackcraig Hill.
A 207 Blackcraig Hill.
A 208 Blackcraig Hill.
A 209 Blackcraig Hill.
A 210 Blackcraig Hill.
A 211 Blackcraig Hill.
A 212 Blackcraig Hill.
A 214 Gray Burn.
A 215 Langlee Burn.
A 216 Langlee Burn.
A 217 Dingle Brae.
A 218 Dingle Brae.
A 219 Pollach Burn.
A 221 March Burn.
A 222 March Burn.
A 225 Lochbrowan Hill.
A 227 Lochbrowan Hill.
A 228 Lochbrowan Hill.
A 229 Lochbrowan Hill.
A 232 Dalhanna Burn.
A 233 Dalhanna Burn.
A 234 Dalhanna Burn.
N 237 March Burn.
N 238 March Burn.
N 239 March Burn.

N 241	March Burn.	K 327	Carcarse Burn.
N 242	March Burn.	K 328	Carcarse Burn.
N 250	Polmarlach Burn.	K 330	Kello Water.
N 251	Polmarlach Burn.	K 331	March Burn.
N 252	Polmarlach Burn.	K 333	Kello Water.
N 253	Polmarlach Burn.		
N 255	Polmarlach Burn.	A 334	Bolt Burn.
N 256	Polmarlach Burn.	A 335	Bolt Burn.
N 257	Polmarlach Burn.	A 336	Bolt Burn.
N 258	Polmarlach Burn.	A 337	Bolt Burn.
N 259	Polmarlach Burn.	A 338	Bolt Burn.
N 260	Polmarlach Burn.	A 340	Bolt Burn.
N 261	Polmarlach Burn.	D 344	Reeve Craigs.
N 262	Polmarlach Burn.		
N 263	Polmarlach Burn.	S 345	Scar Water.
N 265	Polhote Burn.	S 348	Scar Water.
N 267	Polhote Burn.	S 350	Scar Water.
N 268	Polhote Burn.	S 351	Scar Water.
N 269	Polhote Burn.	S 352	Dalganar.
N 270	Polhote Burn.	S 354	Scar Water.
N 274	Polneul Burn.	S 355	Scar Water.
		S 356	Scar Water.
K 280	Mynwhirr Burn.	S 359	Scar Water.
K 284	Mynwhirr Burn.	S 360	Scar Water.
		S 361	Scar Water.
N 292	Redree Burn.		
N 294	Dalhanna Hill.	A 369	Quintin Knowe.
		A 370	Quintin Knowe.
A 297	Afton Water.		
A 299	Afton Water.	K 373	Bottan Burn.
A 300	Afton Dam.		
A 301	Afton Dam.	A 374	Langlee Burn.
A 302	Mantraw Burn.	A 377	Dingle Brae.
A 303	Mantraw Burn.	A 378	Gray Burn.
A 304	Mantraw Burn.		
A 305	Mantraw Burn.	W 379	A 713, Dalmellington.
A 306	Mantraw Burn.	W 380	A 713, Glenmuck.
A 307	Mantraw Burn.	W 382	A 713, Glenmuck.
A 308	Mantraw Burn.	W 383	A 713, Glenmuck.
A 309	Mantraw Burn.	W 384	Loch Muck.
A 310	Mantraw Burn.	W 385	Loch Muck.
A 311	Meikledodd Hill.	W 386	A 713, Meadowhead.
A 313	Alwhat.	W 387	Water of Deugh.
A 314	Alwhat.	W 388	Bow Burn, Water of Deugh.
A 315	Langlee Burn.	W 389	A 713, Carsphairn.
K 317	Kello Water.		
K 318	Kello Water.	E 391	Poltallan Burn.
K 321	Kello Water.		
K 322	Kello Water.	A 393	Blacklorg Hill.
K 323	Kello Water.		
K 325	Carcarse Burn.	K 394	Kello Water.
		K 395	Kello Water.

- A 396 Blacklorg Hill.
N 397 Polmarlach Burn.
L 399 Mennock Water.
N 400 Burnsands Burn.
N 401 Burnsands Burn.
N 402 Burnsands Burn.
N 403 River Nith.
E 404 Glenlarie Burn.
E 407 Glenlarie Burn.
E 408 Collar Knowe.
E 409 Collar Knowe.
N 410 Polmarlach Burn.
N 413 Nethertown Burn.
N 426 Nether Cairn.
N 430 March Burn.
N 431 March Burn.
N 433 Nether Cairn Farm.
A 434 Carcow Burn.
A 439 Lochingirroch Burn.
A 440 Glenshalloch Burn.
A 441 Glenshalloch Burn.
A 443 Ashmark Hill.
A 444 Ashmark Hill.
A 445 Ashmark Hill.
N 447 Gatelock Craigs.
S 448 Scar Water.
S 449 Rashy Grain.
S 450 Dalganar Cleuch.
E 452 Poltallon Burn.
N 453 River Nith.
N 454 River Nith.
N 456 River Nith.
N 459 Gatelock Craigs.
N 460 Rye Burn, New Cumnock.
K 462 Polhigh Burn.
A 463 Craig Burn, Glen Afton.
S 464 Druidhill Burn.
S 466 Druidhill Burn.
C 469 Ashmark Hill.
C 470 Ashmark Hill.
C 471 Ashmark Hill.
C 472 Connel Burn.
C 473 Connel Burn.
C 474 Connel Burn.
N 476 Spout Burn.
N 478 March Burn.
N 480 March Burn.
N 481 Docken Burn.
N 485 Hare Sike.
N 486 Polmarlach Burn.
A 487 Langlee Burn.
A 488 Langlee Burn.
S 491 Glenwhem Burn.
S 492 Glenwhem Burn.
S 494 Glenwhem Burn.
S 496 Glenwhem Burn.
S 497 Glenwhem Burn.
S 498 Druidhill Burn.
S 499 Druidhill Burn.
E 503 Whing Burn.
N 506 Hall Burn, Glenmuckloch.
N 507 Burnsands Burn.
L 515 Dinabid Linn, Dalveen Pass.
L 520 Dinabid Linn, Dalveen Pass.
L 522 Potrenick Burn, Dalveen Pass.
L 527 Glenimshaw Burn.
L 528 Glenimshaw Burn.
S 529 Cairn Burn.
S 531 Cairn Burn.
S 532 Cairn Burn.
S 533 Cairn Burn.
A 535 Glen Afton.
A 536 Glen Afton.
N 540 March Burn.
N 542 March Burn.
N 543 March Burn.
L 548 WH 3 Borehole, Wanlockhead.
L 554 WH 3 Borehole, Wanlockhead.
L 559 WH 6 Borehole, Wanlockhead.
L 562 WH 6 Borehole, Wanlockhead.
L 566 WH 6 Borehole, Wanlockhead.

L 572 WH 7 Borehole, Wanlockhead.

W 580 Loch Braden.

W 581 Loch Braden.

W 582 Loch Braden.

L 584 Lime Cleuch.

L 585 Lime Cleuch.

L 586 Lime Cleuch.

L 587 Lime Cleuch.

L 589 Lime Cleuch.

L 590 Lime Cleuchfoot.

L 591 March Burn.

N 592 March Burn.

N 593 March Burn.

N 594 March Burn.

N 595 March Burn.

N 597 March Burn.

W 598 Loch Braden.

W 599 Loch Braden.

W 602 Witches Bridge.

W 603 Balloch Burn.

W 604 Loch Doon.

W 606 Pinwherry.

W 607 Albany Burn.

W 608 Portandea.

W 609 Portandea.

N 610 Docken Burn.

N 611 Docken Burn.

N 612 Docken Burn.

S 615 Hall Burn.

S 616 Scar Water.

S 617 Scar Water.

S 618 Scar Water.

N 619 Kiln Burn.

S 622 Scar Water.

S 623 Carlinstane Burn.

S 624 Carlinstane Burn.

A 629 Glen Afton.

ZK 377 Frigg Gas Pipeline, Craig Hill.

ZK 379 Frigg Gas Pipeline, Craig Hill.

ZK 380 Frigg Gas Pipeline, Craig Hill.

APPENDIX A5.2 : WEST COAST TRAVERSE

PDW	1	Currarie Port	PDW	51	Boak Port
PDW	2	Currarie Port	PDW	52	Lady Cave
PDW	3	Craigangal	PDW	53	Bradock
PDW	4	Craigangal	PDW	54	Burnfoot
PDW	5	Brackness Hole	PDW	55	Dundream
PDW	6	Brackness Hole	PDW	56	Port Mullin
PDW	7	Tongue	PDW	57	Portaclearys
PDW	8	Burnt Foot	PDW	58	Ochley Point
PDW	9	Glendrisaig Farm	PDW	59	Well Isle
PDW	10	Turf Hill	PDW	60	Dunskirloch
PDW	11	Turf Hill	PDW	61	Corsesnall Point
PDW	12	Portandea	PDW	62	Slouchlaw
PDW	13	Portandea	PDW	63	Ships Slouch
PDW	14	Portandea	PDW	64	Horseback Rock
PDW	15	Finnarts Hill	PDW	65	Bloody Rock
PDW	16	Finnarts Point	PDW	66	Bloody Rock
PDW	17	Nelsons Cove	PDW	67	Barrack Point
PDW	18	Dyke Foot	PDW	68	Braid Port
PDW	19	Dyke Foot	PDW	69	Braid Port
PDW	20	Garry Point	PDW	70	Genoch Rocks
PDW	21	Garry Point	PDW	71	Genoch Rocks
PDW	22	Finnarts Bay	PDW	72	Genoch Rocks
PDW	23	Port Sally	PDW	73	Port Gavillan
PDW	24	Port Sally	PDW	74	Port Gavillan
PDW	25	Staling Knowe	PDW	75	Portnaughan Bay
PDW	26	Altehit Burn	PDW	76	Portnaughan Bay
PDW	27	Galloway Burn	PDW	77	Portnaughan Bay
PDW	28	White Cave	PDW	78	South Cairn
PDW	29	Black Cave	PDW	79	Portlong Bay
PDW	30	Polymodie Bridge	PDW	80	Laggan Hill
PDW	31	Clachan Heughs	PDW	81	Dally Bay
PDW	32	Clachan Heughs	PDW	82	Dounan Bay
PDW	33	Portbeg	PDW	83	Dinbonnet
PDW	34	Jamiesons Point	PDW	84	Portsand
PDW	35	Jamiesons Point	PDW	85	Portsand
PDW	36	Jamiesons Point	PDW	86	March Port
PDW	37	Portmore	PDW	87	Castle Butt
PDW	38	Yellow Craig	PDW	88	Castle Butt
PDW	39	Lady Bay	PDW	89	Carrick Fundle
PDW	40	Broadport	PDW	90	Salt Pan Bay
PDW	41	Marsh Slung	PDW	91	Salt Pan Bay
PDW	42	McMeckans Rocks	PDW	92	Salt Pan Bay
PDW	43	The Beef Barrel	PDW	93	Salt Pan Bay
PDW	44	The Beef Barrel	PDW	94	Portobello
PDW	45	Port Nauchtry	PDW	95	Portobello
PDW	46	Port Nauchtry	PDW	96	Dounan Knowe
PDW	47	Port Nauchtry	PDW	97	Dounan Knowe
PDW	48	Millev Point	PDW	98	Strool Bay
PDW	49	Millev Point	PDW	99	Strool Bay
PDW	50	Millev Point	PDW	100	Strool Bay
			PDW	101	Strool Bay
			PDW	102	Juniper Rock

PDW	104	High Mark	PDW	156	Port Morn
PDW	105	High Mark	PDW	157	Yellow Isle
PDW	106	High Mark	PDW	158	Yellow Isle
PDW	107	Slouchnawen Bay	PDW	159	Portpatrick
PDW	108	Slouchnawen Bay	PDW	160	Portpatrick
PDW	109	Slouchnawen Bay	PDW	161	Portpatrick
PDW	110	Galdenoch Burn	PDW	162	Portpatrick
PDW	111	Meikle Galdenoch	PDW	163	Castle Point
PDW	112	Meikle Galdenoch	PDW	164	Castle Point
PDW	113	Meikle Galdenoch	PDW	165	Castle Point
PDW	114	Galdenoch Moor	PDW	166	Castle Point
PDW	115	Galdenoch Moor	PDW	167	Tandoo Point
PDW	116	Galdenoch Moor	PDW	168	Tandoo Point
PDW	117	Galdenoch Moor	PDW	169	Tandoo Point
PDW	118	Galdenoch Moor	PDW	170	Morroch Bay
PDW	119	Salt Pans Bay	PDW	171	Morroch Bay
PDW	120	Salt Pans Bay	PDW	172	Morroch Bay
PDW	121	Salt Pans Bay	PDW	173	Morroch Bay
PDW	122	Cranberry Point	PDW	174	Morroch Bay
PDW	123	Cranberry Point	PDW	175	Finloch Bay
PDW	124	Cranberry Point	PDW	176	Finloch Bay
PDW	125	Cranberry Point	PDW	177	Finloch Bay
PDW	126	Cranberry Point	PDW	178	Dunanrea Bay
PDW	127	Broadsea Bay	PDW	179	Dunanrea Bay
PDW	128	Broadsea Bay	PDW	180	Portayew
PDW	129	Broadsea Bay	PDW	181	Portayew
PDW	130	Broadsea Bay	PDW	182	Cairngarroch Bay
PDW	131	Broadsea Bay	PDW	183	Cairngarroch Bay
PDW	132	Knockgour	PDW	184	Cairngarroch Bay
PDW	133	Knockgour	PDW	185	Cairngarroch Bay
PDW	134	Knockgour	PDW	186	Cairngarroch Bay
PDW	135	Portslogan	PDW	187	Cairnmon Fell
PDW	136	Portslogan	PDW	188	Cairnmon Fell
PDW	137	Portslogan	PDW	189	Scarty Head
PDW	138	Cable House	PDW	190	Scarty Head
PDW	139	Cable House	PDW	191	Money Head
PDW	140	Knock Bay	PDW	192	Money Head
PDW	141	Knock Bay	PDW	193	Money Head
PDW	142	Knock Bay	PDW	194	Money Head
PDW	143	Killantringan Bay	PDW	195	Slunkrainy
PDW	144	Killantringan Bay	PDW	196	Slunkrainy
PDW	145	Killantringan Bay	PDW	197	Slunkrainy
PDW	146	Black Head	PDW	198	Float Bay
PDW	147	Black Head	PDW	199	Float Bay
PDW	148	Portamaggie	PDW	200	Float Bay
PDW	149	Portamaggie	PDW	201	Float Bay
PDW	150	Portamaggie	PDW	202	Float Bay
PDW	151	Portayaddie	PDW	203	Hole Stone Bay
PDW	152	Portayaddie	PDW	204	Hole Stone Bay
PDW	153	Stronie	PDW	205	Hole Stone Bay
PDW	154	Catebraid	PDW	206	Hole Stone Bay
PDW	155	Port Kale	PDW	207	Salt Pans

PDW	208	Salt Pans	PDW	260	Port Mona
PDW	209	Salt Pans	PDW	261	Port Mona
PDW	210	Ardwell Bay	PDW	262	Port Kemin
PDW	211	Ardwell Bay	PDW	263	Port Kemin
PDW	212	Ardwell Bay	PDW	264	Port Kemin
PDW	213	Ardwell Point	PDW	265	Port Kemin
PDW	214	Ardwell Point	PDW	266	Port Kemin
PDW	215	Ardwell Point	PDW	267	Port Kemin
PDW	216	Ardwell Point	PDW	268	Port Kemin
PDW	217	Grennan Point	PDW	269	Port Kemin
PDW	218	Grennan Point	PDW	270	Port Kemin
PDW	219	Grennan Point	PDW	271	West Tarbet
PDW	220	Drumoreddan Bay	PDW	272	West Tarbet
PDW	221	Drumoreddan Bay	PDW	273	West Tarbet
PDW	222	Drumoreddan Bay	PDW	274	West Tarbet
PDW	223	Port Lochan	PDW	275	West Tarbet
PDW	224	Port Gill	PDW	276	Kennedy's Cairn
PDW	225	Duniehinnie Fort	PDW	277	Kennedy's cairn
PDW	226	Duniehinnie Fort	PDW	278	Gallie Craig
PDW	227	Duniehinnie Fort	PDW	279	Gallie Craig
PDW	228	Mull of Logan	PDW	280	Wigtown Castle
PDW	229	Mull of Logan	PDW	281	Baldoon Mains
PDW	230	Mull of Logan	PDW	282	Braehead
PDW	231	Cairnie Finnart	PDW	283	Skellarie Rock
PDW	232	Cairnie Finnart	PDW	284	Orchardton
PDW	233	Cairnie Finnart	PDW	285	Orchardton
PDW	234	Port Nessock	PDW	286	Orchardton
PDW	235	Port Nessock	PDW	287	Orchardton
PDW	236	Muldaddie	PDW	288	Orchardton
PDW	237	Muldaddie	PDW	289	Innerwell Port
PDW	238	Cairnywellan Head	PDW	290	Innerwell Port
PDW	239	Cairnywellan Head	PDW	291	Innerwell Port
PDW	240	Slouchnamorroch Bay	PDW	292	Innerwell Port
PDW	241	Clanyard Bay	PDW	293	Innerwell Port
PDW	242	Clanyard Bay	PDW	294	Jultock Point
PDW	243	Clanyard Bay	PDW	295	Jultock Point
PDW	244	Clanyard Bay	PDW	296	Jultock Point
PDW	245	Muddioch Rock	PDW	297	Jultock Point
PDW	246	Breddoch Bay	PDW	298	Port McGean
PDW	247	Breddoch Bay	PDW	299	Port McGean
PDW	248	Breddoch Bay	PDW	300	Port McGean
PDW	249	Breddoch Bay	PDW	301	Port McGean
PDW	250	Breddoch Bay	PDW	302	Port McGean
PDW	251	Portdown Bay	PDW	303	Port McGean
PDW	252	Portdown Bay	PDW	304	Eggerness Point
PDW	253	Portdown Bay	PDW	305	Eggerness Point
PDW	254	Portdown Bay	PDW	306	Eggerness Point
PDW	255	Portdown Bay	PDW	307	Eggerness Point
PDW	256	Port Mona	PDW	308	Cruggleton Bay
PDW	257	Port Mona	PDW	309	Cruggleton Bay
PDW	258	Port Mona	PDW	310	Cruggleton Bay
PDW	259	Port Mona	PDW	311	Sliddery Point

PDW	312	Slidderly Point	PDW	364	Manor Point
PDW	313	Slidderly Point	PDW	365	Thunder Hole
PDW	314	Cruggleton	PDW	366	Brighthouse Bay
PDW	315	Cruggleton	PDW	367	Brighthouse Bay
PDW	316	Cruggleton	PDW	368	Brighthouse Bay
PDW	317	Palmallet Point	PDW	369	Brighthouse Bay
PDW	318	Palmallet Point	PDW	370	White Beach
PDW	319	Palmallet Point	PDW	371	Mull Point
PDW	320	Port Allen	PDW	372	Mull Point
PDW	321	Port Allen	PDW	373	Mull Point
PDW	322	Port Allen	PDW	374	Mull Point
PDW	323	Port Allen	PDW	375	Mull Point
PDW	324	Port Allen	PDW	376	Fauldbog Bay
PDW	325	Port Allen	PDW	377	Fauldbog Bay
PDW	326	Port Allen			
PDW	327	Portyerrock Bay			
PDW	328	Portyerrock Bay			
PDW	329	Portyerrock Bay			
PDW	330	Portyerrock Bay			
PDW	331	Portyerrock Bay			
PDW	332	Portyerrock Bay			
PDW	333	Portyerrock Bay			
PDW	334	Portyerrock Bay			
PDW	335	Cairn Head			
PDW	336	Cairn Head			
PDW	337	Cairn Head			
PDW	338	Cairn Head			
PDW	339	Cairn Head			
PDW	340	Stein Head			
PDW	341	Stein Head			
PDW	342	Stein Head			
PDW	343	Isle of Whithorn			
PDW	344	Isle of Whithorn			
PDW	345	Isle of Whithorn			
PDW	346	Isle of Whithorn			
PDW	347	Bysbie Cott			
PDW	348	Bysbie Cott			
PDW	349	Broom Point			
PDW	350	Broom Point			
PDW	351	Broom Point			
PDW	352	Balmangan			
PDW	353	Balmangan			
PDW	354	Shaw Hole			
PDW	355	Senwick Wood			
PDW	356	Bar Point			
PDW	357	Bar Point			
PDW	358	Bar Point			
PDW	359	Bar Point			
PDW	360	Ross Bay			
PDW	361	Ross Bay Cottage			
PDW	362	Blackstone			
PDW	363	Manor Hole			

GY 1 Storr Haven.
GY 5 NE Luce Bay.
GY 7 W of Kilfillan.
GY 8 W of Kilfillan.
GY 10 N of Kilfillan Point.
GY 14 Borlochart Fell.
GY 16 WNW Green House Bridge.
GY 17 SE end, Rocks of Garheugh.
GY 20 Comrie Fell.
GY 21 Comrie Fell.
GY 22 WNW of Castle Sinniness.
GY 27 W of Castle Sinniness.
GY 28 W of Castle Sinniness.
GY 32 SW of Castle Sinniness.
GY 34 Comrie Sheepfold.
GY 37 SE of Lough Sinniness.
GY 39 Mull of Sinniness.
GY 40 Mull of Sinniness.
GY 45 Comrie Burn, Craigenholly.
GY 52 Borlochart Fell.
GY 54 Borlochart Fell.
GY 60 S of Bolcarry No 1.
GY 64 Comrie Fell.
GY 65 Borlochart Fell.
GY 68 NW of Gillespie.
GY 72 NW of Barhaskine.
GY 74 WSW of Barhaskine.
GY 83 SE of Collies Port.
GY 97 Carleton.
GY 98 NW of Carleton.
GY 105 NE of High Glenjorrie.
GY 106 Glenluce.
GY 107 NE of High Glenjorrie.
GY 108 SE of High Glenjorrie.
GY 109 S of High Glenjorrie.
GY 117 Gabsnout Burn.
GY 118 Gabsnout Burn.
GY 119 Glenhowl.
GY 121 Garheugh Farm.
GY 122 Garheugh Farm.
GY 123 Blackloch, Garheugh.
GY 129 S bank, Alticry Burn.
GY 131 Carsgreugh Fell.
GY 132 NNW of Cornwall.
GY 133 NE of Cornwall.
GY 134 NE of Cornwall.
GY 135 NE of Cornwall.
GY 136 NNW of Chippermere.
GY 137 Chippermere.
GY 139 E side of Bennan Hill.
GY 141 Drumblair.
GY 143 Drumblair.

GY 144 Drumblair.
GY 153 SSW of Barhaskine.
GY 154 SW of Barhaskine.
GY 155 Craignarget Hill.
GY 157 Airyolland.
GY 158 S side of Milton Fell.
GY 159 S side of Milton Fell.
GY 160 NNW of High Milton.
GY 163 Eldrig.
GY 172 East Barr.
GY 173 Corhulloch.
GY 177 Balcraig Moor.
GY 178 SE of Balcraig Moor.
GY 179 W of Barwinnock.
GY 181 Boreland of Longcastle.
GY 182 Boreland of Longcastle.
GY 185 Cairndoon.
GY 186 Whouphill Railway Cutting.
GY 187 Culbae.
GY 188 Dowies.
GY 189 NE of Blairbuie.
GY 190 N of Lorroch.
GY 192 Kirkmaiden
GY 199 Burrow Head.
GY 204 Burrow Head.
GY 205 Burrow Head.
GY 214 Rock of Providence.
GY 215 Carg Hisvon, Burrow Head.
GY 218 S of Mary Mine, Burrow Head.
GY 220 S of High Rouchan.
GY 226 Black Rocks, Monreith.
GY 227 S of Clarksburn.
GY 228 SW of Home Farm, Glasserton.
GY 233 Claymoddie.
GY 235 Gabsnout Burn.
GY 237 Hill of Glasserton.
GY 252 Carghidown.
GY 253 SE of Lobbocks.
GY 254 SE of Lobbocks.
GY 262 Port Castle Bay.
GY 263 SE of Port of Counan.
GY 267 W of Burrow Head.
GY 268 W of Burrow Head.
GY 269 W of Burrow Head.
GY 270 W of Burrow Head.
GY 271 Burrow Head.
GY 276 Machermore.
GY 277 NW of Culroy.
GY 283 Back Boy, Monreith.
GY 284 Northouse Burn
GY 285 Northouse Burn
GY 286 Northouse Burn

APPENDIX 5.3 Glendinning Exploration Sites.

DJR	1	Corbie Shank	DJR	51	Glenshanna Burn
DJR	2	Corbie Shank	DJR	52	Glenshanna Burn
DJR	3	Caple Rig	DJR	53	Glenshanna Burn
DJR	4	Caple Rig	DJR	54	Glenshanna Burn
DJR	5	Caple Rig	DJR	55	Glenshanna Burn
DJR	6	Fawside Burn	DJR	56	Glenshanna Burn
DJR	7	Fawside Burn	DJR	57	Glenshanna Burn
DJR	8	Upper Stennieswater	DJR	58	Glenshanna Burn
DJR	9	Upper Stennieswater	DJR	59	Glenshanna Burn
DJR	10	Upper Stennieswater	DJR	60	Glenshanna Burn
DJR	11	Upper Stennieswater	DJR	61	Glenshanna Burn
DJR	12	Upper Stennieswater	DJR	62	Glenshanna Burn
DJR	13	Under Stennieswater	DJR	700	Lyneholm
DJR	14	Jamestown	DJR	701	Skelfhill Pen
DJR	15	Crooks	DJR	702	Skelfhill Pen
DJR	16	Effgill	DJR	703	Southdean Burn
DJR	17	Stennieswater	DJR	704	Southdean Burn
DJR	18	Stennieswater	DJR	705	Southdean Burn
DJR	19	Stennieswater	DJR	706	Cotterscleuch Shiel
DJR	20	Stennieswater	DJR	707	Gledsneest
DJR	21	Stennieswater	DJR	708	Gledsneest
DJR	22	Stennieswater	DJR	709	Cotterscleuch Monument
DJR	23	Stennieswater	DJR	710	Cotterscleuch Monument
DJR	24	Stennieswater	DJR	711	Cotterscleuch Monument
DJR	25	Stennieswater	DJR	712	Cotterscleuch Monument
DJR	26	Under Stennieswater	DJR	713	Cotterscleuch Monument
DJR	27	Under Stennieswater	DJR	714	Cotterscleuch Monument
DJR	28	Under Stennieswater	DJR	715	Cotterscleuch Monument
DJR	29	Glenshanna Burn	DJR	716	Dryden Fell
DJR	30	Glenshanna Burn	DJR	717	Dryden Fell
DJR	31	Glenshanna Burn	DJR	718	Dryden Fell
DJR	32	Munshiel Hill	DJR	719	High Seat
DJR	33	Trough Hope	DJR	720	High Seat
DJR	34	Trough Hope	DJR	721	High Seat
DJR	35	Trough Hope	DJR	722	High Seat
DJR	36	Trough Hope	DJR	723	High Seat
DJR	37	Trough Hope	DJR	724	Dryden Fell
DJR	38	Trough Hope	DJR	725	Dryden Fell
DJR	39	Trough Hope	DJR	726	Bowanhill
DJR	40	Trough Hope	DJR	727	Bowanhill
DJR	41	Megdale	DJR	728	Teviothead
DJR	42	Meggat Water	DJR	729	Teviothead
DJR	43	Meggat Water	DJR	730	Teviothead
DJR	44	Meggat Water	DJR	731	Gledsneest
DJR	45	Meggat Water	DJR	732	Gledsneest
DJR	46	Meggat Water	DJR	733	Gledsneest
DJR	47	Meggat Water	DJR	734	Northouse Burn
DJR	48	Meggat Water	DJR	735	Northouse Burn
DJR	49	Meggat Water	DJR	736	Northouse Burn
DJR	50	Meggat Water	DJR	737	Northouse Burn
			DJR	738	Northouse Burn
			DJR	739	Northouse Burn

DJR	740	Northouse Burn	DJR	799	Binks Burn
DJR	741	Gledsnest	DJR	800	The Shoulder
DJR	742	Gledsnest	DJR	801	The Shoulder
DJR	743	Gledsnest	DJR	802	The Shoulder
DJR	751	Fawside Burn	DJR	803	The Shoulder
DJR	752	Meikledale Burn	DJR	804	The Shoulder
DJR	753	Meikledale Burn	DJR	805	River Teviot
DJR	754	Meikledale Burn	DJR	806	River Teviot
DJR	755	Meikledale Burn	DJR	807	River Teviot
DJR	756	Meikledale Burn	DJR	808	Rashiegrain
DJR	757	Meikledale Burn	DJR	809	Rashiegrain
DJR	758	Meikledale Burn	DJR	810	River Teviot
DJR	759	Meikledale Burn	DJR	811	Greatmoor Hill
DJR	760	Meikledale Burn	DJR	812	Greatmoor Hill
DJR	761	Meikledale Burn	DJR	813	Greatmoor Hill
DJR	762	Meikledale Burn	DJR	814	Phaup Burn
DJR	763	Meikledale Burn	DJR	815	Phaup Burn
DJR	764	Newmill	DJR	816	Phaup Burn
DJR	765	Newmill	DJR	817	Phaup Burn
DJR	766	Newmill	DJR	818	Phaup Burn
DJR	767	Newmill	DJR	819	Phaup Burn
DJR	768	Newmill	DJR	820	Phaup Burn
DJR	769	Frostlie Burn	DJR	821	Phaup Burn
DJR	770	Frostlie Burn	DJR	822	Phaup Burn
DJR	771	Rams Cleuch	DJR	823	Phaup Burn
DJR	772	Blackcleuch	DJR	824	Castleweary
DJR	773	Blackcleuch	DJR	825	Castleweary
DJR	774	Limiecleuch Burn	DJR	826	Far Height
DJR	775	Limiecleuch Burn	DJR	827	Binks Burn
DJR	776	Limiecleuch Burn	DJR	828	Binks Burn
DJR	777	Limiecleuch Burn	DJR	829	Binks Burn
DJR	778	Meikledale Burn	DJR	830	Binks Burn
DJR	779	Meikledale Burn	DJR	831	Birkiebrae
DJR	780	Meikledale Burn	DJR	832	Birkiebrae
DJR	781	Meikledale Burn	DJR	833	Birkiebrae
DJR	782	Meikledale Burn	DJR	834	Lairhope
DJR	783	Meikledale Burn	DJR	835	Lairhope
DJR	784	Yadgair Edge	DJR	836	Lairhope Burn
DJR	785	Yadgair Edge	DJR	837	Lairhope Burn
DJR	786	Yadgair Edge	DJR	838	Lairhope Burn
DJR	787	Yadgair Edge	DJR	839	Lairhope Burn
DJR	788	Yadgair Edge	DJR	840	Rashy Hill
DJR	789	Yadgair Edge	DJR	841	Lairhope Burn
DJR	790	Rams Cleuch	DJR	842	Pike Hill
DJR	791	Rams Cleuch	DJR	843	Rashy Hill
DJR	792	Rams Cleuch	DJR	844	Old Howpasley
DJR	793	Rams Cleuch	DJR	845	Lairhope Burn
DJR	794	Hill Head	DJR	846	Lairhope
DJR	795	Binks	DJR	847	Lairhope Burn
DJR	796	Binks Burn	DJR	848	Meggat Water
DJR	797	Binks Burn	DJR	849	Corlaw Burn
DJR	798	Binks Burn	DJR	850	Birkiebrae

DJR	851	Wester Rig	DJR	903	Whin Fell
DJR	852	Wester Rig	DJR	904	Ewenshope Fell
DJR	853	Wester Rig	DJR	905	Ewenshope Fell
DJR	854	Calfshaw Head	DJR	906	Wrangway Burn
DJR	855	Calfshaw Head	DJR	907	Linhope Burn
DJR	856	Calfshaw Head	DJR	908	Linhope Burn
DJR	857	Midhill	DJR	909	Linhope Burn
DJR	858	Philhope Loch	DJR	910	Linhope Burn
DJR	859	Philhope Loch	DJR	911	Linhope Burn
DJR	860	Philhope Loch	DJR	912	Frostlie Burn
DJR	861	Corlaw Burn	DJR	913	Wisp Hill
DJR	862	Corlaw Burn	DJR	914	Limiecleuch Burn
DJR	863	Corlaw Burn	DJR	915	Wisp Hill
DJR	864	Corlaw Burn	DJR	916	Commonbrae
DJR	865	Corlaw Burn	DJR	917	Commonbrae
DJR	866	Corlaw Burn	DJR	918	River Teviot
DJR	867	Corlaw Burn	DJR	919	River Teviot
DJR	868	Corlaw Burn	DJR	920	White Knowe
DJR	869	Corlaw Burn	DJR	921	White Knowe
DJR	870	Corlaw Burn	DJR	922	White Knowe
DJR	871	Corlaw	DJR	923	Worms Cleuch
DJR	872	Corlaw	DJR	924	Worms Cleuch
DJR	873	Black Burn	DJR	925	Worms Cleuch
DJR	874	Haregrain Burn	DJR	926	Worms Cleuch
DJR	875	Haregrain Burn	DJR	927	Ramsay Cleuch Burn
DJR	876	Black Burn	DJR	928	Ewesdown Sike
DJR	877	Blaeberry Hill	DJR	929	Ewesdown Sike
DJR	878	Blaeberry Hill	DJR	930	Crooked Braes
DJR	879	Blaeberry Hill	DJR	931	Ewesdown Sike
DJR	880	South Grain Pike	DJR	932	Rams Cleuch
DJR	881	Loath Knowe	DJR	933	Rams Cleuch
DJR	882	South Grain	DJR	934	Rams Cleuch
DJR	883	South Grain	DJR	935	Rams Cleuch
DJR	884	South Grain	DJR	936	Rams Cleuch
DJR	885	Raeburnhead	DJR	937	Rams Cleuch
DJR	886	South Grain Rig	DJR	938	Rams Cleuch
DJR	887	Yade Sike	DJR	939	Ewesdown Sike
DJR	888	Yade Sike	DJR	940	River Teviot
DJR	889	Yade Sike Rig	DJR	941	River Teviot
DJR	890	Roman Signal Station	DJR	942	River Teviot
DJR	891	Toddle Knowe	DJR	943	Stibbiegill Head
DJR	892	Brunt Rig	DJR	944	Swin-Gill
DJR	893	Cat Rig	DJR	945	Swin-Gill
DJR	894	Cat Rig	DJR	946	Swin-Gill
DJR	895	Meggat Water	DJR	947	Swin-Gill
DJR	896	Meggat Water	DJR	948	Swin-Gill
DJR	897	Kirk Cleuch Rig	DJR	949	Swin-Gill
DJR	898	Meggat Water	DJR	950	Swin-Gill
DJR	899	Eweslees	DJR	951	Swin-Gill
DJR	900	Eweslees Burn	DJR	952	Swin-Gill
DJR	901	Whin Fell			
DJR	902	Whin Fell			

APPENDIX A5.4 : WALLROCK ALTERATION SUITE.

<u>No.</u>	<u>Sample No.</u>	<u>Location</u>	<u>Notes</u>
1	PDK 1	The Knipe	Wallrock samples (main dump).
2	PDK 2	The Knipe	Wallrock samples (main dump).
3	PDK 3	The Knipe	Wallrock samples (main dump).
4	TALAS 1	Talnotry	Arsenopyrite-quartz vein.
5	PDTAL 1	Talnotry	Wallrock to chalcopryite lens.
6	PDMIN 1	Cairngarroch	Vein (Bleached Zone).
7	PDMIN 2	Cairngarroch	Vein (8-10cm).
8	PDMIN 3	Cairngarroch	Wallrock (18-100cm from vein).
9	PDMIN 4	Cairngarroch	Wallrock (8-18 cm from vein).
10	PDMIN 5	Cairngarroch	Wallrock (1-1.5 m from vein).
11	PDMIN10	Cairngarroch	Vein 50m north (30cm wide).
12	PDL 1	Leadhills	Suzannah Pb-Zn vein.
13	PDT 1	Tongerhie (shaft 2)	Greywacke (2.5-5m from vein).
14	PDT 2	Tongerhie (shaft 2)	Greywacke (1-2.5m from vein).
15	PDT 4	Tongerhie (shaft 2)	Greywacke (0-1.0m from vein).
16	PDT 5	Tongerhie	Sorting floor.

APPENDIX A5.5 : POLISHED THIN SECTION INDEX.

<u>Section No.</u>	<u>Sample No.</u>	<u>Location.</u>
5852	CXD 1505	Glendinning : BH 1 75.42 - 75.49m
5853	CXD 1506	Glendinning : BH 1 76.94 - 76.97m
5854	CXD 1512	Glendinning : BH 3 80.87 - 80.90m
5855	CXD 1516	Glendinning : BH 3 106.19 - 106.26m
5856	CXD 1527	Glendinning : BH 3 176.82 - 176.92m
5857	CXD 1528	Glendinning : BH 3 177.08 - 177.15m
5859	CXD 1537	Glendinning : BH 1 31.75 - 31.79m
5860	CXD 1538	Glendinning : BH 1 36.50 - 36.56m
5861	CXD 1507	Glendinning : BH 1 79.16 - 79.22m
5863	CXD 1514	Glendinning : BH 3 86.93 - 86.02m
5864	CXD 1517	Glendinning : BH 3 109.23 - 109.31m
5865	CXD 1518	Glendinning : BH 3 128.49 - 128.61m
5866	CXD 1519	Glendinning : BH 3 134.63 - 134.69m
5867	CXD 1521	Glendinning : BH 3 139.63 - 139.74m
5868	CXD 1522	Glendinning : BH 3 145.05 - 145.11m
5869	CXD 1523	Glendinning : BH 3 157.63 - 156.69m
5870	CXD 1524	Glendinning : BH 3 165.75 - 165.80m
5871	CXD 1526	Glendinning : BH 3 175.27 - 175.30m
5873	CXD 1540	Glendinning : BH 4 26.92 - 26.96m
5874	CXD 1541	Glendinning : BH 4 29.41 - 29.50m
5875	CXD 1535	Glendinning : BH 4 33.17 - 33.22m
6021	CXD 1552	Glendinning : BH 3 165.40 - 165.55m
6022	CXD 1558	Glendinning : BH 2 98.57 - 98.62m
6023	CXD 1559	Glendinning : BH 2 100.23 - 100.30m
6024	CXD 1560	Glendinning : BH 2 44.25 - 44.30m
6025	CXD 1561	Glendinning : BH 2 46.25 - 46.29m
6026	CXD 1562	Glendinning : BH 2 49.11 - 49.18m
6027	CXD 1563	Glendinning : BH 2 57.42 - 57.47m
6028	CXD 1564	Glendinning : BH 2 60.14 - 60.20m
6029	CXD 1565	Glendinning : BH 3 145.17 - 145.24m
6030	CXD 1566	Glendinning : BH 3 148.07 - 148.24m
6031	CXD 1567	Glendinning : BH 2 112.87 - 112.97m
6032	CXD 1568	Glendinning : BH 3 178.64 - 178.69m
6033	CXD 1569	Glendinning : BH 3 49.05 - 49.13m
6034	CXD 1570	Glendinning : BH 3 57.85 - 57.95m
6035	CXD 1572	Glendinning : BH 2 168.62 - 168.73m
6036	CXD 1574	Glendinning : BH 4 22.62 - 27.67m
6357	CXD 1575	Glendinning : BH 1 54.86 - 54.94m
6358	CXD 1576	Glendinning : BH 1 83.56 - 83.75m
6359	CXD 1577	Glendinning : BH 1 47.54 - 47.62m
6360	CXD 1573	Glendinning : BH 3 92.35 - 92.49m
6361	CXD 1585	Glendinning : BH 2 48.68 - 48.77m
6362	CXD 1593	Glendinning : BH 3 65.93 - 66.05m
6501	DJR 762	Glendinning : Regional
6502	DJR 821	Glendinning : Regional
6503	DJR 857	Glendinning : Regional
6504	DJR 875	Glendinning : Regional
6505	DJR 937	Glendinning : Regional
6506	DJR 1764	Glendinning : Regional
6507	DJR 1892	Glendinning : Regional
6508	DJR 1894	Glendinning : Regional

APPENDIX A5.5 : POLISHED THIN SECTION INDEX (Cont.).

<u>Section No.</u>	<u>Sample No.</u>	<u>Location.</u>
6509	PDMIN1	Cairngarroch Bay
6510	PDMIN2	Cairngarroch Bay
6511 (w)	PDMIN3	Cairngarroch Bay
6512	PDMIN4	Cairngarroch Bay
6513 (w)	PDMIN5	Cairngarroch Bay
6514	PDMIN6	Cairngarroch Bay
6515	PDW182	Cairngarroch Bay
6516 (w)	PDK1	The Knipe, Hare Hill.
6517 (w)	PDK2	The Knipe, Hare Hill.
6518 (w)	PDK3	The Knipe, Hare Hill.
6520	PDC 1.1	Clontibret
6521	PDC 1.2	Clontibret
6522	PDC 1.3	Clontibret
6523	PDC 1.4	Clontibret
6524	PDC 1.5	Clontibret
6526	PDC 2.5	Clontibret
6527 (w)	PDC 3.1	Clontibret
6528 (w)	PDC 5.6	Clontibret
6529 (w)	PDC 6.2	Clontibret
6530 (w)	PDC 6.6	Clontibret
6531	PDC 10.0	Clontibret
6534	PDC 11.1	Clontibret
6535 (w)	PDC 14.3	Clontibret
6536	PDC 16.1	Clontibret
6537	PDC 16.3	Clontibret
6538	PDC 16.4	Clontibret
6539 (w)	PDC 18.1	Clontibret
6540	PDC 19.1	Clontibret
6541	PDC 19.2	Clontibret
6542	PDC 20.1	Clontibret
6545 (w)	DTQ 1	Langholm Quarry
6546 (w)	DTQ 2	Langholm Quarry
6560	GLN 7	White Birren Quarry
6549	TALN1	Talnotry massive sulphide ore lens.
6550	TALN2	Talnotry massive sulphide ore lens.
6551 (w)	TALN3	Talnotry arsenopyrite vein.
6552	PD01	Tonderghie
6553	PD02	Tonderghie
6554	GLN1	Glendinning Mine Dump.
6555	GLN2	Glendinning Mine Dump.
6556	GLN3	Glendinning Mine Dump.
6557	GLN4	Glendinning Mine Dump.
6558 (w)	GLN5	Glendinning Mine Dump.
6561 (w)	GLN8	Glendinning Mine Dump.

Southern Uplands Composite Traverse : Sample Position and Location.

Position No.	Sample No.	Easting	Northing
1	AX-54	29102	62609
2	AX-156	30286	63328
3	AX-214	29717	62910
4	AX-215	29674	62960
5	AX-216	29643	62902
6	AX-217	29647	62912
7	AX-224	30284	63330
8	AX-292	27473	61739
9	AX-293	27431	61734
10	AX-294	27407	61736
11	A1	26302	60544
12	A232	26226	61065
13	A233	26210	61059
14	A234	26200	61065
15	N237	26719	61272
16	N238	26720	61261
17	N241	26721	61228
18	N292	26243	61192
19	N294	26251	61139
20	A297	26147	61119
21	A299	26141	61142
22	W379	24969	60358
23	W380	25050	60280
24	N413	26743	61374
25	N426	26675	61289
26	N430	26723	61233
27	N431	26722	61232
28	N433	26612	61272
29	C469	26060	60939
30	C472	26017	60980
31	C473	26001	61014
32	C474	26003	60991
33	N476	26710	61258
34	N478	26721	61253
35	N480	26720	61262
36	W506	26858	61360
37	N542	26727	61294
38	N543	26718	61273
39	N591	26722	61239
40	W603	23350	59470
41	W604	24850	60280
42	N610	26682	61238
43	N619	26646	61315
44	AX866	30223	63199
45	AX-62	29274	62080
46	AX-63	29101	62545
47	AX-131	23525	59069
48	AX-132	23532	58945
49	AX-133	23653	58150
50	AX-134	23490	58460

Southern Uplands Composite Traverse : Sample Position and Location.

Position No.	Sample No.	Easting	Northing
51	AX-135	23390	58350
52	AX-136	23285	58090
53	AX-137	23540	58178
54	AX-140	24920	59705
55	AX-141	24868	59822
56	AX-149	23758	58941
57	AX-169	30321	63052
58	AX-170	30269	63083
59	AX-171	30392	63217
60	AX-172	30384	63258
61	AX-202	30031	62856
62	AX-204	30172	62900
63	AX-222	30237	63181
64	AX-223	30252	63225
65	AX-296	27572	61478
66	AX-298	27615	61455
67	AX-299	27642	61449
68	AX-300	27670	61448
69	AX-301	27681	61425
70	AX-302	27681	61414
71	AX-305	27712	61357
72	AX-306	27714	61354
73	AX-307	27721	61338
74	AX-308	27741	61319
75	AX-311	27792	61284
76	DTIA-131	25246	59144
77	DTIA-212	26118	60347
78	E146	27395	60621
79	E148	27392	60644
80	E150	27423	60662
81	E151	27423	60672
82	E152	27421	60681
83	E153	27421	60689
84	E155	27441	60709
85	E156	27452	60726
86	E157	27437	60731
87	E159	27419	60743
88	E160	27317	60715
89	E161	27314	60725
90	E162	27308	60735
91	E163	27303	60746
92	E164	27296	60752
93	E165	27284	60759
94	E166	27280	60769
95	E168	27260	60791
96	E171	27246	60819
97	E172	27263	60854
98	E173	27272	60867
99	E174	27286	60844
100	E175	27287	60833

Southern Uplands Composite Traverse : Sample Position and Location.

Position No.	Sample No.	Easting	Northing
101	E176	27281	60821
102	E177	27267	60782
103	A181	26461	60436
104	A186	26437	60480
105	A187	26432	60492
106	A188	26427	60501
107	A189	26423	60511
108	A190	26420	60519
109	A191	26418	60527
110	A192	26412	60538
111	A193	26407	60547
112	A216	26361	60824
113	A219	26327	60891
114	A221	26314	60909
115	A222	26302	60916
116	A225	26273	60963
117	A227	26257	60980
118	A228	26247	60988
119	A229	26237	60991
120	N242	26721	61219
121	N250	26752	61079
122	N251	26758	61087
123	N252	26760	61097
124	N253	26764	61106
125	N255	26802	61182
126	N256	26799	61174
127	N257	26795	61168
128	N258	26793	61161
129	N259	26792	61155
130	N260	26779	61134
131	N261	26775	61127
132	N262	26770	61119
133	N263	26768	61113
134	N265	26860	61084
135	N267	26849	61070
136	N268	26842	61065
137	N269	26839	61057
138	N270	26832	61051
139	N274	26936	60984
140	K280	26887	60944
141	A302	26387	60363
142	A303	26394	60358
143	A304	26402	60349
144	A305	26412	60351
145	A306	26425	60347
146	A307	26434	60346
147	N308	26443	60344
148	A309	26482	60329
149	A310	26489	60326
150	A311	26528	60266

Southern Uplands Composite Traverse : Sample Position and Location.

Position No.	Sample No.	Easting	Northing
151	A313	26505	60228
152	A315	26368	60821
153	K317	26898	60903
154	K318	26908	60899
155	K321	26947	60881
156	K322	26963	60878
157	K323	27000	60893
158	K325	27009	60879
159	K327	26990	60861
160	K328	26986	60852
161	K330	27123	60880
162	K331	27200	60874
163	A334	26284	60899
164	A335	26268	60832
165	A336	26264	60809
166	A337	26254	60796
167	K337	26254	60796
168	A338	26246	60789
169	K373	26651	60742
170	A377	26394	60866
171	W382	25100	60230
172	W383	25130	60199
173	W384	25100	60120
174	W385	25110	60080
175	W386	25190	59970
176	W387	25460	59840
177	W388	25580	59800
178	W389	25430	59590
179	E391	26960	60701
180	K394	26455	60485
181	K395	26560	60503
182	A396	26478	60447
183	N397	26778	61141
184	E404	27330	60568
185	E407	27340	60558
186	N410	26792	61152
187	S449	26910	60360
188	S450	26935	60340
189	E452	26964	60694
190	K462	26622	60849
191	A463	26399	60561
192	N486	26782	61141
193	E503	27646	60739
194	W580	24340	59920
195	W582	24340	59810
196	N602	23430	59350
197	N612	26672	61207
198	AX857	30196	62954
199	AX-288	27504	61523
200	AX-289	27495	61590

Southern Uplands Composite Traverse : Sample Position and Location.

Position No.	Sample No.	Easting	Northing
201	AX-290	27495	61590
202	A2	26303	60549
203	A6	26282	60535
204	A7	26282	60529
205	A12	26293	60517
206	A13	26294	60512
207	A14	26298	60508
208	A15	26303	60503
209	A17	26279	60549
210	A18	26278	60554
211	A19	26277	60558
212	A20	26276	60567
213	A21	26277	60571
214	A22	26279	60574
215	A23	26281	60576
216	A24	26282	60581
217	A26	26286	60589
218	A33	26305	60617
219	A35	26397	60615
220	A36	26398	60612
221	A43	26387	60705
222	A45	26387	60714
223	A46	26386	60718
224	A49	26396	60728
225	A51	26357	60734
226	A195	26396	60564
227	A197	26386	60580
228	A198	26381	60587
229	A199	26383	60685
230	A200	26384	60677
231	A201	26385	60668
232	A202	26387	60659
233	A203	26385	60649
234	A204	26385	60641
235	A205	26386	60631
236	A207	26371	60743
237	A208	26370	60752
238	A209	26372	60760
239	A210	26374	60768
240	A211	26377	60776
241	A212	26378	60784
242	A214	26380	60810
243	A215	26376	60822
244	K284	26882	60912
245	A300	26306	60594
246	A301	26302	60483
247	A340	26244	60765
248	D344	26136	60410
249	A369	26541	60782
250	A370	26543	60794

Southern Uplands Composite Traverse : Sample Position and Location.

Position No.	Sample No.	Easting	Northing
251	A374	26438	60811
252	A378	26370	60815
253	A439	26168	60734
254	A440	26080	60661
255	A441	26079	60669
256	N487	26391	60818
257	A488	26391	60818
258	W581	24340	59880
259	W599	24340	59850
260	AX-2	32773	64746
261	AX-67	29460	61782
262	AX-68	29456	61793
263	AX-73	29350	61953
264	AX-75	29385	61893
265	AX-111	23612	57482
266	AX-112	23792	57509
267	AX-113	23809	57430
268	AX-117	23867	57694
269	AX-118	23872	57730
270	AX-119	23970	57835
271	AX-122	23661	57420
272	AX-123	23676	57297
273	AX-124	23708	57262
274	AX-130	23658	57381
275	AX-157	30342	62877
276	AX-158	30379	62754
277	AX-159	30357	62811
278	AX-163	30717	62835
279	AX-168	30342	63041
280	AX-180	29902	62278
281	AX-181	29618	62177
282	AX-190	30141	62401
283	AX-191	30014	62270
284	AX-200	30358	62477
285	AX-201	30187	62505
286	AX-206	30333	62770
287	AX-210	30461	62697
288	AX-211	30427	62767
289	AX-212	30341	62837
290	AX-213	30324	62904
291	AX-275	34065	65402
292	AX-277	33973	65644
293	AX-278	33974	65615
294	AX-279	33978	65554
295	DTIA-103	25454	58667
296	DTIA-104	25452	58668
297	DTIA-211	25980	59318
298	S-251	23802	57473
299	S-252	23577	57527
300	S75	27661	60123

Southern Uplands Composite Traverse : Sample Position and Location.

Position No.	Sample No.	Easting	Northing
301	S77	27628	60125
302	S85	27634	60299
303	S95	27599	60356
304	S96	27592	60363
305	S97	27585	60368
306	S99	27580	60371
307	S100	27641	60256
308	S102	27622	60261
309	S104	27653	60245
310	S105	27664	60239
311	S110	27686	60201
312	S111	27566	60349
313	S113	27548	60359
314	S114	27542	60365
315	S115	27532	60366
316	S116	27526	60372
317	E117	27442	60520
318	S118	27452	60512
319	S119	27456	60503
320	S120	27455	60491
321	S121	27466	60483
322	S122	27462	60474
323	S123	27476	60469
324	S124	27462	60447
325	S125	27460	60434
326	S126	27454	60422
327	S127	27465	60418
328	S128	27471	60410
329	S129	27480	60402
330	S130	27487	60393
331	S131	27493	60388
332	S133	27509	60378
333	S134	27517	60375
334	E135	27468	60533
335	E136	27459	60541
336	E139	27424	60548
337	E140	27415	60554
338	S356	27629	60142
339	L399	28320	60960
340	E408	27335	60503
341	E409	27359	60498
342	S491	28060	60358
343	L527	28543	60759
344	L528	28494	60828
345	L548	28683	61372
346	L554	28683	61372
347	L559	28626	61360
348	L562	28626	61360
349	L566	28626	61360
350	L572	28777	61324

Southern Uplands Composite Traverse : Sample Position and Location.

Position No.	Sample No.	Easting	Northing
351	L584	28484	60647
352	L585	28487	60658
353	L586	28507	60680
354	N615	27712	60227
355	S618	27622	60261
356	AX852	30382	62677
357	AX873	30515	63108
358	AK336	33650	65289
359	AK778	33470	65320
360	AX-1	33020	64609
361	AX-36	35792	66685
362	AX-37	35865	66837
363	AX-38	35873	66813
364	AX-127	26070	58390
365	AX-143	26040	58410
366	AX-164	30719	62771
367	AX-177	30281	62235
368	AX-189	30035	61949
369	AX-226	29737	61572
370	AX-229	28062	59663
371	AX-230	28067	59638
372	AX-231	28099	59616
373	AX-235	29552	61627
374	AX-236	29528	61643
375	AX-246	31580	63641
376	AX-276	34125	65320
377	AX-287	34111	65253
378	DTIA-47	25623	58238
379	S-6	26080	58350
380	S54	27886	60031
381	S56	27873	60042
382	S57	27869	60048
383	S58	27858	60056
384	S59	27851	60057
385	S60	27844	60063
386	S62	27825	60069
387	S64	27811	60075
388	S65	27801	60082
389	S67	27774	60093
390	S70	27734	60105
391	S345	27903	60009
392	S348	27942	59977
393	S350	27987	59946
394	S351	27991	59937
395	S354	27796	60081
396	S355	27754	60092
397	S359	28023	59903
398	S360	28025	59883
399	S361	28025	59849
400	N400	28406	60453

Southern Uplands Composite Traverse : Sample Position and Location.

Position No.	Sample No.	Easting	Northing
401	N401	28404	60487
402	N402	28394	60502
403	S448	28049	59614
404	N456	28387	60529
405	S464	28076	59812
406	S466	28089	59813
407	S492	28068	60243
408	S494	28078	60322
409	S496	28092	60301
410	S497	28094	60300
411	S498	28109	60166
412	S499	28095	60116
413	W507	28308	60427
414	L515	28928	60932
415	L520	28986	60848
416	L522	29310	61019
417	S529	28029	60208
418	S531	28019	60216
419	S532	28010	60227
420	S533	28003	60234
421	L587	28508	60679
422	L589	28489	60673
423	L590	28468	60534
424	S623	27785	60122
425	S624	27783	60117
426	AX753	31319	63546
427	AX800	30452	62280
428	AK3	34068	65403
429	AK391	33548	65107
430	AK397	33683	65085
431	AX-4	33065	64420
432	AX-5	32935	64578
433	AX-150	30977	62434
434	AX-151	31080	62290
435	AX-155	31034	62358
436	AX-182	30040	61638
437	AX-187	30132	61882
438	AX-194	29880	61594
439	AX-195	29908	61615
440	AX-196	29941	61618
441	AX-197	29972	61616
442	AX-198	30000	61615
443	AX-199	30026	61614
444	AX-219	30125	61541
445	AX-221	30075	61607
446	AX-234	28192	59537
447	AX-274	34235	65062
448	AX-286	34293	65006
449	DTIA-5	26130	58240
450	DTIA-27	25630	57889

Southern Uplands Composite Traverse : Sample Position and Location.

Position No.	Sample No.	Easting	Northing
451	DTIA-41	25507	58077
452	DTIA-42	25533	58126
453	S-4	26140	58230
454	AX657	31025	62448
455	AX659	30709	62228
456	AX781	30517	61869
457	AX782	30517	61869
458	AX783	30640	62200
459	AX784	30674	62034
460	AX789	30689	62085
461	AX790	30692	62154
462	AX791	30809	62012
463	AX796	30727	61757
464	AX797	30662	62143
465	AX802	30557	62187
466	AX803	30528	62112
467	AX805	30534	62025
468	AX861	30578	61862
469	AK1	34215	65071
470	AK83	34242	65096
471	AK88	34256	65057
472	AK390	33587	65038
473	AK454	33712	64806
474	AX-40	30643	60192
475	AX-43	30549	60302
476	AX-44	30514	60330
477	AX-46	30400	60404
478	AX-47	30395	60410
479	AX-48	30395	60424
480	AX-5	29889	60980
481	AX-79	30342	60549
482	AX-80	30328	60569
483	AX-83	30248	60616
484	AX-87	29977	60867
485	AX-94	31418	62008
486	AX-95	32354	62320
487	AX-96	31755	61810
488	AX-97	31855	61930
489	AX-99	31957	62164
490	AX-100	32178	62330
491	AX-102	32141	62381
492	AX-103	32133	62403
493	AX-104	23881	57331
494	AX-105	24864	57373
495	AX-106	24911	57515
496	AX-107	24895	57565
497	AX-108	24895	57565
498	AX-109	25013	57684
499	AX-179	30370	61306
500	AX-249	31959	61584

Southern Uplands Composite Traverse : Sample Position and Location.

Position No.	Sample No.	Easting	Northing
501	AX-251	33428	63738
502	AX-272	34485	64557
503	AX-273	34808	63850
504	AX-280	34779	63791
505	AX-281	34493	64170
506	AX-283	34605	63970
507	AX-284	34518	64476
508	AX-285	34477	64351
509	ZK-343	30843	59641
510	ZK-344	30826	59703
511	ZK-349	30660	60163
512	DTIA-2	26260	58030
513	DTIA-3	26260	58030
514	S-250	24916	57446
515	S-70109	36389	66236
516	S-70110	36391	66232
517	S-70111	36393	66221
518	S-70112	36393	66222
519	S-70115	35990	66801
520	S-70116	36004	66783
521	S-70118	36037	66743
522	S-70119	35992	66798
523	S-70120	36004	66782
524	S-70121	36079	66700
525	S-70122	36036	66745
526	S-70123	36036	66745
527	S-70124	36080	66699
528	S-70125	36110	66664
529	S-70126	36128	66643
530	S-70127	36140	66629
531	S-70128	36231	66522
532	S-70131	36865	65875
533	S-70132	36861	65879
534	S-70133	36720	65991
535	S-70134	36715	65995
536	S-70135	36711	66001
537	S-70136	36708	66003
538	S-70137	36697	66012
539	S-70141	36619	66056
540	S-70152	36414	66191
541	AX604	31413	62010
542	AX840	30661	61572
543	AX841	30569	61674
544	AX842	30720	61565
545	AX847	30853	61404
546	AX851	30710	61483
547	AK33	34383	64628
548	AK223	34335	64793
549	AK502	33817	64645
550	AK509	33952	64788

Southern Uplands Composite Traverse : Sample Position and Location.

Position No.	Sample No.	Easting	Northing
551	AK551	33800	64588
552	AK674	33973	64218
553	AX-271	34441	64616
554	AX-282	34579	64082
555	AK4	34441	64615
556	AK13	34368	63941
557	AK17	34380	63927
558	AK20	34398	63948
559	AK25	34323	63871
560	AK30	34461	64382
561	AK52	34677	63730
562	AK58	34782	63795
563	AK63	34491	63516
564	AX-114	23920	57569
565	AX-115	23811	57591
566	AX-116	23920	57664
567	AX-121	23638	57469
568	S-70113	36452	66164
569	S-70114	36452	66164
570	S-70138	36640	66046
571	S-70139	36639	66046
572	S-70140	36634	66049
573	S-70142	36610	66060
574	S-70143	36605	66062
575	S-70148	36474	66143
576	S-70149	36472	66144
577	S-70150	36461	66157
578	S-70151	36453	66163
579	S-70154	36619	66056
580	DJR-1	33555	59802
581	DJR-2	33535	59800
582	DJR-3	33500	59778
583	DJR-4	33464	59755
584	DJR-5	33447	59736
585	DJR-6	33388	59666
586	DJR-7	33409	59650
587	DJR-8	33370	59615
588	DJR-9	33358	59598
589	DJR-10	33330	59563
590	DJR-11	33321	59542
591	DJR-12	33310	59522
592	DJR-13	33271	59507
593	DJR-14	32997	59661
594	DJR-16	32998	59273
595	DJR-29	33102	59635
596	DJR-30	33108	59631
597	DJR-31	33114	59628
598	DJR-32	33111	59589
599	DJR-33	33093	59586
600	DJR-34	33087	59572

Southern Uplands Composite Traverse : Sample Position and Location.

Position No.	Sample No.	Easting	Northing
601	DJR-35	33082	59564
602	DJR-36	33070	59555
603	DJR-37	33055	59550
604	DJR-38	33047	59546
605	DJR-39	33037	59543
606	DJR-40	33028	59538
607	DJR-41	33018	59534
608	DJR-42	32990	59596
609	DJR-43	32994	59578
610	DJR-44	33006	59553
611	DJR-45	33010	59525
612	DJR-46	33002	59502
613	DJR-47	32980	59448
614	DJR-48	32911	59478
615	DJR-49	32960	59390
616	DJR-50	32964	59370
617	DJR-51	33120	59666
618	DJR-52	33116	59658
619	DJR-53	33114	59659
620	DJR-54	33109	59661
621	DJR-55	33105	59671
622	DJR-56	33102	59678
623	DJR-57	33082	59692
624	DJR-58	33066	59698
625	DJR-59	33059	59698
626	DJR-60	33037	59698
627	DJR-61	33020	59698
628	DJR-62	33004	59694
629	DJR63	33140	59686
630	DJR64	33140	59686
631	DJR65	33140	59686
632	DJR66	33140	59686
633	DJR-700	32742	59175
634	DJR-702	34361	60352
635	DJR-703	34287	60479
636	DJR-704	34276	60483
637	DJR-705	34284	60490
638	DJR-706	34197	60505
639	DJR-707	34165	60536
640	DJR-708	34168	60540
641	DJR-709	34105	60647
642	DJR-710	34101	60652
643	DJR-711	34107	60654
644	DJR-712	34109	60659
645	DJR-713	34084	60685
646	DJR-714	34044	60735
647	DJR-715	34046	60730
648	DJR-716	34007	60778
649	DJR-717	34002	60772
650	DJR-720	34020	60927

Southern Uplands Composite Traverse : Sample Position and Location.

Position No.	Sample No.	Easting	Northing
651	DJR-721	33995	60895
652	DJR-722	34001	60888
653	DJR-723	34006	60869
654	DJR-724	34004	60823
655	DJR-726	34118	60562
656	DJR-727	34112	60543
657	DJR-728	34111	60533
658	DJR-729	34120	60511
659	DJR-730	34166	60493
660	DJR-731	34211	60557
661	DJR-732	34215	60555
662	DJR-733	34212	60568
663	DJR-734	34373	60750
664	DJR-735	34396	60734
665	DJR-736	34398	60724
666	DJR-737	34400	60715
667	DJR-738	34428	60693
668	DJR-739	34395	60651
669	DJR-740	34372	60598
670	DJR-741	34189	60538
671	DJR-742	34199	60588
672	DJR-743	34172	60614
673	DJR-751	33560	59750
674	DJR-764	34540	61066
675	DJR-765	34551	61078
676	DJR-766	34544	61072
677	DJR-767	34493	61022
678	DJR-768	34488	61012
679	DJR-769	34065	60313
680	DJR-770	34065	60290
681	DJR-771	33649	60117
682	DJR-772	33787	60227
683	DJR-773	33814	60264
684	DJR-774	33880	60348
685	DJR-775	33918	60389
686	DJR-776	33951	60430
687	DJR-777	33967	60450
688	DJR-783	33714	59360
689	DJR-784	33562	60236
690	DJR-785	33551	60259
691	DJR-786	33553	60251
692	DJR-787	33555	60240
693	DJR-788	33555	60223
694	DJR-789	33503	60255
695	DJR-790	33580	60201
696	DJR-791	33596	60179
697	DJR-792	33597	60155
698	DJR-793	33620	60132
699	DJR-794	33612	60100
700	DJR-795	34067	60483

Southern Uplands Composite Traverse : Sample Position and Location.

Position No.	Sample No.	Easting	Northing
701	DJR-796	34078	60478
702	DJR-797	34090	60470
703	DJR-798	34100	60464
704	DJR-799	34101	60451
705	DJR-800	33552	59938
706	DJR-801	33544	59948
707	DJR-802	33538	59963
708	DJR-803	33530	59971
709	DJR-804	33522	59983
710	DJR-805	33520	59996
711	DJR-806	33520	60005
712	DJR-807	33510	60015
713	DJR-808	33494	60032
714	DJR-809	33473	60031
715	DJR-810	33548	60020
716	DJR-814	34274	60267
717	DJR-815	34270	60270
718	DJR-816	34257	60290
719	DJR-817	34235	60294
720	DJR-818	34210	60294
721	DJR-819	34193	60300
722	DJR-820	34173	60314
723	DJR-821	34158	60327
724	DJR-822	34125	60329
725	DJR-823	34101	60340
726	DJR-824	34076	60350
727	DJR-825	34050	60365
728	DJR-826	34120	60443
729	DJR-827	34121	60432
730	DJR-828	34131	60420
731	DJR-829	34149	60410
732	DJR-830	34160	60394
733	DJR-831	33930	60653
734	DJR-832	33946	60643
735	DJR-833	33955	60630
736	DJR-834	33814	60636
737	DJR-835	33784	60627
738	DJR-836	33746	60626
739	DJR-837	33707	60633
740	DJR-838	33684	60630
741	DJR-839	33650	60631
742	DJR-840	33619	60630
743	DJR-841	33593	60630
744	DJR-842	33569	60600
745	DJR-843	33560	60663
746	DJR-844	33530	60678
747	DJR-845	33599	60625
748	DJR-846	33865	60614
749	DJR-847	33716	60620
750	DJR-848	33036	59759

Southern Uplands Composite Traverse : Sample Position and Location.

Position No.	Sample No.	Easting	Northing
751	DJR-849	33121	59738
752	DJR-850	33940	60622
753	DJR-851	33924	60641
754	DJR-852	33897	60659
755	DJR-853	33872	60685
756	DJR-854	33872	60720
757	DJR-855	33842	60763
758	DJR-856	33826	60770
759	DJR-857	33828	60798
760	DJR-858	33820	60850
761	DJR-860	33810	60870
762	DJR-861	33133	59739
763	DJR-862	33149	59738
764	DJR-863	33176	59734
765	DJR-864	33205	59726
766	DJR-865	33220	59708
767	DJR-866	33240	59728
768	DJR-867	33230	59775
769	DJR-868	33196	59778
770	DJR-869	33177	59778
771	DJR-870	33161	59782
772	DJR-871	33097	59797
773	DJR-872	33070	59795
774	DJR-873	33140	59829
775	DJR-874	33242	59935
776	DJR-875	33260	59950
777	DJR-876	33174	59832
778	DJR-877	32870	60147
779	DJR-878	32904	60143
780	DJR-879	32910	60142
781	DJR-880	32992	60149
782	DJR-881	33110	60064
783	DJR-882	33008	60176
784	DJR-883	32960	60200
785	DJR-884	32920	60197
786	DJR-885	32858	60207
787	DJR-886	32936	60270
788	DJR-887	33005	60305
789	DJR-888	33060	60312
790	DJR-889	33036	60410
791	DJR-890	33068	60448
792	DJR-891	33085	60292
793	DJR-892	33218	60243
794	DJR-893	33272	60131
795	DJR-894	33272	60070
796	DJR-895	33080	59980
797	DJR-896	33047	59947
798	DJR-897	33009	59820
799	DJR-898	33014	59785
800	DJR-903	33830	59881

Southern Uplands Composite Traverse : Sample Position and Location.

Position No.	Sample No.	Easting	Northing
801	DJR-904	33807	59925
802	DJR-905	33796	59946
803	DJR-906	33780	59968
804	DJR-912	34072	60183
805	DJR-913	33748	60067
806	DJR-914	33818	60151
807	DJR-915	33797	60107
808	DJR-916	33749	60158
809	DJR-917	33756	60194
810	DJR-918	33460	59916
811	DJR-919	33490	59953
812	DJR-920	33430	60258
813	DJR-921	33416	60286
814	DJR-922	33452	60246
815	DJR-923	33433	60222
816	DJR-924	33404	60245
817	DJR-925	33346	60263
818	DJR-926	33302	60277
819	DJR-927	33360	60200
820	DJR-928	33359	60178
821	DJR-929	33368	60127
822	DJR-930	33435	60114
823	DJR-931	33469	60164
824	DJR-932	33507	60234
825	DJR-933	33502	60242
826	DJR-934	33498	60247
827	DJR-935	33495	60253
828	DJR-936	33490	60266
829	DJR-937	33538	60169
830	DJR-938	33530	60208
831	DJR-939	33504	60205
832	DJR-940	33565	60030
833	DJR-941	33595	60050
834	DJR-942	33564	60052
835	DJR-943	33830	59463
836	DJR-946	33505	59580
837	DJR-947	33545	59568
838	DJR-15	32980	59234
839	DJR-17	33052	59275
840	DJR-18	33081	59280
841	DJR-20	33112	59314
842	DJR-21	33156	59321
843	DJR-22	33180	59320
844	DJR-23	33219	59355
845	DJR-24	33250	59380
846	DJR-25	33258	59403
847	DJR-26	33273	59467
848	DJR-27	33270	59457
849	DJR-28	33274	59448
850	DJR-752	33601	59718

Southern Uplands Composite Traverse : Sample Position and Location.

Position No.	Sample No.	Easting	Northing
851	DJR-753	33644	59680
852	DJR-754	33654	59667
853	DJR-755	33661	59658
854	DJR-756	33667	59644
855	DJR-757	33669	59627
856	DJR-758	33678	59617
857	DJR-759	33687	59590
858	DJR-760	33686	59562
859	DJR-761	33686	59544
860	DJR-762	33690	59528
861	DJR-763	33689	59511
862	DJR-778	33690	59478
863	DJR-779	33705	59455
864	DJR-780	33692	59428
865	DJR-781	33680	59411
866	DJR-782	33680	59398
867	DJR-811	34325	60248
868	DJR-812	34306	60239
869	DJR-813	34289	60250
870	DJR-899	33875	59752
871	DJR-900	33843	59780
872	DJR-901	33817	59829
873	DJR-902	33823	59853
874	DJR-908	34198	59945
875	DJR-909	34210	59995
876	DJR-910	34205	60012
877	DJR-911	34103	60110
878	DJR-944	33516	59609
879	DJR-945	33522	59581
880	DJR-948	33552	59554
881	DJR-949	33582	59523
882	DJR-950	33606	59510
883	DJR-951	33635	59510
884	DJR-952	33655	59507

Glendinning Regional Traverses : Sample Position and Location.

Position No.	Sample No.	Easting	Northing
1	BLANK	0	0
2	BLANK	0	0
3	BLANK	0	0
4	BLANK	0	0
5	BLANK	0	0
6	DJR-15	32980	59234
7	DJR-17	33052	59275
8	DJR-18	33081	59280
9	DJR-20	33112	59314
10	DJR-21	33156	59321
11	DJR-22	33180	59320
12	DJR-23	33219	59355
13	DJR-24	33250	59380
14	DJR-25	33258	59403
15	DJR-26	33273	59467
16	DJR-27	33270	59457
17	DJR-28	33274	59448
18	DJR-752	33601	59718
19	DJR-753	33644	59680
20	DJR-754	33654	59667
21	DJR-755	33661	59658
22	DJR-756	33667	59644
23	DJR-757	33669	59627
24	DJR-758	33678	59617
25	DJR-759	33687	59590
26	DJR-760	33686	59562
27	DJR-761	33686	59544
28	DJR-762	33690	59528
29	DJR-763	33689	59511
30	DJR-778	33690	59478
31	DJR-779	33705	59455
32	DJR-780	33692	59428
33	DJR-781	33680	59411
34	DJR-782	33680	59398
35	DJR-811	34325	60248
36	DJR-812	34306	60239
37	DJR-813	34289	60250
38	DJR-899	33875	59752
39	DJR-900	33843	59780
40	DJR-901	33817	59829
41	DJR-902	33823	59853
42	DJR-908	34198	59945
43	DJR-909	34210	59995
44	DJR-910	34205	60012
45	DJR-911	34103	60110
46	DJR-944	33516	59609
47	DJR-945	33522	59581
48	DJR-948	33552	59554
49	DJR-949	33582	59523
50	DJR-950	33606	59510

Glendinning Regional Traverses : Sample Position and Location.

Position No.	Sample No.	Easting	Northing
51	DJR-951	33635	59510
52	DJR-952	33655	59507
53	BLANK	0	0
54	BLANK	0	0
55	BLANK	0	0
56	BLANK	0	0
57	BLANK	0	0
58	DJR-1	33555	59802
59	DJR-2	33535	59800
60	DJR-3	33500	59778
61	DJR-4	33464	59755
62	DJR-5	33447	59736
63	DJR-6	33388	59666
64	DJR-7	33409	59650
65	DJR-8	33370	59615
66	DJR-9	33358	59598
67	DJR-10	33330	59563
68	DJR-11	33321	59542
69	DJR-12	33310	59522
70	DJR-13	33271	59507
71	DJR-14	32997	59661
72	DJR-16	32998	59273
73	DJR-29	33102	59635
74	DJR-30	33108	59631
75	DJR-31	33114	59628
76	DJR-32	33111	59589
77	DJR-33	33093	59586
78	DJR-34	33087	59572
79	DJR-35	33082	59564
80	DJR-36	33070	59555
81	DJR-37	33055	59550
82	DJR-38	33047	59546
83	DJR-39	33037	59543
84	DJR-40	33028	59538
85	DJR-41	33018	59534
86	DJR-42	32990	59596
87	DJR-43	32994	59578
88	DJR-44	33006	59553
89	DJR-45	33010	59525
90	DJR-46	33002	59502
91	DJR-47	32980	59448
92	DJR-48	32911	59478
93	DJR-49	32960	59390
94	DJR-50	32964	59370
95	DJR-51	33120	59666
96	DJR-52	33116	59658
97	DJR-53	33114	59659
98	DJR-54	33109	59661
99	DJR-55	33105	59671
100	DJR-56	33102	59678

Glendinning Regional Traverses : Sample Position and Location.

Position No.	Sample No.	Easting	Northing
101	DJR-57	33082	59692
102	DJR-58	33066	59698
103	DJR-59	33059	59698
104	DJR-60	33037	59698
105	DJR-61	33020	59698
106	DJR-62	33004	59694
107	DJR-63	33140	59686
108	DJR-64	33140	59686
109	DJR-65	33140	59686
110	DJR-66	33140	59686
111	DJR-700	32742	59175
112	DJR-702	34361	60352
113	DJR-703	34287	60479
114	DJR-704	34276	60483
115	DJR-705	34284	60490
116	DJR-706	34197	60505
117	DJR-707	34165	60536
118	DJR-708	34168	60540
119	DJR-709	34105	60647
120	DJR-710	34101	60652
121	DJR-711	34107	60654
122	DJR-712	34109	60659
123	DJR-713	34084	60685
124	DJR-714	34044	60735
125	DJR-715	34046	60730
126	DJR-716	34007	60778
127	DJR-717	34002	60772
128	DJR-720	34020	60927
129	DJR-721	33995	60895
130	DJR-722	34001	60888
131	DJR-723	34006	60869
132	DJR-724	34004	60823
133	DJR-726	34118	60562
134	DJR-727	34112	60543
135	DJR-728	34111	60533
136	DJR-729	34120	60511
137	DJR-730	34166	60493
138	DJR-731	34211	60557
139	DJR-732	34215	60555
140	DJR-733	34212	60568
141	DJR-734	34373	60750
142	DJR-735	34396	60734
143	DJR-736	34398	60724
144	DJR-737	34400	60715
145	DJR-738	34428	60693
146	DJR-739	34395	60651
147	DJR-740	34372	60598
148	DJR-741	34189	60538
149	DJR-742	34199	60588
150	DJR-743	34172	60614

Glendinning Regional Traverses : Sample Position and Location.

Position No.	Sample No.	Easting	Northing
151	DJR-751	33560	59750
152	DJR-764	34540	61066
153	DJR-765	34551	61078
154	DJR-766	34544	61072
155	DJR-767	34493	61022
156	DJR-768	34488	61012
157	DJR-769	34065	60313
158	DJR-770	34065	60290
159	DJR-771	33649	60117
160	DJR-772	33787	60227
161	DJR-773	33814	60264
162	DJR-774	33880	60348
163	DJR-775	33918	60389
164	DJR-776	33951	60430
165	DJR-777	33967	60450
166	DJR-783	33714	59360
167	DJR-784	33562	60236
168	DJR-785	33551	60259
169	DJR-786	33553	60251
170	DJR-787	33555	60240
171	DJR-788	33555	60223
172	DJR-789	33503	60255
173	DJR-790	33580	60201
174	DJR-791	33596	60179
175	DJR-792	33597	60155
176	DJR-793	33620	60132
177	DJR-794	33612	60100
178	DJR-795	34067	60483
179	DJR-796	34078	60478
180	DJR-797	34090	60470
181	DJR-798	34100	60464
182	DJR-799	34101	60451
183	DJR-800	33552	59938
184	DJR-801	33544	59948
185	DJR-802	33538	59963
186	DJR-803	33530	59971
187	DJR-804	33522	59983
188	DJR-805	33520	59996
189	DJR-806	33520	60005
190	DJR-807	33510	60015
191	DJR-808	33494	60032
192	DJR-809	33473	60031
193	DJR-810	33548	60020
194	DJR-814	34274	60267
195	DJR-815	34270	60270
196	DJR-816	34257	60290
197	DJR-817	34235	60294
198	DJR-818	34210	60294
199	DJR-819	34193	60300
200	DJR-820	34173	60314

Glendinning Regional Traverses : Sample Position and Location.

Position No.	Sample No.	Easting	Northing
201	DJR-821	34158	60327
202	DJR-822	34125	60329
203	DJR-823	34101	60340
204	DJR-824	34076	60350
205	DJR-825	34050	60365
206	DJR-826	34120	60443
207	DJR-827	34121	60432
208	DJR-828	34131	60420
209	DJR-829	34149	60410
210	DJR-830	34160	60394
211	DJR-831	33930	60653
212	DJR-832	33946	60643
213	DJR-833	33955	60630
214	DJR-834	33814	60636
215	DJR-835	33784	60627
216	DJR-836	33746	60626
217	DJR-837	33707	60633
218	DJR-838	33684	60630
219	DJR-839	33650	60631
220	DJR-840	33619	60630
221	DJR-841	33593	60630
222	DJR-842	33569	60600
223	DJR-843	33560	60663
224	DJR-844	33530	60678
225	DJR-845	33599	60625
226	DJR-846	33865	60614
227	DJR-847	33716	60620
228	DJR-848	33036	59759
229	DJR-849	33121	59738
230	DJR-850	33940	60622
231	DJR-851	33924	60641
232	DJR-852	33897	60659
233	DJR-853	33872	60685
234	DJR-854	33872	60720
235	DJR-855	33842	60763
236	DJR-856	33826	60770
237	DJR-857	33828	60798
238	DJR-858	33820	60850
239	DJR-860	33810	60870
240	DJR-861	33133	59739
241	DJR-862	33149	59738
242	DJR-863	33176	59734
243	DJR-864	33205	59726
244	DJR-865	33220	59708
245	DJR-866	33240	59728
246	DJR-867	33230	59775
247	DJR-868	33196	59778
248	DJR-869	33177	59778
249	DJR-870	33161	59782
250	DJR-871	33097	59797

Glendinning Regional Traverses : Sample Position and Location.

Position No.	Sample No.	Easting	Northing
251	DJR-872	33070	59795
252	DJR-873	33140	59829
253	DJR-874	33242	59935
254	DJR-875	33260	59950
255	DJR-876	33174	59832
256	DJR-877	32870	60147
257	DJR-878	32904	60143
258	DJR-879	32910	60142
259	DJR-880	32992	60149
260	DJR-881	33110	60064
261	DJR-882	33008	60176
262	DJR-883	32960	60200
263	DJR-884	32920	60197
264	DJR-885	32858	60207
265	DJR-886	32936	60270
266	DJR-887	33005	60305
267	DJR-888	33060	60312
268	DJR-889	33036	60410
269	DJR-890	33068	60448
270	DJR-891	33085	60292
271	DJR-892	33218	60243
272	DJR-893	33272	60131
273	DJR-894	33272	60070
274	DJR-895	33080	59980
275	DJR-896	33047	59947
276	DJR-897	33009	59820
277	DJR-898	33014	59785
278	DJR-903	33830	59881
279	DJR-904	33807	59925
280	DJR-905	33796	59946
281	DJR-906	33780	59968
282	DJR-912	34072	60183
283	DJR-913	33748	60067
284	DJR-914	33818	60151
285	DJR-915	33797	60107
286	DJR-916	33749	60158
287	DJR-917	33756	60194
288	DJR-918	33460	59916
289	DJR-919	33490	59953
290	DJR-920	33430	60258
291	DJR-921	33416	60286
292	DJR-922	33452	60246
293	DJR-923	33433	60222
294	DJR-924	33404	60245
295	DJR-925	33346	60263
296	DJR-926	33302	60277
297	DJR-927	33360	60200
298	DJR-928	33359	60178
299	DJR-929	33368	60127
300	DJR-930	33435	60114

Glendinning Regional Traverses : Sample Position and Location.

Position No.	Sample No.	Easting	Northing
301	DJR-931	33469	60164
302	DJR-932	33507	60234
303	DJR-933	33502	60242
304	DJR-934	33498	60247
305	DJR-935	33495	60253
306	DJR-936	33490	60266
307	DJR-937	33538	60169
308	DJR-938	33530	60208
309	DJR-939	33504	60205
310	DJR-940	33565	60030
311	DJR-941	33595	60050
312	DJR-942	33564	60052
313	DJR-943	33830	59463
314	DJR-946	33505	59580
315	DJR-947	33545	59568
316	BLANK	0	0
317	BLANK	0	0
318	BLANK	0	0
319	BLANK	0	0
320	BLANK	0	0
321	DJR-1017	33052	59275
322	DJR-1018	33081	59280
323	DJR-1019	33103	59301
324	DJR-1020	33112	59314
325	DJR-1021	33156	59321
326	DJR-1022	33180	59320
327	DJR-1023	33219	59355
328	DJR-1024	33250	59380
329	DJR-1025	33258	59403
330	DJR-1026	33273	59467
331	DJR-1027	33270	59457
332	DJR-1028	33274	59448
333	DJR-1761	33686	59544
334	DJR-1781	33680	59411
335	DJR-1782	33680	59398
336	DJR-1811	34325	60248
337	DJR-1812	34306	60239
338	DJR-1899	33875	59752
339	DJR-1900	33843	59780
340	DJR-1901	33817	59829
341	DJR-1903	33830	59881
342	DJR-1908	34198	59945
343	DJR-1909	34210	59995
344	DJR-1910	34205	60012
345	DJR-1911	34103	60110
346	DJR-1947	33545	59568
347	DJR-1948	33552	59554
348	DJR-1949	33582	59523
349	DJR-1950	33606	59510
350	DJR-1951	33635	59510

Glendinning Regional Traverses : Sample Position and Location.

Position No.	Sample No.	Easting	Northing
351	DJR-1952	33655	59507
352	BLANK	0	0
353	BLANK	0	0
354	BLANK	0	0
355	BLANK	0	0
356	BLANK	0	0
357	DJR-1001	33555	59802
358	DJR-1002	33535	59800
359	DJR-1003	33500	59778
360	DJR-1004	33464	59755
361	DJR-1005	33447	59736
362	DJR-1006	33388	59666
363	DJR-1007	33409	59650
364	DJR-1008	33370	59615
365	DJR-1009	33358	59598
366	DJR-1010	33330	59563
367	DJR-1011	33321	59542
368	DJR-1012	33310	59522
369	DJR-1013	33271	59507
370	DJR-1029	33102	59635
371	DJR-1031	33114	59628
372	DJR-1033	33093	59586
373	DJR-1034	33087	59572
374	DJR-1035	33082	59564
375	DJR-1036	33070	59555
376	DJR-1037	33055	59550
377	DJR-1038	33047	59546
378	DJR-1039	33037	59543
379	DJR-1040	33028	59538
380	DJR-1041	33018	59534
381	DJR-1042	32990	59596
382	DJR-1043	32994	59578
383	DJR-1044	33006	59553
384	DJR-1045	33010	59525
385	DJR-1046	33002	59502
386	DJR-1047	32980	59448
387	DJR-1048	32911	59478
388	DJR-1049	32960	59390
389	DJR-1050	32964	59370
390	DJR-1052	33116	59658
391	DJR-1053	33114	59659
392	DJR-1054	33109	59661
393	DJR-1055	33105	59671
394	DJR-1056	33102	59678
395	DJR-1057	33082	59692
396	DJR-1058	33066	59698
397	DJR-1059	33059	59698
398	DJR-1060	33037	59698
399	DJR-1061	33020	59698
400	DJR-1062	33004	59694

Glendinning Regional Traverses : Sample Position and Location.

Position No.	Sample No.	Easting	Northing
401	DJR-1702	34361	60352
402	DJR-1704	34276	60483
403	DJR-1705	34284	60490
404	DJR-1708	34168	60540
405	DJR-1711	34107	60654
406	DJR-1715	34046	60730
407	DJR-1716	34007	60778
408	DJR-1719	34018	60939
409	DJR-1728	34111	60533
410	DJR-1734	34373	60750
411	DJR-1754	33654	59667
412	DJR-1757	33669	59627
413	DJR-1759	33687	59590
414	DJR-1764	34540	61066
415	DJR-1765	34551	61078
416	DJR-1766	34544	61072
417	DJR-1767	34493	61022
418	DJR-1768	34488	61012
419	DJR-1769	34065	60313
420	DJR-1770	34065	60290
421	DJR-1771	33649	60117
422	DJR-1772	33787	60227
423	DJR-1776	33951	60430
424	DJR-1777	33967	60450
425	DJR-1784	33562	60236
426	DJR-1788	33555	60223
427	DJR-1791	33596	60179
428	DJR-1792	33597	60155
429	DJR-1794	33612	60100
430	DJR-1798	34100	60464
431	DJR-1799	34101	60451
432	DJR-1801	33544	59948
433	DJR-1802	33538	59963
434	DJR-1804	33522	59983
435	DJR-1814	34274	60267
436	DJR-1815	34270	60270
437	DJR-1816	34257	60290
438	DJR-1817	34235	60294
439	DJR-1818	34210	60294
440	DJR-1819	34193	60300
441	DJR-1820	34173	60314
442	DJR-1822	34125	60329
443	DJR-1823	34101	60340
444	DJR-1825	34050	60365
445	DJR-1828	34131	60420
446	DJR-1830	34160	60394
447	DJR-1834	33814	60636
448	DJR-1835	33784	60627
449	DJR-1836	33746	60626
450	DJR-1837	33707	60633

Glendinning Regional Traverses : Sample Position and Location.

Position No.	Sample No.	Easting	Northing
451	DJR-1838	33684	60630
452	DJR-1839	33650	60631
453	DJR-1840	33619	60630
454	DJR-1841	33593	60630
455	DJR-1842	33569	60600
456	DJR-1844	33530	60678
457	DJR-1845	33599	60625
458	DJR-1846	33865	60614
459	DJR-1848	33036	59759
460	DJR-1850	33940	60622
461	DJR-1851	33924	60641
462	DJR-1857	33828	60798
463	DJR-1858	33820	60850
464	DJR-1860	33810	60870
465	DJR-1861	33133	59739
466	DJR-1862	33149	59738
467	DJR-1864	33205	59726
468	DJR-1868	33196	59778
469	DJR-1869	33177	59778
470	DJR-1870	33161	59782
471	DJR-1871	33097	59797
472	DJR-1872	33070	59795
473	DJR-1873	33140	59829
474	DJR-1874	33242	59935
475	DJR-1875	33260	59950
476	DJR-1877	32870	60147
477	DJR-1878	32904	60143
478	DJR-1879	32910	60142
479	DJR-1880	32992	60149
480	DJR-1881	33110	60064
481	DJR-1883	32960	60200
482	DJR-1884	32920	60197
483	DJR-1885	32858	60207
484	DJR-1886	32936	60270
485	DJR-1888	33060	60312
486	DJR-1889	33036	60410
487	DJR-1890	33068	60448
488	DJR-1891	33085	60292
489	DJR-1892	33218	60243
490	DJR-1893	33272	60131
491	DJR-1894	33272	60070
492	DJR-1895	33080	59980
493	DJR-1896	33047	59947
494	DJR-1898	33014	59785
495	DJR-1912	34072	60183
496	DJR-1913	33748	60067
497	DJR-1914	33818	60151
498	DJR-1916	33749	60158
499	DJR-1917	33756	60194
500	DJR-1918	33460	59916

Glendinning Regional Traverses : Sample Position and Location.

Position No.	Sample No.	Easting	Northing
501	DJR-1919	33490	59953
502	DJR-1920	33430	60258
503	DJR-1921	33416	60286
504	DJR-1922	33452	60246
505	DJR-1923	33433	60222
506	DJR-1925	33346	60263
507	DJR-1926	33302	60277
508	DJR-1927	33360	60200
509	DJR-1928	33359	60178
510	DJR-1929	33368	60127
511	DJR-1930	33435	60114
512	DJR-1931	33469	60164
513	DJR-1933	33502	60242
514	DJR-1934	33498	60247
515	DJR-1936	33490	60266
516	DJR-1937	33538	60169
517	DJR-1938	33530	60208
518	DJR-1939	33504	60205
519	DJR-1940	33565	60030
520	DJR-1941	33595	60050
521	DJR-1942	33564	60052
522	DJR-1943	33830	59463

The Longford Down Traverse : Sample Position and Location.

Position No.	Sample No.	Easting	Northing
1	84-01283	20322	29609
2	84-01284	20319	29602
3	84-01290	20050	28805
4	84-01291	20051	28849
5	84-01292	19997	28744
6	84-01296	19813	28395
7	84-01297	19821	28393
8	BLANK	0	0
9	BLANK	0	0
10	BLANK	0	0
11	BLANK	0	0
12	84-01298	19783	28262
13	84-01299	19749	28230
14	84-01300	19547	27414
15	84-01301	19547	27560
16	84-01302	19586	27581
17	84-01304	19517	27606
18	84-01305	19424	27455
19	84-01306	19434	27450
20	84-01307	19500	27490
21	BLANK	0	0
22	BLANK	0	0
23	BLANK	0	0
24	BLANK	0	0
25	84-01199	21927	29037
26	84-01200	21648	29108
27	84-01201	21709	29300
28	84-01235	22478	29860
29	84-01236	22355	29765
30	84-01237	22103	29923
31	84-01238	22157	29957
32	84-01239	22109	29968
33	84-01240	22070	29945
34	84-01241	21895	29163
35	84-01242	22045	29034
36	84-01245	22274	29548
37	84-01246	22296	29563
38	84-01247	22355	29765
39	84-01249	22405	30543
40	84-01250	22510	30665
41	84-01251	22540	30640
42	84-01252	22540	30610
43	84-01253	22360	30415
44	84-01254	22324	30455
45	84-01255	22312	30470
46	84-01256	22312	30295
47	84-01257	22310	30320
48	84-01258	22540	30662
49	84-01259	22453	30135
50	84-01260	22226	30220

The Longford Down Traverse : Sample Position and Location.

Position No.	Sample No.	Easting	Northing
51	84-01261	22223	30219
52	84-01262	22215	30189
53	84-01263	22268	30199
54	84-01264	22276	30185
55	84-01265	22275	30150
56	84-01266	22204	30085
57	84-01267	22196	30104
58	84-01268	22090	30160
59	84-01269	22081	30169
60	84-01270	22063	30217
61	84-01271	22068	30207
62	84-01272	22177	30266
63	84-01273	22026	29975
64	84-01274	22078	29995
65	84-01275	22074	29985
66	84-01276	22072	29973
67	84-01277	20486	29287
68	84-01278	20486	29286
69	84-01279	20415	29390
70	84-01280	20415	29281
71	84-01281	20375	29312
72	84-01282	20398	29400
73	84-01285	20273	28775
74	84-01286	20277	28726
75	84-01287	20072	28785
76	84-01288	20082	28792
77	84-01289	20148	28798
78	84-01293	20110	28835
79	84-01294	20114	28846
80	84-01295	20128	28849
81	BLANK	0	0
82	BLANK	0	0
83	BLANK	0	0
84	BLANK	0	0
85	84-01182	21820	28440
86	84-01183	21802	28420
87	84-01184	21511	28407
88	84-01185	21502	28429
89	84-01186	21520	28460
90	84-01187	21563	28608
91	84-01188	21559	28634
92	84-01189	21572	28790
93	84-01190	21587	28610
94	84-01191	21613	28525
95	84-01192	21698	28613
96	84-01193	21680	28593
97	84-01194	21663	28626
98	84-01195	21787	28717
99	84-01196	21820	28768
100	84-01197	21996	28875

The Longford Down Traverse : Sample Position and Location.

Position No.	Sample No.	Easting	Northing
101	84-01198	21797	28950
102	84-01202	22041	29038
103	84-01203	22175	29155
104	84-01204	23023	29904
105	84-01205	23028	29884
106	84-01206	23014	29933
107	84-01207	23065	29865
108	84-01208	23085	29864
109	84-01209	23095	29858
110	84-01210	23045	29871
111	84-01211	23135	29865
112	84-01212	23135	29865
113	84-01213	23135	29865
114	84-01214	23182	29880
115	84-01215	23195	29870
116	84-01216	23208	29855
117	84-01217	23221	29848
118	84-01231	22500	29455
119	84-01232	22545	29503
120	84-01233	22608	29648
121	84-01234	22600	29646
122	84-01243	21995	29198
123	84-01244	22047	29366
124	84-01248	22388	29337
125	BLANK	0	0
126	BLANK	0	0
127	BLANK	0	0
128	BLANK	0	0
129	84-01172	22215	28686
130	84-01180	21950	28457
131	84-01181	21950	28476
132	BLANK	0	0
133	BLANK	0	0
134	BLANK	0	0
135	BLANK	0	0
136	84-01171	22203	28619
137	84-01173	22344	28511
138	84-01174	22420	28595
139	84-01175	22402	28730
140	84-01228	22938	29323
141	84-01229	22915	29341
142	84-01230	22739	29010
143	BLANK	0	0
144	BLANK	0	0
145	BLANK	0	0
146	BLANK	0	0
147	84-01169	22288	28270
148	84-01170	22284	28302
149	84-01176	22657	28816
150	84-01177	22585	28572

The Longford Down Traverse : Sample Position and Location.

Position No.	Sample No.	Easting	Northing
151	BLANK	0	0
152	BLANK	0	0
153	BLANK	0	0
154	BLANK	0	0
155	84-01178	22590	28389
156	84-01179	22060	28281
157	84-01220	23468	29601
158	84-01221	23458	29615
159	84-01222	23353	29508
160	84-01223	23337	29417
161	84-01224	23350	29403
162	84-01225	23436	29339
163	84-01226	23345	29304
164	84-01227	23093	29315
165	BLANK	0	0
166	BLANK	0	0
167	BLANK	0	0
168	BLANK	0	0
169	84-01162	24627	30076
170	84-01163	24606	30078
171	84-01168	24790	30093
172	BLANK	0	0
173	BLANK	0	0
174	BLANK	0	0
175	BLANK	0	0
176	84-01001	30615	28865
177	84-01002	30695	28960
178	84-01003	30712	28883
179	84-01004	29742	29012
180	84-01005	29820	28300
181	84-01006	29745	28467
182	84-01007	29910	28383
183	84-01008	29926	28552
184	84-01009	29970	28590
185	84-01010	29935	28560
186	84-01011	29980	28645
187	84-01012	29760	28740
188	84-01013	29677	29013
189	84-01014	29525	30243
190	84-01015	29510	30305
191	84-01016	29510	30350
192	84-01017	29508	30388
193	84-01018	29475	30514
194	84-01019	29414	30644
195	84-01020	29384	30665
196	84-01022	29493	30397
197	84-01023	29276	30347
198	84-01024	29150	30338
199	84-01025	29115	30240
200	84-01026	29190	30213

The Longford Down Traverse : Sample Position and Location.

Position No.	Sample No.	Easting	Northing
201	84-01027	29187	30174
202	84-01028	29703	29205
203	84-01029	29772	29274
204	84-01030	29870	29239
205	84-01031	30026	29217
206	84-01032	29997	29305
207	84-01033	29504	29582
208	84-01034	29669	29660
209	84-01035	29570	29760
210	84-01036	29582	29735
211	84-01037	29418	29959
212	84-01038	29496	29916
213	84-01039	29535	29805
214	84-01040	29571	29840
215	84-01041	29420	29681
216	84-01042	29389	29622
217	84-01044	29393	29595
218	84-01045	29736	29969
219	84-01046	29746	30030
220	84-01047	29955	30065
221	84-01048	29994	30086
222	84-01049	30050	30374
223	84-01050	30013	30385
224	84-01051	29960	30364
225	84-01052	29910	30391
226	84-01053	29910	30332
227	84-01054	29863	30308
228	84-01055	29850	30287
229	84-01056	29835	30270
230	84-01057	29666	30085
231	84-01058	29584	30346
232	84-01059	29655	30386
233	84-01060	29673	30400
234	84-01061	29715	30068
235	84-01062	29733	30043
236	84-01063	29813	30105
237	84-01064	29843	30506
238	84-01065	29819	30473
239	84-01066	29775	30456
240	84-01067	29759	30458
241	84-01068	29657	30458
242	84-01069	29623	30496
243	84-01070	29626	30516
244	84-01071	29604	30530
245	84-01072	29555	30558
246	84-01073	29551	30574
247	84-01074	29533	30640
248	84-01075	29513	30645
249	84-01076	29495	30657
250	84-01077	29460	30699

The Rhyns Traverse : Sample Position and Location.

Position No.	Sample No.	Easting	Northing
1	BLANK	0	0
2	BLANK	0	0
3	BLANK	0	0
4	BLANK	0	0
5	BLANK	0	0
6	PDW1	20558	57786
7	PDW2	20540	57778
8	PDW3	20537	57762
9	PDW4	20525	57736
10	PDW5	20513	57711
11	PDW6	20510	57675
12	PDW7	20515	57654
13	PDW8	20515	57637
14	PDW9	20504	57608
15	PDW10	20499	57591
16	PDW11	20493	57567
17	PDW12	20482	57547
18	PDW13	20486	57530
19	PDW14	20480	57519
20	PDW15	20452	57449
21	PDW16	20460	57403
22	PDW17	20471	57377
23	PDW18	20480	57351
24	PDW19	20484	57320
25	PDW20	20479	57298
26	PDW21	20483	57280
27	PDW22	20510	57260
28	PDW23	20509	57241
29	PDW24	20513	57228
30	PDW25	20536	57197
31	PDW26	20552	57175
32	PDW27	20570	57128
33	PDW28	20569	57107
34	PDW29	20589	57072
35	PDW30	20594	57030
36	BLANK	0	0
37	BLANK	0	0
38	BLANK	0	0
39	BLANK	0	0
40	BLANK	0	0
41	PDW49	20205	57361
42	PDW48	20219	57350
43	PDW47	20224	57340
44	PDW46	20235	57324
45	PDW45	20242	57306
46	PDW44	20245	57290
47	PDW43	20249	57275
48	PDW42	20253	57257
49	PDW41	20261	57224
50	PDW40	20266	57211

The Rhyns Traverse : Sample Position and Location.

Position No.	Sample No.	Easting	Northing
51	PDW39	20280	57185
52	PDW38	20291	57152
53	PDW37	20305	57140
54	PDW36	20319	57130
55	PDW35	20332	57117
56	PDW34	20336	57102
57	PDW33	20336	57071
58	PDW32	20350	57049
59	PDW31	20362	57038
60	BLANK	0	0
61	BLANK	0	0
62	BLANK	0	0
63	BLANK	0	0
64	BLANK	0	0
65	PDW50	20188	57368
66	PDW51	20160	57368
67	PDW52	20143	57367
68	PDW53	20113	57363
69	PDW54	20044	57306
70	PDW55	19979	57286
71	PDW56	19904	57275
72	PDW57	19865	57264
73	PDW58	19851	57278
74	PDW59	19840	57271
75	PDW60	19826	57276
76	PDW61	19800	57258
77	PDW62	19798	57253
78	PDW63	19778	57206
79	PDW64	19761	57197
80	PDW65	19743	57169
81	PDW66	19731	57157
82	PDW67	19718	57141
83	PDW68	19717	57112
84	PDW69	19716	57094
85	PDW70	19705	57081
86	PDW71	19698	57070
87	PDW72	19692	57051
88	PDW73	19680	57035
89	PDW74	19670	57017
90	PDW75	19665	57004
91	PDW76	19670	56993
92	PDW77	19656	56980
93	PDW78	19643	56962
94	PDW79	19626	56943
95	PDW80	19622	56927
96	PDW81	19617	56909
97	PDW82	19668	56874
98	PDW83	19660	56858
99	PDW84	19667	56840
100	PDW85	19668	56817

The Rhyns Traverse : Sample Position and Location.

Position No.	Sample No.	Easting	Northing
101	PDW86	19662	56802
102	PDW87	19652	56785
103	PDW88	19652	56772
104	PDW89	19647	56754
105	PDW90	19631	56729
106	PDW91	19630	56715
107	PDW92	19620	56690
108	PDW93	19612	56678
109	PDW94	19608	56658
110	PDW95	19603	56638
111	PDW96	19608	56611
112	PDW97	19601	56597
113	PDW98	19601	56584
114	PDW99	19609	56568
115	PDW100	19606	56544
116	PDW101	19603	56528
117	PDW102	19601	56506
118	PDW103	19599	56475
119	PDW104	19595	56456
120	PDW105	19598	56438
121	PDW106	19593	56420
122	PDW107	19592	56402
123	PDW108	19600	56391
124	PDW109	19602	56369
125	PDW110	19594	56350
126	PDW111	19593	56332
127	PDW112	19599	56310
128	PDW113	19598	56290
129	PDW114	19596	56271
130	PDW115	19599	56253
131	PDW116	19604	56230
132	PDW117	19612	56202
133	PDW118	19627	56174
134	PDW119	19643	56156
135	PDW120	19650	56138
136	PDW121	19655	56122
137	PDW122	19660	56104
138	PDW123	19667	56086
139	PDW124	19674	56075
140	PDW125	19690	56062
141	PDW126	19701	56046
142	PDW127	19711	56029
143	PDW128	19719	56014
144	PDW129	19730	55994
145	PDW130	19740	55980
146	PDW131	19755	55954
147	PDW132	19760	55932
148	PDW133	19761	55911
149	PDW134	19763	55892
150	PDW135	19770	55874

The Rhyns Traverse : Sample Position and Location.

Position No.	Sample No.	Easting	Northing
151	PDW136	19770	55857
152	PDW137	19780	55836
153	PDW138	19793	55816
154	PDW139	19793	55797
155	PDW140	19810	55777
156	PDW141	19830	55755
157	PDW142	19830	55738
158	PDW143	19833	55716
159	PDW144	19830	55700
160	PDW145	19811	55682
161	PDW146	19810	55668
162	PDW147	19803	55648
163	PDW148	19821	55631
164	PDW149	19823	55613
165	PDW150	19826	55598
166	PDW151	19848	55588
167	PDW152	19853	55572
168	PDW153	19865	55542
169	PDW154	19872	55524
170	PDW155	19895	55522
171	PDW156	19922	55510
172	PDW157	19922	55486
173	PDW158	19935	55450
174	PDW159	19959	55427
175	PDW160	19980	55405
176	PDW161	19995	55389
177	PDW162	20010	55374
178	PDW163	20019	55360
179	PDW164	20040	55347
180	PDW165	20060	55328
181	PDW166	20051	55308
182	PDW167	20064	55289
183	PDW168	20080	55272
184	PDW169	20120	55260
185	PDW170	20148	55261
186	PDW171	20178	55239
187	PDW172	20185	55223
188	PDW173	20199	55204
189	PDW174	20220	55170
190	PDW175	20232	55136
191	PDW176	20250	55110
192	PDW177	20278	55102
193	PDW178	20303	55091
194	PDW179	20338	55074
195	PDW180	20364	55059
196	PDW181	20398	55037
197	PDW182	20435	54963
198	PDW183	20443	54962
199	PDW184	20449	54952
200	PDW185	20463	54930

The Rhyns Traverse : Sample Position and Location.

Position No.	Sample No.	Easting	Northing
201	PDW186	20468	54923
202	PDW187	20467	54908
203	PDW188	20461	54900
204	PDW189	20462	54884
205	PDW190	20451	54862
206	PDW191	20455	54843
207	PDW192	20468	54829
208	PDW193	20488	54828
209	PDW194	20502	54816
210	PDW195	20520	54810
211	PDW196	20536	54793
212	PDW197	20555	54769
213	PDW198	20588	54730
214	PDW199	20600	54719
215	PDW200	20623	54724
216	PDW201	20644	54716
217	PDW202	20639	54700
218	PDW203	20649	54684
219	PDW204	20665	54664
220	PDW205	20670	54650
221	PDW206	20677	54634
222	PDW207	20696	54619
223	PDW208	20703	54603
224	PDW209	20713	54588
225	PDW210	20710	54571
226	PDW211	20712	54552
227	PDW212	20710	54530
228	PDW213	20671	54489
229	PDW214	20678	54462
230	PDW215	20683	54439
231	PDW216	20681	54420
232	PDW217	20699	54406
233	PDW218	20721	54391
234	PDW219	20741	54389
235	PDW220	20750	54368
236	PDW221	20774	54360
237	PDW222	20783	54340
238	PDW223	20770	54315
239	PDW224	20775	54291
240	PDW225	20766	54268
241	PDW226	20761	54243
242	PDW227	20753	54218
243	PDW228	20746	54196
244	PDW229	20762	54177
245	PDW230	20798	54160
246	PDW231	20840	54164
247	PDW232	20870	54157
248	PDW233	20888	54140
249	PDW234	20911	54130
250	PDW235	20933	54126

The Rhyns Traverse : Sample Position and Location.

Position No.	Sample No.	Easting	Northing
251	PDW236	20937	54043
252	PDW237	20920	54023
253	PDW238	20908	54002
254	PDW239	20921	53965
255	PDW240	20933	53944
256	PDW241	20969	53852
257	PDW242	20988	53823
258	PDW243	21000	53813
259	PDW244	20960	53760
260	PDW245	20943	53750
261	PDW246	20927	53731
262	PDW247	20891	53695
263	PDW248	20877	53687
264	PDW249	20861	53681
265	PDW250	20863	53672
266	BLANK	0	0
267	BLANK	0	0
268	BLANK	0	0
269	BLANK	0	0
270	BLANK	0	0
271	PDW251	20953	53380
272	PDW252	20960	53376
273	PDW253	20971	53361
274	PDW254	20988	53352
275	PDW255	20992	53331
276	PDW256	21030	53285
277	PDW257	21053	53264
278	PDW258	21069	53241
279	PDW259	21083	53221
280	PDW260	21093	53211
281	PDW261	21120	53201
282	PDW262	21155	53167
283	PDW263	21168	53153
284	PDW264	21187	53140

Interformational Traverses : Sample Position and Location.

Position No. Sample No.

1	AX97212
2	AX97211
3	AX97210
4	AX97209
5	AX97208
6	AX97207
7	AX97206
8	AX97205
9	AX97204
10	AX97203
11	AX97202
12	AX97201
13	BLANK
14	BLANK
15	BLANK
16	BLANK
17	BLANK
18	AX575
19	AX576
20	AX577
21	AX578
22	AX579
23	AX580
24	AX581
25	AX588
26	AX589
27	AX590
28	AX591
29	AX592
30	AX593
31	AX594
32	AX595
33	AX596
34	AX597
35	AX598
36	AX599
37	AX600

Leadhills Alteration Traverse : Sample Position and Location.

Position No. Sample No.

1	PDL-2
2	PDL-3
3	PDL-4
4	PDL-5
5	PDL-6
6	PDL-7
7	PDL-8
8	PDL-9
9	PDL-10
10	PDL-11
11	PDL-12
12	PDL-13
13	PDL-14
14	PDL-15
15	PDL-16
16	PDL-17
17	PDL-18
18	PDL-19
19	PDL-20
20	PDL-21
21	PDL-22
22	PDL-23
23	PDL-24
24	PDL-25
25	PDL-26
26	PDL-27
27	PDL-28
28	PDL-29

Glendinning Borehole Geochemistry : Sample Positions.

Position No. Sample No.

1	CXD1005
2	CXD1006
3	CXD1007
4	CXD1008
5	CXD1009
6	CXD1010
7	CXD1011
8	CXD1012
9	CXD1013
10	CXD1014
11	CXD1015
12	CXD1016
13	CXD1017
14	CXD1018
15	CXD1019
16	CXD1020
17	CXD1021
18	CXD1022
19	CXD1023
20	CXD1024
21	CXD1025
22	CXD1030
23	CXD1031
24	CXD1032
25	CXD1033
26	CXD1034
27	CXD1035
28	CXD1036
29	CXD1037
30	CXD1038
31	CXD1039
32	CXD1040
33	CXD1128
34	CXD1129
35	CXD1130
36	CXD1131
37	CXD1132
38	CXD1133
39	CXD1134
40	CXD1135
41	CXD1136
42	CXD1137
43	CXD1138
44	CXD1139
45	CXD1140
46	CXD1141
47	CXD1142
48	CXD1143
49	CXD1144
50	CXD1145

Glendinning Borehole Geochemistry : Sample Positions.

Position No. Sample No.

51 CXD1146
52 CXD1147
53 CXD1148
54 CXD1149
55 CXD1150
56 CXD1151
57 CXD1152
58 CXD1153
59 CXD1154
60 CXD1155
61 CXD1156
62 CXD1157
63 CXD1158
64 CXD1159
65 CXD1160
66 CXD1161
67 CXD1162
68 CXD1163
69 CXD1164
70 CXD1165
71 CXD1166
72 CXD1167
73 CXD1168
74 CXD1169
75 CXD1170
76 CXD1048
77 CXD1049
78 CXD1050
79 CXD1051
80 CXD1052
81 CXD1053
82 CXD1054
83 CXD1055
84 CXD1056
85 CXD1057
86 CXD1058
87 CXD1059
88 CXD1060
89 CXD1061
90 CXD1062
91 CXD1063
92 CXD1064
93 CXD1065
94 CXD1066
95 CXD1067
96 CXD1068
97 CXD1069
98 CXD1070
99 CXD1071
100 CXD1072

Glendinning Borehole Geochemistry : Sample Positions.

Position No. Sample No.

101	CXD1073
102	CXD1074
103	CXD1075
104	CXD1076
105	CXD1077
106	CXD1078
107	CXD1079
108	CXD1080
109	CXD1081
110	CXD1082
111	CXD1083
112	CXD1084
113	CXD1085
114	CXD1086
115	CXD1087
116	CXD1088
117	CXD1089
118	CXD1090
119	CXD1091
120	CXD1092
121	CXD1093
122	CXD1094
123	CXD1095
124	CXD1096
125	CXD1097
126	CXD1098
127	CXD1099
128	CXD1100
129	CXD1101
130	CXD1102
131	CXD1103
132	CXD1104
133	CXD1105
134	CXD1106
135	CXD1107
136	CXD1108
137	CXD1109
138	CXD1110
139	CXD1111
140	CXD1112
141	CXD1113
142	CXD1114
143	CXD1115
144	CXD1116
145	CXD1117
146	CXD1118
147	CXD1119
148	CXD1120
149	CXD1121
150	CXD1122

Glendinning Borehole Geochemistry : Sample Positions.

Position No. Sample No.

151 CXD1123
152 CXD1124
153 CXD1125
154 CXD1126
155 CXD1127
156 CXD1041
157 CXD1042
158 CXD1043
159 CXD1044
160 CXD1026
161 CXD1027
162 CXD1028
163 CXD1029
164 CXD1045
165 CXD1046
166 CXD1047

APPENDIX 6 : SEMI-QUANTITATIVE X-RAY DIFFRACTION ANALYSIS

Whole rock and clay fraction samples were prepared for analysis in accordance with the following methods (after Bridges, 1986 pers. com.):

A6.1 : Whole Rock Preparation

The sample is gently disaggregated under alcohol in an agate mortar. The resulting slurry is transferred to a micronising mill and ground in alcohol for a period of 15 minutes. The sample is then dried and back-filled into an aluminium holder to produce an aggregate of randomly orientated crystallites.

A6.2 : Extraction of the Clay Fraction (<2microns)

Initial disaggregation is conducted under distilled water in an agate mortar. The sample is then transferred to a suitable beaker together with a dispersing agent in order to prevent flocculation. Liberation of the clay component is facilitated by standing the beaker in an ultrasonic bath for 30 minutes. The >2micron fraction is removed from suspension by centrifuge and the remaining clay is decanted off, sodium saturated and filtered under vacuum onto a membrane. The resulting clay film is transferred to a pyrex glass disk by membrane filter peel technique. Four XRD traces were run for each sample:

1. After drying the clay mount at room temperature and humidity.
2. After ethylene glycol solvation at room temperature for 24 hours (in order to detect the presence of swelling clays).
3. Immediately following heating to 375°C for 30 minutes (this causes illite-smectite and discrete illite to coincide at 10 angstroms).
4. After heating to 550°C for 90 minutes (causing the collapse of kaolinite and the collapse of the brucite layer within chlorite).

In cases where chlorite masks the presence of kaolinite a further trace may be run using sample material that has been treated with 6 molar hydrochloric acid. This collapses the chlorite peaks allowing verification and quantification of kaolinite. Where present, carbonates are removed from the samples during the early stages of preparation using a solution of 3% acetic acid buffered to pH 5 with sodium acetate, thus avoiding damage to sensitive clay minerals.

APPENDIX SEVEN : COMPUTER PROGRAMS

The following interactive Fortran '77 programs are menu driven and provide 'on-line' help in the form of a series of explanatory notes and comments relating to the available options. All file handling and data manipulations are carried out within/by the RAW system programs. Hardcopy output is obtained using Calcomp or HP compatible pen plotters, daisywheel printers and/or laser printers. Output from each of the RAW suite of programs is prefixed by a user selected name and suffixed by the file type relating to the specific program (ie. the RAW program outputs a .RAW file). The RAW system programs were written by the author to assist all aspects of data management and processing during the tenure of this Ph.D. The RAW system programs include:

Program Name		Output File Type
RAW	Numerical Database Management System	.RAW
HIS	Histogram Package	.HIS
STA	Statistical Package	.STA
RAT	Ratio Calculation Package	.RAW
DIS	Simple Discriminant Analysis	.DIS
TRV	Geochemical Traverse Plotter	.TRV
SIF	Sifting utility using KEYS	.RAW
SOR	Sorting/Extraction utility by variable	.RAW

Graphics programs PLOTLIB and SCATCHEM were developed within the Computer Centre and Applied Geology Departments of Strathclyde University, respectively.

0001 PROGRAM RAW

0002 C
0003 C
0004 C
0005 C
0006 C
0007 C
0008 C
0009 C
0010 C
0011 C
0012 C
0013 C
0014 C
0015 C
0016 C
0017 C
0018 C
0019 C
0020 C
0021 C
0022 C
0023 C
0024 C
0025 C
0026 C
0027 C
0028 C
0029 C
0030 C
0031 C
0032 C
0033 C
0034 C
0035 C
0036 C
0037 C
0038 C
0039 C
0040 C
0041 C
0042 C
0043 C
0044 C
0045 C
0046 C
0047 C
0048 C
0049 C
0050 C
0051 C
0052 C
0053 C
0054 C
0055 C
0056 C
0057 C
0058 C
0059 C
0060 C
0061 C
0062 C
0063 C
0064 C
0065 C
0066 C
0067 C
0068 C
0069 C

```

*****      *****      *
*          *      *          *
*      *      *      *      *
*****      *****      *
*      *      *      *      *
*      *      *      *      *
*          *      *          *

```

PAUL R. DULLER
DEPARTMENT OF APPLIED GEOLOGY
THE UNIVERSITY OF STRATHCLYDE
GLASGOW

JUNE 1985.

***** INTRODUCTION *****

THIS PROGRAM IS DESIGNED TO PRODUCE A SELF DESCRIBING
GENERAL PURPOSE DATA FILE, GENERATED BY THE USER FROM
DATA INPUT THROUGH THE TERMINAL.

THE PROGRAM IS ASSIGNED TO READ SAMPLE NAMES TOGETHER
WITH THE DATA MATRIX AND OUTPUT THE DATA TO A .RAW FILE
TOGETHER WITH THE SELF DESCRIBING FILE "HEADER".

THE OBJECT OF THIS PROGRAM IS TO FACILITATE RAPID
MANUAL INPUT OF DATA, AND STANDARDISE A NUMERIC FILE
STRUCTURE WHICH WHEN REINPUT TO THIS PROGRAM WILL
FACILITATE EASE OF MANIPULATION OF DATA AND WILL
ALLOW RAPID IMPLEMENTATION OF DATA IN USER'S OWN
PROGRAMS.

ADDITIONAL FACILITIES WITHIN 'RAW' INCLUDE THE ABILITY TO;

APPEND FILES
MERGE FILES
DELETE RECORDS
REFORMAT OUTPUT (TABULATE)
SAMPLE ORIENTATED EDITING
VARIABLE ORIENTATED EDITING

THE FORMAT OF THE OUTPUT FILE STRUCTURE IS:

RECORD 1 A80	TITLE
RECORD 2 A80	FORMAT OF DATA - USUALLY F13.4
RECORD 3 2I2	NO OF VARIABLES AND NO OF RECORDS, OR 0
RECORD4+ 8(X,A8)	VARIABLE NAMES, 8 PER LINE
RECORD N A12	SAMPLE NAME
RECORD N+	RAW DATA (SEE RECORD 2)

++++++
++++++ END OF INTRODUCTION ++++++
++++++

INTEGER X,Y,A,I,J,K,L,M,M1,M2,N1,N2,O,P,Q,X1,I1,D,E,DEL(2000)
INTEGER DELNO,DECT
INTEGER R,MATH,DEC(100),IDATA(100,2000),LS,LP,LQ,F,Z,J1,J2,NO
REAL DATA(100,2000),DAT,CON1,CON2
CHARACTER TITLE*80,FORM*80,SAMPLE(2000)*10,NAME(100)*8,B*1,OUT*12
CHARACTER SUN(100)*12,BIN*12,C*1,SAMPLE1(2000)*10,KEY(2000)*2

```

0076 CHARACTER FORMX*10,FORM1*10,SAMP*10,NAM*8,NAME2(100)*8,SAMPLE2*10
0077 CHARACTER KEY2*2
0078 C
0079 C
0080 C
0081 C *****
0082 C ***** DETAILS FOR OTHER PROGRAMMERS *****
0083 C *****
0084 C
0085 C M1 = NO OF VARIABLES
0086 C N1 = NO OF RECORDS
0087 C
0088 C B = CONTROL VALUES INPUT FROM THE TERMINAL BY THE
0089 C USER TO INFORM THE PROGRAM OF PROPOSED WORK.
0090 C
0091 C DATA = INPUT DATA VALUES (FREE FORMAT)
0092 C DEC = NO. OF DECIMAL PLACES REQUIRED FOR TABLES
0093 C TITLE = TITLE OF FILE (TO IDENTIFY DATAFILE TO USER)
0094 C FORM = FORMAT OF OUTPUT DATA
0095 C NAME = ARRAY 1 TO M CONTAINING VARIABLE NAMES
0096 C BIN = INPUT .RAW FILE NAME
0097 C OUT = INPUT/CREATION .RAW FILE NAME
0098 C SAMPLE= ARRAY 1 TO N CONTAINING SAMPLE NAMES
0099 C SUN = ARRAY CONTAINING A SUBSET OF SAMPLE NAMES FOR SORTING
0100 C KEY = A TWO SYMBOL CODE ATTACHED TO THE END OF THE
0101 C SAMPLE NAME. BY DEFAULT NORMALLY IS " ".
0102 C DEL = INTEGER ARRAY CONTAINING PRINT(1) OR DELETE(0) CODES
0103 C TO CONTROL OUTPUT.
0104 C
0105 C ++++++
0106 C ++++++ END OF DETAILS ++++++
0107 C ++++++
0108 C
0109 C
0110 C
0111 C *****
0112 C ***** RAW HEADER ***** RAW HEADER *****
0113 C *****
0114 C
0115 C
0116 C 1 WRITE(6,40)
0117 C READ(5,500)B
0118 C IF(B.EQ.'/')THEN
0119 C GOTO 999
0120 C END IF
0121 C IF(B.NE.'C')THEN
0122 C GOTO 1
0123 C END IF
0124 C
0125 C ++++++
0126 C ++++++ END OF RAW HEADER ++++++
0127 C ++++++
0128 C
0129 C
0130 C *****
0131 C ***** SET UP PRINTOUT SWITCHES *****
0132 C *****
0133 C
0134 C ARRAY DEL(1 TO 1000) CONTROLS THE OUTPUT OF SAMPLE RECORDS
0135 C IF DEL(I)=1 THEN RECORD NO. I OUTPUT, =0 THEN NOT OUTPUT.
0136 C DELNO PROVIDES A MEASURE OF THE NUMBER OF SAMPLE RECORDS THAT
0137 C ARE NOT TO BE OUTPUT.
0138 C VALUES FOR DEL AND DELNO ARE ALTERED BY THE SAMPLE ORIENTATED
0139 C MODE OF THE EDIT PROGRAM.
0140 C
0141 C DO 150 I=1,2000
0142 C DEL(I)= 1
0143 C 150 CONTINUE
0144 C DELNO=0
0145 C
0146 C ++++++
0147 C ++++++ END OF SET UP ++++++
0148 C ++++++
0149 C
0150 C

```

```

0151 C *****
0152 C ***** INFORM THE USER OF OPTIONS *****
0153 C *****
0154 C
0155     128 WRITE(6,100)
0156 C
0157 C     FIND OUT FROM THE USER WHAT IS REQUIRED
0158 C
0159     READ (5,500)B
0160 C
0161 C     EXIT
0162 C
0163     IF(B.EQ.'/')THEN
0164     WRITE(6,210)
0165     GOTO 999
0166     END IF
0167 C
0168 C     APPEND
0169 C
0170     IF(B.EQ.'A')THEN
0171     GOTO 121
0172     END IF
0173 C
0174 C     EDIT
0175 C
0176     IF(B.EQ.'E')THEN
0177     GOTO 401
0178     END IF
0179 C
0180 C
0181 C     REFORMAT
0182 C
0183     IF(B.EQ.'R')THEN
0184     GOTO 125
0185     END IF
0186 C
0187 C     EXIT FROM PROGRAM
0188 C
0189     IF(B.EQ.'/')THEN
0190     GOTO 750
0191     END IF
0192 C
0193 C     CREATE
0194 C
0195     IF (B.EQ.'C')THEN
0196     GOTO 126
0197     END IF
0198 C
0199     GOTO 128
0200 C
0201 C ++++++
0202 C ++++++ END OF OPTIONS ++++++
0203 C ++++++
0204 C
0205 C
0206 C
0207 C *****
0208 C ***** CREATE *****
0209 C *****
0210 C
0211 C
0212 C     OUTPUT HEADER FOR CREATE AND PROVIDE USER WITH
0213 C     DETAILS OF THE PROGRAM.
0214 C
0215     104 WRITE(6,481)
0216     READ(5,500)B
0217 C
0218 C     CHECK THAT OPTIONS ARE ACCEPTABLE
0219 C
0220     IF(B.EQ.'/')THEN
0221     GOTO 128
0222     END IF
0223     IF(B.NE.'C')THEN
0224     GOTO 104
0225     END IF

```

```
0226 C
0227 C
0228 C ASK THE USER TO TYPE IN THE FULL .RAW FILENAME
0229 C
0230 126 WRITE(6,101)
0231 READ(5,501)OUT
0232 C CHECK THAT A NAME HAS BEEN INPUT
0233 C
0234 IF(OUT.EQ.' ')THEN
0235 GOTO 126
0236 END IF
0237 C
0238 C
0239 C ASK THE USER TO TYPE IN A TITLE FOR THE FILE
0240 C
0241 488 WRITE(6,129)
0242 READ(5,139)TITLE
0243 C
0244 C CHECK THAT A CHARACTER HAS BEEN INPUT
0245 C
0246 IF(TITLE.EQ.' ')THEN
0247 GOTO 488
0248 END IF
0249
0250 C
0251 C OPEN INPUT CHANNEL
0252 C
0253 OPEN(2,FILE=OUT,DEFAULT FILE='.RAW',STATUS='NEW')
0254 C INPUT THE NUMBER OF VARIABLES (M1)
0255 C
0256 489 WRITE(6,102)
0257 READ(5,*)M1
0258 IF(M1.EQ.0)THEN
0259 GOTO 489
0260 END IF
0261 IF(M1.GE.51)THEN
0262 WRITE(6,491)
0263 GOTO 489
0264 END IF
0265 C CHECK THAT M1 LIES WITHIN THE CORRECT LIMITS
0266 C
0267 C
0268 C INPUT THE VARIABLE NAMES AND STORE IN ARRAY NAME
0269 C
0270 DO 10 I=1,M1
0271 WRITE(6,103)I
0272 READ (5,503)NAME(I)
0273 10 CONTINUE
0274 K=1
0275 N1=0
0276 C
0277 C OUTPUT MESSAGE RELATING TO UNIQUE SAMPLE/ROW NO.
0278 C
0279 WRITE(6,243)
0280 C
0281 C
0282 C SET UP FORMAT STATEMENT
0283 C
0284 FORM='6F13.4'
0285 C
0287 C
0288 50 WRITE(6,106)
0289 725 READ(5,506)SAMPLE(K)
0290 C
0291 C CHECK TO SEE IF A SAMPLE NAME HAS BEEN INPUT
0292 C IF NOT CHECK WITH THE USER TO SEE IF THIS IS
0292 C IF NOT CHECK WITH THE USER TO SEE IF THIS IS
0293 C SATISFACTORY
0294 C
0295 IF(K.GE.2)THEN
0296 C
0297 C FIRST FIND OUT IF A BLANK SAMPLE NAME INPUT
0298 C
0299 IF(SAMPLE(K).EQ.' ')THEN
0300 GOTO 230
```



```
0301      END IF
0302      C
0303      C      IF NOT, CHECK THE UNIQUENESS OF SAMPLE NAME
0304      C
0305      L=K-1
0306      DO 244 I=1,L
0307      IF (SAMPLE(K).EQ.SAMPLE(I))THEN
0308      WRITE(6,246)
0309      GOTO 50
0310      END IF
0311      244 CONTINUE
0312      C
0313      END IF
0314      C
0315      230 IF (SAMPLE(K).EQ.' ')THEN
0316      WRITE(6,492)
0317      ELSE
0318      GOTO 495
0319      END IF
0320      READ(5,500)B
0321      IF (B.EQ.'Y')THEN
0322      GOTO 495
0323      END IF
0324      GOTO 50
0325      C
0326      C      CHECK TO SEE IF OPERATOR WANTS TO QUIT
0327      C
0328      495 IF (SAMPLE(K).EQ.'/')THEN
0329      WRITE(6,459)
0330      C
0331      C      CHECK THAT THE USER DOES WISH TO QUIT
0332      C
0333      READ(5,500)B
0334      IF (B.EQ.'/')THEN
0335      C
0336      C      THE OPERATOR DOES WANT TO QUIT
0337      C
0338      GOTO 750
0339      END IF
0340      GOTO 50
0341      END IF
0342      C
0343      C      CONTINUE WITH THE CREATION PROGRAM
0344      C
0345      KEY(K)=' '
0346      N1=N1+1
0347      C
0348      C      READ IN A SINGLE COMPLETE SAMPLE RECORD
0349      C      CONTAINING THE VALUES FOR EACH OF M1 VARIABLES
0350      C
0351      DO 20 J=1,M1
0352      C
0353      C      ASK FOR THE VALUES OF EACH VARIABLE IN ORDER
0354      C
0355      WRITE(6,107)NAME(J)
0356      READ(5,*)DATA(J,K)
0357      20 CONTINUE
0358      C
0359      C      INCREMENT K AND READ NEXT RECORD
0360      C
0361      K=K+1
0362      GOTO 50
0363      C
0364      C      FIND OUT IF ANY DATA HAS BEEN TYPED IN
0365      C      IF NOT EXIT PROGRAM WITH APPROPRIATE MESSAGE
0366      C
0367      750 IF (K.LE.1)THEN
0368      GOTO 997
0369      C
0370      C      IF SO DO NOT SET UP HEADED OUTPUT FILE
0371      C
0372      END IF
0373      C
0374      C      IF K IS GREATER THAN 1 THEN
0375      C
```

```

0376 C *****
0377 C ***** SET UP OUTPUT FILE WITH HEADER *****
0378 C *****
0379 C
0380 800 BIN=OUT
0381 OPEN(1,FILE=BIN, DEFAULT FILE='.RAW',STATUS='NEW')
0382 WRITE(1,108)TITLE
0383 WRITE(1,109)FORM
0384 C
0385 C CHECK THAT NO RECORDS ARE SCHEDULED TO BE DELETED
0386 C INCREMENT N1 (NO OF RECORDS) ACCORDINGLY
0387 C
0388 N1=N1-DELNO
0389 WRITE(1,110)M1,N1
0390 N1=N1+DELNO
0391 C
0392 C FIND OUT HOW MANY COMPLETE LINES (L) OF SAMPLE NAMES
0393 C ARE REQUIRED TO BE OUTPUT
0394 C
0395 L=1
0396 Q=M1
0397 780 IF(Q.GE.9) THEN
0398 L=L+1
0399 Q=Q-8
0400 GOTO 780
0401 END IF
0402 C
0403 C P IS THE NO OF REMAINING SAMPLE NAMES (LESS THAN 8)
0404 C
0405 P=Q
0406 Y=0
0407 C
0408 C OUTPUT VARIABLE NAMES TO HEADER IN CORRECT FORMAT
0409 C BUT FIRST CHECK OUT HAW MANY PARTLINES REQUIRED
0410 C
0411 L=L-1
0412 IF(L.EQ.0)THEN
0413 GOTO 135
0414 END IF
0415 DO 28 I=1,L
0416 X=Y+1
0417 Y=Y+8
0418 WRITE (1,111)(NAME(J),J=X,Y)
0419 28 CONTINUE
0420 C
0421 135 IF(P.EQ.0)THEN
0422 GOTO 136
0423 END IF
0424 Y=M1-P+1
0425 WRITE(1,111)(NAME(J),J=Y,M1)
0426 C
0427 C
0428 C FIND OUT HOW MANY COMPLETE LINES OF F13.4 DATA
0429 C PER RECORD.
0430 C
0431 136 L=1
0432 Q=M1
0433 785 IF(Q.GE.7)THEN
0434 L=L+1
0435 Q=Q-6
0436 GOTO 785
0437 END IF
0438 P=Q
0439 Y=0
0440 C
0441 C
0442 C *****
0443 C ***** OUTPUT SAMPLE DATA IN CORRECT FORMAT *****
0444 C *****
0445 C
0446 C CHECK THE DEL ARRAY (PRINT RECORD SWITCH 0 OR 1)
0447 C
0448 L=L-1
0449 DO 31 A=1,N1
0450 IF(DEL(A).EQ.1)THEN

```

```

0451 C
0452 C WRITE SAMPLE NAME
0453 C
0454 WRITE (1,484)SAMPLE(A),KEY(A)
0455 IF(L.EQ.0)THEN
0456 GOTO 134
0457 END IF
0458 Y=0
0459 C
0460 C CHECK TO SEE IF AT LEAST ONE COMPLETE 6F13.4 RECORD
0461 C IS PRESENT FOR OUTPUT
0462 C
0463 DO 33 I=1,L
0464 X=Y+1
0465 Y=Y+6
0466 C
0467 C WRITE ONE COMPLETE DATA RECORD TO FILE
0468 C
0469 WRITE(1,113)(DATA(J,A),J=X,Y)
0470 33 CONTINUE
0471 134 IF(P.EQ.0)THEN
0472 GOTO 31
0473 END IF
0474 Y=M1-P+1
0475 WRITE(1,113)(DATA(J,A),J=Y,M1)
0476 END IF
0477 31 CONTINUE
0478 C
0479 C WRITE END OF FILE CHARACTERS
0480 C
0481 WRITE(1,114)
0482 GOTO 998
0483 C
0484 C ++++++
0485 C ++++++ END OF CREATE ++++++
0486 C ++++++
0487 C
0488 C
0489 C
0490 C *****
0491 C ***** APPEND *****
0492 C *****
0493 C
0494 C
0495 C WRITE HEADER FOR APPEND PROGRAM
0496 C
0497 121 WRITE(6,466)
0498 C
0499 C READ OPTION
0500 C
0501 477 READ(5,500)B
0502 C
0503 C
0504 C CHECK OPTION
0505 C
0506 IF(B.EQ.'/')THEN
0507 GOTO 997
0508 C
0509 C AUTO EXIT
0510 C
0511 END IF
0512 IF(B.EQ.'E')THEN
0513 GOTO 122
0514 C
0515 C GO TO THE EDIT ROUTINE
0516 C
0517 END IF
0518 C
0519 C CHECK TO SEE IF MERGE REQUIRED
0520 C
0521 IF(B.EQ.'M')THEN
0522 GOTO 1500
0523 END IF
0524 IF(B.NE.'A')THEN
0525 GOTO 121

```

```
0526      ELSE
0527      GOTO 493
0528      END IF
0529      C
0530      C *****
0531      C ***** MERGE *****
0532      C *****
0533      C
0534      C      ASK FOR FILENAME
0535      C
0536      1500 WRITE(6,1501)
0537      READ(5,501)OUT
0538      OPEN(2,FILE=OUT,DEFAULT FILE='.RAW',STATUS='OLD')
0539      C
0540      C      READ FILE HEADER AND DATA
0541      C
0542      READ(2,108)TITLE
0543      READ(2,109)FORM
0544      READ(2,110)M1,N1
0545      READ(2,111)(NAME(I),I=1,M1)
0546
0547      DO 1435 I=1,N1
0548      READ(2,484)SAMPLE(I),KEY(I)
0549      READ(2,113)(DATA(J,I),J=1,M1)
0550      1435 CONTINUE
0551      C
0552      C      ASK USER FOR TYPE OF MERGE REQUIRED
0553      C      ie. ADDITIONAL SAMPLES WITH SAME VARIABLES
0554      C      OR ADDITIONAL VARIABLES FOR THE SAME SAMPLES.
0555      C
0556      1506 WRITE(6,1502)
0557      READ(5,1503)I2
0558      IF(I2.EQ.1)THEN
0559      GOTO 1504
0560      END IF
0561      IF(I2.EQ.2)THEN
0562      GOTO 1505
0563      ELSE
0564      GOTO 1506
0565      END IF
0566      C
0567      C *****
0568      C ***** STYLE 1: *****
0569      C ***** ADDITIONAL SAMPLES *****
0570      C *****
0571      C
0572      C      ASK USER FOR ADDITIONAL FILENAME
0573      C      AND READ TITLE2,FORM2,M2,N2,NAME2
0574      C
0575      C      CHECK M1 AND M2 ARE IDENTICAL AND THAT
0576      C      ARRAYS NAME AND NAME2 CONTAIN THE SAME
0577      C      VARIABLE NAMES IN THE SAME ORDER
0578      C      IF SO INCREMENT N1 AND ADD DATA TO THE
0579      C      ARRAY DATA.
0580      C
0581      1504 WRITE(6,2115)
0582      READ(5,501)OUT
0583
0584      IF(OUT.EQ.'/')THEN
0585      GOTO 999
0586      END IF
0587
0588      OPEN(2,FILE=OUT,DEFAULT FILE='.RAW',STATUS='OLD')
0589      C
0590      C      READ FILE HEADER AND DATA
0591      C
0592      READ(2,108)TITLE
0593      READ(2,109)FORM
0594      READ(2,110)M2,N2
0595      READ(2,111)(NAME2(I),I=1,M1)
0596      C
0597      C      CHECK M1 vs. M2
0598      C
0599      IF(M1.NE.M2)THEN
0600      C      OUTPUT ERROR MESSAGE AND RETURN USER TO START
```

```
0601      WRITE(6,1600)
0602      GOTO 1504
0603      END IF
0604      C
0605      C      CHECK NAMES (ie.NAME(I) = NAME2(I) FOR M1 SAMPLES)
0606      C
0607      DO 1700 I=1,M1
0608
0609      IF(NAME(I).NE.NAME2(I))THEN
0610      C      OUTPUT ERROR MESSAGE AND RETURN USER TO START
0611      WRITE(6,1601)
0612      GOTO 1504
0613      END IF
0614
0615      1700 CONTINUE
0616      C
0617      C      BOTH NUMBER AND POSITION OF VARIABLES IDENTICAL,
0618      C      DATAMERGE CAN NOW PROCEED.
0619      C
0620      P=N1+1
0621      Q=N1+N2
0622
0623      DO 1488 I=P,Q
0624      READ(2,484)SAMPLE(I),KEY(I)
0625      READ(2,113)(DATA(J,I),J=1,M1)
0626      1488 CONTINUE
0627
0628      N1=N1+N2
0629      C
0630      C      MERGE COMPLETE - INFORM USER OF OPTIONS
0631      C
0632      1670 WRITE(6,1602)
0633      READ(5,500)B
0634
0635      IF(B.EQ.'2')THEN
0636      C      CONTINUE MERGE
0637      GOTO 1504
0638      END IF
0639
0640      IF(B.EQ.'1')THEN
0641
0642      C      ASK USER FOR NEW FILENAME AND OUTPUT MERGED DATAFILE
0643
0644      WRITE(6,101)
0645      READ(5,501)OUT
0646      OPEN(2,FILE=OUT,DEFAULT FILE='.RAW',STATUS='NEW')
0647
0648      C      ASK USER FOR A NEW TITLE
0649
0650      WRITE(6,129)
0651      READ(5,139)TITLE
0652      C
0653      C      MOVE TO CREATE SECTION FOR FINAL OUTPUT
0654      C
0655      GOTO 800
0656      END IF
0657
0658      GOTO 1670
0659
0660      C
0661      C      *****
0662      C      ***** END OF STYLE 1 *****
0663      C      *****
0664
0665      C      *****
0666      C      ***** STYLE 2 *****
0667      C      ***** ADDITIONAL VARIABLES *****
0668      C      *****
0669      C
0670      C
0671      C      ASK USER FOR ADDITIONAL FILENAME
0672      C      AND READ TITLE2,FORM2,M2,N2,SAMPLE2
0673      C
0674      C      CHECK N1 AND N2 ARE IDENTICAL AND THAT
0675      C      ARRAYS SAMPLE AND SAMPLE2 CONTAIN THE SAME
```

```

0676 C      SAMPLE NAMES IN THE SAME ORDER:
0677 C      IF SO INCREMENT M1 AND ADD NEW VARIABLES TO THE
0678 C      EXISTING SAMPLE RECORDS.
0679 C
0680 1505 WRITE(6,2115)
0681      READ(5,501)OUT
0682
0683      IF(OUT.EQ.'/')THEN
0684          GOTO 999
0685      END IF
0686
0687      OPEN(2,FILE=OUT,DEFAULT FILE='.RAW',STATUS='OLD')
0688 C
0689 C      READ FILE HEADER AND DATA
0690 C
0691      READ(2,108)TITLE
0692      READ(2,109)FORM
0693      READ(2,110)M2,N2
0694      READ(2,111)(NAME2(I),I=1,M2)
0695 C
0696 C      CHECK THAT BOTH NUMBER AND POSITION OF SAMPLES IDENTICAL,
0697 C      ONLY THEN CAN DATAMERGE PROCEEDE.
0698 C
0699      IF(N1.NE.N2)THEN
0700 C      OUTPUT ERROR MESSAGE AND RETURN TO START
0701      WRITE(6,1620)
0702      GOTO 1505
0703      END IF
0704
0705      DO 1438 I=1,N1
0706      READ(2,484)SAMPLE2,KEY2
0707
0708 C      CHECK SAMPLE NAMES
0709
0710      IF(SAMPLE(I).NE.SAMPLE2)THEN
0711 C      OUTPUT ERROR MESSAGE AND RETURN TO START
0712      WRITE(6,1621)SAMPLE(I),SAMPLE2
0713      GOTO 1505
0714      END IF
0715
0716      READ(2,113)(DATA(J,I),J=M1+1,M1+M2)
0717
0718 1438 CONTINUE
0719
0720      DO 1750 I=1,M2
0721      NAME(M1+I)=NAME2(I)
0722 1750 CONTINUE
0723
0724      M1=M1+M2
0725
0726 C
0727 C      MERGE COMPLETE - INFORM USER OF OPTIONS
0728 C
0729 1727 WRITE(6,1602)
0730      READ(5,500)B
0731
0732      IF(B.EQ.'2')THEN
0733 C      CONTINUE MERGE
0734      GOTO 1505
0735      END IF
0736
0737      IF(B.EQ.'1')THEN
0738
0739 C      ASK USER FOR NEW FILENAME AND OUTPUT MERGED DATAFILE
0740
0741      WRITE(6,101)
0742      READ(5,501)OUT
0743      OPEN(2,FILE=OUT,DEFAULT FILE='.RAW',STATUS='NEW')
0744
0745 C      ASK USER FOR A NEW TITLE
0746
0747      WRITE(6,129)
0748      READ(5,139)TITLE
0749 C
0750 C      MOVE TO CREATE SECTION FOR FINAL OUTPUT

```



```

0751 C
0752     GOTO 800
0753     END IF
0754
0755     GOTO 1727
0756 C
0757 C *****
0758 C ***** APPEND *****
0759 C *****
0760 C
0761 C     ASK FOR FILENAME
0762 C
0763     493 WRITE(6,115)
0764     READ(5,501)OUT
0765     OPEN(2,FILE=OUT,DEFAULT FILE='.RAW',STATUS='OLD')
0766 C
0767 C     READ FILE HEADER AND DATA
0768 C
0769     READ(2,108)TITLE
0770     READ(2,109)FORM
0771     READ(2,110)M1,N1
0772     READ(2,111)(NAME(I),I=1,M1)
0773     DO 435 I=1,N1
0774     READ(2,484)SAMPLE(I),KEY(I)
0775     READ(2,113)(DATA(J,I),J=1,M1)
0776     435 CONTINUE
0777 C
0778 C     INCREMENT K TO GENERATE FURTHER SAMPLE LOCATIONS
0779 C
0780     434 K=N1+1
0781     GOTO 50
0782 C
0783 C     RETURN TO USER TERMINAL INPUT OF ADDED DATA
0784 C
0785 C ++++++
0786 C ++++++ END OF APPEND ++++++
0787 C ++++++
0788 C
0789 C
0790 C *****
0791 C ***** EDIT *****
0792 C *****
0793 C
0794 C
0795 C     ASK FOR FILENAME
0796 C
0797     401 WRITE(6,485)
0798     READ(5,501)OUT
0799     OPEN(2,FILE=OUT,DEFAULT FILE='.RAW',STATUS='OLD')
0800 C
0801 C
0802 C     DATA INPUT
0803 C
0804 C     READ FILE HEADER AND DATA
0805 C
0806     READ(2,108)TITLE
0807     READ(2,109)FORM
0808     READ(2,110)M1,N1
0809     READ(2,111)(NAME(I),I=1,M1)
0810
0811     DO 403 I=1,N1
0812     READ(2,484)SAMPLE(I),KEY(I)
0813     READ(2,113)(DATA(J,I),J=1,M1)
0814     403 CONTINUE
0815 C
0816 C     INCREMENT K TO GENERATE FURTHER SAMPLE LOCATIONS
0817 C
0818     404 K=N1
0819 C
0820 C     WRITE HEADER FOR PROGRAM
0821 C
0822     122 WRITE(6,467)
0823     486 READ(5,500)B
0824 C
0825 C *****

```

```
0826 C ***** SELECT OPTION *****
0827 C *****
0828 C
0829 C     READ OPTION
0830 C
0831 C     IF(B.EQ.'/')THEN
0832 C     GOTO 800
0833 C     END IF
0834 C
0835 C     IF(B.EQ.'S') THEN
0836 C
0837 C     CALL SAMPLE ORIENTATED PROGRAM HEADER
0838 C
0839 C     7 WRITE(6,469)
0840 C 473 READ(5,500)C
0841 C
0842 C     ASK FOR OPTION
0843 C
0844 C     IF(C.EQ.'/')THEN
0845 C
0846 C     RETURN TO MAIN EDIT PROGRAM
0847 C
0848 C     GOTO 122
0849 C     END IF
0850 C
0851 C     IF(C.EQ.'D')THEN
0852 C     GOTO 41
0853 C     END IF
0854 C     IF(C.EQ.'C')THEN
0855 C     GOTO 42
0856 C     END IF
0857 C     GOTO 7
0858 C     END IF
0859 C
0860 C
0861 C     IF OPTION = V THEN ENTER VARIABLE ORIENTATED HEADER
0862 C
0863 C     IF(B.EQ.'V')THEN
0864 C     8 WRITE(6,468)
0865 C 474 READ(5,500)C
0866 C
0867 C     CHECK OPTION
0868 C
0869 C     IF(C.EQ.'/')THEN
0870 C     GOTO 122
0871 C     END IF
0872 C     IF(C.EQ.'G')THEN
0873 C     GOTO 80
0874 C     END IF
0875 C     IF(C.EQ.'I')THEN
0876 C     GOTO 81
0877 C     END IF
0878 C     IF(C.EQ.'M')THEN
0879 C     GOTO 82
0880 C     END IF
0881 C     IF(C.EQ.'T')THEN
0882 C     GOTO 83
0883 C     END IF
0884 C     IF(C.EQ.'D')THEN
0885 C     GOTO 84
0886 C     END IF
0887 C     GOTO 8
0888 C     END IF
0889 C
0890 C ++++++
0891 C ++++++ END OF SELECTION ++++++
0892 C ++++++
0893 C
0894 C
0895 C *****
0896 C ***** OPTIONS *****
0897 C *****
0898 C
0899 C
0900 C *****
```

```

0901 C ***** DELETE *****
0902 C *****
0903 C
0904 C
0905 41 DELNO=0
0906 56 WRITE(6,51)
0907 C
0908 C OUTPUT DETAILS OF DELETE FUNCTIONS AND
0909 C ASK THE USER FOR OPTION.
0910 C
0911 55 READ(5,500)B
0912 C
0913 C CHECK OPTION
0914 C
0915 IF(B.EQ.'S')THEN
0916 GOTO 52
0917 END IF
0918 IF(B.EQ.'T')THEN
0919 GOTO 53
0920 END IF
0921 IF(B.EQ.'R')THEN
0922 GOTO 54
0923 END IF
0924 IF(B.EQ.' ')THEN
0925 WRITE(6,127)
0926 GOTO 55
0927 END IF
0928 IF (B.EQ.'/')THEN
0929 GOTO 800
0930 END IF
0931 IF(B.NE.' ')THEN
0932 GOTO 56
0933 END IF
0934 C
0935 C *****
0936 C ***** SELECTIVE DELETE *****
0937 C *****
0938 C
0939 52 WRITE(6,57)
0940 C
0941 C
0942 C INFORM USER OF OPTIONS AND ASK FOR ONE TO BE SELECTED
0943 C
0944 READ(5,500)B
0945 C
0946 C CHECK OPTION
0947 C
0948 IF(B.EQ.'/')THEN
0949 GOTO 56
0950 END IF
0951 IF(B.EQ.'C')THEN
0952 GOTO 370
0953 END IF
0954 GOTO 52
0955 C
0956 370 L=1
0957 Q=N1
0958 63 IF(Q.GE.9)THEN
0959 L=L+1
0960 Q=Q-8
0961 GOTO 63
0962 END IF
0963 P=Q
0964 Y=0
0965 L=L-1
0966 C
0967 C WRITE HEADER
0968 C
0969 WRITE(6,262)
0970 C
0971 DO 255 I=1,L
0972 X=Y+1
0973 Y=Y+8
0974 C
0975 C OUTPUT RECORD/SAMPLE NAMES

```

```

0976 C
0977 WRITE(6,265)(SAMPLE(J),J=X,Y)
0978 255 CONTINUE
0979 IF(P.EQ.0)THEN
0980 GOTO 257
0981 END IF
0982 C
0983 C OUTPUT REMAINING RECORD/SAMPLE NAMES
0984 C
0985 Y=N1-P+1
0986 WRITE(6,265)(SAMPLE(I),I=Y,N1)
0987 C
0988 C
0989 257 WRITE(6,62)
0990 C
0991 C ASK THE USER FOR SAMPLE NAME
0992 C
0993 READ(5,506)SAMP
0994 C
0995 C CHECK THAT THIS RECORD NAME EXISTS WITHIN ARRAY SAMPLE
0996 C AND LOCATE THE POSITION AT WHICH IT OCCURS IN THE
0997 C ARRAY (Q)
0998 C
0999 I=1
1000 58 IF(SAMP.EQ.SAMPLE(I))THEN
1001 Q=I
1002 DELNO=DELNO+1
1003 GOTO 59
1004 END IF
1005 C
1006 C CHECK THAT THE LAST SAMPLE HAS NOT BEEN REACHED
1007 C
1008 IF(I.NE.N1)THEN
1009 I=I+1
1010 GOTO 58
1011 END IF
1012 C
1013 C IF I IS EQUAL TO N1 THEN OUTPUT ERROR MESSAGE
1014 C SAMPLE RECORD HAS NOT BEEN LOCATED.
1015 C
1016 WRITE(6,61)SAMP
1017 GOTO 52
1018 C
1019 C
1020 C ARRAY POSITION Q WITHIN ARRAY SAMPLE IS REQUIRED TO BE
1021 C DELETED. IE SET DEL(Q)=0 THEN SAMPLE(Q) NOT PRINTED.
1022 C
1023 59 DEL(Q)=0
1024 C
1025 C INFORM USER THAT A SAMPLE HAS BEEN DELETED
1026 C
1027 WRITE(6,64)SAMP
1028 GOTO 52
1029 C
1030 C ++++++
1031 C ++++++ END OF SELECTIVE DELETE ++++++
1032 C ++++++
1033 C
1034 C
1035 C *****
1036 C ***** TOTAL DELETE *****
1037 C *****
1038 C
1039 C INFORM THE USER OF OPTIONS
1040 C
1041 53 WRITE(6,65)
1042 READ(5,500)B
1043 C
1044 C CHECK OPTION
1045 C
1046 IF(B.EQ.'/')THEN
1047 GOTO 56
1048 END IF
1049 IF(B.NE.'C')THEN
1050 GOTO 53

```

```

1051      END IF
1052      C
1053      C      ALL SAMPLE RECORDS TO BE DELETED (NOT OUPUT AT THE
1054      C      FILE TRANSFER STAGE.
1055      C
1056      DELNO=N1
1057      DO 66 I=1,N1
1058      DEL(I)=0
1059      66  CONTINUE
1060      C
1061      C
1062      68  WRITE(6,67)
1063      READ(5,500)B
1064      C
1065      C      CHECK OPTION
1066      C
1067      IF(B.EQ.'/')THEN
1068      GOTO 56
1069      END IF
1070      IF(B.NE.'R')THEN
1071      GOTO 68
1072      END IF
1073      C
1074      C ++++++
1075      C ++++++ END OF TOTAL DELETE ++++++
1076      C ++++++
1077      C
1078      C *****
1079      C ***** REINSTATE *****
1080      C *****
1081      C
1082      54  WRITE(6,69)
1083      READ(5,500)B
1084      C
1085      C      CHECK OPTIONS
1086      C
1087      IF(B.EQ.'/')THEN
1088      GOTO 56
1089      END IF
1090      IF(B.NE.'R')THEN
1091      GOTO 54
1092      END IF
1093      C
1094      C      LIST SAMPLE/ROW NUMBERS
1095      C      SO THAT THE USER MAY CHOOSE ONE TO BE REINSTATED
1096      C
1097      L=1
1098      Q=N1
1099      813  IF(Q.GE.9)THEN
1100      L=L+1
1101      Q=Q-8
1102      GOTO 813
1103      END IF
1104      P=Q
1105      Y=0
1106      L=L-1
1107      C
1108      C      WRITE HEADER
1109      C
1110      WRITE(6,262)
1111      C
1112      DO 814 I=1,L
1113      X=Y+1
1114      Y=Y+8
1115      C
1116      C      OUTPUT RECORD/SAMPLE NAMES
1117      C
1118      WRITE(6,265)(SAMPLE(J),J=X,Y)
1119      814  CONTINUE
1120      IF(P.EQ.0)THEN
1121      GOTO 815
1122      END IF
1123      C
1124      C      OUTPUT REMAINING RECORD/SAMPLE NAMES
1125      C

```

```

1126      Y=M1-P+1
1127      WRITE(6,265)(SAMPLE(I),I=Y,M1)
1128      C
1129
1130      C      ASK USER FOR THE RECORD NUMBER TO BE REINSTATED
1131      C
1132      815 WRITE(6,70)
1133      READ(5,506)SAMP
1134      C
1135      C      CHECK THAT THE RECORD NAME SAMP EXISTS
1136      C      AND HAS BEEN DELETED.
1137      C
1138      I=1
1139      71 IF(SAMP.EQ.SAMPLE(I))THEN
1140      Q=I
1141      GOTO 72
1142      END IF
1143      C
1144      C      CHECK THAT THE END OF DATA HAS NOT BEEN REACHED
1145      C
1146      IF(I.NE.N1)THEN
1147      I=I+1
1148      GOTO 71
1149      END IF
1150      C
1151      C      OUTPUT AN ERROR MESSAGE AS SAMPLE IS NOT FOUND
1152      C
1153      WRITE(6,61)SAMP
1154      GOTO 54
1155      C
1156      C      REINSTATE THE SAMPLE RECORD LOCATED AT POSITION Q
1157      C      AND CHANGE THE DEL(Q) PRINT SWITCH FROM 0 TO 1.
1158      C
1159      72 DEL(Q)=1
1160      DELNO=DELNO-1
1161      C
1162      C      RETURN TO REINSTATE WITH APPROPRIATE MESSAGE
1163      C
1164      WRITE(6,73)SAMP
1165      GOTO 54
1166      C
1167      C ++++++
1168      C ++++++ END OF REINSTATE ++++++
1169      C ++++++
1170      C
1171      C ++++++
1172      C ++++++ END OF DELETE PACKAGE ++++++
1173      C ++++++
1174      C
1175      C
1176      C *****
1177      C ***** CORRECT *****
1178      C *****
1179      C
1180      C      OUTPUT HEADER AND INFORM THE USER OF OPTIONS
1181      C
1182      42 WRITE(6,43)
1183      READ(5,500)B
1184      C
1185      C      CHECK OPTION
1186      C
1187      IF(B.EQ.'/')THEN
1188      GOTO 122
1189      END IF
1190      IF(B.EQ.'L')THEN
1191      GOTO 49
1192      END IF
1193      IF(B.EQ.'S')THEN
1194      GOTO 817
1195      END IF
1196      IF(B.NE.'C')THEN
1197      GOTO 42
1198      END IF
1199      C
1200      C      ASK THE USER FOR THE SAMPLE NAME TO BE CORRECTED

```



```

1201 C
1202 24 WRITE(6,44)
1203 READ(5,506)SAMP
1204 C
1205 C CHECK THAT THE SAMPLE NAME RELATES TO A KNOWN
1206 C RECORD OF DATA.
1207 C
1208 45 I=1
1209 845 IF(SAMP.EQ.SAMPLE(I))THEN
1210 Q=I
1211 GOTO 46
1212 END IF
1213 IF(I.NE.N1)THEN
1214 I=I+1
1215 GOTO 845
1216 END IF
1217 C
1218 C OUTPUT ERROR MESSAGE - SAMPLE NOT FOUND
1219 C
1220 WRITE(6,61)SAMP
1221 GOTO 42
1222 C
1223 C
1224 C CORRECT
1225 C
1226 C
1227 C FIND OUT HOW MANY COMPLETE LINES OF TEXT ARE TO
1228 C BE OUTPUT TO THE SCREEN.
1229 C
1230 46 L=0
1231 P=M1
1232 39 IF(P.GE.3)THEN
1233 L=L+1
1234 P=P-2
1235 GOTO 39
1236 END IF
1237 C
1238 C P IS THE REMAINING NO OF SAMPLES FORMING LESS THAN
1239 C A COMPLETE ROW OF OUTPUT
1240 C
1241 C OUTPUT DATA VALUES FOR RECORD AT LOCATION SAMPLE(Q)
1242 C
1243 Z=0
1244 850 Y=0
1245 WRITE(6,847)
1246 IF(M1.LE.2)THEN
1247 GOTO 816
1248 END IF
1249 C
1250 DO 48 I=1,L
1251 X=Y+1
1252 Y=Y+2
1253 WRITE(6,47)((J,NAME(J),DATA(J,Q)),J=X,Y)
1254 48 CONTINUE
1255 C
1256 C
1257 IF(P.EQ.0)THEN
1258 GOTO 38
1259 END IF
1260 C
1261 C
1262 816 Y=M1-P+1
1263 WRITE(6,47)((J,NAME(J),DATA(J,Q)), J=Y,M1)
1264 C
1265 IF(Z.NE.0)THEN
1266 GOTO 25
1267 END IF
1268 C ASK USER TO SELECT THE DATA ITEM FOR CORRECTION
1269 C
1270 38 WRITE(6,36)
1271 C
1272 C INPUT DATA ITEM POSITION (M2) TO BE CORRECTED
1273 C
1274 READ(5,*)M2
1275 C

```

```
1276 C CHECK THAT M2 IS ACCEPTABLE
1277 C
1278 IF (M2.EQ.999) THEN
1279 GOTO 42
1280 END IF
1281 C
1282 IF (M2.LE.0) THEN
1283 GOTO 38
1284 END IF
1285 C
1286 IF (M2.LE.M1) THEN
1287 GOTO 32
1288 END IF
1289 C
1290 C THE LOCATION NO REQUESTED IS GREATER THAN THOSE
1291 C AVAILABLE - ASK THE USER TO TRY AGAIN
1292 C
1293 WRITE(6,30)
1294 GOTO 38
1295 C
1296 C ASK THE USER TO INPUT A NEW VALUE FOR M2
1297 C
1298 32 WRITE(6,27) M2
1299 READ(5,*) DATA(M2,Q)
1300 C
1301 Z=Z+1
1302 GOTO 850
1303 C INFORM THE USER THAT THE CORRECTION HAS BEEN MADE
1304 C AND INFORM OF OPTIONS.
1305 C
1306 25 WRITE(6,26)
1307 Z=Z-1
1308 C
1309 C ASK USER FOR OPTION
1310 C
1311 READ(5,500) B
1312 IF (B.EQ.'/') THEN
1313 GOTO 42
1314 END IF
1315 IF (B.EQ.'N') THEN
1316 GOTO 24
1317 END IF
1318 IF (B.NE.'S') THEN
1319 GOTO 25
1320 END IF
1321 GOTO 38
1322 C
1323 C LIST SAMPLE/ROW NAMES
1324 C
1325 C
1326 C LIST SAMPLE/ROW NUMBERS
1327 C SO THAT THE USER MAY CHOOSE ONE TO BE REINSTATED
1328 C
1329 817 L=0
1330 Q=N1
1331 366 IF (Q.GE.9) THEN
1332 L=L+1
1333 Q=Q-8
1334 GOTO 366
1335 END IF
1336 C
1337 P=Q
1338 Y=0
1339 C
1340 IF (L.EQ.0) THEN
1341 GOTO 365
1342 END IF
1343 C
1344 C WRITE HEADER
1345 C
1346 WRITE(6,262)
1347 C
1348 DO 818 I=1,L
1349 X=8*(I-1)+1
1350 Y=8*(I-1)+8
```

```

1351 C
1352 C OUTPUT RECORD/SAMPLE NAMES
1353 C
1354 WRITE(6,265)(SAMPLE(J),J=X,Y)
1355 818 CONTINUE
1356 365 IF(P.EQ.0)THEN
1357 GOTO 337
1358 END IF
1359 C
1360 C OUTPUT REMAINING RECORD/SAMPLE NAMES
1361 C
1362 Y=N1-P+1
1363 WRITE(6,265)(SAMPLE(I),I=Y,N1)
1364 337 WRITE(6,206)
1365 READ(5,207)B
1366 IF(B.EQ.'C')THEN
1367 GOTO 42
1368 END IF
1369 GOTO 337
1370 C
1371 C ++++++
1372 C ++++++ END OF CORRECT ++++++
1373 C ++++++
1374 C
1375 C
1376 C *****
1377 C ***** LIST VARIABLES *****
1378 C *****
1379 C
1380 49 L=0
1381 P=M1
1382 11 IF(P.GE.3)THEN
1383 L=L+1
1384 P=P-2
1385 GOTO 11
1386 END IF
1387 C
1388 C OUTPUT HEADER
1389 C
1390 WRITE(6,369)
1391 C
1392 C NO OF REMAINING SAMPLES FORMING LESS THAN ONE COMPLETE
1393 C ROW (P).
1394 C
1395 C OUTPUT VARIABLE NAMES FOR THIS FILE
1396 C
1397 Y=0
1398 IF(L.EQ.0)THEN
1399 GOTO 819
1400 END IF
1401 DO 5 I=1,L
1402 X=Y+1
1403 Y=Y+2
1404 WRITE(6,6)((J,NAME(J)),J=X,Y)
1405 5 CONTINUE
1406 C
1407 C
1408 819 IF(P.EQ.0)THEN
1409 GOTO 205
1410 END IF
1411 C
1412 Y=M1-P+1
1413 WRITE(6,6)((J,NAME(J)),J=Y,M1)
1414 205 WRITE(6,206)
1415 READ(5,207)B
1416 IF(B.EQ.'C')THEN
1417 GOTO 42
1418 END IF
1419 GOTO 205
1420 C
1421 C
1422 C ++++++
1423 C ++++++ END OF LIST ++++++
1424 C ++++++
1425 C

```

```

1426 C
1427 C ++++++
1428 C ++++++ END OF SAMPLE ORIENTATED EDITING ++++++
1429 C ++++++
1430 C
1431 C
1432 C
1433 C *****
1434 C ***** VARIABLE ORIENTATED EDITING *****
1435 C *****
1436 C
1437 C     GENERATING A NEW VARIABLE NAME
1438 C
1439 C
1440 C     INFORM USER OF OPTIONS AND ASK FOR SELECTION
1441 C
1442 C     80 WRITE(6,19)
1443 C     READ(5,500)B
1444 C
1445 C     CHECK OPTION
1446 C
1447 C     IF(B.EQ. '/') THEN
1448 C     GOTO 8
1449 C     END IF
1450 C     IF(B.EQ. 'C') THEN
1451 C     GOTO 12
1452 C     END IF
1453 C     GOTO 80
1454 C
1455 C     INSERT NEW VARIABLE AT ADDRESS M1+1 AND SET ALL
1456 C     INITIAL VALUES TO ZERO.
1457 C
1458 C     12 M1=M1+1
1459 C     DO 21 I=1,N1
1460 C     DATA(M1,I)=0
1461 C     21 CONTINUE
1462 C
1463 C     ASK THE USER FOR THE NEW VARIABLE NAME
1464 C
1465 C     WRITE(6,22)
1466 C     READ(5,506)NAME(M1)
1467 C     GOTO 8
1468 C
1469 C
1470 C ++++++
1471 C ++++++ END OF GENERATE ++++++
1472 C ++++++
1473 C
1474 C
1475 C *****
1476 C ***** INSERT *****
1477 C *****
1478 C
1479 C
1480 C     81 WRITE(6,85)
1481 C
1482 C     ASK THE USER TO SELECT AN OPTION
1483 C
1484 C     READ(5,500)B
1485 C
1486 C     CHECK THE OPTION
1487 C
1488 C     IF(B.EQ. '/') THEN
1489 C     GOTO 122
1490 C     END IF
1491 C     IF(B.EQ. 'N') THEN
1492 C     GOTO 91
1493 C     END IF
1494 C     IF(B.EQ. 'S') THEN
1495 C     GOTO 99
1496 C     END IF
1497 C     IF(B.EQ. 'I') THEN
1498 C     GOTO 42
1499 C     END IF
1500 C     GOTO 81

```

```

1501 C
1502 C *****
1503 C *** NORMAL INSERT MODE *****
1504 C *****
1505 C
1506 C
1507     91 L=0
1508         P=M1
1509     511 IF(P.GE.3)THEN
1510         L=L+1
1511         P=P-2
1512         GOTO 511
1513     END IF
1514 C
1515 C     OUTPUT HEADER
1516 C
1517     WRITE(6,340)
1518     WRITE(6,368)
1519 C
1520 C     NO OF REMAINING SAMPLES FORMING LESS THAN ONE COMPLETE
1521 C     ROW (P).
1522 C
1523 C     OUTPUT VARIABLE NAMES FOR THIS FILE
1524 C
1525     Y=0
1526     IF(L.EQ.0)THEN
1527         GOTO 509
1528     END IF
1529     DO 504 I=1,L
1530         X=Y+1
1531         Y=Y+2
1532         WRITE(6,6)((J,NAME(J)),J=X,Y)
1533     504 CONTINUE
1534 C
1535 C
1536     509 IF(P.EQ.0)THEN
1537         GOTO 429
1538     END IF
1539     Y=M1-P+1
1540     WRITE(6,6)((J,NAME(J)),J=Y,M1)
1541     GOTO 429
1542 C
1543     429 WRITE(6,92)
1544     READ(5,503)NAM
1545 C
1546 C     CHECK THAT THE VARIABLE NAME EXISTS
1547 C
1548     IF(NAM.EQ.'/')THEN
1549         GOTO 81
1550     END IF
1551 C
1552     DO 290 I=1,M1
1553         IF (NAM.EQ.NAME(I))THEN
1554             Q=I
1555             GOTO 89
1556         END IF
1557     290 CONTINUE
1558 C
1559 C     NAME NOT FOUND - ERROR MESSAGE
1560 C
1561     WRITE(6,90)
1562     GOTO 91
1563 C
1564 C     THE VARIABLE OCCURS AT POSITION Q IN THE ARRAY
1565 C
1566     89 DO 93 I=1,N1
1567         WRITE(6,94) I,SAMPLE(I),NAME(Q)
1568         READ(5,*)DAT
1569 C
1570 C     CHECK THAT THE USER DOES NOT WANT TO AUTO-EXIT
1571 C
1572     IF(DAT.EQ.999.999)THEN
1573     297 WRITE(6,97)I
1574 C
1575 C

```

```

1576      WRITE(6,459)
1577      READ(5,500)B
1578      C
1579      C      CHECK OPTION
1580      C
1581      IF(B.EQ.'/')THEN
1582      GOTO 81
1583      END IF
1584      IF(B.NE.'/')THEN
1585      GOTO 297
1586      END IF
1587      END IF
1588      C
1589      C      USER WISHES TO CONTINUE
1590      C
1591      DATA(Q,I)=DAT
1592      93 CONTINUE
1593      GOTO 81
1594      C
1595      C      ++++++
1596      C      ++++++ END OF NORMAL INSERT MODE ++++++
1597      C      ++++++
1598      C
1599      C
1600      C
1601      C      *****
1602      C      ***** SELECTIVE INSERT MODE *****
1603      C      *****
1604      C
1605      C
1606      C      ASK THE USER TO SELECT THE VARIABLE NAME FROM THE
1607      C      LIST PROVIDED.
1608      C
1609      99 L=0
1610      P=M1
1611      381 IF(P.GE.3)THEN
1612      L=L+1
1613      P=P-2
1614      GOTO 381
1615      END IF
1616      C
1617      C      OUTPUT HEADER
1618      C
1619      WRITE(6,340)
1620      WRITE(6,368)
1621      C
1622      C      NO OF REMAINING SAMPLES FORMING LESS THAN ONE COMPLETE
1623      C      ROW (P).
1624      C
1625      C      OUTPUT VARIABLE NAMES FOR THIS FILE
1626      C
1627      Y=0
1628      IF(L.EQ.0)THEN
1629      GOTO 510
1630      END IF
1631      DO 508 I=1,L
1632      X=Y+1
1633      Y=Y+2
1634      WRITE(6,6)((J,NAME(J)),J=X,Y)
1635      508 CONTINUE
1636      C
1637      510 IF(P.EQ.0)THEN
1638      GOTO 512
1639      END IF
1640      Y=M1-P+1
1641      WRITE(6,6)((J,NAME(J)),J=Y,M1)
1642      C
1643      512 WRITE(6,92)
1644      C
1645      C      ASK USER FOR NAME
1646      C
1647      READ(5,503)NAM
1648      C
1649      C      CHECK THAT THE VARIABLE NAME EXISTS
1650      C

```



```

1651         IF(NAM.EQ.'/')THEN
1652             GOTO 81
1653         END IF
1654     C
1655         DO 298 I=1,M1
1656             IF(NAM.EQ.NAME(I))THEN
1657                 Q=I
1658                 GOTO 98
1659             END IF
1660         298 CONTINUE
1661     C
1662         ERROR MESSAGE - VARIABLE NOT FOUND
1663     C
1664         WRITE(6,90)
1665         GOTO 99
1666     C
1667         ASK THE USER FOR THE NEW STARTING POSITION
1668     C
1669         98 WRITE(6,118)N1
1670            READ(5,*)J
1671     C
1672         THE VARIABLE WHERE INSERT TO TAKE PLACE IS
1673         LOCATED AT POSITION Q.
1674     C
1675         DO 117 I=J,N1
1676             WRITE(6,94)I,SAMPLE(I),NAME(Q)
1677             READ(5,*)DAT
1678     C
1679         CHECK THAT THE USER DOES NOT WANT TO AUTO-EXIT
1680     C
1681         IF(DAT.EQ.999.999)THEN
1682     C
1683     C
1684         119 WRITE(6,97)I
1685            WRITE(6,459)
1686            READ(5,500)B
1687            IF(B.EQ.'/')THEN
1688                GOTO 800
1689            END IF
1690            GOTO 119
1691        END IF
1692     C
1693         USER WISHES TO CONTINUE
1694     C
1695         DATA(Q,I)=DAT
1696         117 CONTINUE
1697         GOTO 81
1698     C
1699     C ++++++
1700 C ++++++ END OF SELECTIVE INSERT MODE ++++++
1701 C ++++++
1702 C
1703 C ++++++
1704 C ++++++ END OF INSERT ++++++
1705 C ++++++
1706 C
1707 C
1708 C
1709 C *****
1710 C ***** TRANSFORM *****
1711 C *****
1712 C
1713 C
1714 C     INFORM USER OF OPTIONS : WRITE HEADER
1715     C
1716         83 WRITE(6,173)
1717            READ(5,500)B
1718     C
1719         P=0
1720         Q=0
1721     C
1722         CHECK OPTIONS
1723     C
1724         IF(B.EQ.'/')THEN
1725             GOTO 122

```

```

1726      END IF
1727      IF (B.NE.'C') THEN
1728      GOTO 83
1729      END IF
1730      C
1731      C
1732      L=1
1733      Q=M1
1734      263 IF (Q.GE.9) THEN
1735      L=L+1
1736      Q=Q-8
1737      GOTO 263
1738      END IF
1739      P=Q
1740      Y=0
1741      L=L-1
1742      C
1743      C      WRITE HEADER
1744      C
1745      WRITE(6,261)
1746      DO 258 I=1,L
1747      X=Y+1
1748      Y=Y+8
1749      C
1750      C      OUTPUT VARIABLE NAMES
1751      C
1752      WRITE(6,260)(NAME(J),J=X,Y)
1753      258 CONTINUE
1754      IF (P.EQ.0) THEN
1755      GOTO 177
1756      END IF
1757      C
1758      C      OUTPUT REMAINING VARIABLE NAMES
1759      C
1760      Y=M1-P+1
1761      WRITE(6,260)(NAME(J),J=Y,M1)
1762      C
1763      C
1764      C      ASK USER FOR VARIABLE 1
1765      C
1766      177 WRITE(6,174)
1767      READ(5,503)NAM
1768      C
1769      C      CHECK THAT CONSTANT (C1) NOT REQUIRED
1770      C
1771      IF (NAM.EQ.'/') THEN
1772      GOTO 178
1773      END IF
1774      C
1775      C      CHECK THAT NAM EXISTS
1776      C
1777      DO 175 I=1,M1
1778      IF (NAM.EQ.NAME(I)) THEN
1779      Q=I
1780      GOTO 176
1781      END IF
1782      175 CONTINUE
1783      C
1784      C      ERROR MESSAGE - VARIABLE NAME NOT FOUND
1785      C
1786      WRITE(6,90)
1787      GOTO 177
1788      C
1789      C      VARIABLE NAME 1 ACCEPTED - ASK USER FOR FUNCTION
1790      C
1791      176 WRITE(6,180)
1792      READ(5,500)B
1793      C
1794      C      CHECK OPTION - SET FUNCTION SWITCHES
1795      C
1796      C      ++++++
1797      C
1798      IF (B.EQ.'+') THEN
1799      MATH=1
1800      GOTO 181

```

```

1801      END IF
1802      C
1803      C -----
1804      C
1805      IF(B.EQ.'-')THEN
1806      MATH=2
1807      GOTO 181
1808      END IF
1809      C
1810      C //////////////////////////////////////
1811      C
1812      IF(B.EQ.'/')THEN
1813      MATH=3
1814      GOTO 181
1815      END IF
1816      C
1817      C *****
1818      C
1819      IF(B.EQ.'*')THEN
1820      MATH=4
1821      GOTO 181
1822      END IF
1823      C
1824      C LLLLLLLLLLLLLLLLLLLLLLLLLLLLLLLLLLLLLLLLLLLLLLLLLLLLLLLLL
1825      C
1826      IF(B.EQ.'L')THEN
1827      MATH=5
1828      GOTO 186
1829      END IF
1830      C
1831      C PPPPPPPPPPPPPPPPPPPPPPPPPPPPPPPPPPPPPPPPPPPPPPPPPPPPPPPPPPPPP
1832      C
1833      IF(B.EQ.'P')THEN
1834      MATH=7
1835      GOTO 181
1836      END IF
1837      C
1838      C NNNNNNNNNNNNNNNNNNNNNNNNNNNNNNNNNNNNNNNNNNNNNNNNNNNNNNNNNNNNN
1839      C
1840      IF(B.EQ.'N')THEN
1841      MATH=6
1842      GOTO 186
1843      END IF
1844      GOTO 176
1845      C
1846      C ASK THE USER FOR THE SECOND VARIABLE NAME
1847      C
1848      181 WRITE(6,183)
1849      READ(5,503)NAM
1850      C
1851      C CHECK TO SEE IF A CONSTANT IS REQUIRED
1852      C
1853      IF(NAM.EQ.'/')THEN
1854      GOTO 184
1855      END IF
1856      C
1857      C CHECK THAT THE VARIABLE NAME EXISTS
1858      C
1859      DO 185 I=1,M1
1860      IF(NAM.EQ.NAME(I))THEN
1861      P=I
1862      GOTO 186
1863      END IF
1864      185 CONTINUE
1865      C
1866      C ERROR MESSAGE - VARIABLE NAME NOT FOUND
1867      C
1868      WRITE(6,90)
1869      GOTO 181
1870      C
1871      C
1872      C VARIABLE NAME 2 ACCEPTED
1873      C ASK THE USER FOR THE NAME OF THE RESULTS VARIABLE
1874      C
1875      186 WRITE(6,187)

```

```

1876      READ(5,503)NAM
1877      C
1878      C      CHECK THAT THE NAME EXISTS
1879      C
1880      DO 188 I=1,M1
1881      IF(NAM.EQ.NAME(I)) THEN
1882      R=I
1883      GOTO 189
1884      END IF
1885      188 CONTINUE
1886      C
1887      C      ERROR MESSAGE - VARIABLE NAME 3 NOT FOUND
1888      C
1889      WRITE(6,90)
1890      GOTO 186
1891      C
1892      C *****
1893      C ***** CONSTANTS *****
1894      C *****
1895      C
1896      C      CON1
1897      C
1898      178 WRITE(6,191)
1899      READ(5,*)CON1
1900      Q=0
1901      C
1902      C      ASK FOR THE MATHS FUNCTION
1903      C
1904      GOTO 176
1905      C
1906      C
1907      C      CON2
1908      C
1909      184 WRITE(6,192)
1910      READ(5,*)CON2
1911      P=0
1912      C
1913      C      ASK FOR RESULTS VARIABLE NAME
1914      C
1915      GOTO 186
1916      C
1917      C
1918      C
1919      C *****
1920      C ***** SELECT MATHS FUNCTIONS *****
1921      C *****
1922      C
1923      C      BY THIS STAGE ALL THE VARIABLE / CONSTANTS AND FUNCTIONS
1924      C      SWITCHES SHOULD BE SELECTED AT THE CORRECT VALUES.
1925      C      FOR THE PROGRAM TO DECIDE WHICH OPTION TO TAKE, A STUDY
1926      C      OF THE RESPECTIVE VALUES OF P AND Q ARE REQUIRED.
1927      C      IF EITHER OR BOTH OF THESE VALUES ARE = 0 (IE A CONSTANT
1928      C      HAS BEEN INPUT THROUGH THE TERMINAL) THEN THE APPROPRIATE
1929      C      ACTION IS TAKEN.
1930      C      NB. IF Q=0 THEN CONSTANT SELECTED AT POSITION 1
1931      C      IF P=0 THEN CONSTANT SELECTED AT POSITION 2
1932      C      THE PROGRAM WILL AUTOMATICALLY REJECT ANY EXPRESSION
1933      C      CONTAINING TWO CONSTANTS.
1934      C
1935      C
1936      189 IF(Q.NE.0)THEN
1937      IF(P.NE.0)THEN
1938      GOTO 213
1939      C
1940      C      MATHS FUNCTIONS 1 SELECTED.
1941      C
1942      END IF
1943      C
1944      C
1945      IF(P.EQ.0)THEN
1946      GOTO 214
1947      C
1948      C      MATHS STYLE 2 SELECTED
1949      C
1950      END IF

```

```

1951      END IF
1952      C
1953      C
1954      IF(Q.EQ.0)THEN
1955      IF(P.EQ.0)THEN
1956      GOTO 194
1957      C
1958      C      ERROR MESSAGE - TWO CONSTANTS
1959      C
1960      END IF
1961      GOTO 193
1962      C
1963      C      MATHS FUNCTION 3 SELECTED!
1964      C
1965      END IF
1966      C
1967      C
1968      C *****
1969      C ***** MATHS STYLE 1: VAR3 = VAR1 f VAR2 *****
1970      C *****
1971      C
1972      C
1973      213 DO 199 I=1,N1
1974      C
1975      IF(MATH.EQ.1)THEN
1976      DATA(R,I)=DATA(Q,I)+DATA(P,I)
1977      GOTO 199
1978      END IF
1979      C
1980      IF(MATH.EQ.2)THEN
1981      DATA(R,I)=DATA(Q,I)-DATA(P,I)
1982      GOTO 199
1983      END IF
1984      C
1985      IF(MATH.EQ.3)THEN
1986      C
1987      C      CHECK FOR ZERO
1988      C
1989      IF(DATA(P,I).EQ.0.0)THEN
1990      DATA(R,I)=0.0
1991      C      OUTPUT ERROR MESSAGE : DIVISION BY ZERO ENCOUNTERED !!
1992      WRITE(6,264)
1993      GOTO 199
1994      END IF
1995
1996      DATA(R,I)=DATA(Q,I)/DATA(P,I)
1997
1998      GOTO 199
1999      END IF
2000      C
2001      C
2002      C
2003      IF(MATH.EQ.4)THEN
2004      DATA(R,I)=DATA(Q,I)*DATA(P,I)
2005      GOTO 199
2006      END IF
2007      C
2008      IF(MATH.EQ.5)THEN
2009
2010      IF(DATA(Q,I).EQ.0.00)THEN
2011      DATA(R,I)=0.00
2012      GOTO 199
2013      END IF
2014
2015      DATA(R,I)=ALOG10(DATA(Q,I))
2016      GOTO 199
2017      END IF
2018      C
2019      IF(MATH.EQ.6)THEN
2020      GOTO 299
2021      END IF
2022      C
2023      IF(MATH.EQ.7)THEN
2024      DATA(R,I)=DATA(Q,I)**DATA(P,I)
2025      GOTO 199

```

```

2026         END IF
2027     C
2028     199 CONTINUE
2029     C
2030     C     INFORM USER - TRANSFORM COMPLETE
2031     C
2032         WRITE(6,198)
2033         GOTO 83
2034     C
2035     C ***** NO FUNCTION *****
2036     C
2037     299 IF(MATH.EQ.6)THEN
2038         DO 196 I=1,N1
2039         DATA(R,I)=DATA(Q,I)
2040     196 CONTINUE
2041         END IF
2042         GOTO 83
2043     C
2044     C
2045     C *****
2046     C ***** MATHS STYLE 2 : VAR1 f CON2 =VAR3 *****
2047     C *****
2048     C
2049     C
2050     214 DO 195 I=1,N1
2051         IF(MATH.EQ.1)THEN
2052             DATA(R,I)=DATA(Q,I)+CON2
2053             GOTO 195
2054             END IF
2055     C
2056         IF(MATH.EQ.2)THEN
2057             DATA(R,I)=DATA(Q,I)-CON2
2058             GOTO 195
2059             END IF
2060     C
2061         IF(MATH.EQ.3)THEN
2062     C
2063     C     CHECK FOR ZERO
2064     C
2065         IF(CON2.EQ.0.0)THEN
2066             DATA(R,I)=999999.9999
2067     C
2068     C     OUTPUT ERROR MESSAGE : DIVISION BY ZERO ENCOUNTERED !!
2069     C
2070         WRITE(6,264)
2071         GOTO 195
2072         END IF
2073     C
2074     C
2075         DATA(R,I)=DATA(Q,I)/CON2 .
2076         GOTO 195
2077         END IF
2078     C
2079         IF(MATH.EQ.4)THEN
2080             DATA(R,I)=DATA(Q,I)*CON2
2081             GOTO 195
2082             END IF
2083     C
2084         IF(MATH.EQ.7)THEN
2085             DATA(R,I)=DATA(Q,I)**CON2
2086             GOTO 195
2087             END IF
2088     C
2089     195 CONTINUE
2090     C
2091     C     ERROR MESSAGE - TWO CONSTANTS
2092     C
2093     194 WRITE(6,215)
2094         GOTO 83
2095     C
2096     C
2097     C *****
2098     C ***** MATHS STYLE 3: CON1 f VAR2 = VAR3 *****
2099     C *****
2100     C

```



```

2101 C
2102 193 DO 153 I=1,N1
2103 C
2104 IF(MATH.EQ.1)THEN
2105 DATA(R,I)=CON1+DATA(P,I)
2106 GOTO 153
2107 END IF
2108 C
2109 IF(MATH.EQ.2)THEN
2110 DATA(R,I)=CON1-DATA(P,I)
2111 GOTO 153
2112 END IF
2113 C
2114 IF(MATH.EQ.3)THEN
2115 C
2116 C CHECK FOR ZERO
2117 C
2118 IF(DATA(P,I).EQ.0.0)THEN
2119 DATA(R,I)=999999.9999
2120 C
2121 C OUTPUT ERROR MESSAGE : DIVISION BY ZERO ENCOUNTERED !!
2122 C
2123 WRITE(6,264)
2124 GOTO 153
2125 END IF
2126 C
2127 DATA(R,I)=CON1/DATA(P,I)
2128 GOTO 153
2129 END IF
2130 C
2131 IF(MATH.EQ.4)THEN
2132 DATA(R,I)=CON1*DATA(P,I)
2133 GOTO 153
2134 END IF
2135 C
2136 IF(MATH.EQ.5)THEN
2137 DATA(R,I)=ALOG10(CON1)
2138 GOTO 153
2139 END IF
2140 C
2141 IF(MATH.EQ.7)THEN
2142 DATA(R,I)=CON1**DATA(P,I)
2143 GOTO 153
2144 END IF
2145 C
2146 IF(MATH.EQ.6)THEN
2147 DATA(R,I)=CON1
2148 GOTO 153
2149 END IF
2150 C
2151 C
2152 153 CONTINUE
2153 C
2154 C INFORM USER - TRANSFORM COMPLETE
2155 C
2156 WRITE(6,198)
2157 GOTO 83
2158 C
2159 C
2160 C ++++++
2161 C ++++++ END OF TRANSFORM ++++++
2162 C ++++++
2163 C
2164 C
2165 C *****
2166 C ***** MOVE *****
2167 C *****
2168 C
2169 C INFORM USER OF OPTIONS
2170 C
2171 C
2172 82 WRITE(6,142)
2173 READ(5,500)B
2174 J=0
2175 C

```

```

2176 C CHECK OPTION
2177 C
2178 IF(B.EQ.'/')THEN
2179 GOTO 8
2180 END IF
2181 C
2182 IF(B.NE.'C')THEN
2183 GOTO 82
2184 END IF
2185 C
2186 C OUTPUT LIST OF VARIABLES THEN ASK USER TO
2187 C SELECT ONE
2188 C
2189 C
2190 C LIST VARIABLES
2191 C
2192 249 L=0
2193 P=M1
2194 211 IF(P.GE.3)THEN
2195 L=L+1
2196 P=P-2
2197 GOTO 211
2198 END IF
2199 C
2200 C NO OF REMAINING SAMPLES FORMING LESS THAN ONE COMPLETE
2201 C ROW (P).
2202 C
2203 C OUTPUT VARIABLE NAMES FOR THIS FILE
2204 C
2205 Y=0
2206 WRITE(6,340)
2207 IF(M1.LT.3)THEN
2208 GOTO 801
2209 END IF
2210 DO 245 I=1,L
2211 X=Y+1
2212 Y=Y+2
2213 WRITE(6,6)((J,NAME(J)),J=X,Y)
2214 245 CONTINUE
2215 IF(P.EQ.0)THEN
2216 GOTO 242
2217 END IF
2218 801 Y=M1-P+1
2219 WRITE(6,6)((J,NAME(J)),J=Y,M1)
2220 GOTO 242
2221 C
2222 242 WRITE(6,155)
2223 READ(5,503)NAM
2224 C
2225 C CHECK IF EXIT REQUIRED
2226 C
2227 IF(NAM.EQ.'/')THEN
2228 GOTO 82
2229 END IF
2230 C
2231 C CHECK THAT NAME EXISTS AND FIND ITS LOCATION (Q)
2232 C
2233 DO 248 I=1,M1
2234 IF(NAM.EQ.NAME(I))THEN
2235 Q=I
2236 GOTO 247
2237 END IF
2238 248 CONTINUE
2239 C
2240 C ERROR MESSAGE NAME NOT DETECTED
2241 C
2242 WRITE(6,90)
2243 GOTO 242
2244 C
2245 247 WRITE(6,156)M1
2246 READ(5,*)M2
2247 C
2248 C FIND OUT IF M2 IS < > or = Q
2249 C
2250 IF(Q.EQ.M2)THEN

```

```

2251      WRITE(6,157)
2252      GOTO 82
2253      END IF
2254      IF(Q.GE.M2)THEN
2255      GOTO 158
2256      END IF
2257      C
2258      C      SHUFFLE DATA DOWN
2259      C      NEW LOCATION HIGHER THAN PRESENT LOCATION IN ARRAY
2260      C
2261      X=3
2262      C
2263      168 DO 159 I=1,N1
2264      P=Q+1
2265      DAT=DATA(Q,I)
2266      DO 160 J=P,M2
2267      R=J-1
2268      DATA(R,I)=DATA(J,I)
2269      160 CONTINUE
2270      DATA(M2,I)=DAT
2271      159 CONTINUE
2272      C
2273      C      ALSO REARRANGE VARIABLE NAMES
2274      C
2275      P=Q+1
2276      NAM=NAME(Q)
2277      DO 162 I=P,M2
2278      R=I-1
2279      NAME(R)=NAME(I)
2280      162 CONTINUE
2281      NAME(M2)=NAM
2282      C
2283      C
2284      IF(X.GT.2)THEN
2285      C
2286      C      INFORM THE USER THAT MOVE COMPLETED
2287      C
2288      WRITE(6,161)
2289      GOTO 82
2290      END IF
2291      C
2292      C      MESSAGE TO SAY DELETE CARRIED OUT SUCCESSFULLY
2293      C
2294      WRITE(6,167)
2295      M1=M1-1
2296      GOTO 84
2297      C
2298      C      RETURN TO MAIN PROGRAM
2299      C
2300      C
2301      C
2302      C      SHUFFLE UP
2303      C      NEW LOCATION LOCATED AT A POSITION LOWER THAN THE
2304      C      PRESENT LOCATION Q IN THE ARRAY.
2305      C
2306      158 DO 163 I=1,N1
2307      P=Q-1
2308      DAT=DATA(Q,I)
2309      DO 165 J=P,M2,-1
2310      R=J+1
2311      DATA(R,I)=DATA(J,I)
2312      165 CONTINUE
2313      DATA(M2,I)=DAT
2314      163 CONTINUE
2315      C
2316      C
2317      C      ALSO SHUFFLE VARIABLE NAMES
2318      C
2319      P=Q-1
2320      NAM=NAME(Q)
2321      DO 164 I=P,M2,-1
2322      R=I+1
2323      NAME(R)=NAME(I)
2324      164 CONTINUE
2325      C

```

```

2326 C
2327 NAME(M2)=NAM
2328 C
2329 C INFORM USER MOVE COMPLETE
2330 C
2331 WRITE(6,161)
2332 GOTO 82
2333 C
2334 C
2335 C ++++++
2336 C ++++++ END OF MOVE ++++++
2337 C ++++++
2338 C
2339 C
2340 C
2341 C *****
2342 C ***** DELETE *****
2343 C *****
2344 C
2345 C INFORM USER OF OPTIONS
2346 C
2347 84 WRITE(6,201)
2348 READ(5,500)B
2349 C
2350 C CHECK OPTIONS
2351 C
2352 IF(B.EQ.'/')THEN
2353 GOTO 8
2354 END IF
2355 C
2356 C OUTPUT LIST OF VARIABLES THEN ASK USER TO
2357 C SELECT ONE
2358 C
2359 C
2360 C LIST VARIABLES
2361 C
2362 802 L=0
2363 P=M1
2364 803 IF(P.GE.3)THEN
2365 L=L+1
2366 P=P-2
2367 GOTO 803
2368 END IF
2369 C
2370 C NO OF REMAINING SAMPLES FORMING LESS THAN ONE COMPLETE
2371 C ROW (P).
2372 C
2373 C OUTPUT VARIABLE NAMES FOR THIS FILE
2374 C
2375 Y=0
2376 IF(M1.LT.3)THEN
2377 GOTO 804
2378 END IF
2379 DO 805 I=1,L
2380 X=Y+1
2381 Y=Y+2
2382 WRITE(6,6)((J,NAME(J)),J=X,Y)
2383 805 CONTINUE
2384 IF(P.EQ.0)THEN
2385 GOTO 253
2386 END IF
2387 804 Y=M1-P+1
2388 WRITE(6,6)((J,NAME(J)),J=Y,M1)
2389 GOTO 253
2390 C
2391 C A DELETE FUNCTION IS CARRIED OUT ON A VARIABLE
2392 C BY 1) MOVING THE VARIABLE TO THE END OF FILE
2393 C 2) DECREASE THE VARIABLE NAME COUNTER BY 1
2394 C
2395 C ASK THE USER FOR THE VARIABLE NAME TO BE DELETED
2396 C
2397 253 WRITE(6,166)
2398 READ(5,503)NAM
2399 C
2400 C CHECK THAT NAM EXISTS AND POSITION IS NOT = M1

```

```

2401 C
2402     IF(NAM.EQ.'XXXX')THEN
2403     GOTO 84
2404     END IF
2405 C
2406     DO 251 I=1,M1
2407     IF(NAM.EQ.NAME(I))THEN
2408     Q=I
2409     GOTO 252
2410     END IF
2411 251 CONTINUE
2412 C
2413 C     ERROR MESSAGE NAME NOT DETECTED
2414 C
2415     WRITE(6,90)
2416     GOTO 253
2417 C
2418 252 IF(Q.EQ.M1)THEN
2419     M1=M1-1
2420     WRITE(6,167)
2421     GOTO 8
2422     END IF
2423     M2=M1
2424     X=1
2425     GOTO 168
2426 C
2427 C ++++++
2428 C ++++++ END OF DELETE ++++++
2429 C ++++++
2430 C
2431 C
2432 C ++++++
2433 C ++++++ END OF EDIT ++++++
2434 C ++++++
2435 C
2436 C
2437 C
2438 C
2439 C *****
2440 C ***** REFORMAT/OUTPUT *****
2441 C *****
2442 C
2443 C
2444 C
2445 C     OUTPUT TITLE PAGE FOR REFORMAT
2446 C
2447 125 WRITE(6,141)
2448     READ(5,422)B
2449     IF(B.EQ.'/')THEN
2450     GOTO 997
2451     END IF
2452     IF(B.NE.'C')THEN
2453     GOTO 125
2454     END IF
2455 C
2456 C     INFORM USER OF THE TWO DIFFERENT STYLES OF OUTPUT
2457 C     AND SELECT THE OPTION REQUIRED.
2458 C
2459 271 WRITE(6,270)
2460     READ(5,422)B
2461     IF(B.EQ.'1')THEN
2462     GOTO 494
2463     END IF
2464     IF(B.EQ.'2')THEN
2465     GOTO 273
2466     END IF
2467     IF(B.EQ.'/')THEN
2468     GOTO 125
2469     END IF
2470     GOTO 271
2471 C
2472 C *****
2473 C ***** REFORMAT: STYLE 1 *****
2474 C *****
2475 C

```

```

2476      494  WRITE(6,405)
2477      READ(5,501)OUT
2478      IF(OUT.EQ.' ')THEN
2479      GOTO 494
2480      END IF
2481      C
2482      C      OPEN INPUT CHANNEL
2483      C
2484      OPEN(1,FILE=OUT,DEFAULT FILE='.RAW',STATUS='OLD')
2485      C
2486      C
2487      C      READ FILE HEADER AND DATA
2488      C
2489      READ(1,108)TITLE
2490      READ(1,109)FORM
2491      READ(1,110)M1,N1
2492      READ(1,111)(NAME(I),I=1,M1)
2493
2494      DO 441 I=1,N1
2495      READ(1,484)SAMPLE(I),KEY(I)
2496      READ(1,113)(DATA(J,I),J=1,M1)
2497      441  CONTINUE
2498      C
2499      C      ASK USER FOR OUTPUT .TAB FILENAME
2500      C
2501      440  WRITE(6,442)
2502      READ(5,443)BIN
2503      C
2504      C      OPEN OUTPUT CHANNEL
2505      C
2506      C      TABLES OF REFORMATTED DATA ARE OUTPUT
2507      C      AUTOMATICALLY TO A .TAB FILE BY DEFAULT
2508      C
2509      C
2510      OPEN(2,FILE=BIN,DEFAULT FILE='.TAB',STATUS='NEW')
2511      C
2512      C      LIST THE CONTENTS OF THE INPUT .RAW FILE TO BE ALTERED
2513      C
2514      WRITE(6,406)OUT
2515      WRITE(6,407)M1
2516      WRITE(6,408)N1
2517      WRITE(6,409)(NAME(I),I=1,M1)
2518      WRITE(6,417)TITLE
2519      C
2520      C      ASK USER IF A TITLE CHANGE IS REQUIRED
2521      C
2522      496  WRITE(6,418)
2523      READ(5,419)B
2524      IF(B.EQ.'Y')THEN
2525      WRITE(6,470)
2526      READ(5,419)TITLE
2527      END IF
2528      IF(B.NE.'N')THEN
2529      GOTO 496
2530      END IF
2531      C
2532      C      ASK USER IF THE TITLE IS REQUIRED ON EACH PART
2533      C      OF OUTPUT
2534      C
2535      497  WRITE(6,421)
2536      READ(5,422)B
2537      IF(B.EQ.'Y')THEN
2538      GOTO 498
2539      END IF
2540      IF(B.NE.'N')THEN
2541      GOTO 497
2542      END IF
2543      C
2544      C      ASK THE USER IF AN INCREMENTAL PART NUMBER
2545      C      IS REQUIRED ON EACH PAGE OF OUTPUT
2546      C
2547      498  WRITE(6,424)
2548      READ(5,425)C
2549      IF(C.EQ.'Y')THEN
2550

```



```

2551 C      ASK THE USER FOR THE FIRST PAGE NUMBER
2552 C
2553      WRITE(6,426)
2554      READ(5,*)D
2555      GOTO 239
2556      END IF
2557 C
2558      IF(C.EQ.'N')THEN
2559      GOTO 239
2560      END IF
2561 C
2562      GOTO 498
2563 C
2564 C      ASK THE USER HOW MANY SAMPLES (E) PER PAGE (1-10)
2565 C
2566 239 WRITE(6,455)
2567      READ(5,*)E
2568 C
2569 C      IF B = Y THEN TITLE PRINTED
2570 C      IF C = Y THEN TITLE AND PART NO PRINTED
2571 C          NB. THE PART NO IS INITIALISED TO D
2572 C
2573 C      NOW FIND OUT HOW MANY COMPLETE BLOCKS (L) OF
2574 C      DATA (IE 6 RECORDS IN LENGTH) ARE REQUIRED.
2575 C
2576      L=0
2577      Q=N1
2578 410 IF(Q.GE.E)THEN
2579      L=L+1
2580      Q=Q-E
2581      GOTO 410
2582      END IF
2583      P=Q
2584 C
2585 C      P IS THE NO OF SAMPLES FORMING AN INCOMPLETE
2586 C      LAST BLOCK OF DATA
2587 C
2588 C
2589 C      ASK THE USER IF HE REQUIRES AN AMMENDMENT TO THE
2590 C      PRESET OUTPUT FORMAT OF F10.2.
2591 C
2592 319 WRITE(6,13)
2593      READ(5,422)F
2594      IF(F.EQ.'N')THEN
2595      GOTO 14
2596      END IF
2597 C
2598      IF(F.EQ.'Y')THEN
2599      DO 17 I=1,M1
2600 C
2601 C      ASK USER FOR THE NUMBER OF DECIMAL PLACES REQUIRED
2602 C
2603 320 WRITE(6,2015)NAME(I)
2604      READ(5,16)DEC(I)
2605 C
2606 C      CHECK THAT THIS NO. DOES NOT EXCEED 4
2607 C
2608      IF(DEC(I).GE.5)THEN
2609      GOTO 320
2610      END IF
2611 C
2612 17 CONTINUE
2613 C
2614      GOTO 18
2615      END IF
2616      GOTO 319
2617 C
2618 C
2619 C *****
2620 C ***** SET UP REFORMATTED OUTPUT FILES : STYLE 1 *****
2621 C *****
2622 C ***** F 10.2 STANDARD FORMAT *****
2623 C *****
2624 C
2625 14 X=0

```

```

2626 C
2627 C RIGHT JUSTIFY ALL SAMPLE NAMES
2628 C FORM AND FORM1 ARE CHARACTER BUFFERS
2629 C NB ARRAY KEY IS UNAFFECTED
2630 C
2631 DO 4 R=1,N1
2632 FORMX=SAMPLE(R)
2633 DO 3 I1=10,1,-1
2634 IF(FORMX(I1:11).NE.' ')THEN
2635 GOTO 2
2636 END IF
2637 3 CONTINUE
2638 I1=1
2639 2 FORM1=' '
2640 J=10-I1+1
2641 FORM1(J:10)=FORMX(1:I1)
2642 SAMP1(R)=FORM1
2643 4 CONTINUE
2644
2645 Y=0
2646 IF(L.EQ.0)THEN
2647 GOTO 412
2648 END IF
2649 C
2650 DO 411 I=1,L
2651 C
2652 C L IS THE NUMBER OF COMPLETE BLOCKS
2653 C
2654 X=E*(I-1)+1
2655 Y=E*(I-1)+E
2656 C
2657 C
2658 IF(B.EQ.'Y') THEN
2659 IF(C.EQ.'Y') THEN
2660 WRITE(2,416)TITLE,D
2661 GOTO 445
2662 END IF
2663 WRITE(2,427)TITLE
2664 END IF
2665 C
2666 C INCREMENT D
2667 C
2668 445 D=D+1
2669 C
2670 C PRINT OUT ONE COMPLETE BLOCK OF DATA
2671 C
2672 C HEADING
2673 C
2674 WRITE(2,413)(SAMPLE(K),K=X,Y)
2675 C
2676 C DATA
2677 C
2678 DO 414 J=1,M1
2679 WRITE(2,415)(NAME(J),(DATA(J,K),K=X,Y))
2680 414 CONTINUE
2681
2682 WRITE(2,1000)
2683
2684 C
2685 C WRITE NEXT BLOCK OF DATA
2686 C
2687 411 CONTINUE
2688 C
2689 C
2690 C
2691 C ARE THERE ANY INCOMPLETE DATA BLOCKS TO BE OUTPUT
2692 C CHECK
2693 C
2694 412 IF(P.EQ.0)THEN
2695 GOTO 453
2696 END IF
2697 C
2698 C PRINT REMAINING INCOMPLETE BLOCK
2699 C
2700 X=Y+1

```

```

2701      Y=Y+P
2702      C
2703      IF(B.EQ.'Y') THEN
2704      IF(C.EQ.'Y') THEN
2705      WRITE(2,416) TITLE,D
2706      GOTO 452
2707      END IF
2708      WRITE(2,427)TITLE
2709      END IF
2710      C
2711      C      HEADING
2712      C
2713      452 WRITE(2,1413)(SAMPLE(K),K=X,Y)
2714      C
2715      C      DATA
2716      C
2717      DO 464 J=1,M1
2718      WRITE(2,415)NAME(J),(DATA(J,K),K=X,Y)
2719      464 CONTINUE
2720
2721      WRITE(2,1000)
2722      C
2723      C      INFORM USER THAT REFORMAT COMPLETE
2724      C
2725      453 WRITE(6,454)
2726      GOTO 998
2727      C
2728      C ++++++
2729      C ++++++ END OF STANDARD FORMAT : STYLE 1 ++++++
2730      C ++++++
2731      C
2732      C
2733      C *****
2734      C ***** SET UP USER FORMATTED OUTPUT FILES : STYLE 1 *****
2735      C *****
2736      C
2737      18 X=0
2738      C
2739      C      RIGHT JUSTIFY ALL SAMPLE NAMES
2740      C      FORM AND FORM1 ARE CHARACTER BUFFERS
2741      C      NB ARRAY KEY IS UNAFFECTED
2742      C
2743      DO 301 R=1,N1
2744      FORMX=SAMPLE(R)
2745      DO 302 I1=10,1,-1
2746      IF(FORMX(I1:11).NE.' ')THEN
2747      GOTO 303
2748      END IF
2749      302 CONTINUE
2750      I1=1
2751      303 FORM1=' '
2752      J=10-I1+1
2753      FORM1(J:10)=FORMX(1:I1)
2754      SAMPLE(R)=FORM1
2755      301 CONTINUE
2756
2757      Y=0
2758      IF(L.EQ.0)THEN
2759      GOTO 304
2760      END IF
2761      C
2762      DO 305 I=1,L
2763      C
2764      C      L IS THE NUMBER OF COMPLETE BLOCKS
2765      C
2766      X=E*(I-1)+1
2767      Y=E*(I-1)+E
2768      C
2769      C
2770      IF(B.EQ.'Y') THEN
2771      IF(C.EQ.'Y') THEN
2772      WRITE(2,416)TITLE,D
2773      GOTO 306
2774      END IF
2775      WRITE(2,427)TITLE

```

```

2776      END IF
2777      C
2778      C      INCREMENT D
2779      C
2780      306 D=D+1
2781      C
2782      C      PRINT OUT ONE COMPLETE BLOCK OF DATA
2783      C
2784      C      HEADING
2785      C
2786      C      WRITE(2,413)(SAMPLE(K),K=X,Y)
2787      C
2788      C      DATA
2789      C
2790      C      DO 307 J=1,M1
2791      C
2792      C      IF(DEC(J).EQ.1)THEN
2793      C      WRITE(2,310)(NAME(J),(DATA(J,K),K=X,Y))
2794      C      END IF
2795      C
2796      C      IF(DEC(J).EQ.2)THEN
2797      C      WRITE(2,415)(NAME(J),(DATA(J,K),K=X,Y))
2798      C      END IF
2799      C
2800      C      IF(DEC(J).EQ.3)THEN
2801      C      WRITE(2,311)(NAME(J),(DATA(J,K),K=X,Y))
2802      C      END IF
2803      C
2804      C      IF(DEC(J).EQ.4)THEN
2805      C      WRITE(2,312)(NAME(J),(DATA(J,K),K=X,Y))
2806      C      END IF
2807      C
2808      C
2809      C      IF(DEC(J).EQ.0)THEN
2810      C      DO 322 K=X,Y
2811      C      IDATA(J,K)=INT(DATA(J,K))
2812      C      322 CONTINUE
2813      C      WRITE(2,313)(NAME(J),(IDATA(J,K),K=X,Y))
2814      C      END IF
2815      C
2816      C      307 CONTINUE
2817      C
2818      C      WRITE(2,1000)
2819      C
2820      C      WRITE NEXT BLOCK OF DATA
2821      C
2822      C      305 CONTINUE
2823      C
2824      C      ARE THERE ANY INCOMPLETE DATA BLOCKS TO BE OUTPUT
2825      C      CHECK
2826      C
2827      C      304 IF(P.EQ.0)THEN
2828      C      GOTO 314
2829      C      END IF
2830      C
2831      C      PRINT REMAINING INCOMPLETE BLOCK
2832      C
2833      C      X=Y+1
2834      C      Y=Y+P
2835      C
2836      C      IF(B.EQ.'Y') THEN
2837      C      IF(C.EQ.'Y') THEN
2838      C      WRITE(2,416) TITLE,D
2839      C      GOTO 308
2840      C      END IF
2841      C      WRITE(2,427)TITLE
2842      C      END IF
2843      C
2844      C      HEADING
2845      C
2846      C      308 WRITE(2,1413)(SAMPLE(K),K=X,Y)
2847      C
2848      C      DATA
2849      C
2850      C      DO 309 J=1,M1

```

```

2851 C
2852 C
2853 IF(DEC(J).EQ.1)THEN
2854 WRITE(2,310)(NAME(J),(DATA(J,K),K=X,Y))
2855 END IF
2856 C
2857 IF(DEC(J).EQ.2)THEN
2858 WRITE(2,415)(NAME(J),(DATA(J,K),K=X,Y))
2859 END IF
2860 C
2861 IF(DEC(J).EQ.3)THEN
2862 WRITE(2,311)(NAME(J),(DATA(J,K),K=X,Y))
2863 END IF
2864 C
2865 IF(DEC(J).EQ.4)THEN
2866 WRITE(2,312)(NAME(J),(DATA(J,K),K=X,Y))
2867 END IF
2868 C
2869 IF(DEC(J).EQ.0)THEN
2870 DO 321 K=X,Y
2871 IDATA(J,K)=INT(DATA(J,K))
2872 321 CONTINUE
2873 WRITE(2,313)(NAME(J),(IDATA(J,K),K=X,Y))
2874 END IF
2875 C
2876 309 CONTINUE
2877 C
2878 WRITE(2,1000)
2879 C
2880 C INFORM USER THAT REFORMAT COMPLETE
2881 C
2882 314 WRITE(6,454)
2883 GOTO 998
2884 C
2885 C ++++++
2886 C ++++++ END OF USER REFORMAT: STYLE 1 ++++++
2887 C ++++++
2888 C
2889 C
2890 C *****
2891 C ***** REFORMAT: STYLE 2 *****
2892 C *****
2893 C
2894 273 WRITE(6,405)
2895 READ(5,501)OUT
2896 IF(OUT.EQ.' ')THEN
2897 GOTO 494
2898 END IF
2899 C
2900 C OPEN INPUT CHANNEL
2901 C
2902 C OPEN(1,FILE=OUT,DEFAULT FILE='.RAW',STATUS='OLD')
2903 C
2904 C
2905 C READ FILE HEADER AND DATA
2906 C
2907 READ(1,108)TITLE
2908 READ(1,109)FORM
2909 READ(1,110)M1,N1
2910 C
2911 READ(1,111)(NAME(I),I=1,M1)
2912 C
2913 DO 275 I=1,N1
2914 READ(1,484)SAMPLE(I),KEY(I)
2915 READ(1,113)(DATA(J,I),J=1,M1)
2916 275 CONTINUE
2917 C
2918 C ASK USER FOR OUTPUT .TAB FILENAME
2919 C
2920 274 WRITE(6,442)
2921 READ(5,443)BIN
2922 C
2923 C OPEN OUTPUT CHANNEL
2924 C
2925 C TABLES OF REFORMATTED DATA ARE OUTPUT

```

```

2926 C      AUTOMATICALLY TO A .TAB FILE BY DEFAULT
2927 C
2928      OPEN(2,FILE=BIN,DEFAULT FILE='.TAB',STATUS='NEW')
2929 C
2930 C      LIST THE CONTENTS OF THE INPUT .RAW FILE TO BE ALTERED
2931 C
2932      WRITE(6,406)OUT
2933      WRITE(6,407)M1
2934      WRITE(6,408)N1
2935      WRITE(6,409)(NAME(I),I=1,M1)
2936      WRITE(6,417)TITLE
2937
2938      IF(M1.GT.10)THEN
2939      WRITE(6,1417)
2940      GOTO 496
2941      END IF
2942 C
2943 C      ASK USER IF A TITLE CHANGE IS REQUIRED
2944 C
2945      276 WRITE(6,418)
2946      READ(5,419)B
2947      IF(B.EQ.'Y')THEN
2948      WRITE(6,470)
2949      READ(5,419)TITLE
2950      END IF
2951      IF(B.NE.'N')THEN
2952      GOTO 276
2953      END IF
2954 C
2955 C      ASK USER IF THE TITLE IS REQUIRED ON EACH PART
2956 C      OF OUTPUT
2957 C
2958      277 WRITE(6,421)
2959      READ(5,422)B
2960      IF(B.EQ.'Y')THEN
2961      GOTO 278
2962      END IF
2963      IF(B.NE.'N')THEN
2964      GOTO 277
2965      END IF
2966 C
2967 C      ASK THE USER IF AN INCREMENTAL PART NUMBER
2968 C      IS REQUIRED ON EACH PAGE OF OUTPUT
2969 C
2970      278 WRITE(6,424)
2971      READ(5,425)C
2972      IF(C.EQ.'Y')THEN
2973      C
2974      C      ASK THE USER FOR THE FIRST PAGE NUMBER
2975      C
2976      WRITE(6,426)
2977      READ(5,*)D
2978      GOTO 240
2979      END IF
2980 C
2981      IF(C.EQ.'N')THEN
2982      GOTO 240
2983      END IF
2984      GOTO 278
2985 C
2986 C      ASK THE USER HOW MANY SAMPLE RECORDS PER PAGE (1-50)?.
2987 C
2988      240 WRITE(6,522)
2989      READ(5,*)F
2990 C
2991 C      THE OUTPUT FROM THIS REFORMAT ROUTINE CONSISTS OF A
2992 C      SUCCESSION OF DATA BLOCKS.
2993 C      A SINGLE COMPLETE BLOCK CONTAINS AN ARRAY OF
2994 C      ('M1' VARIABLES x 'F' SAMPLES).
2995 C      EACH BLOCK IS SEPERATED FROM THE NEXT BY A FORM FEED,
2996 C      THUS THE OUTPUT FORMAT IS 1 BLOCK PER PAGE.
2997 C
2998 C      THE NUMBER OF COMPLETE BLOCKS OF THIS TYPE, IS DEPENDANT
2999 C      UPON THE NUMBER OF SAMPLES REQUIRED PER PAGE (F) AND THE
3000 C      TOTAL NUMBER OF SAMPLES/ROWS (N1), AS INPUT BY THE USER.

```



```

3001 C
3002 C
3003 C      SET UP OUTPUT PAGE
3004 C
3005 C      NB.
3006 C      IF B = Y THEN TITLE PRINTED
3007 C      IF C = Y THEN TITLE AND PART NO PRINTED
3008 C      THE PART NO IS INITIALISED TO D
3009 C
3010 C
3011 C      FIND OUT HOW MANY COMPLETE BLOCKS (L) OF DATA
3012 C      (IE. 'E' VARIABLES ACROSS AND 'F' SAMPLES DOWN, PER
3013 C      PAGE) ARE REQUIRED.
3014 C
3015 C      NB.
3016 C      DATA IN STYLE 2 IS OUTPUT IN M1 COLUMN BLOCKS (1-10).
3017 C
3018 C      L=0
3019 C      Q=N1
3020 C      279 IF(Q.GE.F)THEN
3021 C          L=L+1
3022 C          Q=Q-F
3023 C          GOTO 279
3024 C      END IF
3025 C      P=Q
3026 C
3027 C      L IS NO. OF COMPLETE BLOCKS OF DATA (M1 VARIABLES LONG)
3028 C      AND P IS NO. OF SAMPLES IN THE INCOMPLETE LAST BLOCK.
3029 C
3030 C      ASK THE USER IF HE REQUIRES AN AMMENDMENT TO THE
3031 C      PRESET OUTPUT FORMAT OF F10.2 ?.
3032 C
3033 C      280 WRITE(6,13)
3034 C          READ(5,422)G
3035 C          IF(G.EQ.'N')THEN
3036 C              GOTO 281
3037 C          END IF
3038 C
3039 C          IF(G.EQ.'Y')THEN
3040 C
3041 C      ASK USER FOR THE NUMBER OF DECIMAL PLACES REQUIRED
3042 C
3043 C      881 WRITE(6,15)
3044 C          READ(5,16)DECT
3045 C
3046 C      CHECK THAT THIS NO. DOES NOT EXCEED 4
3047 C
3048 C          IF(DECT.GE.5)THEN
3049 C              GOTO 881
3050 C          END IF
3051 C          GOTO 283
3052 C          END IF
3053 C          GOTO 280
3054 C
3055 C
3056 C *****
3057 C ***** SET UP REFORMATTED OUTPUT FILES : STYLE 2 *****
3058 C *****
3059 C ***** F 10.2 STANDARD FORMAT *****
3060 C *****
3061 C
3062 C      281 X=0
3063 C
3064 C
3065 C      RIGHT JUSTIFY ALL VARIABLE NAMES
3066 C      FORM AND FORM1 ARE CHARACTER BUFFERS
3067 C      NB ARRAY KEY IS UNAFFECTED
3068 C
3069 C      DO 284 R=1,M1
3070 C          FORMX=NAME(R)
3071 C          DO 285 I1=8,1,-1
3072 C              IF(FORMX(I1:11).NE.' ')THEN
3073 C                  GOTO 286
3074 C              END IF
3075 C      285 CONTINUE

```

```

3076      I1=1
3077      286 FORM1=' '
3078          J=8-I1+1
3079          FORM1(J:8)=FORMX(1:I1)
3080          NAME(R)=FORM1
3081      284 CONTINUE
3082      C
3083          Y=0
3084          IF(L.EQ.0)THEN
3085              GOTO 287
3086          END IF
3087      C
3088      C      SET UP A LOOP TO PRINT ALL COMPLETE BLOCKS, AND
3089      C      THEN PRINT THE LAST INCOMPLETE BLOCK, SHOULD THERE BE ONE.
3090      C
3091          DO 345 Z=1,L
3092      C
3093      C      *****
3094      C      FIRST PASS OUTPUT CONTROLLED BY J IN MULTIPLES OF F
3095      C      (IE. A SERIES OF PAGES EACH CONTAINING F SAMPLE RECORDS).
3096      C      *****
3097      C
3098          J1=F*(Z-1)+1
3099          J2=F*(Z-1)+F
3100      C
3101          IF(B.EQ.'Y') THEN
3102              IF(C.EQ.'Y') THEN
3103                  WRITE(2,416)TITLE,D
3104                  GOTO 289
3105              END IF
3106              WRITE(2,427)TITLE
3107              END IF
3108      C
3109      C      INCREMENT D
3110      C
3111          289 D=D+1
3112      C
3113      C
3114      C      PRINT OUT ONE COMPLETE BLOCK OF DATA
3115      C
3116      C      HEADING
3117      C
3118          WRITE(2,513)(NAME(K),K=1,M1)
3119          WRITE(2,465)
3120      C
3121      C      DATA
3122      C
3123          DO 291 J=J1,J2
3124              WRITE(2,515)(SAMPLE(J),(DATA(K,J),K=1,M1))
3125      C
3126          291 CONTINUE
3127      C
3128          WRITE(2,1000)
3129
3130          345 CONTINUE
3131      C
3132      C      ARE THERE ANY INCOMPLETE DATA BLOCKS TO BE OUTPUT
3133      C      CHECK
3134      C
3135          287 IF(P.EQ.0)THEN
3136              GOTO 346
3137          END IF
3138      C
3139      C      PRINT REMAINING INCOMPLETE BLOCK
3140      C
3141          IF(B.EQ.'Y') THEN
3142              IF(C.EQ.'Y') THEN
3143                  WRITE(2,416) TITLE,D
3144                  GOTO 293
3145              END IF
3146              WRITE(2,427)TITLE
3147              END IF
3148      C
3149      C      HEADING
3150      C

```

```

3151      293 WRITE(2,513)(NAME(K),K=1,M1)
3152      WRITE(2,465)
3153      C
3154      C      DATA
3155      C
3156      J1=N1-P+1
3157      J2=N1
3158
3159      DO 894 J=J1,J2
3160      WRITE(2,515)SAMPLE(J),(DATA(K,J),K=1,M1)
3161      894 CONTINUE
3162
3163      WRITE(2,1000)
3164      C
3165      C      INFORM USER THAT REFORMAT COMPLETE
3166      C
3167      346 WRITE(6,454)
3168      GOTO 998
3169      C
3170      C ++++++
3171      C ++++++ END OF STANDARD FORMAT : STYLE 2 ++++++
3172      C ++++++
3173      C
3174      C
3175      C *****
3176      C ***** SET UP USER FORMATTED OUTPUT FILES : STYLE 2 *****
3177      C *****
3178      C
3179      283 X=0
3180      C
3181      C      RIGHT JUSTIFY ALL VARIABLE NAMES
3182      C      FORM AND FORM1 ARE CHARACTER BUFFERS
3183      C      NB ARRAY KEY IS UNAFFECTED
3184      C
3185      DO 294 R=1,M1
3186      FORMX=NAME(R)
3187      DO 295 I1=8,1,-1
3188      IF(FORMX(I1:I1).NE.' ')THEN
3189      GOTO 296
3190      END IF
3191      295 CONTINUE
3192      I1=1
3193      296 FORM1=' '
3194      J=8-I1+1
3195      FORM1(J:8)=FORMX(1:I1)
3196      NAME(R)=FORM1
3197      294 CONTINUE
3198      C
3199      Y=0
3200      IF(L.EQ.0)THEN
3201      GOTO 324
3202      END IF
3203      C
3204      C *****
3205      C FIRST PASS OUTPUT CONTROLLED BY J IN MULTIPLES OF F.
3206      C IE. A SERIES OF PAGES EACH CONTAINING F SAMPLE RECORDS
3207      C *****
3208      C
3209      DO 347 Z=1,L
3210      C
3211      J1=F*(Z-1)+1
3212      J2=F*(Z-1)+F
3213      C
3214      C      L IS THE NUMBER OF COMPLETE BLOCKS
3215      C
3216      IF(B.EQ.'Y') THEN
3217      IF(C.EQ.'Y') THEN
3218
3219      WRITE(2,416)TITLE,D
3220      GOTO 326
3221      END IF
3222      WRITE(2,427)TITLE
3223      END IF
3224      C
3225      C      INCREMENT D

```

```

3226 C
3227 326 D=D+1
3228 C
3229 C PRINT OUT ONE COMPLETE BLOCK OF DATA
3230 C
3231 C HEADING
3232 C
3233 C WRITE(2,513)(NAME(K),K=1,M1)
3234 C
3235 C WRITE(2,465)
3236 C
3237 C DATA
3238 C
3239 C DO 327 J=J1,J2
3240 C
3241 C IF(DECT.EQ.1)THEN
3242 C WRITE(2,516)(SAMPLE(J),(DATA(K,J),K=1,M1))
3243 C END IF
3244 C
3245 C IF(DECT.EQ.2)THEN
3246 C WRITE(2,517)(SAMPLE(J),(DATA(K,J),K=1,M1))
3247 C END IF
3248 C
3249 C IF(DECT.EQ.3)THEN
3250 C WRITE(2,518)(SAMPLE(J),(DATA(K,J),K=1,M1))
3251 C END IF
3252 C
3253 C IF(DECT.EQ.4)THEN
3254 C WRITE(2,519)(SAMPLE(J),(DATA(K,J),K=1,M1))
3255 C END IF
3256 C
3257 C IF(DECT.EQ.0)THEN
3258 C
3259 C DO 328 K=1,M1
3260 C IDATA(K,J)=INT(DATA(K,J))
3261 328 CONTINUE
3262 C
3263 C WRITE(2,520)(SAMPLE(J),(IDATA(K,J),K=1,M1))
3264 C END IF
3265 C
3266 327 CONTINUE
3267 C
3268 C WRITE(2,1000)
3269 C
3270 C WRITE NEXT BLOCK OF DATA
3271 C
3272 347 CONTINUE
3273 C
3274 C ARE THERE ANY INCOMPLETE DATA BLOCKS TO BE OUTPUT
3275 C CHECK
3276 C
3277 324 IF(P.EQ.0)THEN
3278 C GOTO 329
3279 C END IF
3280 C
3281 C PRINT REMAINING INCOMPLETE BLOCK
3282 C
3283 C IF(B.EQ.'Y') THEN
3284 C IF(C.EQ.'Y') THEN
3285 C WRITE(2,416) TITLE,D
3286 C GOTO 330
3287 C END IF
3288 C WRITE(2,427)TITLE
3289 C END IF
3290 C
3291 C D=D+1
3292 C
3293 C HEADING
3294 C
3295 330 WRITE(2,513)(NAME(K),K=1,M1)
3296 C WRITE(2,465)
3297 C
3298 C DATA
3299 C J1=N1-P+1
3300 C J2=N1

```

```

3301 C
3302 DO 331 J=J1,J2
3303 C
3304 IF(DECT.EQ.1)THEN
3305 WRITE(2,516)(SAMPLE(J),(DATA(K,J),K=1,M1))
3306 END IF
3307 C
3308 IF(DECT.EQ.2)THEN
3309 WRITE(2,517)(SAMPLE(J),(DATA(K,J),K=1,M1))
3310 END IF
3311 C
3312 IF(DECT.EQ.3)THEN
3313 WRITE(2,518)(SAMPLE(J),(DATA(K,J),K=1,M1))
3314 END IF
3315 C
3316 IF(DECT.EQ.4)THEN
3317 WRITE(2,519)(SAMPLE(J),(DATA(K,J),K=1,M1))
3318 END IF
3319 C
3320 IF(DECT.EQ.0)THEN
3321
3322 DO 332 K=1,M1
3323 IDATA(K,J)=INT(DATA(K,J))
3324 332 CONTINUE
3325 WRITE(2,520)(SAMPLE(J),(IDATA(K,J),K=1,M1))
3326 END IF
3327 C
3328 331 CONTINUE
3329 C
3330 WRITE(2,1000)
3331 C
3332 C INFORM USER THAT REFORMAT COMPLETE
3333 C
3334 329 WRITE(6,454)
3335 GOTO 998
3336 C
3337 C ++++++
3338 C ++++++ END OF USER REFORMAT : STYLE 2 ++++++
3339 C ++++++
3340 C
3341 C ++++++
3342 C ++++++ END OF REFORMAT ++++++
3343 C ++++++
3344 C
3345 C
3346 C
3347 C *****
3348 C ***** ADDITIONAL OPTIONS *****
3349 C *****
3350 C
3351 C
3352 C INFORM USER OF AUTO EXIT - NO FILE TRANSFER
3353 C
3354 997 WRITE(6,210)
3355 GOTO 999
3356 C
3357 C INFORM THE USE THAT THE FILE HAS BEEN CREATED AND
3358 C TRANSFERED TO ITS .RAW FILE, THEN EXIT PROGRAM
3359 C
3360 998 WRITE(6,200)OUT,TITLE
3361 C
3362 CLOSE(1)
3363 CLOSE(2)
3364 C
3365 C
3366 C ++++++
3367 C ++++++ END OF ADDITIONAL OPTIONS ++++++
3368 C ++++++
3369 C
3370 C
3371 C
3372 C *****
3373 C INPUT/OUTPUT FORMATS AND DIALOGUE
3374 C *****
3375 C

```

```

3376 C
3377 6 FORMAT(1X,2(8X,I3,': ',A8))
3378 13 FORMAT(////////
3379 1/' Change output format of your data (Y/N).....> ', $)
3380 15 FORMAT(//
3381 1 ' The number of decimal places required.....> ', $)
3382 16 FORMAT(I1)
3383 19 FORMAT(//////////
3384 1/' ***** GENERATE *****'/
3385 2/' This program allows the user to GENERATE a new VARIABLE name,'
3386 3/' for each of the records within the .RAW datafile.'
3387 4/' The values contained within the variable are set to zero on'
3388 5/' CREATION and may be changed through the INSERT or TRANSFORM'
3389 6/' commands.'
3390 7//
3391 8/' Options available C - Continue with GENERATE '
3392 9/' / - EXIT'
3393 1///' Select your option.....> ', $)
3394 C
3395 22 FORMAT(///' New Variable Name..... > ', $)
3396 23 FORMAT(///' ***** Variable ',A10,'GENERATED *****'///)
3397 C
3398 26 FORMAT(///
3399 1 ' ***** CORRECTIONS COMPLETE *****'/
3400 1/' Options available S - Correct SAME sample.'
3401 2/' N - Correct NEW sample.'
3402 3/' / - EXIT'
3403 4///' Select option.....> ', $)
3404 27 FORMAT(///' The new value of item ',I3,' is.....> ', $)
3405 30 FORMAT(////' WARNING: Item No. selected out of range!!!'///)
3406 36 FORMAT(////' CHANGE item number (999 to EXIT).....> '$)
3407 C
3408 40 FORMAT(////
3409 1' ***** *
3410 2' * * * * *
3411 3' * * * * *
3412 4' ***** * * * * *
3413 5' * * * * *
3414 6' * * * * *
3415 7' * * * * *
3416 8////
3417 9' Options available C - CONTINUE'/
3418 1' / - EXIT'/
3419 2////' SELECT YOUR OPTION.....> ', $)
3420 C
3421 43 FORMAT(//////////
3422 1' ***** CORRECT *****'/
3423 3/' This option allows mistakes within one or more individual'
3424 4/' records to be corrected. This section of RAW may only be'
3425 5/' applied to records where SAMPLE/ROW No. were input during'
3426 6/' the CREATION of the .RAW datafile, as records are located'
3427 7/' by their respective SAMPLE/ROW number.'/
3428 8/' Options available C - CORRECT'
3429 9/' L - LIST VARIABLE NAMES'
3430 1/' S - LIST SAMPLE NAMES'
3431 1/' / - EXIT'
3432 3///' Select Option.....> ', $)
3433 44 FORMAT(///' SAMPLE Name / ROW Number to be CORRECTED.....> ', $)
3434 47 FORMAT(2(8X,I2,': ',A8,': ',F13.4))
3435 51 FORMAT(///
3436 1/' ***** DELETE *****'/
3437 2/' This program has the ability to delete any or all sample'
3438 3/' records from the input .RAW file, and REINSTATE any or'
3439 4/' all of the deleted records.'
3440 5/' NB. Sample records are not REINSTATEABLE once the user'
3441 6/' has exited from the RAW system.'/
3442 7/' Two main styles of DELETE are available to the user:/'
3443 8/' A SELECTIVE DELETE, This allows individual SAMPLES/ROWS'
3444 9/' to be deleted by name.'/
3445 1/' A TOTAL DELETE, Removes ALL records from the file.'
3446 2/' Individual records may then be'
3447 3/' REINSTATED using the SAMPLE/ROW No.'/
3448 4/' Options available S - SELECTIVE DELETE.'
3449 5/' T - TOTAL DELETE.'
3450 6/' R - REINSTATE.'

```



```

3451      7/' / - EXIT.'/
3452      8/' Select option.....> ', $)
3453      57 FORMAT(///
3454      1/' ***** SELECTIVE DELETE *****'//
3455      2/' This function allows individual sample records to be '
3456      3/' deleted by SAMPLE/ROW name.'////
3457      4/' Options available      C - CONTINUE.'
3458      5/' / - EXIT.'//
3459      6/' Select option.....> ', $)
3460      C
3461      C
3462      61 FORMAT(///
3463      1/' ***** SAMPLE RECORD ',A10,' NOT FOUND *****'
3464      C
3465      C
3466      62 FORMAT(///' Enter sample name to be deleted....> ', $)
3467      64 FORMAT(///' NOTE: SAMPLE RECORD ',A10,' SUCCESSFULLY DELETED')
3468      65 FORMAT(////////
3469      1/' ***** TOTAL DELETED *****'//
3470      2//
3471      3/' This function will delete all sample records within the'
3472      4/' .RAW file. (ie. allowing a large number of individual'
3473      5/' records to be deleted by a single command).'
3474      6/' Individual sample records may be "undeleted" by the use'
3475      7/' of the REINSTATE command.'///
3476      8/' Options available      C - CONTINUE'
3477      9/' / - EXIT'///
3478      1/' Select option.....> ', $)
3479      67 FORMAT(///' ***** ALL RECORDS SUCCESSFULLY DELETED *****'//
3480      1//
3481      2/' Options available      R - REINSTATE'
3482      3/' / - EXIT'///
3483      4/' Select option.....> ', $)
3484      69 FORMAT(////////
3485      1/' ***** REINSTATE *****'//
3486      2/' This function will allow the user to reinsert one or'
3487      3/' more SAMPLE record or ROW of data, previously removed'
3488      3/' by the DELETE or TOTAL DELETE command.'///
3489      4/' Options available      R - REINSTATE'
3490      5/' / - EXIT'////
3491      6/' Select option.....> ', $)
3492      70 FORMAT(///' Record/sample name to be reinstated...> ', $)
3493      73 FORMAT(///' Record/sample name ',A10,'reinstated!!.'////////)
3494      85 FORMAT(////////
3495      1/' ***** INSERT *****'//
3496      2/' This option may be used to systematically insert new'
3497      3/' data into any given variable for all or a selected No.'
3498      4/' of incremental records. No discrimination is made'
3499      5/' between preexisting variables and those created within'
3500      6/' the EDIT program by the CREATE command.'/
3501      1/' In unforeseen circumstances, you may find it necessary to'
3502      2/' EXIT before the INSERT operation is completed.'/
3503      3/' This is carried out by typing 999.999. The program will'
3504      4/' then provide you with the last completed record number'
3505      5/' which should be noted, and then retyped later in the'
3506      6/' SELECTIVE INSERT mode to complete the INSERT operation.'/
3507      7/' Options available      N - NORMAL INSERT      All records'
3508      8/'                          S - SELECTIVE INSERT Records X to N'
3509      9/'                          I - INDIVIDUAL INSERT'
3510      1/' / - EXIT'
3511      2/' Select option.....> ', $)
3512      C
3513      C
3514      C
3515      90 FORMAT(///' ***** VARIABLE NAME NOT FOUND *****'///)
3516      92 FORMAT(///' Select Variable (type / to EXIT)....> ', $)
3517      94 FORMAT(///1X,I5,': Sample Name.. ',A8,' Variable ',A8,'....'
3518      1'> ', $)
3519      97 FORMAT(///
3520      1/' *****'//
3521      1/' ***** AUTO-EXIT forced by 999.999 command *****'//
3522      2/' The next record number to undergo INSERT would have been'
3523      3/'-----> ',I3,' <-----'
3524      4/' Please note for future reference !!!!!/
3525      5/' *****'//)

```

```

3526 C
3527 C
3528 C
3529 100 FORMAT(///
3530 1' ***** WELCOME TO RAW *****'//
3531 1' This program is designed to CREATE or MANIPULATE a self'//
3532 2' addressing standard numeric datafile which may then be'//
3533 3' used as input to PLOTLIB, SPSS or USERS OWN programs.'//
3534 4' The output from this package is a self headed .RAW data'//
3535 6' file, which may be read into Fortran programs, edited'//
3536 7' under normal ED commands or modified from within RAW.'//
3537 8 ///
3538 5' To proceed:'//
3539 9'         Type C for CREATE'//
3540 1'         Type A for APPEND (ie Add to CREATED files)'//
3541 2'         Type E for EDIT (ie Change CREATED files)'//
3542 5'         Type R for REFORMAT (ie Thesis-ready tables)'//
3543 6'         Type / to EXIT'///
3544 7' Select your option.....> ', $)
3545 C
3546 101 FORMAT(///' Type in your new .RAW filename .....> ', $)
3547 102 FORMAT(///' How many variables.....> ', $)
3548 103 FORMAT(///' Variable Name', I2, '.....> ', $)
3549 106 FORMAT(///' Sample/Row Number (type / to exit).....> ', $)
3550 107 FORMAT(///' Enter the value of', I1, 'A8, '.....> ', $)
3551 108 FORMAT(I1, A79)
3552 109 FORMAT(I1, A79)
3553 110 FORMAT(2I6)
3554 111 FORMAT(8(I1, A8))
3555 112 FORMAT(I1, A12)
3556 113 FORMAT(I1, 6F13.4)
3557 114 FORMAT('*****')
3558 115 FORMAT(///' Type .RAW filename to be appended .....> ', $)
3559 118 FORMAT(///' Select your new starting position (1 to', I4, ').'> ', $)
3560 127 FORMAT(////
3561 1' ***** SORRY *****'
3562 1/' The option you have chosen is currently under development'
3563 2///' Please choose another option.....> ', $)
3564 129 FORMAT(///' Type in a TITLE for a the file.....> ', $)
3565 139 FORMAT(A79)
3566 C
3567 C
3568 C
3569 141 FORMAT(////
3570 1' ***** REFORMAT *****'
3571 1/' This program is used to create a .TAB "thesis ready" output'
3572 2/' file from data stored in a self formatting .RAW file format.'
3573 3/' Options incorporated within this package include the ability'
3574 4/' to select and print a titled table heading on each page of'
3575 5/' output, together with the facility to number each separate'
3576 6/' page as an incremented part of the main table. In addition'
3577 6/' the output format for each variable may be altered from that'
3578 6/' of the default value (2 decimal places).'
3579 6///' NB - A useful tip is when renaming the title, use the form;'
3580 6/'         TABLE 1 : Results Experiment No.1'
3581 7///'         Options available:'
3582 8///'         Type C to Continue'
3583 9/'         type / to Exit'
3584 1///' Please select your option.....> ', $)
3585 C
3586 C
3587 C
3588 142 FORMAT(////
3589 1/' ***** MOVE *****'
3590 2/' This program allows the user to MOVE the position of any'
3591 3/' variable name (and the related data) to any given location'
3592 4/' within the data array. The remaining data is automatically'
3593 5/' "shuffled" to allow space for the variable being MOVED.'
3594 5/'
3595 6/' An example of the use of this facility is to MOVE a newly'
3596 7/' GENERATED variable from the end of the variable list, to'
3597 8/' any given location in that list.'/
3598 9/'         Options available:         C - CONTINUE'
3599 1/'         / - EXIT'///
3600 2/' Select your option .....> ', $)

```

```

3601 154 FORMAT(///
3602 1/'***** ERROR ***** ERROR *****'
3603 2/' Two CONSTANTS found to occur in expression '
3604 3/' This is NOT acceptable, Reinput one value ONLY!!!!!!.'//
3605 4/'***** ERROR ***** ERROR *****')
3606 155 FORMAT(///' Variable name to be moved (/ to exit).....> ', $)
3607 156 FORMAT(///' New location of Variable (1 to', I2,').....> ', $)
3608 157 FORMAT(///' ***** STALEMATE : NO MOVE POSSIBLE *****'////////)
3609 161 FORMAT(///' ***** MOVE COMPLETED *****'////////)
3610 166 FORMAT(///' Name to be deleted (XXXX to EXIT).....> ', $)
3611 167 FORMAT(///' ***** VARIABLE DELETED *****')
3612 173 FORMAT(////////)
3613 1' ***** TRANSFORM *****
3614 2/' This program allows the user to TRANSFORM one or more'
3615 3/' variables by the use the mathematical commands:/'
3616 4/' + (add) - (subtract) / (divide) * (multiply)'
3617 5/' L (log10) P (exponential) N (No maths ie A=B) '/'
3618 6/' Operations are carried out by any given VARIABLE upon any'
3619 7/' other VARIABLE (or itself). The results of the operation'
3620 8/' may be stored in any VARIABLE location. '
3621 9/' Examples:'
3622 9/' VARIABLE 1 + VARIABLE 2 = VARIABLE 3'
3623 1/' VARIABLE 1 L = VARIABLE 3'
3624 2/' VARIABLE 1 N = VARIABLE 3'
3625 3/' Variable names 1, 2 and 3 are requested individually by'
3626 4/' the program. However, a CONSTANT can replace names 1 or 2.'
3627 5/' When prompted for name 1 or 2 type / to input a CONSTANT.'
3628 6/' OPTIONS C - CONTINUE'
3629 7/' / - EXIT '/'
3630 8/' Select your option.....> ', $)
3631 174 FORMAT(////' Variable name 1.....> ', $)
3632 180 FORMAT(///' Transform function (+, /, -, *, L, P, N).....> ', $)
3633 183 FORMAT(///' Variable name 2.....> ', $)
3634 187 FORMAT(///' Variable name 3 (Results).....> ', $)
3635 191 FORMAT(///' Constant 1 value.....> ', $)
3636 192 FORMAT(///' Constant 2 value.....> ', $)
3637 198 FORMAT(///
3638 1'***** TRANSFORM COMPLETED *****')
3639 200 FORMAT(///
3640 1' *****'//
3641 2' ***** FILE TRANSFERED : 'A10' *****'//
3642 3' *****'//
3643 4' FILE TITLE : '/'
3644 4 1X, A78//
3645 5' *****'//
3646 6' ***** HAVE A NICE DAY !!!!! *****'//
3647 7' *****'//)
3648 201 FORMAT(///
3649 1/' ***** DELETE *****'
3650 2///
3651 3/' This program allows the user to DELETE one or more VARIABLES.'
3652 4//
3653 5/' Options available D - DELETE'
3654 6/' / - EXIT '/'
3655 7/' Select option.....> ', $)
3656 206 FORMAT(///' Type C to CONTINUE.....> ', $)
3657 207 FORMAT(A1)
3658 210 FORMAT(///
3659 1' *****'//
3660 1' ***** AUTO-EXIT ***** No files CREATED or TRANSFERED ****'/
3661 1' *****'//
3662 2' ***** Better luck next time!!!!!!!!!!!!!!!!!!!! *****'//
3663 3' *****'//
3664 3' ***** Bye ***** Bye ***** Bye ***** Bye *****'//
3665 4' *****'//)
3666 215 FORMAT(///' ERROR - TWO CONSTANTS !!!!!'////////)
3667 243 FORMAT(////
3668 1/' PLEASE NOTE :/'
3669 1/' To use all the facilities available within RAW (such as the'
3670 2/' EDIT command) it is recommended that you allocate a SAMPLE'
3671 3/' name or ROW number for each RECORD of data. '/'
3672 4/' NB. Both numbers and/or character symbols are acceptable as'
3673 4/' SAMPLE/ROW identifiers.'/
3674 4/' A maximum number of 8 characters are allowed for each'
3675 4/' SAMPLE/ROW identifier.'/

```

```

3676      4/'      Each SAMPLE or ROW number should be  UNIQUE  within any'
3677      5/'      individual file and a test will be carried out to check'
3678      6/'      this.'
3679      7/'      You may now proceed to type in your data:- '///  

3680      246  FORMAT(//  

3681      1/'      ++++++  

3682      1/'      The SAMPLE/ROW name selected already exists.'  

3683      2/'      Please select an alternative name,Thank you.'  

3684      3/'      ++++++///  

3685  

3686      C      260  FORMAT(//8(1X,A8))  

3687      261  FORMAT(/////////' Variable names : '///  

3688      262  FORMAT(/////////' Sample names   : '///  

3689      264  FORMAT(///  

3690      1/'      *****  

3691      1/'      *****  

3692      2/'      ***** ERROR ***** ERROR ***** ERROR *****  

3693      3/'      *****  

3694      4/'      ***** DIVIDE BY ZERO ATTEMPTED - RESULT SET TO 99999.999 *****  

3695      5/'      *****  

3696      6/'      *****  

3697      7/' )  

3698      265  FORMAT(8(1X,A8))  

3699      270  FORMAT(///  

3700      1'      *****/  

3701      1'      *****/  

3702      1'      Two styles of output are available from the REFORMAT package:/'  

3703      2'      Output Style 1 -  SAMPLES/ROWS by VARIABLES./'  

3704      3'                        (ie. Samples across and variables down).///  

3705      4'      Output Style 2 -  VARIABLES by SAMPLES/ROWS./'  

3706      5'                        (ie. Variables across and samples down).///  

3707      6'      These options will allow you to generate two different styles/'  

3708      7'      of "thesis ready" tables from your .RAW datafiles. '///  

3709      8'      Please experiment with both options and then select the table/'  

3710      9'      style which best suits your own requirements.///  

3711      1'      Options available          1 - Style 1/'  

3712      2'                                2 - Style 2/'  

3713      3'                                / - Exit.///  

3714      4'      Select Option.....> '$)  

3715      310  FORMAT(10X,A8,4X,10F10.1)  

3716      311  FORMAT(10X,A8,4X,10F10.3)  

3717      312  FORMAT(10X,A8,4X,10F10.4)  

3718      313  FORMAT(10X,A8,4X,10I10)  

3719      340  FORMAT(/////////  

3720      368  FORMAT(/////////1X,'Variable names:/'  

3721      369  FORMAT(/////////1X,'Variable names:/'  

3722      405  FORMAT(// ' Type .RAW filename to be reformatted .....> ',  

3723      406  FORMAT(// ' REFORMAT : Data file ',A12,' read in correctly///  

3724      407  FORMAT(// ' The number of variables are.....> ',I3)  

3725      408  FORMAT(// ' The number of samples are.....> ',I3)  

3726      409  FORMAT(// ' The variable names are: '/(5X,6A8)/)  

3727      1413  FORMAT(10X,'VAR. / ID. ',<P>A10,/  

3728      413  FORMAT(10X,'VAR. / ID. ',10A10,/  

3729      415  FORMAT(10X,A8,4X,10F10.2)  

3730      416  FORMAT('1',////////,10X,A55,'Part ..... ',I3///  

3731      417  FORMAT(////,1X,A79)  

3732      418  FORMAT(// ' Do you wish to change the title (Y or N).....> ',  

3733      419  FORMAT(A79)  

3734      420  FORMAT(A79)  

3735      421  FORMAT(// ' Do you require the title on each page (Y or N)...> ',  

3736      422  FORMAT(A1)  

3737      424  FORMAT(// ' Do you require an incremented part number on/'  

3738      1'      each page of output (Y or N).....> ',  

3739      425  FORMAT(A1)  

3740      426  FORMAT(// ' Initial part number .....> ',  

3741      427  FORMAT('1',////////,11X,A79,///  

3742      442  FORMAT(// ' The .TAB output filename is (in full).....> ',  

3743      443  FORMAT(A12)  

3744      454  FORMAT(//  

3745      1'      *****/  

3746      1'      ***** REFORMAT COMPLETED *****/  

3747      2'      *****/  

3748      455  FORMAT(// ' How many SAMPLES per table page (1-10) .....> ',  

3749      459  FORMAT(1X,// ' Type / to complete EXIT.....> ',  

3750      465  FORMAT(//

```

```

3751 466 FORMAT(/////////
3752 1 ' ***** APPEND *****'
3753 1/' This program allows the user to both read and append .RAW'
3754 2/' formatted data files. As in the CREATE routine, additional'
3755 3/' data RECORDS may be input, then added to an existing file.'/
3756 4/' Output from this program is in the form of an incremented'
3757 5/' version of the original .RAW filename. Therefore extreme'
3758 6/' care is required with system PURGE commands after APPEND.'/
3759 7/' The naming, number and order of the variables are defined'
3760 8/' previously by the .RAW file which will be appended.'/
3761 9/' The ability to modify the output file generated by this'
3762 1/' program, is incorporated within the RAW package, and may'
3763 2/' be accessed through the EDIT (sample / variable editor)'
3764 3/' option.'/
3765 4/' Options available..... Type A - APPEND'
3766 5/' Type E - EDIT'
3767 5/' Type M - MERGE'
3768 6/' Type / - EXIT'/
3769 7/' Select your option.....> ', $)
3770
C
3771 467 FORMAT(/////////
3772 1' ***** EDIT *****'/
3773 1/' This program allows the user to both read, manipulate and/or'
3774 2/' correct .RAW formatted datafiles.'/
3775 3/' Numerous options are available to allow data manipulations'
3776 4/' however, these fall into two main editing categories:'/
3777 5/' SAMPLE ORIENTATED - To correct or change individual items'
3778 6/' or values within a single SAMPLE / ROW'
3779 7/' and/or delete a complete data record.'/
3780 8/' VARIABLE ORIENTATED - To create, delete or mathematically'
3781 9/' manipulate data contained within any'
3782 1/' variable array.'
3783 2/' ie. A= 10, or A=A+B etc.....'/
3784 3/' Options available - Type S - SAMPLE Editor'
3785 4/' Type V - VARIABLE Editor'
3786 5/' Type / - EXIT '/
3787 6/' Select your option.....> ', $)
3788
C
3789 468 FORMAT(/////////
3790 1 ' ***** VARIABLE ORIENTATED EDITOR *****'//
3791 1/' This editor allows data to be modified, created or deleted'
3792 2/' by variable name. New names have to be GENERATED, and are'
3793 3/' placed at the end of the variable list. Variable values'
3794 3/' may then be INSERTED by direct input from the keyboard or'
3795 5/' produced by a TRANSFORM applied to one or more variables.'
3796 6/' Pre-existing variables may also be TRANSFORMED using the'
3797 7/' maths options or DELETED. (NB. ALL sample records are'
3798 8/' modified by the use of the VARIABLE ORIENTATED editor.)'/
3799 9/' Options available : Type I - INSERT new variable data'
3800 2/' Type M - MOVE variable position'
3801 2/' Type M - MOVE variable position'
3802 3/' Type T - TRANSFORM old variables'
3803 4/' Type D - DELETE old variables'
3804 5/' Type / - EXIT.'/
3805 6/' Select option.....> ', $)
3806
469 FORMAT(/////////
3808 1' ***** SAMPLE ORIENTATED EDITOR *****'
3809 1/' This editor allows individual sample records to be accessed'
3810 2/' and allows the modification of items from any specific file.'
3811 3/' Any number of selected samples/rows may be corrected in this'
3812 4/' way before returning to the main EDIT program and exiting.'
3813 5/' An added function of this program is the ability to delete'
3814 6/' individual records by their unique sample/row name.'
3815 7/' By the careful use of CREATE, APPEND and EDIT most, if not'
3816 8/' all data handling and manipulation operations may be carried'
3817 9/' out, on an interactive basis in this user friendly mode.'
3818 1/' Options Available : Type D - DELETE'
3819 2/' Type C - CORRECT individual samples'
3820 3/' Type / - Return to EDIT'
3821 4/' Select option.....> ', $)
3822
C
3823 470 FORMAT(' Title....> ', $)
3824 484 FORMAT(1X,A10,A2)
3825 485 FORMAT(' Type .RAW filename to be EDITED.....> ', $)

```



```

3826 491 FORMAT(// ' The maximum number of variables (50) has'
3827 1' been exceeded!!!!!!')
3828 492 FORMAT(// ' A sample name has not been input'
3829 1// ' Is this OK! (Y or N).....> ', $)
3830 C
3831 481 FORMAT(////////
3832 1' ***** CREATE *****'
3833 2/ ' This program allows the user to CREATE a .RAW datafile,'
3834 3/ ' from data input via a keyboard to a filename of your own'
3835 4/ ' choice. Any RAW file contains the following information:'
3836 5/ ' TITLE Datafile identifier and title for pages of'
3837 6/ ' tabulated data (See REFORMAT).'
3838 7/ ' VARIABLES A list of the user defined VARIABLE names.'
3839 8/ ' M,N The No.of VARIABLES and SAMPLES/ROWS.'
3840 9/ ' RECORDS An array containing the numeric data input'
3841 1/ ' for each SAMPLE/ROW of the M VARIABLES.'
3842 2/ ' SAMPLE NAMES As each RECORD is created it is assigned a'
3843 3/ ' name to distinguish it from other records.'
3844 4/ ' SAMPLE/ROW NUMBERS, provide an ability to'
3845 5/ ' locate any given record, and thus allows'
3846 6/ ' rapid correction or manipulation of data.'
3847 7// ' OPTIONS C CONTINUE'
3848 8/ ' / EXIT'
3849 9/ ' Select your option.....> ', $)
3850 C
3851 500 FORMAT(A1)
3852 501 FORMAT(A12)
3853 503 FORMAT(A8)
3854 506 FORMAT(A10)
3855 507 FORMAT(6F13.4)
3856 513 FORMAT(10X, 'ID. / VAR. ', <M1>(2X, A8))
3857 515 FORMAT(10X, A8, 4X, <M1>F10.2)
3858 516 FORMAT(10X, A8, 4X, <M1>F10.1)
3859 517 FORMAT(10X, A8, 4X, <M1>F10.2)
3860 518 FORMAT(10X, A8, 4X, <M1>F10.3)
3861 519 FORMAT(10X, A8, 4X, <M1>F10.4)
3862 520 FORMAT(10X, A8, 4X, <M1>I10)
3863 521 FORMAT(// ' How many VARIABLES per table page (1-10).....> ', $)
3864 522 FORMAT(// ' How many SAMPLES per table page (1-50).....> ', $)
3865 847 FORMAT(//
3866 1' The data for your chosen SAMPLE/ROW is as follows://)
3867 1000 FORMAT(16(//))
3868 1417 FORMAT(//////////
3869 1' *****'
3870 2/ ' ***** ERROR *****'
3871 3/ ' *****'
3872 4// ' The number of variables is greater than 10, therefore '
3873 5/ ' OUTPUT STYLE 1 is forced.'
3874 6/ ' *****'
3875 7////////)
3876 1501 FORMAT(/// ' Type .RAW filename to be merged .....> ', $)
3877 1502 FORMAT(//////////
3878 1' *****'/
3879 2' ***** MERGE *****'/
3880 3' *****'/
3881 4//
3882 5' Two possible styles of MERGE are available://
3883 6' 1- Additional sample records containing the same variables'/
3884 7' 2- Additional variables for existing sample records'///
3885 8' Please Select Option.....> ', $)
3886 1503 FORMAT(I1)
3887 1507 FORMAT(////
3888 1' Any further datafiles for MERGE (Y or N)....> ', $)
3889 1600 FORMAT(//////////
3890 1' *****'/
3891 1' ***** ERROR - Number of variables differ!! *****'/
3892 1' *****'
3893 1////////)
3894 1601 FORMAT(//////////
3895 1' *****'/
3896 1' ***** ERROR - Variable Names differ!! *****'/
3897 1' *****'
3898 1////////)
3899 1602 FORMAT(//////////
3900 1' *****'/

```



```

3901      2' ***** MERGE COMPLETE *****'/
3902      3' *****'/
3903      4 ///
3904      5/' Options:          1 - Store merged datafile'
3905      6/'                  2 - Merge additional file'
3906      7///' Select Option.....> ', $)
3907 1620 FORMAT(/////////)
3908      1'*****'/
3909      1'***** ERROR - No of sample records differ!! *****'/
3910      1'*****'/
3911      1////////)
3912 1621 FORMAT(/////////)
3913      1'*****'/
3914      1'***** ERROR - Position of sample Names differ!! *****'/
3915      1'*****'/
3916      1//
3917      1/' Offending Samples: ',A8,' and ',A8
3918      1/' *****'
3919      1////////)
3920 2115 FORMAT(///' Type .RAW filename to be merged (/ to exit)..> ', $)
3921 2015 FORMAT(//
3922      1 ' The number of decimal places (1-4) for ',A8,'....> ', $)
3923
3924 C ++++++
3925 C ++++++ END OF OUTPUT FORMATS/DIALOGUE ++++++
3926 C ++++++
3927 C
3928 C
3929      999  END

```

```

0001      PROGRAM HIS
0002      C
0003      C
0004      C
0005      C
0006      C          *      *      *****      *
0007      C          *      *      *      *
0008      C          *      *      *      *
0009      C          *****      *      *****
0010      C          *      *      *      *
0011      C          *      *      *      *
0012      C          *      *      *****      *
0013      C
0014      C
0015      C
0016      C
0017      C      PAUL R. DULLER
0018      C      DEPARTMENT OF APPLIED GEOLOGY
0019      C      THE UNIVERSITY OF STRATHCLYDE
0020      C      GLASGOW
0021      C
0022      C
0023      C *****
0024      C ***** INTRODUCTION *****
0025      C *****
0026      C
0027      C      THIS PROGRAM IS DESIGNED TO GRAPHICALLY ASSESS A
0028      C      GENERAL PURPOSE DATA FILE, GENERATED BY THE USER FROM
0029      C      DATA INPUT THROUGH THE RAG SYSTEM.
0030      C
0031      C      INTEGER NUMTOPLOT,SCALE,TEST,COUNT
0032      C      INTEGER X,I,J,L,M,N,O,P,Q,R,S,T,M1,N1,CLASSES,MAXCLASS
0033      C      INTEGER CLASS(50,50),NUMINCLASS(50),CUMFA,M10,N10
0034      C      REAL MAXCL(50)
0035      C      REAL DATA(50,2000),MIN(50),MAX(50),MEANA(50),MEANG(50)
0036      C      REAL RANGE(50),VAR(50),SDEV(50),SKEW(50),KURT(50),M4(50)
0037      C      REAL SUMX(50),SUMX2(50),V1(50),V2(50),V3(50),V4(50),M2(50)
0038      C      REAL TABLE(50,10),CV(50),K,K1,M3(50),MIDPOINT(50),BOUND(50,2)
0039      C      REAL CF(50,100),CUMF(50,100),INT(50),CELL(50),CLASSINT(50)
0040      C      CHARACTER TITLE*80,FORM*80,SAMPLE(2000)*10,NAME(50)*8,IN*12
0041      C      CHARACTER KEY(2000)*2,FORM1*10,FORMX*10,SAMPLE1(2000)*8
0042      C      CHARACTER HIST*50,CZ*1,BIN*12,TITLE2*80,NAME2(50)*8,CT*1
0043      C
0044      C *****
0045      C ***** OUTPUT HEADER *****
0046      C *****
0047      C
0048      43  WRITE(6,40)
0049      READ(5,41)B
0050      IF(B.EQ.'C')THEN
0051      GOTO 42
0052      END IF
0053      GOTO 43
0054      C
0055      C *****
0056      C ***** INPUT .RAWFILE *****
0057      C *****
0058      C
0059      C      ASK FOR FILENAME
0060      C
0061      42  WRITE(6,100)
0062      COUNT=0
0063      P=1
0064      READ(5,601)IN
0065      OPEN(1,FILE=IN,DEFAULT FILE='.RAW',STATUS='OLD')
0066      OPEN(2,FILE=IN,DEFAULT FILE='.HIS',STATUS='NEW')
0067      C
0068      C      READ FILE HEADER AND DATA
0069      C
0070      READ(1,108)TITLE
0071      READ(1,109)FORM
0072      READ(1,110)M1,N1
0073      C
0074      READ(1,111)(NAME(I),I=1,M1)
0075

```

```

0076      DO 475 I=1,N1
0077      READ(1,484)SAMPLE(I),KEY(I)
0078      READ(1,113)(DATA(J,I),J=1,M1)
0079 475 CONTINUE
0080      C
0081      C
0082      C *****
0083      C ***** STATISTICS *****
0084      C *****
0085      C
0086      C *****
0087      C      MINIMUM, MAXIMUM AND RANGE
0088      C      *****
0089      C
0090      C      TO COMPUTE THE MINIMUM,MAXIMUM AND RANGE
0091      C      OF N1 SAMPLES FOR M1 VARIABLES
0092      C
0093      C      SET SUM TO ZERO
0094      C
0095      DO 98 I=1,M1
0096      J=1
0097      SUMX(I)=DATA(I,J)
0098      SUMX2(I)=DATA(I,J)
0099
0100      DO 95 J=2,N1
0101
0102      K=DATA(I,J)
0103
0104      IF(K.GT.SUMX(I))THEN
0105      SUMX(I)=K
0106      END IF
0107
0108      IF(K.LT.SUMX2(I))THEN
0109      SUMX2(I)=K
0110      END IF
0111
0112 95 CONTINUE
0113      C
0114      MAX(I)=SUMX(I)
0115      MIN(I)=SUMX2(I)
0116      RANGE(I)=MAX(I)-MIN(I)
0117 98 CONTINUE
0118
0119      C
0120      C *****
0121      C      SKEWNESS AND KURTOSIS
0122      C      *****
0123      C
0124      C      THE SKEWNESS AND KURTOSIS CALCULATED IN THIS PROGRAM
0125      C      MAKE USE OF THE SAMPLE CENTRAL MOMENTS AS DEFINED BY
0126      C      BENNETT AND FRANKLIN (1954) STATISTICAL ANALYSIS IN
0127      C      CHEMISTRY AND THE CHEMICAL INDUSTRY. WILEY 724pp.
0128      C
0129      DO 80 I=1,M1
0130
0131      SKEW(I)=0.00
0132      KURT(I)=0.00
0133      V1(I)=0
0134      V2(I)=0
0135      V3(I)=0
0136      V4(I)=0
0137
0138      DO 81 J=1,N1
0139
0140      V1(I)=V1(I)+DATA(I,J)
0141      V2(I)=V2(I)+DATA(I,J)**2
0142      V3(I)=V3(I)+DATA(I,J)**3
0143      V4(I)=V4(I)+DATA(I,J)**4
0144
0145 81 CONTINUE
0146
0147      V1(I)=V1(I)/N1
0148      V2(I)=V2(I)/N1
0149      V3(I)=V3(I)/N1
0150      V4(I)=V4(I)/N1

```

```

0151      M2(I)=V2(I)-(V1(I)**2)
0152      M3(I)=V3(I)-(3*V2(I)*V1(I))+(2*V1(I)**3)
0153      M4(I)=V4(I)-(4*V3(I)*V1(I))+(6*V2(I)*V1(I)**2)-(3*V1(I)**4)
0154
0155
0156      SKEW(I)=M3(I)/(M2(I)**1.5)
0157      KURT(I)=M4(I)/(M2(I)**2.0)
0158
0159      80  CONTINUE
0160
0161      GOTO 1002
0162  C
0163  C *****
0164  C ***** CUMULATIVE FREQUENCY *****
0165  C *****
0166  C
0167      1000 X2=1.00/N1
0168          X2=X2*100
0169
0170          DO 48 I=1,M1
0171          DO 49 J=1,CLASSES
0172              CF(I,J)=0.0000
0173      49  CONTINUE
0174      48  CONTINUE
0175
0176          DO 943 I=1,M1
0177          DO 944 J=1,N1
0178              INT(I)=RANGE(I)/CLASSES
0179              K=MIN(I)
0180              K1=MIN(I)+INT(I)
0181              L=1
0182
0183              IF (DATA(I,J).EQ.MIN(I)) THEN
0184                  CF(I,L)=CF(I,L)+X2
0185              END IF
0186
0187      69  IF (DATA(I,J).GT.K) THEN
0188              IF (DATA(I,J).LE.K1) THEN
0189
0190                  CF(I,L)=CF(I,L)+X2
0191                  GOTO 944
0192              END IF
0193              END IF
0194
0195              K=K+INT(I)
0196              K1=K1+INT(I)
0197              L=L+1
0198
0199              L3=CLASSES+1
0200
0201              IF (L.EQ.L3) THEN
0202                  GOTO 944
0203              END IF
0204
0205              GOTO 69
0206
0207      944  CONTINUE
0208      943  CONTINUE
0209
0210          DO 333 I1=1,M1
0211              CUMF(I1,1)=CF(I1,1)
0212          DO 334 J1=2,CLASSES
0213              L=J1-1
0214              CUMF(I1,J1)=CUMF(I1,L)+CF(I1,J1)
0215      334  CONTINUE
0216      333  CONTINUE
0217  C
0218      GOTO 1001
0219
0220  C *****
0221  C ***** OPTIONS *****
0222  C *****
0223  C
0224  C      RIGHT JUSTIFICATION OF SAMPLE NAMES
0225  C

```

```

0226      1002 DO 4 R=1,N1
0227          FORMX=SAMPLE1(R)
0228          DO 3 I1=8,1,-1
0229              IF(FORMX(I1:I1).NE.' ')THEN
0230                  GOTO 2
0231              END IF
0232          3 CONTINUE
0233              I1=1
0234          2 FORM1=' '
0235              J1=8-I1+1
0236              FORM1(J1:8)=FORMX(1:I1)
0237              SAMPLE1(R)=FORM1
0238          4 CONTINUE
0239              Y=0
0240      C
0241      C *****
0242      C
0243      C OUTPUT MESSAGE TO THE USER AND ASK USER IF HE
0244      C REQUIRES OUTPUT TO BE:
0245      C
0246      C 1. FULLY AUTOMATED DATA PROCESSING
0247      C 2. FULLY AUTOMATED DATA PROCESSING WITH PRESET RANGE.
0248      C 3. MANUAL PROCESSING.
0249      C *****
0250      C
0251      C
0252
0253      994 WRITE(6,990)
0254          READ(5,991)TEST
0255
0256          IF(TEST.EQ.1)THEN
0257              GOTO 731
0258          END IF
0259
0260          IF(TEST.EQ.2)THEN
0261              GOTO 732
0262          END IF
0263
0264          IF(TEST.EQ.3)THEN
0265              GOTO 733
0266          END IF
0267
0268          GOTO 994
0269
0270      C *****
0271      C ***** MANUAL PROCESSING *****
0272      C *****
0273      C
0274      C *****
0275      C ***** LIST VARIABLES *****
0276      C *****
0277      C
0278
0279      733 L=0
0280          P1=M1
0281      11 IF(P1.GE.2)THEN
0282          L=L+1
0283          P1=P1-2
0284          GOTO 11
0285          END IF
0286      C
0287      C NO OF REMAINING SAMPLES FORMING LESS THAN ONE COMPLETE
0288      C ROW (P1).
0289      C
0290      C OUTPUT VARIABLE NAMES
0291      C
0292          Y=0
0293          IF(M1.EQ.0)THEN
0294              GOTO 15
0295          END IF
0296      C
0297          WRITE(6,5)
0298
0299          DO 13 I3=1,L
0300              X=Y+1

```

```

0301      Y=Y+2
0302      WRITE(6,6)((J3,NAME(J3)),J3=X,Y)
0303 13 CONTINUE
0304
0305      IF(P1.EQ.0)THEN
0306      GOTO 15
0307      END IF
0308      Y=M1-1
0309      WRITE(6,6)M1,NAME(M1)
0310 15 X=0
0311 C
0312 C      ***** ASK USER TO SELECT VARIABLE *****
0313 C
0314 63 WRITE(6,171)
0315      READ(5,172)NUMTOPLOT
0316 C
0317 C      ***** ASK USER TO SELECT THE NUMBER OF CLASSES *****
0318 C
0319 996 IF(COUNT.EQ.0)THEN
0320      WRITE(6,350)
0321      READ(5,*)CLASSES
0322      END IF
0323 C
0324 C      ***** ASK USER TO SELECT THE TYPE OF PLOT *****
0325 C
0326      WRITE(6,175)
0327      READ(5,176)CZ
0328
0329      IF(P.GE.2)THEN
0330      GOTO 10
0331      END IF
0332
0333 C
0334 C      ***** CHECK THAT MIN AND MAX ACCEPTABLE *****
0335 C
0336 66 WRITE(6,60)MIN(NUMTOPLOT),MAX(NUMTOPLOT)
0337      READ(6,61)CT
0338      IF(CT.EQ.'N')THEN
0339      RANGE(NUMTOPLOT)=MAX(NUMTOPLOT)-MIN(NUMTOPLOT)
0340      GOTO 10
0341      END IF
0342      IF(CT.EQ.'1')THEN
0343      WRITE(6,64)
0344      READ(6,*)MIN(NUMTOPLOT)
0345      GOTO 66
0346      END IF
0347      IF(CT.EQ.'2')THEN
0348      WRITE(6,65)
0349      READ(6,*)MAX(NUMTOPLOT)
0350      GOTO 66
0351      END IF
0352      GOTO 63
0353 C
0354 C      CHECK TO SEE IF AUTOPROCESSING REQUIRED
0355 C      IF SO ONLY CALCULATE CF% ONCE
0356 C
0357 10 IF(TEST.NE.3)THEN
0358      IF(NUMTOPLOT.NE.1)THEN
0359      GOTO 1001
0360      END IF
0361      END IF
0362
0363      GOTO 1000
0364
0365 1001 CELL(NUMTOPLOT)=RANGE(NUMTOPLOT)/CLASSES
0366
0367      DO 177 I=1,CLASSES
0368
0369 C      CALCULATE THE UPPER LIMIT OF EACH CLASS INTERVAL
0370
0371      CLASSINT(I)=MIN(NUMTOPLOT) + (I*CELL(NUMTOPLOT))
0372 C
0373 C      CALCULATE THE MIDPOINT OF EACH CLASS INTERVAL
0374
0375      MIDPOINT(I)=MIN(NUMTOPLOT) + (I-0.5)*CELL(NUMTOPLOT)

```



```

0376
0377 177 CONTINUE
0378 C
0379 C SET ALL VALUES TO ZERO
0380 C
0381 DO 327 I=1,CLASSES
0382 CLASS(I,NUMTOPLOT)=0
0383 327 CONTINUE
0384
0385 C
0386 C CACULATE THE NUMBER OF MEMBERS OF EACH CLASS (NUMINCLASS) FOR THE
0387 C PARTICULAR VARIABLE REQUESTED (NUMTOPLOT).
0388
0389 DO 187 J=1,N1
0390
0391 K=0
0392
0393 DO 188 I=1,CLASSES
0394
0395 IF(DATA(NUMTOPLOT,J).GT.CLASSINT(I))THEN
0396 GOTO 188
0397 END IF
0398
0399 IF(K.EQ.0)THEN
0400 K=1
0401 CLASS(I,NUMTOPLOT)=CLASS(I,NUMTOPLOT)+1
0402 END IF
0403
0404 188 CONTINUE
0405 187 CONTINUE
0406
0407 C SCALE DOWN ARRAYS TO FIT INTO THE HISTOGRAM
0408 C
0409 IF(P.EQ.2)THEN
0410 MAXCLASS=MAXCL(NUMTOPLOT)
0411 GOTO 1045
0412 END IF
0413
0414 DO 44 I=1,M1
0415 MAXCL(I)=0.00
0416 44 CONTINUE
0417
0418 MAXCLASS=MAXCL(NUMTOPLOT)
0419
0420 DO 17 I=1,CLASSES-1
0421 J=I+1
0422 IF(CLASS(I,NUMTOPLOT).GT.CLASS(J,NUMTOPLOT))THEN
0423 IF(CLASS(I,NUMTOPLOT).GT.MAXCLASS)THEN
0424 IF(MAXCL(NUMTOPLOT).EQ.0.00)THEN
0425 MAXCLASS=CLASS(I,NUMTOPLOT)
0426 END IF
0427 END IF
0428 END IF
0429 17 CONTINUE
0430
0431 IF(MAXCLASS.EQ.50)THEN
0432 GOTO 649
0433 ELSE
0434
0435 1045 DO 18 I=1,CLASSES
0436
0437 IF(CLASS(I,NUMTOPLOT).EQ.0)THEN
0438 GOTO 18
0439 END IF
0440
0441 IF(MAXCLASS.EQ.0)THEN
0442 GOTO 18
0443 END IF
0444
0445 CLASS(I,NUMTOPLOT)=(CLASS(I,NUMTOPLOT)*50)/MAXCLASS
0446
0447 18 CONTINUE
0448 649 END IF
0449
0450 SCALE=MAXCLASS

```

```

0451 C
0452 C *****
0453 C ***** SET UP OUTPUT FILES *****
0454 C *****
0455 C
0456 992 IF (TEST.EQ.3) THEN
0457 WRITE(6,117) TITLE, NAME (NUMTOPLOT)
0458 IF (CZ.NE.'2') THEN
0459 WRITE(6,667) SCALE
0460 ELSE
0461 WRITE(6,502)
0462 SCALE=100
0463 WRITE(6,501) SCALE
0464 END IF
0465
0466 WRITE(6,499) MIN(NUMTOPLOT)
0467
0468 DO 20 J=1, CLASSES
0469 DO 57 I=1, 50
0470 HIST(I:)= ' '
0471 IF (I.GT.CLASS(J, NUMTOPLOT)) THEN
0472 GOTO 57
0473 END IF
0474 HIST(I:)= ']'
0475 57 CONTINUE
0476
0477 IF (CZ.EQ.'1') THEN
0478 WRITE(6,901) HIST, MIDPOINT(J), CUMF (NUMTOPLOT, J)
0479 END IF
0480
0481 IF (CZ.EQ.'2') THEN
0482 IF (CUMFA.LT.0) THEN
0483 CUMFA=0
0484 END IF
0485 IF (CUMFA.LT.49) THEN
0486 Q=49-CUMFA
0487 WRITE(6,53) MIDPOINT(J), CUMF (NUMTOPLOT, J)
0488 ELSE
0489 WRITE(6,54) MIDPOINT(J), CUMF (NUMTOPLOT, J)
0490 END IF
0491 END IF
0492
0493 IF (CZ.EQ.'3') THEN
0494 CUMFA=(CUMF (NUMTOPLOT, J))/2)
0495 HIST(CUMFA:CUMFA)= '*'
0496 WRITE(6,901) HIST, MIDPOINT(J), CUMF (NUMTOPLOT, J)
0497 END IF
0498
0499 20 CONTINUE
0500
0501 SCALE=100
0502 WRITE(6,499) MAX(NUMTOPLOT)
0503
0504 IF (CZ.EQ.'1') THEN
0505 WRITE(6,1501) SCALE
0506 WRITE(6,666) N1
0507 GOTO 747
0508 END IF
0509
0510 WRITE(6,501) SCALE
0511 WRITE(6,666) N1
0512
0513 C
0514 C ASK USER FOR STORAGE, NEW VARIABLE OR QUIT
0515 C
0516 747 WRITE(6,669)
0517 READ(5,991) J4
0518
0519 IF (J4.EQ.1) THEN
0520 GOTO 701
0521 END IF
0522 IF (J4.EQ.2) THEN
0523 GOTO 702
0524 END IF
0525 IF (J4.EQ.3) THEN

```

```

0526      GOTO 733
0527      END IF
0528      GOTO 747
0529      C
0530      C      INFORM USER THAT HISTOGRAMS COMPLETED AND EXIT
0531      C
0532      701 WRITE(6,454)
0533      GOTO 999
0534      END IF
0535
0536      702 IF(COUNT.EQ.0)THEN
0537      WRITE(2,117)TITLE,NAME(NUMTOPLOT)
0538      COUNT=1
0539      ELSE
0540      WRITE(2,1117)NAME(NUMTOPLOT)
0541      END IF
0542
0543      SCALE=MAXCLASS
0544      IF(CZ.NE.'2')THEN
0545      WRITE(2,667)SCALE
0546      ELSE
0547      WRITE(2,502)
0548      SCALE=100
0549      WRITE(2,501)SCALE
0550      END IF
0551
0552      WRITE(2,499)MIN(NUMTOPLOT)
0553
0554      DO 21 J5=1,CLASSES
0555      DO 51 I=1,50
0556      HIST(I:)= ' '
0557      IF(I.GT.CLASS(J5,NUMTOPLOT)) THEN
0558      GOTO 51
0559      END IF
0560      HIST(I:)=']'
0561      51 CONTINUE
0562
0563      IF(CZ.EQ.'1')THEN
0564      WRITE(2,901)HIST,MIDPOINT(J5),CUMF(NUMTOPLOT,J5)
0565      END IF
0566
0567      IF(CZ.EQ.'2')THEN
0568      CUMFA=(CUMF(NUMTOPLOT,J5)/2)-1
0569      IF(CUMFA.LT.0)THEN
0570      CUMFA=0
0571      END IF
0572      IF(CUMFA.LT.49)THEN
0573      Q=49-CUMFA
0574      WRITE(2,53)MIDPOINT(J5),CUMF(NUMTOPLOT,J5)
0575      ELSE
0576      WRITE(2,54)MIDPOINT(J5),CUMF(NUMTOPLOT,J5)
0577      END IF
0578      END IF
0579
0580      IF(CZ.EQ.'3')THEN
0581      CUMFA=(CUMF(NUMTOPLOT,J5)/2)
0582      HIST(CUMFA:CUMFA)='*'
0583      WRITE(2,901)HIST,MIDPOINT(J5),CUMF(NUMTOPLOT,J5)
0584      END IF
0585
0586      21 CONTINUE
0587      I=SCALE
0588      SCALE=100
0589      WRITE(2,499)MAX(NUMTOPLOT)
0590      IF(CZ.EQ.'1')THEN
0591      WRITE(2,1501)I
0592      WRITE(2,1666)N1
0593      GOTO 537
0594      END IF
0595
0596      WRITE(2,501)SCALE
0597      WRITE(2,1666)N1
0598
0599      537 IF(TEST.EQ.1)THEN
0600      GOTO 993

```

```

0601      END IF
0602
0603      IF(TEST.EQ.2)THEN
0604      GOTO 874
0605      END IF
0606
0607      GOTO 747
0608  C
0609  C *****
0610  C ***** FULLY AUTOMATED PROCESSING *****
0611  C ***** PRESET RANGE *****
0612  C *****
0613
0614
0615  C      INFORM USER OF SELECTED OPTION
0616
0617      732 WRITE(6,871)
0618
0619  C      ASK FOR RANGE FILES
0620
0621      WRITE(6,872)
0622      READ(5,601)BIN
0623  C
0624  C      ASK THE USER IF MAXIMUM CLASS INTERVALS ARE TO BE PRESET
0625  C
0626      1011 WRITE(6,1010)
0627      READ(6,*)P
0628      IF(P.NE.1)THEN
0629      IF(P.NE.2)THEN
0630      GOTO 1011
0631      END IF
0632      END IF
0633
0634      OPEN(3,FILE=BIN,DEFAULT FILE='.RAW',STATUS='OLD')
0635      READ(3,108)TITLE2
0636      READ(3,109)FORM
0637      READ(3,110)M10,N10
0638      READ(3,111)(NAME2(I),I=1,M10)
0639      READ(3,484)SAMPLE1(1),KEY(1)
0640      READ(3,113)(MIN(J),J=1,M10)
0641      READ(3,484)SAMPLE1(2),KEY(2)
0642      READ(3,113)(MAX(J),J=1,M10)
0643
0644      IF(P.NE.2)THEN
0645      GOTO 1012
0646      END IF
0647
0648      READ(3,484)SAMPLE1(2),KEY(2)
0649      READ(3,113)(MAXCL(J),J=1,M10)
0650
0651      1012 DO 873 I=1,M10
0652      RANGE(I)=MAX(I)-MIN(I)
0653      873 CONTINUE
0654  C
0655  C ***** CHECK *****
0656  C
0657      IF(M1.NE.M10)THEN
0658      WRITE(6,878)
0659      GOTO 999
0660      END IF
0661
0662      DO 444 I=1,M1
0663      IF(NAME(I).NE.NAME2(I))THEN
0664      WRITE(6,879)
0665      GOTO 999
0666      END IF
0667      444 CONTINUE
0668  C
0669  C ***** END OF CHECK *****
0670  C
0671      DO 874 NUMTOPLOT=1,M1
0672      IF(NUMTOPLOT.EQ.1)THEN
0673      GOTO 996
0674      ELSE
0675      GOTO 10

```

```

0676      END IF
0677 874    CONTINUE
0678
0679      WRITE(6,454)
0680      GOTO 999
0681
0682 C      *****
0683 C      ***** AUTOMATED PROCESSING *****
0684 C      *****
0685
0686 731    WRITE(6,997)
0687      P=3
0688      DO 993 NUMTOPLOT=1,M1
0689          IF(NUMTOPLOT.EQ.1)THEN
0690              GOTO 996
0691          ELSE
0692              GOTO 10
0693          END IF
0694 993    CONTINUE
0695      WRITE(6,454)
0696      GOTO 999
0697
0698 C      *****
0699 C      ***** INPUT/OUTPUT FORMATS AND DIALOGUE *****
0700 C      *****
0701 C
0702      5  FORMAT(//1X,'Variable names: '//)
0703      6  FORMAT(2(10X,I3,' ':',A8))
0704      7  FORMAT(//,1X,A75,///
0705      1' Do you wish to change this title (Y or N).....> ', $)
0706      8  FORMAT(A1)
0707 40     FORMAT(//////////
0708      1/'          *          *          *          *          '
0709      2/'          *          *          *          *          '
0710      3/'          *          *          *          *          '
0711      4/'          *          *          *          *          '
0712      5/'          *          *          *          *          '
0713      6/'          *          *          *          *          '
0714      7/'          *          *          *          *          '
0715      8////////
0716      9'          Type C to Continue.....> ', $)
0717 41     FORMAT(A1)
0718 53     FORMAT(10X,': ',<CUMFA>X,'*',<Q>X,1X,F10.2,F7.2)
0719 54     FORMAT(10X,': ',<CUMFA>X,'*',1X,F10.2,F7.2)
0720 60     FORMAT(//////////
0721 1'*****'/
0722 2'*****'/
0723 3////
0724 4'          Minimum - ',F11.2,/
0725 5'          Maximum - ',F11.2,/
0726 6'          N - No Changes.'/
0727 7'          1 - Change Minimum.'/
0728 8'          2 - Change Maximum.'/////
0729 9'          Select Option.....> ', $)
0730 61     FORMAT(A1)
0731 64     FORMAT(//'          Minimum.....> ', $)
0732 65     FORMAT(//'          Maximum.....> ', $)
0733 100    FORMAT(//
0734 1'          Type the .RAW filename for analysis.....> ', $)
0735 107    FORMAT(A79)
0736 108    FORMAT(1X,A79)
0737 109    FORMAT(1X,A79)
0738 110    FORMAT(216)
0739 111    FORMAT(8(1X,A8))
0740 112    FORMAT(//////////1X,A78/)
0741 113    FORMAT(1X,6F13.4)
0742 118    FORMAT(//////////2X,A78/)
0743 115    FORMAT(2X,A8,2X,9F10.2)
0744 125    FORMAT(' ')
0745 117    FORMAT(///,10X,A69,///,10X,'Variable: ',A8)
0746 1117   FORMAT(///,10X,'Variable: ',A8)
0747 171    FORMAT(// 'No. of variable to be processed.....> ', $)
0748 172    FORMAT(12)
0749 175    FORMAT(//////////
0750 1'*****'/

```

```

0751 2' ***** OPTIONS *****'/
0752 3' *****'/
0753 4/' The following output formats are available:/'
0754 5/' 1 - Histograms.'
0755 6/' 2 - Cumulative Frequency Curves.'
0756 7/' 3 - Both (ie.superimposed).'/
0757 8/' Select Option....> ', $)
0758 176 FORMAT(A1)
0759 200 FORMAT(//
0760 1' *****'/
0761 2' ***** FILE TRANSFERED : 'A10' *****'/
0762 3' *****'/
0763 4' FILE TITLE : '//
0764 4 1X,A78//
0765 5' *****'/
0766 6' ***** HAVE A NICE DAY !!!!! *****'/
0767 7' *****'/
0768 350 FORMAT(//1X,'No of Class intervals (5-50).....> ', $)
0769 520 FORMAT(A79)
0770 522 FORMAT(A1)
0771 523 FORMAT(1X,A79)
0772 525 FORMAT(A1)
0773 527 FORMAT('1',////////,11X,A79)
0774 543 FORMAT(A12)
0775 454 FORMAT(//////////)
0776 1' *****'/
0777 1' ***** HISTOGRAMS COMPLETED *****'/
0778 2' *****'/
0779 3 //)
0780 484 FORMAT(1X,A10,A2)
0781 499 FORMAT(1X,F8.2,1X,
0782 1' .-----:-----:-----:-----: ')
0783 500 FORMAT(1X,F8.2,1X,
0784 1' .-----:-----:-----:-----: ')
0785 1/69X,I7)
0786 1501 FORMAT(58X,I4)
0787 501 FORMAT(58X,I4,'%')
0788 502 FORMAT(64X,' Mid.Pt Cf%')
0789 526 FORMAT(60X)
0790 570 FORMAT(1X,'I=',I3)
0791 571 FORMAT(1X,'CELL=',F10.2)
0792 572 FORMAT(1X,'MIN =',F10.2)
0793 575 FORMAT(1X,'CLASSINT=',F10.2)
0794 601 FORMAT(A12)
0795 666 FORMAT(10X,' n =',I4)
0796 1666 FORMAT(10X,' n =',I4,///)
0797 667 FORMAT(64X,' Mid.Pt Cf%',/,56X,I6)
0798 669 FORMAT(
0799 1/' OPTIONS: 1=Quit, 2=Store, 3=Continue .....> ', $)
0800 700 FORMAT(F8.2)
0801 708 FORMAT(1X,'Q=',I4,'CUMFA=',I4)
0802 738 FORMAT(I1)
0803 871 FORMAT(//////////)
0804 1/' *****'/
0805 1/' ***** AUTOMATED PROCESSING *****'/
0806 2/' ***** PRESELECTED RANGE REQUIRED *****'/
0807 2/' *****'////)
0808 872 FORMAT(1X,'Range Filename.....> ', $)
0809 878 FORMAT(//////////)
0810 1/' ***** ERROR *****'/
0811 2/' No. of variables in two data sets incompatable!!',///)
0812 879 FORMAT(//////////)
0813 1/' ***** ERROR *****'/
0814 2/' Order of Names differs in each file!!!!',////)
0815 901 FORMAT(10X,':',A50,1X,F10.2,F7.2)
0816 990 FORMAT(//////////)
0817 1/' ***** HIS *****'/
0818 2/' This program generates HISTOGRAMS from data created'
0819 3/' and stored using the RAW system.'
0820 4/' Histograms can be obtained in three ways:'
0821 5/' 1) Fully automated processing.'
0822 6/' 2) Fully automated processing (fixed class intervals).'
0823 7/' 3) Manual processing (on screen) and selective storage.'
0824 8/' Option No. 2 requires the use of an additional .RAW'
0825 9/' file other than the main data file, which must contain'

```



```
0826      1/' MIN and MAX, the respective Minimum and Maximum values'
0827      1/' required for histogram generation.'/
0828      1/' Select Option.....> ', $)
0829 991  FORMAT(I1)
0830 997  FORMAT(//////////)
0831      1/' *****'
0832      1/' *****  AUTOMATIC PROCESSING  *****'
0833      1/' *****'//)
0834 1010 FORMAT(//////////)
0835      1/' *****'
0836      1/' *****'//
0837      1'      Do you require a preset maximum scale '/'
0838      1'      (if so a third record of MAXIMUM must '/'
0839      2'      be present in the RANGE file.)'//
0840      2'///  Option (1=No, 2=Yes).....> ', $)
0841
0842 999  END
```

```

0001      PROGRAM STA
0002      C
0003      C
0004      C
0005      C
0006      C          *****      *****      *****
0007      C          *              *              *
0008      C          *              *              *
0009      C          *****      *      *****
0010      C              *              *              *
0011      C              *              *              *
0012      C          *****      *              *
0013      C
0014      C
0015      C
0016      C
0017      C      PAUL R. DULLER
0018      C      DEPARTMENT OF APPLIED GEOLOGY
0019      C      THE UNIVERSITY OF STRATHCLYDE
0020      C      GLASGOW
0021      C
0022      C
0023      C      *****
0024      C      ***** INTRODUCTION *****
0025      C      *****
0026      C
0027      C      THIS PROGRAM IS DESIGNED TO STATISTICALLY ASSESS A
0028      C      GENERAL PURPOSE DATA FILE, GENERATED BY THE USER FROM
0029      C      DATA INPUT THROUGH THE .RAW SYSTEM. OUTPUT IS IN THE FORM
0030      C      OF CUSTOMISED 'THESIS READY' SUMMARY TABLES AND OPTIONAL
0031      C      CORRELATION MATRICES.
0032      C
0033      C
0034      C      ++++++
0035      C      ++++++ END OF INTRODUCTION ++++++
0036      C      ++++++
0037      C
0038      C
0039      C      INTEGER X,I,J,L,M,N,O,P,Q,R,S,T,M1,N1,T1,SKIP,Z
0040      C      REAL DATA(100,2000),MIN(100),MAX(100),MEANA(100),MEANG(100)
0041      C      REAL RANGE(100),VAR(100),SDEV(100),SKEW(100),KURT(100),M4(100)
0042      C      REAL SUMX(100),SUMX2(100),V1(100),V2(100),V3(100),V4(100),M2(100)
0043      C      REAL M3(100),SQU1(100),SQU2(100),SQU3(100,100),SQU4(100,100)
0044      C      REAL TABLE(100,10),CV(100),K,SUM(100),COEF(100,100),SQU9(100,100)
0045      C      CHARACTER TITLE*80,FORM*80,SAMPLE(2000)*10,NAME(100)*8,IN*12
0046      C      CHARACTER KEY(2000)*2,SAMPLE1(100)*8,B*1
0047      C      CHARACTER NAME2(100)*8,FORM1*8,FORMX*8,C*1
0048      C
0049      C
0050      C
0051      C      *****
0052      C      ***** DETAILS FOR OTHER PROGRAMMERS *****
0053      C      *****
0054      C
0055      C      M1      = NO OF VARIABLES
0056      C      N1      = NO OF RECORDS
0057      C
0058      C      M2      = SAMPLE MOMENT 2
0059      C      M3      = SAMPLE MOMENT 3
0060      C      M4      = SAMPLE MOMENT 4
0061      C
0062      C      V1      = MEAN
0063      C      V2      = VARIANCE
0064      C      V3      = 3rd Higher MOMENT about the origin
0065      C      V4      = 4th Higher MOMENT about the origin.
0066      C
0067      C      DATA   = INPUT DATA VALUES (FREE FORMAT)
0068      C      TITLE   = TITLE OF FILE (TO IDENTIFY DATAFILE TO USER)
0069      C      FORM    = FORMAT OF OUTPUT DATA
0070      C      NAME    = ARRAY 1 TO M CONTAINING VARIABLE NAMES

```

```

0071 C OUT = INPUT/CREATION .RAW FILE NAME
0072 C SAMPLE= ARRAY 1 TO N CONTAINING SAMPLE NAMES
0073 C KEY = A TWO SYMBOL CODE ATTACHED TO THE END OF THE
0074 C SAMPLE NAME. BY DEFAULT NORMALLY IS " ".
0075 C
0076 C ++++++
0077 C ++++++ END OF DETAILS ++++++
0078 C ++++++
0079 C
0080 C *****
0081 C ***** OUTPUT HEADER *****
0082 C *****
0083 C
0084 43 WRITE(6,40)
0085 READ(5,41)C
0086 IF(C.EQ.'C')THEN
0087 GOTO 42
0088 END IF
0089 GOTO 43
0090 C
0091 C ++++++
0092 C ++++++
0093 C ++++++
0094 C
0095 C
0096 C *****
0097 C ***** INPUT .RAWFILE *****
0098 C *****
0099 C
0100 C ASK FOR FILENAME
0101 C
0102 42 WRITE(6,100)
0103 READ(5,501)IN
0104 OPEN(2,FILE=IN,DEFAULT FILE='.RAW',STATUS='OLD')
0105 C
0106 C READ FILE HEADER AND DATA
0107 C
0108 READ(2,108)TITLE
0109 READ(2,109)FORM
0110 READ(2,110)M1,N1
0111 T1=N1
0112 READ(2,111)(NAME(I),I=1,M1)
0113
0114 DO 435 I=1,N1
0115 READ(2,484)SAMPLE(I),KEY(I)
0116 READ(2,113)(DATA(J,I),J=1,M1)
0117 435 CONTINUE
0118 C
0119 C SELECT OPTION
0120 C
0121 79 WRITE(6,881)
0122 READ(5,8)C
0123
0124 IF(C.EQ.'2')THEN
0125 GOTO 1998
0126 END IF
0127
0128 IF(C.EQ.'1')THEN
0129 GOTO 79
0130 END IF
0131
0132 C *****
0133 C ***** STATISTICAL PACKAGE *****
0134 C *****
0135 C
0136 C *****
0137 C ARITHMETIC MEAN
0138 C *****
0139 C
0140 C TO COMPUTE THE MEAN OF N1 SAMPLES FOR M1 VARIABLES
0141 C
0142 104 DO 99 I=1,M1
0143 SUMX(I)=0.00
0144 DO 114 J=1,N1
0145 SUMX(I)=SUMX(I)+DATA(I,J)

```

```

0146      114 CONTINUE
0147
0148      MEANA(I)=SUMX(I)/N1
0149      99 CONTINUE
0150      C
0151      C *****
0152      C GEOMETRIC MEAN
0153      C *****
0154      C
0155      C TO COMPUTE THE GEOMETRIC MEAN OF N1 SAMPLES FOR M1 VARIABLES
0156      C
0157      DO 85 I=1,M1
0158      T=1
0159      777 IF(DATA(I,T).EQ.0.00)THEN
0160
0161      IF(T.EQ.N1)THEN
0162      MEANG(I)=0.00
0163      GOTO 85
0164      END IF
0165
0166      T=T+1
0167      GOTO 777
0168      END IF
0169
0170      SUMX(I)=LOG(DATA(I,T))
0171
0172      T=T+1
0173      DO 84 J=T,N1
0174      IF(DATA(I,J).LE.0.00)THEN
0175      GOTO 84
0176      END IF
0177      SUMX(I)=SUMX(I)+LOG(DATA(I,J))
0178      84 CONTINUE
0179      SUMX(I)=SUMX(I)/N1
0180      MEANG(I)=EXP(SUMX(I))
0181      85 CONTINUE
0182
0183      C *****
0184      C VARIANCE AND STANDARD DEVIATION
0185      C *****
0186      C
0187      DO 97 I=1,M1
0188
0189      SUMX(I)=0.00
0190      SUMX2(I)=0.00
0191
0192      DO 96 J=1,N1
0193
0194      SUMX(I)=SUMX(I)+DATA(I,J)
0195      SUMX2(I)=SUMX2(I)+DATA(I,J)*DATA(I,J)
0196
0197      96 CONTINUE
0198
0199      VAR(I) =(SUMX2(I)-N1*MEANA(I)**2)/(N1-1)
0200
0201      IF(VAR(I).LT.0.0000)THEN
0202      VAR(I)=0.0000
0203      SDEV(I)=0.0000
0204      GOTO 97
0205      END IF
0206
0207      SDEV(I)=SQRT(VAR(I))
0208
0209      97 CONTINUE
0210      C
0211      C *****
0212      C MINIMUM, MAXIMUM AND RANGE
0213      C *****
0214      C
0215      C TO COMPUTE THE MINIMUM,MAXIMUM AND RANGE
0216      C OF N1 SAMPLES FOR M1 VARIABLES
0217      C
0218      C SET SUM TO ZERO
0219      C
0220      C

```

```

0221
0222      DO 98 I=1,M1
0223      J=1
0224      SUMX(I)=DATA(I,J)
0225      SUMX2(I)=DATA(I,J)
0226
0227      DO 95 J=2,N1
0228
0229      K=DATA(I,J)
0230
0231      IF (K.GT.SUMX(I)) THEN
0232      SUMX(I)=K
0233      END IF
0234
0235      IF (K.LT.SUMX2(I)) THEN
0236      SUMX2(I)=K
0237      END IF
0238
0239      95 CONTINUE
0240  C
0241      MAX(I)=SUMX(I)
0242      MIN(I)=SUMX2(I)
0243      RANGE(I)=MAX(I)-MIN(I)
0244
0245      98 CONTINUE
0246
0247  C *****
0248  C COEFFICIENT OF VARIABILITY : %CV
0249  C *****
0250
0251      DO 778 I=1,M1
0252      IF (MEANA(I).EQ.0) THEN
0253      CV(I)=0.0
0254      GOTO 778
0255      END IF
0256      CV(I)=(SDEV(I)/MEANA(I))*100
0257      778 CONTINUE
0258
0259  C *****
0260  C SKEWNESS AND KURTOSIS
0261  C *****
0262  C
0263  C THE SKEWNESS AND KURTOSIS CALCULATED IN THIS PROGRAM
0264  C MAKE USE OF THE SAMPLE CENTRAL MOMENTS AS DEFINED BY
0265  C BENNETT AND FRANKLIN (1954) STATISTICAL ANALYSIS IN
0266  C CHEMISTRY AND THE CHEMICAL INDUSTRY. WILEY 724pp.
0267  C
0268  C
0269      DO 80 I=1,M1
0270
0271      SKEW(I)=0.00
0272      KURT(I)=0.00
0273      V1(I)=0
0274      V2(I)=0
0275      V3(I)=0
0276      V4(I)=0
0277
0278      DO 81 J=1,N1
0279
0280      V1(I)=V1(I)+DATA(I,J)
0281      V2(I)=V2(I)+DATA(I,J)**2
0282      V3(I)=V3(I)+DATA(I,J)**3
0283      V4(I)=V4(I)+DATA(I,J)**4
0284
0285      81 CONTINUE
0286
0287      V1(I)=V1(I)/N1
0288      V2(I)=V2(I)/N1
0289      V3(I)=V3(I)/N1
0290      V4(I)=V4(I)/N1
0291
0292      M2(I)=V2(I)-(V1(I)**2)
0293      M3(I)=V3(I)-(3*V2(I)*V1(I))+(2*V1(I)**3)
0294      M4(I)=V4(I)-(4*V3(I)*V1(I))+(6*V2(I)*V1(I)**2)-(3*V1(I)**4)
0295
0296      IF (M2(I).LE.0) THEN

```

```

0297      SKEW(I)=0.0
0298      KURT(I)=0.0
0299      GOTO 80
0300      END IF
0301
0302      SKEW(I)=M3(I)/(M2(I)**1.5)
0303      KURT(I)=M4(I)/(M2(I)**2.0)
0304
0305      80  CONTINUE
0306
0307      GOTO 1010
0308
0309      C
0310      C *****
0311      C CORRELATION COEFFICIENTS
0312      C *****
0313      C
0314      C The correlation coefficients calculated within this program
0315      C make use of the algorithms defined by DAVIS (1973) Statistics
0316      C and Data analysis in Geology.
0317      C
0318      998 WRITE(6,800)
0319      READ(5,8)B
0320
0321      IF(B.EQ.'N')THEN
0322      GOTO 999
0323      END IF
0324
0325      IF(B.NE.'Y')THEN
0326      GOTO 998
0327      END IF
0328
0329      1998 DO 1000 I=1,M1
0330      SUM(I)=0
0331      DO 1001 J=1,N1
0332      SUM(I)=SUM(I)+DATA(I,J)
0333      1001 CONTINUE
0334      1000 CONTINUE
0335
0336      DO 1002 I=1,M1
0337      SQU1(I)=0
0338      DO 1003 J=1,N1
0339      SQU1(I)=SQU1(I)+DATA(I,J)*DATA(I,J)
0340      1003 CONTINUE
0341      1002 CONTINUE
0342      DO 1004 I=1,M1
0343      SQU2(I)=(SUM(I)*SUM(I))/N1
0344      1004 CONTINUE
0345
0346      DO 1005 I=1,M1
0347      DO 1006 J=1,M1
0348      SQU3(I,J)=(SUM(I)*SUM(J))/N1
0349      SQU4(I,J)=0
0350
0351      DO 1007 K=1,N1
0352      SQU4(I,J)=SQU4(I,J)+(DATA(I,K)*DATA(J,K))
0353      1007 CONTINUE
0354
0355      SQU4(I,J)=SQU4(I,J)-SQU3(I,J)
0356      SQU9(I,J)=SQRT((SQU1(I)-SQU2(I))*(SQU1(J)-SQU2(J)))
0357      COEF(I,J)=SQU4(I,J)/SQU9(I,J)
0358
0359      1006 CONTINUE
0360      1005 CONTINUE
0361
0362      GOTO 1111
0363
0364      C
0365      C ++++++
0366      C ++++++ END OF STATISTICAL ASSESSMENT ++++++
0367      C ++++++
0368      C
0369
0370
0371      C

```



```

0372 C *****
0373 C ***** SET UP OUTPUT FILES *****
0374 C *****
0375 C
0376 C *****
0377 C STATISTICS TABLES
0378 C *****
0379 C
0380 C FOR THE OUTPUT SECTION OF THIS PACKAGE N1 (No. OF SAMPLES)
0381 C IS REASSIGNED TO N THE NUMBER OF STATISTICAL FUNCTIONS CARRIED
0382 C OUT, TOGETHER WITH SAMPLE, WHICH IS ASSIGNED THE RESPECTIVE
0383 C NAMES OF EACH OF THE FUNCTIONS, AND TABLE, AN ARRAY CONTAINING
0384 C THE RESPECTIVE STATISTICAL RESULTS.
0385 C
0386 1010 N=9
0387 SAMPLE1(1)='Min'
0388 SAMPLE1(2)='Max'
0389 SAMPLE1(3)='Mean'
0390 SAMPLE1(4)='Range'
0391 SAMPLE1(5)='St.Dev'
0392 SAMPLE1(6)='Skew'
0393 SAMPLE1(7)='Kurt'
0394 SAMPLE1(8)='G.Mean'
0395 SAMPLE1(9)='%CV'
0396
0397 DO 75 I=1,M1
0398
0399 TABLE(1,I)=MIN(I)
0400 TABLE(2,I)=MAX(I)
0401 TABLE(3,I)=MEANA(I)
0402 TABLE(4,I)=RANGE(I)
0403 TABLE(5,I)=SDEV(I)
0404 TABLE(6,I)=SKEW(I)
0405 TABLE(7,I)=KURT(I)
0406 TABLE(8,I)=MEANG(I)
0407 TABLE(9,I)=CV(I)
0408
0409 75 CONTINUE
0410 C
0411 C *****
0412 C ***** STATISTICAL TABLES STYLE 1 *****
0413 C *****
0414 C
0415 C RIGHT JUSTIFY ALL SAMPLE NAMES
0416 C FORM AND FORM1 ARE CHARACTER BUFFERS
0417 C NB ARRAY KEY IS UNAFFECTED
0418 C
0419 DO 4 I=1,N
0420 FORMX=SAMPLE1(I)
0421 DO 3 I1=8,1,-1
0422 IF(FORMX(I1:I1).NE.' ')THEN
0423 GOTO 2
0424 END IF
0425 3 CONTINUE
0426 I1=1
0427 2 FORM1=' '
0428 J=8-I1+1
0429 FORM1(J:8)=FORMX(1:I1)
0430 SAMPLE1(I)=FORM1
0431 4 CONTINUE
0432
0433 Y=0
0434 C
0435 C OUTPUT STATISTICS TO THE VDU AND ASK USER IF HE
0436 C REQUIRES OUTPUT TO BE STORED FOR LATER PLOTTING.
0437 C
0438 C
0439 C VDU HEADING
0440 C *****
0441 C
0442 WRITE(6,413)IN,(SAMPLE1(K),K=1,N)
0443 WRITE(6,125)
0444 C
0445 C VDU DATA
0446 C *****

```

```

0447 C
0448 DO 414 J=1,M1
0449 WRITE(6,415)(NAME(J),(TABLE(K,J),K=1,N))
0450 414 CONTINUE
0451 C
0452 C *****
0453 C ASK USER IF HE REQUIRES DATA TO BE STORED/ARCHIVED
0454 C *****
0455 C
0456
0457 994 WRITE(6,990)
0458 READ(5,991)B
0459
0460 IF(B.EQ.'N')THEN
0461 GOTO 998
0462 END IF
0463
0464 IF(B.NE.'Y')THEN
0465 GOTO 994
0466 END IF
0467
0468 WRITE(6,7)TITLE
0469 READ(5,8)B
0470 IF(B.EQ.'Y')THEN
0471 WRITE(6,117)
0472 READ(5,107)TITLE
0473 END IF
0474 C
0475 C *****
0476 C TABLES OF STATISTICS ARE AUTOMATICALLY OUTPUT TO
0477 C A .STA FILE, HAVING THE SAME NAME AS THE ORIGINAL
0478 C .RAWFILE ON WHICH THE ANALYSES WERE CARRIED OUT.
0479 C *****
0480 C
0481 802 OPEN(2,FILE=IN,DEFAULT FILE='.STA',STATUS='NEW')
0482 C
0483 C GIVE USER THE OPERTUNITY TO REMOVE ONE OR MORE
0484 C PARAMETERS.
0485 C
0486 WRITE(6,737)
0487 READ(5,738)N
0488 C
0489 C OUTPUT/STORAGE HEADING
0490 C *****
0491 C
0492 992 WRITE(2,118)TITLE
0493 WRITE(2,116)(SAMPLE1(K),K=1,N)
0494 WRITE(2,125)
0495 C
0496 C STORAGE DATA
0497 C *****
0498 C
0499 DO 421 J=1,M1
0500 WRITE(2,115)(NAME(J),(TABLE(K,J),K=1,N))
0501 421 CONTINUE
0502 C
0503 WRITE(2,995)T1
0504 C
0505 C INFORM USER THAT TABLES COMPLETE
0506 C
0507 453 WRITE(6,454)
0508 GOTO 998
0509 C
0510 C *****
0511 C CORRELATION COEFFICIENT TABLES
0512 C *****
0513 C
0514 C PRODUCE AN ARRAY OF RIGHT JUSTIFIED VARIABLE NAMES FOR
0515 C THE TOP ROW OF THE OUTPUT TABLES
0516 C
0517 C FORM AND FORM1 ARE CHARACTER BUFFERS
0518 C
0519 1111 IF(C.EQ.'2')THEN
0520 OPEN(2,FILE=IN,DEFAULT FILE='.STA',STATUS='NEW')
0521 END IF

```

```

0522
0523      DO 14 P=1,M1
0524      FORMX=NAME(P)
0525      DO 13 I=8,1,-1
0526      IF (FORMX(I:I).NE.' ') THEN
0527      GOTO 12
0528      END IF
0529      13 CONTINUE
0530      I=1
0531      12 FORM1=' '
0532      J=8-I+1
0533      FORM1(J:8)=FORMX(1:I)
0534      NAME2(P)=FORM1
0535      14 CONTINUE
0536      C
0537      C      LABELS FOR CORRELATION MATRIX NAME2(M1) x NAME(M1)
0538      C
0539      C      DEFINE THE NUMBER OF COMPLETE PAGES (L) REQUIRED FOR THE
0540      C      OUTPUT TABLE AND THE NUMBER OF INCOMPLETE RECORDS IN THE
0541      C      LAST BLOCK (Q).
0542      C
0543      L1=0
0544      Q=M1
0545      830 IF (Q.GE.10) THEN
0546      L1=L1+1
0547      Q=Q-10
0548      GOTO 830
0549      END IF
0550      C
0551      C      INFORM USER OF OUTPUT FORMATS AVAILABLE
0552      C
0553      1114 WRITE(6,820)
0554      READ(5,8)B
0555
0556      IF (B.EQ.'1') THEN
0557      GOTO 1113
0558      END IF
0559
0560      IF (B.NE.'2') THEN
0561      GOTO 1114
0562      END IF
0563
0564      GOTO 1115
0565      C
0566      C      *****
0567      C      COMPLETE MATRIX
0568      C      *****
0569      C
0570      C      SET UP OUTPUT TABLE
0571      C
0572      1113 DO 850 I=1,L1
0573
0574      X=10*(I-1)+1
0575      Y=10*(I-1)+10
0576
0577      C      PRINT ONE COMPLETE PAGE
0578
0579      C      HEADING LISTED ONLY ONCE
0580      IF (I.LE.1) THEN
0581      WRITE(2,300) TITLE
0582      ELSE
0583      WRITE(2,301)
0584      END IF
0585
0586      WRITE(2,860) (NAME2(K), K=X,Y)
0587
0588      DO 861 J=1,M1
0589      WRITE(2,862) NAME(J), (COEF(K,J), K=X,Y)
0590      861 CONTINUE
0591
0592      IF (I.EQ.1) THEN
0593      WRITE(2,2000) N1
0594      END IF
0595
0596      850 CONTINUE

```

```

0597 C
0598 C CHECK IF ANY INCOMPLETE PAGES REMAIN TO BE PRINTED
0599 C
0600 IF(Q.LT.1)THEN
0601 WRITE(2,2001)
0602 GOTO 871
0603 END IF
0604 C
0605 C PRINT REMAINING INCOMPLETE PAGE
0606 C
0607 X=Y+1
0608 Y=Y+Q
0609
0610 WRITE(2,301)
0611 WRITE(2,860)(NAME2(K),K=X,Y)
0612 DO 875 J=1,M1
0613 WRITE(2,862)NAME(J),(COEF(K,J),K=X,Y)
0614 875 CONTINUE
0615 WRITE(2,2001)
0616 C INFORM USER MATRIX COMPLETE
0617 871 WRITE(6,810)
0618 GOTO 999
0619 C
0620 C
0621 C *****
0622 C HALF MATRIX
0623 C *****
0624 C
0625 1115 DO 857 I=1,L1
0626
0627 X=10*(I-1)+1
0628 Y=10*(I-1)+9
0629
0630 C PRINT ONE COMPLETE PAGE WITH HEADING LISTED ONLY ONCE
0631
0632 IF(I.LE.1)THEN
0633 WRITE(2,300)TITLE
0634 ELSE
0635 WRITE(2,301)
0636 END IF
0637
0638 L=Y+1
0639 WRITE(2,860)(NAME2(K),K=X,L)
0640
0641 L=0
0642 SKIP=0
0643
0644 IF(I.GT.1)THEN
0645 SKIP=10*(I-1)
0646
0647 DO 666 J=1,SKIP
0648 WRITE(2,1871)NAME(J)
0649 666 CONTINUE
0650
0651 END IF
0652
0653 L=SKIP
0654 DO 833 J=X,M1
0655 IF(L.LE.Y)THEN
0656 L=L+1
0657 END IF
0658 WRITE(2,862)NAME(J),(COEF(K,J),K=X,L)
0659 833 CONTINUE
0660
0661 IF(I.EQ.1)THEN
0662 WRITE(2,2000)N1
0663 END IF
0664
0665 857 CONTINUE
0666 C
0667 C CHECK IF ANY INCOMPLETE PAGES REMAIN TO BE PRINTED
0668 C
0669 IF(Q.LT.1)THEN
0670 WRITE(2,2001)
0671 GOTO 871

```

```

0672      END IF
0673      C
0674      C *****
0675      C PRINT REMAINING INCOMPLETE PAGE
0676      C *****
0677
0678      X=10*L1+1
0679      Y=M1
0680
0681      WRITE(2,301)
0682      WRITE(2,1860)(NAME2(K),K=X,Y)
0683      WRITE(2,1861)
0684      L=0
0685      I=L1+1
0686
0687      IF(I.GT.1)THEN
0688      SKIP=10*L1
0689      DO 667 J=1,SKIP
0690      WRITE(2,1871)NAME(J)
0691      667 CONTINUE
0692      END IF
0693
0694      L=SKIP
0695
0696      DO 888 J=X,M1
0697      IF(L.LE.Y)THEN
0698      L=L+1
0699      END IF
0700      WRITE(2,862)NAME(J),(COEF(K,J),K=X,L)
0701      888 CONTINUE
0702      C
0703      C INFORM USER MATRIX COMPLETED
0704      C
0705      WRITE(2,2001)
0706      WRITE(6,810)
0707      GOTO 999
0708
0709      C ++++++
0710      C ++++++ END OF OUTPUT TABLES ++++++
0711      C ++++++
0712      C
0713      C *****
0714      C ***** INPUT/OUTPUT FORMATS AND DIALOGUE *****
0715      C *****
0717      5 FORMAT(//1X,'Variable names: '//)
0718      6 FORMAT(2(10X,I3,': ',A8))
0719      7 FORMAT(//,1X,A75,///)
0720      1' Do you wish to change this title (Y or N).....> ', $)
0721      8 FORMAT(A1)
0722      40 FORMAT(//////////)
0723      1/' *****
0724      2/' * * * * *
0725      3/' * * * * *
0726      4/' *****
0727      5/' * * * * *
0728      6/' * * * * *
0729      7/' *****
0730      8////////
0731      9' Type C to Continue.....> ', $)
0732      41 FORMAT(A1)
0733      100 FORMAT(///)
0734      1' Type the .RAW filename for analysis.....> ', $)
0735      107 FORMAT(A79)
0736      108 FORMAT(1X,A79)
0737      109 FORMAT(1X,A79)
0738      110 FORMAT(2I6)
0739      111 FORMAT(8(1X,A8))
0740      112 FORMAT(//////////1X,A78/)
0741      113 FORMAT(1X,6F13.4)
0742      116 FORMAT(20X,'VAR. / STAT.',A8,8(2X,A8))
0743      115 FORMAT(20X,A8,2X,9F10.2)
0744      118 FORMAT(//////////,20X,A78,/,20X,'Summary Statistics:',/)
0745      125 FORMAT(' ')
0746      117 FORMAT(///' Type new TITLE .....> ', $)

```

```

0747 200 FORMAT(//
0748 1' *****'//
0749 2' ***** FILE TRANSFERED : 'A10' *****'//
0750 3' *****'//
0751 4' FILE TITLE : '//
0752 4 1X,A78//
0753 5' *****'//
0754 6' ***** HAVE A NICE DAY !!!!! *****'//
0755 7' *****')
0756 300 FORMAT(1X,A78,/' Correlation Coefficients:',/)
0757 301 FORMAT(////////)
0758 407 FORMAT('/ The number of variables are.....> ',I2)
0759 408 FORMAT('/ The number of samples are.....> ',I2)
0760 409 FORMAT('/ The variable names are: '/(5X,6A8)/)
0761 413 FORMAT(//////////1X,10A8)
0762 415 FORMAT(1X,A8,9F8.2)
0763 417 FORMAT(////////11X,A79)
0764 418 FORMAT('/ Change title (Y or N).....> ', $)
0765 419 FORMAT(A79)
0766 420 FORMAT(A79)
0767 422 FORMAT(A1)
0768 423 FORMAT(1X,A79)
0769 425 FORMAT(A1)
0770 427 FORMAT('1',////////,11X,A79)
0771 443 FORMAT(A12)
0772 454 FORMAT(//////////)
0773 1' *****'//
0774 1' ***** STATISTICS COMPLETED *****'//
0775 2' *****'//
0776 3 ///)
0777 484 FORMAT(1X,A10,A2)
0778 501 FORMAT(A12)
0779 737 FORMAT(////////)
0780 1/' *****'
0781 1/' *****'
0782 2/' STA is able to reduce the number of statistical variables'
0783 3/' transfered to the results file. '//
0784 5/' 1. Min.'
0785 6/' 2. ....+Max.'
0786 7/' 3. ....+Mean.'
0787 8/' 4. ....+Range.'
0788 1/' 5. ....+St.Dev.'
0789 5/' 6. ....+Skew.'
0790 8/' 7. ....+Kurt.'
0791 8/' 8. ....+G.Mean.'
0792 8/' 9. ....+ CV%.'//
0793 4/' Select the number of variables you require (1-9)....> ', $)
0794 738 FORMAT(I1)
0795 800 FORMAT(//////////)
0796 1' Do you require Correlation Coefficients (Y or N)....> ', $)
0797 810 FORMAT(//////////)
0798 1/' *****'
0799 2/' ** CORRELATION MATRIX COMPLETED AND STORED IN .STA FILE **'
0800 3/' *****'
0801 4/' ***** BYE ! *****'
0802 5/' *****'
0803 6////////)
0804 820 FORMAT(//////////)
0805 1/' *****'
0806 2/' ***** CORRELATION COEFFICIENTS *****'
0807 3/' *****'
0808 3//' Two possible output formats are available:'
0809 3//' 1 - Complete matrix.'
0810 3//' 2 - Half matrix.'//
0811 3//' Please select your option.....> ', $)
0812 860 FORMAT(16X,10(1X,A8),/)
0813 1860 FORMAT(16X,10(1X,A8))
0814 1861 FORMAT()
0815 862 FORMAT(1X,A8,7X,10F9.2)
0816 863 FORMAT(16X,10F9.2)
0817 1871 FORMAT(1X,A8)
0818 881 FORMAT(//////////)
0819 1/' *****'
0820 1/' ***** OPTIONS *****'
0821 1/' *****'

```



```

0822      1/////      1 - Basic Stats.'
0823      2/'          2 - Correlation Coefficients.'
0824      3/////
0825      4'          Please select your option.....> ', $)
0826
0827 990 FORMAT(/
0828      1 ' Store in .STA format (Y or N).....> ', $)
0829 991 FORMAT(A1)
0830 995 FORMAT(/,20X,'n = ',I4,24(/))
0831 2000 FORMAT('/' n =',I4)
0832 2001 FORMAT(//////////)
0833 999 END

```

```

0001      PROGRAM RAT
0002      C
0003      C
0004      C
0005      C
0006      C
0007      C          *****      *****      *****
0008      C          *      *      *      *      *
0009      C          *      *      *      *      *
0010      C          *****      *****      *
0011      C          *      *      *      *      *
0012      C          *      *      *      *      *
0013      C          *      *      *      *      *
0014      C
0015      C
0016      C
0017      C
0018      C      PAUL R. DULLER
0019      C      DEPARTMENT OF APPLIED GEOLOGY
0020      C      THE UNIVERSITY OF STRATHCLYDE
0021      C      GLASGOW
0022      C
0023      C
0024      C      ***** INTRODUCTION *****
0025      C
0026      C      THIS PROGRAM IS DESIGNED TO READ      A SELF DESCRIBING
0027      C      GENERAL PURPOSE DATA FILE, GENERATED BY THE USER FROM
0028      C      DATA INPUT THROUGH THE RAW SYSTEM.
0029      C
0030      C      THE OBJECT OF THIS PROGRAM IS TO CALCULATE A SERIES OF
0031      C      COMPLEX RATIOS FROM THE STANDARD NUMERIC DATAFILE AND
0032      C      APPEND THIS DATA TO THE OUTPUT DATAFILE.
0033      C
0034      C      THE FORMAT OF THE INPUT FILE STRUCTURE IS:
0035      C
0036      C      RECORD 1 A80      TITLE
0037      C      RECORD 2 A80      FORMAT OF DATA - USUALLY F13.4
0038      C      RECORD 3 2I2      NO OF VARIABLES AND NO OF RECORDS, OR 0
0039      C
0040      C      RECORD4+ 8(X,A8)      VARIABLE NAMES, 8 PER LINE
0041      C
0042      C      RECORD N A12      SAMPLE NAME
0043      C
0044      C      RECORD N+      RAW DATA (SEE RECORD 2)
0045      C
0046      C
0047      C      INTEGER X,I,J,K,M1,N1,M2,M3
0048      C      INTEGER POS1,POS2,POS3,POS4,POS5,POS6,POS7,POS8,POS9,POS10
0049      C      INTEGER POS11,POS12,POS13,POS14,POS15,POS16,POS17,POS18
0050      C      REAL DATA(100,2000),SUM
0051      C      CHARACTER TITLE*80,FORM*80,SAMPLE(2000)*10,NAME(100)*8,IN*12
0052      C      CHARACTER BIN*12,KEY(2000)*2
0053      C
0054      C      ***** DETAILS FOR OTHER PROGRAMMERS *****
0055      C
0056      C      M1      = NO OF VARIABLES
0057      C      N1      = NO OF RECORDS
0058      C      DATA   = INPUT DATA VALUES (FREE FORMAT)
0059      C      TITLE   = TITLE OF FILE (TO IDENTIFY DATAFILE TO USER)
0060      C      FORM    = FORMAT OF OUTPUT DATA
0061      C      NAME    = ARRAY 1 TO M CONTAINING VARIABLE NAMES
0062      C      OUT     = INPUT/CREATION .RAW FILE NAME
0063      C      SAMPLE  = ARRAY 1 TO N CONTAINING SAMPLE NAMES
0064      C      KEY     = A TWO SYMBOL CODE ATTACHED TO THE END OF THE
0065      C                  SAMPLE NAME. BY DEFAULT NORMALLY IS ' '.
0066      C
0067      C      ASK FOR FILENAME
0068      C      *****
0069      C
0070      C      WRITE(6,100)
0071      C      READ(5,501)IN
0072      C      OPEN(2,FILE=IN,DEFAULT FILE='.RAW',STATUS='OLD')
0073      C
0074      C
0075      C      READ FILE HEADER AND DATA

```

```

0076 C *****
0077 C
0078 READ(2,108)TITLE
0079 READ(2,109)FORM
0080 READ(2,110)M1,N1
0081 READ(2,111)(NAME(I),I=1,M1)
0082
0083 DO 435 I=1,N1
0084 READ(2,484)SAMPLE(I),KEY(I)
0085 READ(2,113)(DATA(J,I),J=1,M1)
0086 435 CONTINUE
0087
0088 C ***** LIST VARIABLES *****
0089
0090 104 L=0
0091 P1=M1
0092 11 IF(P1.GE.3)THEN
0093 L=L+1
0094 P1=P1-2
0095 GOTO 11
0096 END IF
0097
0098 C NO OF REMAINING SAMPLES FORMING LESS THAN ONE COMPLETE
0099 C ROW = P1.
0100
0101 C OUTPUT VARIABLE NAMES
0102 C *****
0103
0104 Y=0
0105 IF(L.EQ.0)THEN
0106 GOTO 12
0107 END IF
0108 C
0109 WRITE(6,5)
0110 DO 13 I=1,L
0111 X=Y+1
0112 Y=Y+2
0113 WRITE(6,6)((J,NAME(J)),J=X,Y)
0114 13 CONTINUE
0115 IF(P1.EQ.0)THEN
0116 GOTO 15
0117 END IF
0118 12 Y=M1-P1+1
0119 WRITE(6,6)((J,NAME(J)),J=Y,M1)
0120 GOTO 15
0121 15 X=0
0122 C
0123 C ***** CHECK THAT ALL THE VARIABLES REQUIRED EXIST
0124 C AND DEFINE THEIR POSITION IN THE DATA ARRAY
0125 C
0126 K=0
0127
0128 DO 1499 I=1,M1
0129
0130 IF(NAME(I).EQ.'SiO2')then
0131 POS1=I
0132 K=K+1
0133 GOTO 1499
0134 END IF
0135
0136 IF(NAME(I).EQ.'Al2O3')then
0137 POS2=I
0138 K=K+1
0139 GOTO 1499
0140 END IF
0141
0142 IF(NAME(I).EQ.'Fe2O3')then
0143 POS3=I
0144 K=K+1
0145 GOTO 1499
0146 END IF
0147
0148 IF(NAME(I).EQ.'MgO')then
0149 POS4=I
0150 K=K+1

```

```
0151      GOTO 1499
0152      END IF
0153
0154      IF (NAME(I).EQ.'CaO')then
0155      POS5=I
0156      K=K+1
0157      GOTO 1499
0158      END IF
0159
0160      IF (NAME(I).EQ.'Na2O')then
0161      POS6=I
0162      K=K+1
0163      GOTO 1499
0164      END IF
0165
0166      IF (NAME(I).EQ.'K2O')then
0167      POS7=I
0168      K=K+1
0169      GOTO 1499
0170      END IF
0171
0172      IF (NAME(I).EQ.'La')then
0173      POS8=I
0174      K=K+1
0175      GOTO 1499
0176      END IF
0177
0178      IF (NAME(I).EQ.'Y')then
0179      POS9=I
0180      K=K+1
0181      GOTO 1499
0182      END IF
0183
0184      IF (NAME(I).EQ.'Nb')then
0185      POS10=I
0186      K=K+1
0187      GOTO 1499
0188      END IF
0189
0190      IF (NAME(I).EQ.'P2O5')then
0191      POS11=I
0192      K=K+1
0193      GOTO 1499
0194      END IF
0195
0196      IF (NAME(I).EQ.'Rb')then
0197      POS12=I
0198      K=K+1
0199      GOTO 1499
0200      END IF
0201
0202      IF (NAME(I).EQ.'Sr')then
0203      POS13=I
0204      K=K+1
0205      GOTO 1499
0206      END IF
0207
0208      IF (NAME(I).EQ.'Ni')then
0209      POS14=I
0210      K=K+1
0211      GOTO 1499
0212      END IF
0213
0214      IF (NAME(I).EQ.'Co')then
0215      POS15=I
0216      K=K+1
0217      GOTO 1499
0218      END IF
0219
0220      IF (NAME(I).EQ.'Cu')then
0221      POS16=I
0222      K=K+1
0223      GOTO 1499
0224      END IF
0225
```

```

0226      IF (NAME(I).EQ.'Zr')then
0227      POS17=I
0228      K=K+1
0229      GOTO 1499
0230      END IF
0231
0232      IF (NAME(I).EQ.'Zn')then
0233      POS18=I
0234      K=K+1
0235      GOTO 1499
0236      END IF
0237
0238
0239      1499 CONTINUE
0240
0241      IF (K.NE.18)THEN
0242      C
0243      C      WRITE ERROR MESSAGE - TOO FEW VARIABLES PRESENT
0244      C
0245      K=18-K
0246      WRITE(6,1500)K
0247      GOTO 999
0248      END IF
0249      C
0250      C      SET UP NEW VARIABLE NAMES
0251      C
0252      M2=M1+1
0253      NAME(M2)='K/Na'
0254
0255      M2=M2+1
0256      NAME(M2)='Al/Si'
0257
0258      M2=M2+1
0259      NAME(M2)='Fe/Mg'
0260
0261      M2=M2+1
0262      NAME(M2)='Fe/Mg'
0263
0264      M2=M2+1
0265      NAME(M2)='Al/Ca+Na'
0266
0267      M2=M2+1
0268      NAME(M2)='La/Y'
0269
0270      M2=M2+1
0271      NAME(M2)='Nb/Y'
0272
0273      M2=M2+1
0274      NAME(M2)='Nb/P'
0275
0276      M2=M2+1
0277      NAME(M2)='Rb/Sr'
0278
0279      M2=M2+1
0280      NAME(M2)='Ni/Co'
0281
0282      M2=M2+1
0283      NAME(M2)='Cu/Co'
0284
0285      M2=M2+1
0286      NAME(M2)='Zn/Co'
0287
0288      M2=M2+1
0289      NAME(M2)='Zr/Nb'
0290
0291      M2=M2+1
0292      NAME(M2)='K/K+Na'
0293
0294      M2=M2+1
0295      NAME(M2)='K+Na'
0296
0297      J=M1+1
0298
0299      DO 1501 I=J,M2
0300      WRITE(6,1502)NAME(I)

```

```

0301      1501 CONTINUE
0302
0303      C ***** CACULATE RATIO'S *****
0304
0305          DO 1505 I=1,N1
0306      C
0307      C      K2O/Na2O
0308      C      *****
0309
0310          M2=M1+1
0311
0312          IF (DATA(POS7,I).EQ.0.00)THEN
0313              DATA(M2,I)=0
0314              GOTO 301
0315          END IF
0316
0317          IF (DATA(POS6,I).EQ.0.00)THEN
0318              DATA(M2,I)=0
0319              GOTO 301
0320          END IF
0321
0322          DATA(M2,I)=DATA(POS7,I)/DATA(POS6,I)
0323      C
0324      C      AL2O3/SiO2
0325      C      *****
0326
0327      301 M2=M2+1
0328
0329          IF (DATA(POS2,I).EQ.0.00)THEN
0330              DATA(M2,I)=0
0331              GOTO 302
0332          END IF
0333          IF (DATA(POS1,I).EQ.0.00)THEN
0334              DATA(M2,I)=0
0335              GOTO 302
0336          END IF
0337
0338          DATA(M2,I)=DATA(POS2,I)/DATA(POS1,I)
0339      C
0340      C      FE2O3/MGO
0341      C      *****
0342      302 M2=M2+1
0343          DATA(M2,I)=DATA(POS3,I)+DATA(POS4,I)
0344      C
0345      C      FE2O3/MGO
0346      C      *****
0347
0348          M2=M2+1
0349          IF (DATA(POS3,I).EQ.0.00)THEN
0350              DATA(M2,I)=0
0351              GOTO 303
0352          END IF
0353          IF (DATA(POS4,I).EQ.0.00)THEN
0354              DATA(M2,I)=0
0355              GOTO 303
0356          END IF
0357          DATA(M2,I)=DATA(POS3,I)/DATA(POS4,I)
0358      C
0359      C      AL2O3/(CAO+NA2O)
0360      C      *****
0361
0362      303 M2=M2+1
0363          IF (DATA(POS2,I).EQ.0.00)THEN
0364              DATA(M2,I)=0
0365              GOTO 304
0366          END IF
0367
0368          SUM=DATA(POS5,I)+DATA(POS6,I)
0369
0370          IF (SUM.EQ.0.00)THEN
0371              DATA(M2,I)=0
0372              GOTO 304
0373          END IF
0374
0375          DATA(M2,I)=DATA(POS2,I)/(DATA(POS5,I)+DATA(POS6,I))

```



```

0376 C
0377 C LA/Y
0378 C ****
0379
0380 304 M2=M2+1
0381 IF (DATA(POS8,I).EQ.0.00)THEN
0382 DATA(M2,I)=0
0383 GOTO 305
0384 END IF
0385 IF (DATA(POS9,I).EQ.0.00)THEN
0386 DATA(M2,I)=0
0387 GOTO 305
0388 END IF
0389 DATA(M2,I)=DATA(POS8,I)/DATA(POS9,I)
0390 C
0391 C NB/Y
0392 C ****
0393
0394 305 M2=M2+1
0395 IF (DATA(POS10,I).EQ.0.00)THEN
0396 DATA(M2,I)=0
0397 GOTO 306
0398 END IF
0399 IF (DATA(POS9,I).EQ.0.00)THEN
0400 DATA(M2,I)=0
0401 GOTO 306
0402 END IF
0403 DATA(M2,I)=DATA(POS10,I)/DATA(POS9,I)
0404 C
0405 C NB/P205
0406 C *****
0407
0408 306 M2=M2+1
0409 IF (DATA(POS10,I).EQ.0.00)THEN
0410 DATA(M2,I)=0
0411 GOTO 307
0412 END IF
0413 IF (DATA(POS11,I).EQ.0.00)THEN
0414 DATA(M2,I)=0
0415 GOTO 307
0416 END IF
0417 DATA(M2,I)=DATA(POS10,I)/DATA(POS11,I)
0418 C
0419 C RB/SR
0420 C *****
0421
0422 307 M2=M2+1
0423 IF (DATA(POS12,I).EQ.0.00)THEN
0424 DATA(M2,I)=0
0425 GOTO 308
0426 END IF
0427 IF (DATA(POS13,I).EQ.0.00)THEN
0428 DATA(M2,I)=0
0429 GOTO 308
0430 END IF
0431 DATA(M2,I)=DATA(POS12,I)/DATA(POS13,I)
0432 C
0433 C NI/CO
0434 C *****
0435
0436 308 M2=M2+1
0437 IF (DATA(POS14,I).EQ.0.00)THEN
0438 DATA(M2,I)=0
0439 GOTO 309
0440 END IF
0441 IF (DATA(POS15,I).EQ.0.00)THEN
0442 DATA(M2,I)=0
0443 GOTO 309
0444 END IF
0445 DATA(M2,I)=DATA(POS14,I)/DATA(POS15,I)
0446 C
0447 C CU/CO
0448 C *****
0449
0450 309 M2=M2+1

```

```

0451      IF (DATA(POS16,I).EQ.0.00)THEN
0452      DATA(M2,I)=0
0453      GOTO 310
0454      END IF
0455      IF (DATA(POS15,I).EQ.0.00)THEN
0456      DATA(M2,I)=0
0457      GOTO 310
0458      END IF
0459      DATA(M2,I)=DATA(POS16,I)/DATA(POS15,I)
0460      C
0461      C      ZN/CO
0462      C      *****
0463
0464      310 M2=M2+1
0465      IF (DATA(POS18,I).EQ.0.00)THEN
0466      DATA(M2,I)=0
0467      GOTO 311
0468      END IF
0469      IF (DATA(POS15,I).EQ.0.00)THEN
0470      DATA(M2,I)=0
0471      GOTO 311
0472      END IF
0473      DATA(M2,I)=DATA(POS18,I)/DATA(POS15,I)
0474      C
0475      C      ZR/NB
0476      C      *****
0477
0478      311 M2=M2+1
0479      IF (DATA(POS17,I).EQ.0.00)THEN
0480      DATA(M2,I)=0
0481      GOTO 312
0482      END IF
0483      IF (DATA(POS10,I).EQ.0.00)THEN
0484      DATA(M2,I)=0
0485      GOTO 312
0486      END IF
0487      DATA(M2,I)=DATA(POS17,I)/DATA(POS10,I)
0488      C
0489      C      (K20/(K20+NA20))*100
0490      C      *****
0491
0492      312 M2=M2+1
0493      IF (DATA(POS7,I).EQ.0.00)THEN
0494      DATA(M2,I)=0
0495      GOTO 313
0496      END IF
0497
0498      SUM=DATA(POS7,I)+DATA(POS6,I)
0499
0500      IF (SUM.EQ.0.00)THEN
0501      DATA(M2,I)=0
0502      GOTO 313
0503      END IF
0504      DATA(M2,I)=DATA(POS7,I)/(DATA(POS7,I)+DATA(POS6,I))
0505      DATA(M2,I)=DATA(M2,I)*100
0506      C
0507      C      K20+NA20
0508      C
0509
0510      313 M2=M2+1
0511      DATA(M2,I)=DATA(POS7,I)+DATA(POS6,I)
0512
0513      1505 CONTINUE
0514
0515      C *****
0516      C ***** SET UP OUTPUT FILES *****
0517      C *****
0518
0519      C      ASK FOR FILENAME
0520      C      *****
0521      C
0522      WRITE(6,1100)
0523      READ(5,501)IN
0524      OPEN(1,FILE=IN,DEFAULT FILE='.RAW',STATUS='NEW')
0525      C

```

```

0526 C
0527 C WRITE FILE HEADER AND DATA
0528 C *****
0529 C
0530 M2=M1+15
0531
0532 WRITE(1,108)TITLE
0533 WRITE(1,109)FORM
0534 WRITE(1,110)M2,N1
0535 WRITE(1,111)(NAME(I),I=1,M2)
0536
0537 DO 1435 I=1,N1
0538 WRITE(1,484)SAMPLE(I),KEY(I)
0539 WRITE(1,113)(DATA(J,I),J=1,M2)
0540 1435 CONTINUE
0541
0542 C *****
0543 C ***** INPUT/OUTPUT FORMATS AND DIALOGUE *****
0544 C *****
0545
0546 1500 FORMAT(//1X,'There are ',I1,' variables missing from the data'/
0547 1' No calculations will be carried out until this is corrected.'
0548 2//)
0549 1502 FORMAT(1X,'New variable created ....>',A8)
0550 5 FORMAT(//1X,'Variable names: '//)
0551 6 FORMAT(2(10X,I3,' ':',A8))
0552 100 FORMAT(///' Type in the .RAW filename required.....> ',,$)
0553 1100 FORMAT(///' Type in the .RAW output filename .....> ',,$)
0554 108 FORMAT(1X,A79)
0555 109 FORMAT(1X,A79)
0556 110 FORMAT(2I6)
0557 111 FORMAT(8(1X,A8))
0558 113 FORMAT(6F13.4)
0559 484 FORMAT(1X,A10,A2)
0560 501 FORMAT(A12)
0561 999 END

```

```

0001      PROGRAM DIS
0002      C
0003      C
0004      C
0005      C
0006      C
0007      C      *****
0008      C      *      *      *      *
0009      C      *      *      *      *
0010      C      *      *      *      *****
0011      C      *      *      *      *
0012      C      *      *      *      *
0013      C      *****
0014      C
0015      C
0016      C
0017      C      PAUL R. DULLER
0018      C      DEPARTMENT OF APPLIED GEOLOGY
0019      C      THE UNIVERSITY OF STRATHCLYDE
0020      C      GLASGOW
0021      C
0022      C
0023      C
0024      C
0025      C      *****
0026      C      ***** INTRODUCTION *****
0027      C      *****
0028      C
0029      C      THIS PROGRAM IS DESIGNED TO READ ONE OR MORE SELF DESCRIBING
0030      C      .RAW DATA FILES, PREVIOUSLY GENERATED BY THE USER FROM DATA
0031      C      INPUT THROUGH THE RAW SYSTEM.
0032      C
0033      C      THE OBJECT OF THIS PROGRAM IS TO FACILITATE RAPID
0034      C      DISCRIMINATORY DATA ANALYSIS ON ONE OR MORE .RAW FILES AND
0035      C      OUTPUT THE DATA IN A TABULATED, EASILY INTERPRETABLE FORM.
0036      C
0037      C      THE FORMAT OF THE INPUT FILE STRUCTURE OF EACH .RAW FILE IS:
0038      C
0039      C      RECORD 1 A80      TITLE
0040      C      RECORD 2 A80      FORMAT OF DATA - USUALLY F13.4
0041      C      RECORD 3 212      NO OF VARIABLES AND NO OF RECORDS, OR 0
0042      C
0043      C      RECORD4+ 8(X,A8)      VARIABLE NAMES, 8 PER LINE
0044      C
0045      C      RECORD N A12      SAMPLE NAME
0046      C
0047      C      RECORD N+      RAW DATA (SEE RECORD 2)
0048      C
0049      C
0050      C      ++++++
0051      C      ++++++ END OF INTRODUCTION ++++++
0052      C      ++++++
0053      C
0054      C
0055      C      INTEGER X,I,J,K,M1,N1,P1,TOTAL(2000),Q,R,S,LOC(100),COUNT
0056      C      REAL DATA(100,2000),NUM(100),MIN,MAX
0057      C      CHARACTER TITLE*80,FORM*80,SAMPLE(2000)*10,NAME(100)*8,OUT*12
0058      C      CHARACTER BIN*12,KEY(1000)*2,FACTOR(50)*1
0059      C      CHARACTER VAR(100)*2,HEAD*80,RESULT(100,2000),P*1
0060      C
0061      C
0062      C
0063      C      *****
0064      C      ***** DETAILS FOR OTHER PROGRAMMERS *****
0065      C      *****
0066      C
0067      C      M1      = NO OF VARIABLES
0068      C      N1      = NO OF RECORDS
0069      C      DATA   = INPUT DATA VALUES (FREE FORMAT)
0070      C      TITLE   = TITLE OF FILE (TO IDENTIFY DATAFILE TO USER)
0071      C      FORM    = FORMAT OF OUTPUT DATA
0072      C      NAME    = ARRAY 1 TO M CONTAINING VARIABLE NAMES
0073      C      OUT     = INPUT/CREATION .RAW FILE NAME
0074      C      SAMPLE = ARRAY 1 TO N CONTAINING SAMPLE NAMES
0075      C      KEY    = A TWO SYMBOL CODE ATTACHED TO THE END OF THE

```

```

0076 C          SAMPLE NAME. BY DEFAULT NORMALLY IS " ".
0077 C
0078 C *****
0079 C ***** HEADER *****
0080 C *****
0081 C
0082 96 WRITE(6,99)
0083 READ(5,98)B
0084 IF(B.EQ.'C')THEN
0085 GOTO 97
0086 END IF
0087 GOTO 96
0088 97 WRITE(6,95)
0089 READ(5,98)B
0090 IF(B.EQ.'C')THEN
0091 GOTO 94
0092 END IF
0093 GOTO 97
0094 C
0095 C *****
0096 C ***** DATA INPUT *****
0097 C *****
0098 C
0099 C ASK FOR FILENAME
0100 C
0101 94 WRITE(6,100)
0102 READ(5,501)OUT
0103 OPEN(2,FILE=OUT,DEFAULT FILE='.RAW',STATUS='OLD')
0104 C
0105 C
0106 C READ FILE HEADER AND DATA
0107 C
0108 READ(2,108)TITLE
0109 READ(2,109)FORM
0110 READ(2,110)M1,N1
0111 READ(2,111)(NAME(I),I=1,M1)
0112 DO 435 I=1,N1
0113 READ(2,484)SAMPLE(I),KEY(I)
0114 READ(2,113)(DATA(J,I),J=1,M1)
0115 435 CONTINUE
0116 C
0117 C ++++++
0118 C ++++++ END OF DATA INPUT ++++++
0119 C ++++++
0120 C
0121 C
0122 C
0123 C *****
0124 C ***** LIST VARIABLES *****
0125 C *****
0126 C
0127 K=0
0128 50 L=0
0129 P1=M1
0130 11 IF(P1.GE.3)THEN
0131 L=L+1
0132 P1=P1-2
0133 GOTO 11
0134 END IF
0135 C
0136 C NO OF REMAINING SAMPLES FORMING LESS THAN ONE COMPLETE
0137 C ROW (P1).
0138 C
0139 C OUTPUT VARIABLE NAMES
0140 C
0141 Y=0
0142 IF(L.EQ.0)THEN
0143 GOTO 12
0144 END IF
0145 C
0146 WRITE(6,5)
0147 C
0148 DO 13 I=1,L
0149 X=Y+1
0150 Y=Y+2

```

```

0151      WRITE(6,6)((J,NAME(J)),J=X,Y)
0152      13 CONTINUE
0153      C
0154      IF(P1.EQ.0)THEN
0155      GOTO 104
0156      END IF
0157      C
0158      12 Y=M1-P1+1
0159      WRITE(6,6)((J,NAME(J)),J=Y,M1)
0160      C
0161      IF(K.EQ.0)THEN
0162      GOTO 104
0163      END IF
0164      IF(K.EQ.4)THEN
0165      GOTO 207
0166      END IF
0167      C
0168      C *****
0169      C ***** SIMPLE NUMERIC DISCRIMINATION *****
0170      C *****
0171      C
0172      C      ASK THE USER HOW MANY DISCRIMINATIONS (P) ?
0173      C
0174      104 WRITE(6,302)
0175      READ(5,105)P
0176
0177      IF(P.EQ.'L')THEN
0178      GOTO 1000
0179      END IF
0180
0181      IF(P.NE.'G')THEN
0182      GOTO 104
0183      END IF
0184
0185      C
0186      C *****
0187      C ***** DISCRIMINATION *****
0188      C *****
0189      C
0190      1000 WRITE(6,309)
0191      K=4
0192      C      LIST VARIABLES AND THEN RETURN
0193      GOTO 50
0194      C
0195      C      FIND OUT THE ARRAY POSITION OF THE VARIABLES TO BE TESTED.
0196      C
0197      207 WRITE(6,301)
0198      READ(5,300)M2
0199      C
0200      C      CACULATE MINIMUM AND MAXIMUM VALUES
0201      C
0202      MAX=DATA(M2,1)
0203      MIN=DATA(M2,1)
0204      C
0205      DO 53 I=2,N1
0206      IF(DATA(M2,I).LE.MIN)THEN
0207      MIN=DATA(M2,I)
0208      END IF
0209      IF(DATA(M2,I).GE.MAX)THEN
0210      MIN=DATA(M2,I)
0211      END IF
0212      53 CONTINUE
0213      C
0214      C      ASK THE USER FOR THRESHOLD VALUE
0215      C
0216      WRITE(6,500)NAME(M2),MIN,MAX
0217      WRITE(6,306)
0218      READ(5,*)NUM(M2)
0219      C
0220      C      ASSESS EACH RECORD WITHIN THE FILE
0221      C
0222      COUNT=0
0223
0224      IF(P.EQ.'L')THEN
0225

```



```

0226      DO 20 I=1,N1
0227          TOTAL(I)=0
0228          IF(DATA(M2,I).LE.NUM(M2)) THEN
0229              COUNT=COUNT+1
0230              TOTAL(I)=TOTAL(I)+1
0231          END IF
0232      20  CONTINUE
0233          WRITE(6,669)COUNT,NUM(M2)
0234          GOTO 1500
0235          END IF
0236
0237          IF(P.EQ.'G')THEN
0238
0239              DO 120 I=1,N1
0240                  TOTAL(I)=0
0241                  IF(DATA(M2,I).GE.NUM(M2)) THEN
0242                      TOTAL(I)=TOTAL(I)+1
0243                      COUNT=COUNT+1
0244                  END IF
0245              120 CONTINUE
0246                  WRITE(6,700)COUNT,NUM(M2)
0247                  END IF
0248
0249      C
0250      C      SET UP OUTPUT FILES
0251      C
0252      C ++++++
0253      C ++++++ End of DISCRIMINATION STUDIES ++++++
0254      C ++++++
0255      C
0256      C *****
0257      C ***** SET UP OUTPUT TABLE *****
0258      C *****
0259      C
0260      C      ASK THE USER IF A CHANGE OF HEADING FOR THE OUTPUT OTHER
0261      C      THAN THE TITLE IS REQUIRED.
0262      C
0263      1500 WRITE(6,403)TITLE
0264          READ(5,98)B
0265          IF(B.EQ.'Y')THEN
0266              GOTO 90
0267          END IF
0268          IF(B.NE.'N')THEN
0269              GOTO 1500
0270          END IF
0271          GOTO 406
0272
0273      90  WRITE(6,308)
0274          READ(5,198)TITLE
0275      C
0276      C      ASK FOR OUTPUT FILENAME
0277      C
0278      406 WRITE(6,114)
0279          READ(5,501)OUT
0280
0281          OPEN(1,FILE=OUT,DEFAULT FILE='.RAW',STATUS='NEW')
0282      C
0283      C      ASK THE USER IF ALL OF THE DATA IS REQUIRED OR ONLY THE
0284      C      VARIABLE OF INTEREST.
0285      C
0286      753 WRITE(6,750)
0287          READ(5,751)P
0288          IF(P.EQ.'Y')THEN
0289              GOTO 752
0290          END IF
0291          IF(P.NE.'N')THEN
0292              GOTO 753
0293          END IF
0294      C
0295      C      WRITE FILE HEADER AND DATA
0296      C
0297      752 IF(P.EQ.'N')THEN
0298
0299          M1=1
0300

```

```

0301      WRITE(1,108)TITLE
0302      WRITE(1,109)FORM
0303      WRITE(1,110)M1,COUNT
0304      WRITE(1,111)NAME(M2)
0305
0306      DO 2435 I=1,N1
0307
0308          IF (TOTAL(I).EQ.1)THEN
0309              WRITE(1,484)SAMPLE(I),KEY(I)
0310              WRITE(1,113)DATA(M2,I)
0311          END IF
0312
0313      2435 CONTINUE
0314          GOTO 999
0315      END IF
0316  C
0317  C OTHERWISE
0318  C
0319      WRITE(1,108)TITLE
0320      WRITE(1,109)FORM
0321      WRITE(1,110)M1,COUNT
0322      WRITE(1,111)(NAME(I),I=1,M1)
0323
0324      DO 1435 I=1,N1
0325          IF (TOTAL(I).EQ.1)THEN
0326              WRITE(1,484)SAMPLE(I),KEY(I)
0327              WRITE(1,113)(DATA(J,I),J=1,M1)
0328          END IF
0329      1435 CONTINUE
0330  C
0331  C
0332  C      *****
0333  C      INPUT/OUTPUT FORMATS AND DIALOGUE
0334  C      *****
0335      5  FORMAT(////////1X,'Variable names: '//)
0336      6  FORMAT(2(10X,I3,': ',A8))
0337      95  FORMAT(////////)
0338      1' ***** SIMPLE DISCRIMINANT ANALYSIS *****'//
0339      2' This program is designed to read any self-describing data'//
0340      3' files, previously generated by the user from data input'//
0341      4' through the "RAW" package.'//
0342      5' The object of this program is to facilitate rapid, SIMPLE'//
0343      6' DISCRIMINANT ANALYSIS and output results to a .RAW file'
0344      7' which may then be used to generate Thesis-Ready tables.'//
0345      8' This program has two main analytical objectives:'//
0346      9' 1 - To review a data file and select individual SAMPLES'//
0347      1'   which contain values for any given VARIABLE'//
0348      2'   GREATER THAN a User defined THRESHOLD.'//
0349      9' 2 - To review a data file and select individual SAMPLES'//
0350      1'   which contain values for any given VARIABLE'//
0351      2'   LESS THAN a user defined THRESHOLD.'//
0352      2'   Type C to Continue....> ', $)
0353      98  FORMAT(A1)
0354      99  FORMAT(////////)
0355      1/'      *****      *****      *****      '
0356      2/'      *      *      *      *      '
0357      3/'      *      *      *      *      '
0358      4/'      *      *      *      *****      '
0359      5/'      *      *      *      *      '
0360      6/'      *      *      *      *      '
0361      7/'      *****      *****      *****      '///
0362      8'////'      Type C to continue...> ', $)
0363      100 FORMAT(////)
0364      1' Type in the .RAW filename required .....> ', $)
0365      101 FORMAT(I3)
0366      102 FORMAT(X,A12)
0367      114 FORMAT(/)
0368      1' Type in a Results .RAW filename.....> ', $)
0369      105 FORMAT(A1)
0370      106 FORMAT(A2)
0371      107 FORMAT(I2)
0372      108 FORMAT(1X,A79)
0373      109 FORMAT(1X,A79)
0374      110 FORMAT(2I6)
0375      111 FORMAT(8(1X,A8))

```

```

0376 113 FORMAT(6F13.4)
0377 198 FORMAT(A79)
0378 199 FORMAT(1X,A79,/)
0379 300 FORMAT(I2)
0380 301 FORMAT(/
0381 1/' Type Variable No. for assessment.....> ' $)
0382 302 FORMAT(/
0383 1/' "Greater than" or "Less than"option (G or L)....> ', $)
0384 306 FORMAT(/
0385 1' Select threshold value .....> ', $)
0386 307 FORMAT(/
0387 1' GREATER THAN OPTION '
0388 2' *****'/)
0389 308 FORMAT(///
0390 1' Type a TITLE for your results.....> ', $)
0391 309 FORMAT(/
0392 1' LESS THAN OPTION'
0393 2/' *****'/)
0394 310 FORMAT(/////////
0395 1/' *****'
0396 1/' ***** DISCRIMINATION ANALYSIS COMPLETE *****'
0397 1/' *****'
0398 2/' ***** BYE !!! *****'
0399 3/' *****'
0400 4/////////)
0401 403 FORMAT(//////////1X,':',A78//
0402 1/' Do you require a new title (Y or N).....> ', $)
0403 484 FORMAT(1X,A10,A2)
0404 500 FORMAT(/1X
0405 1A8,/' Minimum value : ',F10.2,/' Maximum value : ',F10.2,/)
0406 501 FORMAT(A12)
0407 669 FORMAT(/1X,I3,1X,
0408 1'Samples have been classified as LESS THAN',F11.3)
0409 700 FORMAT(/1X,I3,1X,
0410 1'Samples have been classified as GREATER THAN',F11.3)
0411 750 FORMAT(///' ALL variables in results file (Y or N)...> ', $)
0412 751 format(A1)
0413 C
0414 C ++++++
0415 C ++++++ END OF INPUT/OUTPUT FORMAT ++++++
0416 C ++++++
0417 C
0418 999 END

```

```

0001      PROGRAM TRV
0002      C
0003      C
0004      C
0005      C
0006      C          *****      *      *
0007      C          *      *      *      *      *
0008      C          *      *      *      *      *
0009      C          *      *      *      *      *
0010      C          *      *      *      *      *
0011      C          *      *      *      *      *
0012      C          *      *      *      *      *
0013      C
0014      C
0015      C
0016      C
0017      C      PAUL R. DULLER
0018      C      DEPARTMENT OF APPLIED GEOLOGY
0019      C      THE UNIVERSITY OF STRATHCLYDE
0020      C      GLASGOW
0021      C
0022      C
0023      C      *****
0024      C      ***** INTRODUCTION *****
0025      C      *****
0026      C
0027      C      THIS PROGRAM IS DESIGNED TO GENERATE TRAVERSES FROM A
0028      C      GENERAL PURPOSE DATA FILE, GENERATED BY THE USER FROM
0029      C      DATA INPUT THROUGH THE RAW SYSTEM.
0030      C
0031      C      INTEGER NUMTOPLOT,SCALE,TEST
0032      C      INTEGER X,I,J,L,M,N,O,P,Q,R,S,T,M1,N1,CLASSES,MAXCLASS
0033      C      INTEGER CLASS(50,50),NUMINCLASS(50),CUMFA,M10,N10
0034      C
0035      C      REAL DATA(50,1000),MIN(50),MAX(50),MEANA(50),MEANG(50)
0036      C      REAL RANGE(50),VAR(50),SDEV(50),SKEW(50),KURT(50),M4(50)
0037      C      REAL SUMX(50),SUMX2(50),V1(50),V2(50),V3(50),V4(50),M2(50)
0038      C      REAL TABLE(50,10),CV(50),K,K1,M3(50),MIDPOINT(50),BOUND(50,2)
0039      C      REAL CF(50,100),CUMF(50,100),INT(50),CELL(50),CLASSINT(50)
0040      C      CHARACTER TITLE*80,FORM*80,SAMPLE(1000)*10,NAME(50)*8,IN*12
0041      C      CHARACTER KEY(1000)*2,FORM1*10,FORMX*10,SAMPLE1(1000)*8
0042      C      CHARACTER HIST*50,CZ*1,BIN*12,TITLE2*80,NAME2(50)*8,PIN*1
0043      C
0044      C      *****
0045      C      ***** OUTPUT HEADER *****
0046      C      *****
0047      C
0048      C      43  WRITE(6,40)
0049      C          READ(5,41)B
0050      C          IF(B.EQ.'C')THEN
0051      C              GOTO 42
0052      C          END IF
0053      C          GOTO 43
0054      C
0055      C      *****
0056      C      ***** INPUT .RAWFILE *****
0057      C      *****
0058      C
0059      C      ASK FOR FILENAME
0060      C
0061      C      42  WRITE(6,100)
0062      C          READ(5,601)IN
0063      C          OPEN(1,FILE=IN,DEFAULT FILE='.RAW',STATUS='OLD')
0064      C          OPEN(2,FILE=IN,DEFAULT FILE='.TRV',STATUS='NEW')
0065      C
0066      C      READ FILE HEADER AND DATA
0067      C
0068      C      READ(1,108)TITLE
0069      C      READ(1,109)FORM
0070      C      READ(1,110)M1,N1
0071      C
0072      C      READ(1,111)(NAME(I),I=1,M1)
0073      C
0074      C      DO 475 I=1,N1
0075      C          READ(1,484)SAMPLE(I),KEY(I)

```

```

0076      READ(1,113)(DATA(J,I),J=1,M1)
0077 475 CONTINUE
0078 C
0079 C
0080 C *****
0081 C ***** STATISTICS *****
0082 C *****
0083 C
0084 C *****
0085 C MINIMUM, MAXIMUM AND RANGE
0086 C *****
0087 C
0088 C TO COMPUTE THE MINIMUM,MAXIMUM AND RANGE
0089 C OF N1 SAMPLES FOR M1 VARIABLES
0090 C
0091 C SET SUM TO ZERO
0092 C
0093 C DO 98 I=1,M1
0094 C J=1
0095 C SUMX(I)=DATA(I,J)
0096 C SUMX2(I)=DATA(I,J)
0097 C
0098 C DO 95 J=2,N1
0099 C
0100 C K=DATA(I,J)
0101 C
0102 C IF(K.GT.SUMX(I))THEN
0103 C SUMX(I)=K
0104 C END IF
0105 C
0106 C IF(K.LT.SUMX2(I))THEN
0107 C SUMX2(I)=K
0108 C END IF
0109 C
0110 C 95 CONTINUE
0111 C
0112 C MAX(I)=SUMX(I)
0113 C MIN(I)=SUMX2(I)
0114 C RANGE(I)=MAX(I)-MIN(I)
0115 C 98 CONTINUE
0116 C
0117 C *****
0118 C ***** OPTIONS *****
0119 C
0120 C
0121 C ***** LIST VARIABLES *****
0122 C
0123 C
0124 C 733 L=0
0125 C P1=M1
0126 C 11 IF(P1.GE.2)THEN
0127 C L=L+1
0128 C P1=P1-2
0129 C GOTO 11
0130 C END IF
0131 C
0132 C NO OF REMAINING SAMPLES FORMING LESS THAN ONE COMPLETE
0133 C ROW (P1).
0134 C
0135 C OUTPUT VARIABLE NAMES
0136 C
0137 C Y=0
0138 C IF(M1.EQ.0)THEN
0139 C GOTO 63
0140 C END IF
0141 C
0142 C WRITE(6,5)
0143 C
0144 C DO 13 I3=1,L
0145 C X=Y+1
0146 C Y=Y+2
0147 C WRITE(6,6)((J3,NAME(J3)),J3=X,Y)
0148 C 13 CONTINUE
0149 C
0150 C IF(P1.EQ.0)THEN

```

```

0151      GOTO 63
0152      END IF
0153      WRITE(6,6)M1,NAME(M1)
0154      C
0155      C      ***** ASK USER TO SELECT VARIABLE *****
0156      C
0157      63 WRITE(6,171)
0158      READ(5,172)NUMTOPLOT
0159      C
0160      C      INFORM USER OF MIN,MAX AND RANGE OF DATA
0161      C
0162      66 WRITE(6,60)MIN(NUMTOPLOT),MAX(NUMTOPLOT)
0163      READ(6,61)CZ
0164      IF(CZ.EQ.'N')THEN
0165      GOTO 277
0166      END IF
0167      IF(CZ.EQ.'1')THEN
0168      WRITE(6,64)
0169      READ(6,*)MIN(NUMTOPLOT)
0170      GOTO 66
0171      END IF
0172      IF(CZ.EQ.'2')THEN
0173      WRITE(6,65)
0174      READ(6,*)MAX(NUMTOPLOT)
0175      GOTO 66
0176      END IF
0177      GOTO 63
0178      C
0179      C      ***** ASK USER TO SELECT OPTIONS *****
0180      C
0181      277 WRITE(6,175)
0182      READ(5,176)J5
0183      IF(J5.EQ.1)THEN
0184      GOTO 278
0185      ELSE
0186      IF(J5.EQ.2)THEN
0187      GOTO 279
0188      END IF
0189      END IF
0190      GO TO 277
0191
0192      C      *****
0193      C      ***** SET UP OUTPUT FILES *****
0194      C      ***** STYLE 1 *****
0195      C      *****
0196      C
0197      C      ASK USER IF SAMPLE NUMBERS ARE REQUIRED FOR OUTPUT
0198      C      ALONGSIDE THE TRAVERSE SECTION.
0199      C
0200      278 WRITE(6,400)
0201      READ(5,401)PIN
0202      IF(PIN.EQ.'N')THEN
0203      GOTO 403
0204      END IF
0205      IF(PIN.EQ.'Y')THEN
0206      GOTO 278
0207      END IF
0208
0209      403 WRITE(6,117)TITLE,NAME(NUMTOPLOT)
0210      WRITE(6,501)MIN(NUMTOPLOT),MAX(NUMTOPLOT)
0211      WRITE(6,499)
0212      RANGE(NUMTOPLOT)=MAX(NUMTOPLOT)-MIN(NUMTOPLOT)
0213      DO 20 J=1,N1
0214      K=0
0215      K=(DATA(NUMTOPLOT,J)-MIN(NUMTOPLOT))
0216      K=(K/RANGE(NUMTOPLOT))*50
0217
0218      DO 24 I=1,50
0219      HIST(I:)= ' '
0220      24 CONTINUE
0221
0222      HIST(K:K)='*'
0223
0224      IF(PIN.EQ.'N')THEN
0225      WRITE(6,402)HIST

```



```

0226      GOTO 20
0227      END IF
0228
0229      WRITE(6,901)SAMPLE(J),HIST
0230
0231      20  CONTINUE
0232
0233      WRITE(6,499)
0234      WRITE(6,501)MIN(NUMTOPLOT),MAX(NUMTOPLOT)
0235      C
0236      C      ASK USER FOR STORAGE, NEW VARIABLE OR QUIT
0237      C
0238      747 WRITE(6,669)
0239      READ(5,991)J4
0240
0241      IF(J4.EQ.1)THEN
0242      GOTO 701
0243      END IF
0244      IF(J4.EQ.2)THEN
0245      GOTO 702
0246      END IF
0247      IF(J4.EQ.3)THEN
0248      GOTO 733
0249      END IF
0250      GOTO 747
0251      C
0252      C      INFORM USER THAT DIAGRAMS COMPLETED AND EXIT
0253      C
0254      701 WRITE(6,454)
0255      GOTO 999
0256
0257      702 WRITE(2,117)TITLE,NAME(NUMTOPLOT)
0258      WRITE(2,501)MIN(NUMTOPLOT),MAX(NUMTOPLOT)
0259      WRITE(2,499)
0260      RANGE(NUMTOPLOT)=MAX(NUMTOPLOT)-MIN(NUMTOPLOT)
0261      DO 21 J=1,N1
0262      K=0
0263      K=(DATA(NUMTOPLOT,J)-MIN(NUMTOPLOT))
0264      K=(K/RANGE(NUMTOPLOT))*50
0265
0266      DO 25 I=1,50
0267      HIST(I:)= ' '
0268      25  CONTINUE
0269
0270      HIST(K:K)='*'
0271
0272      IF(PIN.EQ.'N')THEN
0273      WRITE(2,402)HIST
0274      GOTO 21
0275      END IF
0276
0277      WRITE(2,901)SAMPLE(J),HIST
0278
0279      21  CONTINUE
0280
0281      WRITE(2,499)
0282      WRITE(2,501)MIN(NUMTOPLOT),MAX(NUMTOPLOT)
0283      WRITE(2,2000)
0284      GOTO 747
0285
0286      C      *****
0287      C      ***** SET UP OUTPUT FILES *****
0288      C      ***** STYLE 2 *****
0289      C      *****
0290      C
0291      C      ASK USER IF SAMPLE NUMBERS ARE REQUIRED FOR OUTPUT
0292      C      ALONGSIDE THE TRAVERSE SECTION.
0293      C
0294      279 WRITE(6,400)
0295      READ(5,401)PIN
0296      IF(PIN.EQ.'N')THEN
0297      GOTO 405
0298      END IF
0299      IF(PIN.NE.'Y')THEN
0300      GOTO 279

```

```

0301      END IF
0302
0303      405 WRITE(6,117)TITLE,NAME(NUMTOPLOT)
0304      WRITE(6,501)MIN(NUMTOPLOT),MAX(NUMTOPLOT)
0305      WRITE(6,499)
0306      RANGE(NUMTOPLOT)=MAX(NUMTOPLOT)-MIN(NUMTOPLOT)
0307      DO 120 J=1,N1
0308      K=0
0309      K=(DATA(NUMTOPLOT,J)-MIN(NUMTOPLOT))
0310      K=(K/RANGE(NUMTOPLOT))*50
0311
0312      DO 124 I=1,50
0313      HIST(I:)= ' '
0314      IF (I.GT.K)THEN
0315      GOTO 124
0316      END IF
0317      HIST(I:)= ']'
0318 124  CONTINUE
0319
0320      IF (PIN.EQ.'N')THEN
0321      WRITE(6,402)HIST
0322      GOTO 120
0323      END IF
0324
0325      WRITE(6,901)SAMPLE(J),HIST
0326
0327 120  CONTINUE
0328
0329      WRITE(6,499)
0330      WRITE(6,501)MIN(NUMTOPLOT),MAX(NUMTOPLOT)
0331  C
0332  C      ASK USER FOR STOREAGE, NEW VARIABLE OR QUIT
0333  C
0334 1747 WRITE(6,669)
0335      READ(5,991)J4
0336
0337      IF (J4.EQ.1)THEN
0338      GOTO 1701
0339      END IF
0340      IF (J4.EQ.2)THEN
0341      GOTO 1702
0342      END IF
0343      IF (J4.EQ.3)THEN
0344      GOTO 733
0345      END IF
0346      GOTO 1747
0347  C
0348  C      INFORM USER THAT DIAGRAMS COMPLETED AND EXIT
0349  C
0350 1701 WRITE(6,454)
0351      GOTO 999
0352
0353 1702 WRITE(2,117)TITLE,NAME(NUMTOPLOT)
0354      WRITE(2,501)MIN(NUMTOPLOT),MAX(NUMTOPLOT)
0355      WRITE(2,499)
0356
0357      DO 121 J=1,N1
0358      K=0
0359      K=(DATA(NUMTOPLOT,J)-MIN(NUMTOPLOT))
0360      K=(K/RANGE(NUMTOPLOT))*50
0361
0362      DO 125 I=1,50
0363      HIST(I:)= ' '
0364      IF (I.GT.K)THEN
0365      GOTO 125
0366      END IF
0367      HIST(I:)= ']'
0368 125  CONTINUE
0369
0370      IF (PIN.EQ.'N')THEN
0371      WRITE(2,402)HIST
0372      GOTO 121
0373      END IF
0374
0375      WRITE(2,901)SAMPLE(J),HIST

```

```

0376
0377 121 CONTINUE
0378
0379 WRITE(2,499)
0380 WRITE(2,501)MIN(NUMTOPLOT),MAX(NUMTOPLOT)
0381 WRITE(2,2000)
0382 GOTO 1747
0383
0384 C *****
0385 C ***** INPUT/OUTPUT FORMATS AND DIALOGUE *****
0386 C *****
0387 C
0388 5 FORMAT(//////////1X,'Variable names: '//)
0389 6 FORMAT(2(10X,I3,': ',A8))
0390 8 FORMAT(A1)
0391 40 FORMAT(//////////
0392 1/' ***** * * * * *
0393 1/' * * * * *
0394 1/' * * * * *
0395 1/' * * * * *
0396 1/' * * * * *
0397 1/' * * * * *
0398 1/' * * * * * PRD'///
0399 9///
0400 1' Type C to Continue.....> ', $)
0401 41 FORMAT(A1)
0402 60 FORMAT(//////////
0403 1' *****'/
0404 1' *****'/
0405 2' Minimum - ',F11.2,/
0406 2' Maximum - ',F11.2,///
0407 2' N - No Changes.'/
0408 3' 1 - Change Minimum'/
0409 3' 2 - Change Maximum'/////
0410 4' Select Option...> ', $)
0411 61 FORMAT(A1)
0412 64 FORMAT(//' Minimum.....> ', $)
0413 65 FORMAT(//' Maximum.....> ', $)
0414 100 FORMAT(//////////
0415 1' Type the .RAW filename for analysis.....> ', $)
0416 107 FORMAT(A79)
0417 108 FORMAT(1X,A79)
0418 109 FORMAT(1X,A79)
0419 110 FORMAT(2I6)
0420 111 FORMAT(8(1X,A8))
0421 112 FORMAT(//////////1X,A78/)
0422 113 FORMAT(1X,6F13.4)
0423 118 FORMAT(////2X,A78/)
0424 115 FORMAT(2X,A8,2X,9F10.2)
0425 117 FORMAT(///,10X,A69,///,10X,'Variable: ',A8,///,9X,
0426 1'Min',48X,'Max'//)
0427 171 FORMAT(//' No. of variable to be processed.....> ', $)
0428 172 FORMAT(I2)
0429 175 FORMAT(//////////
0430 1' *****'/
0431 2' ***** OPTIONS *****'/
0432 3' *****'/
0433 3///' 1 - Single position markers'
0434 3/' 2 - Bar charts'///
0435 8/' Select Option...> ', $)
0436 176 FORMAT(I1)
0437 400 FORMAT(//////////
0438 1' Do you require Sample Numbers on the plot (Y or N).....> ', $)
0439 401 FORMAT(A1)
0440 402 FORMAT(10X,': ',A50)
0441 454 FORMAT(//////////
0442 1' *****'/
0443 1' ***** TRAVERSES COMPLETED *****'/
0444 2' *****'/
0445 3//////////)
0446 484 FORMAT(1X,A10,A2)
0447 499 FORMAT(10X,
0448 1'-----:-----:-----:-----: ')
0449 501 FORMAT(3X,F10.2,40X,F10.2)
0450 520 FORMAT(A79)

```

```

0451 522 FORMAT(A1)
0452 523 FORMAT(1X,A79)
0453 525 FORMAT(A1)
0454 527 FORMAT('1',////////,11X,A79)
0455 543 FORMAT(A12)
0456 601 FORMAT(A12)
0457 669 FORMAT(
0458 1/' OPTIONS: 1=Quit, 2=Store, 3=Continue .....> ', $)
0459 700 FORMAT(F8.2)
0460 738 FORMAT(I1)
0461 901 FORMAT(1X,A9,':',A50)
0462 991 FORMAT(I1)
0463 2000 FORMAT(/////////)
0464 999 END

```

```

0001      PROGRAM SIF
0002      C
0003      C
0004      C
0005      C
0006      C
0007      C          *****
0008      C          *           *           *
0009      C          *           *           *
0010      C          *****           *           *****
0011      C          *           *           *
0012      C          *           *           *
0013      C          *****           *           *****
0014      C
0015      C
0016      C
0017      C
0018      C      PAUL R. DULLER
0019      C      DEPARTMENT OF APPLIED GEOLOGY
0020      C      THE UNIVERSITY OF STRATHCLYDE
0021      C      GLASGOW
0022      C
0023      C
0024      C      *****
0025      C      ***** INTRODUCTION *****
0026      C      *****
0027      C
0028      C      THIS PROGRAM IS DESIGNED TO SIFT A SELF DESCRIBING
0029      C      GENERAL PURPOSE DATA FILE, GENERATED BY THE USER FROM
0030      C      DATA INPUT THROUGH THE RAW SYSTEM.
0031      C
0032      C      OBJECTIVES :
0033      C
0034      C          TO SELECT A SUBGROUP OF SAMPLE RECORDS,
0035      C      FROM A .RAW FILE ON THE BASIS OF THE "KEY" AND OUTPUT
0036      C      THE DATA TO A NEW .RAW FILE OF THE USERS CHOICE.
0037      C
0038      C
0039      C
0040      C
0041      C
0042      C      THE FORMAT OF THE INPUT/OUTPUT FILE STRUCTURE IS:
0043      C
0044      C      RECORD 1 A80      TITLE
0045      C      RECORD 2 A80      FORMAT OF DATA - F10.2(IN),F13.4(OUT)
0046      C      RECORD 3 212      NO OF VARIABLES AND NO OF RECORDS, OR 0
0047      C
0048      C      RECORD4+ 8(X,A8)   VARIABLE NAMES, 8 PER LINE
0049      C
0050      C      RECORD N A12      SAMPLE NAME
0051      C
0052      C      RECORD N+      RAW DATA (SEE RECORD 2)
0053      C
0054      C      ++++++
0055      C      ++++++ END OF INTRODUCTION ++++++
0056      C      ++++++
0057      C
0058      C
0059      C      INTEGER X,I,J,M1,N1,N2
0060      C      REAL DATA(50,1000)
0061      C      CHARACTER TITLE*80,FORM*80,SAMPLE(1000)*10,NAME(50)*8,OUT*12
0062      C      CHARACTER BIN*12,KEY(1000)*2,SIFT*2,B*1,K*2
0063      C
0064      C
0065      C
0066      C      *****
0067      C      ***** DETAILS FOR OTHER PROGRAMMERS *****
0068      C      *****
0069      C
0070      C      M1      = NO OF VARIABLES
0071      C      N1      = NO OF RECORDS
0072      C      DATA   = INPUT DATA VALUES (FREE FORMAT)
0073      C      TITLE  = TITLE OF FILE (TO IDENTIFY DATAFILE TO USER)
0074      C      FORM   = FORMAT OF OUTPUT DATA
0075      C      NAME   = ARRAY 1 TO M CONTAINING VARIABLE NAMES

```

```

0076 C      OUT  = INPUT/CREATION .RAW FILE NAME
0077 C      SAMPLE= ARRAY 1 TO N CONTAINING SAMPLE NAMES
0078 C      KEY   = A TWO SYMBOL CODE ATTACHED TO THE END OF THE
0079 C             SAMPLE NAME. BY DEFAULT NORMALLY IS "  ".
0080 C
0081 C ++++++
0082 C ++++++ END OF DETAILS ++++++
0083 C ++++++
0084 C
0085 C
0086 C      ASK FOR FILENAME
0087 C
0088 C      WRITE(6,100)
0089 C      READ(5,501)OUT
0090 C      OPEN(2,FILE=OUT,DEFAULT FILE='.RAW',STATUS='OLD')
0091 C
0092 C
0093 C      READ FILE HEADER AND DATA
0094 C
0095 C      READ(2,108)TITLE
0096 C      READ(2,109)FORM
0097 C      READ(2,110)M1,N1
0098 C      READ(2,111)(NAME(I),I=1,M1)
0099 C
0100 C      DO 435 I=1,N1
0101 C          READ(2,484)SAMPLE(I),KEY(I)
0102 C          READ(2,901)(DATA(J,I),J=1,M1)
0103 C      435 CONTINUE
0104 C
0105 C *****
0106 C ***** LIST VARIABLES *****
0107 C *****
0108 C
0109 C      104 L=0
0110 C          P1=M1
0111 C          11 IF(P1.GE.3)THEN
0112 C              L=L+1
0113 C              P1=P1-2
0114 C              GOTO 11
0115 C          END IF
0116 C
0117 C      NO OF REMAINING SAMPLES FORMING LESS THAN ONE COMPLETE
0118 C      ROW (P1).
0119 C      OUTPUT VARIABLE NAMES
0120 C
0121 C      Y=0
0122 C      IF(L.EQ.0)THEN
0123 C          GOTO 12
0124 C      END IF
0125 C      WRITE(6,1000)
0126 C      WRITE(6,108)TITLE
0127 C
0128 C      WRITE(6,5)
0129 C      DO 13 I=1,L
0130 C          X=Y+1
0131 C          Y=Y+2
0132 C          WRITE(6,6)((J,NAME(J)),J=X,Y)
0133 C      13 CONTINUE
0134 C          IF(P1.EQ.0)THEN
0135 C              GOTO 15
0136 C          END IF
0137 C      12 Y=M1-P1+1
0138 C          WRITE(6,6)((J,NAME(J)),J=Y,M1)
0139 C          GOTO 15
0140 C      15 X=0
0141 C
0142 C *****
0143 C ***** SET UP KEYS IF REQUIRED *****
0144 C *****
0145 C
0146 C      ASK USER IF HE WISHES TO INPUT KEYS
0147 C
0148 C      786 WRITE(6,777)
0149 C      READ(5,916)B
0150 C

```



```

0151      IF(B.EQ.'Y')THEN
0152      DO 778 I=1,N1
0153      WRITE(6,779)SAMPLE(I),KEY(I)
0154      READ(5,789)K
0155      IF(K.EQ.'.')THEN
0156      GOTO 778
0157      END IF
0158      KEY(I)=K
0159 778 CONTINUE
0160      GOTO 785
0161      END IF
0162
0163      IF(B.NE.'N')THEN
0164      GOTO 786
0165      END IF
0166
0167  C
0168  C
0169  C
0170  C *****
0171  C ***** SET UP REFORMATTED OUTPUT FILE *****
0172  C *****
0173  C
0174  C      ASK USER IF HE WISHES TO VIEW THE POSSIBLE "KEYS"
0175  C
0176 785 WRITE(6,915)
0177      READ(5,916)B
0178      IF(B.EQ.'Y')THEN
0179      WRITE(6,917)(KEY(I),I=1,N1)
0180      GOTO 784
0181      END IF
0182      IF(B.NE.'N')THEN
0183      GOTO 785
0184      END IF
0185  C
0186  C      ASK THE USER IF HE REQUIRES TO SORT THE KEYS
0187  C
0188 784 WRITE(6,783)
0189      READ(5,916)B
0190      IF(B.EQ.'N')THEN
0191      GOTO 222
0192      END IF
0193  C
0194      IF(B.NE.'Y')THEN
0195      GOTO 784
0196      END IF
0197
0198  C      ASK FOR REFORMATTED DATA FILENAME
0199  C
0200      WRITE(6,900)
0201      READ(5,501)BIN
0202      OPEN(1,FILE=BIN,DEFAULT FILE='.RAW',STATUS='NEW')
0203  C
0204  C      ASK IF A NEW TITLE OF THE FILE IS REQUIRED
0205  C
0206      WRITE(6,444)
0207      READ(5,916)B
0208      IF(B.EQ.'Y')THEN
0209      WRITE(6,446)
0210      READ(5,445)TITLE
0211      END IF
0212  C
0213  C      ASK FOR THE TWO LETTER NEMONIC TO BE USED AS THE SELECTION
0214  C      PARAMETER ie. THE KEY.
0215  C
0216      WRITE(6,910)
0217      READ(5,911)SIFT
0218  C
0219  C      WRITE FILE HEADER AND DATA
0220  C
0221      N2=0
0222  C
0223      DO 929 I=1,N1
0224      IF(SIFT.EQ.KEY(I))THEN
0225      N2=N2+1

```

```

0226      END IF
0227      929 CONTINUE
0228
0229      WRITE(1,108)TITLE
0230      WRITE(1,109)FORM
0231      WRITE(1,110)M1,N2
0232  C
0233      WRITE(1,111)(NAME(I),I=1,M1)
0234  C
0235      DO 902 I=1,N1
0236      IF(SIFT.EQ.KEY(I))THEN
0237      WRITE(1,484)SAMPLE(I),KEY(I)
0238      WRITE(1,901)(DATA(J,I),J=1,M1)
0239      END IF
0240      902 CONTINUE
0241  C
0242      WRITE(1,903)
0243      GO TO 999
0244  C
0245      SET UP GENERAL OUTPUT FILE
0246  C
0247      222 BIN=OUT
0248      OPEN(1,FILE=BIN,DEFAULT FILE='.RAW',STATUS='NEW')
0249  C
0250      WRITE FILE HEADER AND DATA
0251  C
0252      WRITE(1,108)TITLE
0253      WRITE(1,109)FORM
0254      WRITE(1,110)M1,N1
0255      WRITE(1,111)(NAME(I),I=1,M1)
0256      DO 223 I=1,N1
0257      WRITE(1,484)SAMPLE(I),KEY(I)
0258      WRITE(1,901)(DATA(J,I),J=1,M1)
0259      223 CONTINUE
0260      WRITE(1,903)
0261      GOTO 999
0262  C
0263  C ++++++
0264  C ++++++ END OF REFORMATTED DATA OUTPUT ++++++
0265  C ++++++
0266  C
0267  C
0268  C
0269  C
0270  C *****
0271  C ***** INPUT/OUTPUT FORMATS AND DIALOGUE *****
0272  C *****
0273  C
0274      5  FORMAT(//1X,'Variable names: '//)
0275      6  FORMAT(2(10X,I3,' ':',A8))
0276      100 FORMAT(///' Type in the .RAW filename required.....> ', $)
0277      108 FORMAT(1X,A79)
0278      109 FORMAT(1X,A79)
0279      110 FORMAT(2I6)
0280      111 FORMAT(8(1X,A8))
0281      444 FORMAT(///' Is a new TITLE required (Y or N).....> ', $)
0282      445 FORMAT(A79)
0283      446 FORMAT(///' Title....> ', $)
0284      484 FORMAT(1X,A10,A2)
0285      501 FORMAT(A12)
0286      777 FORMAT(///' Input a KEY to your data (Y or N).....> ', $)
0287      779 FORMAT(///' Sample ',A8,' (New KEY or . to pass) Key= '
0288      1,A2,' .....> ', $)
0289      789 FORMAT(A2)
0290      783 FORMAT(///' Do you require SORT (Y or N).....> ', $)
0291      900 FORMAT(///' The name for the new SIFTED .RAW datafile..> ', $)
0292      901 FORMAT(1X,6F13.4)
0293      903 FORMAT(1X,'*****')
0294      910 FORMAT(1X,'Select the two letter nemonic for SIFT.....> ', $)
0295      911 FORMAT(A2)
0296      915 FORMAT(///' Do you want to list the "KEYS" (Y or N).....> ', $)
0297      916 FORMAT(A1)
0298      917 FORMAT(19(2X,A2))
0299      1000 FORMAT(///)
0300      999  END

```

```

0001      PROGRAM SOR
0002      C
0003      C
0004      C
0005      C
0006      C
0007      C          *****      *****      *****
0008      C          *          *          *          *          *
0009      C          *          *          *          *          *
0010      C          *****      *          *          *****
0011      C          *          *          *          *          *
0012      C          *          *          *          *          *
0013      C          *****      *****      *          *
0014      C
0015      C
0016      C
0017      C
0018      C      PAUL R. DULLER
0019      C      DEPARTMENT OF APPLIED GEOLOGY
0020      C      THE UNIVERSITY OF STRATHCLYDE
0021      C      GLASGOW
0022      C
0023      C
0024      C      JUNE 1986.
0025      C
0026      C      *****
0027      C      ***** INTRODUCTION *****
0028      C      *****
0029      C      THIS PROGRAM IS DESIGNED TO SORT A SELF DESCRIBING
0030      C      GENERAL PURPOSE DATA FILE, GENERATED BY THE USER FROM
0031      C      DATA INPUT THROUGH THE TERMINAL.
0032      C
0033      C      OBJECTIVES :
0034      C      1) TO REORGANISE THE STRUCTURE AND ORDER OF
0035      C      SAMPLE RECORDS CONTAINED WITHIN A .RAW FILE, CONTROLLED BY
0036      C      THE VALUE OF THE 'KEY' ( OR ANY VARIABLE).
0037      C      2) TO SUBSAMPLE AND EXTRACT ANY NUMBER OF
0038      C      VARIABLES FROM THE .RAW FILE.
0039      C
0040      C      RESULTS ARE NORMALLY OUTPUT TO A NEW, USER SELECTED .RAW
0041      C      FILE, HOWEVER IN A EXTRACT OPTION .RAW OR .DAT OUTPUT
0042      C      FILES MAY BE SELECTED.
0043      C
0044      C      THE FORMAT OF THE INPUT/OUTPUT FILE STRUCTURE IS:
0045      C
0046      C      RECORD 1 A80      TITLE
0047      C      RECORD 2 A80      FORMAT OF DATA - F10.2(IN),F13.4(OUT)
0048      C      RECORD 3 A12      NO OF VARIABLES AND NO OF RECORDS, OR 0
0049      C
0050      C      RECORD4+ 8(X,A8)  VARIABLE NAMES, 8 PER LINE
0051      C
0052      C      RECORD N A12      SAMPLE NAME
0053      C
0054      C      RECORD N+      RAW DATA (SEE RECORD 2)
0055      C
0056      C      ++++++ END OF INTRODUCTION ++++++
0057      C      ++++++
0058      C
0059      C      INTEGER X,I,J,M1,N,N1,N2,KEY(2000),POS,VARNO,EXTRACT,POSIT(100)
0060      C      REAL DATA(100,2000),DAT,DATA2(100,2000)
0061      C      CHARACTER TITLE*80,FORM*80,SAMPLE(2000)*10,NAME(100)*8,OUT*12
0062      C      CHARACTER BIN*12,SORT*2,B*1,K*2,NAME2(100)*8,SELECT*1
0063      C
0064      C      *****
0065      C      ***** DETAILS FOR OTHER PROGRAMMERS *****
0066      C      *****
0067      C
0068      C      M1 = NO OF VARIABLES
0069      C      N1 = NO OF RECORDS
0070      C      DATA = INPUT DATA VALUES (FREE FORMAT)
0071      C      TITLE = TITLE OF FILE (TO IDENTIFY DATAFILE TO USER)
0072      C      FORM = FORMAT OF OUTPUT DATA
0073      C      NAME = ARRAY 1 TO M CONTAINING VARIABLE NAMES
0074      C      OUT = INPUT/CREATION .RAW FILE NAME
0075      C      SAMPLE= ARRAY 1 TO N CONTAINING SAMPLE NAMES

```

```

0076 C KEY = A TWO SYMBOL CODE ATTACHED TO THE END OF THE
0077 C SAMPLE NAME. BY DEFAULT NORMALLY IS " ".
0078 C (NB. THIS PROGRAM ASSUMES KEY IS NUMERIC)
0079 C
0080 C ++++++
0081 C ++++++ END OF DETAILS ++++++
0082 C ++++++
0083 C
0084 C
0085 C ASK FOR FILENAME
0086 C
0087 C WRITE(6,100)
0088 C READ(5,501)OUT
0089 C OPEN(2,FILE=OUT,DEFAULT FILE='.RAW',STATUS='OLD')
0090 C
0091 C INFORM USE OF THE STYLES OF SORT AVAILABLE
0092 C
0093 302 WRITE(6,910)
0094 READ(5,911)SORT
0095 IF(SORT.EQ.'/')THEN
0096 GOTO 999
0097 END IF
0098 IF(SORT.EQ.'K')THEN
0099 GOTO 300
0100 END IF
0101 IF(SORT.EQ.'V')THEN
0102 GOTO 301
0103 END IF
0104 IF(SORT.EQ.'E')THEN
0105 GOTO 4000
0106 END IF
0107 GOTO 302
0108 C
0109 C *****
0110 C ***** SELECTIVE EXTRACTION *****
0111 C *****
0112 C
0113 C READ FILE HEADER AND DATA
0114 C
0115 4000 READ(2,108)TITLE
0116 READ(2,109)FORM
0117 READ(2,110)M1,N1
0118 READ(2,111)(NAME(I),I=1,M1)
0119
0120 DO 2435 I=1,N1
0121 READ(2,483)SAMPLE(I),KEY(I)
0122 READ(2,901)(DATA(J,I),J=1,M1)
0123 2435 CONTINUE
0124 C
0125 C ASK THE USER FOR THE NUMBER OF VARIABLES
0126 C TO BE EXTRACTED
0127 C *****
0128 C
0129 C WRITE(6,2020)
0130 C READ(5,*)EXTRACT
0131 C
0132 C READ IN THE POSITIONS OF EACH VARIABLE
0133 C TO BE EXTRACTED
0134 C *****
0135 C
0136 C DO 2022 I=1,EXTRACT
0137 C
0138 C LIST VARIABLES
0139 C *****
0140 C
0141 3104 L=0
0142 P1=M1
0143 3011 IF(P1.GE.3)THEN
0144 L=L+1
0145 P1=P1-2
0146 GOTO 3011
0147 END IF
0148 C
0149 C NO OF REMAINING SAMPLES FORMING LESS THAN ONE COMPLETE
0150 C ROW (=P1).

```

```

0151 C
0152 C   OUTPUT VARIABLE NAMES
0153 C
0154     Y=0
0155     IF(L.EQ.0)THEN
0156     GOTO 3012
0157     END IF
0158     WRITE(6,1000)
0159     WRITE(6,108)TITLE
0160
0161     WRITE(6,5)
0162     DO 3013 I1=1,L
0163     X=Y+1
0164     Y=Y+2
0165     WRITE(6,6)((J,NAME(J)),J=X,Y)
0166 3013 CONTINUE
0167     IF(P1.EQ.0)THEN
0168     GOTO 15
0169     END IF
0170 3012 Y=M1-P1+1
0171     WRITE(6,6)((J,NAME(J)),J=Y,M1)
0172 C
0173 C   ASK USER FOR VARIABLE NUMBER
0174 C   *****
0175 C
0176     WRITE(6,2023)
0177     READ(5,*)POSIT(I)
0178
0179 2022 CONTINUE
0180 C
0181 C   ASK FOR REFORMATTED DATA FILENAME
0182 C
0183     WRITE(6,900)
0184     READ(5,501)BIN
0185 C
0186 C   GENERATE NEW ARRAYS FOR THE REQUIRED VARIABLE NAMES
0187 C   PRIOR TO OUTPUT
0188 C
0189     DO 2300 I=1,N1
0190     DO 2301 J=1,EXTRACT
0191
0192     DATA2(J,I)=DATA(POSIT(J),I)
0193     NAME2(J)=NAME(POSIT(J))
0194
0195 2301 CONTINUE
0196 2300 CONTINUE
0197 C
0198 C   OUTPUT EXTRACTED DATA
0199 C   *****
0200 C
0201 C   ASK THE USER IF A RAW OR DAT FILE IS REQUIRED
0202 C
0203 2044 WRITE(6,2040)
0204     READ(5,2041)SELECT
0205     IF(SELECT.EQ.'R')THEN
0206     GOTO 2042
0207     END IF
0208     IF(SELECT.EQ.'D')THEN
0209     GOTO 2043
0210     END IF
0211     GOTO 2044
0212 C
0213 C   WRITE RAW FILE
0214 C   *****
0215 C
0216 2042 OPEN(1,FILE=BIN,DEFAULT FILE='.RAW',STATUS='NEW')
0217
0218     WRITE(1,108)TITLE
0219     WRITE(1,109)FORM
0220     WRITE(1,110)EXTRACT,N1
0221     WRITE(1,111)(NAME2(I),I=1,EXTRACT)
0222
0223     DO 2010 I=1,N1
0224     WRITE(1,483)SAMPLE(I),KEY(I)
0225     WRITE(1,901)(DATA2(J,I),J=1,EXTRACT)

```

```

0226      2010 CONTINUE
0227
0228          WRITE(6,350)
0229          GOTO 999
0230      C
0231      C      WRITE DAT FILE
0232      C      *****
0233      C
0234      2043 WRITE(6,2046)N1
0235
0236          OPEN(1,FILE=BIN,DEFAULT FILE='.DAT',STATUS='NEW')
0237
0238          DO 2482 I=1,N1
0239              WRITE(1,2483)SAMPLE(I)
0240              WRITE(1,901)(DATA2(J,I),J=1,EXTRACT)
0241      2482 CONTINUE
0242
0243          WRITE(6,350)
0244          GOTO 999
0245      C
0246      C      *****
0247      C      ***** SORT USING KEYS *****
0248      C      *****
0249      C
0250      C      READ FILE HEADER AND DATA
0251      C
0252      300 READ(2,108)TITLE
0253          READ(2,109)FORM
0254          READ(2,110)M1,N1
0255          READ(2,111)(NAME(I),I=1,M1)
0256
0257          DO 435 I=1,N1
0258              READ(2,483)SAMPLE(I),KEY(I)
0259              READ(2,901)(DATA(J,I),J=1,M1)
0260      435 CONTINUE
0261      C
0262      C      CHECK IF No.of Samples > 99
0263      C
0264          IF(N1.GE.100)THEN
0265              WRITE(6,305)
0266          END IF
0267      C
0268      C      ASK FOR REFORMATTED DATA FILENAME
0269      C
0270          WRITE(6,900)
0271          READ(5,501)BIN
0272          OPEN(1,FILE=BIN,DEFAULT FILE='.RAW',STATUS='NEW')
0273      C
0274      C      SCAN THE KEYS AND DELETE ALL "0" KEYS
0275      C      *****
0276      C
0277          I=1
0278      1400 IF (KEY(I).EQ.0)THEN
0279
0280      C      MOVE ALL DATA RECORDS AFTER RECORD I FORWARD BY 1
0281
0282          DO 1310 I1=I+1,N1
0283              SAMPLE(I1-1)=SAMPLE(I1)
0284              KEY(I1-1)=KEY(I1)
0285              DO 1311 J=1,M1
0286                  DATA(J,I1-1)=DATA(J,I1)
0287      1311 CONTINUE
0288      1310 CONTINUE
0289
0290          N1=N1-1
0291
0292          IF(I.GT.N1)THEN
0293
0294              N=2
0295
0296              WRITE(1,108)TITLE
0297              WRITE(1,109)FORM
0298              WRITE(1,110)M1,N1
0299              WRITE(1,111)(NAME(I),I=1,M1)
0300

```



```

0301      GOTO 313
0302      END IF
0303
0304      GOTO 1400
0305      END IF
0306
0307      I=I+1
0308
0309      GOTO 1400
0310      C
0311      C      SCAN THE KEYS TO FIND THE LOWEST
0312      C      *****
0313      C
0314      313 POS=KEY(2)
0315
0316      IF (KEY(1).GT.KEY(2)) THEN
0317      C
0318      C      SWOP POSITIONS
0319      C
0320      KEY(1999)=KEY(1)
0321      KEY(1)=KEY(2)
0322      KEY(2)=KEY(1999)
0323
0324      SAMPLE(1999)=SAMPLE(1)
0325      SAMPLE(1)=SAMPLE(2)
0326      SAMPLE(2)=SAMPLE(1999)
0327
0328      DO 1200 J=1,M1
0329
0330      DATA(J,1999)=DATA(J,1)
0331      DATA(J,1)=DATA(J,2)
0332      DATA(J,2)=DATA(J,1)
0333
0334      1200 CONTINUE
0335
0336      POS=KEY(2)
0337      END IF
0338
0339
0340      DO 307 I=1,N1
0341      IF (KEY(I).LT.POS) THEN
0342      N=I
0343      POS=KEY(I)
0344      END IF
0345      307 CONTINUE
0346
0347      IF (N1.EQ.1) THEN
0348      N=1
0349      END IF
0350      C
0351      C      WE NOW HAVE N, THE POSITION OF THE LOWEST KEY/RECORD IN ARRAY
0352      C      AND CAN THEREFORE WRITE A SINGLE DATA RECORD (N)
0353      C
0354      WRITE(1,483) SAMPLE(N), KEY(N)
0355      WRITE(1,901) (DATA(J,N), J=1,M1)
0356      C
0357      C      CHECK TO SEE THAT THE RECORD IN QUESTION WAS NOT AT THE END
0358      C      OF THE LIST OF RECORDS
0359
0360      IF (N1.EQ.1) THEN
0361      WRITE(6,350)
0362      GOTO 999
0363      END IF
0364      C
0365      C      IF THE LAST RECORD IS THE ONE TO BE PRINTED THEN NO RESHUFFLE
0366      C      IS REQUIRED ONLY DECREASE ARRAY SIZE BY 1.
0367      C
0368      IF (N1.EQ.N) THEN
0369      N1=N1-1
0370      N=1
0371      GOTO 313
0372      END IF
0373      C
0374      C
0375      C      MOVE ALL DATA RECORDS AFTER RECORD N FORWARD BY 1

```

```

0376 C
0377 DO 310 I=N+1,N1
0378 SAMPLE(I-1)=SAMPLE(I)
0379
0380 KEY(I-1)=KEY(I)
0381
0382 DO 311 J=1,M1
0383 DATA(J,I-1)=DATA(J,I)
0384 311 CONTINUE
0385 310 CONTINUE
0386 N1=N1-1
0387
0388 GOTO 313
0389 C
0390 C LOOP N1 TIMES!!
0391 C
0392 C *****
0393 C ***** SORT USING VARIABLES *****
0394 C *****
0395 C
0396 C READ FILE HEADER AND DATA
0397 C
0398 301 READ(2,108)TITLE
0399 READ(2,109)FORM
0400 READ(2,110)M1,N1
0401 READ(2,111)(NAME(I),I=1,M1)
0402
0403 DO 385 I=1,N1
0404 READ(2,484)SAMPLE(I),KEY(I)
0405 READ(2,901)(DATA(J,I),J=1,M1)
0406 385 CONTINUE
0407 C
0408 C LIST VARIABLES
0409 C
0410 104 L=0
0411 P1=M1
0412 11 IF(P1.GE.3)THEN
0413 L=L+1
0414 P1=P1-2
0415 GOTO 11
0416 END IF
0417 C
0418 C NO OF REMAINING SAMPLES FORMING LESS THAN ONE COMPLETE
0419 C ROW (P1).
0420 C OUTPUT VARIABLE NAMES
0421 C
0422 Y=0
0423 IF(L.EQ.0)THEN
0424 GOTO 12
0425 END IF
0426 WRITE(6,1000)
0427 WRITE(6,108)TITLE
0428
0429 WRITE(6,5)
0430 DO 13 I=1,L
0431 X=Y+1
0432 Y=Y+2
0433 WRITE(6,6)((J,NAME(J)),J=X,Y)
0434 13 CONTINUE
0435 IF(P1.EQ.0)THEN
0436 GOTO 15
0437 END IF
0438 12 Y=M1-P1+1
0439 WRITE(6,6)((J,NAME(J)),J=Y,M1)
0440 C
0441 C ASK USER TO SELECT VARIABLE NAME FOR SORT
0442 C
0443 WRITE(6,366)
0444 READ(5,*)VARNO
0445
0446 C ASK FOR REFORMATTED DATA FILENAME
0447 C
0448 15 WRITE(6,900)
0449 READ(5,501)BIN
0450

```

```

0451      OPEN(1,FILE=BIN,DEFAULT FILE='.RAW',STATUS='NEW')
0452      C
0453      C      WRITE FILE HEADER AND DATA
0454      C
0455      WRITE(1,108)TITLE
0456      WRITE(1,109)FORM
0457      WRITE(1,110)M1,N1
0458      WRITE(1,111)(NAME(I),I=1,M1)
0459      C
0460      C      SCAN THE VARIABLE (VARNO) TO FIND THE LOWEST
0461      C      *****
0462      C
0463      399 DAT=DATA(VARNO,1)
0464      DO 320 I=1,N1
0465      IF (DATA(VARNO,I).LT.DAT)THEN
0466      N=I
0467      DAT=DATA(VARNO,I)
0468      END IF
0469      320 CONTINUE
0470
0471      IF(N1.EQ.1)THEN
0472      N=1
0473      END IF
0474
0475      C
0476      C      WE NOW HAVE N, THE POSITION OF THE LOWEST KEY/RECORD IN ARRAY
0477      C      AND CAN THEREFORE WRITE A SINGLE DATA RECORD (N)
0478      C
0479      WRITE(1,484)SAMPLE(N),KEY(N)
0480      WRITE(1,901)(DATA(J,N),J=1,M1)
0481      C
0482      C      CHECK TO SEE THAT THIS WAS NOT THE LAST SAMPLE
0483      C
0484      IF(N1.EQ.1)THEN
0485      WRITE(6,350)
0486      GOTO 999
0487      END IF
0488
0489      IF(N1.EQ.N)THEN
0490      N1=N1-1
0491      N=1
0492      GOTO 399
0493      END IF
0494      C
0495      C      MOVE ALL DATA RECORDS AFTER RECORD N FORWARD BY 1
0496      C
0497      DO 381 I=N+1,N1
0498      SAMPLE(I-1)=SAMPLE(I)
0499      KEY(I-1)=KEY(I)
0500
0501      DO 382 J=1,M1
0502      DATA(J,I-1)=DATA(J,I)
0503      382 CONTINUE
0504      381 CONTINUE
0505
0506      N1=N1-1
0507
0508      GOTO 399
0509      C
0510      C      LOOP N1 TIMES!!
0511      C
0512      C      *****
0513      C      ***** END OF PROCESSING *****
0514      C      *****
0515      C
0516      C      *****
0517      C      ***** INPUT/OUTPUT FORMATS AND DIALOGUE *****
0518      C      *****
0519      C
0520      5  FORMAT(//1X,'Variable names: '//)
0521      6  FORMAT(2(10X,I3,' : ',A8))
0522      100 FORMAT(///' Type in the .RAW filename required.....> ', $)
0523      108 FORMAT(1X,A79)
0524      109 FORMAT(1X,A79)
0525      110 FORMAT(2I6)

```

```

0526 111  FORMAT(8(1X,A8))
0527 305  FORMAT(///
0528 1' WARNING: No. of sample records exceeds 99!!'///)
0529 350  FORMAT(/////
0530 1' *****' /
0531 2' ***** SORT COMPLETED *****' /
0532 3' *****' ///)
0533 366  FORMAT(//' Select Variable No.....> ', $)
0534 444  FORMAT(//' Is a new TITLE required (Y or N).....> ', $)
0535 445  FORMAT(A79)
0536 446  FORMAT(//' Title....> ', $)
0537 2483 FORMAT(1X,A10,';')
0538 483  FORMAT(1X,A10,A2)
0539 484  FORMAT(1X,A10,A2)
0540 501  FORMAT(A12)
0541 777  FORMAT(//' Input a KEY to your data (Y or N).....> ', $)
0542 779  FORMAT(//' Sample ',A8,' (New KEY or . to pass) Key= '
0543 1,A2,' ....> ', $)
0544 789  FORMAT(A2)
0545 783  FORMAT(//' Do you require SORT (Y or N).....> ', $)
0546 890  FORMAT(' N=',I3,' N1=',I3)
0547 900  FORMAT(//' Select a name for the new SORTED datafile....> ', $)
0548 901  FORMAT(1X,6F13.4)
0549 903  FORMAT(1X,'*****')
0550 910  FORMAT(/////
0551 1 ' *****' /
0552 2 ' ***** SORT *****' /
0553 3 ' *****' /
0554 4/' Two types of sort are available to reorder the datafile:/'
0555 5/' KEY Sort:      Records are placed in order of ascending'
0556 6/'              Key values. (All keys are asumed to be'
0557 7/'              numeric and values of zero are deleted.)/'
0558 8/' VARIABLE Sort: Records are placed in order of ascending'
0559 9/'              variable values. (Any variable may be '
0560 9/'              selected for sorting). '/'
0561 9/' EXTRACT Sort: Any number of variables may be selected'
0562 9/'              for EXTRACTION from the datafile. '/'
0563 9/' Select Sort Style (K,V,E or / to Exit).....> ', $)
0564 911  FORMAT(A2)
0565 915  FORMAT(//' Do you want to list the "KEYS" (Y or N).....> ', $)
0566 916  FORMAT(A1)
0567 917  FORMAT(19(2X,A2))
0568 1000 FORMAT(///)
0569 2000 FORMAT(1X,I2)
0570 2020 FORMAT(//' How many variables are to be extracted.....> ', $)
0571 2023 FORMAT(//' Select variable number for extraction .....> ', $)
0572 2040 FORMAT(//' Select RAW or DAT file (R or D).....> ', $)
0573 2041 FORMAT(A1)
0574 2046 FORMAT(//' No of Records in the DAT file = ',I4)
0575 999  END

```